



Best Available Mercury Reduction Technology Analysis and Proposed Alternative Mercury Emissions Reduction Plan

Prepared for
ArcelorMittal Minorca Mine Inc.



ArcelorMittal

December 2018

Appendix B (B-1 through B-4)

Historical Mercury Reduction Research Reports

Appendix B

Historical Mercury Reduction Research Reports

Appendix B-1

Pre-TMDL Implementation Plan DNR Research

Contents

B-1-1: Mercury Removal from Induration Off Gas by Wet Scrubbers (November 15, 2001).....	B-1-1
B-1-2: On the Distribution of Mercury in Taconite Plant Scrubber Systems (October 15, 2003)	B-1-40
B-1-3: Mercury and Mining in Minnesota (October 15, 2003)	B-1-71
B-1-4: Mercury Capture at Taconite Processing Facilities: Update on DNR Research Activities (October 1, 2004)	B-1-134
B-1-5: Mercury Transport in Taconite Processing Facilities: (I) Release and Capture During Induration (August 15, 2005)	B-1-153
B-1-6: Mercury Vaporization Characteristics of Taconite Pellets (October 2005).....	B-1-214
B-1-7: Mercury Chemistry and Mossbauer Spectroscopy of Iron Oxides During Taconite Processing on Minnesota's Iron Range (December 31, 2005)	B-1-239
B-1-8: Mercury Transport in Taconite Processing Facilities: (II) Fate of Mercury Captured by Wet Scrubbers (December 31, 2005).....	B-1-255
B-1-9: Email communication from Anne Jackson (MPCA) to Cliff Twaroski (Barr). Mercury Speciation Profiles (October 11, 2006).....	B-1-268
B-1-10: Methods Testing for Measurement of Mercury Speciation for High-Reactive Dust (April 2007)	B-1-292
B-1-11: Mercury Control Technologies for the Taconite Industry (June 2007).....	B-1-307
B-1-12: Mercury Transport in Taconite Processing Facilities: (III) Control Method Test Results (December 31, 2007)	B-1-344
B-1-13: Bench Scale Tests to Separate Mercury from Wet-Scrubber Solids from Taconite Plants (January 7, 2008)	B-1-393
B-1-14: On the Measurement of Stack Emissions at Taconite Processing Plants (May 30, 2008).....	B-1-420
B-1-15: Proof-of-concept Testing of Novel Mercury Control Technology for a Minnesota Taconite Plant (July 2008)	B-1-444
B-1-16: Demonstration of Mercury Capture in a Fixed Bed (June 2009).....	B-1-460
B-1-17: Assessment of Potential Corrosion Induced by Bromine Species used for Mercury Reduction in a Taconite Facility (August 2009)	B-1-511
B-1-18: A Brief Summary of Hg Control Test Results for Br Injection into Taconite Induration Furnaces (April 10, 2011)	B-1-594
B-1-19: Email communication from Michael Berndt (DNR) to Ryan Siats (Barr). Data from Previous Mercury Reduction Research (September 15, 2016).....	B-1-602

Appendix B-1-1

Mercury Removal from Induration Off Gas by Wet Scrubbers

November 15, 2001

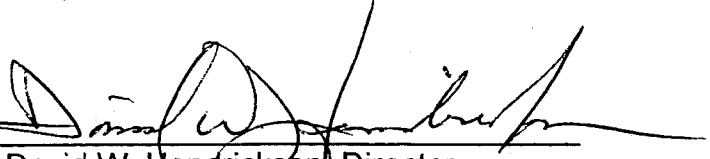
MAY 03 2002

**MERCURY REMOVAL
FROM INDURATION OFF GAS
BY WET SCRUBBERS**

COLERAINE MINERALS RESEARCH LABORATORY

November 15, 2001

By 
Blair R. Benner
Program Director – Minerals

Approved by 
David W. Hendrickson, Director
Coleraine Minerals Research Laboratory

Project #5601403
CMRL/TR-01-19
NRRI/TR-2001/37

University of Minnesota Duluth
Natural Resources Research Institute
5013 Miller Trunk Highway
Duluth, Minnesota 55811

Coleraine Minerals Research Laboratory
P O Box 188
One Gayley Avenue
Coleraine, Minnesota 55722

Mercury Removal from Induration Off Gas by Wet Scrubbers

SUMMARY

During the induration of taconite pellets, green balls are heated to greater than 2200°F. A previous study¹ indicated that greater than 90 percent of the mercury contained in the green balls is volatilized during induration. Some of the volatilized mercury is removed by the gas scrubbers. Studies²⁻⁴ on coal burning power plants indicate that the mercury in flue gas is present as either elemental mercury or as divalent mercury. In power plant scrubbers, the majority of the divalent mercury is removed, but very little elemental mercury is removed by the scrubbers. The particulate matter in the off gas appears to remove a significant portion of the mercury that is removed. It is thought that the off gas chemistry and the scrubber water chemistry could affect the removal of mercury. To determine if the scrubber water chemistry could affect the removal of mercury from taconite pelletizing off gases, the Minnesota Department of Natural Resources' (MNDNR) environmental cooperative funded a study to sample around the scrubbers from the plants equipped with wet scrubbers to determine if water chemistry affects mercury removal. Another objective of the study was to determine the role of solids entrained in the off gases and removed by the scrubbers. These solids are returned to the process. If they were discarded, then some amount of mercury could be eliminated from the system, but at a cost of iron units.

Samples were obtained from Minntac, EVTAC, Minorca, Hibtac and Northshore. With the exception of the mercury analyses, all chemical analyses were conducted at Coleraine. Mercury analyses were run by Frontier Geosciences of Seattle, Washington.

While the various plants have different scrubber configurations and scrubber water chemistries, these differences appeared to have no significant affect on mercury removal. Accurate mercury balances were not possible because mercury content in the fired pellets from all of the plants was below the detection limit of about 0.6 parts per billion (ppb). Solids entrained in the off gases removed significantly more mercury than the scrubber water. Of the mercury removed in the scrubber systems, the amount contained in the solids ranged from 75 percent at Northshore to greater than 99 percent at EVTAC. The minus 10 micron fraction of the solids in the off gases appears to remove the most mercury. Analysis of the solids that are continually recycled to the Minorca wet scrubbers indicates a high capacity for mercury removal (the solids assayed over 3000 ppb mercury). This result indicates that the mercury should remain with the solids and should not leach if the solids were sent to the tailings basin.

INTRODUCTION

During the pelletizing process, the majority of mercury contained in the green balls is vaporized and leaves with the off gases. Wet scrubbers remove some of this mercury. Mercury that is removed is either dissolved in the water or is associated with the solids entrained in the off gas stream. It is generally assumed that mercury removed by the scrubber water and solids is present as divalent mercury and mercury that is not removed by the scrubbers is present as elemental mercury. Based on research on coal fired power plant emissions, most of the removed mercury is associated with the solids that are generally recovered in the electrostatic precipitators and that the amount of carbon, chlorine, and sulfur in the off gas can affect the amount of mercury removed. It is possible that other elements in the indurating off gas may also affect the amount of mercury removed by the wet scrubbers.

In most cases, the solids contained in the scrubber water are recovered and are recycled to green ball feed. This practice tends to increase the amount of mercury in the green balls. One of the objectives of this program is to determine how much mercury is being recycled and how much iron would be lost if the material was wasted instead of recycled.

The MNDNR's environmental cooperative funded a study by the Coleraine Minerals Research Laboratory (CMRL) to sample the various plants and conduct chemical analyses of the various streams. Sampling was conducted at the five operating taconite plants (Hibtac, Minntac, EVTAC, Minorca, and Northshore) that are equipped with some type of wet scrubbers on the indurating off gases. The main objective of the sampling program was to determine if scrubber water chemistry could be related to mercury removal by the wet scrubbers. The test program was **not** designed to provide a mercury balance around the indurating plant. Data contained in this report cannot be used to accurately calculate the amount of mercury being released to the atmosphere by any of the sampled plants.

SAMPLING PROGRAM

Grab samples were taken of the materials entering the system: green balls, solid fuel (if any), and scrubber inlet water; and exiting the system: fired pellets, scrubber water out, and multiclone solids (if any). Sampling devices were cleaned with dilute acid and distilled water prior to the sampling. Each of the sampling devices were purged with the material being sampled. All samples were brought to the Coleraine Minerals Research Laboratory (CMRL) for filtering and chemical analysis. (Samples from Hibtac were from a previous sampling program conducted by Hibtac in October of 1998.) All liquid samples were filtered through 0.45 micron paper, with the solids content being measured. All solids samples were dried, with the moisture content being recorded. All solids processing equipment was thoroughly cleaned and was purged with the material being processed (when possible). Splits of the solids and water samples were sent to Frontier Geosciences in Seattle for mercury analysis. All remaining analyses were run at CMRL by ICP.

OFF GAS TREATMENT SCHEMES

Each of the plants has slightly different wet scrubbers. Minntac has the simplest flowsheet, Figure 1, where the exhaust from the grate-kiln system is sent to one scrubber per line, fresh water is added to the scrubber, and the water with entrained solids is removed and sent to a thickener. Both the water and solids are eventually recycled to the process, but nothing is recycled to the scrubber.

EVTAC also employs the grate-kiln system, but has a more complicated scrubber flowsheet, as shown schematically in Figure 2. EVTAC's system consists of a scrubber and a de-misting tank. Fresh water is added through slats in the top of the de-misting tank. That water plus the water and solids from the scrubber are sent to a thickener. The thickener overflow is recycled to the scrubber. Thickener underflow is sent back to the process. In steady state, the water added at the slats (slat water) is equal to the amount of water removed with the thickener underflow.

Minorca has a traveling grate machine with two separate gas streams going to the scrubber as shown in Figure 3. The first (hood exhaust) goes directly to the scrubber, while the second and larger stream (window exhaust) goes to a series of "multi clones" to remove most of the entrained dust. Gas from the multi clones goes to the scrubber. Water to the scrubbers is continuously recycled, with fresh water being added to maintain sump level.

Hibtac is similar to Minorca in that it has a traveling grate and a dry dust removal step prior to the wet scrubbers, as shown schematically in Figure 4. It is not known if all of the off gas passes through the dry dust removal section, but all of the off gas is treated by the wet scrubbers. Scrubber water is not recycled directly to the scrubber.

Northshore also employs a traveling grate machine and has two off gas streams, as shown in Figure 5. Unlike Minorca and Hibtac, there is no dust removal prior to the scrubbers and there are separate scrubbers for each exhaust stream. Fresh water is added to the scrubbers with no direct recycle.

WATER CHEMISTRY

Chemical analyses for the water samples taken in the test program are given in Table I. All of the analyses are in parts per million (ppm) except for the mercury analyses, which are in nanograms per liter (ng/l) or parts per trillion (ppt).

For Minntac there were only two water samples; scrubber water in and scrubber water out. Looking at the Minntac analysis in Table I, the mercury results appear to be wrong in that the scrubber in water has more mercury than the water out. Previous work¹ showed a mercury content of 2.05 ng/l in the water in and 491.55 ng/l in the scrubber out water. The scrubber in water analysis was a quality control sample for Frontier, which means that it was run in duplicate and was run with a known addition. The duplicate analyses were 74.5 and 83.3 ng/l for an average of 78.9 ng/l report in Table I. Frontier's reports for all samples with the quality control results are given in Appendix I. Since the duplicate analyses were reasonably close, it appears that the mercury analysis of the

scrubber in water is truly the mercury content on the sample sent to Frontier. It is possible that the scrubber out sample was accidentally poured into both the scrubber in and scrubber out bottles that were sent to Frontier. Based on the cation and anion analyses for the Minntac waters (Table I), samples were taken of the scrubber in and scrubber out waters.

For EVTAC there were five water samples as shown in Table I. EVTAC has two thickeners for the scrubbers; therefore, there is an overflow and underflow sample for each thickener as well as the makeup water (slat spray water). Again, there appears to be a problem with the mercury analyses. In this case, thickener overflow 2A appears to be too high in mercury. The other analyses look appropriate.

For Northshore there were also five water samples (Table I), since both lines 11 and 12 were sampled. With the exception of the Waste Gas Water from line 11, the analyses look consistent. The reason for the low cation and anion concentrations in line 11 waste gas water is unknown. Northshore has the most unique water chemistry due to the addition of soda ash to soften the water.

Only two water samples were obtained from Minorca - the recycled scrubber water and the make up water. As would be expected from recycling the water, the Minorca scrubber water had the highest mercury content of 112 ppt.

Hibtac supplied three water samples for analyses. It appears that only the make-up water and the scrubber water are germane to this study.

As mentioned above, some sampling of scrubber water was conducted as part of a previous study in 1997¹. Mercury analyses of those waters were significantly different from the current study, as shown in Table II. For Minntac and Hibtac, there was a large decrease in the mercury content of the water coming out of the scrubber, while the mercury concentration in the water from the Northshore scrubbers increased, especially line 11: For Hibtac and Northshore, the mercury content in the scrubber input water had increased. The 1997 mercury analyses were also conducted by Frontier Geosciences.

SOLIDS CHEMISTRY

Solids from the sampling program were analyzed for mercury by Frontier. The samples were analyzed at Coleraine for total iron, ferrous iron, silica, CaO, MgO, alumina, sulfur and carbon (coal sample only). Results are given in Table III. Frontier Geosciences' reports of mercury analysis for the solid samples are included in Appendix I. Values in Table III are in dry weight percent except for the mercury, which are in ng/g (ppb).

For Minntac there were four solid samples: the greenballs, fired pellets, solids contained in the scrubber discharge, and coal. Fired pellet mercury content was below the detection limit of 0.6 ppb. For Minorca there were also four solid samples: the greenballs, fired pellets, multiclone dust, and the solids in the recycling scrubber water. As with the Minntac sample, the fired pellet mercury content was below detection limits. For EVTAC there were 7 solid samples: greenballs, fired pellets, coal, two thickener underflows (A & B), and two thickener overflows. Again, the fired pellets were below the mercury detection limits (0.69 ppb in this case). Hibtac provided 7 solid samples: filtercake, concentrate, greenballs, limestone, bentonite, fired pellets and multi-tube dust.

Unfortunately, Hibtac did not supply a sample of the solids in the scrubber discharge. Again, the fired pellets were below the mercury detection limits of 0.69 ppb. For Northshore there were eight samples (four per line): greenballs, fired pellets, solids from the hood exhaust scrubber and solids from the waste gas scrubber. Line 12 fired pellets were reported to contain 1.85 ppb mercury, which is most likely a mistake. Line 11 fired pellets were below the detection limit as were all the other fired pellet samples from the other plants.

Comparing the greenball mercury analysis with the 1997 study indicated essentially the same mercury concentration for both studies, as shown in Table IV.

Part of the work on the solids included screening selected samples on a 10 micron screen and having mercury analyses run on the size fractions. Samples screened were the two thickener underflow samples from EVTAC and the multitube dust from Hibtac. Results are given in Table V. As was expected, there was very little minus 10 micron material in the multitube dust. About 30 percent of the thickener underflow solids was minus 10 micron. Due to the relatively small amount of minus 10 micron material, no analysis was performed on that fraction. Mercury concentration in the minus 10 micron fraction was calculated from the head mercury, the mercury in the plus 10 micron fraction and the weight split. Mercury was concentrated in the minus 10 mesh fractions. All of the minus 10 mesh material had a calculated mercury concentration of greater than 1 ppm.

ESTIMATED MERCURY BALANCES

Estimated mercury balances for the various plant scrubbers are given in Table VI. Since all of the fired pellet mercury analyses were below detection limits, a value of 0.5 ng/g (ppb) was assumed for all fired pellets. Also included in Table VI is the mercury balance if the pellets contain 0 ng/g and 0.69 ng/g (detection limit).

Minntac - For the period tested, the greenball feed rate was 450 tph at a moisture of 9.5 percent. Coal was added at the rate of 13,000 lb/hr and the flow rate to the scrubber was 2,960 gpm. As shown in Table VI, the greenballs added 3.355 grams per hour (g/hr) of mercury to the system; the coal added 0.149 g/hr and the scrubber water added 0.0067 g/hr. (a value of 10 ng/l was assumed for the scrubber in water). Coming out of the system the fired pellets (at the assumed mercury content) removed 0.194 g/hr mercury; the solids with the scrubber water removed 0.115 g/hr and the scrubber water removed 0.0447 g/hr. Based on the calculated tonnage of solids with the scrubber water and the iron analysis (Table III) of the scrubber, there are about 0.832 tph of iron in the scrubber solids. Assuming 100 percent operating time (8,760 hours per year), not recycling the scrubber solids would result in about 2.2 pounds of mercury being removed from the system with a loss of about 7,300 tons of iron units per year.

Northshore - Line 11 was being fed 196 tph of greenballs at 10.1 percent moisture with an estimated scrubber feed rate of 1,000 gpm. As shown in Table VI, this results in 0.258 g/hr mercury being added to the system with the greenballs and 0.0016 g/hr being added with the scrubber water. Coming out of the system, the fired pellets removed 0.0847 g/hr (using the assumed mercury content in the fired pellets); the combined scrubber solids removed 0.021 g/hr; and the combined scrubber water removed

0.007 g/hr. Line 12 was very similar, as shown in Table VI. As was the case for Minntac, more mercury was removed with the scrubber solids than with the scrubber water.

EVTAC - The system was being fed 600 ltp of greenballs at 9.5 percent moisture. Coal was being added at a rate of 7.52 ltp and slat water at 980 gpm. At these rates, the greenballs added 6.627 g/hr mercury; the coal added 0.0788 g/hr; and the slat water added 0.0012 g/hr as shown in Table VI. Exiting the system, the fired pellets removed 0.2619 g/hr mercury, the combined solids in the thickener underflows removed 0.7761 g/hr mercury; and the thickener underflow water removed 0.0040 g/hr mercury. Assuming 100 percent operating time, discarding the thickener underflow solids would remove 14.99 pounds of mercury a year from the system with a loss of about 5,423 tons of iron units.

Minorca - Since there was no estimate of the amount of dust from the multiclone, there was no way to estimate a mercury balance. It is of interest to note the high mercury concentration (3.179 ppm) in the solids recycled with the scrubber. This indicates that magnetite dust has a high capacity for removing mercury and would suggest that any scrubber solids sent to the tailing basin would not be leached by the water.

Hibtac - As with Minorca, there was no estimate of the rate of multitube dust production. That, combined with a lack of the solids contained with the scrubber water, precluded the calculation of a mercury balance.

CONCLUSIONS

Sampling around the scrubbers at five taconite plants has indicated that the majority of the mercury that is removed by the various scrubbers is removed by the solids, either wet or dry. Mercury in the solids appears to be concentrated in the minus 10 micron fractions. There was no indication that the scrubber water chemistry had any affect on the amount of mercury removed by the water. Discarding the solids from the scrubber system could remove significant amounts of mercury from the system without a catastrophic loss of iron units. Results from Minorca's scrubber solids recycling indicates that the scrubber solids have a relatively high capacity for the deposition of mercury, which implies that the scrubber solids would retain the mercury in the tailings basin. Since the fired pellet mercury analyses were all below detection limits, no accurate mercury balances could be calculated. Using an assumed value of 0.5 ng/g mercury in the fired pellets, the fired pellets removed a significant amount of mercury compared to the scrubber solids and water.

REFERENCES

1. Engesser and Niles, Mercury Emissions for Taconite Pellet Production, Technical Report CMRL/TR-97-11, September 1997.
2. Meij, Vredenburg, and Winkel, The Fate of Mercury in Coal-Fired Power Plants, The A&WMA Specialty Conference on Mercury Emissions: Fate, Effects, and Control, Chicago, IL, August, 2001.
3. Gibb, Clarke, and Mehta, The Fate of Coal Mercury During Combustion, Fuel Processing Technology, Vol. 65-66, pp 365-377, 2000.
4. Galbreath and Zygarlicke, Mercury Speciation in Coal Combustion and Gasification Flue Gases, Environmental Science and Technology, Vol. 30, No. 8, page 2421, 1996.

Table I - Chemical Analysis of Water Samples

	Hg, ng/g	pH	IC	Na	K	Ca	Mg	SO4	Cl	F	TOC
Minntac						ppm					
Scrub in	78.90	8.11	41.00	73.23	26.26	117.14	176.81	717.60	141.80	2.91	3.70
Scrub out	66.50	6.62	5.60	74.57	27.47	135.63	180.27	878.10	163.80	8.00	2.80
Inland				2%	5%	15%	2%	2%	16%	175%	
Process water	5.67	7.88	37.10	41.41	9.72	32.69	52.46	74.70	82.00	5.79	3.80
Scrub out	112.00	4.57	1.40	52.07	14.61	62.03	73.63	154.20	205.70	47.50	2.80
Northshore											
Feed Water	7.05	9.71	36.90	738.50	53.33	22.57	6.08	426.30	395.00	35.80	6.70
Hood Exhaust 11	32.80	7.65	30.30	780.60	56.01	24.32	7.12	531.60	436.30	130.90	6.80
Hood Exhaust 12	15.70	7.54	31.40	808.30	53.01	23.42	7.00	504.30	458.30	136.30	7.80
Waste Gas Wat 11	29.10	7.81	34.20	441.40	33.70	19.65	7.17	279.30	266.70	68.50	5.00
Waste Gas Wat 12	15.70	7.79	44.60	851.30	63.77	25.29	7.34	518.10	487.20	130.90	9.10
Evtac											
Thick unflo 2A	15.48	4.44	2.76	103.38	20.83	175.16	67.73	752.10	79.50	31.70	5.12
Thick oflo 2A	82.22	3.92	2.96	103.50	20.26	168.11	65.29	766.50	84.10	45.70	5.81
Thick unflo 2B	18.12	4.49	2.61	100.26	18.82	146.36	67.62	704.10	76.00	38.80	5.44
Thick oflo 2B	24.35	4.53	3.32	98.92	18.69	136.31	65.30	668.40	78.20	40.40	5.17
Slat Spray Water	5.25	7.25	29.24	74.30	10.89	44.57	55.74	246.60	55.00	12.00	6.41
Hibtac											
Conc water	8.61	7.99	90.89	58.75	10.80	74.79	128.89	265.20	64.20	8.30	7.92
Make-up water	5.37	8.00	40.79	58.31	16.26	40.32	74.58	204.90	57.20	9.80	3.62
Scrub water	11.95	7.63	22.79	58.95	16.94	41.23	74.77	267.60	62.30	18.00	2.84

**Table II - Comparison of Mercury Content in Water Samples
From 1997 and Current Study.**

		Hg, ng/l		
		1997	Current	Current
Minntac	Scrubber in	2.05	78.9	
	Scrubber out	491.55	66.5	
Hibtac	Scrubber in	2.81	5.37	
	Scrubber out	63.35	11.95	
Northshore			Line 11	Line 12
	Scrubbers in	2.21	7.05	7.05
	Hood Exhaust out	6.61	32.8	15.7
	Waste Gas out	10.87	29.1	15.7

Table III - Chemical Analyses of Solid Samples

	Hg, ng/g	Fe	SiO ₂	CaO	Percent		Sat Mag	Fe+2	S	C
					MgO	Al ₂ O ₃				
Evtac Greenball	12.00	66.60	6.14	0.80	0.48	0.10	66.53	22.92	0.016	
Evtac Fired Pellet	<0.69	64.90	6.18	0.72	0.48	0.10	0.58	0.79	0.003	
Evtac Coal	10.30	0.09	2.01			0.95			2.980	74.63
Evtac Thickner Unflow 2A	527.00	55.00	17.56	0.98	1.25	0.74	39.56	14.50	0.064	
Evtac Thickner Oflow 2A	233.00	49.60	23.64	0.85	1.68	1.08	28.53	11.89	0.083	
Evtac Thickner Unflow 2B	367.00	57.20	15.53	0.87	1.06	0.53	43.86	14.93	0.099	
Evtac Thickner Oflow 2B	826.00	48.30	24.21	1.31	1.81	0.90	28.47	11.83	0.074	
Hibtac Filter Cake	13.90	67.90	4.17	0.31	0.30	0.07	68.90	22.88	0.015	
Hibtac Concentrate	18.20	68.40	3.97	0.16	0.28	0.05	68.12	23.24	0.005	
Hibtac Limestone	3.72	0.02	0.46	55.05	0.69	0.11			0.285	
Hibtac Multi-tube Dust	154.00	66.90	4.56	0.28	0.32	0.13	38.01	12.58	0.028	
Hibtac Greenball	16.70	67.60	4.69	0.31	0.30	0.18	68.67	21.39	0.022	
Hibtac Bentonite	26.40	3.03	61.47	0.09	1.91	17.60			0.295	
Hibtac Fired Pellet	<0.69	66.20	4.62	0.31	0.33	0.17	1.99	1.09	0.000	
Northshore Waste Gas 11	211.00	61.20	5.94	3.80	1.25	0.35	52.76	16.49	0.030	
Northshore Waste Gas 12	110.00	62.20	4.34	3.96	1.12	0.32	52.74	16.40	0.022	
Northshore Hood Exhaust 11	26.00	63.20	3.92	3.68	1.02	0.33	56.68	18.53	0.030	
Northshore Hood Exhaust 12	26.40	62.70	4.56	3.72	1.04	0.35	54.26	17.01	0.031	
Northshore Greenball 11	1.44	63.20	3.86	3.85	1.03	0.28	63.33	20.73	0.013	
Northshore Greenball 12	1.10	63.10	4.06	3.85	1.04	0.32	62.81	20.29	0.018	
Northshore Fired Pellet 11	<0.69	63.30	4.42	3.91	1.05	0.34	2.01	0.21	0.011	
Northshore Fired Pellet 12	1.85	63.20	4.25	3.94	1.04	0.33	1.76	0.18	0.014	
Minntac greenball	8.10	62.90	4.48	3.27	1.12	0.18	62.88	21.00	0.016	
Minntac fired pellet	<0.6	63.60	4.64	5.58	1.13	0.20	1.45	0.20	0.014	
Minntac scrubber out	87.00	64.00	4.57	2.19	1.10	0.25	52.50	15.20	0.015	
Minntac coal	25.30	0.20	0.86			0.74			0.327	66.39
Minorca scrubber solids	3179.00	55.40	14.13	2.88	1.78	0.22	13.85	4.38	0.050	
Minorca multiclone dust	193.00	49.40	5.18	9.63	4.94	0.15	13.47	4.26	0.058	
Minorca green balls	7.80	61.10	4.29	4.35	1.39	0.15	61.00	20.99	0.014	
Minorca fired pellet	<0.6	62.60	4.38	4.52	1.45	0.15	6.44	1.47	0.004	

Table IV - Comparison of Mercury Content in Greenballs and Fired Pellets From 1997 and Current Study.

		Hg, ng/g		
		1997	Current	Current
Minntac	Greenballs	7.5	8.1	
	Fired Pellets	0.65	<0.60	
Hibtac	Greenballs	16.2	16.7	
	Fired Pellets	0.94	<0.69	
Northshore			Line 11	Line 12
	Greenballs	0.83	1.44	1.1
	Fired Pellets	0.29	<0.69	<0.69

Table V - Distribution of Mercury Between Plus and Minus 10 Micron Fractions

	Sample	Wt, g	Wt %	Hg, ng/g	Hg Dist, %
EVTAC Un'flow 2A	+10 microns	2.75	66.91	38.8	4.93
	-10 microns head	1.36	33.09	1514.2 527.0	95.07
Un'flow 2B	+10 microns	4.70	73.90	48.6	9.79
	-10 microns head	1.66	26.10	1268.5 367.0	90.21
Hibtac Multitube Dust	+10 microns	5.40	93.43	86.8	52.66
	-10 microns head	0.38	6.57	1108.9 154.0	47.34

Table VI - Estimated Mercury Balances for the Various Plants

		Hg	Flow	Total Hg	
	IN	Analysis	Rate	g/hr	% solids
Minntac	Greenball	8.1 ng/g	450 ltp	3.3547	90.50
	Coal	25.3 ng/g	13000 lb/hr	0.1493	
	Scrubber water	10 ng/l	2960 gpm	0.0067	
	Total in			3.5107	
	OUT				
	Pellets	0.5 ng/g	382.5 ltp	0.1945	
	Scrubber solids	87 ng/g	1.33 tph	0.1150	
	Scrubber water	66.5 ng/l	2960 gpm	0.0447	0.18
Total out			0.3542		
Northshore Line 11	IN				
	Green Balls	1.44 ng/g	196 ltp	0.2583	89.90
	Scrubber water	7.05 ng/l	1000 gpm	0.0016	
	Total in			0.2599	
	OUT				
	Pellets	0.5 ng/g	166.6 ltp	0.0847	
	Waste Gas Solids	211 ng/g	0.08 tph	0.0171	0.08
	Waste Gas water	29.1 ng/l	400 gpm	0.0026	
Exhaust Solids	26 ng/g	0.15 tph	0.0039	0.10	
Exhaust water	32.8 ng/l	600 gpm	0.0045		
Total out			0.1129		
Line 12	IN				
	Green Balls	1.1 ng/g	184 ltp	0.1852	90.00
	Scrubber water	7.05 ng/l	1000 gpm	0.0016	
	Total in			0.1869	
	OUT				
	Pellets	0.5 ng/g	156.4 ltp	0.0795	
	Waste Gas Solids	110 ng/g	0.09 tph	0.0100	0.09
	Waste Gas water	15.7 ng/l	400 gpm	0.0014	
Exhaust Solids	26.4 ng/g	0.09 tph	0.0024	0.06	
Exhaust water	15.7 ng/l	600 gpm	0.0021		
Total out			0.0955		
EVTAC	IN				
	Green balls	12 ng/g	600 ltp	6.6265	90.50
	Slat water	5.25 ng/l	980 gpm	0.0012	
	Coal	10.3 ng/g	7.52 ltp	0.0788	
	Total in			6.7064	
	OUT				
	Fired pellets	0.5 ng/g	515 ltp	0.2619	
	Underflow water	18.12 ng/l	980 gpm	0.0040	
Underflow solids a	527 ng/g	0.49 tph	0.2621	0.40	
Underflow solids b	826 ng/g	0.61 tph	0.5140	0.50	
Total out			1.0420		

Total Hg in Solids (University of Minnesota)

analyzed by:

Frontier Geosciences R&C 414 Pontius Avenue North, Suite B, Seattle WA 98109

phone: (206) 622-6960 fax: (206) 622-6870 email: nicolasb@frontier.wa.com

Sample Identification	Dry Fraction	Total Hg, ng/g*	
		wet wt basis	dry wt basis
Evtac Green Ball	1.000	12.0	12.0
Evtac Final Pellet	0.999	ND(<0.69)	ND(<0.69)
Evtac Coal	0.998	10.3	10.3
Evtac Thickener Un'flow 2A	0.999	526	527
Evtac Thickener O'flow 2A	0.998	233	233
Evtac Thickener Un'flow 2B	0.997	366	367
Evtac Thickener O'flow 2B	0.996	823	826
Hibtac Filter Cake	0.998	13.9	13.9
Hibtac Concentrate	0.999	18.2	18.2
Hibtac Limestone	0.999	3.72	3.72
Hibtac Mult-tube Dust	1.000	154	154
Hibtac Green Ball	1.000	16.7	16.7
Hibtac Bentonite	0.980	25.9	26.4
Hibtac Fired Pellet	1.000	ND(<0.69)	ND(<0.69)
North Shore Waste Gas Line 11	0.999	211	211
North Shore Waste Gas Line 12	0.999	110	110
North Shore Hood Exhaust Line 11	0.998	25.9	26.0
North Shore Hood Exhaust Line 12	1.000	26.4	26.4
North Shore Green Ball Line 11	0.999	1.44	1.44
North Shore Green Ball Line 12	1.000	1.10	1.10
North Shore Fired Pellet Line 11	0.999	ND(<0.69)	ND(<0.69)
North Shore Fired Pellet Line 12	1.000	1.85	1.85

*Blank corrected

ND-less than estimated MDL

Total Hg in Solids (University of Minnesota)

analyzed by:

Frontier Geosciences R&C 414 Pontius Avenue North, Suite B, Seattle WA 98109

phone: (206) 622-6960 fax: (206) 622-6870 email: nicolasb@frontier.wa.com

Sample Identification	Dry Fraction	Total Hg, ng/g	
		wet wt basis	dry wt basis

Method Blanks

Blank-1		0.89	
Blank-2		1.96 ^a	
Blank-3		0.49	
Blank-4		0.49	
Mean method blank		0.62	
Estimated MDL		0.69	

^aExcluded from calculation of mean method blank

Standard Reference Materials

NIST-2709		1,529	
recovery		109.2%	
reference value		1,400	

Total Hg in Solids (University of Minnesota)

analyzed by:

Frontier Geosciences R&C 414 Pontius Avenue North, Suite B, Seattle WA 98109

phone: (206) 622-6960 fax: (206) 622-6870 email: nicolasb@frontier.wa.com

Sample Identification	Dry Fraction	Total Hg, ng/g*	
		wet wt basis	dry wt basis

Matrix Duplicates

North Shore Hood Exhaust Line 11		25.89	
North Shore Hood Exhaust Line 11 MD		25.85	
Mean		25.87	
RPD		0.2%	
North Shore Fired Pellet Line 11		-0.01	
North Shore Fired Pellet Line 11 MD		1.32	
Mean		0.66	
RPD		203.1%	
Evtac Green Ball		11.98	
Evtac Green Ball MD		11.95	
Mean		11.97	
RPD		0.3%	

Matrix Spikes

North Shore Fired Pellet Line 11 MS		9,980	
spiking level		9,488	
net		9,979	
recovery		105.2%	
North Shore Fired Pellet Line 11 MSD		9,868	
spiking level		9,901	
net		9,867	
recovery		99.7%	
RPD		5.4%	

*Blank corrected

Total Mercury in Process Water (University of Minnesota)

analyzed by

Frontier Geosciences R&C 414 Pontius North, Suite B Seattle WA 98109

phone: 206-622-6960 fax: 206-622-6870 e-mail: nicolasb@frontier.wa.com

sample ID	description	[Hg], ng/L	comments
#8	evtac thickener u'flow water 2A	15.48	
#20	evtac concentrate water	8.61	
#12	evtac slat spray water	5.25	
#10	evtac thickener u'flow water 2B	18.12	
#22	hibtac scrubber water	11.95	
#21	hibtac makeup water	5.37	
#9	evtac thickener o'flow water 2A	82.22	
#11	evtac thickener o'flow water 2B	24.35	
B-1	blank-1	0.12	
B-2	blank-2	0.16	
B-3	blank-3	0.16	
	mean	0.15	
	estimated MDL	0.07	
#12	evtac slat spray water rep 1	4.97	
#12	evtac slat spray water rep 2	6.21	
	mean	5.25	10.5% RPD
	matrix spike level	40.40	
#8	evtac thickener u'flow water 2A + MS	53.71	94.6% recovery
#8	evtac thickener u'flow water 2A + MSD	54.77	97.3% recovery
	mean	52.24	2.1% RPD
NIST-1641d	NIST certified water CRM rep 1	7,751	diluted 200x
NIST-1641d	NIST certified water CRM rep 2	7,054	diluted 200x
	mean	7,403	9.4% RPD
	certified value	7,950	93.1% recovery
	analysis date	2-Jul-01	

Total Mercury in Process Water (University of Minnesota)

analyzed by

Frontier Geosciences R&C 414 Pontius Avenue North, Suite B Seattle WA 98109

phone: (206) 622-6960 fax: (206) 622-6870 email: ericv@frontier.wa.com

sample ID	description	[Hg], ng/L	comments
#9	N.S. Feed Water	7.05	
#10	N.S. Hood Exhaust Water Line 11	32.8	
#11	N.S. Hood Exhaust Water Line 12	15.7	
#12	N.S. Waste Gas Water Line 11	29.1	
#13	N.S. Waste Gas Water Line 12	15.7	
B-1	blank-1	0.05	
B-2	blank-2	0.10	
B-3	blank-3	0.05	
	mean	0.06	
	estimated MDL	0.09	
#11	N.S. Hood Exhaust Water Line 12	15.72	
#11	N.S. Hood Exhaust Water Line 12	17.67	
	mean	15.89	11.7% RPD
	matrix spike level	40.40	
#11	N.S. Hood Exhaust Water Line 12 + MS	57.94	97.2% recovery
#11	N.S. Hood Exhaust Water Line 12+ MSD	56.11	92.9% recovery
	mean	57.03	3.2% RPD
NIST-1641d	NIST certified CRM (diluted 200x)	8,042	101.2% recovery
	certified value	7,950	
	analysis date	July 9, 2001	

Total Mercury in Taconite Mill Substances (Coleraine Minerals Research Lab)

analyzed by

Frontier Geosciences Inc. 414 Pontius North, Seattle WA 98109

phone: 206-622-6960 fax: 206-622-6870 e-mail: nicolasb@frontier.wa.com

sample #	sample description	[Hg]	units	date analyzed	comment
#01	Mintac scrubber in water	78.9	ng/L	18-Jul-01	QC sample
#02	Mintac Scrubber out water	66.5	ng/L	18-Jul-01	
#03	Inland process water	5.67	ng/L	18-Jul-01	
#04	Inland scrubber water	112	ng/L	18-Jul-01	
#05	Mintac greenball	8.1	ng/g	31-Aug-01	QC sample
#06	Mintac fired pellet	< 0.6	ng/g	31-Aug-01	
#07	Mintac scrubber out solids	87.0	ng/g	31-Aug-01	
#08	Mintac coal	25.3	ng/g	31-Aug-01	
#09	Inland scrubber water solids	3,179	ng/g	31-Aug-01	
#10	Inland multi-clone dust	193	ng/g	31-Aug-01	
#11	Inland fired pellet	< 0.6	ng/g	31-Aug-01	
#12	Inland greenball	7.8	ng/g	31-Aug-01	
#13	Evtac thickener 2A + 10m	38.8	ng/g	31-Aug-01	
#14	Evtac thickener 2B + 10m	48.6	ng/g	31-Aug-01	
#15	Hibtac multi-tube dust + 10m	86.8	ng/g	31-Aug-01	
	solids blank #1	0.4	ng/g	31-Aug-01	
	solids blank #2	0.4	ng/g	31-Aug-01	
	solids blank #3	0.2	ng/g	31-Aug-01	
	solids blank #4	0.8	ng/g	31-Aug-01	
	solids blank #5	0.3	ng/g	31-Aug-01	
	solids blank #6	0.2	ng/g	31-Aug-01	
	mean	0.4	ng/g	31-Aug-01	estimated MDL = 0.6 ng/g
	water blank #1	0.05	ng/L	18-Jul-01	
	water blank #2	0.06	ng/L	18-Jul-01	
	water blank #3	0.09	ng/L	18-Jul-01	
	mean	0.07	ng/L	18-Jul-01	estimated MDL = 0.06 ng/L

Total Mercury in Taconite Mill Substances (Coleraine Minerals Research Lab)

analyzed by

Frontier Geosciences Inc. 414 Pontius North, Seattle WA 98109

phone: 206-622-6960 fax: 206-622-6870 e-mail: nicolasb@frontier.wa.com

sample #	sample description	[Hg]	units	date analyzed	comment
#05	Mintac greenball	8.3	ng/g	31-Aug-01	
#05	Mintac greenball dup	7.8	ng/g	31-Aug-01	
	mean	8.1	ng/g	31-Aug-01	6.2% RPD
#05	Mintac greenball + 93.5 ng/g MS	97.4	ng/g	31-Aug-01	
	% recovery	95.6			
#05	Mintac greenball + 99.7 ng/g MSD	107.2	ng/g	31-Aug-01	
	% recovery	99.4			3.9% RPD
	NIST-2709 (soil)	1,367	ng/g	31-Aug-01	certified = 1,400 ng/g
	% recovery	97.6			
#01	Mintac scrubber in water	74.5	ng/L	18-Jul-01	
#01	Mintac scrubber in water dup	83.3	ng/L	18-Jul-01	
	mean	78.9	ng/L	18-Jul-01	11.2% RPD
#01	Mintac scrubber in water + 202 ng/L MS	292.5	ng/L	18-Jul-01	
	% recovery	105.7			
#01	Mintac scrubber in water + 202 ng/L MSD	279.7	ng/L	18-Jul-01	
	% recovery	99.4			6.4% RPD
	NIST-1641d (water)	7,926	ng/L	18-Jul-01	certified 7,950 ng/L @ 200x dilution
	% recovery	99.7			

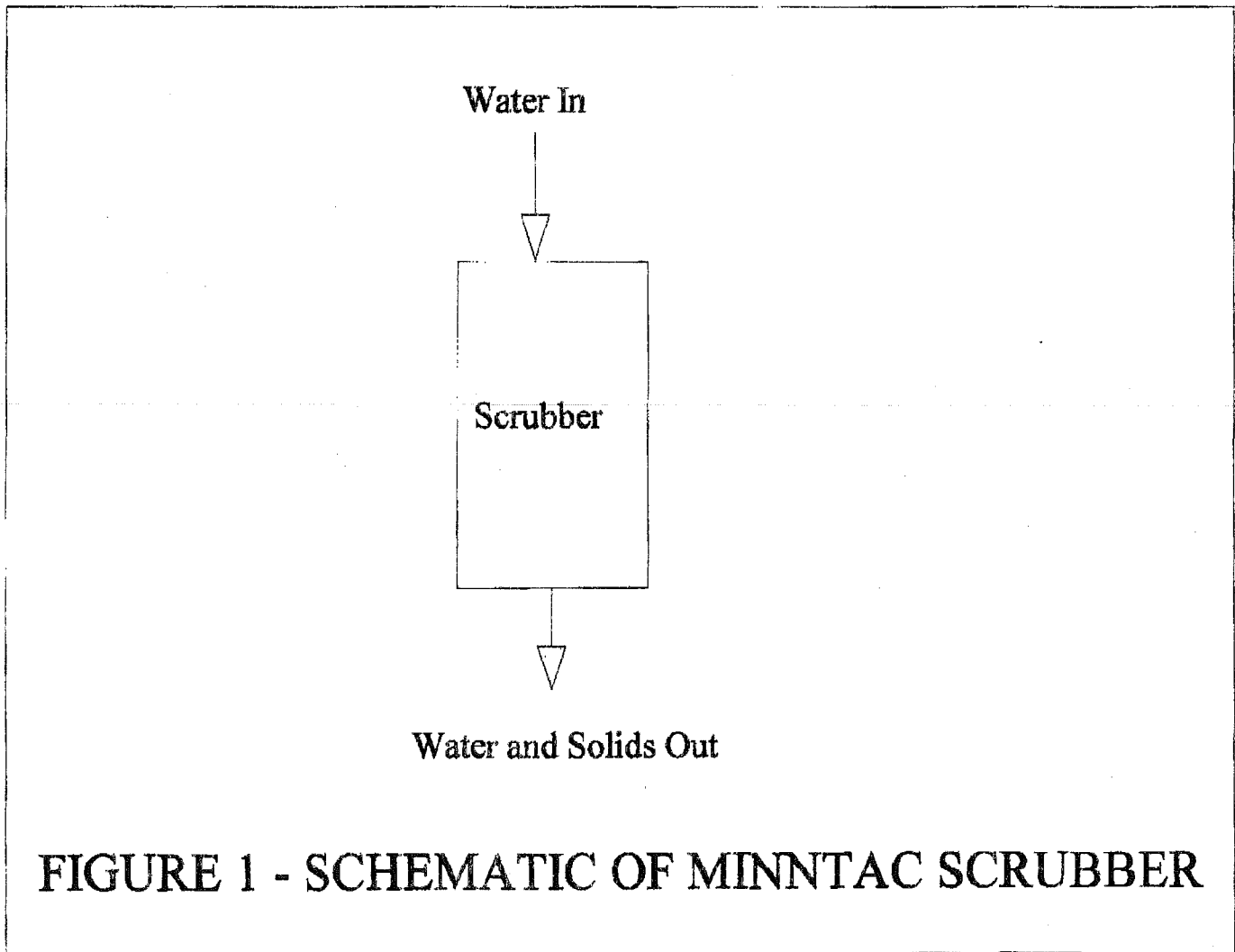
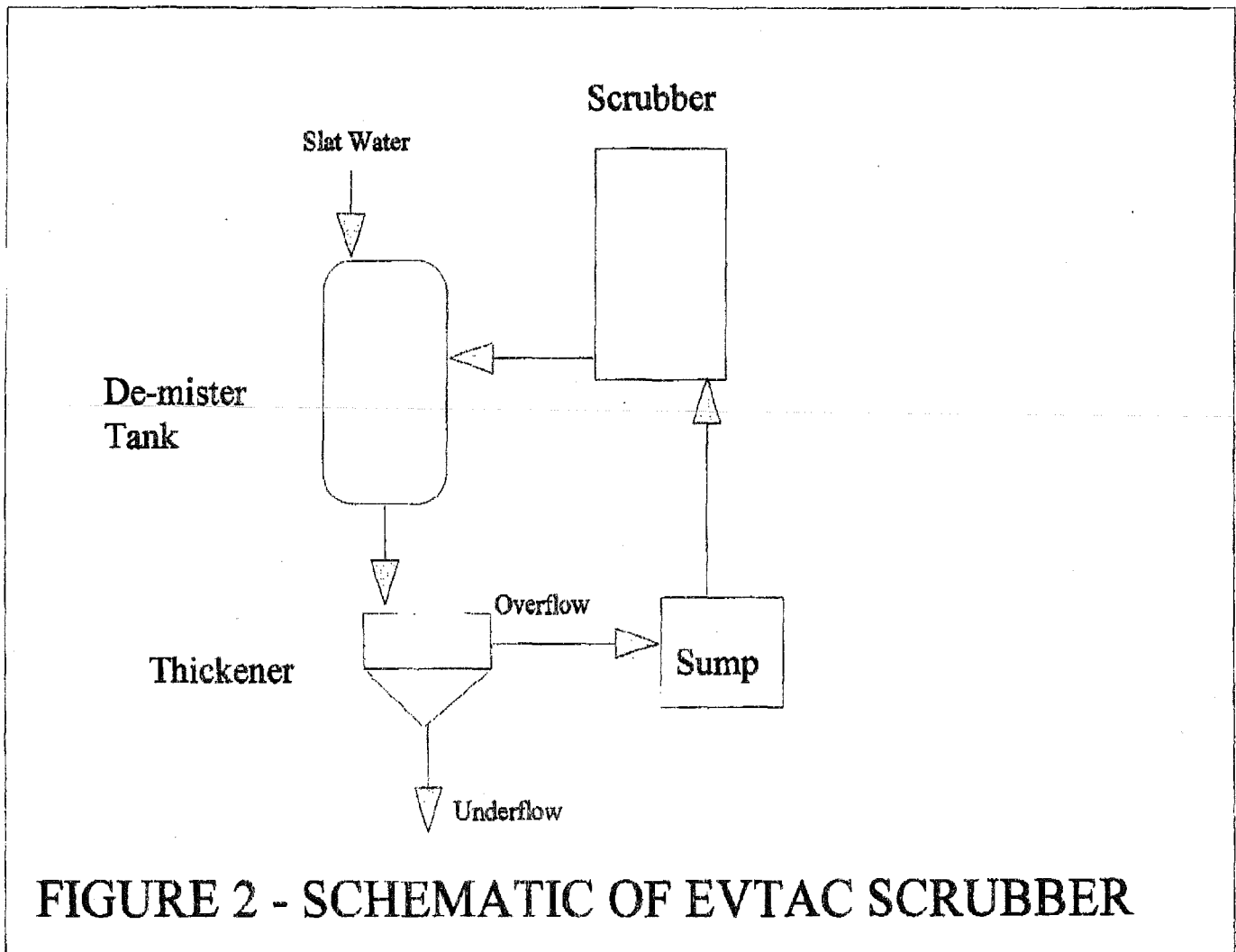
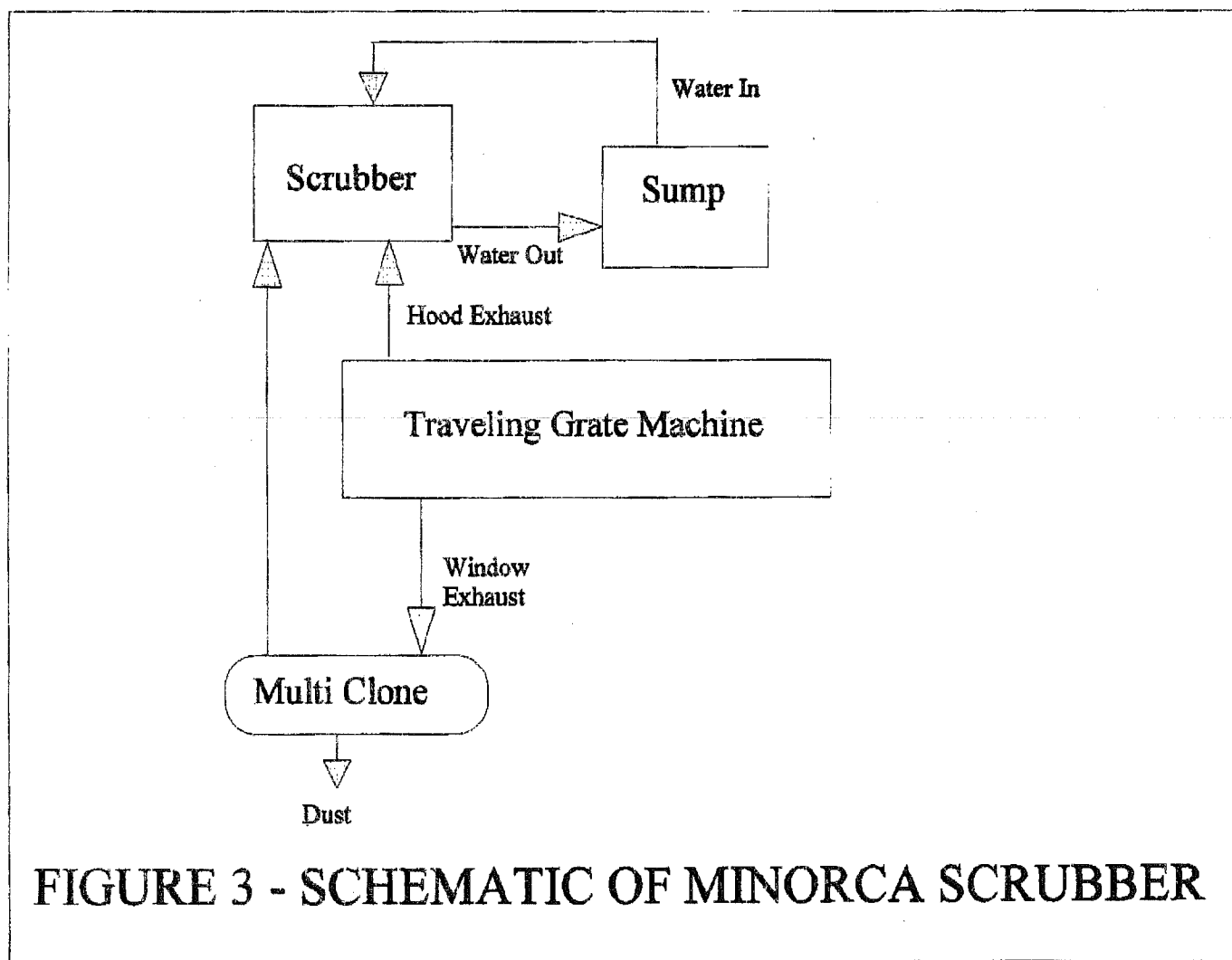


FIGURE 1 - SCHEMATIC OF MINNTAC SCRUBBER





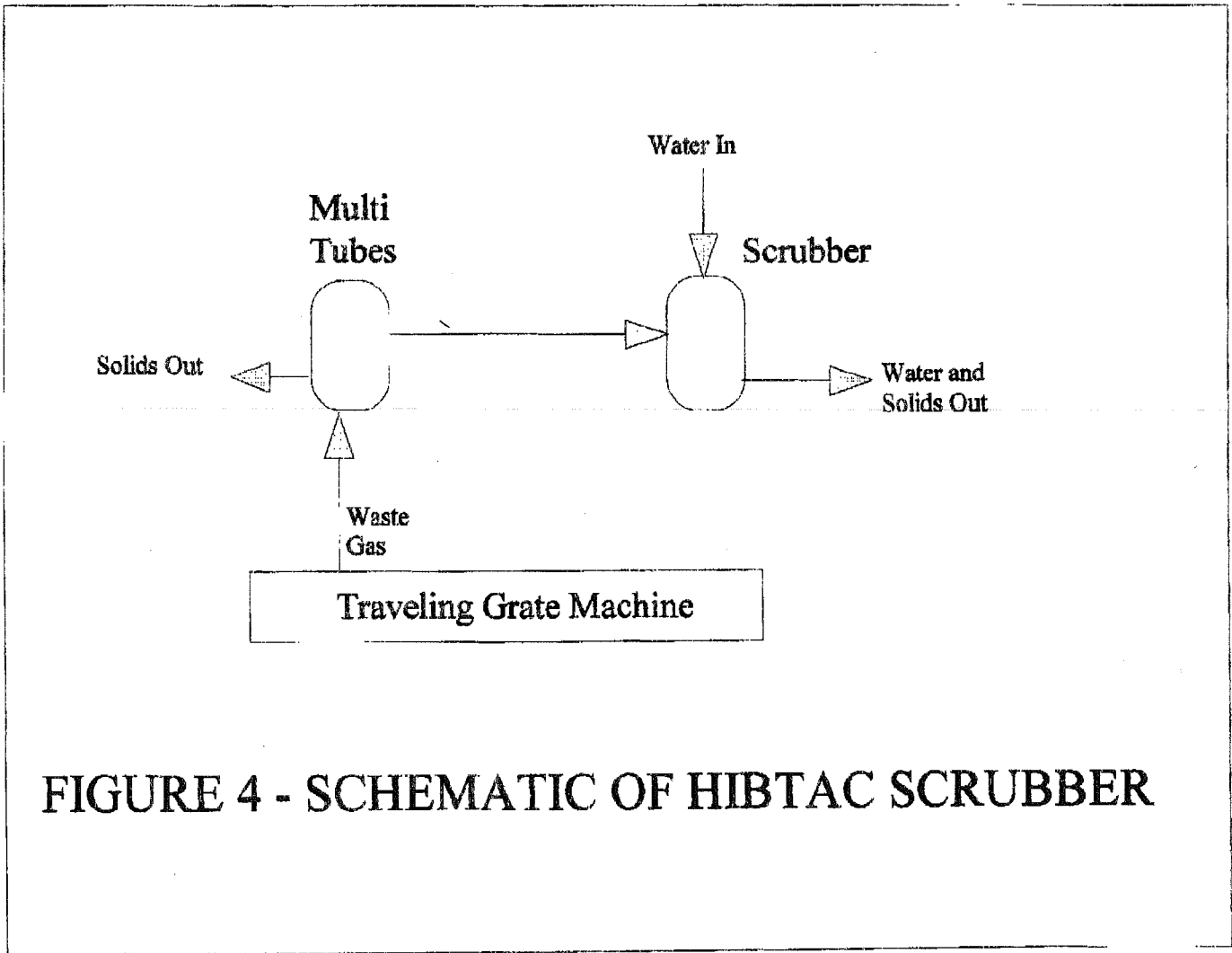


FIGURE 4 - SCHEMATIC OF HIBTAC SCRUBBER

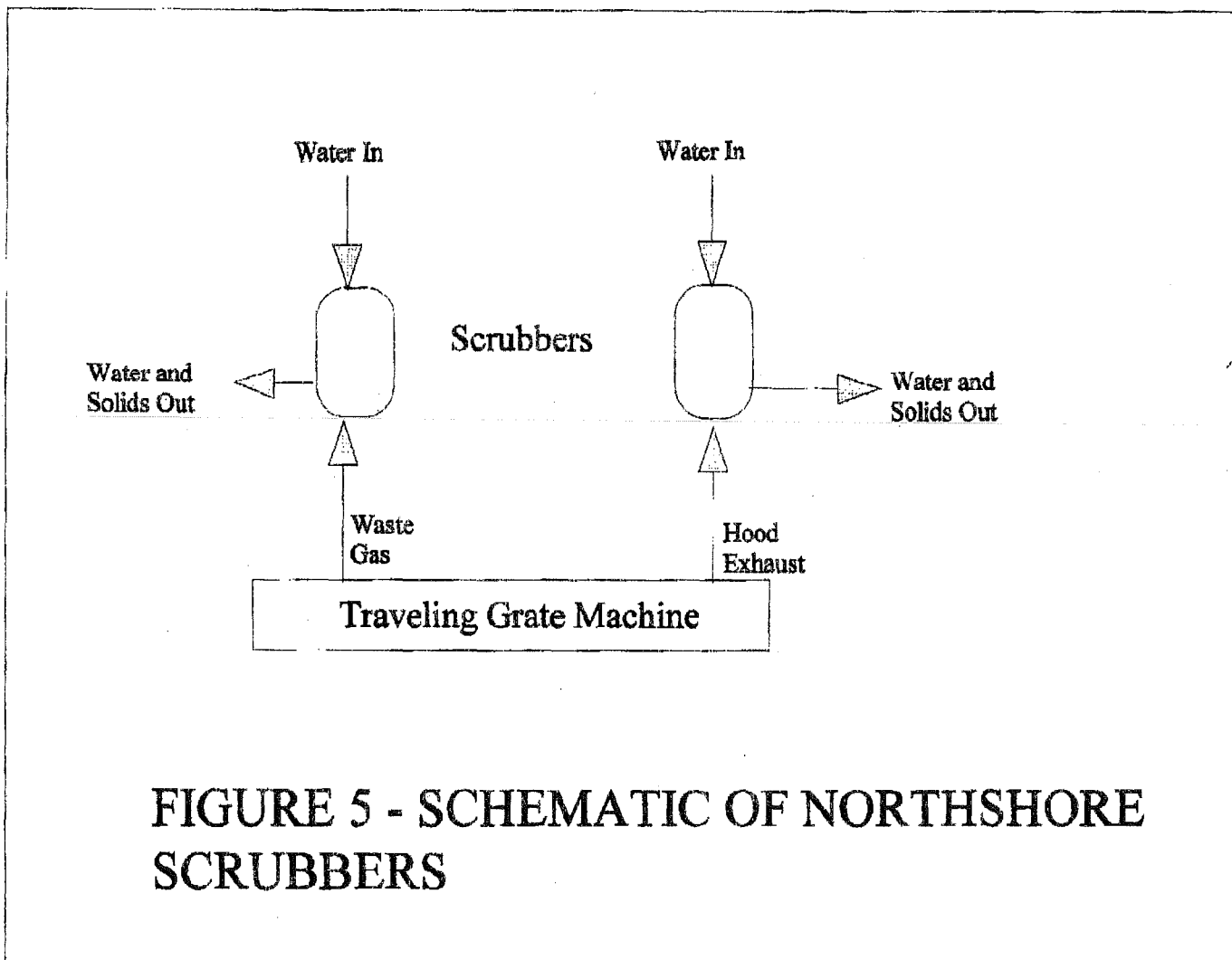


FIGURE 5 - SCHEMATIC OF NORTHSORE SCRUBBERS

**APPENDIX I - MERCURY ANALYSES REPORTS FROM FRONTIER
GEOSCIENCE**

Total Hg in Solids (University of Minnesota)*analyzed by:*

Frontier Geosciences R&C 414 Pontius Avenue North, Suite B, Seattle WA 98109

phone: (206) 622-6960 fax: (206) 622-6870 email: nicolasb@frontier.wa.com

Sample Identification	Dry Fraction	Total Hg, ng/g*	
		wet wt basis	dry wt basis
Evtac Green Ball	1.000	12.0	12.0
Evtac Final Pellet	0.999	ND(<0.69)	ND(<0.69)
Evtac Coal	0.998	10.3	10.3
Evtac Thickener Un'flow 2A	0.999	526	527
Evtac Thickener O'flow 2A	0.998	233	233
Evtac Thickener Un'flow 2B	0.997	366	367
Evtac Thickener O'flow 2B	0.996	823	826
Hibtac Filter Cake	0.998	13.9	13.9
Hibtac Concentrate	0.999	18.2	18.2
Hibtac Limestone	0.999	3.72	3.72
Hibtac Multi-tube Dust	1.000	154	154
Hibtac Green Ball	1.000	16.7	16.7
Hibtac Bentonite	0.980	25.9	26.4
Hibtac Fired Pellet	1.000	ND(<0.69)	ND(<0.69)
North Shore Waste Gas Line 11	0.999	211	211
North Shore Waste Gas Line 12	0.999	110	110
North Shore Hood Exhaust Line 11	0.998	25.9	26.0
North Shore Hood Exhaust Line 12	1.000	26.4	26.4
North Shore Green Ball Line 11	0.999	1.44	1.44
North Shore Green Ball Line 12	1.000	1.10	1.10
North Shore Fired Pellet Line 11	0.999	ND(<0.69)	ND(<0.69)
North Shore Fired Pellet Line 12	1.000	1.85	1.85

*Blank corrected

ND-less than estimated MDL

Total Hg in Solids (University of Minnesota)*analyzed by:*

Frontier Geosciences R&C 414 Pontius Avenue North, Suite B, Seattle WA 98109

phone: (206) 622-6960 fax: (206) 622-6870 email: nicolasb@frontier.wa.com

Sample Identification	Dry Fraction	Total Hg, ng/g	
		wet wt basis	dry wt basis

Method Blanks

Blank-1		0.89	
Blank-2		1.96 ^a	
Blank-3		0.49	
Blank-4		0.49	
Mean method blank		0.62	
Estimated MDL		0.69	

^aExcluded from calculation of mean method blank**Standard Reference Materials**

NIST-2709		1,529	
recovery		109.2%	
reference value		1,400	

Total Hg in Solids (University of Minnesota)*analyzed by:*

Frontier Geosciences R&C 414 Pontius Avenue North, Suite B, Seattle WA 98109

phone: (206) 622-6960 fax: (206) 622-6870 email: nicolasb@frontier.wa.com

Sample Identification	Dry Fraction	Total Hg, ng/g*	
		wet wt basis	dry wt basis

Matrix Duplicates

North Shore Hood Exhaust Line 11		25.89	
North Shore Hood Exhaust Line 11 MD		25.85	
Mean		25.87	
RPD		0.2%	
North Shore Fired Pellet Line 11		-0.01	
North Shore Fired Pellet Line 11 MD		1.32	
Mean		0.66	
RPD		203.1%	
Evtac Green Ball		11.98	
Evtac Green Ball MD		11.95	
Mean		11.97	
RPD		0.3%	

Matrix Spikes

North Shore Fired Pellet Line 11 MS		9,980	
spiking level		9,488	
net		9,979	
recovery		105.2%	
North Shore Fired Pellet Line 11 MSD		9,868	
spiking level		9,901	
net		9,867	
recovery		99.7%	
RPD		5.4%	

*Blank corrected

Total Mercury in Process Water (University of Minnesota)			
<i>analyzed by</i>			
Frontier Geosciences R&C 414 Pontius North, Suite B Seattle WA 98109			
phone: 206-622-6960 fax: 206-622-6870 e-mail: nicolasb@frontier.wa.com			
sample ID	description	[Hg], ng/L	comments
#8	evtac thickener u'flow water 2A	15.48	
#20	evtac concentrate water	8.61	
#12	evtac slat spray water	5.25	
#10	evtac thickener u'flow water 2B	18.12	
#22	hibtac scrubber water	11.95	
#21	hibtac makeup water	5.37	
#9	evtac thickener o'flow water 2A	82.22	
#11	evtac thickener o'flow water 2B	24.35	
B-1	blank-1	0.12	
B-2	blank-2	0.16	
B-3	blank-3	0.16	
	mean	0.15	
	estimated MDL	0.07	
#12	evtac slat spray water rep 1	4.97	
#12	evtac slat spray water rep 2	6.21	
	mean	5.25	10.5% RPD
	matrix spike level	40.40	
#8	evtac thickener u'flow water 2A + MS	53.71	94.6% recovery
#8	evtac thickener u'flow water 2A + MSD	54.77	97.3% recovery
	mean	52.24	2.1% RPD
NIST-1641d	NIST certified water CRM rep 1	7,751	diluted 200x
NIST-1641d	NIST certified water CRM rep 2	7,054	diluted 200x
	mean	7,403	9.4% RPD
	certified value	7,950	93.1% recovery
	analysis date	2-Jul-01	

Total Mercury in Process Water (University of Minnesota)

analyzed by

Frontier Geosciences R&C 414 Pontius Avenue North, Suite B Seattle WA 98109

phone: (206) 622-6960 fax: (206) 622-6870 email: ericv@frontier.wa.com

sample ID	description	[Hg], ng/L	comments
#9	N.S. Feed Water	7.05	
#10	N.S. Hood Exhaust Water Line 11	32.8	
#11	N.S. Hood Exhaust Water Line 12	15.7	
#12	N.S. Waste Gas Water Line 11	29.1	
#13	N.S. Waste Gas Water Line 12	15.7	
B-1	blank-1	0.05	
B-2	blank-2	0.10	
B-3	blank-3	0.05	
	mean	0.06	
	estimated MDL	0.09	
#11	N.S. Hood Exhaust Water Line 12	15.72	
#11	N.S. Hood Exhaust Water Line 12	17.67	
	mean	15.89	11.7% RPD
	matrix spike level	40.40	
#11	N.S. Hood Exhaust Water Line 12 + MS	57.94	97.2% recovery
#11	N.S. Hood Exhaust Water Line 12+ MSD	56.11	92.9% recovery
	mean	57.03	3.2% RPD
NIST-1641d	NIST certified CRM (diluted 200x)	8,042	101.2% recovery
	certified value	7,950	
	analysis date	July 9, 2001	

Total Mercury in Taconite Mill Substances (Coleraine Minerals Research Lab)

analyzed by

Frontier Geosciences Inc. 414 Pontius North, Seattle WA 98109

phone: 206-622-6960 fax: 206-622-6870 e-mail: nicolasb@frontier.wa.com

sample #	sample description	[Hg]	units	date analyzed	comment
#01	Mintac scrubber in water	78.9	ng/L	18-Jul-01	QC sample
#02	Mintac Scrubber out water	66.5	ng/L	18-Jul-01	
#03	Inland process water	5.67	ng/L	18-Jul-01	
#04	Inland scrubber water	112	ng/L	18-Jul-01	
#05	Mintac greenball	8.1	ng/g	31-Aug-01	QC sample
#06	Mintac fired pellet	< 0.6	ng/g	31-Aug-01	
#07	Mintac scrubber out solids	87.0	ng/g	31-Aug-01	
#08	Mintac coal	25.3	ng/g	31-Aug-01	
#09	Inland scrubber water solids	3,179	ng/g	31-Aug-01	
#10	Inland multi-clone dust	193	ng/g	31-Aug-01	
#11	Inland fired pellet	< 0.6	ng/g	31-Aug-01	
#12	Inland greenball	7.8	ng/g	31-Aug-01	
#13	Evtac thickener 2A + 10m	38.8	ng/g	31-Aug-01	
#14	Evtac thickener 2B + 10m	48.6	ng/g	31-Aug-01	
#15	Hibtac multi-tube dust + 10m	86.8	ng/g	31-Aug-01	
	solids blank #1	0.4	ng/g	31-Aug-01	
	solids blank #2	0.4	ng/g	31-Aug-01	
	solids blank #3	0.2	ng/g	31-Aug-01	
	solids blank #4	0.8	ng/g	31-Aug-01	
	solids blank #5	0.3	ng/g	31-Aug-01	
	solids blank #6	0.2	ng/g	31-Aug-01	
	mean	0.4	ng/g	31-Aug-01	estimated MDL = 0.6 ng/g
	water blank #1	0.05	ng/L	18-Jul-01	
	water blank #2	0.06	ng/L	18-Jul-01	
	water blank #3	0.09	ng/L	18-Jul-01	
	mean	0.07	ng/L	18-Jul-01	estimated MDL = 0.06 ng/L

Total Mercury in Taconite Mill Substances (Coleraine Minerals Research Lab)

analyzed by

Frontier Geosciences Inc. 414 Pontius North, Seattle WA 98109

phone: 206-622-6960 fax: 206-622-5870 e-mail: nicolasb@frontier.wa.com

sample #	sample description	[Hg]	units	date analyzed	comment
#05	Mintac greenball	8.3	ng/g	31-Aug-01	
#05	Mintac greenball dup	7.8	ng/g	31-Aug-01	
	mean	8.1	ng/g	31-Aug-01	6.2% RPD
#05	Mintac greenball + 93.5 ng/g MS	97.4	ng/g	31-Aug-01	
	% recovery	95.6			
#05	Mintac greenball + 99.7 ng/g MSD	107.2	ng/g	31-Aug-01	
	% recovery	99.4			3.9% RPD
	NIST-2709 (soil)	1,367	ng/g	31-Aug-01	certified = 1,400 ng/g
	% recovery	97.6			
#01	Mintac scrubber in water	74.5	ng/L	18-Jul-01	
#01	Mintac scrubber in water dup	83.3	ng/L	18-Jul-01	
	mean	78.9	ng/L	18-Jul-01	11.2% RPD
#01	Mintac scrubber in water + 202 ng/L MS	292.5	ng/L	18-Jul-01	
	% recovery	105.7			
#01	Mintac scrubber in water + 202 ng/L MSD	279.7	ng/L	18-Jul-01	
	% recovery	99.4			6.4% RPD
	NIST-1641d (water)	7,926	ng/L	18-Jul-01	certified 7,950 ng/L @ 200x dilution
	% recovery	99.7			

Frontier Geosciences Inc.

Environmental Research & Specialty Analytical Laboratory

414 Pontius Ave N · Seattle WA 98109

Mr. Blair Benner
University of Minnesota Duluth
Coleraine Minerals Research Lab
P.O. Box 188
Coleraine, MN 55722

July 16, 2001

Dear Mr. Blair,

Enclosed please find our results for the determination of total Hg in 22 solids samples which were received on June 25 and July 2, 2001 and 8 water samples received on July 2. Following receipt, the water samples were preserved with 1% (v/v) 0.2N BrCl and allowed to oxidize at least overnight prior to analysis.

One gram aliquots of the samples were accurately weighed into HF cleaned Teflon bombs, and 25 mL of a mixture of 2:1:1 (v/v) HNO₃ + HF + HCl were added. The samples were digested for 12 hours at 100°C. We find that even though common soils and rocks will easily go into solution in less than 4 hours under these conditions, the "conc." and "pellet" samples did not fully solubilize even after the full 12 hours. Although certain ores, including taconite and bauxite, do not fully solubilize during digestion, we have performed intercomparison exercises with thermal volatilization and aqua regia digestion which suggest that grinding to a powder, followed by HF/HNO₃/HCl digestion is never-the-less the most effective way to liberate the Hg for analysis.

After digestion, the samples were cooled and diluted to 100 mL with reagent water, and stored in their respective digestion bombs until analysis. Aliquots (2.0 mL) of the digests were analyzed using SnCl₂ reduction, purge and trapping on gold coated sand, and cold vapor atomic fluorescence spectrometry (CVAFS) detection. Overall, the analysis went very well, with excellent spike and CRM recoveries, and low blanks. One of the four blanks prepared and analyzed with the set was noted to be higher than the other three, and was excluded from calculation of the mean blank employed to blank correct the data.

206 622 6960
fax 206 622 6870
email: info@Frontier.WA.com
www.FrontierGeosciences.com

Frontier Geosciences Inc.

Environmental Research & Specialty Analytical Laboratory
414 Pontius Ave N · Seattle WA 98109

July 24, 2001

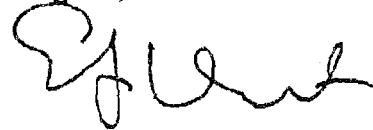
Mr. Blair Benner
University of Minnesota-Duluth
Coleraine Minerals Research Lab
P.O. Box 188
Coleraine, MN 55722

Dear Mr. Benner,

Enclosed please find our results for the determination of total mercury in process water samples received on July 2, 2001. The samples were received in good condition and immediately oxidized with 1% (v/v) 0.2N BrCl. All samples were allowed to oxidize at least overnight prior to analysis.

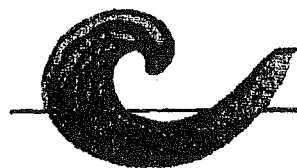
Aliquots of each sample were analyzed using SnCl₂ reduction, dual gold amalgamation, and cold vapor atomic fluorescence (CVAFS) detection. Analysis went very well, with no analytical problems encountered. Please feel free to contact me if you have any questions regarding these results.

Regards,



Eric J. von der Geest
Analytical Chemist

206 622 6960
fax 206 622 6870
email: info@Frontier.WA.com
www.FrontierGeosciences.com



FRONTIER GEOSCIENCES INC.

ENVIRONMENTAL RESEARCH & SPECIALTY ANALYTICAL LABORATORY

(206) 622-6960 • FAX: (206) 622-6870

E-MAIL: info@FRONTIER.WA.COM

414 PONIUS NORTH • SEATTLE, WA 98109

Mr. Blair Benner
University of Minnesota Duluth
Coleraine Minerals Research Lab
P.O. Box 188
Coleraine, MN 55722

September 9, 2001

Dear Mr. Blair,

Enclosed please find our results for the determination of total Hg in 11 taconite process solid samples and 4 waters, which were received on July 16, 2001. This is a hard copy report of the data table already forwarded to you by e-mail on September 8, 2001.

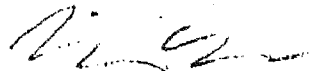
One gram aliquots of the solid samples were accurately weighed into HF cleaned Teflon bombs, and 25 mL of a mixture of 2:1:1 (v/v) HNO₃ + HF + HCl were added. The samples were digested for 12 hours at 100°C. We find that even though common soils and rocks will easily go into solution in less than 4 hours under these conditions, some ore samples do not fully solubilize even after the full 12 hours. Although certain ores, including taconite and bauxite, do not fully solubilize during digestion, we have performed intercomparison exercises with thermal volatilization and aqua regia digestion which suggest that grinding to a powder, followed by HF/HNO₃/HCl digestion is never-the-less the most effective way to liberate the Hg for analysis. After digestion, the samples were cooled and diluted to 100 mL with reagent water, and stored in their respective digestion bombs until analysis. Water samples were digested by the addition of 1% (v/v) of 0.2 N BrCl in 12N HCl to the original sample bottle, and allowing to sit over night at room temperature prior to analysis.

Aliquots (0.1-2.0 mL of the solids digests, or 5-50 mL of the waters) were analyzed using SnCl₂ reduction, purge and trapping on gold coated sand, and cold vapor atomic fluorescence spectrometry (CVAFS) detection. Overall, the analysis went very well, with excellent spike and CRM recoveries, and low

blanks. One sample (Inland scrubber water solids) went off scale, but was re-analyzed on a different analyzer on the same day.

Please feel free to call or e-mail me if you have any questions, or are in need of additional analytical or contract research services.

Best Wishes,



Nicolas Bloom
Sr. Research Scientist

Appendix B-1-2

On the Distribution of Mercury in Taconite Plant Scrubber Systems

October 15, 2003

On the distribution of mercury in taconite plant scrubber systems

Michael E. Berndt¹

John Engesser²

and

Andrea Johnson²

Submitted June 30, 2003

Revised Oct. 15, 2003

Minnesota Department of Natural Resources
Division of Lands and Minerals

¹500 Lafayette Road
St. Paul, Minnesota 55155

²1525 Third Avenue E.
Hibbing Minnesota 55746

Summary

Water samples containing suspended solids (“scrubber dust”) were collected from wet scrubber systems of four taconite processing plants on Minnesota’s Iron Range. Mercury in scrubber water and scrubber dust were analyzed separately following field and laboratory filtration. Results indicated that mercury redistribution among water and particles occurred when samples were brought from the field and shipped to the analytical laboratory. Mercury in the water tended to adsorb to particles. Although the time dependency of the adsorption process was not established in this study, the results demonstrate that dissolved and adsorbed mercury components must both be considered in any inventory and process evaluation for taconite scrubber systems.

Considerable short- and long-term variation in total mercury concentration was found in all of the systems studied. Short-term variability could be attributed to the inhomogeneous nature of taconite processing and gas stream chemistry, but the long-term mercury variations imply relationships between processing technique and mercury recovery. For example, mercury captured by the scrubber system at Minntac (line 4) was approximately an order of magnitude greater when the company was making “acid” pellets as compared to “fluxed” pellets. It is possible that the additional heating required to fire fluxed pellets resulted in greater volatilization (conversion of Hg^{+2} to volatile Hg^0) of mercury in the gas stream. However, Ispat-Inland Mining Company was also generating acid pellets during one of our visits and fluxed pellets during another. In this case, mercury capture by the scrubber system appeared to be significantly greater during fluxed pellet production. This reversal (compared to Minntac) may be related to the fact that Ispat-Inland uses a straight-grate induration system, while Minntac uses a grate-kiln system, however, Ispat-Inland’s practice of recirculating water within its scrubber system complicates the interpretation.

In two process lines (Ispat-Inland and Hibtac), a multiclone dry dust collector is employed upstream from the wet-scrubber system. In both cases, the mercury concentration of dry dust was found to be much lower than that of dust collected by the wet scrubber system. This difference suggests that Hg^{+2} is either being generated or transported within the non-particulate fraction of the gas phase. Adsorption of this mercury fraction to particulates appears to take place at lower temperatures and within the aqueous phase beginning from the time that it is captured by the wet scrubber system until the time that suspended particulates are separated from the water.

Verification of the results is needed, because it is possible that day-to-day changes in mineral source and processing could account for some of the observed variation. Planned future studies of these and other relationships for mercury in taconite processing plants may lead to better inventory assessments of mercury emissions from taconite companies, and may ultimately help to identify a cost effective means to reduce mercury emissions from taconite processing plants.

Introduction

Taconite mineral processing in Minnesota contributes an estimated 250 to 350 kg of volatile mercury to the atmosphere each year, increasing when mining production rates are high and decreasing when production is low (Engesser and Niles, 1997; Jiang et al., 1999; Berndt, 2002). The mercury is released when taconite pellets are exposed to high temperatures during the induration or hardening process. Reduced and oxidized mercury enter the process gas stream during heating and are either captured in plant scrubbers or released to the environment as stack emissions. It is generally thought that most of the mercury released to the gas phase during induration is “elemental” or “volatile” mercury, Hg^0 . This form of mercury is insoluble in water and does not adsorb to most solids, and is, therefore, not captured by taconite scrubber systems.

However, recent research performed at the Coleraine Minerals Research Laboratory (Benner, 2001) determined that the concentration of mercury on particles suspended in scrubber waters (filtered upon return to the laboratory) is, in some cases, quite large, and may represent as much as 10% or more of the inventory of mercury in taconite plant emissions. This mercury probably represents the oxidized fraction of the mercury, Hg^{+2} . Oxidized mercury is both water-soluble and adsorbs to particles and is, therefore, mostly captured by wet scrubbers. Benner believed that all or most of the mercury captured by wet scrubbers is adsorbed to the solid phase, which in many plants is recycled back to the induration furnaces. Thus, his results suggested that one pathway to reduce mercury emissions might be to eliminate recycling of some or all scrubber solids to induration furnaces.

The Department of Natural Resources undertook the present study with guidance and funding from the Minnesota Pollution Control Agency. The purpose of the study was to evaluate more closely the inventory of mercury in plant scrubber systems and to determine how best to optimize sampling and experimentation methods associated with mercury reduction projects anticipated over the next two years. This report presents the results and interpretations from the initial six months of what is expected to be a two to three year study.

Methods

Plant participation and sample site selection

Four companies were selected for participation based on the presence of a wet scrubber system. These companies included Hibbing Taconite Company (Hibtac), United States Steel Corporation Minnesota Ore Operations (Minntac), EVTAC Mining (Evtac), and Ispat-Inland Mining Company. In each case, sampling sites were chosen in consultation with mining personnel. Diagrams for each of the scrubber systems are presented in the appendix.

There were two sample points at Hibtac. Scrubber water samples were taken from a pipe containing the combined effluent from two separate induration lines. Samples were also collected from Hibtac’s “multiclone” dry dust collection system, which removes particles from process gases upstream from the wet scrubber system. Samples from the second site provide information on the mercury concentration of dust prior to capture by the wet scrubber

system. Mr. Rod Heikkila of Hibbing Taconite Company assisted the DNR in identifying the sampling points.

Only one sample point was selected at Minntac. This site was at a valve located on the scrubber discharge pipe from the “Line 4” agglomeration unit. Mr. Tom Moe and Mr. Ron Braski of USS Minntac assisted the DNR in identifying the sample point. Minntac does not use a multiclone system, so no dry dust samples could be collected from that system.

Only one sample collection point was identified at EVTAC, and this was located at the scrubber-thickener-underflow-discharge pipe. No valve was available to sample direct scrubber outflow which feeds directly into the thickener system. It was decided that for this initial phase of the study, we would focus attention on the underflow portion of the thickener because of its higher suspended solids and the greater ease with which it could be accessed (less potential for contamination). Mr. Bradley Anderson of EVTAC Mining assisted the DNR in identifying this sampling point.

Two sample points were found for Ispat-Inland Mining Company. In this case, scrubber effluent was sampled from a valve located upstream from a scrubber-water storage tank, but directly downstream from the scrubber itself. Like Hibtac, Ispat-Inland also uses a multiclone system to collect dry dust directly upstream from the wet scrubber system. Samples were also obtained from this site during one of our visits, once again to provide a reference for the concentration of mercury on dust prior to capture in the wet scrubber system. Mr. Gus Josephson assisted the DNR in identifying the sample points at Ispat-Inland.

Dates and more detailed processing information for each sampling site are provided in Table 1. An important distinction between the facilities is that two of the operations are “grate-kiln” facilities (Evtac and Minntac diagrammed in Fig. 1) and two are “straight grate” (Ispat-Inland and Hibbtac, diagrammed in Fig. 2). This fundamental difference in plant design, when superimposed with other less distinct differences in plant operation procedures makes every plant on the iron range unique. Thus, while some aspects of mercury chemistry will likely remain consistent in all taconite processing plants, subtleties associated with mineral processing and plant engineering for each processing plant need to be considered to understand mercury pathways in specific taconite processing operations.

Water sampling and analysis:

At each plant, water samples were collected in a clean two-liter plastic bottle from which sub-samples were decanted. Samples that were to be filtered in the laboratory were decanted quickly (prior to settling) into specially purchased, pre-acid washed 250 mL glass sample jars with Teflon-lined lids. Samples filtered on-site were forced through membrane filters (0.45µm, Pall Corporation) and the resulting water and filtrate were placed into separate 250 ml jars.

All samples for mercury analyses were collected using “clean-hands, dirty-hands” procedures, whereby the clean bottles were placed into sealed plastic bags prior to leaving the laboratory and not opened except during sampling. Only the designated clean-hands person, wearing clean plastic gloves, handled the sample bottles when they were outside of the plastic bag. All other sample processing was conducted quickly and efficiently by so-called “dirty-hands” personnel. These procedures were implemented to minimize the risk of contamination from plant dust and of cross-contamination between samples.

In addition to these special precautions, procedures were extensively evaluated during our second sampling round to assess the degree of mercury contamination associated with filtration and sampling. A series of procedural blanks were collected at each site. One bottle was filled with deionized water prior to leaving the laboratory and another was filled at the sampling site with deionized water brought from the lab. In addition, deionized water was filtered at the sampling location and both the water and the filter were saved for analysis. An empty bottle was also sealed into a plastic bag, brought to the sampling site, and then later filled with water at the mercury analytical laboratory. Finally, an unused filter was placed into a 250 ml bottle and also analyzed for total mercury. The level of contamination introduced by our procedures was insignificant relative to the concentration of mercury found in samples analyzed in this study (see Table 2). The importance of this step cannot be overstated, as it implies that variation in mercury concentration observed among samples is unlikely due to contamination.

Samples were analyzed by Cebam Analytical, Inc., located in Seattle, Washington. Filtered water samples were digested with BrCl over night, and then analyzed by SnCl₂ reduction, gold trap collection, and CVAFS detection (modified EPA1631).

Temperature, pH, and conductivity were measured on site. Temperature and pH were measured using a Beckman Model 11 meter with a Ross Model 8165BN combination pH electrode and a Beckman Model 5981150 temperature probe, while specific conductance was measured with a Myron L EP series conductivity meter.

For cations and trace metals, samples were acidified in the field using nitric acid and analyzed by inductively coupled plasma mass spectrometry (ICP-MS) at the University of Minnesota, Department of Geology and Geophysics. For anions, samples were stored in clean plastic bottles and analyzed using ion-chromatography (IC, Dionex Ion Chromatograph fitted with a GP40 gradient pump, CD20 conductivity detector, and two AS4 anion exchange columns) at the University of Minnesota, Department of Geology and Geophysics.

Finally, an attempt was made to evaluate exchangeability of adsorbed Hg⁺⁺. H₂SO₄ and NaOH were added to unfiltered samples collected during our first visit to Minntac, and reaction enhanced by placing the samples on a bottle roller at the DNR laboratory in Hibbing for 24 hours prior to shipment and later filtration at Cebam, Inc. By measuring distribution as a function of pH, we could assess potential for pH adjustments in scrubber systems to be used in Hg⁺² control strategies.

Suspended solids (scrubber dust)

Filters containing the solids from the above procedures were dried at 104C for analysis, weighed, and digested in hot acid (HCl/HNO₃, 3/1). Particulate mercury was analyzed using SnCl₂ reduction and gold trap collection, followed by CVAFS detection (modified EPA1631). Certified reference materials WS-68, NIST2709, and GSR-2 were used to assess recovery and analytical accuracy.

Total suspended solids (TSS) were analyzed by filtering a two-liter sample of scrubber water collected specifically for this purpose. Solids from this sample were collected on a glass fiber filter (0.7μ), dried at 100° C overnight, and weighed.

Selected dust samples were sent to Blair Benner at the Coleraine Minerals Research Laboratory – Natural Resources Research Institute (CMRL-NRRI), University of Minnesota, Duluth for determination of percentage magnetite using a Satmagan analyzer. Solids were also examined by Scanning Electron Microscopy (SEM) to assess mineralogy, texture, and grain size. These analyses were conducted by Peter McSwiggen and Associates in New Brighton, MN on a JEOL Microprobe.

Results and Discussion

Mercury data for scrubber water and suspended particulates are provided in Tables 3 through 6 and plotted in Figures 3 through 6. Concentrations varied greatly between operations on both short and long time scales and also depended on the timing of filtration. However, the aforementioned differences in mineral processing make it difficult to compare directly the mercury distributions and abundances observed at different plants. We will discuss mercury distributions, therefore, on a detailed plant specific basis in following sections, but prior to that we present less detailed discussion of other components measured in our study.

Temperature, TSS, pH, and water chemistry for the scrubber waters are reported in Table 7. All of the scrubber waters were warm (27.4 to 44.6°C) and slightly acidic to near-neutral in pH (4.2 to 7.38). Suspended solids were highest at EVTAC where we sampled the underflow, and lowest at Hibtac, where a multiclone dry-dust collection unit removes much of the dust from the gas stream before it enters the wet scrubber. Because scrubbers capture volatile gases generated during heating of taconite ore and burning of fuels, they contain relatively high concentrations of F (from HF), Cl (from HCl), and SO_4^{2-} (oxidation of SO_2).

An important indication of process origin for the dust is the percentage of material captured that is still magnetic. Induration converts the taconite pellets that are composed initially of magnetite (magnetic) to hematite and other non-magnetic iron-oxides. Satmagan analysis of the dust samples (Table 8) reveals that only a small fraction of the dust collected at Ispat-Inland was magnetic (17 to 20%), and 52 to 81% of the taconite dust from the other companies was magnetic. This low value for Ispat-Inland dust samples suggests composite exposure of the captured dust to higher temperatures compared to scrubber-dust from other companies.

SEM images for the solids are shown in Figures 8 through 12. Not surprisingly, the dust from all of the processing plants was relatively similar in appearance in terms of mineralogy, texture, and grain size. Dust samples from Evtac appeared to contain many particles larger than those in samples from the other companies (250 microns as opposed to 100 microns), while samples from Ispat-Inland's scrubber system appeared to have a finer upper limit on particle size (50 microns). Conspicuous in the material from Evtac and also, to a lesser degree, in samples from Minntac, were small round spherical particles suggestive of melt formation somewhere in the process lines or gas streams at those two plants. Although the dust samples were, of course, composed primarily of iron-oxides, occasional grains of silicate and carbonate phases were also observed.

Hibtac:

A total of eight water samples and nine dust samples were collected and analyzed for mercury during two visits to Hibtac. The highest concentration of mercury in dust was 5027 ng/g, which was found in a sample that was filtered by Cebam, Inc. (Figure 3, Table 3). This concentration was much higher than the 1405 ng/g measured for dust collected on the same visit, but filtered immediately after collection. Dissolved mercury for these two samples was 255.5 ng/L in the sample filtered at the plant, but only 13.6 ng/L in the water sampled after shipment to the analytical facility, implying that the increased mercury on solids came from the water in which the solid was suspended. Apparently, most mercury in Hibtac's scrubber system is initially dissolved, but then, given time, adsorbs onto the suspended dust particles.

A similar observation was made in a second sampling round in May. Then, dust obtained by on-site filtration averaged approximately 600 ng/L mercury while dust filtered in the lab averaged approximately 1540 ng/L. Dissolved mercury in the corresponding water samples decreased from 340 ng/L to 13 ng/L. The increase for particulate mercury was not as large as we observed previously, most likely due to the increased total suspended solids (350 mg/L compared to 70 mg/L in the first visit). The five-fold increase in suspended solids in the second sampling visit effectively diminishes the effect of mercury adsorption on particulate mercury concentration.

Multiclone dust also contains mercury, but the concentration was much less than that of the scrubber dust. Dust collected in the multiclone has a grain size coarser than that collected "down-stream" in the plant scrubber system, and the lower specific surface area combined with hotter trapping temperatures may account for the lower mercury concentration. It is also possible that not all of the oxidized mercury carried in taconite gas streams is carried on the particulate phases. If it were, one might expect better agreement between concentration of mercury for dust samples collected from the multiclone and wet scrubber systems. Furthermore, the great difference in mercury distribution for lab and field filtered wet-scrubber samples suggests an overall process whereby at least some oxidized mercury is transported or produced in the gas phase, captured by the wet scrubber system, and only then begins to adsorb to the captured particulate phases.

Minntac:

Two sets of samples were collected at Minntac, and, importantly, while the plant was operating under distinctly different conditions. In particular, the first sample set from Minntac was obtained on February 19, 2003, when the company was processing "acid" pellets, while the second set of samples was obtained on May 9, 2003, when Minntac was producing "fluxed" pellets. This difference, in terms of mercury capture by plant scrubbers, turned out to be quite large, with nearly an order of magnitude increase in mercury captured by plant scrubbers during production of acid compared to fluxed pellets.

The mercury concentration in dust filtered on-site from scrubber water was 1285 ng/g during the first visit, but only about 160 ng/g in the second visit. The water, meanwhile, contained approximately 115 and 80 ng/l dissolved mercury, during acid and fluxed pellet production, respectively. For samples filtered after shipping to Cebam, the concentration of mercury in the dust increased to over 2000 ng/g for acid pellet, versus 180 ng/g for fluxed

pellet production. The corresponding water for samples filtered by Cebam decreased in all cases to values close to 25 ng/L.

Water chemistry might be one way to account for differences in the adsorptive behavior of mercury. For example, adsorption to iron oxides is supposed to decrease with decreasing pH. However, we tested the effect of pH on mercury adsorption (Table 4) and found that the mercury tends to adsorb to scrubber dust (long exposure time) for the entire pH range we expected to encounter (3 to 9) in taconite processing plants. When the pH was lowered to 2.96 by addition of H₂SO₄, the concentration of mercury in the scrubber water was 68.3 ng/L but when NaOH was added to the water, bringing the pH up to 9, dissolved mercury in scrubber water was 16.9 ng/L Hg. Because the dissolved mercury concentration in water filtered on-site was higher than either value, the results imply that adsorption to solids dominated mercury distribution, regardless of pH. The amount that adsorbs over an extended period of time (6 days) decreases with decreasing pH, but these differences pale in comparison to differences in overall mercury concentrations associated with production of acid versus fluxed pellets.

Another potential cause for the differences observed during our two sampling visits to Minntac include the fact that TSS was much higher in the later sample sample (3870 mg/L as compared to 860 mg/L). Particulate mercury concentration would be lower for adsorption in solutions containing higher TSS. However, this effect is insufficient to account for all of the observed difference in mercury for fluxed and acid pellet production because the difference in TSS is only about 5X, while that for mercury concentration is approximately 12X. This implies that the delivery rate for oxidized mercury to the wet scrubber systems, whether originally adsorbed to particulates or not, was greater during acid pellet production than during fluxed pellet production.

One possibility to account for this might be the differences in heat management and distribution for production of the two types of pellets. Owing to differences in heat capacity and chemical energy release upon heating, significantly greater amounts of energy are required to produce fluxed pellets than are needed for acid pellets. Because of this, auxiliary burners have been added in the pre-heat zone at Minntac, which are activated only when fluxed pellets are being generated (Fig. 1). The hotter gas temperatures in the preheat zone could cause a larger share of the Hg²⁺ released during induration to become chemically reduced to volatile Hg⁰. Because only the oxidized form, Hg⁺², is captured by the wet scrubber systems during production of either type of pellet, this would result in less capture of mercury in wet scrubbers during fluxed pellet production. It is interesting to note that the lower concentrations of mercury observed in this study during fluxed pellet production are similar to those reported by Benner (2001) who also sampled scrubber effluents at a time when Minntac was producing fluxed pellets.

Evtac

The scrubber at Evtac was only sampled once owing to temporary shutdown during the second sampling round. This turned out to be unfortunate for our study, because we obtained fewer samples for this plant than others in our initial visit, and for those few samples we did collect, the behavior of mercury appeared to be unique compared to that observed at

the other plants. Unlike Hibbtac and Minntac, the highest particulate mercury concentrations were found during on-site filtration (980 ng/g compared to 490 ng/g mercury for samples filtered at Cebam). The corresponding concentration for dissolved mercury (filtered scrubber water) was 64 ng/L for on-site filtration which increased to an average of approximately 90 ng/l when filtered at Cebam, Inc. The cause for this variation is unknown, but one possibility under consideration is a chemical reaction with SO₂ (or H₂SO₃ when dissolved in water), which owing to Evtac's use of coal as a fuel source, may be more abundant than at the other plants. If, this molecule reacts with Hg⁺² on the solid phase, it would likely convert it to Hg⁰ and volatilize it. On-site filtration, in effect, would isolate adsorbed Hg⁺² from the H₂SO₃ and prevent its loss, while waiting and filtering samples at the lab might provide time for the reaction to take place and reduce the overall amount of mercury in the sample. Due to the limited number of samples taken at EVTAC, however, it is also possible that the time-dependency of mercury distribution that we observed is only reflecting the simple short-term variation in the mercury distributions in EVTAC's process stream. Nevertheless, possible reaction with H₂SO₃ will be tested further in future studies.

Ispat-Inland Mining Company

Like Hibbtac, Ispat-Inland also employs a dry multiclone scrubber system to remove some of the dust from their gas stream prior to collection in the wet scrubber system. Unlike Hibbtac, however, the water and fine particles in Inland's system are recirculated within the scrubber and only periodically dumped. Because of this, components like Hg²⁺ may build up for a period of time within the scrubber system and grow to higher concentrations than might be expected in a "single-pass" scrubber system. Owing to this, the mercury distribution is more difficult to characterize for Ispat-Inland's system than for the other plants, however, this procedure could offer potential advantages since it is possible that Hg-adsorbing fine particles will adsorb proportionately large amounts of mercury by reacting with fresh Hg-bearing processing gas streams many times before being dumped.

One important observation is the fact that the dry dust captured by the multiclone system at Ispat-Inland was found to be quite low (only 6.4 ng/l), which is consistent with a component that may have been heated to high temperatures and lost most of its mercury. A high temperature origin for this dust is also consistent with the low percentage magnetite for Inland dust samples.

In contrast, mercury concentrations in the wet scrubber samples were consistently high. During acid pellet production (2/20/03 samples) on-site filtration yielded 1215 ng/L dissolved mercury and 616 ng/g for particulate mercury. The percent magnetite, meanwhile, was very low (19%), however, suggesting a common high-temperature heritage with the multicyclone dust. This implies that most of the mercury captured by Ispat-Inland's wet scrubber system was NOT transported there on particulate phases, but was transported there in the gaseous phase, perhaps as minute particles of mercury-oxide or mercury salts.

Another important observation appears to be related to the fact that mercury concentrations appeared to be higher when Ispat-Inland was producing fluxed pellets compared to when they were producing acid pellets. This is the opposite of what was observed for Minntac. Dissolved mercury for scrubber water during fluxed pellet production at Ispat Inland was approximately 840 ng/L for samples filtered on-site and only 550 ng/L for samples filtered by Cebam. Particulate mercury concentrations, meanwhile, increased from

1560 ng/g to 3460 ng/g for samples filtered in the field and lab, respectively. The fact that a large fraction of the mercury remained in solution in these samples suggests that the solids may have reached their capacity to adsorb mercury.

Unfortunately, the recirculating nature of Inland's wet scrubber system makes it difficult to determine if the increase in mercury concentrations for fluxed pellet production were related to the change in process, or to greater accumulation due to increased recycling time. If the later case were true, however, one might expect other components in the scrubber fluid (F, Br, SO_4^{2-}) to be enriched in similar fashion to mercury, which they were not. Thus, for the limited samples that we now have, it appears that production of fluxed pellets results in increased capture of mercury at Ispat-Inland, but reduced capture of mercury at Minntac. Whether this represents a fundamental difference between Ispat Inlands use of a straight grate line compared to Minntac's use of a grate-kiln system, remains to be determined in future studies.

Conclusions

It is apparent from the results collected in this study that the distribution of mercury in wet scrubber systems is highly dependent on a number of variables, only a few of which were addressed in this preliminary study. Other variables not addressed might include variations in the mercury concentration and distribution in the ore source, or slight differences in crushing and milling. In general, however, it appears that it is important to take into account the mercury concentrations in both the aqueous and particulate phases to provide a full accounting of mercury cycling in taconite scrubber systems. Furthermore, there appears to be significant differences in the rate at which mercury is captured when companies produce acid or fluxed pellets. Studying these differences may lead, ultimately to an understanding of the processes most important in controlling mercury release (heating effects on Hg volatilization, catalysis of mercury oxidation and reduction processes in scrubber streams). Finally, in plants that contained both multiclone dust collectors and wet scrubbers, the concentration of mercury was much higher on the dust particles captured by the wet scrubbers than they were upstream in the dry multiclone dust collectors. This, and the finding of considerable dissolved mercury in scrubber waters immediately upon sampling suggest strongly that non-particulate, oxidized mercury is being transported or generated within the gas stream at taconite plants. This mercury readily adsorbs to particulates suspended in the water at room temperatures following sample collection. Thus, accurate assessment of mercury distribution within wet scrubber systems necessarily requires on-site filtration.

Future studies on possible mercury control should be directed toward better defining the rates of mercury adsorption in aqueous solutions, the dependence of this rate on temperature and water chemistry, and the degree to which changes in mineral processing affect mercury volatilization and transport. Until the relative importance of these factors can be better understood, it is likely premature to estimate the potential savings in mercury emissions that might be found by making adjustments to mineral processing techniques (e.g., discarding rather than recycling scrubber fines, Benner, 2001). The relatively high flow rates and high concentrations of mercury in some of the aqueous and particulate samples collected by Benner (2001) and in the present study suggest, however, that cost effective means to reduce mercury emissions using some form of scrubber water and scrubber dust method may be found.

References

Benner, B. (2001) Mercury removal from induration off gas by wet scrubbers. Coleraine Minerals Research Laboratory Technical Report #CMRL/TR-01-19. 7 pages plus table figures and appendices.

Berndt, M. E. (2002) Mercury and Mining in Minnesota, Minerals Coordinating Committee Year 1 Status Report, Minnesota Department of Natural Resources Report, 57 pages.

Engesser, J., and Niles, H. B. (1997) Mercury emissions from taconite pellet production. Coleraine Minerals Research Laboratory Report: University of Minnesota Contract: #1663-187-6253. Coleraine Minerals Research Laboratory Report. 16 p. plus appendices.

Jiang, H., Arkly, S., and Wickman,, T. (2000) Mercury emissions from taconite concentrate pellets- stack testing results from facilities in Minnesota. Presented at USEPA conference "Assessing and managing mercury from historic and current mining activities". San Francisco, November 28-30, 18 pages.

Table 1: Taconite Plant data.

Taconite Plant	Sample Date	Scrubber Flow Rate (gpm)	Green Ball Feed Rate (Lton/hr)	Pellet Type	Fuel Type	Furnace Type	Notes
Hibtac	2/20/03	6600	450/ furnace	Acid	Natural gas	Straight grate	Two of 3 furnaces operating
Hibtac	5/8/03	6627	~450/ furnace	Acid	Natural gas	Straight grate	Two of 3 furnaces operating
Minntac	2/19/03	2650	600	Acid	Wood to kiln, no preheat burners	Grate kiln	
Minntac	5/9/03	2645	540	Flux	Wood to kiln, natural gas to preheat burners	Grate kiln	
EVTAC	2/18/03	2300	600	Acid	Pet-coke, coal (3% S)	Grate kiln	
Inland	2/20/03	1000	240	Acid	Natural gas	Straight grate	
Inland	5/8/03	1000	340	Flux	Natural gas	Straight grate	

Table 2: Blanks and Standards

Sample type	Filtration	Hg in water (ng/L)	Hg in filtrate (ng/g)	Notes
Hibtac-Blank 1			0.9	Filter (new) (assuming 1 gram of filtrate)
Hibtac-Blank 2	Cebam (6 days)	1.5		Cebam DDW water placed in sealed bottle
Hibtac-Blank 3		1.2		DNR DDW water - bottle filled at lab and brought to plant sealed
Hibtac-Blank 4		1.3		DNR DDW water - bottle filled at the plant (unfiltered)
Hibtac-Blank 5	Immediate	1.3		DNR DDW water - filtered at the plant
Hibtac-Blank 6			2.9	Filter from Blank 5 (assuming 1 gram of filtrate)
Minntac-Blank 1			0.9	Filter (new) (assuming 1 gram of filtrate)
Minntac-Blank 2	Cebam (5 days)	1.4		Cebam DDW water
Minntac-Blank 3		5.5		DNR DDW water - bottle filled at lab and brought to plant sealed
Minntac-Blank 4		2.1		DNR DDW water - bottle filled at the plant (unfiltered)
Minntac-Blank 5	Immediate	1.9		DNR DDW water - filtered at the plant
Minntac-Blank 6			3.0	Filter from Blank 5 (assuming 1 gram of filtrate)
Inland-Blank 1			0.8	Filter (new) (assuming 1 gram of filtrate)
Inland-Blank 2	Cebam (6 days)	1.1		Cebam DDW water
Inland-Blank 3		1.5		DNR DDW water - bottle filled at lab and brought to plant sealed
Inland-Blank 4		1.5		DNR DDW water - bottle filled at the plant (unfiltered)
Inland-Blank 5	Immediate	1.5		DNR DDW water - filtered at the plant
Inland-Blank 6			2.6	Filter from Blank 5 (assuming 1 gram of filtrate)

DDW = doubly deionized water

Table 3: Hibtac Mercury Data

Sample type	ID	Filtration	Hg in water (ng/L)	Hg in filtrate (ng/g)	Notes
Scrubber water (2/20/03)	Hg6	Cebam (5 days)	13.6	5027.4	
Scrubber water (2/20/03)	Hg8	immediate	255.5	1405.5	
Scrubber water (5/08/03)	2-1	immediate	337.3	420.5	
Scrubber water (5/08/03)	2-3	immediate	340.8	808.1	
Scrubber water (5/08/03)	2-5	Cebam (6 days)	13.6	1519.0	
Scrubber water (5/08/03)	2-6	Cebam (6 days)	13.0	1539.3	
Multiclone water (2/20/03)	Hg1	Cebam (5 days)	5.2	175.2	
Multiclone water (2/20/03)	Hg3	Cebam (5 days)	12.7	129.9	0.5mL 1N H ₂ SO ₄ (pH=2.96)
Multiclone dust (2/20/03)	dust			63.5	

Table 4: Minntac Mercury Data

Sample type	ID	Filtration	Hg in water (ng/L)	Hg in filtrate (ng/g)	Notes
Scrubber water (2/19/03)	Hg1	Cebam (6 days)	26.7	2292.7	
Scrubber water (2/19/03)	Hg2	Cebam (6 days)	21.7	1864.2	
Scrubber water (2/19/03)	Hg3	immediate	115.8	1284.8	
Scrubber water (2/19/03)	Hg5	Cebam (6 days)	68.3	1970.3	0.5mL 1N H ₂ SO ₄ (pH= 2.96)
Scrubber water (2/19/03)	Hg6	Cebam (6 days)	22.3	2093.7	0.5mL 0.1N H ₂ SO ₄ (pH= 4.51)
Scrubber water (2/19/03)	Hg8	Cebam (6 days)	16.9	2607.7	0.5mL 0.5N NaOH (pH= 8.99)
Scrubber water (5/09/03)	2-1	immediate	89.8	153.0	
Scrubber water (5/09/03)	2-3	immediate	72.6	167.6	
Scrubber water (5/09/03)	2-5	Cebam (5 days)	25.7	179.9	
Scrubber water (5/09/03)	2-6	Cebam (5 days)	26.7	173.8	

Table 5: Evtac Mercury Data

Sample type	ID	Filtration	Hg in water (ng/L)	Hg in filtrate (ng/g)	Notes
Scrubber water (2/18/03)	Hg1	Cebam (7 days)	107.5	496.6	
Scrubber water (2/18/03)	Hg2	Cebam (7 days)	76.4	436.6	
Scrubber water (2/18/03)	Hg3	immediate	64.2	978.7	

Table 6: Inland Mercury Data

Sample type	ID	Filtration	Hg in water (ng/L)	Hg in filtrate (ng/g)	Notes
Scrubber water (2/20/03)	Hg1	Cebam (5 days)	35.9	1105.3	
Scrubber water (2/20/03)	Hg2	Cebam (5 days)	33.7	1012.6	
Scrubber water (2/20/03)	Hg3	immediate	1215.5	616.8	
Multiclone dust (2/20/03)	dust			6.4	
Scrubber water (5/08/03)	2-1	immediate	836.6	4378.8	
Scrubber water (5/08/03)	2-3	immediate	853.2	1560.2	
Scrubber water (5/08/03)	2-5	Cebam (6 days)	585.2	3382.9	
Scrubber water (5/08/03)	2-6	Cebam (6 days)	529.1	3550.1	

Table 7: TSS and Water Chemistry for scrubber water samples.

Parameter	Hibtac (2/20/03)	Hibtac ¹ (2/20/03)	Hibtac (5/08/03)	Minntac (2/19/03)	Minntac (5/9/03)	Inland (2/20/03)	Inland (5/8/03)	EVTAC (2/18/03)
Temp. (C)	27.4	4.0	34.1	35.1	42.2	36.6	44.6	40.8
Conductivity (μ S/cm)	1350	850	1050	2300	1950	1000	1250	1800
pH	6.67	7.00	7.38	5.62 (4.25)	6.42	6.67	6.42	4.20
% Solids	0.007		0.035	0.086	0.387	0.328	0.142	1.34
Anions (ppm)								
F	22.33	6.80	19.09	23.07	6.94	47.69	42.65	43.19
Cl	85.94	39.52	64.90	196.1	175.5	108.7	208.6	58.5
NO2-N	0.22	0.020	0.187	0.15	0.176	0.19	0.395	<0.050
Br	0.327	0.148	0.280	1.408	1.279	0.701	1.697	0.337
NO3-N	7.226	3.543	5.123	3.286	3.156	1.746	1.688	3.165
PO4-P	<0.020	<0.020	<0.020	<0.020	<0.020	0.022	0.021	0.025
SO4	325.5	154.5	243.4	994.6	859.25	159.2	193.9	710.7
Cations (ppm)								
Na	74.89	37.08	51.93	103.7	88.21	51.20	57.22	55.07
Mg	98.73	61.34	77.25	193.85	174.03	67.68	78.39	44.14
Al	0.011	0.056	0.008	0.023	0.01	0.014	0.032	1.299
Si	12.11	8.79	10.30	8.05	4.31	8.63	15.29	10.18
P	0.012	0.005	0.003	0.058	0.022	0.034	0.008	0.069
K	16.84	8.24	17.88	29.63	25.39	9.24	11.54	13.09
Ca	57.55	56.83	43.25	137.88	129.10	45.19	66.08	179.73
Fe	0.025	0.631	0.003	0.111	0.047	0.029	0.0002	9.46
Mn	0.112	0.141	0.068	0.147	0.152	0.122	0.258	0.780
Sr	0.206	0.161	0.146	0.435	0.385	0.185	0.232	0.409
Ba	0.012	0.010	0.007	0.059	0.040	0.009	0.013	0.042
Trace (ppb)								
Li	22.22	12.62	16.58	24.79	20.21	23.35	27.08	14.64
B	116.25	53.12	96.57	147.65	108.97	121.5	169.57	127.65
Al	5.40	50.11	5.60	16.58	8.15	12.14	26.15	1251.5
P	6.19	2.53	4.79	33.47	24.34	14.96	11.22	38.83
S	133750	50945	78337	373450	269833	53135	61987	266750
Cl	83285	31755	63677	176900	161700	108700	194200	42285
Cr	0.40	0.41	0.16	1.83	1.02	0.39	0.60	15.15
Fe	1.32	493.95	9.39	29.44	55.81	0.12	14.45	7823
Mn	92.83	118.70	61.59	115.55	138.93	101.8	234.60	699.35
Co	0.32	0.42	0.22	0.53	0.58	0.37	0.31	2.97
Ni	1.03	2.22	1.25	4.66	7.43	3.74	5.39	82.75
Cu	0.99	0.43	1.95	2.82	1.63	1.67	2.49	45.99
Zn	2.69	1.46	2.20	6.86	10.59	2.72	10.84	14.39
As	40.16	9.69	63.19	30.72	1.48	11.43	3.10	82.42
Br	357.80	158.80	289.03	1434	1260.33	732.75	1765.33	359.85
Se	19.61	5.51	18.15	17.71	6.95	54.58	28.34	48.26
Rb	10.73	5.72	11.01	27.45	22.65	8.47	15.18	17.13
Sr	192.3	153.65	137.60	391.00	345.10	174.90	215.93	373.65
Mo	26.57	10.70	25.04	65.04	67.98	126.15	149.63	51.61
Cd	0.05	0.06	0.03	0.17	0.11	0.20	0.21	0.19
Cs	0.53	0.29	0.57	2.51	3.97	1.52	6.69	3.75
Ba	10.20	8.85	6.50	49.34	34.86	7.94	11.90	36.71
W	1.81	0.26	0.70	0.69	1.12	1.33	0.88	1.79
Ti	0.61	0.49	0.50	2.08	3.45	1.00	1.21	3.68
Pb	0.11	0.03	0.07	3.25	0.30	0.10	0.24	1.19
Th	0.47	0.02	0.38	0.10	0.88	0.15	0.36	0.96
U	1.25	0.90	1.30	0.95	1.15	0.51	0.44	1.13

¹ Hibtac multicloned water sample

Table 8. Satmagan analysis of magnetite for taconite scrubber and multiclone dust.

Taconite Plant	Sample Date	Sample Type	Magnetite %	Notes
Hibtac	2/20/03	Multiclone	51.87	
Minntac	2/19/03	Scrubber water	73.73	
Minntac	5/9/03	Scrubber water	80.80	
EVTAC	2/18/03	Scrubber water	55.11	
Inland	2/20/03	Scrubber water	13.20	
Inland	2/20/03	Multiclone	16.50	
Inland	5/8/03	Scrubber water	19.80	small sample size

analysis by CMRL-NRRI.

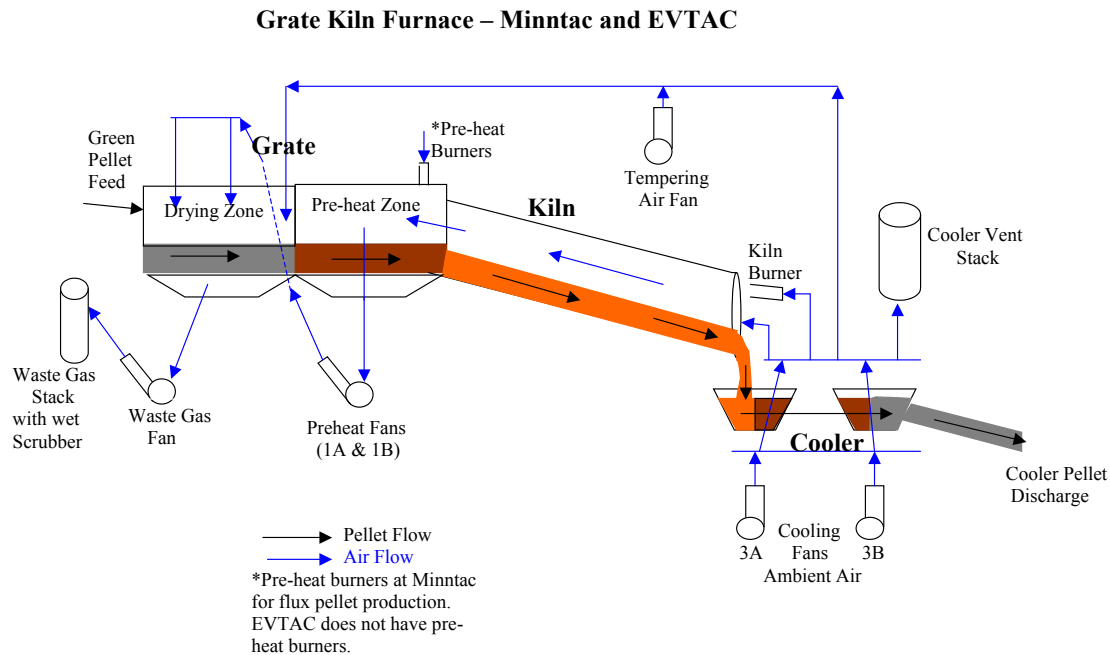


Figure 1. Diagram of a grate-kiln taconite pellet indurating process. Fresh, wet pellets (termed green balls) fed into the system (on the left side) are systematically dried, heated, and hardened into pellets as they pass from the drying zone and through a large, rotating kiln. Drying and heating is accomplished using gases, that are generated by cooling of the hot pellets and burning of fresh fuels in the kiln. The gases interact with pellets in the kiln, and are passed through pellet beds in the drying and pre-heat zones. The gases carry mercury and dust to the wet scrubber systems that were sampled in our study. The preheat burner near the center of the diagram is used only for fluxed pellet production.

Straight Grate Furnace – Ispat Inland and Hibbing Taconite

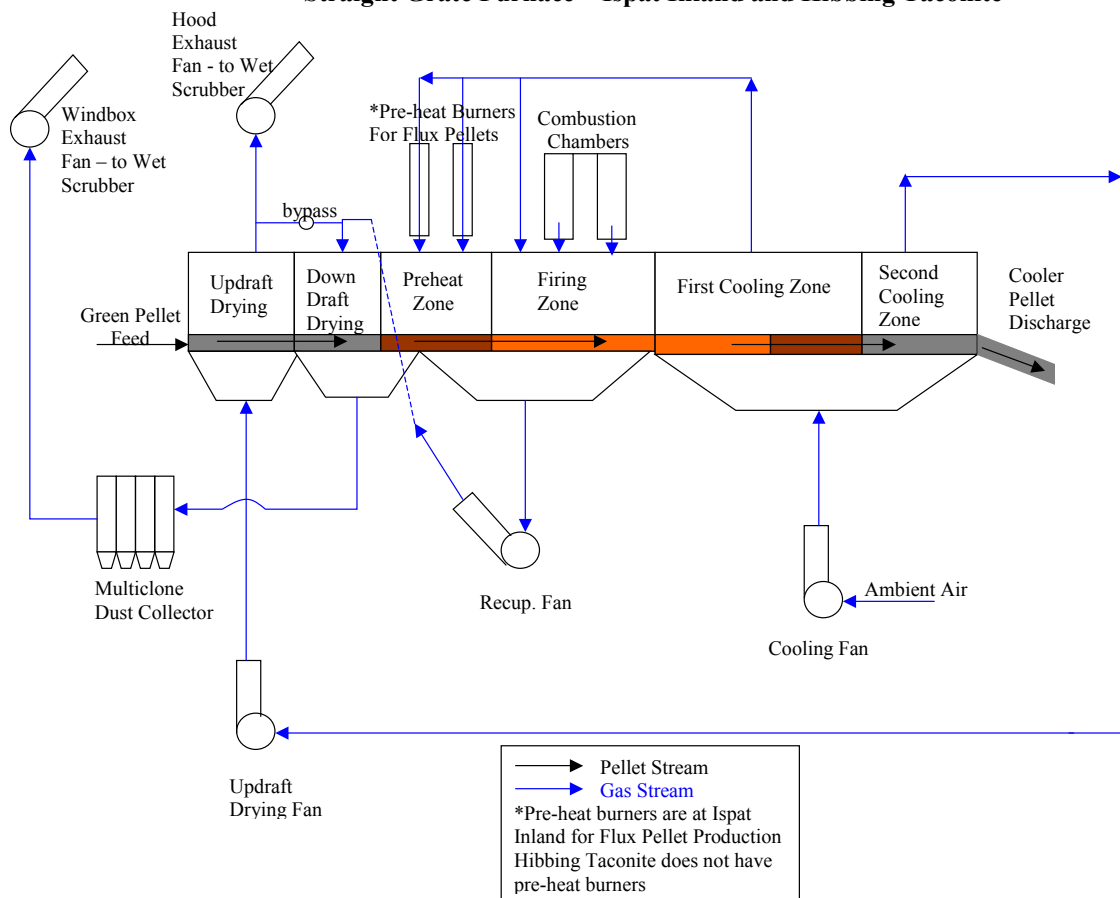


Figure 2. Diagram of a straight-grate taconite pellet indurating process. Fresh pellets are carried on a grate through a furnace and cooled by fresh air passed through the pellet bed. The air used for cooling and gases generated in the firing zone are used for drying and heating the pellets. In this case, the gases are passed through a dry “multiclone” dust collector that collects relatively hot, coarse particulates before they pass through the wet scrubber system. In this study, dust was collected from the multiclone collector and water containing particulates was sampled from the wet scrubbers.

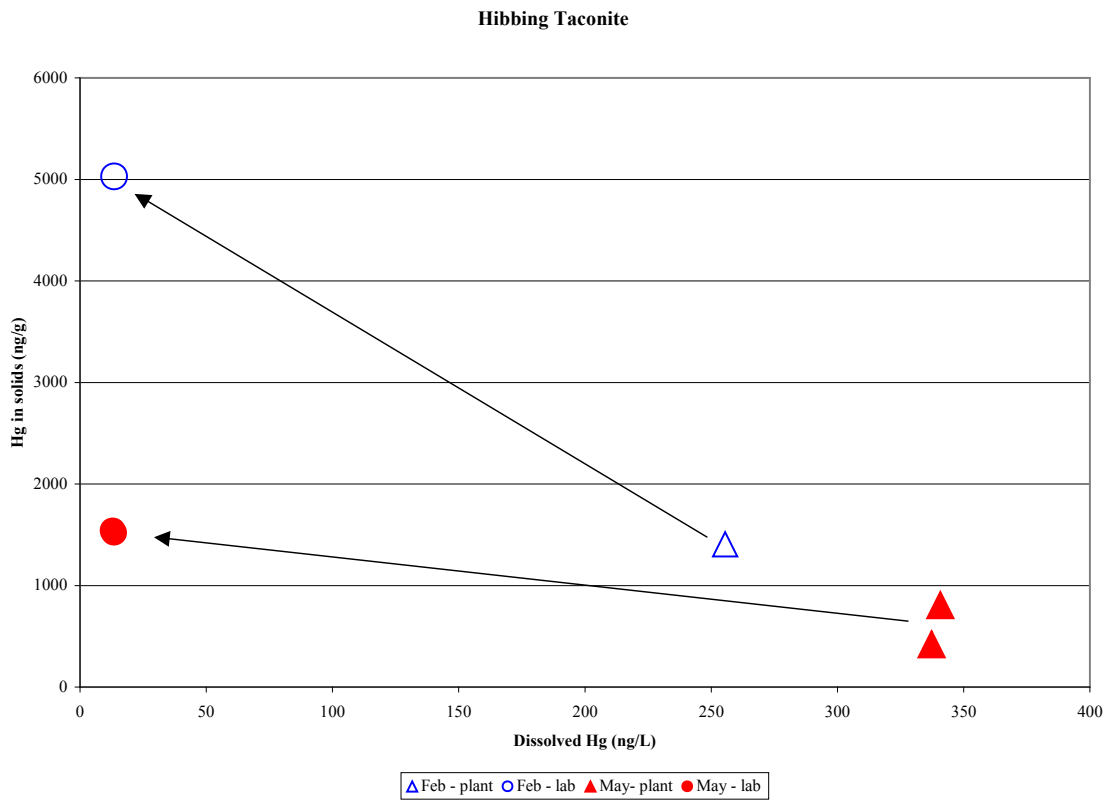


Figure 3. Mercury distribution in wet scrubber samples collected from Hibtac. Open symbols are for the first sampling round, close symbols are for the second sampling round. Triangles are results for samples filtered on-site, while circles are for samples that were filtered at the analytical laboratory, usually about six days after the sample was collected.

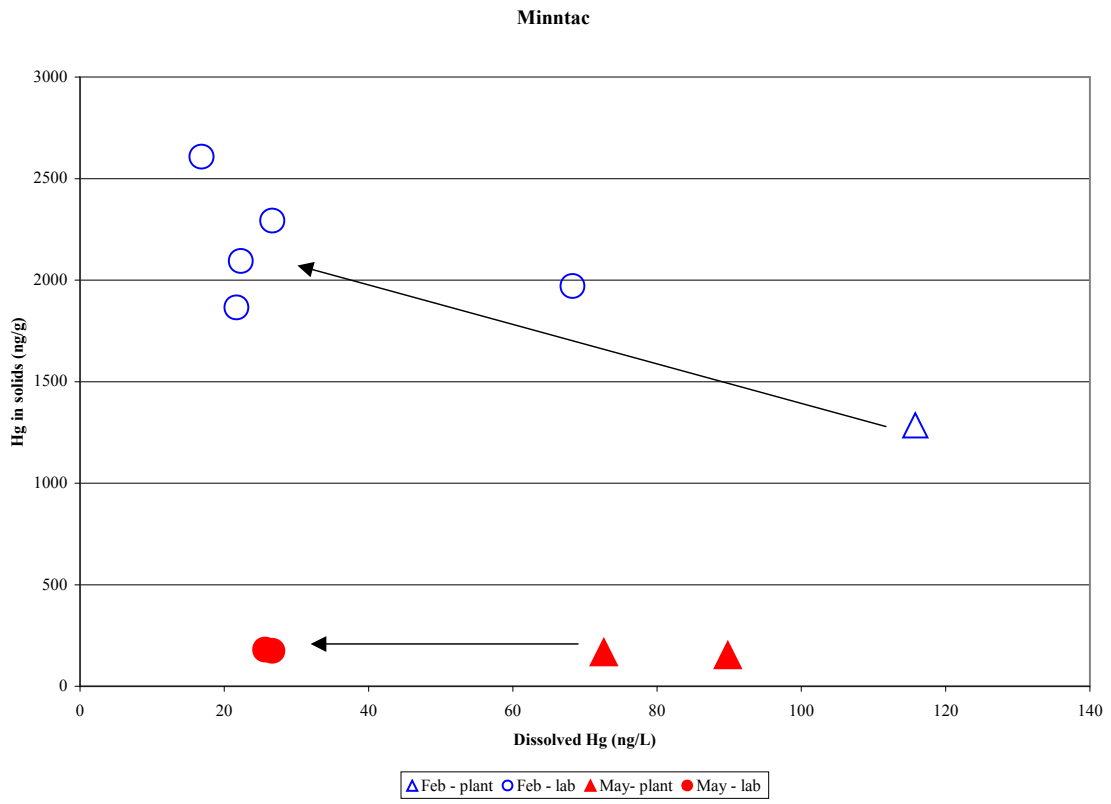


Figure 4. Mercury distribution in wet scrubber samples collected from Minntac. Symbols are the same as described in the caption for Figure 3.

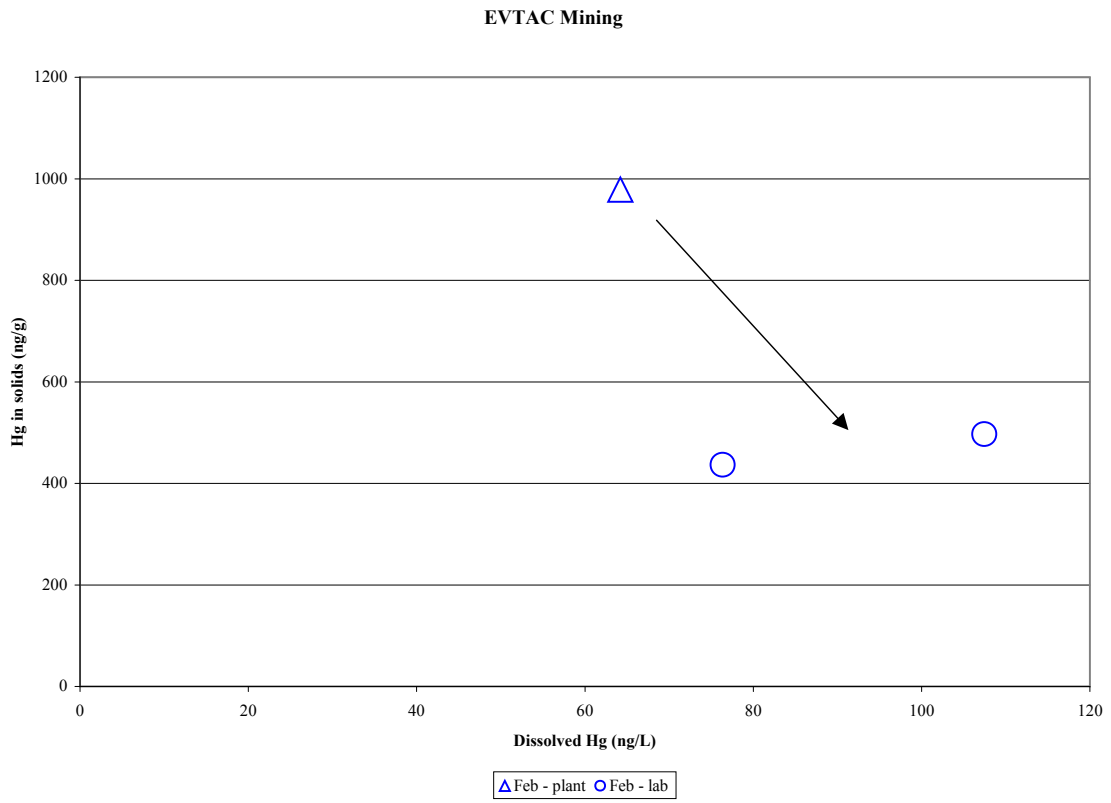


Figure 5. Mercury distribution in wet scrubber samples collected from Evtac. Symbols are the same as described in the caption for Figure 3.

Ispat Inland Mining

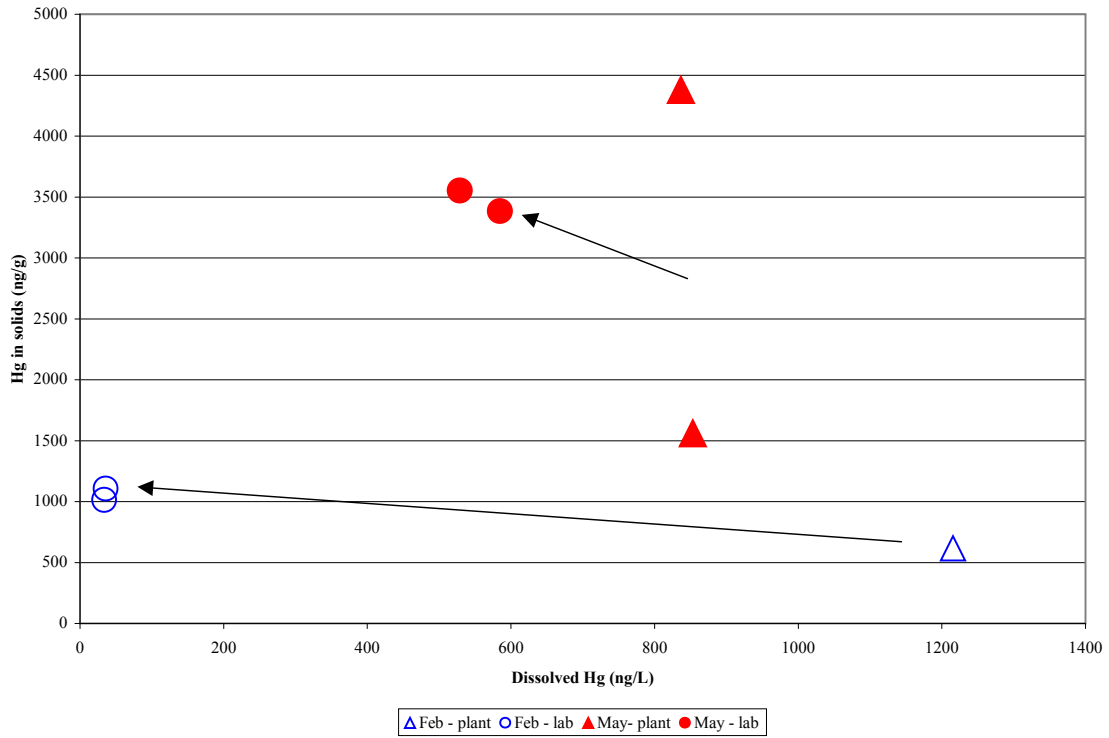


Figure 6. Mercury distribution in wet scrubber samples collected from Ispat-Inland. Symbols are the same as described in the caption for Figure 3.

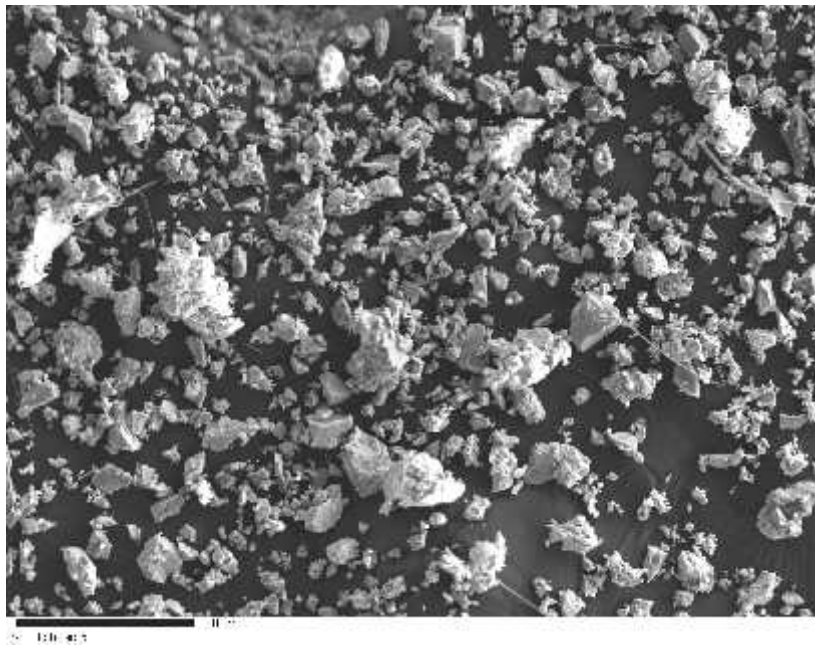
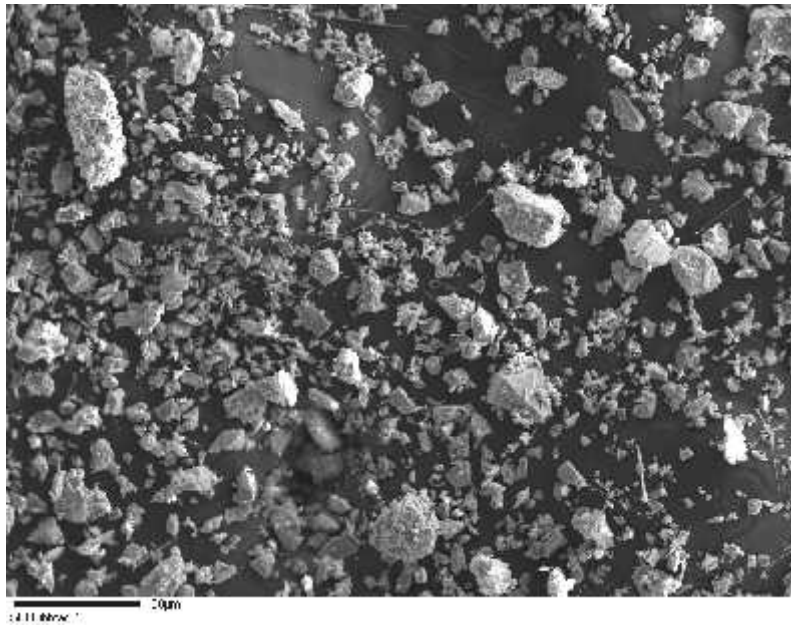


Figure 7. SEM images of dust samples filtered from samples collected at Hibtac. Larger grains range up to approximately 100 microns, but most are in the 5 to 30 micron range. Most of the sample is composed of iron-oxides (approximately 51% magnetic).

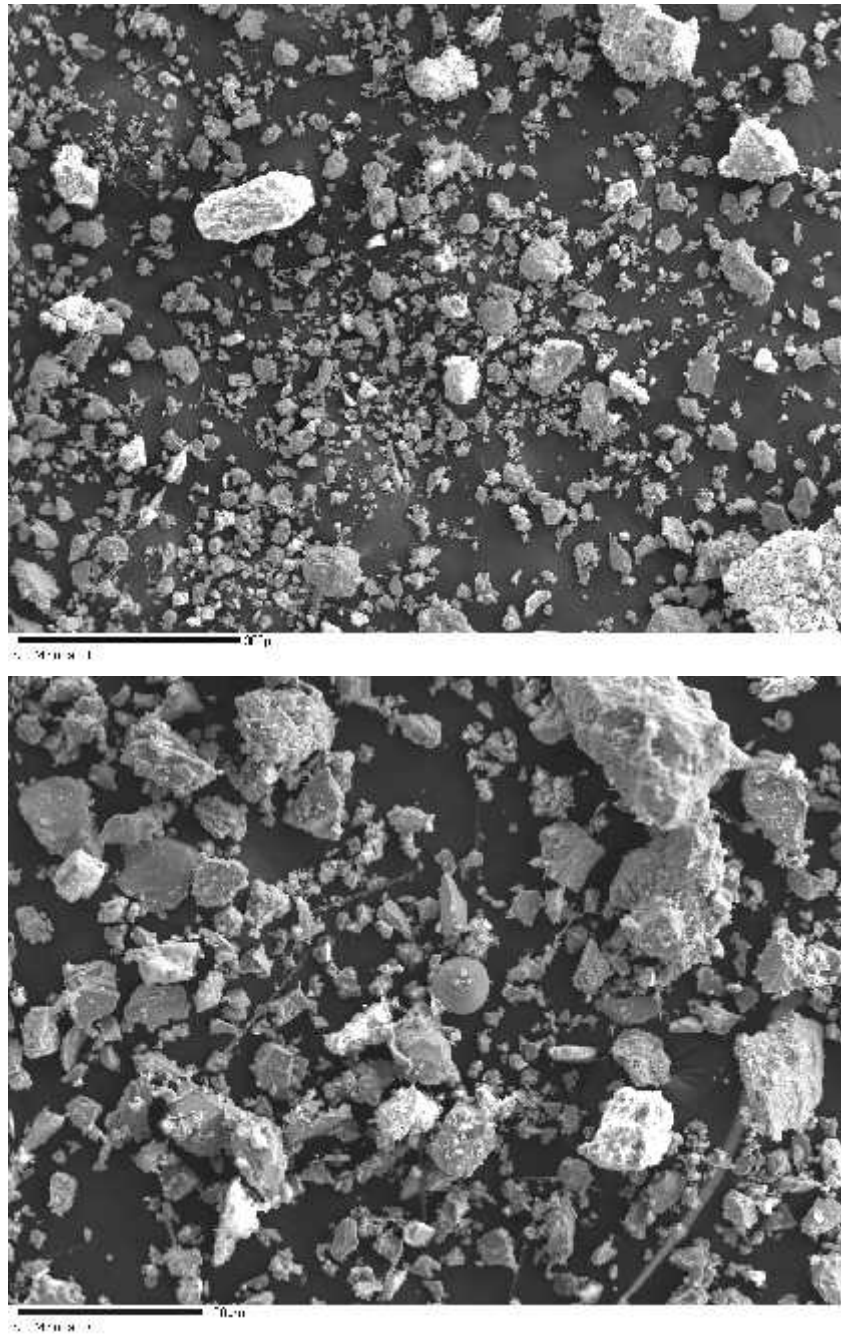


Figure 8. Secondary electron images showing grain size distribution for Minntac scrubber dust. Larger grains are around 100 microns across but most of the dust is between approximately 10 and 50 microns. The spherical object in the center is composed of iron-oxide. In addition to the dominant iron oxides, small amounts of carbonate and silicate grains were present. 80% of the sample was magnetic.

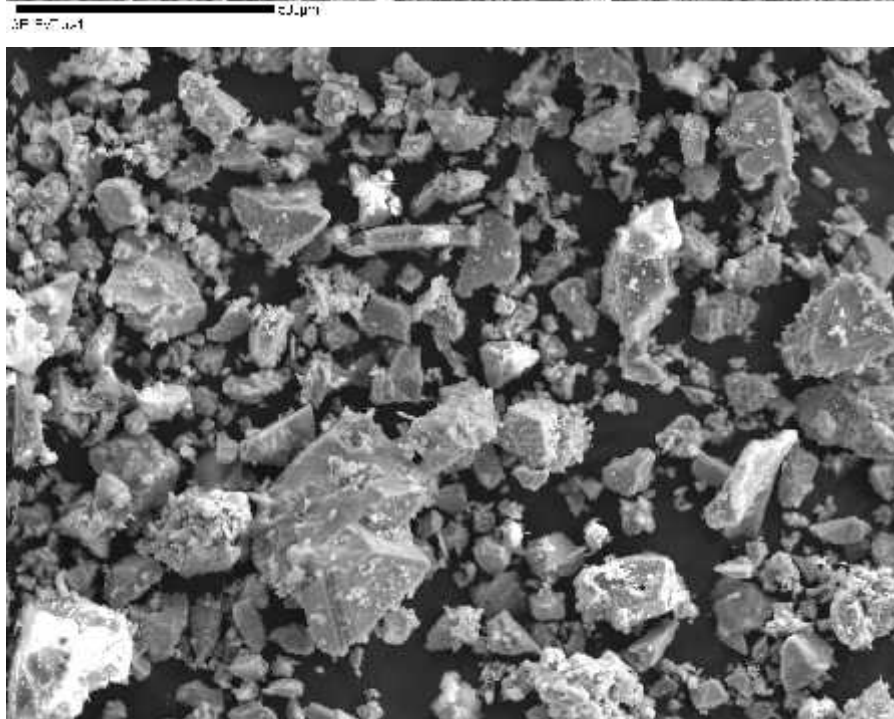
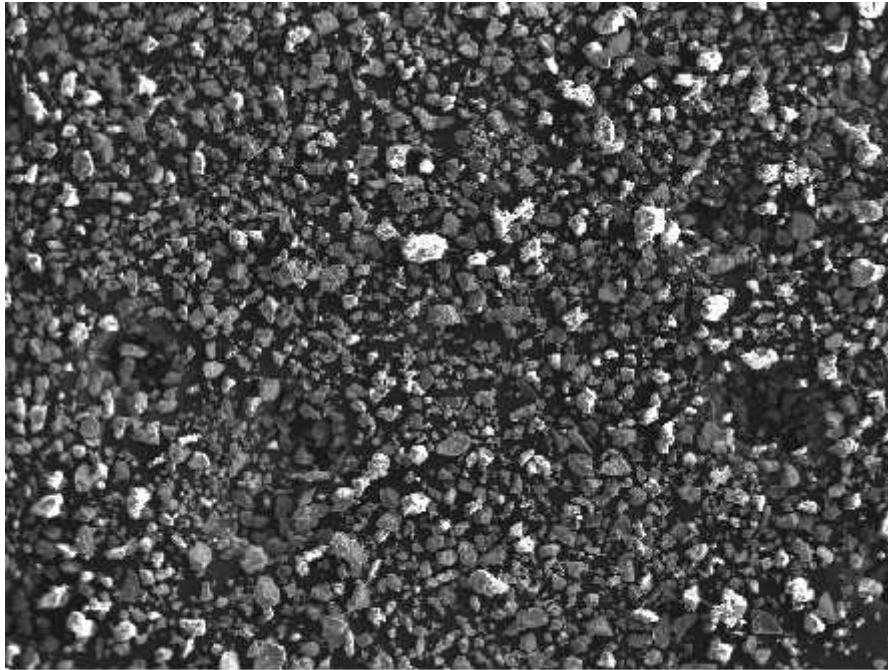
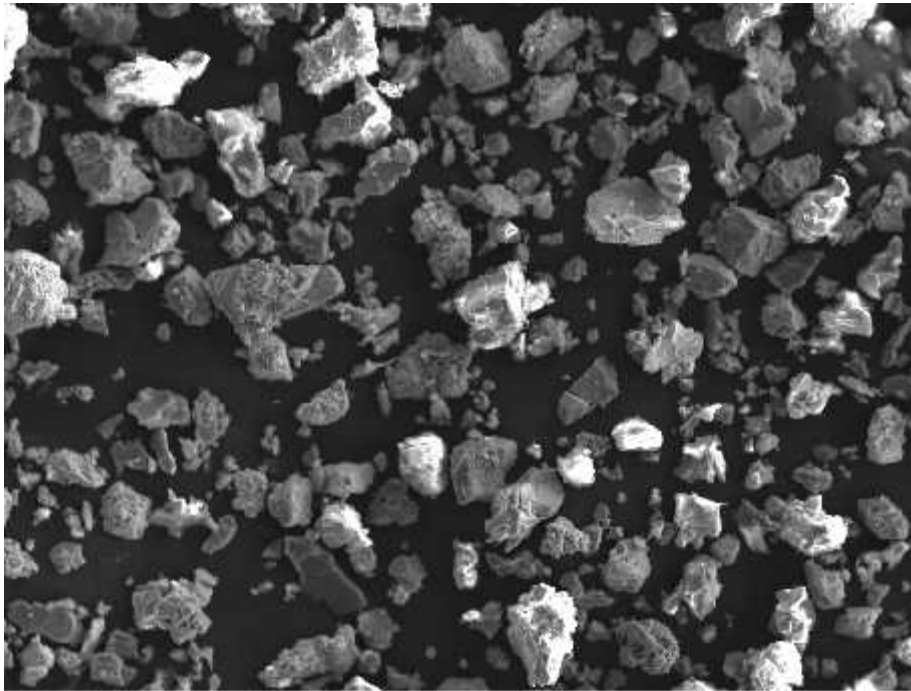


Figure 9. SEM images of scrubber dust samples from Evtac. The larger grains are 100 to 250 microns across, while the smaller grains tend to be in the 5 to 30 microns range. Numerous spherical objects were present. Interpreted as melt products, they were composed of iron silicate, iron-oxides, and aluminum silicate. The sample was 55% magnetic.



SEI100k1

100µm



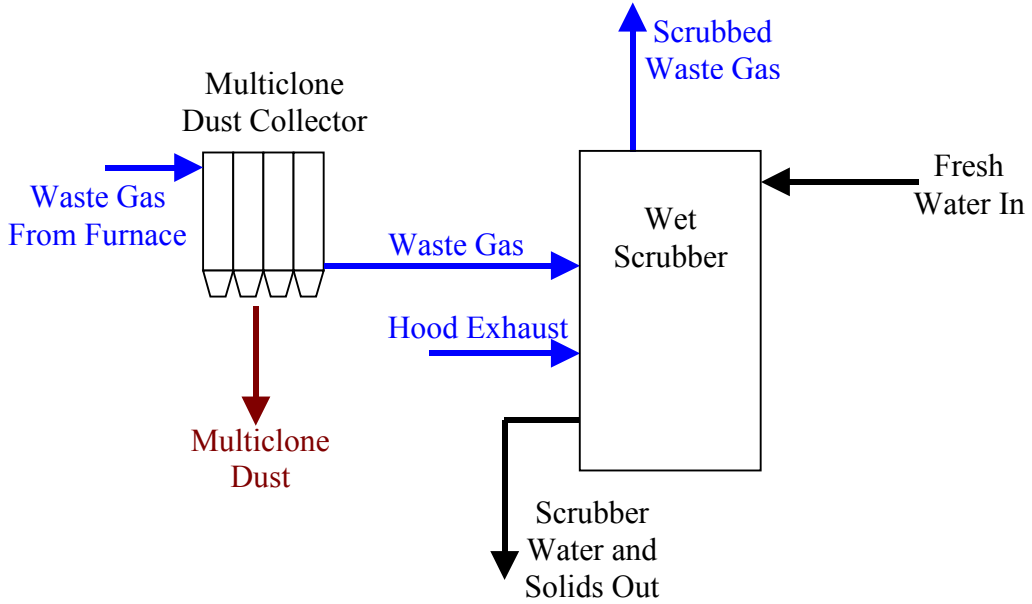
SEI1000k1

100µm

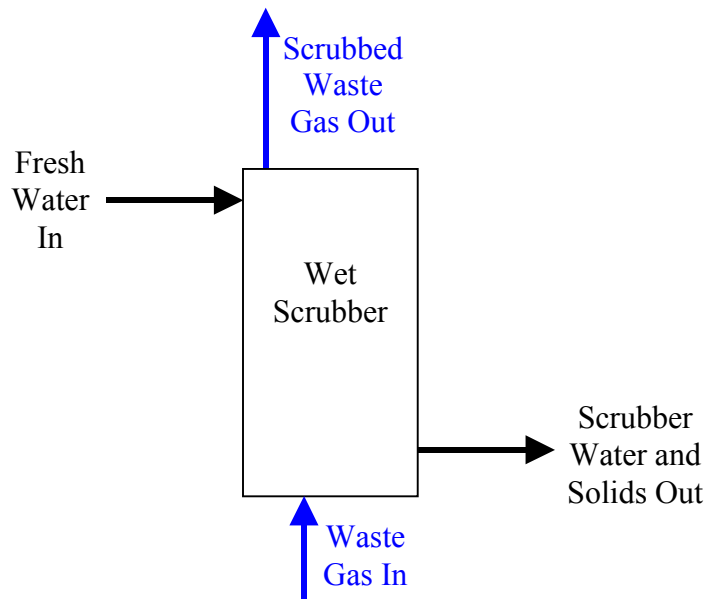
Figure 10. SEM images for scrubber dust samples from Ispat-Inland. Larger grains are around 50 microns across, but typical grain size is in the range of 5 to 30 microns.

Appendix: Wet scrubber schematic diagrams

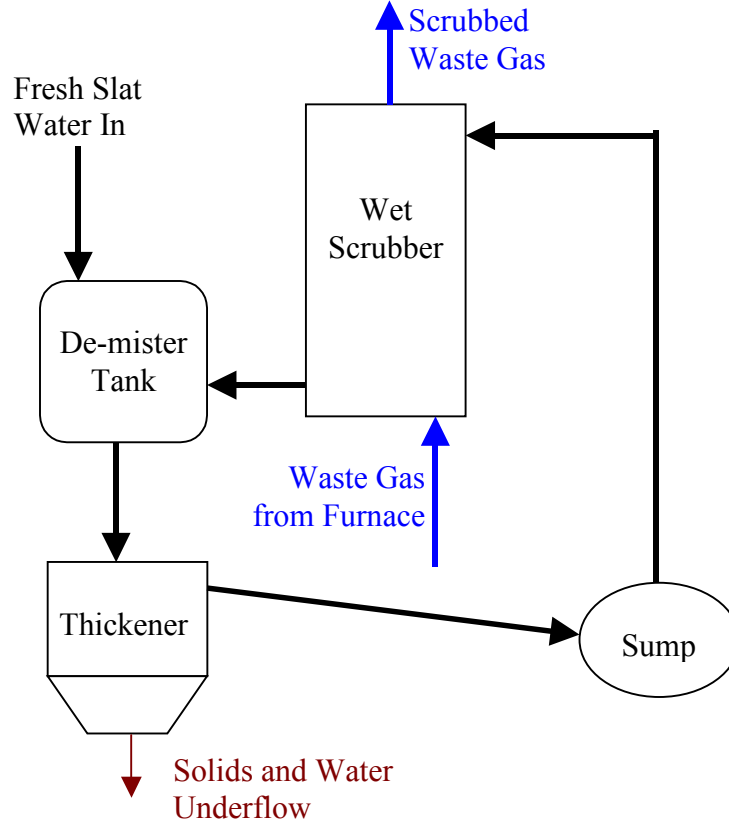
Hibbing Taconite Company Scrubber Flow Diagram



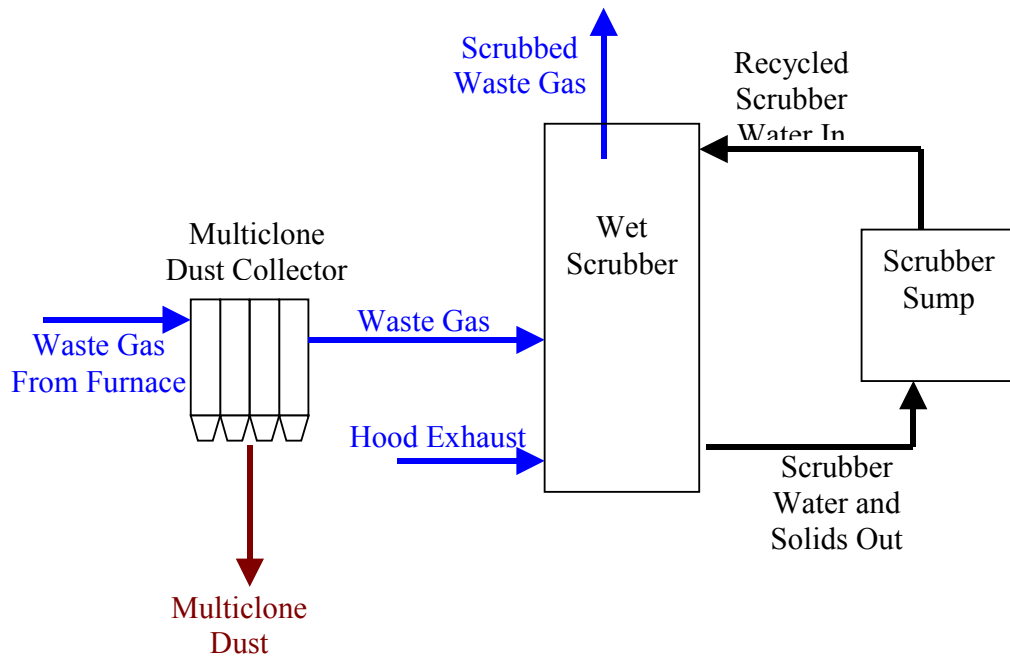
Minntac Scrubber Flow Diagram



EVTAC Mining Scrubber Flow Diagram



Ispat-Inland Scrubber Flow Diagram



Appendix B-1-3

Mercury and Mining in Minnesota

October 15, 2003

Mercury and Mining in Minnesota

Minerals Coordinating Committee
Final Report

Submitted June 30, 2003
Revised Oct. 15, 2003

Michael E. Berndt
Minnesota Department of Natural Resources
Division of Lands and Minerals
500 Lafayette Road
St. Paul, Minnesota, 55155

Summary

Mercury is a naturally occurring element that is ubiquitous in the earth's crust. It is released to the environment by natural processes and anthropogenic activities and transported worldwide through atmospheric and aquatic reservoirs. Increased Hg loading to the environment has ultimately led to increased Hg in freshwater fish, often to levels considered unsafe for human consumption. This has, in turn, led to global, national, and statewide efforts to reduce mercury emissions. The present document summarizes mercury cycling in NE Minnesota where an economically important iron-mining district ("taconite") operates within a region prized for its many fishing lakes.

As is the case in most regions, mercury loading in NE Minnesota is dominated by atmospheric deposition. Most mercury deposited on land is revolatilized, but a significant fraction is incorporated into local soils with only a relatively small component transported to lakes. Only a tiny fraction of the mercury deposited in any region is converted to methylmercury (CH_3Hg^+), the type of mercury that accumulates in fish. Considerable uncertainty exists concerning relationships between mercury emission, deposition, methylation, and bioaccumulation. However, recent research (METAALICUS) suggests much of the methylated mercury in a lake is generated in surface sediments but comes from "new mercury" that was recently deposited on the lake surface (e.g., precipitation within the last season) and conveyed to the bottom via particle transport.

Average mercury concentration in NE Minnesota precipitation is higher than dissolved mercury in most streams and lakes, underscoring the importance of sedimentation and uptake by soils and vegetation in regional mercury cycles. Atmospheric deposition of mercury from precipitation appears to be increasing or holding steady since 1990 despite large reductions in Minnesota's statewide emission rates. Lake sediment records indicate that mercury is being delivered to lakes at rates much greater now than in pre-industrial times, but some lakes reveal recent declines. Mercury concentrations in fish inhabiting surface waters are sufficiently high to trigger consumption advisories, but in more lakes than not, fish-Hg levels are declining.

Taconite processing in NE Minnesota potentially participates in the mercury cycle in three ways: (1) by releasing spent water that was originally obtained from precipitation and other freshwater supplies, (2) by generating tailings that interact with the environment, and (3) by emitting mercury to the atmosphere through stack emissions. Release of mercury to waters during taconite processing appears to be insignificant since the water sampled from tailings basins has mercury concentrations that are lower than local precipitation and similar to normal surface waters. Most of the dissolved mercury in taconite tailings basins may have come from atmospheric sources, rather than from mineral processing. Stack emissions are clearly the dominant pathway of mercury release from taconite processing on the iron range. Hg(II) in ore concentrate is converted to Hg(0) during the firing of pellets and released to the atmosphere in stack emissions. Emission factors reflect primary distribution of mercury in the ore body, and generally

increase in a westward direction across the district from 1 to 17 kg Hg per million long tons of pellets.

Atmospheric Hg emissions from taconite processing exceeded 100 kg/yr in the late 1960's, and have ranged between approximately 200 and 400 kg/yr ever since. The great majority of this mercury is transported out of the state and distributed globally, contributing approximately 0.24% and 0.007%, respectively, to national and global totals. No suitable technology has been found to curtail taconite mercury emissions. Regardless of whether currently active research on the iron range provides a cost efficient and effective method to limit mercury emissions from taconite processing, significant reduction of mercury deposition to Minnesota lakes will require global reductions in mercury emissions.

Table of Contents

1. Introduction.....	1
2. Mercury Chemistry	1
3. Mercury Distribution in NE Minnesota	4
3.1 Precipitation	4
3.2 Lakes and Streams	5
3.3 Fish.....	6
3.4 Historical Deposition	7
4. Iron Mining in Minnesota.....	8
4.1 Introduction.....	8
4.2 Taconite and the Biwabik Iron Formation	9
5. Mercury Release from Taconite.....	9
5.1 Mercury in Taconite Ore.....	10
5.2 Tailings Basins.....	12
5.3 Stack Emissions	14
5.3.1 Historical stack emissions.....	15
5.3.2 Comparison to other sources.....	17
5.3.2 Potential control.....	17
6. Cost and Benefit.....	18
7. Additional Studies.....	19
8. Summary	20
9. References.....	22
10. Tables.....	28
11. Figures.....	35
Appendices.....	45
Appendix 1: Hg Concentrations at Taconite Plants.....	46
Appendix 2: Historical Pellet Production	55
Appendix 3: Historical Mercury Emissions.....	57

1. Introduction

Human activities since the industrial revolution have increased atmospheric deposition of mercury to lakes compared to pre-industrial times (Swain et al., 1992; Engstrom and Swain, 1997; Engstrom et al., 1999; Fitzgerald et al., 1998). The resulting increased environmental availability of mercury has led, in turn, to increased uptake of the element by many aquatic organisms, including fish that may be consumed by humans. Mercury in fish tissue is now the leading cause for issuance of consumption advisories for fish captured in Minnesota lakes, just as it is at many localities throughout the US.

In an attempt to reduce mercury deposition to lakes, US legislation has mandated emission regulations for coal-fired power plants, previously identified as the largest anthropogenic emitter of mercury to the atmosphere (EPA, 1997). Decreased emissions from this and other sources will likely help Minnesota to reach statewide mercury emission reduction goals which were set during 1999 state legislation, and include reducing mercury emissions from 1990 levels by 60% in 2000 and 70% by 2005. Already, decreases in Hg release from industrial sectors where effective control measures are easiest to implement have led to large reductions in Minnesota statewide mercury emissions. At the same time, however, these decreases have effectively increased the proportion of current statewide Hg emissions for industries where control measures are either not available or difficult to implement. One such industry is taconite processing, which has seen its share of statewide emissions increase from 16% in 1995 to 20% in 2000, making it the second largest current source of Hg emissions in Minnesota (Table 1). As the primary domestic supplier of iron ore to US steel manufacturing companies, however, Minnesota is the only state where taconite processing is considered a major emitter of mercury. Important timelines for reduction of Hg from this source may include 2007 and 2010 when mercury “total-maximum-daily-load” (TMDL) limits must be set for the Great Lakes Basin and Minnesota (statewide), respectively (MPCA, 2001).

Northeastern Minnesota is a region prized not only for its economically important taconite mining industry, but also for its many wetlands and fishing lakes. Thus, the Minnesota Department of Natural Resources has undertaken this two-year study on mercury cycling and distribution in northeastern Minnesota, with emphasis on taconite processing. The overall goal of this study is to provide a technical foundation and background that can be used to guide mercury research and future discussions regarding the development and application of mercury regulations to Minnesota’s taconite industry.

2. Mercury Chemistry

Mercury occurs in the environment in two forms: zero-valent Hg(0) (or elemental mercury) and doubly charged Hg(II) (or oxidized mercury). Hg(0) is a liquid in pure form at room conditions, but vaporizes when in contact with the atmosphere. Because it has low solubility in water and does not adsorb readily to solids, Hg(0) emitted into the atmosphere generally remains there until it is oxidized to Hg(II). Hg(II) readily combines with other compounds to form non-volatile species that are both water-soluble and adsorb to solids. These properties promote a return of the element to terrestrial and aquatic environments through wet and dry deposition. While much of the mercury deposited

from the atmosphere in terrestrial environments may be revolatilized and returned to the atmosphere, a significant fraction is retained in local soils, sediments, and biota. Ultimately, only a very small fraction of mercury deposited in a region is incorporated in the tissues of fish.

Seasonal, annual, and spatial variations, as well as the high cost and technical specialization associated with low-level mercury analysis, make it difficult to determine an absolute mercury budget for any single watershed. However, based on a review of data from forested watersheds in temperate and boreal zones, Grigal (2002) provided a general description and semi-quantitative understanding of the most important processes. In detail, mercury deposition in a region can be divided into three distinct categories: that associated with litterfall (captured by and transported with falling vegetation), that in throughfall (rinsed from vegetation during precipitation), and mercury deposited in open precipitation (direct dry and wet deposition). Mean reported flux values for these three transport mechanisms for a region like NE Minnesota are approximately 21, 17, and 10 $\mu\text{g m}^{-2} \text{a}^{-1}$, respectively. Grigal suggested that the dominance of the first two terms (21 and 17) over the last (10) indicates the relative importance of vegetative matter as a trap and transport mechanism for mercury. These data further indicate that the flux of mercury to the forested portion of a watershed can be much greater than that for open water (approximately 4x or $(21+17+10)/10$).

On the other hand, most mercury deposited in a forested watershed appears to be revolatilized (e.g., mean value is 32 $\mu\text{g m}^{-2} \text{a}^{-1}$) by poorly understood processes. The primary step must involve reduction of Hg(II) back to Hg(0), but how this occurs is uncertain. Most of the remaining non-volatilized mercury is sequestered by soils (5 $\mu\text{g m}^{-2} \text{a}^{-1}$) and only a small fraction is transported out in streams (e.g., 1.7 $\mu\text{g m}^{-2} \text{a}^{-1}$) (Grigal, 2002). As a result, only about 5-25% of the mercury deposited on forested lands typically winds up in streams and lakes but, depending on the relative surface area of lakes and lands, this can account for between about 5 and 85% of the mercury delivered to lakes.

Mercury sequestration and transport in terrestrial and aquatic environments most commonly involves complexation with organic molecules, the most important of which appear to be fulvic and humic acids. A particularly strong affinity exists between Hg(II) and reduced-sulfur functional groups such as thiol (Skylberg et al., 2000). The capacity for organic molecules to bind with mercury in soils and streams typically exceeds mercury availability, meaning that any unbound Hg(II) is “captured” and transported with organic “captors”. As a consequence, strong correlations are often found between mercury concentration and dissolved or particulate organic carbon (Sorenson et al., 1990; Fleck, 1999; Kolka et al., 1999). The later correlation becomes more important in watersheds characterized by draining of peat lands, which, owing to slow growth and efficient adsorption of mercury, can accumulate mercury deposited from many centuries of precipitation. Groundwaters, by contrast, typically have little or no detectable mercury because nearly all of the mercury in infiltrating waters is captured by soils.

Although most terrestrial and aquatic mercury interactions involve organic compounds, one reaction that deserves special consideration is methylation, or the generation of methyl-mercury (CH_3Hg^+ or “MeHg”). This species, although representing only a small fraction of dissolved mercury in lakes, accounts for nearly all of the mercury

present in the tissues of fish. MeHg is a persistent bioaccumulative compound, meaning that once formed, it can remain in the environment where, owing to a high affinity for living tissues, it accumulates up the food chain. MeHg is not “emitted” into the environment, but rather produced from Hg(II) that is present in the environment. Gilmour et al. (1992) were the first to recognize that bacterial reduction of SO_4^- to S^- is associated with increased generation of methylmercury. Benoit et al. (1999) hypothesized later that methylation of mercury occurs at the transition zone between oxidizing and reducing conditions, where dissolved neutral Hg-sulfur species, having the ability to penetrate the cell membranes of methylating bacteria, are most likely to form. Their results, which revealed a direct correlation between calculated abundances of neutral Hg-sulfide complexes and rates of mercury methylation, support this idea. Kelley et al. (2003) recently provided data disagreeing with this model, however, and suggested an alternative explanation involving an H^+ facilitated mechanism for cell-uptake of mercury.

Hg(II) can also form complexes with other inorganic species (e.g., Cl^-), and can adsorb to solids. Indeed, most of the mercury in wet and dry precipitation is inorganically bound Hg(II), but most of this mercury quickly combines with organic carbon or sulfide in terrestrial and lake environments. Owing to the low solubility of HgS (cinnabar), dissolved Hg(II) is virtually absent from solutions when sulfide ion becomes abundant.

Although much has been learned about specific reactions that might affect mercury distribution, a more important question concerns identification of the most important pathways that exist between anthropogenically released mercury and fish uptake. The chain connecting mercury deposited from the atmosphere to mercury taken up by fish has many links, many of which are not fully understood. However, a multi-institutional collaborative study named “METAALICUS” (Mercury Experiment To Assess Atmospheric Loading In Canada and the United States, Hintelmann et al., 2002) has recently provided clues to the more important processes by introducing isotopically labeled Hg to a lake and its watershed and tracking its dispersal in the environment.

In an initial phase of the study, most of the mercury applied to a forested area surrounding a small Canadian lake (Hintelmann et al., 2002) remained bound to vegetation and soils in the application area. Less than 1% of the new mercury was rinsed into the lake and approximately 8% was revolatilized. In a more recent study phase, ^{202}Hg was added directly to the lake surface and other isotopes, ^{200}Hg and ^{198}Hg , were added to surrounding wetland and upland areas, respectively (Krabbenhoft and Goodrich-Mahoney, 2003). The ^{202}Hg isotope spike was found in sediment traps on the lake bottom within six days of application and continued to accumulate throughout the summer months. Simultaneously, Me^{202}Hg spread upward from the sediments into the water column. The isotope spikes added to the land around the lake did not contribute significantly to any of the various lake-mercury reservoirs (water column, sediments, MeHg). Although full results and discussion have not yet been published, the data provide evidence that mercury deposited on the surface of a lake is conveyed relatively rapidly to the sediments via particle transport, and it is this “new” mercury that appears to provide the dominant source of bioaccumulative MeHg to the water column.

3. Mercury Distribution in NE Minnesota

As is apparent from the discussion above, concentration of mercury in a lake or stream, or in the tissues of fish or in other aquatic species that inhabit a watershed may be functions of a large number of parameters (Glass et al., 1990). Considering the seasonal and annual variations in precipitation and the fact that no two lakes are identical (e.g., underlying geology and topography, vegetation, soil development, relative distributions of forest, wetland, and open water), it is not surprising that there is considerable variation in the mercury levels of northeastern Minnesota lakes. Moreover, mercury appears to be very transient in its behavior, meaning that relatively recent effects (rainfall, enhanced sedimentation or runoff, filtration) can cause the concentration at a single location to vary, depending on when and how the sample was collected. For an organism such as a fish, mercury may accumulate through its lifetime and mercury concentration may reflect a time-integrated snapshot of mercury uptake processes.

The following brief summary of mercury distribution in NE Minnesota is meant to provide information on the quality and quantity of mercury data that exist for the region.

3.1 Precipitation

A considerable database has been developed on recent precipitation in the US, largely through efforts of the Mercury Deposition Network (MDN) which is part of the National Atmospheric Deposition Program (NADP) (Vermette et al., 1995; Glass et al., 1999; NADP, 2002). Currently, there are over fifty MDN sites nationwide that collect and report high quality mercury data for precipitation. Four of these sites are located in Minnesota: including one near Ely and another at the Marcel research center near Grand Rapids.

Both Ely and Marcel stations began reporting on mercury deposition in early spring of 1995. Additional mercury data for precipitation in NE Minnesota are reported for the period 1990 to 1995 by Glass and Sorenson (1999). In that report, data are included for stations located in or near Duluth, Finland, International Falls, and Ely. Data for 1988 and 1989 are also available for Marcel, Ely, and Duluth (Sorenson et al., 1990; Glass et al., 1991), however, the reported concentrations were conspicuously elevated compared to those in the later two datasets and compared to precipitation in many other similar stations elsewhere in the world. Noting this discrepancy, Sorenson et al. (1994) reported that the higher values for 1988 and 1989, as compared to 1990 or 1991 may have been related to either a change in sampling procedures or to changing local emissions, and did not include the data in subsequent studies. The 1988 and 1989 data are also excluded here.

Combining data from 1990 to 1995 from Glass and Sorenson (1999) and the data collected since then from northern Minnesota MDN sites (Marcel and Ely), we can evaluate trends in mercury concentration for precipitation (Figure 1a) and for wet deposition (Figure 1b) on an annualized basis for the twelve-year period extending from 1990 through 2001. Data in Figure 1a suggest that the volume-averaged concentration of mercury in regional precipitation in northern Minnesota have been relatively level or slightly rising in the last decade. Data in Figure 1b suggest that total wet deposition of

mercury is also relatively level, or slightly increasing in the region, although the dataset is noisier than that for concentration.

Because data from the beginning and end portions of the twelve-year period were generated by two different research groups, it is possible that the apparent increasing trends could be related to minor differences in sampling or analytical procedures. However, Glass and Sorenson (1999) argue that increases in wet mercury deposition for the abbreviated time period of their study (1990-1996) were already statistically meaningful. They suggested that the increasing trend is due to an increase in atmospheric mercury owing to increased coal consumption in the region.

Increasing mercury in precipitation is in direct contrast to global atmospheric data (Slemr et al., 2003) and also to data from 1994 through 1999 generated at the Trout Lake station in northern Wisconsin. Atmospheric mercury as measured at various stations in the Northern Hemisphere appears to have decreased greatly during the early 1990's and leveled off in the period since 1996 (Slemr et al., 2003). Meanwhile, mercury in both precipitation and surface waters from the precipitation-dominated Trout Lake in Northern Wisconsin appeared to be on a decreasing trend (Watras et al., 2000). Moreover, many, but not all, lakes in Minnesota record decreasing mercury accumulation in sediments following periods of peak accumulation in the 1960's and 1970's (see section 3.4 below). Spatial and temporal changes of mercury in precipitation are apparently very complicated on a regional scale, but the twelve years of continuous precipitation records in NE Minnesota suggest mercury concentrations may have been increasing, or at least not decreasing.

3.2 Lakes and Streams

A search of the US EPA's "STORET" database (EPA, 2002) provided mercury concentrations for 84 lakes in NE Minnesota, nearly all of which were sampled in 1991 and referenced to the MPCA. Samples were collected just beneath the surface of the lake using clean techniques and analyzed by a sensitive technique (cold vapor atomic fluorescence spectroscopy or "CVAFS") (Swain, E., MPCA, personal communication). Additional data for approximately 80 lakes sampled in 1996 were found in a recent report by Glass et al. (1999). Samples for this study were also collected using clean techniques, but from a 1-meter depth and then analyzed using a less sensitive, but widely accepted method (Cold vapor atomic absorption spectroscopy or "CVAAS"). Finally, data from an additional 80 lakes in NE Minnesota sampled in 1988 were found in Sorenson et al. (1989, 1990). Hg data from the lakes where samples were analyzed by the more sensitive CVAFS technique are shown in Figure 2. As can be seen, considerable variability exists for lake mercury, but the values are all less than that of average precipitation.

The most striking difference between the different datasets is they had greatly different ranges in mercury concentration. The STORET database values range up to 10 ng/L while mercury concentrations reported by Glass et al. (1999) are all less than 3 ng/L for a similar set of lakes. Hg concentrations in the Sorenson et al. study are similar to the 1991 STORET data, ranging in concentration up to 7 ng/L. In that study, a significant positive correlation was found for total Hg and total organic carbon (TOC), consistent with the general consensus that most mercury in lakes is associated with organic carbon. Similar correlations and concentration ranges have been reported elsewhere, including

New York (Driscoll et al., 1995) and Wisconsin (Watras et al., 1995). The reason for the different ranges in mercury concentrations is unknown.

There is a near complete absence of readily available information on mercury concentrations in lake waters for the region extending southeastward from the iron range to the Lake Superior shoreline. Some indication of mercury levels in that area can also be found in stream data. The EPA's STORET database reported mercury concentration data for six rivers draining into Lake Superior from NE, Minnesota. Samples were collected on monthly intervals during the summer of 1996 (Figure 3). Again, the data were collected and analyzed using clean techniques by the MPCA. Concentrations generally varied from 2 to 6 ng/L (reported as total mercury recovered), but two concentrations reported for the Knife River were well above these values (9 and 14). With the exception of those two higher values the concentrations are similar to those reported for area lakes in the STORET database.

Abundant stream data has also been reported from the Marcel research station near Grand Rapids, MN, for an area characterized by upland forests and bogs (Kolka et al., 1999). Mercury concentrations up to 50 ng/L were reported for streams draining bogs during periods of high flow, and most of this mercury was bound to particulate organic carbon. Because this form of carbon settles from the water column under calmer conditions, streams often have much higher total mercury concentrations than lakes.

3.3 Fish

Fish have many orders of magnitude higher mercury concentrations than the waters they grow in. The concentration varies among lakes and species, but within a single lake, mercury in fish tends to increase with size and age. In order to compare mercury concentrations in fish from different lakes, therefore, it is important to compare similar sized fish of the same species.

Two of the largest databases on Minnesota fish mercury levels were generated by Glass et al (1999) and Sorenson et al. (1990). Jeremiason (2002) combined these data with other fish mercury data collected by Minnesota state agencies through 1999 and produced an extensive database of normalized fish-mercury concentrations which allowed assessment of spatial and temporal trends. Empirical relationships were developed to estimate mercury concentrations for a 55 cm northern pike (NP₅₅) using mercury concentrations measured in northern pike of other sizes or fish of other species (Sorenson et al., 1990; Jeremiason, 2002).

Recent NP₅₅ fish mercury concentrations in NE Minnesota range up to approximately 2 µg/g (Fig. 4). For comparison, recent fish consumption advisories began to take effect at a level of 0.038 µg/g Hg, but fish containing 2 µg/g Hg were to be consumed no more than once per month by most people, and no more than approximately once per year by young children or by women of child-bearing age (Table 2). These levels are subject to change as more becomes known about health effects of Hg consumption.

A number of lakes in extreme northern Minnesota have relatively high fish-mercury concentrations, as do some located near the iron range but none of these appear to be close to the highest level for fish consumption advisories. The highest Np₅₅ mercury

concentrations near the iron range are in Wynne (Np55= 0.60 and 1.11 µg/g in 1996), Esquagama (0.64 and 0.66 µg/g in 1999), Colby (0.82 µg/g in 2000), and Embarrass Lakes (0.64 and 0.94 µg/g in 1999) located on or just south of the eastern side of the Mesabi Iron Range. These values are for a standard sized northern pike of 55 cm as reported by Jeremiason (2002 and personal communication).

Determining whether fish mercury is increasing or decreasing in Minnesota is a difficult task owing to the slow rate at which changes take place and to a relatively sparse dataset for lakes that have had fish measured at least twice over a long period of time. Statewide, Jeremiason (2002) found 114 lakes that had fish mercury data available for 1995 and later and which had been sampled at least 5 years previous. Of these, fish-Hg declined in 63 cases, increased in 22 cases, and stayed approximately the same for 29 lakes, suggesting that fish mercury levels, on average, may be declining. On the other hand, when measurements of fish mercury were grouped according to year, regardless of which lakes were sampled, a regression of fish mercury levels versus time resulted in no significant change with time. Likely, it is too early to tell whether state, national, and international efforts to reduce mercury emissions are having a direct impact on the mercury levels in Minnesota fish.

3.4 Historical Deposition

Much of the mercury delivered to a lake in the form of precipitation or runoff is deposited and stored permanently in sediments. Thus, coring and age-dating the sediments from a lake make it possible to evaluate historical changes in Hg deposition and to evaluate changing mercury transport characteristics for a watershed. Two recent lake sediment studies conducted on lakes in Minnesota include Swain et al. (1992) and Engstrom and Swain (1997), who reported age-dated sediment data from 12 lakes including four in NE Minnesota, and Engstrom et al. (1999) who report data from 50 Minnesota lakes including 20 in NE Minnesota. Actual mercury accumulation rates are highly variable owing to geographic and geologic differences, but cores consistently record increasing mercury accumulation rates since pre-industrial times (Figure 5). These increases can be attributed to increased erosion of soils within disturbed watersheds and to increased global and regional atmospheric deposition.

Not surprisingly, the greatest changes in Hg fluxes to lakes in Minnesota occur in the east central part of the state, near Minneapolis and St. Paul, where watersheds are most likely to have been disturbed and where lakes are located closest to a number of potential mercury sources (e.g., coal combustion, waste incinerators). As is the case for Hg data from lakes and rivers, however, few cores exist to evaluate changes in Hg accumulation rates on or near the iron range. A group of lakes cored near Grand Rapids is well west, and generally “upwind” of the areas currently being mined. Another group of lakes cored near Silver Bay, meanwhile, are relatively close to Northshore mining’s processing plant, but as will be discussed later, the ore processed at this site has much lower mercury concentration than ore mined by the other companies on the iron range.

4. Iron Mining in Minnesota

4.1 Introduction

The iron mining industry in Minnesota began with discoveries of iron ore in the late 1860's, production on the Vermilion Range in the 1880's, and rapid expansion to the Mesabi Iron Range in the early 1890's and Cuyuna Range in the early 1910's (Emmons and Grout, 1943; Hatcher, 1950; Engesser and Niles, 1997). The so called "natural ore" mined during the first half of the 20th century was high grade, having been oxidized and enriched by extensive weathering near the surface. Most ore of this type required little or no processing before being shipped through the Great Lakes to iron and steel manufacturing facilities in the eastern United States, but beneficiation increased gradually during the early part of the 1900's. From 1906 to 1936, the percentage of ore beneficiated increased in five-year periods as follows: 0.6, 8.9, 9.6, 18.3, 36.3, 35, and 42.0, and increasing to over 50% by 1940 (Emmons and Grout, 1943). Most beneficiation in these early periods involved simple crushing, screening, washing, and drying of the ore, all processes that likely did not result in release of significant mercury.

Mining and beneficiation of taconite, a very hard, relatively low grade, siliceous ore that forms the basis of the iron industry in Minnesota today, began in 1949 after years of research determined how best to utilize this large resource. While the "natural" direct-shipping ore has been largely mined out, it is estimated that there may still be over 200 years of taconite reserves remaining in Minnesota (Ojakangas and Matsch, 1982). Taconite production involves the fine grinding and magnetic separation of ore, and importantly, the conversion of concentrate into pellets. Because, as will be discussed later, Hg release is intrinsically linked to the firing of pellets, airborne Hg emissions from Minnesota's iron industry effectively began with taconite processing in 1949.

In 2003, at the beginning of the year, six active taconite companies remained, all of which mine on the Mesabi Iron Range (Fig. 6). These include, from west to east: National Steel Pellet Company (NSPC) near Keewatin (recently purchased by US-Steel and called Keewatin Taconite Minnesota Ore Operations), Hibbing Taconite (HibTac) near Hibbing, US Steel-Minntac (Minntac), near Mountain Iron, EVTAC Mining (EVTAC), near Eveleth, Ispat-Inland Mining Company (IIMC), near Virginia, and, finally, Northshore (NS) Mining, with mines located near Babbitt and ore processing facility located on the shore of Lake Superior in Silver Bay. EVTAC was in a temporary shut down mode at the time this document was prepared. LTV-Steel Mining company (LTVSMC) is a Cliffs-Erie facility that mined and processed ore on the iron range until 2001, at a site near Hoyt Lakes and located between IIMC and Northshore. In more recent developments on the iron range, newer Direct-Reduction-Iron (DRI) and pig-iron nugget technologies are being considered for mining operations near Nashwauk (the former Butler mine site) and Northshore, respectively. These and similar products, with their higher iron contents, may represent the future of mining production in Minnesota and elsewhere in the world.

4.2 Taconite and the Biwabik Iron Formation

All taconite companies in Minnesota currently mine ore from the Biwabik Iron Formation. This formation is similar to banded iron formations found throughout the world, all of which were deposited primarily from 1.8 to 2.6 billion years ago, during a period of time when oxygen in the Earth's atmosphere was becoming more available. This oxidation led to world-wide deposition of iron from seawater. In Minnesota, near-surface exposure of the Biwabik Iron Formation strikes east-northeast in a continuous band extending approximately 120 miles from a location southeast of Grand Rapids to a point near Babbitt, where it is truncated by the Duluth Complex. Sandwiched between the Pokegama Quartzite below and the Virginia Formation above, the Biwabik Iron Formation ranges in thickness from about 200 to 750 feet, and dips approximate 5 to 15° towards the southeast (Morey, 1972). The relatively planar feature is interrupted by several major structural features, the most prominent of which is the so-called "Virginia Horn". This feature, consisting of the Virginia syncline and parallel Eveleth anticline, produces, in surface expression, a seven-mile curved offset of the formation between EVTAC and Minntac (Fig. 6). The crest of the Eveleth anticline, traced using geophysical methods, plunges into the subsurface in a southwesterly direction (Morey, 1972).

Taconite is a sedimentary rock, probably deposited originally as a mixture of $\text{Fe}(\text{OH})_3$ and varying proportions of other common material (silica, carbonates, organic carbon, iron-sulfides, clays) and converted to present form during diagenesis or low-grade regional metamorphism (Morey, 1972; Perry et al., 1983; Thode and Goodwin, 1983; Bauer et al., 1985). Eastern sections of the formation have been subjected to thermal metamorphism, especially near Babbitt, where intense heating occurred during intrusion of the Duluth Complex (Morey, 1972; Ojakangas and Matsch, 1982). Although the metamorphism in that area has not seriously affected the major element geochemistry, it has certainly affected mineralogy, as the primary low temperature silicate phases (minnesotaite, greenalite, stilpnomelane, and chamosite) have been replaced by a compositionally equivalent high temperature phase assemblage (quartz, amphibole, magnetite, pyroxene, fayalite, cummingtonite). By comparison, isotopic data on minerals recovered from the western side of the district suggest peak "metamorphic" temperatures were less than 100 or 150° C (Morey, 1972).

5. Mercury Release from Taconite Processing

There are two potential primary sources of mercury during taconite processing: (1) mercury released from processing of the ore and (2) mercury released from fuels used when processing the ore. Of these two categories, the first is clearly dominant and will be discussed in detail below. Coal is the primary source of mercury in fuels used by mining companies, but only Minntac and EVTAC commonly use coal to fire their pellets. However, it takes only about 20 to 30 lbs of coal to fire one long ton of pellets (Engesser, personal communication), so for this to be a significant source of mercury compared to pellets, the concentration would have to be much higher. Mercury concentrations for coal used by mining companies (included in the appendix) are similar to those in the unprocessed ore, so this report focuses on mercury distribution in the ore.

5.1 Mercury in Taconite Ore

Mercury concentrations in the Biwabik Iron Formation reflect concentrations of the element deposited with the original sediment as modified by diagenetic, metamorphic, and weathering processes. Despite a significant amount of chemical work on the Biwabik Iron Formation, relatively few data exist which can be used to confidently quantify the abundance and distribution of mercury in taconite ore. Data from the most extensive study of mercury distributions in the Biwabik Iron Formation (Morey and Lively, 1999) cannot be easily reconciled with data from numerous other studies conducted on samples collected from mineral processing facilities (Appendix I). Both datasets are described here along with possible explanations for observed discrepancies.

Morey and Lively (1999) reported mercury concentrations for approximately 200 samples collected from drill core at three sites south of the present area of mining. Collectively, the samples had a mean value of 79.2 ng/g (ppb) for mercury concentration, but the ore zone had slightly lower mercury concentrations near Biwabik (56.82 ppb, n=13) and Keewatin (70.9 ppb, n=12) and slightly higher near Buhl (90.2 ppb, n=10). Replicate analyses were made at three other laboratories. Results from Frontier Geosciences, Seattle Washington, who employed a more sensitive technique (cold-vapor atomic fluorescence spectrometry, or CVAFS with detection limit of approximately 0.5 ppb) than that used in the rest of the study (cold vapor atomic *absorption* spectroscopy or CVAAS; detection limit about 5 to 10 ppb) proved to be systematically lower than values obtained from the other three labs, sometimes by more than 70%. Morey and Lively noted this, as well as the large differences between concentrations they measured and those reported for materials presently being mined (Engesser and Niles, 1997). Further research and appropriate iron formation standards were needed to explain the disparate results.

As a result of limitations in the above data, mercury measurements from a large number of studies conducted at taconite processing facilities (Engesser and Niles, 1997; Engesser, 1998a,b, 2000; Monson et al., 2000; Lapakko and Jakel, 2000; Benner, 2001a,b) were compiled (Appendix 1) and summarized in Table 3 and Figure 7. Mercury concentrations from freshly crushed, non-beneficiated ore samples ranged in value from 0.6 up to a maximum of only 32 ppb, well below the values reported by Morey and Lively (including the subset of samples analyzed by Frontier Geosciences). Moreover, there is general agreement among data collected in various studies, providing evidence of a relatively clear trend in mercury concentration for unprocessed ore. Mercury concentration at the west end of the district is only about 20 ppb but increases gradually eastward to a maximum of 32 ppb and then decreases gradually again to a value less than 1 ppb in thermally metamorphosed ore at Northshore. A similar geographic trend is present in the Morey and Lively data, but their reported concentrations are elevated over those at the present mining surface by approximately 50 ppb.

Engesser and Niles (1997) noted an association between mercury and sulfur concentrations at Minntac and LTVSMC's facilities. This introduces the possibility that higher Hg concentrations reported by Morey and Lively (1999) for deep drill core might be related to the presence of higher sulfur concentrations than near the surface. Thus, mercury concentrations from Morey and Lively (1999) were plotted as a function of

sulfur concentration (for the same core intervals as reported earlier by Morey, 1992) and compared to similar data for presently mined ore from Engesser and Niles (1997) (Fig. 8). The mercury values reported by Morey and Lively (1999) are clearly elevated for samples having similar sulfur as reported by Engesser and Niles (1997), indicating that the high mercury cannot be attributed to increased sulfur.

Another possibility to consider is that of Hg contamination for the dataset reporting the higher numbers: Morey and Lively (1999). In this regard, the potential for significant mercury contamination in powdered samples is demonstrated by the results of mercury adsorption experiments conducted by Fang (1978). This study found that 2.0 gram powdered mineralogical samples adsorbed up to 5 µg of Hg from air containing 79.2 µg/m³ Hg(0) in a few weeks. Furthermore, mercury was still rapidly adsorbing to the solids when the experiments ended and the adsorbed mercury was not later released when samples were placed into a vacuum. These data indicate that powders exposed to air for long periods of time could experience increasing concentrations of mercury.

Of relevance to the contamination question, in this case, is the fact that samples collected by Morey and Lively (1999) were garnered from a previous study (Pfleider et al., 1968), and had been stored as powders for approximately 30 years prior to being analyzed for mercury. Although Hg concentrations typical for indoor air are three orders of magnitude less than those used in Fang's experiments (Carpi and Chen, 2001), the powders analyzed by Morey and Lively were exposed for a much longer period of time than that used in the experiments. Furthermore, because the samples analyzed by Morey and Lively (1999) were stored in cardboard boxes, rather than in air-tight glass or plastic containers, temporary exposure to air containing high levels of Hg from common products, such as latex paints, pesticides, fungicides, or detergents or from the accidental breakage of Hg-containing devices (fluorescent lights, tilt switches, thermostats), cannot be ruled out. Because of the possibility of mercury adsorption from air, data from Morey and Lively (1999) are not considered further in the present study. Distribution of mercury in ores deep in the subsurface may well be similar to those in ore presently being mined today (See Fig. 7), but the possibility of elevated Hg values should not be ignored. Conducting further analyses on fresh core samples could potentially clarify this issue.

Perhaps more significant than bulk mercury concentration, especially regarding atmospheric emissions, is the concentration of mercury in magnetite, the primary ore mineral from which iron is derived. During processing, magnetite is magnetically separated from other solids in the composite ore and the resulting concentrate is rolled with other minor components (fluxing agents, binders) into balls (greenballs). It is the magnetite dominated "greenballs" that are introduced into the indurating furnaces where mercury emissions are generated. Mercury concentrations in "concentrate" and "greenball" were found to be statistically similar to each other, and these concentrations were almost always lower than concentrations in the bulk ore, especially at IIMC and Minntac (Fig. 7). Because magnetite is, by far and away, the dominant mineral in concentrate and greenballs, these concentrations probably represent mercury associated with magnetite in the primary ore. Correspondingly, tailings from Minntac, EVTAC, and IIMC have the highest mercury of all samples collected (averages of 39.5, 40.2, and 35.4 ppb, respectively), consistent with the idea that selective removal of low-Hg magnetite from the bulk ore results in selective enrichment of mercury in tailings (Fig. 7).

Engesser and Niles (1997) noted mercury concentrations at some facilities (Minntac and LTVSMC) were closely associated to sulfur concentrations. In these cases, a relatively small percentage of the mercury in the primary ore was routed into the pelletizing plant. Apparently, pyrite, which is non-magnetic and is sent, therefore, to tailings basins, provides an important host for the trace mercury at Minntac and LTVSMC. Little correlation was observed by Engesser and Niles between mercury and sulfur at HibTac and Northshore mining, however, and the result was that a higher percentage of the mercury was routed with concentrate into the pellet plant at those facilities. Nevertheless, significant mercury was routed into the tailings basins when no correlation with sulfur could be made. This indicates that, in addition to magnetite and sulfide minerals, some mercury resides in other phases in the ore matrix (non-magnetic iron oxides, silicates, and carbonates). No attempt has been made to establish the distribution of mercury among these other minerals.

Other sample types were collected at some of the processing sites, including dust from scrubbers and various filtrates. Values are reported in the appendix, but have little application to the present study, which focused on the broader question of mercury distribution in the Biwabik Iron Formation and release during mineral processing.

5.2 Tailings Basins

Fine tailings generated at most mining operations are slurried with processing waters and pumped into large man-made impoundments called tailings basins. There, the tailings settle from the discharged waters, and most of the water is recycled to the plant for reuse. IIMC previously disposed tailings in a tailings basin but in December, 2001, began disposing tailings and recycling water in an abandoned open-pit mine located near their processing facility (Minorca Pit). An important question for all of these operations relates to the effect of tailings disposal on mercury distributions in NE Minnesota.

As discussed previously, and shown in Figure 7, the concentration of mercury in tailings is usually greater than the concentration of mercury in the concentrate. Furthermore, the mass of tailings released to tailings basins is typically two to three times the mass of pellets generated (Engesser and Niles, 1997, Skillings, 2001). Thus, the total mass of mercury that reports to tailings basins must be larger than that which is emitted to the atmosphere. At least two pathways need to be considered for release of mercury from tailings basins: (1) transport out of the system in waters that leak or are intentionally discharged from the tailings basin and (2) direct release of mercury to the atmosphere as Hg(0).

Averaged mercury concentrations for tailings basin waters are compiled in Table 4. The averaged values range from 1.23 to 3.48 ng/L for basin waters and from 0.72 to 2.44 ng/L for seeps. These values are similar to those measured in lakes and streams (see above), but much less than that of recent precipitation (most recently about 12 ng/L). In fact, calculations suggest that a relatively large fraction of the mercury present in tailings basins waters may have been supplied by precipitation. According to Cl concentration data available in Berndt et al. (1999), it can be shown that water discharged to tailings basin at NSPC from 1996 to 1999 was diluted by an average 21% by precipitation falling on the basin. Assuming 21% dilution in 1999 when mercury concentrations were measured in NSPC's basin, and considering that precipitation contained an average 12

ng/L in the area for that year, precipitation alone would account for at least 2.54 ng/L mercury. Although this calculation does not take into account mercury added by dry deposition or further concentration of dissolved elements by evaporation, the average value of dissolved mercury in NSPC's tailings basin was 2.52 ng/L. Thus, wet and dry precipitation alone, combined with evaporative increase, more than accounts for all of the dissolved mercury in tailings basins. This is not particularly surprising, as the same can be said for many lakes in NE Minnesota. However, it does demonstrate that tailings are not a significant source of dissolved mercury.

Minntac performed a study to evaluate mercury released during seepage from tailings basins (US Steel, 2000) (See Table 4 and Appendix 1). Water within the tailings basin had an average of 1.1 ng/L Hg during the study in 1999. This is considerably less than the single value of 4.23 ng/L reported by Engesser and Niles (1997) for a sample collected in 1996. Seepage during 1999 averaged only 0.73 ng/L, indicating that reaction of water with tailings does not result in an increase in the concentration of mercury and may, in fact, result in a decrease in concentration. The mercury concentrations in waters seeping from the tailings basins were found to be lower than concentrations in surrounding surface waters. Similar findings were made at Northshore by Monson et al. (2000) who determined that the net effect of discharge from the tailings basin was to decrease the concentration of mercury in the river receiving the discharge.

It is important to note that just because an industry discharges water with a concentration that is less than that of the water it takes in does not mean it will meet water quality standards. Currently, two major water quality standards are in effect, depending on which drainage basin the discharge is located. Tailings basins for Northshore, Evtac, and the former LTVSMC as well as Ispat-Inland's Minorca Pit disposal facility are all located in the Lake Superior watershed, which currently has a Class 2B mercury discharge standard for mercury of 1.3 ng/L. The current standard for IIMC's inactive tailings basin and for Hibbtac, National, and Minntac, all of which have tailings basins located in the Red and Mississippi River watersheds, is 6.9 ng/L. Currently, it appears that all of the mining companies meet the higher water quality standard, but water in some tailings basins and seepages are above the stricter 1.3 ng/L water standard.

Finally, volatilization is an important natural process in forested watersheds where it has been estimated that a mean value of 32 ug of mercury is volatilized (or deposited and revolatilized) per square meter per year (Grigal, 2002). Thus, a screening study was conducted to evaluate mercury volatilization rates from taconite tailings basins (Swain, 2002). Rates of measurement for the 20 minute intervals used in the study, which was conducted in the fall under daylight conditions, cannot be extrapolated for the year nor can it be applied to nighttime conditions. Nevertheless, the data suggest that some mercury does appear to volatilize from unvegetated tailings, and that this amount is different for different tailings. Rates of volatilization ranged from 24 to 44 ng/m²/hr at Evtac, 29 to 34 ng/m²/hr at Minntac, and were indistinguishable from the control at Northshore. No volatilization was detected above ponded water in the tailings basin. If tailings volatilized approximately 30 ng/m²/hr for a full year, then a total of 263 ug m⁻² a⁻¹ would be released. Although this is greater than that estimated for natural background volatilization (32 ug m⁻² a⁻¹), extrapolating this rate to a tailings basin having a size of

300 hectares (Evtac's tailings basin area), results in an estimate of approximately 0.8 kg a^{-1} . This would represent a relatively small addition to EVTAC's mercury emissions, which as will be shown in the next section, already commonly exceed 50 kg a^{-1} . Moreover, closure of tailings basins involves a revegetation of the surface. It is unknown, what effect this will have on mercury volatilization.

5.3 Stack Emissions

Engesser and Niles (1997) realized that emission rates (per ton of ore produced) increased in a westward direction across the Mesabi Iron Range. This trend can be attributed to a combination of effects including low levels of mercury in ore from the eastern side of the district and sulfide enhanced mercury levels in the center of the district. Highest mercury emission rates were found on the western side of the district, where the mercury was neither diminished by metamorphism nor sequestered into easily separable sulfide minerals. However, because stack emissions weren't measured directly by Engesser and Niles (1997), they had to be estimated by difference and by assuming a value for scrubber efficiency for mercury removal from stack effluents. Stack emissions have since been measured directly at all taconite facilities on the Iron Range and results have been compiled and summarized by Jiang et al. (2000). In general, these stack emission tests have corroborated and better refined the trends noticed by Engesser and Niles.

An important parameter for estimating emissions from taconite companies is the "emission factor", which represents the mass of mercury released divided by the mass of pellets produced. Probably the most convenient unit for presenting emission factors is kg mercury per million long tons of pellets produced ($\text{kg}/10^6\text{LT}$). Not only are taconite production figures often provided in units of long tons, but one long ton of solid containing 1 ppb (or $1 \mu\text{g}/\text{kg}$) mercury is capable of releasing a numerically similar amount of mercury in kg (1.016 kg) ($1 \text{ ppb} = 1.016 \text{ kg}/10^6\text{LT}$).

Emission factors reported by Jiang et al. (2000) are listed in Table 5 and plotted with concentration data as a function of distance from Northshore's mine in Figure 7, a procedure first adopted by Engesser and Niles (1997). Several important observations can be made, including: (1) emission factors and concentrations are extremely low on the eastern side of the district (Northshore); (2) mercury in the concentrate and/or green ball generally increases westward across the district; and (3) despite its location at the center of the district, EVTAC's emissions and mercury levels in concentrate or greenball are closer to values characteristic of facilities on the western side of the district (NSPC and HibTac).

It is generally recognized that low mercury in Northshore ore is related to past geological processes, whereby mercury was expelled during intense heating associated with emplacement of the Duluth Complex. A possibility to account for the other noted trends might involve heating to lesser degrees due to (1) increasing distance from the Duluth Complex or (2) range-wide differences in the peak depth of burial. Indeed, ore across the district exhibits increasing metamorphism and recrystallization from west to east on the iron range (Morey, 1972). Increasing recrystallization of magnetite may have systematically released a greater percentage of mercury from the magnetite.

The portion of the Biwabik Iron Formation currently mined by EVTAC, is somewhat unique compared to other parts of the formation because it is positioned at the top of the Eveleth anticline. Whether this ultimately affected the depth to which this section of the formation was buried, or whether it affected the degree to which it was affected by igneous intrusion during emplacement of the Duluth Complex, is beyond the scope of this paper. Indeed, with the collection of more data, it may turn out that the higher mercury at EVTAC relative to other nearby operations is a statistical anomaly, or may be rooted in differences in mineral processing technique (IIMC and Minntac use flotation to refine their concentrate, while EVTAC does not).

Whatever the cause of the mercury emission trends, it is generally assumed that the mercury that is emitted from stacks is predominantly in elemental form. Although this has not been verified at every plant, a study conducted at HibTac indicated that an average of 93.3% of mercury emissions were in Hg(0) form, with almost all of the remainder emitted as Hg(II) (Jiang et al., 2000). Very little particulate mercury was emitted. The form of mercury is important for determining where the element is deposited. Elemental mercury can be transported in the atmosphere for years prior to being deposited, while particulate and charged forms may be deposited much more locally.

5.3.1 Historical stack emissions

Because mining companies keep relatively complete production records, and because mercury stack emissions are believed to be directly proportional to mining production, it is possible to estimate historical mercury release levels for taconite mining operations since the industry began. Such records may have value for evaluating links between mercury emissions and local mercury accumulation.

Records of annual concentrate production were compiled for Minnesota taconite mining companies through 1995 by Engesser and Niles (1997). Similar data were also obtained for the present study for the years 1995 through 2003 (estimated) in Skillings (2003). All concentrate production data were converted to pellet production numbers using recent conversion factors (pellet mass/ concentrate mass) and are plotted as a function of time for individual mining companies in Figure 9. Resulting values were multiplied by emission factors from 1995 to 1997 reported by Jiang et al. (2000) (Table 5) to provide estimates of annual atmospheric emission since initiation of taconite mining in 1949. Prior to this, nearly all ore and concentrate shipped to ports in the eastern US were mined and processed using techniques involving little or no intense heating. While emission factors may have varied through time, data presented in Figure 7 suggest that emissions are closely linked to concentration of mercury in the concentrate, which appears to be closely related to geographic location of the mine. Thus, by multiplying geographically appropriate emission factors by production figures for individual taconite plants, reasonable estimates of historical atmospheric emissions can be achieved (Appendix 3).

No mercury data are available for the former Butler site, so production at this site was assumed to have an emission factor similar to that of NSPC, the nearest site. LTVSMC operated the Dunka mine, which, with its location immediately adjacent to the

Duluth Complex, probably contained very little mercury. IIMC, meanwhile, extracted ore from the Minorca pit, located near Virginia Minnesota (on the Virginia anticline) between Minntac and EVTAC until 1993, but has since switched to its current mine location, between EVTAC and LTVSMC. These and other possible geographic shifts in mining operations were not taken into account here.

With the exception of a few subtle differences, the historical patterns of mercury emission (Fig. 9) are, of course, similar to historical patterns of taconite production (Fig. 10). Because early pellet production was concentrated on the east end of the range (Northshore and LTVSMC) where emission factors are low, initial mercury emission rates were also initially low relative to production. In contrast, a peak in taconite production that occurred from 1979 to 1981 involved the opening and rapid expansion of companies on the western side of the district, where mercury emission factors are comparatively high. This westward shift in mining led to an acceleration of mercury emissions relative to production. Annual mercury emissions exceeded the 100 kg mark in 1967, leveled off at approximately 200 kg at the end of the 1970's, and then abruptly and temporarily increased to the 350 kg range from 1978 through 1981. Following that, annual mercury emissions abruptly decreased to 200 kg but then increased gradually through the 1980's and eventually leveled off between 300 and 350 kg/year through the 1990's.

The closing of LTVSMC, and production decreases in 2001 at other companies, have resulted in a correspondingly large reduction in mercury emissions from taconite companies in recent years. If other companies on the western side of the district had picked up the reduced pellet production caused by LTVSMC's closing, then emissions would likely have increased slightly owing to the higher emission factors for those companies. However, LTVSMC's closing does not appear to have bolstered pellet production at other Minnesota companies. Hg emissions have, therefore, decreased substantially.

Based on the most recent precipitation records available from the National Atmospheric Deposition Program (NADP, 2002; Vermette et al., 1995), the annual atmospheric Hg release from taconite mining is approximately two to three times that deposited from precipitation over an area the size of St. Louis County in NE Minnesota. Thus, if only a fraction of the Hg released by taconite processing were deposited locally, it should be recorded in Hg distributions in sediments from nearby lakes. Because of the global nature of mercury dispersal, a link between mercury emission and deposition is not always established in an area. This appears also to be the case here, where an assessment of Minnesota lake sediment data by Engstrom et al. (1999) found that mercury accumulation rates for lakes closest to the iron range (e.g., near Silver Bay) did not obviously reflect taconite emission data. This is consistent with the notion that most Hg emissions from taconite companies are airborne and not deposited locally. Because Hg(0) released to the atmosphere remains in the atmosphere for a long period of time before being precipitated (approximately half will be oxidized and precipitated out every 1 to 3.5 yrs; Mason et al., 1994, Pirrone et al., 2000), mercury in Minnesota taconite stack emissions is probably dispersed globally before being deposited.

5.3.2 Comparison to other sources

While the amount of mercury released to the atmosphere by taconite mining companies is second (in Minnesota) to that of power companies, the total is relatively small compared to emissions from other national and international sources (Table 6). An estimated maximum of 388 kg of mercury was released by the taconite industry in 1979. Mercury emission data from other iron producers world-wide was not readily available, except for an estimate of 4360 kg released annually by the steel and iron industry in the Mediterranean area of Europe (Pirrone et al., 2001). The later number, which may include mercury released by scrap iron processing (a considerable source due to presence of mercury bearing equipment in scrapped automobiles), is similar to Minnesota's entire 1990 annual output of 5,305 kg, but much higher than Minnesota's entire annual output in 2000, estimated at 1720 kg (MPCA, 2002).

US emissions were estimated to be approximately 144,000 kg in 1994 to 1995 (EPA, 1997), less than half of North America's estimated 1992 total of 301,000 kg. Global anthropogenic emissions are approximately 1,450,000 to 2,000,000 kg, which is less than half of the estimated total global Hg emissions to the atmosphere (anthropogenic + natural) of 5,000,000 kg/yr (EPA, 1997). Based on these figures, taconite emissions represent about 0.24% of the US anthropogenic releases in 1994/1995, 0.1% of North American anthropogenic Hg emissions to the atmosphere, and about 0.007 % of total global emissions (anthropogenic plus natural).

5.3.2 Potential control

As part of a statewide plan to reach emission reduction goals, many taconite companies have entered into voluntary mercury reduction agreements with the MPCA. Although significant steps have indeed been taken by all of the taconite companies to eliminate and/or control use of Hg bearing chemicals and equipment (IMA, 2001), these sources were not even considered in the MPCA's prior assessment of taconite companies, which focused exclusively on mercury in stack emissions (Engesser and Niles, 1997; Jiang et al, 2000). As discussed above, mercury present in taconite occurs as a trace element, and cannot be eliminated by simply using a different fuel source or by eliminating mercury-bearing components from material to be combusted.

A recent study by the Coleraine Minerals Research Laboratory (CMRL-NRRI), University of Minnesota, suggested that some emission control may be obtained by modifying the current practice of recycling the dust from wet scrubbers into the indurating furnaces (Benner, 2001b). Benner (2001b) found that this dust contains extremely high mercury concentrations, and if this material, particularly the fine fraction, was channeled into the waste stream (rather than recycled to the indurator), mercury emissions could be cut. Estimated savings in terms of mercury release to the environment are shown in Table 7, but it is important to note that these estimates are based on one time measurements, and are based on many assumptions.

For example, Berndt et al. (2003) showed that considerable mercury is present in dissolved form in plant scrubber systems and that with passage of time this mercury adsorbs to the suspended dust. The concentration of mercury measured on dust, therefore, can vary considerably depending on when the filtration was performed.

Because most previous studies collected samples at the plant and processed them at the laboratory (after adsorption occurred), the amount of mercury adsorbed to dust has probably been previously over-estimated.

In addition, Berndt et al. (2003) found that the amount of mercury captured in wet scrubbers depends greatly on whether the processing facility is producing fluxed or acid pellets. At Minntac, mercury capture by the plant scrubber system was nearly an order of magnitude greater when the company was producing acid pellets compared to fluxed pellets. Thus, the combined mercury captured by scrubber waters and suspended solids can, at times, represent a significant fraction of the mercury released during taconite processing. This is a continuing area of active research on the iron range (see section 7 below) and may potentially lead to re-estimates of taconite plant emissions (taking into account increased capture during acid pellet production) and/or more cost effective means to eliminate at least some of the mercury from taconite air emissions.

6. Cost and Benefit

Cost-benefit analyses attempt to weigh the costs of implementing control measures against the benefit in terms of environmental and public health. Technologies to reduce mercury emission from taconite processing have only recently begun to be addressed (see above) so the cost of reducing mercury from emissions is unknown.

Hagen et al. (1999) surveyed and interviewed Minnesota residents to help arrive at a dollar figure for the value of reduced mercury deposition to Minnesotans. They first educated a large number of Minnesota residents on mercury issues, and then asked how much they would be willing to pay for mercury reductions. 2500 Minnesotans were surveyed and an additional 250 were interviewed. For a 12% reduction in mercury deposition, the surveyed households were willing to pay an average of \$118.91 per year while those interviewed were willing to pay an average \$198.03 per year. The lower figure translates to a value of approximately 212 million dollars for Minnesota as a whole.

Lutter and Irwin (2002) reviewed literature on health effects and mercury exposure and estimated the cost per child of controlling mercury from coal burning power plants. They claim that “approximately 6000 children in the US would experience improvements in specific, narrow measures of neurological performance (between 13 and 22 percent of a standard deviation)” upon the complete elimination of mercury from fish. The authors noted that even sharp cuts to the power industry would not achieve such improvements owing to the fact that many other industries and activities emit mercury to the atmosphere. Using what the authors claimed to be conservative choices, the cost of implementing mercury control on coal-fired power plants (\$1.1 billion to \$1.7 billion per year) amounted to spending approximately \$10,000.00 per affected US child. The authors indicated, however, that the positive effects of reduced mercury exposure would likely be hard to measure or detect.

The taconite industry emits much less mercury to the atmosphere than coal-fired power plants and, in fact, it is clear from data in Table 6 that cutting even 100% of the mercury from taconite stack emissions would have only a small impact on the national and world inventories of mercury. If mercury in the environment is to be controlled, it

must involve a global effort, placing emphasis on curtailing emissions from the largest sources that are easiest to control. Mercury control methods and costs are only beginning to be established for taconite processing companies, but even if an economic means is found to remove this source of mercury, continued efforts will be needed to reduce mercury emissions elsewhere to have significant impact on mercury deposited in Minnesota.

7. Additional Studies

Studies are being conducted at Coleraine Minerals Research Laboratory and by the Department of Natural Resources which could help to improve our understanding of mercury concentrations and distribution in taconite ore and also help to control emissions. Funding from the Minerals Coordinating Committee (MCC), the Iron Ore Cooperative Research Fund (IOCR), and the Permanent University Trust Fund (PUTF) is being used for conducting mercury balance studies around the concentrators at EVTAC, IIMC, Minntac, and HibTac. Results from this study are due out shortly. CMRL is also studying removal of elemental mercury from flue gases using a copper-coated magnetite injection process at Clay-Boswell, using funding from PUTF and the Federal Government Economic Development Administration (EDA).

Other studies are being conducted by the Minnesota Department of Natural Resources to evaluate mercury exchange between water and solids in processing lines and to determine if minor processing changes can lower mercury emissions to the atmosphere. This work is funded partially by IOCR, Environmental Cooperative Research (ECR), and the Great Lakes Nation Program Office (GLNPO-EPA). The idea is to maximize mercury oxidation in processing lines, eliminate recycling of oxidized mercury captured by plant scrubbers (to the induration furnace), and to ensure permanent disposal of the mercury in tailings basins. A secondary objective is to better evaluate the relative sources of mercury in tailings basin water (precipitation?). These studies are expected to take two years, with start times ranging from July to October, 2003.

8. Summary

This study summarizes and presents available data on mercury distributions in and around the taconite mining region in Minnesota. Twelve years of deposition records suggest a stable to increasing trend of mercury concentration in precipitation and mercury deposition, while sediment records indicate a recent decreasing trend for selected localities within NE Minnesota. Two large datasets on the total mercury concentration in lakes yield conflicting results, one suggesting much higher concentrations than the other. Neither dataset provide concentration of mercury for lakes in a large region extending from the iron range southeastward to Lake Superior. Fish mercury is decreasing in more lakes than it is increasing in, but the overall record is insufficient to prove a declining trend in fish mercury levels. Recent research reveals that the mercury in precipitation that falls directly on a lake is much more available for methylation than that which falls on (and runs off from) land.

Mercury is present in small quantities in primary taconite ore, ranging in concentrations from approximately 20 ppb on the western edge of the active area, up to approximate 32 ppb at Minntac, near the center of the mining district, and decreasing again eastward to approximately 1 ppb in Northshore's ore. Mercury in Northshore's ore is low owing to effects of extensive thermal metamorphism that occurred during intrusion of the Duluth Complex. Data from a study on drill core suggest that mercury concentration increases by approximately 50 ppb down-dip in the iron formation, however, the possibility that samples analyzed in that study were affected by Hg-adsorption from air makes this an unresolved issue.

Waters existing in and being discharged or seeping from tailings basins have mercury concentrations similar to and possibly lower than rivers and lakes in the region and much lower than local precipitation. Class 2b water quality standards for total mercury in NE Minnesota are 6.9 ng/L for waters discharged into the Red and Mississippi River Drainage basins and 1.3 ng/L total mercury for waters discharged into the Lake Superior basin. All tailings basin waters and seeps have concentrations less than the higher standard, and a few have concentrations that are below the much stricter Lake Superior basin standard. No mercury appears to be volatilized from tailings basin ponds, but small amounts are volatilized from the tailings themselves.

The primary source of mercury from taconite mining are stack emissions. The amount of mercury released per kg of pellets produced is a plant-specific quantity related more to the distribution of mercury within the primary ore than to bulk concentration in the ore, itself. Mercury release to the atmosphere increases westward across the range from a value less than 1.0 kg per million long tons at the eastern edge of the mined area to about 15 to 17 kg per million long tons on the western side of the district. The exception to this trend is EVTAC, located in the center of the district at the top of a prominent geologic feature (the Eveleth anticline). This company releases mercury at a rate similar to taconite producers located on the western side of the district. The notion that most mercury emitted is in elemental form, Hg(0), has been tested and confirmed by stack emission measurements at HibTac. Most mercury emitted in this form would be dispersed worldwide.

Present day emission factors were combined with past production records to estimate annual Hg release since taconite mining began in NE Minnesota (1949). Results suggest that atmospheric Hg emissions exceeded 100 kg/yr in the late 1960s, and have ranged between approximately 200 and 350 kg/yr ever since, with a peak occurring from 1979 to 1981, corresponding to a peak in taconite pellet production. Taconite emissions represent about 0.24% of the US anthropogenic releases (1994-1995), 0.1% of North American anthropogenic Hg emissions to the atmosphere, and about 0.007% of estimated total annual global emissions (anthropogenic plus natural). Thus, although taconite processing is a sufficiently large industry that it is one of the biggest emitters of mercury in the state of Minnesota and to the Lake Superior Basin, it is not so large as to significantly impact national and international mercury atmospheric budgets. Current efforts to reduce mercury emissions from taconite processing reflect Minnesota's desire and commitment to reach state-wide reduction goals as a part of national and international cooperative efforts to reduce mercury in the environment.

9. References

- Bauer, M. E., Hayes, J. M., Studley, S. A., and Walter, M. R. (1985) Millimeter-scale variations of stable isotope abundances in carbonates from banded iron-formations in the Hammersly Group of Western Australia. *Econ. Geol.* 80, 270-282.
- Benner, B. R. (2001a) Preparation of mercury standards from taconite. Coleraine Minerals Research Laboratory Report # TR-01-16. 10 pages plus appendices.
- Benner, B. R. (2001b) Mercury removal from induration off gas by wet scrubbers. Coleraine Minerals Research Laboratory Draft Report. 18 pages plus appendices.
- Benoit, J. M., Gilmour, C. C., Mason, R. P., and Heyes, A. (1999) Sulfide controls on mercury speciation and bioavailability to methylating bacteria in sediment pore waters. *Env. Sci. Technol.* 33, 951-957.
- Berndt, M. E. (2002) Mercury and Mining in Minnesota. Minerals Coordinating Committee Year One Status Report. Minnesota Department of Natural Resources Report. 57 pages.
- Berndt, M. E., Engesser, J., and Johnson, A. (2003) On the distribution of mercury in taconite plant scrubber systems. Minnesota Department of Natural Resources Report. 30 pages.
- Berndt, M. E., Lapakko, K. and Jakel, E. M. (1999) In-Pit Disposal of Taconite Tailings: Geochemistry. Minnesota Department of Natural Resources Report. 77 pages plus appendices.
- Carpi, A. and Chen, Y. (2001) Gaseous elemental mercury as an indoor air pollutant. *Environ. Sci. Tech.* 35, 4170-4173.
- Driscoll, C. T., Blette, V., Yan, C., Schofield, C. L., Munson, R., and Holsapple, J. (1995) The role of dissolved organic carbon in the chemistry and bioavailability of mercury in remote Adirondack lakes. *Water, Air, Soil Pollut.*, 80, 499-508.
- Emmons, W. H., and Grout, F. F. (1943) Mineral Resources of Minnesota. Minnesota Geological Survey Bulletin, V. 30. University of Minnesota Press, Minneapolis, MN. 147 pages.
- Engesser, J. (1998a) Mercury balance at Minntac line 7 agglomerator Sept. 3, 1997. Coleraine Minerals Research Laboratory Report. 4 pages plus tables and figures.
- Engesser, J. (1998b) Mercury balance at EVTAC. Coleraine Minerals Research Laboratory Report.

Engesser, J. (2000) National Steel Pellet Company mercury balance. NRRI-Coleraine Minerals Research Laboratory report. 11 pages plus appendices.

Engesser, J. and Niles, H. (1997) Mercury emissions from taconite pellet production. Coleraine Minerals Research Laboratory, Report to MPCA: U of M contract # 1663-187-6253. 16 pages plus tables, figures and appendices.

Engstrom, D. A. and Swain, E. (1997) Recent declines in atmospheric mercury deposition in the upper Midwest. *Environ. Sci. Technol.* 31, 960-967.

Engstrom, D. A., Thomas, K., Balogh, S., Swain, E. B., and Post, H. A. (1999) Trends in atmospheric mercury deposition across Minnesota: evidence from dated sediment cores from 50 Minnesota lakes. Final Report to the Legislative Commission on Minnesota Resources. 32 pages plus tables and figures.

EPA (1997) Mercury Study Report to Congress. EPA Report # EPA-452/R-97-003.

EPA (2002) <http://www.epa.gov/storet/> (Last accessed 6/27/02)

Fang, S. C. (1978) Sorption and transformation of mercury vapor by dry soil. *Env. Sci. Technology*, 12, 285-288.

Fitzgerald, W. F., Engstrom, D. R., Mason, R. P., and Nator, E. A. (1998) The case for atmospheric mercury contamination in remote areas. *Env. Sci. Technol.* 32, 1-7.

Fleck, J. A. (1999) Mercury transport through northern forested watersheds. M. S. Thesis. University of Minnesota, St. Paul, MN.

Gilmour, C., Henry, E., and Mitchell, R. (1992) Sulfate stimulation of mercury methylation in freshwater sediments. *Env. Sci. Tech.* 26, 2281-2287.

Glass, G. E. and Sorenson, J. A. (1999) Six Year Trend (1990-1995) of Wet Mercury Deposition in the Upper Midwest, USA. *Env. Sci. Technol.* 33, 3303-3312.

Glass, G. E., Sorenson, J. A., and Rapp, G. R., Jr. (1999) Mercury deposition and lake quality trends. Final Report for project I-11/I-15. (Note: Copy was dated 2/15/1999 and marked for peer review, acquired from LCMR)

Glass, G. E., Sorenson, J. A., Schmidt, K. W., Rapp, G. R., Jr., Yap, D., and Fraser, D. (1991) *Water, Air, Soil Pollut.* 56, 235-2249.

Grigal, D. F. (2002) Inputs and outputs of mercury from terrestrial watersheds: a review. *Environ. Rev.* 10, 1-39.

Hagen, D. A., Vincent, J. W., and Welle, P. G. (1999) Economic benefits of reducing mercury deposition in Minnesota. Report prepared on behalf of the Minnesota Pollution Control Agency and Legislative Commission on Minnesota Resources. 63 pages.

Hatcher, H (1950) A century of iron and men, Bobbs -Merrill, NY, 295 p.

Hintelmann, H., Harris, R., Heyes, A., Hurley, J. P., Kelly, C. A., Krabbenhoft, D. P., Lindberg, S., Rudd, J. W. M., Scott, K. J., and St. Louis, V. L. (2002) Reactivity and mobility of new and old mercury deposition in a boreal forest ecosystem during the first year of the METAALICUS study. *Env. Sci. Tech.* 36, 5034-5040.

IMA (2001) Taconite industry voluntary mercury reduction progress report submitted to the MPCA pursuant to individual mine voluntary mercury reduction agreements. Iron Mining Association Report. 20 pages.

Jeremiason, J. (2002) Mercury in Minnesota Fish, 1998-1999: Temporal and Spatial Trends. Minnesota Pollution Control Agency Technical Report. 13 pages plus appendices.

Jiang, H., Arkly, S., and Wickman, T (2000) Mercury emissions from taconite concentrate pellets- stack testing results from facilities in Minnesota. Presented at USEPA conference "Assessing and managing mercury from historic and current mining activities". San Francisco, November 28-30, 18 pages.

Kelley, C. A., Rudd, J. W. M., and Holoka, M. H. (2003) Effect of pH on mercury uptake by an aquatic bacterium: Implications for Hg cycling. *Env. Sci. Tech.*, 37, 2941-2946.

Krabbenhoft, D. and Goodrich-Mahoney (2003) Mercury transformations on land and water (METAALACUS) Valuing Externalities Workshop Proceedings. NETL Publications, February 20-21, 2003. Last accessed on 5/27/03 at <http://www.netl.doe.gov/publications/proceedings/03/valuing-ext/v-ext03.html>.

Kolka, R. K., Grigal, D. F., Verry, E. S., and Nater, E. A. (1999) Mercury and organic carbon relationships in streams draining forested upland/peatland watersheds. *J. Env. Qual.*, 28, 766-775.

Lapakko, K. and Jakel, E. (2000) Detailed analysis of potential environmental impacts of taconite tailings disposal in the Minorca Pit on water quality in the Missabe Mountain Pit. Final Report. Minnesota Department of Natural Resources. 83 pages plus appendices.

Lutter, R., and Irwin, E. (2002) Mercury in the environment: a volatile problem. *Environment*. 44, #9, 24-40.

Mason, R. P., Fitzgerald, W. F., and Morel, F. M. M. (1994) The biogeochemical cycling of elemental mercury: Anthropogenic influences. *Geochim. Cosmochim. Acta*, 58, 3191-3198.

Monson, B. A., Pruchnofski, G. J., Wagner, D., Osmundson, M. and Twaroski, C. J. (2000) Estimated mercury emissions, deposition and tailings basin discharge from a proposed expansion of a taconite processing facility in northeastern Minnesota. Air and Waste Mgmt Assoc. Annual Conference, June 18-21. 17 pages.

Morey, G. B. (1972) Mesabi Range. In: *Geology of Minnesota: A centennial volume*. P.K. Sims and G. B. Morey (eds), Minnesota Geological Survey, St. Paul, MN. 204-217.

Morey, G. B. (1992) Chemical composition of the eastern Biwabik Iron Formation (Early Proterozoic), Mesabi range, Minnesota. *Economic Geology*, 87, 1649-1658.

Morey, G. B. and Lively, R. S. (1999) Background levels of mercury and arsenic in paleoproterozoic rocks of the Mesabi Iron Range, Northern Minnesota. *Minnesota Geological Survey Informational Circular 43*. 14 p.

MPCA (2001) Interim MPCA Mercury Policy (Revised staff draft, July 2001). MPCA report, 40 p.

MPCA (2002) Mercury Reduction Program: Progress report to the Minnesota Legislature. 23 p.

NADP (2002) National Atmospheric Deposition Program, <http://nadp.sws.uiuc.edu/mdn>

Ojakangas, R. W. and Matsch, C. L. (1982) *Minnesota's Geology*. University of Minnesota Press, Minneapolis. 255 p.

Pacyna, J. M. and Pacyna, P. E. (1996) Global emissions of mercury to the atmosphere. Emission from anthropogenic sources. A report for the Arctic monitoring and assessment programme (AMAP), Oslo, June 1996)

Perry, E. C., Jr., Tan, F. C., and Morey, G. B. (1973) Geology and stable isotope geochemistry of the Biwabik iron-formations. *Econ. Geol.* 68, 1110-1125.

Pfleider, E. P., Morey, G. B., and Bleifuss, R. L. (1968) Mesabi deep drilling project: Progress report No. 1. In: *Proceedings of the 29th Annual Mining Symposium, and 41st Annual Meeting of American Institute of Mining and Metallurgical Engineers, Minnesota Section, Duluth, University of Minnesota*, p 59-92.

Pirrone, N., Allegrini, I., Keeler, G. J., Nriagu, J. O., Rossman, R., and Robbins, J. A. (1998) Historical atmospheric mercury emissions and deposition in North America compared to mercury accumulations in sedimentary records. *Atmospheric Environment*, 32, 929-940.

Pirrone, N., Costa, P., Pacyna, J. M., and Ferrara, R. (2001) Mercury emissions to the atmosphere from natural and anthropogenic sources in the Mediterranean region. *Atmospheric Environment*, 35, 2997-3006.

Pirrone, N., Keeler, G. J., and Nriagu, J. O. (1996) Regional differences in worldwide emissions of mercury to the atmosphere. *Atmospheric Environment*. 30, 2981-2987.

Rae, D. Impacts of mercury reductions in Minnesota. Report to the Minnesota Pollution Control Agency. St. Paul, MN, 1997.

Skillings (2003) Skillings Minnesota Mining Directory 2003, Westmorelandflint Publishing, Duluth, MN. 181 pages.

Skyllberg, U., Xia, K., Bloom, P. R., Nater, E. A., and Bleam, W. F. (2000) Binding of Mercury(II) to Reduced Sulfur in Soil Organic Matter Along Upland-Peat Transects. *J. Environ. Qual.*, 29, 855-865.

Slemr, F., Brunke, E.-G., Ebinghaus, R., Temme, C., Munthe, J., Wangberg, I., Schroeder, W., Steffen, A., and Berg, T. (2003) Worldwide trend of atmospheric mercury since 1977, *Geophys. Res. Lett.*, 30, 1516-1519.

Sorenson, J. A., Glass, G. E., and Schmidt, K. W. (1994) Regional patterns of wet mercury deposition. *Env. Sci. Tech.* 28, 2025-2032.

Sorenson, J. A., Glass, G. E., Schmidt, K. W., Huber, J. K., and Rapp, G. R., Jr. (1990) Airborne Mercury Deposition and Watershed Characteristics in Relation to Mercury Concentrations in Water, Sediments, Plankton, and Fish of Eighty Northern Minnesota Lakes. *Environ. Sci. Technol.*, 24, 1716-1727.

Sorenson, J. A., Glass, G. E., Schmidt, K. W., Huber, J. K., and Rapp, G. R., Jr. (1989) Airborne Mercury Deposition and Watershed Characteristics in Relation to Mercury Concentrations in Water, Sediments, Plankton, and Fish of Eighty Northern Minnesota Lakes. Chapter 5 in Swain, E. B., Editor., *Assessment of Mercury Contamination in Selected Minnesota Lakes*, Report to the Legislative Commission on Minnesota Resources., MPCA, 36 pages plus appendices.

Swain, E. B. (2002) Mercury volatilization associated with taconite tailings: a screening study. Report to Minnesota Department of Natural Resources.

Swain, E. B., Engstrom, D. A., Brigham, M. E., Henning, T. A., and Brezonik, P. L. (1992) Increasing rates of atmospheric mercury deposition in mid-continental North America. *Science*, 257, 784-787.

Swain, E. D., and Helwig, D. (1989) Mercury in fish from northeastern Minnesota lakes: historical trends, environmental correlates, and potential sources. *J. Minn. Acad. Sci.* 55: 103-109.

Thode, H. G. and Goodwin, A. M. (1983) Further sulfur and carbon isotope studies of late Archaen Iron-Formations of the Canadian Shield and the rise of sulfate reducing bacteria. *Precambrian Research*, 20, 337-356.

US Steel (2000) USS-Minntac low level mercury testing at various water locations. Data submitted to MPCA in association with permit # MN0057207.

US-EPA (2001) Mercury Maps: A quantitative spatial link between air-deposition and fish tissue. Peer Reviewed Final Report. EPA-823-R-01-009. 21 pages + appendices and review comments.

Vermette, S., Lindberg, S., and Bloom, N. (1995) Field Tests for a Regional Mercury Deposition Network - Sampling Design and Preliminary Test Results. *Atmospheric Environment*, 29, 1247-1251.

Watras, C. J., Morrison, K. A., and Back, R. C. (1996) Mass balance studies of mercury and methyl mercury in small temperate/boreal lakes of the Northern Hemisphere. In *Global and regional mercury cycles: sources, fluxes, and mass balances*. W. Baeyens, R. Ebinghaus, and O. Vasiliev, Eds., NATO-ASI-series, V. 21, Kluwer Academic Publishers, Dordrecht, The Netherlands, 329-358.

Watras, C. J., Morrison, K. A., Hudson, R. J. M., Frost, T. M. and Kratz, T. K. (2000) Decreasing mercury in Northern Wisconsin: Temporal Patterns in Bulk Precipitation and a Precipitation-Dominated Lake. *Environ. Sci. Technol.* 34, 4051-4057.

10. Tables

Table 1. Estimates of Minnesota mercury emissions for 1990, 1995, and 2000 (MPCA, 2002).

Source	1990		1995		2000	
	Kg	%	Kg	%	Kg	%
Coal-fired power plants	711	13.4	737	34.6	820	47.7
Latex Paint	1725	32.5	0	0.0	0	0.0
Municipal Solid Waste Combustion	820	15.4	288	13.5	73	4.3
Household Waste Incineration	302	5.7	123	5.8	82	4.8
Taconite Processing	333	6.3	352	16.5	342	19.9
Volatilization from Solid Waste	592	11.1	196	9.2	131	7.6
Medical Waste Combustion	234	4.4	16	0.8	4	0.2
All Other	594	11.2	419	19.7	268	15.6
Total	5312	100.0	2131	100.0	1719	100.0

Table 2. Fish consumption advisories for Minnesota. Advisories vary by group depending on susceptibility and how often fish are eaten (e.g., only on vacation, only during fishing season, or year round. “Susceptible groups” in this table refers to young children and women of child-bearing age. Data on Minnesota lakes is from Jeremiason (2002). Fish advisories are subject to change as more data become available. Up-to-date fish advisories can be found on the internet at <http://www.health.state.mn.us/divs/eh/fish/safeeating/safeeating.html>.

Mercury Level	Advisory	% MN Lakes (1998/1999)
0-0.038	Unlimited consumption for all groups	2.4
0.038-0.16	Vacation: Unlimited Seasonal: Unlimited for most, 2 meals/wk for susceptible groups Annual: 2 meals/wk for most, 1 meal/wk for susceptible groups	35.2
0.16-0.65	Vacation: Unlimited for most, 1 meal/wk for susceptible groups Seasonal: 2 meals/wk for most, 2 meals/mo for susceptible groups Annual: 1 meal/wk for most, 1 meal/mo for susceptible groups	54.1
0.65-2.8	Vacation: 1 meal/wk for most, 1 meal/year for susceptible groups Seasonal: 2 meals/mo for most, 1 meal/2 mo for suscept. groups Annual: 1 meal/mo for most, none for suscept. groups	8.1
>2.8	Vacation: 1 meal/yr for most, none for suscept. groups Seasonal: 1 meal/mo for most, none for suscept, groups Annual: do not eat	0.2

Table 3. Summarized data for Hg concentrations (ppb or ng/g) and number of samples analyzed (n) from taconite mining operations in Minnesota. Full data set is included in the appendix.

Company	Miles from Northshore	Raw ore	n	Concentrate or "greenball"	n	Tailings	n
NSPC	51	21	3	15.2	3	20.4	6
HibTac	46	24	4	16.6	7	26.0	6
Minntac	30	32	2	8.2	7	39.5	7
EVTAC ¹	29	32	0	11.4	3	40.2	3 ²
IIMC	23	27	1	7.8	1	35.4	1
LTVSMC	12	11	2	4.0	3	12.2	3
Northshore	0	0.6	3	1.1	5	1.1	8

¹ No estimated or measured value was available for raw ore from EVTAC so a value was calculated using reported values for "greenball" and tailings and assuming 31.5 % recovery rate (Skillings, 2003).

² A single sample with a high value of 130 was not included in the average.

Table 4. Averaged mercury concentrations in tailings basin waters and seeps. The full data set can be found in the appendix.

Site	Hg (Total) (ng/L)	Hg (Filtered) (ng/L)	MeHg (ng/L)
NSPC: Basin	2.52 (n=3)		
Monitoring well	2.69 (n=1)		
Hibbing Taconite: Basin	2.24 (n=1)		
US Steel (Minntac): Basin	1.72 (n=5)	0.42 (n=4)	<0.008 (n=4)
Seep	0.72 (n=3)	0.77 (n=3)	<0.016 (n=3)
EVTAC			
IIMC: Seeps and wells	2.9 (n=3)		
LTV: Basin	3.48 (n=1)		
Seep	2.44 (n=1)		
Northshore: Basin	1.23 (n=5)		

Table 5. Air emission factors for taconite production from Jiang et al. (2000). These factors have been multiplied by production figures to estimate yearly mercury emissions to air in Minnesota since taconite mining began in 1949. Hg values measured for greenball and concentrate from Table 3 are provided for direct comparison.

Company	Air Emission Factor (kg Hg/10 ⁶ LT pellet) Jiang et al (2000)	Hg (ppb) in “greenball” or concentrate Average value
National Steel Pellet Company (NSPC)	10.1	15.2
Hibbing Taconite	12.6	16.6
U.S. Steel (Minntac)	5.3	8.2
EVTAC	11.4	11.4
Inland Steel (IIMC)	5.4	7.8
LTVSMC Steel	5.1	4.0
Northshore Mining Company	1.8	1.1

Table 6: Comparison of taconite stack air emissions with emissions from other sources and regions throughout the world. It is important to note that emission records for mercury are uncertain and subject to change with increasing information. These data are presented for relative comparison purposes only.

Source	Hg Emission (kg/yr)	Reference
MN Taconite industry ¹ : peak (1979)	388	This report
1995-1997	347	Jiang et al. (2000)
2000	342	This report
Steel and Iron Industry in Mediterranean Area (1995)	4,360	Pirrone et al. (2001)
Minnesota anthropogenic 1990	5,305	MPCA (2002)
1995	2,120	MPCA (2002)
2000 (est.)	1,720	MPCA (2002)
US total anthropogenic emissions (1990)	144,000	EPA (1997)
North America anthropogenic Emissions (1992)	301,000	Pirrone et al. (1998)
Global emissions (anthropogenic)	1,450,000	Pacyna and Pacyna (1996)
	2,000,000	Pirrone et al. (1996)
Global total Hg emissions (anthropogenic + natural)	5,000,000	EPA (1997)

¹Taconite values are for air emissions only. Hg reductions relating to recycling or discontinued use of Hg-bearing equipment and chemicals are reported in IMA (2001) but have not been factored in here.

Table 7. Cost estimate figures for mercury reduction from stack emissions. Estimates were made by John Engessor (MnDNR, personal communication), using data in the listed references, extrapolated from one time results to a full year of production.

Taconite company: Reference	Recycled dust (lt/yr)	Value of recycled dust assuming \$25/lt	Hg saved (lbs/yr) by discarding rather than recycling the dust	Cost of technology (\$ per lb Hg)
EVTAC:				
Benner (2001b)	8343	\$208,575.00	15	\$13,905.00
Engesser and Niles (1998b)	27600	\$690,000.00	19	\$36,315.79
Minntac:				
Benner (2001b)	11231	\$280,775.00	2.2	\$127,625.00
Engesser (1998a)	39900	\$997,500.00	22.6	\$44,137.17

11. Figures

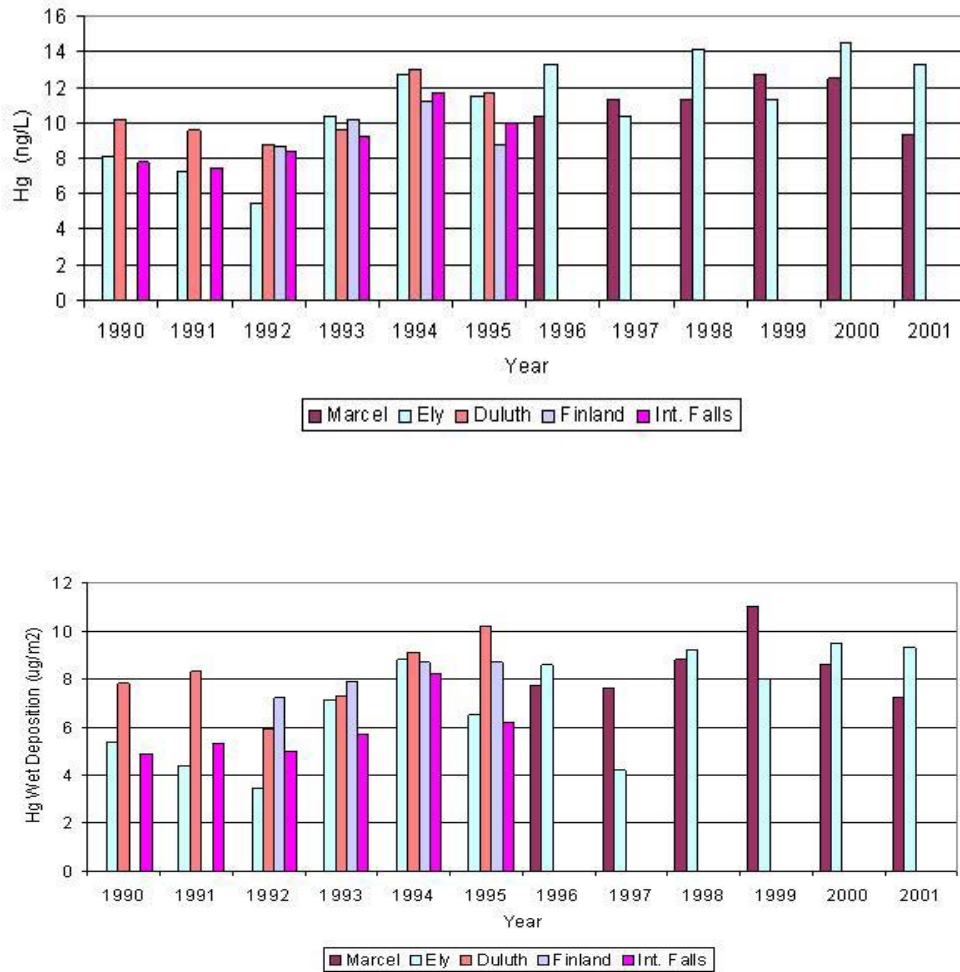


Figure 1. (A) Concentration and (B) annual deposition rate (wet) of Hg in precipitation in NE Minnesota. 1990-1995 data from Glass et al. (1999); 1996-2001 data from NADP (2002). The data appear to reveal a trend of increasing mercury concentration and mercury deposition in NE Minnesota over the last twelve years.

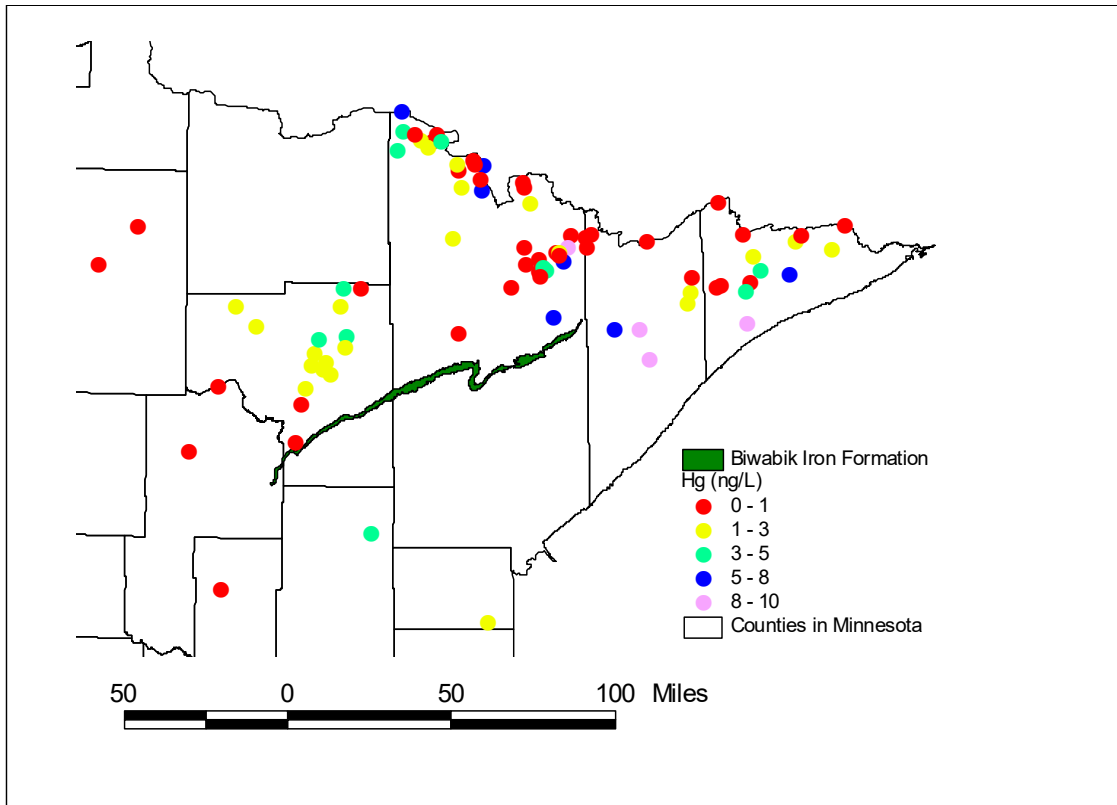


Figure 2. Total Hg in water from lakes in Northeastern Minnesota. Data are from STORET database that for this region consisted almost exclusively of 1991 values.

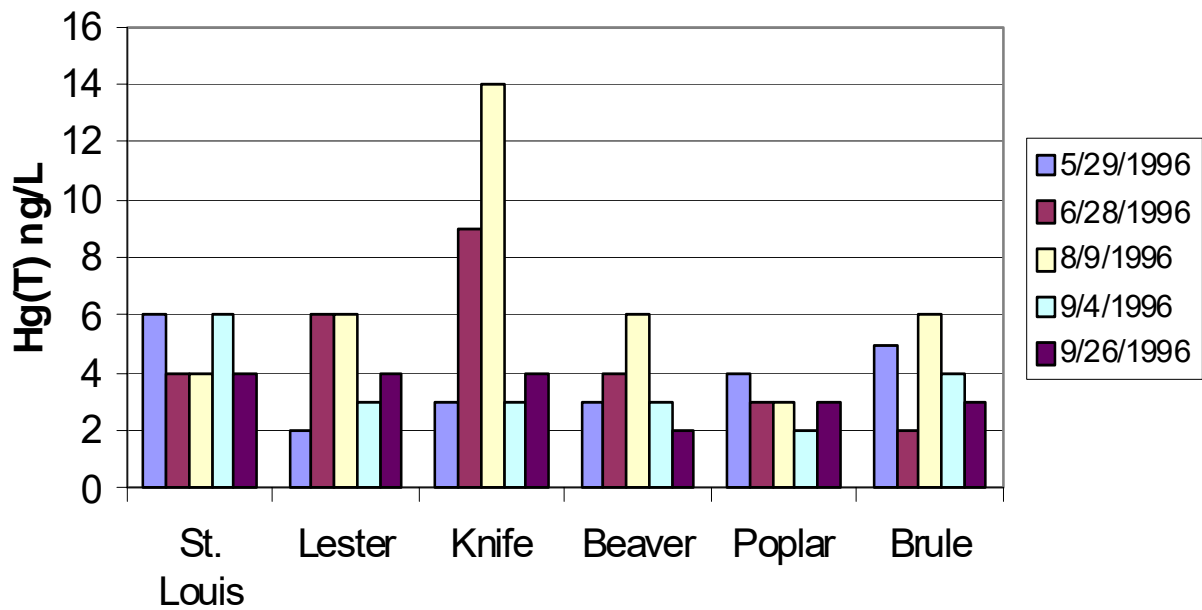


Figure 3. Mercury concentrations for rivers entering Lake Superior from NE Minnesota. Average value for all measured concentrations is 4.3 ± 2.8 . Data are from MPCA STORET database. Dates of sample collection are ± 1 day.

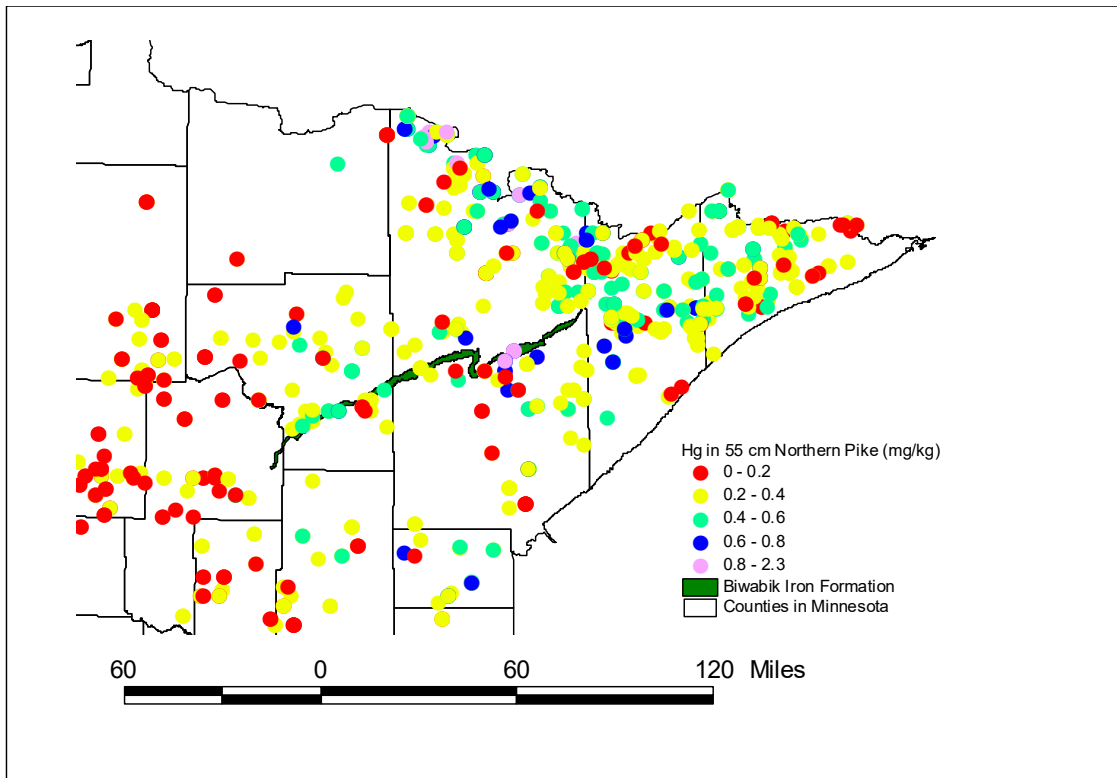


Figure 4. Mercury levels in standard sized (55 cm) Northern Pike Fish. Data are from samples collected in the 1990's as compiled by Jeremiason (2002). The database for fish mercury is considerably larger than that for lake water chemistry.

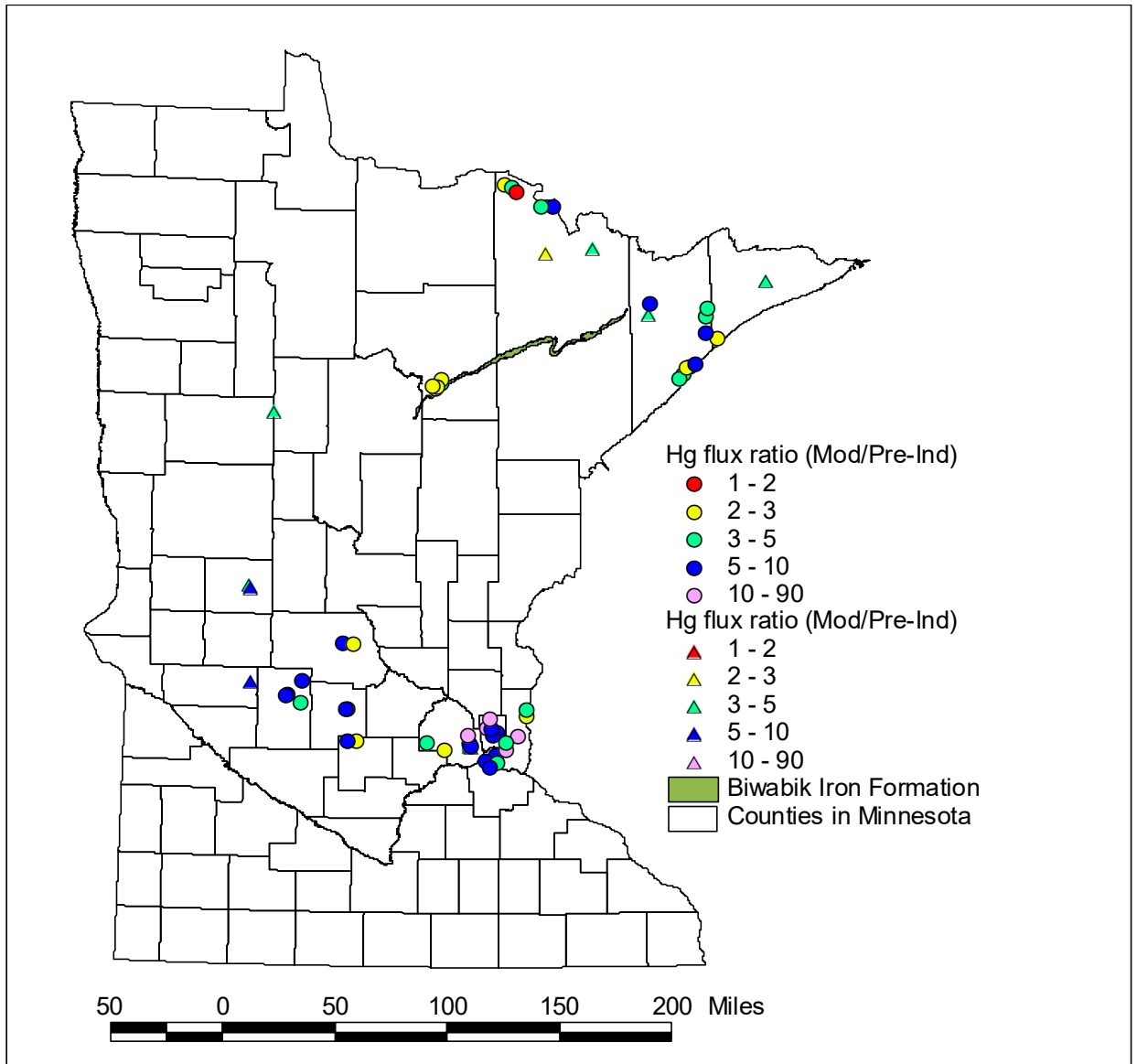


Figure 5. Ratio of Hg flux (modern versus pre-industrial) as estimated from age-dated lake sediment cores. Circles are data from Engstrom et al. (1999) and triangles are data from Engstrom and Swain (1997). As is the case for most lakes world-wide, the current mercury flux to lakes is much greater than in pre-industrial times. In Minnesota, greater increases in mercury flux have occurred near heavily populated and agricultural regions, owing most likely to increased erosion of soils. An approximate three to four-fold increase in Hg in precipitation since pre-industrial times has also caused mercury fluxes to increase to lakes in remote areas.

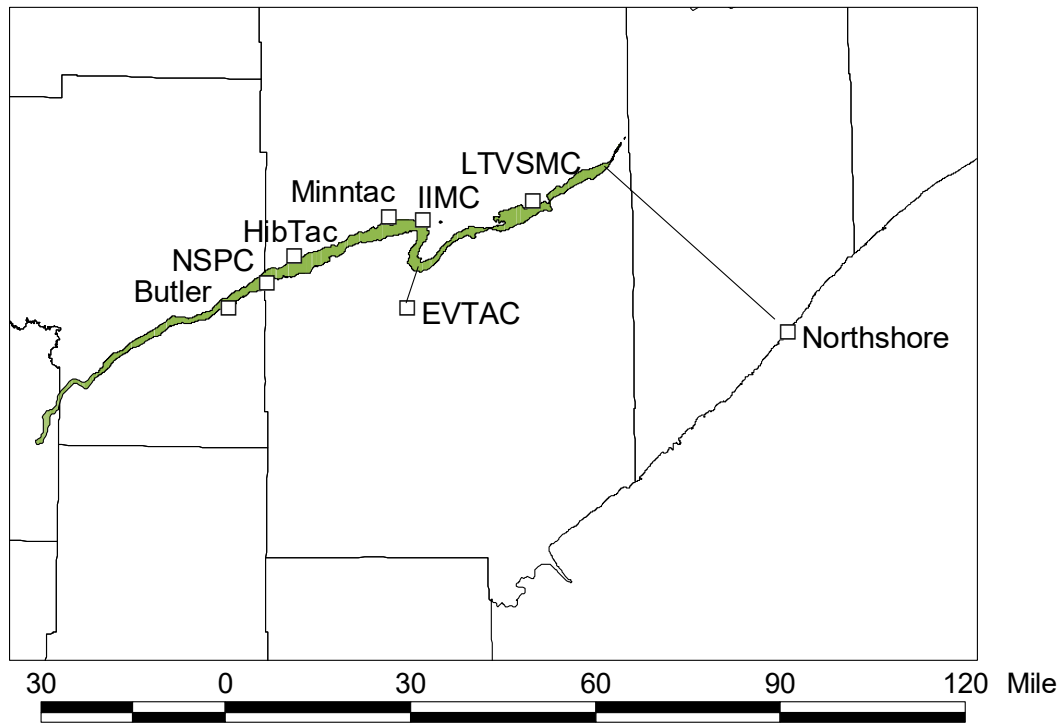


Figure 6. Location map showing location of the Mesabi Iron Range and taconite processing plants in northern Minnesota. Butler and LTVSMC plants are not currently operational, but are included for completeness. EVTAC was temporarily shut down beginning in May, 2003. The Biwabik Iron formation, which is currently the source of all iron mined in Minnesota, is shown for comparison. The formation is a broad planar feature, dipping 5 to 15 degrees to the southeast, but interrupted near the center of the district by a large fold structure known as the Virginia Horn, which is itself, composed of the Virginia syncline and Eveleth anticline. EVTAC's ore bodies are located on the Eveleth anticline.

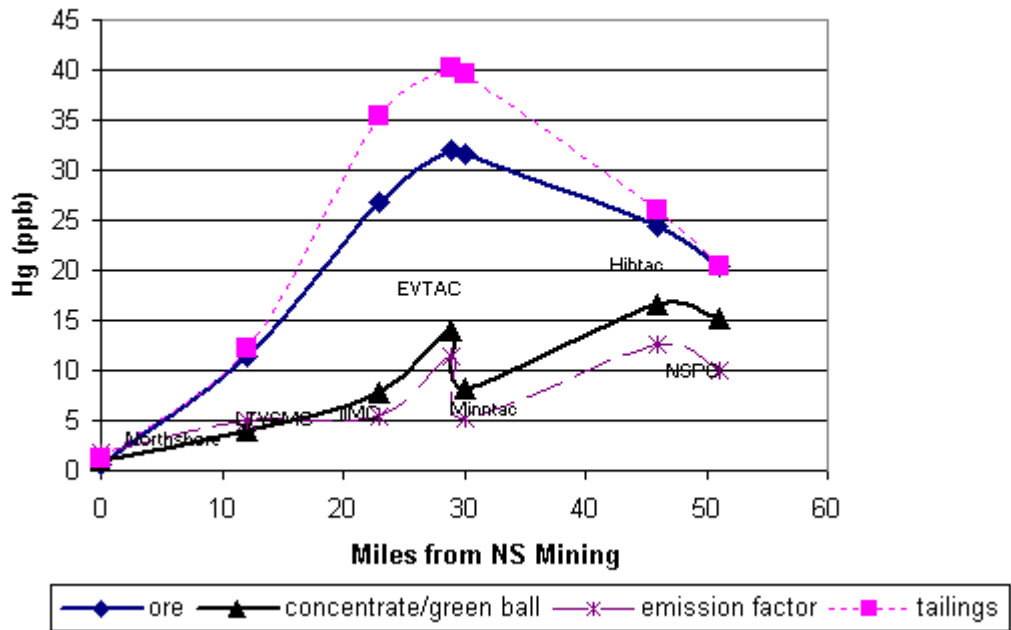


Figure 7. Mercury concentration in ore, concentrate, and tailings as a function of distance from Northshore (located on the east edge of the district). The concentration of mercury in “green ball” was considered to be within the error of measurement for mercury concentration in “concentrate” and the two were combined to provide better statistics. In addition, emission factors (in units $\text{kg}/10^6\text{LT}$) are similar to concentration units presented in ppb ($1 \text{ ppb} = 1.016 \text{ kg}/10^6\text{LT}$), so these parameters can be compared directly. No data were available for raw ore or tailings at EVTAC. The concentration of mercury approaches zero at Northshore where the ore has been thermally metamorphosed, but increases to highest values in the center of the mining district. Emissions and concentrations of mercury in the concentrate (and “greenball”) generally increase with distance from Northshore mine pits, with the exception of EVTAC.

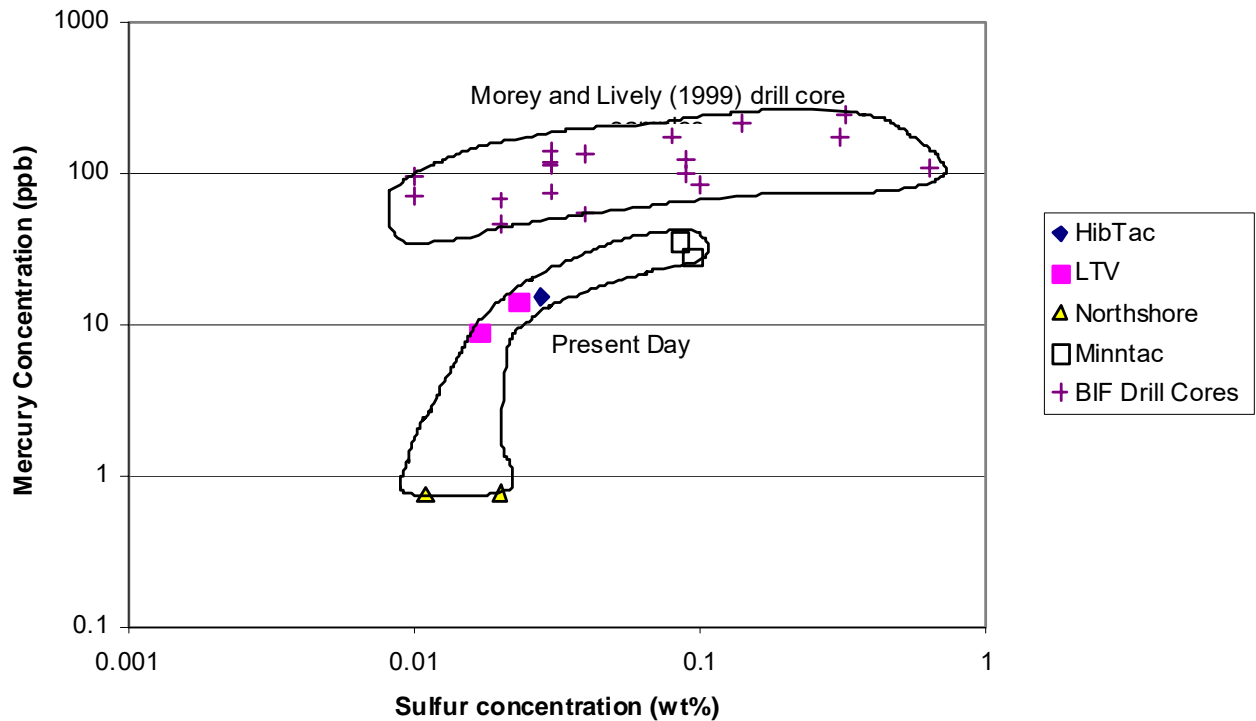


Figure 8. Mercury concentration as a function of total sulfur in Biwabik Iron Formation rocks. “Present day” samples represent ore mined at the surface and processed at the listed facility. Morey and Lively’s samples were collected from drill core locations down dip from the current mining horizon, but were powdered and stored in cardboard boxes for thirty years prior to analysis for mercury. If mercury concentration in the Biwabik Iron Formation actually does increase down dip from the current mining horizon, it is not related to increased presence of sulfur (or pyrite). Alternatively, the long-term storage of the powdered drill core samples might have led to inadvertent contamination by Hg adsorbed from air as demonstrated by experiments on other mineralogical powders by Fang (1978).

Minnesota Historical Taconite Production

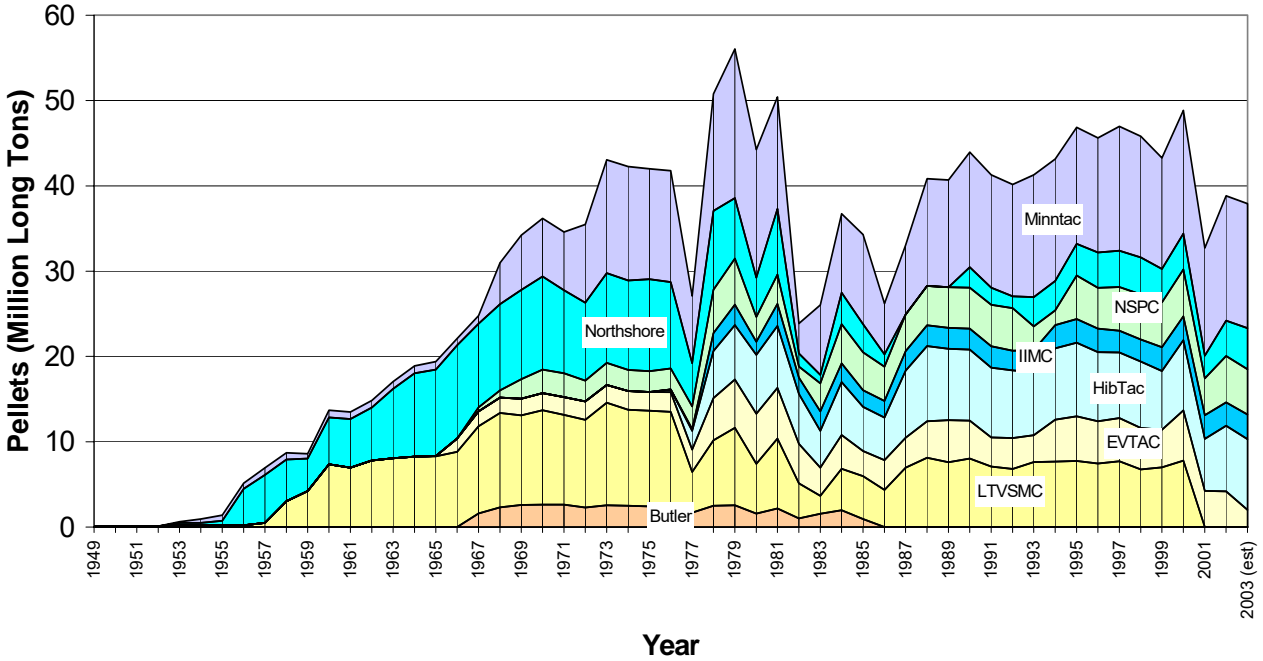


Figure 9. Taconite pellet production by Minnesota taconite companies since 1949. Production reached a peak in the late 1970's, declined sharply, in the early 1980's, but then increased gradually again, leveling off in the 1990's. After a major decline in 2001 when LTV closed, pellet production rebounded slightly in 2002 and 2003.

Estimated Hg emissions from Minnesota Taconite mining operations

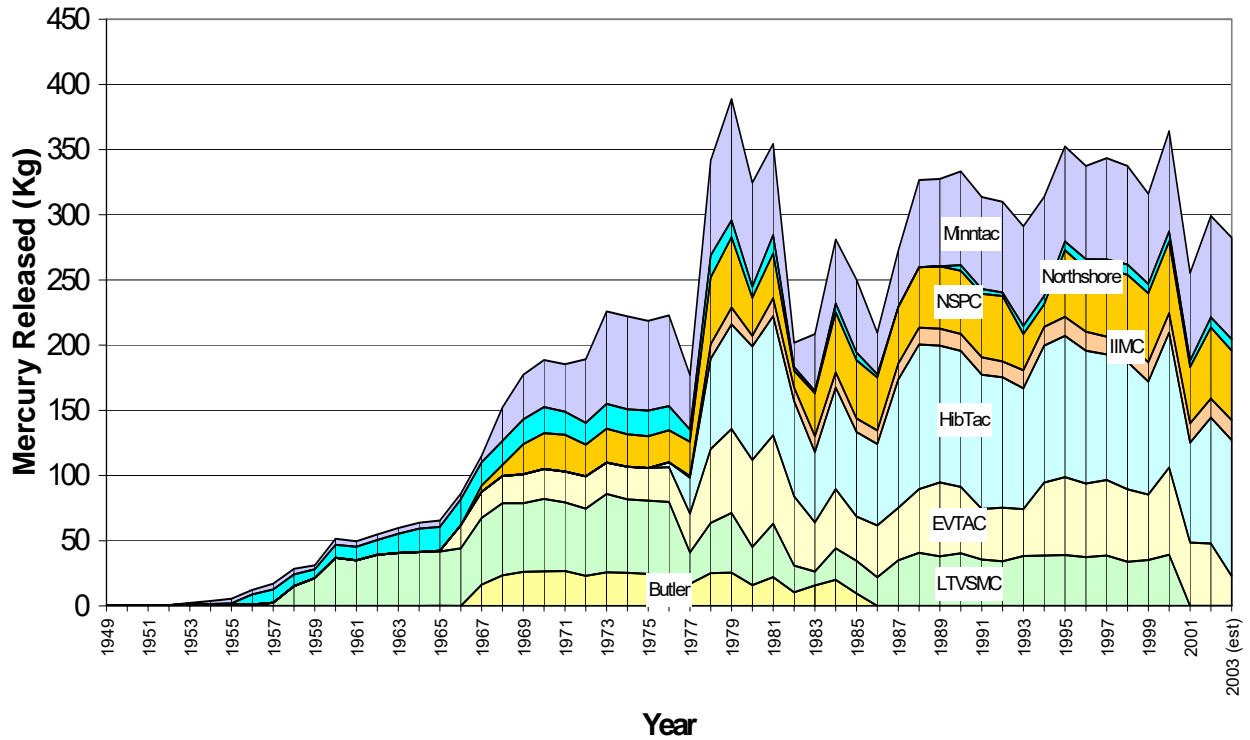


Figure 10. Estimated stack emissions of Hg from Minnesota taconite companies since 1949. Mercury emission estimates are generally similar to pellet production (Fig. 9), but with subtle differences owing to differences in mercury emission factors across the range (See Fig. 7).

Appendices

Appendix 1: Hg Concentrations at Taconite Plants

Compiled data on concentration of mercury in water and solids from taconite mining companies. Note: Many of the water samples collected from processing lines were apparently unfiltered. Water samples having high concentrations of mercury may have entrained solids containing adsorbed Hg.

Location	Sample Description	Source	Hg(T)	Date	Hg(TD)	MeHg
			ng/l (water)			ng/L
			ng/g (solid)			
NSPC	Tailings Basin Monitoring Well	Lapakko (2000)	2.69			
NSPC	Tailings Basin Clear Pool	Engesser (2000)	1.7	08/10/99		
NSPC	Tailings Return Water	Engesser (2000)	3.03			
NSPC	Tailings Return Water	Engesser (2000)	2.83			
Hibtac	Concentrator	Benner (2001b)	8.61	10/15/98		
Hibtac	Make-up	Benner (2001b)	5.37	10/15/98		
Hibtac	Scrubber Water	Benner (2001b)	11.96	10/15/98		
Hibtac	Scrubber Water In (average)	Engesser and Niles (1997)	2.81	02/04/97		
Hibtac	Scrubber Water Out (average)	Engesser and Niles (1997)	63.35	02/04/97		
Hibtac	Tailings Basin	Engesser and Niles (1997)	2.24	09/19/96		
Minntac	Scrubber Water Out	Benner (2001b)	66.5	07/18/01		
Minntac	Scrubber Water In	Engesser and Niles (1997)	2.05	02/04/97		
Minntac	Scrubber Water Out	Engesser and Niles (1997)	491.55	02/04/97		
Minntac	Tailings Basin Water	Engesser and Niles (1997)	4.23	09/19/96		
Minntac	Tailings Basin Water (TB1-2')	USX(2000)	1.54	09/22/99		
Minntac	Tailings Basin Water (TB1-2')	USX(2000)	1.06	09/22/99		
Minntac	Tailings Basin Water (TB1-2')	USX(2000)	0.99	Nov. 1999	0.41	<0.008
Minntac	Tailings Basin Water (TB1-27')	USX(2000)		Nov. 1999	0.36	<0.008

Minntac	Tailings Basin Water (TB2-2')	USX(2000)	0.76	Nov. 1999	0.41	<0.008
Minntac	Tailings Basin Water (TB1-32')	USX(2000)		Nov. 1999	0.51	<0.008
Minntac	West Seepage (O2O)	USX(2000)	1.17	Nov. 1999	1.33	<0.008
Minntac	Dark River (Cty Rd 668)	USX(2000)	1.12	Nov. 1999		0.091
Minntac	Dark River (US For Rd 271)	USX(2000)	1.66	Nov. 1999		0.056
Minntac	Sturgeon River (Cty Rd 107)	USX(2000)	2.77	Nov. 1999		0.128
Minntac	East Seepage (030)	USX(2000)	0.44	09/22/99	0.27	0.033
Minntac	East Seepage (030)	USX(2000)	0.54	Nov. 1999	0.7	<0.008
Minntac	Sandy River (Hwy 53)	USX(2000)	3.56	09/22/99		0.67
Minntac	Sandy River (Hwy 53)	USX(2000)	1.3	Nov. 1999		0.089
Minntac	Sandy River (Hwy 169)	USX(2000)	3.85	09/22/99		
Minntac	Sandy River (Hwy 169)	USX(2000)	2.19	Nov. 1999		0.162
Minntac	Pike River (Hwy 169)	USX(2000)	2.82	Nov. 1999		0.238
Minntac	Step III Scrubber	USX(2000)		Nov. 1999	3.42	0.288
Minntac	Step II Scrubber (L7)	USX(2000)		Nov. 1999	6.04	0.174
Minntac	Step III Loadout Discharge	USX(2000)		Nov. 1999	1.23	0.026
Minntac	Scrubber Water Rec. Pond	USX(2000)		Nov. 1999	0.8	<.02
Minntac	Scrubber Water Rec. Pond	USX(2000)		Nov. 1999	3.42	0.288
Minntac	Step I Ditch	USX(2000)		Nov. 1999	0.65	<.02
Minntac	Step II Ditch	USX(2000)		Nov. 1999	0.29	<.02
Minntac	Step III Ditch	USX(2000)		Nov. 1999	0.59	<.02
EVTAC	Thickener Underflow 2A	Benner (2001b)	15.5			
EVTAC	Thickener Overflow 2A	Benner (2001b)	82.2			
EVTAC	Thickener Underflow 2B	Benner (2001b)	18.1			
EVTAC	Thickener Overflow 2B	Benner (2001b)	24.35			
EVTAC	Slat Spray Water	Benner (2001b)	5.25			
EVTAC	Slat Spray Water	Engesser (1998b)	2.46	11/18/97		
EVTAC	Slat Spray Water	Engesser (1998b)	2.15	11/18/97		
EVTAC	Thickener overflow	Engesser (1998b)	199.6	11/18/97		
EVTAC	Thickener overflow	Engesser (1998b)	293.6	11/18/97		

IIMC	Process Water	Benner (2001b)	5.67	07/18/01		
IIMC	Scrubber Water	Benner (2001b)	112	07/18/01		
IIMC	Tailings Basin Seep	Lapakko (2000)	2.99			
IIMC	Tailings Basin monitoring well	Lapakko (2000)	2.83			
IIMC	Tailings Basin monitoring well	Lapakko (2000)	2.86			
LTVSMC	Tailings Basin Water	Engesser and Niles (1997)	3.48	09/19/96		
LTVSMC	Tailings Basin Seep	Lapakko (2000)	2.44			
Northshore	Tailings Basin Water	Swain (2002)	1.1	Sept. 2000		
Northshore	Tailings Basin Water	Swain (2002)	1.3	Sept. 2000		
Northshore	Tailings Basin Water	Swain (2002)	1.9	Sept. 2000		
Northshore	Lake Superior	Monson et al. (2000)	1.02			
Northshore	Return water	Monson et al. (2000)	0.96			0.025
Northshore	Discharge to Beaver River	Monson et al. (2000)	0.73			<0.009
Northshore	Process Water	Monson et al. (2000)	1.12			0.237
Northshore	Beaver River	Monson et al. (2000)	6.15			0.271
Northshore	Beaver River	Monson et al. (2000)	5.78			0.294
Northshore	Upstream of MP7 Discharge	Monson et al. (2000)	4.02			0.262
Northshore	Downstream of MP7 Discharge	Monson et al. (2000)	3.48			0.248
Northshore	Feedwater	Benner (2001b)	7.05			
Northshore	Hood Exhaust 11	Benner (2001b)	32.8			
Northshore	Hood Exhaust 12	Benner (2001b)	15.7			
Northshore	Waste Gas Wet 11	Benner (2001b)	29.1			
Northshore	Waste Gas Wet 12	Benner (2001b)	15.7			
Northshore	Thickener Overflow	Engesser and Niles (1997)	2.21	09/20/96		
Northshore	Hood Exhaust Out	Engesser and Niles (1997)	6.61	09/20/96		
Northshore	Waste Gas Out	Engesser and Niles (1997)	10.87	09/20/96		

Northshore	Lake Superior	Engesser and Niles (1997)	2.18	09/20/96		
Northshore	Tailings Basin Water	Engesser and Niles (1997)	0.9	09/20/96		
NSPC	Sag Mill Discharge	Benner (2001a)	20.3			
NSPC	Sag Mill Discharge	Engesser (2000)	21.5	08/10/99		
NSPC	Sag Mill Discharge	Engesser (2000)	19.7	08/10/99		
NSPC	Coarse Tailings	Engesser (2000)	17.1	08/10/99		
NSPC	Coarse Tailings	Engesser (2000)	14	08/10/99		
NSPC	Fine Tailings	Engesser (2000)	25.5	08/10/99		
NSPC	Fine Tailings	Engesser (2000)	29	08/10/99		
NSPC	Concentrate	Engesser (2000)	16.5	08/10/99		
NSPC	Concentrate	Engesser (2000)	15.2	08/10/99		
NSPC	Concentrate	Benner (2001a)	14			
NSPC	Fired Pellet	Engesser (2000)	2.85	08/10/99		
NSPC	Fired Pellet	Engesser (2000)	5.73	08/10/99		
NSPC	Tailings	Lapakko(2000)	17.1			
NSPC	Tailings	Lapakko(2000)	19.5			
Hibtac	Filter Cake	Benner (2001b)	13.9			
Hibtac	Concentrate	Benner (2001b)	18.2			
Hibtac	Limestone	Benner (2001b)	3.72			
Hibtac	Multi-tube dust	Benner (2001b)	154			
Hibtac	Greenball	Benner (2001b)	16.7			
Hibtac	Bentonite	Benner (2001b)	26.4			
Hibtac	Pellet	Benner (2001b)	<0.69			
Hibtac	Mill Feed	Engesser and Niles (1997)	14.89	07/24/96		
Hibtac	Calculated Mill Feed	Engesser and Niles (1997)	22.41	07/24/96		
Hibtac	Concentrate	Engesser and Niles (1997)	14.85	07/24/96		
Hibtac	Tailings	Engesser and Niles (1997)	25.03	07/24/96		
Hibtac	Calculated Mill Feed	Engesser and Niles (1997)	23.24	12/10/96		
Hibtac	Concentrate	Engesser and Niles	15.4	12/10/96		

		(1997)				
Hibtac	Tailings 1	Engesser and Niles (1997)	24.6	12/10/96		
Hibtac	Tailings 2	Engesser and Niles (1997)	27.5	12/10/96		
Hibtac	Calculated Mill Feed	Engesser and Niles (1997)	23.78	12/13/96		
Hibtac	Concentrate	Engesser and Niles (1997)	13.2	12/13/96		
Hibtac	Tailings 1	Engesser and Niles (1997)	22.6	12/13/96		
Hibtac	Tailings 2	Engesser and Niles (1997)	25.8	12/13/96		
Hibtac	Calculated Mill Feed	Engesser and Niles (1997)	28.3	01/28/97		
Hibtac	Final Concentrate	Engesser and Niles (1997)	21.87	01/28/97		
Hibtac	Tailings	Engesser and Niles (1997)	30.54	01/28/97		
Hibtac	Fired Pellets	Engesser and Niles (1997)	0.48	07/24/96		
Hibtac	Bentonite	Engesser and Niles (1997)	22.39	07/24/96		
Hibtac	Limestone	Engesser and Niles (1997)	5.89	07/24/96		
Hibtac	Greenball	Engesser and Niles (1997)	16.2	01/28/97		
Hibtac	Fired Pellets	Engesser and Niles (1997)	0.94	01/28/97		
Hibtac	Bentonite	Engesser and Niles (1997)	12.56	01/28/97		
Hibtac	Limestone	Engesser and Niles (1997)	91.6	01/28/97		
Minntac	Fine Tailings	Swain (2002)	29.6	Sept. 2000		
Minntac	Fine Tailings	Swain (2002)	35.1	Sept. 2000		
Minntac	Greenball	Benner (2001b)	8.1	08/31/01		
Minntac	Pellet	Benner (2001b)	<0.6	08/31/01		
Minntac	Scrubber Filtrate	Benner (2001b)	87	08/31/01		
Minntac	Coal	Benner (2001b)	25.3	08/31/01		
Minntac	Rod Mill Feed	Engesser and Niles (1997)	35.09	07/09/96		

Minntac	Final Concentrate	Engesser and Niles (1997)	8.12	07/09/96		
Minntac	Coarse Tailings	Engesser and Niles (1997)	45.93	07/09/96		
Minntac	Fine Tailings	Engesser and Niles (1997)	38.97	07/09/96		
Minntac	Rod Mill Feed	Engesser and Niles (1997)	27.97	01/23/97		
Minntac	Final Concentrate	Engesser and Niles (1997)	8.22	01/23/97		
Minntac	Coarse Tailings	Engesser and Niles (1997)	43.54	01/23/97		
Minntac	Fine Tailings	Engesser and Niles (1997)	36.96	01/23/97		
Minntac	Filter Cake	Engesser and Niles (1997)	7.19	07/10/96		
Minntac	Greenball	Engesser and Niles (1997)	7.5	07/10/96		
Minntac	Fired Pellets	Engesser and Niles (1997)	0.65	07/10/96		
Minntac	Bentonite	Engesser and Niles (1997)	7.42	07/10/96		
Minntac	Fluxstone	Engesser and Niles (1997)	1.97	07/09/96		
Minntac	Greenball	Engesser and Niles (1997)	8.79	01/24/97		
Minntac	Fired Pellets	Engesser and Niles (1997)	0.57	01/24/97		
Minntac	Bentonite	Engesser and Niles (1997)	12.36	01/24/97		
Minntac	Fluxstone	Engesser and Niles (1997)	3.26	01/24/97		
Minntac	Wood chips	Engesser and Niles (1997)	6.01	01/24/97		
Minntac	Wood chip ash	Engesser and Niles (1997)	11.85	01/24/97		
Minntac	Greenball	Engesser (1998a)	8.62	09/03/97		
Minntac	Greenball	Engesser (1998a)	7.76	09/03/97		
Minntac	Fired Pellets	Engesser (1998a)	0.76	09/03/97		
Minntac	Fired Pellets	Engesser (1998a)	0.72	09/03/97		
Minntac	Scrubber Solids Out	Engesser (1998a)	252.7	09/03/97		
Minntac	Drying furnace solids	Engesser (1998a)	12.77	09/03/97		

Minntac	Tailings	Lapakko(2000)	46.6			
EVTAC	Coarse Tailings	Swain (2002)	24.7			
EVTAC	Coarse Tailings	Swain (2002)	130.2			
EVTAC	Fine Tailings	Swain (2002)	44			
EVTAC	Fine Tailings	Swain (2002)	51.9			
EVTAC	Greenball	Benner (2001b)	12			
EVTAC	Pellet	Benner (2001b)	<0.69			
EVTAC	Coal	Benner (2001b)	10.3			
EVTAC	Thickener underflow 2A	Benner (2001b)	527			
EVTAC	Thickener overflow 2A	Benner (2001b)	233			
EVTAC	Thickener underflow 2B	Benner (2001b)	367			
EVTAC	Thickener overflow 2B	Benner (2001b)	826			
EVTAC	Final Pellet	Engesser (1998b)	0.36	11/18/97		
EVTAC	Final Pellet	Engesser (1998b)	0.34	11/18/97		
EVTAC	Green Ball	Engesser (1998b)	17	11/18/97		
EVTAC	Green Ball	Engesser (1998b)	13	11/18/97		
EVTAC	Ball Mill	Engesser (1998b)	2.84	11/18/97		
EVTAC	Ball Mill	Engesser (1998b)	2.44	11/18/97		
EVTAC	Classifier Overflow	Engesser (1998b)	11.99	11/18/97		
EVTAC	Classifier Overflow	Engesser (1998b)	10.62	11/18/97		
EVTAC	Thickener Underflow	Engesser (1998b)	286.4	11/18/97		
EVTAC	Thickener Underflow	Engesser (1998b)	243.5	11/18/97		
IIMC	Scrubber Filtrate	Benner (2001b)	3179	08/31/01		
IIMC	Multiclone dust	Benner (2001b)	193	08/31/01		
IIMC	Greenball	Benner (2001b)	7.8	08/31/01		
IIMC	Pellet	Benner (2001b)	<0.6	08/31/01		
IIMC	Tailings	Lapakko (2000)	35.4			
LTVSMC	Rod Mill Feed	Engesser and Niles (1997)	14.05	08/06/96		
LTVSMC	Final Concentrate	Engesser and Niles (1997)	4.87	08/06/96		
LTVSMC	Total Tailings	Engesser and Niles (1997)	17.86	08/06/96		

LTVSMC	Rod Mill Feed	Engesser and Niles (1997)	8.86	02/06/96		
LTVSMC	Final Concentrate	Engesser and Niles (1997)	3.73	02/06/96		
LTVSMC	Total Tailings	Engesser and Niles (1997)	11.61	02/06/96		
LTVSMC	Fired Pellets	Engesser and Niles (1997)	0.16	08/06/96		
LTVSMC	Pellet Chips	Engesser and Niles (1997)	0.42	08/06/96		
LTVSMC	Bentonite	Engesser and Niles (1997)	9.41	08/06/96		
LTVSMC	Filter Feed	Engesser and Niles (1997)	5.72	08/06/96		
LTVSMC	Fired Pellets	Engesser and Niles (1997)	2.17	02/06/96		
LTVSMC	Pellet Chips	Engesser and Niles (1997)	2.88	02/06/96		
LTVSMC	Bentonite	Engesser and Niles (1997)	14.81	02/06/96		
LTVSMC	Green Balls	Engesser and Niles (1997)	3.49	02/06/96		
LTVSMC	Total Tailings	Lapakko (2000)	7			
Northshore	Coarse Tailings	Swain (2002)	0.43			
Northshore	Fine Tailings	Swain (2002)	1.2			
Northshore	Fine Tailings	Swain (2002)	3.2			
Northshore	Wastegas 11 filtrate	Benner (2001b)	211			
Northshore	Wastegas 12 filtrate	Benner (2001b)	110			
Northshore	Hood exhaust 11 filtrate	Benner (2001b)	26			
Northshore	Hood exhaust 12 filtrate	Benner (2001b)	26.4			
Northshore	Greenball 11	Benner (2001b)	1.44			
Northshore	Greenball 12	Benner (2001b)	1.1			
Northshore	Pellet 11	Benner (2001b)	<.69			
Northshore	Pellet 12	Benner (2001b)	1.85			
Northshore	Dry Cobber Feed	Engesser and Niles (1997)	0.75			
Northshore	Final Concentrate	Engesser and Niles (1997)	0.82			
Northshore	Dry Cobber Tailings	Engesser and Niles	0.28			

		(1997)				
Northshore	Coarse Tailings	Engesser and Niles (1997)	0.83			
Northshore	Fine Tailings	Engesser and Niles (1997)	1.07			
Northshore	Dry Cobber Feed	Engesser and Niles (1997)	0.76			
Northshore	Final Concentrate	Engesser and Niles (1997)	1.13			
Northshore	Dry Cobber Tailings	Engesser and Niles (1997)	0.77			
Northshore	Coarse Tailings	Engesser and Niles (1997)	0.54			
Northshore	Fine Tailings	Engesser and Niles (1997)	1.64			
Northshore	Acid Pellets	Engesser and Niles (1997)	0.22			
Northshore	Flux Pellets	Engesser and Niles (1997)	0.04			
Northshore	Limestone	Engesser and Niles (1997)	0.48			
Northshore	Bentonite	Engesser and Niles (1997)	19.4			
Northshore	Oriox	Engesser and Niles (1997)	1.09			
Northshore	Green Balls	Engesser and Niles (1997)	0.83			
Northshore	Fired Pellets	Engesser and Niles (1997)	0.29			
Northshore	Limestone	Engesser and Niles (1997)	0.91			
Northshore	Bentonite	Engesser and Niles (1997)	14.69			
Northshore	Oriox	Engesser and Niles (1997)	1.46			
Northshore	Coal	Engesser and Niles (1997)	15.61			
Northshore	Coal Ash	Engesser and Niles (1997)	86.76			

Appendix 2: Historical Pellet Production

Pellets produced (Million Long Tons) by individual mining companies. Sources included compilation of concentrate produced as reported by Engesser and Niles (1997) multiplied by a conversion factor (mass pellets/mass concentrate) and direct report of pellets production as reported by Skillings (2003).

	Butler	LTVSMC	EVTAC	Hibbing	IIMC	NSPC	Northshore	Minntac
1949		0.05						
1950		0.13						
1951		0.10						
1952		0.10					0.01	0.00
1953		0.24					0.26	0.14
1954		0.19					0.32	0.43
1955		0.21					0.53	0.66
1956		0.22					4.28	0.66
1957		0.50					5.62	0.82
1958		3.04					4.89	0.80
1959		4.23					3.80	0.57
1960		7.35					5.50	0.85
1961		6.97					5.71	0.81
1962		7.82					6.21	0.82
1963		8.09					8.12	0.85
1964		8.25					9.77	0.88
1965	0.01	8.28	0.05				10.12	0.93
1966		8.81	1.56				10.94	0.81
1967	1.62	10.20	1.76			0.47	9.80	0.94
1968	2.33	11.04	1.82			0.84	10.10	4.84
1969	2.6	10.51	1.94			2.29	10.45	6.42
1970	2.64	11.06	2.01			2.73	10.94	6.82
1971	2.65	10.50	2.08			2.81	9.73	6.83
1972	2.3	10.27	2.16			2.42	9.13	9.19
1973	2.56	12.01	2.09			2.58	10.52	13.29
1974	2.52	11.23	2.19			2.48	10.47	13.38
1975	2.44	11.21	2.18			2.43	10.81	12.92
1976	2.4	11.10	2.31	0.31		2.46	10.15	13.03
1977	1.69	4.79	2.60	2.19	0.25	2.62	5.08	7.88

1978	2.51	7.64	4.97	5.52	2.08	5.10	9.24	13.71
1979	2.55	9.08	5.66	6.38	2.42	5.37	7.10	17.48
1980	1.58	5.85	5.84	6.94	1.52	2.90	4.63	15.00
1981	2.19	8.18	5.94	7.27	2.58	3.42	7.72	13.12
1982	1.04	4.08	4.66	5.81	1.93	1.29	1.54	3.51
1983	1.56	2.11	3.30	4.29	2.31	3.27	1.00	8.17
1984	1.99	4.84	3.97	6.20	2.19	4.58	3.71	9.23
1985	0.95	5.01	2.97	5.16	1.97	4.43	3.31	10.50
1986		4.36	3.49	4.98	1.95	4.02	1.44	5.96
1987		6.97	3.51	7.84	2.29	4.31	0.00	8.13
1988		8.13	4.28	8.82	2.43	4.61	0.00	12.56
1989		7.59	4.96	8.35	2.45	4.75	0.00	12.56
1990		8.03	4.46	8.30	2.45	4.81	2.40	13.47
1991		7.10	3.40	8.18	2.53	4.85	2.01	13.22
1992		6.82	3.61	7.96	2.28	5.00	1.40	13.09
1993		7.62	3.15	7.38	2.59	2.76	3.44	14.32
1994		7.69	4.91	8.35	2.71	1.73	3.46	14.28
1995		7.76	5.24	8.62	2.77	5.08	3.71	13.65
1996		7.46	4.94	8.12	2.74	4.77	4.16	13.42
1997		7.71	5.07	7.67	2.58	5.11	4.25	14.58
1998		6.75	4.87	7.78	2.58	5.28	4.35	14.19
1999		7.00	4.40	6.90	2.80	5.25	3.91	13.01
2000		7.80	5.87	8.23	2.81	5.47	4.20	14.44
2001			4.26	6.10	2.77	4.30	2.65	12.64
2002			4.19	7.70	2.73	5.44	4.14	14.64
2003 (est)			2.00	8.30	2.90	5.30	4.80	14.61

Appendix 3: Historical Mercury Emissions

Mercury (kg) emitted from taconite mining companies. Estimates were made by multiplying past production records with present day emission factors.

kg Hg	Butler	LTVSMC	EVTAC	Hibbing	IIMC	NSPC	Northshore	Minntac	Total	Cumulative
1949		0.23							0.23	0.23
1950		0.67							0.67	0.90
1951		0.52							0.52	1.42
1952		0.52					0.02		0.54	1.96
1953		1.19					0.48	0.73	2.40	4.36
1954		0.93					0.59	2.32	3.84	8.19
1955		1.03					0.96	3.50	5.49	13.69
1956		1.09					7.79	3.50	12.38	26.07
1957		2.53					10.22	4.35	17.10	43.17
1958		15.25					8.90	4.24	28.39	71.56
1959		21.25					6.91	3.05	31.21	102.78
1960		36.92					10.02	4.52	51.46	154.23
1961		35.00					10.39	4.29	49.68	203.92
1962		39.24					11.30	4.35	54.90	258.82
1963		40.59					14.78	4.52	59.89	318.70
1964		41.42					17.78	4.69	63.88	382.59
1965	0.10	41.57	0.58				18.42	4.97	65.64	448.23
1966		44.21	17.76				19.91	4.29	86.17	534.40
1967	16.30	51.19	20.07			4.73	17.83	5.03	115.14	649.54
1968	23.44	55.43	20.76			8.45	18.38	25.82	152.28	801.82
1969	26.16	52.74	22.15			23.04	19.03	34.24	177.34	979.17
1970	26.56	55.53	22.95			27.46	19.91	36.33	188.74	1167.91
1971	26.66	52.69	23.76			28.27	17.70	36.38	185.46	1353.37
1972	23.14	51.55	24.68			24.35	16.62	48.98	189.32	1542.69
1973	25.75	60.29	23.88			25.95	19.15	70.85	225.88	1768.57
1974	25.35	56.36	25.03			24.95	19.06	71.30	222.05	1990.62
1975	24.55	56.26	24.91			24.45	19.67	68.87	218.70	2209.32
1976	24.14	55.74	26.41	3.84		24.75	18.47	69.44	222.80	2432.12
1977	17.00	24.04	29.64	27.54	1.32	26.36	9.25	41.98	177.13	2609.25
1978	25.25	38.37	56.75	69.31	11.09	51.31	16.82	73.05	341.94	2951.19

1979	25.65	45.60	64.59	80.07	12.87	54.02	12.92	93.17	388.90	3340.09
1980	15.89	29.37	66.67	87.12	8.10	29.17	8.42	79.94	324.69	3664.78
1981	22.03	41.05	67.82	91.34	13.73	34.41	14.04	69.94	354.38	4019.15
1982	10.46	20.48	53.17	73.02	10.28	12.98	2.79	18.70	201.89	4221.04
1983	15.69	10.60	37.72	53.94	12.30	32.90	1.82	43.56	208.52	4429.56
1984	20.02	24.30	45.33	77.89	11.66	46.07	6.75	49.21	281.24	4710.80
1985	9.56	25.13	33.91	64.82	10.46	44.57	6.03	55.99	250.46	4961.26
1986		21.87	39.91	62.52	10.40	40.44	2.63	31.75	209.52	5170.78
1987		35.00	40.14	98.52	12.18	43.36	0.00	43.33	272.54	5443.32
1988		40.80	48.91	110.82	12.93	46.38	0.00	66.95	326.77	5770.09
1989		38.11	56.63	104.92	13.04	47.79	0.00	66.95	327.44	6097.53
1990		40.33	50.98	104.28	13.04	48.39	4.37	71.81	333.21	6430.74
1991		35.63	38.87	102.75	13.44	48.79	3.66	70.45	313.59	6744.33
1992		34.23	41.18	99.93	12.12	50.30	2.56	69.78	310.09	7054.42
1993		38.26	35.99	92.75	13.79	27.77	6.27	76.33	291.15	7345.57
1994		38.62	56.06	104.92	14.42	17.40	6.31	76.10	313.84	7659.41
1995		38.96	59.84	108.27	14.74	51.10	6.75	72.75	352.41	8011.82
1996		37.43	56.43	101.99	14.56	47.99	7.57	71.53	337.50	8349.32
1997		38.70	57.85	96.34	13.74	51.37	7.74	77.70	343.43	8692.75
1998		33.89	55.57	97.68	13.74	53.12	7.92	75.63	337.54	9030.28
1999		35.14	50.25	86.66	14.90	52.78	7.11	69.35	316.19	9346.48
2000		39.16	67.04	103.38	14.97	55.03	7.64	76.97	364.18	9710.66
2001			48.65	76.62	14.74	43.26	4.82	67.34	255.43	9966.08
2002			47.80	96.71	14.53	54.70	7.54	78.04	299.31	10265.40
2003 (est)			22.84	104.25	15.43	53.32	8.74	77.84	282.41	10547.81

Appendix B-1-4

Mercury Capture at Taconite Processing Facilities: Update on DNR Research Activities

October 1, 2004

**Mercury Capture at Taconite Processing Facilities:
Update on DNR Research Activities**

Michael Berndt¹ and John Engesser²

Minnesota Department of Natural Resources
Division of Lands and Minerals

¹500 Lafayette Road
St. Paul, Minnesota 55155

²1525 Third Avenue E.
Hibbing Minnesota 55746

October 1, 2004

Table of Contents

Table of Contents.....	2
Introduction.....	3
Mercury Capture by Wet Scrubbers	3
Scrubber efficiency and possible link to heating rate.....	3
Mercury oxidation state and maghemite.....	4
On the Fate of Captured Mercury	6
Summary.....	7
References.....	8
Tables.....	9
Figures	11

Introduction

The Minnesota Department of Natural Resources (DNR) has been studying wet scrubbers and process lines at four taconite processing facilities to evaluate potential mercury control options for stack emissions. Projects are funded by Iron Ore Cooperative Research (IOCR) and the Environmental Protection Agency-Great Lakes National Program Office (EPA-GLNPO). In addition, this research is supplemented by funds from the Department of Natural Resources-Environmental Cooperative Research (DNR-ECR) fund. The IOCR project is more concerned with evaluating mercury release and capture mechanisms while the EPA-GLNPO funds were solicited with the objective of evaluating the ultimate fate of oxidized mercury once it has been captured by the wet scrubbers. However, because processes of capture and fate have been found to be inextricably linked, we combine and discuss details from each study in a single document for distribution to all concerned parties. Results are also combined with data from our earlier study (Berndt and Engesser, 2003) and essential findings are summarized here. It is important to recognize that data and discussion in this document have not been through the review process and should therefore be considered as preliminary.

Mercury Capture by Wet Scrubbers

Four taconite companies have participated in our study: Hibtac, Minntac, United Taconite (formerly Evtac), and Ispat-Inland. Scrubber water and other samples were collected from each company to help estimate the fraction of mercury released from pellets that is captured by the wet scrubber (Table 1, Figure 1). The fraction of mercury captured varied considerably between processing plants and within individual plants sampled at different times. Note that in this discussion, we only evaluate the mercury captured by the wet scrubber without regard to its ultimate fate. As we show in a later section, much of the mercury can be recycled to the induration furnace and re-released. Nevertheless, the data have important use as a means to provide information on processes that lead, respectively, to low and high mercury capture rates.

Variation in capture rates is likely linked to differences in the temperature distributions in induration furnaces as well as to changes in gas and dust composition. Thus, we focused on these parameters when comparing data from different taconite processing lines.

Scrubber efficiency and possible link to heating rate

A key variable affecting scrubber efficiency appears to be the rate of heating of taconite pellets in induration furnaces. For example, Minntac generates both standard and fluxed pellets in their “line 4” processing line. Scrubber efficiency (for Hg capture) was higher when the company was producing standard pellets than when producing fluxed pellets. Fluxed pellet production involves additional heating, and therefore, higher furnace temperatures than standard pellet production. This is because the heating of the flux material (CaCO_3/CaO) is highly endothermic (requiring heat), while oxidation of

magnetite is exothermic (generates heat). Thus, Minntac activates preheat burners during induration of fluxed pellets that are not used during standard pellet production. This additional heating may be the primary mechanism leading to reduced mercury capture, although differences in scrubber dust and gas composition cannot be ruled out.

In addition, we note great differences in the rate of mercury capture by otherwise similar wet scrubbers at Minntac for lines 4 and 7 during production of fluxed pellets. Line 4 employs a standard kiln while line 7 employs a sophisticated ported kiln. Because the ported kiln makes more effective use of the chemical heat derived from magnetite oxidation, less heat is added throughout the process, and the heating in the kiln takes place under smaller thermal gradients. Thus, our observation of significantly greater mercury capture by the scrubber system in line 7 compared to line 4 during fluxed pellet production (Table 1) suggests a possible link between heating rate and mercury capture. Because the product being generated is the same for this particular comparison, the dust particles and gas chemistry would be expected to be similar among the two lines. Thus, most of the difference in mercury capture is probably related to differences in temperature distribution.

Finally, we note the relative efficiencies for mercury capture for Hibtac and Minntac wet scrubbers (Fig. 1). Owing to differences in system design (straight grate for Hibtac, grate-kiln for Minntac), significant differences in heat input are required for induration of standard pellets at these plants. Analysis of furnace temperatures during production of standard pellets show that heating in Minntac's line occurs much more evenly than it does at Hibtac (Fig. 2). The increased heating rate at Hibtac, specifically above a temperature of 500C may be partially responsible for the less efficient mercury capture rates at Hibtac compared to Minntac, however, we also notice that the amount of dust generated at Minntac is also higher than that at Hibbtac. Taken together with the observed dependence of scrubber efficiency for production of fluxed and non-fluxed pellets in ported and non-ported kilns at Minntac, the results suggest a possible (but non-conclusive) link between heating rate and mercury capture by wet scrubbers.

Mercury oxidation state and maghemite

Any link between temperature distribution in the furnace and scrubber efficiency for Hg implies a link between temperature and mercury oxidation state in the gas phase. This is because oxidized mercury, Hg(II), is captured in wet scrubber systems while reduced mercury, Hg(0), is not. Thus, any factor affecting the oxidation state of mercury in gases passing through the scrubber system affects the scrubber efficiency in terms of Hg removal.

One model to account for our observations would involve a relationship between heating rate and the oxidation state of mercury released from pellets during heating. If, for example, faster heating and higher temperatures result in release of mercury with high Hg(0)/Hg(II) ratio, then mercury capture rates should decrease with increased heating rate, as has been observed. Alternatively, a temperature dependence for the oxidation rate of reduced mercury (*in-flight*) could account for the observed trends. Thus, current and future DNR research efforts have been designed to evaluate whether mercury capture is related to differences in the primary oxidation state of mercury released from pellets in furnaces or to subsequent oxidation of mercury within the gas phase.

Of potential significance for taconite processing facilities is the Fe-oxide mineral maghemite. This mineral has been identified as a powerful oxidant for reduced mercury when it exists in the flue-gases of coal fired power plants (Zygarlicke, et al. 2003). This phase is also expected to form during moderate heating of taconite pellets up to temperatures of approximately 750 F (Papanatassiou, 1970). If this phase is generated and released (as dust) into process gases, it potentially impacts the oxidation state of mercury and mercury capture rate in wet scrubbers. Because of the potential importance of this phase, the DNR conducted a mossbauer spectroscopic study to determine whether maghemite was present in dust samples and, if so, whether a link could be established between mercury capture and maghemite abundance. Mossbauer spectroscopy is a sensitive technique that can distinguish maghemite from other Fe-oxide minerals in mixed samples of hematite, magnetite, and/or other phases.

In this case, studies were designed to specifically evaluate temperature, mercury capture, and maghemite in dust produced under normal mineral processing conditions at Hibtac and Minntac.

At Hibtac, dust samples were collected from wind boxes at various locations along the straight grate (Fig. 3) as the pellets were heated to high temperatures. Dust from the pellets becomes trapped beneath the grate in “wind boxes” in the approximate temperature zones where the dust was generated. The dust samples from these windboxes were dry-sieved to remove the larger chips, and subsequently analyzed for mercury concentration and maghemite abundance. Mercury concentration in dust increased greatly in windboxes 12 through 16 with a large peak for dust from windbox 14. The average temperature (average in gas from above and below the pellet bed) was approximately 750 F at the peak mercury concentration. Interestingly, magnetite is oxidized to maghemite in air between 400 and 750 F but to hematite at temperatures above 750 F (Papanatassiou, 1970). Peak mercury concentration was found in a zone where maghemite formation is expected to occur.

Mossbauer analysis of selected samples from Hibtac revealed formation of a small but significant component of maghemite in the sample from windbox 14. However, maghemite was not detected in the unheated green-ball feed sample (Fig. 4). Thus, the maghemite must have formed during heating of the pellets. Maghemite was also found in the dust collected from higher temperature zones in the furnace (windbox 18), but in this case, the hematite fraction had also increased significantly above that for the greenball feed sample. We hypothesize, therefore, that the maghemite formed at temperatures below 750 F is overprinted by hematite on the surfaces of dust grains heated to temperatures above 750 F. This overprinting may “deactivate” the dust grains with respect to mercury oxidation (Fig. 4) and prevent capture of mercury. If correct, this could help to account for observed relationships between temperature distribution and mercury capture in taconite processing plants.

Two samples from Minntac were also analyzed by mossbauer spectroscopy for maghemite to determine if a link exists between scrubber efficiency and maghemite abundance in scrubber dust. Dust filtered from scrubber water collected at a time when mercury capture rate was high contained a small amount of maghemite as well as some hematite, and was similar in composition to the sample collected from Hibtac in windbox 14. Dust filtered from scrubber water collected at a time when mercury capture rate was relatively low revealed enhanced hematite formation and was similar in composition to

the Hibtac sample from windbox 18 (hot). These data suggest a possible link between maghemite formation and mercury capture in taconite processing facilities. If substantiated, a promising technique to reduce mercury emissions may involve control and distribution of maghemite and hematite dust in taconite process gases.

Samples were also recently collected from beneath the grate and preheat zones at Minntac in July, 2004 (Figure 5). The samples revealed that unlike the case at Hibtac, mercury is concentrated more generally throughout the pellet bed. Plans are currently underway to subject these and other scrubber dust solids to Mossbauer spectroscopic analysis to determine whether the association between maghemite and mercury capture at taconite processing plants is robust.

While the mossbauer results suggest a possible correlation between maghemite formation and mercury capture efficiency in taconite processing plants, our results are not yet conclusive. It is still possible that maghemite formation and mercury capture are affected by temperature distributions for reasons that are independent from each other. Indeed, the reaction rates for Hg(0) and maghemite may well be too slow for significant oxidation to occur in the short residence times applicable to taconite processing gas streams. To better understand mercury emissions in taconite process streams the DNR plans to determine relationships between heating rate, release temperatures (of mercury to air), and the primary oxidation state of the mercury released to the gas phase. While we are not equipped to perform the needed experiments, we have been making efforts to secure funds for this research and to identify a laboratory to do the needed additional work.

On the Fate of Captured Mercury

Once captured by a wet scrubber, mercury needs to be disposed in a manner where it does not enter the environment through other pathways. Thus, an important component of the DNR Hg research program has been to evaluate the fate of mercury captured by the scrubber systems. Samples have been collected “downstream” from the scrubber systems in taconite processing plants in order to determine the fraction of captured mercury that is currently routed to the tailings basin. For the purposes of our study, we consider mercury to be permanently disposed of only after it reaches the tailings basin.

We note that the mercury captured by scrubber systems occurs in two states (1) dissolved in water and (2) adsorbed to particulates (Fig. 6). It is important to consider both forms of mercury, especially in plants where the distribution of mercury is relatively evenly divided between dissolved and adsorbed components. In addition, experiments conducted by our group on samples from Minntac and Hibtac indicate that mercury adsorption to solids in scrubber waters is a dynamic process, occurring with reaction times measured in minutes to hours (Figs. 7,8). This time frame is important because it impacts the manner in which mercury removal systems might be studied and subsequently designed. Furthermore, these results imply that samples collected for mercury analysis may need to be filtered immediately upon collection to prevent misleading results on dissolved and particulate loads. Collecting samples at the plant, and waiting to filter back at the lab will typically result in an over-reporting of the

particulate fraction and under-representation of the dissolved component for scrubber waters.

Each of the four taconite companies in our study routes their scrubber waters differently, but the overall results for at least three of the companies appears to be the same: most of the captured mercury is recycled back to the induration furnaces and not currently routed to tailings basins.

Minntac sends their scrubber solids to a thickener where they are mixed with chip regrind and other solids. Most of the scrubber water overflows the scrubber thickener. Sample analyses indicate that most of the mercury that was in the scrubber water adsorbs to the solids in the scrubber-thickener underflow. These scrubber-thickener underflow solids eventually mix with the concentrate which is rolled into greenballs. This means that most of the mercury captured in the scrubbers is recycled back to the greenballs. Thus, the percentage of captured mercury that is currently sent to the tailings basin at this plant appears to be small.

Ispat-Inland sends their scrubber solids to the concentrate filter and we find that little mercury remains dissolved in the water following the process. Thus, most of the captured mercury at this plant also appears to recycle back to the induration furnace and probably only a small fraction is directed to the tailings basin.

United Taconite sends their scrubber waters and solids to a chip regrind mill where it is reground, rolled into greenballs, and sent to the induration furnace. Because only a very small fraction of the mercury captured at United Taconite is initially dissolved in the water, most of the captured mercury at this plant is probably recycled back to the induration furnace.

The case for mercury recycling back to the induration furnace is less clear at Hibtac because a high fraction of the mercury is dissolved, and because scrubber waters are introduced into the grinding mills where background mercury in the primary ore interferes with the analyses. While our present studies have demonstrated that the dissolved mercury from the added scrubber water adsorbs to phases in the grinding mills, the percentage adsorbing to magnetic versus nonmagnetic minerals is more difficult to evaluate. However, experiments recently conducted by us at United Taconite (Table 2) may have bearing on this issue. The results showed that most mercury in tailings/scrubber water mixtures at this plant are adsorbed to the nonmagnetic fraction. If mercury in scrubber waters from Hibtac adsorbs to the nonmagnetic fraction during grinding, it will eventually be routed to the tailings basin and, thus, not recycled to the furnace.

The DNR mercury research program will continue to evaluate mercury partitioning during exposure of scrubber waters and other components of taconite processing streams (tailings, raw process waters) to typical mineral processing procedures (e.g., magnetic separation, elutriation, thickeners, grinding).

Summary

Scrubber efficiency for mercury released during taconite processing has been studied and found to vary widely across the iron range. The capture rate for mercury appears to be plant- and product-dependent owing to differences in heating characteristics associated with process line design (straight-grate versus grate-kiln, ported

versus non-ported kiln) and product heat requirements (fluxed versus standard pellets). There is preliminary evidence pointing to possible importance of a maghemite-catalyzed mercury oxidation process to account for some of the variability between mercury capture rates. One facet of future DNR research will, therefore, study primary processes that control mercury oxidation in taconite process gas streams.

Although each of the four processing plants in our study routes their scrubber water blow down differently, it appears that most of the mercury captured by scrubbers at three of the taconite plants reports back to the induration furnace, where it is likely revolatilized. The fate of mercury at the fourth plant (Hibtac) is less certain, but initial results on mercury partitioning between magnetic and non-magnetic minerals suggest that introducing scrubber water to the grinding mills (as is their practice) may have some benefit in permanent mercury removal. This is because captured mercury appears to adsorb preferentially to the non-magnetic fraction which is, ultimately, routed to the tailings basin.

Optimally, systems will need to be designed to direct higher percentages of the mercury captured by wet scrubbers to the tailing basin. Thus, future DNR research will also focus on evaluating partitioning of dissolved and particulate mercury from scrubber waters during commonly used mineral processing techniques (elutriation, thickening, magnetic separation). Because mercury adsorption to solids is a dynamic process, taking place in minutes to hours, these studies will be conducted on time scales reflecting those of mineral processing at taconite plants.

References

- Berndt, M. E. and Engesser, J. (2003) On the distribution of mercury in taconite plant scrubber systems. Minnesota DNR report prepared for MPCA. 30 p.
- Papanatassiou, D. J. (1970) Mechanisms and Kinetics Underlying the Oxidation of Magnetite in the Induration of Iron Ore Pellets. University of Minnesota, Duluth, Unpublished PHD Thesis. 134 p.
- Zygarlicke, et al. (2003) Experimental Investigations of Mercury Transformations in Pilot-Scale Combustion Systems and a Bench-Scale Entrained-Flow Reactor. University of North Dakota Energy and Environmental Research Center Technical Report. 22 p.

Tables

Table 1: Mercury capture data for taconite wet scrubbers.

Plant/Line	Date	Pellet Type	TSS (wt %)	Hg Tot (ng/L)	% Hg Dissolved ¹	% Hg Captured ²
Minntac L4	2/19/03	Std	0.086	1221	9.5	18.9
Minntac L4	5/9/03	Flux	0.387	700	11.6	12.0
Minntac L4	9/10/03	Std	0.217	1415	33.4	36.7
Minntac L4	1/28/04	Std	0.145	2422	6.8	46.5
Minntac L7	1/28/04	Flux	0.041	1251	17.8	25.0
Minntac L7	5/11/04	Flux	0.052	1707	17.0	39.4
Minntac L7	7/27/04	Flux	0.095	2744	11.1	34.8
Hibtac	2/20/03	Std	0.007	354	72.2	5.1
Hibtac	5/8/03	Std	0.035	769	44.1	11.1
Hibtac	9/11/03	Std	0.038	690	66.9	10.9
Hibtac	1/27/04	Std	0.018	556	52.5	10.2
Hibtac	5/12/04	Std	0.013	501	47.1	9.0
Hibtac	7/27/04	Std	0.014	684	42.9	8.3
Evtac	2/18/03	Std	1.340	13183	0.5	4.9
United Tac	1/28/04	Std	0.903	6140	1.6	2.4
United Tac	5/11/04	Std	1.270	7709	2.1	2.4
United Tac	7/28/04	Std	2.260	10485	1.1	3.3
Ispat-Inland	2/20/03	Std	0.328	3239	37.5	23.0
Ispat-Inland	5/8/03	Flux	0.142	3060	27.6	15.4
Ispat-Inland	9/11/03	Flux	0.175	4685	21.6	14.6
Ispat-Inland	1/27/04	Flux	0.137	3169	32.3	5.3
Ispat-Inland	5/12/04	Flux	0.095	3730	88.8	11.3

¹ “% Hg dissolved” is the percentage of mercury present in scrubber waters that is in the dissolved state (not bound to particulates) immediately after sampling.

² “% Hg captured” is the scrubber efficiency and represents the total mercury captured by the scrubber system (measured) divided by the total mercury available (estimated using mass balance).

Table 2: Results from experiments performed on tailings/scrubber solid mixtures from United Taconite. The solids were mixed together and allowed to react overnight. The magnetic fraction was then separated from the non-magnetic fraction and both separates analyzed for total mercury.

Experiment	Magnetic Fraction (wt%)	% Hg on Magnetic Fraction	Nonmagnetic Fraction (wt%)	%Hg on Nonmagnetic Fraction
Tails	4.3	6.3	95.7	93.7
Tails + Scrubber Solids	14.4	11.6	85.6	88.4
Tails + Scrubber Solids	12.7	10.2	87.3	89.8
Tails + Scrubber Solids	13.4	14.0	86.6	86.0
Scrubber Solids	67.7	23.6	32.3	76.4

Figures

Hg Captured/Volatilized

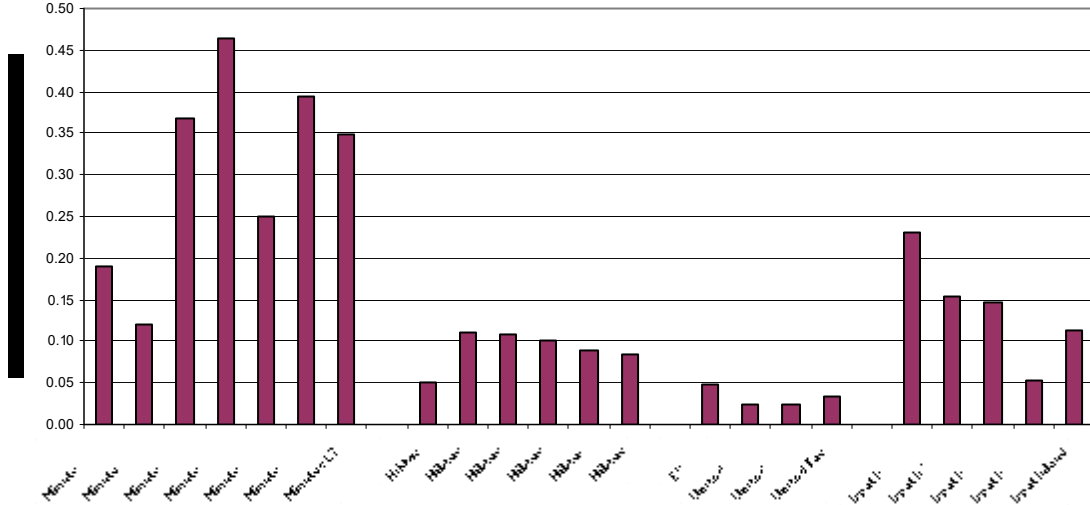


Figure 1. Scrubber efficiency estimates for taconite plants. These values are calculated by dividing the rate of mercury capture by the rate at which mercury is being volatilized in the induration furnace. The rate of capture is estimated by multiplying the scrubber blow-down rate by the concentration of mercury (dissolved plus particulate) in the scrubber water. The volatilization rate is calculated by using an assumed or measured value for green-ball mercury concentration and feed rate, allowing for greenball moisture as well as loss of some mercury via other pathways (green ball attrition and mercury in the final product). These scrubber efficiencies do not necessarily reflect permanent removal of mercury from taconite processing because much of the captured mercury in current plant configurations may be recycled back to the induration furnace and re-released.

Straight Grate and Grate Kiln Average Pellet Temperatures
Standard Pellet Production

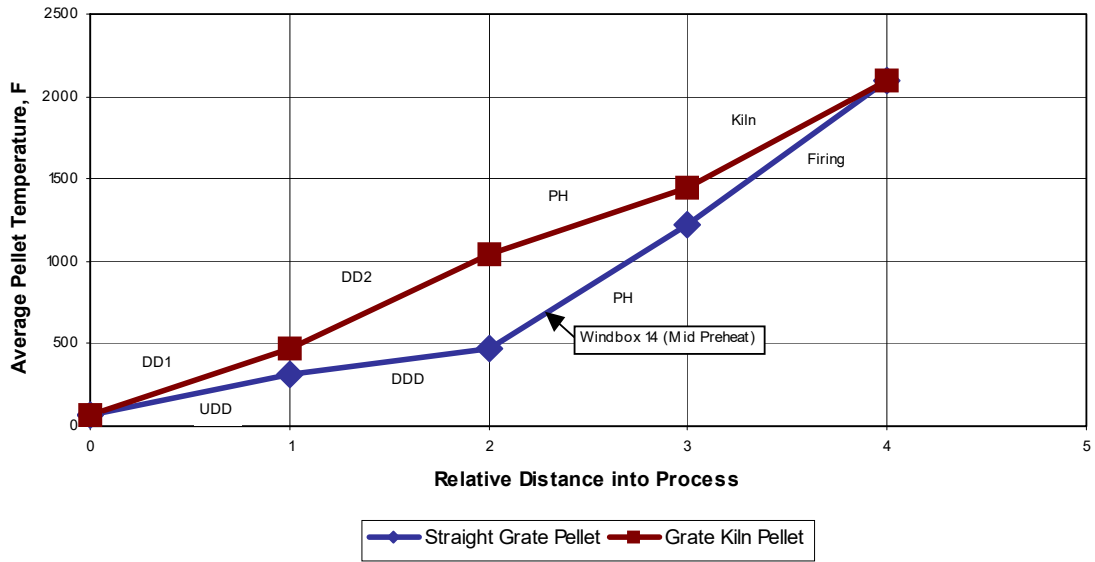


Figure 2. Representative temperature profiles during production of standard pellets at Minntac (Grate-Kiln, Line 4) and Hibtac (Straight Grate).

Mercury in Straight Grate Dust versus Windbox Temperature

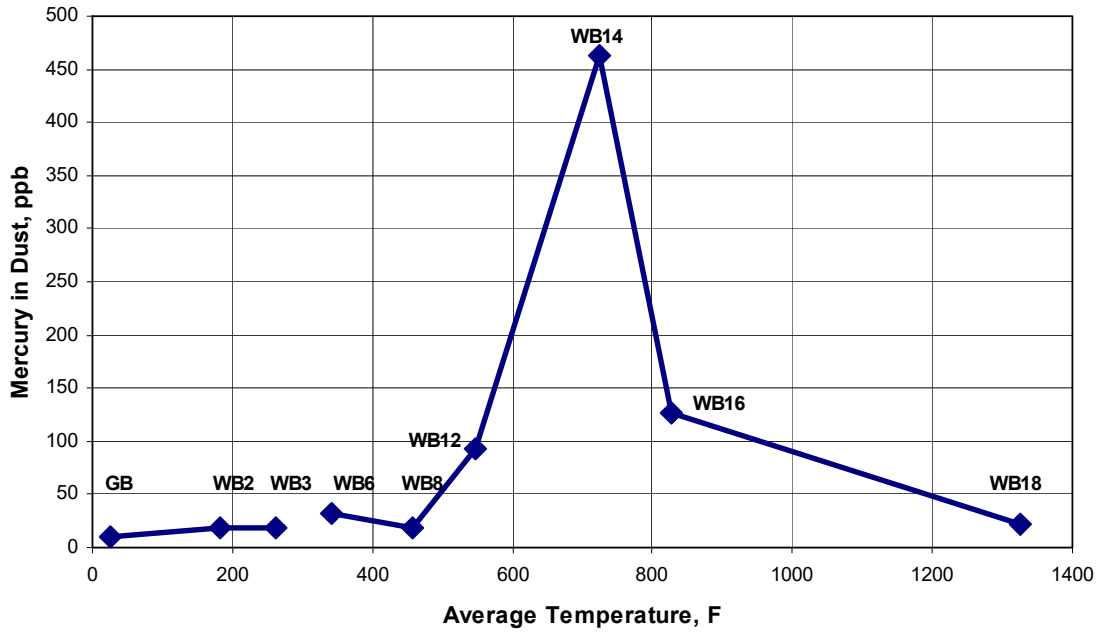


Figure 3. Measured mercury in dust captured from beneath the straight-grate at Hibtac. The temperature was calculated as the average of measurements made above and beneath the grate. The maximum in mercury takes place in the portion of the furnace where average temperature is about 700F. This suggests mercury is released at temperatures of about 800F and above and captured at temperatures below this.

Mossbauer results

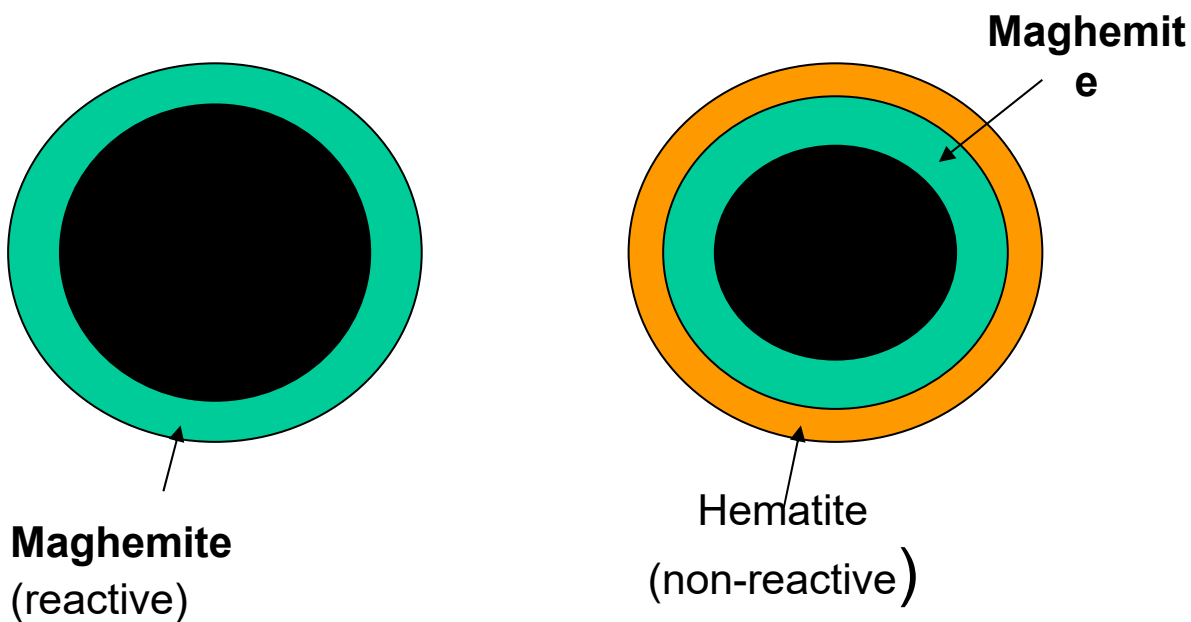
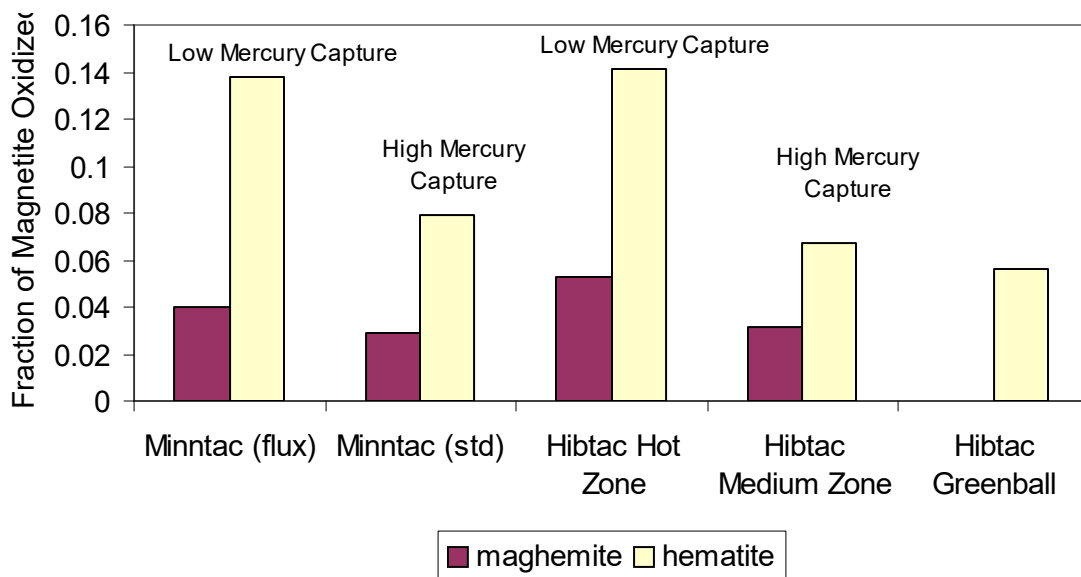


Figure 4. Results and interpretation of Mossbauer study of dust samples collected from Hibtac and Minntac. High mercury capture may result when outer surfaces of dust grains are converted to maghemite which is known to rapidly oxidize Hg(0) to Hg(II). When the dust grains are exposed to high temperature, the outer surfaces are converted to hematite, which does not react with Hg(0).

Mercury versus Distance Into Process

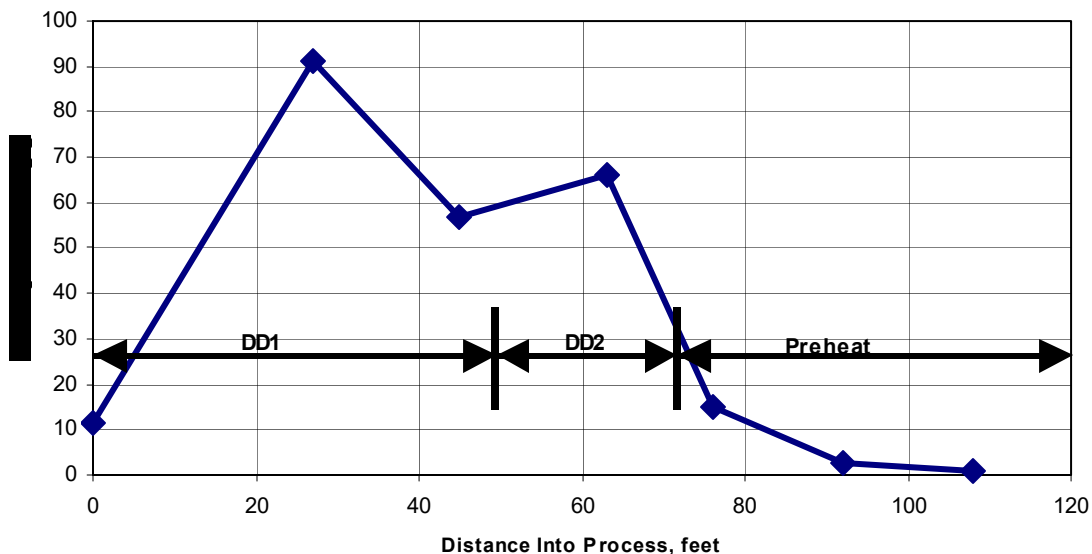


Figure 5. Mercury distribution in dust collected from Minntac's operation. Unlike the case at Hibtac where one distinct mercury maximum was found, there appears to be two mercury maximum zones. Process gas in this case is routed from right to left while pellets move into the process from left to right. Dust from the preheat zone has no mercury, but that in the down draft zones (DD1 and DD2) is enriched in mercury relative to the pellets. These data provide evidence that sufficient oxidized mercury exists in the process gas to dramatically affect the concentration of mercury in particles (by adsorption). Experiments will soon be underway to determine whether this mercury is released in oxidized state or if it is oxidized *in-flight*.

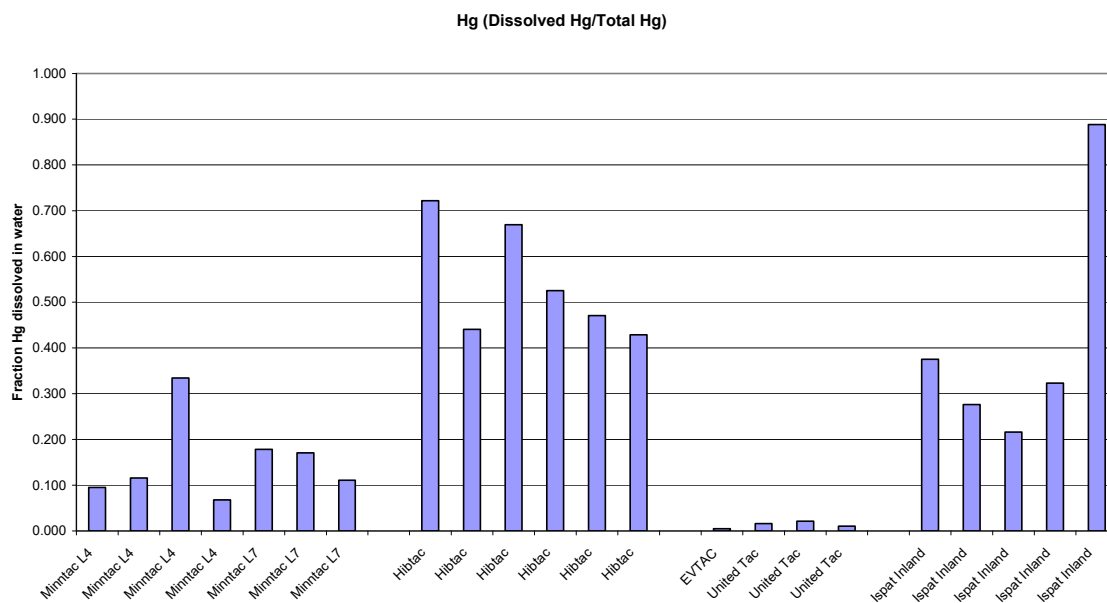


Figure 6. Fraction of mercury in scrubber waters that was initially present in dissolved form. Dissolved and adsorbed forms of mercury must be taken into account when designing mineral processing schemes to focus mercury into tailings basins. The dissolved fraction is higher at Hibtac and Ispat-Inland than it is at Minntac and United Taconite (Formerly Evtac). It is thought that the difference may be chemistry related (SO₂ and HCl).

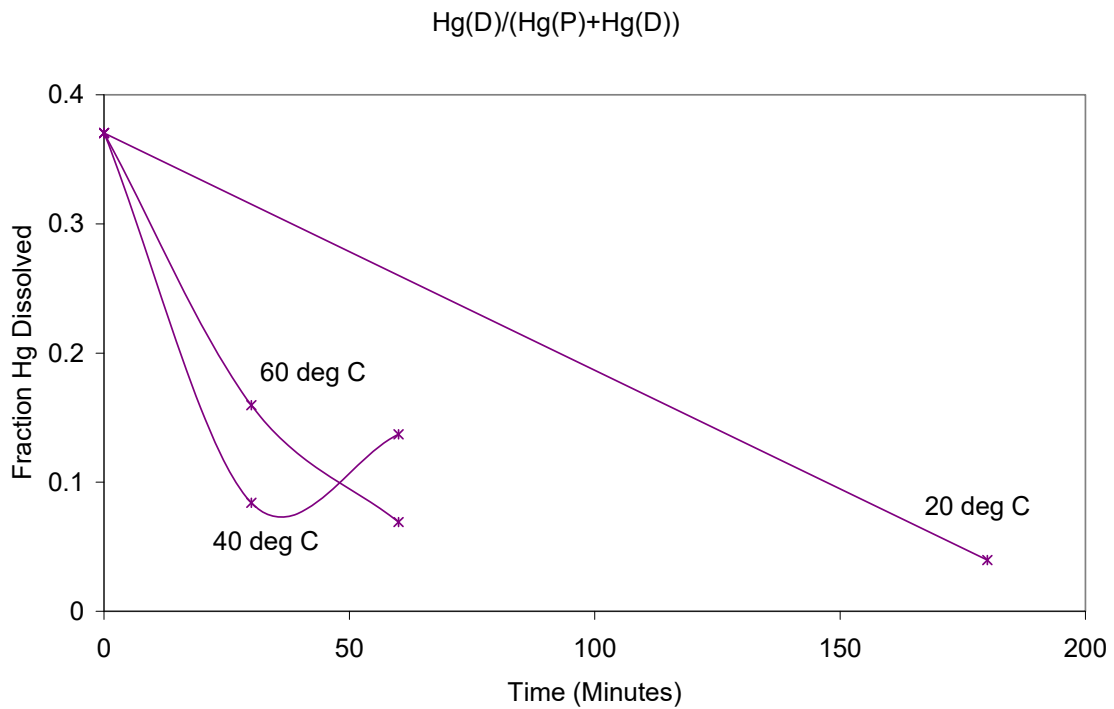


Figure 7. Results from adsorption experiments performed previously at Minntac showing that mercury present in scrubber water adsorbs to scrubber solids over time. These results indicate that filtration must take place immediately upon sampling for applications where knowledge of the fraction of dissolved mercury is needed.

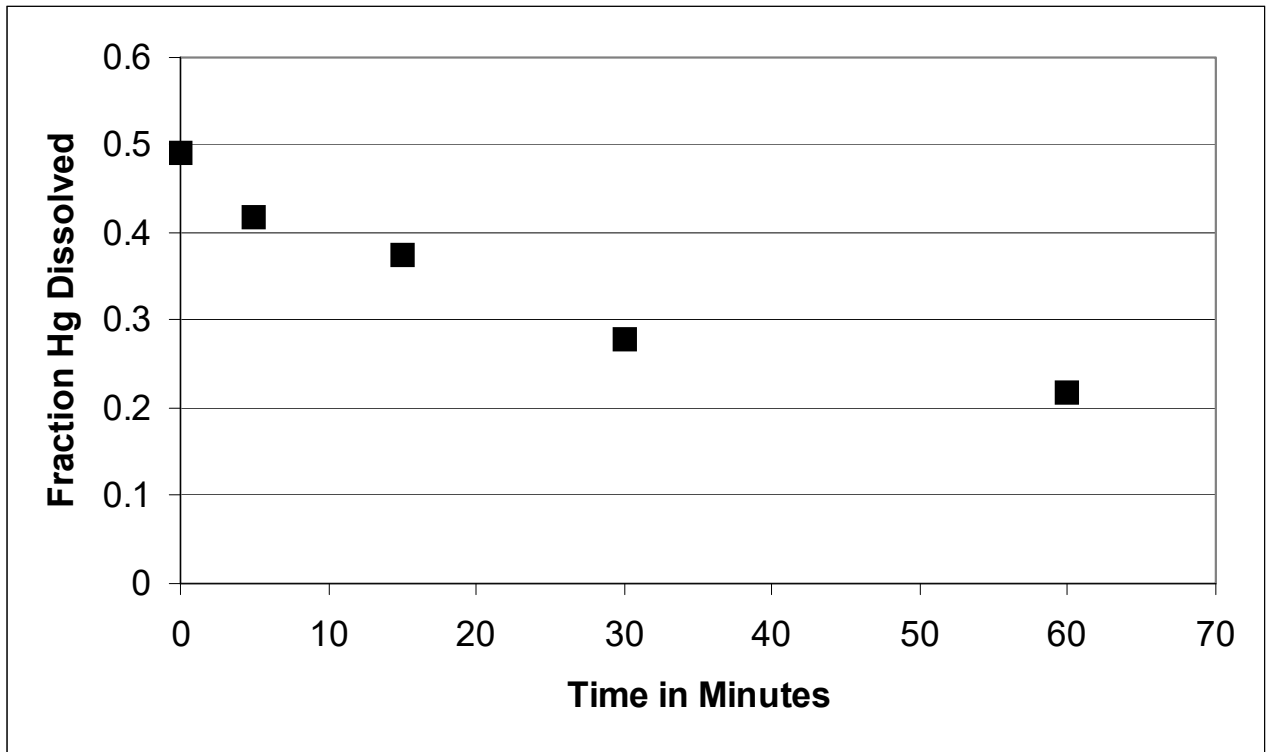


Fig. 8. Results of adsorption experiments performed on scrubber solids at Hibtac. While approximately half of the mercury captured by plant scrubbers in this plant is dissolved (the other half is adsorbed to particulates), the fraction of mercury dissolved decreases to approximately 20% in one hour, even without addition of adsorbing solids.

Appendix B-1-5

Mercury Transport in Taconite Processing Facilities: (I) Release and Capture During Induration

August 15, 2005

**Mercury Transport in Taconite Processing Facilities: (I)
Release and Capture During Induration**

Aug. 15, 2005

**Michael Berndt and John Engesser
Minnesota Department of Natural Resources
Division of Lands and Minerals**

Iron Ore Cooperative Research Final Report

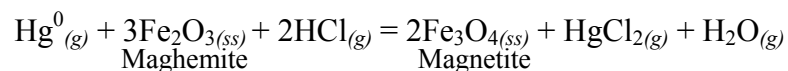
Table of Contents

1. Abstract.....	3
2. Introduction.....	3
3. Methods	5
3.1. Heating Experiments.....	6
3.2. Greenball and Undergrate Dust Sampling	6
3.3. Scrubber Water and Greenball Sampling.....	7
Suspended Solids (scrubber dust)	8
Greenball Samples.....	9
3.4. Mössbauer Spectroscopy.....	9
4. Results	10
4.1. Heating Experiments.....	10
4.2. Undergrate Samples	14
4.3. Scrubber Water and Greenball Composition	17
5. Discussion	23
6. Conclusions	29
7. References	29
8. Acknowledgments	31
9. Appendices.....	32
9.1. Taconite Induration Furnaces.....	32
9.2. Taconite Scrubber Systems.....	34
9.3. Heating Experiments (B. Benner, CRML)	36
9.4. Mössbauer Report (T. Berquo, IRM).....	39
9.5. Raw Mercury Data.....	52
Hibtac	52
Minntac.....	54
U-Tac.....	56
Ispat.....	58

1. Abstract

With the recent emergence of atmospheric mercury as an environmental issue, taconite companies have begun looking for cost effective means to reduce mercury in stack emissions. The Minnesota Department of Natural Resources (DNR) has studied the distribution and fate of mercury at four taconite processing facilities across the Iron Range, focusing specifically on release and transport mechanisms. This document provides a mechanistic interpretation for mercury transport in induration furnaces based on data from heating experiments and from field samples collected from grates and scrubber waters at taconite plants.

During taconite processing, wet “greenballs” consisting predominantly of magnetite and possible other components (limestone flux, organic or bentonite binder, trace non-ore components) are conveyed into a furnace and heated to approximately 1200-1300°C in the presence of air. Data from this study suggest that magnetite is first converted to a magnetite/maghemite solid-solution which attracts and collects mercury released from greenballs deeper in the furnace. Mercury release occurs when magnetite and/or magnetite/maghemite solid-solutions are heated past 450 or 500° C and converted to hematite. Wet scrubbers collect oxidized mercury from flue gases, but not volatile $\text{Hg}^0_{(g)}$. Wet scrubbers sometimes capture over 40% of the mercury released during induration, implying that extensive generation and transport of oxidized mercury can occur. On the other hand, scrubber efficiency can also be less than 10% for mercury, indicating that conditions needed for mercury oxidation are not always present. Plants having the highest capture rates for mercury, also appear to have the highest Cl and particulate fluxes, suggesting a relationship such as:



controls mercury oxidation rates during induration. Future work is planned to verify and refine flux estimates and to determine if relatively simple, passive processes such as Cl injection can increase mercury oxidation.

2. Introduction

Taconite is a very hard, relatively low grade ore that forms the basis of the iron industry in Minnesota. In 2005, six taconite companies were active, all of which mined on the Mesabi Iron Range. These include, from west to east: Keewatin Taconite Minnesota Ore Operations (Keetac), near Keewatin; Hibbing Taconite (Hibtac) near Hibbing, US Steel-Minntac (Minntac), near Mountain Iron, United Taconite (U-Tac), near Eveleth, Ispat-Inland Mining Company (IIMC; recently changed name to Mittal Steel, USA), near Virginia, and, finally, Northshore (NS) Mining, with mines located near Babbitt and ore processing facility located on the shore of Lake Superior in Silver Bay. All of these taconite plants were built decades ago to process low-grade iron ore, at a time when Hg was not an issue. Thus, atmospheric Hg emissions from taconite processing have grown with the industry, exceeding

IOCR Final Report

100 kg/yr in the late 1960's, and ranging between approximately 200 and 400 kg/yr ever since (Engesser and Niles, 1997; Jiang et al., 1999; Berndt, 2003).

The Biwabik Iron Formation strikes east-northeast in a continuous band extending approximately 120 miles across northeastern Minnesota. Iron rich portions of the formation were deposited as sediments, probably as a mixture of $\text{Fe}(\text{OH})_3$ and varying proportions of other common material (silica, carbonates, organic carbon, iron-sulfides, clays) and converted to present mineralogy during diagenesis or low-grade regional metamorphism (Morey, 1972; Perry et al., 1983; Thode and Goodwin, 1983; Bauer et al., 1985) except in the eastern sections of the formation which have been subjected to thermal metamorphism during intrusion of the Duluth Complex (Morey, 1972; Ojakangas and Matsch, 1982). By comparison, isotopic data on minerals collected from the western side of the district suggest peak "metamorphic" temperatures are less than 100 or 150° C (Morey, 1972). Because mercury volatilizes at high temperatures, this difference in metamorphic history has affected mercury distributions. Engesser and Niles (1997) and Berndt (2003) found that Hg emission factors reflected primary distribution of mercury in the concentrate, and generally increased in a westward direction across the district from 1 kg/LT (kg per million long ton) pellets at Northshore on the metamorphosed east end of the range, up to approximately 17 kg/LT on the relatively unmetamorphosed west end of the range.

During processing, magnetite is magnetically separated from other solids in the composite ore and the resulting concentrate is rolled with other minor components (fluxing agents, binders) into balls (greenballs). It is the magnetite dominated "greenballs" that are introduced into the induration furnaces where mercury emissions are generated. Because magnetite is, by far and away, the dominant mineral in concentrate and greenballs, concentrations probably represent mercury that is directly associated with magnetite, although evidence of an association with sulfur can sometimes be found, especially in the primary ore.

It is important to note that mercury emissions from taconite are generated under conditions quite distinct from those in the much better studied coal-fired power plants (see Pavlish et al, 2003, for a review). For example, the primary source of mercury emissions in coal-fired power plants is the fuel, while the primary source of mercury released during taconite processing on Minnesota's Iron Range is typically the ore (Berndt, 2003). This is partly because relatively few companies use coal to fire their pellets, while most other companies use natural gas and/or petroleum coke that contains little or no mercury. Even when coal is used, it takes only about 20 to 30 lbs of coal to fire one long ton of pellets so the amount of mercury released from the magnetite concentrate, especially on the west side of the range, greatly exceeds the amount of mercury available from the coal.

Secondly, taconite processing gases remain more oxidizing than is typical for coal-fired power plants, which consume much of the oxygen in the combustion process (Zahl et al., 1995). Oxygen is an important component for reaction with mercury molecules during transport since oxidized mercury, Hg^{2+} , is much more soluble in scrubber waters than the reduced form, Hg^0 . A more oxidizing flue gas may provide more opportunities in taconite plants to control mercury using simple oxidation pathways.

Third, the released mercury is potentially exposed to large masses of heated iron oxide minerals in taconite companies that may be present, but not nearly as abundant, in power plants. This is significant, since it has been shown that iron-oxide minerals can, in some cases, promote oxidation and capture of Hg^0 (Zygarlicke, 2003; Pavlish, 2003). The more oxidizing conditions and the presence of potentially catalytic and/or reactive minerals in taconite plants can impact mercury transport and chemistry in ways not observed at coal-fired power plants.

However, one important similarity between taconite processing and coal-fired power plants is that flue gases in both types of facilities can contain chloride, an important mercury oxidation agent (Pavlish et al, 2003). In the case of power plants, the fuel is the primary Cl source, but fluxing agents and pore fluids that accompany solids into induration furnaces are the primary source of Cl in taconite processing plants.

The present study, was conducted specifically to evaluate how the presence of iron oxides and Cl in Minnesota's processing plants affect mercury transport in induration furnaces. This report represents the first of two documents being prepared on mercury transport in taconite processing facilities and details specifically mercury release and capture mechanisms that take place during induration. A second, later report will detail the ultimate fate of mercury in taconite processing plants once the mercury has been captured by wet scrubbers.

3. Methods

The present study consists of three distinct but inter-related parts:

- (1) A bench-scale experimental study detailing the relationship between mercury release and mineralogy during the heating of disaggregated greenball samples from two processing plants,
- (2) A field study involving systematic collection and analysis of samples of dust collected from beneath the grates in four induration furnaces, and
- (3) A field study characterizing greenball and scrubber water chemistry to evaluate Hg and Cl transport and capture in four induration furnaces.

The first and second parts of this study were designed to provide fundamental information on the release temperatures and characteristics for mercury in induration furnaces. By analyzing when and where mercury is released in the furnaces, it could help to provide information on potential control options. Moreover, it was important to evaluate how the iron-oxides and volatilized mercury interact with each other. Thus, an important component of these studies was use of Mössbauer spectroscopy to evaluate oxidation of magnetite to various phases, including magnetite, magnetite/maghemite solid-solutions, maghemite, and hematite.

The third part of this study involved the collection of greenball and scrubber samples over a period of time to evaluate capture efficiency for mercury, and the factors that might affect it. Particular attention was also paid to distinguish between particulate and dissolved mercury in scrubber waters, since the relative proportion of each can affect mercury control strategies. However, that component of the study will be discussed in much greater detail in the second document in this series.

3.1. Heating Experiments

Bench-scale heating experiments were contracted with and performed by Blair Benner of the Coleraine Mineral Research Laboratory (CMRL). A full description of procedures is provided in the Appendix (section 9.3). Briefly, greenball samples collected from Hibtac (standard pellets contained about 1% limestone) and Minntac (fluxed pellets containing approximately 10% limestone flux), were dried, crushed, and then heated in either N₂ gas or air for periods of time ranging between 5 and 20 minutes. Temperatures ranged from 300 to 700°C for Minntac samples, and from 300 to 600°C for Hibtac samples. Mercury concentrations of run products were measured and compared to those in splits from the original sample. Iron-oxide mineralogy of selected samples was determined using Mössbauer spectroscopy at the University of Minnesota, Institute for Rock Magnetism (see section 3.4 below).

3.2. Greenball and Under-grate Dust Sampling

To further evaluate mercury transfer processes, samples were collected from beneath the grates in active induration furnaces at each of the four facilities in our study. In each case, sampling sites were chosen in consultation with mining personnel. An important distinction between plants is that two of the operations use “grate-kiln” furnaces (Minntac and United Taconite) while the other two operate “straight-grates” (Hibtac and Ispat-Inland). Grate-Kiln facilities dry and heat pellets on a grate, but final firing is done in a rotating kiln. Drying, heating, and firing procedures are all performed on the grate in a straight-grate facility, however, a “hearth layer” consisting of pre-fired pellets is added beneath fresh greenball samples to protect the grate from the intense heat used in the firing zones. Schematic diagrams for each of the induration plants are presented in the Appendix (section 9.1). This fundamental difference in plant design, when superimposed with other less distinct differences in plant operation procedures makes every plant on the Iron Range unique. Significant differences can even exist between different lines in different plants. For example, Minntac employs both ported and non-ported kilns, which affect the manner in which oxygen is added to the kiln (more exposure to oxygen takes place in a ported kiln). In our case, under-grate dust samples were collected from Line 7, which is a ported kiln. United Taconite is also a grate-kiln facility, and its kiln is non-ported.

The method of sample collection varied depending on the dust collection configuration available at the plant. For the straight-grate plants (Hibtac and Ispat-Inland), windboxes collect dust and pellet chips as the pellets move on the grate from the drying zone into the preheat and firing zones. The dust, in these cases was collected using clean aluminum pans, which were held beneath the windbox ports. The hot dust samples spilled into the pan when

the windboxes opened. Samples were covered and allowed to cool, and then sieved to remove pellet chips back at the laboratory. The <100-mesh material was analyzed for mercury at Cebam, Inc. Selected samples were also analyzed for iron-oxide mineralogy using Mössbauer spectroscopy (see section 3.4 below).

A similar process was used for collection of samples at the grate-kiln plants (Minntac and United Taconite), however, the down draft drying zone samples could not be collected dry at Minntac because the samples were only available after being mixed with process water. Solids for these samples were collected from the laundered samples on a glass fiber filter (0.7 μ) and dried at 100° C overnight prior to being analyzed for mercury and iron oxide mineralogy.

In each case, information on temperature was collected (where available) for the zones where dust was sampled.

3.3. Scrubber Water and Greenball Sampling

The same four companies involved in the under-grate sample part of this project were selected for participation in our scrubber-water and greenball sampling study. Sampling sites were again chosen in consultation with mining personnel. Schematic diagrams for each of the scrubber systems are presented in the Appendix (section 9.2).

Hibtac combines scrubber water effluent from three lines into one stream flow that leads back to the concentrator. A valved sampling site was selected from this stream. Minntac Line 7 dispenses their scrubber effluent into a thickener along with other streams. Scrubber water samples were collected as a split stream of the main flow leading into the thickener. Minntac Line 4 has a valve that can be opened to collect scrubber water samples. United Taconite and Ispat Inland have recirculating scrubber systems, but continuously provide make-up water that replenishes the system and allows a continuous blow-down stream to be maintained, containing dust and dissolved components caught by the scrubber system. A valved port exists at each plant that was used for sampling of the “blow-down” water. United taconite has tandem but identical thickeners, but only one was sampled for all but the final sampling visits when both were sampled.

Berndt et al (2003) showed that scrubber waters contain a significant dissolved component in addition to mercury bound to particulates. They showed further that the ratio of particulate to dissolved mercury increases with time following collection of the sample. The dissolved mercury adsorbs to the solids. Thus, different results are obtained if a sample is filtered at the plant or if the sample is filtered later, just prior to analysis. Subsequent studies showed that the time scale for increased adsorption to particulate is on the order of minutes and hours. For the most accurate results on the relative dissolved and particulate mercury loads, it is necessary, therefore, to filter scrubber water samples within the first few minutes of sampling.

At each plant, water samples were collected in a clean two-liter plastic bottle from which sub-samples were decanted. Filtration was performed immediately using acid washed

IOCR Final Report

filtration units and pre-weighed membrane filters (0.45 μ m, Pall Corporation). The filtered water was placed in an acid washed glass jar with Teflon-lined lid. The filters containing the filtrate were placed into separate 10 ml acid washed jars and the filter weight was recorded.

All samples for mercury analyses were collected using “clean-hands, dirty-hands” procedures, whereby the clean bottles were placed into sealed plastic bags prior to leaving the laboratory and not opened except during sampling, and then again later when the analysis was being conducted. Only the designated clean-hands person, wearing clean plastic gloves, handled the sample bottles when they were outside of the plastic bag. All other sample processing was conducted quickly and efficiently by the so-called “dirty-hands” person. These procedures were implemented to minimize the risk of contamination from plant dust and of cross-contamination between samples.

In addition to these special precautions, procedures were consistently evaluated using blanks to assess the degree of mercury contamination associated with filtration and sampling. Procedural blanks were collected at each site during each visit. One bottle was filled at the sampling site with deionized water brought from the laboratory. In addition, deionized water was filtered at the sampling location and both the water and the filter were saved for analysis. The level of contamination introduced by our procedures was insignificant relative to the concentration of mercury found in samples analyzed in this study. Samples were analyzed by Cebam Analytical, Inc., located in Seattle, Washington. Filtered water samples were digested with BrCl over night, and then analyzed by SnCl₂ reduction, gold trap collection, and CVAFS detection (modified EPA1631). This laboratory participates in many round-robin blind sampling programs and routinely ran duplicates and standards to ensure accuracy.

Temperature, pH, and conductivity were measured on site. Temperature and pH were measured using a Beckman Model 11 meter with a Ross Model 8165BN combination pH electrode and a Beckman Model 5981150 temperature probe, while specific conductance was measured with a Myron L EP series conductivity meter.

For cation (Ca⁺⁺, Mg⁺⁺, K⁺, Na⁺, etc..) analyses, samples were filtered and acidified with nitric acid in the field and then analyzed by inductively coupled plasma mass spectrometry (ICP-MS) at the University of Minnesota, Department of Geology and Geophysics. For anions (Cl⁻, Br⁻, SO₄⁼, etc..), samples were stored in clean plastic bottles and analyzed using ion-chromatography (IC, Dionex Ion Chromatograph fitted with a GP40 gradient pump, CD20 conductivity detector, and two AS4 anion exchange columns) at the University of Minnesota, Department of Geology and Geophysics.

Suspended Solids (scrubber dust)

Filters containing scrubber solids from the above procedures were dried at 104°C for analysis, weighed, and digested in hot acid (HCl/HNO₃, 3/1). Particulate mercury was analyzed using SnCl₂ reduction and gold trap collection, followed by CVAFS detection (modified EPA1631). Certified reference materials WS-68, NIST2709, and GSR-2 were used to assess recovery and analytical accuracy. As was the case for water samples, solids were digested and analyzed by Cebam Analytical, Inc., located in Seattle, Washington.

Total suspended solids (TSS) were analyzed by filtering a two-liter sample of scrubber water collected specifically for this purpose. Solids from this sample were collected on a glass fiber filter (0.7 μ), dried at 104°C overnight, and weighed.

Greenball Samples

Greenball samples were commonly collected as a means to assess mass balance with respect to components entering and leaving the furnace (Cl and Hg, in particular). The sample collection point, in all cases, was at the front end of the induration furnace, just prior to the point where the greenball is fed onto the grate. The samples were placed into clean, acid-washed 250 ml bottles with Teflon-lined lids. The damp greenball samples, which contain approximately 9 to 10% moisture by weight, were dried in the Hibbing laboratory and gently disaggregated prior to sending to Cebam, Inc., for total mercury analysis. Several samples were sent, as well, to the University of Minnesota, IRM, for Mössbauer spectroscopy.

To assess Cl transport and addition of other salts (Na, Ca, K, Br, SO₄) to induration furnaces, 100 grams of dry greenball material from each of the four plants was leached for approximately one week in 100 grams of deionized water. The water was then filtered and analyzed for major cations and anions using ICP-MS and ion-chromatography, respectively, at the University of Minnesota, Department of Geology and Geophysics. The resulting concentrations were reported as water-leachable salts.

3.4. Mössbauer Spectroscopy

Mössbauer spectroscopy is a sensitive technique for measuring the atomic environments of iron atoms in a compound. The technique works by measuring absorption of gamma radiation of very specific wavelengths, generated by an oscillating radioactive source material (⁵⁷Co). The oscillation causes a Doppler shift of the emitted gamma radiation, while a detector records absorption as a function of gamma wave frequency. Thus, results are typically presented in terms of absorption versus velocity of the radioactive source. The details of the technique are not important for this discussion, but it is important to realize that the method permits clear distinction and quantification of the relative amounts of iron that are found in the crystal lattices of magnetite and various oxidation products. Mössbauer spectroscopic measurements were made by Dr. Thelma S. Berquó at the Institute for Rock Magnetism, University of Minnesota, Minneapolis, MN. A detailed discussion of the technique and results are provided in the Appendix (Section 9.4).

Considerable importance in this study was placed on the relative distribution of iron on A and B sites of magnetite grains. As magnetite oxidizes it forms a solid solution between magnetite and maghemite. The oxygen is added by increasing the proportion of oxidized iron in A versus B sites and accommodating this change with the introduction of site vacancies in the B site. Mössbauer spectroscopy not only evaluates mineralogy of iron oxides (e.g., magnetite, maghemite, and hematite), but determines the relative distribution of iron atoms in magnetite that are located on A or B sites. Relationship between relative absorption of gamma rays by iron on magnetite A and B sites has been related to magnetite composition by Coey (1971) and Papamarinopoulos et al. (1982), and is displayed in Figure 3.4.1.

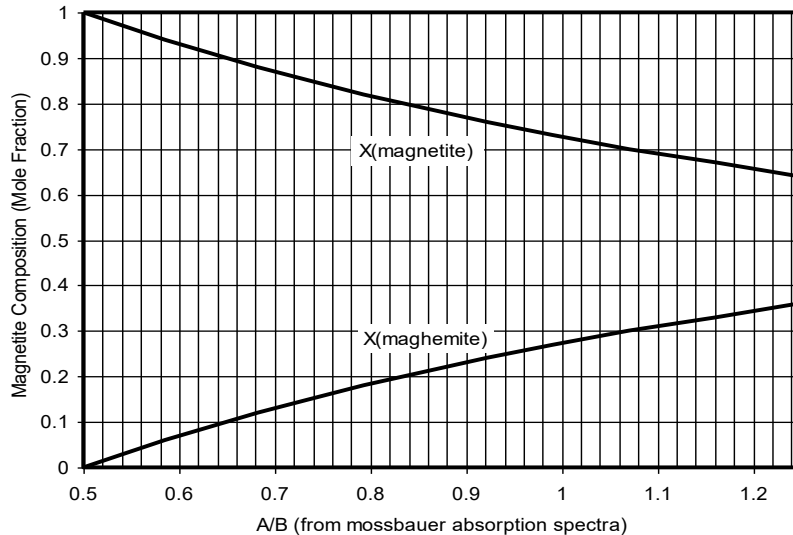


Figure 3.4.1: Ideal relationship between A/B from Mössbauer spectroscopic measurement, and magnetite/maghemite solid solution composition.

4. Results

4.1. Heating Experiments

Results from the heating experiments are provided in Tables 4.1.1 and 4.2.1, displayed in figures 4.1.1 and 4.1.2, and presented in greater detail in the Appendix (Section 9.3).

The mercury in the starting greenball sample from Hibtac was close to 21 ng/g, and the mercury remaining decreased with temperature following heating at 300 to 600°C (Fig 4.1.1), regardless of whether heating occurred in air or in N₂ gas. However, the loss of mercury to N₂ gas was greater than the loss to air at 300 and 400°C. The loss in mercury to N₂ and air was nearly the same, however, once the samples were heated to 500°C. Thus, mercury is apparently less mobile in the presence of magnetite under oxidizing conditions than under a N₂ atmosphere at intermediate temperatures.

Experiments on Hibtac samples heated in air or N₂ at 450°C for different time periods (Fig. 4.1.2) demonstrated that most of the mercury removal is rapid at this temperature, with 75% of the mercury loss occurring within the first five minutes. There was little difference in mercury loss at 450°C for experiments conducted with N₂ or air.

Experiments conducted on Minntac greenball samples (Fig. 4.1.1) showed somewhat similar trends to those shown for Hibtac samples, however, the difference between mercury volatilization in air or N₂ was present at all temperatures, 300 to 700°C. More mercury was released in N₂ such that volatilization was nearly complete by 600°C. However, 27% of the mercury remained during heating of the Minntac greenball for 20 minutes at 700°C.

Four samples from experiments on Minntac greenballs were analyzed by Mössbauer spectroscopy to gauge mineralogic changes occurring to iron oxides in the two types of

IOCR Final Report

experiments (N₂ or air). The starting sample was found to contain magnetite that was slightly oxidized to begin with as indicated by A/B = 0.72 (as opposed to 0.50 for stoichiometric magnetite). Heating this material in N₂ for 20 minutes at 500°C resulted in a decrease in the amount of magnetite and a dramatic shift in magnetite composition (to A/B = 0.59). Some of the magnetite was replaced by a mineral that appeared to be a mix of maghemite and hematite. One possibility is that the initial magnetite simply unmixed into near-stoichiometric magnetite and Fe₂O₃. It appears that much mineralogic change can occur to magnetite while heating to 500°C for only 20 minutes, even in the absence of O₂.

Mössbauer results for samples heated in air at 400 and 500°C revealed systematic mineralogic changes. 11% of the magnetite was replaced by hematite at 400°C while 23% was replaced by hematite during heating at 500°C. Moreover, the magnetite that remained became systematically more oxidized, with A/B increasing from 0.72 in the starting material, to 0.98 at 400 and 1.26 at 500°C (approximately 27 and 36 percent maghemite component, respectively).

Table 4.1.1 Mercury concentrations for samples from heating experiments involving Greenball from Hibtac.

<i>Temperature (°C)</i>	<i>Gas</i>	<i>Time (min)</i>	<i>Hg (ng/g)</i>	
Start			20.69	
			20.34	
			21.39	
			21.01	
300 (572°F)	Air	20	17.68	
	N ₂	20	9.21	
400 (752°F)	Air	20	12.72	
	Air	20	11.43	
450 (842°F)	N ₂	20	4.17	
		Air	5	5.09
		Air	10	3.06
	N ₂	15	1.86	
		5	5.87	
		10	4.63	
500 (932°F)	Air	15	2.46	
		20	2.61	
		20	2.39	
600 (1112°F)	Air	20	1.50	

Table 4.1.2 Mercury concentration and mineralogy of samples from Minntac Greenball heating experiments.

<i>Temperature (°C)</i>	<i>Gas</i>	<i>Time (min)</i>	<i>Hg (ng/g)</i>	<i>Mineralogy*</i>	<i>Magnetite A/B</i>
Start			7.62	100 % mt	0.72
			7.59		
300 (572°F)	Air	20	6.42		
	N ₂	20	2.69		
400 (752°F)	Air	20	2.89	89% mt, 11 % hm	0.98
	N ₂	20	0.75		
500 (932°F)	Air	20	3.70	77% mt, 23% hm	1.26
	N ₂	20	0.92	89% mt, 11% hm?	0.59
600 (1112°F)	Air	20	2.17		
	N ₂	20	0.48		
700 (1292°F)	Air	20	2.07		

* mt = magnetite solid solution, hm=hematite, hm? = sample with ambiguous pattern

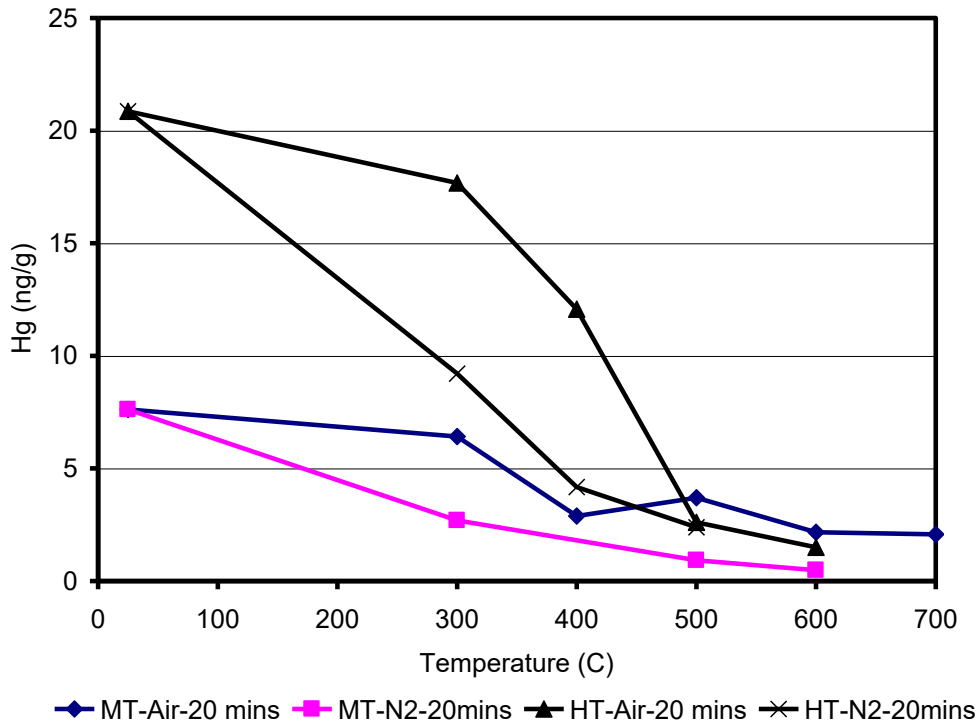


Figure 4.1.1 Mercury remaining in Minntac (MT) and Hibtac (HT) greenball samples after heating in air or nitrogen gas for 20 minutes in a tube furnace at temperatures from 300 to 700°C.

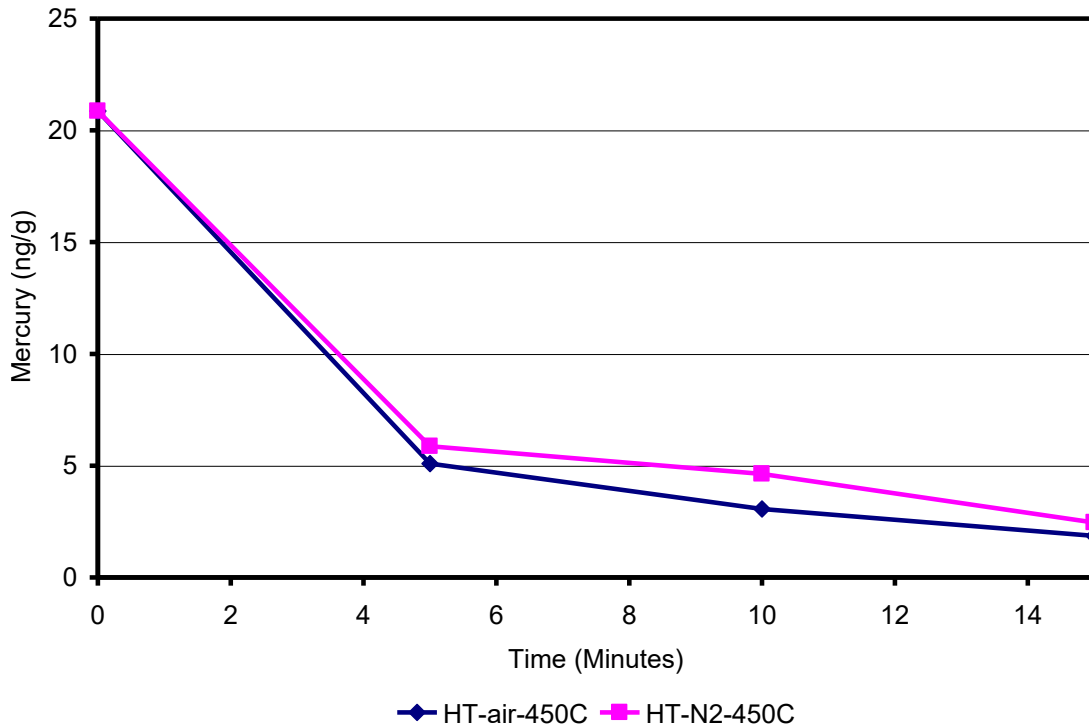


Figure 4.1.2. Concentration of mercury in samples that remained after heating Hibtac Greenball samples in air or N₂ at 450°C for 0 to 15 minutes.

4.2. Under-grate Samples

Numerous dust samples were collected from beneath taconite grates during the course of the study and analyzed for mercury and iron oxide mineralogy (%hematite, % magnetite, % maghemite and relative A/B values (see section 3.4). Locations and dates are provided in Table 4.2.1 along with the pertinent data on location, temperatures, mercury concentration, and iron-oxide mineralogy.

Mercury concentrations were surprisingly elevated in some samples (Fig. 4.2.1). For example, concentrations of mercury reached as high as 464 ng/g in the preheat zone (Windbox 14) at Hibbing Taconite; 91 ng/g at Minntac Line 7 in the down draft drying zone (DD1), and 60 ng/g in the preheat zone at Ispat Inland (Windbox 13). These high mercury concentrations indicate that mercury released from greenball in some parts of the furnace (high temperature) can adsorb to taconite dust at lower, but still elevated, temperatures. The concentration of mercury on dust from United Taconite grates does not reach high levels, owing likely to a large dilution effect with dust that has been heated to high temperatures. Dust generation and collection at United Taconite appeared to be a much more extensive process than at the other plants.

The temperature of this adsorption process is not easy to determine due to the intense thermal gradients that exist in induration furnaces. For example, the pellet bed in taconite furnaces is only 5 to 6 inches thick in grate/kiln furnaces and about 16 inches thick in straight-grate furnaces, including a greenball layer stacked on top of a 3-inch hearth layer of pre-fired pellets. In some parts of the furnaces, depending on the plant, the temperature across the bed can differ by well over 1000°F (or well over 500°C) see Table 4.2.1.

Another difficulty is that although the sampling location for the dust is known, the source of the dust is not well known. Some light can be shed on this from the mineralogy of the iron oxides (Figure 4.2.2). Most of the dust in the United Taconite samples were highly elevated in hematite, suggesting much of this dust had been exposed to very high temperatures, perhaps derived from the kiln. One of the drying zone samples collected at Hibtac also had high hematite, but the source of this hematite may be the hearth layer. A dust sample collected at Minntac from the preheat zone also contained elevated hematite levels, indicating it was derived from a relatively hot zone, most likely the kiln.

Interestingly, all of the samples still contained a significant magnetite component with A/B ratios only slightly modified compared to the starting greenball samples. At Hibtac, A/B for the magnetite component increased gradually from 0.57 in the starting sample only to 0.69 for the sample in the firing zone. The change in A/B at other plants was less systematic. The A/B trend, along with decreased thermal gradients at Hibtac, and the more pronounced Hg peak suggest that the overall heating rate is low at this plant compared to others. Slower heating may lead to more time for magnetite to oxidize without converting to hematite. The oxidation of magnetite to magnetite/maghemite solid-solutions (as indicated by increasing A/B), however, is much less than that observed from the experimental run products discussed in section 4.1 where A/B increased to 0.98 after 20 minutes of heating at 400C.

Table 4.2.1 Locations, temperatures, mercury concentrations, mineralogy and magnetite composition (A/B) of samples collected from taconite plants during this study.

<i>Plant</i>	<i>Location**</i>	<i>Overbed T (°F)</i>	<i>Underbed T(°F)</i>	<i>Hg ng/g</i>	<i>Mineralogy* %mt / %hm / %mh</i>	<i>Magnetite A/B</i>
Hibtac 1/27/04	Greenball			11	96 / 0 / 4	0.57
	UDD WB2.5	342	490	18		
	UDD WB6.5	342	490	32	50 / 50 / 0	0.61
	DDD WB8	573	340	19	94 / 6 / 0	0.62
	PH WB12	897	195	94	90 / 10 / 0	0.64
	PH WB14	1248	202	464	94 / 6 / 0	0.65
	PH WB16	1402	253	127		
	FZ WB18	2300	350	22	88 / 12 / 0	0.69
Minntac Line 7 7/27/04	Greenball			12	100 / 0 / 0	0.61
	DD1	654	199	91	91 / 9 / 0	0.65
	DD2	1049	246	57		
	DD2	1443	493	66	91 / 9 / 0	0.63
	PH WB1	2076	544	15		
	PH WB3	2076	890	2.7	36 / 64 / 0	0.56
	PH WB5	2076	1215	0.7		
United 11/29/04	Greenball			14	100 / 0 / 0	0.59
	DDD	525	384	24		
				24		
				21		
				24	37 / 63 / 0	0.48
	PH	1852	1291	1.7		
				1.6	35 / 65 / 0	0.59
			1.6			
			2.2			
Ispat 2/15/05	Greenball			10		
	DDD WB9	720	250	7	92 / 8 / 0	0.64
	DDD WB 11	720	250	10	87 / 13 / 0	0.61
	PH WB 13	1854	250	60	91 / 9 / 0	0.60
	PH WB17	2257	700	58	92 / 8 / 0	0.61
	FZ WB 19	2332	725	26	74 / 26 / 0	0.61
	FZ WB 21	2313	730	10	63 / 37 / 0	0.75

* mt=magnetite, hm=hematite, mg=%maghemite

** UDD=Updraft drying, WB=windbox, DDD=Downdraft drying, PH=preheat, FZ=Firing Zone.

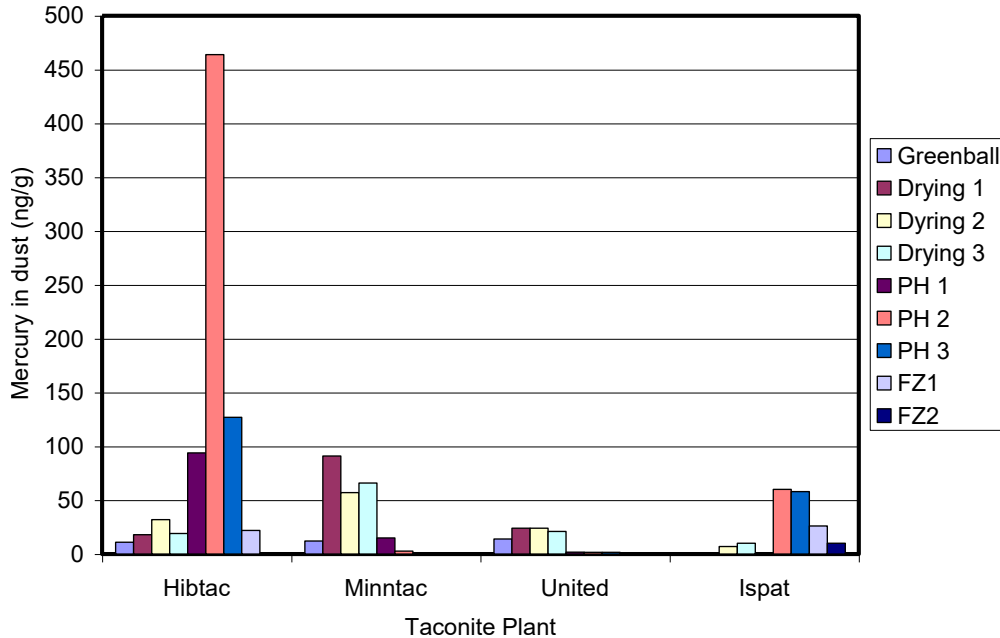


Figure 4.2.1. Mercury concentrations of dust samples collected from grates at taconite plants. Left to right on this graph for each plant represents samples collected from progressively deeper locations in the furnaces: drying zones, preheat, and firing. Hibtac and Ispat samples are from straight grates where highest mercury concentrations appear to be found in dust from preheat zones. Minntac and United, both grate-kiln plants, have their highest mercury levels in dust samples collected from the drying zones. The relative amount of mercury likely depends on the amount of dust generated, the amount of mercury available, and the specific temperatures to which the dust was exposed.

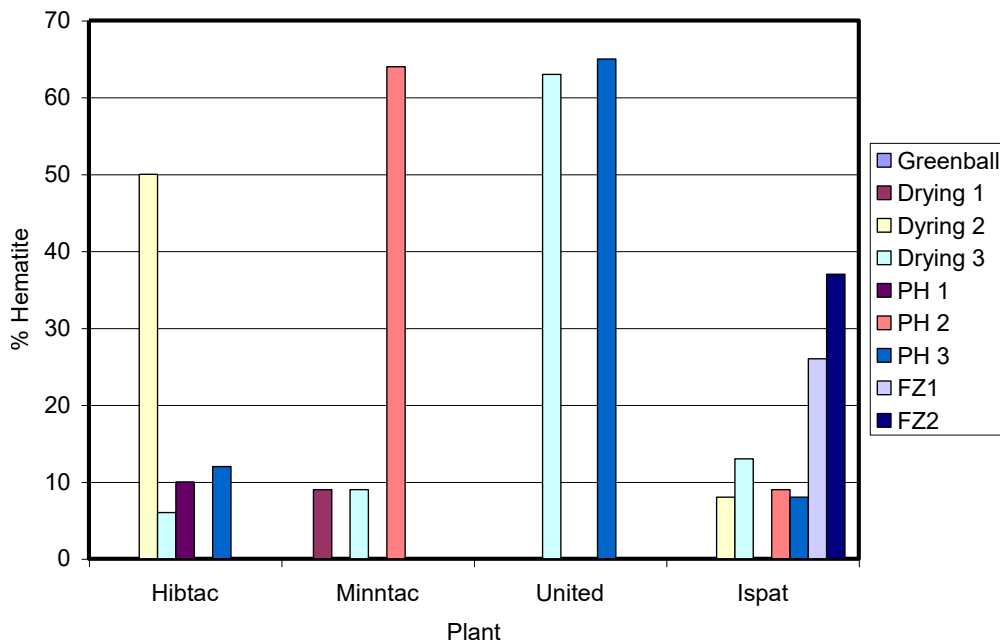


Figure 4.2.2. % Hematite for dust samples collected at taconite plants. None of the greenball samples had significant hematite and so those samples are plotted as zero % hematite on this graph. Samples from the other locations with apparent zero values were not analyzed. Temperatures representative of each zone at the time of collection are shown in Table 4.2.1.

4.3. Scrubber Water and Greenball Composition

The purpose of this portion of the study was to collect data that could be used to calculate mercury, Cl, and particulate flux values for taconite induration furnaces. By collecting information on the composition and mass of solids entering the furnace, the flux of elements and particulates can be estimated. Similarly, by collecting information on the scrubber water composition and flow rate, the flux of mercury being collected by the scrubber system can be estimated.

Greenball feed, pellet production, and scrubber water flow rates for the plants at the time of each visit are provided in Table 4.3.1. Data previous to September 2003 are included in the tables and these data were taken from Berndt *et al.* (2003). It is important to note that greenball feed rates are measured for wet samples, while most analyses are performed on a dry weight basis. Also, many of the greenball samples that are placed on a grate can break up in the furnace and are responsible for creating the dust and chips sampled in section 4.2. Another estimate of overall feed rate, subtracting moisture and loss from pellet degradation can be made using the weight of the pellet product, although in this case, oxygen is added to the Fe-oxide, increasing the weight of the overall solids, while CO₂ liberation from the limestone flux results in approximately 4-5% weight loss for the fluxed pellets produced at Minntac and Ispat-Inland.

Scrubber water flow rates are also subject to some uncertainty, depending on the plant. Hibtac and Minntac both monitor flow rates continuously and so a new reading was made during each visit. However, the flow rates at United Taconite were not measured until recently (Brad Anderson, personal communication). The value obtained (810 gpm total for two scrubbers) was used for the entire study. Plant personnel were relied on to provide flow rate estimates at Ispat-Inland which, like United Taconite, does not provide continuous measurement of flow for its scrubber. The flow rate was assumed equal to the estimated pumping rate of 350 gpm throughout the study period.

Greenball sampling began in January, 2004, and the measured mercury concentrations varied considerably: 18.6 ± 5.7 for Hibtac; 11.3 ± 3.2 for Minntac; 16.6 ± 5.1 at United Taconite; and 8.4 ± 1.3 at Ispat Inland all on a dry weight basis and in units of ng/g. At this point, sampling frequency and absence of procedural blanks was insufficient to determine if the variation was due to handling and analytical error, or if it is caused by real monthly variation in the mercury concentration of greenballs. Multiple greenball samples will be collected and sampling and drying methods will be studied further in future visits.

A similar amount of variation was observed for scrubber water samples. However, in this case, sampling frequency was greater each visit and procedural blanks were collected. At least some of the observed variation in composition is “real”, although several samples with unusual values were encountered and rejected. Full data sets of data for mercury samples are provided in the Appendix (Section 9.5).

IOCR Final Report

Three different mercury concentration numbers are reported in Table 4.3.2. Hg(D) is the dissolved concentration for mercury that was determined on samples that were filtered immediately upon collection in the field, and represents the best value for dissolved mercury in water as the water leaves the scrubber system. Hg(P) is the concentration of mercury in dried filtrate solids (ng/g), but only for those solids filtered from the water immediately upon sampling. Hg(T) is the total mercury in the scrubber water, and this was measured in two different ways. The first method is to add dissolved mercury to particulate mercury (as calculated from separate measurements of Total Suspended Solids, TSS, and the concentration of mercury on the suspended solids on a dry solid basis, Hg(P)). The second method is to collect an unfiltered sample and send it to the laboratory for analysis of total Hg. Both methods were used here, and the average of all values for each sampling round is reported as Hg(T) in Table 4.3.2.

Other parameters of potential use for scrubber waters are reported in Table 4.3.3, including *pH*, indicative of capture of acidic gases, and Cl, Ca, and SO₄, elements that can change rapidly during scrubbing of process gases owing to capture of HCl and H₂SO₄. The source of Ca is unclear, but it was shown to increase significantly in scrubber waters from recirculating systems, possibly in response to reaction between solids and acid. This is demonstrated by the results of a one day test that was conducted on 2/14/05 to 2/16/05 (Table 4.3.4). In this test, scrubber water leaving the system was compared to scrubber water feed, and the change in composition was measured. HF, HCl, and H₂SO₄ (partly from oxidized SO₂) increase the most during scrubbing. Ca increases most rapidly at United Taconite which operates at *pH* between 3.5 and 4.5. Almost no change in Ca is observed at Hibtac and Minntac, which operated at less acidic *pH* values around 7.2 and 5.7, respectively.

Also reported in Table 4.3.4 are the results of greenball leach studies. The values represent leachable salts on a dry-greenball weight basis. Most of the Cl and Br in dried greenballs comes from salts that remain following evaporation of pore fluids. This concentration is used later to estimate Cl flux in furnaces.

IOCR Final Report

Table 4.3.1 Plant parameters at time mercury samples were collected.

<i>Plant</i>	<i>Date</i>	<i>Greenball Feed LT/hr</i>	<i>Pellet Type</i>	<i>Scrubber Flow (gpm)</i>	<i>Prod. Factor.</i>	<i>Pellet Production LT/hr</i>
Hibtac	02/20/03	450	Standard	3300	0.75	338
Hibtac	05/08/03	450	Standard	3315	0.75	338
Hibtac F1-2	09/11/03	354	Standard	3000	0.75	265
Hibtac F1-3	01/27/04	397	Standard	3206	0.75	298
Hibtac F1-3	05/12/04	401	Standard	3453	0.75	301
Hibtac F1-2	07/27/04	417	1% Flux	3372	0.75	312
Hibtac F1-3	02/15/05	415	.4% Flux	3406	0.75	311
Hibtac F1-3	05/19/05	456	.4% Flux	3923	0.75	342
	Average	417		3372	0.75	313
Minntac L4	02/19/03	600	Standard	2650	0.84	504
Minntac L4	05/09/03	540	Fluxed	2645	0.84	454
Minntac L4	09/10/03	403	Standard	2980	0.84	339
Minntac L4	01/28/04	530	Standard	2900	0.84	445
	Average	518		2794	0.84	435
Minntac L7	01/28/04	530	Fluxed	2800	0.78	413
Minntac L7	05/11/04	505	Fluxed	3050	0.78	394
Minntac L7	07/27/04	605	Fluxed	2820	0.75	454
Minntac L7	12/01/04	497	Fluxed	3000	0.85	422
Minntac L7	02/16/05	490	8% Flux	3018	0.84	412
Minntac L7	05/20/05	600	8% Flux	3000	0.84	504
	Average	538		2948	0.81	433
EVTAC	02/18/03	600	Standard	810	0.87	522
United Tac	01/28/04	560	Standard	810	0.87	487
United Tac	05/11/04	604	Standard	810	0.87	525
United Tac	07/28/04	630	Standard	810	0.87	548
United Tac	11/29/04	549	Standard	810	0.87	478
United Tac	02/14/05	435	Standard	810	0.87	378
United Tac	05/19/05	598	Standard	810	0.87	520
	Average	563		810	0.87	490
Ispat Inland	02/20/03	240	Standard	350	0.62	149
Ispat Inland	05/08/03	340	Fluxed	350	0.62	211
Ispat Inland	09/11/03	510	Fluxed	350	0.62	316
Ispat Inland	01/27/04	420	Fluxed	350	0.62	260
Ispat Inland	05/12/04	501	Fluxed	350	0.62	311
Ispat Inland	11/30/04	554	Fluxed	350	0.62	343
Ispat Inland	02/15/05	428	10% Flux	350	0.62	265
Ispat Inland	05/19/05	530	10% Flux	350	0.62	329
	Average	440		350	0.62	273

IOCR Final Report

Table 4.3.2 Mercury concentrations and TSS for greenball and scrubber water samples. Hg(D) = Dissolved mercury, Hg(P) = concentration of mercury in dried filtrate, Hg(T) = total mercury concentration including dissolved and particulate fractions.

<i>Plant</i>	<i>Date</i>	<i>Greenball Hg (ng/g)</i>	<i>Hg(D) (ng/l)</i>	<i>Hg(P) (ng/g)</i>	<i>TSS (wt%)</i>	<i>Hg(T) (ng/l)</i>
Hibtac	2/20/2003		256	1406	0.010	492
	5/8/2003		339	606	0.033	532
	9/11/2003		231	604	0.038	460
	1/27/2004	10.9	292	1484	0.018	556
	5/12/2004	16.5	237	2039	0.013	502
	7/27/2004	20.6	294	2813	0.014	688
	2/15/2005	18.6	721	2874	0.024	1410
	5/19/2005	26.4	234	8396	0.006	731
	Average	18.6	325	2528	0.019	671
	St. Dev.	5.7	164	2525	0.011	314
Minntac Line 4	2/19/2003		116	1285	0.058	1167
	5/9/2003		81	160	0.315	578
	9/10/2003		474	434	0.217	1993
	1/28/2004		164	1557	0.145	2422
	Average		209	859	0.184	1540
	St. Dev.		180	668	0.109	826
Minntac Line 7	1/28/2004		223	2489	0.041	1251
	5/11/2004	8.1	291	2723	0.052	1706
	7/27/2004	11.6	305	2564	0.095	2746
	12/1/2004	8.5	234	2830	0.075	2357
	2/16/2005	12.0	331	2855	0.058	1987
	5/20/2005	16.1	256	1360	0.100	1613
	Average	11.3	273	2470	0.070	1943
	St. Dev.	3.2	42	563	0.024	541
Evtac United	2/18/2003		64	979	0.916	6612
	1/27/2004		273	697	0.903	6571
	5/11/2004	13.2	164	594	1.270	7714
	7/28/2004	12.4	112	459	2.260	10491
	11/29/2004	13.8	32	322	2.410	7791
	2/14/2005	24.3	1440	848	2.180	19923
	5/19/2005	19.5	962	856	1.210	11829
	Average	16.6	542	616	1.866	11550
	St. Dev.	5.1	626	236	0.578	5004
Ispat	2/20/2003		1216	617	0.328	3418
	5/8/2003		852	2970	0.142	5274
	9/11/2003		1032	2094	0.175	4697
	1/27/2004		1025	1563	0.137	3166
	5/12/2004	8.9	3312	440	0.095	3730
	11/30/2004	7.2	388	1975	0.118	2719
	2/15/2005	9.9	304	4032	0.170	7157
	5/19/2005	7.5	465	2774	0.123	3865
	Average	8.4	1117	2305	0.126	4368
	St. Dev.	1.3	1465	1504	0.031	1929

Table 4.3.3 pH, Cl, Ca, and SO₄ concentrations for scrubber waters.

<i>Plant</i>	<i>Date</i>	<i>pH</i>	<i>Cl</i> <i>ppm</i>	<i>Ca</i> <i>ppm</i>	<i>SO₄</i> <i>ppm</i>
Hibtac	2/20/03	6.7	86	58	325
	5/8/03	7.4	65	43	243
	9/11/03	7.5	59	44	
	1/27/04	7.3	91		335
	5/12/04	7.0		40	
	7/27/04	7.2	68	37	261
	7/27/04	7.2			
	2/15/05	7.2	98	60	368
	5/19/05	7.2	60	41	239
Minntac Line 4	2/19/03	5.6	196	138	994
	5/9/03	6.4	176	129	859
	9/10/03	6.1	162	116	
	1/28/04	4.3	194	90	870
Minntac Line 7	1/28/04	5.6	200		901
	5/11/04	5.8		106	
	7/27/04	4.0	231	115	860
	12/1/04	5.5	187	122	924
	2/16/05	5.6	208	131	964
	5/20/05	5.6	180	134	879
Evtac United Tac	2/18/03	4.2	59	180	711
	1/28/04	4.0	60	52	640
	5/11/04	3.7		106	
	7/28/04	3.5	89	140	779
	11/29/04	3.8	95	135	780
	2/14/05	4.5	82	202	780
	5/19/05	3.6	87	105	674
Ispat-Inland	2/20/03	6.7	109	45	159
	5/8/03	6.4	209	66	193
	9/11/03	7.3	160	67	
	1/27/04	6.9	195		233
	5/12/04	6.5		59	
	11/30/04	7.5	206	56	173
	2/15/05	7.2	226	54	216
	5/19/05	6.8	223	50	140

IOCR Final Report

Table 4.3.4 Comparison of Greenball leach analysis and change to chemistry of scrubber water.

	<i>F</i> (mg/kg)	<i>Cl</i> (mg/kg)	<i>Br</i> (mg/kg)	<i>SO₄</i> (mg/kg)	<i>Na</i> (mg/kg)	<i>Mg</i> (mg/kg)	<i>K</i> (mg/kg)	<i>Ca</i> (mg/kg)
Hibtac								
Greenball Leach	2.6	14.8	0.04	98	105	5.6	8.4	9.0
Scrubber Feed	13.9	92	0.41	298	85	110	18.3	61.1
Scrubber Water	22.0	98	0.43	368	85	110	18.3	59.5
Scrubber Change	8.1	6	0.02	70	0	0	0.0	-1.6
Minntac								
Greenball Leach	3.0	31.8	0.22	136	158	2.3	5.3	2.1
Scrubber Feed	3.7	180	1.30	819	105	183	27.4	128
Scrubber Water	7.0	208	1.45	964	106	182	27.6	131
Scrubber Change	3.3	28	0.15	145	1	-1	0.2	3
United Taconite								
Greenball Leach	3.2	6.8	0.05	47	69	7.6	4.4	8.6
Scrubber Feed	11.7	53	0.33	328	56	51	22.8	79
Scrubber Water	30.3	82	0.31	780	57	56	23.7	202
Scrubber Change	18.6	31	-0.02	452	1	5	0.9	123
Ispat Inland								
Greenball Leach	2.1	16.8	0.11	40	82	4.2	6.6	4.6
Scrubber Feed	5.6	109	0.87	86	68	71	8.1	31.5
Scrubber Water	28.1	226	1.95	216	83	83	11.9	53.5
Scrubber Change	22.5	117	1.08	130	15	12	3.8	22.0

5. Discussion

Results from this study have shown that mercury transport during taconite processing involves a relatively complex series of reactions, whereby some of the mercury released at high temperatures in the furnace is recaptured by magnetite and/or magnetite solid-solutions with maghemite (magnetite/maghemite solid-solutions). In all plants, however, there is also mercury captured by scrubber systems that is dissolved in solution, indicating potential importance of a molecular reaction between mercury and gaseous species, most likely Cl. To simplify the release process, we write four reactions that are shown in Table 5.1 as those most likely to impact mercury release from taconite ore. Reactions 1 and 2 represent the relative formation of magnetite/maghemite solid-solutions and hematite, while Reactions 3 and 4 represent release of mercury in reduced and oxidized form, respectively. Each of the reactions in Table 5.1 proceeds from left to right upon heating of magnetite in taconite induration furnaces, and the challenge is to determine specific processes affecting the relative rates of each process.

Magnetite oxidation to maghemite and/or magnetite/maghemite solid-solutions is important because it controls the composition of dust that may or may not react with, and ultimately help trap, reduced mercury ($\text{Hg}^0_{(g)}$) in process gases. Zygarlicke (2003) and Galbreath et al. (2005), for example, demonstrated that maghemite participates in reactions with gaseous mercury, while magnetite and hematite do not. Maghemite forms when oxygen is added to magnetite without modification of the spinel-type crystal lattice. Formation of this mineral has long been considered to take place at intermediate temperatures in induration furnaces (Papanatassiou, 1970), however, its abundance as a mineral phase, and its importance with respect to mercury transport during taconite processing, was previously unknown.

Data in the present study provide an indication of time needed for solid-solutions between magnetite and maghemite to form, but perhaps more importantly, demonstrate that mercury reacts not just with maghemite, but also with magnetite/maghemite solid-solutions that may be close in composition to magnetite. A comparison of A/B site occupancy ratios for Fe^{+3} in magnetite from experiments and grates indicate far greater formation of oxidized solid-solutions in the experiments. A/B values after 20 minutes reaction between greenball and air at temperatures of 400 and 500°C produced magnetite having A/B = 0.98 and 1.26 (Table 4.1.2) consistent with magnetite solid-solutions composed approximately of 27 and 36% maghemite component (see Figure 3.4.1). This compares to the starting material which was composed of magnetite having A/B of 0.72, or approximately a 12% maghemite component. The magnetite in under-grate samples all had A/B between 0.48 and 0.75 (see Table 4.2.1 and compare to Figure 3.4.1) indicating that this dust had not reacted with air at elevated temperatures for sufficiently long time periods to oxidize magnetite to more maghemitic compositions. Indeed, the experiments where maghemite enriched magnetite was generated were conducted for 20 minute time intervals, while solids probably spend less than half that time reaching the firing zone in taconite induration furnaces ($T = 1200$ to 1300 C).

IOCR Final Report

Reaction 1 in Table 5.1, therefore, does not appear to take place on a large scale, to the point where it is easily observable in dust samples from grates. We note, however, that the process may take place on a small scale during pellet induration. This is suggested by the A/B values for samples from Hibtac's grate which increased gradually from 0.57 in the starting solid to 0.69 in the firing zone. It is possible, therefore, if not likely that magnetite/maghemite solid-solutions interact with mercury, even for slight levels of maghemitization. This behavior can be understood, perhaps, by considering in more detail the steps needed for magnetite oxidation to maghemite to take place (Columbo et al., 1965; O'Reilly, 1984; Zhou et al., 2004). First, oxygen must be adsorbed to the surface of the grain. This takes place by reaction of oxygen with electrons from the Fe^{+2} component in magnetite to form Fe^{+3} and O^{-2} ions, which has the effect of extending the mineral lattice. $\text{Fe}^{+3}/\text{Fe}^{+2}$ ratio at the mineral surface increases as a result of this interaction, and a cation site vacancy develops in the vicinity of the added oxygen. Ionic and electronic diffusion then occur to reduce the chemical gradients, and given time, the grain may become homogeneous.

Oxidation of a magnetite grain occurs from the outside in, such that full oxidation of the interior portions is diffusion limited and can only take place only as fast as Fe diffusion permits. The outer surface mineralogy and rate of mineral growth is complex, depending on temperature, humidity, oxygen availability, and nucleation effects, as well as crystal orientation (Zhou et al., 2004). Based on results from experiments and under-grate samples, conversion of magnetite to magnetite/maghemite solid-solutions can take place on relatively short time scales at 400 and 500°C, but time scales for induration furnaces are short, so only the outer-most surfaces of magnetite grains have time to convert to magnetite/maghemite solid-solutions.

Ultimately, nearly all of the magnetite in greenballs is converted to hematite by exposure to air at temperatures of 1200 to 1300C later in the induration process. Hematite is not known as a significant oxidant for Hg^0 in flue gases at power plants (Zygarlicke, 2003). Thus, Reaction 2 in Table 1, conversion of magnetite to hematite may limit mercury oxidation and capture during induration, and the mineralogic conversion process likely signals the final release of mercury to process gases. To understand mercury transport in taconite induration furnaces, therefore, it is important to determine where magnetite and magnetite/maghemite solid-solutions convert to hematite.

For the Minntac greenball samples heated in air, it took 20 minutes of exposure at 400 and 500°C (752 and 932°F) to convert 11 and 23% of the solids, respectively, to hematite. Under-grate samples, obviously, require much higher reaction temperatures for this amount of hematite to form, since reaction times are much less than 20 minutes. Based on results from under-grate samples, significant hematite is observed in dust from preheat zones at both Minntac (Line 7) and United Taconite. At Hibtac and Ispat, hematite did not become a large component of the dust samples until the firing zone. In all four cases, mercury decreases become evident when hematite increases in under-grate samples, consistent with the idea that heating to the temperatures needed to generate hematite is needed to effectively release all of the mercury from magnetite/hematite solid-solutions.

IOCR Final Report

This brings us to consideration of reaction 3: the conversion of mercury from its oxidized immobile form, $\text{HgO}_{(ss)}$, to its reduced and volatile form, $\text{Hg}^0_{(g)}$. The subscript “(ss)” in $\text{HgO}_{(ss)}$ is used to indicate Hg existing in a solid solution within magnetite/maghemite solid-solutions, however, the nature and form of this component is not well known. In primary greenball samples it likely exists initially as an element dispersed throughout the grain or, even perhaps, combined with other trace components such as sulfur. However, the high concentration of mercury observed on dust samples composed exclusively of magnetite/maghemite solid-solutions at Hibtac, leave little doubt that the element exists as a surface adsorbate on magnetite/maghemite solid-solutions in the cooler regions of the furnace where hematite has not yet begun to form. Release temperatures from experiments indicate this process is important in air at temperatures to approximately 400 or 450° (842°F). At temperatures above this, mercury appears to have little affinity to react with magnetite solid-solutions or magnetite, perhaps signifying final conversion of the surfaces of the mineral grains to non-reactive hematite rather than to magnetite/maghemite solid-solutions.

The precise manner in which mercury evolves from the surface of magnetite/maghemite solid-solutions may provide an important constraint on the form of mercury in the resulting process gas, which can impact the behavior of mercury in wet scrubber systems. Reaction 3 in Table 5.1 is a hypothetical mechanism for producing $\text{Hg}^0_{(g)}$, the form of mercury to be avoided, if possible, because it is not captured by wet scrubbers unless subsequent chemical reactions promote oxidation in the process gas phase. One such reaction to oxidize mercury is Reaction 4, a hypothetical mechanism for generating $\text{HgCl}_2^0_{(g)}$, a molecule containing mercury in oxidized form which is easily captured by wet scrubber system and which can adsorb to solids. The relative overall rates of reactions like 3 and 4 will dictate the relative amounts of mercury released in taconite induration furnaces that can be captured either as particulate or dissolved mercury or which will be released to the atmosphere ($\text{Hg}^0_{(g)}$).

The experiments conducted for the present study (Figures 4.1.1 and 4.1.2) were conducted in the absence of HCl and, thus, provide some information on mercury systematics, although reaction times are, as discussed previously, probably too long to provide an exact analogy to processes taking place during taconite induration. For Hibtac and Minntac greenball samples over half of the mercury was released in 20 minutes of reaction at 300°C, but only a small fraction of the mercury was driven off at this temperature during reaction in air. This suggests that at 300°C, mercury that might have been volatilized in N_2 is instead captured and held by magnetite/maghemite solid-solutions that formed as the solid was heated. However, at 400°C nearly half of the total mercury is released within 20 minutes, even in air. If these results were to be extrapolated to the short time scales of heating in taconite induration furnaces, it is likely that the majority of the mercury release would take place at somewhat higher temperatures than this. At 450 and especially 500°, where mercury release during N_2 - and air-based experiments became similar for Hibtac samples, reactions between mercury and the surfaces of oxidation products for magnetite must no longer be as important as they were at the lower temperature. Thus, Reaction 3 in Table 5.1 appears to dominate transport at temperatures between about 300 and 400°C, but then loses significance when temperatures approach 450°C, perhaps commensurate with more rapid conversion of mineral surfaces from magnetite/maghemite solid-solutions to unreactive hematite.

While it is unlikely that the iron-oxide mineralogy would be strongly affected by the presence or absence of $\text{HCl}_{(g)}$ in process gases, there is good reason to expect that the chemistry of mercury reactions taking place at the surfaces of minerals might change to favor Reaction 4 over Reaction 3 in Table 5.1. Galbreath and Zygarlicke (2000), for example, showed that the dominant transformation pathways for mercury in flue gases in coal fired power plants was by chlorination reactions at mineral surfaces on fly-ash. The reaction products were a combination of particle-bound mercury and $\text{HgCl}_{2(g)}$. Results from mercury oxidation experiments involving gas reactions with fly ash have suggested a direct role for Fe-oxides, in particular (Ghiorshi, 1999; Lee *et al.*, 2001).

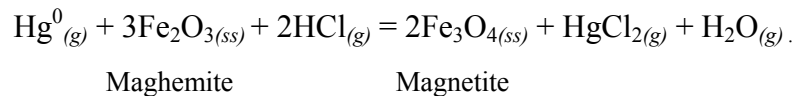
The high mercury concentrations in many of the under-grate samples support this contention, as does the relatively high concentration of mercury in scrubber waters, which are present in both dissolved and particulate form. Before a role for HCl can be assessed, however, it is important to compare the relative source and abundance of HCl in taconite processing gases, as compared to flue gases from power plants. Table 5.2 presents an estimate of HCl abundance in taconite processing gases, based on feed-rate and scrubber water flow data from Table 4.3.1, greenball Cl data from Table 4.3.4, and gas flow data from Zahl *et al.* (1995) and personal communication (Ray Potts for Minntac, Brad Anderson for United Taconite). The predominant source of Cl is thought to be the pore fluid from processing waters and limestone flux material (Minntac and Ispat-Inland), which upon heating to 1200 to 1300°C in the firing zone, is expected to be volatilized as $\text{HCl}^0_{(g)}$. Air containing the $\text{HCl}^0_{(g)}$ travels into the preheat and drying zones where it may react with the mercury bearing iron oxides. Since HCl is likely only released from fired pellets, the mass flux of Cl in our calculations was related to pellet production rate to account for Cl that would likely have fallen along with other material from the grates before it volatilized.

Mass balance results indicate considerable uncertainty in the amount of Cl that is volatilized from pellets, compared to the mass captured in wet scrubbers. Assuming the lower value based on flux from the firing of pellets, however, it is estimated that the taconite processing gases contain from 1 to 10 ppmv Cl. These concentrations are relatively low compared to experimental conditions where Cl generation has been shown to take place in homogenous gas phase reactions (e.g., Widmer *et al.*, 1998) so it is unlikely that homogenous gas reactions with HCl will promote oxidation during taconite induration. However, Edwards *et al.* (2001) showed that the predominant Cl species for mercury oxidation in homogenous reactions were trace molecular species such as $\text{Cl}^0_{(g)}$ and $\text{Cl}_2^0_{(g)}$ which oxidize $\text{Hg}^0_{(g)}$ orders of magnitude more rapidly than HCl. It is unknown whether such metastable species exist in taconite processing gases. Another possibility is that the heterogeneous reactions between HCl and iron oxides that come into contact with the processing gas (Ghiorshi, 1999; Lee *et al.*, 2001; Zygarlicke, 2003, Galbreath *et al.*, 2005). Certainly, there is abundant opportunity for processing gases containing $\text{Hg}^0_{(g)}$ and HCl to come into contact with iron oxides and some of the process gases obviously contain large amounts of oxidized mercury, both adsorbed to particulates and as a molecular form easily caught in wet scrubbers.

Table 5.3 was constructed as an attempt to compare estimated “capture efficiencies” for processing facilities in order to evaluate the relative effects of Cl and availability of dust particles on mercury capture. It should be noted, before comparing these values that the

estimates are highly uncertain. For example, the capture efficiency for Cl was unexpectedly poor in Table 5.2. Cl collected in the scrubber waters for three of the plants was twice as high as that calculated from greenball input values for Cl. Because no other significant source for Cl is known at these plants, it is possible that the scrubber water flow rates or the production rates may not be entirely accurate. Secondly, there is uncertainty associated with the estimate of mercury inputs into the furnace based on processes occurring in the taconite dust itself. It is unknown at this point if the mercury-bearing magnetite spilling from grates is a significant fraction of the total mercury balance, but if it is, then it would cause an underestimate of mercury capture efficiency. Finally, there was no attempt made to provide “closure” to the calculations (e.g., measuring gas chemistry) to ensure accuracy. Mercury capture efficiencies were computed in Table 5.3 for comparison purposes only. It is expected that these issues will be resolved in planned future studies.

Capture efficiencies estimated during the study (Table 5.3) varied from less than 10% to greater than 40%, with the highest recovery values being found at Minntac and United Taconite which use grate-kilns and lower values found at Hibtac and Ispat-Inland, which use straight-grates. While a simple difference in the grate type might be partially responsible for differences in capture efficiency, it is also possible that the trend is tied to differences in the concentrations of reactive components (e.g., HCl and/or iron-oxides). Combining Reactions 1, 3, and 4 in Table 5.1, for example, leads to an overall reaction describing heterogeneous oxidation of mercury by magnetite/maghemite solid-solutions and HCl, as follows:



This reaction shows that if components on the left hand side of the reaction are elevated (maghemite and HCl), it will favor generation of $\text{HgCl}_{2(g)}$ relative to $\text{Hg}_{(g)}^0$ and, thus, greater capture efficiency. The company with the highest average mercury recover rate, Minntac, also has the highest Cl concentration and flux (Table 5.3). United Taconite, on the other hand, has low Cl, but has the highest $F_{\text{particulate}}$ load (also Table 5.3). These data suggest several pathways may be available to limit mercury emissions, including addition of HCl and increasing exposure of gases to maghemite or other solids.

Future studies are planned to measure gas chemistry directly in taconite induration furnaces as well as to test whether Cl injection has a direct impact on mercury oxidation and capture rates in taconite induration furnaces. Additional samples are also being collected to lessen the errors associated in estimating fluxes for Cl, Hg, and particulates. Confirmation of these trends could potentially lead to an increase in capture of mercury across the Iron Range involving manipulation of components already available in all taconite processing plants.

It should be mentioned, however, that just increasing the capture rate for mercury in induration furnaces will be insufficient to reduce mercury in taconite stack emissions. Part II of this series of papers will detail the behavior of mercury in taconite scrubber waters once the mercury is captured. Currently, three out of four plants simply recycle the captured mercury back to the induration plants. Several potential means to ensure the majority of captured mercury is routed to tailings basins, rather than back to the induration plant, are potentially

available, however, the most cost effective means to do this will likely vary at each plant, owing to differences in ore processing techniques.

Table 5.1 Primary chemical reactions that constrain mercury release, transport, and capture in taconite induration furnaces.

<i>Number</i>	<i>Chemical reaction</i>	<i>Importance for Hg transport</i>
(1)	$2\text{Fe}_3\text{O}_{4(ss)} + \frac{1}{2} \text{O}_2(g) = 3\text{Fe}_2\text{O}_{3(ss)}$ Magnetite Maghemite	Maghemite interacts with mercury in flue gases, while magnetite does. The minerals have the same structure and form a solid solution but little is known about how mercury reacts with magnetite solid-solutions.
(2)	$2\text{Fe}_3\text{O}_4 + \frac{1}{2} \text{O}_2(g) = 3\text{Fe}_2\text{O}_3$ Magnetite Hematite	Mercury is released when magnetite is converted to hematite in induration furnaces. Hematite does not interact with mercury in flue gases.
(3)	$\text{HgO}_{(ss)} = \text{Hg}^0_{(g)} + 1/2\text{O}_2(g)$	$\text{Hg}^0_{(g)}$ is insoluble in water and cannot be caught by wet scrubbers. $\text{HgO}_{(ss)}$ represents mercury associated with magnetite and magnetite/maghemite solid-solutions.
(4)	$\text{HgO}_{(ss)} + 2\text{HCl}_{(g)} = \text{HgCl}_{2(g)} + \text{H}_2\text{O}_{(g)}$	$\text{HgCl}_{2(g)}$ is soluble in water and the Hg^{2+} base atom can adsorb to solids. This species is more easily captured by wet scrubbers than is $\text{Hg}^0_{(g)}$.

Table 5.2 Cl-flux calculations for taconite processing facilities.

<i>Plant</i>	<i>Pellet Production Rate (dry,LT/hr)</i>	<i>Scrubber Water flow rate (gpm)</i>	<i>Cl flux into furnace (g/s)</i>	<i>Cl flux out through scrubber (g/s)</i>	<i>Process Gas Flow Rate* (mscfh)</i>	<i>Estimated Total Cl in Gas (ppmv)</i>
Hibtac	311	3406	1.3	1.3	20	5.2
Minntac L7	412	3018	3.7	5.3	28	10.6
United	378	810	0.7	1.4	46	1.2
Ispat Inland	265	350	1.3	2.6	18	5.8

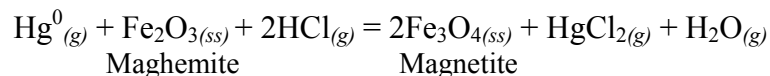
Table 5.3 Flux calculations for taconite facilities in this study.

<i>Plant</i>	<i>Particle flux to scrubber (g/sec)</i>	<i>Cl flux to furnace (g/sec)</i>	<i>Estimated Mercury Capture Efficiency</i>
Hibtac	40	1.3	0.11 ± 0.06
Minntac 7	130	3.7	0.33 ± 0.13
United Taconite	953	0.7	0.27 ± 0.08
Isp. Inland.	25	1.3	0.14 ± 0.06

6. Conclusions

Experiments were performed and samples were collected from beneath grates and wet scrubbers in four induration furnaces to identify the primary processes affecting mercury release and capture for the taconite industry. Magnetite/maghemite solid-solutions formed during heating of the fresh magnetite-dominated greenballs in air and correspondingly, mercury release rates were greatly reduced compared to when the greenballs were heated in N₂. These results agreed with observations from under-grate samples from taconite induration furnaces which revealed considerable uptake of mercury at moderate temperatures. In general, therefore, it appears that mercury release during induration begins at approximately 450°C and continues to unspecified higher temperatures, as the magnetite converts to hematite, which appears to exclude and not react with mercury.

Subsequent to release, mercury can resorb to magnetite/hematite solid-solutions but the overall rate of capture by wet scrubbers appears to depend both on the availability of HCl⁰_(g) and particulate phases, most likely magnetite/maghemite solid-solutions, consistent with a reaction such as:



Despite the considerable uncertainty that exists in computation of mass fluxes for mercury, chloride, and particulates in taconite induration furnaces, the relationships observed in this study provide evidence that relatively simple procedures involving injection of Cl and/or maghemite/magnetite may provide a relatively cheap and simple means to control mercury emissions during induration at taconite processing facilities.

7. References

Bauer, M. E., Hayes, J. M., Studley, S. A., and Walter, M. R. (1985) Millimeter-scale variations of stable isotope abundances in carbonates from banded iron-formations in the Hamersley Group of Western Australia. *Econ. Geol.* 80, 270-282.

IOCR Final Report

Berndt, M. E. (2003) *Mercury and mining in Minnesota*. Final report, Minnesota Department of Natural Resources, 58p.

Berndt, M. E. and Engesser, J. (2003) On the distribution of mercury in taconite plant scrubber systems. Minnesota DNR report prepared for MPCA. 30 p.

Colombo, U., Gazzarrini, F., Lanzavecchia, G., Sironi, G. (1965) Magnetite oxidation: a proposed mechanism. *Science*, 147, 1033.

Coey, J.M.D., Morrish, A. H., Sawatsky, A. Mössbauer study of conduction in magnetite. *J. Phys.* (1971) C1-32, 271-273.

Edwards, J. R., Srivastava, R. K., and Kilgroe, J. D. (2001) A study of gas-phase mercury speciation using detailed chemical kinetics. *J. Air. Waste. Man. Assoc.*, 51, 869-877.

Engesser, J. and Niles, H. (1997) Mercury emissions from taconite pellet production. Coleraine Minerals Research Laboratory, Report to MPCA: U of M contract # 1663-187-6253. 16 pages plus tables, figures and appendices.

Galbreath, K. C. and Zygarlicke, C. J. (2000) Mercury transformation in coal combustion flue gas. *Fuel Processing Tech.* 65, 289-310.

Galbreath, K. C., Zygarlicke, C. J., Tibbetts, J. E., Schulz, R. L., and Dunham, G. E. (2005) Effects of NO_x, α -Fe₂O₃, δ -Fe₂O₃, and HCl on mercury transformations in a 7-kW coal combustion system. *Fuel Processing Technology*, 86, 429-488.

Ghiorshi, B. S. (1999) Study of the fundamentals of mercury speciation in coal-fired boilers under simulated post-combustion conditions. EPA-600/R-99-026, United States EPA Office of Res. and Development, NC.

Jiang, H., Arkly, S., and Wickman, T (2000) Mercury emissions from taconite concentrate pellets- stack testing results from facilities in Minnesota. Presented at USEPA conference "Assessing and managing mercury from historic and current mining activities". San Francisco, November 28-30, 18 pages.

Lee, L. W., Srivastava, R. K., Kilgroe, J. D., and Ghiorshi, S. B. (2001), Effect of iron content in coal combustion fly ashes on speciation of mercury. *Proc. 94th*, A&WMA Annual Meeting, Air and Waste Management Association, Pittsburgh, PA.

Morey, G. B. (1972) Mesabi Range. In: *Geology of Minnesota: A centennial volume*. P.K. Sims and G. B. Morey (eds), Minnesota Geological Survey, St. Paul, MN. 204-217.

Ojakangas, R. W. and Matsch, C. L. (1982) *Minnesota's Geology*. University of Minnesota Press, Minneapolis. 255 p. O'Reilly, W. (1984) *Rocks and Rock Magnetism*, Chapman and Hall, NY.

IOCR Final Report

Papamarinopoulos, S., Readman, P. W., Maniatis, Y., and Simopoulos, A., 1982, Magnetic Characterization and Mössbauer spectroscopy of magnetic concentrates from Greek lake sediments. *Earth Planet Sci. Letters*, 57, 173-181.

Papanatassiou, D. J. (1970) Mechanisms and Kinetics Underlying the Oxidation of Magnetite in the Induration of Iron Ore Pellets. University of Minnesota, Duluth, Unpublished PHD Thesis. 134 p.

Pavlish, J. H., Sondreal, E. A., Mann, M. D., Olson, E. S., Galbreath, K. C., Laudal, D. L., and Benson, S. A. (2003), Status Review of Mercury. Control Options for Coal-fired Power Plants. *Fuel Processing Technology* 82. 89-165.

Perry, E. C., Jr., Tan, F. C., and Morey, G. B. (1973) Geology and stable isotope geochemistry of the Biwabik iron-formations. *Econ. Geol.* 68, 1110-1125.

Thode, H. G. and Goodwin, A. M. (1983) Further sulfur and carbon isotope studies of late Archaen Iron-Formations of the Canadian Shield and the rise of sulfate reducing bacteria. *Precambrian Research*, 20, 337-356.

Widmer, N. C., Cole, J. A., Seeker, W. R., and Gaspar, J. A. (1998) *Combust. Sci. Technol.* 134, 315-326.

Zahl, R., Haas, L, and Engesser, J. (1995) Formation of NO_x in Iron Oxide Pelletizing Furnaces. *Iron Ore Cooperative Research (MnDNR)*, 43 p. plus tables and figures.

Zhou, Y., Xuesong, J., Mukovskii, Y, and Shvets, I. (2004) Kinetics of oxidation of low-index surfaces of magnetite. *J. Phys: Condensed Matter.* 16, 1-12.

Zygarlicke, et al. (2003) Experimental Investigations of Mercury Transformations in Pilot-Scale Combustion Systems and a Bench-Scale Entrained-Flow Reactor. University of North Dakota Energy and Environmental Research Center Technical Report. 22 p.

8. Acknowledgments

This study was supported by funds from Iron Ore Cooperative Research and Environmental Cooperative Research Programs at the Minnesota Department of Natural Resources. Thanks are extended to those who participated in this research, particularly: John Folman, Minnesota Department of Natural Resources who provided dedicated and careful assistance selecting and readying equipment for and participating in field sampling trips; Blair Benner, NRRI, who performed and helped interpret data on taconite heating experiments; and Dr. Thelma Berquó who performed and helped interpret the Mössbauer spectroscopic analyses. We also thank the following mining personnel for helping to arrange our visits to their companies, choosing and readying sampling locations, and/or for providing assistance in interpreting results: Andrea Hayden, Steve Rogers, Dana Koth and Rod Heikkila at Hibtac; Tom Moe and Ron Braski at Minntac, Brad Anderson at United Taconite, and Gus Josephson and Jim Sterle at Ispat-Inland.

9. Appendices

9.1. Taconite Induration Furnaces

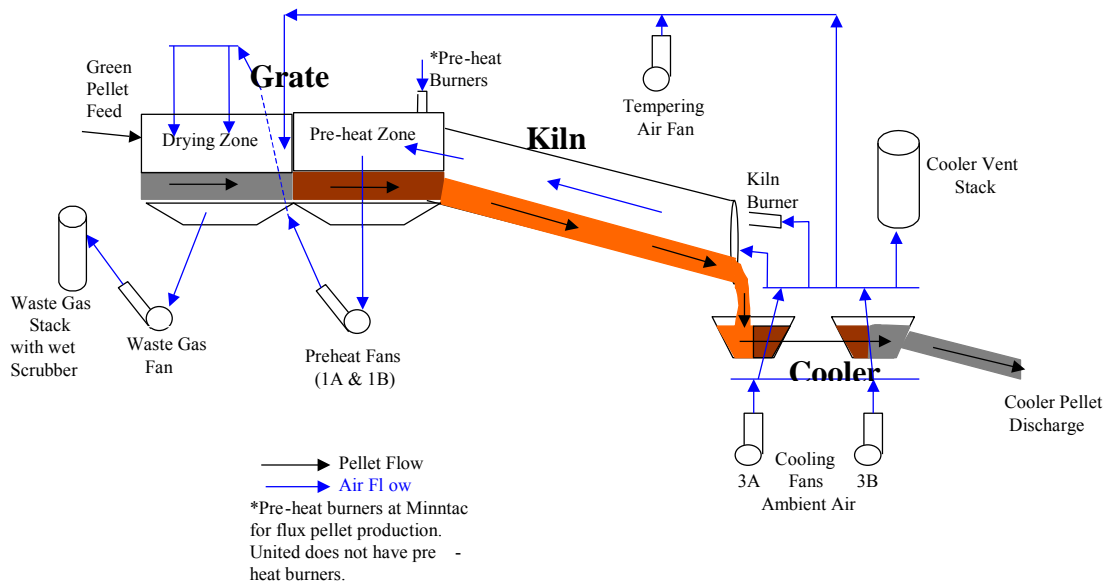


Figure 1. Diagram of a grate-kiln taconite pellet induration process (used at Minntac and United Taconite). Fresh, wet pellets (termed green balls) fed into the system (on the left side) are systematically dried, heated, and hardened into pellets as they pass from the drying zone to the rotating kiln. Drying and heating is accomplished using gases, that are generated by cooling of the hot pellets and burning of fresh fuels in the kiln. The gases interact with pellets in the kiln, and are passed through pellet beds in the drying and pre-heat zones. The gases carry mercury and dust to the wet scrubber systems that were sampled in our study. The preheat burner near the center of the diagram is used only for fluxed pellet production.

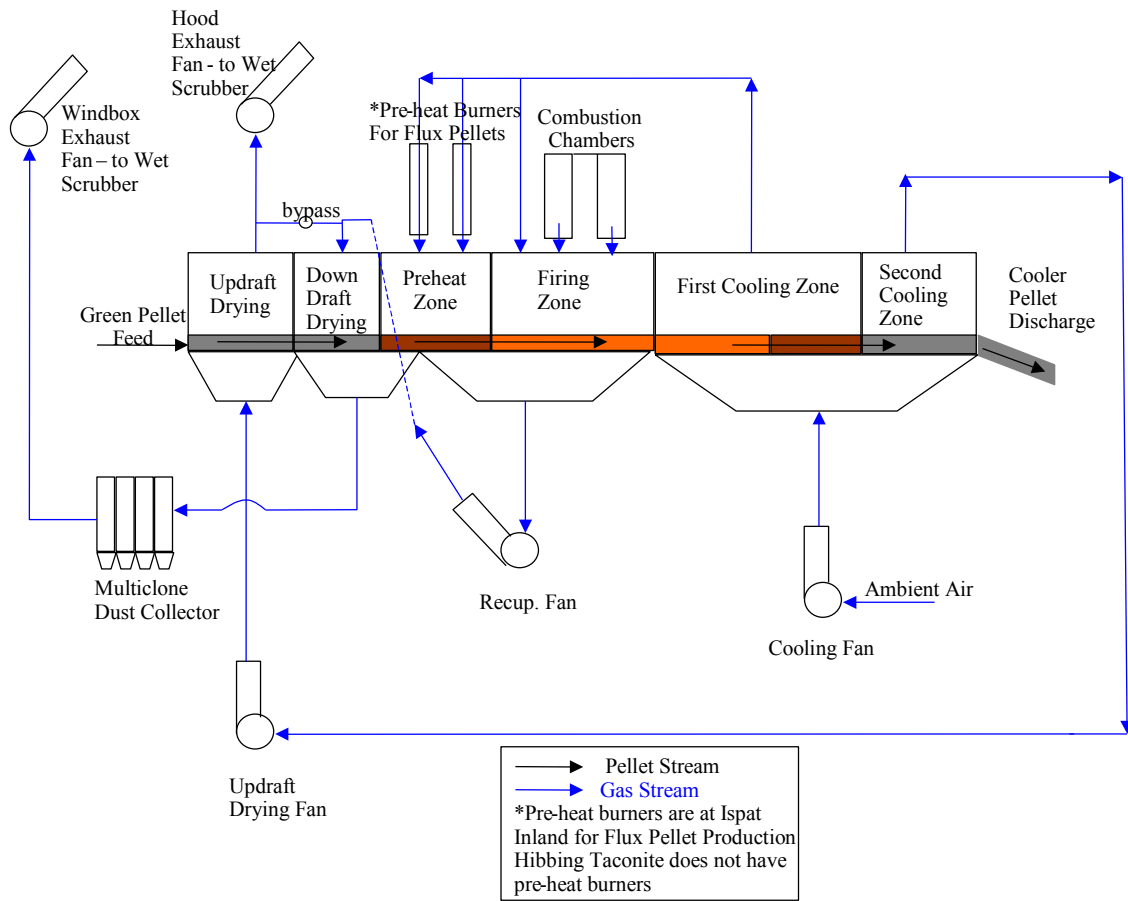
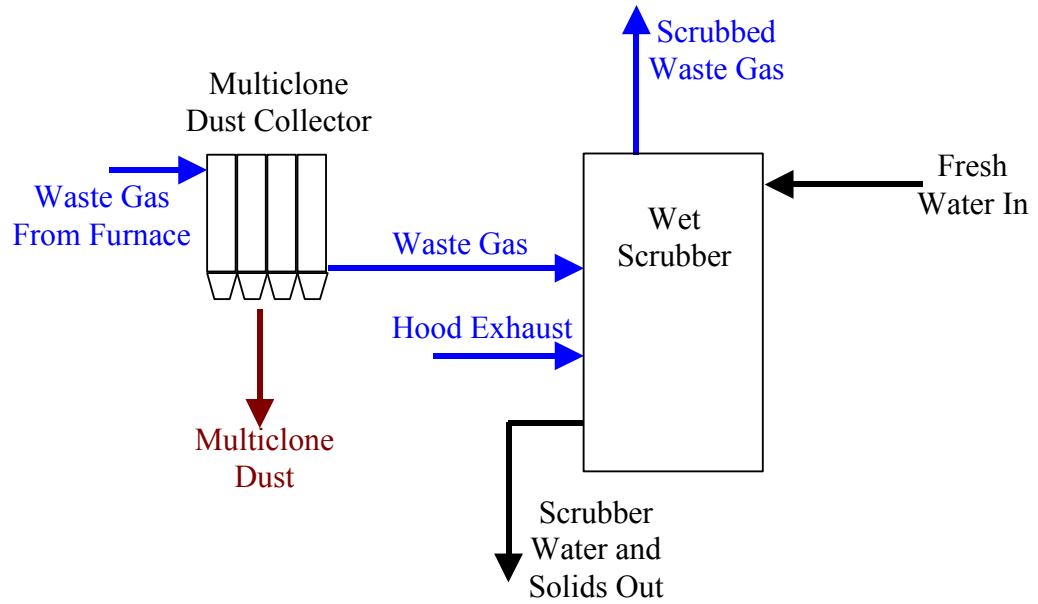


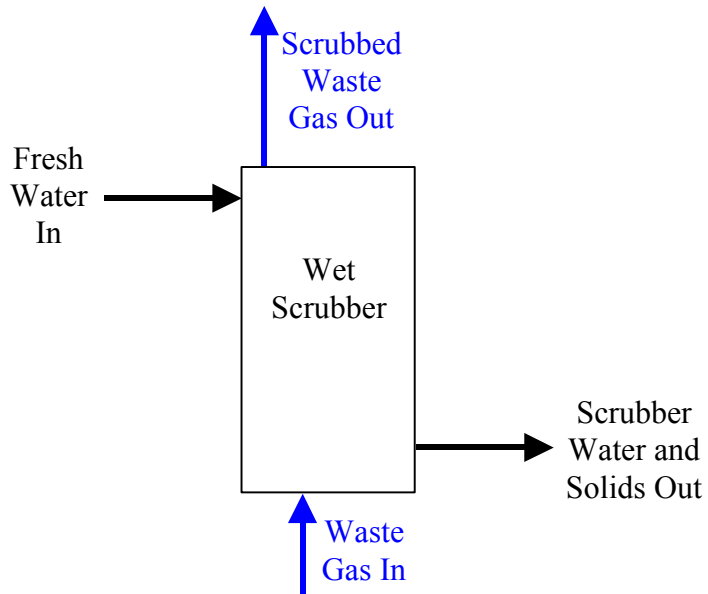
Figure 2. Diagram of a straight-grate taconite pellet induration process (used at Hibtac and Ispat Inland). Fresh pellets are carried on a grate through a furnace and cooled by fresh air passed through the pellet bed. The air used for cooling the hot pellets and gases generated in the firing zone are used for drying and heating the pellets.

9.2. Taconite Scrubber Systems

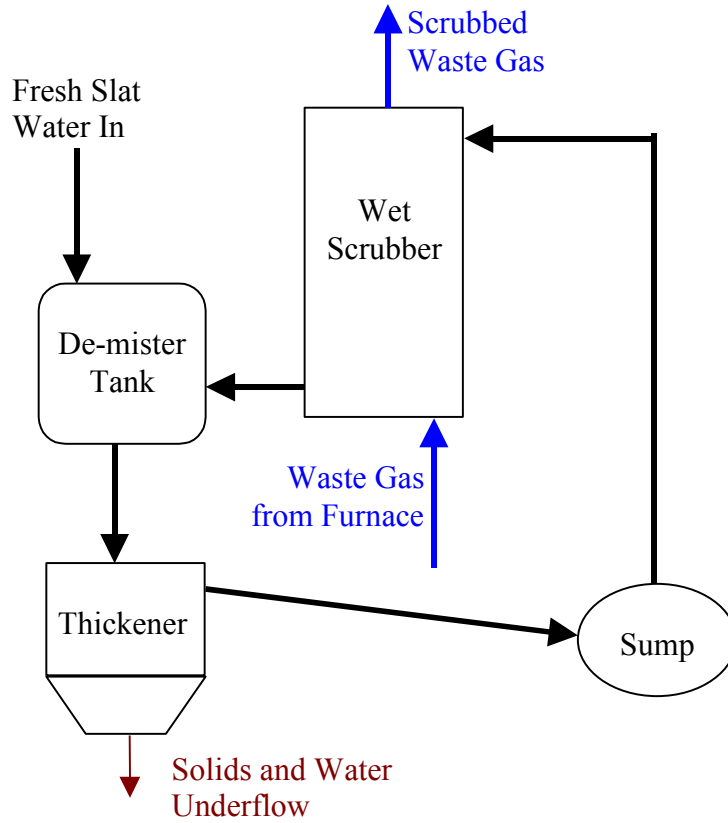
Hibbing Taconite Company Scrubber Flow Diagram



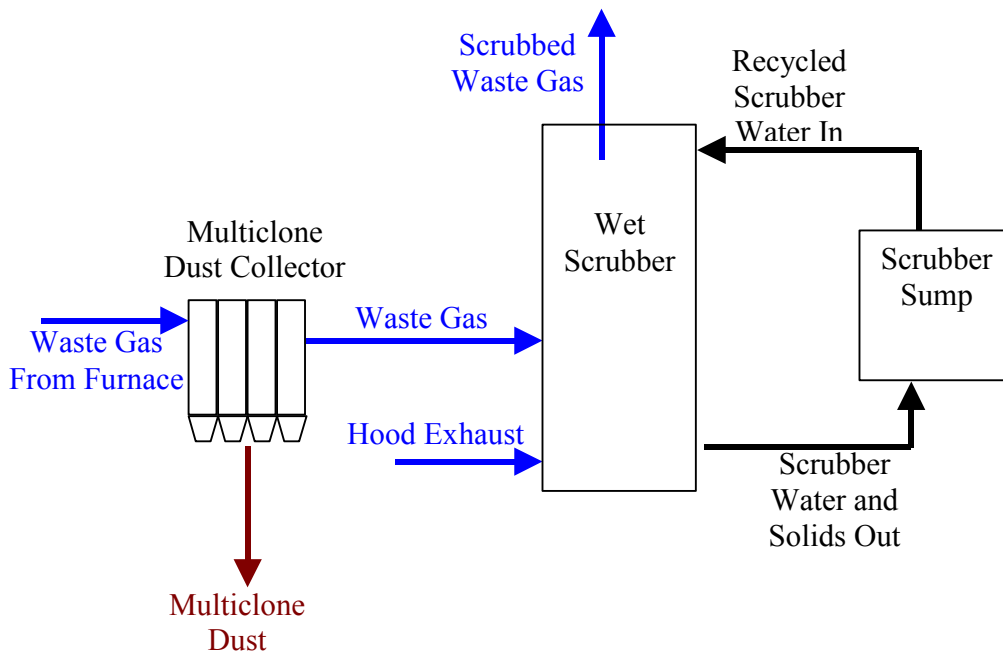
Minntac Scrubber Flow Diagram



United Taconite Scrubber Flow Diagram



Ispat-Inland Scrubber Flow Diagram



9.3. **Heating Experiments (B. Benner, CRML)**

(Scanned text from hard copy original)

Mercury Release from Taconite During Heating

Blair Benner (CMRL report TR-05-06/NRRI/TR-2005-17) June 15, 2005

Introduction:

The taconite industry is under pressure to reduce the emissions of mercury from their induration process. Previous studies have indicated that greater than 90 percent of the mercury in the green balls being fed to the induration process is vaporized during the induration. The Minnesota DNR is in the process of conducting a bench-scale study to determine the rate of mercury release as a function of temperature during the heating of taconite. This program is a supplement to that work. The objectives of this program were to determine the role of oxidation in the release of mercury at various temperatures and to provide samples of heated material for Mossbauer spectroscopic analysis.

Test Procedure and Results:

In consultation with the DNR, samples of green balls were obtained from Minntac (Line 6) and Hibtac. The green balls were dried at 100 C, crushed, and blended to provide two feedstocks for the testing. Head samples were taken for mercury and Mossbauer analyses. An electrically heated tube furnace with a built-in temperature controller was used for all of the tests. A 7/8-inch ID combustion tube was placed inside the tube furnace. Temperature measurements were taken inside the combustion tube at the center and 3/4 and 1.5 inches from each side of the center. The temperatures in the 3 inch zone ranged from 500 to 505 C.

The test procedure was as follows: The furnace was heated to the desired temperature. If the test was to be conducted in a nitrogen atmosphere, the combustion tube was purged for 20 minutes with nitrogen being added at the rate of 0.67 l/min. An empty 3-inch long combustion boat was weighed. The boat was filled with the desired sample of dried green balls and re-weighed. The loaded boat was placed in the center of the heating zone and either air or nitrogen was added to the tube at the rate of 0.67 l/min. After 20 minutes, the boat was removed from the hot zone. In the case of tests in nitrogen, the boat was kept in the cool end of the combustion tube for 10 minutes under nitrogen to prevent oxidation. In the case of tests in air the boat was removed from the combustion tube to cool. A portion of the cooled sample was submitted for mercury analyses and a portion was sent out for Mossbauer analysis. With each set of mercury analyses, a taconite concentrate standard¹ containing 14 +/- 1.2 *ng/g* Hg was also run. The results for the Minntac Line 6 green balls are given in Table I. At all temperatures there was a greater release of mercury in nitrogen than in air. With the exception of the test run at 500 C, there is a steady increase in the amount of mercury released with increasing temperature. The fact that the 500 C tests were the first tests run may have contributed to the slight anomaly. It is apparent that heating in air retards the release of mercury. Even heating to 700 C in air

IOCR Final Report

resulted in more than twice the concentration of mercury remaining in the solids compared with heating to 400 C in nitrogen (2.07 ng/g vs. 0.75 ng/g).

The results for the tests with Hibtac green balls are given on Table II. The results were similar to the ones from the Minntac green balls at lower temperatures. Namely, that more mercury was released in nitrogen than in air. The main difference between the two green balls was seen above 400°C. Above 400°C with the Hibtac green balls there was essentially no difference between air and nitrogen, while with the Minntac green balls there was always a significant difference between air and nitrogen.

To investigate the effect time may have on the mercury release, Hibtac green balls were tested at 450°C. The samples were placed in the furnace for 5, 10 and 15 minutes in air and in nitrogen. The times *refer* to the time from insertion of the boat until removal. In these tests all of the boats including those from the nitrogen tests were removed from the tube to cool. The test results, Table II, indicate that a significant amount of the mercury was released in 5 minutes with the release increasing with time.

Conclusion:

This test work has shown that the release of mercury during induration is related to temperature, time and atmosphere. Since Minntac green balls contain flux and caustic soda, the differences in chemistry may have had an effect on the mercury release. The rapid release of mercury with the Hibtac green balls suggests that in plant practice the mercury is released early in the process. Although time tests were not run on the Minntac green balls, it is probable that the release from Minntac green balls would also be rapid. This would suggest that the mercury is released on the grate in plant practice and, therefore, there should be little difference between straight-grate and grate-kiln plants. Since atmosphere appears to have an effect on mercury release, tests should be run in an atmosphere similar to that found in the plant machines.

Reference:

1. B. R. Benner, "Preparation of Mercury Standard from Taconite," CMRL technical report TR-01-16, September 25,2001.

IOCR Final Report

Table 1- Summary of Tests with Minntac Green Balls Air and Nitrogen Flow Rates = 0.67 l/min

Sample	HQ, ng/g	Sample Wt., g	ng Hg removed
Minntac Line 6 Green Balls	7.62		
Minntac Line 6 Green Balls	7.59		
AVG	7.61		
300°C in Air	6.42	4.6588	5.55
300°C in Nitrogen	2.69	4.7760	23.51
400°C in Air	2.89	4.0025	18.89
400°C in Nitrogen	0.75	4.1379	28.36
Standard (14 +/-1.2 ng/g)	14.20		
500°C in Air	3.70	3.8806	15.17
500°C in Nitrogen	0.92	3.9669	26.53
600°C in Air	2.17	4.7994	26.12
600°C in Nitrogen	0.48	4.7716	34.02
700°C in Air	2.07	5.0308	27.84
Standard (14 +/-1.2 ng/g)	13.57		

Table II - Summary of Tests with Hibtac Green Balls Air and Nitrogen Flow Rates = 0.067 l/min

Sample	HQ, ng/g	Sample Wt., g	ng Hg removed
HTC Green Balls, Head	20.69		
	20.34		
	21.39		
	21.01		
AVG, Head	20.86		
300°C in air	17.68	5.3661	17.05
300°C in nitrogen	9.21	5.2255	60.86
400°C in air	12.72	5.3464	43.50
400°C in air (repeat)	11.43	5.3845	50.77
400°C in nitrogen	4.17	5.3847	89.86
500°C in air	2.61	5.4278	99.02
500°C in nitrogen	2.39	5.5266	102.04
600°C in air	1.50	5.1340	99.40
Standard (14 +/-1.2 ng/g)	13.57		
Standard (14 +/-1.2 ng/g)	14.96		
450°C in air for 5 min	5.09	5.2466	82.69
450°C in air for 10 min	3.06	5.5479	98.71
450°C in air for 15 min	1.86	5.4438	103.39
450°C in N2 for 5 min	5.87	5.2495	78.69
450°C in N2 for 10 min	4.63	5.4550	88.52
450°C in N2 for 15 min	2.46	5.3369	98.19
Standard (14 +/-1.2 ng/g)	15.12		

9.4. Mössbauer Report (T. Berquo, IRM)

Mössbauer spectroscopy analyses of taconite dust samples

Thelma S. Berquó, Institute for Rock magnetism, Department of Geology and Geophysics, University of Minnesota, Minneapolis, MN 55455

1. Introduction

Mössbauer spectroscopy is used routinely as an analytical tool in many different areas of science, for example physics, biology and geology. In geology, materials like soils, sediments and rocks are frequently studied. Murad and Cashion (2004) introduced some useful information related to Mössbauer spectroscopy and mineral processing. This is a powerful technique to study iron ores, since the Fe is extremely abundant and mineral transformations are common during the processing of iron-containing ores. By using Mössbauer spectroscopy it is possible to observe the presence of different iron phases (magnetite, maghemite and hematite) or a mixture of these iron oxides during the processing.

Magnetite is a stable mineral found in iron deposits of northern Minnesota. This mineral oxidizes to Fe³⁺-oxides like maghemite or hematite. The specific mechanism of oxidation is complex and some information can be found at the literature, p. ex., Colombo et al. (1965), O'Reilly (1984) and Zhou et al. (2004).

The iron ore in northern Minnesota contains trace mercury which may be released during mineral processing. This mercury could be released during transformation of magnetite to another phase. The goal of this project is to determine and quantify relationships between iron oxide transformation and mercury release during mineral processing.

Mössbauer spectroscopy is a nuclear technique and has a rich literature where many books (Greenwood and Gibb, 1971, Cornell and Schwertmann, 1996, Murad and Cashion, 2004, among other) discuss the methods in details. Below we present a short introduction to Mössbauer spectroscopy adapted from Dickson and Berry (1983), some information about the hyperfine parameters obtained by the technique and finally the experimental data obtained during this study on taconite processing samples.

2. Mössbauer spectroscopy

The energy of a nucleus situated in an atom and in a solid is modified very slightly by the environment of the nucleus. Mössbauer spectroscopy is a technique which enables these energy levels to be investigated by measuring the energy dependence of the resonant absorption of Mössbauer gamma rays by nuclei. Hence, the hyperfine interaction between the nucleus and its surrounding electrons are investigated by this technique using the nucleus itself to probe its chemical environment.

The most usual experimental arrangement for Mössbauer spectroscopy, and the one used in this study, involves a radioactive source containing the Mössbauer isotope source material in an excited state and material to be investigated containing this same isotope in its ground state. The source used in this work was the normally radioactive ^{57}Co which undergoes a spontaneous electron capture transition to give a metastable state of ^{57}Fe which in turn decays to the ground state via a gamma ray cascade which includes 14.4 keV gamma rays useful for Mössbauer studies of material containing iron atoms. Gamma rays emitted by the source are partially absorbed by the iron atoms before passing through a suitable detector.

A critical aspect of Mössbauer spectroscopy is the systematic varying of gamma ray energy through movement of the source and its resulting Doppler shift. Resonant absorption occurs when the energy of the gamma ray exactly matches the nuclear transition energy for iron nuclei in the absorber and the Doppler shifting of the energy provides the means to precisely match those energies at very specific source velocities. Thus, the resulting Mössbauer spectrum consists of a plot of gamma ray counts against the velocity of the source. The spectrum is accumulated for a period typically of the order of hours or days and is a function of the concentration of Fe atoms in various chemical states within the absorbing material. Relative concentration of different chemical forms for iron atoms in a solid source provides quantitative information on the mineralogy of the samples. Further information, useful for mineralogic identification and provided by the spectrums, include hyperfine parameters: isomer shift (IS), quadrupole splitting (QS) and magnetic hyperfine field (B_{hf}).

The **isomer shift** of the Mössbauer spectrum is a result of the electric monopole interaction between the nuclear charge distribution over the finite nuclear volume and the electronic charge density over this volume. The **quadrupole splitting** obtained from the Mössbauer measurement involves both nuclear quantity, the quadrupole moment, and an electronic quantity, the electric field gradient. This parameter reflects the symmetry of the bonding environment and the local structure in the vicinity of the Mössbauer atom. Finally, the **magnetic hyperfine field** is the interaction between the nuclear magnetic moment and the net effective magnetic field that is felt by the nucleus.

3. The Iron Oxides

Iron occurs in minerals both as a major constituent and also as an impurity. Magnetite, maghemite, and hematite, the three primary minerals of interest here, were characterized with Mössbauer spectroscopy. Detailed Mössbauer information for these minerals, briefly reviewed below, can be found in the following sources: Long and Grandjean, 1993; Vandenberghe et al., 1990; Cornell and Schwertmann, 1996; Vandenberghe et al., 2000; Murad and Cashion, 2004.

Magnetite is a ferrimagnetic mineral and differ from the other iron oxides because contain both divalent an trivalent iron, with structural formula $(\text{Fe}^{3+})_{\text{A}}[\text{Fe}^{2.5+}]_{\text{B}}\text{O}_4$ in which the B site, with ferrous and ferric ions, merge into $\text{Fe}^{2.5+}$ due to a fast electron hopping above the Verwey transition (~ 120 K). Mössbauer spectrum at room temperature

can be fitted with two well-known distinct sextets with typical hyperfine parameter for the sextet corresponding to high spin Fe^{3+} on the tetrahedral site ($B_{\text{hf}}=49.2$ T; $QS=0.02$ mm/s; $IS= 0.26$ mm/s) and the other one to $\text{Fe}^{2.5+}$ on the octahedral site ($B_{\text{hf}}=46.1$ T; $QS=-0.02$ mm/s; $IS= 0.67$ mm/s).

Magnetite forms a complete solid solution series with **maghemite**, a mineral similar to magnetite in structure, but where all or most Fe is in the trivalent state and cation vacancies, which are necessary to compensate for the oxidation of Fe^{2+} , are all located on the B-site; resulting in the formula $(\text{Fe}^{3+})_{\text{A}}[\square_{1/3}\text{Fe}^{3+}_{5/3}]_{\text{B}}\text{O}_4$ (\square represents vacancies). The room temperature Mössbauer spectrum of maghemite consists of a slightly asymmetric sextet with hyperfine parameter $B_{\text{hf}}=50.0$ T, $QS\sim 0$ mm/s and $IS=0.35$ mm/s.

For ideal magnetite the sextet area ratio A/B is 1:2 or 0.5. However, deviations from the ideal ratio are often observed due to oxidizing effects as magnetite becomes more maghemite-like. In such cases, there is a decrease in the $\text{Fe}^{2.5+}$ component and increase in Fe^{3+} component on the B-site. The B-site Fe^{3+} hyperfine parameters are similar from those of the A-site and together with introduction of vacancies this will result in a decrease of the B-site sextet area and an apparent increase of that of the A-site. Thus, the area ratio A/B can be used to determine the degree of oxidation of the magnetite, prior to formation of end-member maghemite or other phases.

Hematite is the most stable iron oxide phase in air and it is represented by the formula Fe_2O_3 . The material has red color and it is an important constituent in iron ores. At room temperature the Mössbauer spectrum of a stoichiometric hematite consists of a sextet with the following hyperfine parameters $B_{\text{hf}}=51.8$ T, $QS=-0.20$ mm/s and $IS=0.37$ mm/s. Hematite has the same chemical composition as maghemite, but it is a distinct mineral with different, generally less reactive, chemical behavior.

4. Taconite study

Taconite production involves the fine grinding and magnetic separation of magnetite from the iron ore and the conversion of the magnetic concentrate into pellets. The magnetic concentrate is composed mostly of magnetite which is rolled with other minor components (fluxing agents, binders, water) into balls (greenballs). The magnetite (or greenballs) is introduced into the indurating furnaces where mercury emissions are generated upon heating to high temperatures (Berndt, 2003).

The samples studied here are from four taconite processing facilities: Hibtac, Minntac, United Taconite and Ispat Inland. All Mössbauer spectra were measured at room temperature. A conventional constant-acceleration spectrometer was used in transmission geometry with a $^{57}\text{Co}/\text{Rh}$ source, using a α - Fe at room temperature to calibrate isomer shifts and velocity scale.

The hyperfine parameters obtained after fitting are presented from Table 1 to 6, as well as the fitted spectra are showed from Figure 1 to 6. Magnetite was noticed in all samples but with slightly changing ratio A/B, which is related to oxidation degree, with the increase

of the heating temperature. The main feature observed in these samples were variations in hematite amount and sometimes magnetite becoming well crystallized (ratio A/B~0.5) upon heating. Thermal treatment is a useful and very common method to provide well crystallized synthetic samples, where crystal defects like vacancies can be eliminated. The hematite is resultant from transformation of magnetite into hematite, the transformation of magnetite grains bigger than 300 nm in air atmosphere will produce hematite, even at low temperatures, and maghemite formation is by-passed (Cornell and Schwertmann, 1996). Maghemite was observed in the starting material from HIBTAC plant, but upon heating only oxidized magnetite ($A/B > 0.5$) and hematite were observed.

Several greenball samples that had been heated to temperatures up to 500° C in either air or N₂ gas for 20 minutes each at another laboratory were analyzed for mineralogy. These data are presented in Table 6 and Figure 6. With increase of the temperature it is possible to observe the increase of hematite amount, for samples heated in air. There is also a temperature dependent increase in A/B for the residual magnetite that does not convert to hematite. This magnetite is being progressively oxidized to magnetite/maghemite solid-solutions. For the sample heated at 500 °C at N₂ atmosphere we could identify the presence of 89% of magnetite which was became more stoichiometric ($A/B=0.59$) and 11% of another phase which could be represented by a combination of maghemite and hematite. The starting mineral appears to have unmixed. Therefore, a mineralogic change was observed in both cases, but each atmosphere produced different final products.

5. References

- Berndt, M. E. (2003) *Mercury and mining in Minnesota*. Final report, Minnesota Department of Natural Resources, 58p.
- Colombo, U., Gazzarrini, F., Lanzavecchia, G., Sironi, G. (1965) Magnetite oxidation: a proposed mechanism. *Science*, 147, 1033.
- Cornell, R. M. and Schwertmann, U. (1996) *The iron Oxides: structure, properties, reactions, occurrence and uses*. VCH, Weinheim, 573p.
- Dickson, D. P. E. and Berry, F. J. (1986) *Mössbauer spectroscopy*. Cambridge University Press, Cambridge, 274p.
- Greenwood, N. N. and Gibb, T. C. (1971) *Mössbauer spectroscopy*. Chapman and Hall, London, 659p.
- Long, G. J. and Grandjean, F. (1993) *Mössbauer spectroscopy applied to magnetism and materials science*. Plenum Press, New York, 479p.

IOCR Final Report

Murad, E. and Cashion, J. (2004) *Mössbauer spectroscopy of environmental materials and their utilization*. Kluwer, Boston, 417p.

O'Reilly, W. (1984) *Rock and mineral magnetism*. Chapman and Hall, London, 220p.

Vandenbergh R. E., De Grave E., Landuydt C., Bowen L. H. (1990) Some aspects concerning the characterization of iron oxides and hydroxides in soils and clays. *Hyp Interact.*, **53**, 175-196.

Vandenbergh R. E., Barrero, C. A., da Costa, G. M., Van San, E., De Grave E. (2000) Mössbauer characterization of iron oxides and (oxy)hydroxides: the present state of the art. *Hyp. Interact.*, **126**, 247-259.

Zhou, Y., Jin, X., Mukovskii, Y. M., Shvets, I. V. (2004) Kinetics of low-index surfaces of magnetite. *J. Phys.:Condens. Matter*, **16**, 1-12.

Table 1 – Hyperfine parameters for Hibtac under-grate samples.

Sample	B_{hf} (T)	QS (mm/s)	IS (mm/s)	%	Site	Ratio	Iron phase
H2P1	51.6(1)	-0.19(1)	0.37(1)	12			Hematite
	49.0(2)	-0.01(1)	0.26(1)	36	A	0.69	Magnetite
	45.9(1)	0.01(1)	0.66(1)	52	B		
H2P3	51.7(1)	-0.17(3)	0.37(1)	6			Hematite
	48.9(1)	-0.02(1)	0.27(1)	37	A	0.65	Magnetite
	45.9(1)	0.01(1)	0.66(1)	57	B		
H2P4	51.8(1)	-0.20(1)	0.38(2)	10			Hematite
	49.1(2)	-0.01(1)	0.27(1)	35	A	0.64	Magnetite
	46.0(1)	0.01(1)	0.65(1)	55	B		
H2P5	51.9(3)	-0.17(3)	0.39(1)	6			Hematite
	49.2(2)	-0.01(2)	0.28(1)	36	A	0.62	Magnetite
	45.9(1)	0.01(1)	0.65(1)	58	B		
H2P6	51.6(1)	-0.18(1)	0.37(1)	50			Hematite
	49.0(2)	-0.02(1)	0.28(1)	19	A	0.61	Magnetite
	46.0(1)	0.01(1)	0.67(1)	31	B		
H2P8	50.5(1)	-0.03(1)	0.48(1)	4			Maghemite
	49.0(1)	-0.01(1)	0.26(1)	35	A	0.57	Magnetite
	45.9(1)	0.02(1)	0.66(1)	61	B		

IOCR Final Report

Table 2 – Hyperfine parameters from Ispat-Inland under-grate samples.

Sample	B _{hf} (T)	QS (mm/s)	IS (mm/s)	%	Site	Ratio	Iron phase
I5S1	49.0(1)	-0.02(1)	0.28(1)	40	A	0.67	Magnetite
	45.9(1)	0.01(1)	0.67(1)	60	B		
	51.9(1)	-0.21(6)	0.38(3)	8			
I6S2	49.0(1)	-0.04(1)	0.27(1)	36	A	0.64	Magnetite
	46.0(1)	0.01(1)	0.68(1)	56	B		
	51.7(1)	-0.17(1)	0.39(2)	13			
I6S3	49.0(2)	-0.01(1)	0.27(1)	33	A	0.64	Magnetite
	46.0(1)	0.01(1)	0.65(1)	54	B		
	51.6(3)	-0.12(6)	0.37(3)	9			
I6S4	48.9(1)	-0.02(2)	0.23(1)	34	A	0.60	Magnetite
	46.0(1)	0.03(1)	0.67(1)	57	B		
	51.4(4)	-0.15(8)	0.35(5)	8			
I6S5	49.1(1)	-0.01(1)	0.26(1)	35	A	0.61	Magnetite
	46.0(1)	0.01(1)	0.65(1)	57	B		
	51.6(3)	-0.18(2)	0.36(1)	26			
I6S6	49.0(1)	-0.03(2)	0.25(1)	28	A	0.60	Magnetite
	46.0(1)	0.02(1)	0.66(1)	46	B		
	51.7(1)	-0.13(1)	0.37(1)	37			
I6S7	48.9(1)	-0.04(1)	0.27(1)	27	A	0.75	Magnetite
	46.1(1)	0.02(1)	0.69(1)	36	B		

Table 3 – Hyperfine parameters from Minntac Line 7 under grate samples.

Sample	B _{hf} (T)	QS (mm/s)	IS (mm/s)	%	Site	Ratio	Iron phase
M4S6	51.6(3)	-0.18(3)	0.37(1)	64		0.57	Magnetite
	48.9(2)	-0.03(2)	0.28(1)	13	A		
	46.1(1)	0.03(1)	0.67(1)	23	B		
M4S4	51.7(1)	-0.18(1)	0.38(2)	9		0.63	Magnetite
	49.0(2)	-0.00(1)	0.27(1)	35	A		
	46.0(1)	0.01(1)	0.65(1)	56	B		
M4S2	51.9(2)	-0.15(4)	0.39(2)	9		0.65	Magnetite
	49.0(1)	-0.01(1)	0.26(1)	36	A		
	46.0(1)	0.01(1)	0.66(1)	55	B		
M5S1	49.0(2)	-0.04(1)	0.27(1)	38	A	0.61	Magnetite
	46.0(1)	0.02(1)	0.67(1)	62	B		

IOCR Final Report

Table 4 – Hyperfine parameters from United Taconite under-grate samples.

Sample	B _{hf} (T)	QS (mm/s)	IS (mm/s)	%	Site	Ratio	Iron phase
U5S1	49.0(1)	-0.03(1)	0.26(1)	39	A	0.55	Magnetite
	46.0(1)	0.01(1)	0.66(1)	66	B		
	51.6(1)	-0.17(3)	0.37(1)	63			Hematite
U5S5	48.9(1)	-0.02(1)	0.26(1)	12	A	0.48	Magnetite
	45.8(1)	0.01(1)	0.70(1)	25	B		
	51.6(1)	-0.18(1)	0.37(2)	65			Hematite
U5S7	48.9(1)	-0.01(2)	0.28(1)	13	A	0.59	Magnetite
	45.9(1)	0.01(1)	0.66(1)	22	B		

Table 5 – Hyperfine parameters from scrubber solids.

Sample	B _{HF} (T)	QS (mm/s)	IS (mm/s)	%	Site	Ratio	Iron phase
Hibtac	51.7	-0.18	0.38	72		0.56	Hematite
	48.9	-0.05	0.30	10	A		Magnetite
	46.1	-0.05	0.71	18	B		
Hibtac 2	51.6	-0.19	0.37	73		0.59	Hematite
	49.0	-0.07	0.26	10	A		Magnetite
	45.9	-0.02	0.69	17	B		
Ispat	51.7	-0.18	0.37	79		0.75	Hematite
	48.5	0.09	0.31	9	A		Magnetite
	45.8	0.03	0.68	12	B		
Minntac	51.7	-0.18	0.36	16		0.71	Hematite
	49.2	-0.05	0.26	35	A		Magnetite
	46.0	-0.03	0.66	49	B		
United	51.7	-0.18	0.36	48		0.73	Hematite
	49.2	-0.07	0.27	22	A		Magnetite
	45.9	0.02	0.67	30	B		

Table 6 – Hyperfine parameters for products from heated greenball experiments.

Sample	B _{HF} (T)	QS (mm/s)	IS (mm/s)	%	Site	Ratio	Iron phase
GB	49.5	-0.02	0.29	42	A	0.72	Magnetite
	45.9	0.00	0.64	58	B		
GB400A	52.0	-0.14	0.39	11		0.98	Hematite
	49.5	-0.04	0.28	44	A		Magnetite
	45.9	0.00	0.65	45	B		
GB500A	51.8	-0.14	0.37	23		1.26	Hematite
	49.1	-0.06	0.26	43	A		Magnetite
	46.3	0.05	0.71	34	B		
GB500N	50.5	0.16	0.43	11		0.59	Hematite (?)
	49.2	-0.07	0.25	33	A		Magnetite
	45.9	0.04	0.65	56	B		

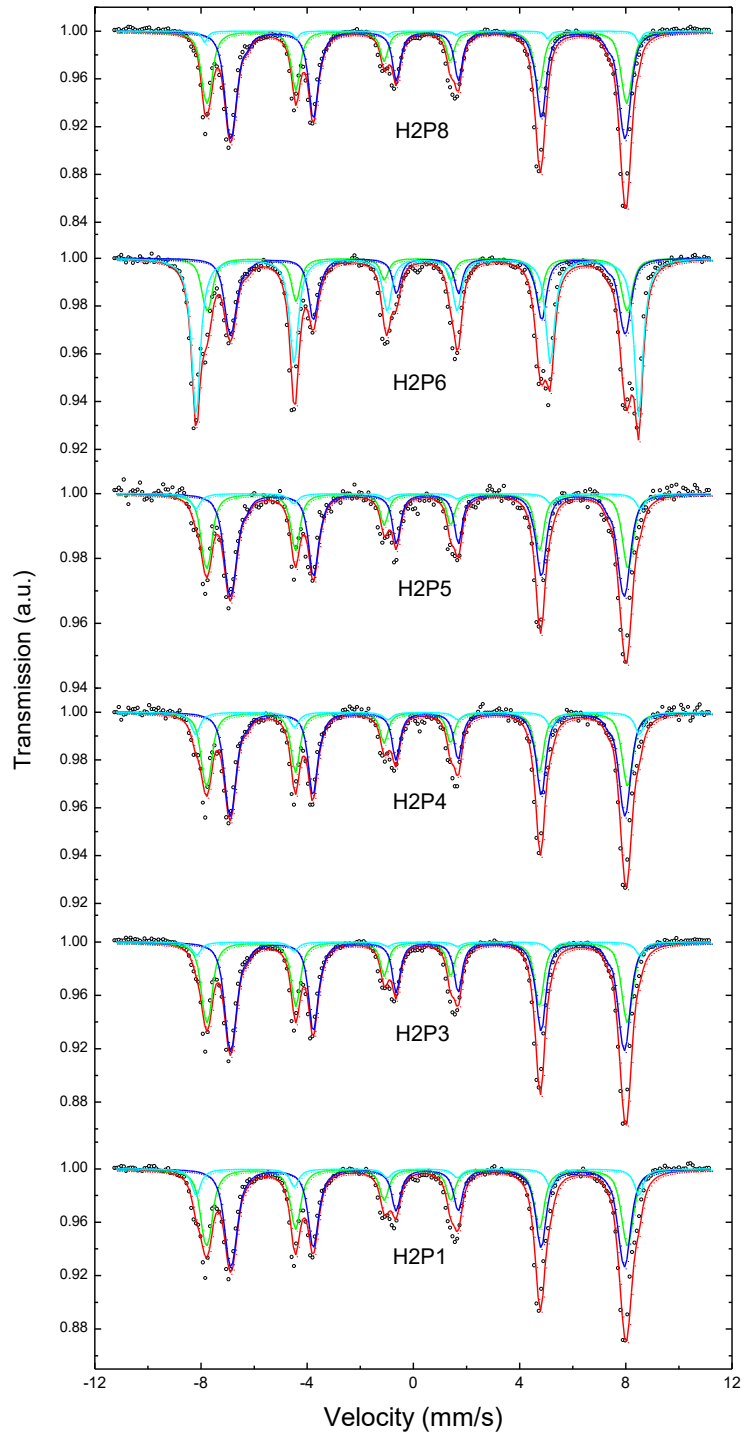


Figure 1 - Mössbauer spectra from Hibtac under-grate samples.

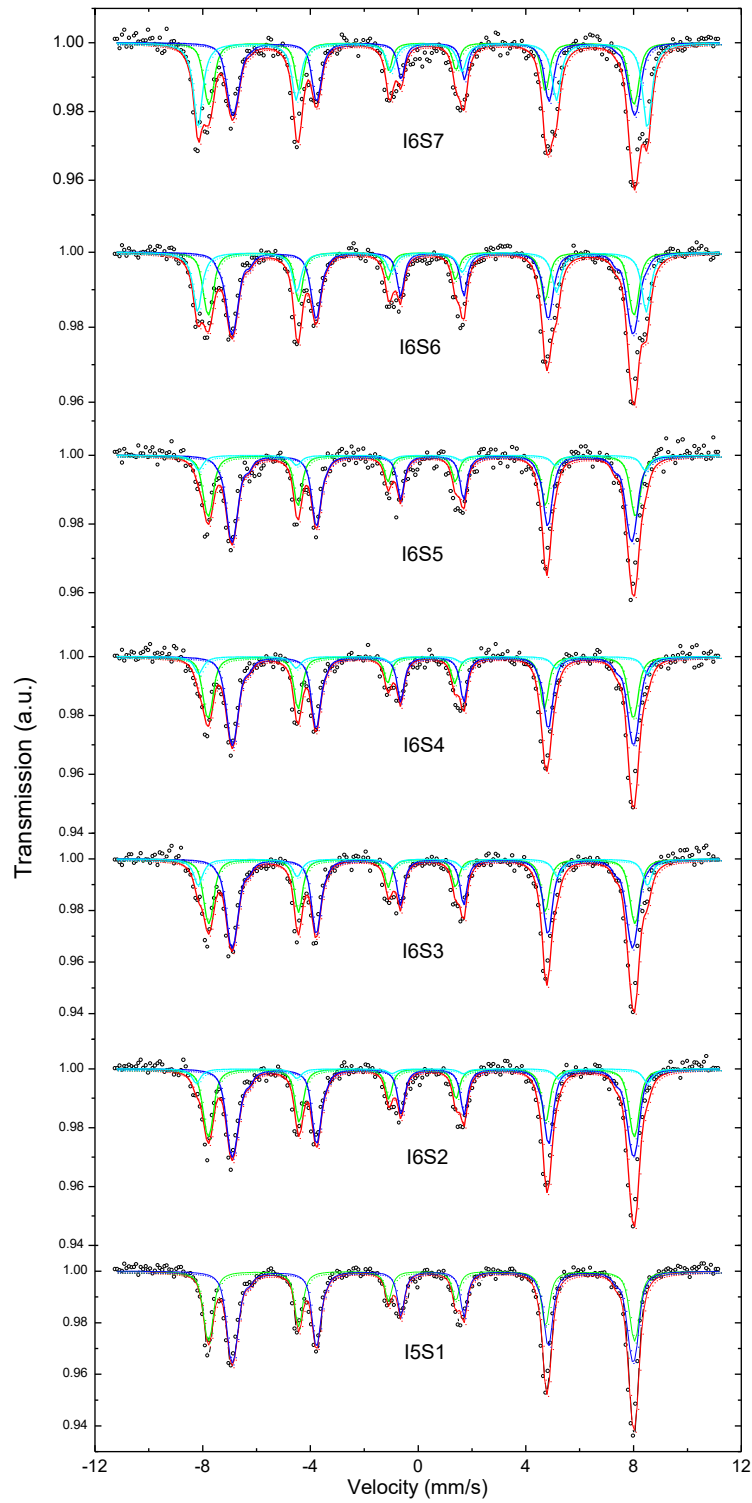


Figure 2 - Mössbauer spectra from Ispat Inland under-grate samples.

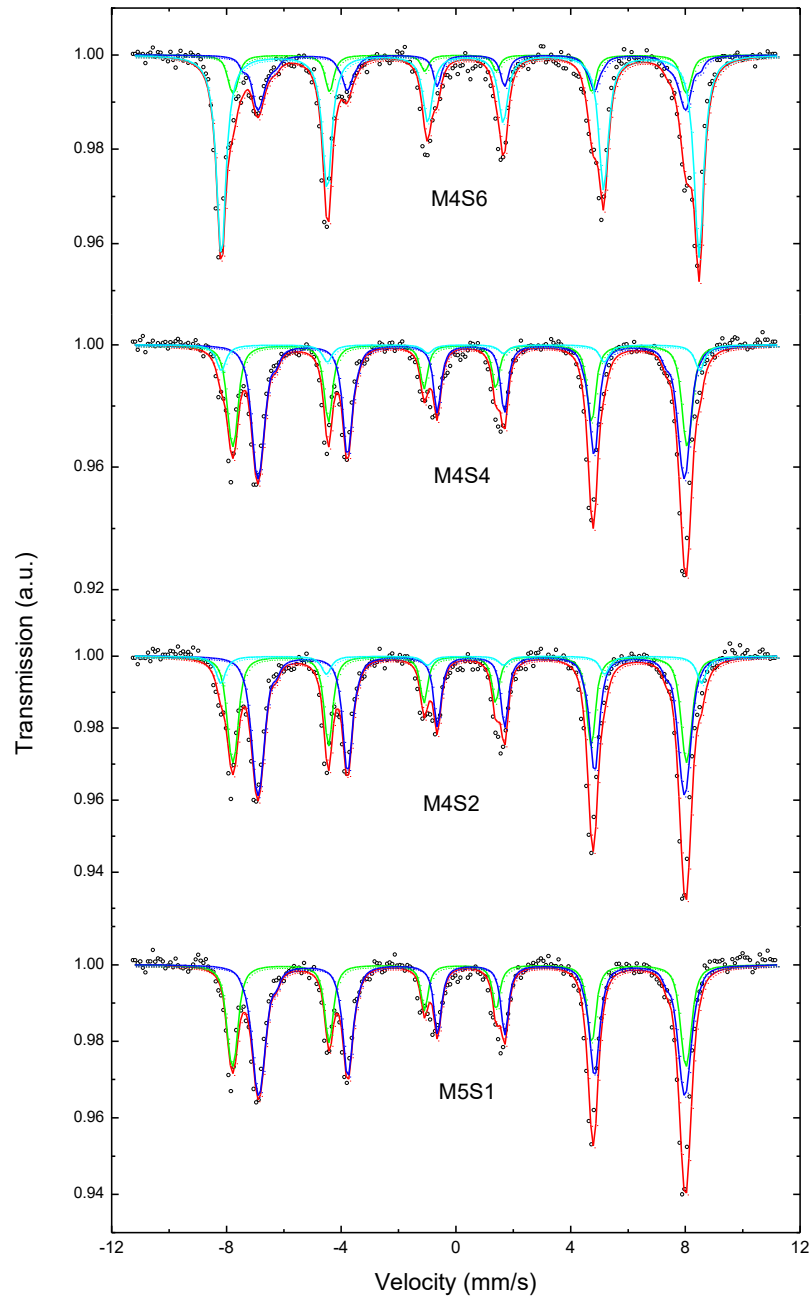


Figure 3 - Mössbauer spectra from Minntac Grate samples.

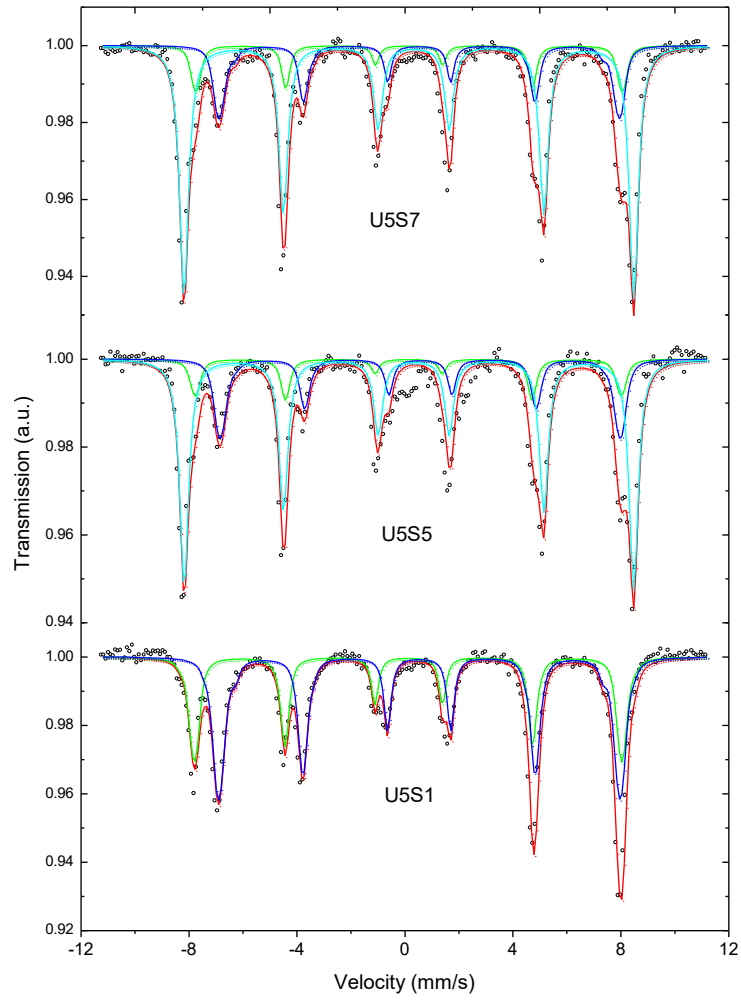


Figure 4 - Mössbauer spectra from United Taconite Grate samples.

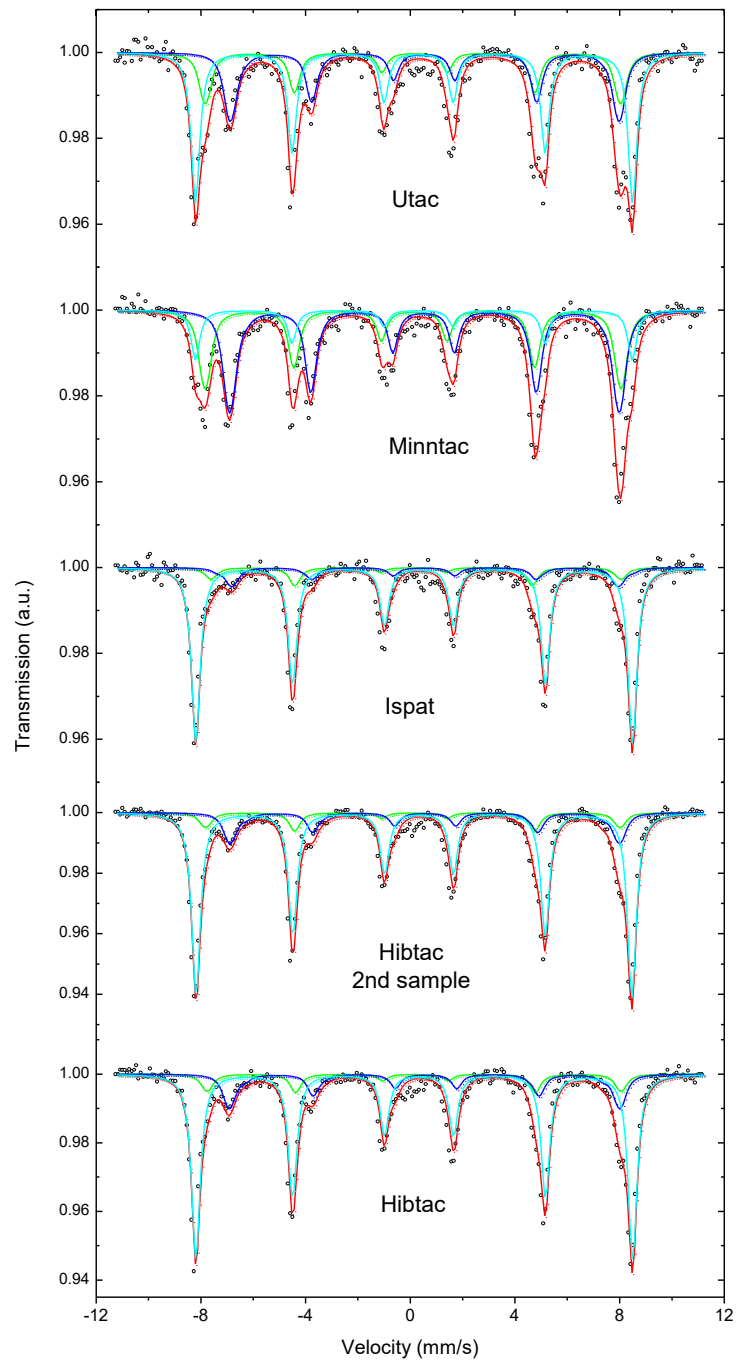


Figure 5 - Mössbauer spectra from scrubber solids.

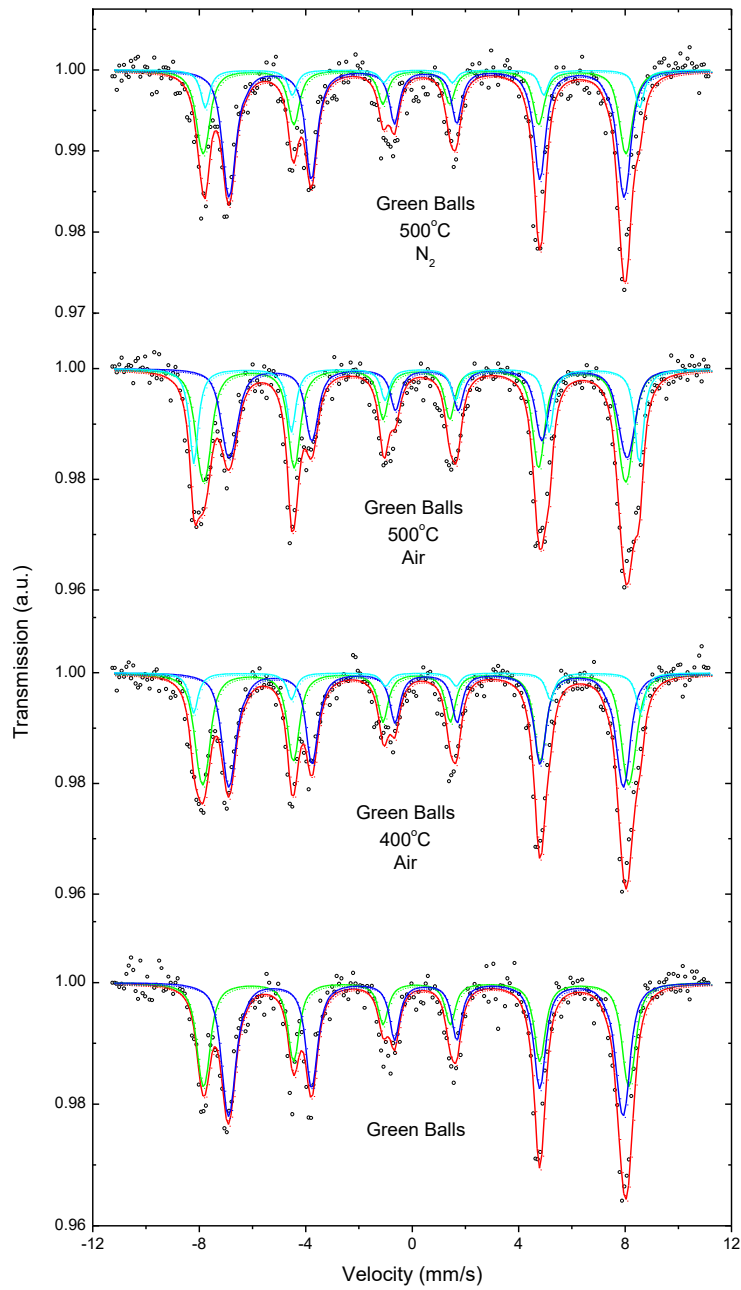


Figure 6 - Mössbauer spectra from heated Minntac greenball samples.

9.5. Raw Mercury Data**Hibtac**

DNR 2003 Study		Hg(D)	Hg(P)	TSS	Hg(T)
2/20/2003		ng/l	ng/g	wt%	ng/l
Hg6	Scrubber Water, filtered after 5 days	13.5	5027.4	0.01226	629.9
Hg8	Scrubber Water, filtered immediately	255.5	1405.5	0.007	353.9
Hg1	Multiclone Dust in proc. water, filtered 5 days	5.2	175.2		
Hg3	Multiclone Dust in proc. water, filtered 5 days	11.7	129.9		
Average		255.5	1405.5	0.00963	492
5/8/2003					
2-1	Scrubber Water, filtered immediately	337.3	420.2	0.035	484.4
2-3	Scrubber Water, filtered immediately	340.8	791	0.035	617.7
2-5	Scrubber Water, filtered after 6 days	13.6	1519	0.0328	511.8
2-6	Scrubber Water, filtered after 6 days	13	1539.3	0.0325	513.3
Average		339.05	605.6	0.033433	532
Round 1					
9/11/2003					
H1W1	Scrubber Water, filtered immediately	257.2	597.1	0.038	484.1
H1W2	Scrubber Water, filtered immediately	204.5	610.2	0.038	436.4
Average		230.85	603.65	0.038	460
1/27/2004 Round 2					
H2W1	Scrubber Water, filtered immediately	301.5	1549	0.0178	577.2
H2W2	Scrubber Water, filtered immediately	281.6	1419	0.0178	534.2
Average		291.55	1484	0.0178	556
H2Blank1	Filtered DI Water				
H2Blank2	Unfiltered DI Water				
H2P1	Grate Dust (Windbox 18)		21.8		
H2P2	Grate Dust (Windbox 16)		127.2		
H2P3	Grate Dust (Windbox 14)		463.6		
H2P4	Grate Dust (Windbox 12)		93.5		
H2P5	Grate Dust (Windbox 8)		19.3		
H2P6	Grate Dust (Scraped between WB 6 and 7)		31.8		
H2P7	Grate Dust (Scraped between WB 2 and 3)		17.9		
H2P8	Greenball (dried)		10.9		
5/12/2004 Round 3					
H3W1	Scrubber Water, filtered immediately	63	2363	0.013	370.2
H3W2	Scrubber Water, filtered immediately	410.4	1715	0.013	633.4
Average		236.7	2039	0.013	502
H3W3	Rougher feed, Decanted, Filtered	4.7			
H3W4	Rougher feed, Decanted, Filtered	4.3			

IOCR Final Report

H3Blank1	Filtered DI Water	1.7
H3Blank2	Unfiltered DI Water	1.1

H3S1	Greenball	16.5
------	-----------	------

7/27/2004 Round 4

H4W1	Scrubber Water, filtered immediately	282.5	2710.9	0.0139	659.3
H4W2	Scrubber Water, filtered immediately	305.4	2914.6	0.0136	701.8
H4W3	Scrubber Water, Filtered at 5 Min	269.5	3096.4	0.0136	690.6
H4W4	Scrubber Water, Filtered at 10 Min	422.3	2712.3	0.0136	791.2
H4W5	Scrubber Water, Filtered at 15 Min	215.1	3300.1	0.0136	663.9
H4W6	Scrubber Water, Filtered at 30 Min	169.8	3581.1	0.0136	656.8
H4W7	Scrubber Water, Filtered at 60 Min	129.9	3859.5	0.0136	654.8
Average		293.95	2812.75	0.013643	688
H4Blank1	Filtered DI Water	3.2			
H4Blank2	Unfiltered DI Water	3.4			
H4S1	Greenball		20.6		

Round 5

Lines shut down when we arrived.

2/15/2005 Round 6

H6W1	Scrubber Water, filtered immediately	607.5	3147.1	0.024	1362.8
H6W2	Scrubber Water, filtered immediately	833.7	2601.3	0.024	1458.0
Average		720.6	2874.2	0.024	1410
H6N1	Non Magnetic Fraction, 5 mls tails, 245 mls scrubber water		1912.4		
H6N3	Non Magnetic Fraction, 10 mls tails, 240 mls scrubber water		1012.1		
H6N4	Non Magnetic Fraction, 10 mls tails, 240 mls di-water		57.7		
H6N5	Non Magnetic Fraction Scrubber Water		7387.1		
H6M1	Magnetic Fraction, 5 mls tails, 245 mls sw		784.8		
H6M3	Magnetic Fraction, 10 mls tails, 240 mls sw		539.8		
H6M4	Magnetic Fraction, 10 mls tails, 240 mls di-water		99.8		
H6M5	Magnetic Fraction Scrubber Water Solids		2521.714		
H6Blank1	Filtered DI Water	2.9			
H6Blank2	Unfiltered DI Water	2.3			
H6S1	Greenball		18.6		

5/19/2005 Round 7

H7W1	Scrubber Water, filtered immediately	258.9	6407	0.0073	726.6
H7W2	Scrubber Water, filtered immediately	249.3	9178	0.0057	772.4
H7W3	Scrubber Water, filtered immediately	194.2	9603	0.0052	693.6
Average		234.1333	8396	0.006067	731

IOCR Final Report

H7B1	Filtered DI Water	2.5	4.9
H7B2	Unfiltered DI Water	1.8	
H7S1	Greenball Feed Sample		26.4

Minntac

Minntac		Hg(D) ng/l	Hg(P) ng/g	TSS wt%	Hg(T) ng/l
DNR 2003 Study					
2/19/2003					
Hg1	Scrubber Water Line 4 (filtered after 6 days)	26.9	2306.5	0.05179	1221.4
Hg2	Scrubber Water Line 4 (filtered after 6 days)	22.9	1864.2	0.06318	1200.7
Hg3	Scrubber Water Line 4 (filtered immediately)	115.8	1284.8	0.086	1220.7
Hg5	Scr. Water Line 4 (acidified to pH 3, filtered 6 days)	68.3	1970.3	0.05789	1208.9
Hg6	Scr. Water Line 4 (acidified to pH 4.5, filtered 6 days)	22.3	2093.7	0.05201	1111.2
Hg8	Scr. Water Line 4 (NaOH add to pH 9, filtered 6 days)	16.9	2607.7	0.0391	1036.5
Average		115.8	1284.8	0.058328	1166.6
5/9/2003					
2-1	scrubber water line 4 filtered immediately	89.8	153	0.387	681.9
2-3	scrubber water line 4 filtered immediately	72.6	167.6	0.387	721.2
2-5	scrubber water (filtered after 6 days)	25.7	179.9	0.2423	461.6
2-6	scrubber water (filtered after 6 days)	26.7	173.8	0.2423	447.8
Average		81.2	160.3	0.31465	578.1
Round 1					
9/10/2003					
M1W1	scrubber water line 4 filtered immediately	264	484.3	0.217	1314.9
M1W2	scrubber water line 4 filtered immediately	684.5	383.2	0.217	1516.0
20t-1	filtered upon return to lab (approx 3 hr, 20C)	92.8	1620	0.217	3608.2
20t-2	filtered after 22 hours (20 C)	51.7	876.5	0.217	1953.7
40t-1	filtered after 30 min. (40 C)	193.8	758.4	0.217	1839.5
40t-2	filtered after 60 min. (40 C)	305.2	634	0.217	1681.0
60t-1	filtered after 30 min.(60 C)	364.3	659.9	0.217	1796.3
60t-2	filtered after 60 min. (60 C)	164.2	953.1	0.217	2232.4
Average		474.25	433.75	0.217	1992.8
1/28/2004 Round 2					
M2W1	scrubber water line 4 filtered immediately	159	1264.4	0.145	1992.4
M2W2	scrubber water line 4 filtered immediately	168	1850.3	0.145	2850.9
Average		163.5	1557.35	0.145	2421.658
M2W7	scrubber water line 7 , filtered immediately	210.6	2647.1	0.0413	1303.9
M2W8	scrubber water line 7 , filtered immediately	235.6	2331.3	0.0413	1198.4
Average		223.1	2489.2	0.0413	1251.14

IOCR Final Report

M2W3	scrubber thickener underflow, filtered immediately	16.3	37.2	35.73	13307.9
M2W5	overflow from scrubber thickener	109.3	325.5	0.0076	134.0
M2W6	overflow from thickener (not filtered)				139.6
5/11/2004 Round 3					
M3W1	scrubber water line 7, filtered immediately	291.3	2182.2	0.052	1426.0
M3W2	scrubber water line 7, filtered immediately	290	3262.8	0.052	1986.7
Average		290.65	2722.5	0.052	1706.35
M3W3	Lines 6 & 7 agglomerator to concentrator, filtered immediately	3.7	55.6	0.12	70.4
M3W4	Lines 6 & 7 agglomerator to concentrator, filtered immediately	5.0	35.1	0.12	47.1
M3B1	filtered DI water	2.3	1.2		
M3B2	unfiltered DI water	1.2			
M3S1	greenball feed sample		8.1		
7/27/2004 Round 4					
M4W1	scrubber water line 7, filtered immediately	269.7	3144.9	0.0952	3263.6
M4W2	scrubber water line 7, filtered immediately	340	1982.7	0.0952	2227.5
Average		304.85	2563.8	0.0952	2745.588
M4B1	filtered DI water	3.7	0.1		
M4B2	unfiltered DI water	2.4			
M4S1	greenball feed sample		11.6		
M4S2	DD1 dust in water, filtered, dried		91.3		
M4S3	DD2 dust in water, filtered, dried		56.6		
M4S4	DD2 dust in water, filtered, dried		66.1		
M4S5	windbox 1 in preheat zone (dry dust)		14.9		
M4S6	windbox 2 in preheat zone (dry dust)		2.8		
M4S7	windbox 3 in preheat zone, (dry dust)		0.7		
12/1/2004 Round 5					
M5W1	scrubber water line 7, filtered immediately	204.8	2942	0.075	2411.3
M5W2	scrubber water line 7, filtered immediately	263.8	2717.5	0.075	2301.9
Average		234.3	2829.75	0.075	2356.613
M5B1	filtered DI water	2.9	2.6		
M5B2	unfiltered DI water	3.2			
M5S1	greenball feed sample		8.5		
M5M1	Magnetic fraction, tails plus scrubber water (20 hrs)		22		
M5M2	Magnetic fraction, tails plus scrubber water		24.8		
M5M3	Magnetic fraction, tails plus scrubber water		26.3		
M5M4	Magnetic fraction, tails plus DI water		24.2		
M5M5	Magnetic fraction, scrubber water		304.7		

IOCR Final Report

M5N1	Non-Magnetic fraction, tails plus scrubber water		44.3
M5N2	Non-Magnetic fraction, tails plus scrubber water		36.1
M5N3	Non-Magnetic fraction, tails plus scrubber water		28
M5N4	Non-Magnetic fraction, tails plus DI water		29.5
M5N5	Non-Magnetic fraction, scrubber water		26072.8

2/16/2005 Round 6

M6W1	line 7 filtered scrubber water	198.7	3171.2	0.058	2038.0
M6W2	line 7 filtered scrubber water	463.7	2538.1	0.058	1935.8
Average		331.2	2854.65	0.058	1986.897

M6B1	filtered DI water	6.5	2.3
M6B2	unfiltered DI water	6.6	
M6S1	greenball feed sample		12
M6N1	non-magnetic fraction of scrubber water (after 1 day)		9190.8
M6M1	magnetic fraction of scrubber water (after 1 day)		221.6

5/20/2005 Round 7

M7W1	scrubber water line 7, filtered immediately	194.5	1424.5	0.097	1576.3
M7W2	scrubber water line 7, filtered immediately	272.9	1426.6	0.098	1671.0
M7W3	scrubber water line 7, filtered immediately	301.5	1228.3	0.105	1591.2
Average		256.3	1359.8	0.1	1612.816

M7B1	Filtered DI water	3.9	9.9
M7B2	Unfiltered DI water	2.3	
M7S1	Greenball Feed Sample		16.1

U-Tac

United Taconite		Hg(D)	Hg(P)	TSS	Hg(T)
		ng/l	ng/g	wt%	ng/l
DNR 2003 Study					
2/18/2003 (EVTAC)					
Hg1	Scrubber thickener underflow (filtered after 7 days)	108.2	496.6	0.5405	2792.3
Hg2	Scrubber thickener underflow (filtered after 7 days)	76.4	436.6	0.8676	3864.3
Hg3	Scrubber thickener underflow (filtered immediately)	64.2	978.7	1.34	13178.8
Average		64.2	978.7	0.916033	6611.8
5/8/2003					
Mine shutdown					
Round 1					
9/11/2003					
Mine shutdown					
1/27/2004 Round 2					
U2W2	Scrubber thickener underflow (filtered immediately)	79.3	644.7	0.903	5900.9

IOCR Final Report

U2W3#	Scrubber thickener underflow (filtered immediately)	815.8#	692.9	0.903	
U2W4	Scrubber thickener underflow (filtered immediately)	79.3	656.1	0.903	6003.9
U2W5	Scrubber thickener underflow (filtered immediately)	119.2	796.1	0.903	7308.0
Average		92.6	698.9667	0.903	6404.269

5/11/2004 Round 3

U3W1	Scrubber thickener underflow (filtered immediately)	242.9	541.4	1.27	7118.7
U3W2	Scrubber thickener underflow (filtered immediately)	85.8	647.5	1.27	8309.1
Average		164.35	594.45	1.27	7713.865

U3W3	agglomerator to concentrator	11.1	115.1	0.497	583.1
U3W4	agglomerator to concentrator	12.9	117	0.497	594.4
U3B1	filtered DI water	1.5			
U3B2	unfiltered DI water	1.3			

U3S1	Greenball feed		13.2		
------	----------------	--	------	--	--

7/28/2004 Round 4

U4W1	Scrubber thickener underflow (filtered immediately)	135.9	357.5	2.26	8215.4
U4W2	Scrubber thickener underflow (filtered immediately)	88.5	561	2.26	12767.1
Average		112.2	459.25	2.26	10491.25

U4B1	filtered DI water	2.3			
U4B2	unfiltered DI water	1.1			
U4M1	Magnetic fraction, tails and s.w. mixture, approx 20 hrs		69		
U4M2	Magnetic fraction, tails and s.w. mixture, approx 20 hrs		58.3		
U4M3	Magnetic fraction, tails and s.w. mixture, approx 20 hrs		64.2		
U4M4	Magnetic fraction, tails(20%) plus DI water, approx 20 hrs		25		
U4M5	Magnetic fraction, scrubber solids, 20 hrs		182.4		
U4N1	Non-Magnetic fraction, tails and sw mixture, 20 hrs		88.3		
U4N2	Non-Magnetic fraction, tails and sw mixture, 20 hrs		74.8		
U4N3	Non-Magnetic fraction, tails and sw mixture, 20 hrs		61.2		
U4N4	Non-Magnetic fraction, tails(20%) plus DI water, 20 hrs		16.7		
U4N5	Non-Magnetic fraction, scrubber solids, 20 hrs		1237.4		

U4S1	Greenball Feed Sample		12.4		
------	-----------------------	--	------	--	--

11/29/2004 Round 5

U5W1	Scrubber thickener underflow (filtered immediately)	38.1	264.9	2.41	6422.2
U5W2	Scrubber thickener underflow (filtered immediately)	26.6	379	2.41	9160.5
Average		32.35	321.95	2.41	7791.345

U5B2	unfiltered DI water	4.6			
U5S1	Greenball Feed Sample		13.8		
U5S2	Launderers in down draft zone, east side line 2		23.9		
U5S3	Launderers in down draft zone, east side line 2		24.2		
U5S4	Launderers in down draft zone, east side line 2		20.5		
U5S5	Launderers in down draft zone, east side line 2		23.5		

IOCR Final Report

U5S6	multi-tube samples, preheat zone	1.7
U5S7	multi-tube samples, preheat zone	1.6
U5S8	multi-tube samples, preheat zone	1.6
U5S9	multi-tube samples, preheat zone	2.4

2/14/2005 Round 6

U6W1	Scrubber thickener underflow (filtered immediately)	1423.8	861.6	2.18	20206.7
U6W2	Scrubber thickener underflow (filtered immediately)	1456.4	834.1	2.18	19639.8
Average		1440.1	847.85	2.18	19923.23
U6B1	filtered DI water	2.9			
U6B2	unfiltered DI water	1.2			
U6S1	Greenball Feed Sample		24.3		
U6N1	Non-Magnetic Fraction (Scrubber Water, 3 days)		1312.4		
U6M1	Magnetic Fraction (Scrubber Water, 3 days)		311.4		

5/19/2005 Round 7

U7W1	Scrubber thickener underflow (filtered immediately)	237	944.4	1.26	12136.4
U7W2#	Scrubber thickener underflow (filtered immediately)	3474#	422.7#	0.86	
U7W3	Scrubber thickener underflow (filtered immediately)	82	1038.3	1.09	11399.5
U7W4	Scrubber thickener underflow (filtered immediately)	54.1	1019.4	1.63	16670.3
Average		124.3667	1000.7	1.21	13402.08
U7B1	Filtered DI water	3.1	7.3		
U7B2	Unfiltered DI water	3			
U7S1	Greenball Feed Sample		19.5		

Ispat

ISPAT

Hg(D)	Hg(P)	TSS	Hg(T)
ng/l	ng/g	wt%	ng/l

DNR 2003 Study

2/20/2003

Hg1	Scrubber water, filtered at lab	35.9	1105.3	0.328	3661.3
Hg2	Scrubber water, filtered at lab	33.7	1012.6	0.328	3355.0
Hg3	Scrubber water, filtered immediately	1215.5	616.8	0.328	3238.6
Average		1215.5	616.8	0.328	3418.3

5/8/2003

2-1	Scrubber water, filtered immediately	849.8	4378.8	0.142	7067.7
2-3	Scrubber water, filtered immediately	853.2	1560.2	0.142	3068.7
2-5	Scrubber water, filtered at lab	585.2	3382.9	0.142	5388.9
2-6	Scrubber water, filtered at lab	529.1	3550.1	0.142	5570.2
Average		851.5	2969.5	0.142	5273.9

Round 1

9/11/2003

I1W2	Scrubber water, filtered immediately	1174.3	2224.35	0.175	5066.9
I1W2-A	Half of filter for I1W2		2169.5		
I1W2-B	Other half of filter for I1W2		2279.2		

IOCR Final Report

I1W3	Scrubber water, filtered immediately	1019.7	1890.7	0.175	4328.4
I1W3-A	Half of filter for I1W3		1778.9		
I1W3-B	Other half of filter for I1W3		2002.5		
I1W4	Scrubber water, filtered immediately	902.6	2168	0.175	4696.6
I1W4-A	Half of filter for I1W4		2232.8		
I1W4-B	Other half of filter for I1W4		2103.2		
Average		1032.2	2094.35	0.175	4697.313

1/27/2004 Round 2

I2W3	Scrubber water, filtered immediately	367.3	2300.6	0.137	3519.1
I2W4	Scrubber water, filtered immediately	1681.9	825.5	0.137	2812.8
Average		1024.6	1563.05	0.137	3165.979

5/12/2004 Round 3

I3W1	Scrubber water, filtered immediately	3536.2	678.1	0.095	4180.4
I3W2	Scrubber water, filtered immediately	3087.5	202.6	0.095	3280.0
Average		3311.85	440.35	0.095	3730.183

I3W3	concentrate filtrate water (I3F3)	7.0	54.4		
I3W4	concentrate filtrate water (I3F4)	4.8	30.3		
I3B1	filtered DI water (I3F5)	2.0	0.9		
I3B2	unfiltered DI water	1.4			

I3S1	Greenball		8.9		
------	-----------	--	-----	--	--

7/27/2004 Round 4

No sample

11/30/2004 Round 5

I5W1	Scrubber water, filtered immediately	375	1632.6	0.118	2301.5
I5W2	Scrubber water, filtered immediately	400.4	2318.1	0.118	3135.8
Average		387.7	1975.35	0.118	2718.613

I5B1	filtered DI water	11.5	1.8		
I5B2	unfiltered DI water	2.8			
I5S1	greenball feed sample		7.2		
I5M1	Magnetic fraction, 137 mls tails to 942 mls sw		47.4		
I5M2	Magnetic fraction, 106 mls tails to 919 mls sw		56.2		
I5M3	Magnetic fraction, 173 mls tails to 970 mls sw		32.4		
I5M4	Magnetic fraction, 202 mls tails to 914 mls sw		23.2		
I5M5	Magnetic fraction, scrubber water only		255.7		
I5N1	Non-Magnetic fraction, 137 mls tails to 942 mls sw		25.5		
I5N2	Non-Magnetic fraction, 106 mls tails to 919 mls sw		38.2		
I5N3	Non-Magnetic fraction, 173 mls tails to 970 mls sw		33.6		
I5N4	Non-Magnetic fraction, 202 mls tails to 914 mls sw		12.3		
I5N5	Non-Magnetic fraction, scrubber water only		2411		

2/15/2005 Round 6

IOCR Final Report

I6W1	Scrubber water, filtered immediately	248	3860.6	0.17	6811.0
I6W2	Scrubber water, filtered immediately	359.4	4202.6	0.17	7503.8
Average		303.7	4031.6	0.17	7157.42

I6B1	filtered DI water	4.1	2.3		
I6B2	unfiltered DI water	2.8			
I6N1	Non-Magnetic fraction, scrubber water only		2766.6		
I6M1	Magnetic fraction, scrubber water only		102.2		
I6S1	greenball feed sample		9.9		
I6S2	under-grate sample		7.3		
I6S3	under-grate sample		10.5		
I6S4	under-grate sample		58.1		
I6S5	under-grate sample		57.6		
I6S6	under-grate sample		25.8		
I6S7	under-grate sample		5		

5/19/2005 Round 7

I7W1	Scrubber water, filtered immediately	410.3	2551	0.112	3267.4
I7W2	Scrubber water, filtered immediately	462	2800.1	0.131	4130.1
I7W3	Scrubber water, filtered immediately	467.8	2747	0.114	3599.4
Average		464.9	2773.55	0.1225	3864.756

I7B1	filtered DI water	10.1	7.5		
I7B2	unfiltered DI water	10.8			
	Greenball Feed Sample		7.1		

Appendix B-1-6

Mercury Vaporization Characteristics of Taconite Pellets

October 2005

October 31, 2005

Dr. Michael Berndt
Senior Project Consultant
Minnesota Department of Natural Resources
Division of Lands and Minerals
500 Lafayette Road
St. Paul, MN 55155-4045

Dear Dr. Berndt:

Subject: Final Report for Mercury Vaporization Characteristics of Taconite Pellets
UND Fund 9089

Enclosed is the final report for the subject project. If you have any questions or comments, I can be reached by phone at (701) 777-5127, by fax at (701) 777-5181, or by e-mail at kgalbreath@undeerc.org.

Sincerely,

Kevin C. Galbreath
Research Manager

KCG/nfp

Enclosure

MERCURY VAPORIZATION CHARACTERISTICS OF TACONITE PELLETS

Final Report

(For the period of April 25–September 30, 2005)

Prepared for:

Dr. Michael Berndt

Senior Project Consultant
Minnesota Department of Natural Resources
Division of Lands and Minerals
500 Lafayette Road
St. Paul, MN 55155-4045

Prepared by:

Kevin C. Galbreath

Energy & Environmental Research Center
University of North Dakota
PO Box 9018
Grand Forks, ND 58202-9018

EERC DISCLAIMER

LEGAL NOTICE This research report was prepared by the Energy & Environmental Research Center (EERC), an agency of the University of North Dakota, as an account of work sponsored by Minnesota Department of Natural Resources. Because of the research nature of the work performed, neither the EERC nor any of its employees makes any warranty, express or implied, or assumes any legal liability or responsibility for the accuracy, completeness, or usefulness of any information, apparatus, product, or process disclosed, or represents that its use would not infringe privately owned rights. Reference herein to any specific commercial product, process, or service by trade name, trademark, manufacturer, or otherwise does not necessarily constitute or imply its endorsement or recommendation by the EERC.

MERCURY VAPORIZATION CHARACTERISTICS OF TACONITE PELLETS

ABSTRACT

The Hg and other volatile components (e.g., H₂O, CO₂, HCl) of Hibtac and Minntac green ball samples were thermally released in air (\pm HCl addition) and 100% N₂ in a stainless steel chamber by heating (\sim 20°C/min) from about 25° to 1000°C. Total Hg and Hg⁰ concentrations in the heated gas stream were measured simultaneously every 10 s using dual individual-channel atomic absorption spectroscopy. The Hg release profiles from Hibtac and Minntac green balls in air were characterized by the rapid release of Hg⁰ at 200°–250°C followed by periodic releases of total Hg that exceeded Hg⁰ concentrations, suggesting that Hg²⁺ was liberated from 235° to 545°C. Hg⁰ and total Hg release concentrations peaked relatively rapidly with increasing temperature and then declined asymmetrically to baseline concentrations by about 600°C.

Primarily Hg⁰ was released from the Hibtac and Minntac green balls in the 100% N₂ atmosphere from about 200° to 650°C. The Hg⁰ release profiles were asymmetrical. The complexity of the Hg release profiles, as defined by the number and intensity of total Hg release peaks, was much less during analyses performed in 100% N₂ relative to those performed in air. The reducing atmosphere inhibited magnetite oxidation and apparently the release of Hg²⁺.

The addition of 50 ppmv HCl to air during the heating of Hibtac green balls simplified the total Hg release profile from 3 or 4 peaks to a single total Hg release peak centered at about 285°C. The difference between total Hg and Hg⁰ release concentrations suggested that, at most, about 40% of the total Hg was being released as Hg²⁺ at any given time and temperature. The addition of 100 ppmv HCl to air during the heating of Minntac green balls promoted the thermal release of total Hg, possibly as HgCl₂, at the expense of Hg⁰.

TABLE OF CONTENTS

LIST OF FIGURES	ii
LIST OF TABLES	ii
INTRODUCTION	1
BACKGROUND	1
EXPERIMENTAL	2
RESULTS AND DISCUSSION	5
Green Ball Hg Contents	5
Evaluation of the Bench-Scale Thermal Release Analyzer	6
Thermal Release Analyses of Green Ball Samples	6
Thermal Release Analysis of Hg from Green Balls in Air (30% O ₂ –70% N ₂).	7
Thermal Release Analysis of Hg from Green Balls in 100% N ₂	10
Thermal Release Analysis of Hg from Green Balls in Air Containing HCl	12
SUMMARY AND CONCLUSIONS	14
REFERENCES	14
PRELIMINARY Hg RELEASE PROFILES FOR Hibtac GREEN BALL	Appendix A

LIST OF FIGURES

1	Schematic of the bench-scale thermal desorption apparatus and CMM system.....	4
2	Photograph of the sample chamber in an oven	4
3	Photograph of the stainless steel heating coil and sample chamber in an oven.....	5
4	Heating profiles for Hibtac green ball in air	8
5	Total Hg and Hg ⁰ release profiles for Hibtac green ball in air	9
6	Heating and total Hg and Hg ⁰ release profiles for Minntac green ball in a 30% O ₂ -70% N ₂ mixture	9
7	Heating profiles for Hibtac green ball in 100% N ₂	11
8	Total Hg and Hg ⁰ release profiles for Hibtac green ball in 100% N ₂	11
9	Heating and total Hg and Hg ⁰ release profiles for Minntac green ball in 100% N ₂	12
10	Heating and total Hg and Hg ⁰ release profiles for Hibtac green ball in 30% O ₂ -70% N ₂ -5% H ₂ O containing 50 ppm HCl	13
11	Heating and total Hg and Hg ⁰ release profiles for Minntac green ball in 30% O ₂ -70% N ₂ -5% H ₂ O containing 100 ppm HCl	13

LIST OF TABLES

1	Physical Properties of Fe ₂ O ₃ Polymorphs	2
2	Replicate Hg Analysis Results, reported on a dry basis	5
3	Green Ball Analysis Matrix	6
4	Mercury Mass Balance Results.....	8

MERCURY VAPORIZATION CHARACTERISTICS OF TACONITE PELLETS

INTRODUCTION

The processing of taconite (iron oxide pellets) in northern Minnesota released about 800 lb of mercury to the environment in 2000, accounting for almost 20% of the state's mercury emission inventory (1–3). Most of the atmospheric mercury emissions resulting from taconite processing occur during the heating of wet “green balls,” consisting predominantly of magnetite (Fe_3O_4) and other components (limestone flux, organic or bentonite binder, and mineral contaminants), and the subsequent oxidation of Fe_3O_4 in induration furnaces (4). Stack mercury speciation measurements by Jiang et al. (5) indicated that, on average, 93.3% of the total mercury emitted was gaseous elemental mercury (Hg^0), and most of the remainder was gaseous inorganic mercuric compounds (Hg^{2+}).

The Minnesota Department of Natural Resources (DNR) has been researching wet scrubbers and process lines at taconite-processing facilities to evaluate potential mercury control options for stack emissions. Wet scrubbers are effective in removing Hg^{2+} but not Hg^0 . According to the DNR, scrubber Hg removal efficiency may be affected by the heating rate of taconite in induration furnaces. The identification of a heating rate that would promote the evolution of Hg^{2+} rather than Hg^0 from taconite would be beneficial for capturing Hg^{2+} using a wet scrubber. In addition, Berndt et al. (6) determined that wet scrubbers more effectively capture the Hg released during acid pellet processing relative to fluxed pellet processing. Calcite (CaCO_3) and lime (CaO) are added as a flux during fluxed pellet processing. CaO , the thermal decomposition product of CaCO_3 , may have reacted with acid and halogen-bearing gases liberated during heating, thus inhibiting the Hg^0 oxidation reactions that occur with such gases. The inhibition of Hg^0 oxidation in the fluxed-pellet induration flue gas may explain the lack of wet scrubber Hg removal.

The Energy & Environmental Research Center (EERC) worked interactively with the DNR to characterize Hg vaporization during the heating and oxidation of green ball in air, nitrogen, and HCl using a thermal release apparatus and continuous mercury monitoring (CMM) system. The EERC has investigated the thermal stability of Hg in, and its release from, coal fly ashes, scrubber sludges, activated carbon sorbents, and amalgams but not green balls (7, 8). The volatilization of Hg^0 and Hg^{2+} as functions of temperature ($<1000^\circ\text{C}$), time, and gas composition were determined on two green ball samples supplied by Hibbing Taconite (Hibtac) and US Steel-Minntac (Minntac).

BACKGROUND

The primary oxidation product of Fe_3O_4 produced during induration is hematite ($\alpha\text{-Fe}_2\text{O}_3$). Maghemite ($\gamma\text{-Fe}_2\text{O}_3$), an intermediate oxidation product of Fe_3O_4 and a polymorph of $\alpha\text{-Fe}_2\text{O}_3$, may also form, especially in the presence of water vapor (9–11). The oxidation of Fe_3O_4 , an inverse spinel structure mineral, to $\gamma\text{-Fe}_2\text{O}_3$ involves the

addition of free oxygen at the surface of the crystal and the diffusion of Fe^{3+} through an oxygen framework to the crystal surface, thus creating cation vacancies in the spinel structure (9). Physical properties of the Fe_2O_3 polymorphs are compared in Table 1. Bench-scale investigations using heated (370°C) simulated flue gases demonstrated that specific metal oxides, including $\alpha\text{-Fe}_2\text{O}_3$, promote the formation of Hg^{2+} in the presence of gaseous hydrogen chloride (HCl) and/or nitrogen oxides (NO_x), possibly via surface redox reactions (12–15). Bench-scale experiments by Miller et al. (16) and Hitchcock (17) indicated that $\gamma\text{-Fe}_2\text{O}_3$ does not catalyze Hg^{2+} formation, but rather it readily reacts with Hg^0 at 155°C , resulting in Hg^0 removal from a simulated coal combustion flue gas. In contrast, pilot-scale coal combustion testing by Galbreath et al. (18) indicated that $\alpha\text{-Fe}_2\text{O}_3$ does not affect Hg^0 oxidation, whereas $\gamma\text{-Fe}_2\text{O}_3$ promoted the conversion of Hg^0 to Hg^{2+} and particle-associated Hg.

EXPERIMENTAL

Green ball samples were analyzed using ASTM International Method D6414-01: Standard Test Method for Total Mercury in Coal and Coal Combustion Residues by Acid Extraction or Wet Oxidation/Cold Vapor Atomic Absorption. This method covers the determination of total Hg in coal, coke, combustion residues, and geologic materials. A nominal 1-gram portion of each sample was mixed with nitric and hydrochloric acids and heated in a hot-water bath at 80°C for 2 hours. Each taconite sample was digested at least three times. The digested samples were then cooled to room temperature, diluted with deionized water to a known volume of 50 mL, filtered, and analyzed by cold-vapor atomic absorption spectroscopy (CVAAS). The instrument used was a CETAC Model M6000A Hg analyzer that was calibrated at 0, 10, 50, and 100 ng/L. Hg concentrations were reported on a $\mu\text{g/g}$ dry basis. The reporting limit for the method is $0.0005 \mu\text{g/g}$ (ppm). For quality control purposes, a Hg standard from taconite was analyzed. The Hg standard, a final concentrate sampled from Keewatin Taconite Minnesota Ore Operations, contains an average Hg content of 14 ppb, with confidence limits ($\pm 95\%$) of 1.2 ppb based on analyses from five laboratories (19).

Table 1. Physical Properties of Fe_2O_3 Polymorphs

Parameter	Hematite ($\alpha\text{-Fe}_2\text{O}_3$)	Maghemite ($\gamma\text{-Fe}_2\text{O}_3$)
Crystal System	Hexagonal–rhombohedral	Cubic
Crystal Structure	Corundum ($\alpha\text{-Al}_2\text{O}_3$) structure; isostructural with eskolaite (Cr_2O_3) and karelianite (V_2O_3)	Cation-deficient ferric spinel with ideal formula $[\text{Fe}] (\text{Fe}_{1.67 \quad 0.33}) \text{O}_4$ where $[\text{Fe}]$ represents a vacancy
Density, g/cm^3	5.27	4.88
Magnetization	Antiferromagnetic (no net magnetization)	Ferrimagnetic

The bench-scale apparatus and CMM system used to analyze the thermal release of Hg from green ball samples are shown schematically in Figure 1. The sample chamber consists of a ¾-in. (1.90-cm)-diameter, 10-in. (25.4-cm)-long stainless steel (Type 316) pipe. Stainless steel was used to construct the thermal release apparatus because, based on EERC experience with bench- and pilot-scale combustion testing equipment, it is chemically inert with respect to Hg. The chamber resides in a 6-ft. (1.8-m)-long tube furnace, as shown in Figure 2, that is temperature-controlled to heat at a nominal rate of 20°C/minute (68°F/min.). The furnace temperature and the gas temperature in the sample chamber were measured using thermocouples. Mass flow controllers were used to meter in various gases including N₂, O₂, H₂O, and HCl. The gases flowed through ¼-in. (0.64-cm) stainless steel tubing into a heating coil within the oven, as shown in Figure 3, before entering the sample chamber. Green ball samples were placed at the bottom of the chamber, and the heated gases flowed over the top. After exiting the sample chamber, the gases were cooled using coiled stainless steel tubing to 300°F (149°C). The gases then passed from the cooling coil, via a heated (300°F, 149°C) Teflon tube, into a PS Analytical (PSA) S235C400 flue gas-conditioning and Hg conversion unit. The S235C400 uses two separate liquid flow paths, one to continuously reduce Hg²⁺ to Hg⁰, resulting in a total gaseous Hg sample, and the other to continuously absorb Hg²⁺, resulting in an Hg⁰ sample. The S235C400 also employs a Peltier thermoelectric module to cool and dry the sample gases prior to analysis.

During the initial thermal release analyses (Analyses 1–3), a Tekran Model 2537A atomic fluorescence-based Hg vapor analyzer was used to measure Hg⁰ and total Hg concentrations online. The Tekran instrument trapped the Hg vapor from the conditioned sample onto an ultra-pure gold sorbent. The amalgamated Hg was then thermally desorbed and detected using atomic fluorescence spectrometry. A dual-cartridge design enabled alternate sampling and desorption cycles, resulting in a nearly continuous measurement of the sample stream. The Tekran instrument was used to measure either total Hg or Hg⁰ approximately every 2.5 minutes. In order to improve the temporal resolution of the Hg release profiles obtained on the green ball samples, a Nippon Instruments Corporation (NIC) DM-6A was used during subsequent experiments (Analyses 4–17). The DM-6A uses dual individual channel atomic absorption spectroscopy to measure Hg⁰ and total Hg concurrently every 10 seconds, and Hg²⁺ was estimated by difference (i.e., total Hg – Hg⁰ = Hg²⁺). An Hg⁰ permeation source was used to calibrate both instruments daily.

Sample preparation consisted of sampling a known amount of green ball, generally ~25 g, in a plastic bag and then crushing by hand. The green balls were then flattened into a thin layer, 3 to 6 mm thick. The resulting green ball cake was then divided using a spatula into small sections (~1-mm squares). The sectioned sample was then placed into the bottom of the sample chamber for testing.

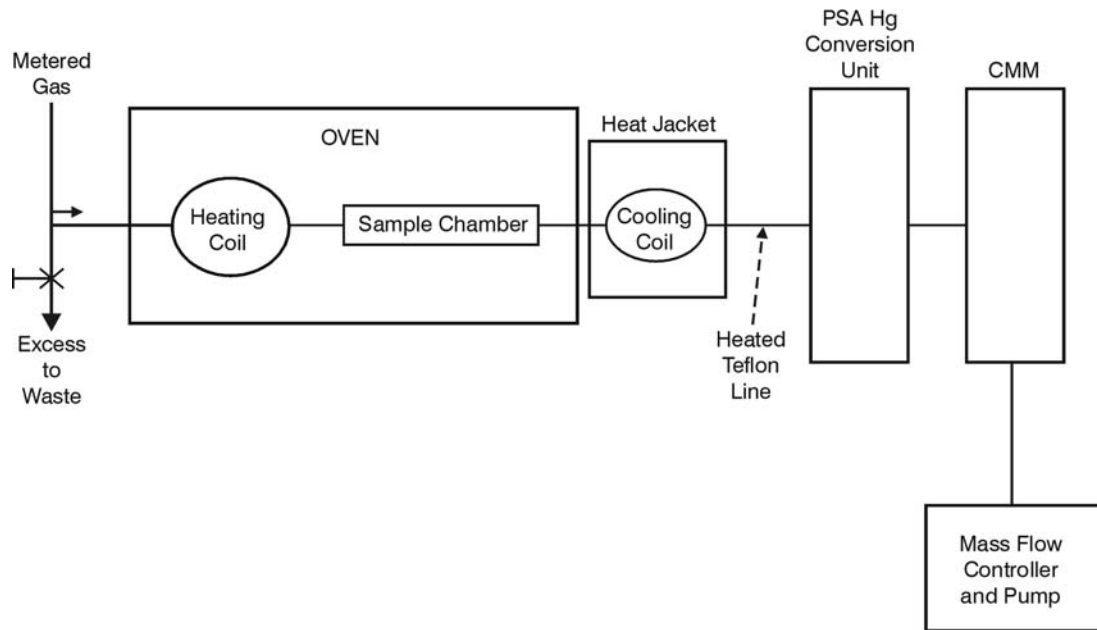


Figure 1. Schematic of the bench-scale thermal desorption apparatus and CMM system.



Figure 2. Photograph of the sample chamber in an oven.



Figure 3. Photograph of the stainless steel heating coil and sample chamber in an oven.

RESULTS AND DISCUSSION

Green Ball Hg Contents

Hg analysis results are presented in Table 2 for the concentrate standard and green ball samples collected from Minntac and Hibtac. The measured Hg content for the concentrate standard is within 9% of the average value of 14 ± 1.2 ng/g (ppb) reported by five laboratories (19). The Hg content of the Hibtac green ball sample is similar to the concentrate standard, whereas the Minntac green ball sample contains significantly lower Hg.

Table 2. Replicate Hg Analysis Results, reported on a dry basis

Sample	Concentrate Standard	Minntac Green Ball	Hibtac Green Ball
Number of measurements	5	3	4
Average Hg, ng/g	15.2	6.23	16.1
$\pm 95\%$ confidence limits, ng/g	1.2	0.06	1.1

Evaluation of the Bench-Scale Thermal Release Analyzer

Initially, the bench-scale thermal release apparatus (Figure 1) was tested with no sample inside to assess Hg contamination. Total Hg and Hg⁰ concentrations during the blank (background) tests were very low at $\leq 0.2 \mu\text{g}/\text{m}^3$. A Hg⁰ permeation source was used to send $20 \mu\text{g}/\text{m}^3$ of Hg⁰ through the system to evaluate Hg recovery. Essentially 100% of the Hg⁰ was recovered, and when the Hg⁰ source was turned off, the Hg⁰ concentration decreased to $<0.1 \mu\text{g}/\text{m}^3$ within about 1–2 s.

Thermal Release Analyses of Green Ball Samples

The green ball analysis matrix is described in Table 3. Analyses were conducted in air (30 vol% O₂–70 vol% N₂) and a reducing atmosphere of 100 vol% N₂. Several HCl addition tests to air were also performed to evaluate whether the added chlorine would promote the thermal release of Hg²⁺. Initial tests (1–3) were performed at a flow rate of 0.25 L/min, whereas subsequent tests (4–17) were performed at 0.5 L/min. As soon as a green ball sample was exposed to the flowing gas, described in Table 3, the furnace was turned on to heat the sample at about 20°C/min. (68°F/min). During heating to about 300°C, the gas temperature fluctuated and was lower relative to the furnace temperature because of cooling associated with moisture evaporation from the green ball samples. The concentrations of total Hg and Hg⁰ released from the green ball samples were plotted as functions of the furnace temperature rather than gas temperature because of the sample-cooling effect. When the furnace peaked at 990° to 1000°C, it was turned off and allowed to cool to $<300^\circ\text{C}$. The sample was then removed from the chamber and placed in a sealed glass vial for analysis.

Table 3. Green Ball Analysis Matrix

Analysis No.	Green Ball Source	Sample Weight, g	O ₂ , vol%	N ₂ , vol%	H ₂ O, vol%	HCl, ppm
1	Hibtac	73.00	30	70	NA ¹	NA
2	Hibtac	15.00	30	70	NA	NA
3	Hibtac	15.00	30	70	NA	NA
4	Hibtac	24.71	30	70	NA	NA
5	Minntac	24.97	30	70	NA	NA
6	Hibtac	24.94	30	70	NA	NA
7	Minntac	25.10	30	70	NA	NA
8	Hibtac	25.40	30	70	NA	NA
9	Minntac	25.09	NA	100	NA	NA
10	Hibtac	24.70	NA	100	NA	NA
11	Minntac	24.71	NA	100	NA	NA
12	Hibtac	25.10	NA	100	NA	NA
13	Hibtac	25.14	NA	100	NA	NA
14	Concentrate	24.77	NA	100	NA	NA
15	Minntac	25.00	30	65	5	100
16	Hibtac	25.10	30	65	5	100
17	Hibtac	25.30	30	65	5	50

¹Not applicable.

After each analysis, the amount of Hg vaporized from the sample was calculated from the thermal release profile. A portion of the green ball residue was also analyzed for Hg. The vaporized and residue Hg concentrations for each analysis are presented in Table 4. Hg mass balances were calculated from the vaporized, residue, and green ball Hg concentrations. As indicated in Table 4, Hg mass balance recoveries range widely from 5% to 305%.

Total Hg and Hg⁰ thermal release profiles for Analyses 9, 14, and 16 are not presented because of very poor Hg mass balance recoveries. The release profiles from Analyses 1–3 are presented in Appendix A for information purposes only because they were obtained using the Tekran CMM, which lacked temporal resolution and could not be used to measure total Hg and Hg⁰ simultaneously. The Tekran results, however, were useful for determining how much green ball sample was appropriate for providing measurable concentrations of total Hg and Hg⁰ during subsequent thermal release analyses.

Thermal Release Analysis of Hg from Green Balls in Air (30% O₂–70% N₂)

Presented in Figures 4 and 5 are three heating profiles and associated total Hg and Hg⁰ release profiles, respectively, for the Hibtac green ball sample in air, Analyses 4, 6, and 8 described in Table 3. Heating rates during Analyses 4 and 8 were similar, whereas the heating rate during Analysis 6 was slightly lower. The heating rate gradually slowed with time, and thus increasing temperature, especially after about 40 min. into the test. The three Hg release profiles in Figure 5 indicate that significant concentrations of Hg were initially liberated at 200°C as Hg⁰. Based on the mass balance closure results in Table 4, Analysis 8 results are probably the most reliable. Analysis 8 results show four distinct peaks associated with the release of total Hg at 235°, 260°, 300°, and 360°C. Total Hg concentrations exceed those of Hg⁰ at these temperatures, suggesting that Hg²⁺ compounds were being released. The liberation of Hg⁰ peaked at 235° and 320°C. In general, Hg⁰ concentrations were greater than total Hg concentrations at ≥320°C, indicating that only Hg⁰ was being liberated from about 320° to 700°C.

Analysis 6 results are similar to those for Analysis 8 in that at about 220°C the total Hg concentration exceeded Hg⁰, suggesting that Hg²⁺ was also being liberated. In addition, three of the four total Hg release peaks are discernable, although not as well resolved, and each occurring at about 10°C higher. Analysis 4 results indicate a total Hg release peak at 350°C that compares favorably with a similar peak at 360°C in the Analysis 8 Hg release profile. The total Hg and Hg⁰ release profiles in Figure 5 are generally asymmetric in that Hg⁰ and total Hg are initially released more rapidly at low temperatures, <300°C, relative to higher temperatures.

Presented in Figure 6 are two heating profiles and associated total Hg and Hg⁰ release profiles for the Minntac green ball sample in air, Analyses 5 and 7 described in Table 3. According to Table 4, the Hg releases during Analyses 5 and 7 were overbalanced by about 40% and 55%, respectively, suggesting that Hg may have

Table 4. Mercury Mass Balance Results

Analysis No.	ng of Hg vaporized per g of sample	Residue Hg, ng/g	Total Hg recovered, ng/g	Recovery, %
1	5.37	0.86	6.23	38.6
2	3.37	0.68	4.05	25.1
3	4.40	0.70	5.10	31.6
4	6.79	<0.5 (0.13) ¹	6.92	42.9
5	8.39	<0.5 (0.29)	8.68	139
6	4.82	<0.5 (0.16)	4.98	30.8
7	9.53	<0.5 (0.15)	9.68	155
8	14.5	<0.5 (0.14)	14.6	90.6
9	18.7	<0.5 (0.33)	19.0	305
10	12.2	<0.5 (0.44)	12.6	78.3
11	7.78	<0.5 (0.31)	8.09	130
12	6.93	0.55	7.48	46.4
13	14.2	0.55	14.8	91.7
14	<0.5 (0.15)	0.58	0.73	4.8
15	3.17	0.60	3.77	60.4
16	2.25	0.80	3.05	18.9
17	8.78	0.60	9.38	58.3

¹ Even though Hg in the sample was below method quantification limits, the instrument display value reported in parentheses was used in the mass balance calculations.

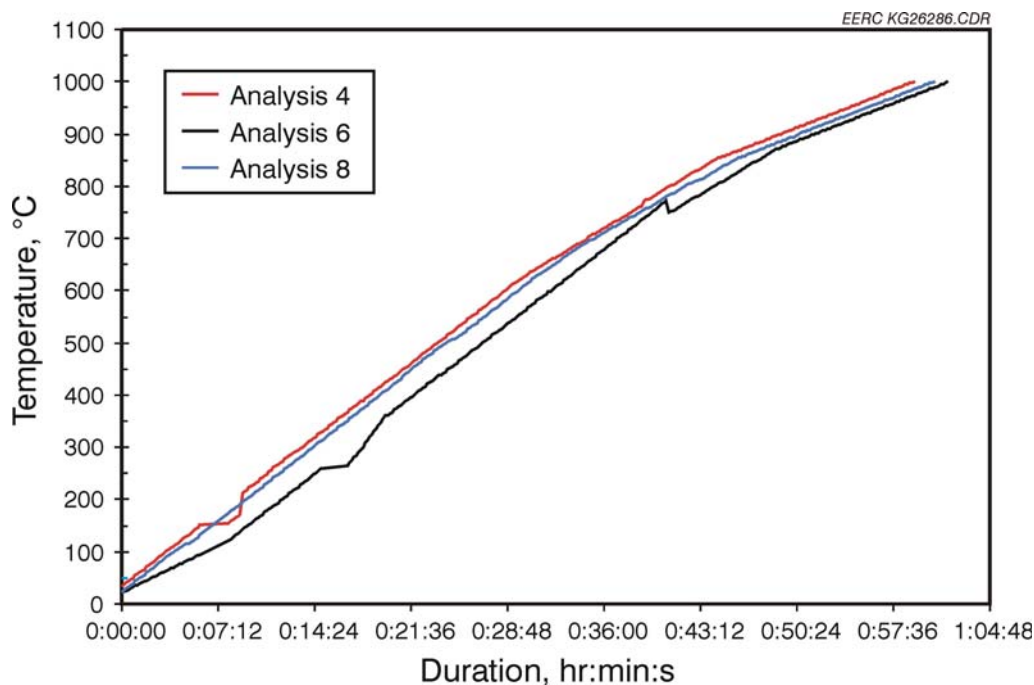


Figure 4. Heating profiles for Hibtac green ball in air.

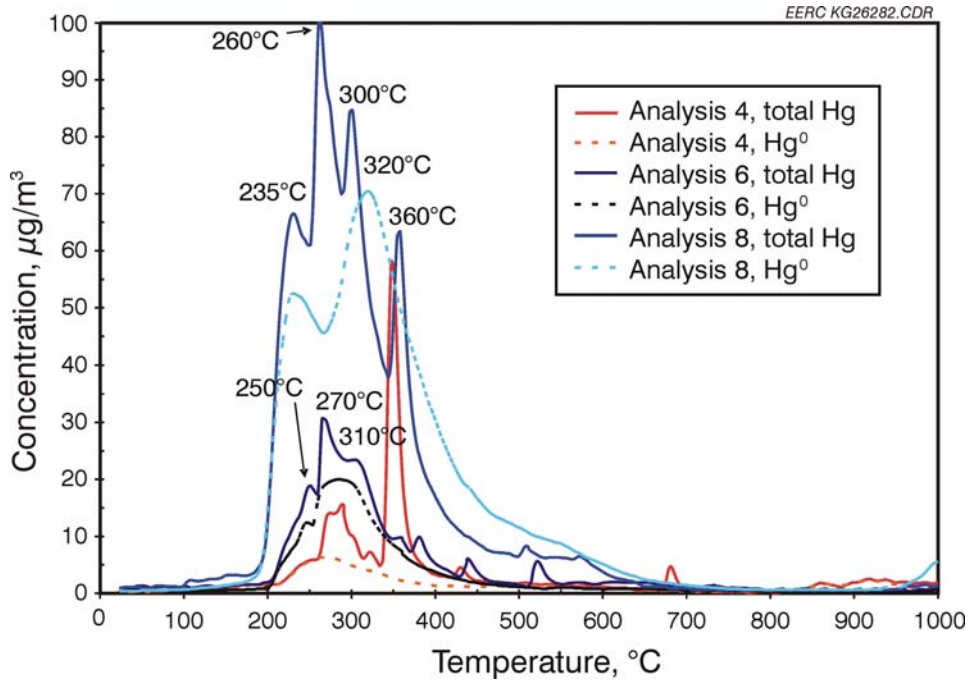


Figure 5. Total Hg and Hg⁰ release profiles for Hibtac green ball in air.

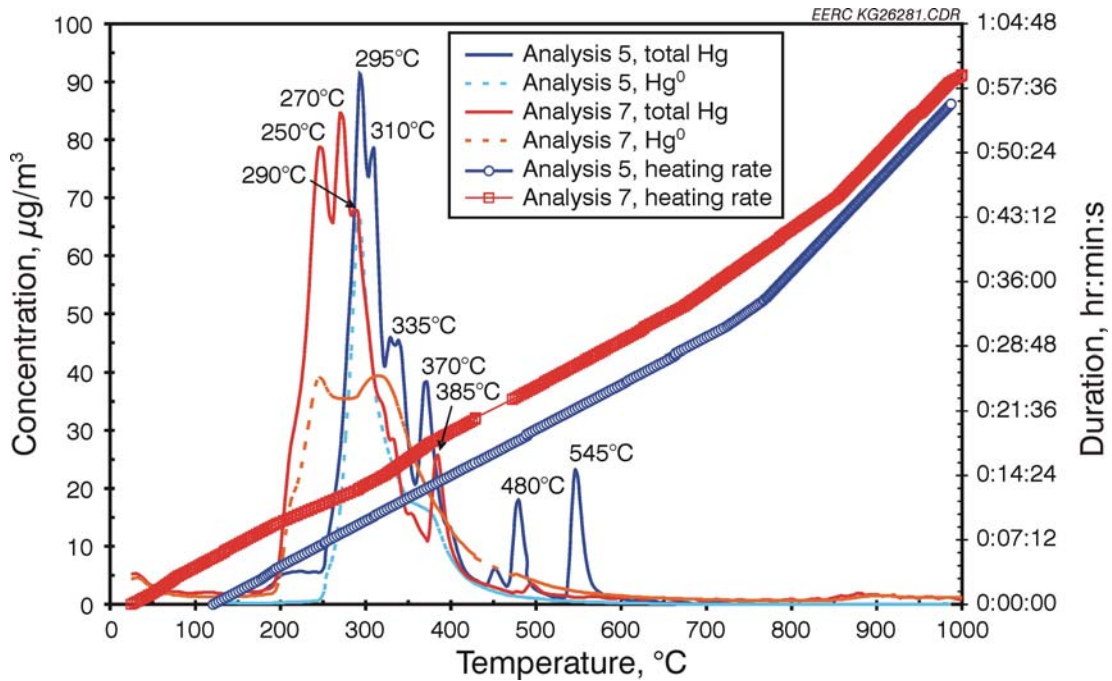


Figure 6. Heating and total Hg and Hg⁰ release profiles for Minntac green ball in a 30% O₂-70% N₂ mixture.

remained in the system as a contaminant from previous analyses. The heating profiles indicate that Analysis 5 was performed too soon after the previous analysis, before the sample chamber was cooled to room temperature. Analysis 5 began at about 125°C compared to 25°C for Analysis 7. Even though Analysis 7 began at a lower temperature relative to Analysis 5, Hg⁰ was initially released at a lower temperature of 195°C compared to 250°C during Analysis 5. Hg⁰ release during Analysis 5 occurred relatively abruptly over a temperature range of 250° to 425°C and peaked at 290°C. In contrast, Hg⁰ release during Analysis 7 occurred over a relatively broad temperature range of 195° to 550°C. Similar to the Hg release profile from the Hibtac green ball sample in Figure 5, the total Hg liberated from the Minntac green ball exceeded Hg⁰, indicating that Hg²⁺ was also probably released from the Minntac green ball sample. Analysis 5 indicated the presence of six prominent total Hg release peaks at about 295°, 310°, 335°, 370°, 480°, and 545°C, whereas Analysis 7 indicated four prominent total Hg release peaks at 250°, 270°, 290°, and 385°C. During both analyses, the Hg⁰ and total Hg release profiles for the Minntac green ball were asymmetric.

Thermal Release Analysis of Hg from Green Balls in 100% N₂

Presented in Figures 7 and 8 are three heating profiles and associated total Hg and Hg⁰ release profiles, respectively, for the Hibtac green ball sample in a 100% N₂ atmosphere, Analyses 10, 12, and 13 described in Table 3. The heating profiles for Analyses 12 and 13 are similar, whereas the heating rate during Analysis 10 was initially greater. Analysis 13 results are probably the most reliable based on the Hg mass balance closures presented in Table 4. In contrast to the analysis results in an oxidizing atmosphere, Figure 5, the relatively small differences in total Hg and Hg⁰ concentrations in Figure 8 suggest that Hg²⁺ liberation from the Hibtac green ball was insignificant in the N₂ atmosphere. The small differences between total Hg and Hg⁰ concentrations are generally within the analytical uncertainties of the flue gas conditioning and Hg conversion unit and CMM. In comparing the most reliable results based on mass balance closures, Analyses 8 and 13 in Figures 5 and 8, respectively, the overall temperature range (~200° to 600°C) and asymmetry of the Hg⁰ releases are similar, but the Hg release profile for Hibtac in air (Figure 5) is much more complex relative to its profile in 100% N₂ (Figure 8).

The heating profile and associated total Hg and Hg⁰ release profiles for the Minntac green ball sample in 100% N₂, Analysis 11 described in Table 3, are presented in Figure 9. As indicated in Table 4, the Hg mass balance for Analysis 11 was 130%. Hg⁰ was initially released from the Minntac green ball at about 210°C. The release of Hg⁰ peaked to ~40 µg/m³ at 295°C and then decreased asymmetrically to baseline concentrations at 645°C. Analysis 11 results show two distinct peaks associated with the release of total Hg at about 300°C and 380°C. Total Hg concentrations significantly exceed those of Hg⁰ at these temperatures, suggesting that Hg²⁺ compounds were being released. Similar to the Hibtac Hg release results, the Hg release profile for Minntac in 100% N₂ (Figure 8) is simpler with fewer Hg⁰ and total Hg peak releases relative to its profile in air (Figure 6).

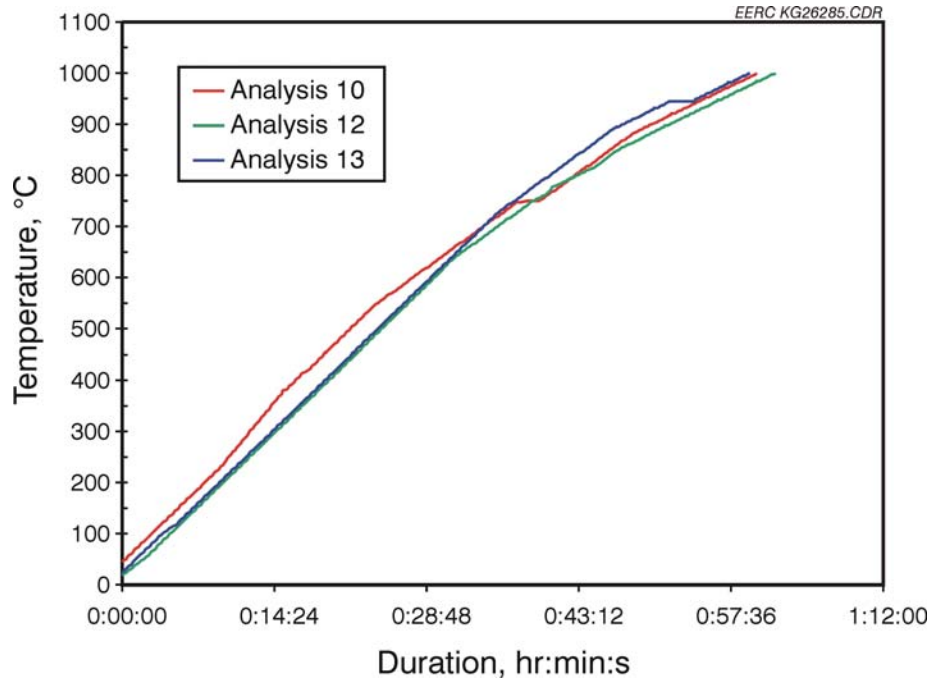


Figure 7. Heating profiles for Hibtac green ball in 100% N₂.

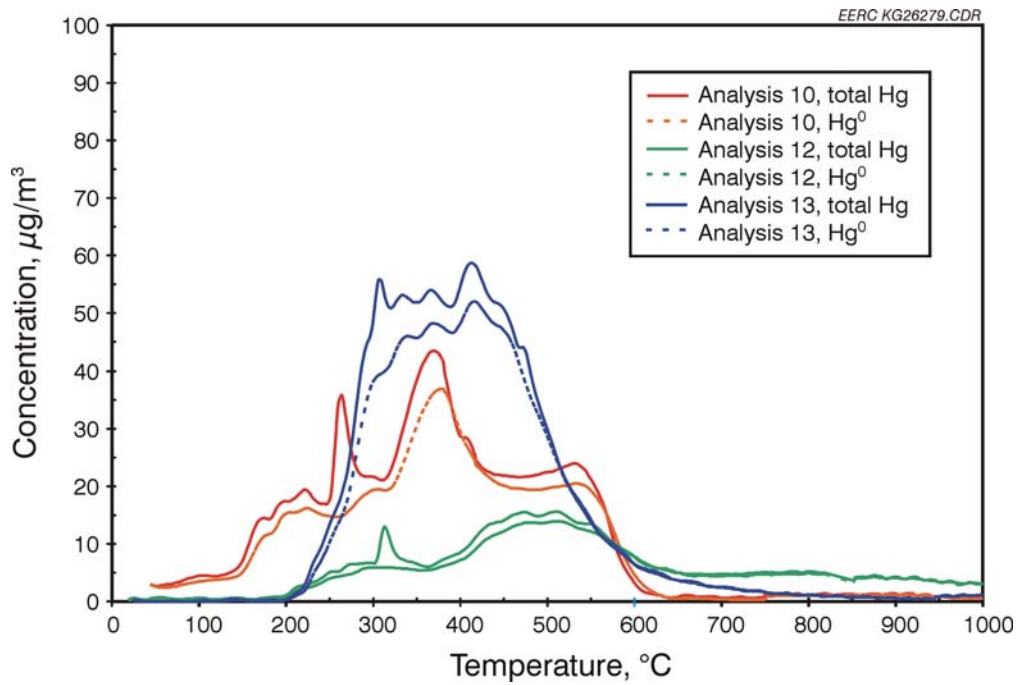


Figure 8. Total Hg and Hg⁰ release profiles for Hibtac green ball in 100% N₂.

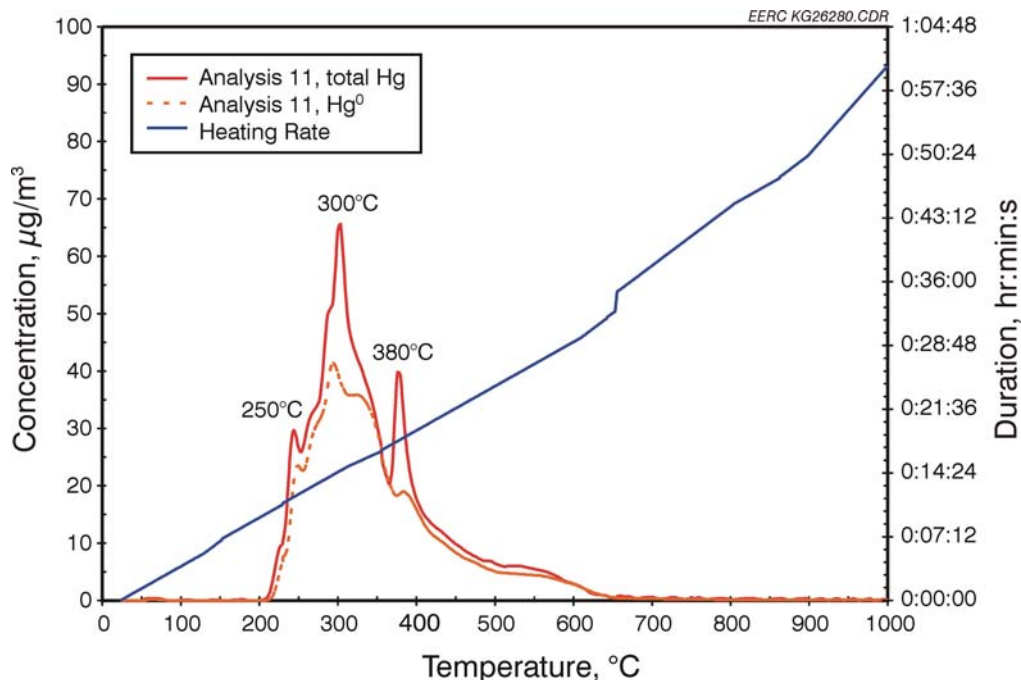


Figure 9. Heating and total Hg and Hg⁰ release profiles for Minntac green ball in 100% N₂.

Thermal Release Analysis of Hg from Green Balls in Air Containing HCl

Compared in Figures 10 and 11 are the heating profiles and total Hg and Hg⁰ release profiles obtained during the analyses of Hibtac and Minntec green ball samples, Analyses 17 and 15 described in Table 3. The heating rates are similar, however, Analysis 15 of the Minntac sample began at a higher temperature relative to Analysis 17 of the Hibtac sample, thus it required more time during the Hibtac analysis for the furnace to attain ~1000°C. As indicated in Table 4, Hg mass balance closures for both analyses were about 60%.

In the presence of 50 ppm HCl, the Hibtac green ball initially released Hg⁰ from about 220° to 270°C as indicated in Figure 10. Total Hg and Hg⁰ were released concurrently from about 260° to 315°C. Total Hg and Hg⁰ release peaked at ~285°C to about 70 and 40 µg/m³, respectively, suggesting that a maximum of about 40% of the total Hg was being liberated as Hg²⁺. Hg⁰ continued to be released from >315°C to about 450°C. Hg release subsided until about 885°C when Hg⁰ release peaked again to about 12 µg/m³. In comparison to the Hibtac Hg release profile in Figure 5, the presence of 50 ppm HCl reduced the complexity of the total Hg release as evidenced by the lack of multiple total Hg release peaks in Figure 10.

During heating of the Minntac green ball in the presence of 100 ppm HCl, low concentrations of Hg⁰, ≤2.0 µg/m³, were initially liberated at about 220°C. Hg⁰ release

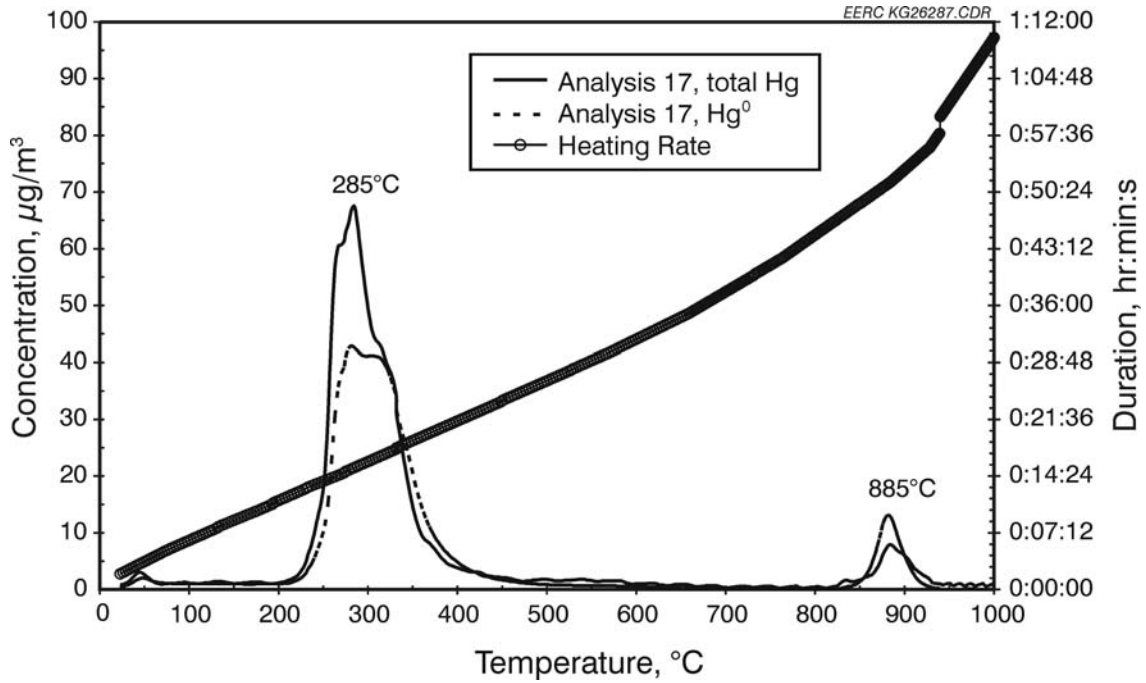


Figure 10. Heating and total Hg and Hg⁰ release profiles for Hibtac green ball in 30% O₂-70% N₂-5% H₂O containing 50 ppm HCl.

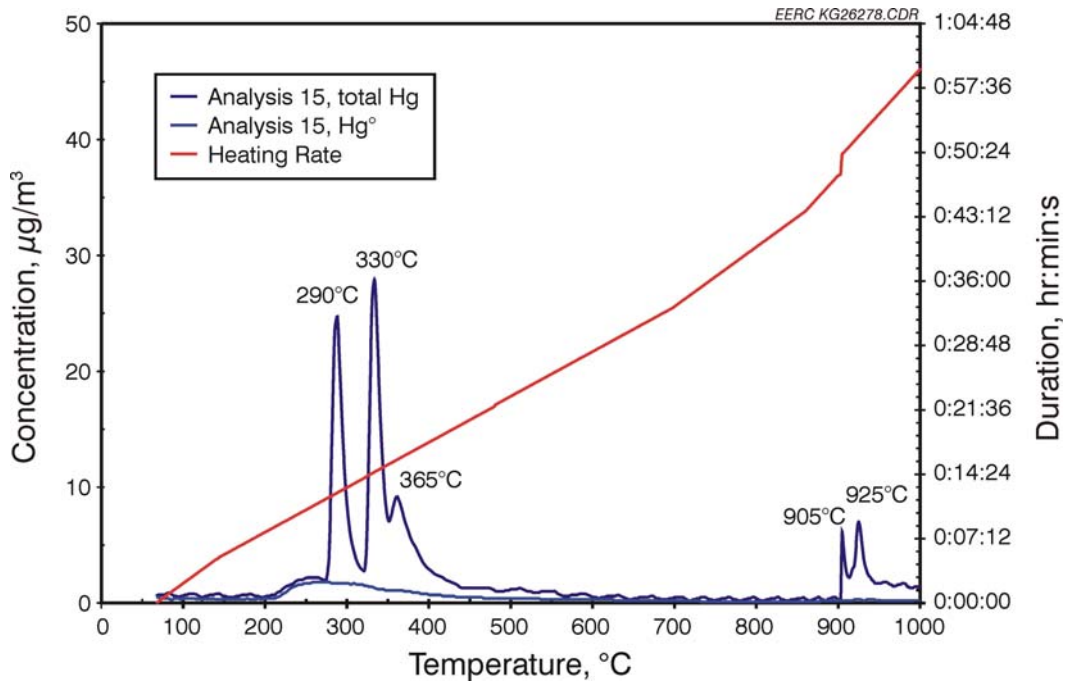


Figure 11. Heating and total Hg and Hg⁰ release profiles for Minntac green ball in 30% O₂-70% N₂-5% H₂O containing 100 ppm HCl.

remained very low and gradually decreased to baseline concentrations at about 450°C. Total Hg, and presumably Hg²⁺, release peaked at 290°, 330°, 365°, 905°, and 925°C. The peak at 905°C is asymmetric because the CMM performed a blank (i.e., zero background) measurement at about 900°C. The presence of 100 ppm HCl significantly decreased Hg⁰/total Hg as indicated by a comparison of Figures 6 and 11, thus implying that it enhanced the thermal release of Hg²⁺. The limestone flux in Minntac green ball did not seem to inhibit Hg⁰ oxidation as was postulated in the introduction section of this report.

SUMMARY AND CONCLUSIONS

The Hg and other volatile components (e.g., H₂O, CO₂, HCl) in Hibtac and Minntac green ball samples were thermally released in air (± HCl addition) and 100% N₂ in a stainless steel chamber by heating (~20°C/min) from about 25° to 1000°C. In general, the Hg release profiles from Hibtac and Minntac green balls in air are characterized initially by the rapid release of Hg⁰ at 200°–250°C followed by periodic releases of total Hg that exceed Hg⁰ concentrations, suggesting Hg²⁺ liberation from 235° to 545°C. With increasing temperature, Hg⁰ and total Hg release concentrations peaked relatively rapidly and then declined asymmetrically to baseline concentrations by about 600°C.

Primarily Hg⁰ was released from the Hibtac and Minntac green balls in the 100% N₂ atmosphere from about 200° to 650°C. The Hg⁰ release profiles were asymmetric. The complexity of the Hg release profiles, as defined by the number and intensity of total Hg release peaks, was much less during analyses performed in 100% N₂ relative to those performed in air. The reducing atmosphere inhibited the magnetite in green ball samples from oxidizing during heating. Apparently, Hg⁰ interactions with magnetite oxidation products, maghemite and hematite, are important for promoting Hg²⁺ formation.

The addition of 50 ppmv HCl to air during the heating of Hibtac green balls simplified the total Hg release profile from 3 or 4 peaks to a single total Hg peak release from about 260° to 315°C. The difference between total Hg and Hg⁰ release concentrations suggested that a maximum of 40% of the total Hg was released as Hg²⁺. The addition of 100 ppmv HCl to air during the heating of Minntac green balls promoted the thermal release of total Hg, possibly as HgCl₂, at the expense of Hg⁰.

REFERENCES

1. Minnesota Pollution Control Agency. Mercury Reduction Program, Progress Report to the Minnesota Legislature, January 2002. Available at: <http://www.pca.state.mn.us/hot/legislature/reports/2002/mercury-02.pdf>.
2. Jackson, A.M.; Swain, E.B.; Andrews, C.A.; Rae, D. Minnesota's Mercury Contamination Reduction Initiative. *Fuel Process. Technol.* **2000**, 65–66, 79–99.

3. Murray, M.; Holmes, S.A. Assessment of Mercury Emissions Inventories for the Great Lakes States. *Environ. Res.* **2004**, *95* (3), 282–297.
4. Berndt, M.E. *Mercury and Mining in Minnesota*; Minnesota Department of Natural Resources, Division of Lands and Minerals, Minerals Coordinating Committee Final Report, October 15, 2003, 66 p.
5. Jiang, H.; Arkly, S.; Wickman, T. Mercury Emissions from Taconite Concentrate Pellets – Stack Testing Results from Facilities in Minnesota. Presented at U.S. Environmental Protection Agency Conference *Assessing and Managing Mercury from Historic and Current Mining Activities*, San Francisco, CA, November 28–30, 2001, 18 p.
6. Berndt, M.E.; Engesser, J.; Johnson, A. *On the Distribution of Mercury in Taconite Plant Scrubber Systems*; Minnesota Department of Natural Resources Report for the Minnesota Pollution Control Agency, 2003, 30 p.
7. Sondreal, E.A.; Benson, S.A.; Pavlish, J.H.; Galbreath, K.C.; Zygarlicke, C.J.; Thompson, J.S.; McCollor, D.P.; Crocker, C.R.; Lillemoen, C.M.; Mann, M.D.; Jensen, R.R.; Weber, G.F. *Center for Air Toxic Metals Final Technical Report Volume III*, October 1, 1996–September 30, 2000; prepared for U.S. Environmental Protection Agency Assistance Agreement R 824854; September 2000.
8. Pavlish, J.P. *Mercury Stability in the Environment*; Final Report Prepared for the Federal Energy Technology Center, U.S. Department of Energy, Pittsburgh, PA, July 1999; Energy & Environmental Research Center Report 99-EERC-09-03, 21 p.
9. D.H. Lindsley, In *Oxide Minerals*, MSA Reviews in Mineralogy Vol. 3, Chap. 1; Rumble III, D., Ed.; Mineralogical Society of America, Washington, DC, **1976**; pp. 1–60.
10. Colombo, U.; Fagherazzi, G.; Gazzarrini, F.; Lanzavecchia, G.; and Sironi, G. Mechanisms in the First Stage of Oxidation of Magnetites. *Nature* **1964**, *202*, 175–176.
11. Colombo, U.; Gazzarrini, F.; Lanzavecchia, G.; and Sironi, G. Magnetite Oxidation: A Proposed Mechanism. *Science* **1965**, *147*, 1033.
12. Ghorish, S.B.; Lee, C.W.; Kilgroe, J.D. Mercury Speciation in Combustion Systems: Studies with Simulated Flue Gases and Model Fly Ashes. Presented at the Air & Waste Management Association’s 92th Annual Meeting & Exhibition, St. Louis, MO, June 20–24, 1999; Paper 99-651.

13. Carey, T.R.; Skarupa, R.C.; Hargrove Jr., O.W. *Enhanced Control of Mercury and Other HAPs by Innovative Modifications to Wet FGD Processes*; Phase I Report for the U.S. Department of Energy, Contract DE-AC22-95PC95260, Aug 28, 1998.
14. Lee, C.W.; Kilgroe, J.D.; Ghorishi, S.B. Speciation of Mercury in the Presence of Coal and Waste Combustion Fly Ashes. Presented at the, 93rd Annual Meeting of the Air & Waste Management Association, Salt Lake City, UT, June 18–22, 2000, Paper 151.
15. Zhuang, Y.; Biswas, P.; Quintan, M.E.; Lee, T.G.; Arar, E. Kinetic Study of Adsorption and Transformation of Mercury on Fly Ash Particles in an Entrained Flow Reactor. Presented at the, 93rd Annual Meeting of the Air & Waste Management Association, Salt Lake City, UT, June 18–22, 2000, Paper 331.
16. Miller, S.J.; Olson, E.S.; Dunham, G.E.; Sharma, R.K. Preparation Methods and Test Protocol for Mercury Sorbents. Presented at the Air & Waste Management Association's 91st Annual Meeting & Exhibition, San Diego, CA, June 14–18, 1998; Paper 98-RA79B.07.
17. Hitchcock, H.L. Mercury Sorption on Metal Oxides. Master of Science Thesis, University of North Dakota, Dec 1996; 83 p.
18. Galbreath, K.C.; Zygarlicke, C.J.; Tibbetts, J.E.; Schulz, R.L.; Dunham, G.E. Effects of NO_x , $\alpha\text{-Fe}_2\text{O}_3$, $\gamma\text{-Fe}_2\text{O}_3$, and HCl on Mercury Transformations in a 7-kW Coal Combustion System. *Fuel Process. Technol.* **2005**, 86 (4), 429–448.
19. Benner, B.R. *Preparation of Mercury Standards from Taconite*; Coleraine Minerals Research Laboratory, Report TR-01-16, 2001, 10 p.

APPENDIX A

**PRELIMINARY Hg RELEASE PROFILES FOR
Hibtac GREEN BALL**

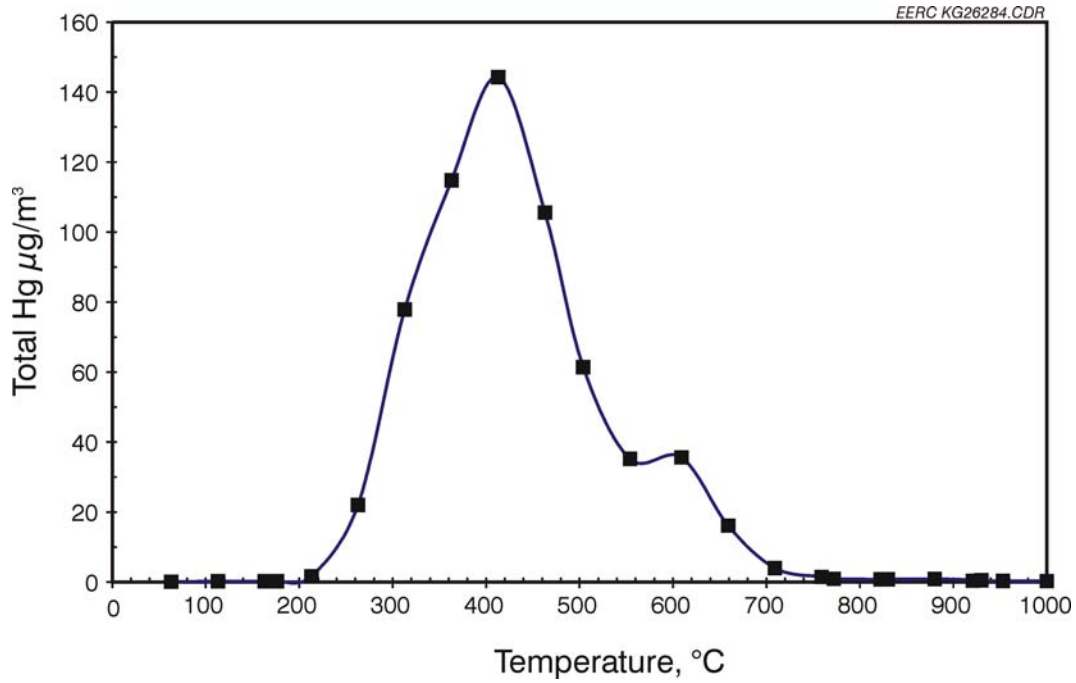


Figure A-1. Total Hg release profile for Hibtac green ball in air.

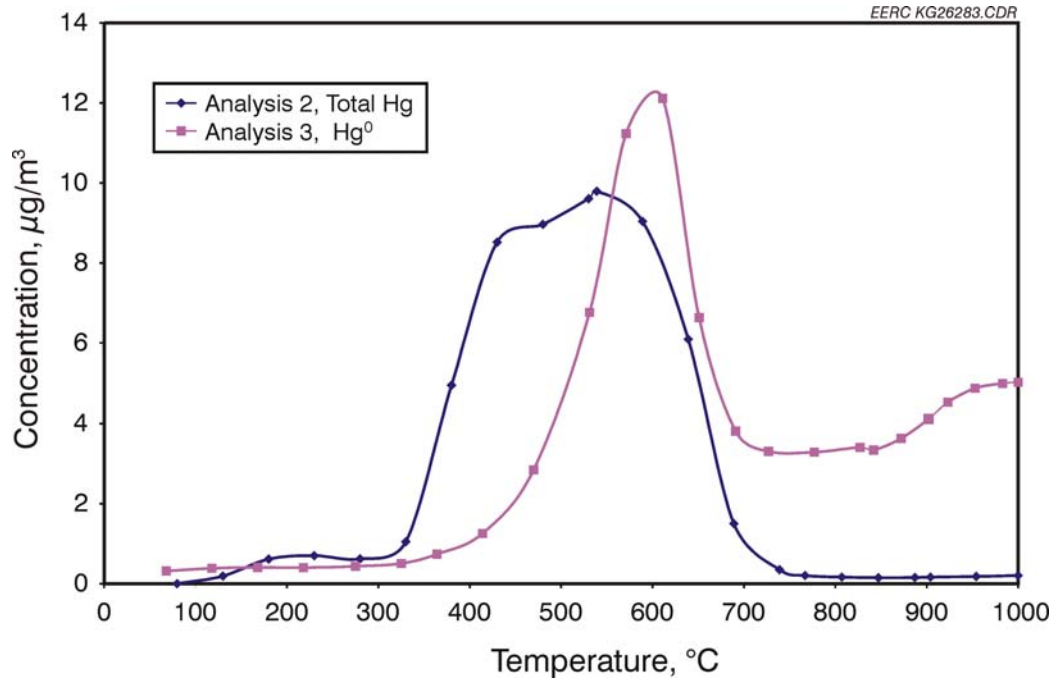


Figure A-2. Total Hg and Hg⁰ release profiles for Hibtac green ball in air.

Appendix B-1-7

Mercury Chemistry and Mossbauer Spectroscopy of Iron Oxides During Taconite Processing on Minnesota's Iron Range

December 31, 2005

Mercury Chemistry and Mössbauer Spectroscopy of Iron Oxides During Taconite Processing on Minnesota's Iron Range

Michael Berndt¹, John Engesser², and Thelma S. Berquó³

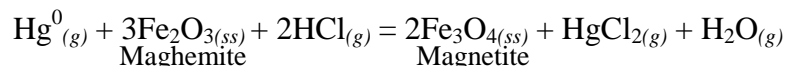
¹MN Dept. of Natural Resources, 500 Lafayette Road St. Paul, MN 55155

²MN Dept. of Natural Resources, 1525 3rd Avenue East Hibbing, MN 55746

³Inst. for Rock Magnetism, 100 Union St., Univ. of MN, Minneapolis, MN, 55455

ABSTRACT

The Minnesota Department of Natural Resources (DNR) has been studying the distribution and fate of mercury at four Minnesota taconite processing facilities. This paper details and interprets mercury concentration data and Mössbauer spectroscopic measurements made on solids generated in heating experiments and collected from taconite plants on Minnesota's Iron Range. During taconite processing, wet "greenballs" consisting predominantly of magnetite and possible other components (limestone flux, organic or bentonite binder, trace non-ore components) are conveyed into a furnace and converted to hematite by heating to 1200-1300°C in the presence of air. Magnetite is first converted to magnetite/maghemite solid-solutions which attract and collect mercury released from greenball samples during conversion to hematite deeper in the furnace. The dual capture and release mechanisms can lead to high mercury concentrations in solids collected from the intermediate zones in the furnaces. Wet scrubbers sometimes capture large amounts of oxidized mercury released from induration, suggesting extensive transport of oxidized mercury takes place in process gases. A relationship such as:



is proposed to control this mercury oxidation rate during taconite induration. Future work is planned to verify the importance of this reaction and to determine if relatively simple, passive processes can be found to enhance mercury oxidation and capture during taconite induration.

INTRODUCTION

Taconite is a very hard, relatively low grade ore that forms the basis of the iron industry in Minnesota today. In 2005, six taconite companies were active, all of which mine on the Mesabi Iron Range. All of these taconite plants were built decades ago to process low-grade iron ore, at a time when Hg was not an issue. Thus, atmospheric Hg emissions from taconite processing have grown with the industry, exceeding 100 kg/yr in the late 1960's, and ranging between approximately 200 and 400 kg/yr ever since (Engesser and Niles, 1997; Jiang et al., 1999; Berndt, 2003; Berndt et al., 2003).

During processing, magnetite is magnetically separated from other solids in the composite ore and the resulting concentrate is rolled with other minor components

(fluxing agents, binders) into balls (“greenballs”). Mercury is released during induration, a process where the greenballs are hardened and converted to hematite by heating to high temperatures (1200 to 1300°C) in air.

Mercury emissions from taconite are generated under conditions quite distinct from those in the much better studied coal-fired power plants (see Pavlish et al, 2003, for a review). For example, the primary source of mercury at coal-fired power plants is the fuel, while the primary source of mercury released during taconite processing on Minnesota’s Iron Range is typically the ore (Berndt, 2003). This is partly because relatively few companies use coal to fire their pellets, but even when coal is used, it takes only about 20 to 30 lbs of coal to fire one long ton of pellets. Unless the plant uses a low-mercury ore and/or high-mercury coal the amount of mercury released from the magnetite concentrate exceeds that derived from the coal.

Secondly, taconite processing gases remain more oxidizing than is typical for coal-fired power plants, which consume much of the oxygen in the combustion process (Zahl et al., 1995). Oxygen is an important component for reaction with mercury molecules during transport since oxidized mercury, Hg^{2+} , is much more soluble in scrubber waters than the volatilized reduced form, Hg^0 . A more oxidizing flue gas may provide opportunities for taconite plants to control mercury through simple oxidation pathways.

Third, mercury released during taconite induration is exposed to large masses of potentially reactive iron oxide minerals. These minerals, although also present in smaller amounts in coal fired power plants, have been shown to promote oxidation and capture of Hg^0 from flue gases (Zygarlicke, 2003; Pavlish, 2003; Galbreath et al., 2005). The increased exposure of process gases to iron oxides during taconite processing may have a fundamental impact on mercury transport processes.

However, one important similarity between taconite processing and coal-fired power plants is that flue gases in both types of facilities can contain chloride, an important mercury oxidation agent, particularly in the presence of iron oxides (Pavlish et al, 2003; Galbreath et al., 2005). In the case of power plants, the fuel is the primary Cl source, but fluxing agents and pore fluids that accompany solids into induration furnaces are the primary source of Cl in taconite processing plants. The present study, was conducted specifically to evaluate how the presence of iron oxides and Cl in Minnesota’s processing plants affect mercury transport in induration furnaces.

METHODS

A major goal of this study was to provide fundamental information on relationships between magnetite oxidation, mercury concentration, and heating in taconite induration furnaces. Samples heated in experiments under various conditions were compared to samples collected in induration furnaces using Mössbauer spectroscopy to evaluate iron-oxide mineralogy and total digestion to analyze mercury.

Solids from bench-scale heating experiments were obtained from Blair Benner of the University of Minnesota-Coleraine Mineral Research Laboratory (CMRL) (Benner, 2005). Benner heated samples from taconite companies in N₂ gas and air for periods of time up to 20 minutes and then measured the remaining mercury. Temperatures ranged from 300 to 700°C. Several of the samples obtained from Benner were analyzed for iron-oxide mineralogy using Mössbauer spectroscopy.

Samples were also collected from beneath the grates in active induration furnaces at four taconite processing facilities. An important distinction between taconite operations is that some use “grate-kiln” furnaces (Fig. 1) while others operate “straight-grates” (Fig. 2). Grate-Kiln facilities dry and heat pellets on a grate, but final firing is done in a rotating kiln. Drying, heating, and firing procedures are all performed on the grate in a straight-grate facility, however, a “hearth layer” consisting of pre-fired pellets is added beneath fresh greenball samples to protect the grate from the intense heat used in the firing zones. This fundamental difference in plant design, when superimposed with other less distinct differences in plant operation procedures makes every plant on the Iron Range unique. Samples in this study were collected from two straight grates and two grate kilns. Samples were sieved (<100-mesh) to remove chips and large grains and then analyzed for total mercury at Cebam, Inc., in Seattle, Washington. Most samples were also analyzed for iron-oxide mineralogy using Mössbauer spectroscopy. In each case, information on temperature was collected for the zones where dust was sampled.

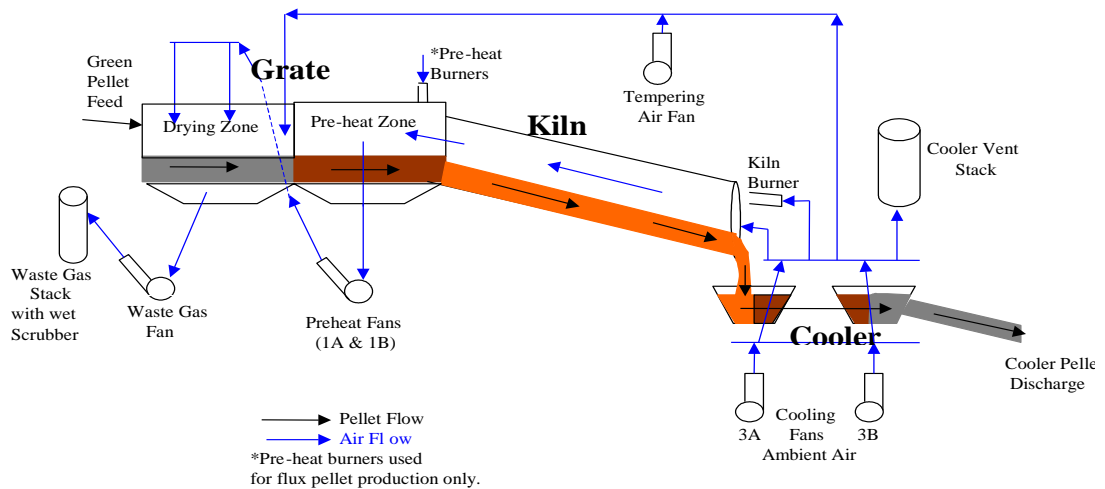


Figure 1. Diagram of a grate-kiln taconite pellet induration process. Fresh, wet pellets (termed green balls) fed into the system are systematically dried, heated, and hardened into pellets as they pass from the drying zone to the rotating kiln. Drying and heating is accomplished using gases, that are generated by cooling of the hot pellets and burning of fresh fuels in the kiln. The gases interact with pellets in the kiln, and are passed through pellet beds in the drying and pre-heat zones. The gases carry mercury and dust to the wet scrubbers. The preheat burner near the center of the diagram is used only for fluxed pellet production.

Fresh greenball and scrubber water samples were also collected from these plants and analyzed for mercury. Water samples were filtered at the plant, reacted with BrCl overnight, and then analyzed using SnCl₂ reduction, gold trap collection, and CVAFS detection (modified EPA 1631). The filters containing the scrubber solids were dried at 104°C for analysis, weighed, and digested in hot acid (HCl/HNO₃, 3/1), and the mercury analyzed also using SnCl₂ reduction and gold trap collection, followed by CVAFS detection (modified EPA 1631). Greenball samples were disaggregated into powder, digested in hot acid prior to analysis for mercury. All mercury analyses for samples collected at the taconite companies were analyzed by Cebam Analytical, Inc., Seattle, Washington. Total suspended solids (TSS) were analyzed by filtering a two-liter sample of scrubber water collected specifically for this purpose. Solids from this sample were collected on a glass fiber filter (0.7µ), dried at 104°C overnight, and weighed.

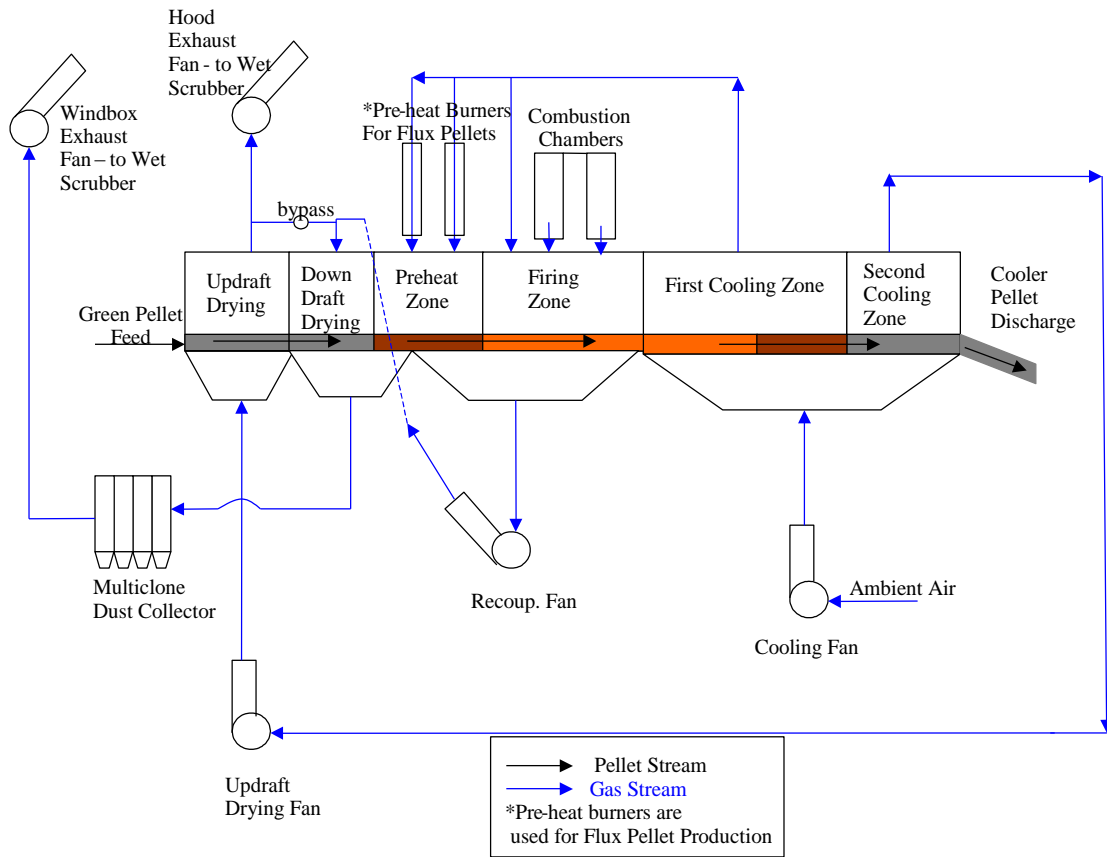


Figure 2. Diagram of a straight-grate taconite induration furnace. Fresh pellets are carried on a grate through a furnace and cooled by fresh air passed through the pellet bed. The air used for cooling the hot pellets and the gases generated in the firing zone are used for drying and heating the pellets.

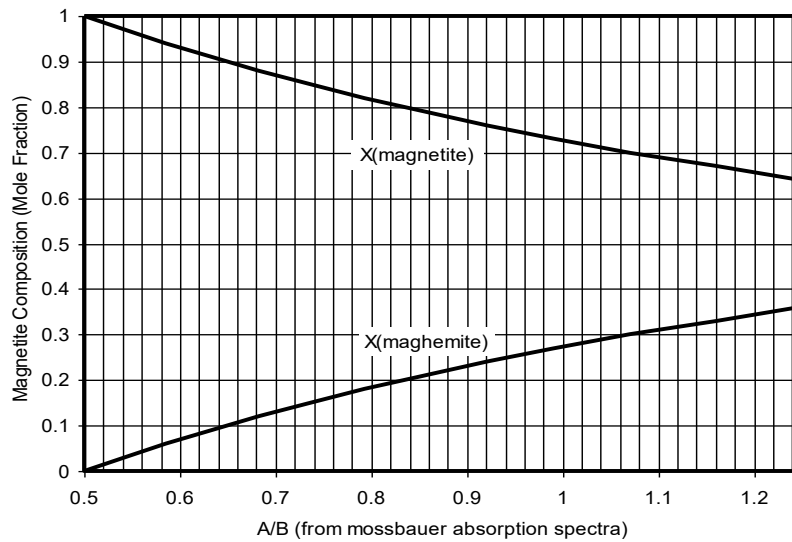


Figure 3: Ideal relationship between A/B from Mössbauer spectroscopic measurements, and magnetite/maghemite solid solution composition.

Mössbauer Spectroscopy

Mössbauer spectroscopy is a sensitive technique for measuring the atomic environments of iron atoms in a compound. The technique works by measuring absorption of gamma radiation of very specific wavelengths, generated by an oscillating radioactive source material (^{57}Co). The oscillation causes a Doppler shift of the emitted gamma radiation, while a detector records absorption as a function of gamma wave frequency. Thus, results are typically presented in terms of absorption versus velocity of the radioactive source. The details of the technique are not important for this discussion, but it is important to realize that the method permits clear distinction and quantification of the relative amounts of iron that are found in the crystal lattices of magnetite and various oxidation products. Mössbauer spectroscopic measurements were made at the University of Minnesota (Minneapolis), Institute for Rock Magnetism.

Considerable importance in this study was placed on the relative distribution of iron on A and B sites of magnetite grains. As magnetite oxidizes it forms a solid solution between magnetite and maghemite. The oxygen is added by increasing the proportion of oxidized iron in A versus B sites and accommodating this change with the introduction of site vacancies in the B site. Mössbauer spectroscopy not only evaluates mineralogy of iron oxides (e.g., magnetite, maghemite or $\gamma\text{-Fe}_2\text{O}_3$, and hematite or $\alpha\text{-Fe}_2\text{O}_3$), but determines the relative distribution of iron atoms in magnetite that are located on A or B sites. Thus, the relative absorption by iron in A and B sites (A/B) reflects magnetite composition (Coey, 1971; Papamarinopoulos et al., 1982; see Fig. 3).

Table 1: Mercury concentration and mineralogy of samples from greenball heating experiments.

<i>Temperature (°C)</i>	<i>Gas</i>	<i>Time (min)</i>	<i>Hg (ng/g)</i>	<i>Mineralogy*</i>	<i>Magnetite A/B</i>
Start			7.62	100 % mt	0.72
			7.59		
300 (572°F)	Air	20	6.42		
	N ₂	20	2.69		
400 (752°F)	Air	20	2.89	89% mt, 11 % hm	0.98
	N ₂	20	0.75		
500 (932°F)	Air	20	3.70	77% mt, 23% hm	1.26
	N ₂	20	0.92	89% mt, 11% hm?	0.59
600 (1112°F)	Air	20	2.17		
	N ₂	20	0.48		
700 (1292°F)	Air	20	2.07		

* mt = magnetite solid-solution, hm=hematite

RESULTS

Results from one set of Benner's (2005) heating experiments are presented in Table 1. Benner (2005) found that most of the mercury in taconite is released at temperatures below 400°C, especially during heating in N₂. However, a larger fraction of the mercury is retained if heating takes place in air, rather than N₂, even to temperatures as high as 700°C.

The starting sample was composed of magnetite that was slightly oxidized even before heating, as indicated by A/B = 0.72 (as opposed to 0.50 for stoichiometric magnetite, see Fig. 3). Heating this material in N₂ for 20 minutes at 500°C resulted in a decrease in the amount of magnetite and a shift in magnetite composition (to A/B = 0.59). Some of the magnetite was replaced by a mineral that appeared to be a mixture of maghemite and hematite. One possibility is that the initial magnetite simply unmixed into near-stoichiometric magnetite and Fe₂O₃, releasing its mercury in the process. It appears that mineralogic changes and mercury release occur rapidly for magnetite, even in the absence of O₂. Mössbauer results for samples heated in air at 400 and 500°C revealed systematic mineralogic changes, as well. 11% of the magnetite was replaced by hematite at 400°C while 23% was replaced by hematite during heating at 500°C. Moreover, the magnetite that remained became systematically more oxidized, with A/B increasing from 0.72 in the starting material, to 0.98 at 400 and 1.26 at 500°C, representing approximately 27 and 36 percent maghemite component, respectively.

Pertinent data on location, temperature, mercury concentration, and iron-oxide mineralogy for dust samples collected from grates at taconite plants are presented in Table 2. Mercury concentrations were surprisingly elevated in some samples. For example, concentrations of mercury reached as high as 464 ng/g in the preheat zone at one company (Fig. 4), which compares to only 11 ng/g in the starting material. Mercury concentrations were also elevated in the preheat zones at all of the companies, suggesting

Table 2 Locations, temperatures, mercury concentrations, mineralogy and magnetite composition (A/B) of samples collected from taconite plants during this study.

<i>Plant</i>	<i>Location**</i>	<i>Overbed T (°F)</i>	<i>Underbed T (°F)</i>	<i>Hg ng/g</i>	<i>Mineralogy* %mt / %hm / %mh</i>	<i>Magnetite A/B</i>
Straight. Grate #1	Greenball			11	96 / 0 / 4	0.57
	UDD WB2.5	342	490	18		
	UDD WB6.5	342	490	32	50 / 50 / 0	0.61
	DDD WB8	573	340	19	94 / 6 / 0	0.62
	PH WB12	897	195	94	90 / 10 / 0	0.64
	PH WB14	1248	202	464	94 / 6 / 0	0.65
	PH WB16	1402	253	127		
	FZ WB18	2300	350	22	88 / 12 / 0	0.69
Grate Kiln #1	Greenball			12	100 / 0 / 0	0.61
	DD1	654	199	91	91 / 9 / 0	0.65
	DD2	1049	246	57		
	DD2	1443	493	66	91 / 9 / 0	0.63
	PH WB1	2076	544	15		
	PH WB3	2076	890	2.7	36 / 64 / 0	0.56
	PH WB5	2076	1215	0.7		
Grate Kiln #2	Greenball			14	100 / 0 / 0	0.59
	DDD	525	384	24		
				24		
				21		
				24	37 / 63 / 0	0.48
	PH	1852	1291	1.7		
				1.6	35 / 65 / 0	0.59
			1.6			
			2.2			
Straight Grate #2	Greenball			10		
	DDD WB9	720	250	7	92 / 8 / 0	0.64
	DDD WB 11	720	250	10	87 / 13 / 0	0.61
	PH WB 13	1854	250	60	91 / 9 / 0	0.60
	PH WB17	2257	700	58	92 / 8 / 0	0.61
	FZ WB 19	2332	725	26	74 / 26 / 0	0.61
	FZ WB 21	2313	730	10	63 / 37 / 0	0.75

* mt=magnetite, hm=hematite, mh=%maghemite

** UDD=Updraft drying, WB=windbox, DDD=Downdraft drying, PH=preheat, FZ=Firing Zone.

a general process whereby mercury released from greenball in some parts of the furnace (high temperature) reabsorbs to greenballs and process dust at lower temperatures. The total amount of mercury collected in dust from each zone likely depends on plant-specific variations in heating rate, gas routing, and mercury concentration in the primary minerals.

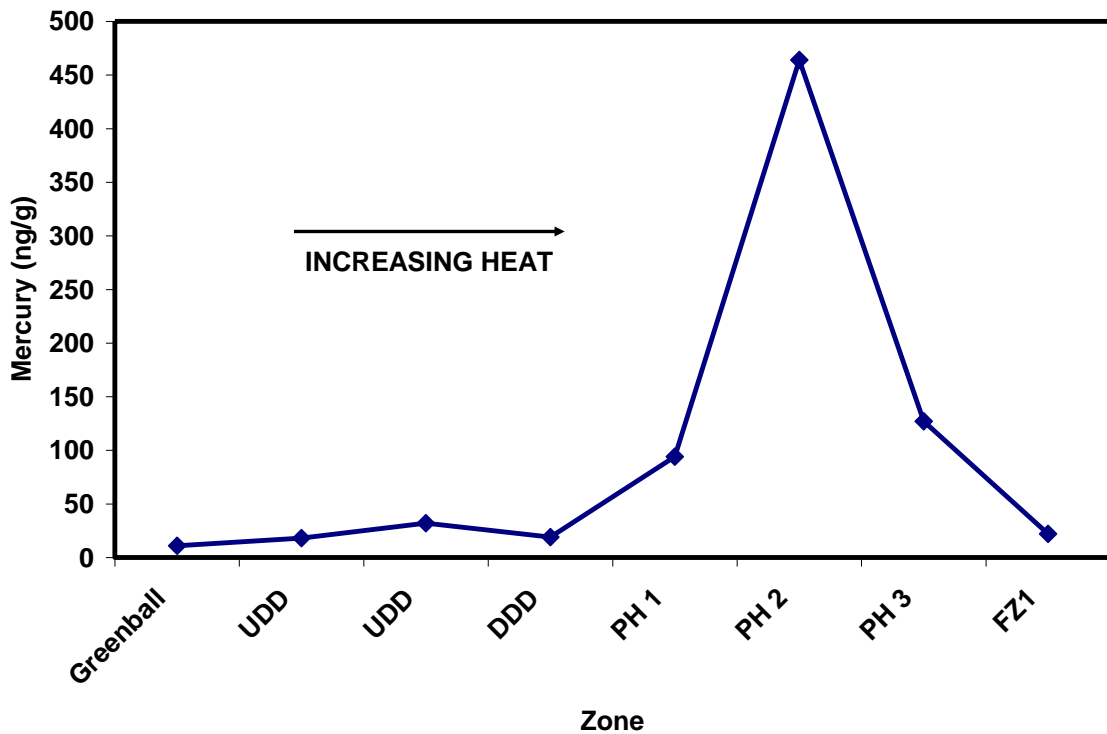


Figure 4. Mercury concentrations in dust samples collected from Straight-Grate #1. Concentrations increased to 464 ng/g in the preheat zone and then decreased again as the firing zone was approached.

The specific temperature range for mercury release and adsorption in taconite plants is not easy to evaluate due to the intense thermal gradients that exist in induration furnaces. Temperatures across the pellet bed can differ by well over 500°C (see Table 2). Samples collected from some locations contain abundant hematite suggesting at least a fraction of the collected material was exposed to very high temperatures, perhaps in the firing zone. In straight grates, hematite can also come from the hearth layer. Even when hematite is present, however, all of the samples contain a significant magnetite component, and the A/B ratios for this magnetite were only slightly shifted compared to the starting greenball samples. A/B for the magnetite component for samples whose mercury concentrations are plotted in Fig. 4 increased gradually from 0.57 in the starting sample to 0.69 for the sample from the firing zone. The change in A/B at other plants was less systematic, but still much less than observed in the heating experiments.

Greenball and scrubber water mercury concentrations (Table 3) varied widely across the range and at each plant during a two year sampling study. However, mercury concentrations were generally high at all plants, especially in the filtered solids. This indicates significant mercury oxidation takes place in induration furnaces. It appears that the oxidized mercury atoms are transported both attached to dust particles and as molecular volatile species such as $\text{HgCl}_{2(g)}$ since both particulate and dissolved mercury concentrations are elevated. Mass balance estimates indicate that over 40% of the

Table 3 Mercury concentrations and TSS for greenball and scrubber water samples. Hg(D) = Dissolved mercury, Hg(P) = concentration of mercury for dried filtrate, Hg(T) = total mercury concentration including dissolved and particulate fractions.

<i>Plant</i>	<i>Date</i>	<i>Greenball Hg (ng/g)</i>	<i>Hg(D) (ng/l)</i>	<i>Hg(P) (ng/g)</i>	<i>TSS (wt%)</i>	<i>Hg(T) (ng/l)</i>
Straight Grate #1	Average	18.6	325	2528	0.019	671
	St. Dev.	5.7	164	2525	0.011	314
Grate Kiln #1	Average	11.3	273	2470	0.070	1943
	St. Dev.	3.2	42	563	0.024	541
Grate Kiln #2	Average	16.6	542	616	1.866	11550
	St. Dev.	5.1	626	236	0.578	5004
Straight Grate #2	Average	8.4	1117	2305	0.126	4368
	St. Dev.	1.3	1465	1504	0.031	1929

released mercury was captured in wet scrubbers some days at some plants. In other cases, capture efficiencies were less than 10%. Understanding the mechanisms and processes leading to the wide variation in mercury speciation (in scrubber water) and capture efficiencies during taconite processing is needed for design of cost-effective mercury technologies for these plants.

DISCUSSION

Results from this study have shown that mercury transport during taconite processing involves a relatively complex series of reactions, whereby some of the mercury released at high temperatures in the furnaces is recaptured by magnetite and/or magnetite/maghemite solid-solutions. To simplify understanding of the release and capture process, four independent reactions (Table 4) can be used to represent processes most likely to impact mercury release during taconite induration. Reactions 1 and 2 represent conversion of magnetite to either magnetite/maghemite solid-solutions or hematite, while Reactions 3 and 4 represent release of mercury in reduced and oxidized forms, respectively. Each of the reactions in Table 4 proceeds from left to right upon heating of magnetite in taconite induration furnaces, and the challenge is to determine specific processes affecting the relative rates of each.

Magnetite oxidation to maghemite is important because it controls the composition of dust that may or may not react with, and ultimately help trap, reduced mercury ($\text{Hg}^0_{(g)}$) in process gases. Zygarlicke (2003), for example, demonstrated that maghemite participates in reactions with gaseous mercury, while magnetite and hematite do not. Maghemite forms when oxygen is added to magnetite without modification of the spinel-type crystal lattice. Formation of this mineral has long been considered to take place at intermediate temperatures in taconite induration furnaces (Papanatassiou, 1970), however, its abundance as a mineral phase, and its importance with respect to mercury transport during taconite processing, was previously unknown. Data in the present study provide an indication of time needed for magnetite to convert to magnetite/maghemite solid-solutions, but perhaps more importantly, demonstrate that mercury reacts not just

with maghemite, but also with magnetite/maghemite solid-solutions that may be close in composition to magnetite.

Reaction 1 in Table 4 does not appear to take place on a scale where it is easily observable in bulk dust samples from grates. We note, however, that the process may take place on a small scale during pellet induration. While A/B values did tend to increase slightly during induration, the amount was not nearly as much as in experiments. This behavior can be understood, perhaps, by considering in more detail the steps needed for magnetite oxidation to maghemite to take place (Columbo et al., 1965; O'Reilly, 1984; Zhou et al., 2004). First, oxygen must be adsorbed to the surface of the grain. This takes place by reaction of oxygen with electrons from the Fe^{+2} component in magnetite to form Fe^{+3} and O^{-2} ions. This has the effect of extending the mineral lattice. $\text{Fe}^{+3}/\text{Fe}^{+2}$ ratio at the mineral surface increases as a result of this interaction, and a cation site vacancy develops in the vicinity of the added oxygen. Ionic and electronic diffusion then occur to reduce the chemical gradients, and given time, the grain may become homogeneous.

If time is insufficient for diffusion to take place, then only the outer boundaries of the grains can convert to maghemite. Oxidation of magnetite grains, thus, occurs from the outside in, such that full oxidation of the interior portions is diffusion limited and can only take place as fast as diffusion permits. The outer surface mineralogy and rate of mineral growth is complex, depending on temperature, humidity, oxygen availability, and nucleation effects, as well as crystal orientation (Zhou et al., 2004). Based on results from experiments and under-grate samples, conversion of magnetite to magnetite/maghemite solid-solutions can take place on relatively short time scales at 400 and 500°C. However, time scales for induration furnaces are even shorter than those used in experiments, so only the outer-most surfaces of magnetite grains have time to convert to magnetite/maghemite solid-solutions. Since only the outer surface of the grains contacts mercury in the process gases, surface conversion of magnetite to maghemite may be all that is needed. Experimental data (Benner, 2005) indicate the process (Reaction 1) begins at temperatures less than 400 °C and will likely continue until eclipsed by conversion to hematite. To understand mercury transport in taconite induration furnaces, therefore, it is important to determine where magnetite and magnetite/maghemite solid-solutions convert to hematite (Reaction 2).

Ultimately, nearly all of the magnetite in greenballs is converted to hematite by exposure to air at temperatures of 1200 to 1300°C later in the induration process. Hematite is not known as a significant oxidant for $\text{Hg}^0_{(g)}$ at power plants (Zygarlicke, 2003). Thus, conversion of magnetite to hematite may limit mercury oxidation and capture during induration, and the mineralogic conversion process likely signals the final release of mercury to process gases during taconite induration.

For greenball samples heated in air, it took 20 minutes of exposure at 400 and 500°C to convert 11 and 23% of the solids, respectively, to hematite. Reaction times are lower, but temperatures are higher during induration. Hematite formation begins to dominate the oxidation process in the preheat zones in grate-kiln furnaces and in the

firing zone at straight grate furnaces. In all four grates sampled, mercury decreases in dust coincide with hematite increases, consistent with the idea that hematite generation effectively releases all of the mercury from magnetite/hematite solid-solutions. It is somewhat paradoxical in terms of predicting mercury release when at least a fraction of the mercury released from hematite formation will be adsorbed to solids and transported directly back to the part of the furnace where it had just been released.

This leads to consideration of the conversion of mercury from its oxidized immobile form, $\text{HgO}_{(ss)}$, to its reduced and volatile form, $\text{Hg}^0_{(g)}$ (Reaction 3). The subscript “(ss)” in $\text{HgO}_{(ss)}$ is used to indicate Hg in magnetite/maghemite solid-solutions, however, the nature and form of this component is not well known. In primary greenball samples Hg may be dispersed throughout the grain or combined with other trace components such as sulfur. However, the high concentration of mercury observed for dust samples composed exclusively of slightly oxidized magnetite in preheat zones (Fig. 4) leaves little doubt that the element exists as a surface adsorbate once it is recaptured by minerals in the furnace.

The precise manner in which mercury evolves from the surface of magnetite/maghemite solid-solutions may provide an important constraint on the form of mercury in the resulting process gas, and can impact the behavior of mercury in wet scrubber systems. Reaction 3 is a hypothetical mechanism for producing $\text{Hg}^0_{(g)}$, the form of mercury to be avoided, if possible, because it is not captured by wet scrubbers unless subsequent chemical reactions promote oxidation in the process gas phase. Reaction 4,

Table 4: Primary chemical reactions that constrain mercury release, transport, and capture in taconite induration furnaces.

<i>Number</i>	<i>Chemical reaction</i>	<i>Importance for Hg transport</i>
(1)	$2\text{Fe}_3\text{O}_{4(ss)} + \frac{1}{2} \text{O}_2(g) = 3\text{Fe}_2\text{O}_{3(ss)}$ <p style="text-align: center;">Magnetite Maghemite</p>	Maghemite interacts with mercury in flue gases, while magnetite does not. The minerals have the same structure and form a solid solution but little is known about how mercury reacts with magnetite solid solutions.
(2)	$2\text{Fe}_3\text{O}_4 + \frac{1}{2} \text{O}_2(g) = 3\text{Fe}_2\text{O}_3$ <p style="text-align: center;">Magnetite Hematite</p>	Mercury is released when magnetite is converted to hematite in induration furnaces. Hematite does not interact with mercury in flue gases.
(3)	$\text{HgO}_{(ss)} = \text{Hg}^0_{(g)} + 1/2\text{O}_2(g)$	$\text{Hg}^0_{(g)}$ is insoluble in water and cannot be caught by wet scrubbers. $\text{HgO}_{(ss)}$ represents mercury associated with magnetite and magnetite/maghemite solid-solutions.
(4)	$\text{HgO}_{(ss)} + 2\text{HCl}_{(g)} = \text{HgCl}_{2(g)} + \text{H}_2\text{O}_{(g)}$	$\text{HgCl}_{2(g)}$ is soluble in water and the Hg^{2+} base atom can adsorb to solids. This species is more easily captured by wet scrubbers than $\text{Hg}^0_{(g)}$.

however, represents a hypothetical mechanism for generating $\text{HgCl}_2^0_{(g)}$, a molecule containing mercury in oxidized form which is easily captured by wet scrubber system and which can adsorb to solids. The relative overall rates of Reactions like 3 and 4 will dictate the relative amounts of mercury released in taconite induration furnaces that can be captured either as particulate or dissolved mercury or which will be released to the atmosphere ($\text{Hg}^0_{(g)}$).

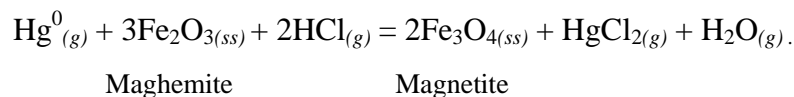
While it is unlikely that the iron-oxide mineralogy would be strongly affected by the presence or absence of small amounts of $\text{HCl}_{(g)}$ in process gases, there is good reason to expect HCl to favor Reaction 4 over Reaction 3 under conditions of relatively modest HCl concentrations. Galbreath and Zygarlicke (2000), for example, showed that the dominant transformation pathways for mercury in flue gases in coal fired power plants was by heterogeneous chlorination reactions taking place at mineral surfaces on fly-ash. The reaction products were a combination of particle-bound mercury and $\text{HgCl}_{2(g)}$. Results from mercury oxidation experiments involving gas reactions with fly ash have suggested a direct role for Fe-oxides, in particular (Ghiorshi, 1999; Lee *et al.*, 2001). Subsequently, Galbreath *et al.* (2005) performed experiments to confirm that reactions between $\text{Hg}^0_{(g)}$, HCl, and maghemite lead to a high degree of oxidation of mercury in flue gases.

The high mercury concentrations in many of the under-grate samples support reactivity of iron oxides with mercury during taconite processing, and the relatively high concentration of mercury in scrubber waters provides evidence that the mercury finally released from induration is sometimes highly oxidized (e.g., 40%). The predominant source of Cl is thought to be the pore fluid from processing waters and lime stone flux material which upon heating to 1200 to 1300°C in the firing zone, is expected to be volatilized as $\text{HCl}^0_{(g)}$. Air containing the $\text{HCl}^0_{(g)}$ travels into the preheat and drying zones where it may react with the mercury bearing iron oxides.

Mass balance results suggest taconite processing gases contain 1 to 10 ppmv Cl, values that are relatively low compared to those needed for homogenous gas phase HCl oxidations to occur (e.g., Widmer *et al.*, 1998). Thus, it is unlikely that homogenous gas reactions with HCl promote oxidation during taconite induration. However, Edwards *et al.* (2001) showed that the predominant Cl species for mercury oxidation in homogenous reactions were trace molecular species such as $\text{Cl}^0_{(g)}$ and $\text{Cl}_2^0_{(g)}$ which oxidize $\text{Hg}^0_{(g)}$ orders of magnitude more rapidly than HCl. It is unknown whether such metastable species exist in taconite processing gases. Alternatively, the heterogeneous reactions between HCl and iron oxides that come into contact with the processing gases can account for the oxidized mercury in scrubber waters (Ghiorshi, 1999; Lee *et al.*, 2001; Zygarlicke, 2003; Galbreath *et al.*, 2005). Certainly, there is abundant opportunity for processing gases containing $\text{Hg}^0_{(g)}$ and HCl to come into contact with iron oxides.

Capture efficiencies range between 9 and 40%, with the highest recovery values found for plants that use grate-kilns. While a simple difference in the grate type might be partially responsible for the difference in capture rates, it is also possible that the trend is related to differences in residence times and concentration of reactive components (e.g.,

HCl and/or iron oxides). An overall reaction describing heterogeneous oxidation of mercury by magnetite/maghemite solid-solutions and HCl can be written:



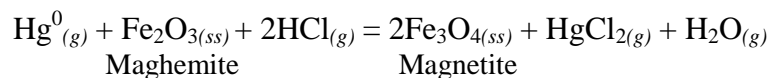
Future studies are planned to measure gas chemistry directly in taconite induration furnaces as well as to test whether Cl injection has a direct impact on mercury oxidation and capture by wet scrubbers.

It should be mentioned, however, that just increasing the capture rate for mercury in induration furnaces will be insufficient to reduce mercury in taconite stack emissions. Currently, three out of the four plants studied here simply recycle most of the captured mercury back to the induration plants. Several potential means to ensure the majority of captured mercury is routed to tailings basins, rather than back to the induration plant, are being investigated.

CONCLUSIONS

Experiments were performed and samples were collected from beneath grates and wet scrubbers in four induration furnaces to identify the primary processes affecting mercury release and capture for the taconite industry. Magnetite/maghemite solid-solutions formed during heating of the fresh magnetite-dominated greenballs in air and correspondingly, mercury release rates were greatly reduced compared to when the greenballs were heated in N₂. These results agreed with observations from under-grate samples from taconite induration furnaces which revealed considerable uptake of mercury at moderate temperatures. In general, therefore, it appears that mercury release during induration begins at approximately 450°C and continues to unspecified higher temperatures, as the magnetite converts to hematite, which appears to exclude and not react with mercury.

Subsequent to release, mercury can readsorb to magnetite/hematite solid-solutions but the overall rate of capture by wet scrubbers appears to depend both on the availability of HCl_(g)⁰ and particulate phases, most likely magnetite/maghemite solid-solutions, consistent with a reaction such as:



Despite the considerable uncertainty that exists in computation of mass fluxes for mercury, chloride, and particulates in taconite induration furnaces, the relationships observed in this study provide evidence that relatively simple procedures involving injection of Cl and/or maghemite/magnetite may provide a relatively cheap and simple means to control mercury emissions during induration at taconite processing facilities.

ACKNOWLEDGMENTS

This study was supported by funds from Iron Ore Cooperative Research and Environmental Cooperative Research Programs at the Minnesota Department of Natural Resources. Thanks are extended to those who participated in this research, particularly: John Folman, Minnesota Department of Natural Resources who provided dedicated and careful assistance selecting and readying equipment for and participating in field sampling trips. We also thank Blair Benner, University of Minnesota, Coleraine Minerals Research Laboratory, who performed and helped interpret data on taconite heating experiments. We also thank personnel from the mining industry for helping to arrange our visits, choosing and readying sampling locations, and/or for providing assistance in interpretation of results.

REFERENCES

- Benner, B. (2005) Mercury release from taconite during heating. CMRL report TR-05-06/NRRI/TR-2005-17, 3 pages.
- Berndt, M. E. (2003) *Mercury and mining in Minnesota*. Final report, Minnesota Department of Natural Resources, 58p.
- Berndt, M. E., Engesser, J., and Anderson, A. (2003) On the distribution of mercury in taconite plant scrubber systems. Minnesota DNR report prepared for MPCA. 30 p.
- Colombo, U., Gazzarrini, F., Lanzavecchia, G., Sironi, G. (1965) Magnetite oxidation: a proposed mechanism. *Science*, 147, 1033.
- Coe, J.M.D., Morrish, A. H., Sawatsky, A. Mössbauer study of conduction in magnetite. *J. Phys.* (1971) C1-32, 271-273.
- Edwards, J. R., Srivatava, R. K., and Kilgroe, J. D. (2001) A study of gas-phase mercury speciation using detailed chemical kinetics. *J. Air. Waste. Man. Assoc.*, 51, 869-877.
- Engesser, J. and Niles, H. (1997) Mercury emissions from taconite pellet production. Coleraine Minerals Research Laboratory, Report to MPCA: U of M contract # 1663-187-6253. 16 pages plus tables, figures and appendices.
- Galbreath, K. C. and Zygarlicke, C. J. (2000) Mercury transformation in coal combustion flue gas. *Fuel Processing Tech.* 65, 289-310.
- Galbreath, K. C., Zygarlicke, C. J., Tibbetts, J. E., Schulz, R. L., and Dunham, G. E. (2005) Effects of NO_x, α -Fe₂O₃, δ -Fe₂O₃, and HCl on mercury transformations in a 7-kW coal combustion system. *Fuel Processing Technology*, 86, 429-488.

Ghiorshi, B. S. (1999) Study of the fundamentals of mercury speciation in coal-fired boilers under simulated post-combustion conditions. EPA-600/R-99-026, United States EPA Office of Res. and Development, NC.

Jiang, H., Arkly, S., and Wickman, T (2000) Mercury emissions from taconite concentrate pellets- stack testing results from facilities in Minnesota. Presented at USEPA conference "Assessing and managing mercury from historic and current mining activities". San Francisco, November 28-30, 18 pages.

Lee, L. W., Srivistava, R. K., Kilgroe, J. D., and Giorshi, S. B. (2001), Effect of iron content in coal combustion fly ashes on speciation of mercury. Proc. 94th, A&WMA Annual Meeting, Air and Waste Management Association, Pittsburgh, PA.

Papamarinopoulos, S., Readman, P. W., Maniatis, Y., and Simopoulos, A., 1982, Magnetic Characterization and Mössbauer spectroscopy of magnetic concentrates from Greek lake sediments. Earth Plant Sci. Letters, 57, 173-181.

Papanatassiou, D. J. (1970) Mechanisms and Kinetics Underlying the Oxidation of Magnetite in the Induration of Iron Ore Pellets. University of Minnesota, Duluth, Unpublished PHD Thesis. 134 p.

Pavlish, J. H., Sondreal, E. A., Mann, M. D., Olson, E. S., Galbreath, K. C., Laudal, D. L., and Benson, S. A. (2003), Status Review of Mercury. Control Options for Coal-fired Power Plants. Fuel Processing Technology 82. 89-165.

Widmer, N. C., Cole, J. A., Seeker, W. R., and Gaspar, J. A. (1998) Combust. Sci. Technol. 134, 315-326.

Zahl, R., Haas, L, and Engesser, J. (1995) Formation of NO_x in Iron Oxide Pelletizing Furnaces. Iron Ore Cooperative Research (MnDNR), 43 p. plus tables and figures.

Zhou, Y., Xuesong, J., Mukovskii, Y, and Shvets, I. (2004) Kinetics of oxidation of low-index surfaces of magnetite. J. Phys: Condensed Matter. 16, 1-12.

Zygarlicke, et al. (2003) Experimental Investigations of Mercury Transformations in Pilot-Scale Combustion Systems and a Bench-Scale Entrained-Flow Reactor. University of North Dakota Energy and Environmental Research Center Technical Report. 22 p.

Appendix B-1-8

Mercury Transport in Taconite Processing Facilities: (II) Fate of Mercury Captured by Wet Scrubbers

December 31, 2005

Submitted December 31, 2005.

Mercury Transport in Taconite Processing Facilities: (II) Fate of Mercury Captured by Wet Scrubbers

Dec. 31, 2005

Michael Berndt and John Engesser
Minnesota Department of Natural Resources
Division of Lands and Minerals

Minnesota Department of Natural Resources Report prepared for:
EPA-Great Lakes National Program Office

Table of Contents

1	Abstract.....	3
2	Introduction.....	3
3	Background.....	4
3.1	Taconite Processing on Minnesota’s Iron Range.....	4
3.2	Mercury Emissions and Capture During Induration.....	4
4	Methods.....	6
4.1	Scrubber Waters: Hg(D), Hg(P), Hg(T) and Other Components	6
4.2	Adsorption Experiments	9
4.3	Davis-Tube Separation.....	10
5	Results and Discussion	11
5.1	Scrubber Water Chemistry.....	11
5.2	Hibtac.....	14
5.3	Minntac Line 7.....	18
5.4	United Taconite.....	21
5.5	Mittal.....	25
6	Conclusions.....	29
7	Acknowledgements.....	30
8	References.....	31

1 Abstract

The taconite industry in northern Minnesota emits approximately 300-400 kgs of mercury to the atmosphere each year. Most of this mercury is emitted as a result of induration, a process where magnetite concentrate from the ore is heated to high temperatures and oxidized to hematite. Hg(0) is released in the process and emitted to the atmosphere. Oxidized mercury (Hg(II)) is also generated during induration, but this species forms water soluble molecules and/or particulate-bound compounds that can be captured by the plants' wet scrubbers. This report details the mercury concentration in scrubber waters, and provides empirical experimental data needed to understand how the captured mercury partitions during subsequent reintroduction to mineral processing lines.

Concentrating iron at taconite plants involves grinding the ore to a fine grain size followed by magnetic separation to release the primary ore mineral, magnetite, from the more abundant non-magnetic gangue minerals (silicates, carbonates, hematite, goethite). Because magnetic separation is the primary means used to concentrate iron from taconite ore, experiments were conducted to determine how mercury partitions between magnetic and non-magnetic minerals. Mercury bound to nonmagnetic minerals will be rejected from the process and report to tailings basins, while mercury associated with magnetic minerals will be agglomerated into greenballs and re-volatilized during induration.

Results indicate that mercury in scrubber waters adsorb predominantly to non-magnetic minerals during taconite processing. This indicates that introducing scrubber waters and solids back into the taconite processing lines before magnetic separation will result in routing of the majority of captured mercury to tailings basins. Several taconite processing plants could cut mercury in stack emissions by sending scrubber waters and/or solids to the concentrator rather than to the agglomerator. The cost of implementing such changes and the likely savings in mercury emissions is dependent on a number of plant-specific parameters requiring further study.

2 Introduction

Stack emissions from taconite plants represent Minnesota's second largest contributor of mercury to the atmosphere. The emissions occur when the magnetic concentrate from taconite ore (magnetite) is heated to high temperatures in a process known as induration (hardening of taconite pellets). Trace mercury in the concentrate is volatilized mostly to Hg(0) which cannot be captured by the existing wet-scrubbers at taconite processing plants. However, a portion of the mercury volatilized during induration is oxidized to Hg(II) and transported as molecular or particulate-bound species that can be captured by wet scrubbers. This is the second report in a two-part series on control of mercury emissions in taconite processing facilities. The first report addressed mercury oxidation and capture during induration while this paper is concerned with the fate of the mercury following its capture in wet scrubbers.

Berndt et al. (2003) showed that mercury in scrubber waters from taconite plants is both dissolved (Hg(D)) and particle-bound (Hg(P)). The behavior of this captured mercury during taconite processing depends, to a large extent, on the minerals in the scrubber water that adsorb mercury and the routing of those minerals within the plant. A

key parameter affecting mercury transport during taconite processing is the relative tendency for the element to adsorb to magnetic (magnetite and maghemite) versus non-magnetic minerals (hematite, quartz, Fe-silicates, and Fe-carbonates, binders or limestone flux). Magnetic separation is the primary method used to concentrate magnetite and reject silicate and carbonate minerals. Thus, mercury adsorbing to magnetic minerals will be directed to the induration furnaces and volatilized. Mercury adsorbing to non-magnetic minerals, meanwhile, will report to tailings basins where, based on low levels of dissolved mercury in tailings waters, disposal appears to be permanent (See Berndt, 2003). This paper provides mercury data from scrubber waters collected over a period of time from four taconite plants and empirical experimental data indicating that most mercury in scrubber waters adsorbs to non-magnetic minerals. This indicates that existing magnetic separators can route most of the captured mercury to tailings basins while selectively recapturing the magnetic iron units from scrubber solids.

3 Background

3.1 Taconite Processing on Minnesota's Iron Range

Taconite is a very hard, relatively low-grade ore that forms the basis of the iron mining industry in Minnesota. In 2005, six taconite companies were active in Minnesota, all of which mined ore on the Mesabi Iron Range. These include, from west to east: US Steel Minnesota Ore Operations-Keewatin Taconite (Keetac), near Keewatin; Hibbing Taconite Company (Hibtac) near Hibbing, US Steel Minnesota Ore Operations-Minntac Plant (Minntac), near Mountain Iron, United Taconite Mines (U-Tac), near Eveleth, Mittal Steel USA Minorca Mine (Mittal; formerly Ispat-Inland Mining Company), near Virginia, and, finally, Northshore (NS) Mining Company, with mines located near Babbitt and ore processing facility located in Silver Bay. All of these taconite plants were built decades ago to process low-grade iron ore, at a time when Hg was not an issue. Thus, atmospheric Hg emissions from taconite processing have grown with the industry, exceeding 100 kg/yr in the late 1960's, and ranging between approximately 200 and 400 kg/yr ever since (Engesser and Niles, 1997; Jiang et al., 1999; Berndt, 2003).

During processing, ore is ground to a fine grain size and magnetite is magnetically separated from other solids producing an iron-rich "concentrate". This concentrate is "rolled" with other minor components (fluxing agents, binders) into wet, friable 1-cm balls (greenballs) in a process known as "agglomeration". The greenballs are then dried and heated to high temperatures during "induration", a process that converts the soft greenballs to hardened pellets composed mostly of hematite. These pellets are durable for shipping and ideal for use in steel-making blast furnaces.

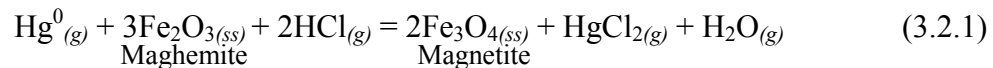
3.2 Mercury Emissions and Capture During Induration

An understanding of mercury release during taconite processing is needed for development of effective control measures for mercury in taconite stack emissions. In Part I of this series, Berndt and Engesser (2005) indicated how mercury release from taconite is distinct from the combustion-related processes that dominate mercury release in coal-fired power plants. First and foremost, the primary source of mercury released during taconite processing on Minnesota's Iron Range is the ore and not the coal or other

Submitted December 31, 2005.

fuel (Berndt, 2003). Relatively few taconite processing companies use coal to fire their pellets and, for those that do, it only takes about 20 to 40 lbs of coal to fire one long ton of pellets.

Another important difference from coal-fired power plants is that mercury released during induration in taconite companies is exposed to large masses of iron-oxide minerals in the pellet bed as well as in dust transported with the volatiles. This is significant because iron oxides are believed to promote oxidation and capture of Hg^0 especially in the presence of HCl (Galbreath and Zygarlicke, 2000; Zygarlicke, 2003; Pavlish, 2003, Galbreath et al., 2005; Berndt and Engesser, 2005, Berndt et al., 2005; Galbreath, 2005). Indeed, Berndt and Engesser (2005) found that taconite plants having the highest apparent capture efficiencies for mercury (by wet scrubbers) also had the highest Cl and particulate fluxes in process gases, and proposed a relationship such as:



to account for mercury oxidation. By this process, maghemite/magnetite solid solutions (indicated by the subscript “ss”) created during induration mediate the oxidation of $\text{Hg}^0_{(g)}$ in the process gas, and Cl from $\text{HCl}_{(g)}$ combines with oxidized mercury to generate a water soluble molecule ($\text{HgCl}_{2(g)}$). Bench scale heating experiments confirmed a relationship like Equation 3.2.1 for release of oxidized mercury from taconite and demonstrated, further, that most of the reaction takes place at temperatures less than 450 or 500°C (Benner, 2005; Galbreath, 2005; Berndt and Engesser, 2005). This release temperature is well below the high temperatures associated with mercury release in coal combustion plants (e.g., approximately 1600°C). Thus, the high- temperature radicals thought important for mercury oxidation in coal-fired power plants (e.g., Edwards et al., 2001) play a subordinate role compared to low-temperature, iron oxide-influenced reactions during taconite processing.

Regardless of the source of mercury in wet scrubbers at taconite plants, its fate during mineral processing depends on a number of factors including plant routing and adsorption to particles in the process stream. Mercury in scrubber waters is initially present as both dissolved and adsorbed species, but adsorption of the dissolved component is progressive and rapid in scrubber waters. Berndt et al. (2003), for example, measured dissolved and adsorbed mercury on samples that were filtered either immediately upon collection or several days later at the analytical facility. Dissolved mercury at one of the taconite plants (Hibtac) was close to 300 ng/l for samples filtered in the field, but dropped to only 13 ng/l for samples filtered at the analytical laboratory. A corresponding increase in particulate mercury was observed indicating that the dissolved mercury had adsorbed to the suspended solids. The meta-stable nature of mercury distribution in scrubber waters complicates the study of mercury fate during mineral processing and obviates the need to consider and note the relative timing between sample collection and filtration.

A common, but non-universal practice among taconite processing plants is to mix the scrubber solids with the concentrate prior to greenball agglomeration. This slightly

Submitted December 31, 2005.

increases the overall efficiency of the plant in terms of iron unit recovery but potentially reintroduces previously captured mercury into the induration furnace. This study investigates magnetic separation as a means to selectively reject mercury-bearing minerals but still recover iron units from the scrubber solids. Little is known about the relative adsorption of mercury to magnetite and other minerals such as hematite, silicates, and carbonates in the taconite-processing stream. The empirical data provided herein permits assessment of the relative efficiency of iron recovery and mercury rejection from scrubber waters for companies sending scrubber waters suspended solids to the plants' concentrator.

4 Methods

Four taconite processing plants participated in the present study: Hibbing Taconite (Hibtac), US Steel-Minntac (Minntac), United Taconite (U-Tac), and Mittal Steel (Mittal). These plants were selected based on the concentration of mercury in stack emissions and the presence of wet scrubber systems. Keewatin Taconite (Keetac) was eliminated based on lack of a wet scrubber during the study period. Keetac has since installed a wet scrubber system that began operation in October 2005. Northshore Mining was eliminated from this study because this company has low mercury emissions owing to low mercury concentrations in their ore. The four plants participating in this study were the same four companies that participated in Part I of the study (Berndt and Engesser, 2005).

4.1 Scrubber Waters: Hg(D), Hg(P), Hg(T) and Other Components

Scrubber water samples were collected routinely as part of both this and the previous study (see Berndt and Engesser (2005)). For all but one plant, scrubber waters were accessed by opening a valve and temporarily diverting part of the flow from a much larger pipe. Minntac, Line 7, was the exception. Scrubber water samples from this plant were collected from a dedicated hose that continuously diverted a small portion of the scrubber water stream into an accessible spot above the concentrate thickener.

Hg(D) in this report represents the concentration of dissolved mercury (ng of mercury per liter of solution) which is, in this case, the mercury concentration remaining in the water after filtration through a 0.45-micron filter (Pall Corporation). Hg(P) represents the concentration of mercury in the filter cake (ng of mercury divided by grams of filter cake). Hg(T) represents the total mercury concentration (in ng per liter) which could be determined in one of two ways. The preferred method for calculating Hg(T) is using the formula:

$$\text{Hg(T)} = \text{Hg(D)} + \text{TSS} \times 10 \times \text{Hg(P)} \quad (4.1.1)$$

where TSS (Total Suspended Solids) is in units of wt%, Hg(D) and Hg(T) are in units of ng/l, and Hg(P) is in units of ng/g. An alternative method to determine Hg(T) is to simply process and analyze unfiltered water samples for mercury, however, this method

Submitted December 31, 2005.

is less desirable because the 250 ml sample may contain a less representative fraction of suspended solids than the larger sample used for measurement of TSS (see below). Most of the mercury in taconite scrubber systems is usually present as species that are adsorbed on the suspended solids.

Although the concentration of mercury in scrubber waters is typically much higher than in waters from lakes and rivers, all water samples for Hg(D), Hg(P), and Hg(T) analyses were collected using “clean-hands, dirty-hands” procedures. Clean acid-washed bottles were placed into sealed plastic bags prior to leaving the laboratory and not opened except during sampling. Only the designated clean-hands person, wearing clean plastic gloves, handled the sample bottles when they were outside of the plastic bag. All other sampling procedures were conducted quickly and efficiently by the so-called “dirty-hands” person. These procedures were implemented to minimize the risk of contamination from plant dust or from cross-contamination between samples.

Filtered water samples were shipped to the analytical laboratory, where they were digested with BrCl and then analyzed by SnCl₂ reduction, gold trap collection, and CVAFS detection (modified EPA1631). All samples were processed and analyzed at Cebam Analytical, Inc., located in Seattle, Washington. This laboratory participates in many round-robin blind sampling programs and routinely ran duplicates and standards to ensure accuracy.

Filters containing scrubber solids from the above procedures were dried at 104°C for analysis, weighed, and digested in hot acid (HCl/HNO₃, 3/1). Particulate mercury was analyzed using SnCl₂ reduction and gold trap collection, followed by CVAFS detection (modified EPA1631). In most cases, the entire filter was processed with the filter cake to ensure that all of the mercury was analyzed and to prevent sampling bias that might result from scraping the filter cake from the filter paper. The filter papers used as procedural blanks typically contained undetectable mercury (<1 ng) or only a tiny fraction of the mercury found in the scrubber solids. Hg(P) could be calculated by dividing the total mercury detected during total digestion of the filter and filter cake by the net weight of the solids (filter plus solids minus filter weight). However, for samples with relatively high TSS, such that digestion of the entire mass was unwieldy, only a portion of the solids was analyzed without the filter.

Certified reference materials WS-68, NIST2709, and GSR-2 were used to assess recovery and analytical accuracy. As was the case for water, solids were digested and analyzed by Cebam Analytical, Inc.

Procedures were consistently evaluated using blanks to assess the degree of mercury contamination associated with filtration and sampling. Procedural blanks were collected at each site during each visit. One bottle was filled at the sampling site with deionized water brought from the laboratory. In addition, deionized water was filtered at the sampling location and both the water and the filter were saved for analysis. The level of contamination introduced by our procedures was usually insignificant compared to the relatively high concentrations of mercury found in scrubbers. The exceptions to this were when the mass of solids available for measurement of Hg(P) was exceptionally small or when the concentration of mercury was exceptionally low. These samples were considered on an individual basis as discussed in the results.

Submitted December 31, 2005.

Total suspended solids (TSS) were analyzed by filtering a two-liter sample of scrubber water collected specifically for this purpose. Solids from this sample were collected on a glass fiber filter (0.7 μ), dried at 104°C overnight, and weighed.

Other samples were routinely collected for measurement of temperature, pH, and conductivity on site. Temperature and pH were measured using a Beckman Model 11 meter with a Ross Model 8165BN combination pH electrode and a Beckman Model 5981150 temperature probe, while specific conductance was measured with a Myron L EP series conductivity meter. For cation (Ca⁺⁺, Mg⁺⁺, K⁺, Na⁺, etc..) analyses, samples were filtered and acidified with nitric acid in the field and then analyzed by inductively coupled plasma mass spectrometry (ICP-MS) at the University of Minnesota, Department of Geology and Geophysics. For anions (Cl⁻, Br⁻, SO₄⁻, etc..), samples were stored in clean plastic bottles and analyzed using ion-chromatography (IC, Dionex Ion Chromatograph fitted with a GP40 gradient pump, CD20 conductivity detector, and two AS4 anion exchange columns) at the University of Minnesota, Department of Geology and Geophysics. Chemical data for pH, Ca, and Cl were reported in Part I of this study, and complete data on other elements can be obtained by contacting the authors of this report.

Other Considerations: Previous sampling at taconite companies revealed that considerable variability could be found for samples collected from the same source during the same trip. Two sets of preliminary tests were conducted for this study to evaluate whether this uncertainty is due to sampling difficulty (e.g., scrubber waters are meta-stable and heterogeneous mixtures of solids and water) or if it is due to imprecision or inaccuracy in the laboratory analysis. The first test examined potential errors associated with analysis of Hg(P) by complete digestion of filters and solids. Three filters containing filter cake from a single sample were cut in half and sent to the analytical facility to be processed independently. Although cutting the filters introduced additional weighing errors, analysis of Hg(P) for the two halves from each filter agreed to within 3.4, 4.2, and 8.4 %, respectively. This suggests errors in Hg(P) greater than about 5 to 10% can be attributed to real variation in Hg(P) in the sample being tested.

A second test evaluated the effect of sample residence time (prior to filtration) on analysis of Hg(D) and Hg(P). In this case, a single two-liter sample of scrubber water was collected, and mixed continuously by hand for a two-hour period. 250 ml aliquots were periodically drawn from the bottle, filtered, and analyzed for Hg(D) and Hg(P). Results are displayed in Figure 4.1.1.

The initial sample from this test contained 0.0136 wt% solids with Hg(P)= 2800 ng/g suspended in a solution containing 300 ng/l Hg(D) for a total Hg concentration, Hg(T), of approximately 700 ng/l. Hg(D) decreased to nearly 200 ng/l within 15 minutes and to 130 ng/l within 2 hrs. Hg(P) simultaneously increased to over 3800 ng/g mercury (not shown), but when multiplied by TSS to calculate total mercury on a per/liter basis (Hg(adsorbed) in Figure 4.1.1) it can be seen that the increase in adsorbed mercury mirrored the decrease in Hg(D). Hg(T) remained nearly constant throughout the experiment, allowing for minor mercury adsorption onto the walls of the plastic bottle. Thus, even though this sample contained only 0.0136 % solids, adsorption processes dramatically affected mercury distribution within minutes of sampling. This test illustrates the important role that sample residence time plays on controlling the mercury

distribution in scrubber water samples. Although scrubber waters sampled in the present study were filtered at the sampling sites within minutes of sample collection, variation in residence time within the scrubber system can cause significant change in mercury distribution.

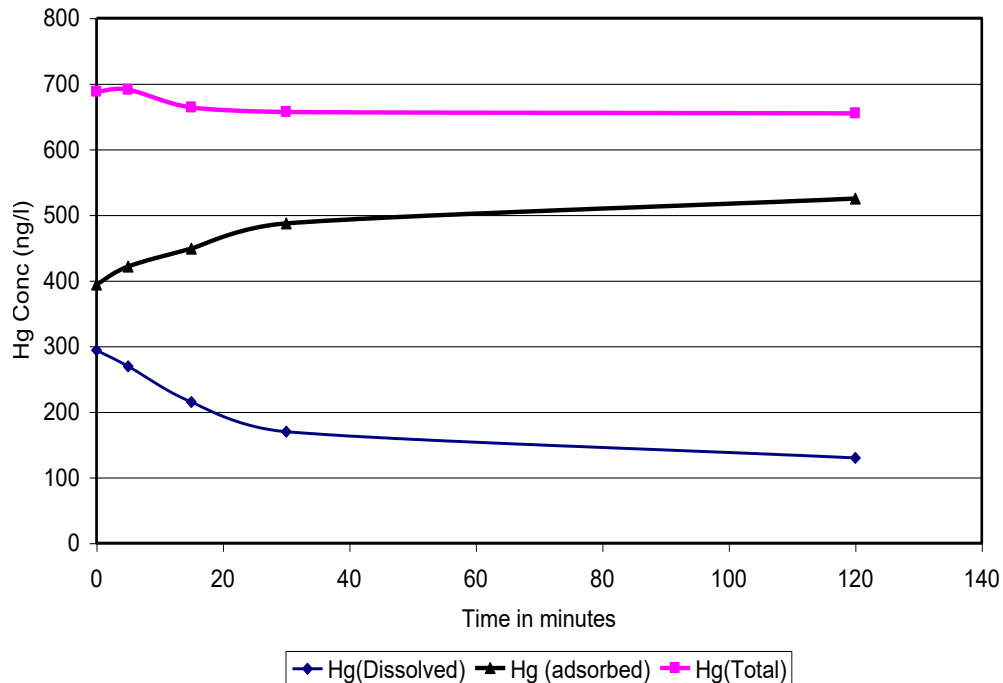


Figure 4.1.1 Results of preliminary time series test from Hibtac. Results demonstrate the rapid transfer of mercury from solution to solids that takes place in scrubber waters. Hg(adsorbed), in this case, is the concentration of adsorbed mercury per liter of water.

4.2 Adsorption Experiments

An important component of this study was to evaluate the relative fractions of mercury adsorbed to magnetic and non-magnetic minerals during mineral processing. Mercury adsorbed to magnetic minerals will follow magnetite through the taconite concentration process, eventually adding to the mercury inventory of “greenballs” that are fed to the taconite induration furnaces while mercury associated with non-magnetic minerals will be rejected from the concentrate and routed to tailings basins. To evaluate the final destination of mercury captured by wet scrubbers, a series of experiments involving mixtures of scrubber waters and tailings was performed and the resulting solids were magnetically separated, filtered, and analyzed for mercury. Scrubber solids are composed mostly of magnetite and other iron oxides containing high mercury, whereas, tailings are essentially composed of non-magnetic minerals containing low mercury. By evaluating the relative distribution of mercury in magnetic and non-magnetic fractions of tailings/scrubber water mixtures, we can establish how mercury captured during induration will behave when introduced to concentrators during taconite processing.

Submitted December 31, 2005.

Experiments were performed by placing the reactants in 250 ml acid-washed glass bottles (Teflon lined lids). The bottles were placed on a bottle-roller overnight prior to separation and/or filtration. The bottles were rotated at approximately 14 revolutions per minute, a speed that appeared adequate for keeping solids in suspension and solutions well mixed.

In all cases, experiments were conducted using reactants immediately after they were collected from the processing plants (scrubber waters and suspended solids, freshly produced tailings slurries). Drying and storage of solid samples potentially changes the composition and reactivity of mineral surfaces, while storage of water samples prior to use can lead to precipitation of super-saturated compounds (e.g., fluorite) and/or a change in oxidation state and speciation of dissolved components. Thus, to most closely approximate processes that can be expected to occur within processing plants, only fresh solutions and solids were used as reactants in experiments.

One disadvantage of using fresh reactants, however, involves a difficulty in precisely controlling the relative amounts of water and solids used in the experiments. For example, many experiments that were conducted involved mixing of two suspensions: scrubber waters and tailings. While the relative amounts of suspensions used in the experiments could be controlled, the mass of solid (tailings or scrubber solids) added in each case was unknown until after the experiment was completed and the filtered solids had been dried and weighed.

Filtered solids were, in this case, analyzed using the same method as listed for Hg(P) in section 4.1. However, because total mass of solids or total mass of mercury on the solids was sometimes small, results are reported in terms of masses found in each fraction (total mass of solids and total mass of mercury for magnetic and nonmagnetic fractions, respectively) rather than concentration. For these experiments, Hg(P) values are of secondary importance compared to relative masses of mercury and solids that partition to the magnetic and non-magnetic fractions, respectively.

4.3 *Davis-Tube Separation*

Magnetic separations were performed using Davis Tubes located at the Coleraine Minerals Research Laboratory, University of Minnesota (CMRL). The tubes are composed of glass and mounted vertically to permit gravity flow. A powerful electromagnet, located near the center of the tube, prevents transport of magnetic minerals but permits transport of water and non-magnetic minerals through an outlet at the base of the tube. The tube was pre-loaded with water until the water line was located above the magnet. The entire sample including water and suspended solids was then loaded into the tube with the magnet in the "on" position. Additional deionized water was then added to transport all of the nonmagnetic minerals through the tube and into a waiting container. This was continued until all of the water beneath the magnet was visibly clear. The magnet was then deactivated and the remaining minerals were all rinsed into a clean bottle. The solids used for mercury analysis were retrieved by filtration of each fraction, magnetic and non-magnetic, onto separate pre-weighed filters.

5 Results and Discussion

5.1 Scrubber Water Chemistry

Scrubber water mercury chemistry is displayed in Table 5.1.1. Various components of scrubber water chemistry displayed include: Hg(D) in ng per liter of filtered water (*in this case, filtered immediately upon sampling*); particulate mercury, Hg(P), in ng per gram of filter cake (*also for samples filtered immediately upon sampling*), total suspended solids (TSS in wt %), and total mercury (Hg(T)). Note that Hg(T) in Table 5.1.1 does not always match what might be expected by application of Equation 4.1.1. This is because Hg(D), Hg(P), and Hg(T) were not always determined on the same set of samples.

One defining characteristic for scrubber water mercury chemistry at taconite plants is the wide variation that occurred throughout the study. For example, the standard deviation (σ) for Hg(D) values for Hibtac was nearly half of the average Hg(D) value. Hg(P) at Hibtac varied by even more, ranging from a low value of 604 ng/g up to a high of 8396 ng/g. Similar or even greater variability was found at all of the plants.

Part of this variability could certainly be attributed to the sampling of a heterogeneous and ever-changing process stream composed of water and suspended solids. However, a closer inspection of the data indicates that not all of the variability shown in Table 5.1.1 can be attributed to this. In particular, analysis of duplicate samples collected during the same visit to a plant usually agreed to much less than 25% of the reported value. Visits for those few times when $\sigma > 25\%$ are marked with an asterisk. The observed differences in mercury concentration and distribution through time at each plant are likely process related, and represent day to day changes in ore composition and plant operation. Any method to route captured mercury to tailings basins must be sufficiently robust to work for a wide range of scrubber water conditions.

Another important result suggested by the data in Table 5.1.1 is that the chemistry of scrubber water is generally different at different plants. United Taconite has generally low Hg(P) but high TSS compared to the other plants. Hg(D) at United and Mittal is more variable and reaches values that can be higher or lower than the less variable Hg(D) concentrations observed at Hibtac and Minntac. Hibtac scrubber water is generally lower in TSS and Hg(T) than scrubber water at the other plants. To account for the difference in mercury distribution at plants, we note that each plant in this study is unique in terms of furnace type and scrubber water handling procedures (Table 5.1.2).

Minntac and United use grate-kiln furnaces where the greenballs are dried and heated on a short grate before being dumped into a rotating kiln where they are fired. Hibtac and Mittal use a straight grate for drying, heating, and firing of the pellets. Abrasion of taconite pellets within the rotating kiln in grate-kilns likely generates more dust than simple transport of pellets along a straight grate. In addition, the straight grate plants use multiclone dust collectors to capture some of the dust prior to the wet scrubber. The result is higher particulate capture rate in grate-kilns as compared to straight-grates.

Another key difference is that United Taconite and Mittal Steel recirculate their scrubber waters while Hibtac and Minntac use “single-pass” scrubber systems.

Submitted December 31, 2005.

Recirculating scrubbers allow mercury and dust to accumulate and react for greater periods of time than single-pass scrubber systems. Hg(T) values reflect both the total mercury capture rate of scrubber systems and the accumulation of mercury due to recirculation in some systems.

Averaged values for Hg(T) are lowest at Hibtac (736 ng/l) because this company has a relatively low capture rate compared to other companies (Berndt and Engesser, 2005) and because the company operates a single-pass scrubber. In contrast, Hg(T) is highest at United Taconite (9867 ng/l) owing to a relatively high mercury capture rate (Berndt and Engesser, 2005) and use of a recirculating scrubber system. Minntac, with an averaged Hg(T) value of 1540 ng/l for Line 4 and 2009 ng/l for Line 7, has a high capture rate but does not recirculate scrubber waters. Mittal, with average Hg(T) of 4867 ng/l has relatively low capture rates for mercury but *does* recirculate scrubber water. Thus, Hg(T) for the latter two companies is intermediate to the values measured at Hibtac and U-Tac.

Accounting for differences in the relative concentrations of individual components such as Hg(D) and Hg(P) is more complicated than accounting for difference in Hg(T). This is because Hg(D) and Hg(P) are affected by adsorption phenomena as described in the methods section (See Figure 4.1.1) and because the relative amount of dust generated and captured at each plant varies. Hg(P) values will increase with increasing Hg capture rates and residence times in the scrubber system, but decrease with increasing TSS. For example, Hg(P) in Hibtac scrubber water, which has low TSS (0.02 wt%), was high (2619 ng/g) compared to U-Tac (609), which had high TSS(1.6 wt%) over the study period. High TSS has a diluting effect on Hg(P) at U-tac; a large amount of captured mercury adsorbed to an even larger mass of suspended solids. Conversely, Hibtac's wet scrubber system has low TSS, and thus, any mercury that is captured adsorbs to fewer solids, and results in proportionately higher Hg(P). It is probably no coincidence that the highest Hg(P) for Hibtac was found on a day when TSS was the lowest.

Hg(D) values are much more variable at plants operating recirculating scrubbers (United Taconite and Mittal Steel) than they are in plants with "single-pass" scrubber systems (Hibtac and Minntac). This effect may be due to incomplete mixing processes in the recirculating scrubbers. If some samples contain water that has recently passed through the scrubber, while other samples contain water that has resided in a "dead" zone for a period of time, then Hg(D) will reflect variable amounts of adsorption within the scrubber system. Moreover, it is uncertain how many times water being sampled at any particular time has been exposed to gases in a recirculating scrubber. Such differences are less likely to occur in a single-pass scrubber system because all of the water passes through the scrubber only once.

Submitted December 31, 2005.

Table 5.1.1: Scrubber Water Chemistry. Year 2003 samples are from Berndt et al. (2003). Number in parenthesis is the number of analyses that were averaged to obtain the shown value. A “*” before the value indicates averaged values with $\sigma > 25\%$.

<i>Plant</i>	<i>Date</i>	<i>Hg(D)</i> <i>(ng/l)</i>	<i>Hg(P)</i> <i>(ng/g)</i>	<i>TSS</i> <i>(wt%)</i>	<i>Hg(T)</i> <i>(ng/l)</i>
<i>Hibtac</i>	2/20/2003	256(1)	1406(1)	0.010(1)	492(1)
	5/8/2003	339(2)	606(2)	0.033(3)	532(4)
	9/11/2003	231(2)	604(2)	0.038(1)	460(2)
	1/27/2004	292(2)	1484(2)	0.018(1)	556(2)
	5/12/2004	*237(2)	*2039(2)	0.013(1)	*502(2)
	7/27/2004	294(2)	2813(2)	0.014(2)	688(7)
	2/15/2005	721(2)	2874(2)	0.024(1)	1410(2)
	5/19/2005	234(3)	8396(3)	0.006(3)	731(3)
	8/15/2005	567(3)	3354(3)	0.021(1)	1250(4)
	<i>Average</i>	352	2619	0.020	736
	<i>St. Dev.</i>	173	2378	0.011	351
<i>Minntac</i> <i>Line 4</i>	2/19/2003	116(1)	1285(1)	0.058(6)	1167(6)
	5/9/2003	81(2)	160(2)	0.315(2)	578(4)
	9/10/2003	474(2)	434(2)	0.217(1)	1993(8)
	1/28/2004	164(2)	1557(2)	0.145(1)	2422(2)
	<i>Average</i>	209	859	0.184	1540
	<i>St. Dev.</i>	180	668	0.109	826
<i>Minntac</i> <i>Line 7</i>	1/28/2004	223(2)	2489(2)	0.041(1)	1251(2)
	5/11/2004	291(2)	2723(2)	0.052(1)	1706(2)
	7/27/2004	305(2)	2564(2)	0.095(1)	2746(2)
	12/1/2004	234(2)	2830(2)	0.075(1)	2357(2)
	2/16/2005	*331(2)	2855(2)	0.058(1)	1987(2)
	5/20/2005	256(3)	1360(3)	0.100(3)	1613(3)
	8/15/2005	338(3)	3001(3)	0.065(1)	2407(4)
	<i>Average</i>	283	2546	0.070	2009
	<i>St. Dev.</i>	46	551	0.022	524
<i>Evtac/</i> <i>United</i>	2/18/2003	64(1)	979(1)	0.916(3)	*6612(3)
	1/27/2004	273(3)	697(3)	0.903(1)	6571(3)
	5/11/2004	164(2)	594(2)	1.270(1)	7714(2)
	7/28/2004	112(2)	459(2)	2.260(1)	10491(2)
	11/29/2004	32(2)	322(2)	2.410(1)	7791(2)
	2/14/2005	1440(2)	848(2)	2.180(1)	19923(2)
	5/19/2005	962(3)	856(3)	1.210(4)	11829(3)
	8/17/2005	25(3)	534(3)	0.295(1)	1605(3)
	<i>Average</i>	456	602	1.604	9892
	<i>St. Dev.</i>	599	214	0.824	6043
<i>Ispat/</i> <i>Mittal</i>	2/20/2003	1216(1)	617(1)	0.328(1)	3418(3)
	5/8/2003	852(2)	*2970(2)	0.142(1)	*5274(4)
	9/11/2003	1032(3)	2094(3)	0.175(1)	4697(3)
	1/27/2004	*1025(2)	*1563(2)	0.137(1)	3166(2)
	5/12/2004	3312(2)	*440(2)	0.095(1)	3730(2)
	11/30/2004	388(2)	1975(2)	0.118(1)	2719(2)
	2/15/2005	304(2)	4032(2)	0.170(1)	7157(2)
	5/19/2005	465(3)	2774(3)	0.123(3)	3865(3)
	8/17/2005	19(2)	8930(2)	0.078(1)	6865(4)
	<i>Average</i>	897	3630	0.117	4867
	<i>St. Dev.</i>	1360	3236	0.035	2009

Table 5.1.2 Data for plants that supplied solids for experiments discussed in this study.

	<i>Indurator type, Fuel</i>	⁺ <i>Additives</i>	<i>Scrubber System</i>	[*] <i>“Blowdown” routing</i>
Hibtac	Straight-Grate, Nat. Gas	0.4 to 1% Flux, Na-Bentonite	Single-Pass	3400 gpm to concentrator
Minntac (L7 only)	Grate-Kiln, Coal, Nat. Gas.	8% Flux Na-Bentonite	Single-Pass	2950 gpm to concentrate thickener
United	Grate-Kiln, Petr. Coke/ Coal	Cellulose Binder	Recirculating	800 gpm to chip regrind
Mittal	Straight-Grate, Nat. Gas	10% Flux, Na-Bentonite	Recirculating	400 gpm to concentrate filter

⁺Flux is a Ca-Mg limestone. ^{*}Blowdown rate is total scrubber water output per induration machine.

5.2 Hibtac

Hibtac operates a straight grate furnace and uses a single-pass scrubber system. This combination produces scrubber water containing low TSS and low total mercury Hg(T), but relatively high Hg(P). The average Hg(D) was 352 ng/l while average Hg(T) was 736 ng/l, meaning that nearly half of the mercury captured by wet scrubbers is dissolved and not initially bound to particulates. Scrubber water at this plant is sent directly to the concentrator, without removal of any suspended solids, and used for grinding coarse taconite ore. Two samples of process water collected from locations in the concentrator close to where the scrubber water and solids are mixed into the concentrator process stream contained only 4.3 and 4.7 ng/l Hg(D), a value only 3.0 ng/l greater than that of the procedural blanks (1.7 ng/l). Thus, it appears that extensive adsorption of Hg(D) occurs within the concentrator immediately upon mixing with the taconite ore. The challenge at this plant is to determine what fraction of the mercury captured by scrubbers is transported back to the induration furnaces and what fraction is routed to tailings basin.

Two series of experiments were conducted on Hibtac scrubber solids to evaluate mercury adsorption on magnetic and non-magnetic minerals (Table 5.2.1). In the first series mercury was allowed to adsorb from solution to scrubber solids overnight and the resulting solids were magnetically separated using the Davis Tube and analyzed for mercury. It was found that 92 % of the adsorbed mercury was associated with the nonmagnetic sample in HB-1-1 and 86% was adsorbed to non-magnetic sample in HB-1-2. The mass of minerals in the scrubber water was small because TSS was low but, based on the relative weights of the filter cake in HB-1-2, 73 % of the scrubber solid was composed of nonmagnetic minerals. Thus, for that sample, 86% of the mercury adsorbed to 73% of the solids.

A second series (HB-2) of experiments was performed to evaluate adsorption of mercury in mixtures of tailings and scrubber waters. In this case, 0, 5, or 10 mls (milliliters) of a suspension containing fine tailings from Hibtac was mixed with

Submitted December 31, 2005.

approximately 240-250 mls of freshly sampled scrubber water (HB-2-1 through HB-2-3, in Table 5.2.1). An additional experiment was performed using tailings and deionized water (HB-2-Tails). The purpose of adding a small amount of tailings to the mixture was to increase the mass of non-magnetic minerals compared to magnetic fraction and observe the relative distribution of mercury following adsorption from solution.

As was the case for experiment HB-1-1, TSS was very low, and so the mass of magnetic minerals in the scrubber solids was difficult to measure with accuracy (approximately 3 mg). Nevertheless, 95 to 96% of the mercury adsorbed to the non-magnetic samples in HB-2-1, HB-2-2, and HB-2-3. The percentage of mercury on non-magnetic minerals in these experiments was nearly the same with or without addition of tailings, indicating that addition of small amounts of tailings had little effect on mercury distribution among magnetic and non-magnetic fractions.

Because mass of mercury and mass of solids was measured in each of the experiments, Hg(P) concentrations could be computed for the magnetic and nonmagnetic fractions and compared to concentrations in bulk samples collected at the same time. Figure 5.2.1 shows Hg(P) for samples collected at the same time that experiments HB-1-1 and HB-1-2 were conducted. In this case three samples were collected and filtered immediately when these experiments were conducted. The bulk solids had an average of 3350 ng/g mercury. A fourth sample of scrubber water was collected at the same time but filtered when the magnetic separations was performed. As expected, the concentration for this bulk solid increased (to 4950 ng/g) due to adsorption of dissolved mercury onto the solids. Non-magnetic samples from the experiments had even higher mercury than this, or approximately 6000 ng/g, while magnetic samples had less, or only about 2500 ng/g.

A similar comparison for mercury concentration in bulk solids, and magnetic and non-magnetic fractions from the HB-2 series of experiments is shown in Figure 5.2.2. As was the case for the first series of experiments, Hg(P) for magnetic minerals was far less than for non-magnetic minerals. This again indicates mercury in scrubber waters preferentially adsorbs to non-magnetic minerals both in scrubber waters and scrubber water/tailings mixtures.

These results imply that scrubber solids at Hibtac are mostly non-magnetic and that mercury is attracted more to non-magnetic minerals (hematite, silicates) than to magnetic minerals (magnetite, maghemite). This has important consequences for mercury cycling at Hibtac's processing plant. The data indicate that very little of the captured mercury is returned to the induration furnaces at this plant. This is because scrubber waters at Hibtac are sent to the concentrator where non-magnetic minerals containing the absorbed mercury are rejected by the magnetic separators. Approximately 90% or more of the captured mercury at this plant is routed to the tailings basin. Future efforts at this plant to oxidize and capture a larger percentage of the mercury from process gases should result in a corresponding decrease in mercury emissions because most of the captured mercury is already routed to tailings basins.

Submitted December 31, 2005.

Table 5.2.1: Total mass and mercury distribution among magnetic and non-magnetic minerals for scrubber water-tailings mixtures at Hibtac. Bracketed numbers represent the actual masses of reactants and mercury on the filters following Davis Tube separation. Total water volume in each case was 250 mls. Unbracketed numbers represent the percentages of the total mass or of total mercury for the magnetic and non-magnetic fractions, respectively.

	Reactants	<i>Magnetic Solids</i>	<i>Nonmag. Solids</i>	<i>Hg in Magnetic Fraction</i>	<i>Hg in Nonmag. Fraction</i>
HB-1-1	Scrubber Water	(? mg)	(24 mg)	8 (12 ng)	92 (152 ng)
HB-1-2	Scrubber Water	27 (8 mg)	73 (22 mg)	14 (20 ng)	86 (128 ng)
HB-2-1	Scrubber Water + 0% Tailings	(3 mg)	(24 mg)	4 (8 ng)	96 (174 ng)
HB-2-2	Scrubber Water + 2% Tailings	8 (11 mg)	92 (116 mg)	4 (8 ng)	96 (221 ng)
HB-2-3	Scrubber Water + 4% Tailings	9 (18 mg)	91 (173 mg)	5 (10 ng)	95 (175 ng)
HB-2-tails	Tailings + DI Water	10 (14 mg)	90 (130 mg)	(<1 ng)	(7 ng)

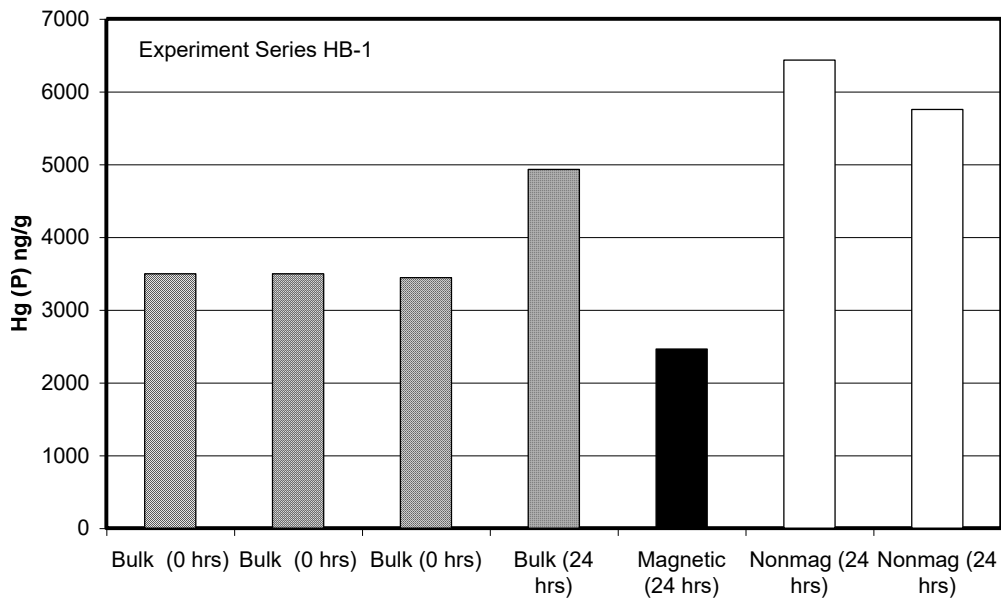


Figure 5.2.1 Hg(P) for solids from Hibtac in scrubber waters and in experiments involving scrubber waters. Bulk solids (hatched pattern) are composed of mixtures of magnetic (black pattern) and non-magnetic (white pattern) minerals, each of which have different mercury concentrations. Hg(P) for the bulk solid increased to close to 5000 ng/g, however, most of this mercury was adsorbed to non-magnetic minerals.

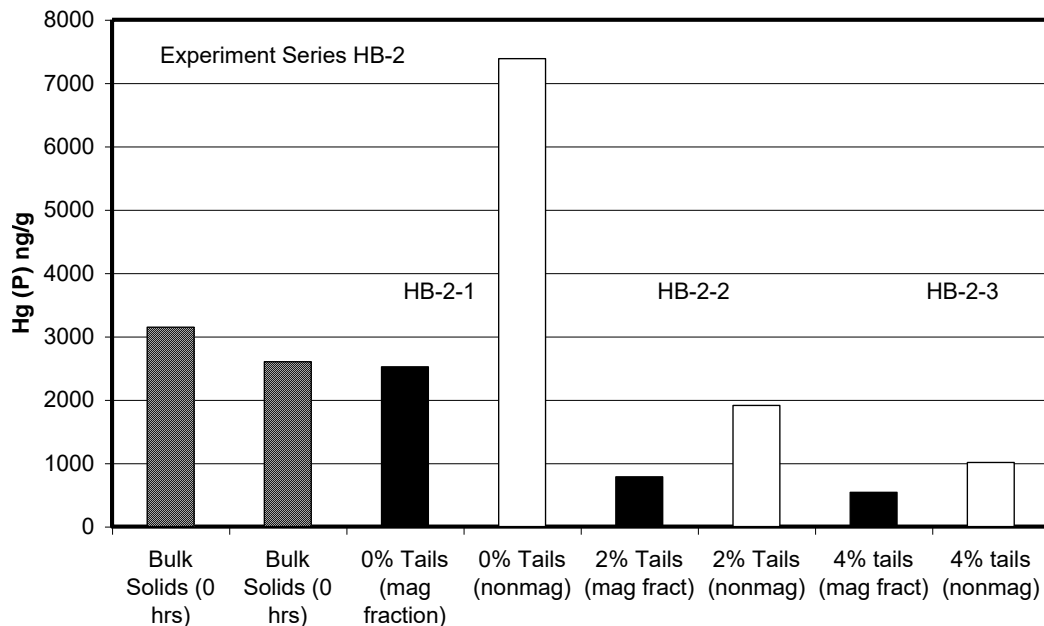


Figure 5.2.2 Hg(P) for solids from Hibtac in scrubber waters and in experiments involving mixtures of scrubber waters and fine tailings. Hg(P) for the nonmagnetic fraction was always greater than for the magnetic fraction, but the concentration in both decreased due to dilution effect from addition of tailings. Patterns are the same as described in Figure 5.2.1.

5.3 *Minntac Line 7*

Minntac sends their scrubber solids to a thickener where they are mixed with grate spill material that has passed through a grinding mill. Most of the scrubber water overflows the scrubber thickener. Sample analyses indicate that most of the mercury that was in the scrubber water adsorbs to the solids that exit through the scrubber-thickener underflow. These scrubber-thickener underflow solids eventually mix with the concentrate that is used to make greenballs. This means that most of the mercury captured in the scrubbers is recycled back to the greenballs. Thus, the percentage of captured mercury that is currently sent to the tailings basin at this plant appears to be small. Nevertheless, if mercury at this plant also adsorbs preferentially to the non-magnetic fraction as at Hibtac, then this plant could immediately cut stack emissions by sending their scrubber solids back to the concentrator rather than mixing them with the concentrate.

Experiments at this plant were conducted during three separate visits as shown in Table 5.3.1. For MN-1-1, MN-2-1, MN-2-2, and MN-3-4, scrubber water was reacted with suspended solids overnight prior to performing a Davis-Tube separation. Unlike Hibtac, scrubber solids at Minntac were predominantly magnetic. Approximately 75 to 94% of the scrubber solids in these experiments were magnetic. As was the case at Hibtac, however, the mercury appeared to adsorb preferentially to non-magnetic minerals suspended in the scrubber water. In fact, 90 to 94% of the mercury was associated with the non-magnetic minerals, even though the mass of non-magnetic minerals was small compared to the mass of magnetic minerals.

Results from experiments involving scrubber waters and tailings mixtures at Minntac were conducted using approximately 50 mls of tailings slurry and 200 mls of scrubber water or, in one case, deionized water. The tailings/solids mixtures resulted in addition of a large mass of magnetic minerals as well as non-magnetic minerals, such that the relative mass of magnetic and non magnetic fractions was approximately the same for all of the experiments. In all of the experiments with tailings, 96 to 98 % of the mercury was found on the non-magnetic solids.

Figures 5.3.1 and 5.3.2 show the relative concentrations for mercury on the magnetic and nonmagnetic fractions as compared to that of the bulk solids collected at the same time as the experiments were begun. Results from MN-1-1 are shown in Figure 5.3.1 where the scrubber water had initial Hg(P) concentration close to 2000 ng/g. The results indicate that the non-magnetic fraction had a mercury concentration approaching 10,000 ng/g, while the magnetic fraction had a relatively low concentration of approximately 220 ng/g.

A similar comparison for experiments MN-2-1 and MN-2-2 is shown in Figure 5.3.2. The scrubber water solids in the these experiments had an average Hg(P) of 3000 ng/g. Results reveal that the non-magnetic fraction had between 40,000 and 50,000 ng/g mercury, while the magnetic fraction only averaged 210 ng/g mercury. Results for MN-3-4 (not shown in a figure) were similar to this.

In the experiments with tailings (Series MN-3 experiments in Table 5.3.1), the mercury concentrations in magnetic and non-magnetic fractions were dominated by their respective concentrations in the primary tailings (Figure 5.3.3). Interestingly, the

Submitted December 31, 2005.

mercury concentration in the magnetic fraction in all three experiments was essentially identical to that of the starting tailings, while that in the non-magnetic fraction was uniformly elevated, owing to sequestration of most of the mercury from the scrubber water.

The results of these experiments imply that Minntac could potentially cut mercury emissions by sending their scrubber solids back to the concentrator grinding mills rather than mixing them with concentrate and sending them to the agglomerator. Recycled mercury to Line 7 would be decreased by 90 to 94% if scrubber water solids were routed to the concentrator. In addition, the magnetic fraction of these solids, or approximately 75 to 94% of the suspended solids for this line, would be recovered in the concentration process.

Table 5.3.1 Mass and mercury distribution among magnetic and non-magnetic minerals for scrubber water-tailings mixtures at Minntac. Bracketed numbers represent the actual masses of reactants and mercury on the filters following Davis Tube separations. Total water volume in each case was 250 mls. Unbracketed numbers represent the percentages of the total mass or of total mercury for the magnetic and non-magnetic fractions, respectively.

	Reactants	<i>Magnetic Solids</i>	<i>Nonmag. Solids</i>	<i>Hg in Magnetic Fraction</i>	<i>Hg in Nonmag. Fraction</i>
MN-1-1	Scrubber Water	74 (56 mg)	26 (20 mg)	6 (12 ng)	94 (181 ng)
MN-2-1	Scrubber Water	94 (94 mg)	6 (7 mg)	7 (19 ng)	93 (262 ng)
MN-2-2	Scrubber Water	94 (80 mg)	6 (5 mg)	6 (17 ng)	94 (283 ng)
MN-3-Tails	Tailings + DI water	5 (1.364 g)	95 (26.74 g)	4 (32 ng)	96 (789 ng)
MN-3-1	Tailings + Scrubber Water	4 (0.919 g)	96 (19.84 g)	2 (20 ng)	98 (879 ng)
MN-3-2	Tailings + Scrubber Water	5 (1.079 g)	95 (22.6 g)	3 (27 ng)	97 (815 ng)
MN-3-3	Tailings + Scrubber Water	4 (0.846 g)	96 (19.3 g)	4 (22 ng)	96 (540 ng)
MN-3-4	Scrubber Water	90 (59 mg)	10 (7 mg)	10 (18 ng)	90 (172 ng)

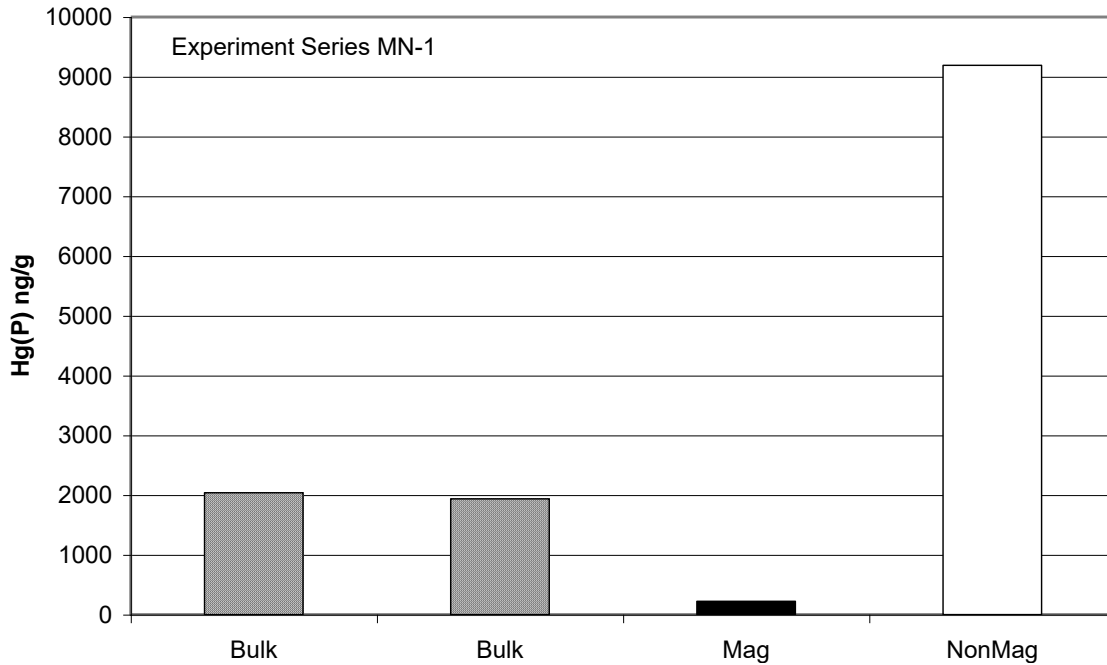


Figure 5.3.1 Hg(P) for solids from MN-1 experiments for Minntac as described in Table 5.3.1. Bulk solids (hatched pattern) are composed of mixtures of magnetic (black pattern) and non-magnetic (white pattern) minerals, each of which have different mercury concentrations. The nonmagnetic fraction was greatly enriched in Hg relative to the bulk solid and magnetic fraction.

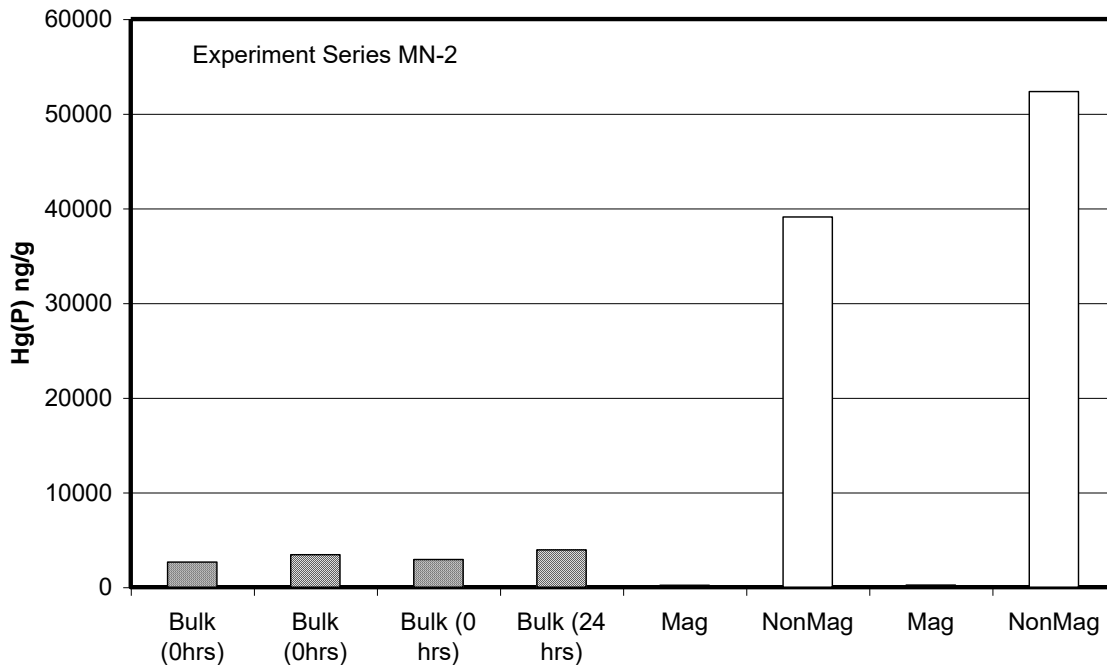


Figure 5.3.2 Hg(P) for solids from MN-2 experiments in Table 5.3.1. Patterns have same meaning as in Fig. 5.3.1. The nonmagnetic fraction was once again greatly enriched in Hg relative to the bulk solid and magnetic fraction, reaching 50000 ng/g.

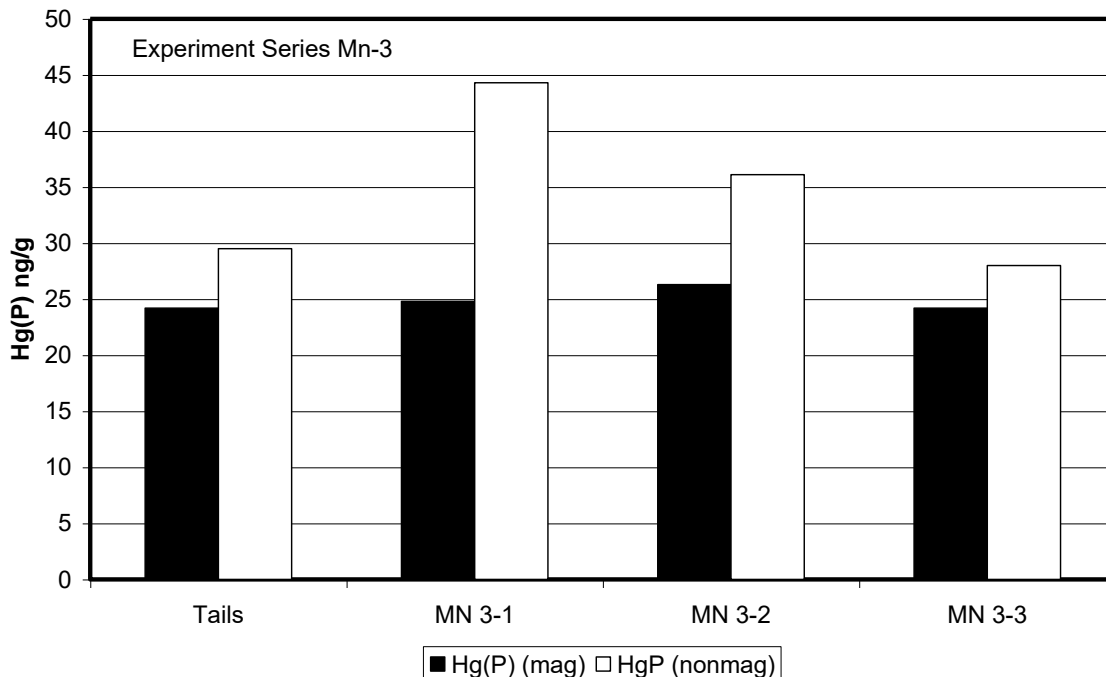


Figure 5.3.3 Hg(P) for solids from MN-3 experiments in Table 5.3.1. Patterns have same meaning as in Fig. 5.3.1. The scale is greatly changed from previous two figures. Adding scrubber water to tailings had little impact on the mercury concentration in the magnetic fraction in the tailings, but increased significantly the mercury concentration in the non-magnetic fraction.

5.4 United Taconite

United Taconite sends their scrubber waters and solids to a chip regrind mill where it is mixed with other solids, reground, and mixed with concentrate from the plant. Because only a very small fraction of the mercury captured at United Taconite is initially dissolved in the water, it was expected that most of the captured mercury at this plant would be recycled back to the induration furnace with the scrubber solids.

However, two samples of the water returning to the concentrator from the agglomerator were collected in one of our visits to the taconite plant. These samples contained lower Hg(D) (= 12 ng/l), Hg(P) (= 117 ng/g), TSS (=0.497 wt%) and Hg(T) (= 589 ng/l) than scrubber water samples, but the concentrations were much higher than expected for a stream containing overflow from a concentrate thickener. It appears that, at least on the day this site was sampled, significant mercury was being sent from the pellet plant back to the concentrator. This stream will be studied in greater detail in future studies. As was the case at Hibtac, the fate of the mercury sent to the concentrator depends on how the element partitions between magnetic and non-magnetic minerals.

Experiments at this plant were conducted during three separate visits as shown in Table 5.4.1. For UN-1-1, UN-2-1, UN-2-2, and UN-3-4, scrubber water was reacted with suspended solids overnight prior to performing a Davis Tube magnetic separation of the solids. The average magnetic and non-magnetic fractions were nearly equal but significant variation was observed: the magnetic fraction ranged from as low as 42

percent of the total mass up to 68 percent. The tendency for mercury to adsorb to non-magnetic minerals was not as strong as was observed at Minntac. Only 76 to 88% of the mercury partitioned onto the non-magnetic minerals in scrubber water at U-Tac while 90 to 94 % of the mercury partitioned into the non-magnetic fraction at Minntac, despite the fact that the scrubber solids from Minntac had a lower non-magnetic fraction than those from U-Tac.

Results from experiments involving scrubber waters and tailings mixtures at United Taconite were conducted by mixing approximately 50 mls of tailings slurry, and 200 ml of freshly collected scrubber water. While magnetic minerals were present in the tailings, the mixture had a net increase in the non-magnetic fraction up to 86 to 87% of the total solids. In the experiments with tailings, 86 to 90 % of the mercury was found on the non-magnetic fraction. Tailings with no addition of scrubber water had 94% of the mercury on the non-magnetic fraction while scrubber water with no addition of tailings for the experiments had only 76 % of the mercury on the non-magnetic fraction.

Figures 5.4.1 and 5.4.2 show the relative concentrations for mercury on the magnetic and nonmagnetic fractions as compared to that of the bulk solids collected at the same time the experiments were performed. Results from test UN-1-1 are shown in Figure 5.4.1. The scrubber water in this test had an initial Hg(P) of approximately 800 ng/g. The Hg(P) of the magnetic fraction was about 300 ng/g and the Hg(P) for the nonmagnetic fraction was more than 1300 ng/g. Experiments UN-2-1 and UN-2-2 are shown (Figure 5.4.2). The solids suspended in the scrubber water for these tests initially had Hg(P) averaging 530 ng/g which is intermediate to the 130 and 710 ng/g values for Hg(P) of the magnetic and nonmagnetic fractions, respectively. For UN-3-4 (not shown in a figure), where the scrubber water had an initial Hg(P) of 460 ng/g, the magnetic fraction had only 182 ng/g mercury, while the non-magnetic fraction contained approximately 1240 ng/g mercury. Thus, as was the case for Hibtac and Minntac, mercury partitions to the non/magnetic fraction of scrubber solids.

In the experiments with tailings (Series UN-3 experiments in Table 5.4.1), the mercury concentrations in magnetic and non-magnetic fractions were dominated by their respective concentrations in the primary tailings (Figure 5.4.3), but the concentration of mercury in both the magnetic and non-magnetic fractions increased relative to tailings. This was expected because the magnetic fraction for solids suspended in the scrubber water at U-Tac had a relatively large fraction of the mercury (24%) when the experiments were performed, and the magnetite in tailings had very little mercury. The concentration of mercury in the magnetic fraction represents a mixture of mercury from the two sources of magnetite – scrubber solids magnetite and tailing magnetite.

Comparing these results with those from Minntac suggests a possible mechanism exists at United Taconite that promotes some adsorption onto the magnetic fraction in scrubber solids. One possibility is that the adsorption of mercury is related to the presence of more oxidized coatings on magnetite grains at Utac than at Minntac. Scrubber solids at U-Tac have a larger non-magnetic fraction than scrubber solids at Minntac. Because the chief non-magnetic mineral in scrubber solids is likely magnetite that has been converted to hematite, a larger non-magnetic component indicates greater oxidation of the solids. However, it is important to note that magnetite grains only

partially converted to hematite will be sufficiently magnetic to partition into the magnetic fraction of solids separated with a Davis Tube.

Another possibility is adsorption of the mercury to silicate gangue minerals associated with the magnetic minerals in the magnetic fraction. Minntac and Mittal use flotation, a process that removes additional silica from concentrate not removed by magnetic separation. United Taconite does not use flotation and, therefore, the mineral gauge concentration associated with magnetic minerals in the concentrate will be higher than at Minntac or Mittal.

Minntac and Mittal Steel also produce fluxed pellets, which introduces carbonate minerals into the agglomeration and induration processes. Fluxed pellets are manufactured by adding 8-10% limestone (dolomite and calcite) to the concentrate prior to producing greenballs for induration. These carbonate minerals potentially affect solution pH in the scrubber waters, although the pH of tailings/scrubber water mixtures in concentrators at taconite plants is typically high (8 to 9).

Table 5.4.1 Mass and mercury distribution among magnetic and non-magnetic minerals for scrubber water-tailings mixtures at U-Tac. Bracketed numbers represent the actual masses of reactants and mercury on the filters following Davis Tube separations. Total water volume in each case was 250 mls. Unbracketed numbers represent the percentages of the total mass or of total mercury for the magnetic and non-magnetic fractions, respectively.

	<i>Reactants</i>	<i>Reactants</i>		<i>Hg in</i>	<i>Hg in</i>
		<i>Magnetic Solids</i>	<i>Nonmag. Solids</i>	<i>Magnetic Fraction</i>	<i>Nonmag. Fraction</i>
UN-1-1	Scrubber Water	51 (826 mg)	49 (801 mg)	20 (257 ng)	80 (1051 ng)
UN-2-1	Scrubber Water	42 (286 mg)	58 (397 mg)	12 (38 ng)	88 (287 ng)
UN-2-2	Scrubber Water	48 (511 mg)	52 (550 mg)	15 (66 ng)	85 (386 ng)
UN-3-Tails	Tailings + DI water	4 (865 mg)	96 (19.35 g)	6 (22 ng)	94 (323 ng)
UN-3-1	Tailings + Scrubber Water	14 (1.542 g)	86 (9.15 g)	12 (106 ng)	88 (808 ng)
UN-3-2	Tailings + Scrubber Water	13 (1.706 g)	87 (11.71 g)	10 (100 ng)	90 (876 ng)
UN-3-3	Tailings + Scrubber Water	13 (2.136 g)	87 (13.77 g)	14 (137 ng)	86 (843 ng)
UN-3-4	Scrubber Water	68 (1.305 g)	32 (624 mg)	24 (238 ng)	76 (772 ng)

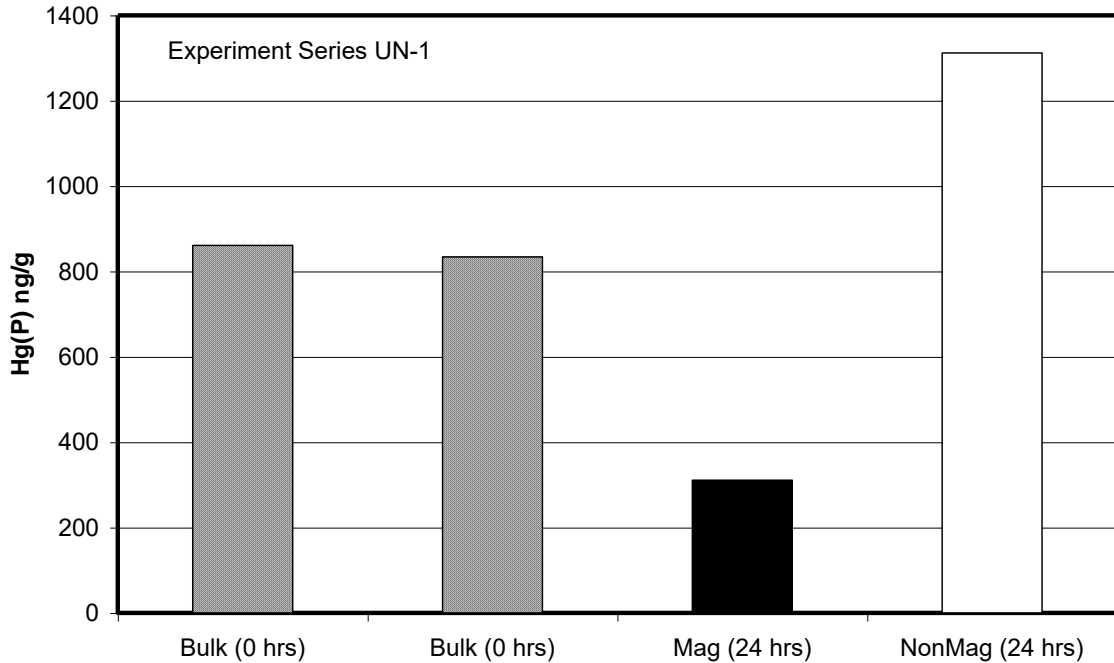


Figure 5.4.1 Hg(P) for solids from UN-1 experiments in Table 5.4.1. Bulk solids (hatched pattern) are composed of mixtures of magnetic (black pattern) and non-magnetic (white pattern) minerals, each of which have different mercury concentrations. As was observed for Hibtac and Minntac, Hg(P) was enhanced in nonmagnetic minerals compared to the bulk solid or to magnetic minerals.

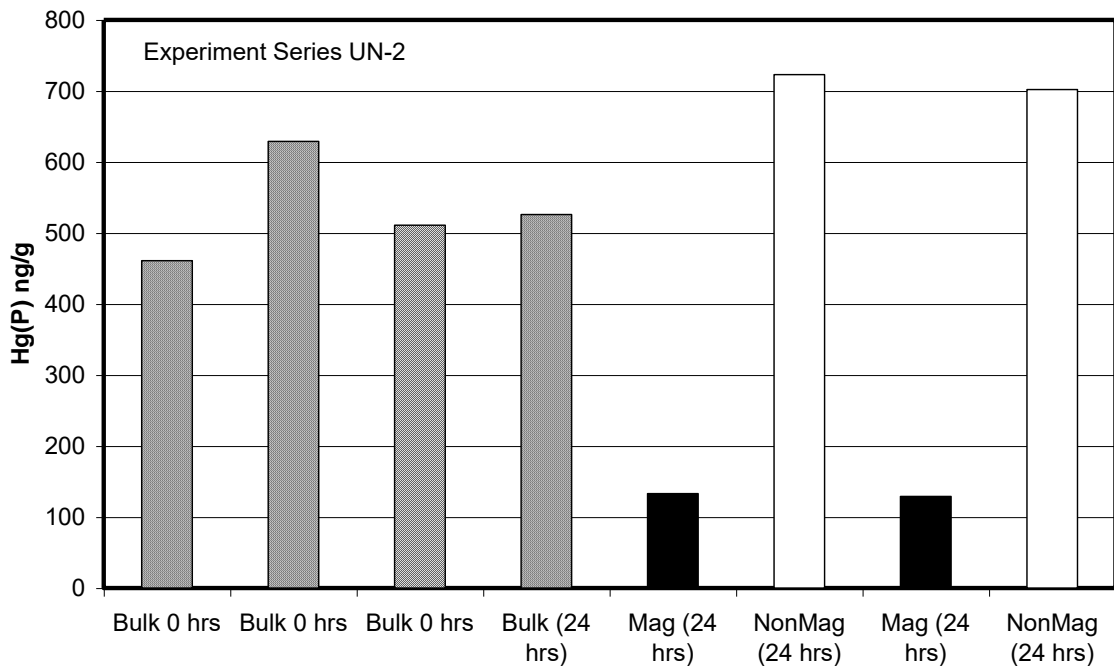


Figure 5.4.2 Hg(P) for solids from UN-2 experiments in Table 5.4.1. Distribution is similar to that shown in Figure 5.4.1, although concentrations for bulk, magnetic, and nonmagnetic fractions are lower.

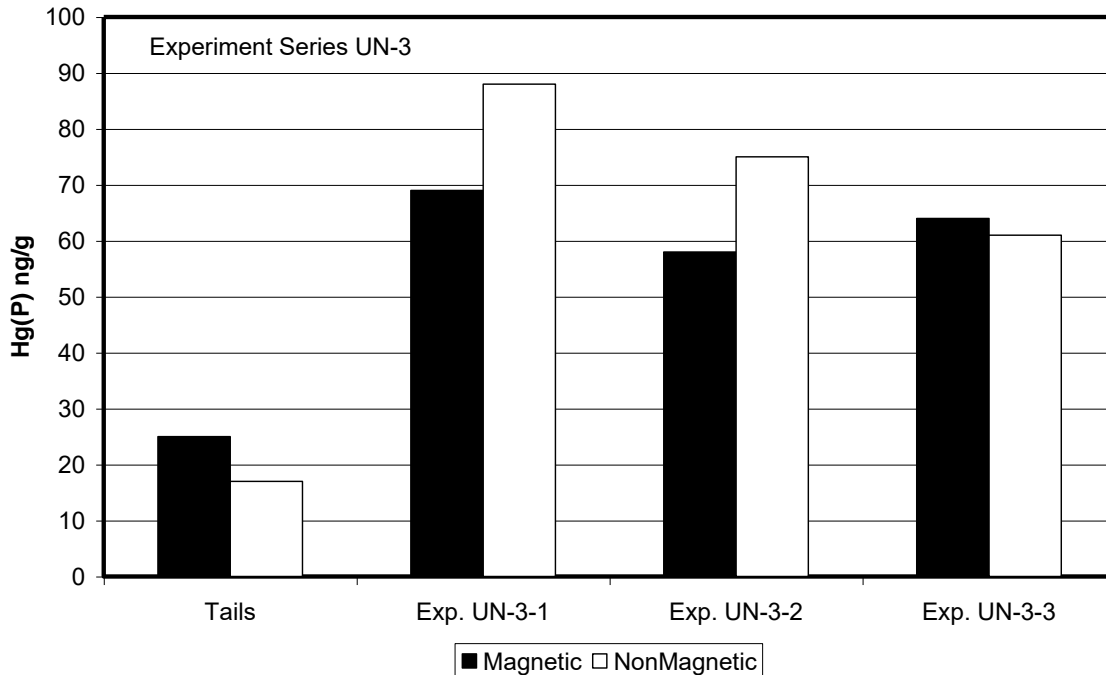


Figure 5.4.3 Hg(P) for solids from UN-3 experiments described in Table 5.4.1. Adding scrubber waters to tailings increased the mercury concentrations in both the magnetic and non-magnetic phase. Solid black pattern represents mercury concentration in the magnetic fraction while white pattern represents the mercury concentration in the corresponding non-magnetic fraction.

5.5 Mittal

Mittal Steel uses a recirculating scrubber and has a relatively low blow-down rate. This means that the average residence time for mercury in the scrubber system is long compared to other systems and thus provides an opportunity for Hg capture and adsorption to occur, potentially leading to very high, but quite variable Hg(D) and Hg(P) values. This company sends their scrubber solids and waters to the concentrate filter and little mercury remains dissolved in the water following the process. Thus, most of the captured mercury at this plant also appears to recycle back to the induration furnace and probably only a small fraction is directed to the tailings basin.

Experiments at this plant were conducted during three separate visits as shown in Table 5.5.1. For ML-1-1, ML-2-1, ML-2-2, and ML-3-4, scrubber water was reacted with suspended solids overnight prior to performing a Davis Tube magnetic separation of the solids. The non-magnetic minerals dominate the scrubber solids at this plant comprising 54 to 73% of the total solids. Moreover, the experiments clearly indicated that mercury adsorbed overwhelmingly to the nonmagnetic minerals (94 to 96% of the total mercury was adsorbed to non-magnetic minerals). Thus, although this plant produces scrubber solids that are even more oxidized than scrubber solids at United Taconite, the mercury avoids adsorption to magnetic minerals in a manner similar to that found at Minntac and Hibtac. When tailings/scrubber water mixtures were used in experiments (See ML-3-1, ML-3-2, and ML-3-3), the fraction of mercury on the non-magnetic minerals dominated that on the magnetic minerals, as well. In particular, 92 to

Submitted December 31, 2005.

96 % of the mercury was associated with the non-magnetic minerals in tailings and tailings/scrubber water mixtures.

Figures 5.5.1 and 5.5.2 provide a comparison of Hg(P) in magnetic and non-magnetic components and bulk solids suspended in scrubber waters. For ML-1-1 (Figure 5.5.1), H(P) for the bulk scrubber water was initially close to 4000 ng/g, but Hg(P) concentrations in the magnetic and nonmagnetic fractions were only 100 and 2770 ng/g, respectively. The low values suggest either that mercury was dissolved from solids during the experiments or that the sample used in the experiments was non-representative of the scrubber water. For ML-2-1 and ML-2-2 (Figure 5.5.2), the Hg(P) of the bulk solution was 8930 ng/l and this value increased to 9200 ng/l during reaction overnight. However, mercury in the samples that underwent magnetic separation averaged only 1090 and 8780 ng/g Hg(P) for the magnetic and nonmagnetic fractions, respectively. The solids in all three of these experiments had lower mercury concentrations than the bulk solution, which suggests that mercury dissolved during the experiments. This loss of mercury did not appear to occur in experiments with scrubber solids from other companies, nor was it noticed in the scrubber solids in experiment ML-3-3 (not shown), where the bulk solid had 1975 ng/g Hg(T), the magnetic fraction contained 260 ng/g, and the non-magnetic fraction concentration was slightly greater than 2411 ng/g.

One possibility to account for the loss of mercury from scrubber solids is that it is the result of an equilibration process whereby solids containing very high mercury concentrations begin to release mercury into the water used in the experiments. It may not be coincidence that the two samples in our study where mercury appeared to be lost involved solids that had the highest concentrations of mercury.

Mercury concentrations for tailings experiments (ML-3 series of experiments in Table 5.5.1 and also shown in Figure 5.5.3) indicate that the mercury concentration in both the magnetic and non-magnetic fractions increased. This was expected based on the relatively low concentration for mercury in both magnetic and non-magnetic fractions of the tailings as compared to the concentrations in the respective fractions for the scrubber solids.

Submitted December 31, 2005.

Table 5.5.1 Mass and mercury distribution among magnetic and non-magnetic minerals for scrubber water-tailings mixtures at Mittal Steel. Bracketed numbers represent the actual masses of reactants and mercury on the filters following Davis Tube separations. Total water volume in each case was 250 mls. Unbracketed numbers represent the percentages of the total mass or of total mercury for the magnetic and non-magnetic fractions, respectively.

	<i>Reactants</i>	<i>Magnetic</i>		<i>Hg in</i>	
		<i>Solids</i>	<i>Nonmag. Solids</i>	<i>Magnetic Fraction</i>	<i>Nonmag. Fraction</i>
ML-1-1	Scrubber Water	46 (78 mg)	54 (91 mg)	3 (8 ng)	97 (252 ng)
ML-2-1	Scrubber Water	27 (28 mg)	73 (73 mg)	5 (30 ng)	95 (636 ng)
ML-2-2	Scrubber Water	34 (38 mg)	66 (76 mg)	6 (42 ng)	94 (671 ng)
ML-3-Tails	Tailings + DI water	4 (404 mg)	96 (11.10 g)	6 (9 ng)	94 (137 ng)
ML-3-1	Tailings + Scrubber Water	5 (385 mg)	95 (8.16 g)	8 (18 ng)	92 (208 ng)
ML-3-2	Tailings + Scrubber Water	5 (343 mg)	95 (6.62 g)	7 (19 ng)	93 (253 ng)
ML-3-3	Tailings + Scrubber Water	5 (522 mg)	95 (11.01 g)	4 (17 ng)	96 (370 ng)
ML-3-4	Scrubber Water	33 (66 mg)	67 (138 mg)	5 (17 ng)	95 (332 ng)

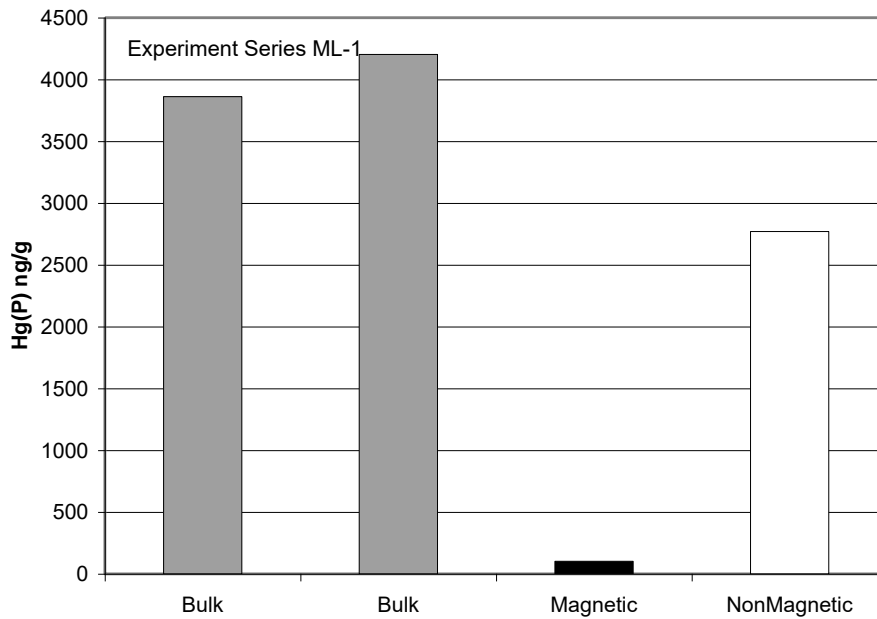


Figure 5.5.1 Hg(P) for magnetic and nonmagnetic minerals in scrubber solids at Mittal for ML-1 experiments described in Table 5.5.1. Patterns are same as in previous figures. Both non-magnetic and magnetic phases had low Hg(P) compared to bulk solids suggesting some redissolution of adsorbed Hg.

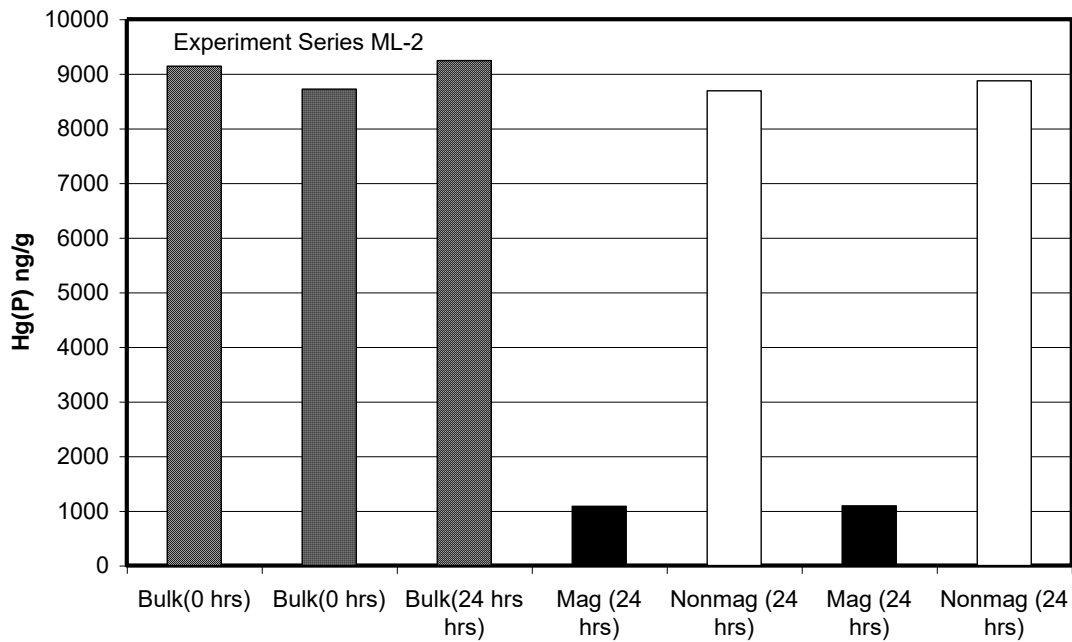


Figure 5.5.2 Hg(P) magnetic and nonmagnetic minerals in scrubber solids at Mittal Steel for ML-2 experiments in Table 5.5.1.

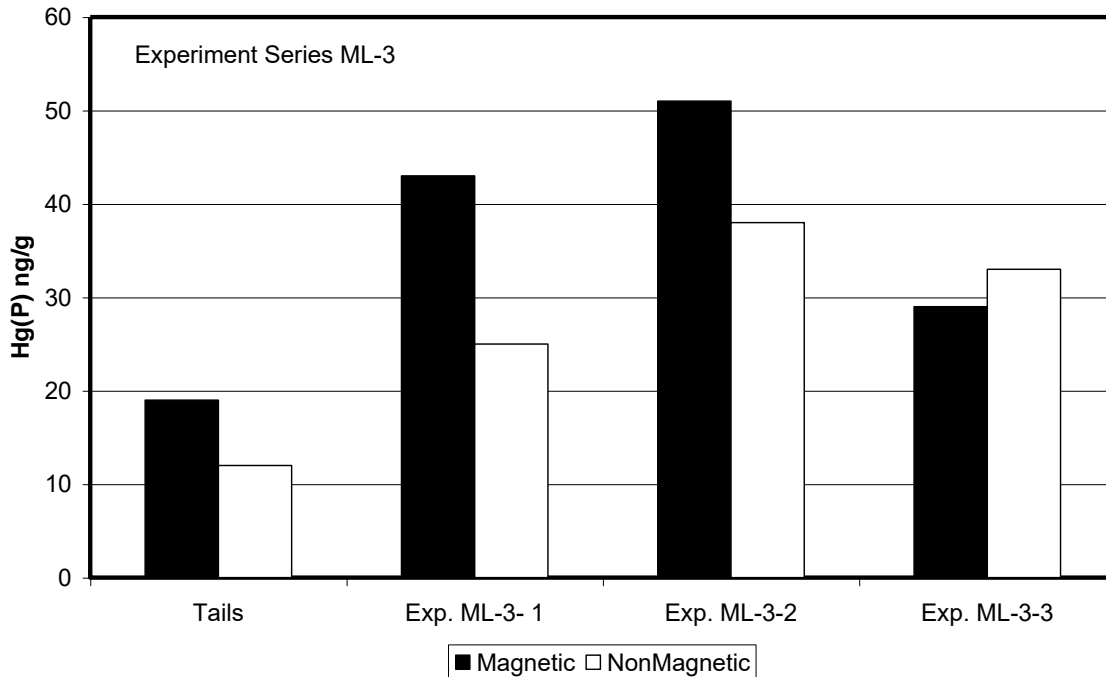


Figure 5.5.3 Hg(P) following addition of scrubber water to tailings at Mittal Steel. The concentration of mercury increased for both magnetic and non-magnetic fractions, however, the total concentration for either fraction remained relatively low.

6 Conclusions

Wholesale recycling of scrubber-solids back to the induration furnace results in recovery of iron-oxide units from the dust, but also results in recycling and release of a large fraction of the captured mercury. One alternative to this practice would be to route all of the scrubber solids to tailings basins or similar disposal sites, but this practice would result in loss of previously processed product. Another alternative involves sending scrubber solids back to the concentrator to permit retrieval of the magnetic components of the scrubber solids while disposing of the non-magnetic components to tailings basins. Projected mercury rejection and iron recovery efficiencies for this process is plant specific (Table 6.1) and depends on the mineralogy and chemistry of scrubber waters and suspended solids:

(1) Magnetic separation of scrubber solids in the concentrator is already practiced at Hibtac. Results from this study suggest this company is eliminating approximately 90-95% of the captured mercury from its process lines. If a means can be found to increase oxidation and capture of mercury from process gases during induration, this company appears to be well poised to reject the additional mercury without further change to its mineral processing lines.

(2) Magnetic separation of scrubber solids would have the greatest impact on decreasing mercury emissions at Minntac. This company has a single pass scrubber that captures dust with a high magnetic content, and with very high levels of mercury in the small non-magnetic fraction. 90 to 94% of the recycled mercury would be rejected if

Submitted December 31, 2005.

Minntac routed the scrubber solids to the grinding mills in the concentrator, and 75 to 94% of the iron units associated with the dust could be recovered. However, it is unknown at this time what implications such routing would have on pellet quality and production rates.

(3) Magnetic separation of scrubber dust does not appear to be as efficient for United Taconite as at Minntac. United Taconite already appears to route most of the captured mercury back to the concentrator; however, not enough samples were obtained to quantify this. If U-Tac routed all of the scrubber solids to the grinding mills in the concentrator, then approximately 75 to 88% of the mercury in the scrubber dust would be rejected with the tailings. The company would lose about half of the iron units associated with the scrubber dust.

(4) Magnetic separation of scrubber dust at Mittal Steel would be highly effective in preventing recycling of captured mercury to the induration furnaces. Mercury concentrations on solids can reach high levels owing to use of a recirculating scrubber at this plant. Mixing tailings with the scrubber waters disperses the mercury onto a larger mass of non-magnetic solids. If Mittal sent their scrubber solids to the concentrator grinding mills, it would prevent recycling of 94 to 97% of mercury contained on the scrubber dust, but they would also lose more than half of the iron units associated with the dust.

Future planned research will compare the feasibility of magnetic separation to reject mercury in taconite plants as opposed to other mineral processing techniques such as rejection of scrubber fines (Benner, 2001) or full disposal of scrubber solids (currently practiced at Keetac).

Table 6.1 Summary of data for scrubber solid recycling at taconite plants.

<i>Plant</i>	<i>*Estimated Mercury Capture Efficiency</i>	<i>Current Hg Rejection Rate</i>	<i>Mercury Rejection Rate for Magnetic Separation</i>	<i>Iron Recovery Rate for Magnetic Separation</i>
Hibtac	0.11 ± 0.06	86-96%	86-96%	10-27%
Minntac 7	0.33 ± 0.13	Near 0%	90-94%	74-94%
United	0.27 ± 0.08	Unknown	76-85%	42-68%
Mittal	0.14 ± 0.06	Near 0%	94-97%	27-46%

*From Berndt and Engesser (2005)

7 Acknowledgements

This study was supported by funds from the U.S. Environmental Protection Agency- Great Lakes National Program Office and from the Iron Ore Cooperative Research and Environmental Cooperative Research Programs at the Minnesota Department of Natural Resources. Thanks are extended to those who participated in this research, particularly: John Folman, Minnesota Department of Natural Resources who provided dedicated and careful assistance selecting and readying equipment for and participating in field sampling trips and Lian Liang from Cebam, Inc., who provided high quality mercury analyses during the study, and to the University of Minnesota's

Submitted December 31, 2005.

Coleraine Minerals Research Laboratory for permitting us to use their Davis Tube separator. We also thank the following mining personnel for helping to arrange our visits to their companies, assisting us in selecting sample locations, and/or for providing assistance in interpreting results: Andrea Hayden, Steve Rogers, Dana Koth and Rod Heikkila at Hibtac; Tom Moe and Ron Braski at Minntac, Brad Anderson at United Taconite, and Gus Josephson and Jim Sterle at Ispat-Inland.

8 References

Benner, B. (2001) Mercury removal from induration off gas by wet scrubbers. Coleraine Minerals Research Laboratory Technical Report #CMRL/TR-01-19. 7 pages plus table figures and appendices.

Benner, B. (2005) Mercury release from taconite during heating. CMRL report TR-05-06/NRRI/TR-2005-17, 3 pages.

Berndt, M. E. (2003) *Mercury and mining in Minnesota*. Final report, Minnesota Department of Natural Resources, 58p.

Berndt, M. E., Engesser, J., and Johnson, A. (2003) On the distribution of mercury in taconite plant scrubber systems. Minnesota DNR report prepared for MPCA. 30 p.

Berndt, M. E. and Engesser, J. (2005) Mercury Transport in Taconite Processing Facilities: (I) Release and Capture During Induration. Iron Ore Cooperative Research Final Report. Minnesota Department of Natural Resources. 31 pages plus appendices.

Berndt, M. E., Engesser, J., and Berquó, T. S. (2005) Mercury Chemistry and Mössbauer Spectroscopy of Iron Oxides During Taconite Processing on Minnesota's Iron Range. In Proceedings Air Quality V, International Conference on Mercury, Trace Elements, SO₃, and Particulate Matter. Washington, DC, Sept. 2005. 15 p.

Edwards, J. R., Srivatava, R. K., and Kilgroe, J. D. (2001) A study of gas-phase mercury speciation using detailed chemical kinetics. J. Air. Waste. Man. Assoc., 51, 869-877.

Engesser, J., and Niles, H. B. (1997) Mercury emissions from taconite pellet production. Coleraine Minerals Research Laboratory Report: University of Minnesota Contract: #1663-187-6253. Coleraine Minerals Research Laboratory Report. 16 p. plus appendices.

Galbreath, K. C. and Zygarlicke, C. J. (2000) Mercury transformation in coal combustion flue gas. Fuel Processing Tech. 65, 289-310.

Galbreath, K. C. (2005) Mercury vaporization characteristics of taconite pellets. University of North Dakota Energy and Environmental Research Center Technical Report. 16 pages plus appendix.

Galbreath, K. C., Zygarlicke, C. J., Tibbetts, J. E., Schulz, R. L., and Dunham, G. E. (2005) Effects of NO_x, α -Fe₂O₃, δ -Fe₂O₃, and HCl on mercury transformations in a 7-kW coal combustion system. Fuel Processing Technology, 86, 429-488.

Submitted December 31, 2005.

Jiang, H., Arkly, S., and Wickman,, T. (2000) Mercury emissions from taconite concentrate pellets- stack testing results from facilities in Minnesota. Presented at USEPA conference "Assessing and managing mercury from historic and current mining activities". San Francisco, November 28-30, 18 pages.

Pavlish, J. H., Sondreal, E. A., Mann, M. D., Olson, E. S., Galbreath, K. C., Laudal, D. L., and Benson, S. A. (2003), Status Review of Mercury. Control Options for Coal-fired Power Plants. Fuel Processing Technology, 82, 89-165.

Zygarlicke, et al. (2003) Experimental Investigations of Mercury Transformations in Pilot-Scale Combustion Systems and a Bench-Scale Entrained-Flow Reactor. University of North Dakota Energy and Environmental Research Center Technical Report. 22 p.

Appendix B-1-9

Email communication from Anne Jackson (MPCA) to Cliff Twaroski
(Barr). Mercury Speciation Profiles

October 11, 2006

Dane G. Jensen

From: Jackson, Anne <Anne.Jackson@state.mn.us>
Sent: Wednesday, October 11, 2006 10:02 AM
To: Cliff J. Twaroski
Cc: Swain, Edward; Mondloch, Mike
Subject: Mercury Speciation profiles
Attachments: Modified_MN_2001_Hg_Ems_EPA05.xls

Ed and I said we'd provide our speciation information. Attached is a spreadsheet prepared by Dr. Dwight Atkinson at EPA, who first prepared the source list and emissions profile. Ed and I messed with it to correct the assumptions he was making about emissions profiles. I've highlighted in yellow on the sheet titled "Major contributors" the emissions profiles we offered to Dr. Atkinson as revisions to his dataset.

The profiles come from various stack tests conducted over time. When mercury tests are done in MN, I usually try to get ahold of them to see whether a profile can be determined.

Anne M. Jackson, P.E.
Minnesota Pollution Control Agency
ph: (651) 296-7949

Emissions were Modified followed instructions provided in the Documents listed below:																
"Summary of 2001 Hg Emissions Inventory Modifications for Minnesota" (dated April 8, 2005)																
"Ed Swain's Comments dated Feb 4, 2005																
Coal Combustion (Utility)																
- Revised Mercury Speciation																
2001 CAMR Emissions										Modified 2001 Emissions						
FIPS	Unit	Plant Name	HG0_1 (tpy)	HG2_1 (tpy)	HGP_1 (tpy)	Total (tpy)	% Total HG0_1	% Total HG2_1	% Total HGP_1	HG0_1 (tpy)	HG2_1 (tpy)	HGP_1 (tpy)	Total (tpy)	% Total HG0_1	% Total HG2_1	% Total HGP_1
27141	1	SherburneCountyGeneratingPlant	0.084	0.005	0.001	0.090	93%	5%	1%	0.081	0.006	0.002	0.090	90.7%	7.1%	2.0%
27141	2	SherburneCountyGeneratingPlant	0.101	0.006	0.002	0.109	93%	5%	1%	0.098	0.008	0.002	0.109	90.7%	7.1%	2.0%
27141	3	SherburneCountyGeneratingPlant	0.088	0.004	0.001	0.092	95%	4%	1%	0.089	0.002	0.002	0.092	96.3%	2.0%	1.7%
Total			0.273	0.014	0.004	0.291	94%	5%	1%	0.269	0.016	0.006	0.291	92%	5%	2%
Note:																
Speciation profiles are modified for all units (unit numbers have been varified with EMAD output)																
27061	1	ClayBoswell	0.001	0.003	0.000	0.003	16%	83%	1%	0.001	0.003	0.000	0.003	16%	83%	1%
27061	2	ClayBoswell	0.001	0.003	0.000	0.004	16%	83%	1%	0.001	0.003	0.000	0.004	16%	83%	1%
27061	3	ClayBoswell	0.061	0.003	0.001	0.066	93%	5%	1%	0.065	0.001	0.000	0.066	98.98%	1.00%	0.02%
27061	4	ClayBoswell	0.090	0.005	0.001	0.096	93%	5%	1%	0.088	0.006	0.003	0.096	91.5%	5.9%	2.6%
Total			0.153	0.014	0.002	0.169	90%	8%	1%	0.154	0.012	0.003	0.169	91%	7%	2%
Note:																
Speciation profiles are modified for units 3 & 4 (unit numbers have been varified with EMAD output)																
27163	1	AllenS.KingGeneratingPlant	0.001	0.004	0.000	0.005	26%	68%	6%	0.005	0.000	0.000	0.005	93.9%	6.1%	0.0%
27163	4	AllenS.KingGeneratingPlant	0.032	0.014	0.000	0.046	69%	31%	0%	0.043	0.003	0.000	0.046	93.9%	6.1%	0.0%
Total			0.033	0.018	0.000	0.051	65%	35%	1%	0.048	0.003	0.000	0.051	94%	6%	0%
Note:																
Revised speciation profile was calculated based on April 13, 2005 table "Allen S. King Plant Mercury Testing"																
Incineration (Waste Disposal)																
- Revised Mercury Speciation																
2001 CAMR Emissions										Modified 2001 Emissions						
FIPS	Plant ID	Plant Name	HG0_1 (tpy)	HG2_1 (tpy)	HGP_1 (tpy)	Total (tpy)	% Total HG0_1	% Total HG2_1	% Total HGP_1	HG0_1 (tpy)	HG2_1 (tpy)	HGP_1 (tpy)	Total (tpy)	% Total HG0_1	% Total HG2_1	% Total HGP_1
27123	N0053	MCESMetropolitanWWTP-StPaul	0.039	0.101	0.035	0.175	22%	58%	20%	0.049	0.002	0.001	0.051	95.3%	3.5%	1.2%
27109	N0001	OlmsteadWTEFacility	0.025	0.066	0.023	0.114	22%	58%	20%	0.004	0.019	0.000	0.024	16.9%	81.2%	2.0%
27111	N0002	PerhamRenewableRF	0.014	0.038	0.013	0.065	22%	58%	20%	0	0	0	0			
27111	N0001	FergusFalls	0.012	0.031	0.011	0.053	22%	58%	20%	0.009	0.000	0.000	0.009	95.3%	3.5%	1.2%
27119	N0001	PolkCo.SolidWasteResourceRecovery	0.010	0.026	0.009	0.045	22%	58%	20%	0.000	0.014	0.000	0.015	0.6%	97.2%	2.2%
Total			0.100	0.262	0.090	0.452	22%	58%	20%	0.061	0.036	0.002	0.099	62%	36%	2%
Note:																
(1) Total Hg emissions were modified using the values provided in Table 2 (Feb 4, 2005)																

(2) The speciation profiles were modified for all five facilities																
Miscellaneous Industrial Processes																
- Revised Mercury Speciation																
2001 CAMR Emissions										Modified 2001 Emissions						
FIPS	Plant ID	Plant Name	HG0_1 (tpy)	HG2_1 (tpy)	HGP_1 (tpy)	Total (tpy)	% Total HG0_1	% Total HG2_1	% Total HGP_1	HG0_1 (tpy)	HG2_1 (tpy)	HGP_1 (tpy)	Total (tpy)	% Total HG0_1	% Total HG2_1	% Total HGP_1
27137	N0005	USSteelMinnOreOperations-Minntac	0.068	0.041	0.027	0.136	50%	30%	20%	0.069	0.005	0.000	0.074	93.3%	6.6%	0.1%
27137	N0061	HibbingTaconiteCo	0.074	0.009	0.009	0.092	80%	10%	10%	0.079	0.006	0.000	0.085	93.3%	6.6%	0.1%
27137	N0113	EVTACMining-Plant	0.051	0.006	0.006	0.064	80%	10%	10%	0.031	0.002	0.000	0.034	93.3%	6.6%	0.1%
27061	TAC1	NationalSteelPelletCo	0.048	0.006	0.006	0.060	80%	10%	10%	0.038	0.005	0.005	0.048	80%	10%	10%
27137	N0009	LTVSteelMining-HoytLakes	0.022	0.013	0.009	0.043	50%	30%	20%	0	0	0	0			
27037	N0011	KochPetroleumGroupLP-PineBend	0.021	0.013	0.009	0.043	50%	30%	20%	0.021	0.013	0.009	0.043	50%	30%	20%
Total			0.284	0.088	0.066	0.438	65%	20%	15%	0.239	0.030	0.013	0.283	85%	11%	5%
Note:																
(1) Total Hg emissions were modified using the values provided in Table 1 (Feb 4, 2005)																
(2) The speciation profiles were modified for US Steel, Hibbing and EVTAC																
Ferrous Metals Processing																
- Revised Mercury Speciation																
2001 CAMR Emissions																
FIPS	Plant ID	Plant Name	HG0_1 (tpy)	HG2_1 (tpy)	HGP_1 (tpy)	Total (tpy)	% Total HG0_1	% Total HG2_1	% Total HGP_1							
27123	N0055	NorthStarSteelMinnesota-StPaul	0.069	0.010	0.009	0.088	78%	11%	11%							

Appendix B-1-10

Methods Testing for Measurement of Mercury Speciation for High- Reactive Dust

April 2007

April 10, 2007

Dr. Mike Berndt
Research Scientist II
Division of Lands and Minerals
Minnesota Department of Natural Resources
500 Lafayette Road
St. Paul, MN 55155-4045

Dear Mike:

Subject: Final Report for Task 2b, "Methods Testing for Measurement of Mercury Speciation for High-Reactive Dust"; Agreement No. A85811; EERC Fund 9301

Enclosed is the final report for the testing that was done at Keewatin Taconite facility to develop a method that would accurately measure speciated mercury in highly reactive dust scenarios. The test was done at the inlet to the scrubber where previous results clearly indicated mercury conversion as a result of reactive dust collecting on a filter. The tests were conducted October 25–30, 2006.

If you have any questions or comments, I can be reached by phone at (701) 777-5138, by fax at (701) 701-5181, or by e-mail at dlaudal@undeerc.org.

Sincerely,

Dennis L. Laudal
Senior Research Advisor

DLL/hmv

Enclosure

c/enc: Anne Jackson, MPCA
Richard Schulz, EERC
Grant Dunham, EERC

METHODS TESTING FOR MEASUREMENT OF MERCURY SPECIATION FOR HIGH-REACTIVE DUST

Final Report

(for the period of March 1, 2006, through June 30, 2007)

Prepared for:

Mike Berndt

Division of Lands and Minerals
Minnesota Department of Natural Resources
500 Lafayette Road
St. Paul, MN 55155-4045

Agreement No. A85811
EERC Fund 9301

Prepared by:

Dennis L. Laudal

Energy & Environmental Research Center
University of North Dakota
15 North 23rd Street, Stop 9018
Grand Forks, ND 58202-9018

April 2007

EERC DISCLAIMER

LEGAL NOTICE. This research report was prepared by the Energy & Environmental Research Center (EERC), an agency of the University of North Dakota, as an account of work sponsored by Minnesota Department of Natural Resources. Because of the research nature of the work performed, neither the EERC nor any of its employees makes any warranty, express or implied, or assumes any legal liability or responsibility for the accuracy, completeness, or usefulness of any information, apparatus, product, or process disclosed or represents that its use would not infringe privately owned rights. Reference herein to any specific commercial product, process, or service by trade name, trademark, manufacturer, or otherwise does not necessarily constitute or imply its endorsement or recommendation by the EERC.

TABLE OF CONTENTS

LIST OF FIGURES	ii
LIST OF TABLES	ii
1.0 INTRODUCTION	1
2.0 PROJECT OBJECTIVES	2
3.0 APPROACH	2
3.1 Plant Description.....	2
3.2 Continuous Mercury Monitor (CMM) Description	2
3.2.1 PS Analytical Conversion Systems.....	2
3.2.2 PS Analytical Sir Galahad Mercury Analyzers	3
3.2.3 Inertial Separation Probe.....	4
3.3 Sampling Approach	4
4.0 RESULTS AND DISCUSSION	5
5.0 CONCLUSIONS.....	9

LIST OF FIGURES

1	Schematic of the modified PS Analytical pretreatment/conversion system	3
2	Diagram of an ISP	4
3	CMM results – October 25, 2006.....	6
4	CMM results – October 26, 2006.....	6
5	CMM results – October 27, 2006.....	7
6	CMM results – October 29, 2006.....	7
7	CMM results – October 30, 2006.....	8

LIST OF TABLES

1	FAMS Mercury Speciation Results at Keetac.....	1
2	CMM Data.....	5
3	Comparison of the Standard FAMS Data to the CMM Data	8
4	FAMS Results Using an ISP	8

METHODS TESTING FOR MEASUREMENT OF MERCURY SPECIATION FOR HIGH-REACTIVE DUSTS

1.0 INTRODUCTION

Previous work at both coal-fired power plants and taconite facilities have shown that reactive dust collected on a filter prior to a mercury measurement method can result in either adsorption of mercury or conversion of mercury across the filter. The dust that is being generated as a result of the taconite processes and being removed by the scrubber consists of a material that has a very high iron concentration. Therefore, this material has the potential to catalyze a wide range of chemical reactions including those of mercury.

Based on tests conducted at Keewatin Taconite (Keetac) by the Coleraine Minerals Research Laboratory in August of 2006 using the Flue-gas Adsorbent Mercury Speciation (FAMS) Method (shown in Table 1), it is clear that conversion of mercury is occurring since the elemental mercury (Hg^0) concentration measured at the scrubber outlet is greater than that measured at the inlet. This can be a result of two mechanisms. The first is that the filter used in front of the FAMS tube is collecting dust and the high level contact between the flue gas and the dust on the filter is resulting in oxidation of the mercury across the filter. As a result, there is a measured high bias for oxidized mercury (Hg^{2+}) or low bias for Hg^0 . In this mechanism, the actual Hg^{2+} in the flue gas is, as expected, captured by the scrubber leaving primarily Hg^0 .

The second mechanism that could explain the results shown in Table 1 is that there was substantial mercury reemission across the scrubber. In this mechanism, the scrubber inlet mercury speciation results are correct; however, a portion of the Hg^{2+} collected by the scrubber is reemitted as Hg^0 . This has been shown to be a result of SO_2/SO_3 reactions. This is unlikely as the scrubbers used in the taconite industry are not typical SO_2 scrubbers but are modified venturi particulate scrubbers. In addition, the SO_2 and, therefore, the SO_3 concentrations entering the scrubber are very low (<75 ppm).

The Minnesota Department of Natural Resources (MDNR) contracted with the Energy & Environmental Research Center (EERC) to test a method that can accurately measure speciated mercury at the inlet to the scrubber.

Table 1. FAMS Mercury Speciation Results at Keetac (8/22/06)

Hg Species	Scrubber Inlet*		Scrubber Outlet*	
	Avg, $\mu g/m^3$	St. Dev., $\mu g/m^3$	Avg, $\mu g/m^3$	St. Dev., $\mu g/m^3$
Hg (part.)	0.35	0.10	0.29	0.11
Hg^{2+}	8.77	1.53	0.61	0.22
Hg^0	1.12	0.61	4.61	1.18
Hg (total)	10.24	1.02	5.51	1.50

* Three tests were conducted.

2.0 PROJECT OBJECTIVES

It was the objective of the project to develop a method that will accurately measure speciated mercury at the inlet of the scrubbers at taconite facilities. Other objectives are as follows:

- The method should be relatively simple to use.
- Evaluate which of the two mechanisms discussed in the introduction is occurring.
- Determine if sorbent traps using an inertial separation probe (ISP) can be used to accurately speciate mercury.

3.0 APPROACH

3.1 Plant Description

The tests were conducted at the Keetac facility owned and operated by United States Steel Corporation. Keetac has 1 grate kiln furnace that has a production rate of 700 long tons per hour. A new scrubber system and coal handling system were installed this year so that the furnace could burn coal. Powder River Basin (PRB) coal is used as the induration fuel. The new scrubber is a recirculating scrubber with lime treatment so the SO₂ removal efficiency is about 70%, which is a higher removal efficiency than most other taconite wet scrubbers. It should be noted that there is a multiclone located prior to the scrubber. Also, based on experience, the dust generated from the burning PRB coal is not very reactive toward mercury.

The plant produces standard (acid) pellets but at times adds approximately 1% limestone to increase pellet strength for shipping purposes. The annual production rate of Keewatin Taconite is 5.5 million long tons of pellets.

3.2 Continuous Mercury Monitor (CMM) Description

All CMMs essentially consist of three sections. These are the probe, pretreatment/conversion system, and the analyzer. The primary equipment that was used for the test includes the following:

- Two modified PS Analytical conversion systems
- Three PS Analytical Sir Galahad mercury analyzers
- One ISP
- FAMS sampling equipment

3.2.1 PS Analytical Conversion Systems

The function of the pretreatment/conversion system is to remove any potential interference gases and to convert all the mercury present in the flue gas to Hg⁰ so that the monitor can

analyze the mercury. A modified wet chemistry PS Analytical pretreatment conversion system was used for this test to ensure accurate speciated mercury measurements were being made. The system is shown in Figure 1. In this system SnCl_2 in a sodium hydroxide solution is used to convert all the mercury to Hg^0 to provide a total mercury concentration. The second half of the system uses a KCl solution to strip out the Hg^{2+} giving the concentration of Hg^0 (the difference between the two values is the concentration of Hg^{2+}).

3.2.2 PS Analytical Sir Galahad Mercury Analyzers

The PS Analytical (PSA) is based on the principle of atomic fluorescence which provides an inherently more sensitive signal than atomic absorption. The system uses a gold-impregnated silica support for preconcentrating the mercury and separating it from potential interferences that degrade sensitivity.

The Sir Galahad requires a 4-step process to obtain a flue gas mercury measurement. In the first step, 2 L of flue gas is pumped through a gold trap which is maintained at a constant temperature. Before the mercury is desorbed from the gold trap, a flushing step is initiated to remove any flue gas that may be present, because it has a damping effect on the mercury fluorescence. When this is completed, the analysis step begins. The heating coil is activated, and the gold trap is heated to approximately 500°C . This desorbs the mercury from the trap, and the mercury is carried into the fluorescence detector. The gold trap is cooled rapidly by pumping argon over it, in preparation for the next sample. The total time for the entire process is about 5 minutes.

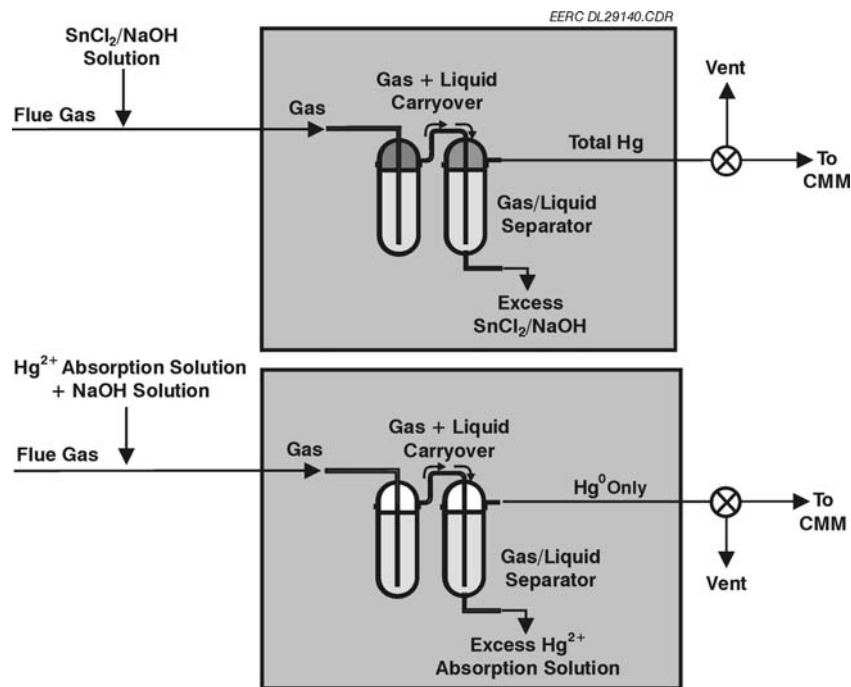


Figure 1. Schematic of the modified PS Analytical pretreatment/conversion system.

The system is calibrated using vapor-phase Hg^0 injections as the primary standard. The Hg^0 is contained in a closed vial which is held in a thermostatic bath. The temperature of the mercury is monitored, and the amount of mercury is measured using vapor pressure calculations. Typically, the calibration of the unit has proven stable over a 24-hour period.

3.2.3 Inertial Separation Probe

The function of the ISP is to remove particulate matter from the gas stream with minimum interaction between the dust and the mercury. This is done by using a sintered metal filter and a very high velocity gas flow that continuously scours the filter. A small portion of the gas that is to be analyzed by the instrument is drawn through the filter with the remainder of the gas being put back into the duct. A diagram of an ISP is shown in Figure 2.

3.3 Sampling Approach

The EERC tested four mercury measurement methods at the inlet to scrubber. The first method was to use two CMMs with a PS Analytical conversion system. To ensure that accurate speciation measurements were being made, several modifications to the system were made for this test. First, the two sides of the conversion system were separated and two analyzers used. This resulted in continuous measurement of total mercury and Hg^0 rather than switching back and forth. Second, the solutions were injected at the probe tip, and no filter was used. Although this method would not be practical as a permanent measurement technique, it does ensure there is little if any biases as a result of the highly reactive dust.

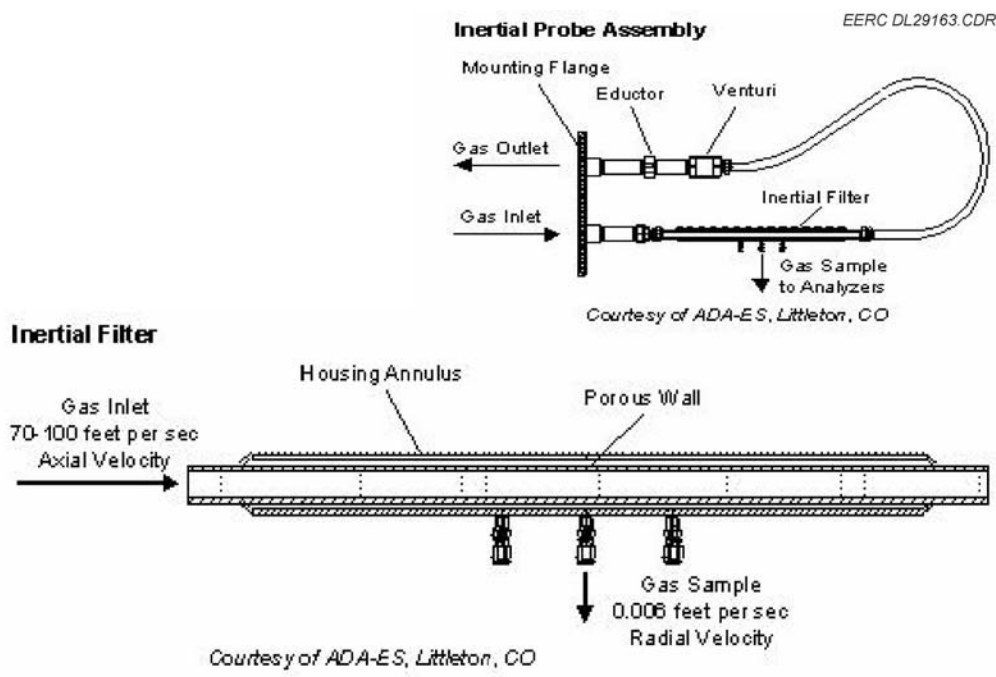


Figure 2. Diagram of an ISP.

The second method was to use an ISP with a CMM. This is the method typically used for coal-fired systems. Although the contact between the dust and the mercury across the filter is minimized, the method is not perfect, and there was concern that the highly reactive nature of the dust of the taconite facility would still impact the mercury speciation. By comparing this result to those obtained using the modified pretreatment/conversion system, the effectiveness of the ISP could be determined.

The third method was to again use the ISP, but rather than using the CMM, tests were conducted using the FAMS sorbent traps. These traps are being evaluated by MDNR for measuring mercury speciation at the various taconite facilities. Although in general the total mercury results have been reasonable, there have been questions as to the data validity. This has been especially true for mercury speciation data. The last method was to do the standard FAMS sampling.

4.0 RESULTS AND DISCUSSION

Table 2 and Figures 3–7 show the results comparing data collected from the two CMMS using the modified PSA conversion systems without a filter and the data collected using a CMM with an ISP. The results show that there is good agreement between the two methods for total mercury, but there was conversion of Hg^0 to Hg^{2+} across the sintered metal filter of the ISP. There also appeared to be more variability in the data when the ISP was used.

As stated previously, tests were conducted using the FAMS method in the standard mode and using an ISP. The results are shown in Table 3. The FAMS results were somewhat lower for total mercury compared to the CMMs. However, the percentage of Hg^0 was about the same comparing the standard FAMS results to those obtained using a CMM with an ISP. In both cases, there appeared to be a high bias for Hg^{2+} compared to the data collected for the CMM that was operated without any filter. The FAMS method did not work at all when used with an ISP. This may have been a result of the flow rates not matching properly or possible contamination in the ISP. The results are shown in Table 4.

Table 2. CMM Data

Date	CMMs without filter					CMM with ISP				
	Total Hg, $\mu\text{g}/\text{m}^3$	St. Dev., $\mu\text{g}/\text{m}^3$	Hg^0 , $\mu\text{g}/\text{m}^3$	St. Dev., $\mu\text{g}/\text{m}^3$	Hg^0 , %	Total Hg, $\mu\text{g}/\text{m}^3$	St. Dev., $\mu\text{g}/\text{m}^3$	Hg^0 , $\mu\text{g}/\text{m}^3$	St. Dev., $\mu\text{g}/\text{m}^3$	Hg^0 , %
10/25/2006	9.65	0.85	6.91	0.38	71.6	9.83	0.15	–	–	–
10/26/2006	8.54	1.18	5.97	0.6	69.9	7.04	0.88	6.05	2.69	85.9
10/27/2006	7.29	0.53	6.22	0.16	85.3	9.55	1.61	5.53	1.45	57.9
10/29/2006	6.36	0.44	5.61	0.21	88.2	6.48	0.85	4.31	0.28	66.5
10/30/2006	6.26	0.83	5.45	0.43	82.1	6.84	1.38	4.35	0.40	67.1

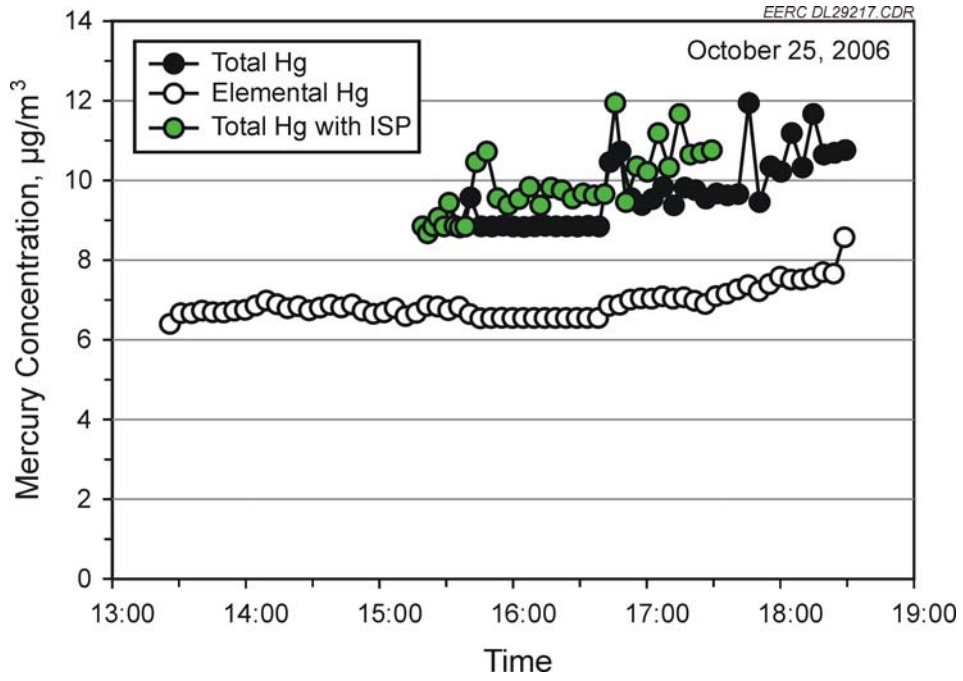


Figure 3. CMM results – October 25, 2006.

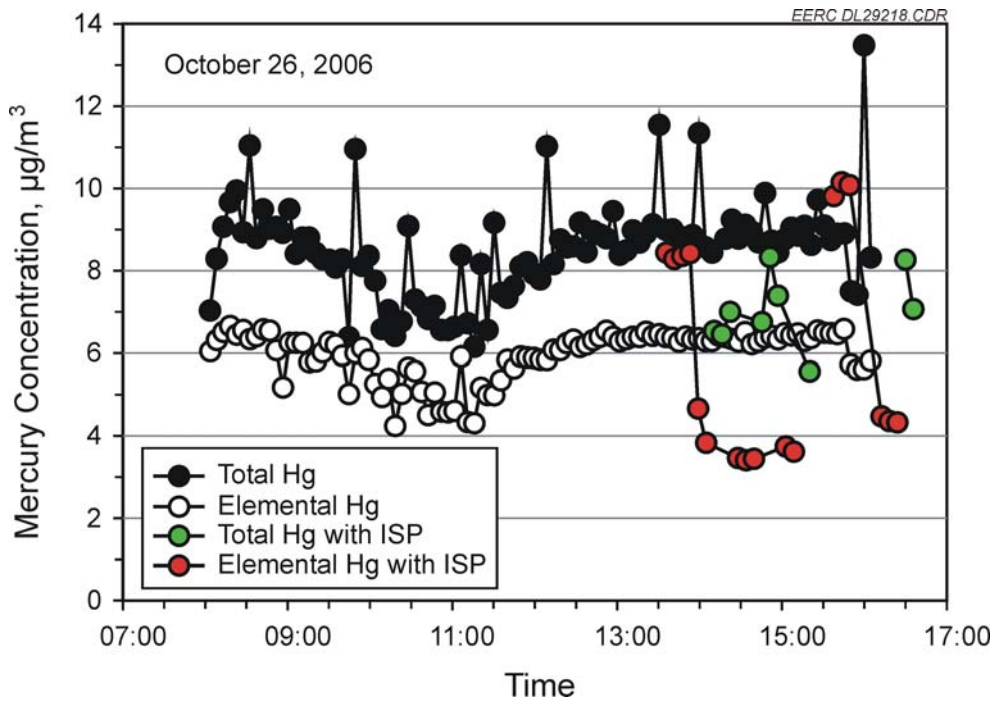


Figure 4. CMM results – October 26, 2006.

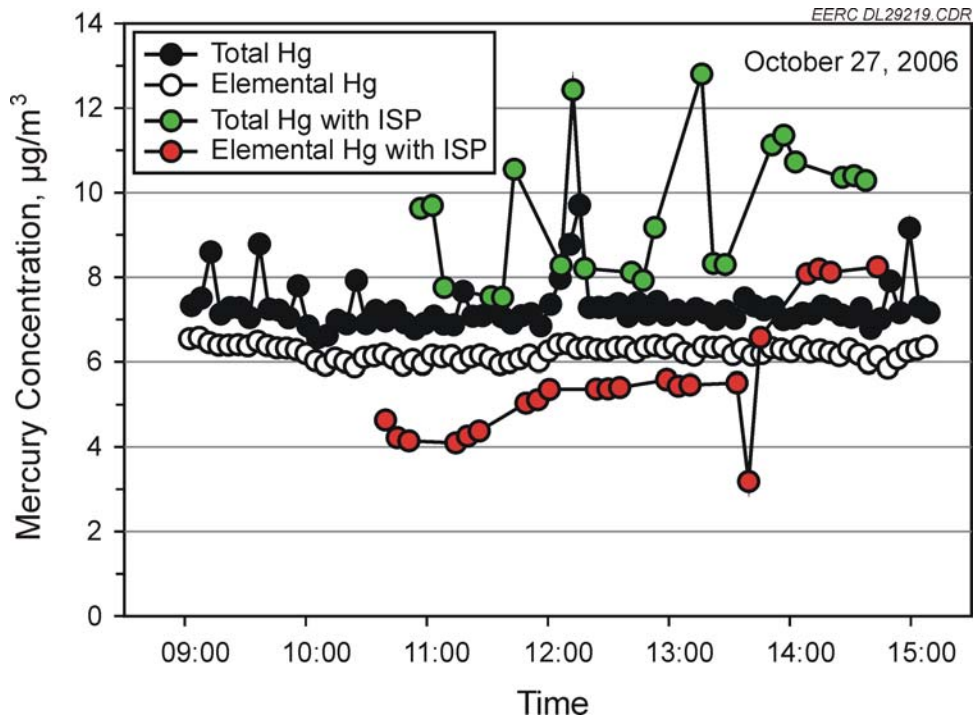


Figure 5. CMM results – October 27, 2006.

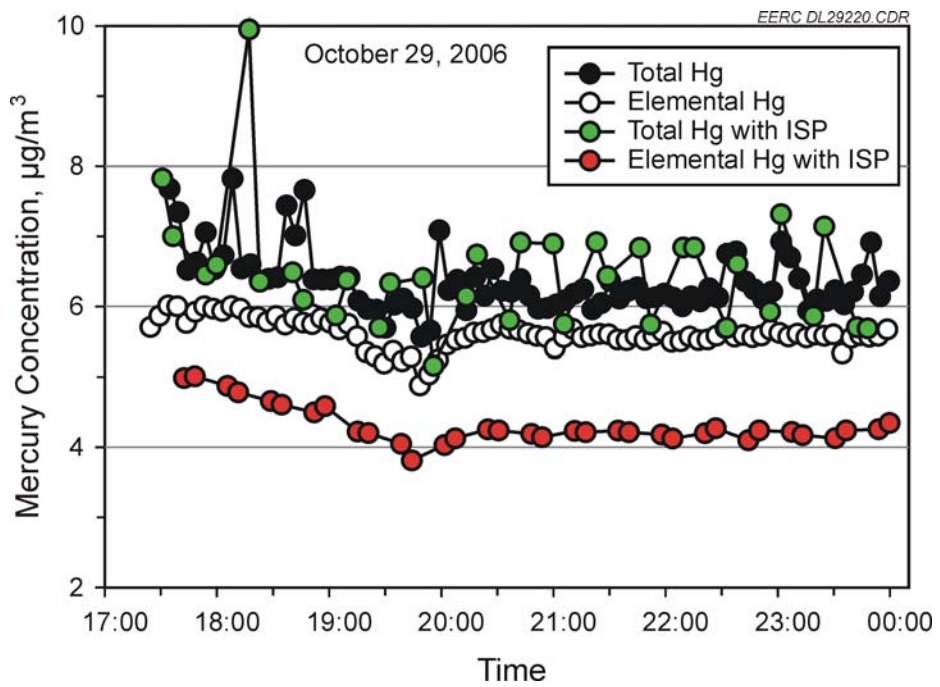


Figure 6. CMM results – October 29, 2006.

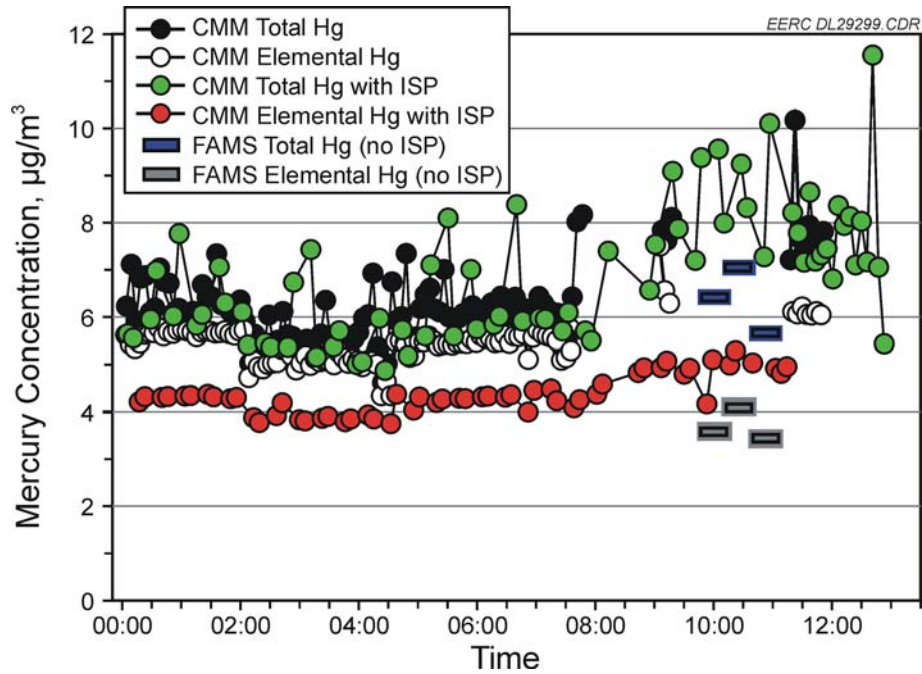


Figure 7. CMM results – October 30, 2006.

Table 3. Comparison of the Standard FAMS Data to the CMM Data

Time Start	FAMS Without ISP			CMMs With ISP			CMMs Without ISP*		
	Total Hg, $\mu\text{g}/\text{m}^3$	Hg^0 , $\mu\text{g}/\text{m}^3$	Hg^0 , %	Total Hg, $\mu\text{g}/\text{m}^3$	Hg^0 , $\mu\text{g}/\text{m}^3$	Hg^0 , %	Total Hg, $\mu\text{g}/\text{m}^3$	Hg^0 , $\mu\text{g}/\text{m}^3$	Hg^0 , %
9:48	6.42	3.59	55.9	8.98	4.75	53.4	8.11	6.29	77.6
10:13	7.04	4.11	58.4	8.52	5.10	60.7			
10:40	5.66	3.43	60.7	8.56	4.99	54.7	7.21	6.11	84.8
Average	6.37	3.71	58.3	8.69	4.94	56.2	7.66	6.20	81.2
St. Dev.	0.69	0.36		0.92	0.33				

* Instrument was not operating in this mode when FAMS samples were taken. Results shown are those just prior to the first FAMS sample and just after the last one.

Table 4. FAMS Results Using an ISP

Time Start	Total Hg, $\mu\text{g}/\text{m}^3$	Hg^0 , $\mu\text{g}/\text{m}^3$	Hg^0 , %
09:48	3.96	2.81	71.0
10:13	21.37	5.53	25.9
10:40	21.30	8.17	38.4
Average	15.54	5.50	45.1
St. Dev.	10.03	2.68	

5.0 CONCLUSIONS

Based on the results of the testing conducted under Task 2b, the following conclusions can be made:

- At Keetac, the use of a filtering device (ISP or filter) prior to the measurement device (CMM or FAMS) resulted in a high bias for Hg^{2+} at the inlet to the particulate scrubber. This was because of oxidation of some of the Hg^0 to Hg^{2+} across the filtering device.
- Compared to the previous testing (August 22, 2006) at Keetac, the results at the scrubber inlet clearly show oxidation of the mercury across the filter. When the CMM without a filter is used to measure the scrubber inlet mercury speciation concentrations, the scrubber outlet data in Table 1 makes more sense.
- Unbiased mercury results could be obtained using a PSA wet chemistry pretreatment/conversion system by completely separating the two sides of the system and injecting the oxidation and stripping solutions at the probe and not using a filter. Although for this test two monitors were used, the same type of data could be obtained by using one monitor and switching between the two sides of the pretreatment/conversion system.
- Compared to CMMs operated without a filter, the ISP resulted in a high bias for Hg^{2+} .
- Compared to the CMMs, FAMS total mercury results were somewhat low.
- Using the FAMS with an ISP did not give good results; however, tests were limited, and it is possible that good total mercury results could be obtained.

Appendix B-1-11

Mercury Control Technologies for the Taconite Industry

June 2007

June 7, 2007

Dr. Michael E. Berndt
Research Scientist III
Minnesota Department of Natural Resources
Division of Lands and Minerals
500 Lafayette Road, Box 45
St. Paul, MN 55155-4045

Dear Dr. Berndt:

Subject: Technical Report Entitled "Mercury Control Technologies for the Taconite Industry"; Agreement No. A85811; EERC Fund 9301

Please find enclosed the subject report. I have incorporated your comments into the final report for the project. Please distribute to the plants for their comments. I will be glad to incorporate any changes they feel are necessary. Please let me know as soon as possible if any changes are needed.

If you have any questions or comments, please contact me by phone at (701) 777-5138, by fax at (701) 777-5181, or by e-mail at dlaudal@undeerc.org.

Sincerely,

Dennis L. Laudal
Senior Research Advisor

DLL/kal

Enclosure

MERCURY CONTROL TECHNOLOGIES FOR THE TACONITE INDUSTRY

Technical Report

Prepared for:

Michael E. Berndt

Minnesota Department of Natural Resources
Division of Lands and Minerals
500 Lafayette Road, Box 45
St. Paul, MN 55155-4045

Agreement No. A85811

Prepared by:

Dennis L. Laudal
Grant E. Dunham

Energy & Environmental Research Center
University of North Dakota
15 North 23rd Street, Stop 9018
Grand Forks, ND 58202-9018

June 2007

EERC DISCLAIMER

LEGAL NOTICE. This research report was prepared by the Energy & Environmental Research Center (EERC), an agency of the University of North Dakota, as an account of work sponsored by the Minnesota Department of Natural Resources. Because of the research nature of the work performed, neither the EERC nor any of its employees makes any warranty, express or implied, or assumes any legal liability or responsibility for the accuracy, completeness, or usefulness of any information, apparatus, product, or process disclosed or represents that its use would not infringe privately owned rights. Reference herein to any specific commercial product, process, or service by trade name, trademark, manufacturer, or otherwise does not necessarily constitute or imply its endorsement or recommendation by the EERC.

TABLE OF CONTENTS

LIST OF FIGURES	ii
LIST OF TABLES	iii
1.0 INTRODUCTION.....	1
1.1 Project Objectives.....	2
1.2 Taconite Industry Background	2
2.0 MERCURY CONTROL TECHNOLOGIES BEING CONSIDERED FOR COAL-FIRED UTILITIES	5
2.1 Precombustion Technologies.....	5
2.2 Sorbent Technologies	6
2.3 Mercury Oxidation Technologies.....	14
3.0 POTENTIAL MERCURY CONTROL TECHNOLOGIES FOR THE TACONITE INDUSTRY	18
3.1 Precombustion Technologies.....	18
3.2 Sorbent Technologies	19
3.3 Oxidation Technologies.....	20
4.0 ECONOMICS OF MERCURY CONTROL FOR TACONITE PLANTS.....	24
5.0 RECOMMENDATIONS	26
6.0 REFERENCES.....	27

LIST OF FIGURES

1	Mechanistic model for mercury capture by activated carbon	8
2	Mercury removal (%) vs. sorbent injection rate (lb/Macf) for tests at three sites.....	9
3	Mercury removal as a function of sorbent injection rate at a plant burning a PRB coal with an ESP	10
4	Mercury removal as a function of sorbent injection rate at a plant burning lignite with a FF.....	10
5	Mercury removal as a function of sorbent/additive injection rate at a plant burning a PRB coal with an ESP	11
6	Mercury removal at a plant with high (>30 ppm) SO ₃	12
7	Impact of SO ₃ concentration on mercury removal.....	13
8	Proposed mechanism for Hg ²⁺ reduction to Hg ⁰ in a wet scrubber.....	14
9	Bench-scale tests using EPA's proprietary oxidant	17
10	Schematic of mercury testing at a straight-grate plant using NaCl.....	21
11	Schematic of testing at a grate kiln plant using NaCl	22
12	Schematic of testing for mercury at a straight-grate plant using bromine and chloride salts.....	23
13	Relative cost for mercury control technologies.....	26

LIST OF TABLES

1	Summary of the Minnesota Taconite Plants	4
2	Mercury Concentrations at Power Plant Firing a High-Sulfur Eastern Bituminous Coal ..	15
3	Fate of Scrubber Materials	23
4	Distribution of Mercury in Scrubber Slurry	24
5	Summary of Costs Associated with ACI for Mercury Control at a Taconite Plant	25

MERCURY CONTROL TECHNOLOGIES FOR THE TACONITE INDUSTRY

1.0 INTRODUCTION

Mercury is a naturally occurring element that is ubiquitous in the Earth's crust. However, both anthropogenic activities such as combustion and mining processes and natural sources such as volcanoes release mercury into the atmosphere. Through transport and deposition, some mercury enters the aquatic systems, resulting in an increase in mercury loading in fish. Over the past 15 years, there has been a concerted effort by national and state agencies to reduce mercury emissions from all sources. In 2005, the U.S. Environmental Protection Agency (EPA) issued the Clean Air Mercury Rule (CAMR) that for first time regulated mercury emissions from coal-fired power plants. In addition, a number of states, including Minnesota, are issuing mercury rules that would be more restrictive than those promulgated by EPA. As it became clear that EPA would eventually regulate mercury, the utility industry, the Electric Power Research Institute (EPRI), and the U.S. Department of Energy (DOE) began funding programs to develop and test potential mercury control technologies for coal-fired boilers.

Although utilities are the largest source of anthropogenic mercury, they are not the only source. States are also reviewing the potential of reducing mercury from these other sources as well. In Minnesota, one of these sources is the taconite industry. It has been estimated that these plants emit 250–350 kg of mercury per year into the atmosphere (1). In 2003, EPA stated “Since specific controls for mercury are not currently present in the industry and operating practices that effectively reduce mercury emission have not been identified, we are selecting no emission reduction as new source MACT” (2). This ruling was controversial, and there is continued pressure on the Minnesota Pollution Control Agency (MPCA) to potentially regulate mercury emissions from taconite plants.

As a result, the Minnesota Department of Natural Resources (MDNR) has been working with MPCA staff, taconite industry personnel, and several research laboratories, including the Energy & Environmental Research Center (EERC), to evaluate the sources, concentrations, chemistry, and potential control strategies for mercury from these facilities. This document is a direct result of these collaborations. In addition to visiting and touring each of the facilities discussed in this document, the EERC participated in frequent mercury research discussions between MDNR research staff and mining personnel. Moreover, the EERC was given full access to data as they were being generated by all of the groups involved in the MDNR research program. Beginning in July 2006, the EERC became an active participant in these studies by providing continuous mercury monitors (CMMs) to measure mercury in the stack gases during four plant-scale tests conducted at taconite-processing facilities. In this report, the EERC draws on its long history of mercury research at coal-fired utilities and its more recent experiences with the taconite industry to provide insights on the feasibility of transferring mercury control technologies between the two industries. The MDNR plant-scale tests for taconite facilities are also discussed briefly, but the results of those tests will be presented in more detail in a forthcoming MDNR report.

1.1 Project Objectives

The overall goal of the project is to provide MDNR and the taconite industry with the information necessary to both assess the current state of mercury control technologies and define the mercury control strategies that are most applicable to the taconite industry. Specific objectives of the effort are to:

- Identify and describe mercury control technologies that are currently being considered for coal-fired electric generator plants.
- Collect and compile the relevant data from each of the taconite plants to aid in determining mercury control options.
- Assess to what degree each of the identified technologies may be applicable to the taconite industry.
- Assess potential balance-of-plant impacts that may occur as a result of installing a mercury control technology.
- Complete a preliminary economic evaluation for potential mercury control technologies that could reasonably be implemented.
- Determine the nature of any waste products that may be formed as a result of each potential control technology and the short- and long-term impacts of these waste products on the environment.
- Provide recommendations as to testing that may be necessary before permanent implementation of mercury control technology can take place. This may include laboratory testing and/or full-scale demonstrations.

1.2 Taconite Industry Background

Six taconite facilities are located in Minnesota, as listed below:

- United States Steel (USS) Keewatin Taconite (Keetac) – located near Keewatin, Minnesota
- Hibbing Taconite Company (Hibtac)– located near Hibbing, Minnesota
- USS Minntac (Minntac) – located near Mountain Iron, Minnesota
- Mittal Steel Minorca Mine – located near Virginia, Minnesota
- United Taconite (U-Tac) – located near Eveleth, Minnesota
- Northshore Mining – located near Silver Bay, Minnesota

Taconite processing has two potential sources of mercury: mercury released from processing the ore and mercury released from the fuels used when the ore is processed. Unlike coal-fired utilities, the major source of mercury is not the combustion fuel but the processing of the ore into taconite pellets. Even for those facilities that fire coal, it only takes 20–30 lb of coal

to process 1 long ton (Lt) of green balls. The concentration of mercury in the unprocessed ore is related to the ore's geographical location in the Biwabik Iron Formation. The mercury concentration in the ore at the west end of the district is about 20 ppb and gradually increases eastward to a maximum of 32 ppb then decreases gradually to less than 1 ppb in the ore at Northshore (3). Although some of the information presented in this report may be relevant to Northshore Mining, this facility was not considered part of this study as the mercury concentration is very low.

Another difference between the two industries that could potentially impact the choice of mercury control technology is that all taconite facilities, with the exception of Northshore which has wet electrostatic precipitators (ESPs), utilize a wet venturi-type scrubber to control particulate matter emissions. This is compared to utilities, which most commonly have ESPs or fabric filters (FFs).

In addition to economic issues, a major constraint is that most taconite plants have severe space limitations that may preclude installing large sorbent injection systems, FFs, etc. At some sites, it may be possible to build these components outside of the existing plant. However, even installing the necessary ducting could be a problem for others.

Finally, taconite plants are much more market-driven than power plants. Depending on the worldwide supply and demand for steel, these plants are more susceptible to boom/bust cycles. Therefore, any mercury control technology selected must have a reasonable cost. If onerous mercury controls were required, economics may dictate closing the plant.

Although each plant is unique in its configuration and operation, there are several general factors that will determine the effectiveness of various mercury control strategies. These include the following:

- Type of induration – straight grate or grate kiln
- Mercury concentration and species generated in the process
- Recycle in the scrubber (both water recycle and recycling the collected dust material back to the processing facility)
- Type of pellets being manufactured – flux or acid pellets (flux pellets have limestone added to the pellets)
- Temperature in various zones of the process
- Fuel

Table 1 provides a summary for each of the plants.

Table 1. Summary of the Minnesota Taconite Plants (1)

Plant (line)	Line Type	Production, Lt/hr	Pellets	Fuel	Airflow Rate, kscfm
Minntac ¹					
3	Grate kiln	200–250	Acid	Natural gas	180–250
4	Grate kiln	400–450	Flux/acid	60% wood–40% natural gas	370–450
5	Grate kiln	400–450	Flux/acid	60% wood–40% natural gas	370–450
6	Grate kiln	400–450	Flux	PRB ² coal	370–450
7	Grate kiln	400–450	Flux	PRB coal	370–450
Hibtac					
1	Straight grate	300–350	Acid	Natural gas	350–400
2	Straight grate	300–350	Acid	Natural gas	350–400
3	Straight grate	300–350	Acid	Natural gas	350–400
United Taconite ³					
1	Grate kiln	200–250	Acid	Natural gas	180–250
2	Grate kiln	400–450	Acid	50%–50% petcoke–eastern bit.	450–600 ⁴
Mittal Steel	Straight grate	350	Flux	Natural gas	350
Keetac ⁵	Grate kiln	700	Acid	PRB coal	550–650

¹ Lines 1 and 2 are not operational.

² Powder River Basin.

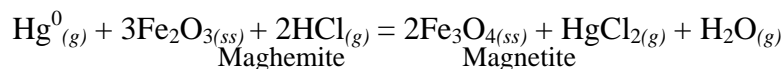
³ Plant uses an organic binder to produce acid pellets.

⁴ The plant has two waste gas fans.

⁵ Scrubber adds lime to enhance SO₂ removal.

As stated earlier, all of the above plants have rod-type venturi scrubbers. The primary purpose of the scrubbers is to remove particulate matter. However, as is shown in Table 1, the new scrubber installed at Keetac was designed to reduce SO₂ by about 70% by adding lime to the slurry. Mittal, Hibtac, and Keetac also have multiclones to aid in reducing particulate matter.

During taconite processing, wet “green balls” consisting predominantly of magnetite and, possibly, other components (limestone flux, organic or bentonite binder, trace nonore components) are conveyed into a furnace and heated to approximately 1200°–1300°C in the presence of air. Data have suggested that magnetite is first converted to a magnetite/maghemite solid solution which attracts and collects mercury released from green balls deeper in the furnace (4). Mercury release occurs when magnetite and/or magnetite/maghemite solid solutions are heated past 450° or 500°C and converted to hematite. Wet scrubbers collect oxidized mercury (Hg²⁺) from flue gases, but not volatile Hg⁰(g). Wet scrubbers sometimes capture over 40% of the mercury released during induration, implying that extensive generation and transport of Hg²⁺ can occur. On the other hand, scrubber efficiency can also be less than 10% for mercury, indicating that conditions needed for mercury oxidation are not always present. Plants having the highest capture rates for mercury also appear to have the highest Cl and particulate fluxes, suggesting a relationship such as the following controls mercury oxidation rates during induration:



2.0 MERCURY CONTROL TECHNOLOGIES BEING CONSIDERED FOR COAL-FIRED UTILITIES

Because of the likelihood of mercury regulations and subsequent promulgation of CAMR, the coal-fired electric utility industry has been the catalyst for most mercury control research. This section will define the technologies that are currently being considered for coal-fired boilers irrespective of their transferability to the taconite industry. Section 3.0 will discuss those technologies that would be applicable to the taconite industry. All mercury control technologies/strategies can then be grouped, based on maturity, into the following three main categories:

- *Commercially available technologies.* These technologies have been tested at the bench-, pilot-, and full-scale level and will be, or could potentially be, commercially available by 2009.
- *Commercially emerging technologies.* These technologies have been tested at the bench- and pilot-scale level and are currently being, or will be, demonstrated at the full-scale level during the next 1–3 years. Some of these technologies may be available by 2009, depending on test schedules and degree of technical and economic success.
- *Developing technologies.* These technologies are defined as those that have had only limited testing at the bench-scale or pilot-scale level but appear to have the potential for removing significant (>50% to 90%) mercury. It is not expected that sufficient demonstration of these technologies would be completed by 2009; therefore, they would not be commercially available until after 2010.

For utilities, mercury control can be accomplished in three fundamental ways:

- *Precombustion technologies.* This can be as simple as changing to a lower-mercury fuel or utilizing complex coal-cleaning techniques.
- *Sorbent technologies.* This strategy uses materials that will adsorb the mercury. The compounds can be injected into the flue gas (i.e., powdered activated carbon injection [ACI]) and then removed by a particulate collection device or utilized as part of a fixed-bed reactor.
- *Oxidation technologies.* These technologies take advantage of the fact that chemically reacted Hg^{2+} is water-soluble and readily removed by a wet scrubber. Therefore, by converting elemental mercury (Hg^0) to Hg^{2+} , the wet scrubber will provide increased mercury removal.

2.1 Precombustion Technologies

Obviously, one method of reducing mercury from coal-fired power plants is to change to a fuel with lower or no mercury, such as natural gas or renewables. In general, in today's market, this is a very limited option or one economically unattractive for existing plants.

Coal cleaning for mercury control could be a very attractive option as it would have limited balance-of-plant impacts. Modifications would not be required for either the combustion process or emission control equipment. However, to date, no economically feasible process for consistently removing >50% of the mercury from all types of coals has been developed and commercialized. Generally, conventional coal cleaning has been limited to bituminous coals, and the process only removes, on average, about 30% of the mercury (5). Technologies have been tested on a limited basis that have the potential to remove >50% of the mercury; however, these technologies are clearly in the developmental stage and include the following:

- Magnetic separation
- Advanced froth flotation
- Selective agglomeration
- Chemical methods
- Biological methods

One precombustion technology that does show promise at the pilot-scale level and will be tested at the full-scale level in 2008 is the Western Research Institute's (WRI's) thermal treatment of coal (6). In this process, the fuel goes through two heating stages. In the first stage, the moisture in the fuel is driven off; in the second stage, coal is heated by nearly inert gas, resulting in significant removal of coal-bound mercury. The inert gas flow is an order of magnitude lower than the combustor flue gas and, hence, the stripping of mercury in the effluent streams becomes easier. The product coal is cooled and then directly fed into the boiler plant pulverizer. Preliminary tests have shown mercury removal of 60%–80%. It is expected that there will be significant reductions in NO_x as a cobenefit of the technology.

2.2 Sorbent Technologies

The most commercially advanced mercury-specific technologies are those using mercury sorbents, specifically ACI. The most important factor influencing the effectiveness of ACI to control mercury emissions resulting from coal combustion is the oxidation state of the mercury in the flue gas. Therefore, the effectiveness of ACI is related to the constituents in the flue gas, in particular, halogens, SO₃, temperature, and residence time. Based on the bench-scale work that has been completed, the following was concluded (7):

- Increasing temperature results in decreased equilibrium adsorption capacity.
- Physical adsorption is not the dominant mechanism, and based on the EERC model, chemisorption of Hg²⁺ to a basic site on the carbon is believed to be the binding site.
- Sorbent particle size determines the minimum sorbent mass requirement necessary to effect mass transfer from the bulk gas to sorbent particles.
- Any water vapor in flue gas decreases the equilibrium sorption capacity because of interactions with NO_x and SO_x species. Water vapor is always present, and there do not appear to be any concentration effects.

- Cl increases the reactivity of activated carbon for mercury.
- SO₂ in the absence of NO_x reduces the equilibrium adsorption capacity dramatically for Hg⁰ and mercuric chloride. The effect of a combination of SO₂ and NO₂ reduces the capture of Hg⁰ even more severely.
- NO_x (10% NO₂ and 90% NO) has an impact on Hg⁰ capacity in the presence of SO₂ and HCl. The equilibrium sorption capacity of Hg⁰ is minimal in the absence of both NO_x and HCl, and it increases as NO_x alone increases. In the presence of HCl, the capacity for Hg⁰ drops as NO_x increases. Bench-scale tests suggest that HCl and NO_x/NO₂ can promote the oxidation and capture of Hg⁰, and little chemisorption capture appears to occur in the absence of mercury oxidation.
- The equilibrium sorption capacity for Hg⁰ increases with increasing levels of oxidation occurring across the carbon test bed, as determined by changing the concentrations of HCl and SO₂. This indicates that mercury oxidation is an essential step in capturing mercury on sorbents.

From the bench- and pilot-scale work completed, a heterogeneous model has been constructed to explain the activated carbon–Hg behavior in coal-fired flue gas shown in Figure 1 (8). Although mercury reactions are complex, essentially Hg⁰ must first be catalytically oxidized by chloride ions and/or NO₂ on the basic carbon sites, thus resulting in mercury capture. Capture continues until the binding sites are used up and breakthrough occurs. However, in the presence of both SO₂ and NO₂, compounds are formed which effectively blind the active sites, preventing long-term mercury capture. Although the mercury is no longer captured, the mercury that breaks through the carbon bed is no longer Hg⁰ but Hg²⁺.

In 1999, DOE issued a request for proposal (RFP) to test mercury control technologies at the full scale. The near-term goal of the RFP was to evaluate technologies that could achieve 50%–70% mercury removal at a cost of less than three-quarters of the estimated cost of \$50,000–\$70,000/lb mercury removed. The longer-term goal was to develop technologies that could provide up to 90% control at a cost of half to three-quarters of ACI technology by the year 2010. Two projects were selected under this RFP:

- Scrubber enhancement – McDermott/Babcock & Wilcox (B&W)
- Activated carbon injection – ADA-ES

The projects were short-term (1–2 weeks) tests that were completed at several different plants. The McDermott/B&W project was to test several additives in attempt to prevent mercury reemission. This project is discussed in Section 2.3. The ADA-ES project was designed to test ACI at plants burning different coals and having different air pollution control equipment. The results of these tests are shown in Figure 2 (9). As was expected, the use of a FF with ACI at the Gaston Plant provided the best mercury removal at the lowest ACI rate. For the same type of coal (low-sulfur bituminous), much higher levels of activated carbon were needed

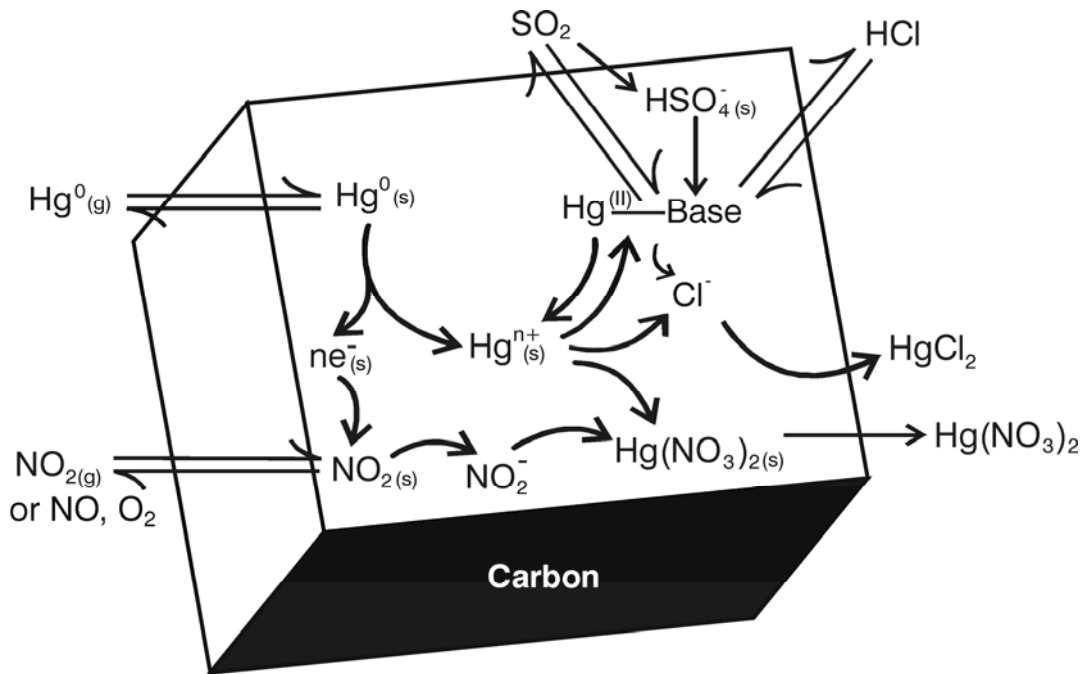


Figure 1. Mechanistic model for mercury capture by activated carbon (8).

to achieve the same level of control when only an ESP was present. For the PRB subbituminous coal with an ESP (Pleasant Prairie), the maximum mercury removal was 66%, regardless of the ACI rate. This clearly demonstrates the effect of fuel type and particulate control device on the effectiveness of ACI for mercury control.

Based on the Phase I results, it appeared that mercury control was going to be more problematic for western lower-rank fuels, lignites, and PRB subbituminous coals. In general, lignites and PRB coals contain significantly lower levels of chlorine and have a much higher concentration of alkali components compared to bituminous coals. As a result, most of the mercury generated is in the form of Hg^0 , which is more difficult to remove. A major focus of DOE Phase II projects was to improve mercury control for these low-rank fuels. Under the Phase II program, the following projects were selected:

- Evaluation of Sorbent Injection for Mercury Control – ADA-ES
- Amended Silicates for Mercury Control – Amended Silicates
- Sorbent Injection for Small ESP Mercury Control – URS Group
- Pilot Testing of Mercury Oxidation Catalysts for Upstream of Wet FGD Systems – URS Group
- Evaluation of MerCAP for Power Plant Mercury Control – URS Group

- Enhancing Carbon Reactivity in Mercury Control in Lignite-Fired Systems – EERC
- Mercury Oxidation Upstream of an ESP and Wet FGD – EERC
- Advanced Utility Mercury-Sorbent Field-Testing Program – Sorbent Technologies

Of these projects, five are attempts to improve mercury capture using various sorbents at plants burning low-rank fuels, including using treated carbons and various additives to improve mercury control. The results of these demonstration programs (Figures 3 and 4) showed that the most effective control methods were to use brominated activated carbon (B-pac from Sorbent Technologies or DARCO Hg-LH from NORIT Americas) or halogenated additives with ACI (9). Although a higher level of mercury control can be achieved at lower ACI rates when a FF is present (Figure 3), a high level of control at reasonable rates can also be achieved with only an ESP when brominated carbons are used (Figure 2).

Rather than using treated carbons, the same improved mercury control was also achieved by using chemical additives with ACI. This provides for more flexibility in that the injection rates of one or both can be controlled. Parametric results for a plant burning a PRB coal with only an ESP are shown in Figure 5 (10). The results shown are similar to those obtained using the treated carbon (Figure 2).

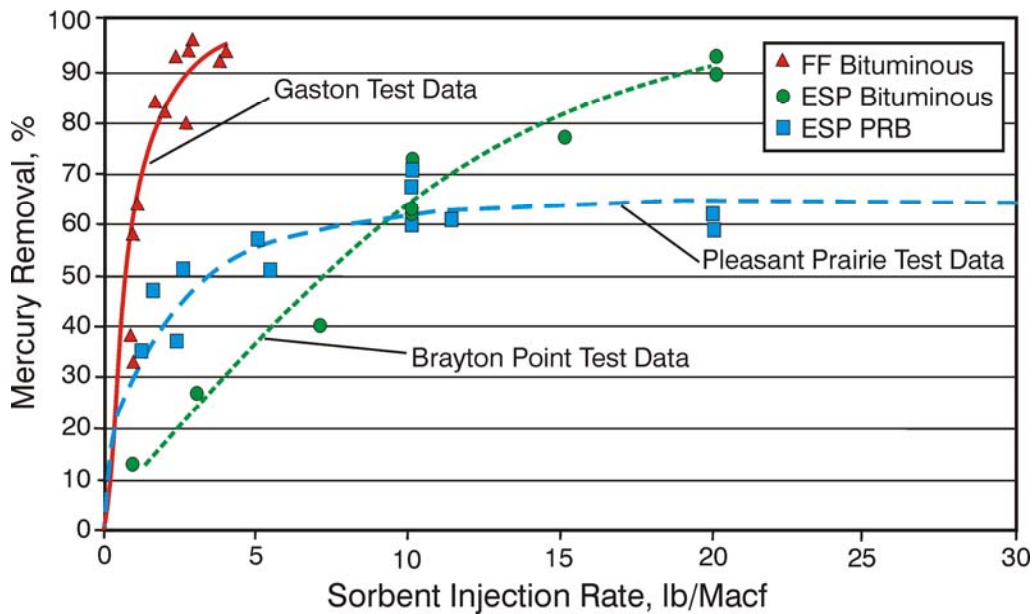


Figure 2. Mercury removal (%) vs. sorbent injection rate (lb/Macf) for tests at three sites (9).

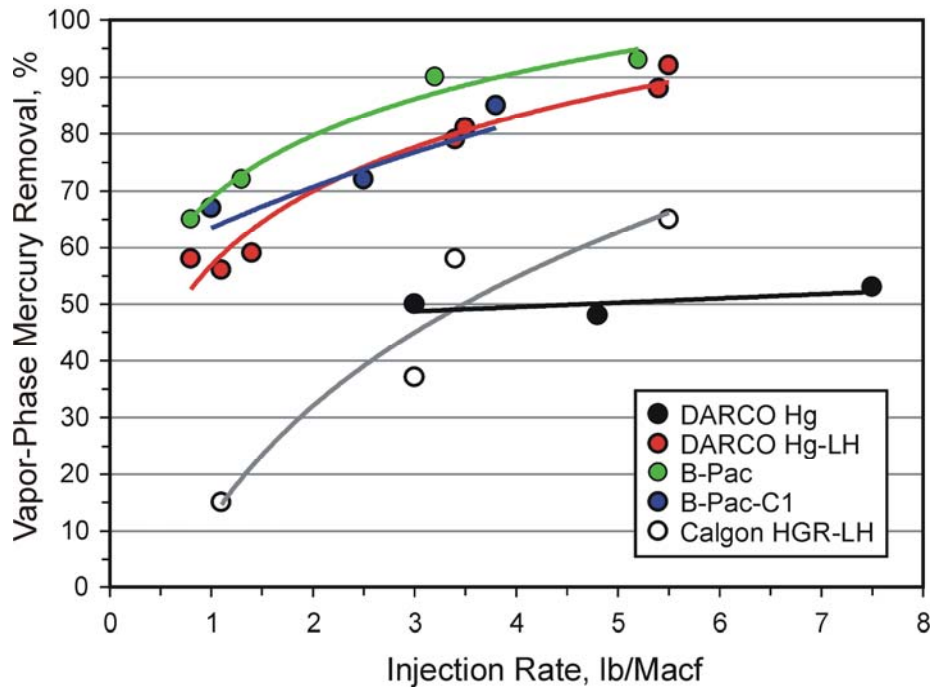


Figure 3. Mercury removal as a function of sorbent injection rate at a plant burning a PRB coal with an ESP (9).

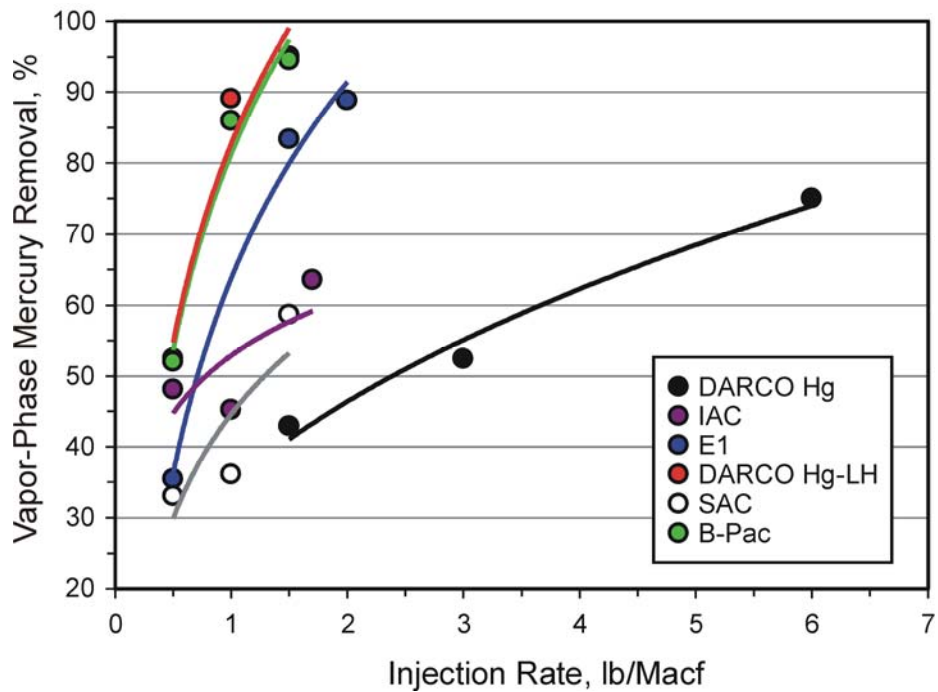


Figure 4. Mercury removal as a function of sorbent injection rate at a plant burning lignite with a fabric filter (9).

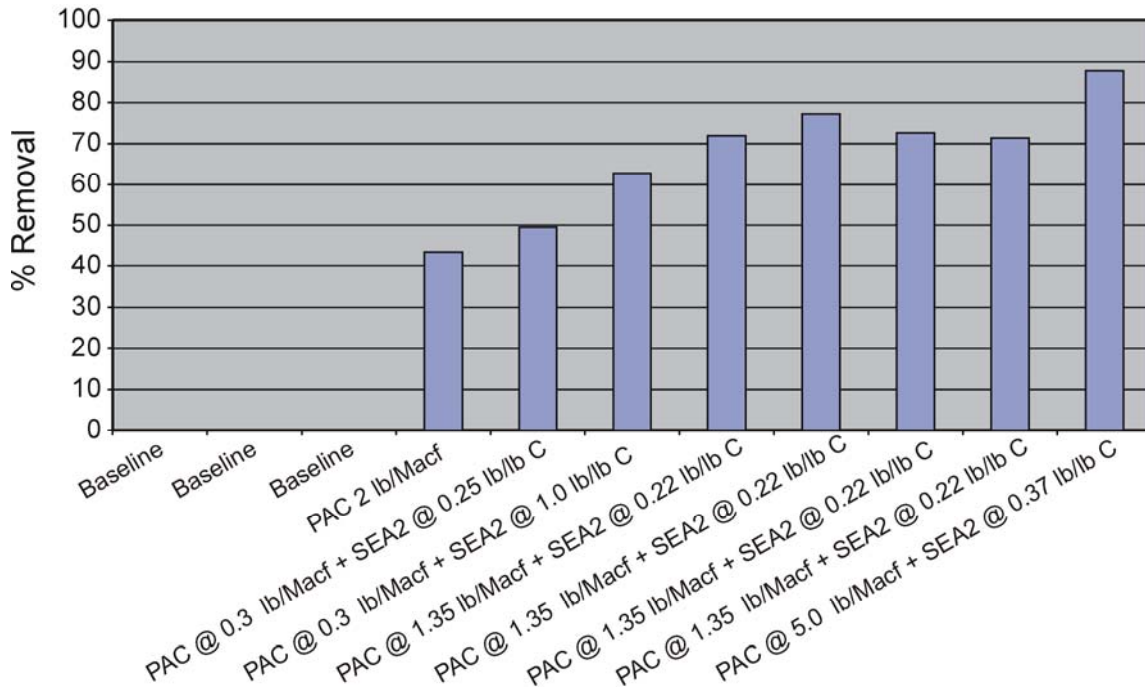


Figure 5. Mercury removal as a function of sorbent/additive injection rate at a plant burning a PRB coal with an ESP (10).

A wide range of non-carbon-based materials have also been tested at the bench-scale level to determine if they are effective in removing mercury. A partial list of these sorbents includes the following:

- Sodium tetrasulfide (Na_2S_4)
- Amended silicates
- Calcium-based sorbents
- Zeolites
- Metal oxide-based sorbents

Although none of these materials are expected to provide substantially better mercury control over carbon-based sorbents, because carbon can limit the resale of fly ash, the materials may find a market at some point in the future.

From the Phase II results it is expected that 80%–90% mercury control can readily be achieved for plants burning low-rank fuels using brominated carbons or halogen additives with ACI. However, it has been found that for high-sulfur eastern bituminous coals achieving a high level of mercury control may be exceedingly difficult. It has been shown that SO_3 greatly decreases the removal efficiency of carbon-based sorbents. As shown in Figure 6, there is at best only a 25%–35% improvement in mercury removal over baseline conditions even using brominated carbons (11). Figure 7 shows that even at low SO_3 concentrations there is an impact on mercury removal (11). Current mercury control research is focusing on methods on minimizing the impact of SO_3 on ACI.

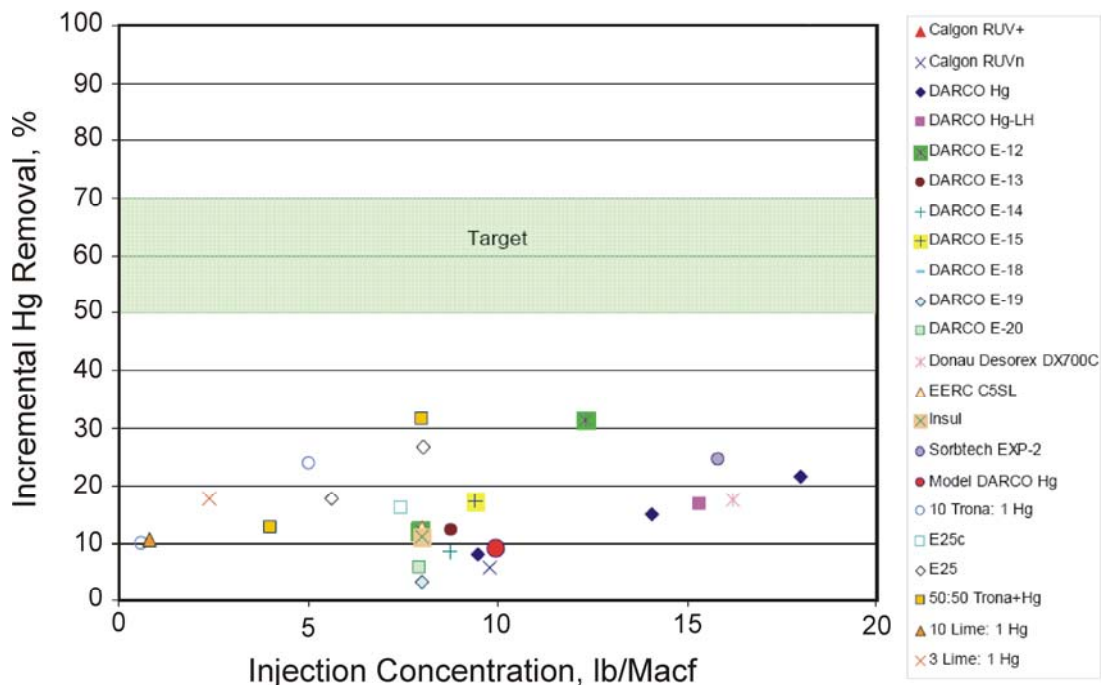


Figure 6. Mercury removal at a plant with high (>30 ppm) SO₃ (11).

Rather than injecting a sorbent into the flue gas, a fixed-carbon reactor can also be used. These systems have been extensively used for mercury control for waste-to-energy systems, particularly in Europe (12). Carbon filter beds have also been used in power plants in Germany since the late 1980s. The primary purpose of these filters is to remove residual SO₂ downstream of a wet flue gas desulfurization (FGD) system and to prevent ammonium sulfate formation in the low-dust selective catalytic reduction (SCR) units. Although not the primary purpose, reduction of mercury is inherent to the control system. A mercury level below 1 µg/dscm has been guaranteed by one vendor (typical power plants have uncontrolled mercury emissions of 5–10 µg/m³).

The most common type of system is the cross-flow filter. In this design, the flue gas flows horizontally through the filter bed. Typically, each filter bed module contains three layers with a total thickness of about 1 meter. Each layer is separated by perforated plates. Fresh carbon is conveyed to and distributed within the bed by a screw conveyor on top of the bed. Discharge cylinders at the bottom allow extraction of carbon from each layer. Pressure drop is usually the parameter that determines the rate of carbon removal. Typically, the pressure drop across the whole system is 305 mm of water (12 inches). Based on typical removal rates, the whole carbon bed is replaced approximately once a year. Note that the bed replacement rate could be expected to increase in the absence of a wet FGD system.

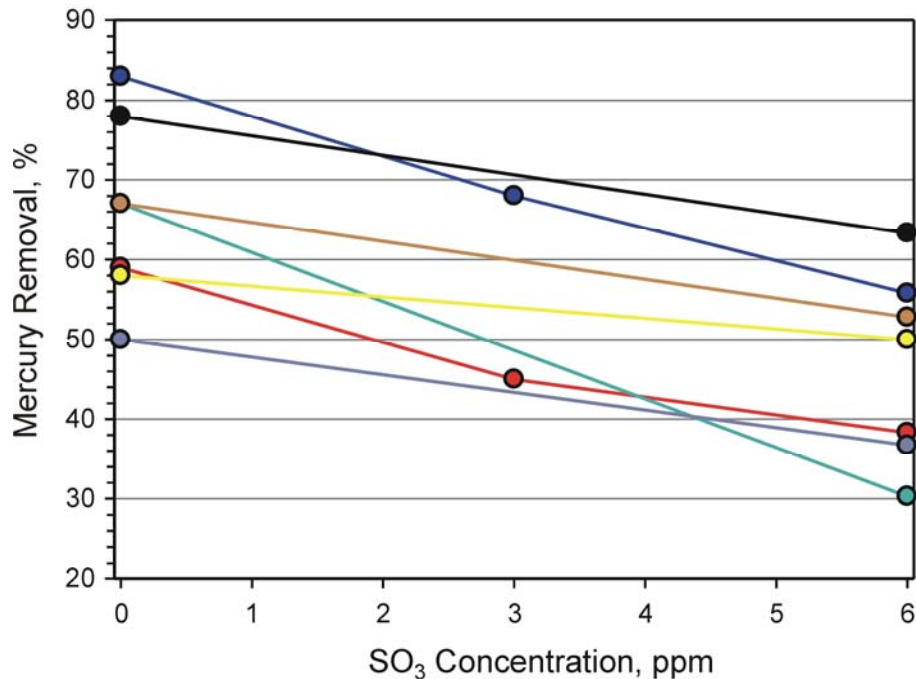


Figure 7. Impact of SO₃ concentration on mercury removal (11).

The primary advantages of a fixed-carbon bed are as follows:

- It is much more flexible, because the mercury removal efficiency does not depend on the type of particulate control device.
- There is the possibility of regenerating the sorbent, reducing costs.
- With a wet FGD system and a fixed-carbon bed, very high mercury removals (>90%) can potentially be achieved. At temperatures typically encountered following a wet FGD, carbon has a high affinity for mercury.

However, there is a strong aversion to widely installing these types of systems on coal-fired electric utilities for the following reasons:

- Flue gas flow rates for utilities are an order of magnitude greater than typical waste-to-energy facilities. This requires substantially more space, and coal-fired utilities are often space-limited.
- Small additional pressure drop is very costly to a large utility.
- To prevent desorption of mercury, a very high level of SO₂, NO_x, and HCl control must be accomplished or the bed replacement rates would need to be increased.

2.3 Mercury Oxidation Technologies

Hg^0 is insoluble, and little if any is removed by wet scrubbers. Therefore, technologies that can result in a higher percentage of the mercury reaching the wet scrubber as Hg^{2+} will provide a greater level of control, but there is a caveat: it must stay captured. There are two primary methods of improving wet scrubber mercury removal efficiency. The first, as mentioned above, is to provide a higher concentration of Hg^{2+} to the scrubber by using a mercury oxidation technology. The second is to ensure that once mercury is captured by the wet scrubber, it remains captured and not reemitted.

Up until the late 1990s, it was assumed that Hg^{2+} was effectively captured by wet scrubbers (>90%), but it was observed that in a number of cases mercury removal was less than expected based on the concentration of Hg^{2+} measured at the inlet to the scrubber. In addition, the concentration of Hg^0 at the scrubber outlet was greater than the scrubber inlet. Initially, this was assumed to be a bias in the measurement because of particulate matter collecting on the filter. This was not the case, however, as it was shown that, depending on scrubber conditions, some of the captured Hg^{2+} can be reduced in the scrubber to Hg^0 and reemitted (13). These mercury reduction reactions are very complex and are not fully understood. A proposed mechanism was developed by URS Corporation and is shown in Figure 8 (14).

An extreme example of reemission is shown in Table 2. The data was generated from a plant burning a high-sulfur bituminous coal that had an SCR, ESP, and wet scrubber. Based on

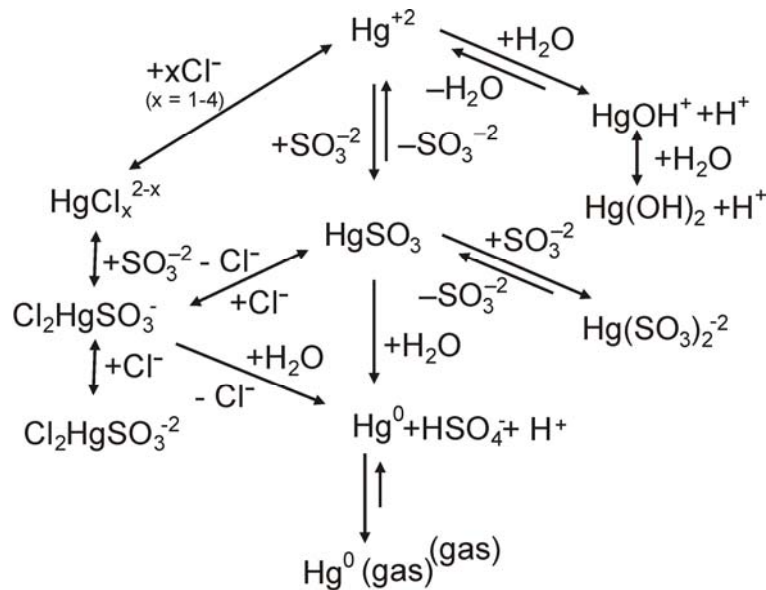


Figure 8. Proposed mechanism for Hg^{2+} reduction to Hg^0 in a wet scrubber (14).

Table 2. Mercury Concentrations at a Power Plant Firing a High-Sulfur Eastern Bituminous Coal*

Sample Location	SCR Inlet, $\mu\text{g}/\text{Nm}^3$	SCR Outlet, $\mu\text{g}/\text{Nm}^3$	Wet FGD		Reduction, %
			Inlet, $\mu\text{g}/\text{Nm}^3$	Stack, $\mu\text{g}/\text{Nm}^3$	
Hg ^p	0.02	0.03	0.00	0.00	
Hg ⁰	8.32	2.83	0.33	3.97	
Hg ²⁺	0.94	5.05	7.60	0.54	
Hg _{total}	9.27	7.90	7.93	4.50	43.3

* All data are corrected to 3% O₂.

the percentage of Hg²⁺ at the wet FGD inlet (>95%), it would be expected the scrubber would provide a very high level of mercury removal, but only 43.3% was removed as a result of mercury reemission as Hg⁰.

As mentioned in Section 2.2, one of the technologies selected under DOE's Phase I program was a project proposed by McDermott/B&W to enhance wet scrubber performance by reducing mercury reemission. Tests were conducted at two different power plants. One had a forced oxidation scrubber, and the other had a magnesium/lime scrubber. McDermott/B&W sprayed a sulfide-containing salt (potassium sulfide, sodium sulfide, and thioacetamide) into the scrubber, which greatly reduced the reemission from the forced oxidation scrubber but had little impact on the magnesium–lime-based scrubber. Since that time, other additives have been studied for preventing mercury reemission from the scrubbers. These include Degussa's TMT-15 additive (15), chelating agents such ethylenediaminetetraacetic acid (EDTA), solid oxides such as aluminum, magnesium and iron oxides, and vanadium pentoxide (16).

The second method for improving mercury removal in a wet scrubber is to use additives or catalysts to increase the concentration of Hg²⁺ in the gas stream or in the scrubber slurry. Any technology that can result in a higher percentage of the mercury reaching the wet scrubber as Hg²⁺ will improve the overall mercury removal efficiency of the system. The following is a list of technologies that have been tested at least at the pilot scale:

- Addition of additives including halogenated compounds
- MercOx process
- Multipollutant control technologies
 - BOC LoTOx™
 - ECO™/PowerSpan
 - EnviroScrub Pahlman™ Process
 - EPA's Multipollutant Scrubber for SO₂, NO_x, and Hg control
 - Airborne Process – sodium bicarbonate scrubbing
- PCO™ Process

- Catalytic oxidation
 - SCR
 - Low-temperature catalytic oxidation (metal oxides and noble metals)

As part of a DOE test program, the EERC sprayed a 30% solution of CaCl_2 onto North Dakota lignite. Full-scale results showed a decrease in Hg^0 from 82% to 65% as a result of adding the equivalent of 500 ppm chloride in the coal (17). At another North Dakota plant, the EERC added a proprietary additive (SEA2) to the coal. The result of injecting this additive was an increase in mercury removal by the wet scrubber from near zero to 45% at an add rate of 100 ppm (10). As was discussed previously, these additives are also being used in conjunction with ACI with very high levels of mercury removal being achieved, particularly for low-rank coals.

A process is being successfully developed in Germany called the MercOx process (18). The process is designed to convert SO_2 to sulfuric acid and Hg^0 to Hg^{2+} . To do this, the MercOx utilizes hydrogen peroxide to oxidize Hg^0 in a specialized scrubber. The scrubber is a packed tower, and flue gas is passed counter to the scrubber liquid (water and hydrogen peroxide). Using a proprietary additive, the mercury is precipitated out as HgS .

The multipollutant control systems are complex and expensive as they are designed to control NO_x , SO_2 , and mercury emissions. Of the three systems listed above, the most commercially advanced system is the PowerSpan reactor (19). A full-scale system is currently being installed at a utility. The PowerSpan process generates high-energy electrons that initiate chemical reactions that lead to the formation of oxygen and hydroxyl radicals. Hg^0 vapor is oxidized to form HgO , which is removed by the wet scrubber/wet ESP.

The BOC LoTOx system is a NO_x removal system that injects ozone into the flue gas stream to oxidize insoluble NO_x to soluble oxidized compounds (20). The mercury removal is achieved by oxidizing Hg^0 with ozone to produce soluble HgO , which is captured in a downstream wet scrubber. The process is very effective for NO_x but the reactions between ozone and mercury are relatively slow and, therefore, the mercury removal is low.

The EnviroScrub Pahlman process uses a regenerated manganese compound to adsorb SO_2 and NO_x . The technology consists of a single-stage, dry system that essentially replaces the wet FGD for SO_2 scrubbing, SCR for NO_x removal, and ACI for mercury reduction (21). High capture percentages coupled with the single-stage capabilities of the system make the technology attractive compared to the standard alternatives of wet FGD, SCR, and ACI systems. Mercury control results from slipstream testing at the Minnesota Power Boswell Station and at Detroit Edison's River Rouge Plant show mercury removals of Hg^0 were achieved up to 99%. Total mercury removals of 94% were also obtained.

The work that is being done by EPA is interesting in that it utilizes a typical lime-based wet scrubber but uses a proprietary oxidant that is added to the scrubber solution to ensure that a high percentage of the mercury is oxidized and that reemission is prevented (22). Bench-scale results are shown in Figure 9. This process is currently being tested at the pilot-scale level.

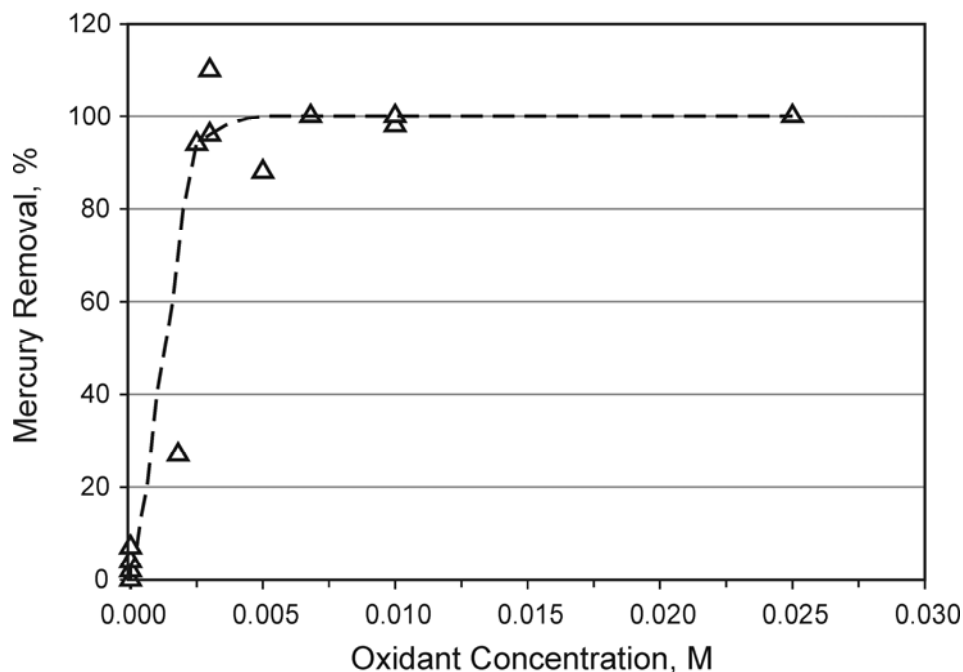


Figure 9. Bench-scale tests using EPA's proprietary oxidant (22).

Airborne Pollution Control's Airborne Process is an advanced pollution control process that employs a sodium bicarbonate scrubbing solution for combined NO_x , SO_x , mercury, and particulate emission reduction. The sodium bicarbonate-based scrubbing is used in conjunction with Airborne's process for the regeneration of the sodium bicarbonate reagent and the production of a high-grade fertilizer by-product. The process has been demonstrated at the 5-MW scale (500 lb/hr of sodium bicarbonate) at Kentucky Utilities' Ghent Generating Station (Ghent, Kentucky), which burns a high-sulfur coal (23). The scrubbing agent was sodium bicarbonate, and the effluent from the oxidizer was predominantly a 20% aqueous solution of sodium sulfate. The regeneration system used ammonium bicarbonate to convert the sodium sulfate into sodium bicarbonate. Mercury control at Ghent depended on the mercury speciation. Particulate mercury was collected in the ESP, and Hg^{2+} was captured in the wet scrubber, as would be expected. Airborne is further investigating the use of an oxidant to convert Hg^0 to Hg^{2+} for improved total mercury capture. The fate of mercury during the regeneration process has not been reported.

The DOE National Energy Technology Laboratory (NETL) has developed a technology to photochemically oxidize mercury in coal-fired power plants. The process is intended to serve as a low-cost mercury oxidation technology that will facilitate Hg^0 removal in a downstream scrubber, wet ESP, or FF. PowerSpan Corporation has licensed the technology and has completed bench- and small-scale pilot testing (24). The technology uses 254-nanometer ultraviolet light to produce an excited mercury species state in the flue gas, leading to oxidation of Hg^0 . Bench-scale testing has indicated that oxidation levels of 86% to 91% can be achieved

using 100% Hg⁰ in a simulated flue gas. The technology is in the early stages of development, and the following issues must still be addressed:

- The practicality of using this approach on very large ducts is uncertain.
- How to maintain a long ultraviolet (UV) path length in a flue gas with ash.
- The fate of the mercury within the scrubber or wet ESP.

Metal oxides have been known to be effective for SO₂ and NO_x control (25). SCR of NO_x using vanadium/titania catalysts has been shown to be an effective method of enhancing mercury oxidation for eastern bituminous coals (26, 27), thereby improving overall mercury capture in wet FGD systems. It appears that the chloride concentration in the flue gas is an important factor. It was thought that other metal oxides may have some potential for oxidizing or removing mercury as well. Although mercury breakthrough occurs very rapidly when acid gases, HCl, SO₂, and NO_x are present, the mercury is nearly 100% oxidized. Metal oxides that have been evaluated include copper, iron, manganese, zinc, and titanium. Noble metals that have been used include gold, palladium, and silver. A slipstream pilot-scale catalytic reactor is currently being tested at five sites (28), including plants burning lignites from North Dakota and Texas, a PRB site, and a site firing an eastern bituminous coal. Depending on the coal type, 50% to 80% mercury oxidation was achieved using noble metal catalysts. These materials are expensive; therefore, to be cost-effective, they must be regenerated.

3.0 POTENTIAL MERCURY CONTROL TECHNOLOGIES FOR THE TACONITE INDUSTRY

There are significant differences between the different taconite facilities and even within lines at the same facility that may impact mercury emissions. As previously stated, the mercury content in the ore is related to the geographic location of the mine. Also, depending on the plant, either a “straight grate” or “grate kiln” operation is used. The fuel to provide the energy for the induration process varies from plant to plant. The primary fuel is either natural gas or coal, but some plant lines use biomass and petroleum coke. Therefore, as is the case for coal-fired power plants, most likely there will not be one technology to fit all plants to reduce mercury emissions.

3.1 Precombustion Technologies

It is highly unlikely that precombustion technologies used for coal (i.e., coal cleaning) will be useful to the taconite industry. Any coal cleaning will have limited value, as the mercury in the coal accounts for only a minor portion of the total mercury emissions. The magnetic separation techniques currently used by the taconite industry to process the ore already remove >80% of the mercury from the raw ore (3). If the overall efficiency of the milling process can be improved, it would not only increase plant efficiency but may also reduce mercury emissions.

3.2 Sorbent Technologies

Using sorbents to remove mercury from the gas stream is a technology that will need to be considered for the taconite industry. Using powdered activated carbon (PAC) or treated PAC injection has several advantages:

- Because mercury control is being done after induration, nothing is added to the pellet-making process to interfere with the iron chemistry, including the initial magnetic separation step, making the green balls, and the induration process.
- To a great degree the effectiveness of the sorbents would be independent of type of furnace, straight grate or grate kiln.
- The technology has been tested extensively for coal-fired systems so the mercury/sorbent chemistry is reasonably well known.
- With the exception of the injection lances, no additional ductwork would be necessary, and the equipment (PAC silo and feeder) could be placed outside of the process building.
- All equipment can be purchased directly from vendors and is very reliable. Depending on the amount of carbon used the annual labor cost for operating and maintaining the equipment can be quite low.

The disadvantages of PAC or treated PAC injection for taconite plants are as follows:

- Although several plants do have multicyclones, the primary particulate control device for the taconite industry is a wet scrubber. Although it is expected that 50%–60% mercury control can be achieved with PAC, all of the removal will be in-duct capture. This will increase the amount of PAC needed to achieve the same level of control as would be the case when an ESP or FF is present. The greater distance upstream of the scrubber the PAC is injected, the better (greater residence time).
- Because of the high-level concentrations of Hg^0 generated at taconite plants, more expensive treated (brominated) carbons may be needed to achieve the desired mercury control at a reasonable cost. The long-term balance-of-plant impacts with these materials is still unknown.
- If a plant is currently concerned about particulate emissions, additional carbon could exacerbate the problem.
- Some plants recycle scrubber solids in the manufacture of the green balls to improve overall iron utilization. Most likely wastewater streams would need to be rerouted to prevent the captured mercury from recycling back to the furnace.

- To ensure good distribution of the PAC, a flow profile of the duct will be needed, and it may be necessary to do modeling of the flow to determine the proper location of the lances.

As an option to using PAC injection, a fixed-bed sorbent reactor could be considered for taconite plants. Almost all the disadvantages of PAC injection no longer pertain:

- The fixed-bed sorbent reactor is much more flexible because the mercury removal efficiency does not depend on the type of particulate control device.
- There is the possibility of regenerating the sorbent, reducing costs.
- With a wet FGD system and a fixed-carbon bed, very high mercury removals (>90%) can potentially be achieved. At temperatures typically encountered following a wet FGD, carbon has a high affinity for mercury.
- Increased particulate emissions would not be a problem.
- There is no impact on the scrubber or recycle of solids.
- There are vendors who currently supply fixed-bed reactors for mercury control.

The disadvantages are as follows:

- A fixed-bed reactor would add 8–14 in. H₂O pressure drop, possibly requiring additional fan power.
- The fixed-bed reactor capital costs will be higher than these PAC injection systems.
- The fixed-bed reactor would require duct modification. Most likely, because of space limitations, the fixed-bed reactor would need to be housed in a separate building located near the process plant. Therefore, additional duct work will be needed from the scrubber to the stack.

Another option that would allow for more flexibility and increased particulate control would be to install a pulse-jet baghouse either in addition to the wet scrubber or as a replacement. Most likely a high level of mercury control could be achieved with a relatively low amount of sorbent. A FF provides an excellent contacting surface for mass transfer for mercury to the carbon. This would be the most expensive option both in capital investment and operating costs. However, if a new plant were to be built, it should be considered a viable option.

3.3 Oxidation Technologies

As all taconite plants have scrubbers for particulate control, it clearly would be advantageous to increase the percentage of Hg²⁺ or particulate-bound mercury at the inlet to the

scrubber. The number of mercury oxidation technologies that could be considered for use within the taconite industry is rather limited. Most likely, multipollutant control technologies that increase Hg^{2+} such as SCRs and ECO™/PowerSpan would not be considered economically viable for the taconite industry. Therefore, the most likely candidates are the addition of chemical additives. Chemical additives that may have potential are as follows:

- Sodium and calcium chloride
- Sodium and calcium bromide
- Hydrogen peroxide
- EPA’s proprietary oxidant
- EERC’s proprietary additive
- Ozone
- Sodium bicarbonate

Beginning in July 2006, MDNR, in collaboration with the EERC and Coleraine Minerals Research Laboratory began conducting plant-scale and bench-scale tests at taconite facilities to evaluate the viability of several of these oxidation technologies. Limited testing has been done with chloride and bromide salts, hydrogen peroxide, and EPA’s proprietary oxidant.

Plant tests were completed at United Taconite (grate kiln) and Hibtac (straight grate), evaluating the impact of adding sodium chloride both directly to the green balls as a solid and adding it as solution to the firing zone at Hibtac and to the kiln at United Taconite. A schematic of the tests is shown in Figures 10 and 11. The results of these tests were somewhat

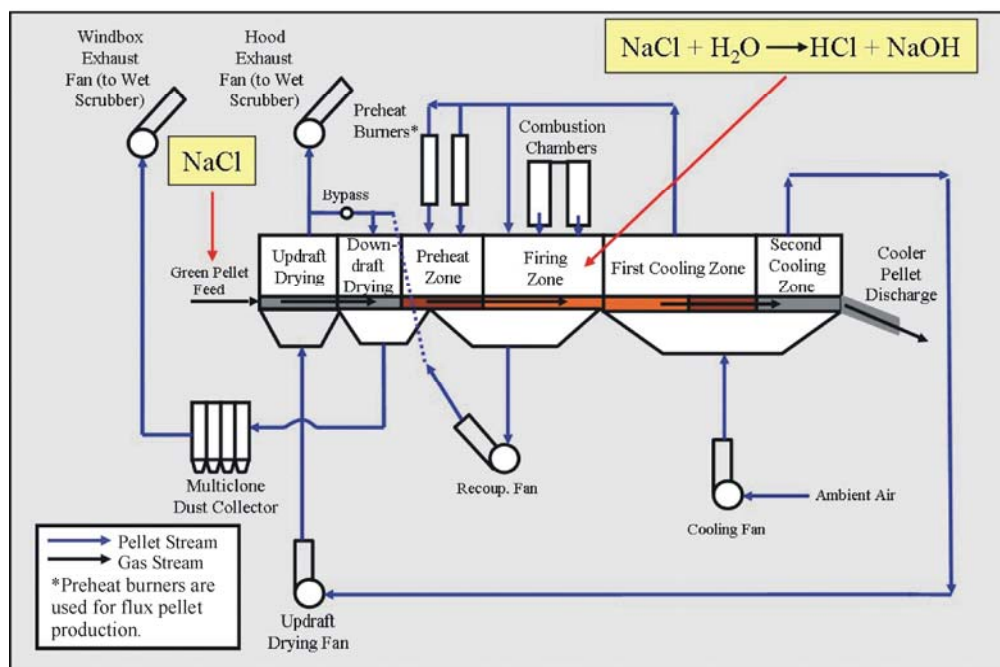


Figure 10. Schematic of mercury testing at a straight-grate plant using NaCl (29).

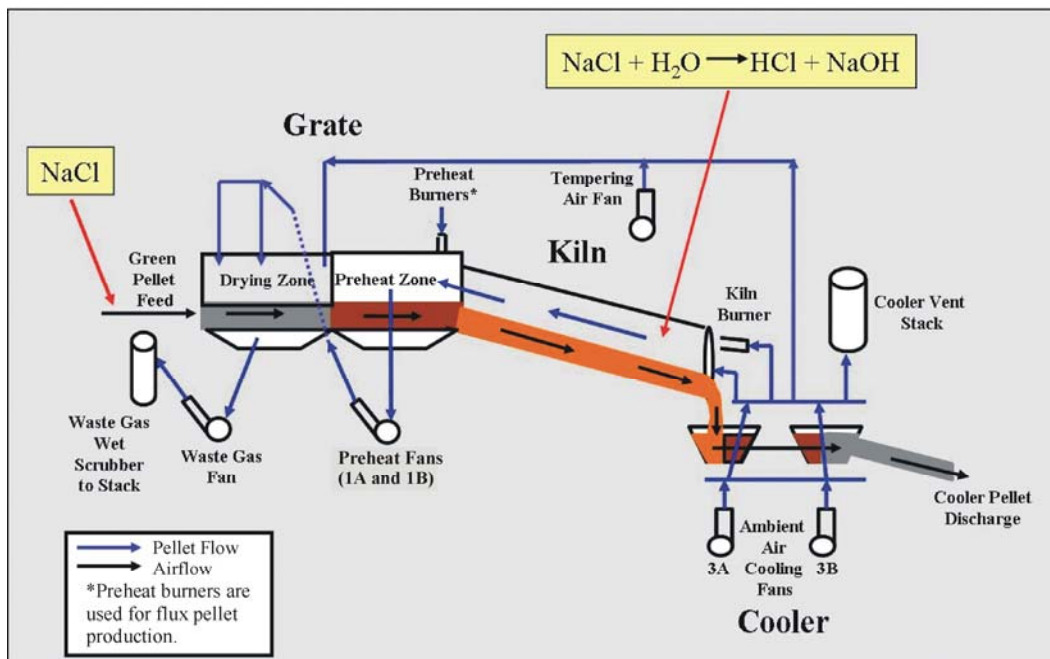


Figure 11. Schematic of testing at a grate kiln plant using NaCl (29).

disappointing at Hibtac but more promising at United Taconite (29). A major difference was that Hibtac had a straight grate compared to a grate kiln at United Taconite. It was believed that in the straight grate most of the mercury is liberated from the ore in the preheat zone (~1500°F).

Additional tests were later conducted at Hibtac where bromine and chloride salts were added as a solution in the preheat zone as shown in Figure 12 (29). The results from these tests showed nearly 70% mercury removal. The results of all tests will be presented in more detail in a report by MDNR.

Bench-scale tests using hydrogen peroxide and EPA's proprietary oxidant in a simulated wet scrubber were also completed by MDNR. The results indicated that hydrogen peroxide did not work well but the EPA oxidant was very promising. It does appear that using additives to increase mercury oxidation and subsequent capture in the scrubber is a promising technology for the taconite industry. However, the overall impact of chemical additives on the induration process is very much an unknown, and additional testing is needed.

Based on the configuration of the taconite plants, high concentration of Hg^0 in the gas stream, and gas temperature, EERC proprietary additive has the potential to provide a high level of mercury oxidation and be very cost-effective. In addition, the additive can be injected almost anywhere in the system, resulting in minimal plant impacts.

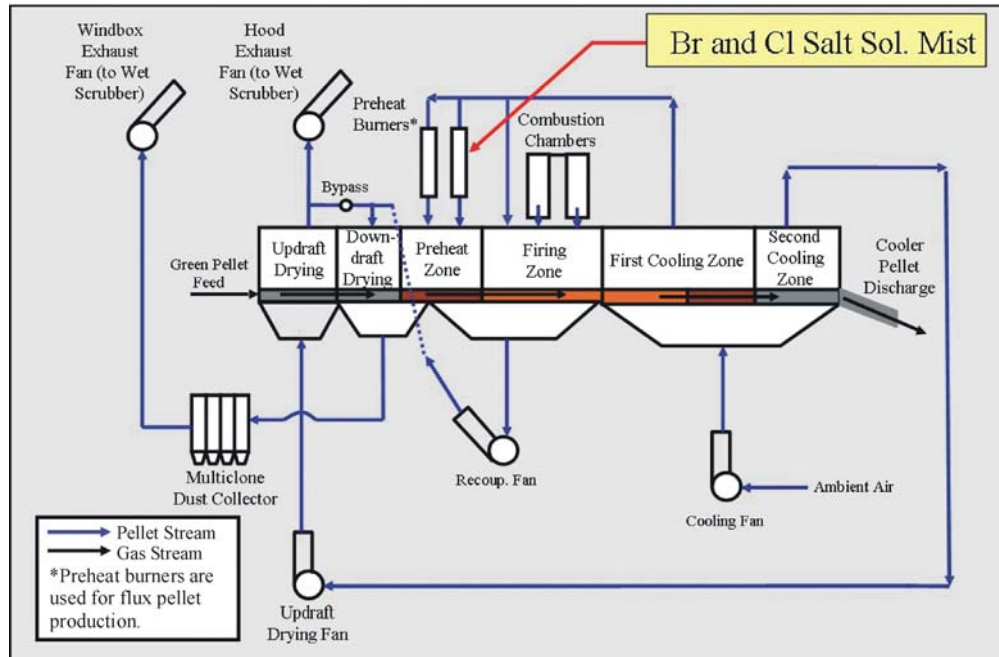


Figure 12. Schematic of testing for mercury at a straight-grate plant using bromine and chloride salts (29).

Another possibility is to use halogenated additives (or potentially others) in conjunction with ACI. By adding small amounts of these additives, the effectiveness of the PAC may be greatly enhanced, resulting in decreased costs. There are several concerns using chemical additives to enhance mercury oxidization. The first is that many of the taconite facilities recycle the scrubber water and send the scrubber solids back to the processing facility to improve the overall plant efficiency by recovering the iron that is in the solids. Table 3 shows how each plant treats the scrubber liquor. At most plants, even if the scrubber is removing the mercury from the gas stream, it is simply being recycled back into the system. Based on the MDNR results presented in a report to the Iron Ore Cooperative Research (4), it appears, with the possible exception of Hibtac, a high percentage (>80%) of the mercury removed by the scrubber reports to the solids. Even though the actual measured concentration is quite variable, the percentage in the solids stays relatively constant as is shown in Table 4. Recycling these solids creates the potential to generate very high mercury concentrations in the slurry, reducing the overall mercury removal. A second concern is the potential for corrosion and erosion. This is particularly true for the halogenated (chlorides and bromides) additives. However, other oxidants also may result in increased equipment maintenance over time. To date, these problems have been minimal in coal-fired boilers, but the tests have been relatively short term. Finally, the overall impact on iron chemistry is unknown.

Table 3. Fate of Scrubber Materials

Plant	No. of Lines	Induration Furnace	Scrubber Type	Scrubber Water	Scrubber Solids
Hibbing Taconite Co.	3	Straight grate	Once through	Grinding mills	Grinding mills
Keewatin	1	Grate kiln	Recirculating	Tailing basin	Landfill
United Taconite Co.	2	Grate kiln	Recirculating	Tailing thickener	Green ball feed
Mittal Steel	1	Straight grate	Recirculating	Tailing thickener	Tailing thickener
Minntac*	4	Grate kiln	Once through	Grinding mills	Green ball feed
Minntac*	1	Grate kiln	Recirculating	Tailing basin	Settling pond

* Lines 4-7 are once through Line 3 is recirculating.

Table 4. Distribution of Mercury in Scrubber Slurry (4)

Plant	Hg(D) ¹ , ng/L		Hg(P) ² , ng/g		TSS ³ , %		Hg(T) ⁴ , ng/L		Hg in Solids, %	
	Avg.	Std. Dev.	Avg.	Std. Dev.	Avg.	Std. Dev.	Avg.	Std. Dev.	Avg.	Std. Dev.
Hibtac	325	164	2528	2525	0.019	0.011	671	314	51.1	9.07
Minntac (Line 4)	209	180	859	668	0.184	0.109	1540	826	86.4	7.39
Minntac (Line 7)	273	42	2470	563	0.070	0.024	1943	541	85.3	3.35
United Taconite	542	626	616	236	1.866	0.578	11550	5004	96.6	2.60
Mittal	1117	465	2305	1504	0.126	0.031	4368	1929	80.5	11.23

¹ Dissolved Hg in filtration liquid.

² Hg in filtration solids.

³ Total suspended solids.

⁴ Total mercury in scrubber slurry.

4.0 ECONOMICS OF MERCURY CONTROL FOR TACONITE PLANTS

Until recently, very little mercury testing has been done at taconite plants. Almost all the testing that has been done has been proof of concept, short-term tests conducted by MDNR and Coleraine Minerals Research Laboratory. To obtain valid economic data, considerably more testing will need to be done, in particular for mercury oxidation technologies. The following information will be needed before a detailed economic study can be constructed for using oxidation technologies to reduce mercury emissions at taconite plants:

- Chemical additive to be used and the cost of the additive
- Amount of additive needed to obtain a specific result
- Feeding devices (solid vs. liquid)
- Impact on scrubber dust and liquid recycle
- Equipment maintenance
- Equipment installation requirements (ducting, utilities, labor)
- Effect on process chemistry, if any

A sensitivity analysis (based on the amount of PAC used) for ACI is shown in Table 5. The data presented in the table are based on an economic study that was done on data from a coal-fired power plant (10). Although the added cost (\$35/ton) of disposal because of the increase in dust due to the carbon is included, the loss of revenue from the disposal of scrubber

Table 5. Summary of Costs Associated with ACI for Mercury Control at a Taconite Plant (Based on 2005 \$)

	Case 1	Case 2	Case 3
Unit Size, kscfm	350	350	350
Particulate Removal	Venturi scrubber	Venturi scrubber	Venturi scrubber
Targeted Mercury Removal	60%	60%	60%
ACI Rate, lb/Macf	10	5	3
ACI Rate, lb/hr	390	145	90
Capital Cost (\$)			
Purchased Equipment	974,000	974,000	974,000
Installation	25,000	25,000	25,000
Total Capital Requirement	999,000	999,000	999,000
Operating and Maintenance (\$/yr)			
Operating Labor	32,000	32,000	32,000
Maintenance Labor	18,240	18,240	18,240
Supervision Labor ¹	4800	4800	4800
Replacement Parts ²	19,480	19,480	19,480
Raw Materials (PAC)	1,312,854	656,427	393,856
Utilities	8775	8775	8775
Disposal of Scrubber Solids Because of Added Carbon	39,414	19,708	11,825
Overhead ³	11,008	11,008	11,008
Taxes, Insurance, Administration ⁴	29,970	29,970	29,970
Fixed Charges	185,571	185,571	185,571
Levelized Annual Costs⁵			
Total Annual Cost, \$/yr	2,090,541	1,200,149	843,993
Mercury Reduction (\$/lb Hg removed)	61,189	35,128	24,703

¹ Based on 15% of operating labor.

² Based on 2% of purchase equipment.

³ Based on 20% of labor costs.

⁴ Based on 3% of total capital requirements.

⁵ The sum of the levelized operating and fixed costs.

dust rather than recycling it back to the milling is not taken into account. Most likely this recycle would not be possible if carbon were to be injected in the scrubber. This also assumes 24-hour operation with 85% uptime.

Although no commercial fixed-carbon beds have been installed in the United States or Canada for mercury control, based on 1996 dollars, EPA estimates the cost for a coal-fired plant using a fixed-carbon bed to be \$37,800 per lb of mercury removed (12). Therefore, a fixed bed would be somewhat more expensive than simply injecting PAC. In general, the capital equipment costs will be higher and the operating costs will be higher because of relatively high pressure drops across the system. It would be expected that sorbent costs will be somewhat less as the filter bed is a better gas sorbent contactor than the venturi scrubber.

Figure 13 shows the relative cost for each of the different technologies, from least expensive to most expensive.

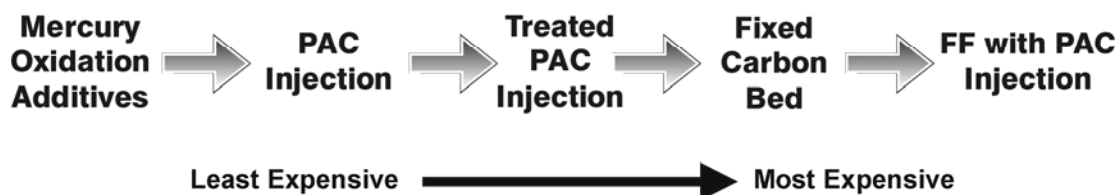


Figure 13. Relative cost for mercury control technologies.

5.0 RECOMMENDATIONS

Unlike the power plant industry, testing of mercury control technologies for the taconite industry is in the very early developmental stage. Although some of the results obtained from testing at coal-fired power plants are valid for taconite plants, there are substantial differences between the two industries that are going to impact on what technologies ultimately are implemented. As has been discussed, there are essentially two types of mercury control technologies that would most likely be considered for the taconite industry. These are mercury oxidization additives and mercury sorbents, of which the oxidation additives will most likely be the cheapest and, possibly, the most effective. However, there are a number of concerns that must be addressed by additional testing, both short and longer term.

A major concern of using oxidants to increase mercury removal in the scrubber is the potential increase in mercury concentration in the scrubber as a result of solids and water recycle loops. As was shown previously in Table 4, a high percentage of the mercury captured by the scrubber is associated with the solids; therefore, recycling the solids could result in very high (and increasing) levels of mercury being recycled. Although these data can only be obtained by conducting long-term testing (several months or more), it is important that the following be evaluated:

- The economics and the practicality of not recycling the solids/water.
- Potential for recycling only a percentage of the solids, thereby reaching some sort of equilibrium.
- Would there be an advantage to recycling the solids back to the grinding mill rather than the green ball feed? It is possible that the mercury-containing solids can be separated during processing. It has shown that the mercury tends to absorb to the nonmagnetic fraction of the scrubber dust. Thus, by sending the scrubber solids back to the grinding mill, the magnetic fraction of these solids without the mercury could be recovered while the high-mercury nonmagnetic fraction would be discarded (30).

Other potential concerns that must be studied are corrosion/erosion of piping and other equipment as a result of the oxidants and the overall impact on system chemistry.

Mercury oxidation is accomplished by either adding the oxidant prior to the scrubber, as would be the case for the EERC additive and halogens such as NaBr or NaCl, or changing the scrubber slurry, as would be the case when using hydrogen peroxide or the EPA oxidant. In either case, there is the potential to change the system chemistry with unknown consequences. If halogens are added, there is the possibility of exacerbating corrosion/erosion problems, resulting in additional system maintenance.

It does appear that the addition of NaBr to the green balls shows promise. Therefore, it is recommended that longer-term testing be completed using NaBr addition in both straight-grate and grate kiln facilities. Initially, testing would be for several days to ensure that the short-term results are valid. Once that is complete, longer-term testing for periods of up to a month should be done. During the longer-term testing, metal coupons will need to be installed to measure corrosion and erosion. During this period, it is essential that measurements be made to evaluate the effect of the water and solids recycle loops on mercury concentration in the scrubber.

Bench-scale testing to screen potential mercury oxidants should continue. In particular additional tests should be conducted utilizing the EPA oxidant, as initial preliminary tests show this additive has promise. If this technology or others continue to be promising, it may be advantageous to build a small slipstream scrubber. This way, tests can be conducted with minimal impact on plant operations.

For coal-fired boilers, the technology of choice appears to be standard ACI or using treated PACs. Depending on several factors, such as future state or federal regulations and the effectiveness and practicality of using mercury oxidants, this technology may need to be evaluated for the taconite industry as well. The effectiveness of these sorbents for removing mercury, the impact on the scrubber and system chemistry, and the impact on the level of particulate emissions is completely unknown at this time. Unfortunately, in order to obtain any meaningful results, testing would have to be conducted at the full-scale level.

One technology that must at least be considered by the industry is to install a carbon fixed bed at the outlet of the scrubber. Depending on fan capacity, this technology would have minimal impact on plant operation. In addition, it is possible to test a slipstream pilot unit to evaluate both standard and treated activated carbons. Although this option would most likely be more expensive than ACI, it could provide the highest level of comfort by not impacting the plant chemistry and recycle systems and at the same time achieve a high level of mercury control. It is possible that by using a halogenated carbon, >90% mercury control could be obtained. Along the same lines, for those facilities interested in reducing particulate emissions, tests could be completed using a slipstream FF with ACI.

6.0 REFERENCES

1. Berndt, M.; Engesser, J.; Johnson, A. *On Distribution of Mercury in Taconite Plant Scrubber Systems*; Submitted to the Minnesota Pollution Control Agency, Oct 2003.

2. Federal Register. National Emission Standards for Hazardous Air Pollutants: Taconite Iron Ore Processing, Final Rule, 40 CFR, Part 63; Oct 30, 2003.
3. Berndt, M. *Mercury and Mining in Minnesota*; Minerals Coordinating Committee Final Report, Oct 2003.
4. Berndt, M.; Engesser, J. *Mercury Transport in Taconite Processing Facilities: (I) Release and Capture During Induration*; Iron Ore Cooperative Research Final Report, April 2003.
5. Pavlish, J.H.; Laudal, D.L.; Holmes, M.J.; Hamre, L.L.; Musich, M.A.; Weber, G.F.; Hajicek, D.A. *Technical Review of Mercury Technology Options for Canadian Utilities – A Report to the Canadian Council of Ministers of the Environment*; Canadian Council of Ministers of the Environment Final Report; March 2005.
6. Brand, A. Pilot Testing of WRI’s Novel Mercury Control Technology by Pre-Combustion Thermal Treatment, In *Proceedings of the 2006 Mercury Control Technology Conference of Coal*; Pittsburgh, PA, Dec 2006.
7. Olson, E.S.; Laumb, J.D.; Benson, S.A.; Dunham, G.E.; Sharma, R.K.; Miller, S.J.; Pavlish, J.H. *Prepr. Pap.—Am. Chem. Soc., Div. Fuel Chem.* **2003**, 48 (1), 30–31.
8. Pavlish, J.H.; Sondreal, E.A.; Mann, M.D.; Olson, E.S.; Galbreath, K.C.; Laudal, D.L.; Benson, S.A. *Status Review of Mercury Control Options for Coal-Fired Power Plants, Fuel* **2003**, 82, 89–165.
9. Feeley, T.J., III; Murphy, J.T.; Hoffmann, J.W.; Granite, E.J.; Renninger, S.A. *DOE/NETL’s Mercury Control Technology Research Program for Coal-Fired Power Plants*; EM 2003; pp 16–23.
10. Wocken, C.A.; Holmes, M.J.; Pavlish, J.H.; Thompson, J.S.; Hill Brandt, K.L.; Pavlish, B.M.; Galbreath, K.C.; Laudal, D.L.; Olderbak, M.R. *Enhancing Carbon Reactivity in Mercury Control in Lignite-Fired Systems*; Draft Final Technical Report for U.S. Department of Energy National Energy Technology Laboratory Cooperative Agreement DE-FC29-03NT4189; Oct 2006; in preparation.
11. Sjostrom, S.M.; Wilson, C.; Bustard, J.; Spitznogle, G.; Toole, A.; O’Palko, A.; Chang, R. Full-Scale Evaluation of Carbon Injection for Mercury Control at a Unit Firing High Sulfur Coal. In *Proceedings of the Power Plant Air Pollutant Control “Mega” Symposium*; Paper No. 14, Baltimore, MD, Aug 2006.
12. U.S. Environmental Protection Agency. *Mercury Study Report to Congress*; Volume VIII: An Evaluation of Mercury Control Technologies and Costs, U.S. Environmental Protection Agency, EPA-452/R-97-010, Dec 1997.
13. McDonald, D.K.; Amrhein, G.T.; Kudlac, G.A.; Yurchison; D.M. *Full-Scale Testing Of Enhanced Mercury Control Technologies for Wet FGD Systems*; Draft Final Report for

- U.S. Department of Energy National Energy Technology Laboratory Cooperative Agreement No. DE-FC26-00NT41006; May 2003.
14. DeBerry, D.W.; Blythe, G.M.; Pletcher, S.; Rhudy, R. Bench-Scale Kinetics Study of Mercury Reactions in FGD Liquors. In *Proceedings of the Power Plant Air Pollutant Control "Mega" Symposium*; Paper No. 47, Baltimore, MD, Aug 2006.
 15. Blythe, G.M.; Miller, C.E.; Rhudy, R.G.; Wiemuth, B.; Kyle, J.; Lally, J. Wet FGD Additive for Enhanced Mercury Control. In *Proceedings of the Power Plant Air Pollutant Control "Mega" Symposium*; Paper No. 36, Baltimore, MD, Aug 2006.
 16. Diaz-Somoano, M.; Unterberger S.; Hein, K.R. Using Wet-FGD Systems for Mercury Removal. *J. Environ. Monit.* **2005**, *9*, 906–909.
 17. McCollor, D.P.; Benson, S.A.; Holmes, M.J.; Libby, S.; Mackenzie, J.; Crocker, C.R.; Kong, L.; Galbreath, K.C. Large-Scale Mercury Control Technology Testing for Lignite-Fired Utilities – Oxidation Systems for Wet FGD. Presented at the 6th Power Plant Air Pollution Mega Symposium, Baltimore, MD, Aug 28–31, 2006.
 18. Korell, J.; Seifert, H.; Paur, H.R.; Anderson, S.; Bolin P. Flue Gas Cleaning with the MercOx Process. *Chem. Eng. Technol.* **2003**, *26* (7), 737–740.
 19. Alix, F.; Boyle, P.D. Commercial Demonstration of ECO[®] Multi-Pollutant Control Technology. Presented at the EUEC 7th Electric Utilities Environmental Conference, Jan 19–22, 2004.
 20. Jarvis, J.B., et al. LoTOx[™] Process Flexibility and Multi-Pollutant Control Capability. Presented at the Combined Power Plant Air Pollutant Control Mega Symposium, Washington, DC, May 19–22, 2003.
 21. Boren, R.M.; Hammel, C.F.; Harris, L.E.; Bleckinger, M.R. Pilot Test Results from Enviroscrub Technologies Multi-Pollutant Pahlman Process[™] Technology for NO_x, SO₂, and Mercury. Presented at the Combined Power Plant Air Pollutant Control Mega Symposium, Washington, DC, Aug 30–Sept 2, 2004.
 22. Hutson, N.; Srivastava, R. A Multipollutant Wet Scrubber for Capture of SO₂, NO_x and Hg. In *Proceeding of the 2006 Mercury Control Technology Conference of Coal*; Pittsburgh, PA, Dec 2006.
 23. Johnson, D.W.; Ehrnschwender, M.S.; Seidman, L. The Airborne Process – Advancement in Multi-Pollutant Emissions Control Technology and By-Product Utilization. In *Proceedings of the Combined Power Plant Air Pollutant Control Mega Symposium*; Washington, DC, Aug 30 – Sept 2, 2004.
 24. McLarnon, C.R.; Granite, E.J.; Pennline, H.W. Initial Testing of Photochemical Oxidation for Elemental Mercury Removal from Subbituminous Flue Gas Streams. Presented at the 19th Annual Western Fuels Symposium; Billings, MT, Sept 2004.

25. Hoffman, J.S.; Yeh, J.T.; Pennline, H.W.; Resnik, K.P.; Vore, P.A. Flue Gas Cleanup Studies with the Moving-Bed Copper Oxide Process. In *Proceedings of the Joint Power and Fuel Systems Contractor Review Meeting*; July 1996.
26. Laudal, D. *Effect of Selective Catalytic Reduction on Mercury, 2002 Field Studies Update*; Final Report; Energy & Environmental Research Center: Grand Forks, ND, Aug 2004.
27. Withum, J.A.; Tseng, S.C.; Locke, J.E. *Mercury Emissions from Coal-Fired Facilities with SCR-FGD Systems*, In *Proceedings of DOE/NETL's Mercury Control Technology R&D Program*; Pittsburgh, PA, July 12–14, 2005.
28. Machalek, T.; Olsen, B. Pilot Testing of Mercury Oxidation Catalysts for Upstream of Wet FGD Systems. Presented at Combined Power Plant Air Pollutant Control Mega Symposium; Baltimore, MD, Aug 28–31, 2006.
29. Berndt, M. E.; Engesser, J. E. Minnesota DNR's Coordinated Hg Research Effort. Presented at the Annual Society of Mining Engineers Meeting: Consolidation, Growth, Technology, Duluth, MN, April 17–18, 2007.
30. Berndt, M. E.; Engesser, J. *Mercury Transport in Taconite Processing Facilities: (II) Fate of Mercury Captured by Wet Scrubbers*; EPA: Great Lakes National Program Office Report, 2005.

Appendix B-1-12

Mercury Transport in Taconite Processing Facilities: (III) Control Method Test Results

December 31, 2007

Mercury Transport in Taconite Processing Facilities: (III) Control Method Test Results

¹Michael E. Berndt and ²John Engesser

Minnesota Dept. of Natural Resources
Division of Lands and Minerals

¹500 Lafayette Road
St. Paul, MN 55155

²1525 3rd Ave. E
Hibbing, MN, 55746

A report submitted to Iron Ore Cooperative Research

Submitted June 30, 2007

Updated Dec. 31, 2007

Table of Contents

1. Summary	3
2. Introduction.....	4
3. Background Information	5
3.1. Previous Research.....	5
3.2. Induration Furnaces and Wet Scrubbers.....	6
4. Methods	9
4.1. NaCl Addition to Greenball: Hibbing Taconite and United Taconite	9
4.1.1. Straight-Grate (Hibbing Taconite).....	9
4.1.2. Grate-Kiln (United Taconite).....	10
4.2. Focused Halide Injection at Hibbing Taconite	10
4.3. In-Scrubber Oxidation: Slip-Stream Test at Keewatin Taconite	11
4.4. Measurement Methods.....	13
4.4.1. Stack-gas Hg Measurement	13
4.4.2. Scrubber Water Sampling and Analysis	14
4.4.3. Greenball Analysis.....	16
4.5. Estimating Mercury Capture Efficiency For Wet Scrubbers	17
5. Results.....	18
5.1. NaCl Addition to Greenball (Hibbing Taconite and United Taconite).....	18
5.1.1. Straight-Grate (Hibbing Taconite).....	18
5.1.2. Grate-Kiln (United Taconite).....	20
5.2. Focused Halide Injection at Hibbing Taconite	23
5.3. In-Scrubber Oxidation: Slip-Stream tests at Keewatin Taconite	26
6. Discussion	29
7. Conclusions.....	34
8. Acknowledgements	35
9. References.....	36
10. Appendices – Miscellaneous Data	39
10.1. Appendix I: Hibbing Taconite NaCl-Addition To Greenball	39
10.2. Appendix II: United Taconite NaCl-Addition to Greenball	43
10.3. Appendix III: Hibbing Taconite Focused Halide Injection Tests.....	47

1. Summary

Short-term tests were conducted at taconite processing facilities as part of a long-term Minnesota DNR study designed to identify potential means to decrease mercury in stack emissions. Three of these tests involved addition of chloride and bromide salts to operating induration furnaces in an attempt to convert elemental mercury (Hg^0) to oxidized mercury (Hg^{+2}), the latter form of which can be captured by existing wet scrubbers. A series of experiments was also performed on “slip-stream” gases from an operating taconite processing plant to evaluate use of chemical oxidants added directly to water in wet scrubbers to enhance capture efficiency for elemental mercury.

NaCl addition to the greenball feed in a straight-grate facility decreased total mercury (Hg(T)) in stack-gases by 5 to 9%, depending on chloride application rate. Injection of NaCl and CaCl_2 salt solutions directly into the preheat zone of a straight-grate furnace decreased Hg(T) in stack-gas by 6 and 13%, respectively. In contrast, NaCl addition to the greenball feed at a grate-kiln facility at rates similar to those used in the straight-grate tests resulted in 18 to 32% decrease in stack-gas Hg(T) . Differences in results for the two types of furnaces can be attributed to differences in gas composition in the preheat zones. HCl is thermally generated from NaCl deep in either type of furnace, but bypasses the preheat zone in straight-grate furnaces and passes directly through the preheat zone in grate-kiln furnaces.

Bromide salts were much more effective than chloride salts at oxidizing mercury in straight-grate furnaces. Injection of NaBr and CaBr_2 salt solutions into the preheat zone of a straight-grate furnace resulted in 62 and 64% decreases in Hg(T) in stack-gas. In addition, mercury passing through the wet scrubber was almost fully oxidized, as measured by a continuous mercury monitor on the stack. These results suggest that at least a portion of the injected Br salts were converted rapidly to highly reactive Br_2 . This gas species effectively oxidized the majority of Hg^0 to Hg^{2+} and enhanced capture of mercury in the wet scrubber. However, Br_2 generation may lead to other corrosion and environmental issues that will need to be studied before this method can be used to control mercury in taconite processing plants.

In slip-stream tests, it was found that hydrogen peroxide (1500 ppm H_2O_2) solutions captured about 10-15% of the mercury in process gas, which was less than the baseline capture rates for weakly buffered NaHCO_3 solutions (2.5 mmolal). However, solutions containing approximately 100 ppm of a proprietary EPA oxidant resulted in mercury capture rates in excess of 80%, pointing to the need for a plant-scale test using this oxidant. A surprising result was that the fraction of mercury captured by NaHCO_3 solution in these tests was much greater than the fraction of mercury present in oxidized form in the raw waste gas. This suggests that an oxidizing component present in waste gas, possibly Cl_2 , oxidizes Hg^0 upon contact of the gas with water.

2. Introduction

The taconite industry arose on Minnesota's Iron Range in the late 1940's and early 1950's as high grade "oxidized" ore declined and technologies to utilize the more extensive but lower grade "taconite" ore were developed. Today, Minnesota supplies approximately 40 to 50 million tons of taconite pellets to steel makers throughout the Great Lakes region each year. The primary iron source is magnetite (Fe_3O_4) which is concentrated from taconite ore by grinding and magnetic separation. This concentrate is combined with either bentonite or an organic binder, rolled into cm-sized balls (referred to as greenballs), and converted to hardened pellets of hematite (Fe_2O_3) by heating in air to high temperatures (2400F) in a process referred to as "induration". In some cases, a limestone fluxing agent, needed for steel making, is added to the greenball prior to induration.

All of Minnesota's existing taconite processing plants were built in the 1950's to 1970's, well before mercury was recognized as a global pollutant. It was only recently recognized that mercury present in taconite concentrate is released to process gases during induration and that the majority of this mercury is not captured by the plants' wet scrubbers, but released to the atmosphere. Collectively, taconite processing in Minnesota releases approximately 350 to 400 kg of mercury to the atmosphere each year (Engesser and Niles, 1997; Jiang et al., 2000; Berndt, 2003; MPCA, 2006). Although this amount is small compared to global emission rates, it represents Minnesota's second largest industrial source of mercury to the atmosphere. It appears, therefore, that reduction in this source will be needed for the state to reach future mercury reduction goals (MPCA, 2006).

This report is the third in a series of studies conducted by the Minnesota Department of Natural Resources in an attempt to find cost effective means to decrease mercury in taconite stack emissions. The first two reports evaluated the source and fate of mercury in taconite processing plants (Berndt and Engesser, 2005 a, b). This report provides results of short-term tests recently conducted at taconite processing facilities to evaluate potential mercury control methods. In addition, the Minnesota DNR commissioned a study by the University of North Dakota's Environment and Energy Research Center (EERC) to independently evaluate feasibility and cost of borrowing other technologies being developed for the coal-fired power industry (Laudal, 2007a). A third study commissioned by the DNR during this biennium was conducted by the University of Minnesota, Coleraine Minerals Research Laboratory, and involves characterization of scrubber solids to determine how best to separate mercury from recoverable iron oxides. The final results from that study were not available at the time this document was being prepared.

3. Background Information

3.1. Previous Research

The DNR conducted its initial study summarizing past data, research, and reports on mercury releases and distribution related to taconite mining in 2003 (Berndt, 2003). Berndt et al. (2003) also conducted a study of scrubber waters in taconite induration plants, showing that large amounts of mercury are captured by existing equipment, and that this mercury is present in both dissolved and particle-bound forms. Following capture from process gas, dissolved mercury decreases while particulate-bound mercury increases in scrubber water on a time scale of minutes to hours.

This study, and an earlier study by Benner (2001), indicated that some control of mercury at taconite plants might be achieved by eliminating the mercury-enriched scrubber solids from processing loops that can recycle solids (and adsorbed mercury) back to the furnace. Based on estimates of Berndt and Engesser (2005a), eliminating mercury recycle loops in taconite companies would remove from 0 to 30% of the mercury currently being emitted. Berndt and Engesser (2005b) and Benner (2007) have worked to identify cost effective means to separate mercury from recyclable iron units. For emission reductions above the 30% level, however, these mercury-recycle loops must be eliminated *and* scrubber capture efficiencies for mercury must be improved.

Berndt and Engesser (2005a) studied the release of mercury in taconite induration plants and found a correlation between capture rate in wet scrubbers and the rates at which HCl and scrubber dust were generated during induration. This study, along with thermal mercury release experiments conducted by Benner (2005) and Galbreath (2005), Mössbauer spectroscopic measurements for heated taconite pellets (Berquó, 2005), and experimental data on adsorption of mercury to maghemite (Galbreath et al., 2005), suggested mercury release during taconite induration is a relatively complex process. Mineralogic conversion of magnetite to maghemite and hematite is closely tied to release of mercury as either Hg^0 or HgCl_2 , depending on availability of HCl in the process gas. This affects scrubber efficiency for mercury capture, since HgCl_2 and other oxidized mercury species are more easily captured by existing wet scrubbers than Hg^0 . Mass balance estimates suggested approximately 10-15% capture of mercury was typical for straight-grates while approximately 30% capture was found at grate-kilns.

Berndt and Engesser (2005b) studied the fate of mercury captured by wet scrubbers in taconite processing plants. They determined that most of the mercury in scrubber waters adsorbs to non-magnetic particles, presumably hematite, and avoids the magnetic particles, maghemite and magnetite. This means that one manner to permanently reduce mercury emissions from taconite processing plants is to increase the fraction of mercury captured by the wet scrubbers and then use mercury adsorption and magnetic separation to focus the captured mercury into tailings basins where the tailings sequester the mercury.

Two primary means to increase oxidation of mercury that were suggested by bench-top experiments included addition of HCl to process gas (Galbreath et al., 2005; Berndt and Engesser, 2005b) and addition of oxidizing compounds to scrubber water (Hutson and Srivistava, 2006). Other methods, such as ozone or activated carbon injection to process gas may also have application to the taconite industry (Laudal, 2007a), however, these methods appear to be more costly to test and implement and have, thus far, not been studied. In addition to HCl, other halide species in gases have been known to oxidize mercury in power plant applications. These include Cl, Cl₂ and especially Br₂ (Liu et al, 2007). Although these gas species are likely expensive and dangerous to inject, they are known to form by thermal decomposition of halide salts during coal combustion (Edwards et al, 2001; Benson, 2006; Liu et al, 2007; Agarwal et al, 2007).

Although similar and more extensive studies have been conducted at other types of facilities (e.g., coal-fired power plants, waste incinerators, gold mining facilities), the taconite industry is intrinsically unique from each of these industries, owing to the widespread occurrence of relatively reactive iron-oxides which have not only been shown to participate in reactions involving mercury transport but can also impact mercury measurement (Laudal, 2007b). The experiments detailed in this report are the first of their kind conducted specifically for the taconite industry, and were, thus, designed to test mercury control methods more on a conceptual level than on a specific practical level.

3.2. Induration Furnaces and Wet Scrubbers

Although all taconite companies use heat and air to oxidize greenballs in induration furnaces, there are two very different types of furnaces used on the Iron Range to accomplish this task: straight-grate and grate-kiln.

Hibbing Taconite, located near Hibbing, MN, and Mittal Steel, located near Virginia, MN, fire greenballs in straight-grate furnaces (Figure 3.2.1). Large combustion chambers located in the center of the furnace provide heat to pellets that move past the firing zone on a large grate. Outside air, heated as it cools the fired pellets in the second cooling zone, dries and heats fresh greenball in the up-draft drying zone. Meanwhile, air introduced in the combustion chambers and/or in the first cooling zone passes through the pellet bed in the firing and preheat zones, and then again in the down-draft drying zone. Northshore Mining, located in Silver Bay, MN, also has straight-grate furnaces, which were the first of their type to be built in Minnesota. These furnaces have a slightly different air flow pattern than do the Hibtac or Mittal straight-grate furnaces.

Keewatin Taconite, near Keewatin, MN, Minntac, near Mountain Iron, MN, and United Taconite, close to Eveleth, MN all operate grate-kiln furnaces (Figure 3.2.2). Most heating in this type of system is provided by a large burner that projects a flame up a large rotating kiln as greenballs, fed from a moving grate, spill through the kiln. Air used to cool pellets in the cooler is cycled into the drying zone, while hot gas from the kiln is passed through the pellet bed in the preheat zone and used ultimately to dry pellets in the down-draft drying zone.

Plants that produce fluxed pellets (Minntac and Mittal) find it necessary to add additional heat to convert the limestone flux to lime. This heat is added through burners located in the preheat zone. United Taconite and Hibtac add small amounts of limestone to the pellets in order to increase pellet strength but at rates much less than used in production of Minntac and Mittal fluxed pellets. Keewatin Taconite does not add limestone to its pellets.

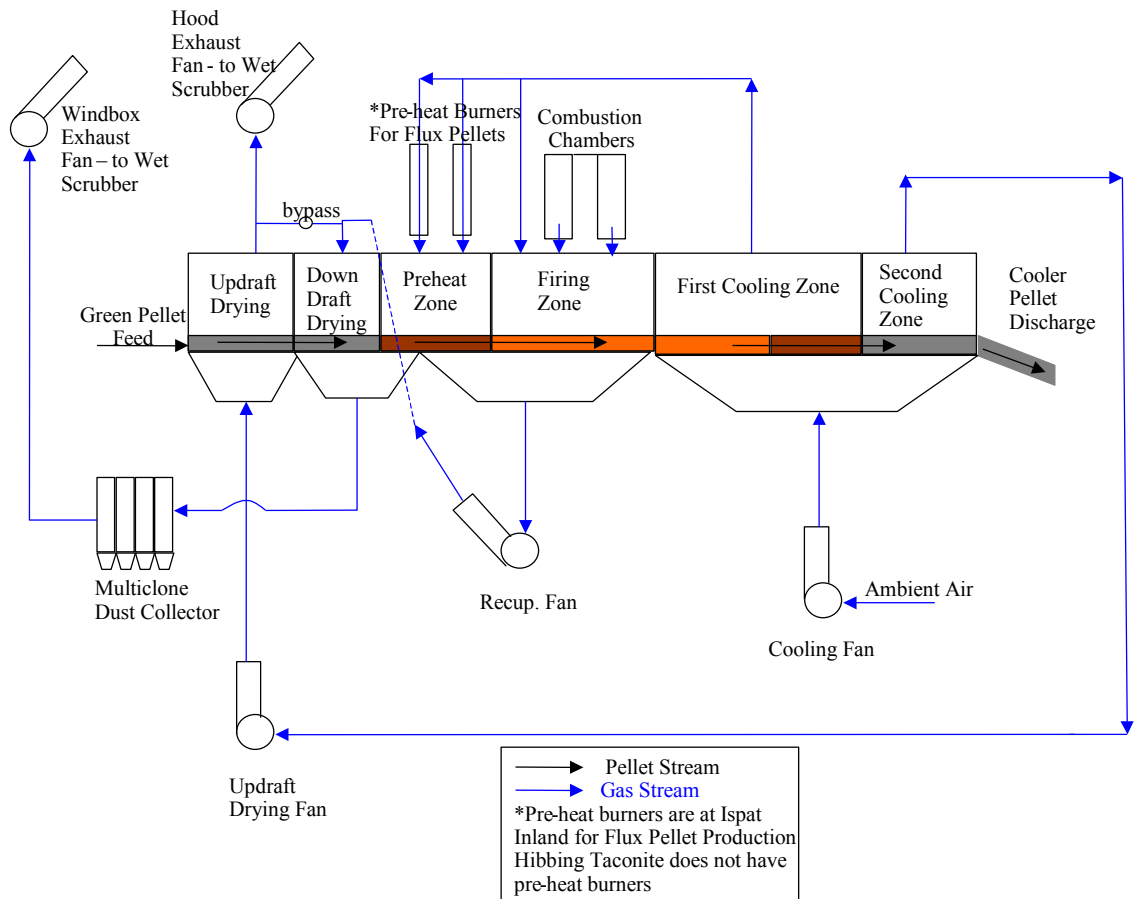


Figure 3.2.2: Diagram of a straight-grate induration furnace. Gases are passed numerous times through the pellet bed in order to dry, heat, and cool the pellets as they pass along a large grate. “Windbox exhaust” gases are derived from the down draft and preheat zones and passed through multiclone dust collectors before entering the wet scrubber/ exhaust system. “Hood exhaust” gases from the updraft drying zone originate from the second cooling zone and pass directly into the wet scrubber/ exhaust system.

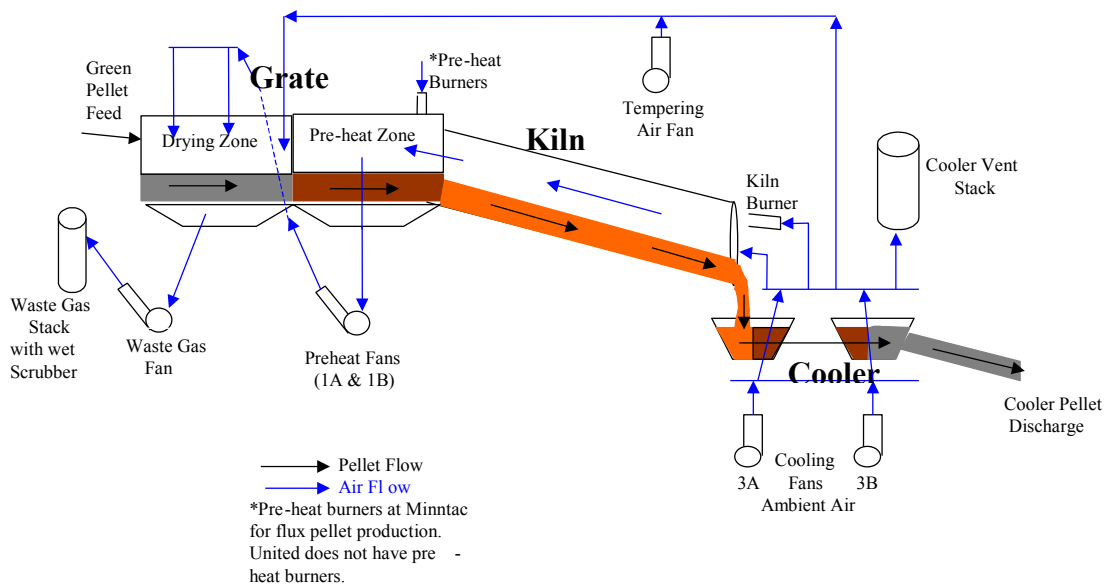


Figure 3.2.2: Diagram of a grate-kiln induration furnace. Combustion gases for heating the pellets are directed up a large rotating kiln and then down through the pellet bed in the preheat zone. The gases are then used for initial heating and drying of the greenball (or pellet) feed. Gases used for cooling the hot pellets are also used to dry and heat the pellets. Depending on the operation, the waste gases are passed through either one or two wet scrubbers and vented through one or two separate stacks.

In addition to differences in furnace types and pellets produced, the facilities use somewhat different methods for removing particles and pollutants from process gas (Table 3.2.1). Keewatin Taconite, United Taconite, and Mittal Steel all have recirculating scrubbers, while Hibbing Taconite has a single-pass scrubber. Minntac has four single-pass scrubbers and one recently built recirculating scrubber. Keewatin Taconite adds lime to control pH in its recirculating scrubber as does Minntac in its new recirculating scrubber. Northshore Mining Co uses wet-wall electrostatic precipitators (WWESPs) and does not use wet scrubbers.

Table 3.2.1: Taconite processing facilities on Minnesota’s Iron Range.

<i>Plant</i>	<i>Lines</i>	<i>Furnace type</i>	<i>Pellets</i>	<i>Scrubber type</i>
US Steel, Keewatin Taconite	1	Grate-Kiln	Standard	Recirculating, Lime added
Hibbing Taconite	3	Straight-Grate	Standard	Single Pass
US Steel, Minntac	5	Grate-Kiln	Standard/ Fluxed	4 Single Pass 1 Recirculating, Lime added
United Taconite	2	Grate-Kiln	Standard	Recirculating
Mittal Steel	1	Straight-Grate	Fluxed	Recirculating
Northshore Mining Co.	3	Straight-Grate	Standard	Wet Wall ESP

4. Methods

4.1. NaCl Addition to Greenball: Hibbing Taconite and United Taconite

Galbreath (2005) achieved approximately 90% oxidation of Hg^0 released from greenball in bench scale tests by adding 100 ppmv HCl to the carrier gases. Although direct addition of HCl to taconite process gas is probably an unreasonable approach, these results suggest that one means to limit mercury emissions during taconite processing is to add components to greenball that can decompose to form HCl during taconite processing. Berndt and Engesser (2005a) showed that Cl salts present in greenball (dissolved in pore fluid) are volatilized quantitatively during induration, most likely as HCl, and carried to the wet scrubber where it is captured along with particles and other water-soluble gases. These results suggested that addition of NaCl to greenball should generate HCl and potentially lead to decreased mercury in stack emissions.

This method was tested at two plants: one (Hibtac) a straight-grate and the other (United Taconite) a grate-kiln plant. These plants were selected specifically because the background Cl⁻ in their processing waters and greenball is lower than at either Mittal or Minntac, and because, at the time these studies were being conducted, Keewatin Taconite's wet scrubber was relatively new and untested. The NaCl addition method may be limited by the potential for corrosive effects of alkali chloride salts on grate bars (Mohanty and Shores, 1993). If the tests for NaCl addition yielded positive results for mercury control, then corrosion studies would be required before mercury control by this method would be considered a viable alternative.

4.1.1. *Straight-Grate (Hibbing Taconite)*

In this test, NaCl was added to the filtered concentrate (filter-cake) at Hibbing Taconite's Line 3. The advantage of adding NaCl by this method is that the NaCl would be reliably mixed throughout the pellet bed as greenballs enter the induration furnace. It was estimated that between one and two hours would be required for NaCl added to filter cake to reach steady-state concentration in the greenball feed to furnaces. This is because filter cake is stored in day-bins, and because considerable cycling takes place in the balling drum circuit owing to transfer inefficiencies associated with greenball sizing. Thus, each test was conducted for a period of three hours: two hours for steady-state NaCl concentration to be achieved in greenballs, and one hour to allow for samples to be collected.

Two tests were conducted, the first adding NaCl at a rate of 25 lbs per hour and the second adding NaCl at a rate of 50 lbs per hour. The greenball feed rate was 500 long tons per hour during these tests and, thus, the application rates were equal to approximately 0.5 and 1.0 lbs of NaCl for every 10 long tons of greenball. Baseline samples for evaluating background concentrations of mercury, chloride, and other elements were collected before the tests were started and following completion of the tests after the added NaCl was cleared from the system.

This plant vents gas through four stacks (Stacks A, B, C, and D) for each production line. Because it was cost prohibitive to measure mercury using continuous mercury monitors (CMMs) (see section 4.4.1) on all four stacks, continuous monitoring was only performed in the stack with the highest mercury concentration. Non-continuous stack-gas mercury measurements were also made using Flue-gas Absorbent-trap Mercury Speciation traps (FAMS; see section 4.4.1) on both stacks A and B during the tests and on all four stacks when the plant was operating under baseline conditions on the day following the Cl-addition tests.

4.1.2. Grate-Kiln (United Taconite)

Owing to much longer residence time for filter cake in the large “day bins” at United Taconite (compared to Hibbing Taconite), NaCl was added at this plant directly to the top of greenballs that had already been formed, rather than to the filter cake feeding the balling drums. The NaCl was added before the balls were tumbled onto the grate, however, to permit as least some distribution of NaCl throughout the pellet bed. All testing at this plant was performed on “Line Two”.

NaCl was added at rates of 30 and 60 lbs per hour. The greenball feed rate was approximately 600 long tons per hour so, as was the case at Hibbing Taconite, application rates were approximately 0.5 and 1.0 lbs of NaCl per 10 long tons of greenball. Baseline samples of scrubber water and greenball were collected to monitor mercury and chloride both shortly before NaCl addition began and again in the morning following completion of the tests. Similar to the straight-grate tests at Hibbing Taconite, each NaCl addition test was run for a period of three hours: two hours for steady-state to be achieved and one hour for measurements to be conducted.

Unlike Hibbing Taconite, which has four stacks releasing gas from one large wet scrubber, United Taconite’s Line Two has two independent scrubbers each venting through its own stack. Beneath each stack is a thickener which helps eliminate particulates in water that recirculates to the scrubber. A sampling port located at the base of each thickener allows sampling of water and scrubber solids from these sites (the “underflow”).

Scrubber thickener underflow water was sampled for both stacks during the tests and analyzed for mercury, cations, and anions. However, gases were monitored by CMM (See section 4.4.1) for only one of the two stacks (2B). This stack was found to have higher Hg concentration than the other stack (2A) during previous visits to the plant. FAMS (See Section 4.4.1) measurements were made on both stacks throughout the tests for comparison purposes.

4.2. Focused Halide Injection at Hibbing Taconite

Halide salts exposed to elevated temperatures in coal-fired utilities generate other gases (HCl, Cl₂, HBr, and Br₂) that can help to oxidize elemental mercury (Edwards et al, 2001; Benson, 2006; Liu et al, 2007; Agarwal et al, 2007). Because little experience exists on the subject of halide behavior in taconite furnaces, a third set of tests was conducted whereby NaCl, NaBr, CaCl₂, and CaBr₂ salts were added directly into the preheat zone at a straight-grate (Hibbing Taconite’s line three). The

chemical and physical behavior of salt solutions sprayed into a taconite furnace is virtually unpredictable, owing to rapid heat transfer and changes in temperature, unknown gas-flow patterns, high vaporization and thermal expansion rates of the resulting steam, and unknown rates for key chemical reactions. Rather than attempt to test or model all of these parameters, it was decided to directly test the method in an operating induration furnace using “best guesses” on flow and spray parameters.

Each of the four salts was sprayed into the furnace at approximately 50 lbs per hour, all dissolved in water as 10 wt% solutions. Because these salts were added directly to the furnace, response was expected to be nearly immediate and so test-periods were shortened to one hour. Following an initial baseline period during which no salt was sprayed, NaCl was first added for a period of one hour. Greenball and scrubber water samples were collected 30 minutes into the test to monitor the behavior of Hg, Cl, Br, and other anions and cations such as Ca and Na in the scrubber water. Following NaCl addition, the other salts were tested sequentially in the order: NaBr, CaCl₂, CaBr₂. Each test followed a one hour period of time during which no salt was sprayed into the furnace. Scrubber water and greenball samples were collected beginning 30 minutes after addition of the salt had begun.

As was the case for NaCl addition to greenball at Hibbing taconite, the CMM was employed on Stack A. This stack was found to have the highest mercury during previous testing at this plant. FAMS was not used to measure mercury in this case because the CMM was considered a more reliable means to assess mercury for this specific application.

It is important to note that halide addition method may be limited by the potential for corrosive effects of alkali chloride salts on grate bars (Mohanty and Shores, 1993). If the tests for halide addition yielded positive results for mercury control, corrosion studies and cost analysis would be required before mercury control by this method would be considered a viable alternative.

4.3. In-Scrubber Oxidation: Slip-Stream Test at Keewatin Taconite

A number of studies have suggested that adding oxidizing chemicals directly to scrubber water (rather than to process gas) may provide an alternative means to control mercury in stack emissions for coal-fired power plants that have wet scrubbers (Overcamp, 1999; Korrell et al, 2003; Hutson and Srivistava, 2006). A preliminary assessment of potential control methods was made based on likely cost, effectiveness, and environmental impact of the oxidants. H₂O₂ was selected as one potential oxidant based on its low cost, widespread availability, its known ability to oxidize mercury at high concentrations, and reported success when using H₂O₂ to control mercury along with other additives in relatively specialized applications (Laudal, 2007a). In addition, H₂O₂ and ferric iron are known, in some cases, to have a synergistic effect on oxidation processes by generating highly oxidizing hydroxyl radicals (e.g., Fenton’s reagent). Another chemical, referred to here as EPA_{OX} was selected following consultation with Nick Hutson, (e.g., Hutson and Srivistava, 2006) after it was determined that this proprietary reagent is also inexpensive, widely available, and likely to decompose to harmless chemicals in the environment.

A special system was designed to screen oxidants for their effectiveness in capturing mercury from taconite process gases (Fig. 4.3.1). This system, referred to here as the Quench Liquid Injection Probe (QLIP) was configured specifically to prevent clogging and interference from accumulating particulates in a frit and to maximize contact between slip-stream gas and the liquids being tested. During a test, the scrubbing solution (with or without oxidant) is continuously circulated to the tip of the sampling probe using a peristaltic pump, and then sucked along with the process gas back into the liquid reservoir. Oxidized mercury and particulates are captured by the liquid, while insoluble gases pass through the system. Any mercury not collected by the “scrubber” solution is collected and speciated by a series of separate dry sorbent traps in the FAMS system (see section 4.4.1).

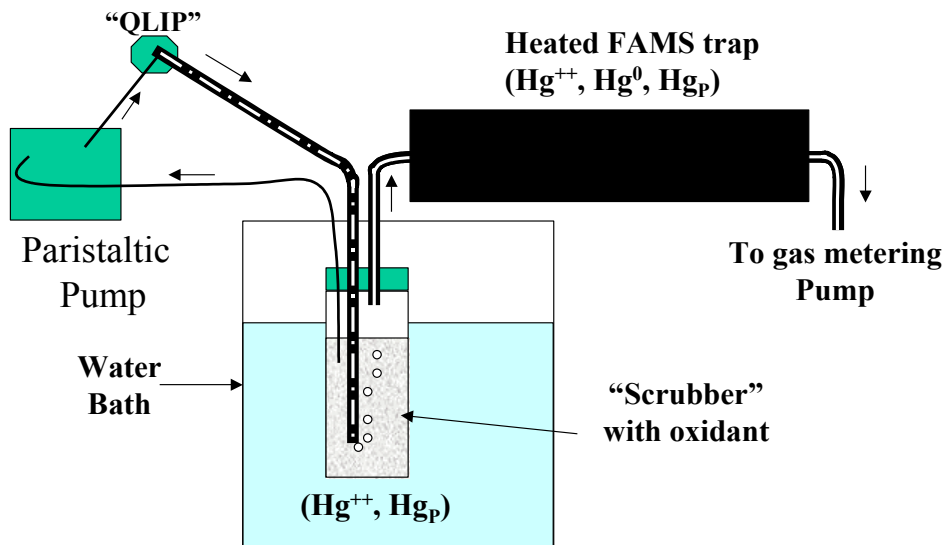


Figure 4.3.1 Quick Liquid Injection Probe (QLIP) designed for use in a slip-stream study. A peristaltic pump injects the scrubber solution containing oxidants into a sampling probe that is inserted into the ductwork at an operating processing facility. This liquid returns to the sampling jar with gases being pumped from the duct. Oxidized mercury is captured in the scrubber while any mercury remaining in the process gas is captured and speciated by the FAMS traps (see section 4.4.1).

Tests were conducted sequentially and side-by-side in the order shown in Table 4.3.1. All scrubber solutions tested were weakly buffered at near-neutral pH conditions using 2.5 mmolal $NaHCO_3$. Baseline conditions were assessed both by using $NaHCO_3$ solutions with no oxidant added and also by conducting tests with no “scrubber” solution added to the QLIP. In between baseline evaluations, solutions containing the same concentration of $NaHCO_3$ and either 1500 ppm H_2O_2 or approximately 100 ppm EPA_{OX} were tested in the apparatus. Following each test, a five ml aliquot of the reactant solution was collected and sent to the University of Minnesota Geochemistry laboratory for analysis by anion chromatography (Cl , Br , NO_2^- , NO_3^- , SO_4^-). Following a final measurement of pH, the remaining solution was preserved with $BrCl$ and shipped to Cebam, Inc., Seattle, WA, for measurement of total captured mercury. The University of Minnesota, NRRI, supplied the constant temperature water bath and FAMS apparatus, including the gas pump. This group also performed mercury analysis on sorbents in the FAMS traps.

Table 4.3.1: Additives used for slip-stream tests at Keewatin Taconite. Baseline tests (NaHCO₃ with QLIP) were conducted in parallel with tests conducted without the QLIP apparatus.

<i>ID</i>	<i>“Scrubber” Solution</i>	<i>Parallel FAMS test w/o QLIP?</i>
Baseline-1	<i>0.0025 M NaHCO₃</i>	Yes
H ₂ O ₂ -1	<i>0.0025 M NaHCO₃+1500 ppm H₂O₂</i>	No
EPA _{OX} -1	<i>0.0025 M NaHCO₃ + 100 ppm EPA_{ox}</i>	No
Baseline-2	<i>0.0025 M NaHCO₃</i>	Yes
H ₂ O ₂ -2	<i>0.0025 M NaHCO₃+1500 ppm H₂O₂</i>	No
EPA _{OX} -2	<i>0.0025 M NaHCO₃ + 100 ppm EPA_{ox}</i>	No
Baseline-3	<i>0.0025 M NaHCO₃</i>	Yes

4.4. Measurement Methods

Extensive sampling and analysis of solids, liquids, and gases was performed prior to and during these tests to evaluate the best means to measure and monitor mercury in various components of the taconite process. However, chemical analysis is a non-trivial issue for mercury measurement in taconite process gases and scrubber waters owing to its relatively low concentrations, the presence of reactive gaseous species in taconite processing streams (such as Br₂, Cl₂, SO₂), and the ubiquitous occurrence of iron-oxide particles that can react with mercury in several ways (Berndt and Engesser, 2005a, 2005b; Laudal, 2007b). These issues will be discussed briefly in this report but are also the subject of continued research in other on-going studies.

4.4.1. Stack-gas Hg Measurement

Two primary methods were used to analyze the composition of stack-gases in this study: CMMs (continuous mercury monitors) and FAMS (flue gas absorbent-trap mercury speciation). CMMs systematically collect and automatically analyze either gaseous elemental mercury, referred to as Hg(0) or Hg⁰, or total mercury, Hg(T), every few minutes. CMMs are the preferred method for gas analysis during plant tests because they provide virtually instantaneous feed-back that is needed when relating changes in process to change in stack-gas chemistry. However, FAMS analysis is a much less expensive method that provides an average value for gas concentration over a period of time and additionally reports values for three forms of gaseous mercury: particulate Hg(P), oxidized gaseous (Hg²⁺), and elemental (Hg⁰). If FAMS could be proven reliable for measuring mercury in taconite stack-gases, it could be used to assess gas composition for plant balance and monitoring applications and to assess mercury speciation in applications where speciation is important.

Several CMM methods were tested and/or used to analyze gases during these tests. The first method, involved filtering the stack-gas at the sampling duct followed by transport to the analytical shed for processing and analysis. This method was used for analyzing mercury in gases during NaCl addition to greenball at Hibbing Taconite

and United Taconite. A second method that was considered involved sampling gases through an ISP (Inertial Separation Probe) that effectively eliminates particles from entering the tubing by increasing the velocity of the gas at the sampling point. This method was tested at a taconite processing facility, but appeared to provide inferior results and so was not used in this study (Laudal, 2007b). A third method involved injecting a conditioning liquid into the duct at the gas sampling site and transporting the resulting gas/liquid mixture through heated tubing to the analytical shed. This method was also tested at a taconite processing facility by Laudal (2007b), and then subsequently used at Hibbing Taconite during the focused halide injection tests.

Collection of samples for FAMS analysis was performed using three different methods. The normal method involved inserting a heated vessel containing the FAMS sorbent train directly into the duct. This method eliminates condensation effects and allows any particulates in the gas phase to collect in a dry filter in the front end of the FAMS trap. This method was used to sample stack-gases when NaCl was added to greenball at the straight-grate and grate-kiln facilities.

The second FAMS method is depicted in Figure 4.3.1. This method involves placing a heated FAMS trap at the end of a liquid injection/trap system (QLIP = Quench Liquid Injection Probe) that removes particulate and oxidized mercury from the process gas during transport to the FAMS device. This system was developed to minimize sampling artifacts related to oxidation and capture of mercury by taconite dust in the sampling tubes. The FAMS method, in this case, only quantifies and speciates mercury that remains in the gas after passing through the QLIP. This method was only used for the slip-stream tests at Keewatin Taconite, although limited testing was also performed under baseline conditions at Hibbing Taconite prior to the focused halide injection tests.

In the third FAMS method, the system was connected to the sampling port by a one-meter long unheated Teflon tube. No effort was made to prevent condensation from occurring in the tube connecting the port to the FAMS. However, the FAMS was kept at high temperature to prevent condensing water from interfering with the material in the dry sorbent traps. This method was only used to provide results to compare to tests conducted when the QLIP system was used.

In all cases, the FAMS sorbent train contains three individual compartments for isolating different forms of mercury. Particulate mercury is isolated using a quartz fiber filter, oxidized mercury is trapped on a solid KCl sorbent material, and elemental mercury is collected with a chemically impregnated solid carbon sorbent. The solids from each compartment are digested and analyzed separately to provide the speciation. All FAMS testing in the study was performed by the University of Minnesota, Coleraine Minerals Research Laboratory.

4.4.2. *Scrubber Water Sampling and Analysis*

In all cases, scrubber water sampling ports were chosen at locations that provided the freshest sample of scrubber water possible. Hibbing Taconite, for example, combines scrubber water effluent from three lines into one stream flow that leads back to the concentrator. The line tested in this case, Line 3, has its own valved

outlet for sampling of the blow-down water before it is added to the larger single stream.

United Taconite recirculates scrubber water using thickeners located beneath the wet scrubbers. The sample ports for scrubber water at United Taconite permit collection of the underflow water from each of its scrubber thickeners. Water from the top of the thickeners is pumped back to the scrubber and reused. This recirculation and thickening of scrubber water results in a much larger amount of suspended solids in United Taconite scrubber water compared to Hibbing Taconite blow-down water. Moreover, the contact time between water and particles prior to sampling is greater at United Taconite compared to single-pass scrubbers such as at Hibbing Taconite.

Scrubber water sampling at Keewatin Taconite is similar to that at United Taconite. There are valves located beneath the scrubber water thickener permitting sampling of the underflow, whereas water from the top of the scrubber is reused by the wet scrubber.

All water samples for mercury analyses were collected using “clean-hands, dirty-hands” procedures, whereby the clean bottles were placed into sealed plastic bags prior to leaving the laboratory and not opened except during sampling, and then again later when the analysis was being conducted. Only the designated clean-hands person, wearing clean plastic gloves (powder-free), handled the sample bottles when they were outside of the plastic bag. All other sample processing was conducted quickly and efficiently by the so-called “dirty-hands” person. These procedures were implemented to minimize the risk of contamination from plant dust and of cross-contamination between samples.

In addition to these special precautions, procedures were consistently evaluated using blanks to assess the degree of mercury contamination associated with filtration and sampling. Procedural blanks were collected at each site during each visit. One bottle was filled at the sampling site with deionized water brought from the laboratory. In addition, deionized water was filtered at the sampling location and both the water and the filter were saved for analysis. The level of contamination introduced by our procedures was insignificant relative to the concentration of mercury found in samples analyzed in this study.

Samples were analyzed by Cebam Analytical, Inc., located in Seattle, Washington. Filtered water samples were digested with BrCl over night, and then analyzed by SnCl₂ reduction, gold trap collection, and CVAFS detection (modified EPA1631). This laboratory participates in many round-robin blind sampling programs and routinely ran duplicates and standards to ensure accuracy.

Mercury concentration of the suspended solids, Hg(P) (in ng/g on a dry particle basis), was determined by analyzing the scrubber solids filtered from the water. Filters containing scrubber solids from the above procedures were dried at 104°C for analysis, weighed, and digested in hot acid (HCl/HNO₃, 3/1). Mercury was analyzed using SnCl₂ reduction and gold trap collection, followed by CVAFS detection (modified EPA1631). Certified reference materials WS-68, NIST2709, and GSR-2 were used to assess recovery and analytical accuracy. As was the case for

water samples, solids were digested and analyzed by Cebam Analytical, Inc., located in Seattle, Washington.

A new method was developed for analysis of total mercury in unfiltered waters containing suspended solids. This method was developed by Cebam, Inc., when lab personnel noticed that emptied sampling bottles left to dry over a period of time took on a reddish color. This reddish color was believed to be due to adherence of fine iron-oxide dust particles to the glass. The new method was developed to allow all of the mercury in a sample, including that on particles adhering to the surface of the bottle, to be analyzed with a single mercury analysis.

By this method, the visible suspended solids were allowed to settle from solution and the bulk of the water containing only the smallest particles was then decanted and treated with BrCl to oxidize the mercury. The remaining slurry was then digested in hot acid (HCl/HNO₃, 3/1) added directly to the sampling jar where it could dissolve mercury from both the visible solids as well as from any mercury on solids adhering to the surface of the sampling bottle. The contents of the jar were then added to the decanted portion and total mercury in the mixture was analyzed by SnCl₂ reduction, gold trap collection, and CVAFS detection (modified EPA 1631).

Importantly, it was found during the study that some scrubber waters contain components that are capable of reducing oxidized mercury to elemental mercury during sample storage. Elemental mercury is lost from the solution when this occurs and will be missed in the analysis. BrCl was routinely added to fix the samples prior to shipment, but not until after it was found that some of the samples in this study had potentially lost mercury due to this reduction process. This will be discussed further in relation to specific tests where it was thought mercury loss occurred (NaCl addition to a straight-grate at United Taconite).

4.4.3. Greenball Analysis

Greenball samples were commonly collected as a means to assess mass balance with respect to components entering and leaving the furnace (Cl and Hg, in particular). The sample collection point, in all cases, was at the front end of the induration furnace, just prior to the point where the greenball is fed onto the grate. The samples were collected using a spatula and placed into clean, acid-washed 20 ml bottles with Teflon-lined lids. The damp greenball samples, which contain approximately 9 to 10% moisture by weight, were shipped to Cebam, Inc., for drying and analysis of mercury. Greenball Hg concentrations were determined on a dry-weight basis by Cebam, Inc., using the same technique described above (Section 4.4.2) for solids filtered from scrubber water.

For Cl addition to straight-grates, the effectiveness of Cl addition to greenball was tested by leaching fresh greenballs with water and analyzing the water by Ion Chromatography. For these tests, 100 grams of dry greenball material was leached for approximately one week in 100 grams of deionized water. The water was then filtered and analyzed by ion-chromatography at the University of Minnesota, Department of Geology and Geophysics. The resulting concentrations were reported as water-leachable salts on a dry weight basis for the pellets.

4.5. Estimating Mercury Capture Efficiency For Wet Scrubbers

Ideally, estimating mercury capture efficiency for wet scrubbers would involve comparing simultaneously measured mercury concentrations in process gas at the scrubber inlet and outlet. The change in mercury concentration across the scrubber could be divided by the mercury concentration in gas entering the scrubber to obtain the capture efficiency. Unfortunately, this straight-forward method is not possible at Hibbing Taconite or United Taconite where the plants tests were performed. United Taconite does not have a suitable gas sampling port in the ducts leading to its wet scrubber. Hibbing Taconite has two ducts with sampling ports leading to the wet scrubber from different parts of the furnace, but the gases from these ducts mix into a common manifold from which four stacks vent waste gas. Gas flow rates and mercury concentrations from both scrubber-inlet ducts and all four stacks would be required to accurately measure scrubber efficiency for mercury at this plant.

An alternative approach that might be considered to measure capture efficiency at taconite processing plants is the mass balance approach used by Engesser and Niles (1997) and Berndt and Engesser (2005a, b), whereby Hg entering the furnace with greenball is compared to mercury exiting the furnace in scrubber water. However, data provided by Berndt and Engesser (2005a) indicate that mercury has a relatively long residence time in furnaces during taconite induration owing to adsorption and desorption of mercury on the surfaces of pellets, dust particles, and ductwork. Owing to this effect, the mercury entering the furnace may be temporarily out of sync with mercury concentrations in gases and scrubber water exiting the furnace. Thus, the mass balance approach is insufficient for estimating scrubber efficiency for short-term tests such as those conducted here, and likely requires the averaging of fluxes of mercury in major components for inputs and outputs to the furnace over a long term to accurately represent an averaged scrubber efficiency.

For the present case, the goal of the experiments was not to estimate scrubber efficiency, but rather to evaluate changes in mercury emission that occurred as a response to addition of a chemical. For this purpose, we relied on changes in the CMM-measured mercury concentrations in a single stack to evaluate cause/effect relations for the tests. For example, if mercury concentration measured in stack-gases is $6.0 \mu\text{g}/\text{m}^3$ before a control method is applied and $4.0 \mu\text{g}/\text{m}^3$ during activation of the control method, and then subsequently returns to $6.0 \mu\text{g}/\text{m}^3$ following the test period, this suggests that the technique decreased the existing emissions by 33% compared to baseline emissions. However, the true efficiency of the wet scrubber could be significantly higher than this, since monitoring only a change in emission does not take into account the fact that some mercury is already removed by the wet scrubber under baseline conditions. Furthermore, true capture efficiency for the scrubber could be lower than this, owing to possible unaccounted for processes, such as increased adsorption to duct walls taking place during the test period. Non-scrubber related adsorption can temporarily remove mercury at locations upstream from the scrubber and, thus, cause the method used in this study to over-estimate long-term scrubber efficiency in short-term tests. In effect, the results from these short-term plant-scale tests represent an intermediate step in a long-term research process;

control method potential must be evaluated in the presence of process parameters not easily simulated in bench –scale tests before longer-termed tests can be designed.

5. Results

5.1. NaCl Addition to Greenball (Hibbing Taconite and United Taconite)

5.1.1. Straight-Grate (Hibbing Taconite)

Baseline mercury concentration in Stack A before and after NaCl was added to greenball at Hibbing Taconite was approximately $4.3 \mu\text{g}/\text{m}^3$ total mercury (Figure 5.1.1.1), although a plant upset shortly before the test resulted in considerable scatter just prior to testing. This concentration dropped to about 4.1 and $3.9 \mu\text{g}/\text{m}^3$ after addition of 25 and 50 lbs/hr of NaCl to greenball, respectively, indicating 5% and 9% reduction in mercury emission compared to baseline mercury removal from gases in Stack A.

FAMS measurements for Stacks A and B were also made before, during, and following the NaCl addition test (Table 5.1.1.1) while Stacks C and D were only monitored for comparison purposes after all testing was completed. Although the FAMS results for total mercury in Stack A are similar to those indicated by the CMM, all of the values were approximately 10% lower. Furthermore, the FAMS Hg(T) measurements for Stack B showed an increase from 2.00 before NaCl addition was started to 2.74 and 2.79 ng/l during the NaCl injection tests. When NaCl addition to greenball ceased, the FAMS Hg(T) in Stack B increased to $3.57 \mu\text{g}/\text{m}^3$. These data do not follow the Hg trend for Stack A. Because of this, and because there are known interferences for FAMS measurements made in taconite processing gases (Laudal, 2007b), these FAMS data are not considered sufficiently reliable for purposes of drawing conclusions in this report. Full FAMS results for this test, including speciation, are provided in the appendix.

A potential complication for interpretation of these data is that the mercury concentration in the greenball feed to the furnace decreased unexpectedly during the testing period (Table 5.1.1.2). Total mercury in greenball averaged 20.4 ng/g for five samples collected just before NaCl addition began, decreased to 15.8 for the first test period, and finally dropped again to 12.0 ng/g for five samples collected during the second testing period. The average mercury concentration in greenball was 11.9 for five samples collected in the morning on the day following the NaCl addition tests. If stack emissions responded directly and immediately to the mass of mercury entering the furnace, a 40% decrease in mercury concentration would have been expected during the testing period even without NaCl addition. These data provide strong evidence that mercury concentrations in gases exiting the furnace responded much more quickly to changes in the chemistry and conditions of the process gas than they did to changing concentration of mercury in the greenball feed.

The total mercury concentration in scrubber water from Line 3 increased during the tests from 738 ng/l before Cl addition began, up to a maximum of 880 ng/l

during the second testing period, and then returned back to 827 ng/l on the day following the tests (Table 5.1.1.2). This small increase in the concentration of mercury in scrubber water during testing provides confirmation that NaCl addition to greenball in a straight-grate slightly improves the mercury capture efficiency of wet scrubbers.

Na and Cl concentrations in scrubber water are reported along with greenball Cl concentration in Table 5.1.1.3. The increase in dissolved Cl, but not Na, in scrubber water during these tests indicates that the Cl from NaCl is volatilized, most likely as HCl and/or Cl₂, in the furnace and carried to the wet scrubber and captured. Na, meanwhile, is not volatilized to a significant degree, but stays with the pellet product. Full chemical data on anions, cations, and pH in scrubber waters during these tests are provided in the appendix.

Table 5.1.1.1 FAMS measurements for total mercury in Hibbing Taconite stacks A through D (µg/m³). Each value represents the average of three separate measurements. The complete data set for individual samples is available in Appendix I.

Hg(T)	Stack A	Stack B	Stack C	Stack D
Baseline	3.90	2.00		
Cl Test 1	3.49	2.74		
Cl Test 2	3.55	2.79		
Baseline	3.83	3.57	1.54	1.19

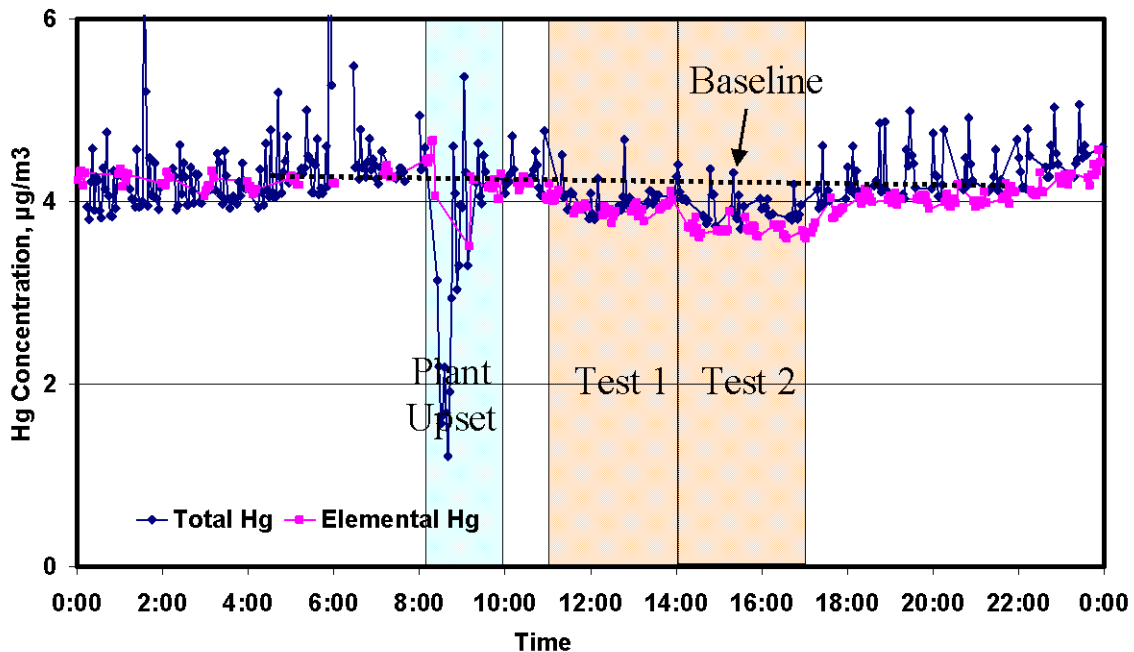


Figure. 5.1.1.1 Total and elemental mercury concentrations as a function of time during addition of NaCl to greenball at a straight-grate (Hibbing Taconite). There was a plant upset (blue) just before the tests were conducted but conditions were stable after that.

Table 5.1.1.2: Mercury concentration in greenballs and scrubber water during the NaCl addition tests performed at Hibbing Taconite. The full data set is provided in Appendix I.

<i>Sample ID</i>	<i>Greenball Hg (ng/g)</i>	<i>Hg(T) (ng/l)</i>	<i>Hg(D) (ng/l)</i>	<i>Hg(P) (ng/g)</i>
Baseline	20.4	738	439	1209
NaCl Add 1	15.8	742	499	1266
NaCl Add 2	12.0	880	587	1394
Baseline	11.9	827	561	1553

Table 5.1.1.3. Greenball Cl concentrations during Cl addition tests at Hibbing Taconite and resulting concentrations for Na and Cl in scrubber water. All concentrations are in units of ppm.

	<i>Greenball Cl (H₂O leachable)</i>	<i>Sodium</i>	<i>Chloride</i>
Make-up	-	-	66.0
Baseline	6.2	60.3	70.4
Cl Addition Test 1	21.0	60.0	75.4
Cl Addition Test 2	42.3	60.2	81.3
Baseline	6.2	60.3	70.7

5.1.2. Grate-Kiln (United Taconite)

As was the case for NaCl addition to Greenball at Hibbing Taconite, there was a plant upset shortly before the NaCl addition test began at United Taconite (Figure 5.1.2.1). There was considerable scatter in the CMM data for Stack 2B, following this time period, but based on concentrations measured shortly before the plant upset and soon after completion of the tests, baseline total mercury concentration in the stack-gas was estimated to be 5.7 $\mu\text{g}/\text{m}^3$. This concentration dropped to about 4.7 and 3.9 $\mu\text{g}/\text{m}^3$, respectively, during the two test periods, suggesting that the Cl-addition to the grate-kiln led to a reduction in mercury emissions from this stack of 18 and 32%, respectively. These changes are significantly higher than those observed for similar levels of NaCl addition to greenball at Hibtac's straight-grate (5 and 9%).

FAMS measurements were collected for both Stacks 2A and 2B during these tests (Table 5.1.2.1). The concentrations measured by FAMS for Stack 2B did not agree well with those reported for the same stack by the CMM. The first baseline FAMS set of samples had an average total mercury concentration of 2.9 $\mu\text{g}/\text{m}^3$, which is about half the value reported by the CMM. Subsequent samples agreed more closely with the CMM data, although total concentrations were generally lower and the oxidized fraction reported by the FAMS is higher than would be expected based on the CMM measurements.

As was the case for the tests at Hibbing Taconite, a close look at the accompanying greenball and scrubber water data present difficulties for data

interpretation (Table 5.1.2.2). First, the greenball mercury concentration appeared to increase from 14.5 ng/g before the tests began up to 18.8 by the end of the second test period. It is unknown whether this effect was due to recycling of excess mercury captured during the test period or if it was due to a change in the concentration of mercury in the concentrate. However, it was also found that the concentration of mercury in the particulates that were being captured by the scrubber for Stack 2B increased from 465 ng/g before the tests began up to 823 ng/g during the first test period and, finally, up to 1165 ng/g by the end of the second test period, before decreasing again to 330 ng/g on the following day. Solids in thickener underflow water for Stack A showed similar increases in the Hg(P) from an initial value of 341 ng/g up to 578 ng/g and 625 ng/g during NaCl addition, and then decreased again to 246 ng/g in the morning of the day after testing was completed. These data suggest that there must have been a relatively large increase in mercury capture rate associated with NaCl addition to greenball at this site.

Unfortunately, mercury concentration in unfiltered scrubber water (Hg(T)) collected during times when mercury should be the highest (since more mercury was being removed from the process gases), turned out to be lower than in unfiltered scrubber water collected under baseline conditions. It is suspected that this was a sampling artifact because most of the mercury in United Taconite's scrubber waters is adsorbed to suspended particles and, thus, the decrease in Hg(T) is inconsistent with the simultaneously measured large increase in Hg(P) values. The conditions for these samples are consistent with those reported previously to cause reemission of Hg from wet scrubbers in the power industry (Currie, 2006): low pH and high SO₂. SO₂ dissolves in water as H₂SO₃, which reacts with dissolved Hg²⁺ by converting it to Hg⁰. Hg⁰ has low solubility in water and volatilizes. If this process affects United Taconite scrubber water samples collected during the tests and shipped to Cebam, then dissolved and particle-adsorbed mercury Hg²⁺ in unfiltered samples and dissolved mercury in filtered samples could be lost during shipping as Hg⁰. The only samples that reflect the true mercury concentration in the scrubber water during the tests would be Hg(P) because filtration and drying of the suspended solids separates the Hg²⁺ from the H₂SO₃ before the two species can react with each other. Thus, the increases in Hg(P) observed during these tests are strong indicators that NaCl addition to greenball resulted in enhanced mercury capture by the wet scrubbers, consistent with the large decrease in Hg(T) in stack-gases reported by the CMMs.

Following this test, BrCl preservative was added to samples right after sampling, rather than after shipment to the analytical laboratory. Addition of BrCl insures that all mercury present in a sample remains oxidized during shipping.

Na and Cl concentrations in scrubber water are reported for both scrubbers in Table 5.1.2.3, along with pH and concentrations of other selected cations and anions (Ca, Fe, and SO₄). More complete data for cations and anions for these experiments are provided in the appendix.

As expected, Cl concentrations in the waters from both scrubbers increased during the experiments, while Na concentrations did not. Sodium concentration, in fact, appeared to decrease with increasing Cl. Interestingly, Ca in scrubber water increased with Cl during NaCl addition to greenball, while Fe concentrations, which

are elevated at the low pH values for these scrubbers, decreased with increasing Cl. These data suggest that addition of NaCl to grate-kilns results in generation of HCl which, in turn, either changes the transport of other elements to the wet scrubber or affects the adsorption and precipitation equilibria among the other compounds within the scrubber.

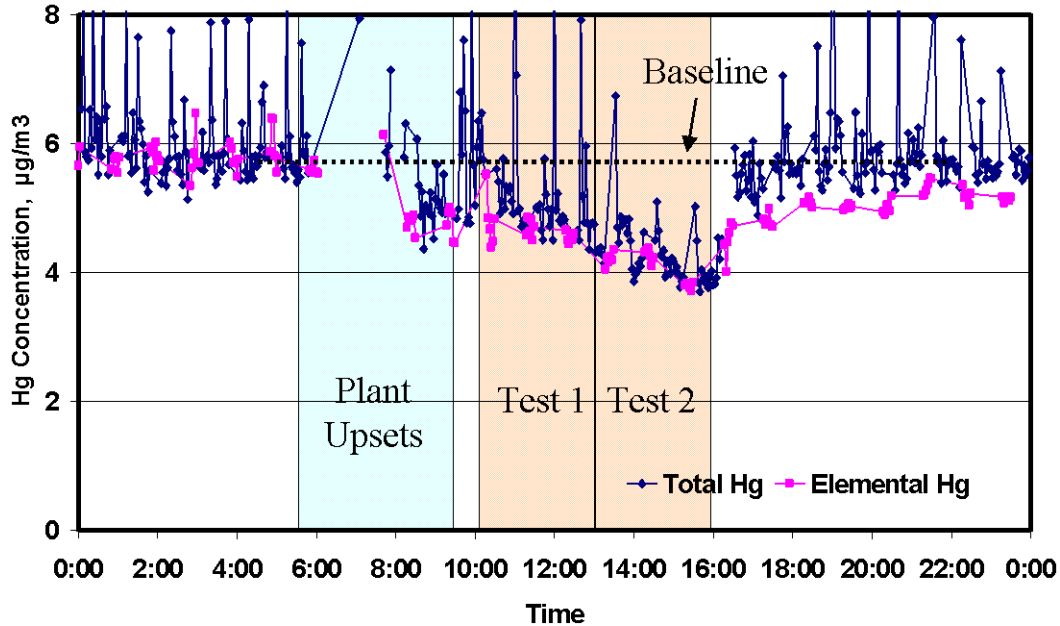


Figure 5.1.2.1 CMM mercury data collected during Cl addition to greenballs at United Taconite’s grate-kiln furnace. The measurements were made on Stack 2B. A plant upset (indicated by blue) occurred just prior to conduction of the tests.

Table 5.1.2.1 FAMS mercury data for Stacks 2B and 2A the United Taconite. CMM data are provided for comparison purposes.

<i>Stack-gas concentrations (µg/m³)</i>	<i>Hg(P)</i>	<i>Hg⁺²</i>	<i>FAMS Hg°</i>	<i>FAMS Hg(T)</i>	<i>CMM Hg°</i>	<i>CMM Hg(T)</i>
<u>Stack 2B</u>						
Baseline	0.18	0.70	2.02	2.90	5.5	5.7
Cl-Test-1	0.20	0.79	2.87	3.86	4.6	4.7
Cl-Test-2	0.15	0.50	3.11	3.75	3.9	3.9
Baseline	0.09	0.88	3.94	4.90	4.8	5.7
<u>Stack 2A</u>						
Baseline	0.21	0.52	4.42	5.15		
Cl-Test-1	0.28	0.25	4.19	4.71		
Cl-Test-2	0.16	0.13	3.61	3.90		
Baseline	0.10	0.19	4.98	5.27		

Table 5.1.2.2 Mercury concentration in greenball and scrubber water during NaCl addition to greenball at United Taconite.

	<i>Hg GB</i> <i>ng/g</i>	<i>Hg(T)</i> <i>ng/l</i>	<i>*Hg(D)</i> <i>ng/l</i>	<i>Hg(P)</i> <i>Ng/g</i>
<u>Stack 2B</u>				
Baseline	14.7	7790	32	465
Cl-Add I	14.5	7916	38	823
Cl-Add 2	18.8	5451	56	1165
Baseline	18.5	7678	144	330
<u>Stack 2A</u>				
Baseline	14.7	4954	187	341
Cl-Add I	14.5	5237	125	578
Cl-Add 2	18.8	3356	99	625
Baseline	18.5	5985	763	246

*Suspect that these samples lost mercury during shipping of samples to the analytical laboratory.

Table 5.1.2.3 Concentration of selected elements in scrubber waters collected during NaCl addition to greenball at United Taconite.

	<i>pH</i>	<i>Na</i> <i>(ppm)</i>	<i>Ca</i> <i>(ppm)</i>	<i>Fe</i> <i>(ppm)</i>	<i>Cl</i> <i>(ppm)</i>	<i>SO4</i> <i>(ppm)</i>
<u>Stack 2B</u>						
Baseline	3.19	113	62	25	85	614
Cl addition-1	3.12	-	-	-	106	589
Cl addition-2	3.13	110	76	17	113	580
Baseline	3.37	-	-	-	88	726
<u>Stack 2A</u>						
Baseline	3.75	116	56	21	84	497
Cl addition-1	3.73	-	-	-	106	479
Cl addition-2	3.88	112	69	10	112	451
Baseline	4.43	-	-	-	91	577

5.2. Focused Halide Injection at Hibbing Taconite

The focused halide injection test at Hibbing Taconite (a straight-grate facility) delivered 10 wt% halide salt solutions directly into the preheat zone as a mist. Stack-gas mercury concentrations during each period of injection decreased within minutes of salt injection and increased rapidly right after injection was stopped (Figure 5.2.1). However, the stack-gas mercury concentration did not always return to the original baseline level when the salt addition was stopped. This created a need to adjust the baseline for latter experiments; particularly following injection of the bromide salts.

Initial injection of NaCl resulted in a 6% decrease in stack-gas mercury concentration from baseline conditions. This decrease is similar to that found when NaCl was added to greenball at this plant, but small compared to the 62% decrease in stack-gas Hg(T) that occurred within minutes of injecting the NaBr solution into the

preheat zone. In fact, Hg^0 reported by the CMM all but disappeared from the emissions during NaBr injection, suggesting the nearly all mercury reaching the detector was oxidized to Hg^{2+} . This suggests either that (1) essentially all mercury passing through the wet scrubber did so as an oxidized species or (2) elemental mercury became oxidized some time after passing through the wet scrubber but before it could be analyzed by the detector. The importance of this distinction will be discussed in greater detail in Section 6.1 of this report.

Once NaBr injection stopped, the concentrations of both elemental and total mercury in stack-gases (Stack A) rapidly increased, though not to the original baseline levels. Thus, a new baseline pattern was assumed for CaCl_2 injection and the total mercury in stack-gas declined by approximately 13% from the adjusted baseline. Stack-gas mercury rapidly returned to the projected baseline levels when CaCl_2 salt injection was stopped.

Subsequently, stack-gas Hg(T) and Hg^0 response to CaBr_2 injection was equally impressive to that observed when NaBr was injected. For CaBr_2 there was an estimated 64% decrease in stack-gas total mercury concentration compared to the adjusted baseline conditions (Fig.5.2.1). When CaBr_2 addition was stopped, there was a rapid rebound in mercury concentration, but, as was noted following injection of NaBr, the concentration did not reach the pre-injection level. Moreover, Hg(T) continued to increase gradually to values above the original baseline, and not decreasing to the original baseline values until after approximately a 12 hour period (not shown) of slightly increased emission. Interestingly, stack-gas Hg^0 concentration, as reported by the CMM, decreased to low levels during injection, but, unlike Hg(T) , never exceeded the original baseline level once bromide injection stopped. This component increased gradually before leveling off at the original baseline value about six hours after the last halide injection test was completed.

Mercury concentration in greenball stayed relatively constant throughout the tests, but the concentrations were generally higher than they were for most of the previous test period when NaCl was added to greenball at this plant. Scrubber water mercury concentrations, meanwhile, increased in approximate proportion to the sequential mercury decreases observed during the series tests (Table 5.2.1). This is consistent with greater capture in the scrubber water leading to reduced mercury emissions in the stack-gases, especially during bromide salt injection.

Na, Ca, Cl, and Br concentrations for scrubber water before, during, and after the test periods are shown in Table 5.2.2. As expected, Na and Ca concentrations changed little during the injection periods, while Br and Cl increased when their respective salts were injected into the preheat zone. This indicates that the cations (Na,Ca) dissociated from Br and Cl during the tests, and combined with solids in the pellets. Only the Cl and Br were volatilized and transported to the wet scrubber. Full chemical data for the scrubber waters in these tests are presented in Appendix 3.

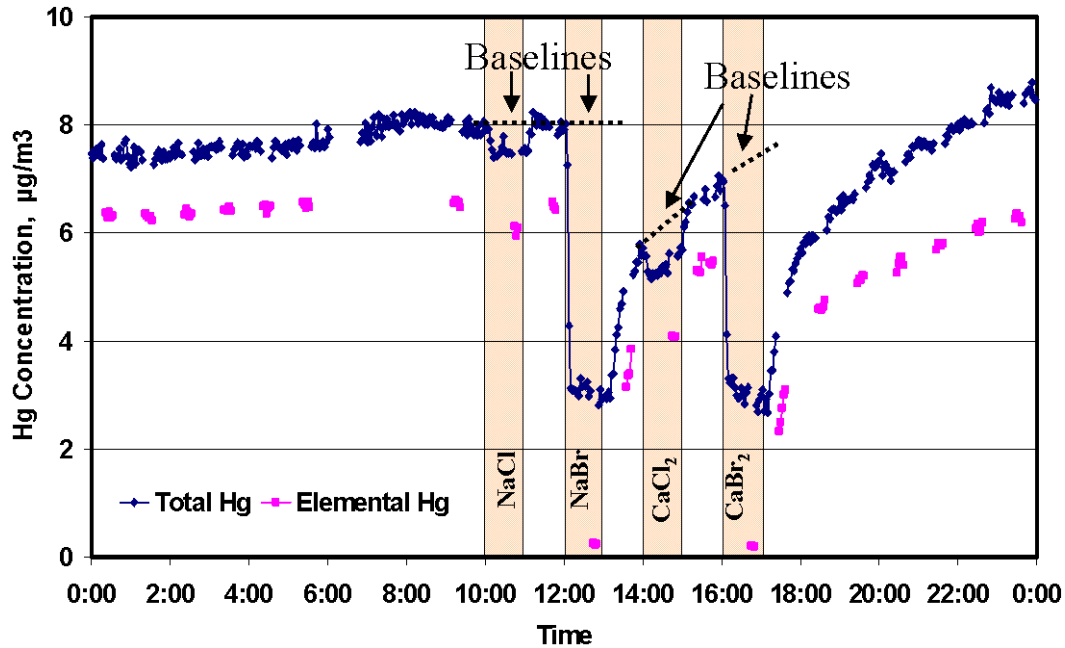


Figure 5.2.1 CMM mercury concentrations reported during halide injection tests at a straight-grate facility (Hibbing Taconite).

Table 5.2.1 Reported mercury concentrations for samples collected during halide injection experiments at Hibbing Taconite.

	<i>Hg GB</i> <i>ng/g</i>	<i>Hg(T)</i> <i>ng/l</i>	<i>Hg(D)</i> <i>ng/l</i>	<i>Hg(P)</i> <i>ng/g</i>
Base1	19.0	1288	1127	162
NaCl	23.9	1453	1210	244
NaBr	19.4	2950	2630	319
CaCl ₂	18.7	1665	1484	181
CaBr ₂	18.7	3072	2799	273
Base2	17.6	1528	1316	212

Table 5.2.2 Concentrations of selected elements in scrubber waters observed during baseline conditions and during injection of halide salts at Hibbing Taconite.

	<i>pH</i>	<i>Na</i> <i>(ppm)</i>	<i>Ca</i> <i>(ppm)</i>	<i>Cl</i> <i>(ppm)</i>	<i>Br</i> <i>(ppm)</i>
Baseline	6.74	49.1	35.9	67.6	0.24
NaCl Injection	6.75	49.8	36.1	78.3	0.24
NaBr Injection	6.77	49.3	36.0	67.1	12.4
CaCl ₂ Injection	6.64	49.2	36.1	79.6	0.42
CaBr ₂ Injection	6.71	49.2	36.0	68.4	13.8
Baseline	6.79	49.2	36.0	67.8	0.61

Table 5.2.3 Concentrations of potential oxidation products for NO_x and SO_x in scrubber waters that were observed under baseline conditions and during injection of halide salts at Hibbing Taconite.

<i>Concentrations (ppm)</i>	<i>NO2-N</i>	<i>NO3-N</i>	<i>SO4</i>
Baseline	0.21	5.45	247
NaCl Injection	0.19	5.47	241
NaBr Injection	0.18	5.46	240
CaCl ₂ Injection	0.19	5.48	242
CaBr ₂ Injection	0.18	5.53	243
Baseline	0.19	5.64	241

Table 5.2.3 lists the dissolved concentrations of NO₂⁻, NO₃⁻, and SO₄⁼ reported during these tests. The results indicate that the injection of halides has little or no effect on capture of NO_x and SO₂ from stack-gases.

5.3. In-Scrubber Oxidation: Slip-Stream tests at Keewatin Taconite

Mercury results for the “in-scrubber” oxidation bench scale tests are shown in Table 5.3.1 and Figure 5.3.1, computed in units of µg per cubic meter of gas that passed through the QLIP and FAMS apparatus. These units allow direct comparison to be made with the FAMS and CMM stack-gas measurements for the rest of this report. The “scrubber Hg” represents the mercury scrubbed by the wet portion of the apparatus, while the other amounts represent mercury in various forms that passed through the wet scrubber and adsorbed to the sequence of dry sorbents in the FAMS trap (See section 4.4.1). The experiments labeled “no scrubber” were run in parallel with the NaHCO₃-only tests, but with an unheated Teflon tube leading from the sampling port to the heated FAMS trap.

An unexpected result was that fraction of mercury identified as particulate and/or oxidized mercury when no solution was used in the QLIP was much less than that trapped by the NaHCO₃ “scrubber” solution in any of the other test. For example, approximately 23% of the mercury was captured in the scrubber portion of the apparatus when no oxidizing compound was added to the solution, but only a tiny fraction was captured when there was no solution. The total mercury measured in these experiments was virtually identical and the tests were conducted over exactly the same time period. These data suggest either that mercury in taconite process gas becomes oxidized when it contacts the water in the QLIP device, or that oxidized mercury is quickly reduced to elemental mercury in empty Teflon tubing. This is a critical observation since it potentially affects interpretation of all mercury data from taconite stacks and wet scrubbers.

Perhaps even more surprising than the high degree of capture by weak NaHCO₃ solutions (compared to the no-scrubber configuration) is the fact that adding H₂O₂ to the NaHCO₃ solution resulted in even less capture of oxidized mercury than when NaHCO₃ solutions were used without an oxidant. A possible explanation for this was provided by the analyst at Cebam, Inc., who reported that the solutions containing H₂O₂ and received by the laboratory did not have the same amber color as

the other solutions in the shipment. The amber color is produced by the preservative, BrCl. The laboratory reported that additional BrCl was added to the solutions but, each time they did this, the color faded with time. This indicated that a reaction was taking place between H_2O_2 and BrCl. The laboratory proceeded to measure mercury in the solutions, but indicated the concentrations may be low because of this apparent interference. Adding H_2O_2 to the scrubber test solutions led to a decrease in the solution's ability to oxidize and capture elemental mercury in taconite process gases, suggesting the possibility that minor Cl_2 is present in taconite process gas, and that its reaction with H_2O_2 *rather than* elemental mercury led to reduced mercury capture efficiency. It appears from these results that H_2O_2 is not a likely candidate for in-scrubber oxidation at taconite processing plants and that, perhaps, it even interferes with the background mercury oxidation process that takes place when no oxidant is added to the water.

Results for EPA_{ox} are quite opposite from those obtained using H_2O_2 . Not only did EPA_{ox} capture much more mercury than the other solutions, but only a small percentage of mercury in the slip-stream gas was able to elude capture by the EPA_{ox} scrubber solution to register a response in the FAMS sorbent traps. 80% and 87% capture was measured for the two experiments. This oxidant is, thus, a good candidate for further testing at taconite plants. It appeared, however, from the high total mercury concentration in all of the traps combined (Figure 5.3.1) that there was contamination in the EPA_{ox} traps, perhaps resulting from additional uptake of Hg^0 from air or another temporary source that came into contact with the solutions. Nevertheless, after discounting this additional source of mercury that greater than 70% of the total mercury in the slip-stream gas was oxidized and captured by water containing the oxidant.

In addition to mercury, the scrubber solutions were tested for NO_2-N , NO_3-N , and SO_4 , to determine if other pollutant species were oxidized along with elemental mercury (Table 5.3.2). Results showed that the EPA_{ox} solutions had the highest concentrations of each of these components indicating that other components in taconite processing gas could potentially interfere with the ability of EPA_{ox} to capture mercury. However, the concentrations of these species suggest recovery rates for NO_x and SO_x were relatively low in these tests.

Table 5.3.1 Mercury trapped from slip-stream gas at Keewatin Taconite during the “in-scrubber” oxidation experiments.

	<i>*Scrubber</i>			
	<i>Hg</i> $\mu\text{g}/\text{m}^3$	<i>**Hg(P)</i> $\mu\text{g}/\text{m}^3$	<i>**Hg²⁺</i> $\mu\text{g}/\text{m}^3$	<i>**Hg⁰</i> $\mu\text{g}/\text{m}^3$
No scrubber	-	0.07	0.13	5.56
No scrubber	-	0.09	0.21	5.78
No scrubber	-	0.07	0.13	5.68
NaHCO ₃	1.27	0.00	0.02	4.23
NaHCO ₃	1.27	0.01	0.03	4.37
NaHCO ₃	1.41	0.02	0.04	4.56
H ₂ O ₂ - NaHCO ₃	0.53	0.03	0.02	4.83
H ₂ O ₂ - NaHCO ₃	0.77	0.04	0.21	4.75
EPAox- NaHCO ₃	6.21	0.06	0.07	0.73
EPAox- NaHCO ₃	5.06	0.08	0.10	1.19

*Scrubber Hg is the total mass of mercury captured in the QLIP apparatus, divided by the total amount of process gas that passed through the system.

** Hg(P), Hg²⁺, and Hg⁰ are, in this case, the total amounts of mercury captured on sorbents in the appropriate FAMS traps divided by the total amount of gas passing through the system.

Table 5.3.2 Anion concentrations in “scrubber water” from slip-stream tests performed at Keewatin Taconite.

	<i>F</i> (ppm)	<i>Cl</i> (ppm)	<i>NO₂-N</i> (ppm)	<i>NO₃-N</i> (ppm)	<i>SO₄</i> (ppm)
NaHCO ₃ start	<0.005	0.08	<0.002	0.17	0.24
NaHCO ₃ -1	1.26	2.22	0.12	0.25	25.9
NaHCO ₃ -2	1.51	5.25	0.12	0.25	29.3
NaHCO ₃ -3	1.46	5.30	0.10	0.14	26.9
H ₂ O ₂ – start	<0.005	0.151	<0.002	0.20	0.37
H ₂ O ₂ – 1	1.276	2.292	0.12	0.11	25.8
H ₂ O ₂ – 2	1.35	4.08	0.11	0.26	26.2
EPAox –start	0.09	12.4	<0.002	0.11	0.37
EPAox –1	1.39	37.7	0.32	1.10	28.3
EPAox –2	1.61	28.5	0.09	0.84	26.4

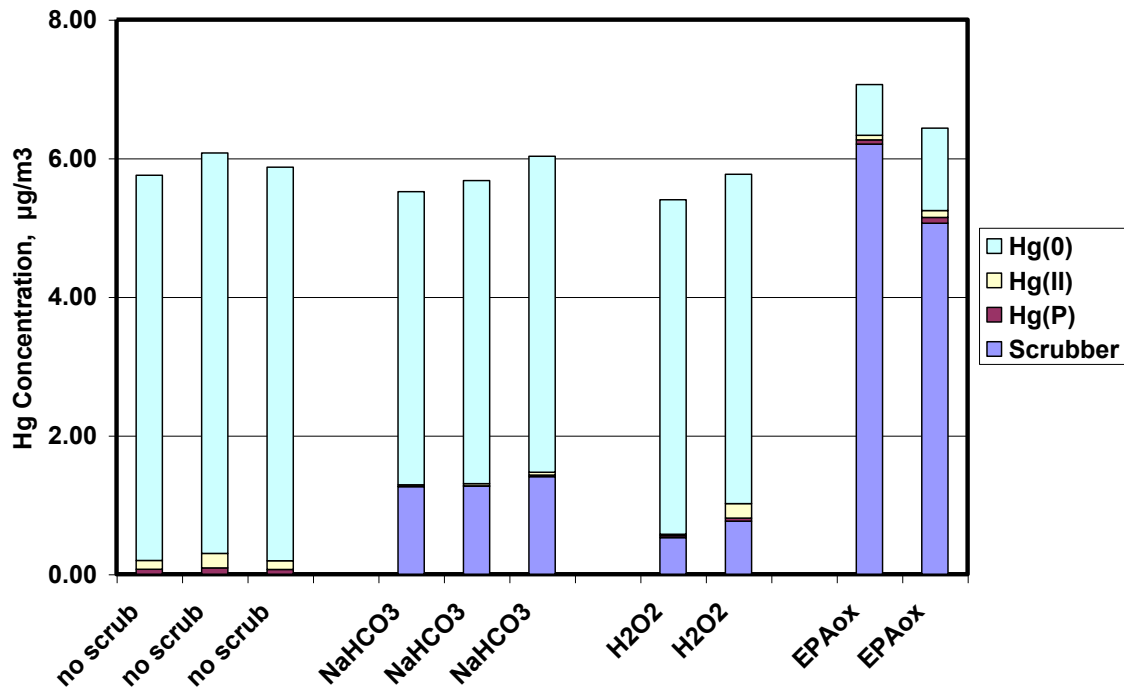


Figure 5.3.1 Mercury captured from slip-stream gas at Keewatin Taconite using the QLIP-FAMS testing system described in section 4.3.

6. Discussion

While it is tempting to begin to analyze potential costs associated with the most promising techniques, such endeavors carried out at a serious level are likely premature as the tests conducted here were short-term and it is likely that improvements in measurement and control methods will be made as experience increases. The tests presented in this study merely reveal that several promising approaches exist for controlling mercury emissions at taconite processing plants. Final evaluation of whether a method is a viable alternative must wait until the time when longer tests can be performed and other hazards of using the techniques can be identified and assessed.

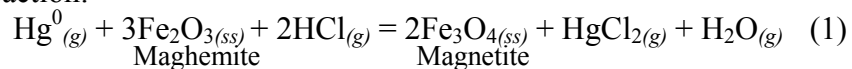
It is important to note that in the process of performing these tests that the empirical relationships obtained between halide addition or injection and mercury oxidation, capture, and measurement are of value regardless of whether they lead directly to a viable control method. A more careful analysis of these results can lead to greater understanding of the physical and chemical processes affecting mercury transport at taconite processing plants needed for future applications. In this regard, at least three results stand out as significant from both practical and conceptual perspectives:

- (1) Addition of NaCl to greenball was more effective at decreasing mercury in stack-gases at the grate-kiln facility than it was at the straight-grate plant, but neither method worked as well as injecting bromide salts into the preheat zone of a straight-grate furnace;

- (2) Elemental mercury in process gas was oxidized and captured upon contact with an aqueous solution, even when no oxidant was added to the solution; and,
- (3) Oxidants added to solutions, EPA_{ox} in particular, have the capacity to oxidize and remove large fractions of the elemental mercury from taconite process gases.

The sodium chloride addition experiments were designed based on models and data presented by Berndt and Engesser (2005a), who found that magnetite is first converted to a magnetite/maghemite solid-solution in the preheat zone, and that this phase plays an important role in regulating mercury capture and release in taconite induration furnaces. In that study, it was found that full mercury release in the absence of added NaCl did not occur until magnetite and/or magnetite/maghemite solid-solutions were heated past approximately 450 or 500° C and converted to hematite. However, mercury released from hotter zones in the furnace could partially collect in the cooler zones where it came into contact with maghemite. This maghemite need only coat the outer surface of a magnetite grain to absorb mercury and, thus, high mercury concentrations are generally found in iron-oxides within the preheat zones of taconite induration furnaces.

Experimental and field data presented by Berndt and Engesser (2005a) suggested that the degree to which Hg was volatilized as either Hg⁰ or HgCl₂ in this zone depended, to some degree, on the availability of HCl, as described by the following reaction:



where the subscripts, “g” and “ss”, represent gaseous and solid-solution components for process gas and iron-oxides, respectively. According to this reaction, increasing HCl in the process gas in the zone of active maghemite generation (e.g., the preheat zone), should lead to increased transport of HgCl₂ to the wet scrubber. This is the presumed dominant volatile form of oxidized mercury, Hg²⁺, which is the form of mercury most easily captured by wet scrubbers.

Cl is present to some extent in all greenball produced on the Iron Range. It is released both from the ore minerals and limestone flux during processing, although most Cl entering an induration furnace at any one time is dissolved in the process water pore fluid of the greenball, which makes up about 10% of the mass of the greenball at the time it enters the furnace. Drying of the greenball in the preheat zones during induration leads to evaporation of the water and residual salt in the greenball pore spaces. These salt components break down into volatile and labile components upon heating to high temperatures. Typically, the most volatile components from these residual salts are the halides, Cl⁻, Br⁻, and F⁻, which are thought to combine with H⁺ to generate mobile acid species HCl, HBr, and HF. These species are generally soluble in water and, as a consequence, are captured by wet scrubbers. Adding NaCl to greenball in the straight-grate experiments was intended to generate HCl which, upon contact with maghemite and adsorbed mercury

in the preheat zone, would mobilize the mercury to the wet scrubber as HgCl_2 (Reaction 1).

While chloride addition increased mercury capture when NaCl was added to the greenball or directly to the preheat zone, the method worked considerably better in the grate-kiln facility compared to at a straight-grate. One important clue for this, perhaps, is provided by considering the somewhat limiting constraint imposed by Reaction (1) requiring HCl generated by the process to directly contact greenball in the preheat zone. More specifically, if HCl fails to contact greenball in the zones where active maghemite formation is occurring (e.g., the preheat zone), then it will not result in significant improvement in the capture of mercury at taconite processing plants.

Examination of the geometry and ducting for straight-grate and grate-kiln furnaces provides a possible explanation for the large difference in mercury capture rates for the two types of plants. At United Taconite, the grate-kiln plant, NaCl addition resulted in 18 and 32% improvement to capture rates which, added to baseline capture rates, suggests that as much as 40 to 50% total recovery of mercury may be achieved (using the estimated normal capture rates reported by Berndt and Engesser, 2005b). It is important to note, however, that any HCl generated in the kiln (e.g., the firing zone) portion of a grate-kiln plant is transported directly to the preheat zone where the gases are passed through the pellet bed. Thus, assuming Reaction 1 is the primary process in this case, and assuming further that HCl (rather than, Cl_2 or other species) is generated in the kiln, this is an ideal situation for using NaCl addition to greenball to control mercury.

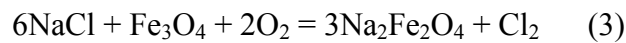
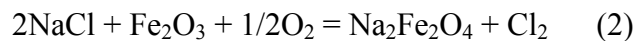
By contrast, HCl generated by NaCl degradation in a straight-grate furnace has two potential pathways through which gases eventually reach the wet scrubber, one leading through the preheat zone, and the other not. Gases generated in the firing zone are transported to the downdraft drying zone, while gases generated in the first cooling zone are fed into the preheat zone. Thus, HCl generated in the firing zone will generally miss the zone of active maghemite formation and proceed directly to a drying zone. This difference can account for the relatively low level of mercury control found when NaCl was added to greenball at the straight-grate facility (Hibbing Taconite).

It was hoped that adding NaCl or CaCl_2 solutions directly to the preheat zone as a mist might better utilize Reaction 1 as a means to control mercury emission at a straight-grate facility in at least one of two ways. First, since the top of the pellet bed in the preheat zone is much hotter than the bottom of the bed, this method of adding NaCl or CaCl_2 should lead to earlier formation of HCl compared to the case where NaCl is distributed throughout the pellet bed. Second, if HCl is generated at the top of the pellet bed, it would be driven through the lower portion of the pellet bed where Reaction 1 may be taking place. This, in turn, could lead to increased oxidation and capture of mercury by the wet scrubber.

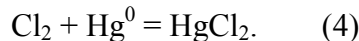
The fact that focused injection of chloride salts did not significantly improve mercury capture rates compared to addition of NaCl to greenball indicates that either the HCl was still generated too deeply in the furnace to make use of Reaction 1 or

that only a small portion of the pellet bed was contacted by the NaCl or CaCl₂ mist in the preheat zone. Whatever the cause, the results suggest that addition of chloride salts is a relatively ineffective means to control mercury at straight-grate facilities.

During the course of this study, an alternative pathway for mercury oxidation related to chloride addition was also considered, based on an entirely different reaction pathway compared to Reaction 1. Edwards et al. (2001), for example, showed that other chloro-based gas species, such as Cl and Cl₂, can oxidize Hg⁰ at rates that are orders of magnitude more rapid than reactions with HCl. It is unknown whether such meta-stable species exist in taconite processing gases. However, exposure of NaCl to high temperatures during induration could conceivably generate at least some of these species. Moreover, data presented and summarized by Radermakers et al, 2002, suggest that reaction of NaCl with iron oxides can lead to heterogeneous reactions that generate Cl₂, as follows:



Generation of Cl₂ by this or any other reaction would almost certainly impact mercury capture since Cl₂ can react directly with mercury by:



This reaction has been found to be especially rapid when Cl₂ and Hg⁰ come into contact with water (Linak et al, 2001; Roy, 2003).

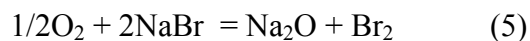
Reaction 4, in fact, may help to account for two unusual results obtained from the in-scrubber oxidation experiments with slip-stream gases: (1) significant mercury was captured from taconite waste gas containing only a small fraction of oxidized mercury even when no oxidant was added to the aqueous solution and (2) H₂O₂ addition to the scrubber actually impeded mercury capture compared to the case where no oxidant was added. If we infer the presence of minor Cl₂ in the slip-stream gas used in those experiments, then Reaction (4) can account for both of these unusual observations. First, Cl₂ in the process gas would behave as a mercury oxidant when the gas contacted the aqueous solution as discussed and shown by Roy (2003). Moreover, it is quite possible that H₂O₂ consumes Cl₂ as effectively as it consumed the similar compound BrCl that was used as a preservative (see section 5.3). In effect, the Cl₂ oxidizes the H₂O₂ to O₂ while it is itself converted to much less reactive (with respect to Hg⁰) HCl. If so, then addition of H₂O₂ to the scrubber water interferes with, rather than enhances capture of mercury from waste gas containing Cl₂. However, this is only indirect evidence for a role for Cl₂ during mercury capture by taconite wet scrubbers. Better data on mercury, chloride, and chlorine gas species in taconite process gases are needed to confirm this mechanism.

Regardless of the mechanism controlling oxidation of mercury by chloride or chlorine in taconite process gases, the tests clearly revealed that bromide salts outperformed chloride salts in terms of increasing mercury capture upon injection into the preheat zone at straight grate facilities. It is apparent that injection of NaBr or CaBr₂ into induration furnaces leads to formation of a very reactive oxidant, most likely Br₂. As was the case for injection of NaCl and CaCl₂, analysis of scrubber

waters during injection of bromide salts into the preheat zone revealed no detectable increases in Na or Ca suggesting that the salts were not transported to the scrubber as aerosols containing NaBr or CaBr₂. The salts injected must have been converted to other Br-bearing species such as HBr or Br₂. Rademakers *et al.* (2002), in a review of the literature on Br speciation, suggest that Br₂ gas forms rapidly from HBr oxidation in “almost entirely a homogeneous reaction” at temperatures between 490°C and 635°C. Thermocouples placed in the area into which the bromide salts were injected into Hibbing Taconite’s furnace registered temperatures close to 750°C which implies this zone was certainly hot enough to heat the injected solutions to the temperature range needed for Br₂ formation.

Whether or not Br₂ or HBr is generated in induration furnaces is important for two reasons. First, Br₂ is a strong oxidant that can cause corrosion in equipment that it contacts and, second, it can pass through the wet scrubber systems and be emitted to the atmosphere. The latter effect may account for the relatively high apparent oxidation state of mercury reported by the CMM during the Br-salt injection tests. Any Br₂ passing through the wet scrubber would be collected with Hg⁰ by the wet injection probe used to sample gases for the CMM during the halide injection tests. Once sampled, the stack-gases were transported in a bubble train through a heated 25 ft hose before being processed for gas analysis by the Tekron instrument used for mercury analysis. If this amount of reaction time is sufficient for Br₂ to oxidize Hg⁰ to Hg²⁺, then it would cause the CMM to over-report oxidized mercury while still reporting a correct value for Hg(T). Thus, although it is possible that the highly oxidized nature of mercury in the stack-gas during bromide injection is real, a more realistic interpretation is that most of the mercury in the stack was unoxidized Hg⁰ that passed through the wet scrubber, but this mercury was oxidized during transport from the stack to the instrument.

The proposed explanation for the mercury data collected during the bromide salt injection tests, therefore, is that the following overall reactions occurred and dominated mercury transport upon bromide injection to the preheat zone:



Br₂ is thermally generated from NaBr in the furnace (Reaction 5), perhaps catalyzed by iron-oxides in the pellet bed. This Br₂ oxidized a majority of the Hg⁰ being transported in process gas, either by gas-phase reactions or following contact with water in the wet scrubber. The data suggest that some of the Br₂ that formed by the process escaped the wet scrubber and continued to oxidize most of the remaining Hg⁰ that also passed through the wet scrubber. This latter oxidation step may have occurred either before or during entrapment by the wet sampling device used by the CMM, in a manner analogous to the Cl₂ and Hg⁰ capture mechanism explored by Roy (2003).

It is somewhat disconcerting that our efforts to speciate taconite stack-gases are still somewhat uncertain. The relative fates of oxidized and elemental mercury from stack emissions make speciation of stack-gas an important unresolved issue. Hg⁰ remains in the atmosphere for long periods of time and is deposited globally,

whereas oxidized mercury in the gas emissions is deposited locally and could lead to generation of local mercury hot-spots if the emitted gases were composed predominantly of oxidized mercury. The interpretation of the gas measurements associated with the stack testing, therefore, has added significance, not only as a means to assess control feasibility, but also if the data are to be used to evaluate environmental consequence of the control method. At the very least, further testing is needed to resolve whether the high oxidation state for mercury indicated by the CMM used in the bromide salt injection tests is an artifact of the method or an indication of a potential secondary environmental issue.

Considering the relatively small increases in mercury capture efficiencies demonstrated for chloride salt addition in straight-grate furnaces, and the potential for corrosion should bromide be injected into taconite furnaces for long periods of time, perhaps the most promising technology studied here is in-scrubber oxidation using EPA_{ox} . Not only was this oxidant effective, but this method does not appear to result in unwanted by-products in stack emissions (such as Br_2), nor does the method introduce corrosive agents to the grates, kiln, or ductwork leading to the scrubber. The instrumentation required to implement in-scrubber oxidation is inexpensive and straight forward since it involves only a tank containing the oxidant and a small pump to feed the material into the scrubber system. However, the potential breakdown products of the chemical to be used and the potential for oxidizing and capturing other components along with mercury must be evaluated before it can be considered a viable mercury reduction method.

The breakdown products for EPA_{ox} will be evaluated in future studies, however, experiments conducted by Hutson and Srivistava (2006) have already indicated that this oxidant can also react extensively with NO_x and SO_x . It is unknown why application of EPA_{ox} in the tests conducted during the present study were much less effective at oxidizing these components in the taconite process gases. It likely results from differences in contact time between water and process (or carrier) gas. If plant-scale application is better approximated by the apparatus used by Hutson and Srivistava (2006), then it implies both a higher consumption rate for the oxidant and a potential for high NO_3^- in the scrubber effluent, which may lead to an eventual water treatment problem that could add further to the cost of using EPA_{ox} to control mercury in taconite plants.

7. Conclusions

Addition of NaCl to greenball provided a more effective means to control mercury emissions at a grate-kiln facility than at a straight-grate facility. Injection of bromide salts into the preheat zone of a straight-grate worked much better to control emissions than chloride injection at either facility. The difference can be attributed to different predominant pathways for dissociation and reaction of chloride and bromide salts in taconite induration furnaces. The results suggest that addition of chloride salt by any method leads to volatilization mostly of less reactive HCl but possibly minor Cl_2 during taconite induration. Bromide salt injection, on the other hand, appears to generate a large amount of much more reactive species such as Br_2 , capable of oxidizing a large fraction of the mercury in taconite process gases.

One important observation is that elemental mercury in process gas appeared to be oxidized upon contact with water in one set of experiments. Although this observation was used to infer presence of Cl_2 in process gas, the relative distribution of HCl and Cl_2 was not measured.

Slip-stream experiments indicate that addition of a proprietary reagent, EPA_{ox} , has the capacity to remove a large fraction of elemental mercury from taconite process gases. Other gaseous oxidation products from pollutants such as NO_x and SO_x were generated in the experiments, but not to the degree observed by Hutson and Srivistava (2006) owing, most likely, to differences in gas/liquid contact time. Plant-scale tests should be conducted to determine effectiveness of this method with the actual gas/liquid contact time for wet scrubbers under normal use conditions.

8. Acknowledgements

This study was conducted using funds provided by Iron Ore Cooperative Research, the DNR's Environmental Cooperative Research, and each of Minnesota's six mining companies: Keewatin Taconite, Hibbing Taconite, Minntac, Mittal Steel, United Taconite, and Northshore Mining Company. Additional support was provided by the Minnesota Pollution Control Agency.

Dennis Laudal and Grant Dunham from the University of North Dakota's Energy and Environmental Research Center are acknowledged for providing CMM measurements during the conduction of plant-scale tests and for providing a sounding board for many of the ideas considered and presented in this report. Blair Benner from the University of Minnesota's Coleraine Minerals Research Center is acknowledged for providing assistance in designing the small scale slip-stream tests and for providing mercury measurements using FAMS during many of the tests conducted during this study.

Lian Liang of Cebam, Inc., is acknowledged for expert analysis of water and solid samples shipped to her laboratory during this study. She also developed a more efficient and reliable method to determine total mercury in taconite scrubber solutions that are particularly difficult to measure due to the recalcitrant nature of fine iron oxides and their tendency to absorb mercury and adhere to the walls of glass sampling jars.

Kenneth Reid from Tetra Chemicals, Texas, provided the NaBr , CaBr_2 , and CaCl_2 used in the focused halide injection tests at Hibbing Taconite.

This study would not have been possible without the efforts of numerous DNR staff, including, especially, John Folman, who helped collect most of the scrubber waters and greenball samples and helped design, test, and operate the devices used in this study. Dave Antonson is acknowledged for building the apparatus used for injection of NaCl , NaBr , CaCl_2 , and CaBr_2 salt solutions into the preheat zone of the straight-grate. Kim Lapakko is acknowledged for his insightful comments provided throughout the study.

9. References

Agarwal, H., Romero, C. E., and Stenger, H. G. (2007) Fuel Processing Technology, 88, 723-730.

Benner, B. R. (2001) Mercury removal from induration off gas by wet scrubbers. Coleraine Minerals Research Laboratory Report. 18 pages plus appendices.

Benner (2005) Mercury Release from Taconite During Heating. CMRL report TR-05-06/NRRI/TR-2005-17 prepared for Minnesota Department of Natural Resources, 3 p.

Benson, S. (2006) Large-Scale Mercury Control Technology Testing for Lignite-Fired Utilities, Oxidation Systems for Wet FGD. DOE/NETL's Mercury Control Technology Conference of Coal; Pittsburgh, PA, Dec. 11-13, 2006, Presentation Summaries and Speaker Bibliographies.

Berndt, M. E. (2003) *Mercury and mining in Minnesota*. Final report, Minnesota Department of Natural Resources, 58p.

Berndt, M. E. and Engesser, J. (2005a) Mercury Transport in Taconite Processing Facilities: (I) Release and Capture During Induration. Iron Ore Cooperative Research Final Report. Minnesota Department of Natural Resources. 31 pages plus appendices.

Berndt, M. E. and Engesser, J. (2005b) Mercury Transport in Taconite Processing Facilities: (II) Fate of Mercury Captured by Wet Scrubbers. EPA: Great Lakes National Program Office Report. 32 pages.

Berndt, M. E., Engesser, J., and Berquó, T. S. (2005) Mercury Chemistry and Mössbauer Spectroscopy of Iron Oxides During Taconite Processing on Minnesota's Iron Range. In Proceedings Air Quality V, International Conference on Mercury, Trace Elements, SO₃, and Particulate Matter. Washington, DC, Sept. 2005. 15 p.

Berndt, M. E., Engesser, J. E., and Johnson, A. (2003) On the distribution of mercury in taconite plant scrubber systems. Technical report submitted to the MPCA, 30 p.

Berquó, T. S. (2005) Mössbauer spectroscopy analyses of taconite dust samples. University of Minnesota Technical Report prepared for Minnesota Department of Natural Resources. 13 p.

Currie, J. (2006) Bench-scale Kinetics Study of Mercury Reactions in FGD Liquors. DOE/NETL's Mercury Control Technology Conference of Coal; Pittsburgh, PA, Dec. 11-13, 2006, Presentation Summaries and Speaker Bibliographies.

Edwards, J. R., Srivatava, R. K., and Kilgroe, J. D. (2001) A study of gas-phase mercury speciation using detailed chemical kinetics. J. Air. Waste. Man. Assoc., 51, 869-877.

Engesser, J. and Niles, H. (1997) Mercury emissions from taconite pellet production. Coleraine Minerals Research Laboratory, Report to MPCA: U of M contract # 1663-187-6253. 16 pages plus tables, figures and appendices.

Galbreath, K. C. (2005) Final Report for Mercury Vaporization Characteristics of Taconite Pellets. UND Environmental and Energy Research Center Technical Report, Prepared for Minnesota Department of Natural Resources. 16 pages plus appendices.

Galbreath, K. C., Zygarlicke, C. J., Tibbetts, J. E., Schulz, R. L., and Dunham, G. E. (2005) Effects of NO_x, α-Fe₂O₃, δ-Fe₂O₃, and HCl on mercury transformations in a 7-kW coal combustion system. *Fuel Processing Technology*, 86, 429-488.

Hutson, N. and Srivistava, R. A. (2006) Multipollutant Wet Scrubber for Capture of SO₂, NO_x, and Hg. DOE/NETL's Mercury Control Technology Conference of Coal; Pittsburgh, PA, Dec. 11-13, 2006, Presentation Summaries and Speaker Bibliographies.

Jiang, H., Arkly, S., and Wickman, T (2000) Mercury emissions from taconite concentrate pellets- stack testing results from facilities in Minnesota. Presented at USEPA conference "Assessing and managing mercury from historic and current mining activities". San Francisco, November 28-30, 18 pages.

Korell, J., Seifert, H, Paur, H. R., Anderson, S., and Bolin, P. (2003) Flue gas cleaning with the MercOx Process. *Chem. Eng. Technol.*, 26, 737-740.

Laudal, D. (2007a) Mercury Control Technologies for the Taconite Industry. EERC Technical Report to Minnesota Department of Natural Resources, Agreement A85811.

Laudal, D. (2007b) "Methods Testing for Measurement of Mercury Speciation for High-Reactive Dust"; Technical Report to Minnesota Department of Natural Resources, UND Fund No. 9301.

Linak, W. P.; Ryan, J. V., Ghorishi, B. S.; and Wendt, J. O. (2001) Issues related to solution chemistry in mercury sampling impingers. *J. Air. Waste Mgmt. Assoc.* 51, 688-698.

Liu, S-H., Yan, N-Q., Liu, Z-R., Wang, H. P., Chang, S-G., and Miller, C. (2007) Using Bromine Gas to Enhance Mercury Removal from Flue Gas of Coal-Fired Power Plants, *Env. Sci. Technol.* 41, 1405-1412.

Mohanty, B. P., and Shores, D. A. (1993) Hot corrosion of grate bars in taconite indruator during fluxed pellet production. Univ. of Minnesota Corrosion Research Center Report to MN DNR. 35 pages.

MPCA (2006) Minnesota Statewide Mercury Total Maximum Daily Load. Minnesota Pollution Control Agency, 56 pages plus appendices.

Overcamp, T. J. (1999) An oxidizing scrubber for the control of Elemental Mercury. Proc. of Mercury in the Environment, A&WMA Specialty Conference, Minneapolis, MN, Sept 15-17, 1999. 13 p.

Rademakers, P, Hesseling, W., and van de Wetering, J., (2002) Review on corrosion in waster incinerators, and possible effect of bromine. TNO Industrial Technology Report, 51 p.

Roy, S. (2002) Absorption of Chlorine and Mercury in Sulfite Solutions. PhD Thesis. University of Texas, El Paso. 219 p.

10. Appendices – Miscellaneous Data

10.1. Appendix I: Hibbing Taconite NaCl-Addition To Greenball

July 18-19, 2006

Stack-gas Chemistry: Stack A

Gas composition - Stack A

Time	% O2	Ppm NO	ppm NOx	ppm NO2	ppm SO2	ppm CO
7:45:35	19.05	107	107	0.3	3	6
7:49:08	19.05	101	101	0	2	7
7:54:05	19.07	104	104	0	2	6
8:04:51	19.05	104	104	0	6	6
8:10:07	19.06	106	106	0	8	6
8:25:16	19.14	105	105	0	8	5
8:37:30	19.09	108	108	0	8	7

FAMS Analysis: Pre-injection baseline, 7/18/06

Stack A	Particulate	Oxidized	Elemental	Total
	0.01	0.37	3.38	3.75
	0.07	0.45	3.13	3.65
	0.08	0.24	3.97	4.29
Average	0.06	0.35	3.49	3.90
STD/AVE	0.733735	0.290023	0.123	0.088531

Stack B	Particulate	Oxidized	Elemental	Total
	0.06	0.42	1.20	1.69
	0.07	0.71	1.06	1.84
	0.10	0.63	1.74	2.47
Average	0.08	0.59	1.34	2.00
STD/AVE	0.239927	0.250434	0.269477	0.20743

FAMS Analysis: Hibbing Taconite Cl-addition I, 7/18/06

Stack A	Particulate	Oxidized	Elemental	Total
	0.13	0.38	2.95	3.46
	0.12	0.34	2.92	3.38
	0.11	0.27	3.26	3.64
Average	0.12	0.33	3.04	3.49
STD/AVE	0.080651	0.17286	0.061804	0.03819

Stack B	Particulate	Oxidized	Elemental	Total
	0.13	0.62	1.89	2.64
	0.18	0.62	2.04	2.84
	0.15	1.52	3.75	5.41 eliminated
Average	0.15	0.62	1.96	2.74
STD/AVE	0.208615	0.006669	0.053706	0.051795

FAMS Analysis: Hibbing Taconite Cl-addition II, 7/18/06

Stack A	Particulate	Oxidized	Elemental	Total
	0.11	0.35	2.81	3.27
	0.17	0.29	3.21	3.67
	0.11	0.30	3.31	3.72
Average	0.13	0.31	3.11	3.55
STD/AVE	0.266218	0.103336	0.084496	0.069163

Stack B	Particulate	Oxidized	Elemental	Total
	0.12	0.55	2.27	2.94
	0.08	0.53	1.85	2.46
	0.09	0.46	2.43	2.97
Average	0.10	0.51	2.18	2.79
STD/AVE	0.206246	0.094606	0.136568	0.103436

FAMS Analysis: Hibbing Taconite Post-Cl-addition baseline, 7/19/06

Stack A	Particulate	Oxidized	Elemental	Total
	0.11	0.35	3.44	3.90
	0.11	0.27	3.19	3.57
	0.10	0.36	3.56	4.03
Average	0.11	0.33	3.40	3.83
STD/AVE	0.049284	0.153162	0.056145	0.061714

Stack B	Particulate	Oxidized	Elemental	Total
	0.17	0.81	2.54	3.53
	0.21	0.70	2.47	3.38
	0.17	0.60	3.04	3.81
Average	0.18	0.71	2.69	3.57
STD/AVE	0.119711	0.150422	0.114967	0.061496

Stack C	Particulate	Oxidized	Elemental	Total
	0.07	0.17	1.17	1.41
	0.12	0.13	1.33	1.58
	0.09	0.13	1.40	1.63
Average	0.09	0.14	1.30	1.54
STD/AVE	0.22701	0.147173	0.09129	0.073395

Stack D	Particulate	Oxidized	Elemental	Total	
	0.07	0.30	0.82	1.20	
	0.06	0.29	0.84	1.19	
	0.06	0.28	1.44	1.79	eliminated
Average	0.07	0.30	0.83	1.19	
STD/AVE	0.084852	0.034837	0.012738	0.004712	

Scrubber water anion concentrations (ppm) compared to makeup water during Hibbing Taconite Cl-addition tests.

	Fluoride	Chloride	Bromide	Sulfate	Nitrite-N	Nitrate-N
Baseline	11.41	5.38	0.02	46.60	0.06	0.15
Cl-ADD 1	11.23	10.43	0.02	47.10	0.05	0.42
Cl-ADD 2	11.13	16.36	0.02	44.80	0.04	0.27
Baseline	11.26	5.72	0.02	50.20	0.06	0.14

Scrubber water major and trace cation concentrations during Hibbing Taconite Cl-addition tests

	Na Ppm	Mg ppm	Si ppm	K ppm	Ca ppm							
Baseline	60.26	74.32	11.50	19.78	43.04							
Cl-ADD 1	59.99	74.38	11.52	19.81	43.08							
Cl-ADD 2	60.24	74.83	11.77	19.79	43.11							
Baseline	60.28	74.65	11.61	19.71	43.01							

	Li ppb	B ppb	Al ppb	P ppb	Cr ppb	Fe ppb	Mn ppb	Co ppb	Ni ppb	Tl ppb	Pb ppb	U ppb
Baseline	15.18	116.70	0.00	2.58	0.24	131.00	5.15	0.34	9.23	0.58	0.50	1.65
Cl-ADD 1	16.43	107.10	0.00	2.52	0.28	77.17	4.60	0.35	8.18	0.37	0.44	1.71
Cl-ADD 2	17.82	120.30	0.19	4.75	1.38	62.60	4.73	0.37	3.69	0.38	0.53	1.79
Baseline	17.73	123.33	0.00	4.73	0.54	44.55	4.56	0.35	4.47	0.29	0.52	1.75

	Cu ppb	Zn ppb	As ppb	Se ppb	Rb ppb	Sr ppb	Mo ppb	Cd ppb	Cs ppb	Ba ppb	W ppb	Tl ppb	Pb ppb	U ppb
Baseline	3.0	21.6	59	21	14.5	162	27.6	0.09	1.10	21	0.34	0.58	0.50	1.65
Cl-ADD 1	3.6	9.1	34	23	15.2	170	28.0	0.09	1.15	22	0.24	0.37	0.44	1.71
Cl-ADD 2	3.2	6.7	38	26	15.9	179	29.5	0.09	1.19	24	0.23	0.38	0.53	1.79
Baseline	3.4	20.5	52	25	15.7	176	29.7	0.10	1.17	23	0.21	0.29	0.52	1.75

Averaged Total (Hg(T)) and Dissolved (Hg(D)) mercury in scrubber waters during NaCl addition to greenball at Hibbing Taconite.

	Hg(T)	Hg(D)	Hg(D)/Hg(T)
Baseline	738	439	0.60
Cl-ADD 1	742	499	0.67
Cl-ADD 2	880	587	0.67
Baseline	827	561	0.68

Hibbing Taconite Chloride Addition to filter cake: field measurements.

Line 3, 7/18/06 and 7/19/06.

Line 3	Baseline	Test 1	Test 2	Baseline
Time	1000	1300	1600	0900
PH	7.28	7.19	7.00	7.01
Temperature(°C)	39.5	40.0	40.9	40.9
Conductivity(μ S/cm)	1050	1050	1050	1050
Total suspended solids (%)	0.023	0.024	0.0235	0.0235

Note: The initial baseline and tests 1 and 2 were conducted on 7/18/06. The second baseline analysis was conducted on 7/19/06.

10.2. Appendix II: United Taconite NaCl-Addition to Greenball

Dates: Sept. 12-13, 2006

Gas Chemistry during NaCl-addition to greenball at United Taconite

9/12/2006 Stack 2B gas analyses

Time	Temp F	% O2	ppm NO	Ppm NOx	ppm NO2	ppm SO2	ppm CO
8:58:06	122.3	18.90	76	76	0	41	7
8:59:26	122.2	18.87	77	77	0	71	7
9:21:05	122.6	18.75	80	80	0	84	8
9:31:11	121.9	18.80	83	83	0	109	8
9:41:12	122.4	18.79	79	79	0	91	8
9:53:35	124.8	18.82	83	83	0	90	6
10:03:05	128.3	18.85	83	83	0	86	7
10:12:45	123.1	18.76	86	86	0	60	8
11:24:52	122.8	18.78	88	88	0	96	7
11:58:06	123.2	18.65	92	92	0	92	9
12:09:49	123.3	18.67	94	94	0	91	8
12:21:45	123.5	18.71	91	91	0	82	8
12:30:47	122.5	18.73	92	92	0	84	8
12:45:16	123.2	18.72	93	93	0	67	8
12:54:47	123.5	18.72	94	94	0	68	9
13:04:29	123.6	18.84	85	85	0	59	8
14:19:49	122.8	18.82	88	88	0	41	9
14:56:27	123.5	18.65	79	79	0	71	7
15:06:21	123.8	18.68	77	77	0	69	8
15:17:56	125.6	18.65	79	79	0	65	7
15:30:36	125.9	18.68	79	79	0	65	8
15:43:52	125.7	18.68	77	77	0.3	65	7
15:55:13	125.4	18.68	78	78	0	60	8
16:03:51	127.5	18.59	82	82	0	67	7
16:05:10	127.6	18.58	81	82	0.3	61	8

9/13/2006	Temp F	% O2	ppm NO	ppm NOx	ppm NO2	ppm SO2	ppm CO
8:59:10	123.7	18.22	105	105	0	133	9
9:09:15	123.2	18.29	99	99	0	120	8
9:21:47	124.2	18.29	99	99	0	109	8
9:31:15	124.9	18.29	101	101	0	114	9
9:46:37	125.2	18.33	100	100	0	101	7
9:55:43	125.4	18.38	101	101	0	109	8
10:07:40	124.9	18.52	92	92	0	83	8

FAMS Hg measurements during NaCl addition to greenball at United Taconite

9/12/2006

Stack	Sample	Total		Percentage
		ng/l	ng/l	
2B 9:00	1 Particles	0.10		3.97
	1 Oxidized	0.46		18.14
	1 Elemental	1.99	2.56	77.88
9:25	2 Particles	0.18		5.47
	2 Oxidized	0.87		26.93
	2 Elemental	2.18	3.22	67.60
9:51	3 Particles	0.26		8.89
	3 Oxidized	0.77		26.34
	3 Elemental	1.88	2.90	64.77
11:55	4 Particles	0.23		5.76
	4 Oxidized	0.92		22.42
	4 Elemental	2.93	4.08	71.82
12:19	5 Particles	0.15		3.97
	5 Oxidized	0.59		16.03
	5 Elemental	2.96	3.70	80.01
12:42	6 Particles	0.22		5.76
	6 Oxidized	0.85		22.42
	6 Elemental	2.73	3.81	71.82
2:55	7 Particles	0.13		3.54
	7 Oxidized	0.43		11.82
	7 Elemental	3.07	3.63	84.63
3:19	8 Particles	0.12		3.08
	8 Oxidized	0.64		16.24
	8 Elemental	3.18	3.95	80.67
3:42	9 Particles	0.20		5.32
	9 Oxidized	0.42		11.44
	9 Elemental	3.07	3.69	83.24

9/13/2006

8:55	1 Particles	0.10		2.24
	1 Oxidized	0.78		17.25
	1 Elemental	3.63	4.51	80.51
9:19	2 Particles	0.07		1.35
	2 Oxidized	0.88		17.42
	2 Elemental	4.12	5.08	81.23
9:43	3 Particles	0.09		1.76
	3 Oxidized	0.97		18.88
	3 Elemental	4.07	5.12	79.36

9/12/2006

Stack	Sample	Total		Percentage
		ng/l	ng/l	
2A 9:00	1 Particles	0.06		1.07
	1 Oxidized	0.54		10.34
	1 Elemental	4.61	5.20	88.59
9:25	2 Particles	0.40		7.96
	2 Oxidized	0.32		6.42
	2 Elemental	4.33	5.06	85.62
9:51	3 Particles	0.17		3.33
	3 Oxidized	0.69		13.21
	3 Elemental	4.33	5.19	83.45
11:55	4 Particles	0.26		5.01
	4 Oxidized	0.27		5.26
	4 Elemental	4.59	5.11	89.73
12:19	5 Particles	0.24		5.13
	5 Oxidized	0.28		5.77
	5 Elemental	4.25	4.77	89.10
12:42	6 Particles	0.33		7.79
	6 Oxidized	0.20		4.80
	6 Elemental	3.72	4.25	87.41
2:55	7 Particles	0.13		2.91
	7 Oxidized	0.30		6.66
	7 Elemental	4.01	4.44	90.43
3:19	8 Particles	0.29		7.66
	8 Oxidized	0.04		1.18
	8 Elemental	3.42	3.76	91.15
3:42	9 Particles	0.05		1.41
	9 Oxidized	0.06		1.69
	9 Elemental	3.40	3.51	96.90

9/13/2006

8:55	1 Particles	0.06		0.95
	1 Oxidized	0.13		2.23
	1 Elemental	5.81	6.00	96.82
9:19	2 Particles	0.08		1.51
	2 Oxidized	0.27		5.23
	2 Elemental	4.87	5.22	93.26
9:43	3 Particles	0.15		3.35
	3 Oxidized	0.18		3.92
	3 Elemental	4.27	4.61	92.73

Cation concentrations in scrubber water before and during Cl-addition to greenball at United Taconite

	Na	Mg	Si	K	Ca	Fe	Mn	Sr	Ba
	ppm	ppm	ppm	ppm	ppm	ppm	ppm	ppb	ppb
Baseline Stack B	113	58	11.6	20.7	62	25	2.8	379	39.6
During Cl-Addition Stack B	110	55	11.1	19.7	76	17	2.2	363	34.3
Baseline A	116	57	10.4	21.2	56	15	1.7	347	28.3
Cl-Addition A	113	55	10.0	20.1	69	10	1.3	335	24.5

Anion concentrations in scrubber water and in Cl-leach samples from greenball for NaCl addition to greenball at United Taconite

Stack 2B	F	Formate	Cl	NO2-N	Br	NO3-N	SO4
	ppm	ppm	ppm	Ppm	ppm	ppm	ppm
Baseline	57.3	2.5	85	0.005	0.52	8.39	614
Cl addition-1	52.0	2.8	106	0.008	0.52	8.43	589
Cl addition-2	52.9	2.8	113	0.003	0.50	8.18	580
Baseline	54.4	3.2	88	0.010	0.55	8.40	726
Stack 2A							
Baseline	54.9	2.0	84	0.016	0.56	8.4	497
Cl addition-1	52.7	2.1	106	0.013	0.53	8.35	479
Cl addition-2	53.2	1.8	112	0.045	0.50	8.23	451
Baseline	53.8	2.8	91	0.018	0.57	8.21	577
UT1 MAKEUP	11.9	0.18	44.4	0.96	0.25	6.12	195
UT4 MAKEUP	11.8	0.18	45.1	1.03	0.25	6.23	196
Cl in Greenball (dry wt basis)	4.6	4.60	6.20	0.032	0.035	0.82	38
Cl in Greenball (dry wt basis)	4.8	8.34	6.37	0.018	0.031	0.73	34

Field data for NaCl addition to greenball at United Taconite

Stack 2B Thickener	Baseline	Test 1	Test 2	Baseline
Time	0900	1200	1500	0900
PH	3.19	3.12	3.13	3.37
Temperature(°C)	41.9	42.9	42.1	41.0
Conductivity(μS/cm)	2000	2050	2000	2200
Total suspended solids(%)	1.00	0.84	0.64	2.46

Stack 2A Thickener	Baseline	Test 1	Test 2	Baseline
Time	0915	1210	1510	0900
PH	3.75	3.73	3.88	4.43
Temperature(°C)	35.5	37.6	36.5	36.0
Conductivity(μS/cm)	1700	1700	1650	1900
Total suspended solids(%)	1.16	1.14	0.80	2.77

10.3. Appendix III: Hibbing Taconite Focused Halide Injection Tests

Dates: May 1-May 3, 2007

Hibbing Taconite halide injection tests conducted on 5/2/07

Field data for focused halide injection tests at Hibbing Taconite

	Baseline	NaCl	NaBr	CaCl ₂	CaBr ₂	Baseline
Time	0845	1043	1245	1445	1646	1745
PH	6.74	6.75	6.77	6.64	6.71	6.79
Temperature(C)	35.6	35.6	35.5	36.3	36.2	35.6
Conductivity(S/cm)	1050	1050	1050	1050	1050	1050

Anion concentrations in scrubber water during focused halide injection at Hibbing Taconite

	F	Cl	NO ₂ -N	Br	NO ₃ -N	SO ₄
	ppm	Ppm	ppm	ppm	Ppm	ppm
Baseline	30.5	67.6	0.21	0.24	5.45	247
NaCl Injection	30.9	78.3	0.19	0.24	5.47	241
NaBr Injection	28.3	67.1	0.18	12.4	5.46	240
CaCl ₂ Injection	29.0	79.6	0.19	0.42	5.48	242
CaBr ₂ Injection	29.7	68.4	0.18	13.8	5.53	243
Baseline	28.4	67.8	0.19	0.61	5.64	241

Cation concentrations in scrubber water during focused halide injection at Hibbing Taconite

SAMPLE DESCRIPTION	Li	Na	NH ₄	K	Mg	Ca
	ppm	ppm	ppm	ppm	Ppm	ppm
HT - H201	0.0147	49.1	1.04	12.8	66.0	35.9
HT - NaCl	0.0147	49.8	1.11	12.8	66.2	36.1
HT - NaBr	0.0149	49.3	0.99	12.8	66.3	36.0
HT - CaCl ₂	0.0149	49.2	0.96	12.8	66.1	36.1
HT - CaBr ₂	0.0146	49.2	0.91	12.8	66.1	36.0
HT - H202	0.0147	49.2	0.95	12.9	66.1	36.0

FAMS baseline sampling results from Hibbing Taconite immediately before focused halide injection tests were performed.

Sample	ppt	ng	l	ng/l	Total ng/l
HFT 1-1 base 1 particles	37.00	0.85	22.7	0.04	
HFT 1-1 base 1 oxidized	114.70	2.64	22.7	0.12	
HFT 1-1 base 1 elemental	5809.38	133.62	22.7	5.89	6.04
HFT 1-2 base 2 particles	22	0.51	23.4	0.02	
HFT 1-2 base 2 oxidized	138.70	3.19	23.4	0.14	
HFT 1-2 base 2 elemental	5492.58	126.33	23.4	5.40	5.56
HFT 1-3 base 3 particles	105.50	2.43	28.5	0.09	
HFT 1-3 base 3 oxidized	98.30	2.26	28.5	0.08	
HFT 1-3 base 3 elemental	8163.55	187.76	28.5	6.59	6.75

HFT1-1 NaHCO3 Scrubber		16.83	31.7	0.53	
HFT 1-1 QLIP 1 particles	7.80	0.18	31.7	0.01	
HFT 1-1 QLIP 1 oxidized	9.30	0.21	31.7	0.01	
HFT 1-1 QLIP 1 elemental	4504.31	103.60	31.7	3.27	3.81
HFT1-2 NaHCO3 Scrubber		17.66	27.1	0.65	
HFT 1-2 QLIP 2 particles	15.10	0.35	27.1	0.01	
HFT 1-2 QLIP 2 oxidized	165.80	3.81	27.1	0.14	
HFT 1-2 QLIP 2 elemental	4600.18	105.80	27.1	3.90	4.71
HFT1-3 NaHCO3 Scrubber		19.73	28.5	0.69	
HFT 1-3 QLIP 3 particles	16.30	0.37	28.5	0.01	
HFT 1-3 QLIP 3 oxidized	37.60	0.86	28.5	0.03	
HFT 1-3 QLIP 3 elemental	5499.63	126.49	28.5	4.44	5.17

Appendix B-1-13

Bench Scale Tests to Separate Mercury from Wet-Scrubber Solids from Taconite Plants

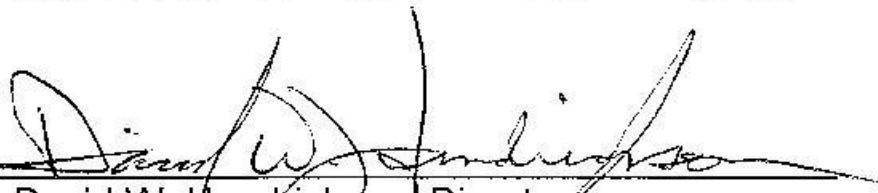
January 7, 2008

**BENCH SCALE TESTS
TO SEPARATE MERCURY
FROM WET-SCRUBBER SOLIDS
FROM TACONITE PLANTS**

COLERAINE MINERALS RESEARCH LABORATORY

Submitted August 17, 2007
Revised January 7, 2008

By 
Blair R. Benner, Program Director - Minerals

Approved by 
David W. Hendrickson, Director
Coleraine Minerals Research Laboratory

CMRL/TR-07-05
NRR/IR-2007/11

University of Minnesota Duluth
Natural Resources Research Institute
5013 Miller Trunk Highway
Duluth, Minnesota 55811

Coleraine Minerals Research Laboratory
One Gayley Avenue
P O Box 188
Coleraine, Minnesota 55722

Bench Scale Tests to Separate Mercury from Wet-Scrubber Solids from Taconite Plants

Summary:

Mercury emissions are a great concern. Initially the emphasis was on the reduction of elemental sources, such as switches, lights, thermometers, dental and medical waste. With those sources greatly diminished, the emphasis has switched to air emissions. The main effort has been in the area of coal-fired power plants, but taconite plants are coming under more scrutiny. Compared to the research on coal-fired power plants, relatively little research has been conducted on taconite plants. The work that has been conducted indicated that the solids in the wet-scrubbers associated with the taconite plants contain a relatively significant amount of mercury and iron units and that this mercury is being recycled back into the process along with the iron. The purpose of this test program was to look at conventional mineral processing steps on the bench scale to determine if the amount of mercury being recycled can be reduced, while at the same time recovering the iron units associated with the scrubber solids. Along with scrubber solids, some of the plants, Minorca, Hibbing Taconite and Keewatin Taconite, also recycle multiclone dust.

Sampling was conducted at Keewatin Taconite (KeeTac), Minntac, Minorca, Hibbing Taconite (Hibtac) and United Taconite (Utac). KeeTac discards all of their scrubber water, and, by permit, are not allowed to recover anything from the scrubber water. They do recycle about 44,700 long tons per year of multiclone dust, which contains about 369 grams of mercury. Some of that mercury is probably removed in a hydraulic classification step prior to the dust going back into the process. No additional beneficiation appears to be necessary. Minorca recycles their multiclone dust and discards a bleed stream of scrubber water. Magnetic separator tests on the scrubber water discard indicated low iron recovery (25%), with a mercury concentration of about 470 ng/g. Minorca's multiclone dust is low in mercury, about 10 ng/g, so there is no need to try to beneficiate that dust. Hibtac also recycles their multiclone dust at a rate of about 990 long tons per year per operating line. Along with that dust, about 174 grams of mercury is recycled. Neither magnetic separation nor hydraulic classification on the dust appeared to reject any significant amount of mercury while still recovering the iron units. When compared to the amount of mercury in the green balls, about 64,000 grams per year, the amount of mercury recycled with the dust is not significant. Hibtac sends their scrubber water to the process water sump in the concentrator, where it is distributed throughout the concentrator. The laboratory tests on Hibtac scrubber water solids indicate that the majority of the mercury is in the minus 8 micron fraction, and, therefore, should stay with the water and report to the tailings basin.

Minntac's scrubber water handling system is a bit more complex than the other plants. The scrubber discharge from each line is sent to a Step wise scrubber thickener, which handles all the scrubber discharge for each Step. So, added to the scrubber thickener is a classifier sand product. The scrubber thickener overflow goes to the pellet plant concentrate thickener, and the overflow from the concentrate thickener goes back to the concentrator. The scrubber thickener underflow goes to the reclaim thickener; the reclaim thickener overflow goes to the reservoir, and the reclaim underflow goes to the concentrate thickener. For two of the six sampling days, the three feeds and two discharges to the Step III scrubber thickener were sampled to obtain a balance around the thickener. Based on the sampling, Minntac scrubbers contain a significant amount of solids, about 4000 long tons per year, containing 7 to 9 pounds of mercury per year.

However, not all of that mercury is recycled. Up to 49 percent of the mercury entering the scrubber thickener reports to the overflow, which in all likelihood ends up in the concentrate thickener overflow and eventually in the tailings basin. Greater than 83 percent of the remaining mercury in the scrubber thickener underflow is in the minus 8 micron fractions. Since the scrubber thickener underflow must pass through two more thickeners before being recycled as pellet feed, it is probable that a significant portion of the minus 8 micron mercury is rejected to the overflows. Additional sampling will be necessary to confirm the above.

For Utac Line 2, there are two parallel scrubbers, one for each side of the machine. Each scrubber discharges under the water level in its own thickener. Also added to each thickener is make up water. The thickener overflows are recirculated to their respective scrubber, and the thickener underflows report to the pellet plant thickener. The combined scrubber thickener underflows send about 3000 long tons of iron and 8.8 pounds of mercury to the pellet plant thickener. With over 50 percent of the mercury in the scrubber thickener underflow being in the minus 10 micron fractions, it is probable that a significant amount of mercury reports to the pellet plant thickener overflow and, therefore, is not recycled. Additional testing will be needed to quantify the amount. Laboratory magnetic separator tests indicate that about 80 percent of the mercury in the scrubber thickener underflows can be rejected, while recovering about 63 percent of the iron. Because of the low percent solids in the thickener underflows, the volumetric loading of the magnetic separator will determine the number of separators needed. Continuous magnetic separator tests will be needed to determine the optimal volumetric loadings.

Introduction:

Mercury in the environment has been a great concern for sometime. Initially the emphasis focused on the reduction of elemental mercury sources such as mercury switches, lights, thermometers, dental waste, medical waste, etc. Great strides have been made in reducing those sources of mercury. While these reductions have been very beneficial to the state, they have elevated the taconite industry from the fourth largest mercury emitter in 1990 to the second largest in 1995¹. The largest source of atmospheric mercury remains coal fired power plants. While emissions from coal fired power plants have been and continue to be extensively studied, there is only a relatively small body of data on taconite plants. The two major sources of information on mercury in the taconite industry have been the Minnesota Department of Natural Resources Division of Lands and Minerals (DNR) and the University of Minnesota Duluth through its Coleraine Minerals Research Laboratory (CMRL). Their work has indicated that each of the six operating taconite plants is unique as far as mercury is concerned. A “snapshot” of mercury distributions around taconite concentrators² in 2003 indicated mercury contents in the crude ranging from a low of 9.44 ppb to a high of 27.90 ppb. The mercury in plant concentrates ranged from 6.19 to 16.10 ppb. There appeared to be no relationship between mercury in the crude and mercury in the concentrate. In general, it appears that greater than 80 percent of the mercury in the crude ore reports to the tailing basin. Recent work by the DNR^{3,4} has focused on the mercury in the induration off-gases, and their interaction with the plant scrubbers. Recently published⁴ data indicate a relatively large variability in the mercury concentration in the green balls feeding the indurating furnaces within a single operation. For example, data for Hibtac showed a greenball mercury concentration of 10.9 ng/g on 1/27/2004, compared to 26.4 ng/g on 5/19/2005. Similarly, greenballs from Minntac ranged from a low of 12.4 to a high of 24.3 ng/g mercury. The large variation in input mercury translates to large variation in the total mercury content of the scrubbers within a plant. For example, corresponding total mercury values (water

plus particles) in the scrubbers at Hibtac ranged from 502 to 1410 ng/l. However, there does not appear to be a direct correlation between mercury in the greenballs and total mercury in the scrubber discharge.

Previous work by CMRL⁵ has indicated that the solids contained in the scrubber water in some of the plants amounts to greater than 5000 tons of iron units annually. Some plants recycle these solids back to the process, which recovers the iron units, but also recycles mercury, a portion of which is probably lost to the atmosphere. Some of the plants send the scrubber solids to the tailings basin, which removes mercury from the system but at a cost of iron units. The objective of this proposal is to determine if standard mineral processing techniques can be used to separate high mercury solids from iron units that can be recycled to the process.

The original test plan called for the collection of bulk composite samples from all of the taconite plants except Northshore, which has very little mercury in the ore. However, after discussions with the DNR and plant personnel, it was decided to take individual samples from each plant, analyze the samples separately, and then composite the solids for bench scale testing.

Sampling Procedure:

With the exception of the 2A and 2B multiclone samples from Keetac, all the samples were collected in acid washed new plastic buckets. The 2A and 2B samples were hot and were collected in metal pails. With the exception of Minntac, all sampling was conducted by CMRL personnel. Minntac sampling was conducted by plant personnel with CMRL supplying the buckets and assisting with the sampling. For the scrubber discharge samples, the slurry pH and temperature were measured and recorded. All samples were brought back to CMRL where the wet weight was measured, the samples were filtered and dried, and the dry weight was used to determine percent solids. Scrubber discharge samples were filtered through #5 paper, which was weighed prior to filtering. Generally, 10 buckets of scrubber discharge were taken for each sample. It was observed that each bucket contained suspended fine solids; therefore, the water column from each bucket was filtered, and then the remaining solids were filtered. For most samples, the same filter paper was used for all buckets; however, for some samples a second paper had to be used due to extremely slow filtering. After drying and weighing the filter paper with solids, the filter cake was removed and the filter paper was weighed to determine the amount of solids remaining in the paper. A portion of the solids was analyzed for total iron, Satmagan iron and mercury. Satmagan iron is a measure of the magnetic iron content of the sample. The filter papers were analyzed for mercury, as was a filter paper blank. Mercury analyses were conducted by dissolution of the samples in a mixture of concentrated hydrochloric and concentrated nitric acid followed by oxidation with bromine mono-chloride. The resultant solutions were analyzed by modified Method 1631 using cold vapor atomic fluorescence spectrometry (CVAFS). Included in each run was a taconite mercury "standard"⁶ for quality control. It is thought to be important to use a standard that has the same matrix as the samples being tested.

One drawback of the sampling procedure is the affinity of the solids to absorb mercury from the scrubber water^{3,4}. The cited work indicated that scrubber discharge samples that were filtered at the plant had consistently lower mercury content in the particles and higher mercury content in the water than samples that were filtered later. Therefore, the mercury values for the scrubber discharge solids reported in this report are probably overstated. Considering the

residence time in the various scrubber thickeners, it is unknown if the thickener samples have the same bias.

Minntac Sampling:

Samples of scrubber discharge were taken from Lines 4 and 7 at Minntac. Both lines were making fluxed pellets. Both lines use a grate-kiln system, with Line 7 having a ported kiln and Line 4 a standard kiln. Line 7 scrubber also had the addition of surfactant ChemTreat 9080 to reduce PM emissions. The scrubber discharges were sampled on six different days. On two days samples were taken around the Step III scrubber thickener (50 foot thickener) as shown in Figure 1. Samples were taken of the streams flowing into the thickener, (Line 6 and 7 scrubber discharges and chip classifier overflow) and flowing out of the thickener, (thickener overflow and underflow). The extra sampling was done to get a better estimate of how much material is being recycled back to the indurating machines. As shown on Figure 1, about 60 percent of the 50' thickener overflow goes to the concentrate thickener. The purpose of that thickener is to densify the concentrate from 45 percent solids to greater than 60 percent solids, with the concentrate thickener overflow going to the concentrator. In essence, the 50' thickener overflow is sent to the concentrator thickener just as a convenient way to get the water back to the concentrator. The remainder of the 50' thickener overflow goes to the plant reservoir. Therefore, it is unlikely that much of material in the 50' thickener overflow is recycled to the indurating machine. The 50' thickener underflow goes to the reclaim thickener, whose overflow goes to process water and whose underflow goes to the concentrate thickener. Therefore, only those solids that settle in the reclaim and concentrate thickener are directly recycled.

Results from the Minntac sampling are given in Table 1. From the mercury analyses of the filter paper, it is obvious that the solids suspended in the water column are very high in mercury compared to the bulk of the solids. The mercury analyses suggest a possible relationship between feed rate to the grate and the mercury content of the scrubber solids for Line 4. On March 14th and 16th, Line 4 was running on low tons due to a balling drum being down. Those are the only two days where Line 4 scrubber solids were lower in mercury than Line 7; however, when the amount of solids in the scrubber discharge is added to the equation (total Hg ng/lb of slurry on Table 1), there is no apparent effect of feed rate. The scrubber solids are highly magnetic, as indicated by the Satmagan iron values (Sat Fe). It is interesting to note that Line 7 scrubber solids always have the highest magnetic iron content, and Line 6 solids are the lowest.

Data from the March 7th and March 14th tests were mass balanced using USIMPAC. A comparison of the computer generated versus actual values is given in Table 2. In general, the agreement is very good, especially for the mercury analyses. Using the balanced data, the annual flow of material can be calculated as shown in Table 3. From this data, it appears that the Step III scrubbers are removing between 7 and 9 lbs of mercury per year, of which about 4.6 to 5.7 lb could be recycling (thickener underflow). Chemistry by size fractions for the thickener underflows from March 7th and 14th, Table 4, indicates that the majority of the mercury is in the minus 500 mesh fraction. Cyclosizer tests, Table 5, on the minus 500 mesh fractions indicate that the majority of the mercury is contained in the minus 8 micron fraction of the thickener underflow. Looking at the total underflow, about 62 percent of the mercury is in the -8 micron fraction for the March 7th sample and about 77 percent for the March 14th sample. Since the 50-foot thickener underflow passes through two additional thickeners (reclaim and concentrate), it is probable that the majority of the minus 8 micron fraction reports to one of the overflows and,

hence, is not recycled. Assuming that each additional thickener removes 1/3 of the minus 8 micron material, then, for the March 7th sample, the total mercury being recycled would be 3.35 lb/yr or about 39 percent of the mercury entering the 50-foot thickener. For the March 14th sample, the mercury recycle would be 2.37 lb/yr, or about 26 percent of the mercury entering the 50-foot thickener. Additional sampling of the other two thickeners would be necessary to determine the actual amount of mercury that is being recycled.

Composites were made of the Line 7 and Line 4 scrubber discharges, so that laboratory concentrating tests could be performed. To simulate the upgrading that could occur in a thickener, elutriation tests were run on the composite discharge samples. The elutriation tests were conducted using a 33 inch long glass tube with diameters ranging from 5/8 inches at the bottom to 1.5 inches at the top with two intermediate diameters between. About 24 inches of the tube has a diameter of 1.5 inches. There is an overflow collection launder at the top. A hose is connected to the bottom and that hose is in turn connected to a glass tee. One leg of the tee is connected to a metered water supply and the other leg, which serves as the drain is clamped off. The test procedure is as follows: The water is set to the desired flow rate, tube is filled about half way with water, the solids are added to the top and the flow is continued until the overflow is clear. The overflow is collected and filtered. The flow rate is increased and the procedure is repeated. When the final flow rate is completed, the drain is opened and the solids are washed out and collected. The Minntac composite discharge samples were run with up flow velocities of 0.0067, 0.0101 and 0.0135 feet per second (as measured in the 1.5 inch diameter portion of the tube). The results shown on Table 6 indicate that greater than 50 percent of the mercury and less than 6 percent of the iron in the scrubber discharge could be removed at the lowest velocity. For comparison purposes, a 50-foot diameter thickener with an overflow of 7000 gpm has an up flow velocity of 0.0079 feet per second.

To determine the effect of magnetic separation, extra 5-gallon pails of Line 4 and Line 7 scrubber discharges were taken with the March 16th sampling. Rather than filtering the two extra pails, they were run as received through the laboratory drum magnetic separator. The results are shown in Table 7. Results from Line 7 are promising, with 49 percent of the mercury and about 8 percent of the iron being rejected. The results for Line 4 scrubber discharge were poor, with only about 18 percent of the mercury being rejected as tailing. It should be noted that the laboratory magnetic separator has a limited feed rate for slurry, which would be impractical in commercial operation. In general, magnetic separation is not run on slurries with such low percent solids. The limiting factor will be the gallons per minute flow to the separators. The closest commercial operation is the pre-classification of flotation feed as currently practiced at Minntac. That operation treats a 17 percent solids stream with an average flow of about 70 gpm per foot of magnet width. Assuming that same flow rate, then each scrubber discharge at 3000 gpm would require at least four single drum machines with 4-ft diameter by 10-ft long drums. Continuous magnetic separator tests on a pilot scale separator would have to be run to determine the effect of volumetric loading and iron recovery and mercury rejection.

Keewatin Taconite Sampling:

The four sets of multiclone discharges were sampled at Keewatin Taconite (KeeTac). KeeTac's scrubber discharge permit precludes recovering any material from the scrubber discharge; therefore, the scrubber discharge was not sampled. The multiclones remove dust from the gas in the grate portion of the grate-kiln machine. The multiclone discharges are double dump valves, which open for a set time. The upper valve opens for a period of time, dumping

the collected dust into a lower chamber. When the upper valve closes, the lower valve closes, dropping the dust into a water swept launder. By measuring the time between consecutive openings of the upper valve, and by collecting all the dust dumped by the lower valve, the rate of dust production can be calculated. There are 4 to 6 discharge valves at each location, and all the valves at a single location open and close at the same time. Therefore, the discharges from all the valves at a single location were composited, and a single time was used to calculate the discharge rate.

Results of the sampling are given on Table 9. There is a significant amount of solids being generated, with the average hourly combined dust being about 11,425 lb/hr or about 5 LTPH with an average mercury of 42.2 mg/hr. The dust from 2 A&B had significantly higher mercury concentrations, (lower weight of solids). The dust at all of the sampling points was high in iron, generally greater than 64 percent, and relatively low in magnetic iron (less than 35 percent). A representative sample from each sampling location for each day was split out and combined to produce a six-day composite for each sampling location. Each composite was screened through 10 microns, and the various fractions were analyzed for total iron, Satmagan iron, and mercury. The results are given on Table 9. The mercury is concentrated in the minus 635 mesh (20 micron) fractions. Generally, the minus 635 mesh fractions are the only ones with mercury concentrations greater than 20 ng/g. There is a trend of increasing magnetic iron with decreasing size fractions for all sampling points. Since the slurried dust goes to a dewatering classifier prior to going back to the process, it is reasonable to assume that the majority of the minus 635 mesh material goes with the water and is not directly recycled to the process. With the relatively low mercury content in the dust, and the probable rejection of close to 40 percent of the mercury in the current process, no further concentrating tests were run on the KeeTac dust.

Minorca:

The Minorca gas cleaning system consists of multiclones to remove the bulk of the dust, followed by 4 wet scrubbers in parallel. The scrubber discharges are collected in a common sump, and the water is recirculated to the scrubbers, with a bleed stream being sent to tailings. Both the bleed stream water and the multiclone dust were sampled. The multiclone dust was not available on the first sampling day due to a plugged hopper. The multiclones operate in the same manner as described for KeeTac, except the cycle period is longer. The results of the sampling are presented in Table 10. The mercury concentration in the multiclone dust sample is low. The mercury in the scrubber water solids is variable, ranging from a low of 111.39 ng/g to a high of 1,246.48 ng/g. The iron in both the dust and scrubber solids is highly oxidized, with a magnetic iron content of between 13.57 and 18.54 percent. Although the current practice at Minorca is to discard the scrubber bleed stream, it may be possible to recover some iron units from that stream. To that end, laboratory magnetic separator tests were run on a sample of scrubber water. The results, Table 11, indicate that although the laboratory drum magnetic separator rejected over 88 percent of the mercury, the mercury concentration of 471 ng/g in the magnetic concentrate is too high to be recycled to the process.

Representative samples of each day's multiclone discharges were composited; a sample of the composite was screened, and the fraction was analyzed, Table 12. The mercury is fairly uniformly distributed across all size fractions, which indicates very little opportunity to reject a high mercury fraction. To confirm this hypothesis, an elutriation test was run on the multiclone composite. The results given in Table 13 indicate little opportunity for mercury rejection.

Hibbing Taconite:

Line 3 was sampled at Hibbing Taconite (Hibtac). The gas treatment scheme is similar to Minorca, employing multiclones to remove dust and then 4 wet scrubbers in parallel. The scrubber discharge is pumped to the concentrator, where it is utilized as process water, with the vast majority of the water ultimately going to the tailings basin. The multiclone dust is pumped to the pellet plant thickener, where whatever does not overflow with the water is added back to the process. The sampling results, Table 14, indicate little variation in the mercury concentration in either the scrubber water or dust. The multiclone dust mercury concentrations are about an order of magnitude higher than the dust from either KeeTac or Minorca. Of the mercury removed from the gas stream, about 13 percent is associated with the multiclone dust.

A multiclone dust composite was made by taking a representative sample from each day's dust. A portion of the multiclone composite was screened, and the fractions were analyzed, Table 15. The mercury content of the fractions between 200 and 635 mesh is fairly uniform and increases significantly in the finer (-635 mesh) fractions. A cyclosizer test was run on the minus 325 mesh fraction of the dust composite, Table 16, which showed little variation except for the minus 8 micron portion, which had a mercury concentration about 3 times higher than the other fractions. These results suggest that only a small amount of mercury is being rejected in the pellet plant thickener overflow.

A laboratory magnet separation test was run on the composite dust, Table 17. Somewhat surprisingly, the mercury was concentrated in the magnetic concentrate. To confirm the magnetic separator results, the test was repeated, with the same results, Table 18. These results clearly eliminate magnetic separation as a means of removing mercury from the multiclone dust while still recovering the iron units.

Although the scrubber solids are being sent to the concentrator and are probably being lost to the process, it may be possible to recover some of the iron units without recovering too much mercury along with the iron. A cyclosizer test was run on a scrubber solids composite, Table 19. The results show a reverse correlation between size and mercury concentration, with the minus 8 micron fraction containing about 69 percent of the mercury. Elutriation tests were also run on the scrubber solids composite, Table 20, which indicated that only a very small up flow velocity will remove a significant amount of mercury. To determine the potential for using magnetic separation for removing mercury and still recovering some of the iron units currently being lost, both Davis tube and laboratory drum magnetic separation tests were run on the scrubber solids composite, Table 21. These results are more typical of what has previously been seen with magnetic separation, namely the concentration of mercury in the non-magnetic portion. Assuming an average scrubber water discharge rate of 2500 gpm at 0.035 percent solids and solids specific gravity of 4.8, then the solids rate in the scrubber water is 423 lb/hour. Based on the magnetic separator tests, about 137 lb per hour or about 600 st/yr could be recovered using magnetic separation. However, along with the iron would come about 48.5 grams per year of mercury. These results assume a sufficient number of magnetic separators to handle the volume of water that needs to be treated with the very low percent solids in the feed.

United Taconite:

United Taconite's (Utac) gas cleaning system is slightly different from the other systems. Utac draws gas from both sides of the indurating line and then treats each side in its own scrubber. Each scrubber discharges under the water level in separate scrubber thickeners. The scrubber thickener overflow is returned to the scrubber, and the underflow goes to the pellet

plant thickener. The Line 2 scrubber system was sampled. Thickener underflows and overflows were taken from both thickeners. The plant designations are thickener 9 and thickener 10. Results of the sampling are given on Table 22. Unfortunately, plant data for the sampling period was not available. Normal operating conditions have a combined (#9 and #10) overflow rate of 1500 gpm and a combined underflow rate of 980 gpm. As would be expected, the thickener overflow solids had a higher mercury concentration than the underflow solids. For thickener #9, the overflow solids averaged 343.3 ng/g mercury, compared to 160.4 ng/g for the underflow solids. Likewise, #10 thickener overflow solids averaged 463.0 ng/g, and the underflow solids averaged 175.1 ng/g. Assuming the average plant values for the flows, then the combined thickener underflows contain, on an annual basis, about 5,170 long tons of solids at 54.7 percent iron (2,968 lt/yr iron) and 8.8 pounds of mercury.

The individual samples from each sampling point were combined to make four overall composites. The composite samples were screened, and the fractions were analyzed for mercury, Table 23. Surprisingly, the mercury concentration on the solids showed a trend of decreasing with decreasing size down to 10 microns. Below 10 microns the mercury concentration increased. Because of the weight distribution of the sizes, the majority of the mercury is contained in the minus 10 micron fractions. This suggests that when the #9 and #10 thickener underflows are sent to the pellet plant thickener, a significant amount of mercury will be removed in the pellet plant thickener overflow.

To determine the potential for magnetic separation, samples of the composite #9 and #10 underflows were diluted to plant percent solids and run through the laboratory drum magnetic separator. The results, Table 24, indicate that about 80 percent of the mercury could be rejected in the non-magnetic portion, while recovering close to 65 percent of the iron in the magnetic portion. On an annual basis, magnetic separation has the potential to recover about 1,900 long tons of iron and reject about 7.1 pounds of mercury. As with the other plants, continuous magnetic separator tests would need to be run to determine the effect of volumetric loading on recovery and mercury rejection.

To estimate the effect of magnetic separation on the thickener overflow, samples of #9 and #10 composites were run in the Davis tube. The results, Table 25, indicate that it would be possible to recover a magnetic product that contained about 11 percent of the mercury and about 60 percent of the iron. The effect of removing the iron from the circulating load of the scrubber is unknown. It may be that removing the iron on a continuous basis would reduce the mercury content of the magnetic concentrate, since it would not be recirculated back to the scrubber. However, it may also mean that the mercury content of the non-magnetic portion would build up even higher before it finally left the scrubber circulating load.

Conclusions:

The sampling and analyses of the solids indicates that, in general, the mercury is concentrated in the minus 10 mesh fractions, which suggests that thickening and or cycloning will remove a significant amount of mercury from the recycle. The sampling has also shown that some scrubber water contains, on an annual basis, greater than 5,000 long tons of solids. However, not all of those solids are recycled.

On a plant by plant basis, Keetac recycles about 44,700 long tons of dust per year, which contains about 369 grams of mercury, some of which is probably removed along with the water in the classifier. There appears to be little need for beneficiation of the dust. Minorca, like Keetac, disposes of their scrubber water bleed stream and only recycles the multiclone dust. On

average, the mercury content of the dust is less than 10 ng/g and, therefore, additional beneficiation is not needed. Hibtac sends their scrubber water to the concentrator process water sump, which essentially removes the mercury in the solids from the recycled material. Some small fraction may be recovered in magnetic separation, but it is impossible to estimate how much. Based on the laboratory tests, it appears that the vast majority of the mercury will remain with the water and exit the plant. Hibtac does recycle their multiclone dust at the rate of about 990 lt/yr per line, containing about 174 grams of mercury. Neither magnetic separation nor hydraulic classification appears to offer much rejection. To put the mercury in the recycled dust in perspective, a line running at 480 ltph with a mercury content of 15 ng/g contains, on an annual basis, about 64,000 grams of mercury.

Minntac scrubbers contain a significant amount of solids, up to 4,000 long tons per year, containing 7 to 9 pounds of mercury per year. However, not all the material in the scrubber water is recycled. As much as 49 percent of the mercury in the scrubbers appears to report to the scrubber thickener overflow, which is sent to the pellet plant concentrate thickener. The concentrate thickener overflow goes to the concentrator as process water and eventually ends up in the tailing basin. Of the mercury remaining in the thickener underflow, greater than 83 percent of that mercury is contained in the minus 8 micron fractions. Since the thickener underflow reports to the reclaim thickener, followed by the concentrate thickener, it is probable that a majority of the minus 8 micron mercury is removed in the overflows. To confirm the mercury rejection, additional sampling should be taken around the various thickeners at Minntac. One way to enhance the mercury rejection would be to cyclone the scrubber thickener underflow prior to the reclaim thickener. The cyclone overflow would report to the thickener overflow, and the underflow to the thickener feed well.

For Utac, the combined #9 and #10 scrubber thickener underflows send about 3,000 long tons of iron and 8.8 pounds of mercury to the pellet plant thickener. Since over 50 percent of the mercury is present in the minus 10 micron fractions, it is probable that a good portion of that mercury overflows to the pellet plant thickener and is effectively removed from the recycle. Additional sampling will be needed to confirm the mercury rejection. The lab testing has shown that magnetic separation of the combined scrubber thickener underflows can reject at least 80 percent of the mercury while recovering about 63 percent of the iron. Continuous magnetic separator tests on the combined scrubber thickener underflows will be necessary to determine the effect of volumetric loading on iron recovery and mercury rejection.

References:

1. Berndt, Michael, "Mercury distribution in the Biwabik Iron Formation and resulting emissions from Minnesota Taconite Companies," Minerals Coordinating Committee Progress Report, Mercury and Mining in Minnesota, January 2002.
2. Benner, B. R., "Mercury Distribution Around Taconite Concentrators," CMRL Technical Report TR-03-10, September 2003.
3. Berndt, Engesser and Johnson, "On the distribution of mercury in taconite plant scrubber systems," Minnesota Department of Natural Resources, October 2003.
4. Berndt, M. and Engesser, J., "Mercury Transport in Taconite Processing Facilities: (I) Release and Capture During Induration," Iron Ore Cooperative Research Final Report, August 2005.
5. Benner, B. R., "Mercury Removal from Induration Off Gas by Wet Scrubbers," CMRL Technical Report TR-01-19, November 2001.

Table 1 - Results from Minntac Sampling

	ng/g Hg				total Hg ng/lb slurry	pH	Temp, C	Fe, %	Sat Fe, %	gpm	Feed LTPH
	% solids	cake	paper **	tot solids							
3/5/2007											
Line 7	0.038	430.56	2158.32	446.78	77.18	6.70	31.2	62.32	57.49	2995	525
Line 4	0.016	1721.32	2263.47	1775.54	131.41	6.61	35.1	60.70	52.99	3040	560
3/7/2007											
Line 7 scrub discharge	0.077	200.38	1122.29	223.76	78.47	6.43	36.4	63.08	57.81	3010	525
Line 4 scrub discharge	0.019	617.78	2773.00	683.09	59.52	6.61	36.1	61.14	52.30	2985	550
Line 6 scrub discharge	0.042	850.82	3697.00	890.91	168.17	6.56	36.7	60.67	46.28	2998	535
50' thick oflow	0.032	280.23	2170.67	314.39	45.03	7.05	34.1	60.13	48.89	6948*	
50' thick unflow	4.143	69.60		69.60	1309.21	7.08	33.7	61.92	50.97	510*	
Line 7 class Oflow	1.320	12.66		12.66	75.89	8.91	24.8	61.28	49.96	1454*	
3/9/2007											
Line 7 scrub discharge	0.054	338.80	3504.00	386.52	94.38	6.42	35.6	62.30	56.44	3000	500
Line 4 scrub discharge	0.013	981.10	894.00	978.20	57.00	6.48	35.3	60.99	51.10	3041	560
3/12/2007											
Line 7 scrub discharge	0.052	413.00	971.60	422.80	99.05	6.24	36.5	63.07	59.02	3000	535
Line 4 scrub discharge	0.038	405.40	1381.30	426.87	74.12	6.41	38.9	61.69	53.80	2975	565
3/14/2007											
Line 7 scrub discharge	0.063	611.25	4306.67	644.49	184.73	6.39	37.0	64.29	59.95	3002	530
Line 4 scrub discharge	0.096	189.61	4337.00	220.27	96.37	6.71	40.0	63.49	58.17	2975	455
Line 4 scrub discharge			2754.67								
Line 6 scrub discharge	0.027	1073.46	2334.67	1132.58	136.68	6.72	37.0	61.72	41.45	3012	525
50' thick oflow	0.047	258.06	812.86	290.16	61.59	6.94	34.6	59.31	44.44	7131*	
50' thick unflow	3.029	76.18		76.18	1047.67	7.19	33.9	62.95	52.36	432*	
Line 7 class Oflow	0.907	1.25		1.25	5.15	9.23	26.6	61.24	52.60	1544*	
3/16/2007											
Line 7 scrub discharge	0.060	600.30	3151.11	635.19	174.29	6.51	37.1	64.72	60.69	3001	540
Line 4 scrub discharge	0.077	430.28	2035.11	445.02	154.57	6.58	38.7	63.27	53.70	3025	450

* Calculated from mass balancing program

** Mercury from digestion of filter paper after removal of filter cake

Table 2 - Mass Balancing around 50-foot Thickener in Step III

	gpm		% solids		Hg, ng/g		Fe, %		Sat Fe, %	
	measured	computer	measured	computer	measured	computer	measured	computer	measured	computer
3/7/2007										
Line 7 scrub dis	3013	3010	0.0772	0.0773	223.76	233.60	63.08	63.10	57.81	57.83
Line 6 scrub dis	2998	2995	0.0416	0.0416	890.91	891.70	60.67	60.68	46.28	46.29
Class oflo		1454	1.3204	1.3321	12.66	13.30	61.28	61.45	49.96	50.08
Thickener Oflow		6948	0.0315	0.0312	314.39	296.30	60.13	60.11	48.89	48.88
Thickener Unflow		510	4.1433	4.0711	69.60	61.10	61.92	61.73	50.97	50.84
	gpm		% solids		Hg, ng/g		Fe, %		Sat Fe, %	
	measured	computer	measured	computer	measured	computer	measured	computer	measured	computer
3/14/2007										
Line 7 scrub dis	3002	3005	0.0631	0.0631	644.49	632.10	64.29	64.34	59.95	59.72
Line 6 scrub dis	3012	3015	0.0266	0.0266	1132.58	1116.40	61.72	61.74	41.45	41.40
Class oflo		1544	0.9074	0.9009	1.25	1.22	61.24	61.60	52.60	51.30
Thickener Oflow		7131	0.0468	0.0472	290.16	308.00	59.31	59.22	44.44	44.67
Thickener Unflow		432	3.0292	3.0670	76.18	81.00	62.95	62.61	52.36	53.59

Table 3 - Calculated Annual Material Flow

3/7/2007	Solids LTPH	lb Hg per yr	LTPY Fe
Line 7 scrub dis	0.53	2.37	3200.2
Line 6 scrub dis	0.28	4.85	1649.4
Class oflo	4.43	1.13	26133.1
Thickener Oflow	0.49	2.80	2841.1
Thickener Unflow	4.85	5.70	28897.4
3/14/2007			
Line 7 scrub dis	0.43	5.22	2656.6
Line 6 scrub dis	0.18	3.90	1077.0
Class oflo	3.19	0.08	18828.2
Thickener Oflow	0.75	4.45	4288.4
Thickener Unflow	2.95	4.62	17947.3

Table 4 - Chemistry by Size for the 50-foot Thickener Underflow Samples

3/7/2007					Distribution, %		
Mesh	wt %	ng/g Hg	% Fe	% Sat Fe	Hg	Fe	Sat Fe
100	4	22.92	59.39	27	1.61	4.09	2.16
150	3.2	46.66	50.55	24.06	2.62	2.79	1.54
200	4.6	31.13	49.29	24.45	2.51	3.91	2.25
270	11.3	42.51	57.76	39.33	8.43	11.25	8.89
325	6.3	22.89	63.45	48.85	2.53	6.89	6.16
400	10.3	18.68	65.51	53.24	3.38	11.63	10.97
500	15.4	15.67	66.26	56.37	4.24	17.58	17.37
-500	44.9	94.76	54.12	56.39	74.68	41.87	50.66

3/14/2007					Distribution, %		
Mesh	wt %	ng/g Hg	% Fe	% Sat Fe	Hg	Fe	Sat Fe
100	3.2	29.43	58.61	26.40	1.54	2.95	1.61
150	2.8	32.14	51.09	22.97	1.47	2.25	1.22
200	3.8	27.55	47.38	24.39	1.71	2.83	1.76
270	10.2	20.68	60.37	42.42	3.44	9.69	8.23
325	5.5	21.61	63.46	59.27	1.94	5.49	6.20
400	10.2	18.32	65.54	56.49	3.05	10.52	10.96
500	15.9	22.51	66.27	58.59	5.84	16.58	17.72
-500	48.4	102.64	65.20	56.81	81.02	49.67	52.30

**Table 5 - Cyclosizer Tests on -500 mesh Fraction
from 50-foot Thickener Underflow**

3/7/2007						Distribution, %		
	wt	wt%	ng/g Hg	% Fe	% Sat Fe	Hg	Fe	Sat Fe
32 u	0.2	0.53	40.63			0.34	0.00	0.00
24 u	3.7	9.89	7.76	71.42	66.19	1.22	11.09	11.72
17 u	9.4	25.13	7.80	69.39	61.95	3.10	27.38	27.87
11 u	9.9	26.47	15.79	64.74	58.10	6.62	26.90	27.53
8 u	3.4	9.09	26.47	64.03	56.26	3.81	9.14	9.15
-8 u	10.3	27.54	191.64	58.98	48.14	83.55	25.50	23.73
Oflow paper	0.5	1.34	64.24			1.36	0.00	0.00
3/14/2007						Distribution, %		
	wt	wt%	ng/g Hg	% Fe	% Sat Fe	Hg	Fe	Sat Fe
32 u	0.2	0.53	185.01			1.56	0.00	0.00
24 u	4.3	11.47	13.40	71.80	66.01	2.43	12.92	13.55
17 u	9.4	25.07	17.44	69.80	62.73	6.92	27.46	28.14
11 u	9.9	26.40	35.42	65.66	59.90	14.80	27.21	28.30
8 u	3.5	9.33	47.99	65.30	56.68	7.09	9.57	9.47
-8 u	9.2	24.53	246.01	60.40	48.64	95.55	23.26	21.36
Oflow paper	1	2.67	17.24			0.73	0.00	0.00

Table 6 - Elutriation Test on Scrubber Discharge Composites

Line 7						Distribution, %		
feet per sec	wt%	ng/g Hg	% Fe	% Sat Fe	Hg	Fe	Sat Fe	
0.0067	6.84	2446.78	34.16	22.21	52.95	3.63	2.59	
0.0101	10.53	273.76	56.42	42.84	9.11	9.23	7.69	
0.0135	41.58	161.59	68.31	63.97	21.25	44.13	45.38	
Unflo	41.05	128.52	67.42	63.3	16.69	43.01	44.34	
Line 4						Distribution, %		
feet per sec	wt%	ng/g Hg	% Fe	% Sat Fe	Hg	Fe	Sat Fe	
0.0067	7.89	3145.97	43.46	27.18	65.18	5.59	3.96	
0.0101	20.79	313.48	64.91	57.61	17.10	22.00	22.08	
0.0135	23.95	133.63	67.44	64.74	8.40	26.32	28.58	
Unflo	44.47	79.81	63.58	55.35	9.32	46.09	45.38	

**Table 7 - Magnetic Separator Tests
on Scrubber Discharges from 3/16/07**

	Wt %	Fe	ng/g, Hg	Fe Dist, %	Hg Dist, %
Line 4 concentrate	82.26	68.23	199.46	96.80	82.37
Line 4 tailing	17.74	10.45	197.89	3.20	17.63
Line 7 concentrate	73.04	70.61	185.84	92.28	50.98
Line 7 tailing	26.96	16.01	484.20	7.72	49.02

Table 8 - KeeTac Multiclone Sampling

Date	Sample	Time, sec	wt	% Fe	% Sat Fe	ng/g Hg	Solids		
							lb/hr	mg Hg/hr	g Hg/yr
2/12/2007 Green ball rate 930 LTPH	1 A	72	16059.8	64.86	21.83	3.70	2558.60	4.30	37.65
	1 B	70	27898.3	64.90	23.48	2.82	4301.50	5.51	48.24
	2 A	36	13910.4	64.90	23.33	39.59	1088.93	19.57	171.45
	2 B	56	6590.5	66.05	33.59	37.74	816.99	14.00	122.62
2/15/2007 Green ball rate 920 LTPH	1 A	72	19926.3	64.90	23.33	3.76	3174.60	5.42	47.47
	1 B	70	32681.7	64.40	22.92	2.01	5039.03	4.60	40.28
	2 A	36	9167.8	64.83	33.37	37.70	717.67	12.28	107.60
	2 B	56	12140.6	64.71	29.48	26.75	1505.01	18.28	160.11
2/16/2007 Green ball rate 920 LTPH	1 A	72	28420.4	65.67	22.76	7.87	4527.86	16.17	141.65
	1 B	70	46217.2	65.73	23.62	2.54	7126.00	8.23	72.09
	2 A	36	9193.5	65.74	33.24	17.16	719.69	5.61	49.11
	2 B	56	9034.6	65.66	29.17	12.31	1119.97	6.26	54.83
2/21/2007 Green ball rate 840 LTPH	1 A	72	16934.2	64.79	23.13	3.67	2697.91	4.50	39.38
	1 B	70	36365.4	64.97	22.74	4.05	5607.00	10.31	90.31
	2 A	36	11304.6	65.16	32.52	28.64	884.95	11.51	100.80
	2 B	56	8580.6	64.59	28.01	27.48	1063.69	13.27	116.25
2/22/2007 Green ball rate 880 LTPH	1 A	72	14437.2	64.67	20.92	4.23	2300.09	4.42	38.69
	1 B	70	38998.6	64.79	22.15	3.12	6013.00	8.52	74.61
	2 A	36	9443.2	64.94	31.40	30.46	739.23	10.22	89.55
	2 B	56	5675	64.50	26.26	20.72	703.50	6.62	57.97
3/6/2007 Green ball rate 930 LTPH	1 A	72	26604.4	64.70	23.05	4.66	4238.54	8.96	78.47
	1 B	70	59746.4	65.21	26.63	4.18	9212.00	17.47	153.02
	2 A	36	10669	63.17	32.93	44.79	835.19	16.99	148.79
	2 B	56	12575.8	64.78	29.15	28.13	1558.96	19.91	174.43

Table 9 - Chemistry by Size for Keetac Multiclone Composite Dust Samples

1A					Distribution, %		
mesh	wt %	% Fe	% Sat Fe	ng/g, Hg	Fe	Sat Fe	Hg
100	8.77	65.81	12.05	2.91	8.97	4.79	4.11
150	7.79	62.34	15.87	2.11	7.55	5.61	2.65
200	15.05	62.95	21.30	2.27	14.72	14.54	5.51
270	24.15	65.56	23.51	1.89	24.61	25.76	7.36
325	10.10	66.49	23.68	2.15	10.43	10.85	3.50
400	6.12	66.88	23.22	2.49	6.36	6.45	2.46
500	13.74	67.02	24.83	2.83	14.30	15.47	6.27
635	6.61	65.90	27.70	3.26	6.77	8.31	3.48
10 u	6.07	66.72	29.84	43.52	6.29	8.22	42.60
-10 u	1.60			85.27	0.00	0.00	22.06
2A					Distribution, %		
mesh	wt %	% Fe	% Sat Fe	ng/g, Hg	Fe	Sat Fe	Hg
100	1.70	63.86	10.71	13.09	1.71	0.58	1.10
150	3.84	61.44	18.08	17.74	3.72	2.23	3.35
200	10.47	62.44	26.92	11.93	10.30	9.04	6.15
270	21.65	65.70	32.34	7.79	22.41	22.45	8.30
325	10.28	66.52	33.21	10.31	10.78	10.95	5.22
400	5.99	66.92	34.45	11.69	6.31	6.61	3.44
500	18.42	67.09	35.12	15.06	19.47	20.74	13.65
635	10.82	66.95	36.03	17.35	11.41	12.50	9.24
10 u	13.31	66.21	34.90	58.88	13.89	14.90	38.57
-10 u	3.52			63.42	0.00	0.00	10.98

Table 9 – Continued

1B					Distribution, %		
mesh	wt %	% Fe	% Sat Fe	ng/g, Hg	Fe	Sat Fe	Hg
100	4.75	65.64	12.18	2.77	4.77	2.46	3.97
150	5.87	61.91	19.12	4.28	5.56	4.77	7.58
200	14.02	62.85	24.30	2.59	13.48	14.47	10.95
270	25.87	65.79	26.36	1.68	26.04	28.96	13.11
325	11.62	66.86	25.67	1.28	11.89	12.67	4.49
400	7.67	67.13	24.01	1.30	7.88	7.82	3.01
500	16.57	67.95	24.00	1.88	17.23	16.89	9.39
635	10.00	66.87	21.89	2.22	10.23	9.30	6.70
10 u	2.87	66.15	21.92	31.97	2.90	2.67	27.66
-10 u	0.76			57.54	0.00	0.00	13.15
2B					Distribution, %		
mesh	wt %	% Fe	% Sat Fe	ng/g, Hg	Fe	Sat Fe	Hg
100	3.09	64.02	11.44	4.45	3.10	1.25	0.79
150	6.88	61.36	20.95	4.68	6.61	5.10	1.85
200	16.03	62.44	27.19	5.74	15.68	15.43	5.28
270	24.13	64.99	28.62	6.73	24.57	24.45	9.33
325	9.84	65.84	29.21	8.03	10.15	10.18	4.54
400	3.28	66.62	27.15	13.20	3.43	3.16	2.49
500	16.73	67.63	32.42	15.98	17.73	19.21	15.36
635	10.80	66.18	32.72	20.30	11.20	12.51	12.59
10 u	7.30	65.72	33.68	86.92	7.52	8.70	36.43
-10 u	1.93			102.34	0.00	0.00	11.33

Table 10 - Results from Sampling at Mittal's Minorca Plant

Sample	% solids	ng/g Hg			total Hg ng/lb slurry	time seconds	Dust lb/hr	Dust Hg mg/hr	pH	Temp, C	% Fe	% Sat Fe
		cake	paper *	tot solids								
3/19/07 scrubber	0.07	645.47	6826.86	681.17	243.92				6.13	40.85	64.16	14.87
			12624.60									
3/20/07scrubber	1.14	111.41	83.11	111.39	578.58				8.08	44.10	60.07	13.82
multiclones		6.68				173.00	1690.75	5.13			62.49	13.57
3/21/07scrubber	0.28	376.10	1323.71	379.56	490.07				7.39	43.75	60.76	17.82
multiclones		9.12				173.00	445.32	1.84			62.27	14.13
3/22/07scrubber	0.10	1227.83	3251.69	1246.48	554.64				6.57	41.33	59.73	14.68
multiclones		11.42				173.00	192.11	1.00			59.88	18.54
3/27/07scrubber	0.12	551.61	9993.71	588.85	333.45				6.65	43.26	60.17	11.23
multiclones		9.98				173.00	280.02	1.27			61.67	14.26
3/28/07scrubber	0.12	607.02	8915.60	639.84	348.70				6.98	42.34	61.73	13.81
multiclones		9.86				173.00	267.42	1.20			60.16	17.15

* Mercury from digestion of filter paper after removal of filtercake.

Table 11 - Magnetic Separator Test on Minorca Scrubber Water

Sample	wt%	% Fe	Hg, ng/g	Distribution, %	
				Fe	Hg
Concentrate	23.08	67.56	471.27	24.95	11.58
Tails	76.92	60.97	1079.39	75.05	88.42

Table 12 - Chemistry by Size for Minorca Multiclone Composite

Mesh	wt %	% Fe	% Sat Fe	Hg, ng/g	Distribution, %		
					Hg	Fe	Sat Fe
100	5.99	60.63	3.57	10.88	6.63	6.08	1.41
150	3.64	55.22	3.82	7.99	2.96	3.37	0.92
200	6.39	50.36	7.36	9.63	6.26	5.38	3.11
270	14.55	55.65	14.02	7.76	11.49	13.55	13.48
325	11.08	61.68	17.99	5.92	6.68	11.44	13.17
400	15.99	63.41	18.94	6.38	10.39	16.97	20.02
500	20.96	65.37	19.01	8.09	17.27	22.93	26.33
635	10.48	65.29	18.25	17.64	18.82	11.45	12.64
10u	8.11	65.10	16.68	16.35	13.50	8.84	8.94
-10u	2.82	-	-	20.85	5.98	-	-

Table 13 - Elutriation Tests on Minorca Multiclone Composite

feet per second	wt %	% Fe	% Sat Fe	Hg, ng/g	Distribution, %		
					Fe	Sat Fe	Hg
0.0135	53.44	60.40	7.58	7.00	52.67	24.08	30.92
0.0169	14.25	61.56	21.28	17.60	14.31	18.03	20.73
Underflow	32.32	62.61	30.14	18.10	33.02	57.90	48.35

Table 14 - Results from Hibtac Sampling

Sample	% solids	ng/g Hg			total Hg	time	Dust	Dust Hg	g Hg/yr	pH	Temp, C	% Fe	% Sat Fe	Scrubber gpm
		cake	paper *	tot solids	ng/lb slurry	seconds	lb/hr	mg/hr						
4/12/2007 scrubber	0.0330	556.83	3325.12	672.71	83.31			892.88	6.88	30.90	67.61	16.43	2442	
multiclones		229.69		229.69		204	225.00	23.46	205.53		66.43	35.56		
4/16/07scrubber	0.0357	587.28	4705.85	690.24	111.83			1219.67	6.91	33.13	65.66	16.05	2485	
multiclones		134.58		134.58		204	257.65	15.74	137.90		66.76	33.57		
4/20/2007 scrubber	0.0344	643.54	5836.31	728.16	113.76			1231.71	7.05	33.97	64.30	12.33	2467	
multiclones		153.32		153.32		204	220.59	15.35	134.51		67.04	29.32		
4/23/07scrubber	0.0332	619.62	3180.00	696.39	105.08			1159.81	6.82	34.32	64.13	16.18	2515	
multiclones		234.32		234.32		204	224.12	23.84	208.86		66.74	36.33		
4/24/07scrubber	0.0306	528.08	3472.00	630.12	87.64			961.59	6.84	33.93	64.68	15.29	2500	
multiclones		222.09		222.09		204	196.76	19.84	173.79		65.93	40.90		
4/25/07scrubber	0.0396	608.58	2461.05	654.41	117.76			1325.09	6.93	34.52	65.34	14.43	2564	
multiclones		116.15		116.15		204	390.00	20.57	180.15		66.41	25.35		

*Mercury from digestion of filter paper after filtercake was removed.

Table 15 - Chemistry by Size for Hibtac Multiclone Composite

mesh	wt %	% Fe	% Sat Fe	Hg, ng/g	Distribution, %		
					Fe	Sat Fe	Hg
65	6.10	65.49	2.13	6.46	6.27	0.40	0.23
100	1.00	62.24	3.88	49.05	0.98	0.12	0.29
150	1.50	52.69	7.15	74.64	1.24	0.33	0.66
200	3.30	50.33	18.69	143.80	2.61	1.90	2.79
270	10.00	62.38	37.29	154.47	9.79	11.47	9.07
325	10.10	66.6	42.92	154.42	10.56	13.33	9.16
400	16.00	67.43	42.62	178.71	16.94	20.97	16.79
500	21.00	68.05	39.12	176.46	22.43	25.26	21.76
635	13.80	67.72	33.20	113.28	14.67	14.09	9.18
10	13.60	67.97	29.01	304.44	14.51	12.13	24.31
-10	3.60	-	-	272.60	-	-	5.76

Table 16 - Cyclosizer Test on Composite Hibtac Multiclone Composite

Sample	wt	wt %	% Fe	% Sat Fe	Hg, ng/g	Distribution, %		
						Fe	Sat Fe	Hg
32 u	6.90	17.88	68.87	27.18	116.92	17.76	22.43	13.80
24 u	18.80	48.70	67.91	21.17	157.66	47.71	47.59	50.71
17 u	9.00	23.32	66.88	18.88	136.08	22.49	20.32	20.95
11 u	3.90	10.10	65.70	15.60	134.07	9.57	7.28	8.94
8 u	Trace							
-8 u	1.00	2.53	66.10	19.98	327.12	2.47	2.39	5.60

Table 17 - Magnetic Separator Test on Composite Hibtac Multiclone Composite

Sample	wt%	% Fe	Hg, ng/g	Distribution, %	
				Fe	Hg
Concentrate	64.27	67.44	199.87	65.32	89.67
Tails	35.73	64.39	41.4	34.68	10.33

Table 18 - Repeat Magnetic Separator Test on Composite Hibtac Multiclone Composite

Sample	wt%	% Fe	Hg, ng/g	Distribution, %	
				Fe	Hg
Concentrate	63.88	67.58	195.23	65.07	87.07
Tails	36.12	63.94	37.6	34.81	9.48

Table 19 - Cyclosizer Test on Composite Hibtac Scrubber Solids

Sample	wt	wt %	% Fe	% Sat Fe	Hg, ng/g	Distribution, %		
						Fe	Sat Fe	Hg
32 u	7.70	20.98	67.50	27.18	54.38	22.04	31.23	5.01
24 u	5.60	15.26	66.82	21.17	77.27	15.87	17.69	5.17
17 u	6.00	16.35	66.36	18.88	81.40	16.88	16.91	5.84
11 u	7.00	19.07	65.08	15.60	102.29	19.32	16.30	8.56
8 u	2.40	6.54	64.74	14.59	132.70	6.59	5.23	3.81
-8 u	7.60	20.71	59.88	11.15	756.79	19.30	12.65	68.77

Table 20 - Elutriation Tests on Composite Hibtac Scrubber Solids

feet per sec	wt%	ng/g Hg	Hg, Dist, %
0.0067	80.99	335.06	93.95
0.0101	5.21	138.52	2.50
Unflo	13.80	74.37	3.55

Table 21 - Magnetic Separator Tests on Composite Hibtac Scrubber Solids

Davis Tube	wt%	% Fe	Hg, ng/g	Distribution, %	
				Fe	Hg
Concentrate	30.34	69.64	126.82	32.48	10.85
Tails	69.66	63.05	453.56	67.52	89.15
Lab Mag Sep					
Concentrate	32.50	67.41	88.73	33.68	8.36
Tails	67.50	63.91	468.39	66.32	91.64

Table 22 - Results from Utac sampling

Sample	% solids	ng/g Hg			total ng/lb slurry	gpm	Solids		pH	Temp, C	% Fe	% Sat Fe
		cake	paper *	tot solids			LTPY	g Hg/yr				
5-7-07 #9 O'flo	0.2132	94.3	192.82	94.93	91.90	750	690.15	302.49			43.79	15.20
5-7-07 #9 Un'flo	0.4448	70.93		70.93	143.24	490	940.65	308.05			48.24	19.81
5-7-07 #10 O'flo	0.1320	782.32	10083.93	968.00	579.94	750	427.12	1908.90			54.52	26.61
5-7-07 #10 Un'flo	1.1396	159.99		159.99	827.76	490	2409.86	1780.10			57.54	31.27
5-8-07 #9 O'flo	0.1310	173.6	501	175.02	104.12	750	424.11	342.72	3.85	43.25	54.59	31.27
5-8-07 #9 Un'flo	1.8870	90.59		90.59	776.08	490	3990.29	1668.96	4.83	42.10	58.35	40.34
5-8-07 #10 O'flo	0.0973	382.445	1940.165	391.85	173.12	750	314.98	569.85	4.04	43.50	57.74	31.05
5-8-07 #10 Un'flo	1.1893	144.42		144.42	779.77	490	2514.87	1676.89	5.03	40.70	57.30	32.04
5-10-07 #9 O'flo	0.1641	341.83	588.38	343.00	255.46	750	530.99	840.88	3.86	43.58	57.99	32.68
5-10-07 #9 Un'flo	2.0015	151.54		151.54	1377.01	490	4232.43	2961.26	4.74	42.80	58.03	33.41
5-10-07 #10 O'flo	0.1034	251.99	353.33	252.62	118.59	750	334.67	390.33			61.15	33.34
5-10-07 #10 Un'flo	1.6701	175.9		175.90	1333.75	490	3531.72	2868.22	4.17	42.70	60.06	31.70
5-11-07 #9 O'flo	0.1459	344.26	396.25	344.47	228.17	750	472.23	751.03	3.80	42.80	52.27	26.28
5-11-07 #9 Un'flo	1.0752	308.48		308.48	1505.75	490	2273.54	3238.10	4.09	40.90	59.42	40.34
5-11-07 #10 O'flo	0.0741	288.88	797.5	290.31	97.64	750	239.78	321.39	3.81	44.00	58.46	32.55
5-11-07 #10 Un'flo	1.1647	270.11		270.11	1428.32	490	2462.99	3071.59	4.37	41.10	56.87	32.56
5-15-07 #9 O'flo	0.1003	590.41	1503.95	600.51	273.40	750	324.59	899.93		.	51.82	27.26
5-15-07 #9 Un'flo	0.9883	159.34		159.34	714.94	490	2089.89	1537.48			53.91	32.64
5-15-07 #10 O'flo	0.1146	590.59	3542.35	628.76	327.06	750	370.84	1076.54			58.53	33.12
5-15-07 #10 Un'flo	1.0941	140.67		140.67	698.73	490	2313.60	1502.62			60.33	36.36
5-16-07 #9 O'flo	0.1284	515.2	271.54	513.42	299.30	750	415.61	985.17	4.03	40.85	54.51	29.90
5-16-07 #9 Un'flo	1.0884	181.75		181.75	898.10	490	2301.59	1931.36	4.62	38.80	58.54	33.11
5-16-07 #10 O'flo	0.0892	481.8	511.71	482.22	195.30	750	288.74	642.85	3.85	42.90	59.71	34.88
5-16-07 #10 Un'flo	0.9270	159.71		159.71	672.12	490	1960.16	1445.38	4.58	40.80	60.24	35.93

* Mercury from digestion of filter paper after filtercake was removed.

Table 23 - Mercury by Size for Utac Composite Samples

		#9 Thickener Underflow			#10 Thickener Underflow		
mesh	wt %	ng/g Hg	Hg Dist	wt %	ng/g Hg	Hg Dist	
100	0.20	2018.33	3.74	1.10	639.55	6.33	
150	0.20	1121.00	2.08	1.00	287.15	2.58	
200	0.80	415.87	3.08	2.30	125.41	2.60	
270	2.80	146.28	3.80	7.10	66.02	4.22	
325	3.10	105.05	3.02	6.00	65.47	3.54	
400	6.00	97.87	5.44	9.40	56.75	4.80	
500	15.00	79.55	11.06	13.30	58.79	7.04	
635	13.30	56.52	6.97	13.70	58.30	7.19	
10	14.90	59.78	8.26	11.00	56.86	5.63	
-10	43.70	129.72	52.55	35.10	177.53	56.08	
		#9 Thickener Overflow			#10 Thickener Overflow		
mesh	wt %	ng/g Hg	Hg Dist	wt %	ng/g Hg	Hg Dist	
100							
150	0.20	350.28	0.25				
200	0.30	316.85	0.34	0.20	371.18	0.22	
270	0.90	151.25	0.49	0.90	128.50	0.34	
325	1.00	114.07	0.41	1.20	107.12	0.38	
400	2.60	94.39	0.89	2.90	85.52	0.73	
500	10.50	94.08	3.58	10.20	89.66	2.68	
635	12.80	68.29	3.17	11.20	76.97	2.53	
10	14.00	73.50	3.73	8.40	90.68	2.24	
-10	57.70	416.40	87.12	65.00	476.50	90.89	

Table 24 - Laboratory Magnetic Separator Tests on Utac Thickener Underflow Composites

	wt%	% Fe	Hg, ng/g	Distribution, %	
				Fe	Hg
#9 Underflow					
Concentrate	54.22	67.86	61.43	65.61	20.76
Tails	45.78	42.13	277.71	34.39	79.24
#10 Underflow					
Concentrate	54.22	66.56	58.79	62.97	18.65
Tails	45.78	50.63	331.78	37.03	81.35

Table 25 - Davis Tube Tests on Utac Thickener Overflow Composites

	wt%	% Fe	Hg, ng/g	Distribution, %	
				Fe	Hg
#9 Underflow					
Concentrate	42.32	68.26	68.44	54.80	11.05
Tails	57.68	41.31	404.42	45.20	88.95
#10 Underflow					
Concentrate	55.56	66.56	58.79	66.26	10.97
Tails	41.02	45.90	646.52	33.74	89.03

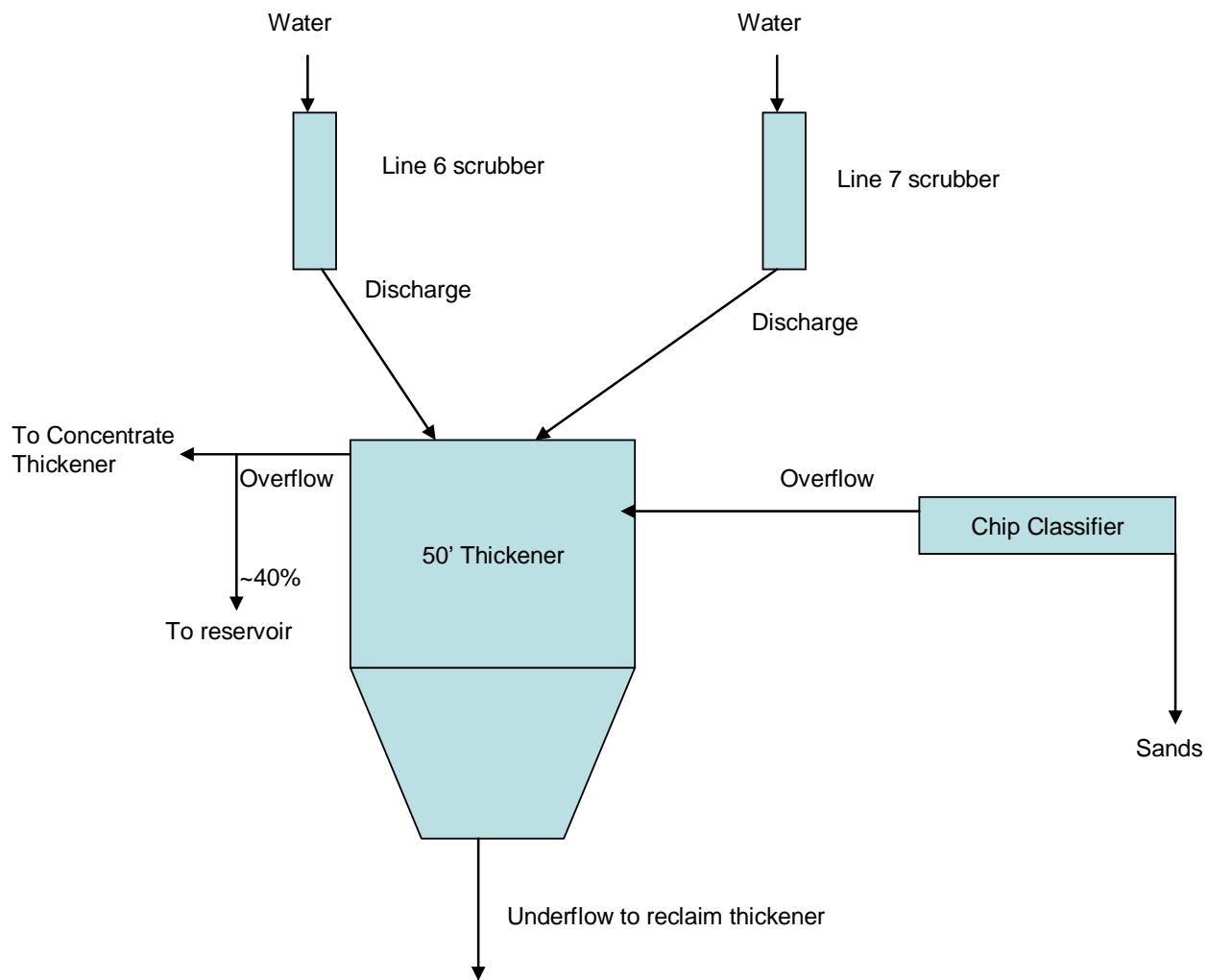


Figure 1 – Schematic of Minntac Step III Sampling

Appendix B-1-14

On the Measurement of Stack Emissions at Taconite Processing Plants

May 30, 2008

On the Measurement of Stack Emissions at Taconite Processing Plants

A progress report submitted to MPCA

Michael E. Berndt
Minnesota Department of Natural Resources
Division of Lands and Minerals
500 Lafayette Rd.
St. Paul, MN 55155

5/30/2008

Table of Contents

Summary 3

Introduction..... 4

Background..... 4

 Stack and process gas measurements..... 5

 Process water and greenball mercury measurements..... 6

A Recent Example: Minntac Hg-control Tests..... 7

Conclusions..... 10

References..... 11

Tables..... 12

Figures 16

Appendix 1: FAMS measurements made at taconite processing facilities..... 19

Appendix 2. Process gas Hg measurements made using FAMS with QLIP modification
..... 23

Summary

The Minnesota Department of Natural Resources is conducting a two year study designed to evaluate potential mercury control technologies. Methods to monitor mercury are being tested and refined during this process in conjunction with these tests, as a part of an interagency agreement between the DNR and MPCA. This paper is a progress report for this study.

Sorbent trap methods (FAMS) were evaluated previously and found to be subject to large interferences, thought to be related to the presence of reactive iron oxide dust in process gases at taconite plants. This method was modified using a wet filtration system, referred to as QLIP, to prevent trapping of oxidized mercury under dry conditions in the sampling filters. Early results were positive, but testing hasn't been pursued during the present study.

Continuous Mercury Monitors (CMMs) have provided mixed results when using dry filtration (DF) systems and/or inertial separation probes (ISPs). The difficulty appears to be related to the presence of reactive iron oxides in the process gas. A new wet filtration system (AWS = advanced wet system) has been developed by the University of North Dakota, EERC, that provides superior results compared to dry filtration, however, it was found that the conditioning liquid used in the method needed to be modified to prevent reaction between molecular halogen gases (Br_2 and Cl_2) and elemental mercury (termed AWSII in this document). The AWSII system is currently the preferred approach for monitoring mercury in stack gases, however, further modifications will be required for use when measuring mercury in process gases prior to the wet scrubbers.

A recent test at Minntac (Line 3) using all of the most methods for analyzing mercury in stack gas, greenball, and scrubber water, provided a reasonable mercury mass balance for the overall induration process when the plant was operating under normal, baseline conditions. However, once mercury control tests were performed involving addition of NaBr to greenball and injection of CaBr_2 to the kiln, the mercury decreases observed in the stack gas were not balanced by comparably sized increases in mercury concentration in the scrubber water. Locating the source of this discrepancy is a major goal for future research.

Introduction

The Minnesota Department of Natural Resources has been conducting mercury research at taconite companies for approximately six years with the purpose being to evaluate mercury transport mechanisms and identify a means to control mercury in taconite stack emissions. Initial studies focused on analysis of samples collected from various locations in processing plants (Berndt et al., 2003, 2005) and conducting bench scale studies to determine how mercury is released from taconite concentrate (Berndt and Engesser, 2005a, 2005b). More recent research, which has focused on conducting short-termed Hg-control tests in active taconite plants (Berndt and Engesser, 2007), has resulted in the need to develop reliable means to assess mercury flow in several process streams (stack and process gases, greenball feed, and blow down water). This document focuses on the monitoring methods being used during many of these tests.

Mercury monitoring methods have been refined continuously over the past several years and will continue to be improved during the next year of Hg control method testing at taconite plants. This document is a progress report for a study being conducted by the DNR to continue development of mercury monitoring technologies under contract with the MPCA. Current methods being used to monitor mercury in taconite processing streams are presented along with results from the most recent full scaled short-termed Hg control test conducted at Minntac in April, 2008. This example demonstrates the complexity associated with measuring plant emissions and estimating capture rates and identifies where updates in mercury monitoring technology are still likely needed for reliable use in taconite processing plants, especially during conduction of plant-scale mercury control tests. Completion of this study is scheduled for June, 2009.

Background

Two primary means have been used to assess mercury emissions from taconite processing plants: (1) direct measurement of mercury in taconite stack gases and (2) calculating stack emissions as the difference between mercury entering the furnace with feed streams and subtracting Hg removed with scrubber blowdown water. Measuring Hg in stack emissions directly is, conceptually, the easiest approach to understand. However, reliable stack gas measurements have been surprisingly difficult to obtain owing to strong interference related to the presence of iron oxides (Berndt et al., 2005a; Laudel, 2007) and the apparent occurrence of Br₂ and Cl₂ or similarly reactive gas species in taconite process gases (Berndt and Engesser, 2007). Moreover, taconite process lines can have as many as four stacks from a single line source, each with different mercury concentrations and flow rates. To monitor all four stacks using specialized continuous mercury monitors (CMMs) is cost prohibitive except in the most extreme cases when stack gas chemistry of all four stacks must be known. The alternative approach of using mass balance estimates to calculate emissions by difference, although not without its own difficulties, may, in some cases provide a substitute means to estimate stack emissions.

Stack and process gas measurements

MN DNR research experience with stack gas and other measurements since 2006 is outlined in Table 1. Initial experience in gas analysis was provided by the University of Minnesota – Natural Resources Research Institute (NRRI), who used sorbent traps to quantify and speciate mercury in stack gas emissions (Berndt and Engesser, 2007). NRRI uses the FAMS technique (Flue gas Absorbant Mercury Speciation), developed by Frontier Geosciences, Inc., (Seattle, WA) to measure gas chemistry. As a part of the present study, all stack gas measurements reported to or used directly in DNR studies have been compiled and are reported in Appendix 1. Generally, these tests revealed considerable variability during repeat analyses and often reported unreasonably high percentages of oxidized mercury, suggesting presence of an interfering component, likely iron oxide particles which are known to react with mercury.

The Minnesota DNR worked with NRRI to help improve the FAMS method for stack gas monitoring, by introducing a wet filtration system to help sample the gases. This method is described by Berndt and Engesser (2007) and referred to as the Quench Liquid Injection Probe (QLIP). By this method, particles and gases in the stack gas or duct first contact a liquid that is injected into the sampling probe. This liquid captures the oxidized and particulate mercury before the gas passes into the sorbent traps. The principle is to prevent gaseous mercury from contacting magnetite (and maghemite) particles in the stack gas that might collect on a dry filter. Varying solution chemistry in the QLIP system provided a range of results, but, in general, reproducibility of results with for a specific solution was acceptable. The technique has not been developed further, since more focus has been placed on direct measurement of stack gases using continuous mercury monitoring. However, results from all FAMS-QLIP tests conducted by the DNR (assisted by NRRI) are reported in Appendix II.

The University of North Dakota, Energy and Environmental Research Center (EERC) has led method development for Continuous Mercury Monitors (CMMS) in taconite process gases under a series of research grants provided by the MN DNR. Initial tests using CMM's were largely consistent over time and responsive to changes in mineral processing conducted in the plant. However, there were periods of considerable instability in the signal, also though to be related to interference with particles trapped in the dry filtration (DF) system used in the earlier techniques. Specific results using DF systems in taconite plant tests are reported in Berndt and Engesser (2007).

Use of an inertial separation probe (ISP) to eliminate this interference in a duct stream was investigated, but did not solve the problem, and generated what appeared to be an unacceptably high percentage of oxidized mercury (Laudel et al., 2007). EERC developed a more promising method, referred to as the "Advanced Wet System" (AWS), to allow collection of the gases without use of a filter. Similar to the QLIP method, sampled gases in the AWS system first contact water that is injected into the sampling probe and can, therefore, prevent reactions from occurring between the mercury in the process gas and the dry, reactive iron oxides. The water/gas mixture is carried to the instrument in two streams, one to convert all of the mercury to elemental form (for

analysis of total mercury) and the other to preserve the current gas-mercury speciation (for analysis of elemental mercury only). Oxidized and particulate mercury in the gas stream is taken as the difference between total and elemental mercury. An important advantage of this system over DF is that it captures and monitors particulate mercury within the total mercury signal. This mercury source is filtered out and missed by CMMs using DF systems.

Initial AWS tests were far superior to the DF system with significantly smoother results and far fewer outliers. However, an unusually high percentage of oxidized mercury was indicated during tests involving introduction of Br salts into the furnace. The most likely interference was expected to be reactions taking place between Hg(0) and Br₂ gas as the gas was being transported from the probe to the instrument. A likely interference was confirmed in side-by-side tests using separate DF and AWS systems during a Hg control study conducted at Keewatin Taconite in September (2007) (See Table 1). The conditioning liquid was subsequently modified to prevent the Br₂/Hg(0) reactions and is referred to in Table 1 as AWSII. This system was used successfully to measure gases at Minntac in April and May, 2008, and partial results from that test are presented below.

Presently, the AWSII system is the preferred approach for stack gas monitoring, however, modifications are still required before the system is suitable for use in gas streams containing high particulate loads. The reason for this is that particulates escaping the conditioning gas have been found to damage the detector (EERC, personal communication). EERC developed a second approach for these gases that contains of both a dry filtration and AWS system, which is referred to in Table 1 as AWSII/DF. Unfortunately, this system suffered from large interferences in its initial tests and will require further modification or redesign.

Process water and greenball mercury measurements

Measurement methods for waters and solids have also been steadily refined by Berndt et al. (2003), Berndt and Engesser (2005), and Berndt et al. (2007). Analyzing mercury in scrubber waters is particularly challenging owing to the fact that the water contains reactive iron oxide particles. Mercury adsorbs to suspended solids which can, in turn, stick to the sampling bottle (even during rinsing). Furthermore, the scrubber solution can contain metastable oxidants (likely SO₃⁻) that convert dissolved, oxidized mercury to elemental mercury which is lost from solution during shipment to the lab. These difficulties have, largely been overcome by collecting multiple samples and using chemical methods as discussed by Berndt and Engesser (2007). In particular, Lian Liang, Cebam, Inc., developed a special method to analyze mercury in waters containing suspended iron oxides that involves decanting the bulk of the solution and performing an acid digestion of the iron oxides within the sample bottle as a part of the analytical technique.

Measurement of concentration in greenball involves a straight-forward acid dissolution method as described by Berndt and Engesser (2007). However, typical errors associated with greenball analysis on samples collected at the same time can, at times, be greater than 10%. Multiple samples must be collected to decrease error and to detect and eliminate outliers.

Numerous greenball and scrubber water samples have been collected over a period of years. The results from many of these studies have been presented by Berndt and Engesser (2005a, 2005b, and 2007). A comprehensive list of all results presented in Table 1 is still being compiled at this time, and will be provided along with interpretation in the final report.

A Recent Example: Minntac Hg-control Tests

This section presents monitoring results from Hg control tests that were conducted at US-Steel's Minntac Operation. The purpose of this is to illustrate the strengths and short-comings of the existing monitoring techniques, especially when used to quantify stack mercury emissions.

The tests were conducted over a period of five days, beginning April 21, 2008. Three one day tests mercury control tests were conducted between April 22 and April 24, with April 21 and 25 being used to set up and dismantle the testing equipment. NaBr was added to greenball pellet feed on the first day of testing, CaBr₂ solutions were injected into the kiln on the second day, and NaClO₂, referred to as EPA_{ox} by Berndt and Engesser (2007), was injected into the wet scrubber on the final day of control method testing.

Tests were conducted on Line 3, which is relatively small sized a Grate-Kiln that typically produces pellets at a rate of about 300 LT/hr. Recent updates were installed to the scrubber system. These include pH monitoring and lime addition to promote acid neutralization and gypsum precipitation, as well as filtering and disposal of scrubber solids. The recirculation tank has a capacity of 25000 gallons and blow down rate is typically between 50 and 60 gpm, monitored every minute.

This site was selected for several reasons, including the fact that there is only one duct leading to the wet scrubber and only a single outlet leading to the waste gas stack. Furthermore, the relatively small size of the line permits testing to be conducted using less chemical and slower injection rates which significantly affects the cost of conducting the test.

Results from these tests will be described in greater detail in future reports, however, monitoring results for process gases are presented in Figures 1 and 2, Scrubber water analysis are presented in Figure 3 and Table 2, and Greenball analysis for these tests are presented in Table 3.

Figure 1 compares Total mercury in stack gas (AWSII) with Total mercury measured in the duct (AWSII/FD) for the time period April 22 through April 25, 2008.

The baseline value for stack gas was approximately 5000 ng m^{-3} , but with transgressions to lower values during a plant upset on April 22, and during NaBr addition to pellets and CaBr₂ injection into the kiln on April 22 and 23, respectively. THg rebound quickly once NaBr addition to pellets was stopped, but return to baseline was very slow following CaBr₂ injection to the kiln. Only a slight decrease in Hg concentration was observed when NaClO₂ was added to the wet scrubber suggesting this technique will not work on this line.

Ideally, gases passing through the duct on the inlet side of the scrubber should have considerably higher THg than stack gas because some Hg is being captured by the wet scrubber. Unfortunately, except for the time period in the afternoon of April 23 and morning of April 25th, THg for the inlet registered well below the stack gas THg concentration. It is clear that interference negatively impacted the scrubber inlet signal, thus complicating interpretation of trap mechanism.

Figure 2 compares total and elemental mercury for the stack gas which, for the most part, appear to be of adequate quality and consistency to provide relatively confident interpretation. First, NaBr addition to pellets resulted in a decrease in the emission of mercury from THg = 5200 ng m^{-3} under baseline conditions to approximately 2400 ng m^{-3} during the short-termed test. This would indicate a 54% mercury reduction compared to baseline capture rates. Similarly, CaBr₂ addition to the kiln resulted in a decline in THg from 5100 to 1400 ng m^{-3} suggesting a 73% reduction compared to baseline capture rates. Difficult to interpret, however, is the relatively long term response from the CaBr₂ test. Is this a result of a monitoring issue or a signal that mercury is being stored somewhere in the process line or worse, somehow being emitted elsewhere?

Table 2 provides THg for scrubber water blowdown water that was sampled under baseline conditions prior to each test and for waters collected at the same location as the testing period was drawing to a close. Standard deviation for samples ranged between 1 and 5% of the total value (sampled in triplicate) which is a satisfactory result, considering that a large fraction of the mercury is adsorbed to particles in the process stream. If the percentage of particles changed greatly during collection of samples, the mercury concentration would reflect this change. However, the scrubber flow appears to be sufficiently homogeneous to allow collection of a representative sample. THg in blow down water increased from 26335 to 35160 ng/l during the NaBr test and from 14992 to 29097 during the CaBr₂ test, mirroring the changes observed in stack emissions. In detail, however, full interpretation depends on comparing the actual mercury mass gains in the scrubber to the total mass of mercury removed from the stack gas (see below).

Mercury speciation in the scrubber water is important for determining ultimate fate of the trapped mercury. The distribution of dissolved and particulate bound mercury is determined by comparing total mercury concentration in filtered and unfiltered scrubber water samples. Typically, only one water sample is filtered for this determination owing to the difficulty involved with filtering these waters, which have high suspended loads, at the plant-site. Failure to filter a sample immediately upon sampling will result in overestimation of the adsorbed fraction since adsorption occurs on

time scales of minutes to hours (Berndt et al., 2003; Berndt and Engesser, 2005b). For the set of solutions collected during the Minntac tests, it was found that the addition of NaBr to the scrubber water resulted in transfer of much of the adsorbed mercury into the water. This is indicated by the fact that Hg(D) increased from a small percentage of the total mercury, while Hg(P) decreased. For the CaBr₂ tests, performed on the day following the NaBr test, H(D) was still relatively high before the test period, and total mercury in the scrubber was significantly less than it was at the start of the previous day. Once CaBr₂ was injected into the kiln, both Hg(D) and Hg(P) increased together. Finally, during the NaClO₂ tests, Hg(D) increased from its baseline value at the expense of Hg(P), resulting in little net gain in Hg(T). This trend indicates that NaClO₂ addition was interfering with the ability of the suspended material to adsorb mercury from solution rather than helping elemental mercury in process gas to oxidize and dissolve in the scrubber water.

Table 3 provides greenball mercury analysis, which were also sampled in triplicate under baseline conditions before the test began, and then while the tests were being conducted. The mercury concentration in greenball is more variable than that measured for scrubber water (Std. Dev. from 0 to 30%), and it is unclear if this is related to analytical or sampling errors. However, these data suggest that the mercury concentration in greenball may have dropped slightly on the second day of testing (e.g., under baseline and test period conditions during the CaBr₂ test).

Mass balance comparison for the three measured process streams are provided in Table 4. These values are calculated based on measured production rates, monitored blowdown rates, and estimated stack gas flow rates. While all of these rates are measured constantly by Minntac for their Line 3, the unit measuring stack gas flow rate was, unfortunately, malfunctioning at the time of the mercury testing. Calculations for stack emissions were made, therefore, using a typical rate for this line (270000 scfm). The values for blowdown water are calculated based on the assumption that the entire contents of the recirculation tank (25000 gallons) changed, but that blow down water was continuously being removed at the measured rate and makeup water containing little mercury was being added. Additionally, feed to grates is typically measured before the pellets are dried and do not take into account loss of greenball during transfer of material to the grate. A so-called "pellet factor" of 0.85 was used for these calculations. These values should be regarded as preliminary.

Ideally, the rate of mercury emission at the stack should balance the mercury delivered to the furnace in greenball minus the mercury trapped in the wet scrubbers, assuming no other significant Hg sources. The company was burning natural gas during this test and pellets have been measured previously and found to have very low mercury, as is the case for the scrubber makeup water. Multiclone dust, measured previously, has been found to have only a small fraction of the mercury generated by greenball firing (Berndt, 2003).

For the initial baseline condition, before tests began, approximately 766 ug/sec Hg was being added to the furnace along with greenballs, but 100 ug/sec was being

captured by the scrubber, leaving a net difference of 666 ug/sec emitted at the stack. This compares with estimated emissions of 675 ug/sec estimated from direct stack gas measurement. A similar level of agreement was obtained for baseline conditions before the CaBr₂ test when stack measurements suggest emission at a rate of 649 ug/sec compared to 672-66 or 606 ug/sec for the mass balance estimate.

In contrast, there is a large divergence in stack emissions estimated by direct measurement and mass balance estimates. For example, direct measurements suggest that 306 and 178 ug/sec Hg was being emitted during the NaBr and CaBr₂ test periods, respectively, while the mass balance estimates suggest much higher values of 738 and 375 ug/sec. Mass balance estimates provide much higher calculated emission rates than those estimated from stack gas chemistry during the NaClO₂ tests. Finding the source of the discrepancy in stack emissions based on the two approaches is a primary goal of the next year of research on stack gas monitoring.

Conclusions

Sufficient experience has been gained to provide a relatively high degree of confidence in our methods for measuring mercury concentration in stack gasses using CMMs (using EERC's AWSII system), however, improvement is needed for measurement of mercury in duct gases prior to particulate control devices. Similar confidence is also found for analytical methods for Hg in scrubber water and greenball, however, the uncertainty associated with greenball concentrations can be relatively high if sampling frequency is low.

When mercury balance estimates were performed under baseline conditions before testing began, it was found that the rate of mercury addition to the furnace (in greenball feed) minus mercury captured by the wet scrubber (in the wet scrubber) balanced mercury emitted in the stacks. However, this steady-state balance was greatly upset once testing began such that the measured stack emissions were far lower than mass balance estimates would suggest. Finding the source or sources of this imbalance is a major goal of the next year of testing at taconite plant facilities.

References

Berndt, M. E. (2003) Mercury and Mining in Minnesota, Minerals Coordinating Committee Final Report. Minnesota Department of Natural Resources Technical Report. 58 p.

Berndt, M. E. and Engesser, J. (2005a) Mercury Transport in Taconite Processing Facilities: (I) Release and Capture During Induration. Iron Ore Cooperative Research Final Report. Minnesota Department of Natural Resources. 31 pages plus appendices.

Berndt, M. E. and Engesser, J. (2005b) Mercury Transport in Taconite Processing Facilities: (II) Fate of Mercury Captured by Wet Scrubbers. EPA: Great Lakes National Program Office Report. 32 pages.

Berndt, M. E. and Engesser, J. (2007) Mercury Transport in Taconite Processing Facilities: (III) Control Method Test Results. Iron Ore Cooperative Research Final Report. Minnesota Department of Natural Resources. 38 pages plus appendices.

Berndt, M. E., Engesser, J. E., and Johnson, A. (2003) On the distribution of mercury in taconite plant scrubber systems. Technical report submitted to the MPCA, 30 p.

Berndt, M. E., Engesser, J., and Berquó, T. S. (2005) Mercury Chemistry and Mössbauer Spectroscopy of Iron Oxides During Taconite Processing on Minnesota's Iron Range. In Proceedings Air Quality V, International Conference on Mercury, Trace Elements, SO₃, and Particulate Matter. Washington, DC, Sept. 2005. 15 p.

Engesser, J. and Niles, H. (1997) Mercury emissions from taconite pellet production. Coleraine Minerals Research Laboratory, Report to MPCA: U of M contract # 1663-187-6253. 16 pages plus tables, figures and appendices.

Laudal, D. (2007) "Methods Testing for Measurement of Mercury Speciation for High-Reactive Dust"; Technical Report to Minnesota Department of Natural Resources, UND Fund No. 9301.

Tables

Table 1: Mercury monitoring at taconite plants since 2006. GB = Greenball samples collected. BD = Blowdown water samples collected. CMM = Continuous Mercury Monitoring. EERC = Energy and Environmental Research Center –University of North Dakota. NRRI = Natural Resources Research Institute, University of Minnesota. FAMS = Flue Gas Absorbant Mercury Speciation. DF = Dry Filtration. AWS = Advanced Wet System. ISP = Inertial Separation Probe.

Dates	Plant and Line	*DNR	**EERC CMM	**NRRI (FAMS)	Result
2/1/2006	Minntac Ln 7			scrubber inlet and outlet ducts	
3/31/2006	Minntac Ln 7	GB BD		scrubber inlet and outlet ducts	
6/6/2006	United Taconite	GB BD		Stacks 2A and 2B	
6/7/2006	Minorca	GB BD		Stacks C,D	
6/8/2006	Hibtac Line 3	GB BD		Stack A	
7/18/2006 and 7/19/2006	Hibtac Line 3	GB BD	Stack A: DF	Stack A, B, C, D	FAMS and CMM with DF disagreed. FAMS data very scattered.
8/22/2006	KeeTac Ln 1	GB BD		Wet scrubber inlet and stack	
9/12/2006 and 9/13/2006	U-Tac Ln 2	GB BD	Stack 2B: DF	Stacks 2A and 2B	FAMS and CMM with DF disagreed. FAMS data very scattered.
10/25/2006 to 10/30/2006	KeeTac Ln 1	GB BD	Inlet Duct: AWS, DF, and ISP	Inlet duct	AWS method proved superior to DF, ISP, and to FAMS.
April 30, 2007	KeeTac Line 1	QLIP		Inlet duct	Hg(0) from ducts oxidized to Hg(II) when gas contacted H ₂ O.
	Hibtac Line 3	GB BD QLIP	Stack A: AWS	Stack A	AWS provides consistent Hg(T), but appeared to under-report Hg(0).
Sept 24 to Sept. 28, 2007	KeeTac Line 1	GB BD	Stack: AWS and DF		AWS system functions better than DF for Hg(T) but appeared to under-report Hg(0).
April 21- May 8, 2008	Minntac Line 3	GB BD	Stack: AWS(II) Scrubber inlet: DF/AWS(II)	Stack: Ohio Lumex CMM	AWSII worked consistently at stack for Hg(T) and Hg(0). Strong interference at scrubber inlet.
Scheduled for July 2008	ArcelorMittal	GB BD	Stack D: AWS(II)	Stack D: Ohio Lumex	Tests conducted during plant-scale Hg control tests.

Table 2: Total Hg in scrubber water during tests conducted at Minntac. For this data set, the standard deviation ranged from 1 to 5% of the average value.

	<i>Hg(ng/l)</i>	<i>Avg.</i>	<i>Std Dev.</i>
	27055		
Baseline	26346	26335	725
	25605		
	35551		
NaBr Test	34692	35160	434
	35236		
	14490		
Baseline	15571	14992	545
	14915		
	29017		
CaBr ₂ Test	29665	29097	533
	28608		
	23897		
Baseline	24386	23982	369
	23664		
	24551		
NaClO ₂ Test	26573	25125	1262
	24253		
	25402		
NaClO ₂ Test	25539	25657	330
	26030		
	23734		
NaClO ₂ Test	25171	24671	812
	25107		

Table 3: Total Hg in greenball feed during tests conducted at Minntac. For this data set, the standard deviation ranged from 0 to 30% of the average value. Even if the 15.8 value measured for greenball during the second baseline test is rejected as an outlier, the standard deviation ranged up to 13%.

	<i>Hg (ng/g)</i>	<i>Avg.</i>	<i>Std Dev.</i>
Baseline	10.3	10.6	0.7
	10.0		
	11.4		
NaBr Test	14.4	13.0	1.7
	11.1		
	13.5		
Baseline	9.1	11.5	3.7
	*15.8		
	9.5		
CaBr ₂ Test	8.5	8.4	0.8
	9.2		
	7.6		
Baseline	11.8	11.5	0.3
	11.3		
	11.3		
NaClO ₂ Test	11.2	11.2	0.0
	11.2		
	11.2		
NaClO ₂ Test	11.7	11.8	0.6
	11.3		
	12.4		
NaClO ₂ Test	11.8	11.4	0.3
	11.1		
	11.3		

*Suspected outlier.

Table 4. Preliminary mercury flux estimates for various processing streams during tests conducted at Minntac in April 2008.

<i>Hg flux, ug/sec</i>	<i>Greenball</i>	<i>Blowdown</i>	<i>Stack Gas</i>
Baseline	766	100	675
NaBr test	939	201	306
Baseline	672	66	649
CaBr2 test	607	232	178
Baseline	831	106	535
NaClO2	809	119	
NaClO2	853	126	509
NaClO2	824	114	

Figures

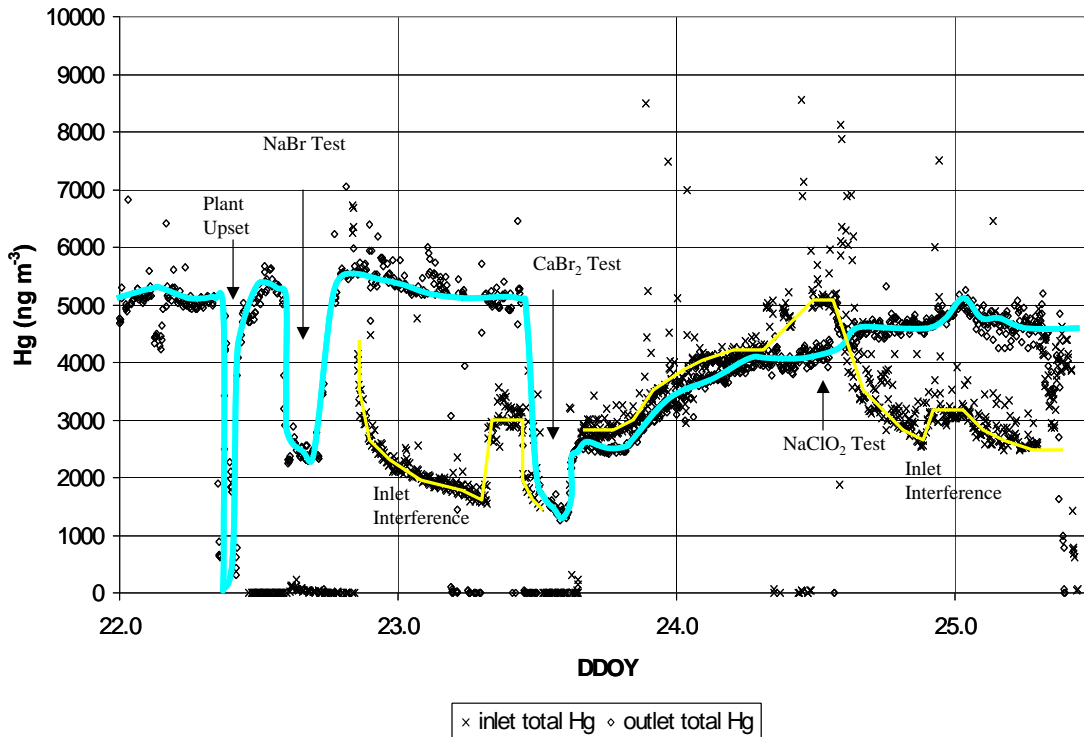


Figure 1: Hg concentration in inlet and outlet to wet scrubber as measured by CMM. Horizontal scale is a digital time scale referring to the dates in April, 2008, when testing was conducted. The inlet concentrations were measured by EERC using AWSII, but modified with a dry filter at the duct (AWS/DF). The outlet concentrations were measured at the stack using EERC's AWSII, the currently preferred method for monitoring mercury in taconite stack emissions. The outlet signal is relatively smooth and responsive to imposed changes in processing. The inlet signal is highly irregular, often revealing concentrations lower than those found in the outlet (e.g., overnight on the 23rd and 25th of April). Beginning with the CaBr₂ test on April 23rd, however, the inlet concentrations were similar to but slightly elevated compared to outlet concentrations. It is believed that the dry filtration unit placed in-line near the sampling probe for the inlet is responsible for this erratic behavior.

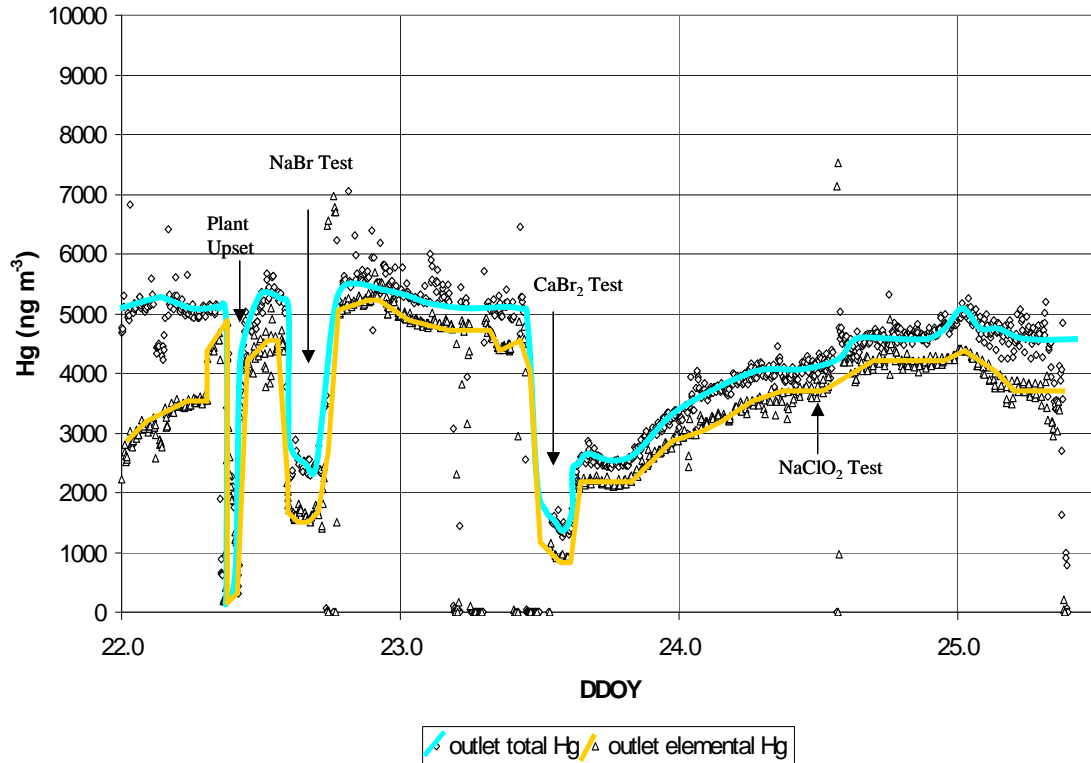


Figure 2: Speciation of Hg as measured by the CMM using the AWS system in Line 3 Stack gases during conduction of mercury control tests at Minntac (Line 3). Horizontal scale is a digital time scale referring to the dates in April, 2008, when testing was conducted. There appeared to be a long warm-up interval for the system early on April 22, when elemental mercury was being under reported, but the results after this appear to be relatively smooth and responsive to the conducted tests. Total and elemental mercury concentrations closely parallel each other, indicating most of the emitted mercury is elemental and not oxidized or particulate mercury.

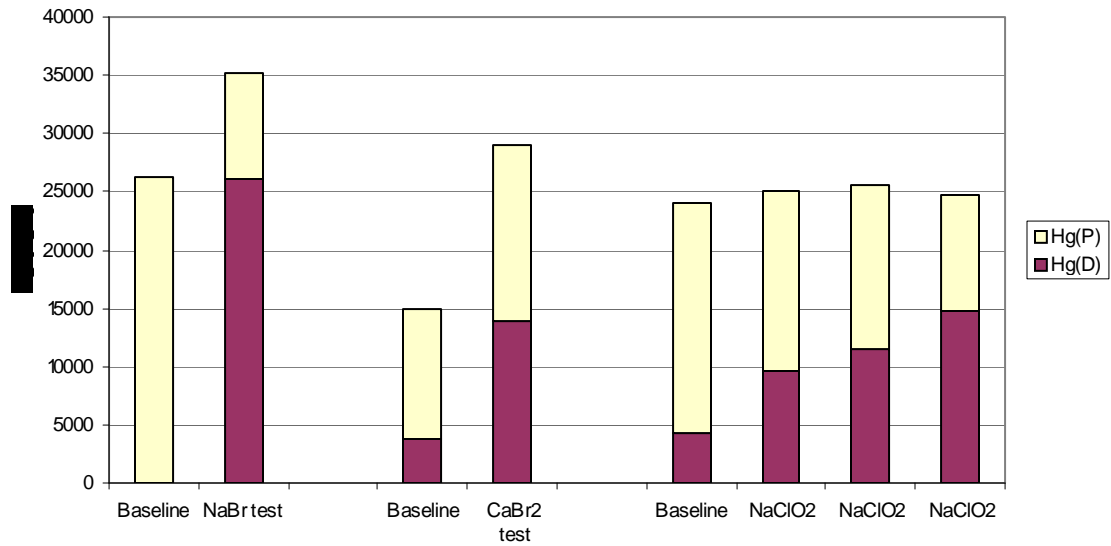


Figure 3: Mercury speciation in scrubber blowdown water during Hg-control testing at Minntac. Note that $\text{Hg(P)} + \text{Hg(D)} = \text{Hg(T)}$ so the change in Hg concentration is reflected by the total height of each of the plotted columns. It was found that addition of NaBr to greenball resulted in a dramatic change in speciation during these tests. In effect, much of the Hg that was originally adsorbed to suspended particles was, instead, dissolved in solution. Injection of CaBr_2 into the kiln also resulted in a change in mercury speciation, but there was still a clear observed increase in particulate mercury. Injection of NaClO_2 into the scrubber water resulted in little net change in Hg(T) , but indicated significant conversion of Hg(P) to Hg(D) .

Appendix 1: FAMS measurements made at taconite processing facilities.

FAMS measurements made by NRRI at taconite processing facilities. Hg(P) is particulate Hg, Hg(Ox) is oxidized gaseous mercury, and Hg(El) is elemental mercury. %Ox is the percentage of total mercury present in particulate or gaseous oxidized forms.

<i>Date</i>	<i>Company</i>	<i>Location</i>	<i>Hg(Part)</i>	<i>Hg(Ox)</i>	<i>Hg(El)</i>	<i>Hg(Tot)</i>	<i>%Ox</i>
1/5/2005	MnTac	Ln6 Inlet	1.13	0.10	4.69	5.92	20.8
			0.52	0.18	4.05	4.75	14.7
			0.71	0.30	4.38	5.39	18.7
1/11/2005	MnTac	Ln6 Inlet	0.17	0.18	6.11	6.46	5.4
			0.28	0.23	5.95	6.46	7.9
			0.84	0.35	6.04	7.23	16.5
1/25/2005	MnTac	Ln6 Inlet	0.88	7.57	4.56	13.01	65.0
			0.13	3.94	6.50	10.57	38.5
			0.29	2.51	6.83	9.63	29.1
2/3/2005	MnTac	Ln6 Inlet	0.05	2.85	4.20	7.10	40.8
			0.12	1.77	3.41	5.30	35.7
			0.39	1.96	1.74	4.09	57.5
1/5/2005	MnTac	L6-Outlet	0.41	0.04	3.15	3.60	12.5
			0.61	0.01	2.80	3.42	18.1
			0.58	0.04	2.01	2.63	23.6
1/11/2005	MnTac	L6-Outlet	0.71	0.87	2.93	4.51	35.0
			0.05	0.69	2.54	3.28	22.6
			0.47	0.48	0.23	1.18	80.5
1/25/2005	MnTac	L6-Outlet	0.62	0.27	2.27	3.16	28.2
			0.35	0.17	1.83	2.35	22.1
			0.48	0.18	1.98	2.64	25.0
2/3/2005	MnTac	L6-Outlet	0.01	0.61	1.53	2.15	28.8
			0.10	0.15	1.73	1.98	12.6
			0.23	0.32	1.64	2.19	25.1
2/1/2006	MnTac	Ln7 Inlet	0.42	1.39	0.54	2.35	77.0
			1.00	2.26	0.40	3.66	89.1
			1.73	1.59	0.76	4.08	81.4
			2.28			4.18	54.5
3/31/2006	Mntac	Ln7 Inlet	1.44	1.60	2.87	5.91	51.4
			1.20	1.58	1.57	4.35	63.9
			0.93	1.66	1.59	4.18	62.0
			1.12	1.24	1.51	3.87	61.0
			0.74	1.39	1.12	3.25	65.5
3/31/2006	Mntac	Ln7 Outlet	0.10	0.07	2.32	2.49	6.8
			0.50	0.11	2.94	3.55	17.2
			0.45	0.09	3.79	4.33	12.5
			0.22	0.06	3.27	3.55	7.9
			0.40	0.04	3.75	4.19	10.5

6/8/2006	HibTac	Ln 3 Inlet	0.28	2.93	0.27	3.48	92.2
			0.46	1.71	0.32	2.49	87.1
			0.59	0.32	0.26	1.17	77.8
6/8/2006	HibTac	Ln3 Hot Stack	0.12	0.45	3.74	4.31	13.2
			0.07	0.54	3.85	4.46	13.7
			0.03	0.47	3.59	4.09	12.2
6/7/2006	Minorca	Stack C	0.04	0.23	0.17	0.44	61.4
			0.06	0.24	0.33	0.63	47.6
			0.19	0.35	0.33	0.87	62.1
		Stack D	0.26	0.22	1.39	1.87	25.7
			0.26	0.35	1.15	1.76	34.7
			0.13	0.11	1.34	1.58	15.2
6/6/2006	Utac	Stack 2A	0.12	0.45	3.54	4.11	13.9
			0.23	0.22	3.45	3.90	11.5
			0.27	0.22	3.42	3.91	12.5
		Stack 2B	0.57	2.56	1.22	4.35	72.0
			0.41	2.01	1.40	3.82	63.4
			0.57	2.06	1.46	4.09	64.3
7/18/2006	HibTac	Stack A	0.01	0.37	3.38	3.76	10.1
			0.07	0.45	3.13	3.65	14.2
			0.08	0.24	3.64	3.96	8.1
		Stack A	0.13	0.38	2.95	3.46	14.7
			0.12	0.34	2.92	3.38	13.6
			0.11	0.27	2.89	3.27	11.6
		Stack A	0.11	0.35	2.81	3.27	14.1
			0.17	0.29	3.21	3.67	12.5
			0.11	0.30	2.90	3.31	12.4
7/19/2006	HibTac	Stack A	0.11	0.35	3.44	3.90	11.8
			0.11	0.27	3.19	3.57	10.6
			0.10	0.36	3.10	3.56	12.9
7/18/2006	HibTac	Stack B	0.06	0.42	1.20	1.68	28.6
			0.07	0.71	1.06	1.84	42.4
			0.10	0.63	1.02	1.75	41.7
		Stack B	0.13	0.62	1.89	2.64	28.4
			0.18	0.62	2.04	2.84	28.2
			0.15	1.52	2.08	3.75	44.5

	HibTac	Stack B	0.12	0.55	2.27	2.94	22.8
			0.08	0.53	1.85	2.46	24.8
			0.09	0.46	1.88	2.43	22.6
7/19/2006	HibTac	Stack B	0.17	0.81	2.54	3.52	27.8
			0.21	0.70	2.47	3.38	26.9
			0.17	0.60	2.27	3.04	25.3
7/19/2006	HibTac	Stack C	0.07	0.17	1.17	1.41	17.0
			0.12	0.13	1.33	1.58	15.8
			0.09	0.13	1.18	1.40	15.7
7/19/2006	HibTac	Stack D	0.07	0.30	0.82	1.19	31.1
			0.06	0.29	0.84	1.19	29.4
			0.06	0.28	1.10	1.44	23.6
8/22/2006	K-Tac	Inlet	0.26	10.48	0.68	11.42	94.0
			0.46	8.33	0.86	9.65	91.1
			0.33	7.51	1.82	9.66	81.2
	K-Tac	Stack	0.42	0.86	5.74	7.02	18.2
			0.23	0.55	4.71	5.49	14.2
			0.21	0.42	3.38	4.01	15.7
9/12/2006	United	Stack 2B	0.10	0.46	1.99	2.55	22.0
			0.18	0.87	2.18	3.23	32.5
			0.27	0.77	1.88	2.92	35.6
			0.23	0.92	2.93	4.08	28.2
			0.15	0.59	2.96	3.70	20.0
			0.22	0.85	2.73	3.80	28.2
			0.13	0.43	3.07	3.63	15.4
			0.12	0.64	3.18	3.94	19.3
			0.20	0.42	3.07	3.69	16.8
		Stack 2A	0.06	0.54	4.61	5.21	11.5
			0.40	0.32	4.33	5.05	14.3
			0.17	0.69	4.33	5.19	16.6
			0.26	0.27	4.59	5.12	10.4
			0.24	0.28	4.25	4.77	10.9
			0.33	0.20	3.72	4.25	12.5
			0.13	0.30	4.01	4.44	9.7
			0.29	0.04	3.42	3.75	8.8
0.05	0.06	3.40	3.51	3.1			
9/13/2006	United	Stack 2B	0.10	0.78	3.63	4.51	19.5
			0.07	0.88	4.12	5.07	18.7
			0.09	0.97	4.07	5.13	20.7
		Stack 2A	0.06	0.13	5.81	6.00	3.2
			0.08	0.27	4.87	5.22	6.7

			0.15	0.18	4.27	4.60	7.2
5/2/2007	Hibtac	Stack A	0.04	0.12	5.89	6.05	2.6
			0.02	0.14	5.40	5.56	2.9
			0.09	0.08	6.59	6.76	2.5

Appendix 2. Process gas Hg measurements made using FAMS with QLIP modification

Appendix 2. Process gas measurements made using FAMS with QLIP modification (Berndt and Engesser, 2007). Hg(P) is particulate Hg, Hg(Ox) is oxidized gaseous mercury, and Hg(El) is elemental mercury that passed through the wet filter. WatSol is the mercury that was collected by the wet filter.

<i>Date</i>	<i>Company</i>	<i>Location</i>	<i>Hg(Part)</i>	<i>Hg(Ox)</i>	<i>Hg(El)</i>	<i>WatSol</i>	<i>Total</i>
4/12/2007	Ktac	Inlet	0.07	0.13	5.56	NA	5.76
			0.09	0.21	5.78	NA	6.08
			0.07	0.13	5.68	NA	5.88
4/12/2007		Inlet*	0.00	0.02	4.23	1.27	5.52
			0.01	0.03	4.37	1.27	5.68
			0.02	0.04	4.56	1.41	6.03
		Inlet**	0.03	0.02	4.83	0.53	5.41
			0.04	0.21	4.75	0.77	5.77
		Inlet***	0.06	0.07	0.73	6.21	7.07
0.08	0.10		1.19	5.06	6.43		
5/2/2007	Hibtac	Stack A	0.04	0.12	5.89	NA	6.05
			0.02	0.14	5.40	NA	5.56
			0.09	0.08	6.59	NA	6.76
		Stack A*	0.01	0.01	3.27	0.53	3.82
			0.01	0.14	3.90	0.65	4.70
			0.01	0.03	4.44	0.69	5.17
* QLIP system with NaHCO ₃ /H ₂ O trap ** QLIP system with H ₂ O ₂ /NaHCO ₃ trap *** QLIP system with NaClO ₂ /NaHCO ₃ trap							

Appendix B-1-15

Proof-of-concept Testing of Novel Mercury Control Technology for a Minnesota Taconite Plant

July 2008



July 1, 2008

Dr. Michael E. Berndt
Research Scientist III
Minnesota Department of Natural Resources
Division of Lands and Minerals
500 Lafayette Road, Box 45
St. Paul, MN 55155-4045

Dear Dr. Berndt:

Subject: Final Report Entitled "Proof-of-Concept Testing of a Novel Mercury Control
Technology for a Minnesota Taconite Plant"
Contract No. B12296; EERC Fund 9752

Enclosed is the subject final report, which details the scope of work and results related to testing a novel technology for mercury removal at a taconite plant. If you have any questions, please feel free to contact me by phone at (701) 777-5268, by fax at (701) 777-5181, or by e-mail at jpavlish@undeerc.org.

Sincerely,

John H. Pavlish
Senior Research Advisor

JHP/dte

Enclosure

c/enc: Ye Zhuang, EERC
Lucinda Hamre, EERC



PROOF-OF-CONCEPT TESTING OF NOVEL MERCURY CONTROL TECHNOLOGY FOR A MINNESOTA TACONITE PLANT

Final Report

(for the period of March 11, 2008, through June 30, 2008)

Prepared for:

Michael E. Berndt

Minnesota Department of Natural Resources
Division of Lands and Minerals
500 Lafayette Road, Box 45
St. Paul, MN 55155-4045

Prepared by:

John H. Pavlish
Ye Zhuang

Energy & Environmental Research Center
University of North Dakota
15 North 23rd Street, Stop 9018
Grand Forks, ND 58202-9018

2008-EERC-07-02

July 2008

EERC DISCLAIMER

LEGAL NOTICE This research report was prepared by the Energy & Environmental Research Center (EERC), an agency of the University of North Dakota, as an account of work sponsored by the Minnesota Department of Natural Resources. Because of the research nature of the work performed, neither the EERC nor any of its employees makes any warranty, express or implied, or assumes any legal liability or responsibility for the accuracy, completeness, or usefulness of any information, apparatus, product, or process disclosed, or represents that its use would not infringe privately owned rights. Reference herein to any specific commercial product, process, or service by trade name, trademark, manufacturer, or otherwise does not necessarily constitute or imply its endorsement or recommendation by the EERC.

PROOF-OF-CONCEPT TESTING OF A NOVEL MERCURY CONTROL TECHNOLOGY FOR A MINNESOTA TACONITE PLANT

ABSTRACT

Mercury control tests using the Energy & Environmental Research Center (EERC) high-energy dissociation technology (HEDT) prototype test unit were completed at Minntac Plant Line 3. Four halogen compounds including NaBr, CaBr₂, NaCl, and NaCl–CaBr₂ mixture were tested in the HEDT unit to evaluate their effectiveness on mercury reduction in taconite flue gas. Mercury continuous mercury monitor (CMM) data for stack gases indicate moderate mercury oxidation by NaBr and CaBr₂ with the HEDT unit but no substantial decrease in mercury emissions. It is suspected that the compromised HEDT injection location, which provided a very short residence time of 0.2 seconds, is part of the reason for the ineffectiveness of mercury oxidation and capture with the existing venturi scrubber. In addition, it is possible that other components in the gas, including fine iron oxide particles and the limestone fluxing material, interfered with mercury oxidation and subsequent capture in the venturi scrubbers. Additional studies on Hg–Br–Fe oxide reactions in taconite flue gas are needed. Possible future HEDT experiments are suggested further upstream of the test location to maximize mercury–bromine reactions at favored flue gas conditions but downstream of the grate to avoid possible corrosion issues.

TABLE OF CONTENTS

LIST OF FIGURES	ii
LIST OF TABLES	ii
INTRODUCTION	1
GOAL AND OBJECTIVES	2
EXPERIMENTAL DESCRIPTION.....	3
RESULTS AND DISCUSSION.....	5
CONCLUSIONS AND RECOMMENDATIONS	7
REFERENCES	7

LIST OF FIGURES

1	Configuration of Minntac Plant Lines 6 and 7, similar in process to Line 3	3
2	Possible injection locations within the Minntac Plant Line 3 ductwork	4
3	EERC HEDT field unit	5
4	Continuous mercury measurement at Minntac Plant Line 3 when NaBr was used with the HEDT	8
5	Continuous mercury measurement at Minntac Plant Line 3 when CaBr ₂ was used with the HEDT	8
6	Continuous mercury measurement at Minntac Plant Line 3 when a CaBr ₂ -NaCl mixture and NaCl alone were used with the HEDT	9
7	Summary of Mercury Testing at Minntac Plant Line 3	9

LIST OF TABLES

1	Test Matrix Completed at Minntac Plant Line 3.....	5
---	--	---

PROOF-OF-CONCEPT TESTING OF A NOVEL MERCURY CONTROL TECHNOLOGY FOR A MINNESOTA TACONITE PLANT

INTRODUCTION

Concerns over bioaccumulation of mercury in tissues of various organisms (including humans) have led the U.S. Environmental Protection Agency (EPA) to determine that it is appropriate to regulate mercury emissions from coal-fired utility plants. Several states have filed state implementation plans to impose strict mercury control and have publicly committed to reducing mercury from all significant sources within their states in order to reduce the potential for mercury hot spots and to hopefully reverse the concentrations of mercury measured in fish tissues and other animals.

The state of Minnesota is targeting an overall mercury reduction of 90%. In order to achieve this level of reduction, all sources of mercury emissions and releases to the environment are being evaluated for potential reductions. In Minnesota, taconite plants are the second largest source of mercury emissions in the state. Mercury emissions result from taconite processing in two ways: those released from the fuel (which is a minor contribution since it only takes 20–30 lb of coal to process 1 long ton [Lt] of iron ore to green balls) and those from the actual processing of the ore, which is the major concern. The concentration of mercury in the unprocessed ore at the west end of the mining region is about 20 ppb and gradually increases eastward to a maximum of 32 ppb then decreases gradually to less than 1 ppb in the ore at the Northshore facility (1). A working group of experts that includes scientists and engineers from the taconite industry, the Minnesota Department of Natural Resources (MNDNR), the Minnesota Pollution Control Agency, and research institutions (University of Minnesota and University of North Dakota) is seeking effective mercury emission reduction strategies that have minimal impacts to the industry, both from an operational standpoint and with respect to the components of the production facility. Discussions are under way to evaluate the most effective means of controlling mercury while minimizing impact on both the operations and economics of Minnesota's taconite plants.

All Minnesota taconite facilities, with the exception of the Northshore facility (which has wet electrostatic precipitators), utilize a wet venturi-type scrubber to control particulate matter emissions (versus removing sulfur compounds as in coal-fired combustors). (2) This scrubber can effectively capture particulate-bound mercury and oxidized mercury (Hg^{+2}), but allows elemental mercury (Hg^0) to be emitted. Therefore, a technology that can promote mercury oxidation should theoretically facilitate capture.

A number of tests of limited duration, involving bench-, slipstream-, and full-scale unit, have been completed to evaluate the effectiveness of various noncarbon additives on mercury reduction in taconite flue gas (2, 3). Chloride and bromide salts have been directly added into the induration furnace, the green ball feed system, and the scrubber liquids in an attempt to convert Hg^0 to Hg^{+2} to facilitate mercury capture. Mercury removals with NaCl_2 and CaCl_2 showed some removal, as was expected; the grate kiln, which is the configuration for the Minntac Plant, showed better removals than straight-grate configurations. A series of experiments were also performed on slipstream gases from an operating taconite-processing

plant to evaluate the use of chemical oxidants added directly to water in wet scrubbers to enhance capture efficiency for elemental mercury.

Most mercury control technologies such as activated carbon injection and chemical additives were originally developed for the coal-fired utility industry and have been proven effective in coal combustion flue gas. However, these technologies may not be applicable to the taconite industry because the process and flue gas conditions for iron ore processing are vastly different (4). In particular, the chemistry and heat profiles of the taconite processes, as well as possible differences in fuel types, are likely to affect the performance of mercury control technologies somewhat differently than when applied to coal-fired utilities. Moreover, iron oxides have been shown to be particularly reactive with mercury in some settings and may, therefore, interfere with control technology applications. Consequently, technologies used by other industries (such as utilities) must be tested to determine their applicability and effectiveness for the taconite industry or new technologies may need to be developed.

The Energy & Environmental Research Center (EERC) at the University of North Dakota is heavily involved in mercury research, from developing protocols for sampling to cost-effective control technologies. The EERC has developed a number of technologies for use at coal-fired power plants that may prove effective for the taconite industry. Based on this experience, the EERC proposed proof-of-concept testing at the Minntac Plant to evaluate an EERC proprietary technology, high-energy dissociation technology (HEDT), for mercury control systems. The proposed technology is thought to have several benefits over standard in-furnace addition, especially in this application. For example, the potential for corrosion is significantly reduced because halogens are not added at locations where can contact the grates at high temperatures. Instead, reactive halogens are generated at high temperatures outside of the taconite process and injected downstream of the grates at low temperatures within the ducts. The technology works by dissociating halogen salts, allowing the use of benign compounds to create halogen radicals that quickly oxidize Hg^0 to Hg^{2+} in flue gas. The oxidized mercury is theoretically removed in downstream equipment such as the wet scrubber. A key advantage of the technology is that injection of the dissociated halogen can occur anywhere in the system, allowing for optimization of injection location and minimization of impacts on system components. By comparison, other technologies require the addition of materials in the hot zone of the induration furnace, which may increase corrosion potentially throughout the entire system.

GOAL AND OBJECTIVES

The overall goal of this project is to evaluate a novel, proprietary EERC process (Patent Application US2007/0051239) by which mercury oxidation can be enhanced by injection of radical halogen species which are created from dissociating halogen salts. Specific objectives are as follows:

- Obtain baseline mercury removals in taconite flue gas.
- Inject variable rates of dissociated halogens to determine improvements in mercury capture and reduction.

- Assess applicability of the halogen dissociation technology to the taconite industry, particularly for a grate–kiln configuration.
- Evaluate initial/potential balance-of-plant impacts that may result from the use of this technology at Minntac and generalize results to other plants.

EXPERIMENTAL DESCRIPTION

The testing that was performed built on and was compared to previous tests that have been conducted under the leadership of Michael Berndt of MNDNR. The on-site evaluation of this technology was conducted at the Minntac Plant Line 3. This facility has a grate–kiln configuration (see Figure 1) that moves high-temperature air counter to the movement of the green balls through the system. Figure 1 shows the configuration for Lines 6 and 7, which are similar in process to Line 3. Line 3 is considerably smaller and is equipped with a recirculating, pH-controlled wet scrubber and updated cyclone for dust collection prior to the scrubber.

Based on a site visit and several follow-up discussions with Minntac personnel, the EERC installed the HEDT field unit at the inlet of the waste gas fan, shown as Location 2 in Figure 2, in which the dissociated halogens were conveyed into the flue gas of Line 3. Location 2 is not optimal since it only provides a nominal ~0.2-second residence time for formed reactive halogen in the taconite flue gas before being scavenged with wet scrubbers. The residence time was estimated based on duct dimensions including duct cross-sectional area, duct length from the HEDT injection location to the scrubber inlet, and typical flue gas flow rate at Line 3. However, other possible injection locations such as Location 1 in Figure 2 were not accessible during the time frame of the project.

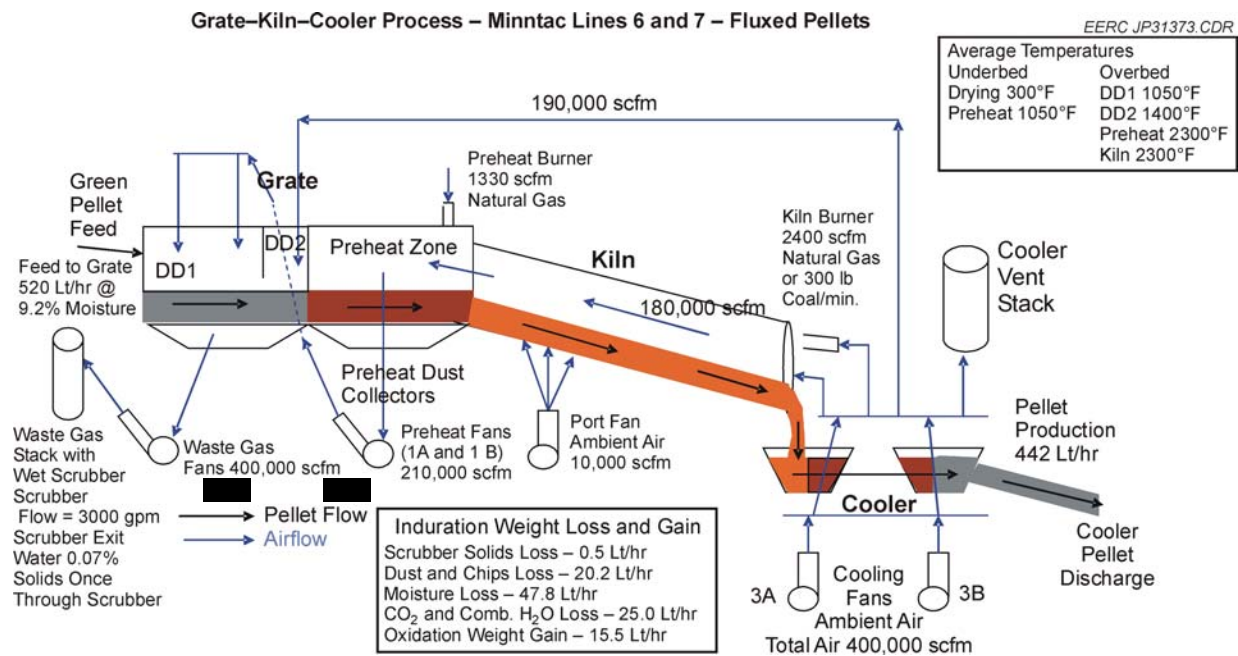


Figure 1. Configuration of Minntac Plant Lines 6 and 7, similar in process to Line 3.

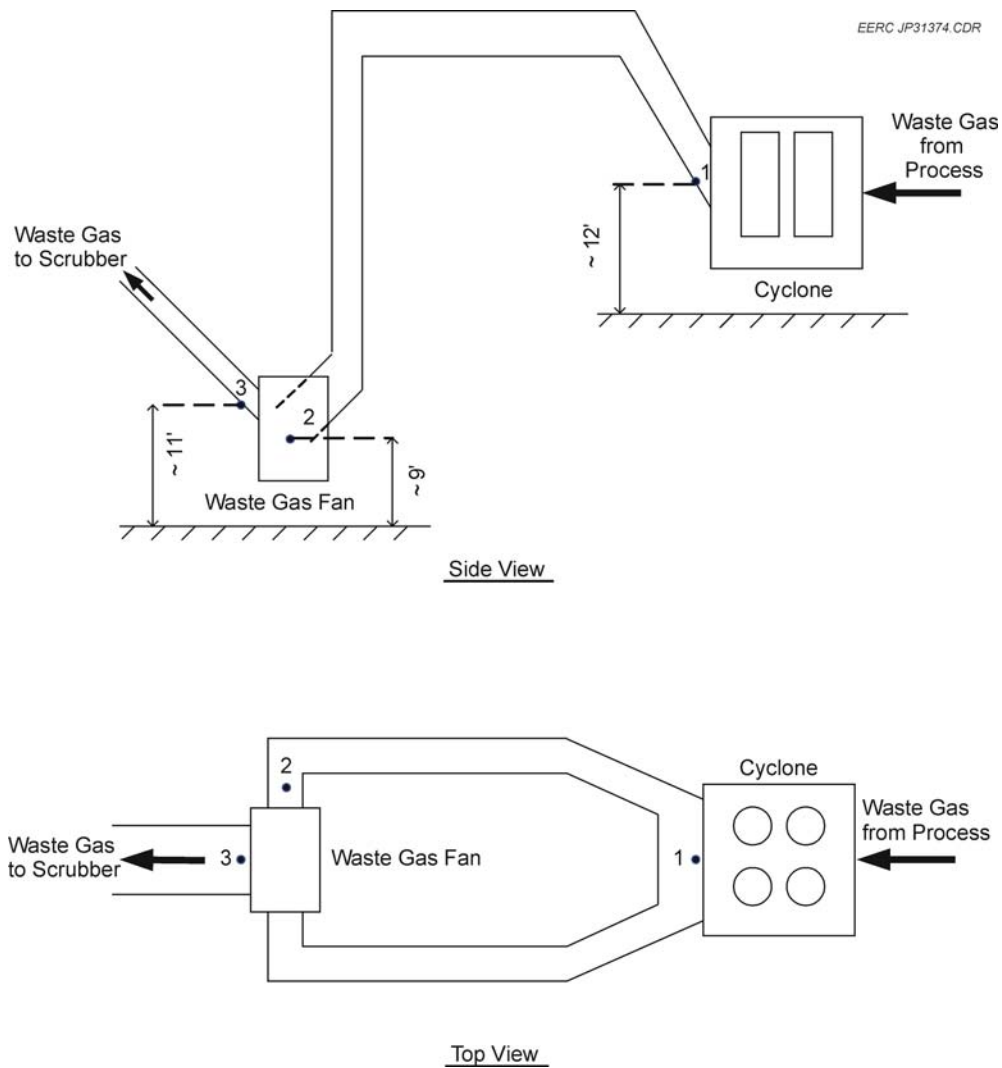


Figure 2. Possible injection locations within the Minntac Plant Line 3 ductwork.

The EERC HEDT field unit, as shown in Figure 3, was shipped to the Minntac Plant and installed at Location No. 2 on Line 3 to test the effectiveness of this technology to generate disassociated halogen radicals for improved mercury oxidation and particulate-bound mercury for subsequent removal by the existing venturi scrubbers.

Sodium bromide, calcium bromide, sodium chloride, and a 50% calcium bromide–50% sodium chloride mixture were evaluated separately for mercury reduction in taconite flue gas using the HEDT unit. The injection rates for each tested chemical additive are listed in Table 1. During the testing period, Minntac was generating fluxed pellets on Line 3, which is different from previous MNDNR test conditions when calcium bromide solution was injected into the kiln (3). In order to evaluate possible interferences on mercury–bromine reactions introduced by the added limestone and changed heating profiles associated with fluxed pellet production, a calcium bromide solution was again injected into the kiln (by DNR personnel) at the end of the EERC tests to compare with previous MNDNR testing results (3).



Figure 3. EERC HEDT field unit.

Table 1. Test Matrix Completed at Minntac Plant Line 3

Test No.	Chemical Additive	Injection Rate, lb/hr	Injecting Location
T-1	NaBr	5, 25	Waste gas fan
T-2	CaBr ₂	5, 14, 25	Waste gas fan
T-3	CaBr ₂ /NaCl	14, 25	Waste gas fan
T-4	NaCl	25	Waste gas fan
A-1*	CaBr ₂ solution	25	Hot zone in kiln

* For comparison, done outside of this project.

Two continuous mercury monitors (CMMs) were used during the tests to measure gaseous mercury species upstream of the HEDT injection location and downstream from the wet scrubber at the stack. To protect the CMM, a filter assembly was installed in the CMM sampling line at the scrubber inlet to capture particulate matter (primarily iron oxide). In doing so, mercury oxidation most likely occurred when elemental mercury came in contact with the iron oxide filter cake. As a result, mercury species sampling at the scrubber inlet had biased low elemental mercury and total gaseous mercury concentration.

RESULTS AND DISCUSSION

Plotted in Figures 4–6 are the temporal variations of gaseous mercury for stack gases for the entire test period. The collected CMM data were then averaged and replotted in Figure 7 to summarize the changes of mercury emissions at the stack when halogen additives were added as defined in Table 1. Mercury CMM data at the stack indicate no significant decrease of mercury emissions but with improved mercury oxidation when dissociated halogens were added into the taconite flue gas. At an injection rate of 25 lb/hr, both NaBr and CaBr₂ enhanced

mercury oxidation by increasing the fraction of oxidized mercury in flue gas: from 8.9% in baseline to 13% for NaBr injection and from 13% in baseline to 38% for CaBr₂ injection. Injections of NaCl and a mixture of CaBr₂-NaCl did not appreciably change mercury speciation in stack flue gas.

The dissociated bromine radicals affect mercury species and subsequent capture by either homogeneously oxidizing elemental mercury followed by adsorption onto particles such as iron oxide or heterogeneously oxidizing mercury on fine particles contained within taconite flue gas. The gas-to-particle transportation is potentially a mass transfer-limiting process, meaning that the residence time for bromine radicals contacting flue gas is very critical. Unfortunately, compared to the ~2 minutes of residence time of bromine species in flue gas when bromide compounds were added into the hot zone of the kiln, only 0.2 seconds of residence time was available during the HEDT tests, which may have been too short for capture by the venturi scrubber.

In addition, since the gas-to-particle transportation rate is inversely correlated with particle size, most of the adsorbed mercury would be enriched within the fine fraction of particulate matter. Allowing adequate residence time, these Hg-enriched fine particles would coagulate with other particles to form large-sized agglomerates that are more easily removed by venturi scrubbers. Coagulation between particles has been recognized as one of the main mechanisms for particle growth in high-dust-loading flue gas, which has been extensively studied elsewhere (5). However, as a result of the short residence time in the current test configuration, the particulate-bound mercury, if formed, would likely remain fine in size and escape the venturi scrubber, which is known for its low collection efficiency for fine particles. Therefore, the Hg-enriched fine particulate matter, most likely in the submicron range, would not be captured and would exit the stack. Additionally, the fine-sized particulate-bound mercury would also travel into the CMM mercury conversion unit in which the particulate-bound mercury would be released, detected, and reported by the CMM as oxidized mercury, adding to the total mercury concentration. It should be noted, that for these tests the CMM was not equipped with an inlet filter as most of the large particulate is scrubbed out by the venturi scrubber.

In order to further evaluate the effect of adding limestone as a fluxing agent, a repeat test injecting CaBr₂ solution into the kiln hot zone was performed (by MNDNR personnel) at the end the HEDT test period. The CMM data are plotted in Figure 6, and averaged data are summarized in Figure 7. It shows mercury emission was reduced to 2.8 µg/m³ with 2.2 µg/m³ of elemental mercury, compared to a decrease of total mercury in stack gases from 5.1 to 1.4 µg/m³ attained in previous MNDNR tests during the production of standard pellets and using the same CaBr₂ injection. From these results, it can be concluded that the added limestone and changed thermal regimes associated with generation of fluxed pellets has a significant negative effect on mercury-bromine chemistry reactions. However, the fact that stack gas mercury decreases occur when CaBr₂ is injected into the kiln while no change or even slight increases of mercury emission occurred when similar species are injected into the duct indicates a fundamental need for more detailed work with Hg-Br-Fe oxide reactions at various temperatures.

CONCLUSIONS AND RECOMMENDATIONS

Experimental data collected at Minntac Plant Line 3 indicate that limited mercury oxidation occurred when reactive bromine species were generated with the EERC HEDT, but with no decrease in total mercury emission at the stack. An increase of oxidized mercury of 4% and 25% was achieved for NaBr and CaBr₂, respectively, at a 25-lb/hr injection rate. The current HEDT injection location, which provided a residence time estimated at 0.2 second, may be one of many factors that limit HEDT performance. Other components in flue gas, including fine iron oxide particles and the limestone fluxing material, may also interfere with mercury oxidation and subsequent capture in the venturi scrubbers.

The repeat MNDNR tests proved that the added limestone and changed thermal regimes associated with generation of fluxed pellets have a significant negative effect on mercury–bromine chemistry reactions.

The EERC HEDT field testing at Minntac Plant Line 3 demonstrated the importance of time–temperature profile on mercury oxidation and/or adsorption in taconite flue gas. The data suggest a need for better understanding of reactions between iron oxides, Br, and Hg as functions of temperature and residence time.

It is recommended that future testing with the HEDT technology be at an injection location further upstream of the location tested for this project, but downstream of the grate to avoid corrosion concerns. For example, at Minntac Plant Line 3, a suggested location would be at the inlet of the fly ash drop box which is upstream of the multicyclone collector.

REFERENCES

1. Berndt, M.E. *Mercury and Mining in Minnesota*; Minerals Coordinating Committee Final Report, Oct 2003.
2. Berndt, M.E.; Engesser, J. *Mercury Transport in Taconite Processing Facilities: (III) Control Method Test Results*; Iron Ore Cooperative Research Final Report, Dec 2007.
3. Berndt, M.E. *On the Measurement of Stack Emissions at Taconite Processing Plants*; Progress Report to Minnesota Pollution Control Agency, May 2008.
4. Laudal, D. *Mercury Control Technologies for the Taconite Industry*; EERC Technical Report to Minnesota Department of Natural Resources; Agreement A85811; 2007.
5. Flagan, R.C.; Seinfeld, J.H. *Fundamentals of Air Pollution Engineering*; Prentice Hall 1988.

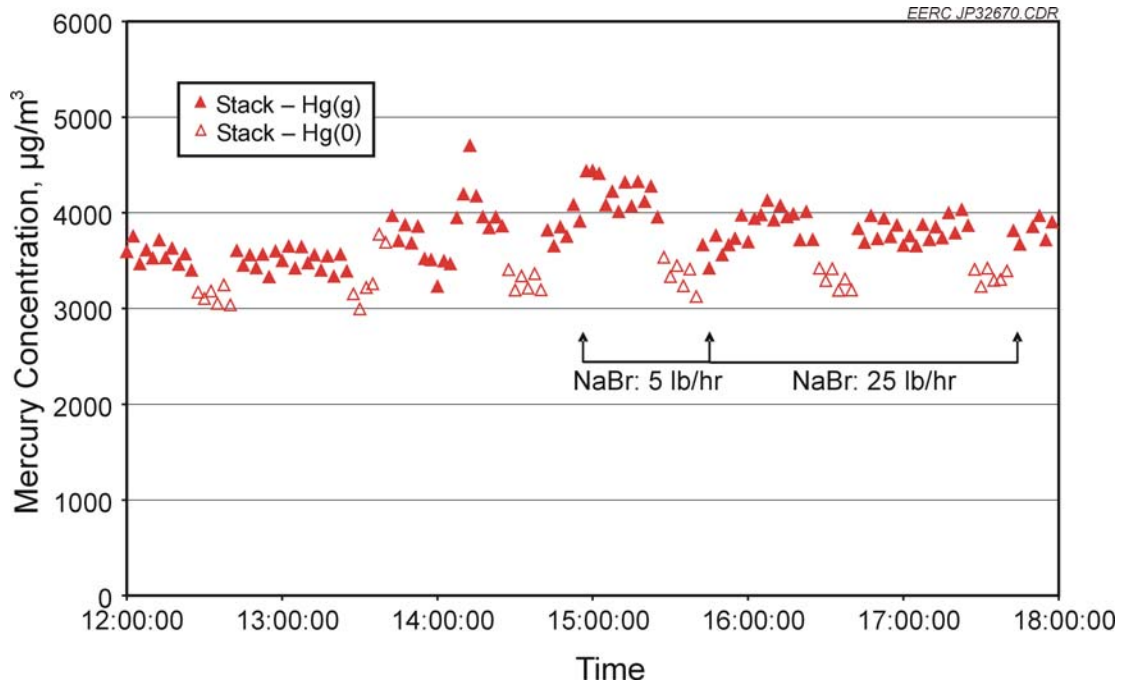


Figure 4. Continuous mercury measurement at Minntac Plant Line 3 when NaBr was used with the HEDT.

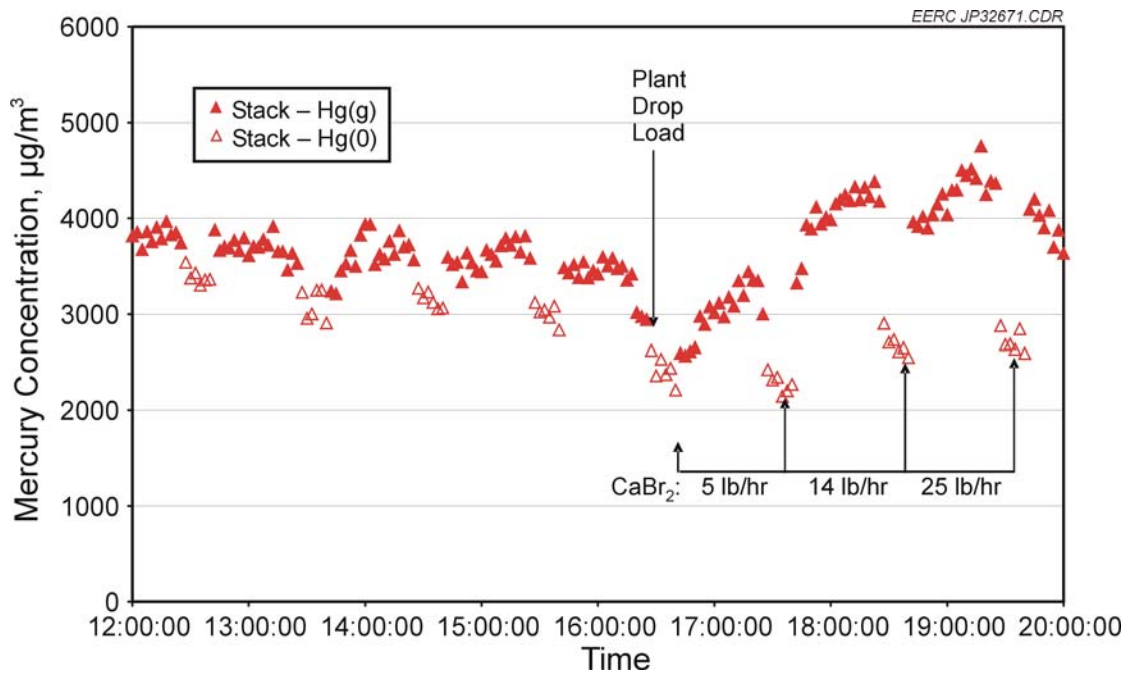


Figure 5. Continuous mercury measurement at Minntac Plant Line 3 when CaBr_2 was used with the HEDT.

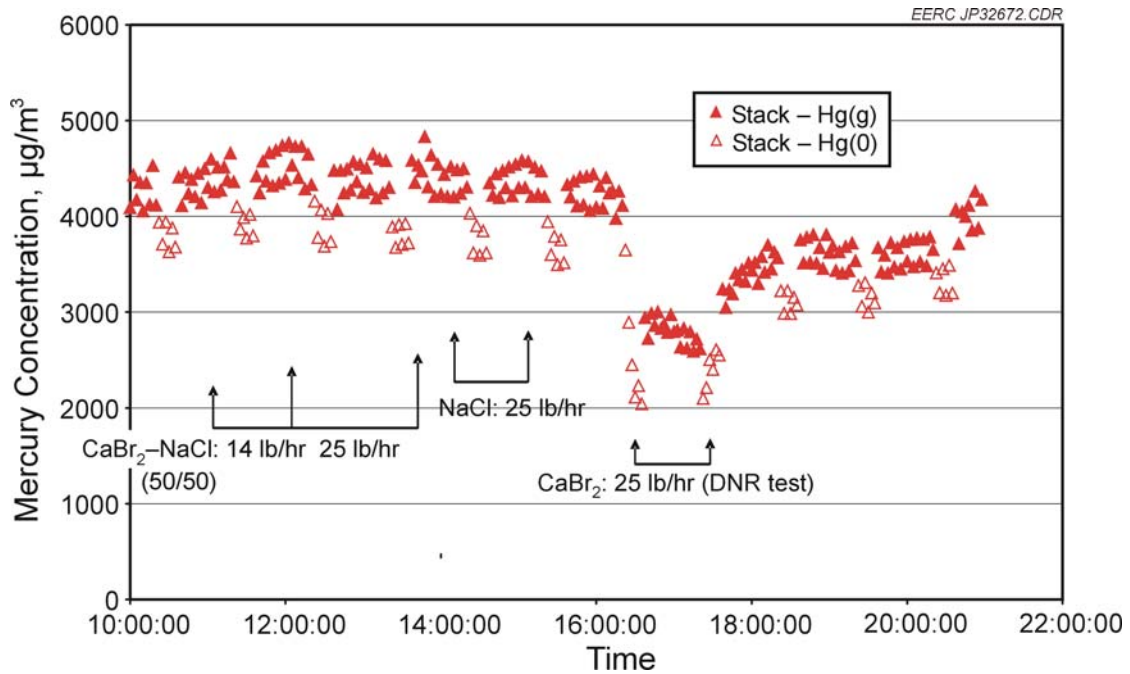


Figure 6. Continuous mercury measurement at Minntac Plant Line 3 when a CaBr₂-NaCl mixture and NaCl alone were used with the HEDT.

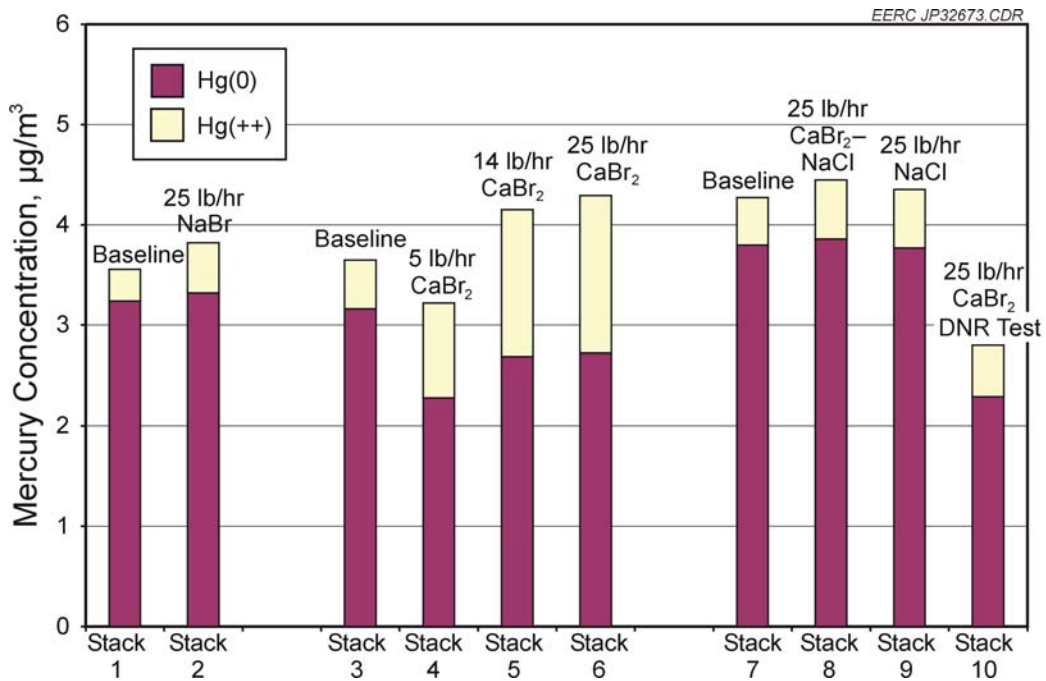


Figure 7. Summary of Mercury Testing at Minntac Plant Line 3.

Appendix B-1-16

Demonstration of Mercury Capture in a Fixed Bed

June 2009



EERC[®]

Energy & Environmental Research Center

UNIVERSITY OF NORTH DAKOTA

15 North 23rd Street — Stop 9018 / Grand Forks, ND 58202-9018 / Phone: (701) 777-5000 Fax: 777-5181
Web Site: www.undeerc.org

June 17, 2009

Dr. Michael Berndt
Research Scientist II
Minnesota Department of Natural Resources
Division of Lands and Minerals
500 Lafayette Road
St. Paul, MN 55155-4045

Dear Dr. Berndt:

Subject: Draft Final Report Entitled "Demonstration of Mercury Capture in a Fixed Bed"
Work Order No. B25018; EERC Fund 14784

Enclosed please find the subject draft final report. If you have any questions or comments, please contact me by phone at (701) 777-5034, by fax at (701) 777-5181, or by e-mail at gdunham@undeerc.org.

Sincerely,

Grant E. Dunham
Research Manager

GED/sah

Enclosure

c/enc: Stan Miller, EERC
David Dunham, EERC



DEMONSTRATION OF MERCURY CAPTURE IN A FIXED BED

Draft Final Report

(for the period of February 10, 2009, through June 30, 2009)

Prepared for:

Michael Berndt

Minnesota Department of Natural Resources
Division of Lands and Minerals
500 Lafayette Road
St. Paul, MN 55155-4045

Work Order No. B25018

Prepared by:

Grant E. Dunham
Stanley J. Miller

Energy & Environmental Research Center
University of North Dakota
15 North 23rd Street, Stop 9018
Grand Forks, ND 58202-9018

June 2009

EERC DISCLAIMER

LEGAL NOTICE. This research report was prepared by the Energy & Environmental Research Center (EERC), an agency of the University of North Dakota, as an account of work sponsored by the Minnesota Department of Natural Resources. Because of the research nature of the work performed, neither the EERC nor any of its employees makes any warranty, express or implied, or assumes any legal liability or responsibility for the accuracy, completeness, or usefulness of any information, apparatus, product, or process disclosed or represents that its use would not infringe privately owned rights. Reference herein to any specific commercial product, process, or service by trade name, trademark, manufacturer, or otherwise does not necessarily constitute or imply its endorsement or recommendation by the EERC.

TABLE OF CONTENTS

LIST OF FIGURES	iii
LIST OF TABLES	v
NOMENCLATURE	vi
1.0 PROJECT SUMMARY	1
2.0 BACKGROUND.....	2
3.0 OBJECTIVES AND APPROACH	3
3.0 SCOPE OF WORK.....	4
3.1 Column Configurations.....	4
3.2 Gas Composition and Conditions	4
3.3 Comparison of Test Conditions to Full-Scale Conditions	5
4.0 EXPERIMENTAL SYSTEM AND PROCEDURES.....	5
4.1 Test Columns	5
4.2 DAC System	9
4.3 Gas Delivery System.....	11
4.4 Mercury Vapor Source.....	12
4.5 Mercury Measurement System	12
4.6 Test Sorbents.....	13
5.0 TEST RUN PERIODS AND POSTRUN ANALYSES	14
5.1 Shakedown.....	14
5.2 Test Run Start-Up and Data Collection	15
5.3 Test Run Periods.....	17
5.4 Postrun Sample Recovery and Analyses.....	18
6.0 RESULTS AND DISCUSSION	18
6.1 Sorbent Mass.....	18
6.2 Process Measurements	19
6.2.1 Gas Flow Measurement	20
6.2.2 Bed Temperatures	21
6.2.3 Column Pressure Drop	23
6.2.4 Mercury Source.....	23
6.3 Mercury Capture and Breakthrough Curves.....	25
6.3.1 Column 1 Breakthrough Curves (DARCO Hg-LH)	26
6.3.2 Column 2 Breakthrough Curves (MERSORB HT-1.5)	31
6.4 Postrun Laboratory Analyses and Mass Balance.....	33

Continued...

TABLE OF CONTENTS (continued)

7.0	DISCUSSION AND CONCLUSIONS.....	37
7.1	Discussion.....	37
7.2	Conclusions.....	39
8.0	REFERENCES.....	40

LIST OF FIGURES

1 Conceptual schematic of one column 6

2 Schematic of the hot box showing sampling configurations 7

3 Photo of the column cabinets and the hot box 8

4 Photo of a loaded column 8

5 Flow balance indicated by orifice ΔP for each column for Phase 2C 21

6 Daily averaged 2C Column 1 bed temperatures 22

7 Daily averaged 2C Column 2 bed temperatures 22

8 Derived carbon bed pressure drop 24

9 Daily averaged mercury source temperatures..... 24

10 Averaged inlet mercury concentrations 25

11 Mercury outlet data for Column 1 containing DARCO Hg-LH compared with target inlet value 27

12 Bed 1 mercury outlet data for Column 1 containing 1 inch of DARCO Hg-LH..... 27

13 Column 1 Bed 1 cumulative mercury capture efficiency 29

14 Bed 2 mercury outlet data for Column 1 containing 2 inches of DARCO Hg-LH 29

15 Column 1 Bed 2 cumulative mercury capture efficiency 30

16 Bed 3 mercury outlet data for Column 1 containing 3 inches of DARCO[®] Hg-LH 30

17 Column 1 Bed 3 mercury cumulative mercury capture efficiency 31

18 Cumulative Hg loading for Beds 1 and 2 32

19 Mercury outlet data for Column 2 containing MERSORB HT-1.5 compared with target inlet value..... 32

20 Bed 1 mercury outlet data for Column 2 containing 1 inch of MERSORB HT-1.5 34

21 Bed 1 cumulative mercury capture efficiency 34

Continued...

LIST OF FIGURES (continued)

22	Bed 2 mercury outlet data for Column 2 containing 2 inches of MERSORB HT-1.5	35
23	Column 2 Bed 2 cumulative mercury capture efficiency	35
24	Column 2 MERSORB HT-1.5 projected stage loading throughout the run.....	36

LIST OF TABLES

1	Column Bed Configurations by Bed Segment.....	4
2	Simulated Flue Gas Inlet Composition and Conditions.....	5
3	Column 1 DARCO Hg-LH Sorbent Mass Before and after the Run.....	19
4	Column 2 MERSORB HT-1.5 Sorbent Mass Before and after the Run	19
5	Column 1 DARCO Hg-LH Sorbent Laboratory Mercury Analyses	36
6	Column 2 MERSORB HT-1.5 Sorbent Laboratory Mercury Analyses	36
7	Mass Balance Closure.....	38

NOMENCLATURE

acfm	actual cubic feet per minute
alpm	actual liter per minute
ARL	Analytical Research Laboratory
ASTM	ASTM International
CMM	continuous mercury monitor
CVAA	cold-vapor atomic absorption
DAC	data acquisition and control
dscm	dry standard cubic meter
dslm	dry standard liter per minute
EERC	Energy & Environmental Research Center
EPA	U.S. Environmental Protection Agency
HEPA	high-efficiency particulate air
Hg ⁰	elemental mercury
Hg ²⁺	oxidized mercury forms
ICP–AES	inductively coupled plasma–atomic emission spectroscopy
lpm	liter per minute
MNDNR	Minnesota Department of Natural Resources
MPCA	Minnesota Pollution Control Agency
MSDS	material safety data sheet
NIST	National Institute of Standards and Technology
NaOH	sodium hydroxide
PSA	P S Analytical
psia	pounds per square inch absolute
sccm	standard cubic centimeter per minute
SIC	sulfur-impregnated carbon
SnCl ₂	stannous chloride
W.C.	water column

DEMONSTRATION OF MERCURY CAPTURE IN A FIXED BED

1.0 PROJECT SUMMARY

The Minnesota Department of Natural Resources (MNDNR) contracted with the Energy & Environmental Research Center (EERC) to conduct a test program to evaluate the performance of activated carbons for mercury capture by fixed-bed mercury adsorption for flue gas generated by taconite-processing facilities.

The work included a 1000-hr test using two parallel columns with fixed beds consisting of multiple stages of selected granular activated carbons. The tests were conducted under constant process conditions for an actual duration of 1009 hours and were completed June 1, 2009.

The purpose of the test was to evaluate carbon performance for mercury abatement in a flue gas environment that simulates that generated in a taconite-processing facility. The test conditions were selected to match the nominal operating conditions downstream of a particulate scrubber.

The test configuration consisted of two columns (designated as Column 1 and Column 2) operated in parallel. Each column has an inside diameter of 3.75 inches and a total depth of 18 inches of carbon adsorbent. The columns were arranged in six bed segments ranging in depth from 1 to 6 inches. Sampling ports were located at the outlet of each bed segment to provide mercury breakthrough concentration data as a function of bed depth and time. The Column 1 carbon was a lignite-based granular brominated carbon (DARCO[®] Hg-LH 4×8) from Norit Americas. The Column 2 adsorbent was NUCON MERSORB HT-1.5 coal-based sulfur impregnated carbon (SIC).

The simulated flue gas composition and operating conditions were selected to represent those of a coal-fired kiln used to process taconite for steel production. The simulated flue gas fed to both columns provided a constant mercury concentration. The target mercury concentration was 6.0 µg/dscm. Mercury breakthrough measurements were taken at specific bed depths from

both columns during the entire run with a continuous mercury monitor (CMM). The same CMM was used to periodically measure the inlet mercury concentration.

Following completion of the test, samples of carbon from each stage were recovered. All stages that were exposed to mercury were analyzed for total mercury content. Good agreement between the independent CMM breakthrough data and the laboratory data along with good mass balance closures provided a strong basis for forming the conclusions.

The results showed that for the conditions evaluated, an 18-inch bed of either brominated granular activated carbon or sulfur-impregnated activated carbon was adequate to provide essentially 100% control of the inlet mercury for more than 1000 hours.

2.0 BACKGROUND

It has been estimated that taconite processing in Minnesota releases approximately 350 to 400 kg of mercury to the atmosphere each year (1–4). Even though this amount is small compared to global emission rates, it represents Minnesota's second largest industrial source of mercury to the atmosphere. Therefore, the Minnesota Pollution Control Agency (MPCA) may regulate mercury emissions from taconite plants.

There are a number of methods to remove mercury from a flue gas stream. With taconite plants, it may be simple to inject additives such as halogens to enhance oxidation of the mercury in the induration furnace and promote capture of the oxidized mercury in the wet particulate scrubbers. Short-term tests (5) indicated 5%–13% capture for a straight-grate facility and 18%–32% for a grate–kiln facility when NaCl was added to the process. The addition of bromide salts was more effective, but still saw reductions of only 62%–64%. The best results (80% capture) were observed when a proprietary U.S. Environmental Protection Agency (EPA) oxidant was added to the scrubber solution. Each of these methods provides some level of mercury capture, but not at a high level (>95%). In addition, there is a possibility of increased corrosion in the system as a result of injecting these additives into the system, and an increase in particulate matter emissions due to additional fine particulate formation.

A fixed bed of activated carbon is preferred over other forms of mercury control for several reasons. Unlike injection of activated carbon upstream of the wet scrubber, a fixed bed will not add to the particulate loading to the scrubber or increase particulate matter emissions at the stack. With a fixed bed, nothing is added to the system that may affect the quality of the product or the life of the system, such as corrosion downstream. There will also be no increase of halogens in the scrubber water.

3.0 OBJECTIVES AND APPROACH

The overall goal of this project was to evaluate the ability of a fixed bed of sorbent material to capture mercury in a flue gas stream that simulates that generated during the processing of taconite for steel production.

The approach used to meet this objective was to utilize two adsorption columns, each configured with an 18-inch depth of carbon adsorbent. Column 1 was loaded with Norit America's DARCO Hg-LH 4×8 brominated lignite-based activated carbon. Column 2 was loaded with MERSORB HT-1.5 coal-based SIC adsorbent. The bed segment configurations in each column were identical. Both carbon adsorbents were selected based on past performance in capturing mercury.

The operating parameters for this test were selected to simulate real process conditions in terms of bed velocity, temperature, flue gas composition, and mercury concentration. The one component missing from the simulated flue gas is particulate matter. Mercury-sampling tests have shown that the dust in the taconite process flue gas is very reactive toward mercury, causing oxidation of elemental mercury (6). Mercury measurements taken at the outlet of the scrubber do not show this oxidation effect to the same degree, indicating the reactive dust has been removed by the scrubber. In support of this, chemical analysis of impactor samples collected at the stack of one taconite facility show the particulate matter downstream of the scrubber is mostly potassium and chloride, most likely as KCl salt (7). Based on these findings, it is likely there is very little reactive dust that would reach the fixed-carbon bed, and any that does would most likely enhance mercury capture rather than hinder it. For these reasons, it was decided to not

include reactive dust as a variable in this test matrix. Using this system rather than pulling a slipstream of real flue gas from one of the taconite facilities also allows for uninterrupted exposure of the samples for an extended period of time in a controlled laboratory environment where all process variables can be controlled.

3.0 SCOPE OF WORK

3.1 Column Configurations

The configuration for the test consisted of two columns operated in parallel; each column had a total depth of 18 inches in six discrete bed segments.

Table 1 provides a segment-by-segment loading schedule for the two columns evaluated during the test. Column 1 consisted of a total of 18 inches of a lignite-based DARCO Hg-LH 4×8, which is brominated. Column 2 consisted of 18 inches of MERSORB HT-1.5 coal-based SIC adsorbent. The bed segment depth configurations were identical for the two columns.

3.2 Gas Composition and Conditions

The simulated flue gas composition used for the test is provided in Table 2. The levels of the gas components and the temperatures are based on actual measurements (8) and suggestions from John Engesser (Principal Engineer for Mineral Development, MNDNR Division of Land and Minerals).

Table 1. Column Bed Configurations by Bed Segment

Bed Segment No.	Bed Segment Sorbent Depth, in.	Cumulative Sorbent Depth at Bed Segment Outlet, in.	Column 1 Segment Loadings	Column 2 Segment Loadings
1	1	1	DARCO Hg-LH	MERSORB HT-1.5
2	2	3	DARCO Hg-LH	MERSORB HT-1.5
3	3	6	DARCO Hg-LH	MERSORB HT-1.5
4	3	9	DARCO Hg-LH	MERSORB HT-1.5
5	3	12	DARCO Hg-LH	MERSORB HT-1.5
6	6	18	DARCO Hg-LH	MERSORB HT-1.5

Table 2. Simulated Flue Gas Inlet Composition and Conditions

Conditions at Hg Adsorption		
Model Column Inlet	Units	Value
Temperature	°F	180
H ₂ O	mol% (wet)	16.0
CO ₂	mol% (dry)	3
O ₂	mol% (dry)	18
N ₂	mol% (dry)	Balance
NO	ppmv (dry)	250
NO ₂	ppmv (dry)	10
SO ₂	ppmv (dry)	20
HCl	ppmv (dry)	2
Hg	µg/dscm	6.0
Superficial Gas Face Velocity	ft/min	23.58

3.3 Comparison of Test Conditions to Full-Scale Conditions

Process conditions from a full-scale system that is used to capture mercury in a similar application were used to select the superficial gas velocity, carbon bulk density, configuration, and residence time per inch of bed. These, along with the temperature, were all held constant between Columns 1 and 2 and the full-scale system. There are no scale-up factors to apply. The mercury entering the system was in elemental form as is the expected case for full-scale operation downstream of a scrubber. The mercury inlet concentration averaged 6.2 µg/dscm.

4.0 EXPERIMENTAL SYSTEM AND PROCEDURES

A system designed and built for evaluating activated carbon for mercury abatement in a high-mercury-concentration flue gas was modified for use in this test program.

4.1 Test Columns

Figure 1 is a conceptual design of a column used for the testing. The system included two parallel columns made up of six separate glass stages separated by perforated Teflon support disks/gaskets. Each stage section was 3.75 inches inside diameter. Steel clamps that were torqued

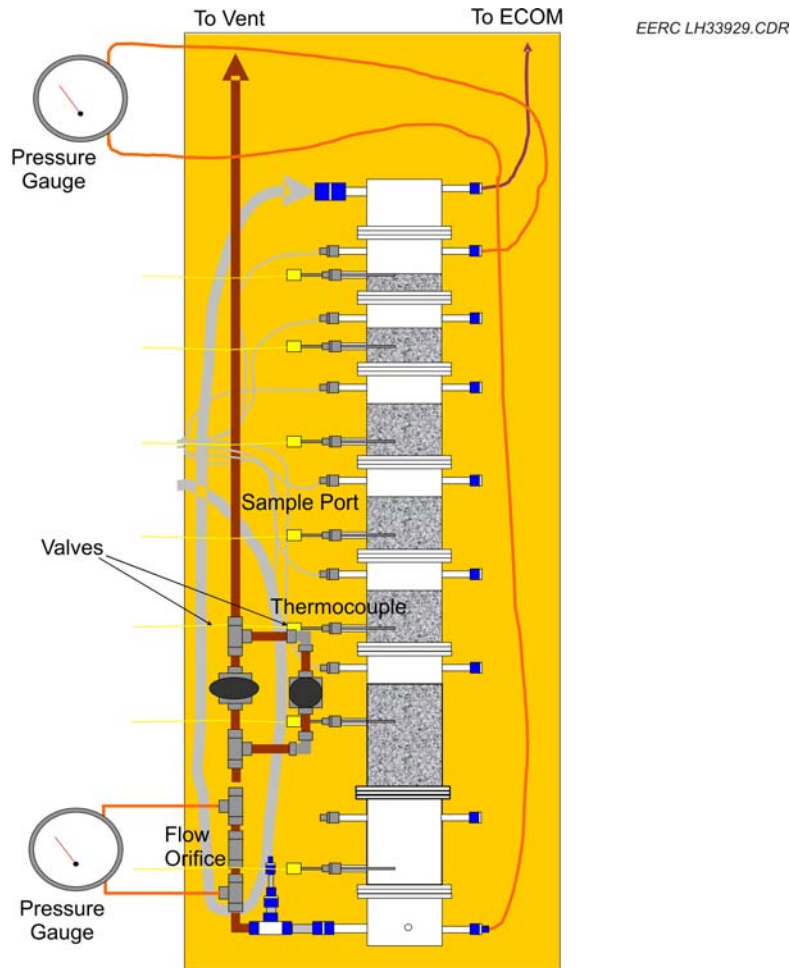


Figure 1. Conceptual schematic of one column.

to a consistent value to ensure a uniform seal held the stages together. Each column was supported the entire length by a threaded rod, which was attached at the top and bottom of the cabinet. Sampling ports were located near the top of each stage. Teflon tubing connected the individual solenoid valves to the ports located in a heated control box between the columns. The common sampling header for this system was also in the heated box. Figure 2 is a conceptual design of the hot box that maintained some of the switching valves and the sampling system at an elevated temperature. The $\frac{1}{8}$ -inch sample lines were joined in a common header. The headers were connected to heated-head sample pumps. The output from the pumps supplied sample to the CMM conditioning/conversion system.

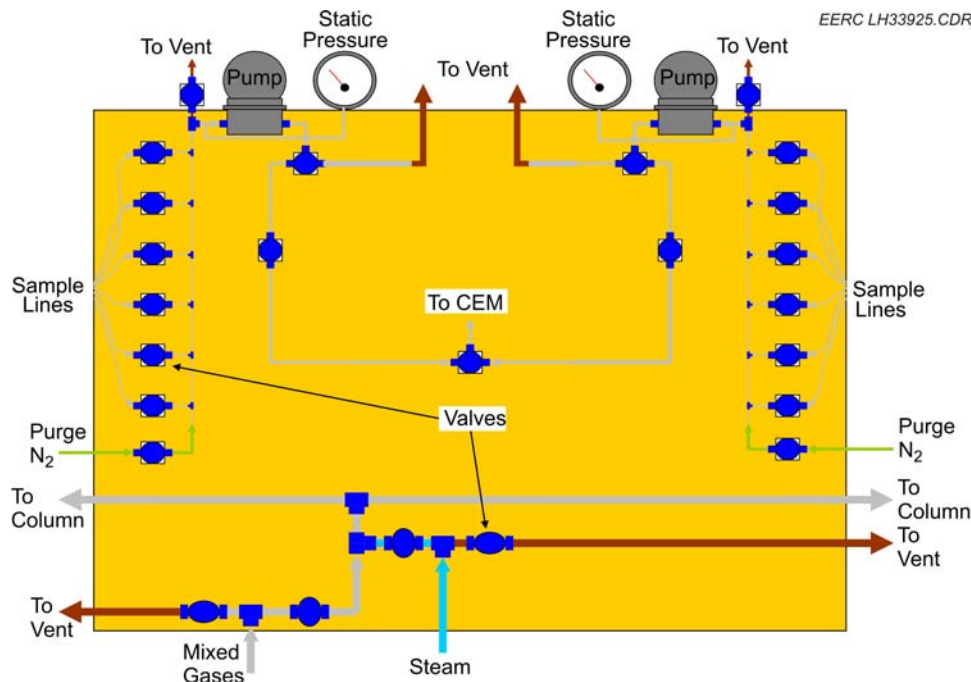


Figure 2. Schematic of the hot box showing sampling configurations.

A data acquisition and control (DAC) system individually controlled each valve. The temperature of each bed was monitored by a thermocouple located near the bottom of each stage section. The cabinets holding the reactor columns were maintained at temperature by using high-temperature blowers to circulate hot air. Heaters were located in an overhead plenum and controlled by external temperature controllers. Figure 3 is a photo of the front of the cabinets holding the columns and the hot box in between. A photo of an example of the carbon bed setup is shown in Figure 4.

The moisture level in the flue gas was controlled by injecting water into a steam generator with a peristaltic pump. The water delivery rate was automatically controlled with the DAC system by monitoring loss of weight of the water reservoir. The mass feed rate of water into the steam generator was independently calibrated by monitoring the pump feed rate. The water feed rate was also monitored with a manual variable-area flowmeter.



Figure 3. Photo of the column cabinets and the hot box.



Figure 4. Photo of a loaded column.

The DAC system was used to select the specific sampling points. A Teflon 3-way valve was used to select between columns. Gases not being sent to the CMM were vented. The common sample headers could also be purged with N₂, either with the exit purge gas going to vent or to the CMM. This provided a means to monitor and clean the system.

4.2 DAC System

National Instruments components were used to construct the DAC system, which was written in LabVIEW graphical language. The front panel of the program acted as the user interface. The DAC system was used to do the following:

- Monitor and control gas flows into the system with mass flow controllers
- Monitor and control the water supply rate to the steam generator
- Monitor flow out of each column
- Monitor system temperatures (beds, cabinets, and steam generation system)
- Control all of the sampling valves
- Integrate with the bed outlet CMM to synchronize sampling
- Log process data every 5 minutes

Metering of component gases into the mixing manifold through the mass flow controllers was controlled by the DAC system. The mass flow controllers were initially calibrated with a Gilibrator bubble-type flowmeter to produce a response curve to convert an input, in units of standard cubic centimeters per minute (sccm), into voltage sent to the flow controller. This calibration was performed with nitrogen for the trace gases that were in a balance of nitrogen and with the gas itself for the CO₂ and O₂. The mass flow controllers have internal closed-loop control to maintain the desired flow and an output representing the actual flow. This voltage was read by the DAC system and converted back into a sccm value, displayed, and recorded.

The flow between the columns was balanced by manually adjusting a back-pressure valve at the exit of each column and by monitoring the pressure drop across a flow orifice at the exit of

each of the columns. Identical 0.25-inch-diameter orifices were installed at the exit of each column to produce a ΔP of 1 to 2 inches W.C. at the desired flow conditions.

System temperatures were monitored with Type K thermocouples and logged by the DAC system. These were wired to input modules designed specifically for thermocouple voltage measurements and mounted on terminal bases intended to minimize thermal gradients in the input module, which would adversely affect the relative accuracy of the different channels. The most recent readings could be viewed on the DAC system screen. The temperatures monitored by the DAC system included the following:

- Individual bed segments
- Upper- and lower-level temperatures in the column enclosure cabinet
- Steam generation system (inlet, interior, and outlet)
- Mercury vapor source oven
- Sampling hot box

The sampling valves for mercury measurement were controlled by the DAC system so that individual points could be selected manually or a sequence of locations could be set so that multiple locations could be sampled for various times over a 24-hour period.

An alarm system was implemented to provide on- and off-site process alerts 24 hours a day, 7 days a week. The system consisted of two levels of alarms for the DAC system. Set points for triggering the alarms were determined during the initial part of the run. The alarm system did not include the CMMs.

Level One: Process Alert and Alarms

The set points for this level of alarm were designed to identify and alarm process instrumentation that was out of the desired range and required test personnel intervention and action to troubleshoot and return the modeling system to normal operation. Short-term excursions of this level were not expected to impact modeling data or personnel safety, but action was required to identify the source of the alarm and perform corrective action within

1–2 hours. Data generated during any system excursion required review and may have been excluded from the data analysis following evaluation.

Level Two: High (critical alarms)

These set points were established to identify immediate control system intervention to protect the modeling equipment, facility, or personnel. These were supported by Level One alarms and were designed to shut down and make safe some or all of the systems in the event of a significant loss of system function or rapidly changing conditions indicating an out-of-control situation.

4.3 Gas Delivery System

All compressed gases for producing the target gas concentrations were purchased from Airgas Specialty Gases. The liquid CO₂ was industrial-grade. The O₂ was obtained from the available house air supply. The CO₂ and air passed through a carbon trap and a HEPA (high-efficiency particulate air) filter before passing through the mass flow controller to ensure no mercury contamination. The SO₂/N₂, HCl/N₂, NO/N₂, and NO₂/N₂ gases were certified standard mixtures. Each of these cylinders came with a certificate of analysis that showed the actual concentration of the desired gas $\pm 2\%$ compared to National Institute of Standards and Technology (NIST)-traceable calibration standards. The flow rates for these gases were adjusted by the DAC system based on the actual concentrations in the cylinders input by the operator. Nitrogen was used as a moisture carrier gas, a mercury source sweep gas, and a mercury sample line purge gas. The source of nitrogen was from a central EERC cryogenic nitrogen supply facility.

Porter mass flow controllers were used to meter the flow of each gas into a gas-mixing manifold. Rotameters were used for backup and as a visual check. Each mass flow controller was calibrated during shakedown with a Gilibrator system, which is a primary standard for flow calibration. The atmospheric pressure and gas temperature were recorded for each calibration, along with the mass flow controller set point and actual measured gas flow rate. Linear

calibration curves were then generated for flow at standard conditions (1 atm and 0°C) as a function of set point.

Mass flow controllers were controlled and monitored by the aforementioned LabVIEW program. Gas concentrations were entered into a Microsoft Excel[®] spreadsheet, which computed the required flow rates for each gas. These flow rates were entered into the LabVIEW program. This software used calibration data for each mass flow controller to adjust the digital-to-analog converter.

The moisture level was controlled by injecting deionized water into a steam generator with a peristaltic pump. The water feed rate was controlled by the DAC. The water feed rate was also monitored with a manual variable-area flowmeter. The steam generator temperatures were monitored and logged with the DAC system.

4.4 Mercury Vapor Source

A mercury vapor source was configured using Hg permeation devices from VICI Metronics. The permeation tubes are small, inert capsules that emit a stable concentration of Hg at a given temperature. The tubes were inserted in a glass reactor supplied with a constant flow of heated carrier gas. The glass reactor was maintained at a constant temperature ($\pm 1^\circ\text{C}$) in a convection oven. A nominal mercury concentration to the columns of $6.0 \mu\text{g}/\text{m}^3$ was established during the weeks prior to the start of the test. The Hg concentration at the inlet to the columns was periodically checked throughout the test to ensure the mercury generation was stable.

4.5 Mercury Measurement System

A CMM was used to measure the mercury at the exit of the individual bed stages for the duration of the test. A conditioning/conversion system was used to remove moisture and acid gases before the analyzer. In order to speciate between elemental and oxidized forms of mercury in the sample gas stream, the conditioning/conversion system either reduced all forms of mercury to elemental mercury for a measurement of total mercury concentration or removed the oxidized

forms of mercury from the sample gas stream for a measurement of elemental mercury concentration. It should be noted that the mercury analyzer was only capable of measuring elemental mercury in the gas stream. The oxidized mercury forms (Hg^{2+}) were reduced to elemental mercury (Hg^0) by passing the sample gas through an impinger containing a solution of 20% sodium hydroxide (NaOH) and 2% stannous chloride (SnCl_2). Each solution also removes the HCl in the sample gas, which can poison the gold traps used to capture and concentrate the mercury. The sample gas exiting each bubbler passed through a chilled gas-liquid separator to dry the sample gas. The difference between the total mercury concentration and the elemental mercury concentration was assumed to be an oxidized form of mercury.

A P S Analytical (PSA) Sir Galahad online mercury analyzer was used for outlet sampling. The analyzer measurement is based on atomic fluorescence using the 253.7-nm line from a mercury vapor lamp. The mercury from the sample stream was concentrated by amalgamation onto a gold trap. The gold trap collected mercury for 2 minutes, after which it was purged with nitrogen and heated. Valves directed the released mercury into the optical stage for analysis. The total analysis time for an individual datum point was approximately 5 minutes.

The CMM was employed to measure the mercury concentration at the exit of each bed intermittently as a function of time. The CMM was set to measure total mercury as the normal operating mode. The priority was to obtain stable total mercury measurements wherever breakthrough had been observed. The intent was to determine the elemental mercury concentration if breakthrough was observed at the exit of the column. There was no interest in determining the mercury speciation between the beds. Since there was no mercury breakthrough at the exit of either column, elemental mercury measurements were not taken. The CMM was calibrated to detect mercury concentrations as low as $0.01 \mu\text{g}/\text{m}^3$.

4.6 Test Sorbents

The two test columns contained DARCO Hg-LH in Column 1 and MERSORB HT-1.5 in Column 2. Each column consisted of six beds loaded with a total of 18 inches of material.

Column 1 was loaded with a sorbent provided to the EERC by Norit Americas. A material safety data sheet (MSDS) was provided to the EERC. The beds contained a granular activated lignite-based brominated activated carbon adsorbent designated by DARCO Hg-LH 4×8 and referred to as DARCO in this report.

Column 2 consisted of beds loaded with MERSORB HT-1.5, a 1.5-mm pelletized bituminous coal-based SIC supplied by NUCON International. A MSDS was provided to the EERC.

5.0 TEST RUN PERIODS AND POSTRUN ANALYSES

5.1 Shakedown

Prior to the formal start of the model run, shakedown testing was conducted to meet the following criteria:

Mercury source mass delivery rate and stability would be demonstrated by continuous monitoring with an independently calibrated CMM. The target Hg permeation rate was 25 µg/hr, which is equivalent to a column inlet mercury concentration of 6 µg/dscm at process conditions with 18% O₂.

System leak integrity was determined by static pressure-testing the entire system. Any observed leaks were corrected so that no leaks were observed at a static pressure greater than the operating pressure of the columns.

Temperature control stability would be demonstrated within the following tolerances:

- Mercury source: $\pm 2^{\circ}\text{F}$
- Heated lines: $\pm 25^{\circ}\text{F}$
- Inlet temperature to columns: $180 \pm 5^{\circ}\text{F}$
- Heated enclosures for columns: $\pm 10^{\circ}\text{F}$

The final set points for the mercury source, heated lines, and column enclosures were determined during the shakedown period.

Gas flow accuracy was demonstrated by independent calibration of the individual mass flow controllers within 5% of individual set points. Balance of flow between the two columns was demonstrated to be within 5% of each other by comparing outlet orifice readings at the exit of each column. A back-pressure valve at the outlet of each column was used for fine adjustment of the balance of flow between the columns.

Performance of DAC data logging was proven by demonstrating successful logging of all system inputs for a 24-hour period.

DAC sampling control was demonstrated by showing that the DAC program could successfully sample at each of the stage outlets. The time required for obtaining steady measurements and for switching from one port to another port depended on the mercury concentrations at the outlet of individual bed segments, and this time changed throughout the run. At the beginning of the run, this time was expected to be approximately 1 hour.

5.2 Test Run Start-Up and Data Collection

Once the shakedown testing was complete, the columns were loaded with sorbent material, and the test run was started.

The DAC system was programmed to log all of the gas component flows, system temperatures, port selection, and continuous mercury data. The system was set up to operate overnight without operator assistance. However, the system was monitored by an operator during a normal 8-hour day shift as well as checked during the evening. In addition, each weekend day, the system was checked twice a day. The operator was responsible for performing, as a minimum, the following checks:

- Compressed gases – document the tank pressures
- Gas component flows – visually check all backup manual flowmeters
- Temperature controllers – verify readouts and set points
- Mercury source – temperature, pressure, and flows
- Mercury conversion system – visual check of bubblers, pumps, and solutions
- Carbon columns – visual check, temperatures, and flow balance
- Mercury analyzer – check data for last 24 hours
- DAC system – check sampling and system-logged data for last 24 hours

In addition to filling out a daily checklist and manually recording data for the system, a daily logbook was maintained and signed by the operator to note any system changes, problems, corrective action, or operational concerns. The following data were collected during the course of the test from the DAC and CMM:

- Cumulative run time (hr)
- Test column number (e.g., L = left = Column 1 filled DARCO Hg-LH lignite-based brominated activated carbon; R = right = Column 2 filled with MERSORB HT-1.5 pelletized bituminous coal-based SIC)
- Bed segment outlet number
- Cumulative bed depth (inches)
- Mercury concentration ($\mu\text{g}/\text{dscm}$)
- Total (full time)

At a minimum, the following Hg-sampling guidelines were observed:

- The primary focus of bed outlet data collection was on beds in both columns that were initially breaking through (e.g., $>0.5 \mu\text{g}/\text{dscm}$) as well as beds immediately before and after the beds that were initially breaking through.

- The secondary focus of data collection was to be on beds that were breaking through at higher mercury concentrations but not at the expense of collecting sufficient-quality data from the beds that were initially breaking through or were indicating nondetectable breakthrough.
- The sequence of bed sampling was from lower-concentration beds to higher-concentration beds except when switching from one column to another when this may not be possible. As a general guideline, when sampling from a given bed (e.g., Bed 2) indicated a total Hg concentration greater than 0.5 $\mu\text{g}/\text{dscm}$, the next sampling cycle in the column began two beds downstream of this bed (e.g., Bed 4) and then proceeded to the next bed upstream (e.g., Bed 3).
- Adequate time was to be allowed for sampling from a given bed to accommodate the time required to purge residual mercury from the sampling line and manifold system.
- Adequate gas sample residence time on the CMM's gold trap was to be provided to give accurate low-mercury-concentration measurements (e.g., $<0.2 \mu\text{g}/\text{dscm}$).
- The calibration of the CMM was checked daily by injecting a known quantity of mercury at the calibration port and determining the percent recovery based on the theoretical mass of mercury injected. If the recovery was greater than $\pm 10\%$, the PSA was recalibrated. The zero of the analyzer was also checked daily.
- Mercury inlet concentration measurements were periodically checked with the CMM.

5.3 Test Run Periods

The test was initially planned as a long-term 1000-hour run. Except for noted minor upset events, operating conditions were held constant during this period. At Run Hour 1009, the Hg, steam, and acid gases were stopped. After a 5-minute purge with dry air and nitrogen, the

remaining dry gases were turned off, and the systems were allowed to cool to room temperature before the carbon samples were removed.

5.4 Postrun Sample Recovery and Analyses

Following completion of the model run, the samples of carbon from each stage were recovered and stored in an appropriately sized glass sample container with a Teflon lid. The postrun sorbent mass of each stage was recorded. To obtain a representative sample for the analyses, each stage was physically mixed by gently tumbling the recovered sorbent material prior to submitting the sample to the EERC Analytical Research Laboratory (ARL).

The first two stages from each column were analyzed for total mercury by taking a representative sample for that stage. Laboratory analyses of the carbons were performed by digesting approximately 1-g samples with concentrated hydrochloric acid and nitric acid (6 and 4 mL, respectively) in a capped digestion vessel. The digestion samples were placed on a dry block heater at 90°C for 4 hours. After digestion, the samples were cooled to room temperature, and the solutions were each brought up to a 50-mL volume. Undiluted samples were analyzed by cold-vapor atomic absorption (CVAA). To fall within the calibration range of the CVAA (0–5 µg/L), the solutions were diluted using volumetric pipettes and flasks.

6.0 RESULTS AND DISCUSSION

6.1 Sorbent Mass

The columns were loaded with as-received carbon samples, and the test was begun April 20, 2009. Tables 3 and 4 show the sorbent mass loaded into each stage of the two columns. At the end of the test, the sorbent from each stage was recovered and weighed, reported in Tables 3 and 4, to determine the mass gain that occurred from exposure to the mercury, flue gas components, and moisture.

Table 3. Column 1 DARCO Hg-LH Sorbent Mass Before and after the Run

Stage	Stage Depth, in.	Cumulative Bed Depth, in.	Loaded Sorbent Mass, g	Postrun Sorbent Mass, g	Mass Gain, g	Mass Gain, %
1	1	1	95.2	149.6	54.4	57.1
2	2	3	190.1	246.6	56.5	29.7
3	3	6	276.5	319.3	42.8	15.5
4	3	9	278.7	293.7	15.0	5.4
5	3	12	262.4	258.1	-4.3	-1.6
6	6	18	525.0	519.7	-5.3	-1.0
Total	18		1627.9	1787.0	159.1	

Table 4. Column 2 MERSORB HT-1.5 Sorbent Mass Before and after the Run

Stage	Stage Depth, in.	Cumulative Bed Depth, in.	Loaded Sorbent Mass, g	Postrun Sorbent Mass, g	Mass Gain, g	Mass Gain, %
1	1	1	103.0	181.9	78.9	76.6
2	2	3	189.8	300.2	110.4	58.2
3	3	6	295.2	390.3	95.1	32.2
4	3	9	281.8	304.6	22.8	8.1
5	3	12	282.4	306.0	23.6	8.4
6	6	18	554.2	596.4	42.2	7.6
Total	18		1706.4	2079.4	373.0	

Given the mercury exposure time for each column, the target mass of added mercury was approximately 13.3 mg to each column. The additional mass gain to each column can be attributed to moisture and acid gases retained by the carbon during the test. The higher weight gain observed with the MERSORB may be caused by the formation of SO₄ from the sulfur already on the carbon.

6.2 Process Measurements

Process data logged by the DAC included gas flow measurements, sorbent bed temperatures, cabinet temperatures, flow balance, and mercury source temperatures. Other aspects of the process were manually recorded daily, including the column pressure drop. Only three minor upset conditions occurred during the 1000-hour run. The first was roughly 156 hours into the test; the SO₂ cylinder ran out, and no alarm was sent. There was no SO₂ gas flow for 9 hours. The second and third upset conditions occurred approximately 180 hours and 206 hours

into the run when the HCl gas cylinder regulator failed. There was no HCl gas flow to the columns for 7 hours and 3 hours, respectively. It was determined that an alarm bypass for the SO₂ and HCl gas flows (used in the previous test program) had been triggered, and no alarms were sent out for any of the upset conditions. The alarm was reset, and there were no further problems. The loss of these gas flows for the short periods of time should not affect the overall performance of the activated carbons to capture mercury.

6.2.1 Gas Flow Measurement

The total and individual dry gas flow rates based on the individual mass flow measurements for the various inlet gases were steady throughout the model run. When a tank of one of the acid gases was changed, that flow was adjusted based on the certified gas concentration of the new tank. With each gas tank change, the nitrogen balance was adjusted to maintain a total constant flow.

The moisture level was controlled by injecting deionized water into a steam generator with a peristaltic pump. The water feed rate was automatically controlled by the DAC based on weight loss measurements from a water supply tank. The water feed rate was monitored manually every day with a variable-area flowmeter.

The individual dry gases were also monitored with rotameters in series with the mass flow controllers. During previous testing, a comparison of the mass flow controller and rotameter data showed that the total dry flow measurements for the mass flow controllers were within 5% of the total flow indicated by the rotameters.

The flow between the columns was balanced by monitoring a flow orifice at the exit of each of the columns. Identical orifices were designed with a 0.25-inch diameter to produce a ΔP of 1 to 2 inches W.C. at the desired flow conditions. The logged orifice ΔP readings for each column, shown in Figure 5, indicate that the orifice readings were well within 0.05 inches of

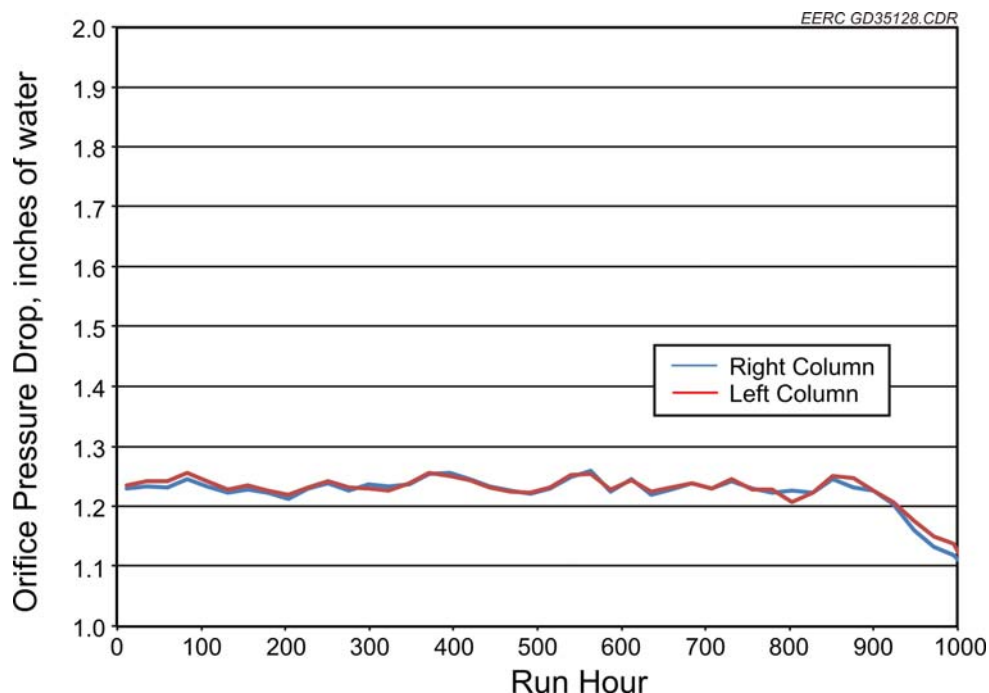


Figure 5. Flow balance indicated by orifice ΔP for each column.

each other for most of the run, which corresponds to the flows balanced to within 2% of each other. The deviation around 800 hours into the run was caused by condensation in one of the lines to the pressure transducers.

6.2.2 Bed Temperatures

The bed temperatures for each stage were logged continuously by the DAC. The temperature recorded for Bed 1 was the temperature of the inlet gas stream since the thermocouple for Bed 1 of each column was above the 1-inch-thick sorbent depth of this stage. For Beds 2–6, the thermocouples were within the carbon sorbent depth. Figure 6 shows the daily averaged temperature throughout the test for Column 1, which contained DARCO Hg-LH. Figure 7 shows the similar information for Column 2, containing MERSORB HT-1.5. The temperatures were within a few degrees of the target temperature of 180°F. The temperatures among the stages were within good general agreement. Initial temperature excursions at start-up

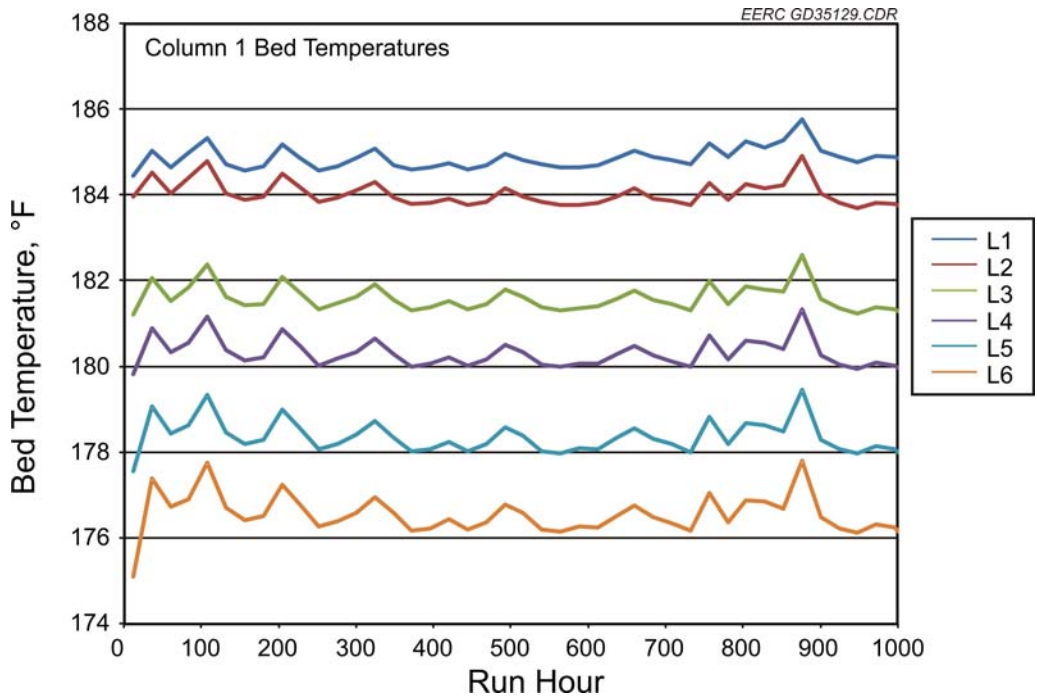


Figure 6. Daily averaged Column 1 bed temperatures.

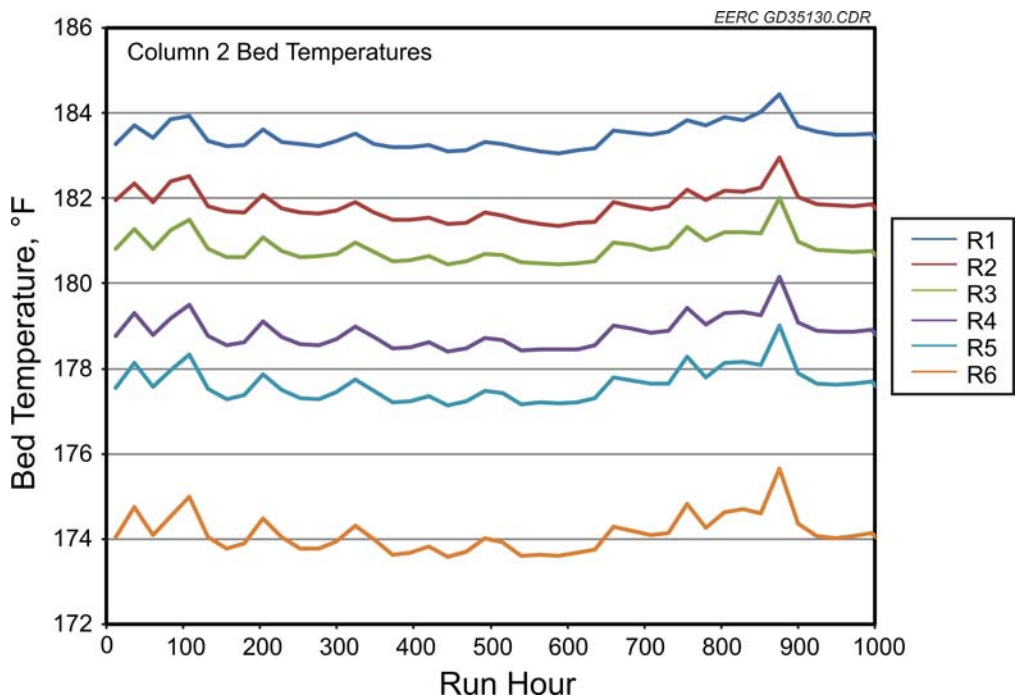


Figure 7. Daily averaged Column 2 bed temperatures.

do not show up on the daily average plot, but they have been seen in previous tests and are attributed to the temperature rise because of the heat of absorption of water when initially exposed to the flue gas.

6.2.3 Column Pressure Drop

Total pressure drop data across the entire column were recorded manually daily for the duration of the run. The total column pressure drop measurements included contributions from the flow resistance through the packed beds of sorbent, the restriction of the perforated flow distribution disks separating each column stage, and the wall friction from flow through the columns. Considering the relatively low gas velocity through the columns, this last component was considered to be negligible compared to the previous two contributors. As part of the previous test program, the pressure drop across the empty system was measured. The contribution of the seven disks to the overall column differential pressure measurements was determined and averaged 2.3 inches of water. The carbon differential pressure was estimated by subtracting the total disk ΔP from the measured total column ΔP measurements, and these data are presented in Figure 8. As indicated in the figure, the normalized differential pressure drop across both carbons increased slightly during the run. Near the end of the test, there was water condensed in the line to one of the pressure transducers used to measure the pressure drop across the flow orifice. After this was cleared, the flow pressure was lower and the pressure drop across the columns was lower. There were no obvious explanations for the changes. All other readings indicated the system was operating normally.

6.2.4 Mercury Source

The mercury source was initially calibrated with the PSA Sir Galahad to deliver 25 μg of mercury per hour (within $\pm 10\%$). This was with a nitrogen sweep gas rate of 0.1 dslm and a mercury source oven temperature of 276°F. The mass flow controller as well as the backup variable-area flowmeter indicated that the sweep flow was constant. The daily averaged source oven temperatures (Figure 9) were also constant throughout the test.

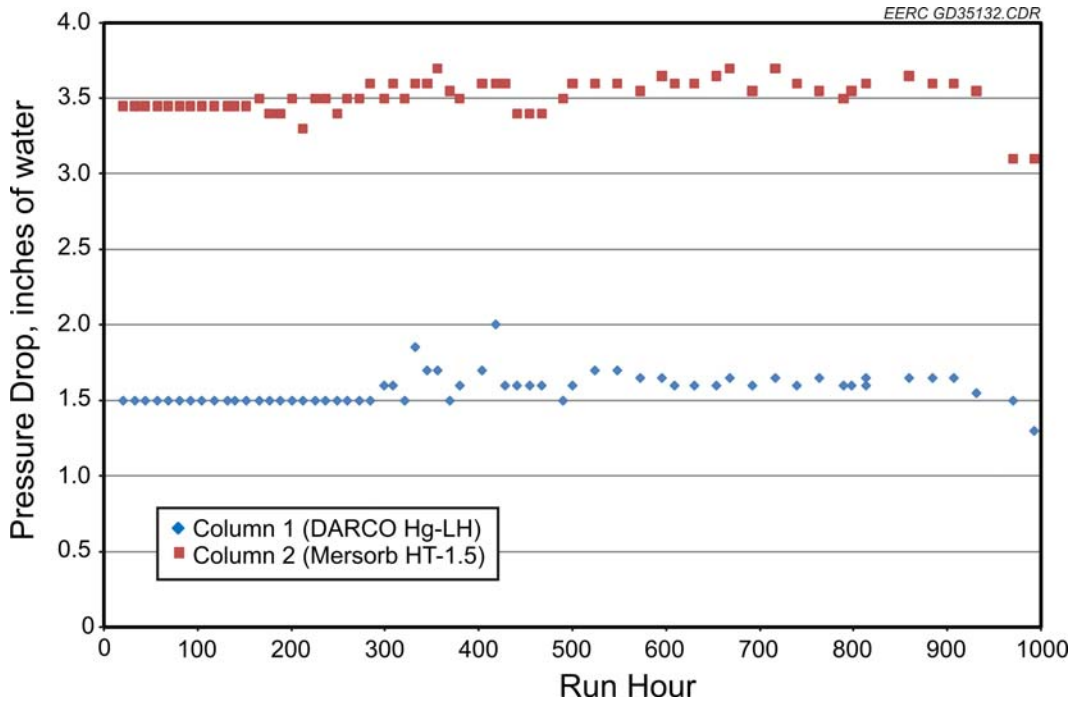


Figure 8. Derived carbon bed pressure drop.

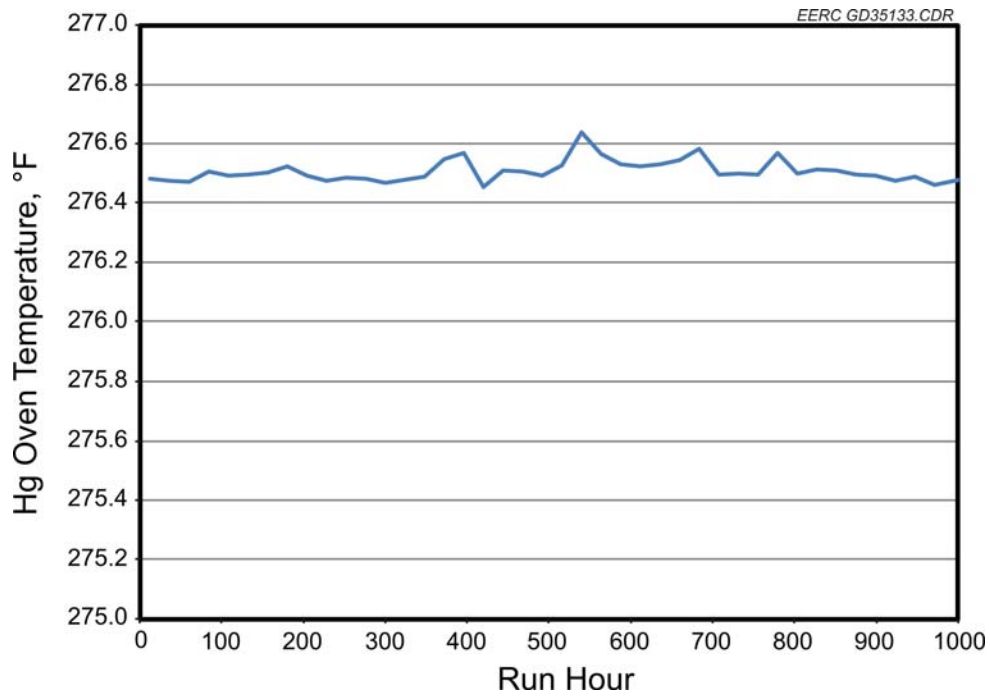


Figure 9. Daily averaged mercury source temperatures.

The averaged measured inlet CMM mercury concentrations to the columns are shown in Figure 10. The inlet concentration to the right column was periodically measured with the PSA CMM. The target inlet mercury rate was 25 $\mu\text{g/hr}$ to achieve the target inlet mercury concentration of 6.0 $\mu\text{g/dscm}$ at the process condition of 18% O_2 .

6.3 Mercury Capture and Breakthrough Curves

A single CMM was used to sample mercury from the exit of selected beds. An individual sample was taken approximately every 5 minutes with the CMM. Data reduction was performed on the sample points obtained from the CMM to reduce noise within the instrument readings, subtract the nitrogen zero level, and apply calculations to present the data in the preferred units.

The primary focus of bed outlet sampling was on beds in both columns that were initially breaking through (e.g., $>0.5 \mu\text{g/dscm}$) as well as beds immediately before and after the beds that were initially breaking through. The general sequence was to sample the nitrogen purge for a

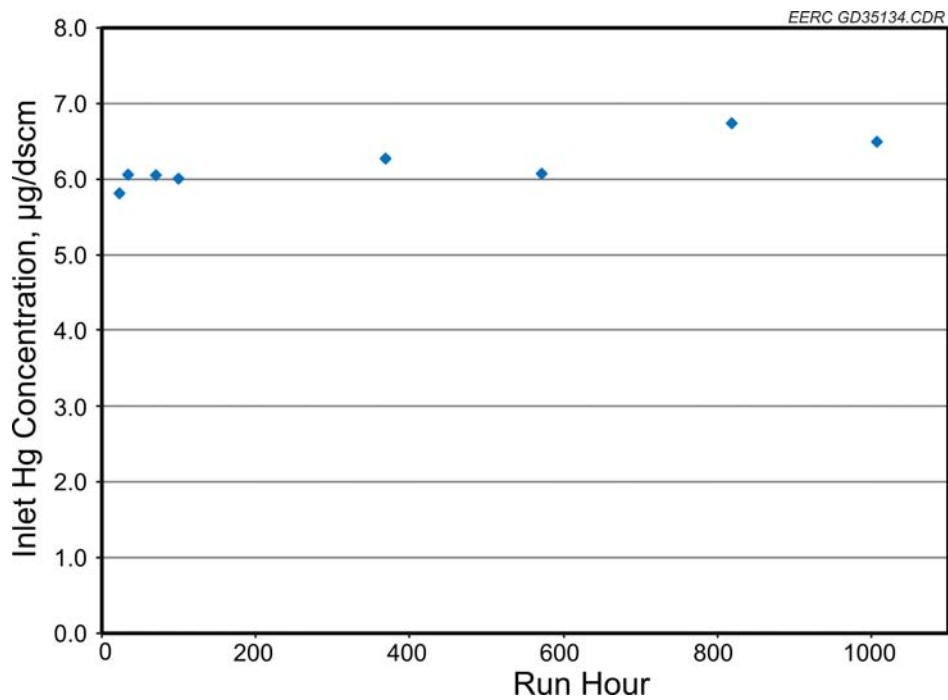


Figure 10. Averaged inlet mercury concentrations.

column and then to sample the outlet mercury from successive beds, including one to two beds past where breakthrough was seen. This procedure was used as an effort to minimize any effect of residual mercury in the sampling lines from a previous stage from biasing the measurement for the next sample. The breakthrough level of 0.5 µg/dscm was considered quantifiable whereas mercury in the 0.1–0.5-µg/dscm range was less certain. The secondary focus was on beds that were breaking through at higher mercury concentrations.

The CMM was calibrated to provide the most accurate readings over the entire measurement range, <0.10 to >6.0 µg/dscm, and additional calibration checks were completed daily to verify that the CMM calibration had not drifted. The CMM was recalibrated if a calibration check indicated it had drifted by more than 10%.

Breakthrough response curves and column-specific results are presented separately for Column 1 in Section 6.3.1 and for Column 2 in Section 6.3.2.

6.3.1 Column 1 Breakthrough Curves (DARCO Hg-LH)

Column 1 contained 18 inches of lignite-based granular brominated carbon (DARCO Hg-LH 4×8) from Norit Americas in six bed segments. Figure 11 shows a plot of all of the reduced Column 1 bed outlet mercury concentration data on the scale of the target inlet concentration. Breakthrough was measured from Bed 1 (1 inch in depth) and, possibly, Bed 2 (cumulative 3 inches in depth). No breakthrough was detected by the CMM for Beds 3 through 6.

Figure 12 plots the mercury concentration at the outlet of Bed 1 as a function of time. One curve represents the “raw” outlet concentration, and the other represents the raw outlet concentration minus the baseline concentration measured while sampling nitrogen through the sampling manifold. The baseline measures the residual mercury in the sampling system. Bed 1, 1-inch depth of DARCO Hg-LH, showed significant mercury breakthrough roughly 300 hours into the run. The breakthrough from Bed 1 then increased throughout the remainder of the test. As the data show, the correction baseline was small compared to the breakthrough levels. By

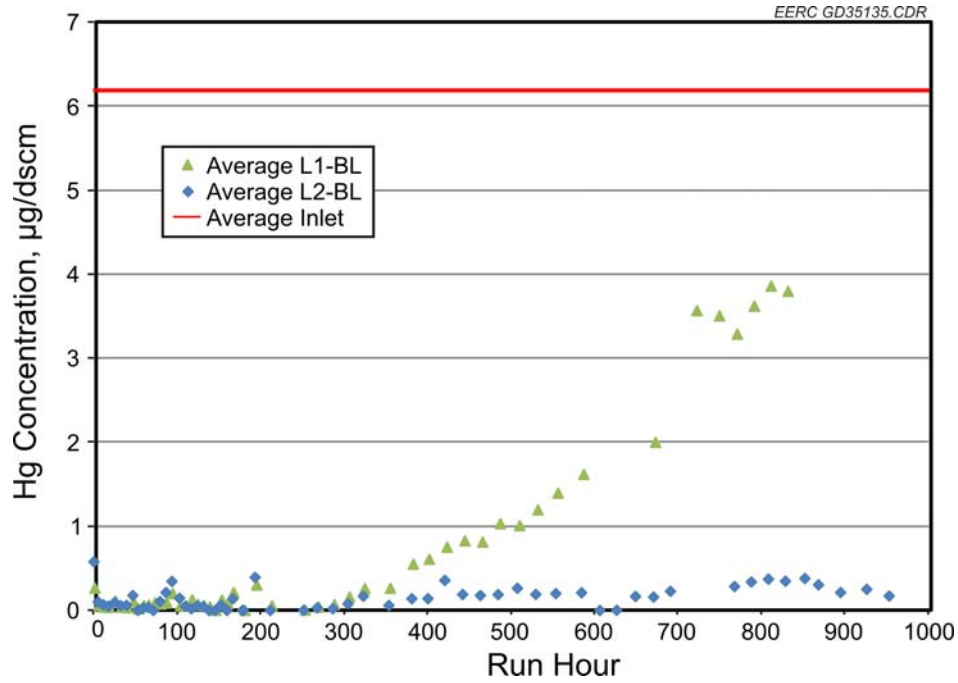


Figure 11. Mercury outlet data for Column 1 containing DARCO Hg-LH compared with target inlet value.

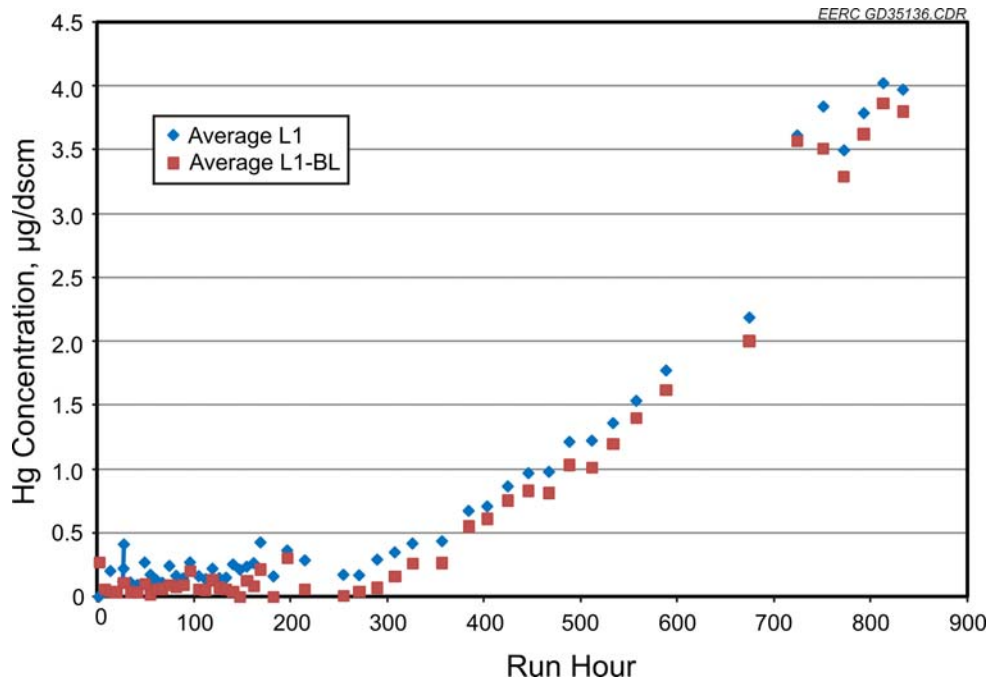


Figure 12. Bed 1 mercury outlet data for Column 1 containing 1 inch of DARCO Hg-LH. The cumulative bed depth is 1 inch.

Run Hour 833, the level of mercury measured at the outlet of Bed 1 was near 4.0 $\mu\text{g}/\text{dscm}$. Measuring mercury at this concentration caused high baseline readings that made it difficult to get an accurate measurement of the mercury concentrations at the exit of Beds 2–6. Therefore, it was decided to stop measuring the mercury concentration at the outlet of the first bed for each column and focus on the low mercury concentrations at the outlet of Beds 2–6. Figure 13 plots the mercury capture efficiency of Bed 1 as a function of time. After 833 hours of exposure, the Hg capture efficiency had dropped to less than 40%, but the remainder of the column was still capturing essentially 100% of the mercury.

All Bed 2 (2-inch depth with a cumulative depth of 3 inches) data are shown in Figure 14. Prior to Run Hour 833, it was not possible to reliably quantify the mercury concentration at the exit of Bed 2 because of the residual mercury in the sampling manifold from measuring the outlet of Bed 1. After discontinuing the measurement of the Bed 1 outlet, it was possible to purge the residual mercury and accurately measure the mercury concentration at the outlet of Bed 2. Figure 15 plots the cumulative capture efficiency at the outlet of Bed 2. For the last 50 hours of the test (when Bed 1 was no longer being measured) the mercury capture efficiency averaged over 97%.

Bed 3 (3-inch depth with a cumulative depth of 6 inches) data are shown in Figure 16. Again, the only reliable outlet mercury concentration data come from the time period after sampling at the outlet of Bed 1 was discontinued. From Run Hour 850 to the end of the test, the mercury concentration at the outlet of Bed 3 dropped. Within the limits of quantification, the data indicate no mercury breakthrough at the exit of Bed 3 by the end of the test. Figure 17 plots the cumulative mercury capture efficiency at the outlet of Bed 3. Over the last 50 hours, the average capture efficiency was 98.9% and increasing. The results show that 6 inches of the DARCO Hg-LH carbon was effective at capturing 100% of the inlet mercury for over 1000 hours.

The cumulative mercury loading for the first two beds was calculated based on the average breakthrough levels observed for each bed for the run and the average inlet mercury

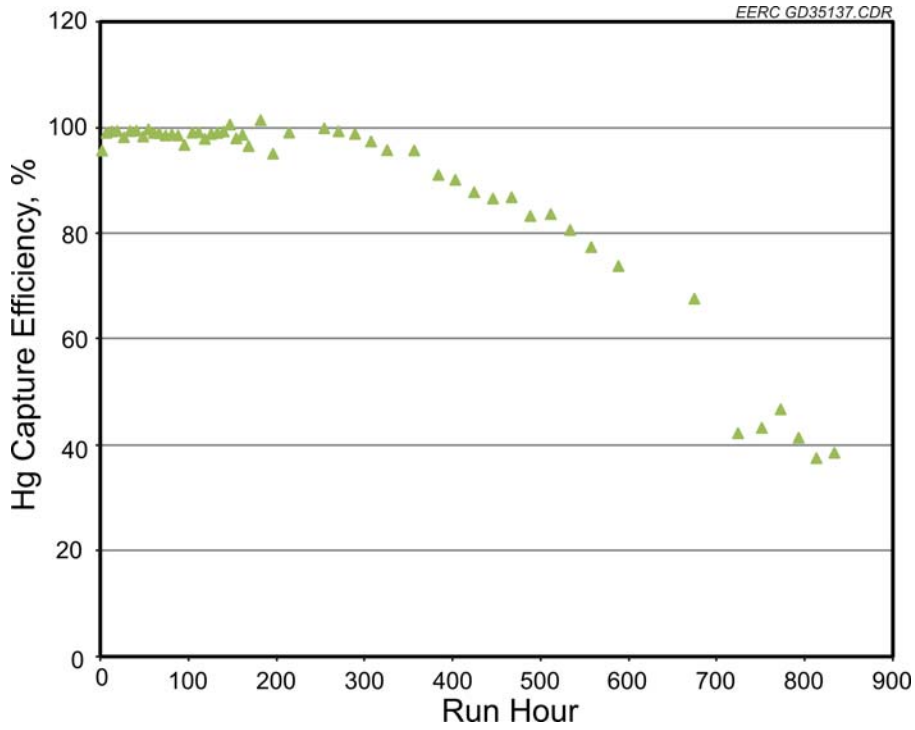


Figure 13. Column 1 Bed 1 cumulative mercury capture efficiency.

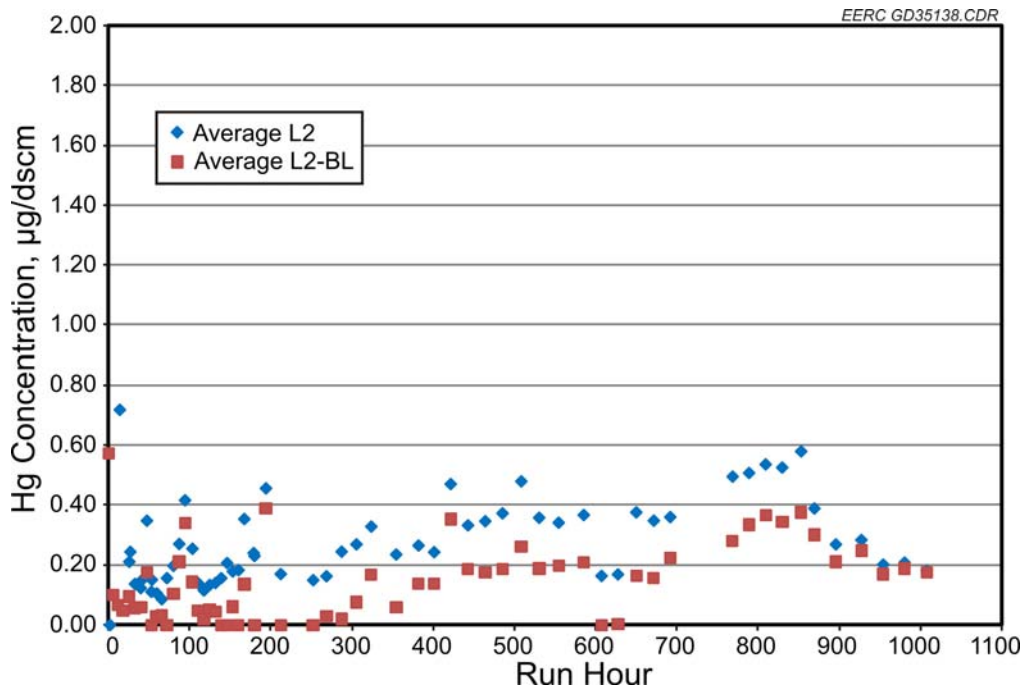


Figure 14. Bed 2 mercury outlet data for Column 1 containing 2 inches of DARCO Hg-LH. The cumulative bed depth is 3 inches.

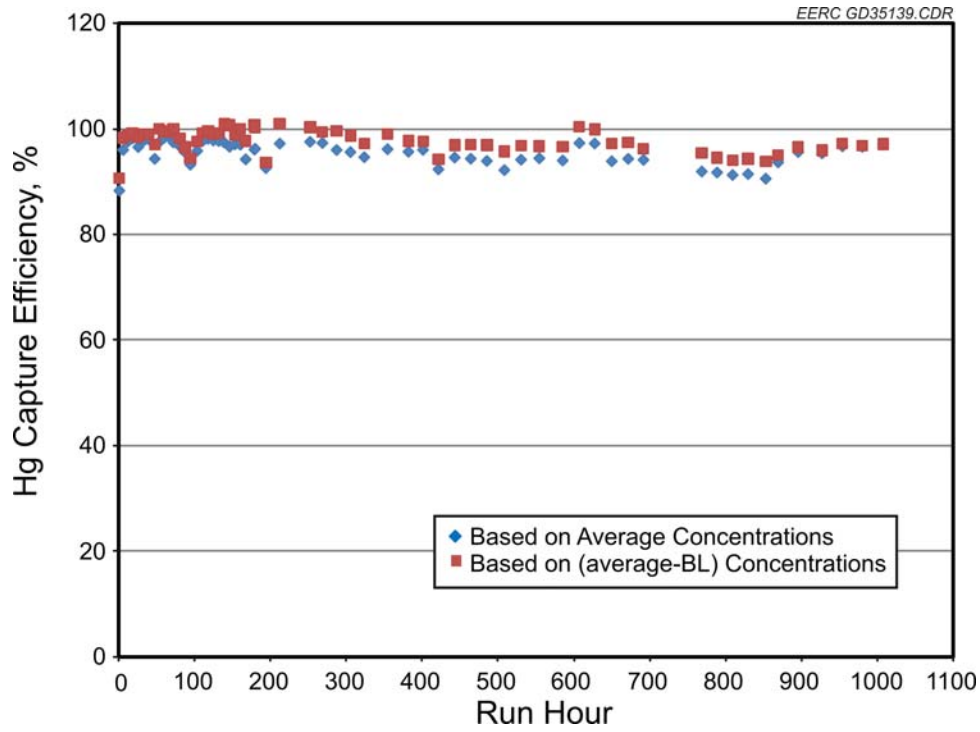


Figure 15. Column 1 Bed 2 cumulative mercury capture efficiency.

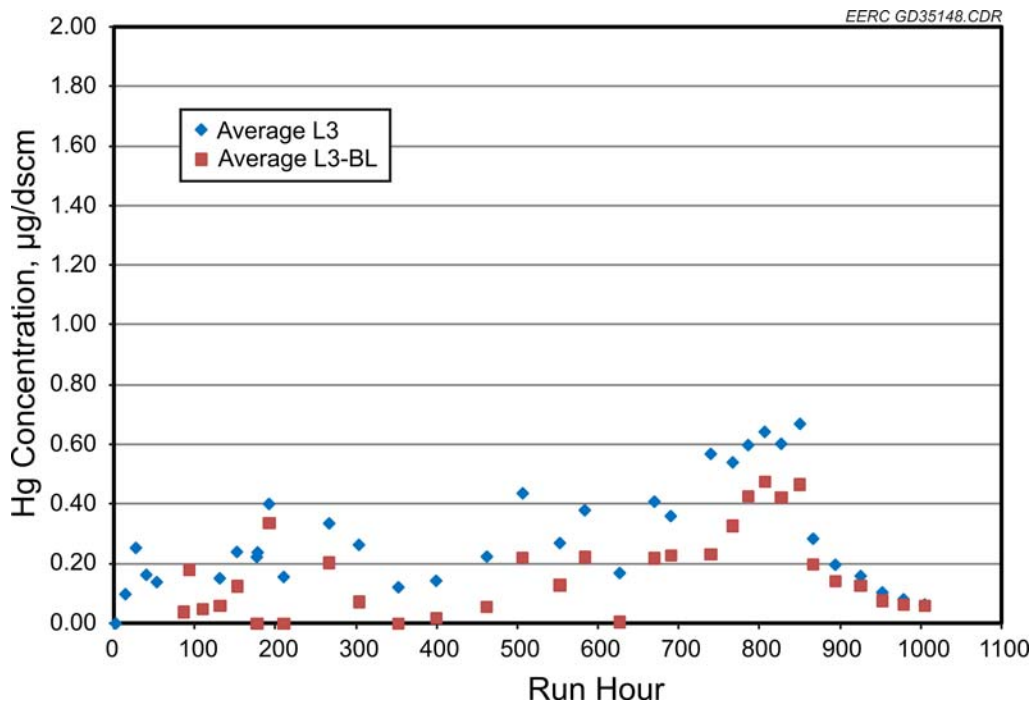


Figure 16. Bed 3 mercury outlet data for Column 1 containing 3 inches of DARCO Hg-LH. The cumulative bed depth is 6 inches.

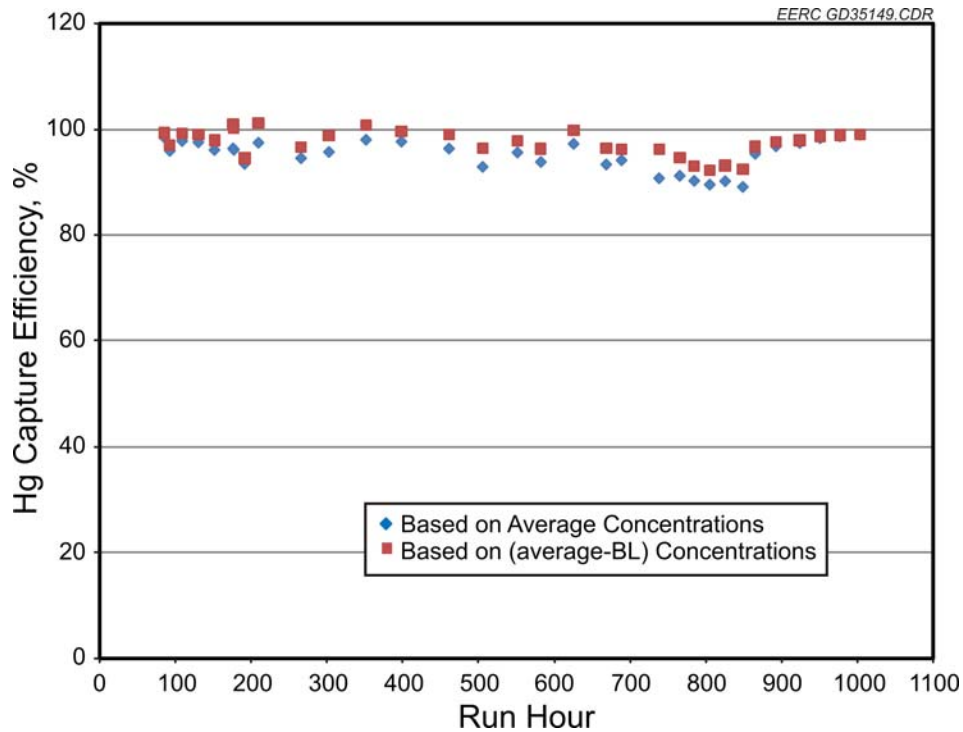


Figure 17. Column 1 Bed 3 mercury cumulative mercury capture efficiency.

concentration measured with the CMM. These data are based entirely on the inlet and outlet CMM data. The data are presented in Figure 18 as cumulative mercury loading in milligrams of mercury per 100 grams of starting carbon mass. The plot only goes up to Run Hour 850 because sampling at the outlet of Bed 1 was discontinued at that time. For comparison, the theoretical cumulative inlet loading to Bed 1 is shown.

6.3.2 Column 2 Breakthrough Curves (MERSORB HT-1.5)

Column 2 contained 18 inches of MERSORB HT-1.5 SIC in six bed segments. Figure 19 shows a plot of all of the Column 2 bed outlet mercury concentration data on the scale of the target inlet concentration. Breakthrough was detected only from Bed 1. Beds 2, 3, and 4 were also monitored.

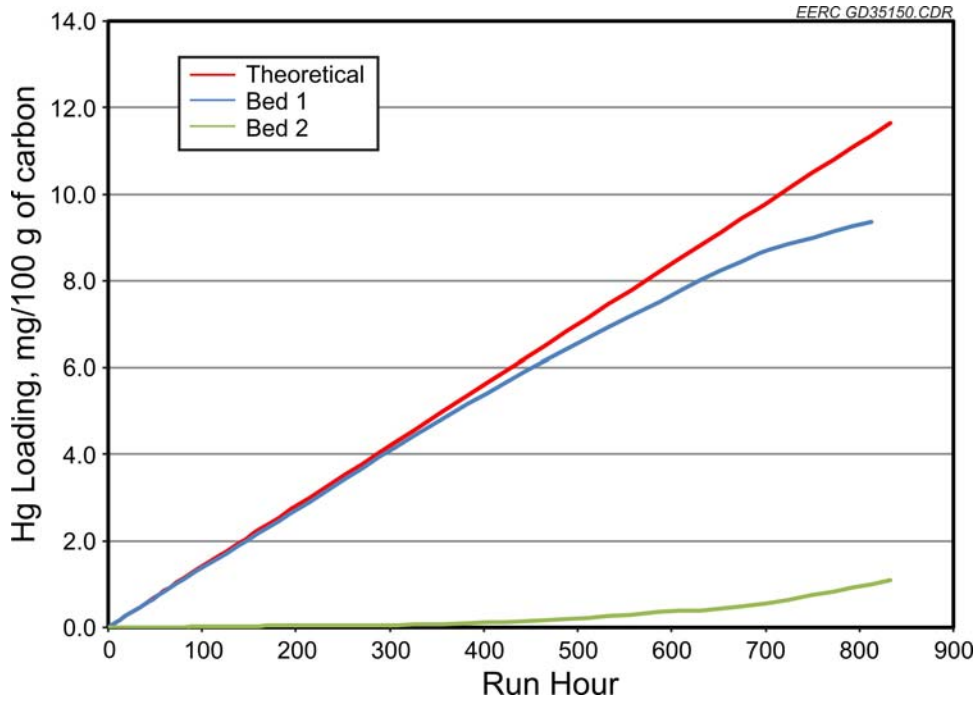


Figure 18. Cumulative Hg loading for Beds 1 and 2.

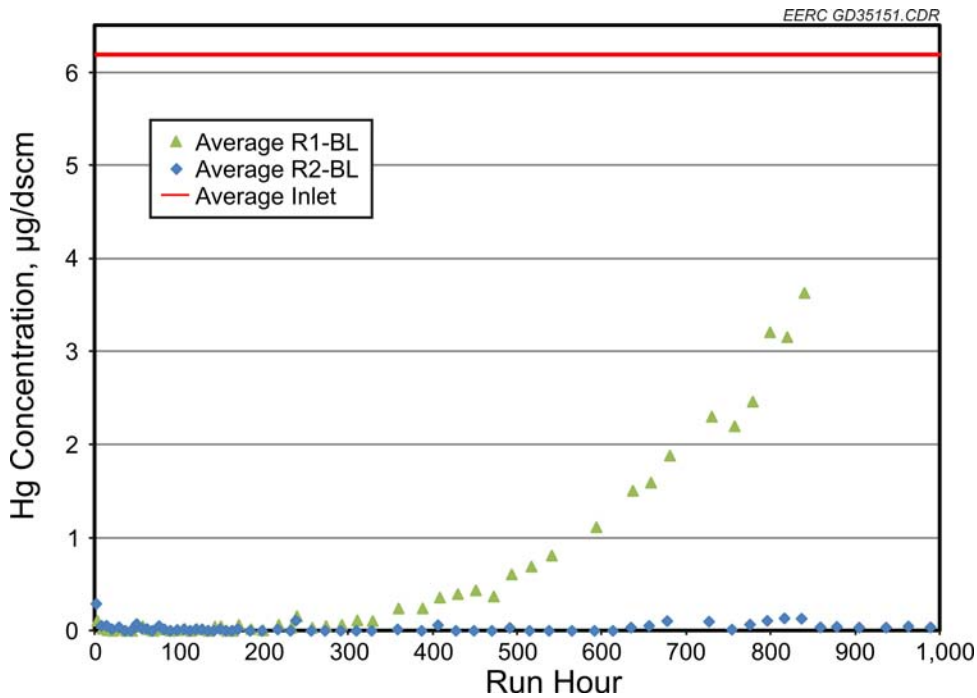


Figure 19. Mercury outlet data for Column 2 containing MERSORB HT-1.5 compared with target inlet value.

Figure 20 plots the mercury concentration at the outlet of Bed 1 as a function of time. Again, the “raw” concentration and the raw minus the baseline concentration are plotted and indicate that the background correction was minor. Bed 1 (1-inch depth of MERSORB HT-1.5) showed quantitative mercury breakthrough roughly 350 hours into the run. The breakthrough from Bed 1 then increased throughout the remainder of the test. By Run Hour 833, the level of mercury measured at the outlet of Bed 1 was near 3.5 $\mu\text{g}/\text{dscm}$. As mentioned above, sampling at the outlet of Bed 1 was discontinued at this time to focus on the low mercury concentrations at the outlet of Beds 2–6. Figure 21 plots the mercury capture efficiency of Bed 1 as a function of time. After 840 hours of exposure, the Hg capture efficiency had dropped to near 40%, but the remainder of the column was still capturing essentially 100% of the mercury.

All Bed 2 (2-inch depth with a cumulative depth of 3 inches) data are shown in Figure 22. Again, as with Column 1, Bed 2 outlet mercury concentrations could not be quantified below 0.2 $\mu\text{g}/\text{dscm}$ until sampling at the outlet of Bed 1 had stopped. By the end of the test, the outlet concentration at the outlet of Bed 2 reached less than 0.05 $\mu\text{g}/\text{dscm}$ which corresponds to greater than 99% capture efficiency. Figure 23 plots the cumulative capture efficiency at the outlet of Bed 2. For the last 100 hours of the test (when Bed 1 was no longer being measured), the mercury capture efficiency averaged 99.4%. Overall, a total of 3 inches of the MERSORB HT-1.5 captured 100% of the inlet mercury for over 1000 hours.

Similar to Column 1, the cumulative mercury loading was calculated for each bed based on the average breakthrough levels observed for each bed for the run and the average inlet mercury concentration measured with the CMM. The data are presented in Figure 24 as cumulative mercury loading in grams of mercury per 100 grams of starting carbon mass, and the cumulative inlet loading to Bed 1 is shown for comparison.

6.4 Postrun Laboratory Analyses and Mass Balance

The results of the mercury content analyses of the individual stages are shown in Tables 5 and 6. Because of the limited number of analyses that could be performed and the difficulty in

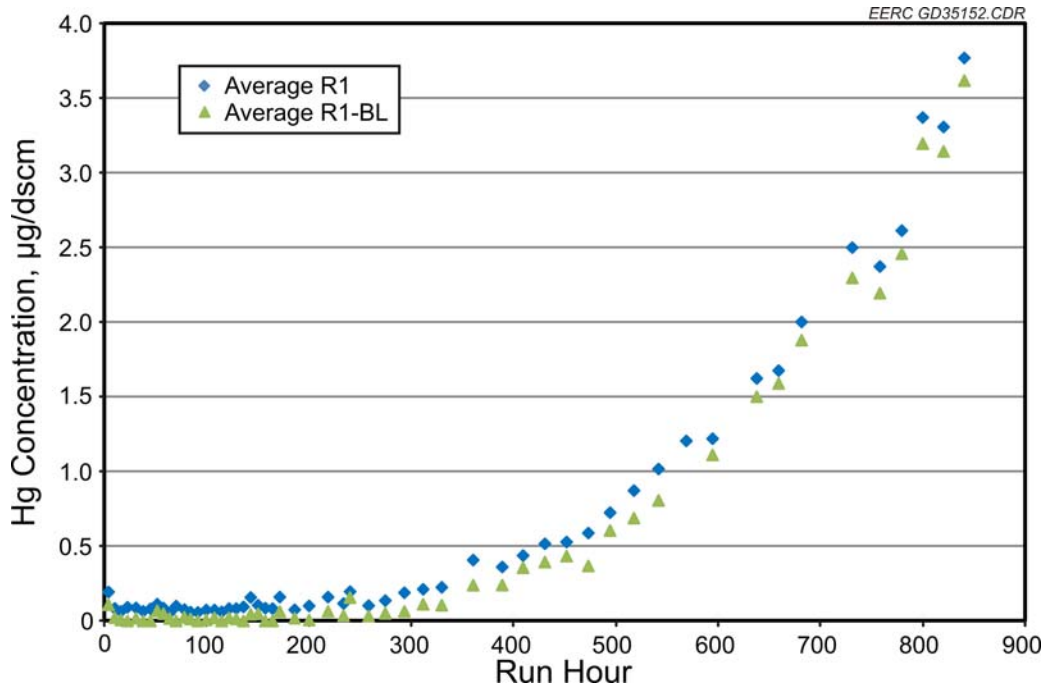


Figure 20. Bed 1 mercury outlet data for Column 2 containing 1 inch of MERSORB HT-1.5. The cumulative bed depth is 1 inch.

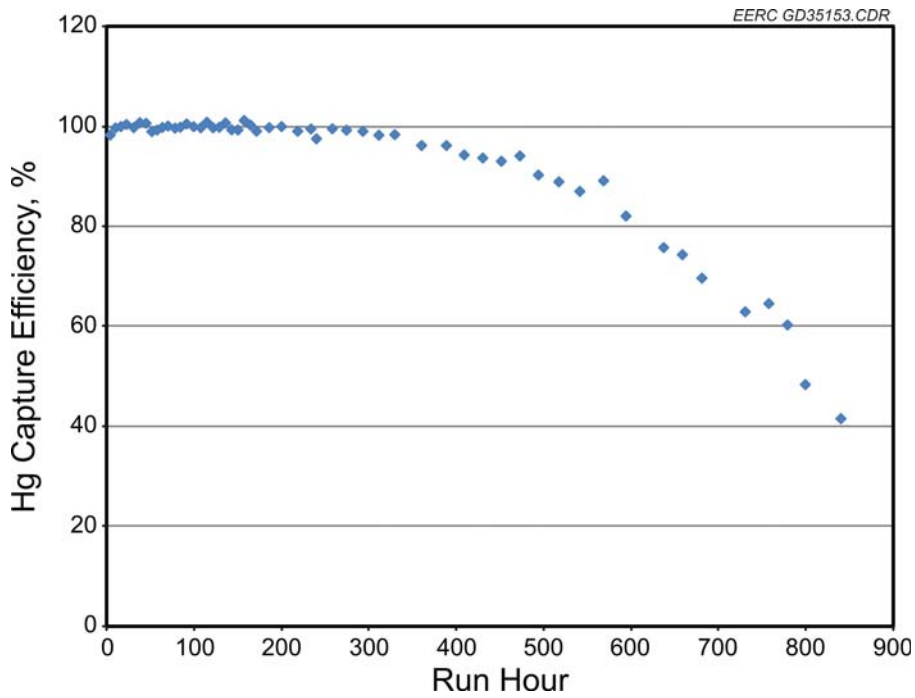


Figure 21. Bed 1 cumulative mercury capture efficiency.

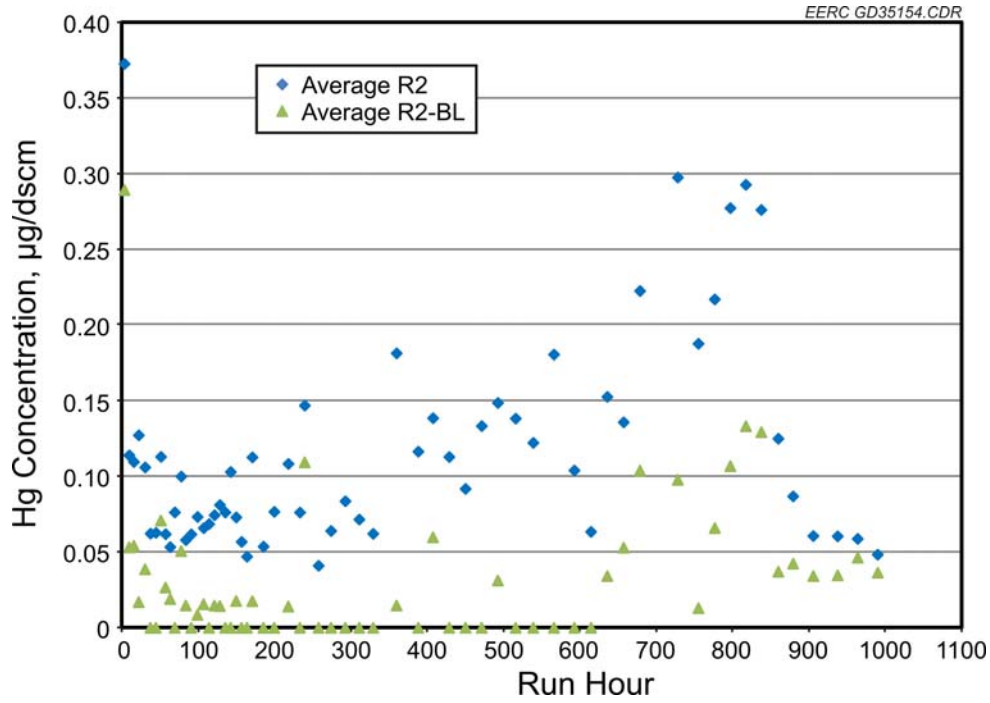


Figure 22. Bed 2 mercury outlet data for Column 2 containing 2 inches of MERSORB HT-1.5. The cumulative bed depth is 3 inches.

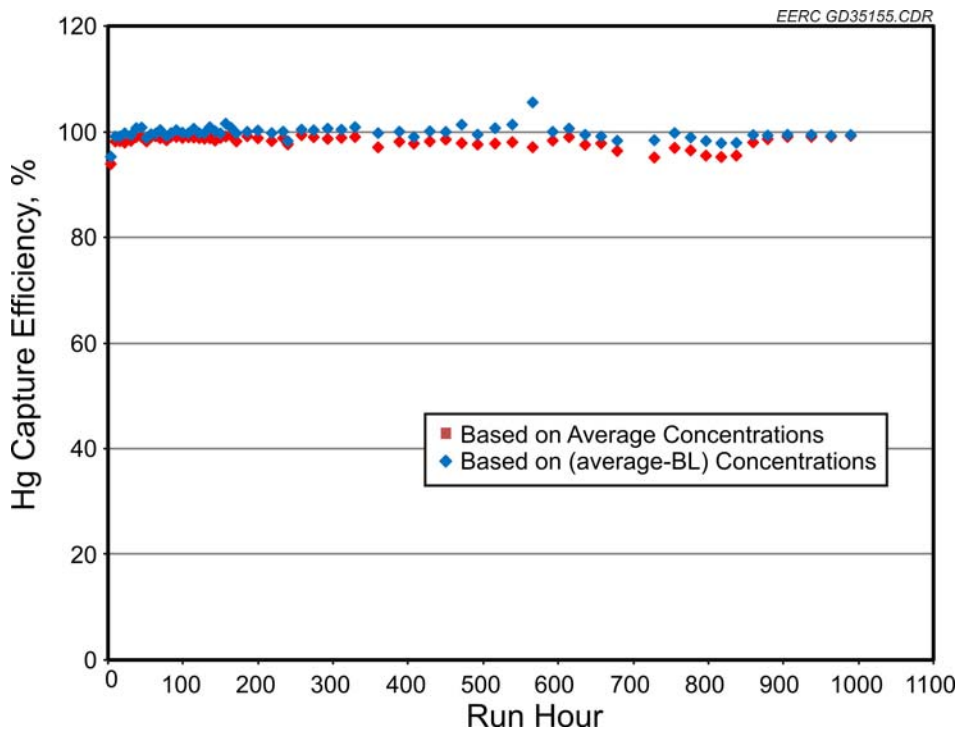


Figure 23. Column 2 Bed 2 cumulative mercury capture efficiency.

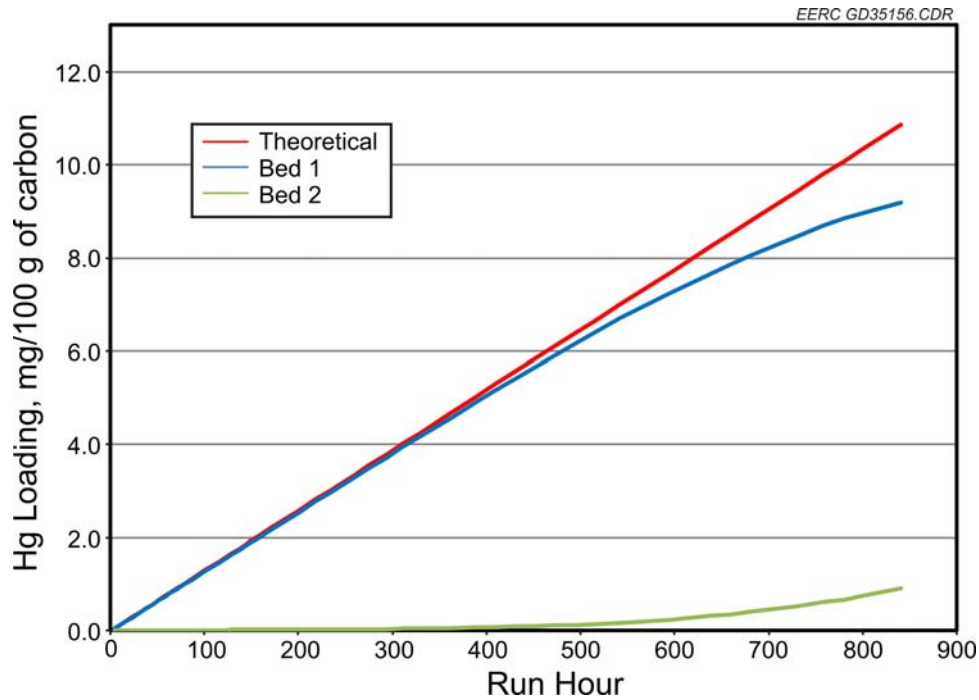


Figure 24. Column 2 MERSORB HT-1.5 projected stage loading throughout the run.

Table 5. Column 1 DARCO Hg-LH Sorbent Laboratory Mercury Analyses

Bed	Stage Depth, in.	Cum. Depth, in.	Prerun Sorbent Mass, g	Postrun Sorbent Mass, g	Mass Gain, %	Hg Conc., µg/g	Total Hg Collected, mg
1	1	1	95.2	149.6	57.1	43.2	6.46
2	2	3	190.1	246.6	29.7	35.5	8.75
Total							15.2

Table 6. Column 2 MERSORB HT-1.5 Sorbent Laboratory Mercury Analyses

Bed	Stage Depth, in.	Cum. Depth, in.	Prerun Sorbent Mass, g	Postrun Sorbent Mass, g	Mass Gain, %	Hg Conc., µg/g	Total Hg Collected, mg
1	1	1	103.0	181.9	76.6	46.0	8.37
2	2	3	189.8	300.2	58.2	26.0	7.81
As-Received Carbon						0.044	
Total							16.2

getting a representative sample from a granular material, the intent of the analysis was not to perform detailed mass balance, but to verify that the mercury was captured by the activated carbon. Calculations of the mercury collected by each stage based on the analytical results and the removal efficiency of each stage are included in the tables. These data are based only on the bed analyses completed after the run and are completely independent from the projected stage loading charts based on the CMM data presented in Figures 18 and 24. The remaining additional mass gain to each column can be attributed to moisture and acid gases retained by the carbon during the run and, possibly, the formation of SO_4 from the existing sulfur on the MERSORB HT-1.5 SIC. It appears more mercury than expected was captured in the second bed of each column. Since sampling at the outlet of Bed 1 was suspended before the end of the test, it is unknown what level of breakthrough was reached or if mercury started to offgas from the first bed and was captured by the second bed. What these analyses do show is that the mercury was captured by the activated carbon in the first two beds.

A comparison that helps to verify the results is the mass balance closure when the total amount of mercury generated based on the inlet CMM data is compared with the amount of mercury recovered based on the laboratory data. Table 7 shows a 118% closure for the bed analysis/CMM inlet average. This level of closure is as good as can be expected considering the limited number of analyses performed.

7.0 DISCUSSION AND CONCLUSIONS

7.1 Discussion

The objective of the test program was to evaluate the ability of a fixed bed of sorbent material to capture mercury in a flue gas stream simulating that generated during the taconite-manufacturing process. The flue gas composition including acid gas and mercury concentrations, the superficial gas velocity, the gas temperature, the carbon bulk density, and the residence time per inch of bed in both Columns 1 and 2 were all selected to be representative of the design for a full-scale system downstream of a venturi scrubber. The CMM results showed that for Column 1,

Table 7. Mass Balance Closure

	CMM Inlet Average, mg	Laboratory Bed Analyses, mg	Bed Analyses/CMM Inlet Average
Column 1	13.3	15.2	114.3%
Column 2	13.3	16.2	121.8%
Total	26.6	31.4	118.1%

which contained an 18-inch depth of DARCO Hg-LH activated carbon, mercury was first detected ($>0.2 \mu\text{g/dscm}$) at the outlet of the 1-inch bed depth at 300 hours and reached a maximum of $3.9 \mu\text{g/dscm}$ by 833 hours into the run. At the 3-inch bed depth, no clear mercury breakthrough $>0.2 \mu\text{g/dscm}$ was seen by the end of the 1000 hours. No mercury was detected at the 6-inch depth or any depth past 6 inches by the end of the run. For Column 2, which contained an 18-inch depth of MERSORB HT-1.5 SIC, mercury $>0.2 \mu\text{g/dscm}$ was first detected at the outlet of the 1-inch bed depth at 300 hours and reached a maximum of $3.6 \mu\text{g/dscm}$ by 840 hours into the run. No mercury was detected by the end of the run at the 3-inch depth or any other depth past 3 inches.

The results from mercury analyses of the individual bed sections at the end of the run verified that the inlet mercury was captured by the first two beds. The mercury analyses of the beds in Column 1 indicated that all of the mercury was collected in the first 3 inches of the bed. Both the mercury analyses data after the run and the CMM data show that 6 inches of DARCO Hg-LH provided essentially 100% mercury capture (to less than the mercury quantification limit) over the entire run. For Column 2, the mercury analyses indicate that all of the mercury was collected in the first 3 inches of the bed. Both mercury analyses data after the run and the CMM data show that 6 inches of MERSORB HT-1.5 SIC also provided essentially 100% mercury capture (to less than the mercury quantification limit) over the run.

The mercury mass balance closure for Column 1 based on the inlet CMM data was 114%. For Column 2, the mercury mass balance was 122% from the CMM data. The overall mass balance closure for both columns was 118% based on the CMM data. Considering the challenges of accurate mercury measurement for gases and solids, the complexity and duration of the run,

and the uncertainty of getting a representative sample from each bed section, these mass balance closures are within expectations. From these results, a primary conclusion is that the commercially available carbons investigated in these tests would be effective for high degrees of mercury abatement, i.e., to levels below the quantification limit, using only six (6) inches of bed depth for the conditions evaluated, which are representative of the expected full-scale operation.

7.2 Conclusions

The following major conclusions are drawn from the 1000-hour test of fixed-bed mercury adsorption performance:

- Based on results from the current test program at the EERC, fixed-bed adsorption using activated carbon as the adsorbent is an extremely effective method of removing mercury from flue gas at process conditions typical of those anticipated for taconite processing.
- Two commercial adsorbents demonstrated good mercury abatement performance in the test: DARCO Hg-LH 4×8 (Norit Americas) and MERSORB HT-1.5 (Nucon International).
- After 1000 hours of run time for both adsorbents, no measurable breakthrough of mercury occurred past the 3-inch bed depth. More run time would be required to reach mercury breakthrough at the 6-inch bed depth.

The data produced in the testing clearly demonstrate the high degree of mercury abatement possible with minimal amounts of commercially available activated carbons. A fixed bed of activated carbon used for mercury control could provide 100% mercury capture for extended periods of time with minimal pressure drop. It should be noted, however, that full-scale mercury abatement in a site fixed bed would not necessarily follow the exact capacity and capture efficiencies demonstrated during this test. Variations in temperature, velocity, mercury concentration as well as other flue gas constituents could lead to different quantitative performance (e.g., bed life and total capacity). In order to develop the most economical design

for a fixed bed, further evaluation of the effects of actual operating conditions such as thermal cycling and gas velocity through the fixed bed will be needed.

8.0 REFERENCES

1. Engesser, J.; Niles, H. *Mercury Emissions from Taconite Pellet Production*; Report to Minnesota Pollution Control Agency; University of Minnesota Contract No. 1663-187-6253; Coleraine Minerals Research Laboratory: Coleraine, MN, 1997; 16 p.
2. Jiang, H.; Arkly, S.; Wickman, T. Mercury Emissions from Taconite Concentrate Pellets – Stack Testing Results from Facilities in Minnesota. Presented at U.S. Environmental Protection Agency Conference Assessing and Managing Mercury from Historic and Current Mining Activities, San Francisco, CA, Nov 28–30, 2000, 18 p.
3. Berndt, M.E. *Mercury and Mining in Minnesota*; Final Report for Minnesota Department of Natural Resources; 2003; 58 p.
4. Minnesota Pollution Control Agency. *Minnesota Statewide Mercury Total Maximum Daily Load*; 2006; 56 p.
5. Berndt, M.E.; Engesser, J. *Mercury Transport in Taconite Processing Facilities: (III) Control Method Test Results*; Final Report to Iron Ore Cooperative Research; Dec 2007.
6. Laudal, D.L. *Methods Testing for Measurement of Mercury Speciation for High-Reactive Dust*; 2007.
7. Miller, S.J. *Results from Line 3 and Line 5 Particulate Sampling January 15–17, 2007, at U.S. Steel Minnesota Ore Operations Minntac Plant*; Final Report to U.S. Steel Minnesota Ore Operations, 2007.

8. Pavlish, J.H.; Zhuang, Y. *Proof-of-Concept Testing of Novel Mercury Control Technology for a Minnesota Taconite Plant*, EERC report to Minnesota Department of Natural Resources, 2008.

Appendix B-1-17

Assessment of Potential Corrosion Induced by Bromine Species used for Mercury Reduction in a Taconite Facility

August 2009

August 28, 2009

Dr. Michael Berndt
Research Scientist II
Minnesota Department of Natural Resources
Division of Lands and Minerals
500 Lafayette Road
St. Paul, MN 55155-4045

Dear Dr. Berndt:

Subject: Revised Final Report Entitled “Assessment of Potential Corrosion Induced by Bromine Species Used for Mercury Reduction in a Taconite Facility”; Work Order Contract No. B24812; EERC Fund 14783

Enclosed please find the subject report. If you have any questions, please contact me by phone at (701) 777-5236 or by e-mail at yzhuang@undeerc.org.

Sincerely,

Ye Zhuang
Research Engineer

YZ/sah

Enclosure

ASSESSMENT OF POTENTIAL CORROSION INDUCED BY BROMINE SPECIES USED FOR MERCURY REDUCTION IN A TACONITE FACILITY

Final Report

(for the period of February 6 through June 30, 2009)

Prepared for:

Michael Berndt

Minnesota Department of Natural Resources
Division of Lands and Minerals
500 Lafayette Road
St. Paul, MN 55155-4045

Work Order Contract No. B24812

Prepared by:

Ye Zhuang
David J. Dunham
John H. Pavlish

Energy & Environmental Research Center
University of North Dakota
15 North 23rd Street, Stop 9018
Grand Forks, ND 58202-9018

EERC DISCLAIMER

LEGAL NOTICE This research report was prepared by the Energy & Environmental Research Center (EERC), an agency of the University of North Dakota, as an account of work sponsored by Minnesota Department of Natural Resources. Because of the research nature of the work performed, neither the EERC nor any of its employees makes any warranty, express or implied, or assumes any legal liability or responsibility for the accuracy, completeness, or usefulness of any information, apparatus, product, or process disclosed or represents that its use would not infringe privately owned rights. Reference herein to any specific commercial product, process, or service by trade name, trademark, manufacturer, or otherwise does not necessarily constitute or imply its endorsement or recommendation by the EERC.

TABLE OF CONTENTS

LIST OF FIGURES	ii
LIST OF TABLES	iv
EXECUTIVE SUMMARY	v
BACKGROUND	1
OBJECTIVES	2
EXPERIMENTAL APPROACH.....	2
EXPERIMENTAL SETUP.....	5
EXPERIMENTAL PROCEDURE.....	6
RESULTS AND DISCUSSIONS.....	7
Macroscopic Surface Analysis	7
Microscopic Analysis	7
United Coupons	8
Minorca Coupons.....	14
USS Minntac Coupons	21
Weight Gain/Loss Measurement.....	25
COMPARISON	27
CONCLUSIONS.....	27
ACKNOWLEDGMENT.....	29
REFERENCES	29
UNITED COUPON SEM ANALYSIS	Appendix A
MINORCA COUPON SEM ANALYSIS	Appendix B
USS MINNTAC COUPON SEM ANALYSIS	Appendix C

LIST OF FIGURES

1	Diagram of a typical taconite process	4
2	Schematic of the exposure testing system.....	5
3	Surface of United coupons after testing	8
4	Surface of Minorca coupons after testing.....	9
5	Surface of USS Minntac coupons after testing	10
6	U7 surface SEM image	11
7	U7 cross-sectional SEM image	11
8	U1 surface SEM image	12
9	U2 surface SEM image	13
10	U3 surface SEM image	13
11	U4 surface SEM image	14
12	U4 cross-sectional SEM image	15
13	M7 surface SEM image.....	16
14	M8 surface SEM image.....	17
15	M9 surface SEM image.....	17
16	M1 surface SEM image.....	18
17	M2 surface SEM image.....	18
18	M3 surface SEM image.....	19
19	M4 surface SEM image.....	19
20	M5 surface SEM image.....	20
21	M6 surface SEM image.....	20

Continued . . .

LIST OF FIGURES (continued)

22	M1 cross-sectional SEM image.....	21
23	M3 cross-sectional SEM image.....	22
24	M5 cross-sectional SEM image.....	22
25	M6 cross-sectional SEM image.....	23
26	UM5 surface SEM image.....	25
27	UM5 cross-sectional SEM image.....	26

LIST OF TABLES

1	Simulated Taconite Flue Gas Baseline Composition	3
2	Exposure Test Matrix	4
3	Coupon Test Layout	6
4	Test Dates	6
5	Normalized Distribution of Elements on United Coupon Surface.....	10
6	Elemental Analysis of U7 Cross Section	12
7	Elemental Analysis of U4 Cross Section	15
8	Normalized Distribution of Elements on Minorca Coupon Surface.....	16
9	Elemental Analysis on M1 Cross Section.....	23
10	Elemental Analysis on M3 Cross Section.....	23
11	Elemental Analysis on M5 Cross Section.....	24
12	Elemental Analysis of M6 Cross Section.....	24
13	Normalized Distribution of Elements on Minorca Coupon Surface.....	24
14	Elemental Analysis of UM5 Cross Section.....	26
15	Weight Gain/Loss of United Coupons	26
16	Weight Gain/Loss of Minorca Coupons.....	27
17	Weight Gain/Loss of USS Minntac Coupons	27
18	Relative Elemental Changes of Cr, Fe, and Ni on Testing Coupon Surface.....	28

ASSESSMENT OF POTENTIAL CORROSION INDUCED BY BROMINE SPECIES USED FOR MERCURY REDUCTION IN A TACONITE FACILITY

EXECUTIVE SUMMARY

Bromine-related mercury control technology has been considered an effective mercury reduction option for the taconite industry even though its impact on taconite facility operation is not well understood. The EERC conducted bench-scale exposure experiments where metal coupons were exposed in simulated taconite flue gas in 40-ppm HBr processing environments. To understand how bromine-induced corrosion may occur in different temperature zones, the designed static-exposure experiments were performed at 500°, 300°, and 150°C to mimic the preheat zone, the drying/cooling zone, and the discharge zone, respectively. The coupons were exposed to flue gas for 30 days and were removed every 10 days during the test for weight measurement. The weight gain/loss was determined by comparing present tested weights to previous weight measurements. The coupons were treated following the ASTM International Standard G1-03 method before the weight measurement. Similar metal coupons were also exposed in taconite flue gas without bromine present for comparison. The metal coupons provided by the taconite industry represented process grate materials used in United Taconite Mine (also U), Minorca Mines (also M), and U.S. Steel (USS) Minntac Mine (UM). At the end of the exposure experiments, morphology as well as the elemental compositions of the corrosion product were then characterized using scanning electron microscopy–energy-dispersive x-ray analysis (SEM–EDX).

The preliminary test results indicated that 1) 40 ppm HBr in taconite process flue gas appears to cause slight surface corrosion of the test coupons. SEM surface microscopy showed small pitting, cracking, and blistering occurred with bromine deposition and losses of Fe, Cr, and Ni; 2) however, coupon cross-sectional analyses indicated that bromine deposition and losses of Fe, Ni, and Cr were mainly confined to the surface of the coupons, and no significant bromine penetration and subsequent elemental changes were observed below the coupon surface after the 30-day exposure experiments; 3) coupon surface corrosion appears to be less with decreasing temperature; 4) three coupon sets showed resistance to bromine attack under testing environments during the 30-day testing period; and 5) deposits of iron oxide and sodium sulfate seem to induce slight chemistry changes on U and M coupons but not on UM coupons.

It should be noted that, because of limited time and scope of work, the completed corrosion exposure tests were carried out in simplified simulated flue gas environments that did not 100% represent 100% actual operating conditions in the taconite process. The original objective of this project was to see if bromine could cause any possible corrosion under selected testing conditions; however, the 30-day exposure testing period may not necessarily be long enough to attain a complete perspective of possible bromine-induced corrosion issues in a taconite facility. Therefore, the project results can be regarded as the first step in the effort to address potential bromine-induced corrosion when bromine is applied to a taconite facility for mercury reduction. Additional bench-scale coupon corrosion tests under continuous thermal cycling with wider temperature regimes and extended exposure times are needed before any large-scale field testing.

ASSESSMENT OF POTENTIAL CORROSION INDUCED BY BROMINE SPECIES USED FOR MERCURY REDUCTION IN A TACONITE FACILITY

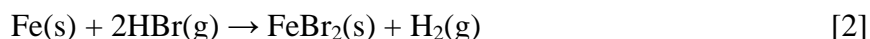
BACKGROUND

The state of Minnesota is targeting an overall mercury reduction of 90%. In Minnesota, taconite plants are the second largest source of mercury emissions in the state, while stack emissions are the dominant pathway of mercury release from taconite processing.

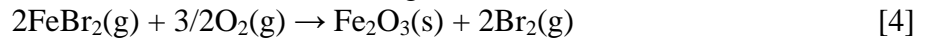
Mercury in a typical taconite flue gas has three basic forms: 1) elemental mercury (Hg^0), 2) oxidized mercury (Hg^{2+}), and 3) particulate-bound mercury ($\text{Hg}[\text{p}]$). It is widely known that both $\text{Hg}[\text{p}]$ and Hg^{2+} can be removed from the gas stream with particulate matter (PM) control devices and/or wet scrubbers, while Hg^0 is not readily removed by existing air pollution control devices (APCDs). Since most taconite facilities are equipped with a wet venturi-type scrubber to control PM emissions (1), the most convenient mercury reduction approach for the taconite industry is to improve conversion of Hg^0 to Hg^{2+} and/or $\text{Hg}[\text{p}]$, so that the mercury can then be removed with existing APCDs without adding new control devices.

Among various mercury reduction technologies being developed, halogens have been widely applied and proven effective in mercury oxidation and adsorption in coal flue gas environments (2–7). However, with the difference between coal flue gas and taconite flue gas, these Hg control technologies have to be tested in taconite flue gas before full-scale application. Both chloride and bromide compounds have been added into the induration furnace, the green ball feed system, and the scrubber liquids to evaluate their effectiveness on mercury reduction in taconite flue gas. So far, bromine compounds have been shown to be the most promising mercury reduction agent that can be directly applied to taconite facilities (1, 8, 9). However, one concern about applying bromide as a mercury reduction agent is that it will induce corrosion and/or accelerate corrosion rates on taconite equipment, such as the feed grate.

Bromine-induced corrosion has been observed in a coal flue gas environment (10) and may be classified as dew point corrosion or active oxidation, depending on the flue gas conditions. Hydrobromic acid is formed with water through multicomponent condensation when flue gas temperature is below a corresponding hydrobromic acid dew point; subsequently, dew point corrosion occurs on the metal surface. At temperatures over the hydrobromic acid dew point, gaseous bromine is capable of diffusing through the oxide layer to the scale–metal interface where it reacts with the iron to form iron bromide through Reactions 1 and/or 2:

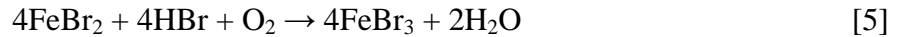


The volatile iron bromide potentially then diffuses outward to the scale surface where it is converted to a solid oxide at the elevated oxygen concentration (Reaction 4):



By Reaction 4, the formed free bromine is either released to the bulk gas or diffuses back to the scale–metal interface, and thus a cycle is formed.

The same bromine corrosion and regeneration cycles may proceed via FeBr_3 , and it is possible for the ferrous iron to be oxidized to the ferric state while the oxidation liberates bromine as well:



Although direct injection of bromide salts, so far, has been shown to be a relatively easy, convenient, and cost-effective mercury control option applicable to the taconite industry (8, 9), most of these tests have been short in duration and have not addressed process concerns and potential impacts to the process and/or processing equipment, including potential bromine-induced corrosion. This project was undertaken to evaluate this potential as a prerequisite to applying bromide salts as a mercury control option for the taconite industry. Therefore, the exposure experiments will help the taconite industry to understand and evaluate the potential side effects that may result from applying bromide-related mercury control technology to the taconite industry.

OBJECTIVES

The objectives of this project included the following:

- Determine if bromine induces and/or increases the metal corrosion of equipment exposed to a typical taconite flue gas environment.
- Determine if the rate of bromine-related corrosion is a function of exposure temperature.
- Determine the mechanisms of bromine-related induced corrosion.

EXPERIMENTAL APPROACH

To meet proposed objectives, the EERC conducted bench-scale exposure experiments where metal coupons were placed in a temperature-controlled chamber filled with simulated taconite flue gas. Table 1 shows the simulated flue gas composition used in the exposure experiments.

Table 1. Simulated Taconite Flue Gas Baseline Composition

Flue Gas Constituent	Concentration ¹
O ₂ , %	14
CO ₂ , %	4.0
H ₂ O, %	20
N ₂ , %	Balance
NO, ppm	600
NO ₂ , ppm	10
CO, ppm	40
SO ₂ , ppm	10
HBr, ppm ²	40

¹ Average value measured in taconite flue gas.

² HBr included in Test Series 2 only.

It should be noted that the taconite flue gas usually has high concentrations of O₂ (~14%) and H₂O (~20%) and small amounts of SO₂ as a result of taconite plants using low-sulfur fuel and moisture from drying the green balls. For the bromine-induced corrosion testing, HBr is added to the matrix in a 40-ppm concentration.

The metal coupons used were provided by three taconite mines and were chosen to closely represent the material of each process grate. The companies supplying coupons were United Taconite Mine (also U), Minorca Mines (also M), and U.S. Steel (USS) Minntac Mine (also UM). In general, the Minorca coupon has a lower Ni content and a higher Fe content than the United and Minntac coupons, while their Cr contents are similar. Each testing coupon was approximately 1 in. × 1 in. The metal coupons were covered with iron oxides to simulate the taconite-processing environment. A parallel exposure experiment was also conducted in which the metal coupons were not covered with iron oxides. The experimental results will determine if iron oxide will affect potential bromine-induced corrosion in taconite flue gas.

It is likely that the grate material will be exposed to bromine species, most likely HBr, throughout the drying zone, preheat zone, firing zone, cooling zone, and stack. Plotted in Figure 1 is a diagram of a typical grate–kiln taconite process. To understand how bromine-induced corrosion may occur at these different temperature zones, the designed static-exposure experiments were performed at 500°, 300°, and 150°C to mimic the preheat zone, the drying/cooling zone, and the discharge zone, respectively. In addition to the bromine-induced corrosion testing, similar metal coupons were also exposed in taconite flue gas without bromine present for comparison. The detailed test matrix is shown in Table 2. The coupons were exposed to flue gas for 30 days and were removed every 10 days during the test for weight measurement. The weight gain/loss was determined through comparison to previous weight measurements. The coupons were treated following the ASTM International Standard G1-03 method before the weight measurement.

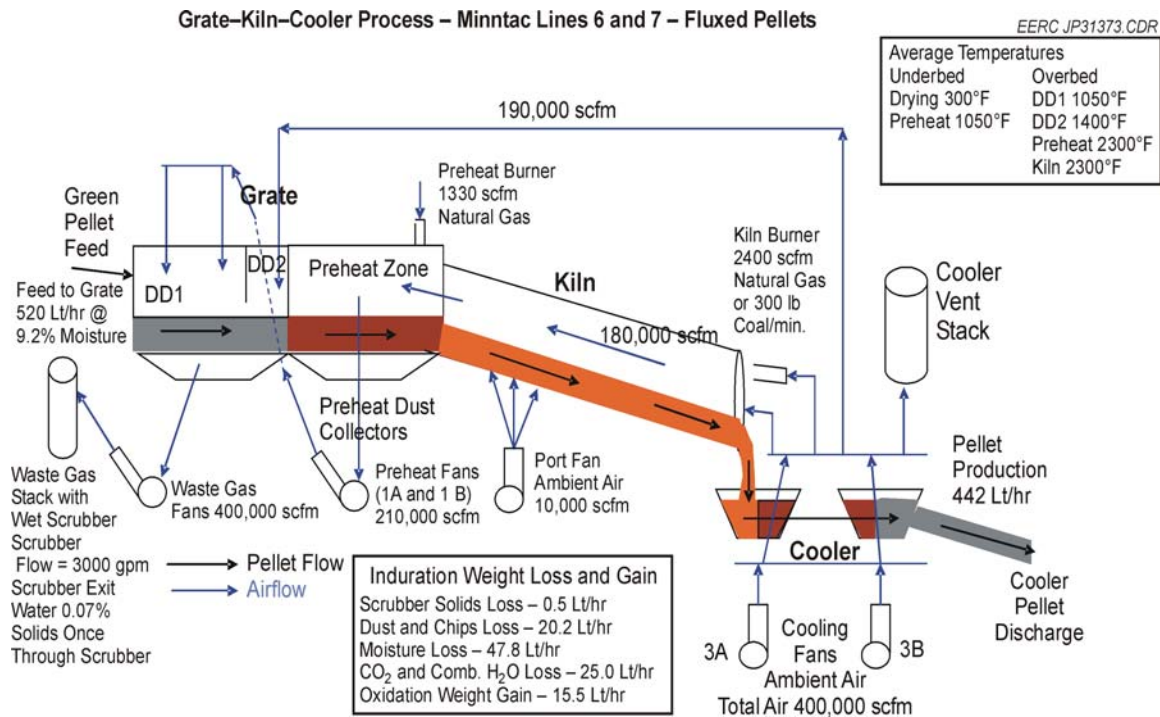


Figure 1. Diagram of a typical taconite process.

Table 2. Exposure Test Matrix

Test No.	Flue Gas Composition	Iron Oxides	Exposure Temperature, °C
I-1	Taconite flue gas baseline	None	500
I-2a	Taconite flue gas baseline plus 40 ppm HBr	None	500
I-2b	Taconite flue gas baseline plus 40 ppm HBr	Yes	500
II-1	Taconite flue gas baseline	None	300
II-2a	Taconite flue gas baseline plus 40 ppm HBr	None	300
II-2b	Taconite flue gas baseline plus 40 ppm HBr	Yes	300
III-1	Taconite flue gas baseline	None	150
III-2a	Taconite flue gas baseline plus 40 ppm HBr	None	150
III-2b	Taconite flue gas baseline plus 40 ppm HBr	Yes	150

At the end of the exposure experiments, the metal coupons were removed and treated following a standard metallographic preparation procedure. Morphology as well as the elemental compositions of the corrosion product was then characterized using scanning electron microscopy–energy-dispersive x-ray analysis (SEM–EDX). This information is presented in the results section of this report.

EXPERIMENTAL SETUP

Bench-scale exposure chambers were designed and set up to provide temperature zones that mimic the taconite process. Two 90-in. ceramic tubes were used as test chambers. One chamber carried flue gas, while a second chamber carried 40 ppm HBr in addition to the flue gas. A tube furnace was used to heat the 500° and 300°C temperature zones. The final zone was wrapped with heat tape and controlled at 150°C. The temperature zones were monitored with a thermocouple/heater controller system. A schematic of the test system is shown in Figure 2.

The gas delivery system of the EERC’s Environmental Control Laboratory was used to provide the flue gas matrix for the test. The system uses mass flow controllers (MFCs) to meter appropriate amounts of each gas constituent. The MFCs are backed up by rotameters to provide a visual check on the gas flows into the mixing manifold. A National Instruments LabVIEW program was written for the test and directed the MFCs to provide required flow rates for each flue gas constituent. The program also logged system temperatures throughout the test. The acid gases, air, nitrogen balance, and carbon dioxide were mixed in a heated manifold before being sent to the test tubes in a heated line. The moisture for the gas matrix was created in a steam generator and combined with a small portion of the nitrogen balance before being sent to the test apparatus in a heated line. The moisture content was regulated with a peristaltic pump which fed the steam generator. It is important to note that heated lines were used to bring all components of the flue gas matrix to the system to allow for preheat and mixing time before entering the test chambers.

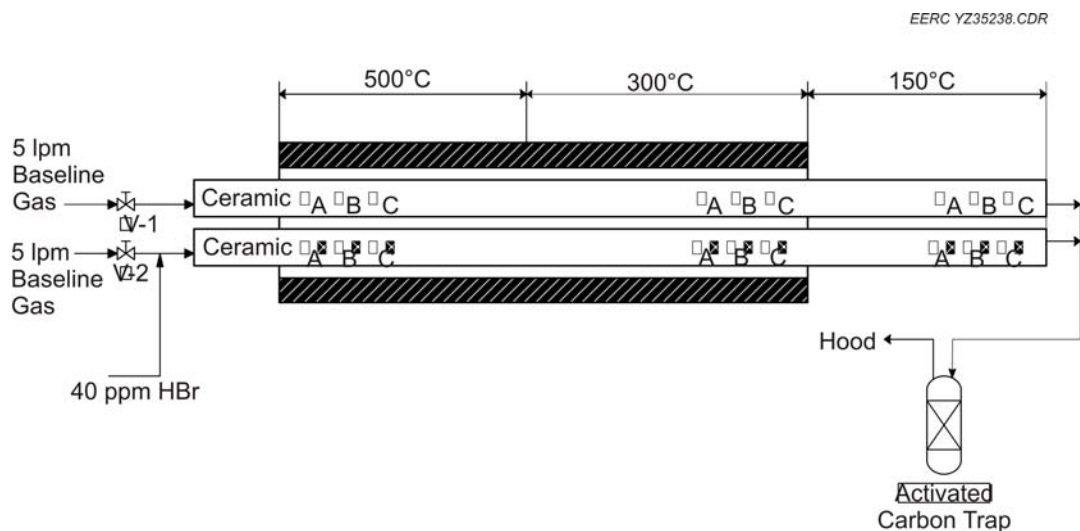


Figure 2. Schematic of the exposure testing system.

EXPERIMENTAL PROCEDURE

The three sets of 1-in. × 1-in. coupons tested were provided by the taconite industry. Before testing, the coupons were prepared by the EERC in the following steps:

- 1) Stamped for identification purposes and labeled 1–9
- 2) Coupons 1–3 of each set drilled to receive iron oxide/sodium sulfate deposit
- 3) Immersed in an acetone bath
- 4) Ultrasonically cleansed for 30 minutes
- 5) Dried in desiccators for 30 minutes
- 6) Weighed

The coupons were loaded into the ceramic test tubes, with the polished surface facing up. Coupons labeled 1–3 received a deposit of iron oxide/sodium sulfate powder (90/10). Table 3 summarizes the layout of testing coupons within the system.

Upon loading, the furnace and heaters were brought up to operating temperature. When the process temperatures were reached, the gases and moisture were turned on. The test ran from April 15 until June 2, 2009. Upon completion of 10 days of testing, the unit was turned off and the coupons removed for weighing and inspection. Because the USS Minntac coupons were received late, they were not included in the first 10 days of testing. Another 10 days of exposure were added at the end of the test to accommodate the Minntac coupon 30-day exposure time. Table 4 lists the start/end date of testing for each coupon set.

Table 3. Coupon Test Layout

Coupons	Deposit	Flue Gas with HBr			Flue Gas Without HBr		
		500°C	300°C	150°C	500°C	300°C	150°C
United	Yes	U1	U2	U3			
	No	U4	U5	U6	U7	U8	U9
Minorca	Yes	M1	M2	M3			
	No	M4	M5	M6	M7	M8	M9
USS Minntac	Yes	UM1	UM2	UM3			
	No	UM4	UM5	UM6	UM7	UM8	UM9

Table 4. Test Dates

	Start Date	End Date
United	4/15/09	5/22/09
Minorca	4/15/09	5/22/09
USS Minntac	4/27/09	6/2/09

Throughout the testing, gas flows, temperatures, and water flows were checked periodically to assure that the test parameters were being met. The gas flows were checked by comparing the rotameter flows with the software readouts from the mass flow controllers. The gas flows remained at their set points throughout the duration of the test. Temperature control was verified several times a day by visual inspection of digital heater control readouts. Water flow input to the system through the steam generator was cross-checked by measuring the mass of water per minute through the peristaltic pump. The water flow was steady at its set point throughout the test.

RESULTS AND DISCUSSIONS

Upon completion of 30 days of testing the coupons were removed and prepared for analysis. The coupons were photographed, weighed, and sent to the EERC's Materials Analysis Laboratory (MAL) for analysis. The MAL used SEM-EDX to determine morphology as well as the elemental compositions of the corrosion product.

Macroscopic Surface Analysis

Figures 3–5 are surface photographs of each coupon after 30 days of flue gas exposure.

United Coupons U1–6 were exposed to flue gas containing HBr while coupons U7–9 were exposed to flue gas only. All of the coupons changed color although the flue gas containing HBr caused more surface discoloration than non-HBr-containing flue gas. Also, the coupons subjected to higher temperatures—U1, 4, and 7—show more surface oxidation than the lower-temperature coupons. The iron oxide/sodium sulfate deposit on U1–3 does not appear to have affected the surface coloration of the United coupons.

For the Minorca coupons, it appears that the exposure to HBr affected surface discoloration but not as greatly as what was seen in the United coupons. Unlike the United coupons, it does not appear that the temperature gradient caused greater surface discoloration across the set. The iron oxide/sodium sulfate deposits on M1–3 appear to have only caused significant surface discoloration on the M1 coupon, which was sitting in the 500°C chamber of the test apparatus.

The surfaces of the USS Minntac coupons are shown in Figure 5. Exposure to higher temperatures caused more discoloration than lower temperatures. The effect of HBr exposure did not induce any additional surface oxidation compared to non-HBr-containing flue gas. A deposit of iron oxide/sodium sulfate on coupons UM1–3 did not cause any additional discoloration when compared to the other coupons.

Microscopic Analysis

Each coupon surface was scanned with SEM-EDX to characterize detailed surface morphology and quantify distribution of metal elements on the coupon surface. Moreover, cross section SEM-EDX analysis was also performed for each coupon to determine degree of potential

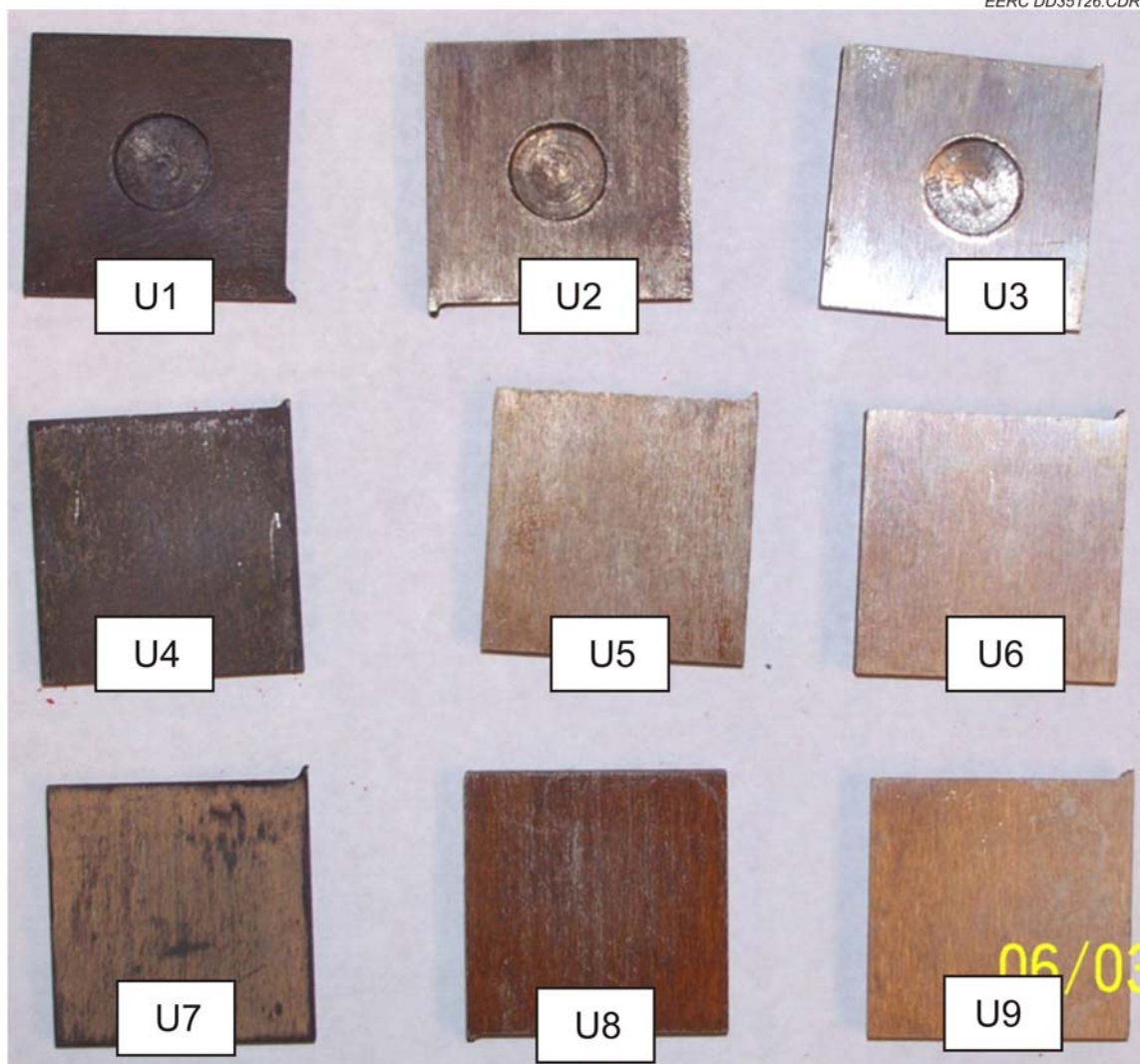


Figure 3. Surface of United coupons after testing.

corrosion. Although all coupons were analyzed, only figures and analyses showing corrosion or other notable characteristics are included in the body of this report. The complete data set of SEM results is included in Appendices A–C for each coupon set.

United Coupons

Table 5 summarizes the elemental distribution on the surfaces of United coupons for the testing conditions. Only averaged data were reported since they best represent the random nature in which the scans were completed. The elemental weight percentage of the United coupons before testing is also included for comparison.

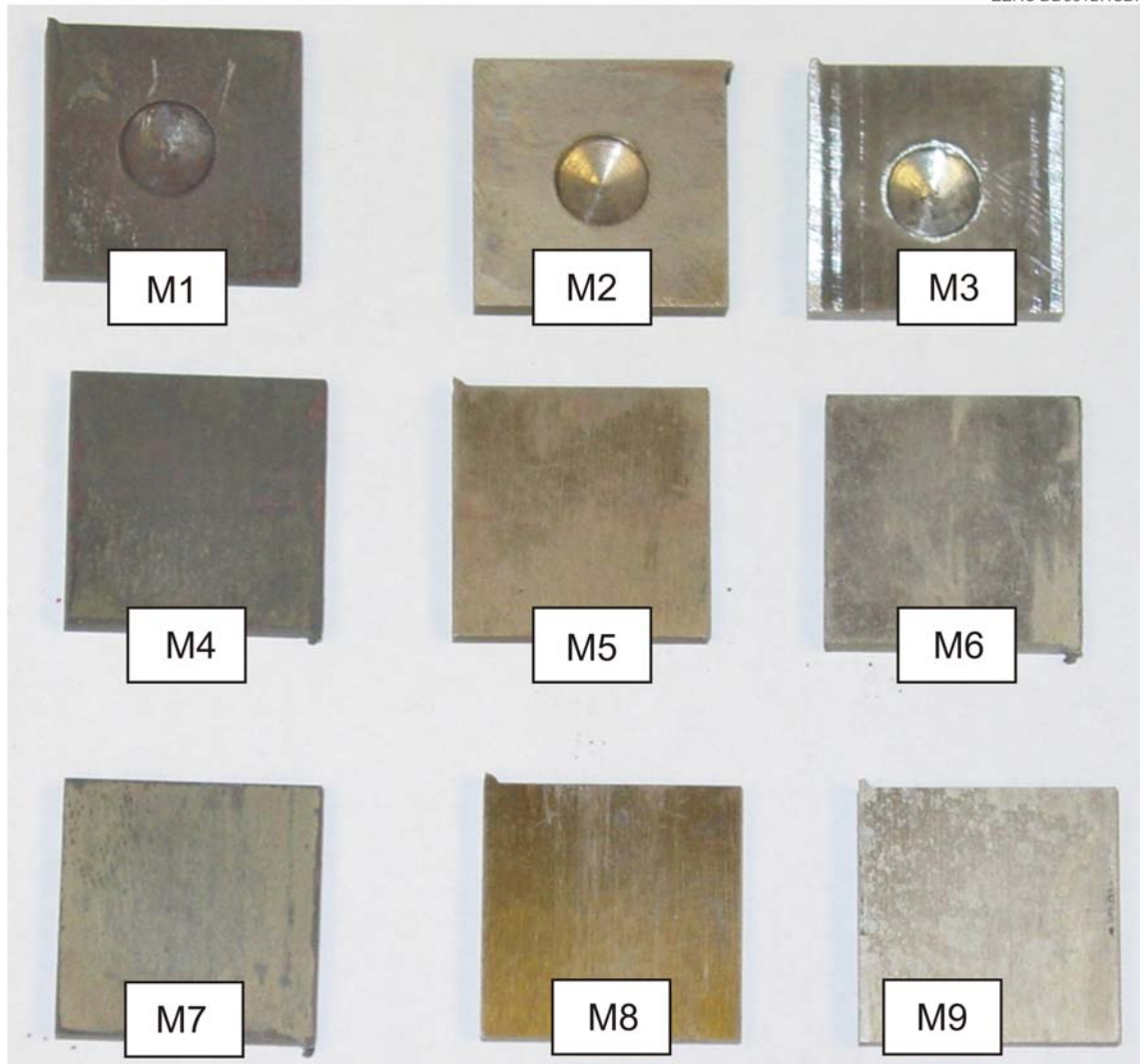


Figure 4. Surface of Minorca coupons after testing.

Compared to the elemental pretest composition, all exposed United coupons experienced some surface corrosion. Coupons exposed to taconite flue gas only, U8 and 9, experienced very few elemental changes, while U7 indicated measurable loss of Ni. The Ni loss can be attributed to sulfur attack. Figures 6 and 7 show SEM images of the U7 surface and cross section, respectively. Table 6 lists measured elemental concentrations along the U7 cross section. The U7 surface appears to have slight surface striations. Although the U7 surface suffered Ni loss, there is no further corrosion penetration.

SEM analyses on the surface and cross section of U8 and U9 show little change in morphology and elemental compositions. The complete analysis details have been included in Appendix A.

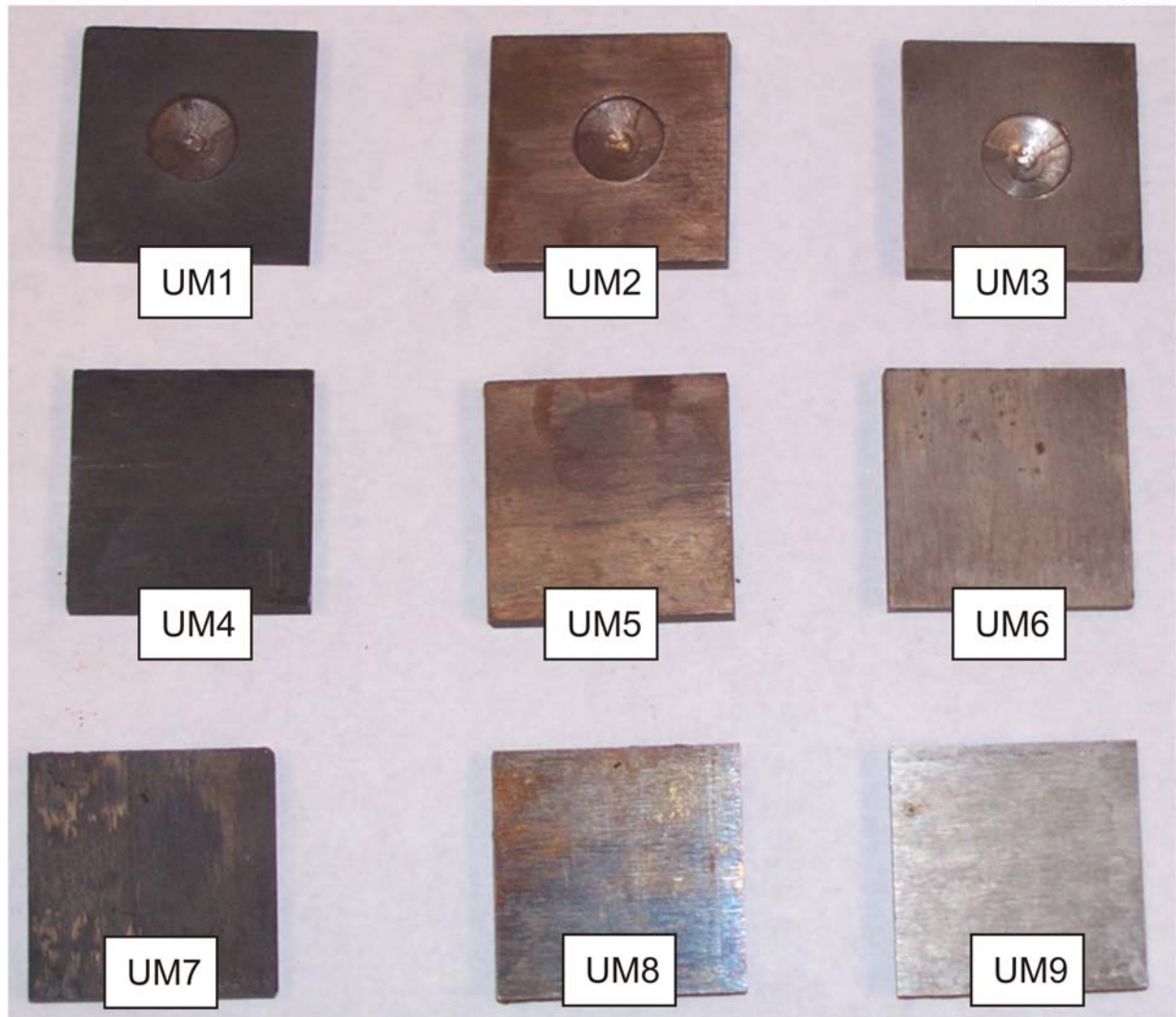


Figure 5. Surface of USS Minntac coupons after testing.

Table 5. Normalized Distribution of Elements on United Coupon Surface, wt%

	Temp., °C	Si	S	Cr	Mn	Fe	Co	Ni	Br
Pretest		4.26	0.50	27.81	0.25	52.42	0.00	14.91	0.00
U1	500	6.18	1.18	21.60	1.69	58.01	0.03	9.00	2.25
U2	300	2.50	0.84	17.90	0.76	67.75	0.20	7.05	2.91
U3	150	1.99	0.57	22.75	0.44	64.81	0.08	7.92	1.35
U4	500	3.09	0.49	21.43	0.90	59.49	0.17	9.09	5.23
U5	300	3.26	1.20	29.98	0.38	48.77	0.00	13.53	2.85
U6	150	3.80	2.86	33.47	0.46	45.47	0.01	12.36	1.31
U7	500	6.44	8.28	39.57	2.90	39.30	0.11	3.22	0.00
U8	300	4.47	2.42	27.09	0.63	52.07	0.09	12.52	0.00
U9	150	4.17	6.34	25.68	0.48	49.82	0.04	13.38	0.00

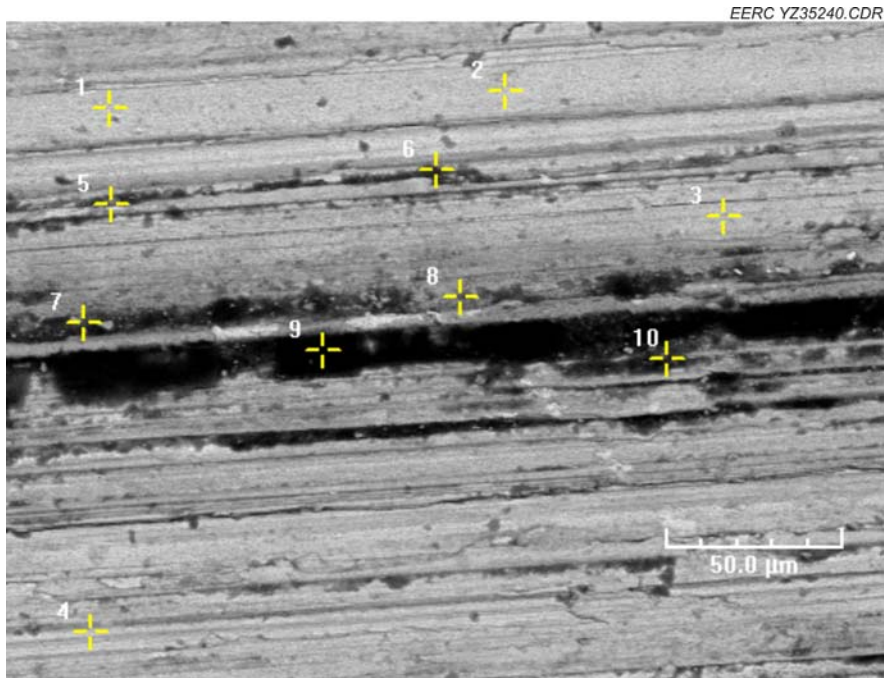


Figure 6. U7 surface SEM image.

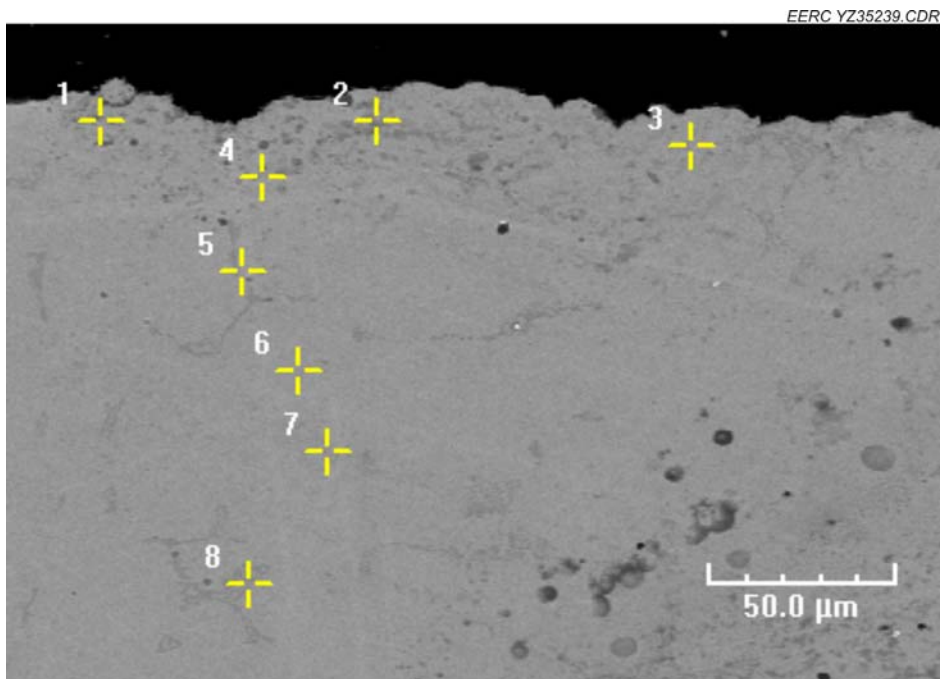


Figure 7. U7 cross-sectional SEM image.

Table 6. Elemental Analysis of U7 Cross Section, wt%

Tag	Si	S	Cr	Mn	Fe	Co	Ni
1	1.78	0.50	50.52	0.71	37.11	0.00	9.34
2	5.68	2.01	26.56	0.23	51.25	0.00	14.02
3	3.19	0.50	26.32	0.43	54.76	0.00	14.71
4	6.63	0.52	26.84	0.15	51.56	0.00	14.29
5	4.23	1.02	28.45	0.17	52.28	0.00	13.81
6	4.69	0.30	24.75	0.37	55.35	0.00	14.45
7	3.04	0.45	26.36	0.18	54.15	0.00	15.72
8	3.73	0.43	27.20	0.78	52.81	0.00	14.96

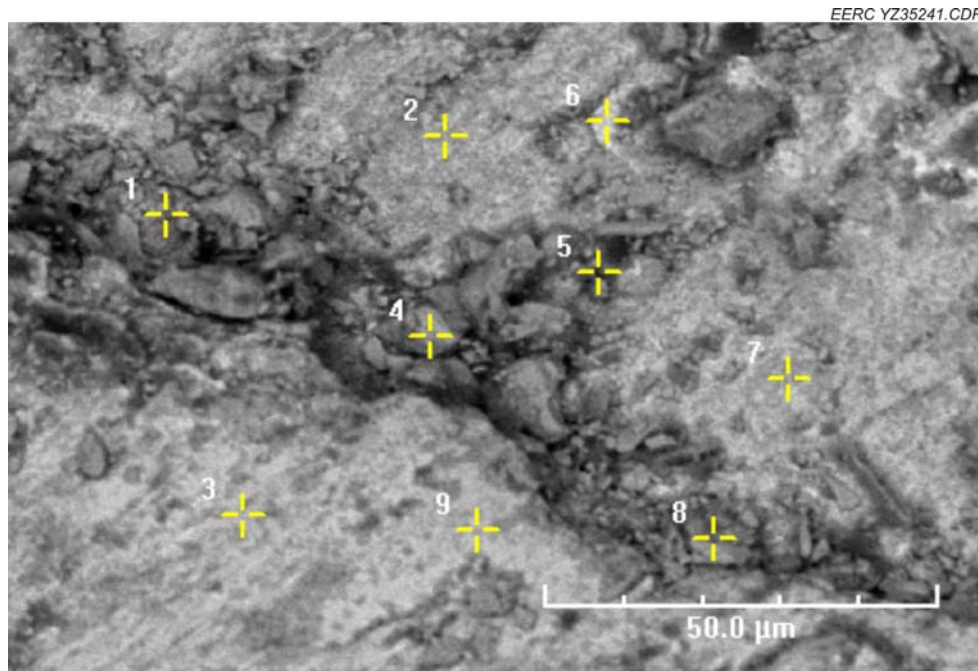


Figure 8. U1 surface SEM image.

Coupons that have been exposed to bromine and taconite flue gas, U1–6, all showed Br deposition in small percentages. As a result, iron, chromium, and nickel elemental averages show small gains/losses depending on the testing conditions. Sulfur and silicon were affected in very small percentages in some coupons. Plotted in Figures 8–11 are the surface SEM images for U1–4 respectively. Compared to surface striations observed on U4, small surface cracks, pits, and chipping on coupons U1–3 were mainly caused by drilling during coupon preparation. Elemental analysis data of the U1–4 surfaces indicate enrichment of Fe and losses of Cr and Ni due to HBr attack. SEM data of U5 and 6 surfaces indicate no large changes in morphology and elemental composition after exposure testing. The complete data set is included in Appendix A.

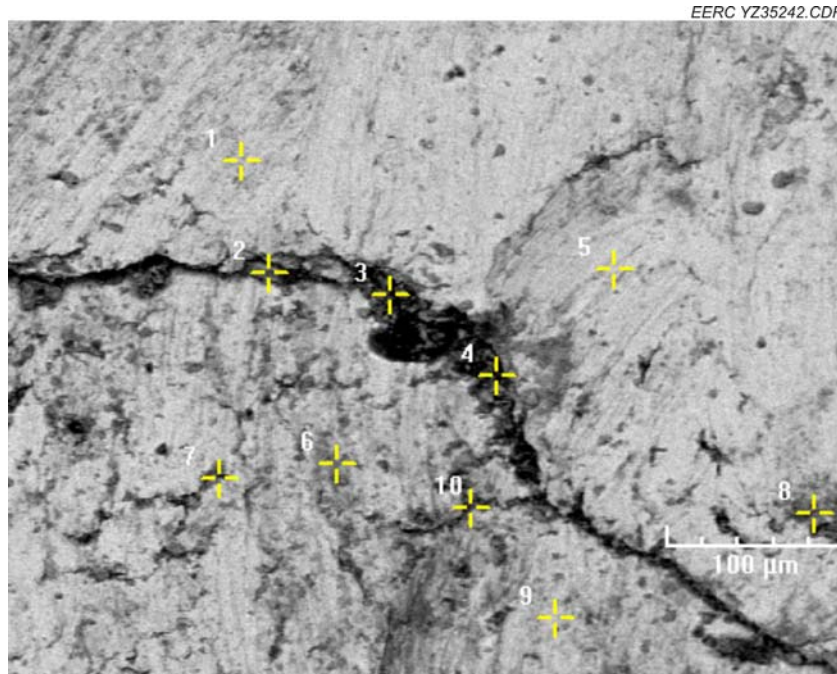


Figure 9. U2 surface SEM image.

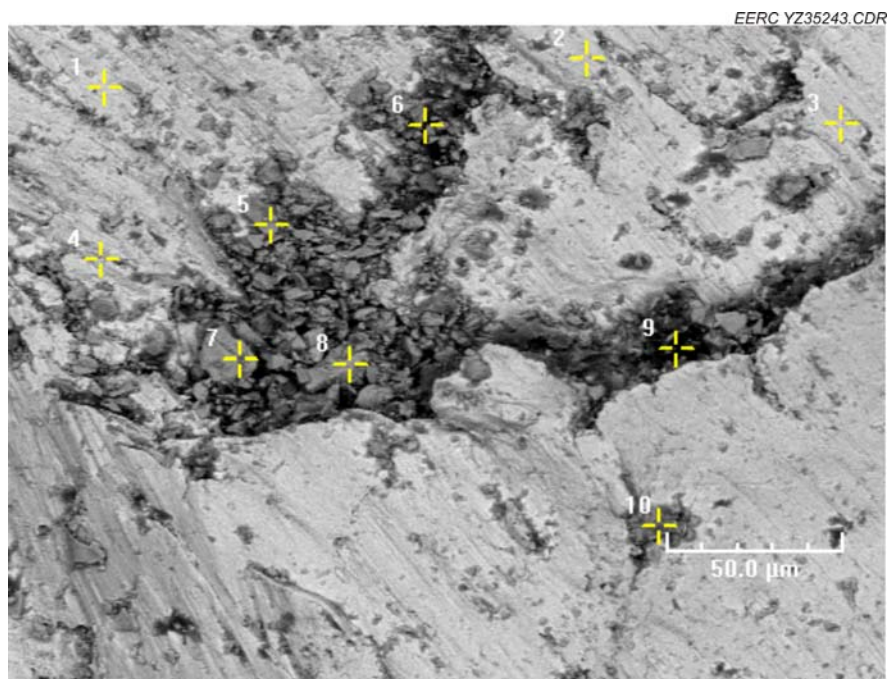


Figure 10. U3 surface SEM image.

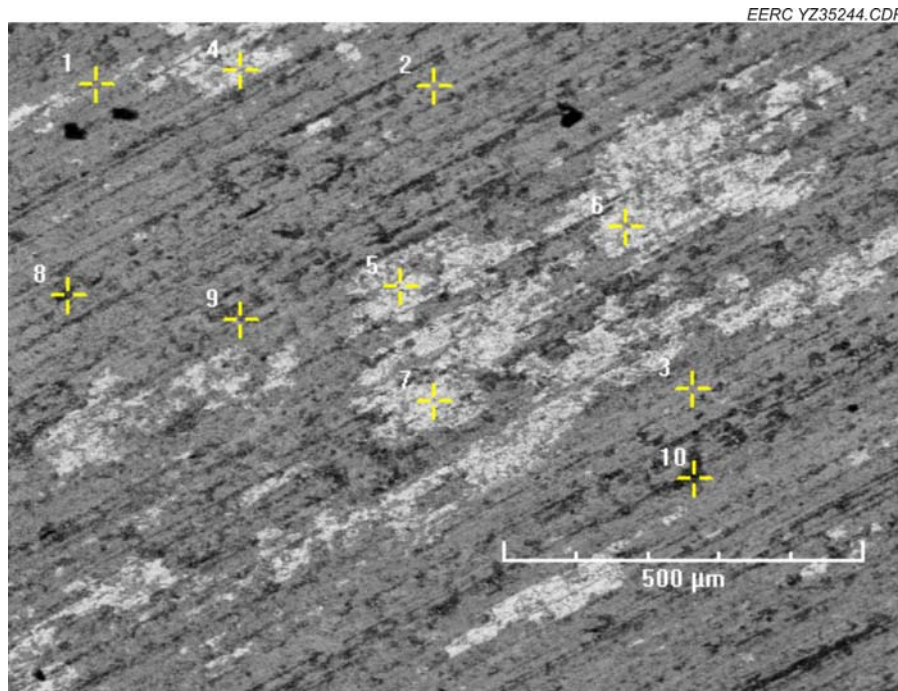


Figure 11. U4 surface SEM image.

The cross-sectional SEM data for United coupons, other than U4, indicate that bromine deposition was confined to the surface of the material and did not impact the elemental composition. Figure 12 is the cross-sectional SEM image for U4, and corresponding elemental distributions are listed in Table 7. The SEM data for U4 indicate slight penetration of bromine species with corresponding losses of Ni and Fe below the coupon surface under 500°C testing conditions. Other SEM cross-sectional data are reported in Appendix A.

In summary, all the United coupons showed very little corrosive deterioration after 30 days of exposure testing. None of the United coupon cross sections showed significant bromine penetration beyond the surface. SEM cross sections showed very small surface chips, cracks, and pits on several of the samples, which most likely were caused by drilling the wells. However, it did not seem to induce any additional corrosive activity. The iron oxide/sodium sulfate deposits showed no more corrosion than the flat areas surrounding them. Although the bromine-exposed coupons saw slightly worse corrosion than those not exposed to bromine, cross-sectional SEM analysis indicates that this oxidation did not penetrate beyond the surface of the coupons.

Minorca Coupons

Listed in Table 8 are the averaged elemental compositions on the surfaces of Minorca coupons under different testing conditions.

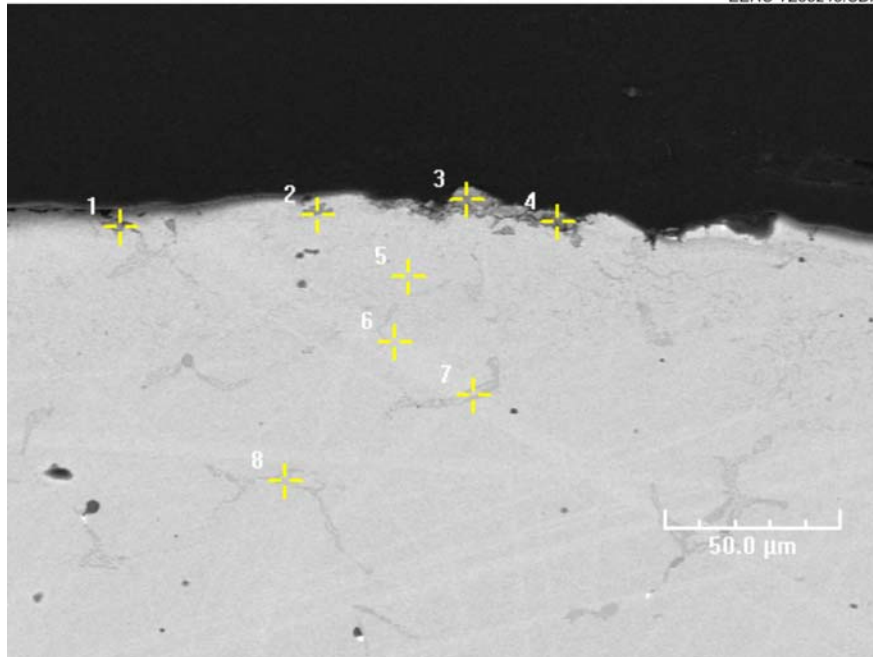


Figure 12. U4 cross-sectional SEM image.

Table 7. Elemental Analysis of U4 Cross Section, wt%

Tag	Si	S	Cr	Mn	Fe	Co	Ni	Br
1	3.09	0.90	16.24	0.00	61.59	0.00	18.08	0.00
2	7.57	0.54	23.58	0.21	50.50	0.00	15.75	1.86
3	5.90	0.58	79.87	3.61	4.82	0.00	1.51	3.71
4	12.35	1.36	55.80	4.43	16.91	0.00	7.38	1.71
5	2.65	0.39	26.22	0.00	55.20	0.00	14.49	0.97
6	3.07	0.51	27.26	0.72	52.08	0.00	14.69	1.66
7	2.40	0.87	60.00	0.07	30.25	0.00	5.32	1.09
8	2.22	0.59	52.67	0.44	35.85	0.01	7.41	0.73

SEM surface analysis of coupons M7–9, which were only exposed to taconite flue gas, indicates gain or loss of Ni, Fe, and Cr, depending on testing conditions. Both Fe and Ni were oxidized or vaporized on the M7 surface under 500°C testing conditions. This resulted in Cr enrichment while little elemental change was observed on M8 at 300°C. The M9 surface appears to have suffered sulfur attack, showing Fe and Cr losses. Plotted in Figures 13–15 are the microscopic surface images of coupons M7–9, respectively. No surface chips, cracks, or pits are visible, but surface striations were observed. Cross-sectional data for M7–9 (reported in Appendix B) show consistent elemental distribution similar to pretest data beyond the coupon surface, proving no penetrated corrosion occurred.

Table 8. Normalized Distribution of Elements on Minorca Coupon Surface, wt%

	Temp., °C	Si	S	Cr	Mn	Fe	Co	Ni	Br
Pretest		5.28	0.31	27.63	0.25	61.66	0.09	4.74	0
M1	500	12.3	0.74	34.95	7.06	41.46	0.06	1.86	1.53
M2	300	1.90	0.24	25.92	0.91	66.94	0.56	2.79	0.76
M3	150	2.67	0.50	14.48	0.43	78.29	0.52	1.86	1.24
M4	500	6.56	0.46	41.54	2.75	43.70	0.43	1.55	3.01
M5	300	3.44	4.25	25.73	0.72	58.61	0.37	3.85	3.03
M6	150	4.35	5.43	26.60	0.38	57.14	0.14	4.03	1.88
M7	500	8.45	0.80	51.78	5.07	32.91	0.00	1.00	0.00
M8	300	3.84	0.39	24.64	0.22	65.90	0.36	4.66	0.00
M9	150	2.96	28.80	15.70	0.50	47.07	0.18	4.39	0.00

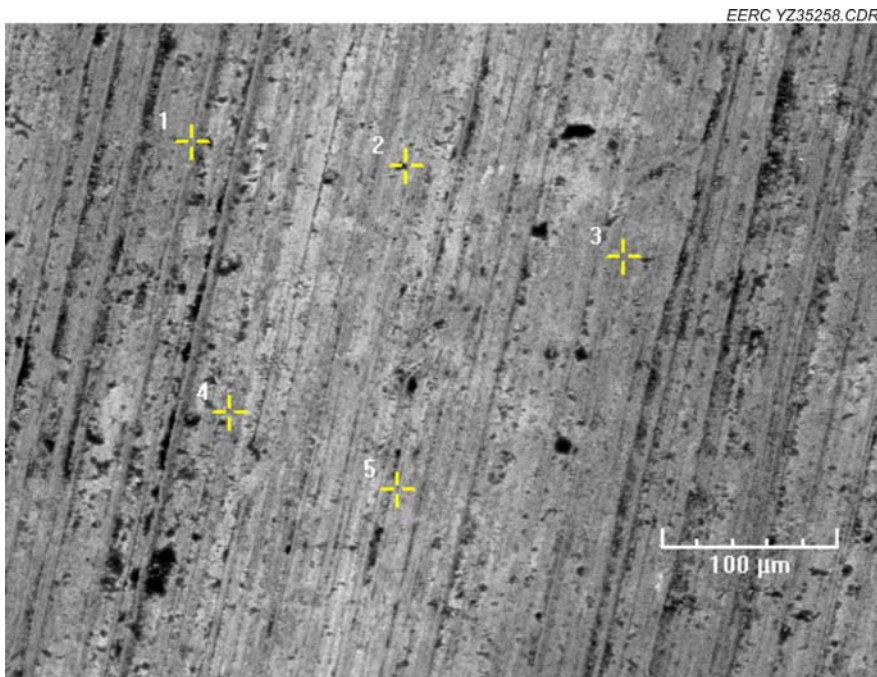


Figure 13. M7 surface SEM image.

The coupons exposed to bromine, M1–6, all showed Br deposition, while bromine concentrations on coupons with iron oxide deposit were less than that without deposition. Plotted in Figures 16–21 are the surface SEM images for coupons M1–6. Small cracking and pitting are observed on M1–3 surfaces, and this was most likely caused by the drilling process. M1 (Figure 16) shows slight blistering, an indication of vaporization at 500°C. Discoloration and striation were seen on M2 and M3. Similar surface striations were also observed for coupons M4–6. As shown in Table 8, consistent losses of Ni were detected on coupon surfaces where they contacted HBr. Iron loss was only detected at the 500°C testing temperature, i.e., M1 and 4.

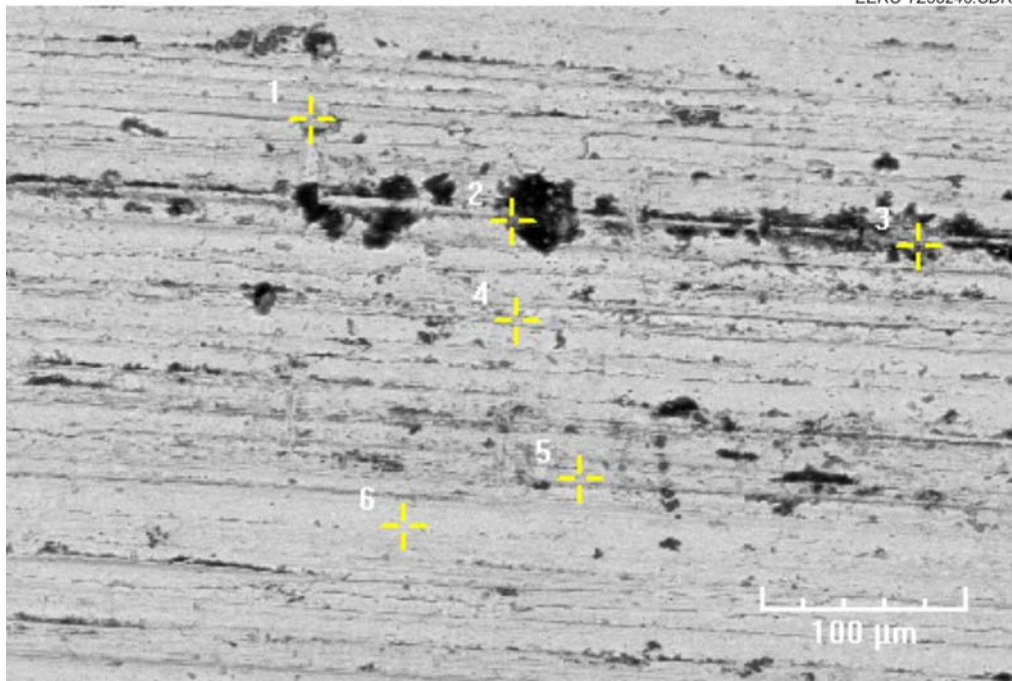


Figure 14. M8 surface SEM image.

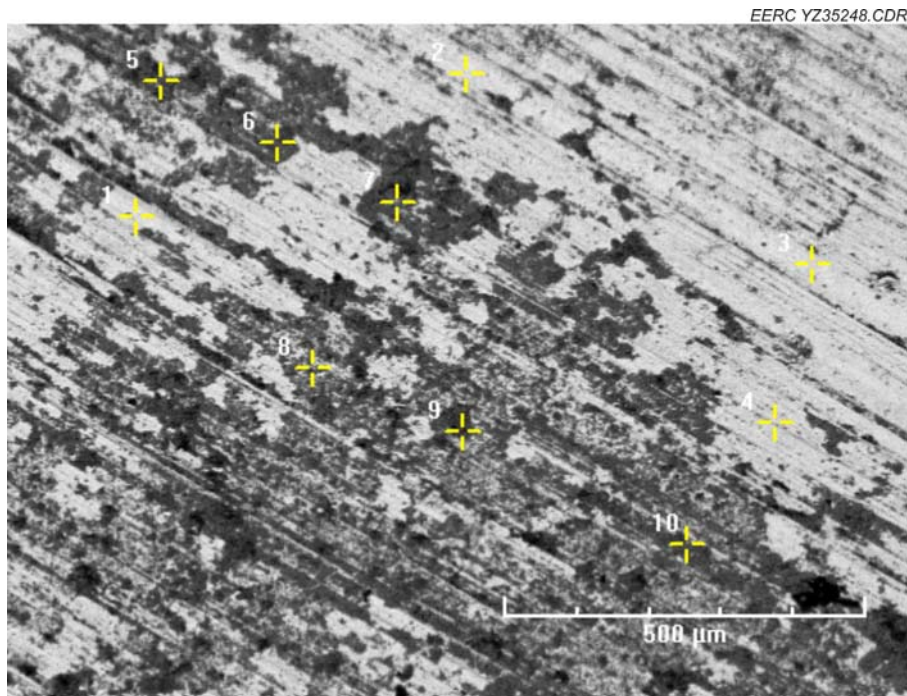


Figure 15. M9 surface SEM image.

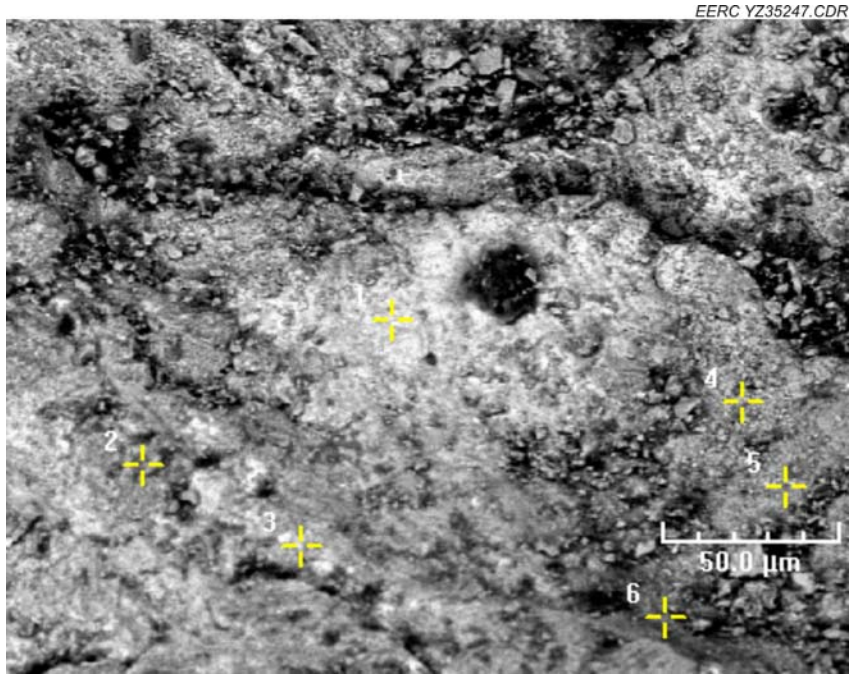


Figure 16. M1 surface SEM image.

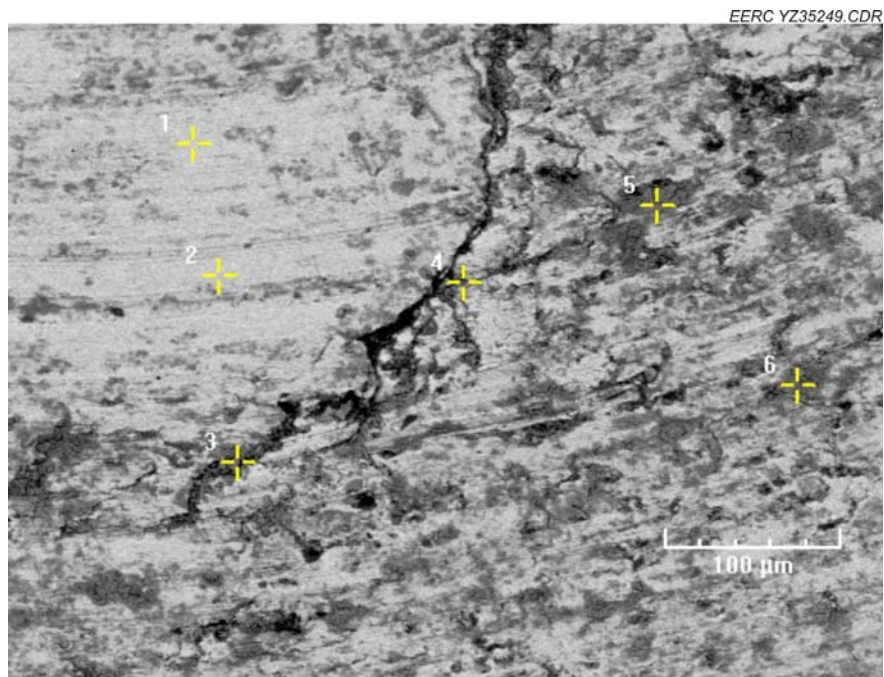


Figure 17. M2 surface SEM image.

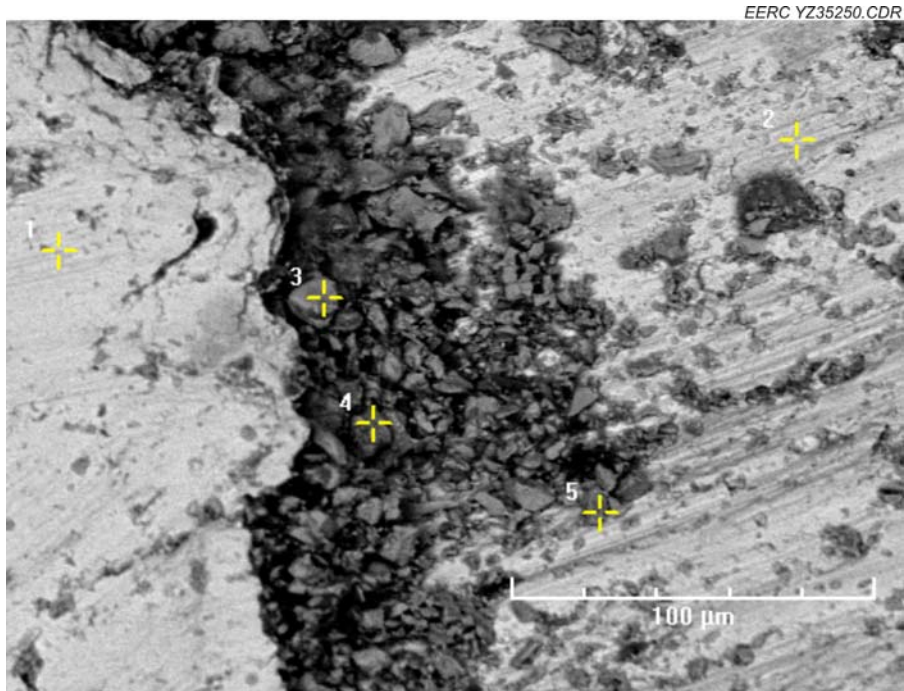


Figure 18. M3 surface SEM image.

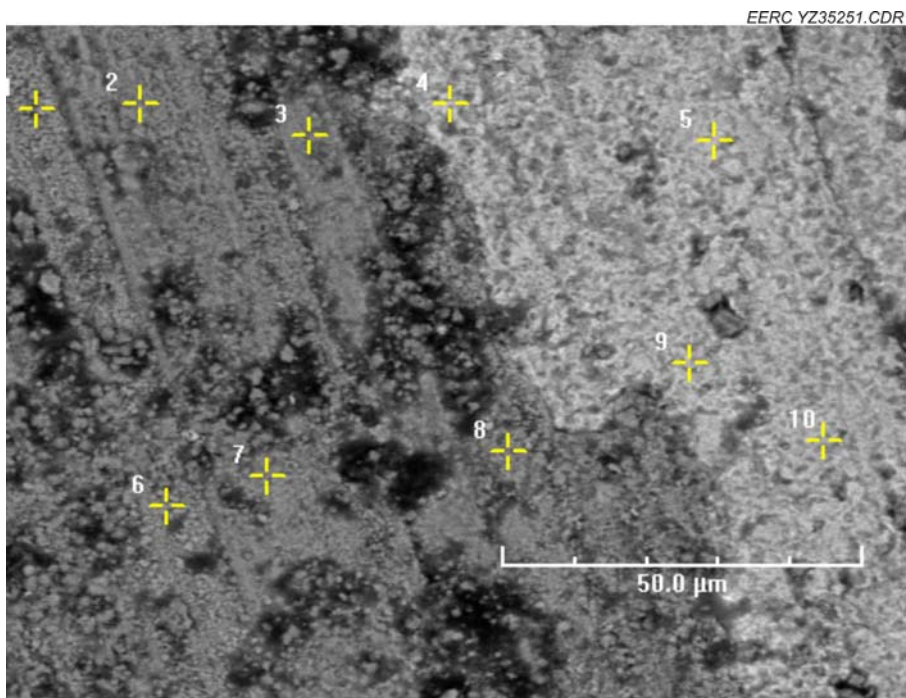


Figure 19. M4 surface SEM image.

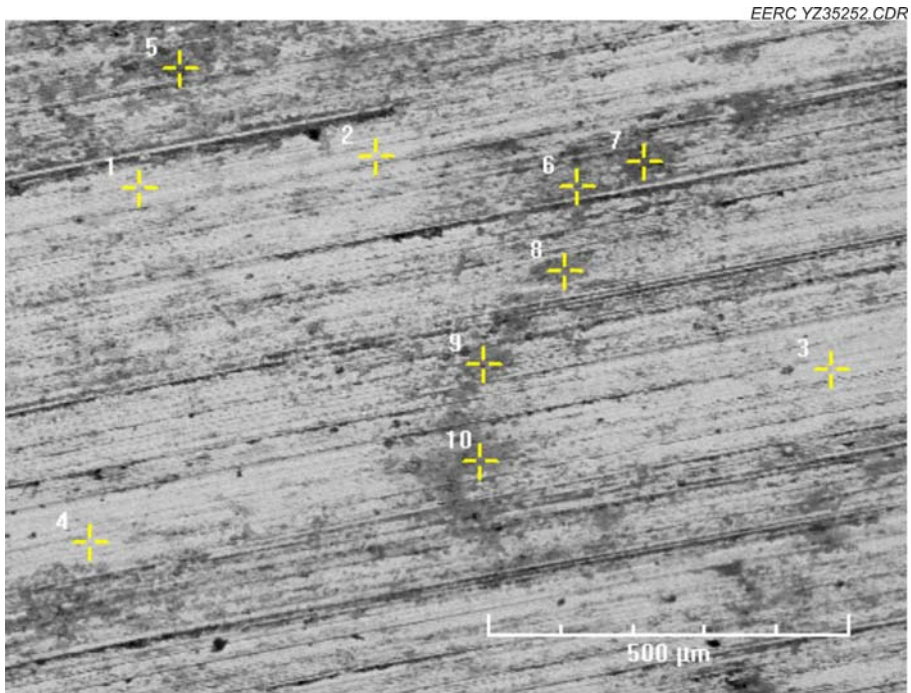


Figure 20. M5 surface SEM image.

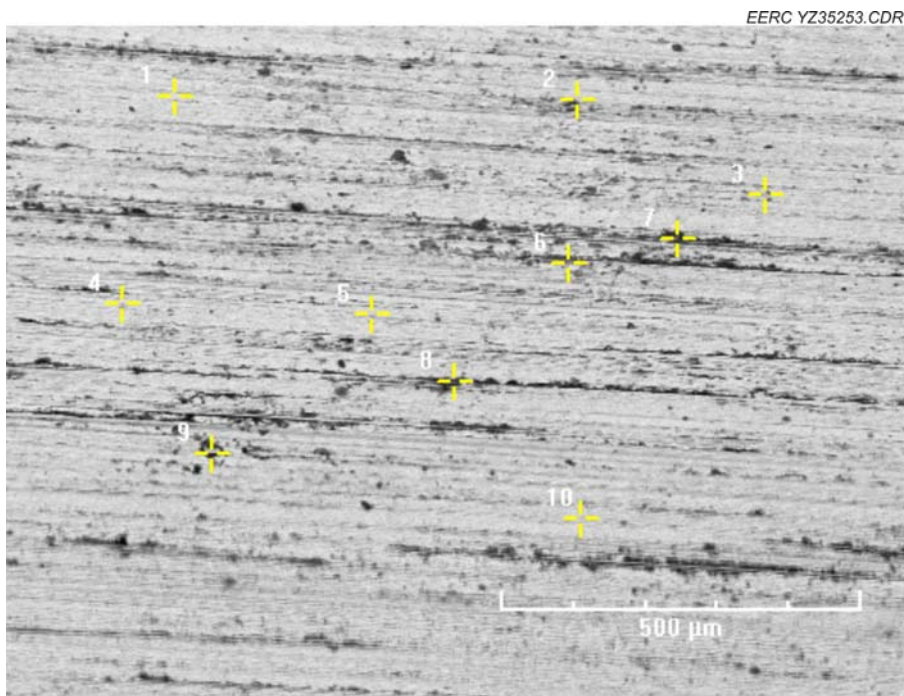


Figure 21. M6 surface SEM image.

Cross-sectional SEM analysis on M1–6 was performed; the complete data set is included in Appendix B. Figures 22–25 are the cross-sectional SEM images for M1, 3, 5, and 6 and show notable changes. M2 and 4 cross-sectional SEMs indicate no corrosion and/or elemental variation compared to pretest data. Cracking through the M1 cross section was due to drilling. However, elemental data (Table 9) show HBr deposits on the surface and no further penetration occurred. Cross-sectional data of M3 (Figure 23 and Table 10) indicate slight Br penetration through intact surface with corresponding Ni loss. Both M5 and M6 cross-sectional SEMs show slight cracking on the coupon surface with elevated Br deposition, but no further elemental changes were observed beyond the surface as listed in Tables 11 and 12.

Overall, microscopic analysis data have confirmed that all bromine attack and corrosion activity did not penetrate beyond the face of the Minorca coupons, although SEM cross sections showed small surface chips, cracks, and pits on several coupons. The wells containing iron oxide/sodium sulfate deposits showed no more corrosion than the flat areas surrounding them. Cracks from drilling the wells were observed in several coupons, although this surface did not attract any additional corrosive activity. All tested coupons have shown minor losses of Fe and Ni on surface, depending on the coupon specific testing conditions. Additional HBr did not induce significant corrosion activities on Minorca coupons under varied testing temperatures.

USS Minntac Coupons

Table 13 shows the averaged elemental compositions on the surfaces of USS Minntac coupons under different testing conditions. The complete SEM data set for surface and cross-sectional analysis are reported in Appendix C.

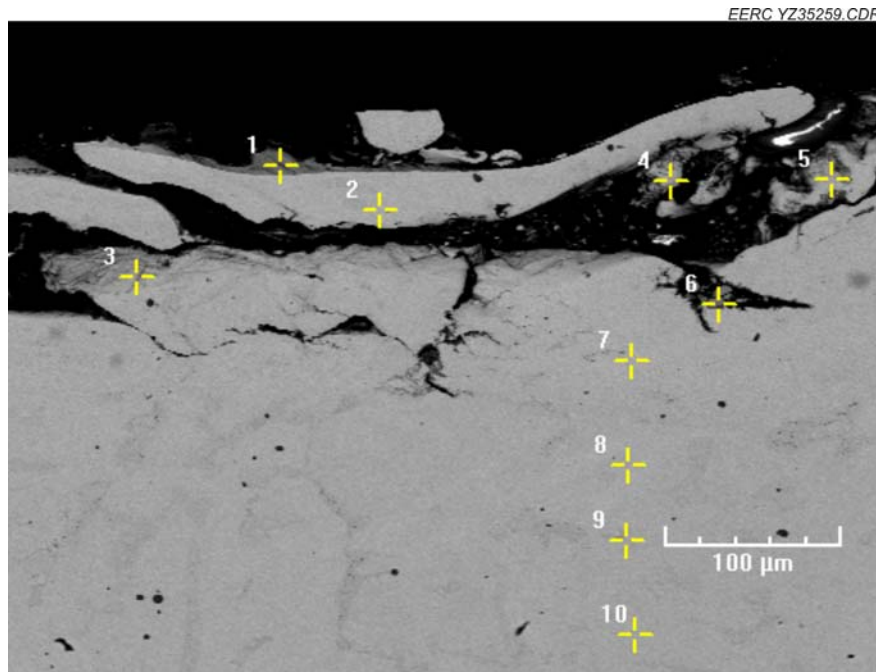


Figure 22. M1 cross-sectional SEM image.

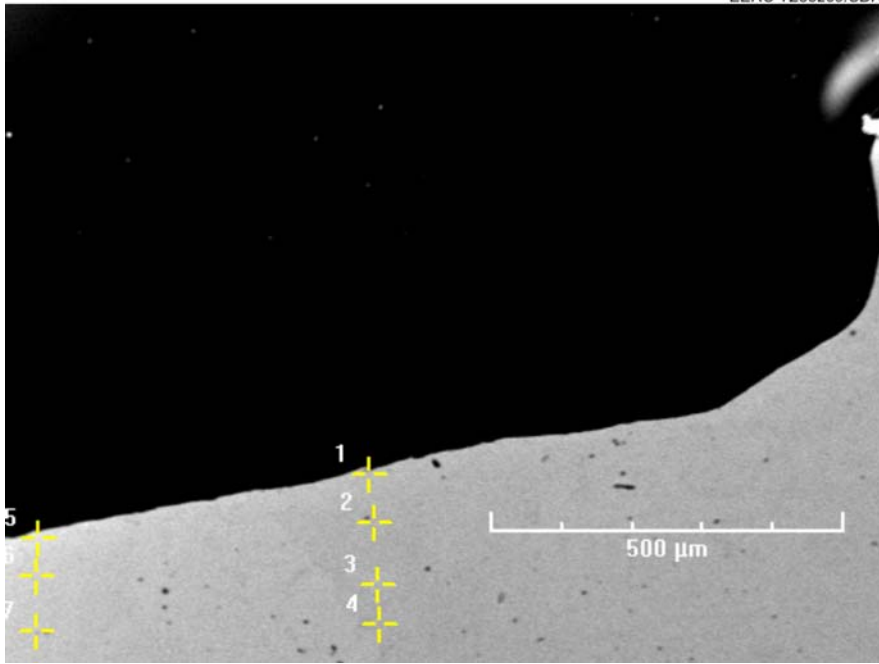


Figure 23. M3 cross-sectional SEM image.

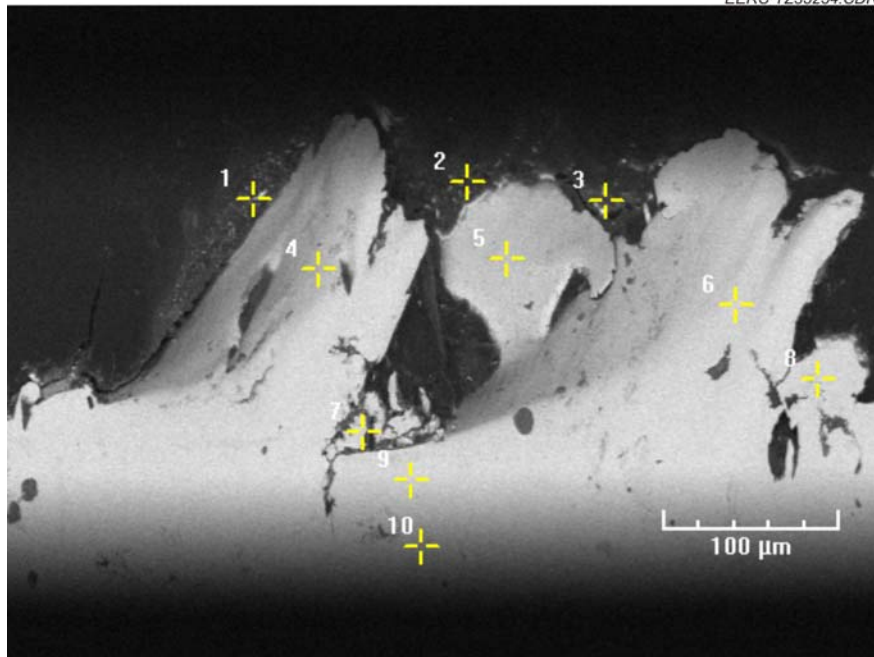


Figure 24. M5 cross-sectional SEM image.

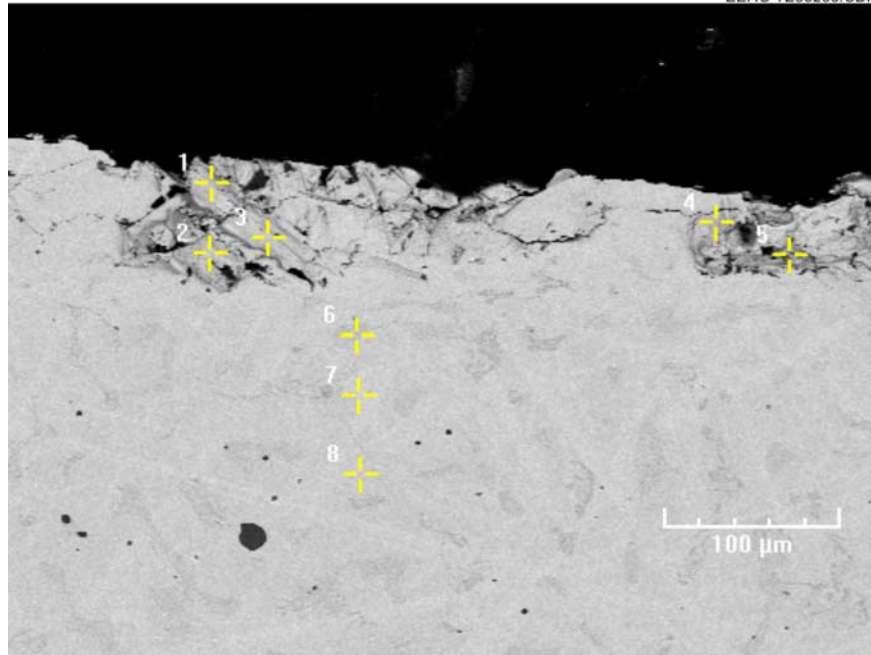


Figure 25. M6 cross-sectional SEM image.

Table 9. Elemental Analysis on M1 Cross Section, wt%

Tag	Si	S	Cr	Mn	Fe	Co	Ni	Br
1	6.14	0.79	22.96	0.00	57.56	0.00	3.55	9.00
2	4.14	0.23	25.42	0.17	63.54	0.00	4.30	2.20
3	4.82	0.32	29.47	0.00	55.97	0.00	3.66	5.76
4	3.32	0.54	16.27	0.00	73.06	0.00	4.58	2.23
5	11.85	0.04	22.64	0.00	62.29	0.00	1.16	2.02
6	1.54	0.57	1.91	0.00	90.98	0.00	0.00	5.00
7	4.13	0.34	26.80	0.09	61.59	0.00	5.19	1.86
8	3.58	0.29	25.38	0.29	64.30	0.02	4.90	1.17
9	3.43	0.28	33.36	0.09	56.94	0.00	4.62	1.25
10	3.39	0.18	26.02	0.18	63.54	0.12	5.13	1.32

Table 10. Elemental Analysis on M3 Cross Section, wt%

Tag	Si	S	Cr	Mn	Fe	Co	Ni	Br
1	9.24	0.00	31.68	0.00	53.12	0.00	1.97	3.86
2	8.07	0.48	28.03	0.00	54.98	0.00	2.30	6.08
3	7.50	0.47	30.11	0.23	55.14	0.00	2.91	3.58
4	7.01	0.13	29.46	0.08	57.41	0.00	2.90	2.81
5	6.88	0.38	27.59	0.00	58.04	0.00	2.50	4.62
6	6.49	0.35	29.54	0.00	58.14	0.00	2.94	2.52
7	6.82	0.15	28.41	0.13	57.49	0.00	2.72	4.28

Table 11. Elemental Analysis on M5 Cross Section, wt%

Tag	Si	S	Cr	Mn	Fe	Co	Ni	Br
1	9.56	1.12	14.04	0.00	33.09	0.00	2.92	39.27
2	19.07	2.54	5.92	0.00	13.68	0.49	3.18	55.12
3	13.59	4.22	7.87	0.81	7.95	0.22	0.32	65.02
4	7.13	0.32	18.97	0.00	46.42	0.00	3.04	24.11
5	5.48	0.45	22.56	0.27	55.29	0.10	4.64	11.20
6	3.75	0.00	25.20	0.06	64.64	0.00	4.86	1.49
7	4.38	0.34	22.22	0.10	65.74	0.08	5.33	1.81
8	3.88	0.24	22.75	0.32	67.42	0.00	4.25	1.00
9	3.08	0.29	24.76	0.17	65.41	0.05	5.08	1.15
10	3.74	0.09	25.84	0.09	63.87	0.00	5.02	1.32

Table 12. Elemental Analysis of M6 Cross Section, wt%

Tag	Si	S	Cr	Mn	Fe	Co	Ni	Br
1	3.57	0.27	25.57	0.06	64.50	0.00	4.68	1.23
2	3.37	0.21	29.81	0.11	61.17	0.00	4.38	0.93
3	3.21	0.25	26.01	0.30	63.89	0.03	5.04	1.25
4	2.84	0.34	27.42	0.13	62.13	0.00	5.23	1.90
5	3.47	0.29	27.54	0.31	61.67	0.00	5.16	1.55
6	3.28	0.26	29.68	0.28	60.28	0.00	5.16	1.01
7	3.14	0.17	24.84	0.36	64.99	0.16	5.13	1.22
8	3.35	0.17	26.06	0.16	65.16	0.00	4.24	0.82

Table 13. Normalized Distribution of Elements on USS Minntac Coupon Surface, wt%

	Temp., °C	Si	S	Cr	Mn	Fe	Co	Ni	Br
Pretest		3.81	0.24	27.24	0.88	50.74	0.03	17.01	0.00
UM1	500	2.34	0.40	19.28	5.30	48.96	0.26	7.20	16.22
UM2	300	2.32	0.91	17.90	0.58	63.86	0.08	9.49	4.80
UM3	150	2.77	0.74	27.26	0.69	48.40	0.05	15.14	4.83
UM4	500	5.76	4.93	48.70	5.54	23.52	0.00	3.63	7.89
UM5	300	2.96	8.71	15.07	0.77	30.64	0.02	11.60	30.09
UM6	150	3.10	41.69	12.70	0.72	27.73	0.09	9.50	3.23
UM7	500	6.59	6.24	56.72	7.24	19.85	0.00	2.62	0.00
UM8	300	5.42	5.00	30.05	1.55	44.98	0.00	12.82	0.00
UM9	150	3.99	8.68	26.63	0.74	46.16	0.00	13.67	0.00

Without HBr in the taconite flue gas, SEM analysis indicates that UM coupons only suffer surface loss of Ni and Fe in a 500°C environment. Discoloration and surface striation were observed for UM7–9. Additional cross-sectional SEM–EDX data show that UM7–9 were well protected and did not experience significant oxidative deterioration.

The coupons exposed to bromine, UM1–6, all showed Br deposition with Ni, Fe, or Cr losses, depending on testing conditions. The highest Br surface concentration was 30.09%, measured on UM5. Figures 26 and 27 and Table 14 are the UM5 microscopic images and cross-sectional analysis, respectively. The UM5 surface shows blistering and cracking, with losses of Ni, Cr, and Fe. Further cross-sectional analysis indicates that although slight Br penetration occurred, no significant elemental disruptions occurred. All other UM coupons exposed to bromine show surface striation but no further corrosion beyond the surface.

Weight Gain/Loss Measurement

Tables 15–17 show the weight gain/loss for each set of coupons during the 30-day testing period.

For the United coupon set, larger weight gains were seen in U1–6, which were exposed to HBr. Coupons U7–9 saw very little weight gain or loss. U1–3 coupons showed a greater weight gain than the non-deposit-containing coupons.

The Minorca coupons exposed to HBr also show a larger weight gain than the non-HBr-exposed coupons. The presence of iron oxide/sodium sulfate deposits on M1–3 did not cause greater weight gain than the M4–6 coupons. For the Minorca coupons, the rate of weight gain was steady throughout the test.

The USS Minntac set showed variable weight gains between the HBr- and non-HBr-exposed coupons.

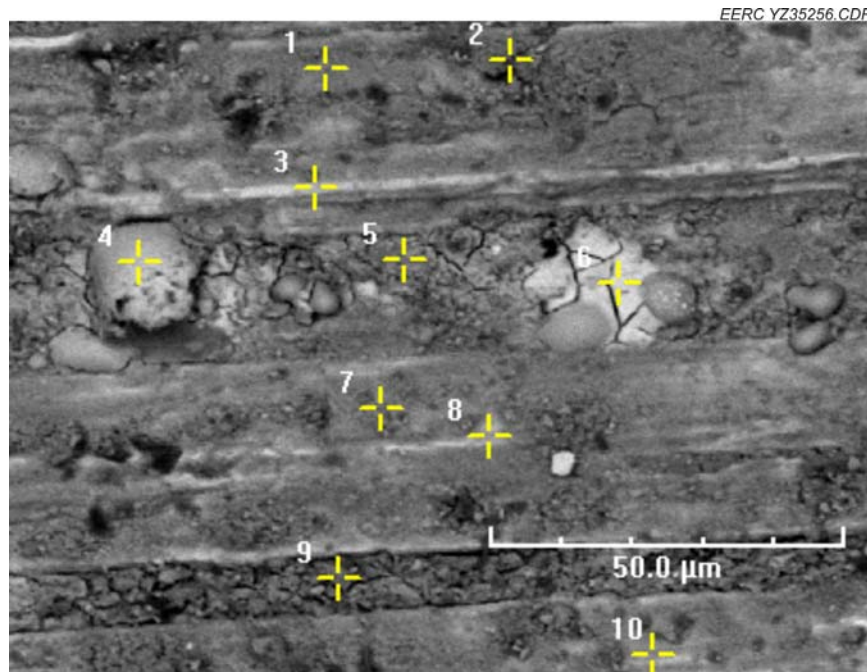


Figure 26. UM5 surface SEM image.

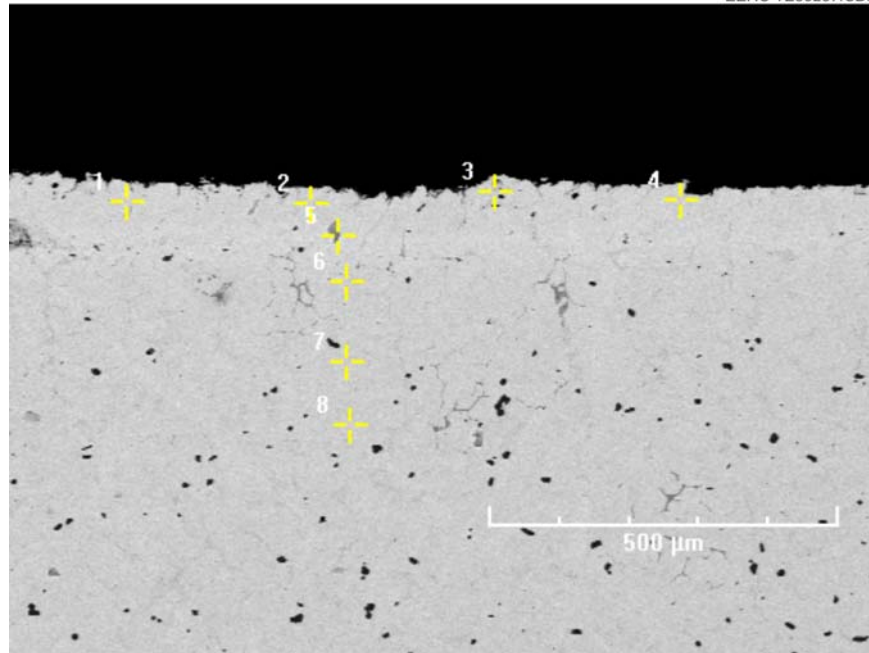


Figure 27. UM5 cross-sectional SEM image

Table 14. Elemental Analysis of UM5 Cross Section, wt%

Tag	Si	S	Cr	Mn	Fe	Co	Ni	Br
1	3.39	0.40	26.51	0.84	46.84	0.00	16.44	5.58
2	2.31	0.31	54.47	0.55	29.91	0.00	9.37	3.09
3	3.04	0.36	24.95	0.19	50.36	0.20	16.47	4.43
4	2.72	0.22	26.61	0.83	48.86	0.00	16.04	4.64
5	3.01	0.12	28.04	0.42	47.69	0.00	15.99	4.73
6	2.84	0.27	27.15	0.75	47.97	0.01	16.23	4.74
7	3.21	0.27	29.13	0.97	44.96	0.00	16.51	4.91
8	2.56	0.31	25.72	0.94	49.02	0.05	16.12	5.20

Table 15. Weight Gain/Loss of United Coupons, mg

Coupon	10 days	20 days	30 days
U1	1.00	2.00	5.00
U2	1.00	4.00	5.00
U3	4.00	3.00	4.00
U4	0.00	-1.00	3.00
U5	0.00	0.00	5.00
U6	0.00	2.00	2.00
U7	1.00	1.00	0.00
U8	-1.00	1.00	-1.00
U9	1.00	0.00	2.00

Table 16. Weight Gain/Loss of Minorca Coupons, mg

Coupon	10 days	20 days	30 days
M1	0.00	2.00	1.00
M2	4.00	7.00	9.00
M3	6.00	4.00	3.00
M4	4.00	6.00	8.00
M5	2.00	5.00	9.00
M6	4.00	5.00	5.00
M7	1.00	2.00	1.00
M8	3.00	2.00	0.00
M9	1.00	2.00	1.00

Table 17. Weight Gain/Loss of USS Minntac Coupons, mg

Coupon	10 days	20 days	30 days
UM1	6.00	3.00	5.00
UM2	0.00	3.00	3.00
UM3	1.00	3.00	1.00
UM4	3.00	3.00	5.00
UM5	-3.00	-2.00	-3.00
UM6	1.00	1.00	-1.00
UM7	7.00	2.00	4.00
UM8	-3.00	-2.00	-2.00
UM9	1.00	-1.00	1.00

COMPARISON

Table 18 provides a summary of relative changes of elements of interest on testing coupon surfaces that experienced different testing conditions. The three coupon sets behaved quite similarly in typical taconite flue gas: limited surface corrosion, mainly with losses of Fe and Ni at 500°C. This corrosion decreased with lowering temperature. As bromine was introduced into the flue gas, all three coupon sets seemed to experience surface attack not only at 500°C but also to some degree at lower temperatures of 300° and 150°C, although corrosion was most obvious at 500°C. The UM coupons seem to indicate more surface reaction than the M and U coupons in bromine-containing taconite flue gas. Iron oxide/sodium sulfate deposition may induce more changes to M and U coupons than UM coupons.

CONCLUSIONS

The EERC was contracted by the Minnesota Department of Natural Resources to perform laboratory corrosion testing on coupons supplied by three Minnesota taconite plants. The bench-scale testing was the first step to determine if the introduction of 40 ppm HBr to flue gas would potentially cause corrosion in taconite facility process equipment. Two simultaneous

Table 18. Relative Elemental Changes of Cr, Fe, and Ni on Testing Coupon Surface

	Cr	Fe	Ni		Cr	Fe	Ni		Cr	Fe	Ni
M1	26.49%	-32.76%	-60.76%	U1	-22.33%	10.66%	-39.64%	UM1	-29.22%	-3.51%	-57.67%
M2	-6.19%	8.56%	-41.14%	U2	-35.63%	29.24%	-52.72%	UM2	-34.29%	25.86%	-44.21%
M3	-47.59%	26.97%	-60.76%	U3	-18.19%	23.64%	-46.88%	UM3	0.07%	-4.61%	-10.99%
M4	50.34%	-29.13%	-67.30%	U4	-22.94%	13.49%	-39.03%	UM4	78.78%	-53.65%	-78.66%
M5	-6.88%	-4.95%	-18.78%	U5	7.80%	-6.96%	-9.26%	UM5	-44.68%	-39.61%	-31.80%
M6	-3.73%	-7.33%	-14.98%	U6	20.35%	-13.26%	-17.10%	UM6	-53.38%	-45.35%	-44.15%
M7	87.40%	-46.63%	-78.90%	U7	42.29%	-25.03%	-78.40%	UM7	108.22%	-60.88%	-84.60%
M8	-10.82%	6.88%	-1.69%	U8	-2.59%	-0.67%	-16.03%	UM8	10.32%	-11.35%	-24.63%
M9	-43.18%	-23.66%	-7.38%	U9	-7.66%	-4.96%	-10.26%	UM9	-2.24%	-9.03%	-19.64%

exposure tests were completed with representative taconite flue gas and flue gas spiked with 40 ppm HBr. The coupon sets were subjected to 30 days of exposure and then analyzed for corrosive activity and bromine deposition. The preliminary test results are given below:

1. Adding 40 ppm HBr to taconite process flue gas appears to cause slight surface corrosion of the test coupons. SEM surface microscopy showed small pitting, cracking, and blistering occurred with bromine deposition and losses of Fe, Cr, and Ni.
2. However, coupon cross-sectional analyses indicated that bromine deposition and losses of Fe, Ni, and Cr were mainly confined to the surface of the coupons, and no significant bromine penetration and subsequent elemental changes were observed below the coupon surface after 30 days of exposure experiments.
3. Coupon surface corrosion appears to be less with decreasing temperature.
4. All three coupon sets show resistance to bromine attack under testing environments during the 30-day testing period.
5. Deposits of iron oxide and sodium sulfate seem to induce slight chemistry changes on U and M coupons but not on UM coupons.

It should be noted that, because of limited time and scope of work, the completed corrosion exposure tests were carried out in simplified simulated flue gas environments that did not represent 100% actual operating conditions in the taconite process. The original objective of this project is to see if bromine could cause any possible corrosion under selected testing conditions, while the 30-day exposure testing period may not necessarily be long enough to attain a complete perspective of possible bromine-induced corrosion issues in a taconite facility. Therefore, the project results can be regarded as the first step in the effort to address potential bromine-induced corrosion as bromine is applied to a taconite facility for mercury reduction. Additional bench-scale coupon corrosion tests under continuous thermal cycling with wider temperature regimes and extended exposure times are needed before any large-scale field testing.

ACKNOWLEDGMENT

The EERC acknowledges the financial support of the Minnesota Department of Natural Resources on this project. The EERC would also like to extend its gratitude to the taconite industry that has provided valuable input on this project. Special thanks to Harold Kokal and Jon Maki from ArcelorMital and Global for helping to prepare the testing coupons.

REFERENCES

1. Berndt, M.E. *On the Measurement of Stack Emissions at Taconite Processing Plants*; Progress Report to Minnesota Pollution Control Agency, May 2008.
2. Zhuang, Y.; Thompson, J.S.; Zygarlicke, C.J.; Pavlish, J.H. Impact of Calcium Chloride Addition on Mercury Transformations and Control in Coal Flue Gas. *Fuel* **2007**, *86* (15), 2351–2359.
3. Zhuang, Y.; Zygarlicke, C.J.; Thompson, J.S.; Pavlish, J.H. Chlorine-Induced Mercury Transformation in a High-Temperature Coal Flue Gas. In *Proceedings of Air Quality V: Mercury, Trace Elements, SO₃, and Particulate Matter Conference*; Arlington, VA, Sept 19–21, 2005.
4. Zhuang, Y.; Laumb, J.; Liggett, R.; Holmes, M.J.; Pavlish, J.H. Impacts of Acid Gases on Mercury Oxidation Across SCR Catalyst. *Fuel Process. Technol.* **2007**, *88*, 929–934.
5. Pavlish, J.H. Understanding Mercury Speciation, Variability, and Operational Impact on Mercury Control. Presented at Mercury 2006, 8th International Conference on Mercury as a Global Pollutant, Madison, WI, Aug 6–11, 2006; Paper No. S-662.
6. Pavlish, J.H.; Sondreal, E.A.; Mann, M.D.; Olson, E.S.; Galbreath, K.C.; Laudal, D.L.; Benson, S.A. A Status Review of Mercury Control Options for Coal-Fired Power Plants. *Special Mercury Issue of Fuel Process. Technol.* **2003**, *82* (2–3), 89–165.
7. Liu, S.; Yan, N.; Liu, Z. Using Bromine Gas to Enhance Mercury Removal from Flue Gas of Coal-Fired Power Plants. *Environ. Sci. Technol.* **2007**, *41* (4) 1405–1412.
8. Berndt, M.E.; Engesser, J. Mercury Transport in Taconite Processing Facilities: (III) Control Method Test Results; Iron Ore Cooperative Research Final Report, Dec 2007.
9. Pavlish, J.H.; Zhuang, Y. *Proof-of-Concept Testing of Novel Mercury Control Technology for a Minnesota Taconite Plant*; EERC Technical Report to Minnesota Department of Natural Resources; 2008-EERC-07-02. Energy & Environmental Research Center: Grand Forks, ND, 2008.
10. Zhuang, Y.; Chen, C.; Timpe, R.; Pavlish, J.H. Investigations on Bromine Corrosion Associated Mercury Control Technologies in Coal Flue Gas. *Fuel* **2008**, *88* (9), 1692–1697.

APPENDIX A

UNITED COUPON SEM ANALYSIS

UNITED COUPON SEM ANALYSIS

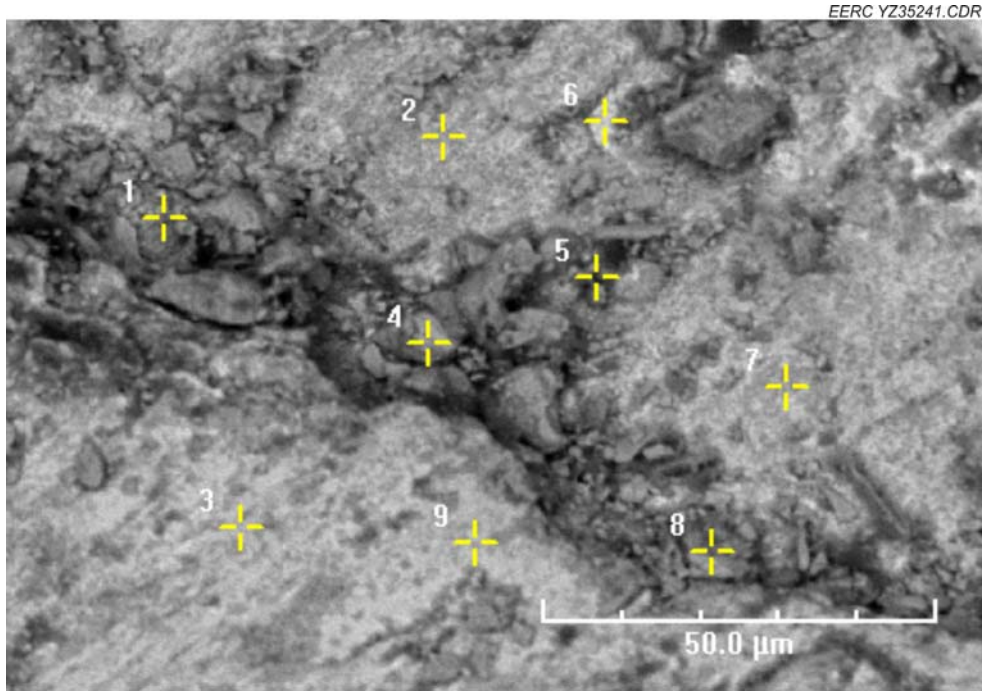


Figure A-1. U1 surface SEM image.

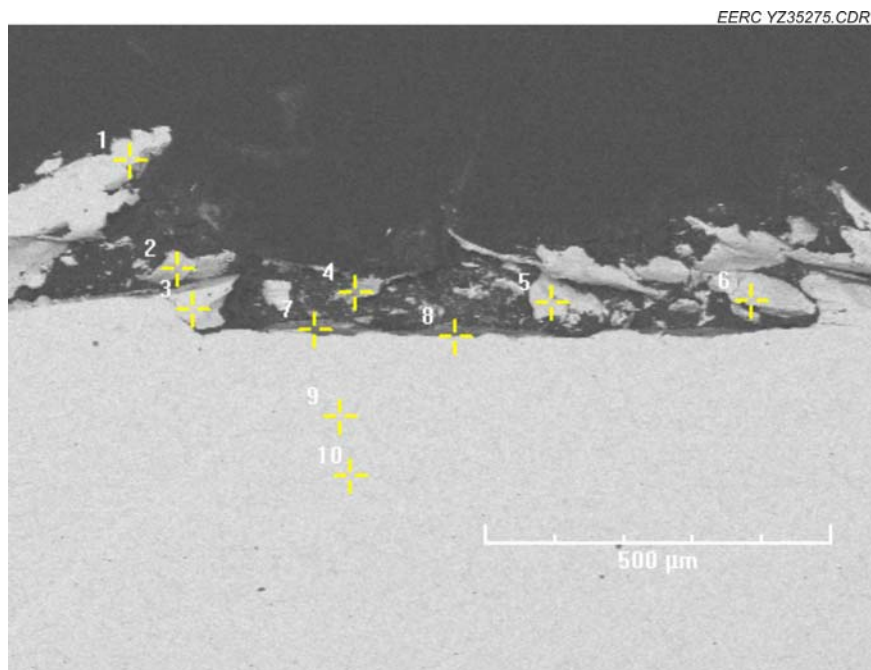


Figure A-2. U1 cross-sectional SEM image.

Table A-1. Elemental Analysis on U1 Cross Section

Tag	Si	S	Cr	Mn	Fe	Co	Ni	Br
1	2.92%	0.52%	24.40%	0.00%	54.96%	0.00%	15.94%	1.24%
2	3.56%	1.03%	28.47%	0.46%	51.50%	0.00%	14.32%	0.65%
3	3.10%	0.89%	28.10%	0.59%	52.33%	0.00%	14.43%	0.57%
4	3.24%	0.70%	29.22%	0.60%	51.62%	0.00%	13.78%	0.84%
5	2.82%	0.32%	25.82%	0.33%	54.85%	0.00%	15.13%	0.73%
6	3.77%	1.10%	39.13%	0.24%	43.24%	0.00%	11.16%	1.35%
7	12.40%	1.01%	47.36%	5.04%	25.36%	0.00%	3.19%	5.49%
8	9.89%	0.88%	30.79%	0.00%	46.92%	0.00%	10.27%	1.25%
9	2.90%	0.25%	25.33%	0.12%	55.07%	0.10%	14.96%	1.26%
10	2.98%	0.41%	26.40%	0.28%	53.73%	0.00%	15.09%	1.12%

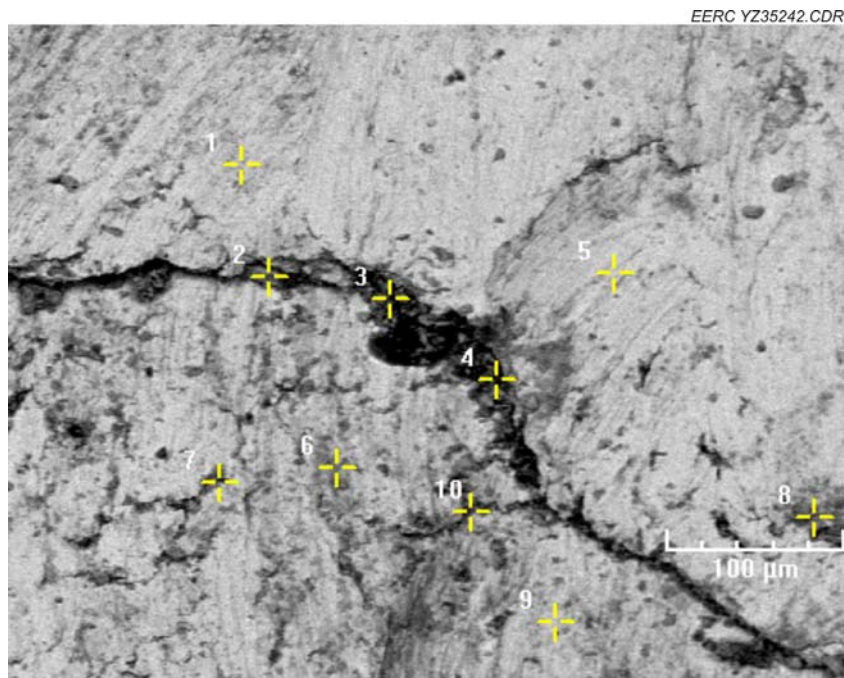


Figure A-3. U2 surface SEM image.

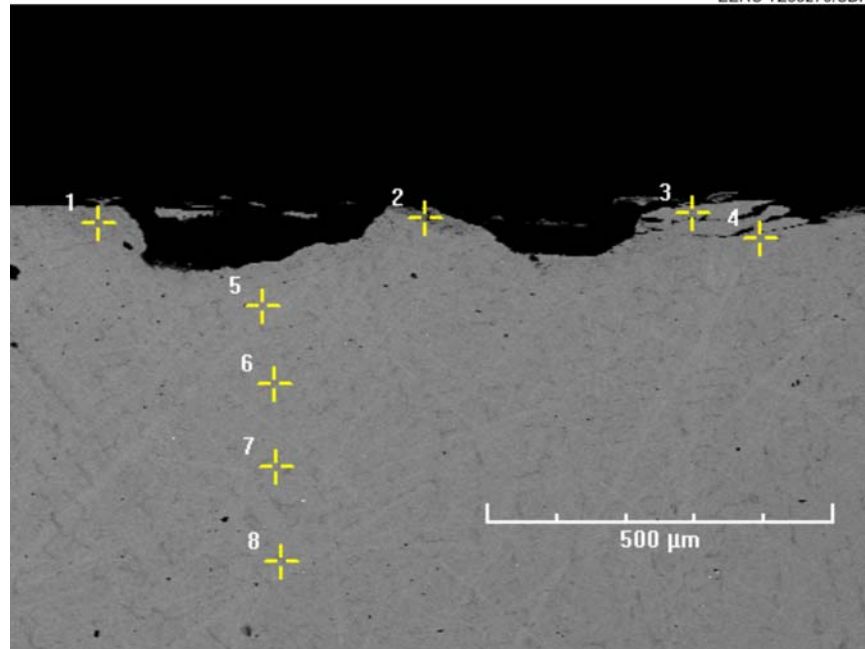


Figure A-4. U2 cross-sectional SEM image.

Table A-2. Elemental Analysis of U2 Cross Section

Tag	Si	S	Cr	Mn	Fe	Co	Ni	Br
1	10.09%	0.58%	26.61%	0.65%	47.72%	0.00%	13.48%	0.82%
2	14.74%	0.48%	26.12%	0.18%	43.42%	0.00%	12.57%	2.40%
3	4.84%	0.37%	24.79%	0.41%	54.39%	0.01%	14.36%	0.81%
4	4.09%	0.39%	27.55%	0.06%	52.58%	0.00%	14.73%	0.60%
5	2.79%	0.39%	27.18%	0.46%	53.14%	0.00%	15.06%	0.97%
6	2.70%	0.26%	26.62%	0.37%	54.42%	0.00%	14.55%	1.05%
7	2.51%	0.38%	25.73%	0.39%	54.63%	0.00%	15.07%	1.23%
8	0.54%	0.68%	85.89%	0.00%	11.45%	0.00%	0.06%	1.33%

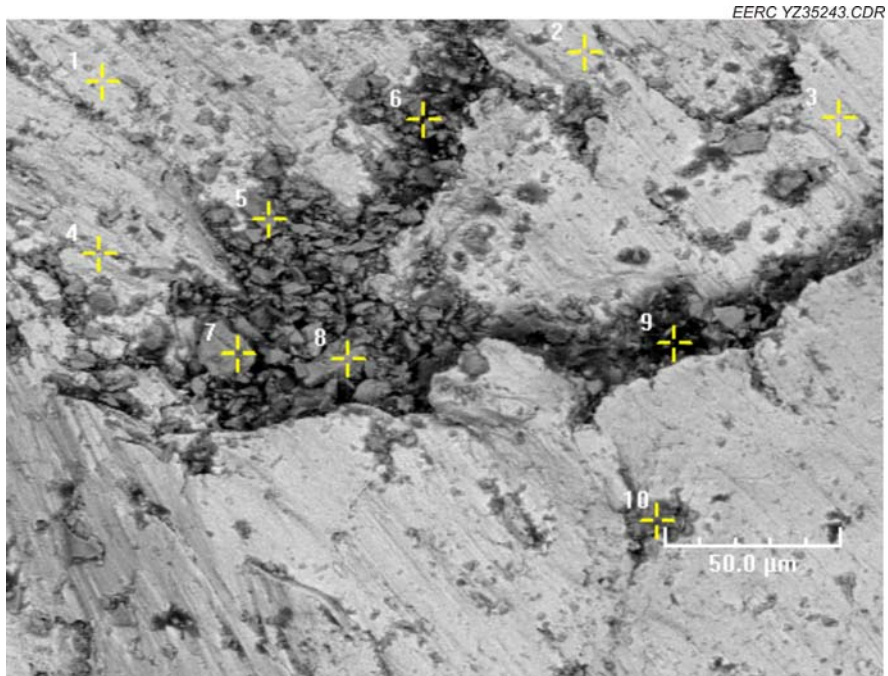


Figure A-5 U3 surface SEM image.

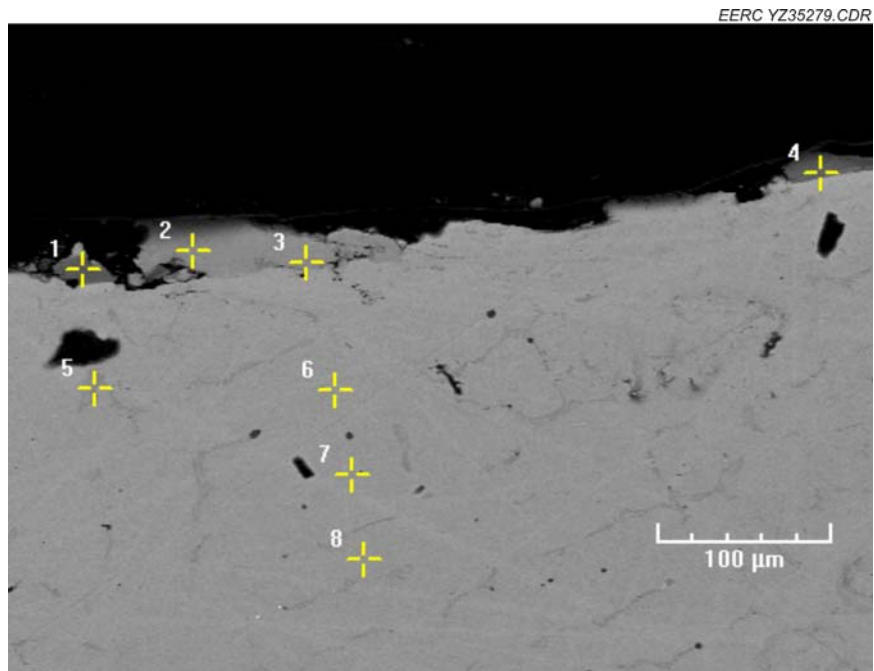


Figure A-6. U3 cross-sectional SEM image.

Table A-3. Elemental Analysis of U3 Cross Section

Tag	Si	S	Cr	Mn	Fe	Co	Ni	Br
1	1.58%	0.04%	30.33%	1.17%	55.04%	0.00%	11.82%	0.00%
2	0.02%	0.00%	25.79%	0.65%	57.47%	0.00%	15.92%	0.00%
3	0.00%	0.00%	26.09%	0.70%	56.22%	0.00%	16.84%	0.00%
4	0.14%	0.00%	27.93%	0.89%	57.51%	0.00%	13.53%	0.00%
5	4.27%	0.44%	26.18%	0.49%	52.59%	0.14%	15.08%	0.80%
6	3.47%	0.40%	26.37%	0.26%	53.70%	0.00%	14.64%	1.14%
7	3.31%	0.38%	30.00%	0.29%	50.71%	0.00%	14.28%	0.92%
8	3.70%	0.34%	25.79%	0.29%	54.65%	0.00%	14.65%	0.59%

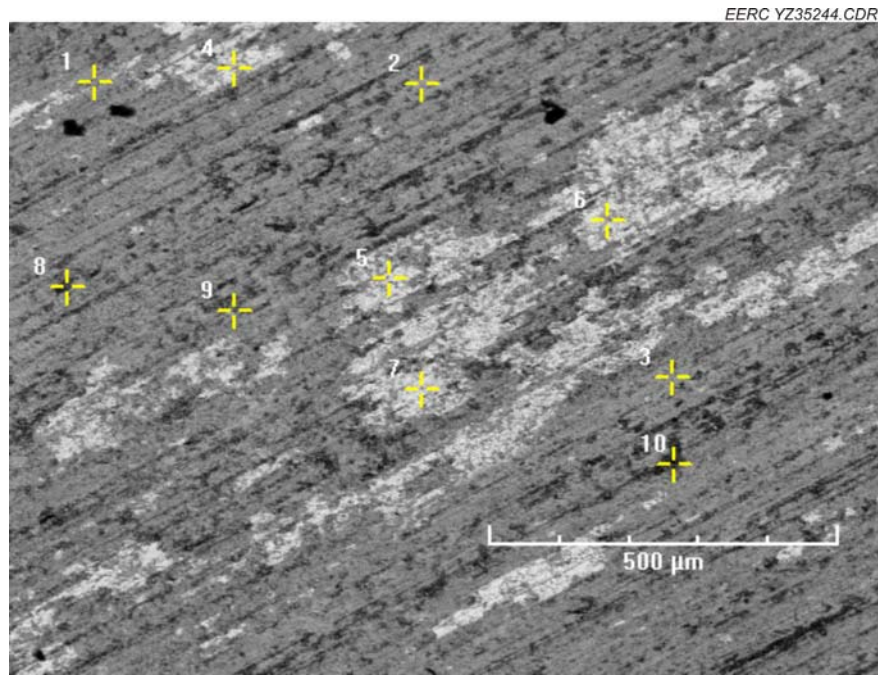


Figure A-7. U4 surface SEM image.

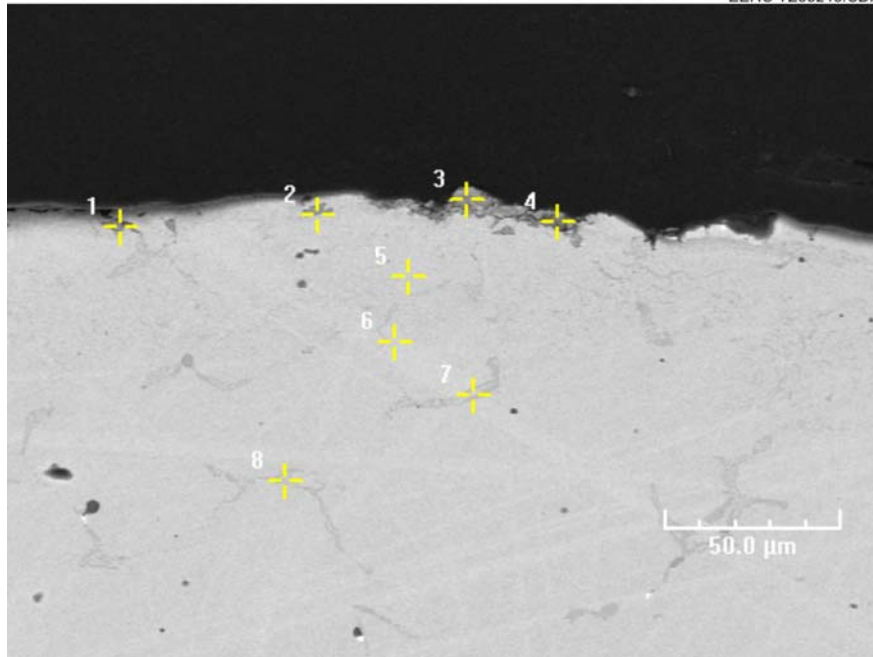


Figure A-8. U4 cross-sectional SEM image.

Table A-4. Elemental Analysis of U4 Cross Section

Tag	Si	S	Cr	Mn	Fe	Co	Ni	Br
1	3.09%	0.90%	16.24%	0.00%	61.59%	0.00%	18.08%	0.00%
2	7.57%	0.54%	23.58%	0.21%	50.50%	0.00%	15.75%	1.86%
3	5.90%	0.58%	79.87%	3.61%	4.82%	0.00%	1.51%	3.71%
4	12.35%	1.36%	55.80%	4.43%	16.91%	0.00%	7.38%	1.71%
5	2.65%	0.39%	26.22%	0.00%	55.20%	0.00%	14.49%	0.97%
6	3.07%	0.51%	27.26%	0.72%	52.08%	0.00%	14.69%	1.66%
7	2.40%	0.87%	60.00%	0.07%	30.25%	0.00%	5.32%	1.09%
8	2.22%	0.59%	52.67%	0.44%	35.85%	0.01%	7.41%	0.73%

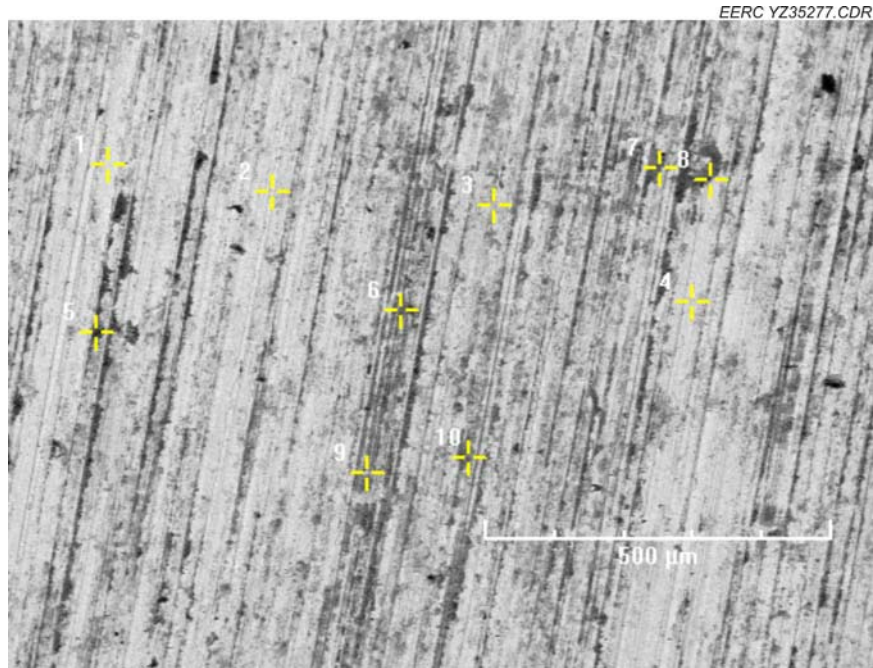


Figure A-9. U5 surface SEM image

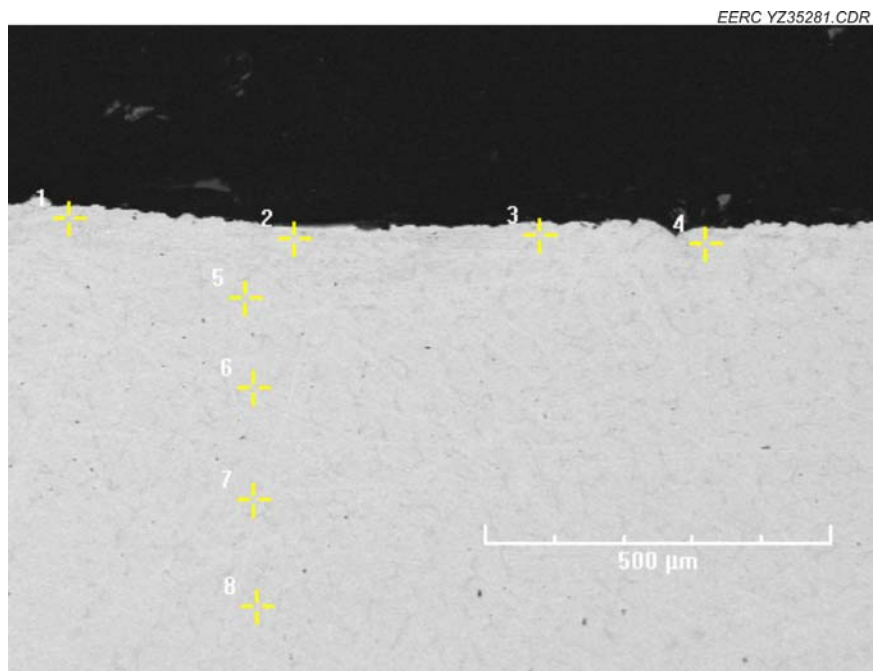


Figure A-10. U5 cross-sectional SEM image.

Table A-5. Elemental Analysis of U5 Cross-Section

Tag	Si	S	Cr	Mn	Fe	Co	Ni	Br
1	3.23%	1.14%	46.18%	0.19%	38.99%	0.00%	9.59%	0.67%
2	4.16%	0.43%	27.70%	0.43%	52.12%	0.00%	13.82%	1.35%
3	3.76%	0.62%	28.76%	0.50%	50.21%	0.00%	15.06%	1.09%
4	2.56%	0.23%	26.44%	0.40%	54.16%	0.00%	14.84%	1.28%
5	2.97%	0.40%	28.62%	0.28%	51.59%	0.00%	15.19%	0.94%
6	2.24%	0.22%	25.64%	0.36%	55.66%	0.00%	14.96%	0.93%
7	2.38%	0.22%	25.56%	0.01%	55.65%	0.00%	15.08%	1.09%
8	2.60%	0.35%	26.02%	0.42%	54.63%	0.00%	14.89%	1.07%

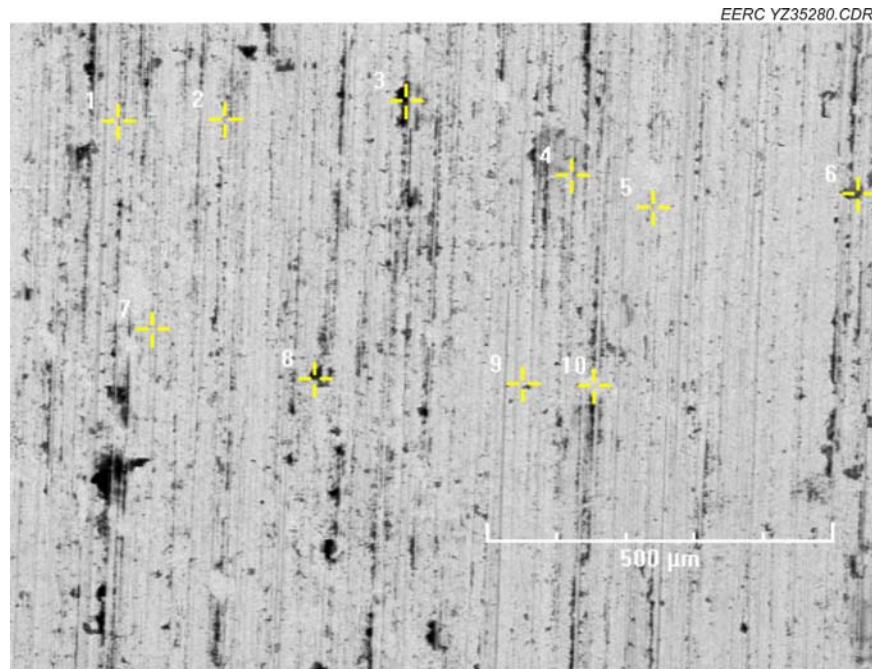


Figure A-11. U6 surface SEM image.

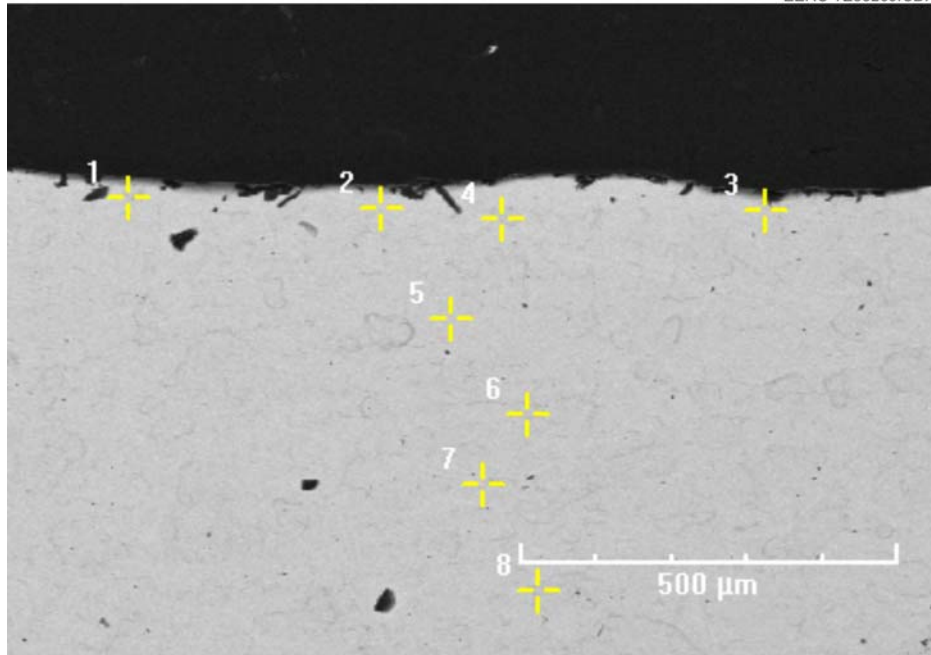


Figure A-12. U6 cross-sectional SEM image.

Table A-6 Elemental Analysis on U6 Cross Section Image

Tag	Si	S	Cr	Mn	Fe	Co	Ni	Br
1	16.33%	1.24%	25.45%	0.27%	44.44%	0.00%	11.66%	0.51%
2	2.97%	0.37%	25.96%	0.34%	54.56%	0.00%	14.92%	0.88%
3	3.30%	0.31%	26.31%	0.54%	53.04%	0.29%	15.06%	1.06%
4	2.52%	0.77%	59.67%	0.00%	29.16%	0.00%	6.95%	0.94%
5	2.55%	0.31%	25.38%	0.39%	54.92%	0.14%	14.96%	1.28%
6	5.30%	0.56%	28.62%	0.56%	48.96%	0.00%	14.56%	1.43%
7	4.41%	0.72%	26.68%	0.51%	51.59%	0.00%	14.76%	1.29%
8	2.96%	0.36%	24.95%	0.43%	55.41%	0.00%	14.69%	1.19%

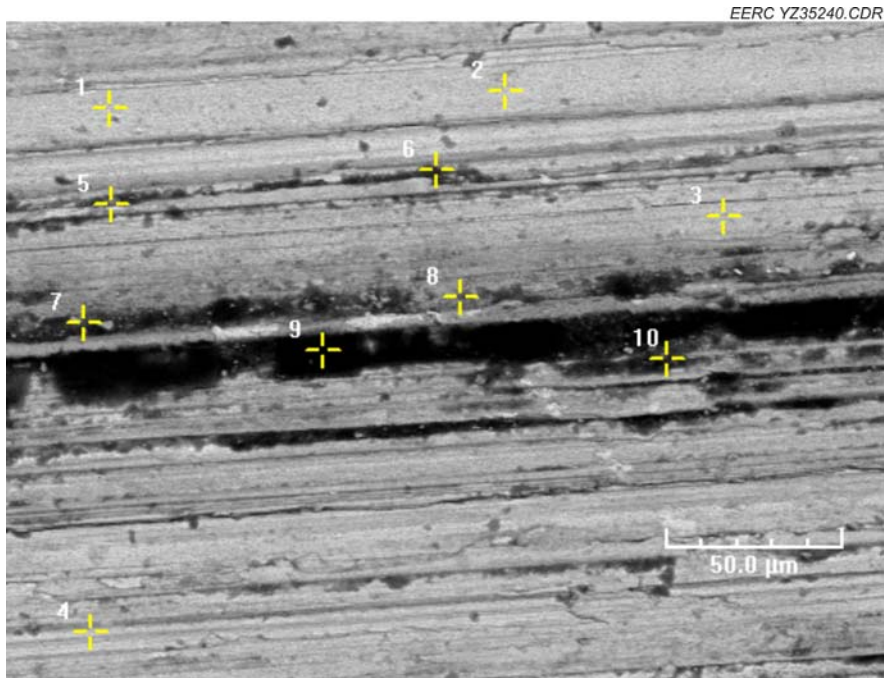


Figure A-13. U7 surface SEM image.

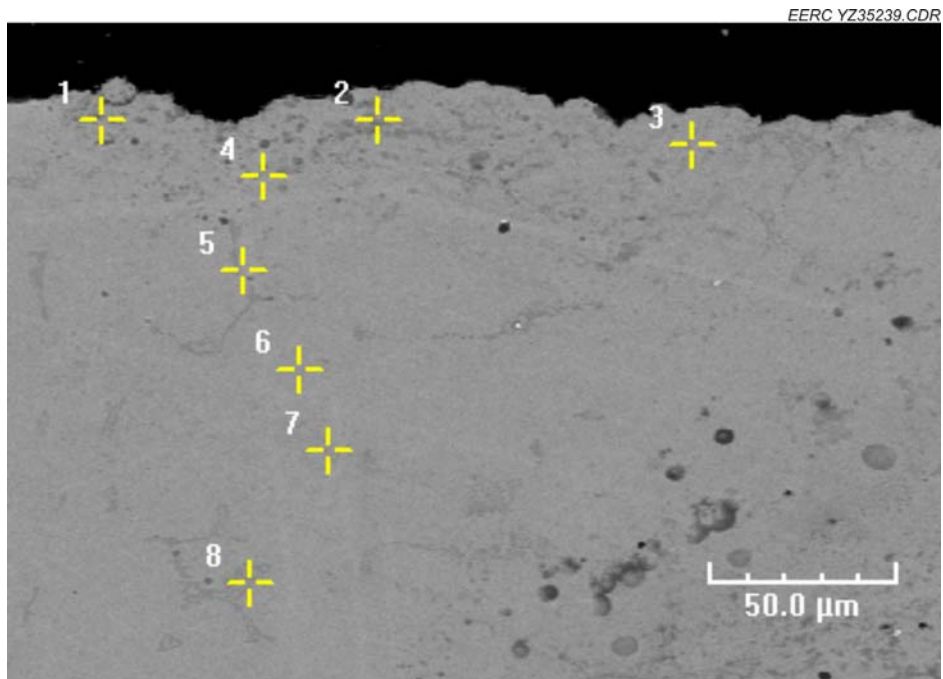


Figure A-14. U7 cross-sectional SEM image.

Table A-7. Elemental Analysis of U7 Cross Section

Tag	Si	S	Cr	Mn	Fe	Co	Ni
1	1.78%	0.50%	50.52%	0.71%	37.11%	0.00%	9.34%
2	5.68%	2.01%	26.56%	0.23%	51.25%	0.00%	14.02%
3	3.19%	0.50%	26.32%	0.43%	54.76%	0.00%	14.71%
4	6.63%	0.52%	26.84%	0.15%	51.56%	0.00%	14.29%
5	4.23%	1.02%	28.45%	0.17%	52.28%	0.00%	13.81%
6	4.69%	0.30%	24.75%	0.37%	55.35%	0.00%	14.45%
7	3.04%	0.45%	26.36%	0.18%	54.15%	0.00%	15.72%
8	3.73%	0.43%	27.20%	0.78%	52.81%	0.00%	14.96%

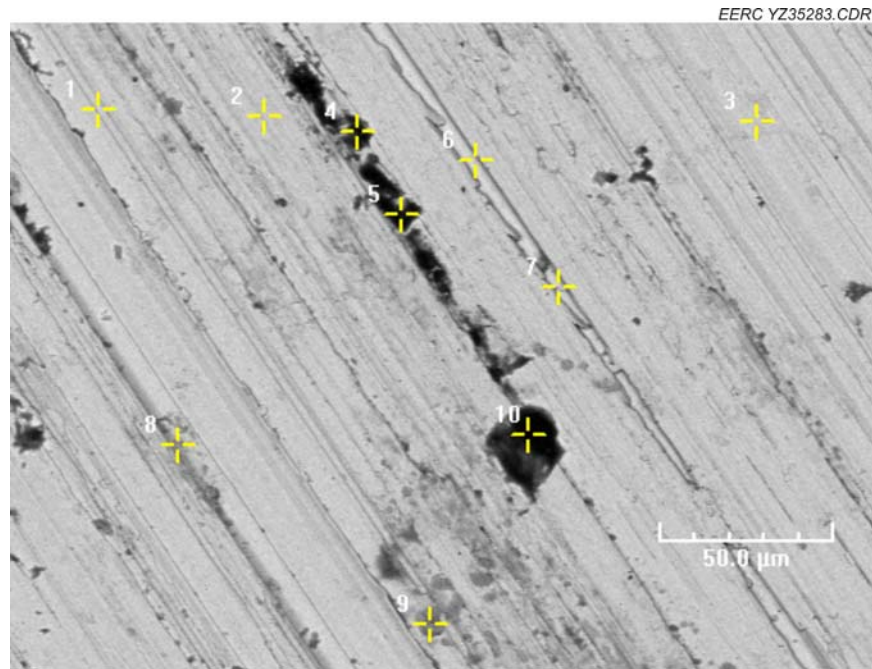


Figure A-15. U8 surface SEM image.

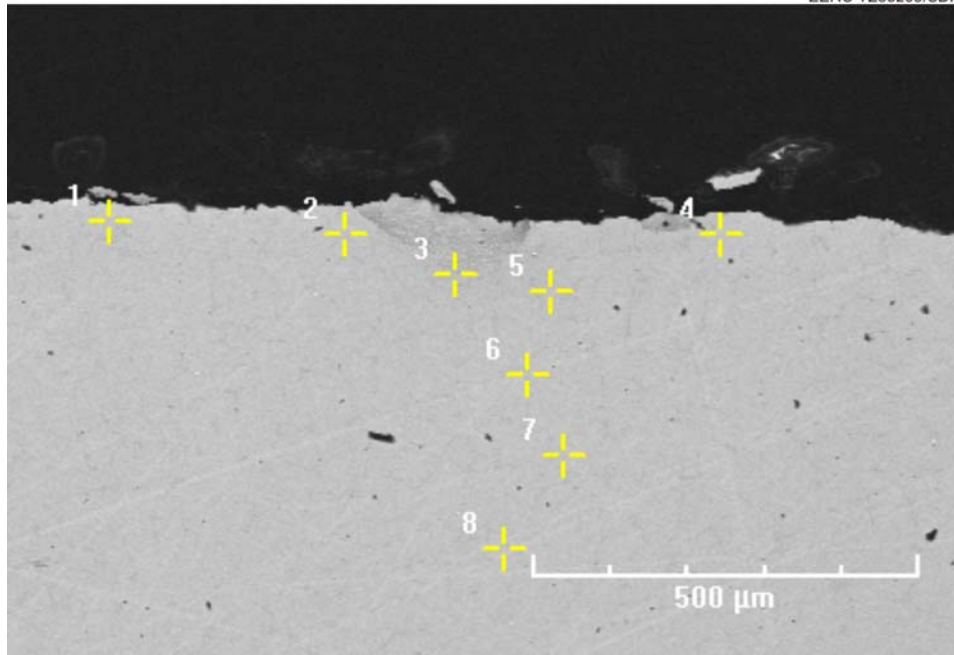


Figure A-16. U8 cross-sectional SEM image.

Table A-8. Elemental Analysis of U8 Cross Section

Tag	Si	S	Cr	Mn	Fe	Co	Ni
1	3.76%	0.62%	45.98%	0.50%	38.91%	0.00%	10.14%
2	5.16%	0.39%	27.95%	0.15%	51.50%	0.00%	14.85%
3	7.39%	0.49%	26.39%	0.61%	50.91%	0.02%	14.18%
4	3.87%	0.20%	26.23%	0.25%	54.65%	0.00%	14.80%
5	4.78%	0.33%	26.00%	0.46%	53.90%	0.00%	14.49%
6	4.00%	0.38%	29.34%	0.13%	51.41%	0.00%	14.75%
7	2.99%	0.31%	27.80%	0.15%	54.19%	0.00%	14.42%
8	2.37%	0.27%	25.48%	0.29%	56.92%	0.00%	14.60%

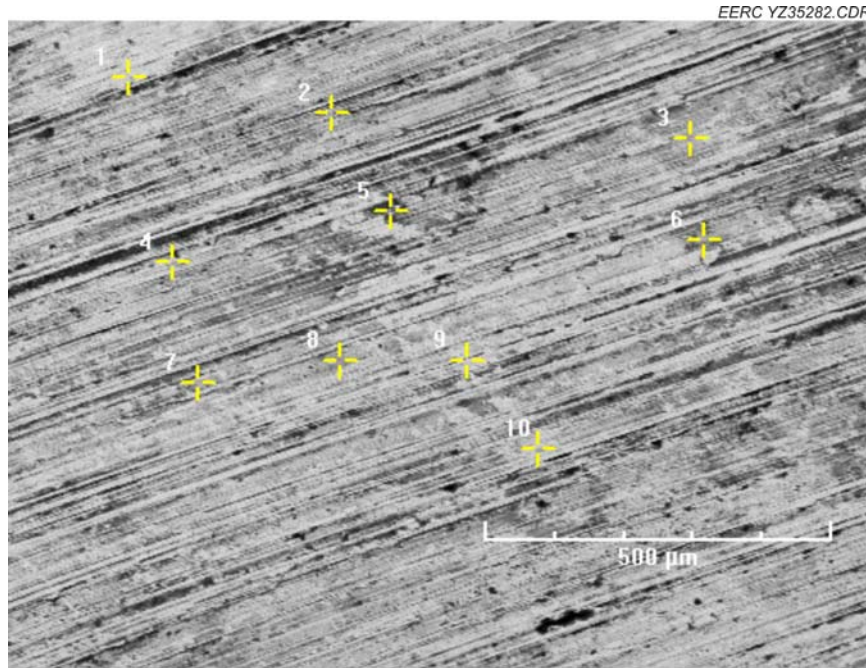


Figure A-17. U9 surface SEM image

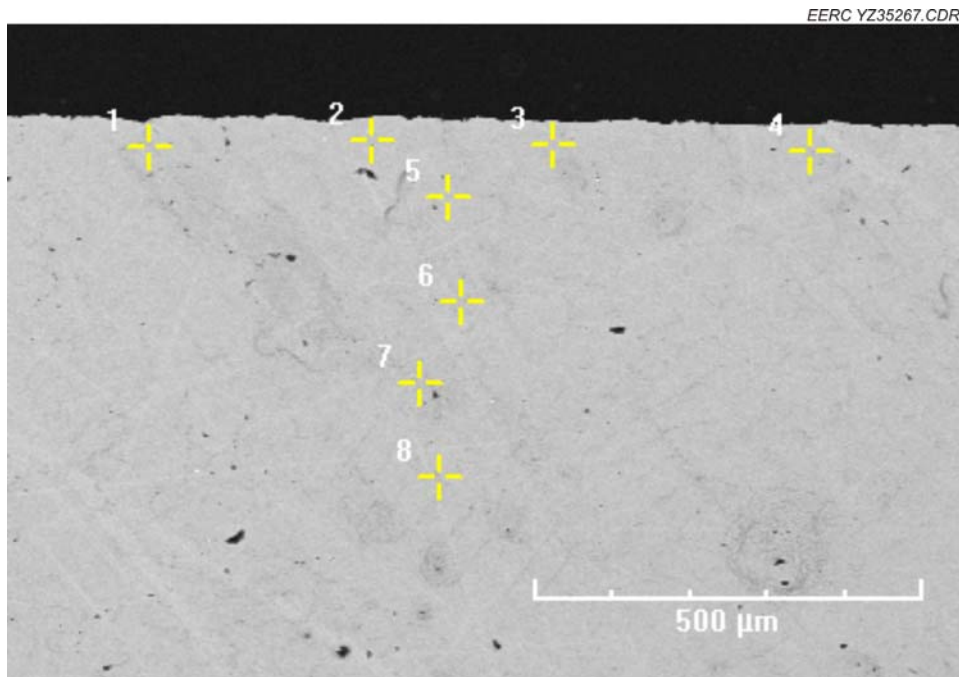


Figure A-18. U9 cross-sectional SEM image.

Table A-9. Elemental Analysis of U9 Cross Section

Tag	Si	S	Cr	Mn	Fe	Co	Ni
1	2.93%	0.32%	25.14%	0.49%	56.54%	0.00%	14.59%
2	3.31%	0.27%	28.23%	0.65%	52.09%	0.19%	15.23%
3	2.94%	0.24%	27.02%	0.21%	54.18%	0.00%	15.42%
4	4.01%	0.53%	29.70%	0.52%	50.64%	0.00%	14.58%
5	4.21%	0.28%	25.78%	0.47%	54.83%	0.00%	14.42%
6	3.43%	0.43%	28.17%	0.42%	51.63%	0.00%	15.83%
7	5.50%	0.56%	29.15%	0.00%	50.16%	0.00%	14.63%
8	4.06%	0.31%	27.86%	0.41%	52.62%	0.00%	14.66%

APPENDIX B

MINORCA COUPON SEM ANALYSIS

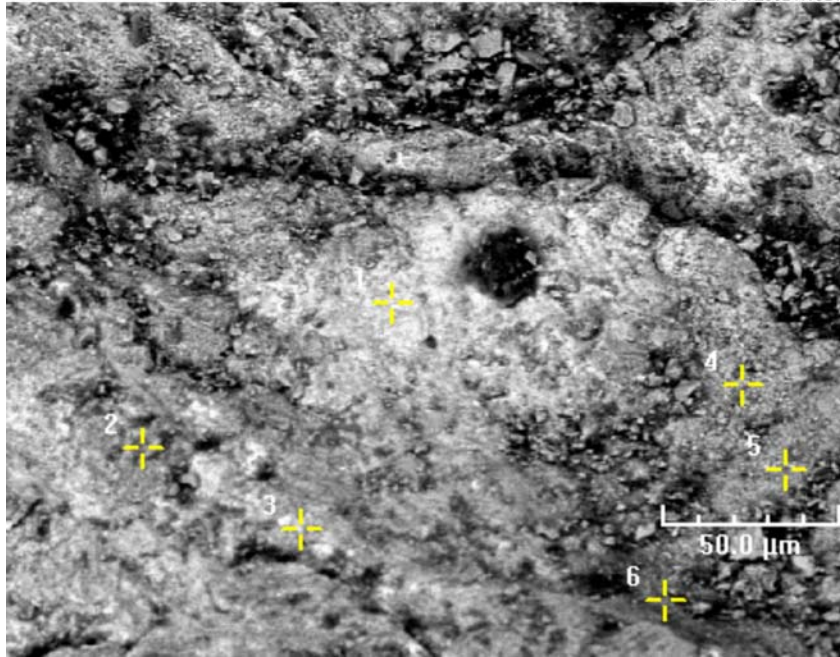


Figure B-1. M1 surface SEM image.

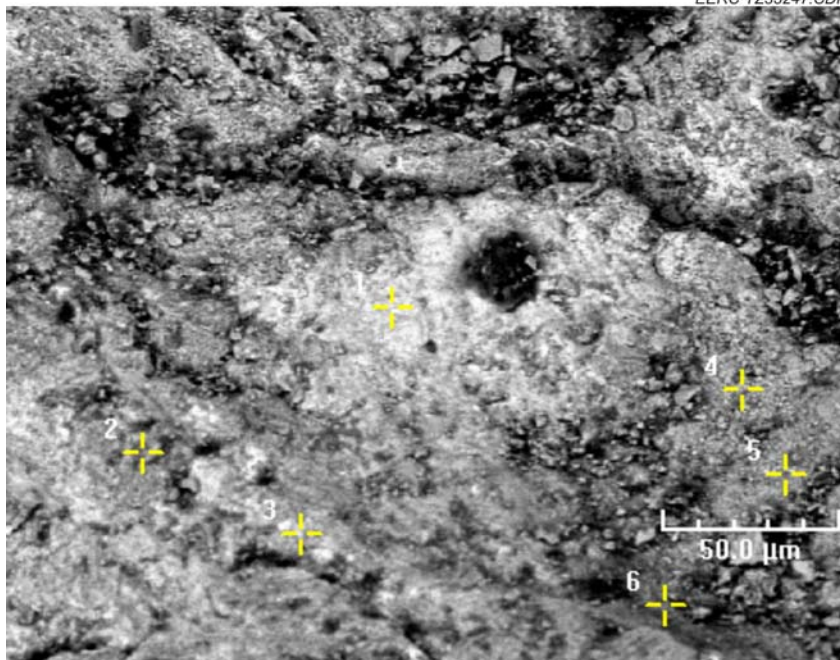


Figure B-2. M1 cross-sectional SEM image.

Table B-1. Elemental Analysis on M1 Cross Section

Tag	Si	S	Cr	Mn	Fe	Co	Ni	Br
1	6.14%	0.79%	22.96%	0.00%	57.56%	0.00%	3.55%	9.00%
2	4.14%	0.23%	25.42%	0.17%	63.54%	0.00%	4.30%	2.20%
3	4.82%	0.32%	29.47%	0.00%	55.97%	0.00%	3.66%	5.76%
4	3.32%	0.54%	16.27%	0.00%	73.06%	0.00%	4.58%	2.23%
5	11.85%	0.04%	22.64%	0.00%	62.29%	0.00%	1.16%	2.02%
6	1.54%	0.57%	1.91%	0.00%	90.98%	0.00%	0.00%	5.00%
7	4.13%	0.34%	26.80%	0.09%	61.59%	0.00%	5.19%	1.86%
8	3.58%	0.29%	25.38%	0.29%	64.30%	0.02%	4.90%	1.17%
9	3.43%	0.28%	33.36%	0.09%	56.94%	0.00%	4.62%	1.25%
10	3.39%	0.18%	26.02%	0.18%	63.54%	0.12%	5.13%	1.32%

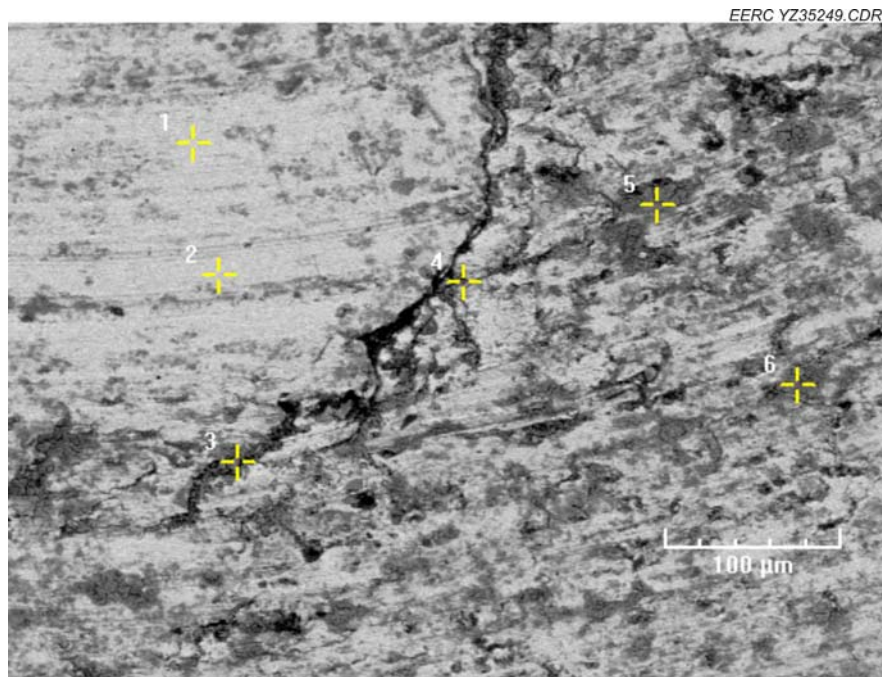


Figure B-3. M2 surface SEM image.

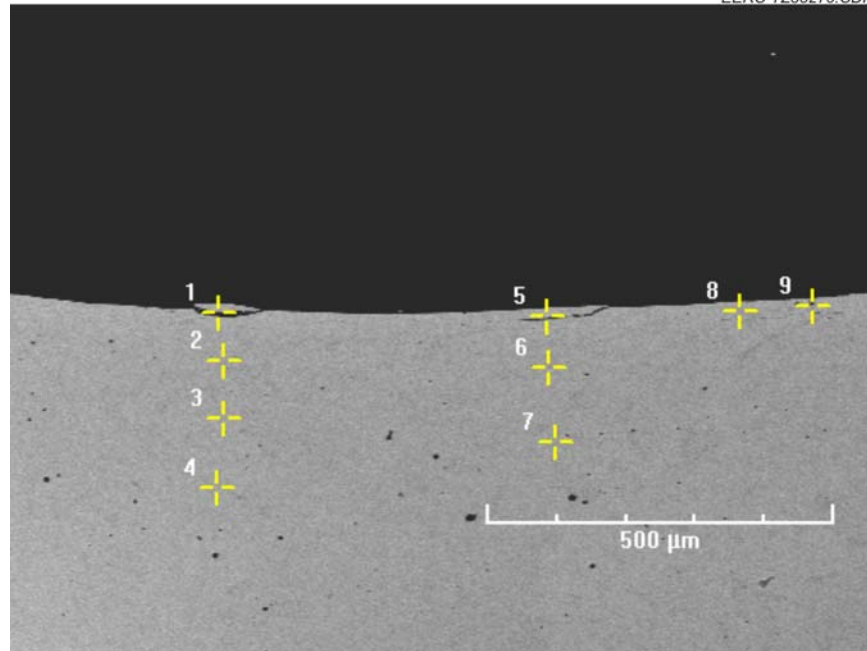


Figure B-4. M2 cross-sectional SEM image.

Table B-2 Elemental Analysis on M2 Cross Section

Tag	Si	S	Cr	Mn	Fe	Co	Ni	Br
1	14.15%	0.20%	10.28%	0.00%	40.67%	0.00%	0.00%	34.66%
2	7.29%	0.43%	29.29%	0.00%	57.24%	0.00%	2.11%	3.64%
3	7.27%	0.37%	29.40%	0.00%	57.35%	0.00%	2.29%	3.33%
4	7.08%	0.27%	29.13%	0.00%	57.32%	0.00%	3.11%	3.01%
5	8.42%	0.00%	25.14%	0.00%	42.16%	0.00%	1.05%	23.23%
6	7.44%	0.25%	30.41%	0.00%	55.06%	0.00%	3.31%	3.53%
7	6.42%	0.16%	28.14%	0.00%	58.75%	0.00%	4.17%	2.36%
8	6.70%	0.14%	31.97%	0.00%	56.49%	0.00%	2.50%	2.17%
9	7.60%	1.10%	29.26%	0.24%	55.55%	0.00%	2.62%	3.63%

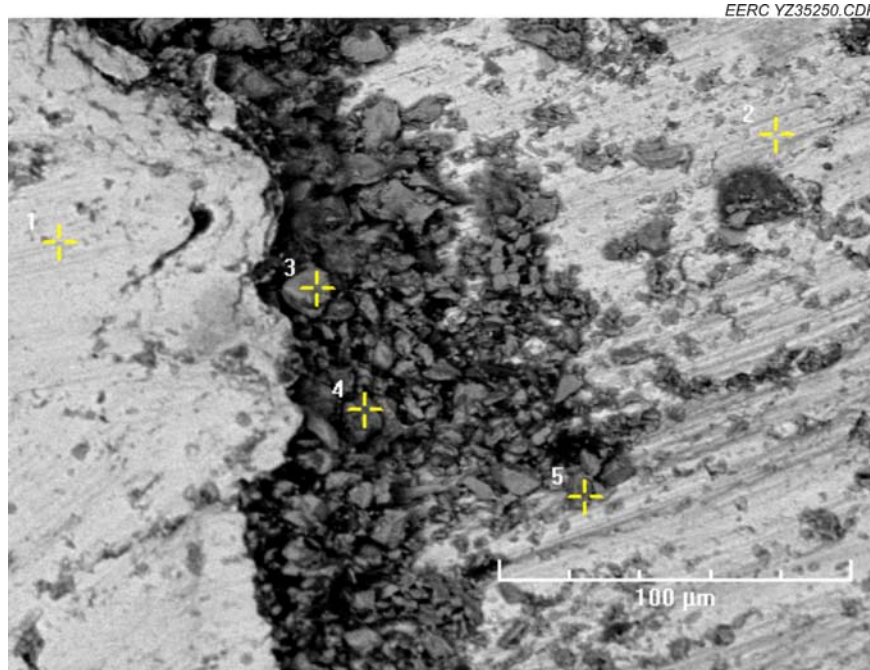


Figure B-5. M3 surface SEM image.

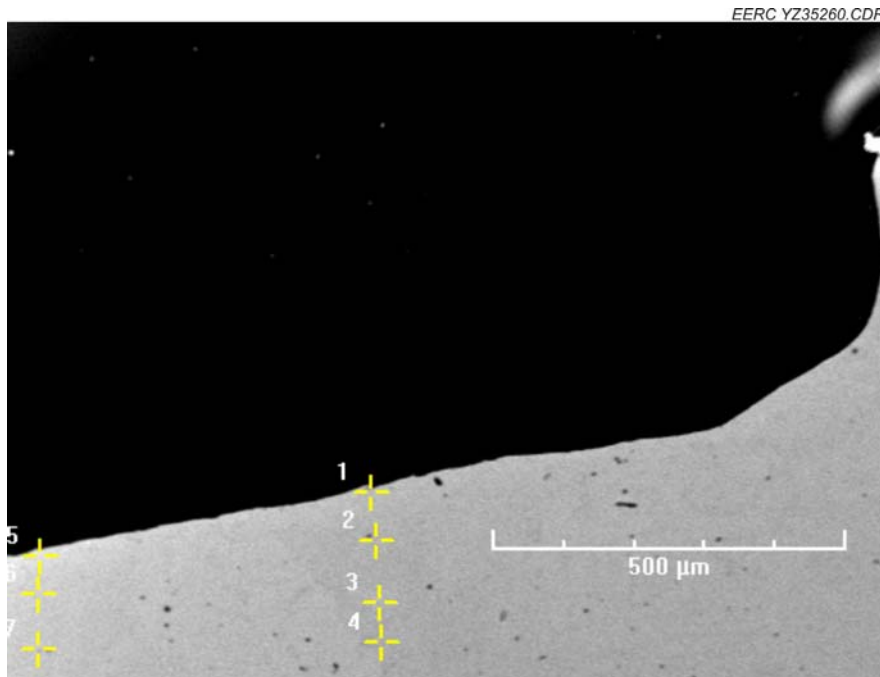


Figure B-6. M3 cross-sectional SEM image.

Table B-3. Elemental Analysis on Cross Section of M3

Tag	Si	S	Cr	Mn	Fe	Co	Ni	Br
1	9.24%	0.00%	31.68%	0.00%	53.12%	0.00%	1.97%	3.86%
2	8.07%	0.48%	28.03%	0.00%	54.98%	0.00%	2.30%	6.08%
3	7.50%	0.47%	30.11%	0.23%	55.14%	0.00%	2.91%	3.58%
4	7.01%	0.13%	29.46%	0.08%	57.41%	0.00%	2.90%	2.81%
5	6.88%	0.38%	27.59%	0.00%	58.04%	0.00%	2.50%	4.62%
6	6.49%	0.35%	29.54%	0.00%	58.14%	0.00%	2.94%	2.52%
7	6.82%	0.15%	28.41%	0.13%	57.49%	0.00%	2.72%	4.28%

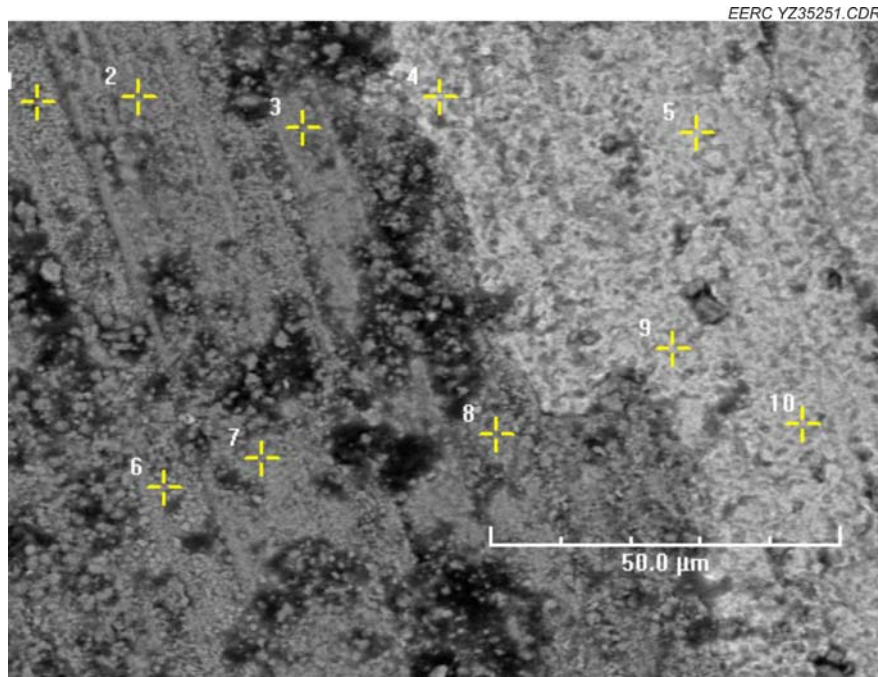


Figure B-7. M4 surface SEM image.

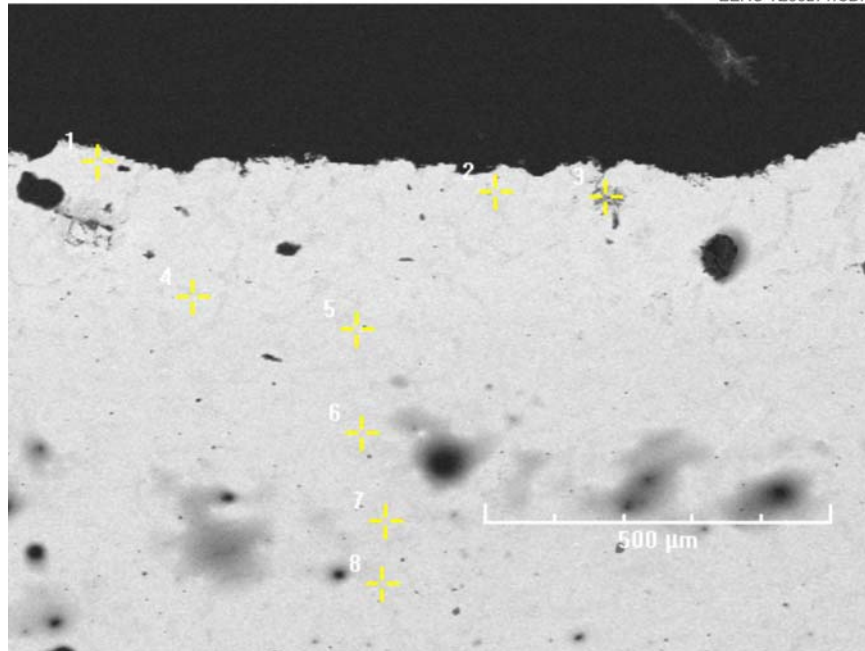


Figure B-8. M4 cross-sectional SEM image.

Table B-4. Elemental Analysis of Cross Section of M4

Tag	Si	S	Cr	Mn	Fe	Co	Ni	Br
1	3.87%	0.35%	24.42%	0.07%	63.83%	0.00%	5.26%	2.15%
2	4.30%	0.16%	25.68%	0.34%	61.38%	0.21%	5.18%	2.76%
3	3.85%	0.58%	26.25%	0.21%	60.70%	0.00%	4.96%	3.46%
4	4.04%	0.08%	25.70%	0.00%	63.82%	0.00%	4.47%	1.80%
5	3.82%	0.19%	27.74%	0.08%	62.15%	0.00%	4.65%	1.36%
6	3.97%	0.37%	26.19%	0.10%	63.11%	0.00%	4.54%	1.69%
7	3.66%	0.25%	26.26%	0.17%	64.73%	0.00%	3.81%	1.06%
8	3.84%	0.28%	27.11%	0.03%	63.50%	0.00%	3.81%	1.40%

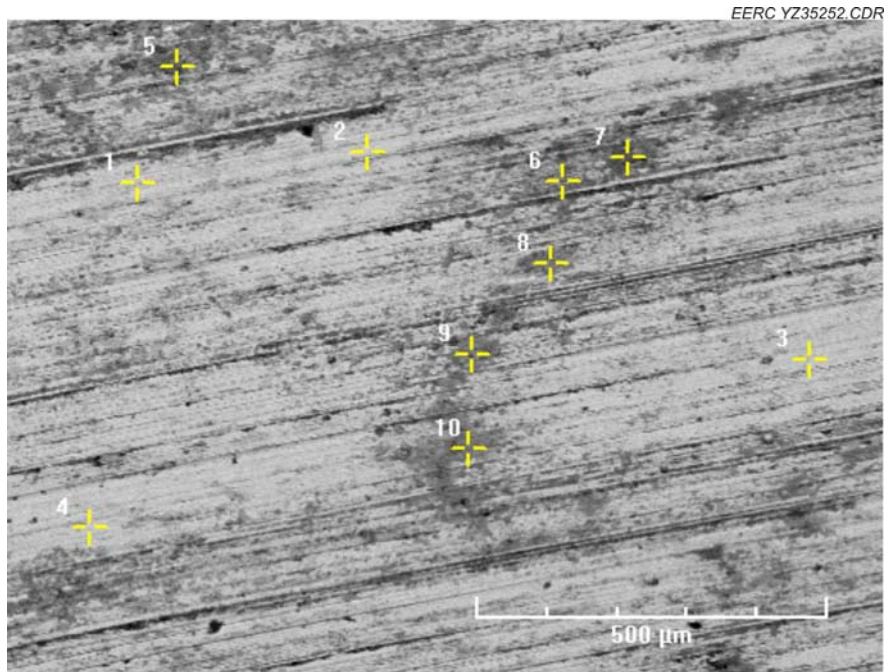


Figure B-9. M5 surface SEM image.

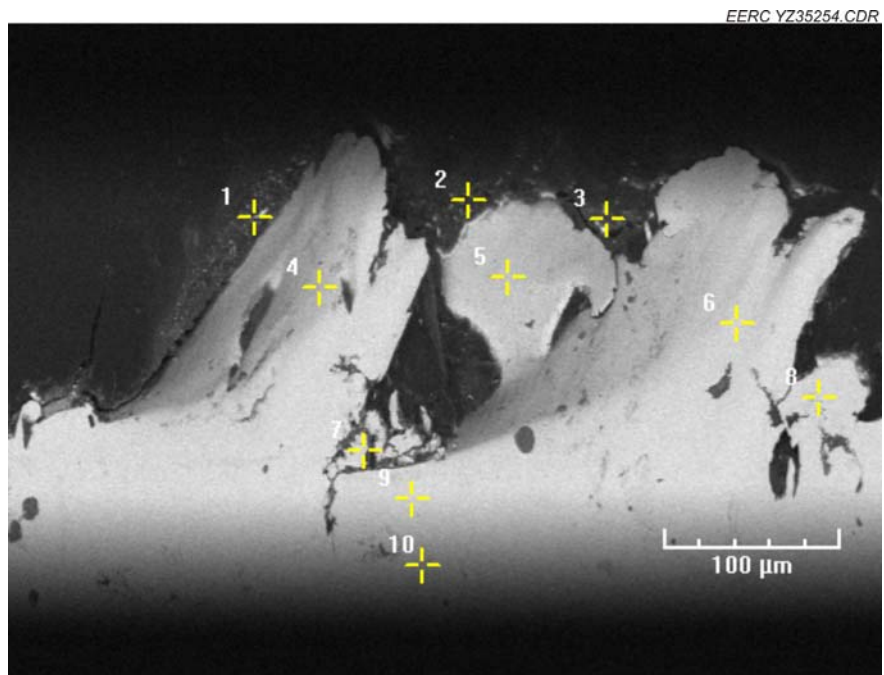


Figure B-10. M5 cross-sectional SEM image.

Table B-5. Elemental Analysis of Cross Section of M5

Tag	Si	S	Cr	Mn	Fe	Co	Ni	Br
1	9.56%	1.12%	14.04%	0.00%	33.09%	0.00%	2.92%	39.27%
2	19.07%	2.54%	5.92%	0.00%	13.68%	0.49%	3.18%	55.12%
3	13.59%	4.22%	7.87%	0.81%	7.95%	0.22%	0.32%	65.02%
4	7.13%	0.32%	18.97%	0.00%	46.42%	0.00%	3.04%	24.11%
5	5.48%	0.45%	22.56%	0.27%	55.29%	0.10%	4.64%	11.20%
6	3.75%	0.00%	25.20%	0.06%	64.64%	0.00%	4.86%	1.49%
7	4.38%	0.34%	22.22%	0.10%	65.74%	0.08%	5.33%	1.81%
8	3.88%	0.24%	22.75%	0.32%	67.42%	0.00%	4.25%	1.00%
9	3.08%	0.29%	24.76%	0.17%	65.41%	0.05%	5.08%	1.15%
10	3.74%	0.09%	25.84%	0.09%	63.87%	0.00%	5.02%	1.32%

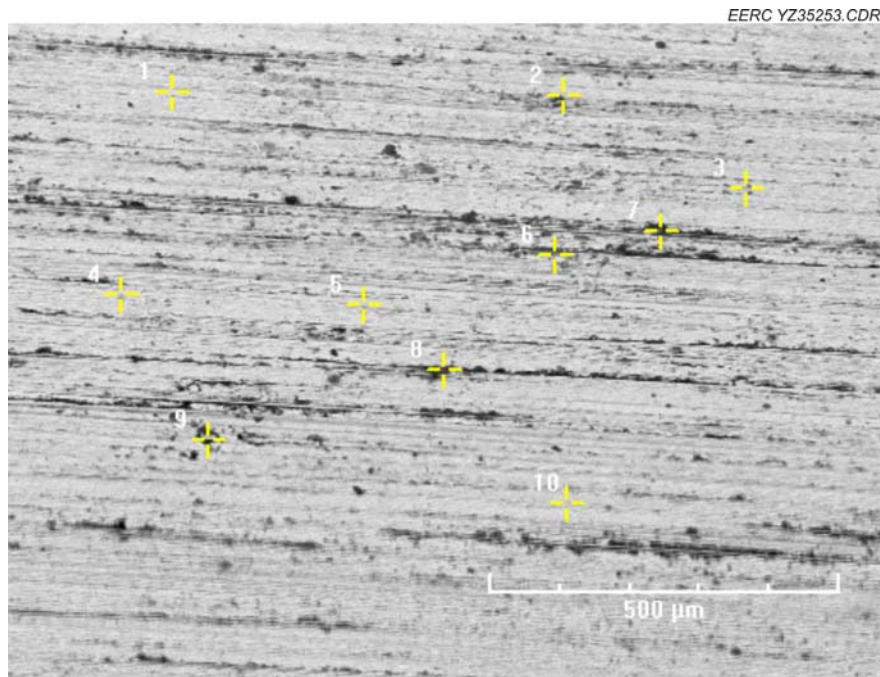


Figure B-11. M6 surface SEM image.

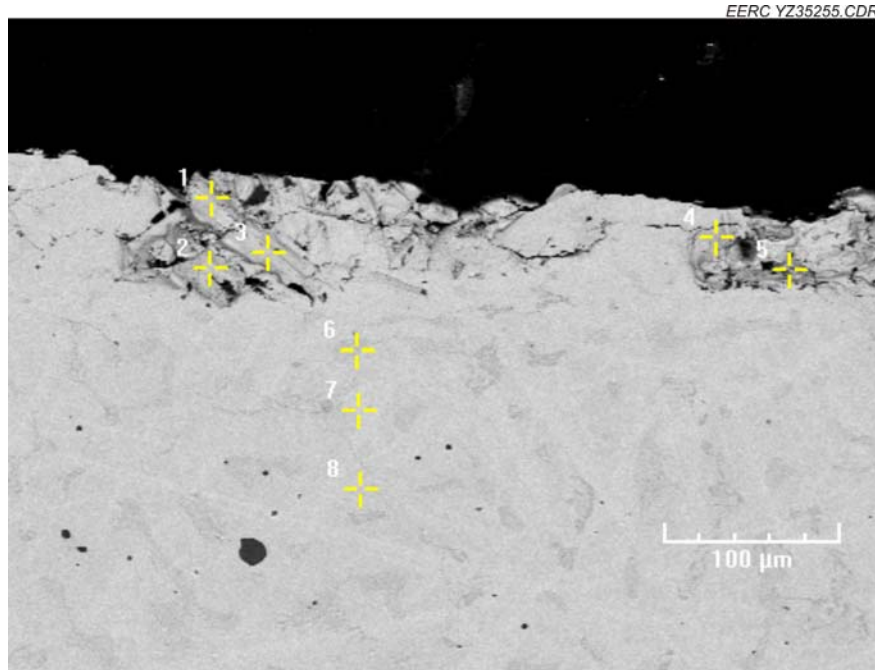


Figure B-12. M6 cross-sectional SEM image.

Table B-6. Elemental Analysis of M6 Cross Section

Tag	Si	S	Cr	Mn	Fe	Co	Ni	Br	K
1	3.57%	0.27%	25.57%	0.06%	64.50%	0.00%	4.68%	1.23%	0.12%
2	3.37%	0.21%	29.81%	0.11%	61.17%	0.00%	4.38%	0.93%	0.01%
3	3.21%	0.25%	26.01%	0.30%	63.89%	0.03%	5.04%	1.25%	0.01%
4	2.84%	0.34%	27.42%	0.13%	62.13%	0.00%	5.23%	1.90%	0.02%
5	3.47%	0.29%	27.54%	0.31%	61.67%	0.00%	5.16%	1.55%	0.00%
6	3.28%	0.26%	29.68%	0.28%	60.28%	0.00%	5.16%	1.01%	0.04%
7	3.14%	0.17%	24.84%	0.36%	64.99%	0.16%	5.13%	1.22%	0.00%
8	3.35%	0.17%	26.06%	0.16%	65.16%	0.00%	4.24%	0.82%	0.05%

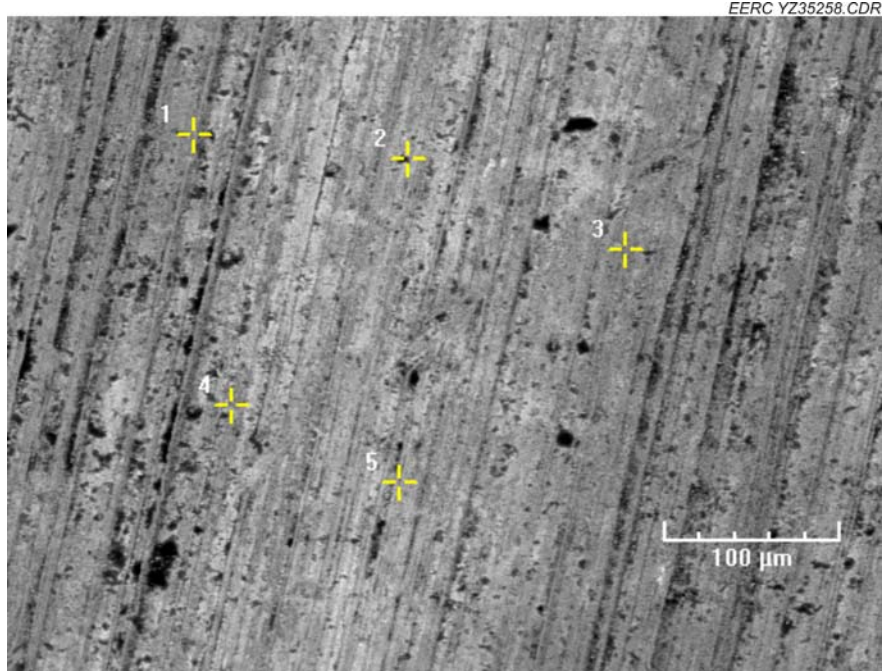


Figure B-13. M7 surface SEM image.

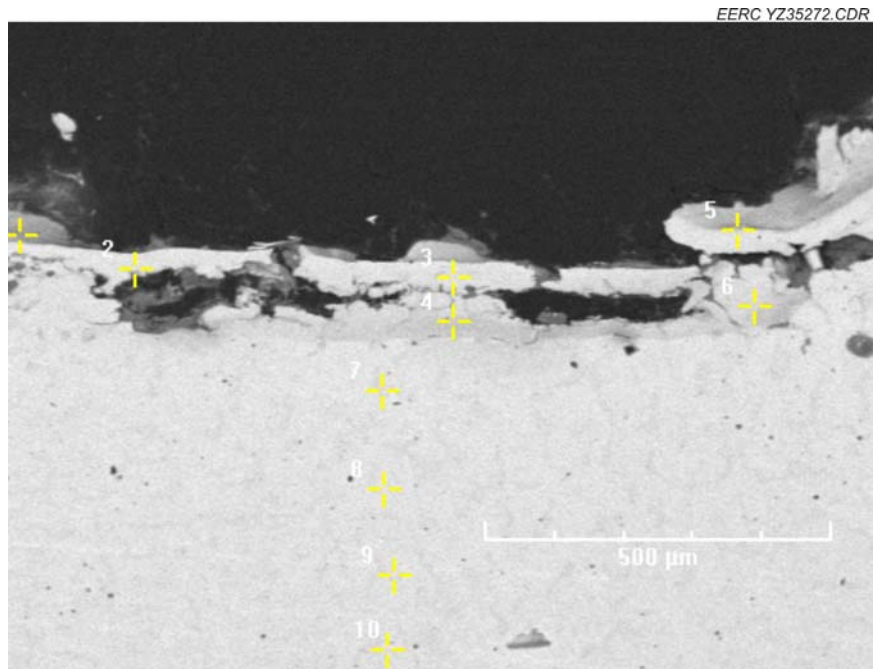


Figure B-14. M7 cross-sectional SEM image.

Table B-7. Element Analysis on M7 Cross Section

Tag	Si	S	Cr	Mn	Fe	Co	Ni	K
1	4.03%	0.43%	26.33%	0.00%	64.44%	0.00%	4.77%	0.00%
2	3.39%	0.17%	27.30%	0.51%	64.00%	0.00%	4.62%	0.00%
3	3.30%	0.23%	25.39%	0.31%	65.68%	0.00%	5.07%	0.01%
4	3.12%	0.44%	26.17%	0.04%	64.91%	0.00%	5.31%	0.00%
5	4.27%	1.11%	28.66%	0.34%	60.61%	0.00%	5.00%	0.00%
6	2.83%	0.32%	25.55%	0.23%	65.64%	0.00%	5.28%	0.16%
7	3.65%	0.15%	30.55%	0.00%	60.45%	0.00%	5.20%	0.00%
8	3.42%	0.24%	26.13%	0.10%	65.55%	0.12%	4.43%	0.00%
9	3.66%	0.28%	24.98%	0.22%	64.95%	0.57%	5.35%	0.00%
10	3.64%	0.10%	26.22%	0.15%	64.81%	0.00%	4.96%	0.12%

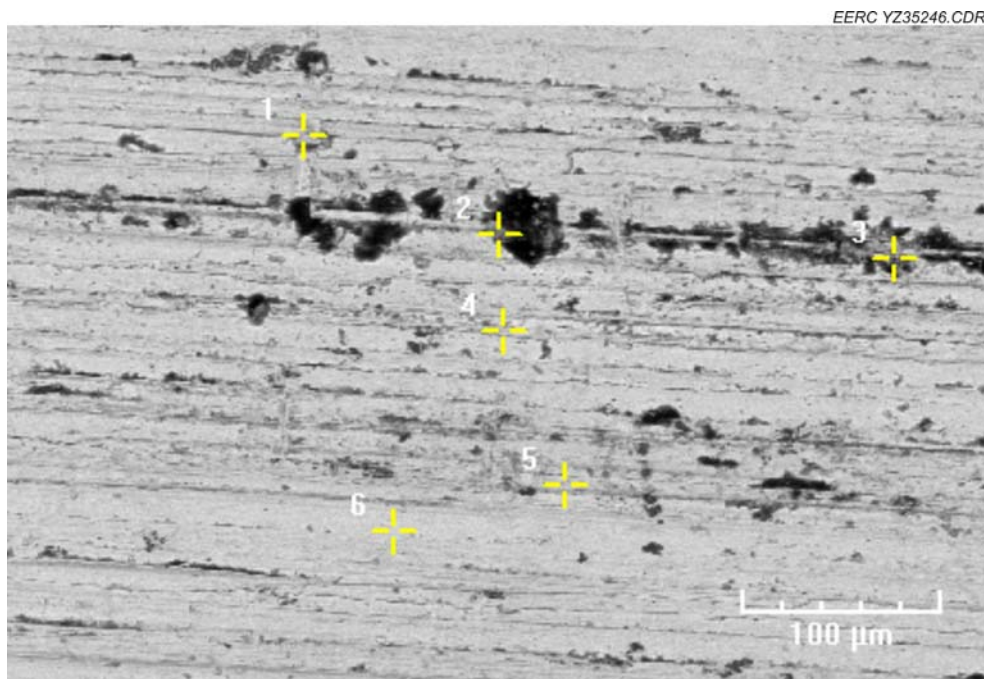


Figure B-15. M8 surface SEM image.

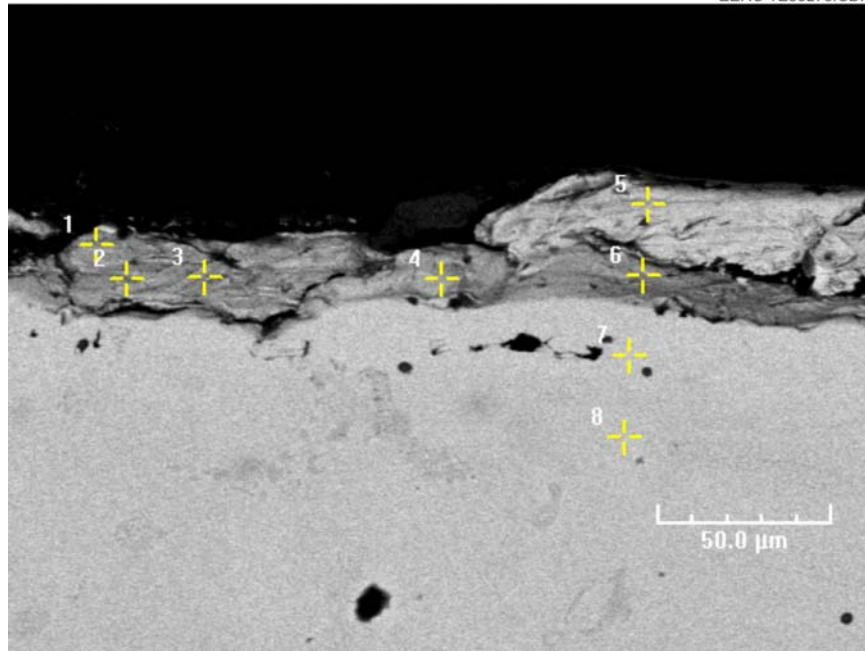


Figure B-16. M8 cross-sectional SEM image.

Table B-8. Elemental Analysis of M8 Cross Section

Tag	Si	S	Cr	Mn	Fe	Co	Ni
1	6.32%	0.41%	26.21%	0.00%	62.00%	0.00%	5.06%
2	3.91%	0.43%	25.67%	0.34%	64.43%	0.00%	5.16%
3	5.01%	0.20%	26.69%	0.35%	63.00%	0.15%	4.60%
4	3.78%	0.20%	26.43%	0.00%	64.82%	0.00%	4.77%
5	3.77%	0.27%	25.95%	0.42%	64.76%	0.00%	4.71%
6	4.47%	0.30%	27.11%	0.17%	63.19%	0.00%	4.76%
7	3.24%	0.28%	24.74%	0.30%	65.82%	0.11%	5.51%
8	3.21%	0.12%	25.93%	0.00%	66.10%	0.00%	4.64%

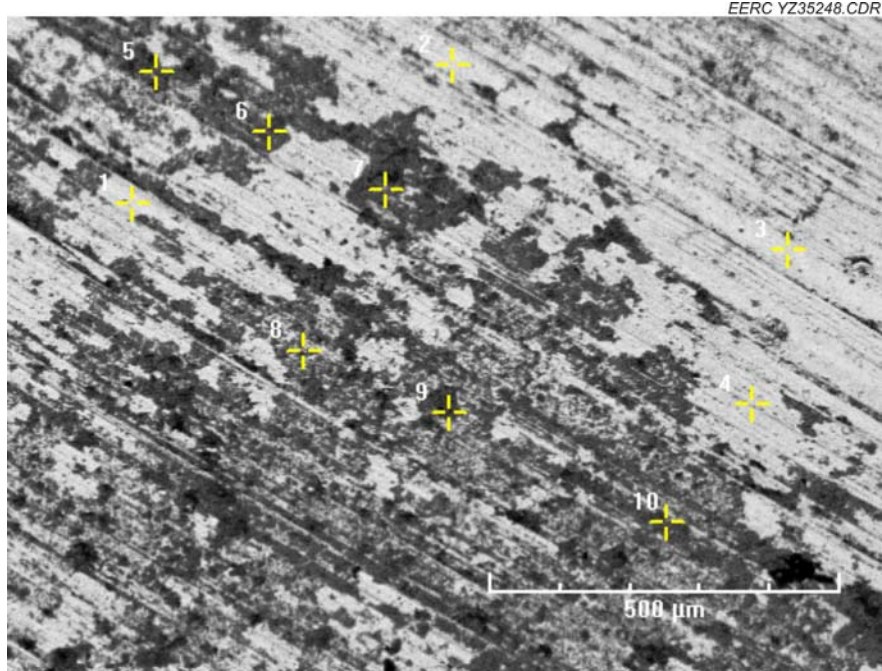


Figure B-17. M9 surface SEM image.

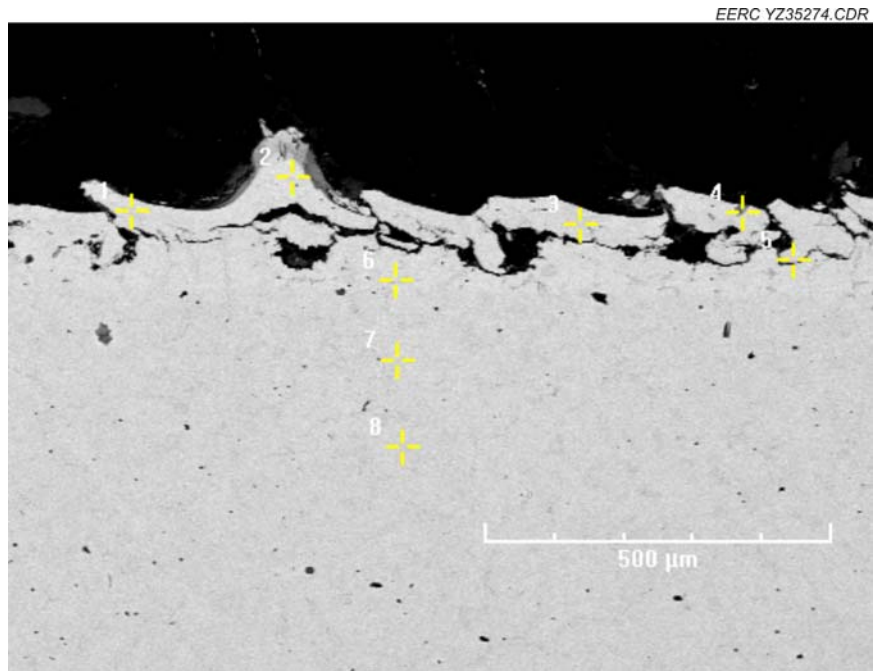


Figure B-18. M9 cross-sectional SEM image.

Table B-9. Elemental Analysis on M9 Cross Section

Tag	Si	S	Cr	Mn	Fe	Co	Ni
1	3.26%	0.23%	28.33%	0.20%	63.27%	0.00%	4.71%
2	3.16%	0.28%	25.36%	0.30%	65.74%	0.00%	5.17%
3	5.43%	0.33%	24.00%	0.31%	66.99%	0.25%	2.67%
4	4.90%	0.24%	25.95%	0.00%	63.31%	0.00%	5.59%
5	3.47%	0.20%	27.13%	0.16%	63.55%	0.00%	5.49%
6	4.32%	0.45%	27.40%	0.00%	63.05%	0.00%	4.74%
7	3.30%	0.32%	25.70%	0.34%	64.83%	0.07%	5.41%
8	3.13%	0.34%	25.83%	0.46%	65.25%	0.00%	4.99%

APPENDIX C

USS MINNTAC COUPON SEM ANALYSIS

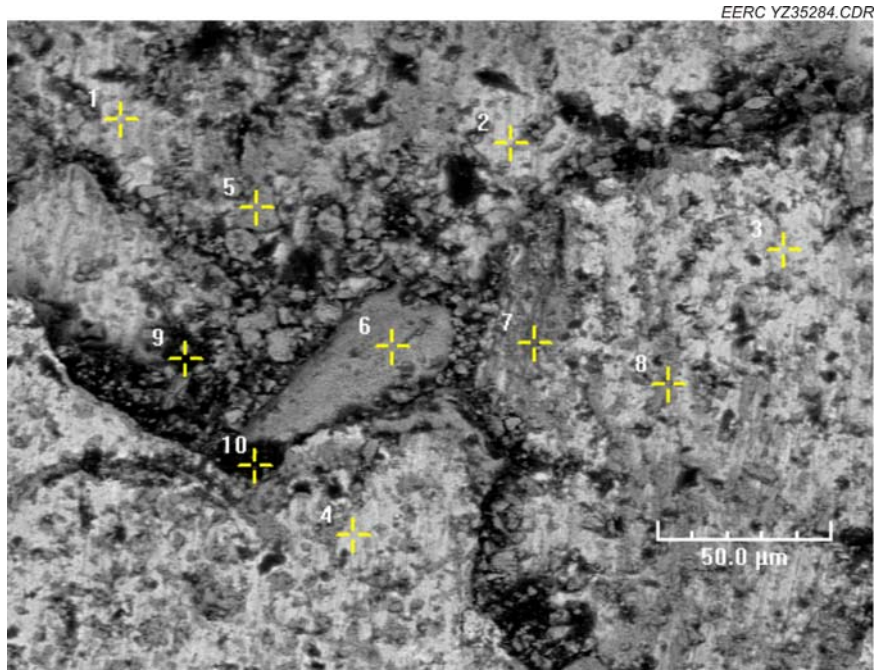


Figure C-1. UM1 surface SEM image.

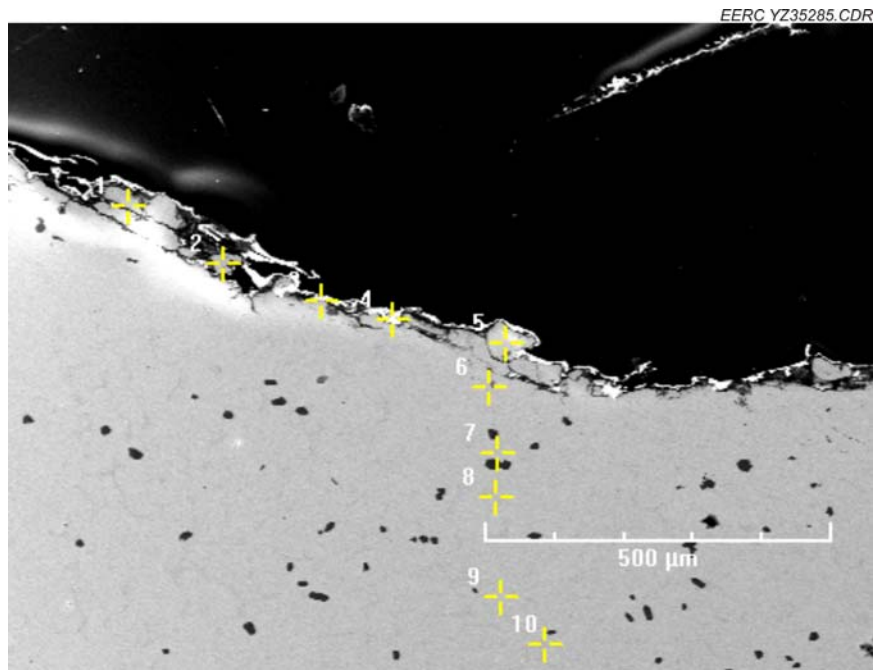


Figure C-2. UM1 cross-sectional SEM image.

Table C-1. Elemental Analysis of UM1 Cross Section

Tag	Si	S	Cr	Mn	Fe	Co	Ni	Br
1	9.38%	0.44%	36.13%	0.23%	35.27%	0.00%	3.99%	14.57%
2	11.97%	0.92%	36.25%	0.00%	34.76%	0.00%	3.35%	12.57%
3	18.72%	0.72%	5.97%	1.62%	10.74%	0.00%	0.76%	61.46%
4	28.82%	0.00%	1.77%	0.00%	14.50%	0.00%	0.46%	54.45%
5	9.66%	1.09%	33.90%	0.00%	36.44%	0.00%	5.10%	13.81%
6	7.33%	0.46%	25.50%	0.25%	37.15%	0.00%	7.00%	22.30%
7	7.75%	0.85%	31.95%	0.61%	40.22%	0.00%	5.93%	12.59%
8	8.53%	0.18%	34.25%	0.33%	37.44%	0.00%	6.09%	13.19%
9	7.24%	0.42%	30.38%	0.63%	40.59%	0.00%	5.43%	15.30%
10	7.67%	0.58%	42.35%	1.33%	31.71%	0.00%	4.51%	11.86%

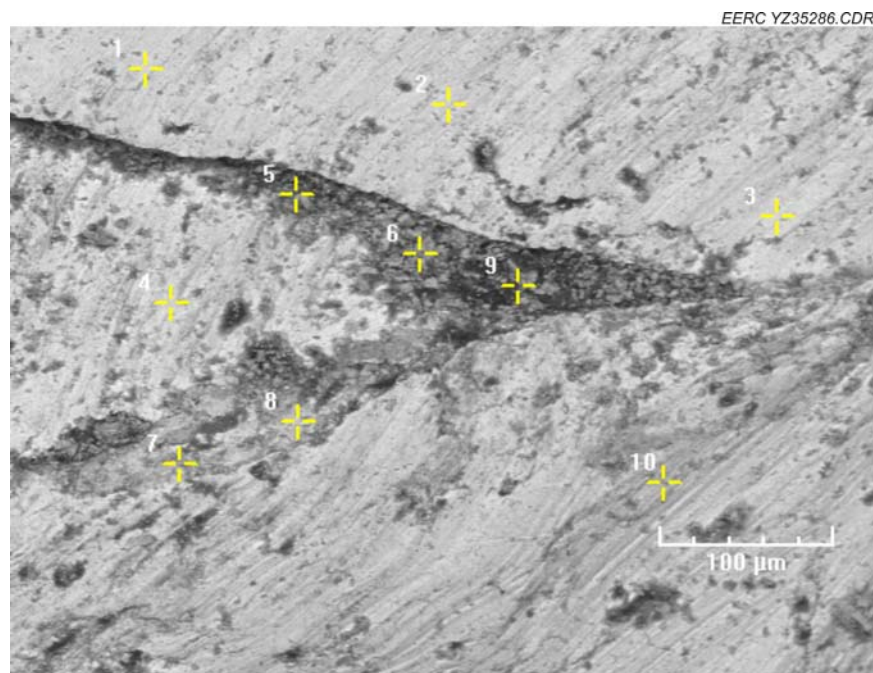


Figure C-3. UM2 surface SEM image.

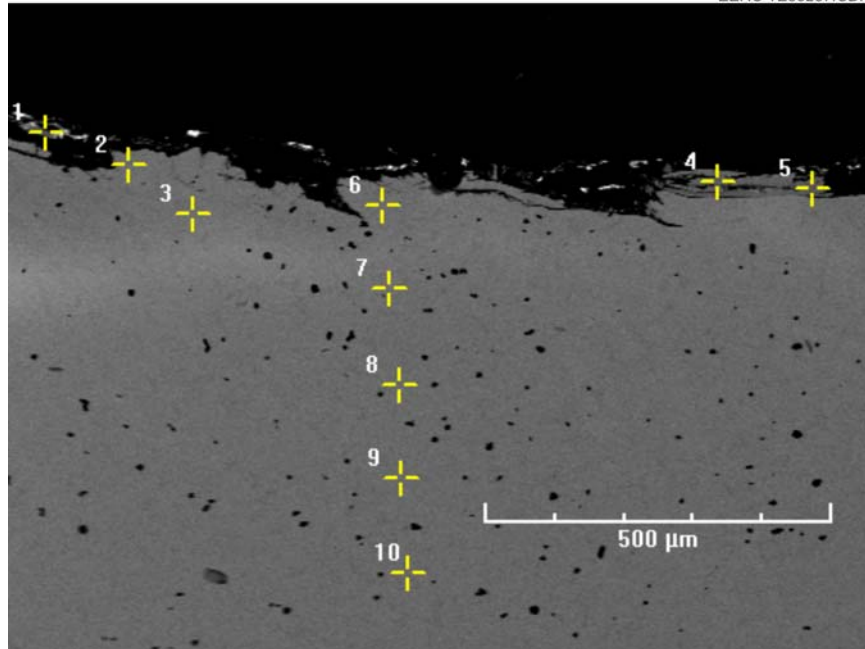


Figure C-4. UM2 cross-sectional SEM image.

Table C-2. Elemental Analysis of UM2 Cross Section

Tag	Si	S	Cr	Mn	Fe	Co	Ni	Br
1	11.82%	0.00%	13.76%	3.77%	19.19%	0.00%	0.00%	51.46%
2	4.64%	0.32%	28.80%	0.68%	44.07%	0.00%	13.46%	8.00%
3	4.04%	0.24%	28.98%	0.95%	44.44%	0.10%	13.57%	7.70%
4	3.82%	0.50%	38.45%	0.34%	39.56%	0.00%	10.79%	6.52%
5	1.26%	0.00%	33.80%	1.79%	48.58%	0.93%	10.17%	3.38%
6	3.65%	0.20%	30.60%	0.87%	44.58%	0.00%	13.58%	6.51%
7	4.39%	0.47%	45.14%	0.86%	34.77%	0.00%	8.58%	5.73%
8	3.92%	0.27%	29.19%	0.49%	46.00%	0.00%	13.45%	6.67%
9	2.96%	0.29%	27.48%	0.38%	48.42%	0.06%	14.44%	5.88%
10	3.46%	0.29%	41.21%	0.40%	39.03%	0.00%	10.45%	5.16%

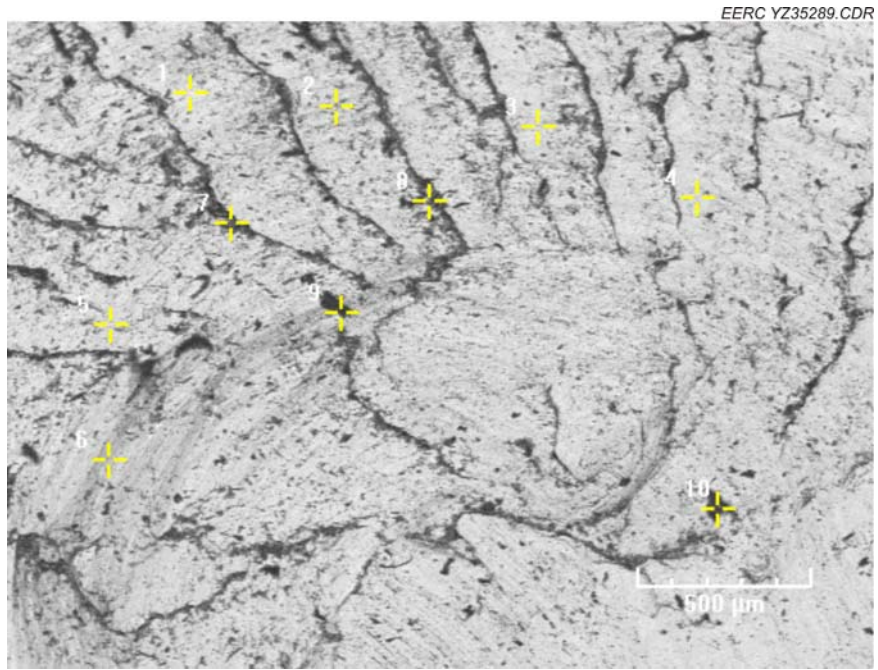


Figure C-5 UM3 surface SEM image.

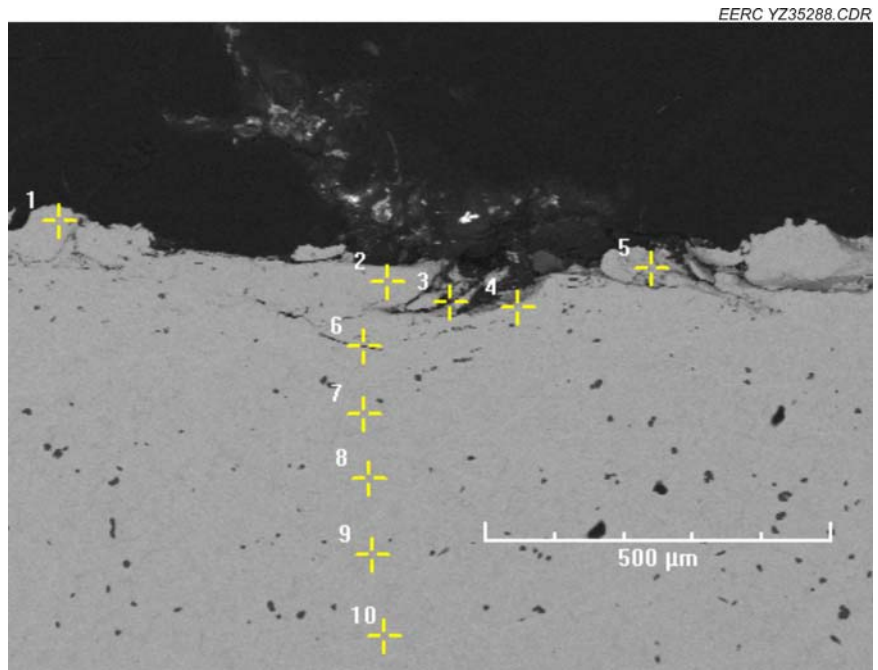


Figure C-6. UM3 cross-sectional SEM image.

Table C-3. Elemental Analysis of UM3 Cross Section

Tag	Si	S	Cr	Mn	Fe	Co	Ni	Br
1	3.39%	0.24%	29.03%	0.69%	45.31%	0.00%	16.15%	5.14%
2	2.81%	0.25%	27.54%	0.65%	48.19%	0.00%	15.61%	4.92%
3	0.25%	0.00%	45.62%	1.48%	45.75%	0.00%	6.19%	0.58%
4	3.13%	0.24%	27.74%	0.68%	46.20%	0.00%	15.90%	6.11%
5	3.60%	0.33%	28.12%	0.33%	46.13%	0.00%	13.98%	7.51%
6	2.98%	0.29%	26.70%	0.80%	47.18%	0.22%	16.14%	5.69%
7	2.50%	0.29%	26.13%	0.66%	49.66%	0.00%	15.80%	4.96%
8	2.88%	0.38%	26.24%	0.70%	47.61%	0.15%	16.56%	5.48%
9	2.77%	0.37%	38.04%	0.75%	40.10%	0.00%	13.65%	4.28%
10	2.48%	0.15%	26.73%	0.73%	49.29%	0.19%	15.21%	5.23%

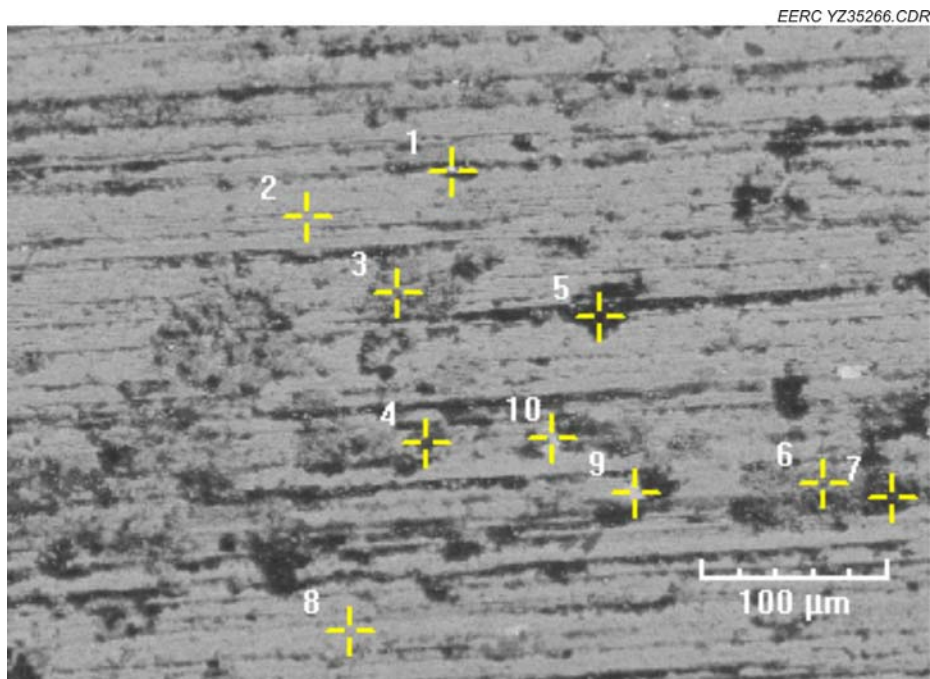


Figure C-7. UM4 surface SEM image.

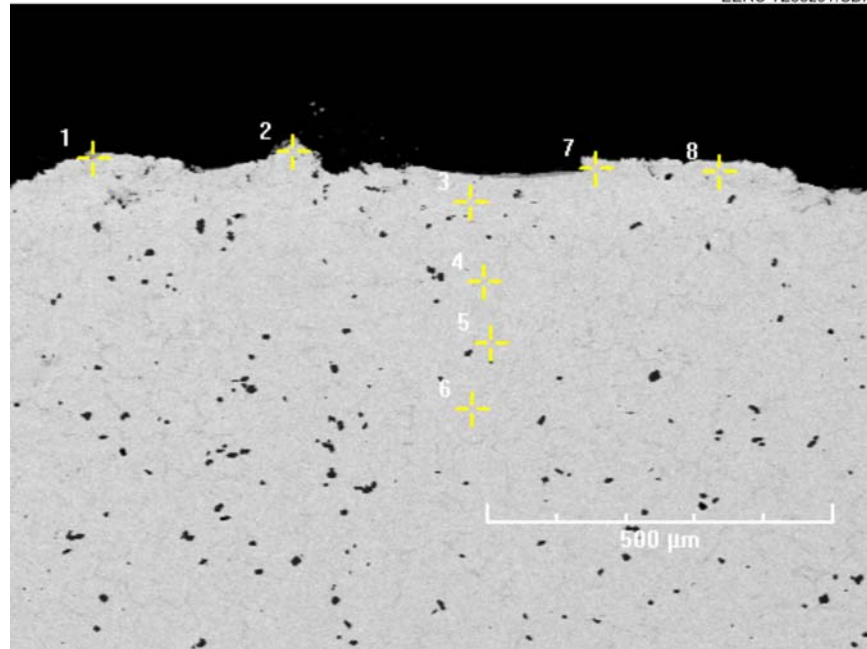


Figure C-8. UM4 cross-sectional SEM image.

Table C-4. Elemental Analysis of UM4 Cross Section

Tag	Si	S	Cr	Mn	Fe	Co	Ni	Br
1	3.28%	0.40%	25.70%	0.28%	49.05%	0.00%	14.33%	6.97%
2	3.25%	0.24%	26.95%	0.24%	47.57%	0.00%	14.90%	6.86%
3	2.99%	0.33%	29.72%	0.54%	47.33%	0.00%	14.16%	4.91%
4	2.96%	0.16%	28.79%	0.57%	47.38%	0.00%	16.07%	4.02%
5	4.44%	0.18%	30.14%	0.41%	52.77%	0.00%	7.21%	4.72%
6	3.22%	0.28%	28.40%	0.84%	45.59%	0.06%	16.87%	4.69%
7	2.56%	0.21%	26.62%	0.65%	48.96%	0.00%	15.73%	5.22%
8	3.02%	0.24%	27.05%	0.63%	47.70%	0.00%	16.06%	5.31%

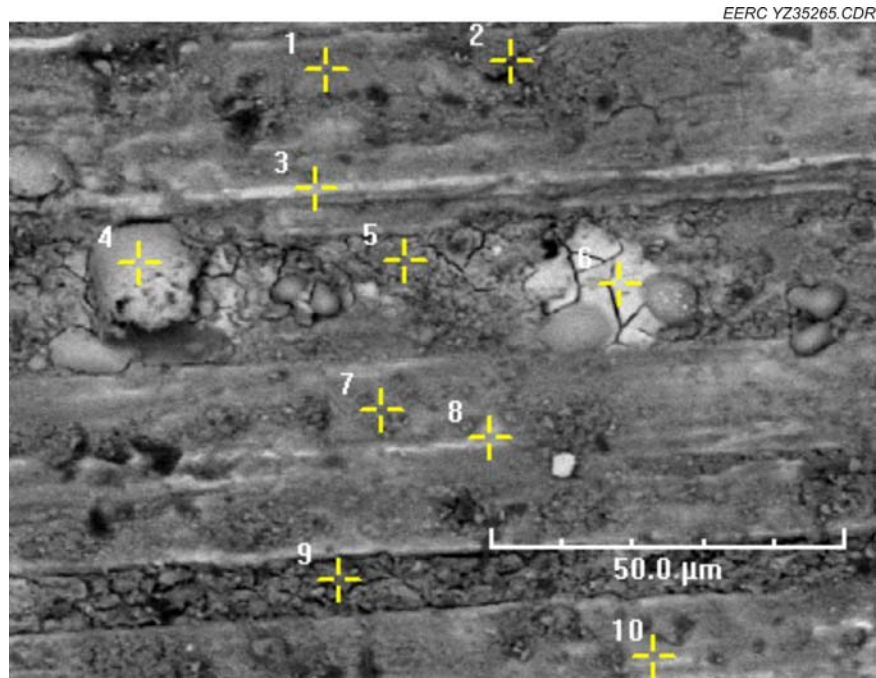


Figure C-9. UM5 surface SEM image.

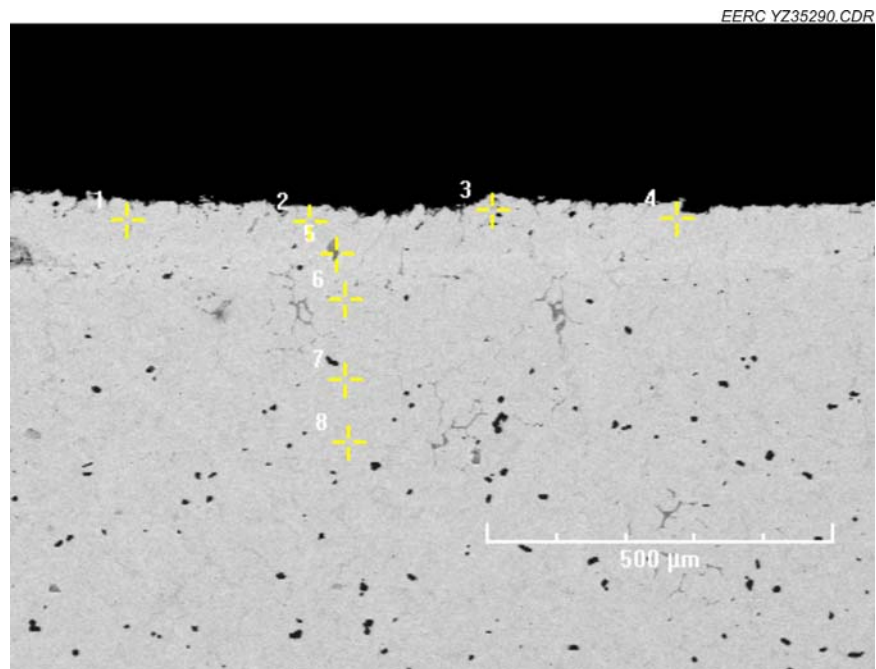


Figure C-10. UM5 cross-sectional SEM image.

Table C-5. Elemental Analysis of Cross-Sectional of UM5

Tag	Si	S	Cr	Mn	Fe	Co	Ni	Br
1	3.39%	0.40%	26.51%	0.84%	46.84%	0.00%	16.44%	5.58%
2	2.31%	0.31%	54.47%	0.55%	29.91%	0.00%	9.37%	3.09%
3	3.04%	0.36%	24.95%	0.19%	50.36%	0.20%	16.47%	4.43%
4	2.72%	0.22%	26.61%	0.83%	48.86%	0.00%	16.04%	4.64%
5	3.01%	0.12%	28.04%	0.42%	47.69%	0.00%	15.99%	4.73%
6	2.84%	0.27%	27.15%	0.75%	47.97%	0.01%	16.23%	4.74%
7	3.21%	0.27%	29.13%	0.97%	44.96%	0.00%	16.51%	4.91%
8	2.56%	0.31%	25.72%	0.94%	49.02%	0.05%	16.12%	5.20%

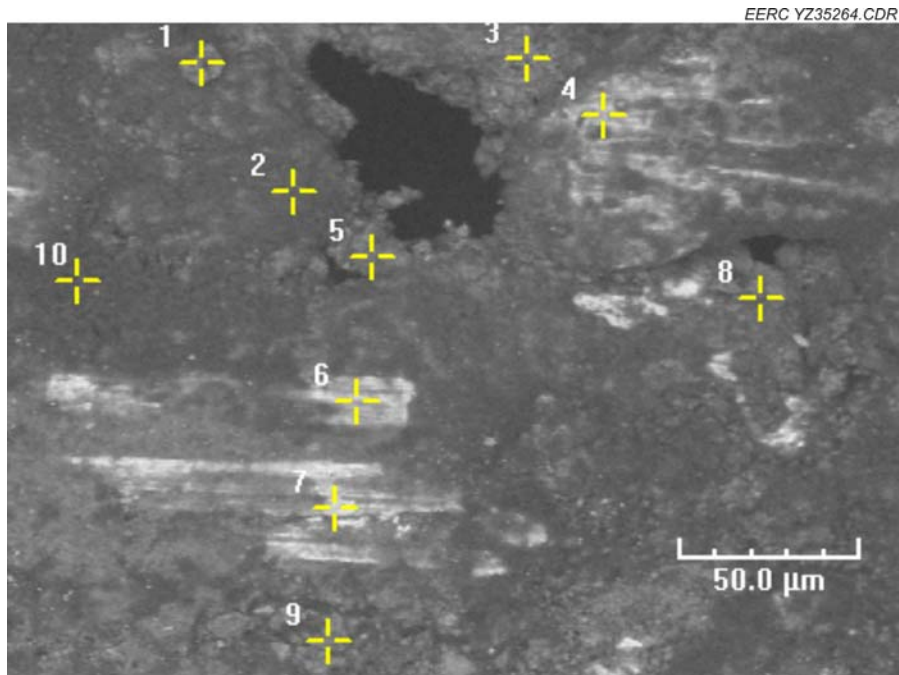


Figure C-11. UM6 surface SEM image.

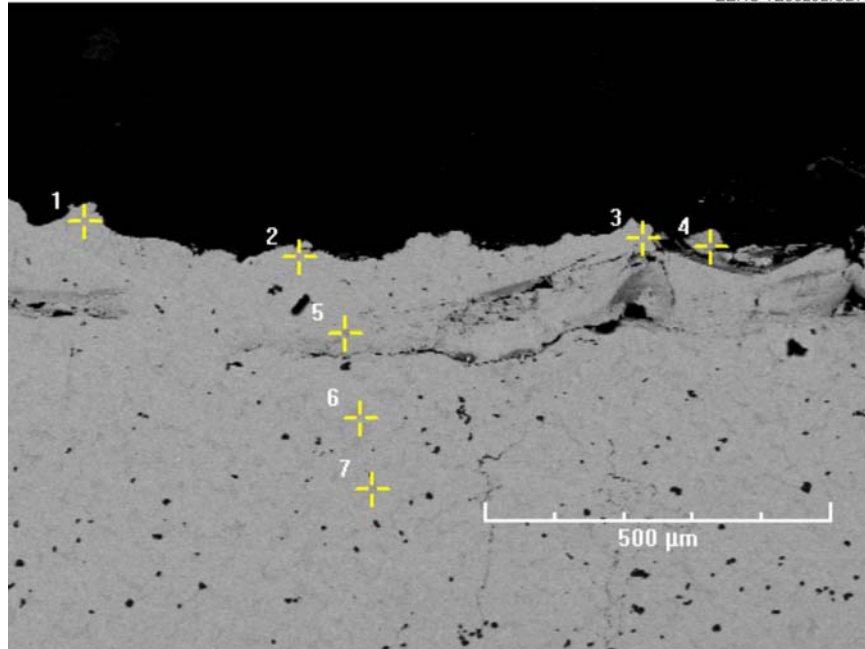


Figure C-12. UM6 cross-sectional SEM image.

Table C-6. Elemental Analysis of UM6 Cross Section

Tag	Si	S	Cr	Mn	Fe	Co	Ni	Br
1	2.88%	0.33%	26.37%	0.39%	47.55%	0.23%	16.87%	5.26%
2	3.27%	0.28%	27.42%	0.41%	48.98%	0.00%	14.60%	4.95%
3	2.84%	0.16%	27.99%	0.33%	48.98%	0.00%	15.73%	3.97%
4	4.44%	0.37%	26.20%	0.66%	45.13%	0.00%	15.47%	7.72%
5	2.59%	0.32%	23.32%	0.75%	43.14%	0.00%	13.73%	16.14%
6	3.25%	0.21%	29.25%	0.58%	46.44%	0.00%	16.02%	4.25%
7	0.78%	0.69%	86.55%	0.38%	9.83%	0.00%	0.10%	1.68%

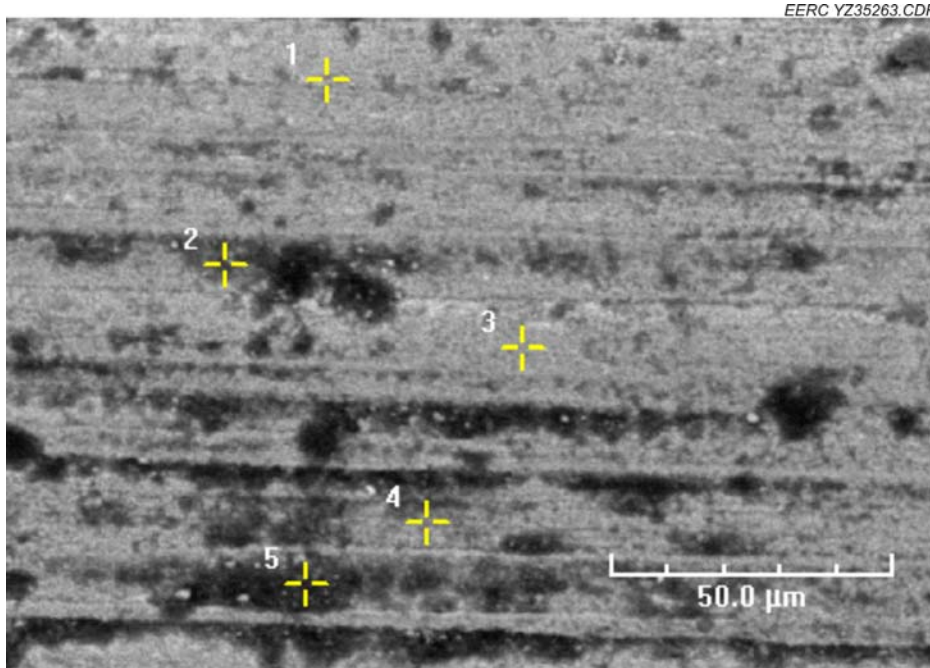


Figure C-13. UM7 surface SEM image.

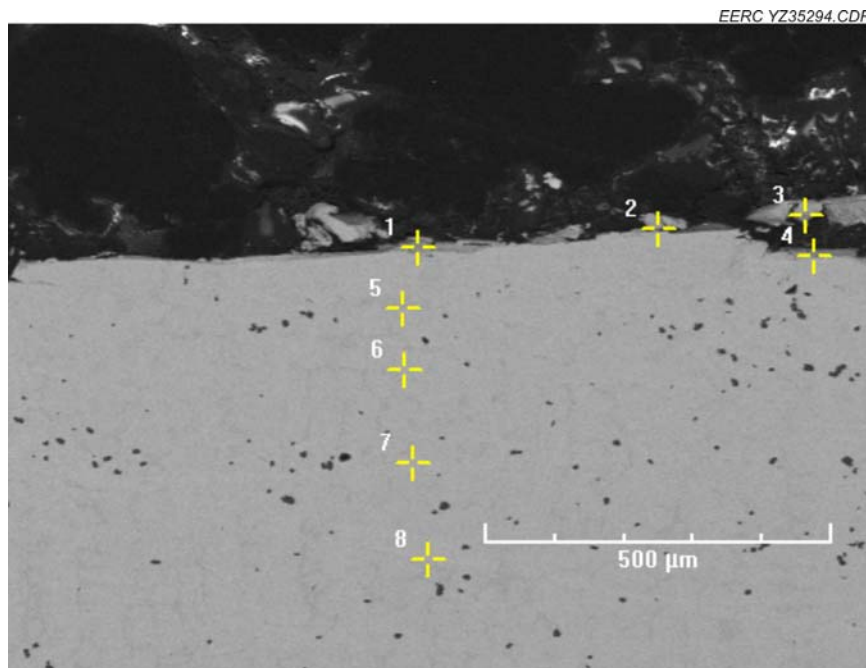


Figure C-14. UM7 cross-sectional SEM image.

Table C-7. Elemental Analysis of UM7 Cross Section

Tag	Si	S	Cr	Mn	Fe	Co	Ni
1	4.34%	0.58%	35.74%	0.58%	43.40%	0.00%	15.37%
2	3.38%	0.39%	29.70%	0.99%	49.54%	0.00%	15.99%
3	3.90%	0.29%	27.36%	0.49%	51.39%	0.00%	16.57%
4	3.88%	0.78%	29.34%	0.83%	49.35%	0.00%	15.81%
5	4.00%	0.85%	37.09%	0.87%	41.46%	0.00%	15.73%
6	2.94%	0.24%	28.50%	0.62%	50.73%	0.00%	16.94%
7	3.06%	0.19%	27.76%	1.09%	51.20%	0.00%	16.69%
8	3.24%	0.30%	28.19%	0.78%	50.71%	0.11%	16.67%

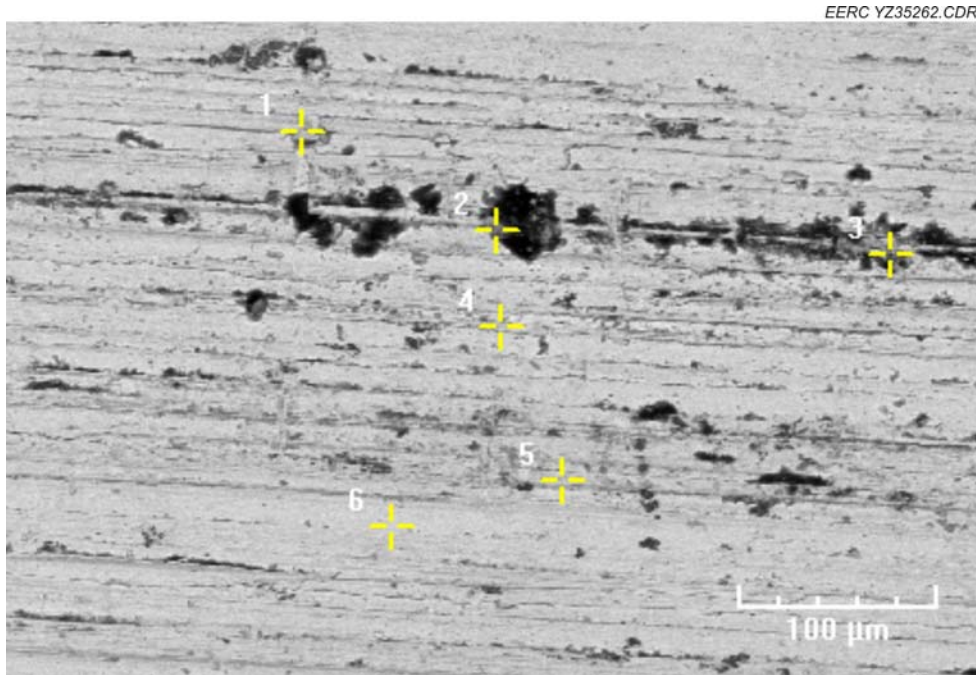


Figure C-15. UM8 surface SEM image.

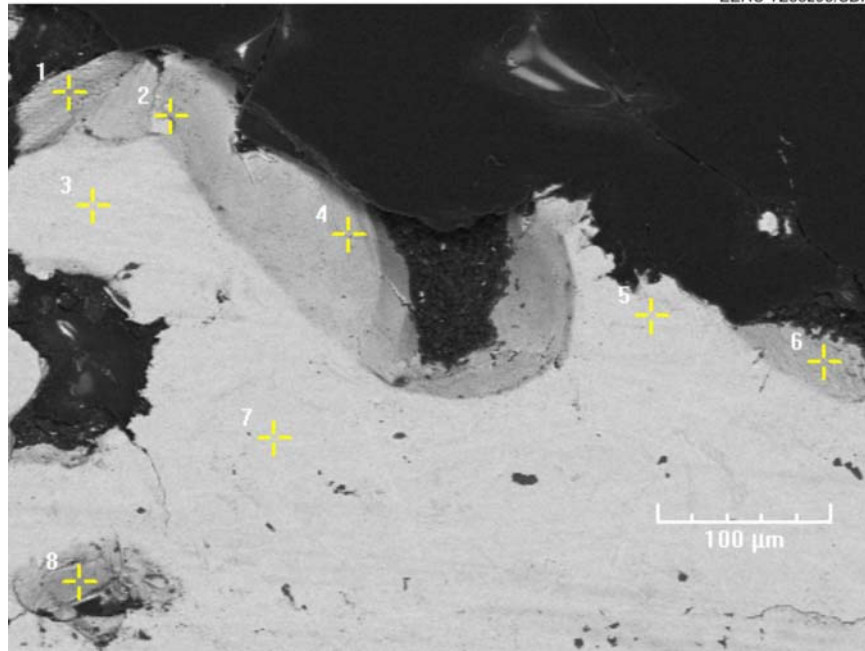


Figure C-16. UM8 cross-sectional SEM image.

Table C-84. Elemental Analysis of Cross-Sectional of UM8

Tag	Si	S	Cr	Mn	Fe	Co	Ni
1	2.86%	0.93%	64.27%	0.26%	25.74%	0.00%	5.95%
2	3.55%	0.49%	29.62%	0.62%	50.78%	0.00%	14.94%
3	3.14%	0.26%	28.05%	0.42%	51.63%	0.00%	16.49%
4	4.13%	0.51%	29.28%	0.09%	50.76%	0.00%	15.21%
5	6.86%	0.66%	35.90%	0.84%	48.36%	0.00%	7.38%
6	3.96%	0.49%	28.62%	0.25%	51.90%	0.00%	14.78%
7	3.58%	0.19%	29.38%	0.78%	49.58%	0.00%	16.50%
8	2.72%	0.46%	35.40%	0.88%	47.15%	0.00%	13.33%

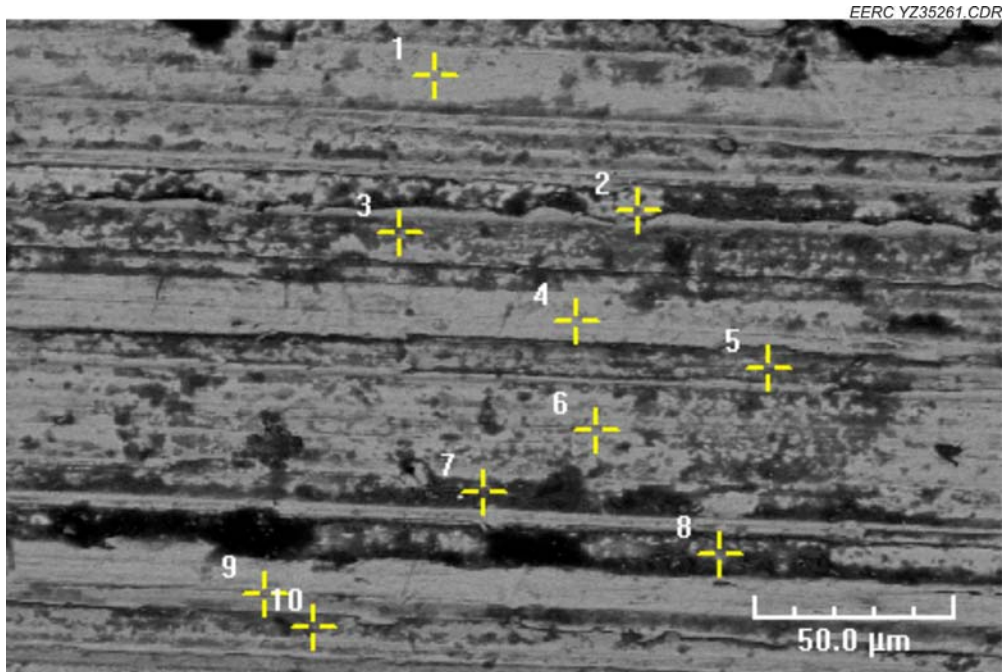


Figure C-17. UM9 surface SEM image.

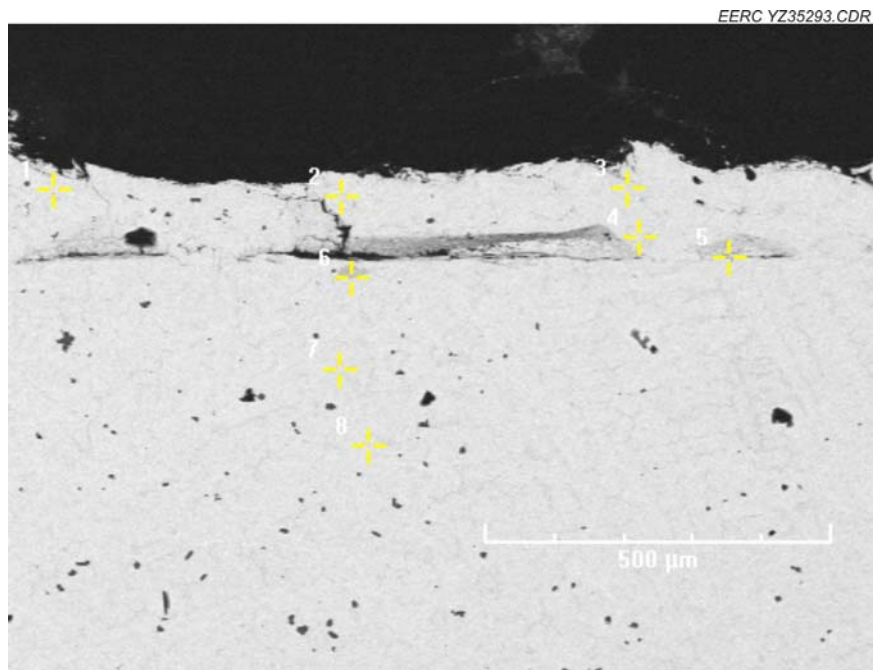


Figure C-18. UM9 cross-sectional SEM image.

Table C-9. Elemental Analysis of UM9 Cross Section

Tag	Si	S	Cr	Mn	Fe	Co	Ni
1	3.05%	0.15%	29.47%	0.86%	49.42%	0.00%	17.06%
2	3.44%	0.30%	29.75%	0.99%	48.71%	0.00%	16.80%
3	2.98%	0.21%	28.54%	0.60%	50.56%	0.00%	17.10%
4	3.17%	0.50%	28.81%	0.75%	49.51%	0.20%	17.06%
5	3.31%	0.26%	28.11%	0.25%	50.49%	0.00%	17.51%
6	4.27%	0.33%	29.07%	0.57%	47.46%	0.07%	18.23%
7	4.07%	0.32%	28.24%	0.97%	49.11%	0.00%	17.29%
8	2.81%	0.20%	27.72%	0.97%	51.36%	0.00%	16.94%

Appendix B-1-18

A Brief Summary of Hg Control Test Results for Br Injection into Taconite Induration Furnaces

April 10, 2011

A Brief Summary of Hg Control Test Results for Br Injection into Taconite Induration Furnaces

Prepared for the Minnesota Taconite Mercury Control Advisory Committee.

Michael E. Berndt (mike.berndt@state.mn.us)
Minnesota Department of Natural Resources
500 Lafayette Rd.
St. Paul, MN, 55455

April 10, 2011

Summary

This report summarizes stack testing data results for Hg control tests performed in 2007 to 2009 when solutions containing dissolved CaBr₂ and NaBr were sprayed into indurating furnaces at five taconite processing plants. Unstable baseline Hg conditions were frequently encountered owing to plant upsets and to slow baseline recovery following injection. Nevertheless, baseline values were estimated to permit a general assessment of the mercury remaining in stack gases when the Br salts were applied. Initial Hg concentrations in stack gases ranged from 2.9 to 8.0 µg/m³, with 12 to 22% of this Hg reported as oxidized Hg. The total Hg remaining in stack gases during tests ranged about 1.4 to 4.6 µg/m³, 25 to 54% of which was oxidized. Thus, the total percentage of Hg remaining in the taconite processing stacks ranged from 27 to 88% of the base value, however, the percentage of mercury emitted in oxidized form increases with Br addition.

Introduction

The Minnesota Department of Natural Resources conducted numerous Hg control tests using Br salt addition to taconite processing plants. This document provides a brief summary of the stack gas Hg concentrations for these tests in graphical form. Numerous additional data accompanied the stack testing during these tests, including full scrubber water chemistry and greenball Hg concentrations. Major flow streams for the taconite processing plants were also provided when automatic readouts were provided. The purpose of this report is to provide the Minnesota Taconite Mercury Control Advisory Committee and research team members with an update on previous Hg testing results and data availability as the effort to find methods to control Hg continues into the future.

Methods

Hg concentrations were measured using CMM (Continuous Mercury Monitors) in stack gases at taconite processing plants before, during, and after spraying of bromide bearing salt solutions into the processing furnaces. For grate kilns, the Br salt addition occurred on the flame end of the kiln. For straight grates, the Br addition was into the second “down-comer” located above the preheat zone. All measurements were made by the Energy and Environmental Research Center (EERC) using their AWS system. While additional data is available on taconite gas process flows (e.g., scrubber water blow down, greenball

feed rate, pellet production, gas temperature, etc..) and composition of the streams, these data are not reported here because the purpose of this document is only to provide a brief overview of the stack gas chemistry, however, these data are available upon request from the author. Furthermore, additional tests were also conducted at these taconite processing facilities involving addition of dry NaBr salt directly to the greenball feed or of NaClO₂ to the scrubber water. Injection of Br salt solutions directly into the furnace typically provided superior results to these other tests and so only these results are presented here.

Results: Br addition tests are summarized in Table 1 and presented in Figures 1 through 6. Typically, two forms of Hg were evaluated: Total Hg and Elemental Hg. Elemental Hg is generally insoluble in water and is thus, not easily captured by taconite processing streams. The difference between the two values (Total minus Elemental Hg) is believed to be present in oxidized form. Initial Hg concentrations in stack gases ranged from 2.9 to 8.0 µg/m³, with 12 to 22% of this Hg apparently present in oxidized form. The total Hg remaining in stack gases during the conduction of tests ranged from 1.4 to 4.6 µg/m³, 25 to 54% of which was present in oxidized form. The total percentage of Hg remaining in the taconite processing stacks ranged from 27 to 88% of the base value, however, the percentage of mercury emitted in oxidized form increases with Br addition.

Table 1 Hg concentrations (µg/m³) in stack gases at taconite processing facilities during Br injection tests conducted by the DNR from 2007 to 2009.

Test	Base THg Conc	Base Elem. Hg	Base % Oxidized	Test Hg Conc	Test Elem. Hg	Test % Ox	% THg Remaining
Keewatin Taconite Ln 2	5.5	4.4	20%	2.4	1.1	54%	44%
Hibbing Taconite Line 3	8	6.5	19%	3.1	NA	NA	39%
Minntac Line 3	5.2	4.6	12%	1.4	0.9	36%	27%
ArcelorMittal	2.9	2.5	14%	2	1.5	25%	69%
United Taconite							
Line 2 Stack A	5.2	4.5	13%	4.6	2.5	46%	88%
Line 2 Stack B	4.6	3.6	22%	3.2	1.8	44%	70%

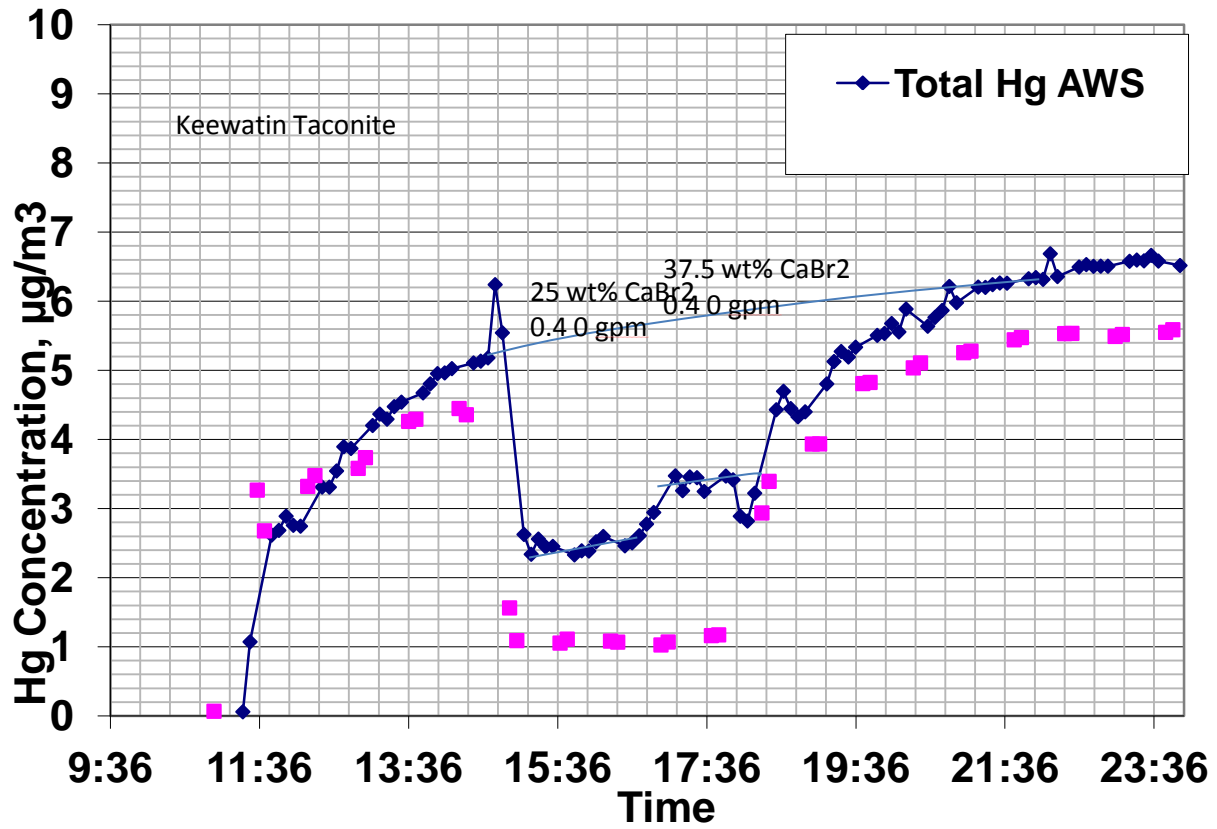


Fig 1. Keewatin Taconite test results. Dark blue diamond shapes represent total Hg. Pink squares represent elemental Hg. A plant upset occurred immediately in the morning when tests were about to begin. The plant came on line again and the test was begun approximately three hours later. It was found that 25 wt% CaBr_2 injection at 0.4 gpm provided better Hg capture than injection of 37.5 wt% CaBr_2 solution at the same rate.

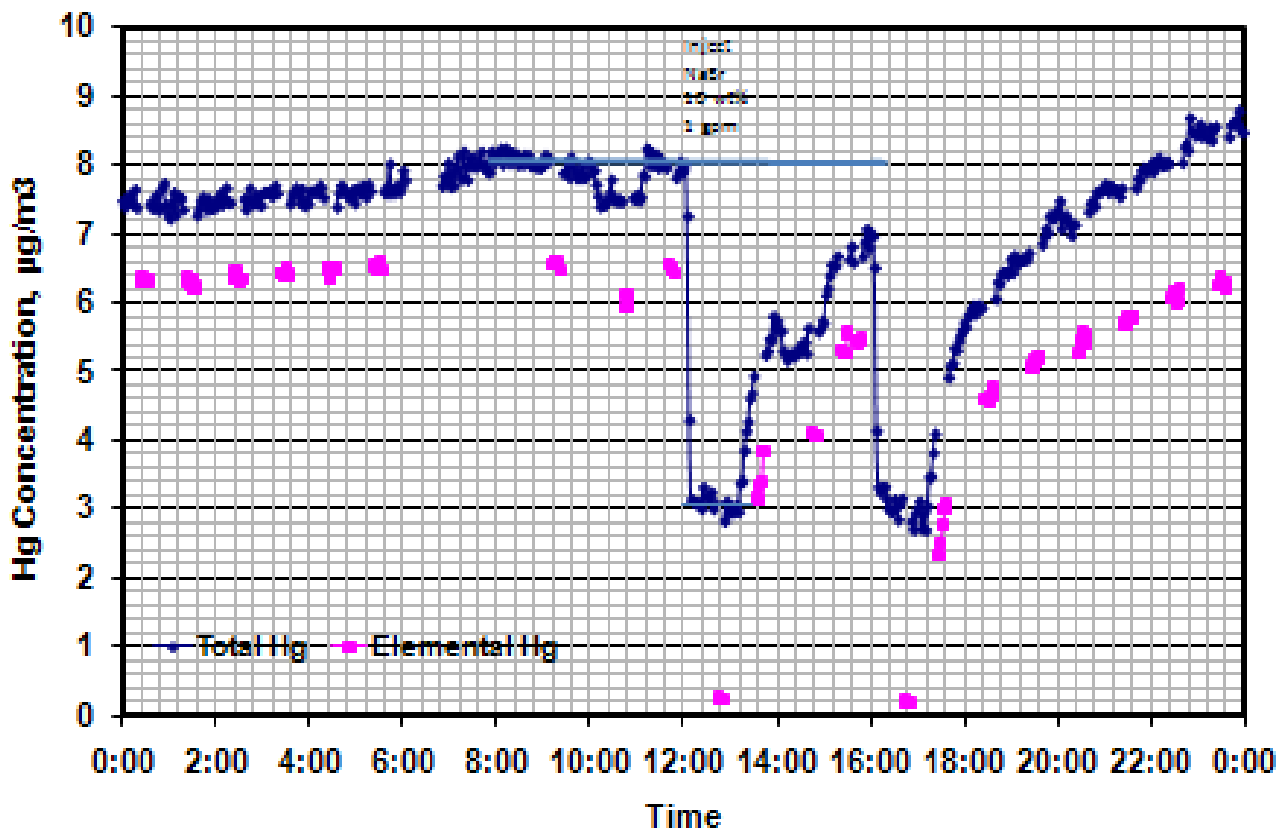


Fig 2. Hibbing Taconite Line 3 test results. Dark blue diamond shapes represent total Hg. Pink squares represent elemental Hg. Several tests were conducted at Hibbing Taconite over a period of approximately eight hours. Only the NaBr injection test, beginning at 12:00 and ending at 13:00 is evaluated here. The smaller dips beginning at 10:00 and 14:00 represent NaCl injection, and the large dip at 16:00 represents CaBr₂ injection. Hg concentration recovery to the pre-test values in the stack gases at this site were very slow following the tests. Note that elemental Hg analysis suggest nearly all of the Hg in the stack gas was present in oxidized form during the Br tests (e.g., very low elemental Hg mercury), but this was later found to be due to an artifact of the method being used to measure Hg. This problem was corrected and is not believed to affect analysis at the other sites.

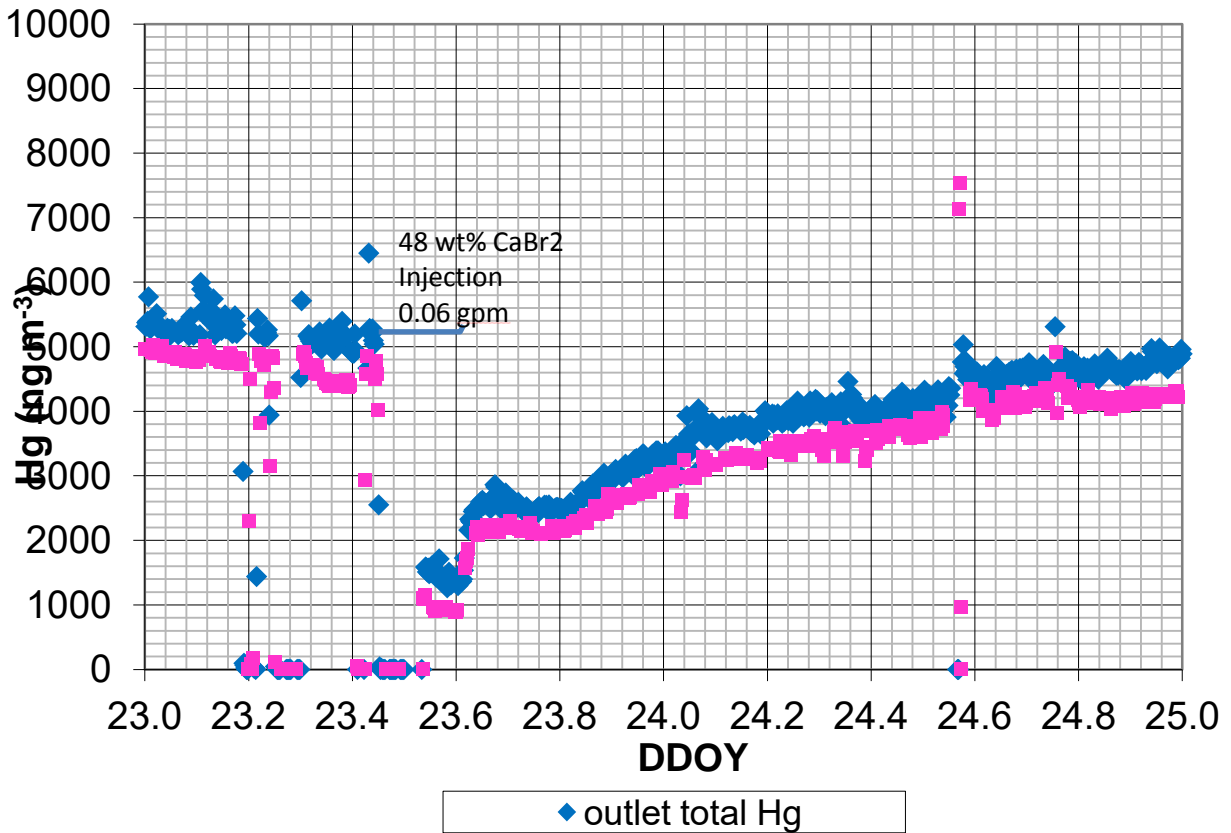


Fig. 3: Hg concentrations resulting from Hg tests conducted on **Minntac Line 3**. Dark blue diamond shapes represent total Hg. Pink squares represent elemental Hg. CaBr₂ addition took place between 23.46 and 23.61 on this time scale (units are in digital days). A temporary monitor malfunction occurred just as the test was scheduled to begin but this was not immediately noticed. It was quickly fixed and readings resumed. As commonly occurred at the other taconite plants, the rebound in Hg concentration in stack gases following the test was very slow.

Arcelor Mittal Tests

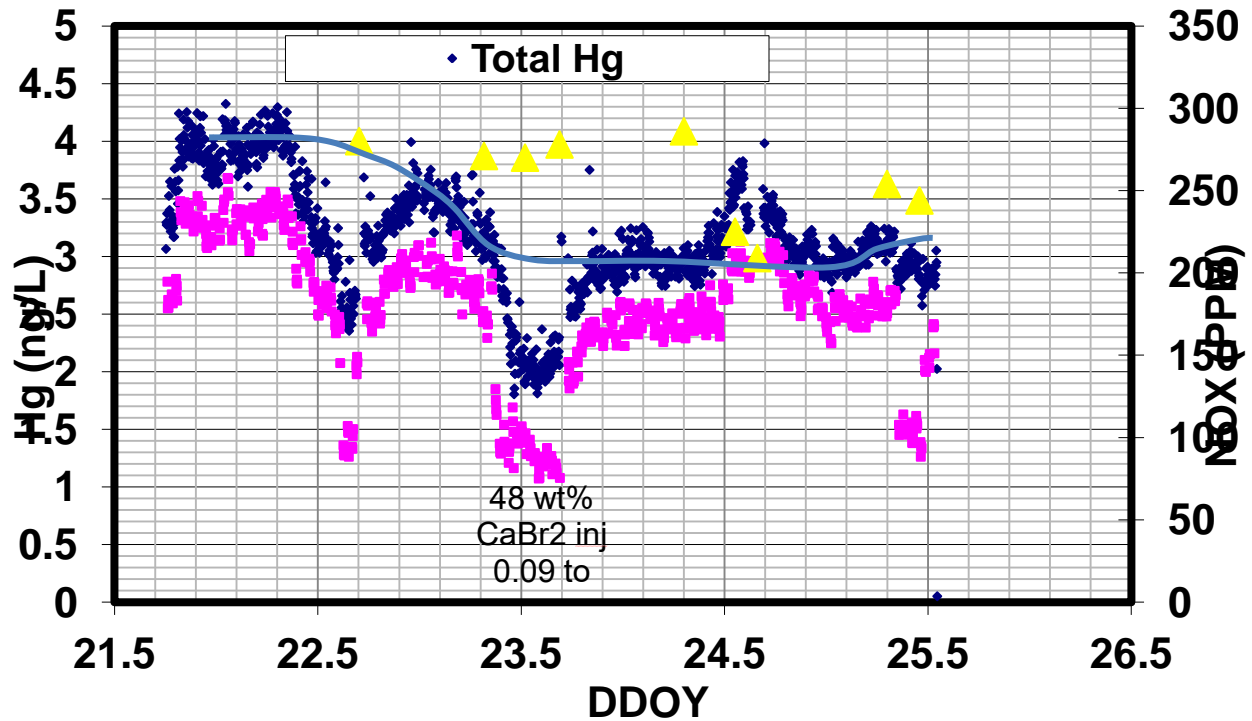


Fig. 4: Hg concentrations resulting from Hg tests conducted on **ArcelorMittal**. Dark blue diamond shapes represent total Hg. Pink squares represent elemental Hg. (yellow triangles are NOX measurements). The baseline shifted greatly prior to this test. Sometime before 22.5, the plant began wasting their scrubber water as a part of the test. Actual CaBr₂ injection occurred between 23.3 and 23.7 on this time scale (digital days).

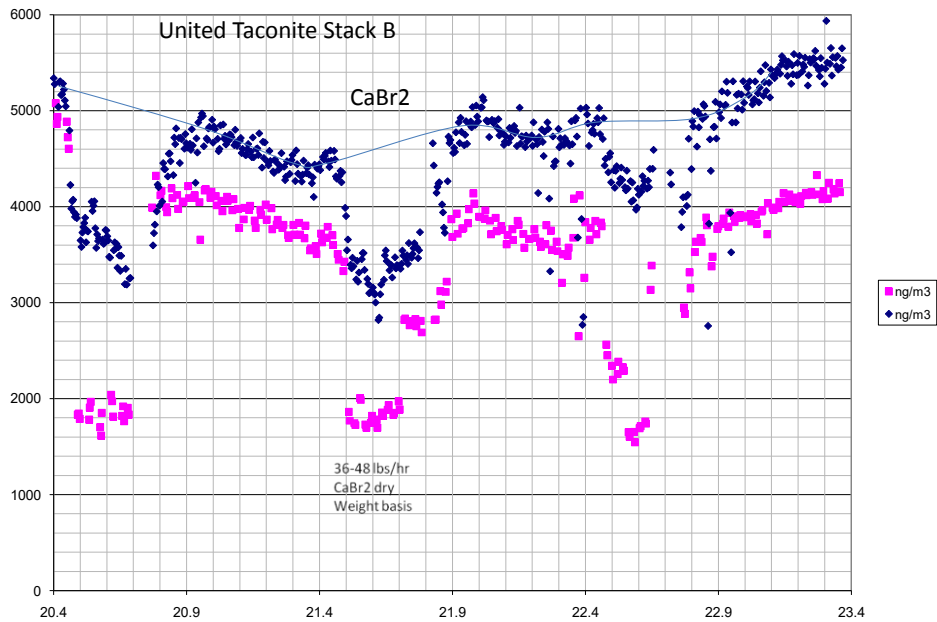
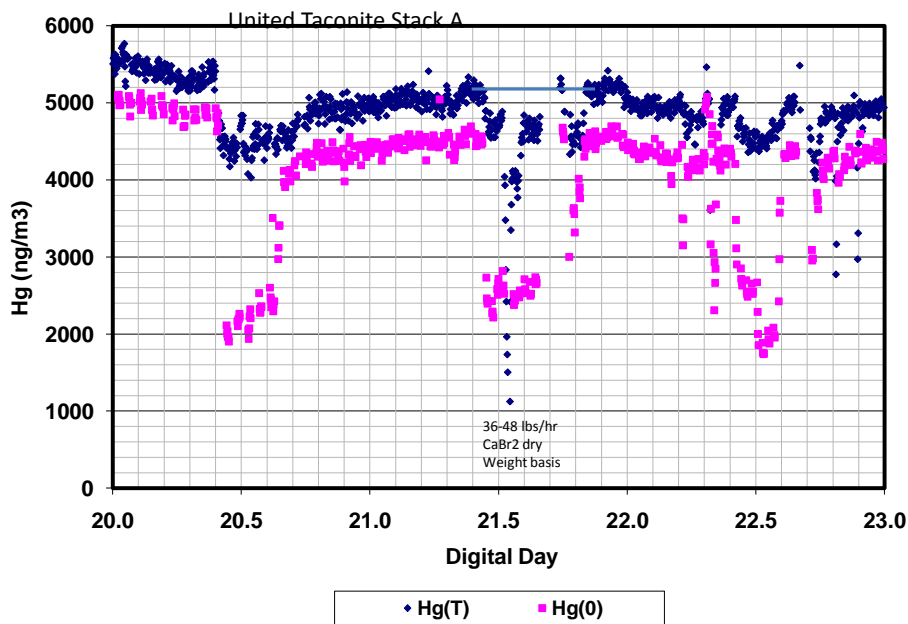


Figure 6. Hg concentration in United Taconite stack emissions during Br injection tests. Dark blue diamond shapes represent total Hg. Pink squares represent elemental Hg. Upper graph is for Stack A and lower graph is for Stack B. CaBr₂ injection occurred between 21.4 and 21.5 on this time scale.

Appendix B-1-19

Email communication from Michael Berndt (DNR) to Ryan Siats (Barr).
Data from Previous Mercury Reduction Research

September 15, 2016

From: "Berndt, Mike (DNR)" <mike.berndt@state.mn.us>
Date: September 15, 2016 at 2:04:53 PM CDT
To: "Ryan D. Siats" <RSiats@barr.com>
Cc: "Olson, Michael (DNR)" <michael.c.olson@state.mn.us>
Subject: RE: Data from previous mercury reduction research

Ryan,
See below. Call or write if you need any additional info.
Mike

From: Ryan D. Siats [<mailto:RSiats@barr.com>]
Sent: Wednesday, September 14, 2016 8:21 AM
To: Berndt, Mike (DNR)
Cc: Dane G. Jensen
Subject: Data from previous mercury reduction research

Good morning Mike,

Barr is currently working on a project for a client (taconite operation) by reviewing previous mercury reduction research. We are looking for information related to mercury control technologies that were previously tested at Arcelor Mittal's Minorca Mine. Could you please review the questions below and respond with anything that the DNR has? We greatly appreciate your help on this.

The DNR published a report in 2011 titled, "*A Brief Summary of Hg Control Test Results for Br Injection into Taconite Induration Furnaces*" (attached). The report presents results from CaBr₂ injection to the preheat zone. However, it also mentioned that tests involving NaBr addition to the furnace/greenballs or NaClO₂ to the scrubber water also occurred. Please refer to each bolded heading below for specific questions about each test.

NaBr Test

- Was this injected into the furnace or to the greenballs? **Powder was sprinkled on greenballs**
 - If injected into the furnace, where specifically? **N/A**
 - If added to the greenballs, was it sprinkled over the greenball feed or added to the concentrate prior to the balling discs? **Greenball feed**
- What was the injection rate? **35 lbs/hr**
- What was the physical state of NaBr – Solid or solution? **powder**

- If solution, please provide the concentration.
- The report mentions that the flue gas was monitored with a continuous mercury monitor (CMM, i.e. vapor Hg phase reduction only). Were other monitoring methods used? **Yes, we took a sample of scrubber water before the NaBr was added and 2 hrs and 45 minutes after the addition had taken place.**
- What was the reported Hg reduction? If this is not known, but you have the CMM data, we could try to estimate. **We attempted a test on 7/22/08, but experienced problems that caused us to abort. We tried and shortened test that ran from 8:00 AM to 11:00 AM on 7/25/08 but then ended the test with no return to baseline. Elemental mercury decreased from about 2.6 ng/ m³ to 1.5 ng/ m³, but total mercury only dropped from about 3.1 to 2.8 ng/m³. I have the raw CMM records stored electronically somewhere and can look for then send them to you if you still want them.**

-

NaClO₂ Test

Are you aware of what company supplied this chemical during testing?

- Where was this injected? **Highly concentrated NaClO₂ was pumped into the scrubber water.**
- What was the Injection rate? **0.186 gpm**
- Was NaClO₂ injected as a solution or pure? **Highly concentrated solution**
 - If solution, please provide the concentration **This is not in my notes, but we still have the drum and so this can be looked up.**
- We are assuming that the same monitoring equipment was used as the NaBr test? **yes**
- What was the reported Hg reduction? If this is not known, but you have the CMM data, we could try to estimate. **Both total and elemental Hg in the stack gases actually increased by about 25% during this test and decreased back to baseline after it. The test ran from 9:30 AM TO 2:10 PM on 7/24/08. I have the raw CMM records stored electronically somewhere and can look for then send them to you if you still want them.**

CaBr₂ Test

- How was this sprayed into the furnace?
 - Where in the furnace was CaBr₂ injected? **Preheat zone**
 - Were injection lances used? **No, it was assumed conversion of the liquid water to steam would disperse the chemical throughout the duct.**
 - If so, do you know who supplied this equipment
 - If not, could you describe in detail the injection setup
 - What kind of pump was used? **I don't have records of this in St. Paul but it was a very small piston pump made of relatively inert materials and it operated very well. We could probably locate the pump if interested. Typically we injected a known amount of concentrated CaBr₂ brine (48% by weight) into a constant stream of DI water that we tried to set**

- at 1 gpm. Brine injection rates were 0.09, 0.06, and 0.045 gpm.
- o Who was the supplier of CaBr_2 ? I do not recall, but we still have some of this left over in our Hibbing Lab and could get the information if it is really important to you.
 - Did you use totes for chemical storage? 55 gallon drums.

If you have any questions please let us know. It may be easier to answer these questions over the phone. If so please give me a call at 218-491-1456.

Thank you for revisiting the past research on this.

Ryan

Ryan D. Siats
Senior Chemical Engineer
Duluth, MN office: 218.788.6364
RSiats@barr.com
www.barr.com



Appendix B-2

Phase I – Minnesota Taconite Mercury Control Advisory Committee

Contents

B-2-1: Minnesota Taconite Mercury Control Advisory Committee: Summary of Phase One Research Results (2010-2012) (November 29, 2012).....	B-2-1
B-2-2: Evaluation of Scrubber Additives and Carbon Injection to Increase Mercury Capture (August 17, 2012)	B-2-27
B-2-3: Mercury Control for Taconite Plants Using Gas-Phase Brominated Sorbents (July 9, 2012).....	B-2-95
B-2-4: Developing Cost-Effective Solutions to Reduce Mercury Emissions from Minnesota Taconite Plants. ArcelorMittal Minorca Mine Inc. Plant (September 2012)	B-2-151
B-2-5: Evaluation of a Slipstream Baghouse for the Taconite Industry (January 2012).....	B-2-303
B-2-6: Phase Two Final Report (July 26, 2012)	B-2-405
B-2-7: Continuation of Corrosion Potential of Bromide Injection under Taconite Operating Conditions (March 2012)	B-2-480

Appendix B-2-1

Minnesota Taconite Mercury Control Advisory Committee: Summary of Phase One Research Results (2010-2012)

November 29, 2012

Minnesota Taconite Mercury Control Advisory Committee: Summary of Phase One Research Results (2010-2012)

A final report submitted to the United State Environmental Protection Agency

Grant Number: *GL00E00655-0*

Project Title: *TACONITE MERCURY EMISSION CONTROL STUDIES: PHASE ONE*

Prepared by:

Michael E Berndt
Minnesota Department of Natural Resources
Division of Lands and Minerals
500 Lafayette Rd
St. Paul, MN 55155

Nov 29, 2012

Summary

The Minnesota Taconite Mercury Control Advisory Committee (MTMCAC), a group of industry, state, and academic technical experts, was formed in 2009 to help the taconite industry achieve a 75% reduction in industry-wide stack gas mercury emissions by 2025. Research conducted by this group from 2010-2012 focused on testing activated and brominated carbon sorbents to improve mercury capture in existing taconite processing plants. Six projects were selected and conducted using combined funds from the Minnesota Department of Natural Resources' Environmental Cooperative Research Program (ECR), six Minnesota participating taconite companies, and the US Environmental Protection Agency, Great Lakes Restoration Initiative (EPA-GLRI).

Two of the studies tested direct injection of powdered activated and brominated carbon directly into process gas streams upstream from existing wet scrubbers. A third study evaluated the capacity of several carbon-based sorbents to remove mercury in gases from active processing plant wet scrubbers. A fourth study used powdered activated and brominated carbon sorbents and a baghouse as a post wet-scrubber polishing process to remove mercury. A fifth study involved adding carbon and brominated carbon to "greenballs" and heating in a laboratory setting to determine if this method could increase oxidation and capture of mercury in process gases and wet scrubbers, respectively. A sixth study, also performed in the laboratory, evaluated the corrosive effects of bromide on grate materials used in taconite processing plants. Of the methods considered, direct carbon injection, fixed bed reactors, and post-scrubber bag houses were all found to have the potential to control mercury at levels needed for the industry to achieve its 75% reduction goal. Direct injection of activated and brominated carbons into process gas streams is considered to be the least expensive of these methods, however, precise cost estimates for application of these technologies for taconite furnaces have not been determined. Future mercury control research efforts will focus on further evaluation of technical and economic feasibility of using this technology to control mercury emissions from Minnesota's taconite industry.

Table of Contents

Summary	2
Introduction	4
Project Summaries	5
Project 1: Evaluation of Scrubber Additives and Carbon Injection to Increase Mercury Capture	5
Project 2: Mercury Control for Taconite Plants Using Gas-Phase Brominated Sorbents	7
Project 3: Developing Cost-Effective Solutions to Reduce Mercury Emissions from Minnesota Taconite Plants.....	8
Sorbent Screening Slipstream Testing	8
Development of Full-Scale, Integrated Fixed-Bed Process Concept.....	8
Pilot Plant Design	9
Techno-Economic Analysis.....	9
Project 4: Evaluation of a slipstream baghouse for the taconite Industry	10
Project 5: Evaluation of a Low Corrosion Method to Increase Mercury Oxidation and Scrubber Capture	11
Project 6: Corrosion Potential of Bromide Injection Under Taconite Operating Conditions	12
Technology Status (September 2012).....	12
Conclusions and Path Forward	15
Acknowledgements.....	16
Technology Research Status Tables	17
References	22
Appendix I: Annual taconite mercury emissions estimated during Minnesota’s Mercury TMDL implementation stake holder process	24
Appendix II. Data for individual taconite processing furnaces where MTMCAC mercury control studies were performed.....	25

Introduction

Taconite mining is a major industry in Northeastern Minnesota that provides the United States with most of its domestic supply of non-recycled iron. Most taconite ore in this region is mined from the Biwabik Iron formation, a thick continuous layer of sedimentary rock that is over 100 miles long and composed of iron oxides, carbonates, silicates and trace mercury. Mercury has been identified as an issue within the last decade because a portion of it is released into the air when ore is concentrated and converted to pellets during taconite processing.

Most of the mercury in taconite ore is diverted to the tailings basin during a mineral separation process that separates the economic mineral, magnetite, from other minerals in the raw ore (Berndt, 2003). The mercury in tailings appears not to be leached into the environment. However, the mercury that remains with the magnetite is converted mostly to elemental mercury and released to the atmosphere during a high-temperature process referred to as induration. Induration is a necessary process in the taconite industry because it converts the powdered magnetite “concentrate” into hardened hematite pellets that are suitable for shipping to sites around the Great Lakes Basin and are ready for conversion to steel in specially designed blast furnaces.

Between 2005 and 2008, the state and industry conducted many studies on mercury cycling in processing plants including mercury generation during induration (Berndt and Engesser, 2005a; Galbreath, 2005; Berndt et al., 2005), its speciation in stack gases (Laudal, 2007; Berndt, 2008); its capture by existing wet scrubbers (Berndt and Engesser, 2005b); and its subsequent cycling within taconite processing plants (Berndt and Engesser, 2005b; Benner, 2008). Laudal and Dunham (2007) evaluated taconite control methods for the industry and concluded that chemical oxidation and sorbent injection methods used or considered for mercury emission control by the power industry may be adapted for use by the taconite industry. This led to the widespread testing of bromide addition in various forms including direct addition of dry salts to greenball, injection of salt brines into process lines, and of heated bromide radicals into waste gas ducts (Berndt and Engesser, 2007; Berndt, 2008, 2011; Pavlish and Zhuang, 2008).

In 2009, the Minnesota Pollution Control Agency (MPCA) developed an Implementation Plan to reduce Minnesota’s statewide mercury Total Maximum Daily Load (TMDL). As part of this plan, the taconite industry and the MPCA set a target of 75% reduction from its 2010 mercury air emission inventory of 841 lbs down to 210 lbs by 2025 (See Appendix A). The Minnesota Taconite Mercury Control Advisory Committee (MTMCAC) was subsequently formed to help the industry achieve this goal. Six Minnesota taconite processing facilities participated in and/or contributed funding to projects: U.S. Steel-Keetac, Hibbing Taconite, U. S. Steel-Minntac, ArcelorMittal Minorca Mine Inc., United Taconite LLC, and Northshore Mining. The MPCA and Minnesota Department of Natural Resources (MDNR) participated in MTMCAC meetings as did the University of Minnesota’s Natural Resources Research Institute (UM-NRRI) and the University of North Dakota’s Energy and Environmental Research Center (UND-EERC). Projects were selected using a rigorous competitive process involving issuance of a request for proposals by the MDNR in November 2009. A total of six projects were selected from among eleven proposals received. Projects were facilitated by the MDNR and coordinated by MTMCAC.

These projects tested carbon injection into the process gases upstream from wet scrubbers at two taconite processing plants, one which has a straight grate furnace and the other a grate kiln. These are the two types of induration furnaces used by the taconite industry in Minnesota. Carbon addition to

greenball was also tested in the laboratory at the bench scale for samples provided by five processing plants. Slip stream tests were conducted involving a bag house located downstream from the scrubber at one of the plants. Capture of mercury in gases passed through fixed beds containing carbon sorbents (located downstream from the scrubber) was evaluated using slip stream studies conducted at three of the plants. A relatively comprehensive bench-scale laboratory study was also conducted to further evaluate the effect of halides (Br and Cl) on corrosion in taconite induration furnaces.

Research into mercury control for taconite industries is an on-going process. This document provides edited summaries for each of the studies completed between 2010 and 2012 and then uses an objective means to represent, track, and compare research results in a series of research status tables. Each of the full reports for the projects is available electronically at the following website: http://www.dnr.state.mn.us/lands_minerals/dnr_hg_research.html.

Project Summaries

Project 1: Evaluation of Scrubber Additives and Carbon Injection to Increase Mercury Capture

http://files.dnr.state.mn.us/lands_minerals/reclamation/benson_nasah_2012a.pdf

Steven A. Benson, Junior Nasah, Charles Thumbi, Shuchita Patwardhan, Lance Yarbrough, Harry Feilen, Scott F. Korom and Srivats Srinivasachar

University of North Dakota, Institute for Energy Studies

August 2012

Project 1 was conducted by the University of North Dakota (UND) and Envergenx LLC team with support from IAC International and Western Kentucky University. The goals of Project 1 included:

- Increasing the degree of oxidation of elemental mercury that is released during induration through the use of additives.

- Maximizing the capture of mercury in the scrubber and preferentially sequestering to the solid non-magnetic portion of the scrubber slurry, providing possible options for further separating and discharging 'mercury-rich' non-magnetic solid fraction.

The scope of work involved bench, pilot and full scale testing to examine the efficiency of various additives to oxidize and sequester the mercury.

To attain the first goal of oxidation and capture, the technology employed two additives: ESORB-HG-11, a proprietary brominated powdered activated carbon provided by Envergenx LLC; and Powdered Activated Carbon (PAC). These additives have been tested and have proven to control mercury emissions in coal-fired power plants. Meanwhile for the second goal, the ability of ESORB-HG-11, PAC and a third additive- diethyl dithiocarbamate (DEDTC), to maximize the sequestration of dissolved mercury was investigated. Sequestering the mercury captured by the scrubber to the solid portion of the slurry and removal of the solids from the process loop would provide an 'exit' for the captured mercury. This can also prevent possible reemission of the captured mercury in the scrubber.

Field tests of the technology were conducted at U.S. Steel Minntac's Line 3 grate kiln. In the grate kiln, the green balls are sequentially dried in a drying zone (downdraft), then heated and oxidized (induration) in both a preheat and kiln zone, respectively. It is believed mercury release from the green

balls begins in the preheat zone. Consequently, the mercury oxidation technology targeted flue gas exiting the preheat zone. The test was divided into four main areas: stack sampling to determine mercury concentration leaving the stack; sampling of green balls to determine mercury input; multiclone dust and scrubber slurry sampling; and injection of the powdered carbon (technology deployment) in the flue gas exiting the preheat zone.

Baseline total mercury stack emissions (during the testing period) from Minntac Line 3 ranged from 3.5 to 8.2 $\mu\text{g}/\text{m}^3$; with most values between 4.0 and 6.2 $\mu\text{g}/\text{m}^3$. Particulate mercury emissions during baseline operation (during test periods) were minimal, with most values below 3% of the total mercury emitted. The predominant form of mercury in the stack emissions was elemental; values ranged between 83 and 90%, with the exception of one measurement.

Of the additives tested, only ESORB-HG-11 showed the potential to attain the target 75% mercury emission reduction. Results from the field testing further indicated significant reductions in vapor phase stack Hg emissions from a test period baseline value of 5.1 $\mu\text{g}/\text{m}^3$ to 0.83 $\mu\text{g}/\text{m}^3$, an 84% reduction, with injection rates of ESORB-HG-11 of 0.5 pound per long ton (150 lb/h of sorbent) of taconite processed. However, reductions in vapor phase mercury during ESORB-HG-11 injection were coupled with an increase in the particulate mercury emissions. Including the added particulate mercury emission, a 71% reduction from the testing baseline value was obtained. While the particulate scrubber is effective for capturing the taconite dust entrained in the flue gas, it is less effective in capturing the powdered carbon additive. Increases in particulate mercury emissions suggest that the tested technology requires higher particulate capture efficiencies to achieve 75% mercury reduction. Another key result from the testing indicated a dramatic decrease in dissolved mercury in the scrubber liquid, (from 3000-5000 ng/L to 20 ng/L) during ESORB-HG-11 injection. This suggests that the dissolved mercury in the scrubber slurry preferentially adsorbed to ESORBHG- 11, a non-magnetic phase, establishing the sequestering capabilities of the additive.

The fate of sequestered mercury associated with ESORB-HG-11 and the scrubber solids depends on the process configuration. On Minntac Line 3, the scrubber slurry is transported to a thickener and the solids are subsequently discharged. This provides an exit for all mercury captured by the system. However, not all taconite plants discharge their solids; instead they are recycled to the front end of the process. This creates a recycle loop for the mercury in the entire process that would lead to increases in the green ball mercury concentrations and a subsequent increase in the stack mercury concentrations. Therefore, for this sorbent injection technology to be effective at mercury oxidation and mercury capture at other facilities, a fraction of their solids from the scrubber would have to be discharged to prevent mercury from accumulating in the system.

Project 2: Mercury Control for Taconite Plants Using Gas-Phase Brominated Sorbents

http://files.dnr.state.mn.us/lands_minerals/reclamation/miller_zerangue_2012.pdf

J. Miller, M. Zerangue, Z. Tang and R. Landreth

Albemarle Environmental Division.

July 2012

In 2011, Albemarle Environmental Division personnel conducted a field trial at Hibbing Taconite to demonstrate the effectiveness of gas-phase brominated sorbents in controlling mercury emissions from taconite facilities. There was a preliminary site visit in March 2011 followed by pre-trial testing in early June 2011. The pre-trial testing determined that the mercury sorbent would have to be injected into both the Windox Exhaust flue gas stream and the Hood Exhaust flue gas stream to achieve the desired 75% mercury removal from the baseline condition.

The equipment was prepared for the trial and the demonstration conducted in September and October 2011. The parametric testing demonstrated that the 75% Hg removal target could be achieved with a gas-phase brominated sorbent injection rate of about 3 lb/MMacf (126 lb/hr). It was demonstrated in a two-week continuous injection run that this removal rate could be achieved over time. This injection rate is higher than expected to achieve the 75% mercury removal but it does not appear to be a problem of the control technique. Rather, the sorbent distribution was sub-optimal due to project limitations. It is believed that better mercury removal results could be achieved with improved sorbent distribution.

Grab samples of green balls, multiclone dust and scrubber water were taken to identify any trends. The green ball mercury content averaged about 15 ng/g and varied randomly by nearly a factor of two from high to low concentration measured. Sorbent was injected before the multiclone and there was a concern that some sorbent would be captured there and decrease the overall Hg removal rate. It was discovered that some sorbent was captured by the multiclone but that its impact on the mercury removal rate was probably small. The Hg content of the scrubber water did not increase during the trial and varied between the high and low levels observed in the baseline testing. Filtering the scrubber water greatly reduced the mercury content since the sorbent contained in the scrubber solids still had Hg capacity.

Project 3: Developing Cost-Effective Solutions to Reduce Mercury Emissions from Minnesota Taconite Plants

http://files.dnr.state.mn.us/lands_minerals/reclamation/schlager_amrhein_2012a.pdf

http://files.dnr.state.mn.us/lands_minerals/reclamation/schlager_amrhein_2012a.pdf

http://files.dnr.state.mn.us/lands_minerals/reclamation/schlager_amrhein_2012a.pdf

Richard Schlager, Jerry Amrhein and Kyle Bowell

ADA-Environmental Solutions

September 2012

ADA Environmental Solutions (ADA) proposed a project to The Minnesota Department of Natural Resources (MnDNR) to develop cost-effective solutions to meet the industry goal by reducing mercury emissions from taconite plants by 75%. ADA was contracted to determine if activated carbon (AC) was a viable sorbent to control mercury in process gas from taconite plants when used in a fixed-bed application. There were four main tasks defined in the Work Scope: (1) Slipstream screening tests evaluating relative performance of test materials in actual process gas, impact of relative humidity on performance, and impact of process gas on mercury capture performance compared to controlled laboratory conditions; (2) develop a full-scale, integrated fixed-bed process concept; (3) pilot-scale fixed-bed design, and (4) techno-economic analysis of mercury control options;

Screening at each plant was conducted using the Mercury Index Method (MIM), a tool based on EPA Reference Method 30B that was developed by ADA for the project. Stack gas from a taconite process was drawn through tubes containing AC sorbents for time periods ranging between 1 and 10 hours. Each tube contained two sections, the first containing the AC under evaluation mixed with sand, and the second containing a standard EPA Method 30B AC. The Method 30B AC was sufficient to capture all the mercury contained in the sample gas for several days to weeks. The effectiveness of the test AC was determined by measuring the mercury captured in both sections and determining the fraction that passed through the first section into the section containing the Method 30B AC.

Sorbent Screening Slipstream Testing

Results indicated that all test AC sorbents were effective for mercury removal. Test sorbents included a sulfonated, granular, coconut shell-based carbon; an untreated, pelletized, anthracite-coal based carbon; and a sulfonated, pelletized, anthracite-coal based carbon. The material that comparatively captured the most mercury at all three plants was the sulfur treated coconut-shell (CR612C-Hg). Performance sensitivity to changes in process conditions will affect the full-scale design. Therefore, CR612C-Hg was tested in process gas with relative humidity between 50% and 70% at Hibbing Taconite, 50 to 81% at Arcelor Mittal, and 50 to 67% at United Taconite. There was no significant impact in mercury capture performance as a result of changes to the relative humidity. Also, mercury removal results from laboratory testing in dry nitrogen were very similar to results from slipstream tests at all three plants, indicating that nothing in the process gases negatively impacted the mercury removal effectiveness.

Development of Full-Scale, Integrated Fixed-Bed Process Concept

Task 1 screening results and full-scale design criteria were used to develop a full-scale fixed-bed conceptual design using design flows of 756,000 ACFM at Hibbing Taconite, 854,000 ACFM at Arcelor

Mittal, and 493,000 ACFM at United Taconite¹. The design incorporates 18, 19, and 11 vessels, respectively, for the plants. Vessels contained beds of carbon that are each 47 feet long and 12-feet wide and 3 feet deep. An estimated 1,252,080 lbs of AC would be required to fill the beds at Hibbing Taconite, which compares to 1,377,288 lbs at Arcelor Mittal, and 813,850 lbs at United Taconite . The estimated pressure drop across the beds in each case is 6 to 12 inches of water. The amount of carbon that would be used per year to maintain 100% mercury capture was projected to be 200,208 lbs at Hibbing Taconite, 117,403 lbs at Arcelor Mittal, and 138,108 lbs at United Taconite. This initial concept design would need to be validated through longer-term pilot testing.

Pilot Plant Design

The estimated cost of a pilot-scale fixed-bed system appropriate to collect detailed information required for a robust full-scale design is \$50,000. All testing costs would be in addition to the cost of the equipment. Task 1 results indicate fixed-beds of activated carbon can reliably achieve the taconite industry's goal of 75% mercury control. However, based on the concept design and the techno-economic analysis (below), a fixed-bed approach to control mercury from the process gas at either HibTac, ArcelorMittal, or UTac is expected to be more costly than other approaches and require multiple, large, interconnected vessels. Therefore, ADA does not recommend continued development and testing of fixed-bed technologies for mercury control from the process gas at these plants.

Techno-Economic Analysis

The relative technical and economic characteristics of seven mercury control technologies were compared using a Kepner-Tregoe (KT) decision-making approach by Stantec Consulting Ltd. The fixed-bed method to control mercury was determined to provide good performance but at relatively high cost compared to other options. The high cost was a result of several factors including the number of vessels required and the associated plant integration, and the expected pressure drop across the beds. AC injection was identified as the most promising technology using this approach.

¹ In a later review of this report, this flow rate was thought to be too low for those typically encountered during normal operation at this plant. A higher flow rate would result in increased costs compared to those estimated in the report.

Project 4: Evaluation of a slipstream baghouse for the taconite Industry

http://files.dnr.state.mn.us/lands_minerals/reclamation/laudal_2012.pdf

Dennis L. Laudal

Energy & Environmental Research Center, University of North Dakota

January 2012

The Energy & Environmental Research Center tested a mercury control technology utilizing a slipstream baghouse with activated carbon injection at the United States Steel Corporation, Minnesota Ore Operations – Keetac Plant. The EERC slipstream baghouse is a trailer-mounted baghouse that was transported to the test site and connected in slipstream fashion to allow for testing “real” flue gases under actual operating conditions. Because the slipstream baghouse was located after a wet scrubber, the flue gas at the inlet was saturated at about 132°F. To avoid wetting the bags and fan, an additional drip leg and heating elements were installed to raise the inlet flue gas temperature to about 165°F. For a full-scale unit, it would be expected that a portion of the flow (prior to the wet scrubber) would be routed to the baghouse to maintain a temperature above the water dew point. For the Keetac test, the baghouse was operated at a nominal air-to-cloth ratio of 6 ft³/min (actual ft³/min of gas per ft² of cloth). Ports were installed so that the mercury concentrations at both the baghouse inlet and outlet could be measured using continuous mercury monitors (CMMs) and sorbent traps. Results showed that by using as little as 2.2 lb/Macf of standard activated carbon or 1.1 lb/Macf of a treated carbon >75% mercury removal can be achieved.

Mercury removal of >75% can be achieved at Keetac with either standard or bromine-treated activated carbon. 2.0 lb/Macf of standard activated carbon and 1.1 lb/Macf of bromine-treated activated carbon are needed when natural gas is used as the fuel. Only 0.6 lb/Macf of bromine-treated activated carbon is needed when a PRB coal is fired. Very low particulate emissions can be achieved in either case.

Because of the relatively high cost of installing a fabric filter, the most economical installation would be for those taconite facilities that require fuel flexibility and/or where additional particulate control is needed. If a baghouse is to be installed at Keetac, 18%–20% flue would need to bypass the wet particulate scrubber to prevent wetting of the bags. Overall, the slipstream baghouse and CMMs operated well during the test period. However, it appears that if the ACI is turned off, there is the potential of (temporarily) high mercury emissions as a result of reemission.

If this is to be a viable technology, the following recommendations are made for future testing:

- (1) Longer-term testing is needed to determine the resultant steady-state pressure drop across the baghouse as a function of air-to-cloth ratio.
- (2) Longer-term tests are also needed to ensure that required mercury control will be maintained.
- (3) It appeared that the bromine-treated activated carbon worked better when firing coal compared to natural gas. The same may be true using standard activated carbon. Therefore, additional coal tests are needed.
- (4) The economic evaluation presented in this report is based on the utility requirements and may or may not be the same for a taconite plant. Therefore, more specific economic data are needed.
- (5) There may be a need to evaluate or update the existing wet scrubber mist eliminators.

Project 5: Evaluation of a Low Corrosion Method to Increase Mercury Oxidation and Scrubber Capture

http://files.dnr.state.mn.us/lands_minerals/reclamation/benson_lentz_2012b.pdf

Steven A. Benson, Nicholas Lentz, Shuchita Patwardhan, Junior Nasah, Charles Thumbi, Harry Feilen and Srivats Srinivasachar

University of North Dakota, Institute for Energy Studies

September 2012

Green balls produced from concentrate/filter cake and additives obtained from five of the taconite facilities operating on the Mesabi Iron Range were combined with trace amounts of ESORB-HG-11. ESORB-HG-11 is a proprietary brominated powdered activated carbon. The green balls containing ESORB-HG-11 were then subjected to laboratory heating experiments to determine the mercury oxidation potential of the additive.

Heating tests of the green balls from four of the facilities gave mercury oxidation levels ranging between 43% and 78%, with averages of 52% ($\pm 8\%$) and 58% ($\pm 11\%$) for additive amounts of 0.1 weight% and 0.5wt%, respectively. Baseline oxidation percentages measured in the laboratory averaged 18% ($\pm 6\%$), while oxidation in green balls mixed with ESORB-HG-11 averaged 42% ($\pm 9\%$) and 48% ($\pm 13\%$) for the 0.1 wt% and 0.5 wt% additive loading experiments respectively. The results confirm preliminary results obtained in Phase 1 of this project, and indicate that the 0.1 weight% ESORB-HG-11 loading is optimal for mercury oxidation, and is recommended for any potential future work involving the technology. The results obtained from a fifth facility, United Taconite, were not included in determining the averages, as they showed significantly lower mercury oxidation increases for ESORB-HG-11-containing green balls. The oxidation levels observed were approximately 10% to 15% lower than those observed for the other plants. The possible reason for this difference was not conclusively established during the testing.

The green balls were produced by the Coleraine Minerals Research Laboratory (CMRL) of the Natural Resources Research Institute (NRRRI). They were then subjected to industry-standard, batch balling tests to determine the possible effects that the additive might have on the physical properties of the green balls. The physical properties investigated consisted of the moisture content, wet drop number, and dry compressive strength. For the samples with 0.1 weight% additive, no significant difference due to addition of ESORB-HG-11 was observed with respect to the baseline standard during the batch balling tests. Slight differences from the baseline standard were observed with the 0.5 weight% additive loading, suggesting that the 0.1 weight% is the optimal additive loading.

Preliminary tests performed during Phase 1 of this project determined that there was little or no gas-phase mercury oxidation occurring during tests performed using the bench scale apparatus. This suggests that the mercury oxidation observed during these tests is a solid phase phenomenon occurring most likely on the carbon surface and within the green ball. Previous work indicates that gas-phase mercury oxidation does occur in taconite facilities with bromide addition to the green ball which enhances baseline (no bromide addition) mercury oxidation values. Consequently, a full-scale demonstration of the technology might result in higher levels of mercury oxidation than observed during the bench scale tests in this project. No tests were performed in this project to determine the impact of the carbon additive on the physical and metallurgical properties of fired taconite pellets; this aspect should be investigated in future testing.

Project 6: Corrosion Potential of Bromide Injection Under Taconite Operating Conditions

http://files.dnr.state.mn.us/lands_minerals/reclamation/zhuang_dunham_2012.pdf

Ye Zhuang, David J. Dunham, John H. Pavlish

Energy & Environmental Research Center, University of North Dakota

June 2012.

The overall goal of this project was to characterize bromine-induced corrosion on taconite processing equipment under simulated but representative taconite processing conditions. Specific objectives of this project included the following: determine Br-induced corrosion on grate bars (metal alloys) and on ductwork materials (low carbon steel) in simulated taconite flue gas containing HBr under thermal cycling conditions, compare the corrosion rates induced by bromine and chlorine, and estimate the life span of test coupons in taconite flue gas containing bromine species.

Comparisons between bromine- and chlorine-induced metal corrosion were made under simulated taconite operating conditions. Blisters and/or pinholes observed on the surface of the grate bar metals indicate that volatile compounds were formed, mainly iron chloride or iron bromide compounds. Temperature is very critical to corrosion, and the maximum temperature seems to be the most important factor.

Active oxidation appears to be the main corrosion mechanism for grate bar samples under elevated temperatures of 500°–950°C, while HBr showed a higher corrosion rate than HCl under similar simulated conditions. As a result, under the same level of halogen exposure with the same thermal cycles, both the Minntac and Minorca grate bar showed more microfracture and weight loss under the bromine condition compared to chlorine, while the main reasons for the weight loss can be ascribed to depletion of iron.

Based upon the measured data, the projected weight loss of Minntac and Minorca grate bar metals over 3 years of operation under HBr conditions is marginal. Minorca grate bar is expected to have 0.84 mm of material depletion in comparison to 0.01 mm of material loss with Minntac grate bar.

By comparison, no significant corrosion was observed for the low-carbon steel from ducts since it only experienced low temperatures of 50°–200°C. The project weight loss of this metal over a 3-year operation under HBr conditions is minimal.

Note that the completed corrosion exposure tests were carried out in a bench-scale experimental system that cannot precisely simulate actual operating conditions in the taconite process. Therefore, the project results can be regarded as a first-step effort to address the potential bromine-induced corrosion as bromine is applied to the taconite facility for mercury reduction. Large-scale field testing is recommended in the future to account for the difference between bench-scale and full-scale systems.

Technology Status (September 2012)

Processing plants and test methods vary so it can become difficult to compare and assess results from competing control methods tested at a variety of processing plants. Some of the variables that need to be considered include furnace type, pellet type produced, binder used in greenballs, scrubber type used to control particulates, fuel type burned, and the number of stacks per line (See Appendix II).

Thus, the MTMCAC adopted a standardized approach to track research status for several different technologies being considered for Hg control by the taconite processing industry. First, each of the contractors performing tests for MTMCAC was required to provide and report the specific details of the equations and extrapolations used to estimate reductions achieved by their methods. These equations and reports were reviewed and validated by an independent third party (Barr Engineering, Minneapolis, MN) to ensure that the reports contained all information and assumptions needed to reproduce the control estimates. Tables 1 to 5 were then constructed to provide a direct comparison of results and to record assumptions made, testing locations and type (e.g., conducted on a bench – slip stream, pilot, or short, or long-term full-plant scale). Results were also extrapolated to other plants to assess the potential Hg reductions that might be realized if the technology were applied on an industry-wide basis. The methods used to make these extrapolations are also tracked in the tables.

The five technologies evaluated include CaBr_2 injection into the process gas stream (Table 1, tested prior to the present study), addition of brominated carbon sorbents to greenball feed (Table 2 – Project 5 in this report), brominated carbon sorbent injection into process gas streams upstream from wet scrubbers (Table 3 – Projects 1 and 2), capture by fixed beds containing several activated carbon types and located downstream from wet scrubbers (Table 4 – Project 3), and post-scrubber injection of sorbents downstream of the scrubber but upstream from a baghouse (Table 5 – Project 4). The mercury reductions were computed from annual baseline values estimated for 2010 (see Appendix 1) which estimated total industry emissions to be 840.6 lbs/year during that year. If a plant had more than one line, then the plant's inventory was partitioned among the separate lines according to their respective production capacities.

These tables include emissions from two companies that did not participate in the present research: Essar Steel and Mesabi Nugget. These companies have permits requiring that they conduct their own research on mercury emission control methods. However, Essar Steel is building a straight-grate taconite processing facility. Therefore, MTMCAC provided estimates for the amount of control they might expect, using each of the five technologies considered here. Results for the studies presented in this report, are not applicable to Mesabi Nugget due to the differences in processing techniques. It was assumed, therefore, that Mesabi Nugget would reach a 75% mercury reduction goal using control methods designed specifically for their process.

Each of the inventories also includes several smaller sources where mercury is unlikely to be controlled or practicable: Northshore, where only 7.3 lbs of Hg is emitted annually from three process lines, and sources unrelated to taconite processing furnaces that emit 1.2 lbs of mercury annually. The inventories presented in Tables 1 through 5 do not assume any control of mercury from these sources.

Estimated annual emissions are provided for each processing line both with and without the technology in place and the total emissions are summed. Costs were evaluated using a relative scale, whereby the technologies were ranked L, M, or H, respectively for those with lowest, medium, or highest estimated costs. Techno-Economic Analysis conducted by Schlager et al. (2003) (Project 3 above) greatly aided this process.

Injection of dissolved CaBr_2 into taconite processing lines (Table 1). Prior to the tests presented in this research summary, extensive testing was conducted to determine whether injection of Br salts into taconite processing furnaces impacts Hg emissions. Test methods involved the direct injection of calcium bromide (CaBr_2) brine into the processing line at rates of approximately 20 to 50 lbs/hr on a dry salt weight basis. The water evaporates and the salts decompose to yield HBr and Br_2 , which can oxidize the mercury. This method was first studied at the Hibbing Taconite processing plant by Berndt and Engesser (2007) and was eventually tested at five processing plants (summarized by Berndt, 2011).

Other methods of Br-salt injection have been tried (addition directly to the greenball feed (Berndt, unpublished data) or direct injection of fired halogens into process gas in the waste gas ducts (Pavlish and Zhuang, 2008), but these methods proved to be less effective than direct injection of CaBr_2 salt solutions into the process gases within the induration furnaces.

Initially, a primary criticism of this method was that the addition of halide salt to the process lines may result in enhanced corrosion and shortened life of furnace grates. Two laboratory studies conducted by Zhuang et al. (2009, 2012 – see summary for Project 6 of this report) on grate materials supplied by industry revealed that although Br addition enhanced corrosion, the rates were relatively slow and would likely have minimal impact on the life spans of the grates.

With or without a corrosion issue, the method was unable to reliably reach the desired 75% capture rate at most of the plants studied (Table 1; Berndt, 2011). It is estimated that although some applications approached 75% capture (Line 3 at Minntac and Line 3 at HibTac), use of this technology would capture only about half of the mercury currently emitted by the industry. Although the cost of this method is considered to be the lowest of those studied, the MTMCAC does not believe it can be used to reach its target reduction goals.

Addition of brominated carbon to greenball feed (Table 2). This process was not tested at any plants but was tested in the laboratory using freshly produced greenball feed from five taconite processing plants (Benson et al., 2012b – See summary for Project 5 of this report). The addition of the brominated carbon to the heated greenball causes an increase in oxidation for Hg released during the induration processes. To estimate the effect of this method on mercury control at taconite processing furnaces, MTMCAC assumed that the increased capture in the wet scrubbers would be proportional to the increased oxidation in the mercury released from the greenball.

Based on this estimation method, none of the companies would reach 75% control of their emissions and the annual total range-wide mercury emissions would drop from approximately 840.6 lbs/year down to 522.6 lbs/year, well short of the 210 lb/year target. Benson et al. (2012) believe that actual control might be better than those estimated by this method due to reactions between bromine and Hg in the gas phase so it is possible that, with further testing at a plant scale, this technique might achieve the 75% reduction level at some plants.

This method has a lower anticipated cost than other sorbent carbon methods but effect on the quality of fired pellets has not been fully evaluated. Engesser (2004), for example, found that addition of 0.6 and 1.0 wt% carbon to greenballs caused a decline in compression strength of the fired pellet.

Injection of gas-phase brominated sorbents into process gas, upstream from wet scrubbers (Table 3). This method involves the injection of brominated carbon-based sorbents into taconite process gases, downstream of the location where the mercury is released, upstream from the wet scrubbers that control particulate emission. This method, which is widely used to control mercury at coal-fired power plants, was tested here at two taconite processing plants: Minntac Line 3 (Benson et al., 2012a; see summary for Project 1) and HibTac Line 1 (Miller et al., 2012; See summary for project 2). Both tests demonstrated that a large percentage of the mercury in taconite stack gases can be removed. Non-brominated activated carbon (PAC) sorbents provided less control of mercury in stack gases but the amount of carbon needed was greatly increased compared to brominated carbon-based sorbents.

It is important to note that Benson et al. (2012a) observed that mercury control by this method at Minntac was accompanied by an increase in particulate mercury emission that was associated with the activated carbon. Total reduction from these tests was approximately 71%, slightly short of the 75% target. It is estimated, therefore, that the technology can reach a 75% or greater mercury control level with improved particulate capture. Tests by Miller et al. (2012) at Hibbing Taconite exceeded the 75%

control goal but they reported that test limitations on injection port locations meant that the amount of sorbent needed to control mercury emissions was larger than expected.

To estimate control levels for the industry, it was simply assumed that the companies would optimize their individual mercury control processes to achieve a 75% (or better) mercury reduction level. In both cases, it appeared that a 75% or greater reduction goal can be achieved using brominated sorbents at taconite plants, and that the total emissions for the industry could potentially be reduced from 840.6 lbs/year to less than 216 lbs/year. Minntac, ArcelorMittal, and United Taconite would also be required to eliminate mercury recycling loops in their induration furnaces (Keetac already discards scrubber solids and the non-magnetic scrubber solids, including the injected sorbent, will be routed to the tailing basins at Hibbing Taconite).

Injection of brominated carbon into process gas downstream of wet scrubbers but upstream from a baghouse (Table 4). The sorbents are injected following the wet scrubber in this polishing technique, and then captured by a baghouse. The sorbents that accumulate in the bag house provide an effective chemical trap for most of the mercury that would otherwise escape the scrubber. Advantages of this method include the fact that it does not interfere directly with the induration process nor does it introduce potentially corrosive bromide into the taconite processing lines. Pellet quality would not be threatened. The slipstream tests conducted by Laudal (2012; See Project 4 summary included in this report) at US Steel Keetac indicated that the method could remove greater than 75% of the mercury that remains in the gas after passage through the scrubber. However, the high initial capitalization and maintenance costs, space limitations, pressure drop across the bags (requiring additional process fans and energy), and the need for heating the process gas stream (or to bypass the wet scrubber with a fraction of the gas) to prevent condensation in the baghouse make this one of the most expensive control methods that was evaluated.

Fixed bed reactors containing activated carbon (Table 5). As with the post-scrubber bag house, this method is a polishing process for the waste gas and so does not interfere directly with the induration process itself and does not increase potentially corrosive bromine to process gases. This method was initially pioneered for taconite processing plants using simulated taconite process gases generated in the laboratory by Dunham and Miller (2009). Schlager et al. (2012 a, b, and c; See Project 3 summary in this report) tested the technique using packed beds exposed for 1 to 10 hrs to actual taconite processing gases at three taconite processing plants. The results suggested that this method could capture greater than 75% of the mercury in taconite processing streams and meet the industry's reduction goals. Furthermore, because it is a polishing technique, located post-scrubber, its use would avoid interference with the taconite induration process, nor would it introduce potentially corrosive bromide to the taconite processing lines. However, this method suffers from many of the same limitations as the post-scrubber baghouse: high initial capitalization and maintenance costs, space limitations, increased pressure drop, and the need for heating of the process gas stream to prevent condensation. It is considered the most expensive method tested.

Conclusions and Path Forward

Six studies were conducted to test a variety of potential carbon-based methods to control mercury levels in stack gases emitted from Minnesota taconite processing facilities. Five of the studies evaluated various activated and brominated carbon applications, while a sixth study evaluated the corrosive effects of halides (bromide and chloride) on the grates that are used in taconite processing facilities. Direct injection of brominated carbon appears to be the least costly of the methods that have

been tested to date that has the potential to help the industry reach its stated goal of 210 lbs Hg emitted per year. Other methods, including (CaBr₂) addition to process gases (tested previously) and brominated carbon addition to greenball feed, are likely less expensive, but neither has been demonstrated to reliably achieve the necessary mercury reduction levels. Polishing techniques located after the scrubber worked well in slipstream experiments, but the costs associated with these techniques are much higher than methods relying on direct injection of brominated carbon to the process gas stream.

Based on mercury research project findings, from 2011 and 2012, the Minnesota taconite industry is planning to conduct long-term testing of gas-phase brominated sorbents. Further, it is the goal of industry to comply with the state of Minnesota's mercury TMDL and to identify a practical, feasible, and cost-effective technology that that not interfere with pellet quality and/or result in additional complex waste streams that will require management. Industry hopes to learn how furnace, fuel, binder and scrubber types may influence results as well the potential operational and capital costs.

Acknowledgements

The research represented in this document was funded, directed, guided, and completed through the combined efforts of a large number of participating groups and agencies. It could not have occurred without funding provided by the MDNR Environmental Cooperative Research program (ECR), the six cooperating Minnesota taconite operations (U.S. Steel-Keetac, Hibbing Taconite, U. S. Steel-Minntac, ArcelorMittal Minorca Mine Inc., United Taconite LLC, Northshore Mining), and especially the United States Environmental Protection Agency, through its Great Lakes Restoration Initiative (EPA-GLRI). John Pavlish (University of North Dakota), Anne Jackson and Mary Jean Fenske (MPCA), and John Engessser (MDNR) are thanked, along with all of the industry MTMCAC representatives who provided consistent and continuous support and encouragement throughout this effort. Keith Hanson and Julianne Hanson, Barr Engineering, are gratefully acknowledged for providing much needed logistical support, including the scheduling of monthly MTMCAC meetings and assistance with keeping all contractors on tight reporting schedules. Tim Russell and Aaron Aamold, Barr Engineering, Inc., are acknowledged for performing data quality verification of the EPA-funded projects. Matt Lindon (Minnesota Pollution Control Agency) provided important assistance in the area of data quality management, as well. Eric Osantowski, EPA, is acknowledged for guiding this project through the federal funding and reporting processes. Daniel Roark, MDNR, is also thanked for navigating the individual contracts through the state and federal funding processes.

Technology Research Status Tables

Table 1: Hg-reduction Technology Status for Injection of calcium bromide (dissolved in water) into the process gas stream. Estimated emissions are listed in pounds of mercury emitted annually with and without the technology in place.

Processing Line	Estimated Baseline Emission	Tests Conducted				Estimated controlled emission	Cost L/M/H	Footnotes
		Bench-Scale Laboratory	Slip Stream	Short Full-Scale	Long Full-Scale			
Keetac 2	105.8			46.6		46.6	L	1,7
HibTac 1	75.7					33.3	L	2,7
HibTac 2	75.7					33.3	L	2,7
HibTac 3	75.7			33.3		33.3	L	1,7
Minntac 3	26.5			7.2		7.2	L	1,7
Minntac 4	39.7					19.9	L	3,6,7
Minntac 5	39.7					19.9	L	3,6,7
Minntac 6	39.7					19.9	L	3,6,7
Minntac 7	39.7					19.9	L	3,6,7
Arc. Mittal 1	33.4			23.0		23.0	L	1,6,7
United Tac 1	66.8					52.8	L	2,6,7
United Tac 2	66.8			52.8		52.8	L	1,6,7
Northshore	7.3					7.3		8
Essar	77.0					41.6	L	4,6,7
Mesabi Nug	70.0					17.5		5
Other	1.2					1.2		9
Rangewide	840.6					429.3		

- 1 Estimate based on full-plant test results from Berndt and Engesser (2007) and Berndt (2011).
- 2 Based on tests conducted on identical processing lines by Berndt and Engesser (2011) and Berndt (2011).
- 3 Calculated using average test result from grate kiln furnaces (50% Hg remained)
- 4 Calculated using average test result from straight grate furnaces (54% Hg remained)
- 5 No applicable results available, but assumes company will reach 75% TMDL Hg reduction goal
- 6 Scrubber solid recirc loop must be eliminated and this could result in improved capture rates.
- 7 Consult Zhuang et al. (2012) to evaluate potential for grate corrosion.
- 8 Small source compared to size of operation, Hg control unlikely to be practicable
- 9 "Other" small sources unrelated to taconite furnaces-Thunderbird and Babbitt boilers

Table 2: Hg-reduction Technology Status for addition of brominated carbon to greenball. Estimated emissions are listed in pounds of mercury emitted annually with and without the technology in place.

Processing Line	Estimated Baseline Emissions	Tests Conducted				Estimated controlled emissions	Cost L/M/H	Footnotes
		Bench-Scale Laboratory	Slip Stream	Short Full-Scale	Long Full-Scale			
Keetac 2	105.8	67.7				67.7	L	1,5,6,9
HibTac 1	75.7	43.1				43.1	L	1,5,6,9
HibTac 2	75.7	43.1				43.1	L	1,5,6,9
HibTac 3	75.7	43.1				43.1	L	1,5,6,9
Minntac 3	26.5	13.5				13.5	L	1,5,6,9
Minntac 4	39.7	20.2				20.2	L	1,5,6,8,9
Minntac 5	39.7	20.2				20.2	L	1,5,6,8,9
Minntac 6	39.7	20.2				20.2	L	1,5,6,8,9
Minntac 7	39.7	20.2				20.2	L	1,5,6,8,9
Arc. Mittal 1	33.4	19.7				19.7	L	1,5,6,8,9
United Tac 1	66.8	54.1				54.1	L	1,5,6,8,9
United Tac 2	66.8	54.1				54.1	L	1,5,6,8,9
Northshore	7.3					7.3		2
Essar	77.0					43.1	L	3,5,6,8,9
Mesabi Nug	70.0					17.5		4
Other	1.2					1.2		7
Rangewide	840.6					488.3		

- 1 Based on bench-scale tests conducted by Benson et al (2012b)
- 2 Small source compared to size of operation, Hg control unlikely to be practicable
- 3 Assumed average for test results from other operations.
- 4 No applicable results available, but assumes company will reach 75% TMDL Hg reduction goal
- 5 This technology is likely to have low cost.
-costs could be higher if Brominated C interferes with pellet quality
- 6 Consult Zhuang et al. (2009, 2012) to assess corrosion potential
- 7 "Other" small sources unrelated to taconite furnaces-Thunderbird and Babbitt heating boilers
- 8 Scrubber solid recirc loop must be eliminated and this could result in improved capture rates.
- 9 Engesser (2004) found addition of 0.6 and 1.0% carbon to greenball decreased pellet strength

Table 3: Hg-reduction Technology Status for injection of brominated carbon sorbents into process gas stream. Estimated emissions are listed in pounds of mercury emitted annually with and without the technology in place.

Processing Line	Estimated Baseline Emissions	Tests Conducted				Estimated controlled emissions	Cost L/M/H	Footnotes
		Bench-Scale Laboratory	Slip Stream	Short Full-Scale	Long Full-Scale			
Keetac 2	105.8					<26.5	L	4,6,7
HibTac 1	75.7			<18.9		<18.9	L	1,5,6,7
HibTac 2	75.7					<18.9	L	3,6,7
HibTac 3	75.7					<18.9	L	3,6,7
Minntac 3	26.5			<6.6		<6.6	L	2,6,7
Minntac 4	39.7					<9.9	L	4,6,7,8
Minntac 5	39.7					<9.9	L	4,6,7,8
Minntac 6	39.7					<9.9	L	4,6,7,8
Minntac 7	39.7					<9.9	L	4,6,7,8
Arc. Mittal 1	33.4					<8.4	L	4,5,6,7,8
United Tac 1	66.8					<16.7	L	4,6,7,8
United Tac 2	66.8					<16.7	L	4,5,6,7,8
Northshore	7.3					7.3		10
Essar	77.0					<19.3	L	4,7,8
Mesabi Nug.	70.0					17.5		9
Other	1.2					1.2		11
Rangewide	840.6					<216.6		

- 1 Based on short term tests conducted by Miller et al. (2012) that showed >75% capture could be achieved
- 2 Based on short term test conducted by Benson et al. (2012a) that showed >75% capture could be achieved
- 3 Based on test results from identical process lines by Miller et al. (2012)
- 4 Based on results from other taconite processing line but no testing was completed on this line.
- 5 Slip stream tests performed on carbon sorbent reactivity this line by ADA-ES (Schlager et al., 2012 a,b,c).
- 6 Adjustment to wet scrubber may be needed to control particulate mercury emissions (Benson et al., 2012a)
- 7 Consult Zhuang et al. (2009, 2012) to evaluate potential for grate corrosion.
- 8 Scrubber solid recirc loop must be eliminated and this could result in improved capture rates.
- 9 No applicable results available, but assumes company will reach 75% TMDL Hg reduction goal
- 10 Small source compared to size of operation, Hg control unlikely to be practicable
- 11 "Other" small sources unrelated to taconite furnaces-Thunderbird and Babbitt boilers

Table 4: Hg-reduction technology status for fixed carbon beds. Estimated emissions are listed in pounds of mercury emitted annually with and without the technology in place.

Processing Line	Estimated Baseline Emissions	Tests Conducted				Estimated controlled emissions	Cost L/M/H	Footnotes
		Bench-Scale Laboratory	Slip Stream	Short Full-Scale	Long Full-Scale			
Keetac 2	105.8					<26.5	H	4,7
HibTac 1	75.7		<18.9			<18.9	H	1,7
HibTac 2	75.7					<18.9	H	4,7
HibTac 3	75.7					<18.9	H	4,7
Minntac 3	26.5					<6.6	H	4,7
Minntac 4	39.7					<9.9	H	4,7
Minntac 5	39.7					<9.9	H	4,7
Minntac 6	39.7					<9.9	H	4,7
Minntac 7	39.7					<9.9	H	4,7
Arc. Mittal 1	33.4		<8.4			<8.4	H	2,7
United Tac 1	66.8					<16.7	H	4,7
United Tac 2	66.8		<16.7			<16.7	H	3,7
Northshore	7.3					7.3		5
Essar	77.0					<19.3	H	4,7
Mesabi Nug	70.0					17.5		6
Other	1.2					1.2		8
Rangewide	840.6					<216.6		

- 1 >75% removal achievable based on slip stream test results (Schlager et al., 2012a)
- 2 >75% removal achievable based on slip stream test results (Schlager et al., 2012b)
- 3 >75% removal achievable based on slip stream test results (Schlager et al., 2012c)
- 4 Based on slip stream results from other processing lines by ADA-ES (Schlager et al., 2012 a,b,c).
- 5 Small source compared to size of operation, Hg control unlikely to be practicable
- 6 No applicable results available, but assumes company will reach 75% TMDL reduction goal
- 7 High cost relative to other technologies based on data available in ADA-ES.
 - Large footprint needed to house exchangeable carbon beds
 - Fans and electrical infrastructure needed to account for increased pressure drop
 - Additional heat may be needed to prevent condensation
- 8 "Other" small sources unrelated to taconite furnaces-Thunderbird and Babbitt boilers

Table 5: Hg-reduction Technology Status for post-scrubber injection of brominated carbon with bag house. Estimated emissions are listed in pounds of mercury emitted annually with and without the technology in place.

Processing Line	Estimated Baseline Emissions	Tests Conducted				Estimated controlled emissions	Cost L/M/H	Footnotes
		Bench-Scale Laboratory	Slip Stream	Short Full-Scale	Long Full-Scale			
Keetac 2	105.8		<26.5			<26.5	H	1, 5
HibTac 1	75.7					<18.9	H	2, 5
HibTac 2	75.7					<18.9	H	2, 5
HibTac 3	75.7					<18.9	H	2, 5
Minntac 3	26.5					<6.6	H	2, 5
Minntac 4	39.7					<9.9	H	2, 5
Minntac 5	39.7					<9.9	H	2, 5
Minntac 6	39.7					<9.9	H	2, 5
Minntac 7	39.7					<9.9	H	2, 5
Arc. Mittal 1	33.4					<8.4	H	2, 5
United Tac 1	66.8					<16.7	H	2, 5
United Tac 2	66.8					<16.7	H	2, 5
Northshore	7.3					7.3		3
Essar	77.0					<19.3	H	2,5
Mesabi Nug	70.0					17.5		4
Other	1.2					1.2		6
Rangewide	840.6					<216.6		

- 1 Slip Stream test results conducted by Laudal (2012).
- 2 Estimated using slip-stream test results for Keetac Line 2 (Laudal, 2012)
- 3 Small source compared to size of operation, Hg control unlikely to be practicable
- 4 No applicable results available, but assumes company will reach 75% TMDL Hg reduction goal
- 5 Costs are estimated to be high relative to other technologies.
 - Retrofit would require considerable re-engineering
 - Large footprint required for bag house
 - Fans and electrical infrastructure needed to account for increased pressure drop
 - Heating or partial scrubber bypass needed to prevent condensation in bag house
- 6 "Other" small sources unrelated to taconite furnaces-Thunderbird and Babbitt boilers

References

Note all DNR reports listed below are available at:

http://www.dnr.state.mn.us/lands_minerals/dnr_hg_research.html

- Benner, B. R. (2008). Bench scale tests to separate mercury from wet-scrubber solids from taconite plants. Minnesota Dept. of Nat. Resources: 26 p.
- Benson, S. A., J. Nasah, et al. (2012a). Evaluation of Scrubber Additives and Carbon Injection to Increase Mercury Capture. Minnesota Dept. of Nat. Resources. St. Paul, MN, : 67 p.
- Benson, S. A., N. Lentz, et al. (2012b). Evaluation of a Low Corrosion Method to Increase Mercury Oxidation and Scrubber Capture. Minnesota Dept. of Nat. Resources. St. Paul, Minnesota: 66 p.
- Berndt, M. and J. Engesser (2005a). Mercury Transport in Taconite Processing Facilities: (I) Release and Capture During Induration. An Iron Ore Cooperative Research Final Report. Minnesota Dept. of Nat. Resources: 60 p.
- Berndt, M. and J. Engesser (2005b). Mercury Transport in Taconite Processing Facilities: (II) Fate of Mercury Captured by Wet Scrubbers. Minnesota Dept. of Nat. Resources: 32 p.
- Berndt, M. and J. Engesser (2007). Mercury Transport in Taconite Processing Facilities: (III) Control Method Test Results - A report submitted to Iron Ore Cooperative Research. Minnesota Dept. of Nat. Resources: 48 p.
- Berndt, M., J. Engesser, et al. (2005). Mercury chemistry and Mossbauer spectroscopy of iron oxides during taconite processing on Minnesota's Iron Range. Air Quality V, Washington, D. C. , Energy and Environmental Research Center. 15 p.
- Berndt, M. E. (2003). Mercury and Mining in Minnesota - A Minerals Coordinating Committee Final Report. Minnesota Dept. of Nat. Resources. St. Paul, MN: 62 p.
- Berndt, M. E. (2008). On the measurement of stack emissions at taconite processing plants - a progress report submitted to MPCA. Minnesota Dept. of Nat. Resources. St. Paul, MN: 23 p.
- Berndt, M. E. (2011). A Brief Summary of Hg Control Test Results for Br Injection into Taconite Induration Furnaces. Minnesota Dept. of Nat. Resources. St. Paul, MN: 7 p.
- Dunham, G. E. and S. J. Miller (2009). Demonstration of mercury capture in a fixed bed. Minnesota Dept. of Nat. Resources. St. Paul, MN: 50 p.
- Engesser, J., 2004. Nitrogen oxide (NO_x) emission reduction during pellet induration by fuel addition to the green pellets and decreased excess air. Minerals and Metallurgical Processing, 24: 9-16.
- Galbreath, K. C. (2005). Mercury Vaporization Characteristics of Taconite Pellets. Minnesota Dept. of Nat. Resources: 24 p.
- Laudal, D. L. (2007). Methods testing for measurement of mercury speciation for high-reactive dust. Minnesota Dept. of Nat. Resources. St. Paul, MN: 14 p.
- Laudal, D. L. (2012). Evaluation of a slipstream baghouse for the taconite industry. Minnesota Dept. of Nat. Resources. St. Paul, Minnesota: 101 p.
- Laudal, D. L. and G. E. Dunham (2007). Mercury control technologies for the taconite industry. Minnesota Dept. of Nat. Resources. St. Paul, MN: 36 p.
- Miller, J., M. Zerangue, et al. (2012). Mercury control for taconite plants using gas-phase brominated sorbents. Minnesota Dept. of Nat. Resources. St. Paul, MN: 55 p.
- Pavlish, J. H. and Y. Zhuang (2008). Proof-of-concept testing of a novel mercury control technology for a Minnesota taconite plant. Minnesota Dept. of Nat. Resources: 15 p.
- Schlager, R., J. Amrhein, et al. (2012a). Developing Cost Effective Solutions to Reduce Mercury from Minnesota Taconite Plants - Hibbing Taconite Plant. Minnesota Dept. of Nat. Resources. St. Paul, MN: 151 p.

- Schlager, R., J. Amrhein, et al. (2012b). Developing cost-effective solutions to reduce mercury emissions from Minnesota taconite plants- ArcelorMittal Minorca Mine Inc. Plant. Minnesota Dept. of Nat. Resources. St. Paul, MN: 151 p.
- Schlager, R., J. Amrhein, et al. (2012c). Developing Cost-Effective Solutions to Reduce Mercury Emissions from Minnesota Taconite Plants - United Taconite Plant. Minnesota Dept. of Nat. Resources: 151 p.
- Zhuang, Y., D. J. Dunham, et al. (2009). Assessment of Potential Corrosion Induced by Bromine Species Used for Mercury Reduction in a Taconite Facility. Minnesota Dept. of Nat. Resources. St. Paul, MN: 82 p.
- Zhuang, Y., D. J. Dunham, et al. (2012). Continuation of Corrosion Potential of Bromide Injection under Taconite Operating Conditions. Minnesota Dept. of Nat. Resources: 33 p.

Appendix I: Annual taconite mercury emissions estimated during Minnesota's Mercury TMDL implementation stake holder process

This is Table 19 from REPORT ON THE MERCURY TMDL IMPLEMENTATION PLAN STAKEHOLDER PROCESS Prepared for the Minnesota Pollution Control Agency by the Minnesota Environmental Initiative July 7, 2008 CFMS Contract No. A99751 most recently downloaded from:
http://www.pca.state.mn.us/index.php/component/option,com_docman/task,doc_view/

Facility	2005	2010	2018
Northshore Mining Co - Silver Bay	7.3	7.3	7.3
US Steel Corp - Minntac	185.3	185.3	185.3
United Taconite LLC - Thunderbird Mine	1.1	1.1	1.1
Hibbing Taconite Co	227.1	227.1	227.1
Ispat Inland Steel Mining - Minorca	33.4	33.4	33.4
US Steel - Keewatin Taconite	146.8	105.8	105.8
United Taconite LLC - Fairlane Plant	133.6	133.6	133.6
Minnesota Steel Industries (MSI)	0.0	77.0	77.0
Mesabi Nugget	0.0	70.0	70.0
Total	734.8	840.6	840.6

Note: Keewatin Taconite had pollution-control equipment installed in Oct 2005, which reduced Hg emissions by 28% after 2005

Appendix II. Data for individual taconite processing furnaces where MTMCAC mercury control studies were performed.

Location	Minntac Line 3	Hibbing Taconite	ArcelorMittal	United Taconite	Keetac
Furnace type	Grate-Kiln	Straight-Grate	Straight-Grate	Grate-Kiln	Grate-Kiln
Pellet type	~8% flux	High compression	~11% flux	~1% standard	~1% flux
Binder for greenballs	Bentonite	Bentonite	Bentonite	Organic	Bentonite
Line used for testing	Line 3	Line 1	Line 1	Line 2	Line 2
Scrubber type	Re-circulating, Discards solids	Single-pass, Solids sent to Concentrator	Re-circulating Solids recycled	Re-circulating, Solids recycled	Re-circulating, Discards solids
Fuel	Natural gas and biomass	Natural gas	Natural gas	Natural gas and coal	Natural gas and coal
No. of stacks/line	1	4	4	2	1

Appendix B-2-2

Evaluation of Scrubber Additives and Carbon Injection to Increase Mercury Capture

August 17, 2012

**EVALUATION OF SCRUBBER ADDITIVES
AND CARBON INJECTION TO INCREASE
MERCURY CAPTURE**

August 17, 2012



Institute for Energy Studies / 243 Centennial Drive Stop 8153 / Grand Forks, ND 58202-8153

701-777-2533 / und.instituteforenergystudies@und.edu / engineering.und.edu/institute-for-energy-studies

UNIVERSITY OF NORTH DAKOTA

FINAL REPORT

Project 1

**EVALUATION OF SCRUBBER ADDITIVES AND CARBON INJECTION TO
INCREASE MERCURY CAPTURE**

**Steven A. Benson, Junior Nasah, Charles Thumbi, Shuchita Patwardhan, Lance
Yarbrough, Harry Feilen and Scott F. Korom**

**University of North Dakota
Institute for Energy Studies
Upson II Room 366
243 Centennial Drive, Stop 8153
Grand Forks, ND 58202-8153**

**Srivats Srinivasachar
Envergex, LLC**

August 17, 2012

Contents

SUMMARY	4
BACKGROUND	6
Problem Description	6
Approach.....	6
Screening Tests	7
Minntac Line 3.....	7
METHODS	9
Testing on Minntac Line 3.....	9
Stack Sampling	12
Green Ball Sampling.....	12
Scrubber Sampling.....	13
Multiclone Solids Sampling.....	13
Field Testing Matrix	14
RESULTS	17
Green Ball Sampling Data	17
Baseline Stack Measurements.....	18
ESORB-HG-11 Testing at Preheat Injection Location	29
Conclusion – ESORB-HG-11 Testing at Preheat Fan Inlet Location.....	42
ESORB-HG-11 Testing at Preheat Grate Injection Location	42
Conclusion – ESORB-HG-11 Testing at Preheat Zone Injection Location.....	47
PAC testing at Preheat Fan Inlet Location.....	47
Conclusion for PAC injection at preheat fan location	50
DEDTC addition to scrubber slurry	50
Conclusion on testing of DEDTC	53
Mercury Reductions with Average Baseline Mercury Emissions	53
CONCLUSION.....	55
REFERENCES	56
APPENDIX A: BENCH AND PILOT RESULTS	57
Bench Testing Summary.....	57
Pilot Testing Summary	58
APPENDIX B – ADDITIONAL FIELD DATA	64

SUMMARY

The results presented in this report are from Project 1 – “Evaluation of Scrubber Additives and Carbon Injection to Increase Mercury Capture.” This project was part of a larger effort coordinated by the Minnesota DNR to examine technologies that have the potential to achieve 75% reduction in mercury emissions from the taconite industry [Taconite Mercury QAPP, 2010]. Project 1 was being conducted by the University of North Dakota (UND) and Envergen LLC team with support from IAC International and Western Kentucky University. The goals of Project 1 include:

- Increasing the degree of oxidation of elemental mercury that is released during induration through the use of additives
- Maximizing the capture of mercury in the scrubber and preferentially sequestering to the solid non-magnetic portion of the scrubber slurry, providing possible options for further separating and discharging ‘mercury-rich’ non-magnetic solid fraction.

The scope of work involved bench, pilot and full scale testing to examine the efficiency of various additives to oxidize and sequester the mercury. The information included in this report is mainly from field tests performed on Minntac Line 3 with supporting data derived from bench and pilot scale testing.

To attain the first goal of oxidation and capture, the technology employed two additives: ESORB-HG-11, a proprietary brominated powdered activated carbon provided by Envergen LLC; and Powdered Activated Carbon (PAC). These additives have been tested and have proven to control mercury emissions in coal-fired power plants. Meanwhile for the second goal, the ability of ESORB-HG-11, PAC and a third additive- diethyl dithiocarbamate (DEDTC), to maximize the sequestration of dissolved mercury was investigated. Sequestering the mercury captured by the scrubber to the solid portion of the slurry and removal of the solids from the process loop would provide an ‘exit’ for the captured mercury. This can also prevent possible re-emission of the captured mercury in the scrubber.

Field tests of the technology were conducted at U.S. Steel Minntac’s Line 3 grate kiln. In the grate kiln, the green balls are sequentially dried in a drying zone (downdraft), then heated and oxidized (induration) in both a preheat and kiln zone, respectively. It is believed mercury release from the green balls begins in the preheat zone. Consequently, the mercury oxidation technology targeted flue gas exiting the preheat zone. The test was divided into four main areas: stack sampling to determine mercury concentration leaving the stack; sampling of green balls to determine mercury input; multiclone dust and scrubber slurry sampling; and injection of the powdered carbon (technology deployment) in the flue gas exiting the preheat zone.

Baseline total mercury stack emissions from Minntac Line 3 ranged from 3.5 to 8.2 $\mu\text{g}/\text{m}^3$; with most values between 4.0 and 6.2 $\mu\text{g}/\text{m}^3$. Particulate mercury emissions during baseline operation were minimal, with most values below 3% of the total mercury emitted. The

predominant form of mercury in the stack emissions was elemental; values ranged between 83 and 90%, with the exception of one measurement.

Of the additives tested, only ESORB-HG-11 showed the potential to attain the target reduction of 75% mercury emission reduction. Results from the field testing further indicated significant reductions in vapor phase stack Hg emissions from a baseline value of $5.1 \mu\text{g}/\text{m}^3$ to $0.83 \mu\text{g}/\text{m}^3$, an 84% reduction, with injection rates of ESORB-HG-11 of 0.5 pound per long ton (150 lb/h of sorbent) of taconite processed. However, reductions in vapor phase mercury during ESORB-HG-11 injection were coupled with an increase in the particulate mercury emissions. Including the particulate mercury emission increased the emission value to $1.5 \mu\text{g}/\text{m}^3$, still a 71% reduction from the baseline values. While the particulate scrubber is effective for capturing the taconite dust entrained in the flue gas, it is less effective in capturing the powdered carbon additive. Increases in particulate mercury emissions suggest that the tested technology requires higher particulate capture efficiencies, which may be achieved by improved operation of the scrubber. Another key result from the testing indicated a dramatic decrease in dissolved mercury in the scrubber liquid, (from 3000-5000 ng/L to 20 ng/L) during ESORB-HG-11 injection. This suggests that the dissolved mercury in the scrubber slurry preferentially adsorbed to ESORB-HG-11, a non-magnetic phase, establishing the sequestering capabilities of the additive.

The fate of sequestered mercury associated with ESORB-HG-11 and the scrubber solids depends on the process configuration. In Minntac Line 3, the scrubber slurry is transported to a thickener and the solids are subsequently discharged. This provides an exit for all mercury captured by the system. However, not all taconite plants discharge their solids; instead they are recycled to the front end of the process. This creates a recycle loop for the mercury in the entire process that would lead to increases in the green ball mercury concentrations and a subsequent increase in the stack mercury concentrations. Therefore, for this sorbent injection technology to be effective at mercury oxidation and mercury capture at other facilities, a fraction of their solids from the scrubber would have to be discharged to prevent building up of the concentration of mercury in the system.

BACKGROUND

Problem Description

The Lake Superior Lakewide Management Plan (LAMP) identified the taconite industry as a major contributor of atmospheric mercury in the Lake Superior basin [Taconite Mercury QAPP]. Mercury is a leading concern among the air toxic metals addressed in the 1990 Clean Air Act Amendments because of its volatility, persistence and bioaccumulation as methylmercury in the environment, and its neurological health impacts.

Current industry wide mercury emissions are estimated at 440-880 lb/yr [Berndt 2003]. In addressing this issue, the Minnesota taconite industry set a goal of achieving a 75% reduction in its mercury emissions by 2025. Several projects were selected by the Minnesota Taconite Mercury Control Advisory Committee (MTMCAC) to identify different mercury-control technologies that have the potential to help the industry achieve this goal.

Previous research work done at taconite processing plants by the Minnesota Department of Natural Resources (MN DNR) suggested that the main source of mercury during taconite processing originates from induration of the ore (heating, oxidizing and sintering), or during the heating of “green balls” to form hardened taconite pellets [Berndt 2003]. Green balls are rolled from a mixture of moist taconite concentrate and a clay binder. Further research suggested that mercury release from the green balls starts at temperatures of approximately 200°C up to 600°C [Galbreath et al 2005], which corresponds to temperatures seen in the preheat zone of the induration furnaces.

Some of the released mercury is captured by a particulate scrubber system; this scrubber is the predominant pollution control device in taconite plants [Berndt et al 2005]. Analysis of scrubber slurry indicated significant mercury concentrations [Berndt et al, 2003], suggesting that some of the mercury released during induration may be oxidized through a variety of oxidation pathways. Oxidized mercury can be captured in a wet particulate scrubber because it is water-soluble; however, elemental mercury cannot. Additional studies also suggest that the mercury captured by the scrubbers in some of the plants adsorbs preferentially to the non-magnetic portion of the scrubber solids [Berndt and Engesser, 2005b].

The University of North (UND) proposed an innovative way of reducing mercury emissions from taconite plants in response to a Request for Proposals (RFP) issued by the MN DNR. This report discusses results of the technological approach taken by UND.

Approach

The approach taken by the UND team comprised the following objectives:

- Use proven mercury control technologies to increase oxidation of mercury in the flue gas upstream of the scrubber. These technologies consisted of injecting plain

Powdered Activated Carbons (PAC) or a proprietary bromated PAC referred to as ESORB-HG-11 in the flue gas and dosing the scrubber recirculation tank with DEDTC.

- Increase the capture of the oxidized mercury by the scrubber through addition of mercury complexing and/or sequestering agents to the scrubber waters; thus reducing the dissolved mercury scrubber concentration, and increasing the driving force for fresh oxidized mercury capture.
- Promote the tendency of the mercury to associate with the non-magnetic portion of the scrubber slurry (complexing/sequestering additives are non-magnetic) while allowing for separation and rejection of the non-magnetic phase as a possible route to sequestering captured mercury and to promote further reduction of recycled mercury by directing it back to the front end of the processing loop.

The information included in this report is mainly from field tests performed on Minntac Line 3 with supporting data provided by screening tests done using bench and pilot-scale equipment at UND.

Screening Tests

Screening tests were performed using bench and pilot-scale equipment to determine the best complexing agents compatible with scrubber slurry chemistry. Initially a series of five different scrubber additives for oxidized mercury capture and sequestration was proposed. They were PAC and ESORB-HG-11 for sequestration, TMT 15, Ca-EDTA (ethylene diamine tetraacetate), and DEDTC (diethyl dithiocarbamate) for complexing. Based on further research covering taconite scrubber chemistry as well as additive efficacy, the additive Ca-EDTA was eliminated. The additives selected from the bench/pilot tests for field testing were ESORB-HG-11, PAC, and DEDTC. The results used to justify their selection are discussed in Appendix A.

Minntac Line 3

Field testing of the technological approach was performed at Line 3 of the Minntac plant located in Virginia, Minnesota. Line 3 is Minntac's smallest line, and operates a grate-kiln furnace with a downdraft drying zone (DD1), followed by a preheat zone, the kiln, and finally the cooler. Mercury release from the green balls is believed to occur in the preheat zone and further down in the kiln. A clear understanding of the flue gas flow is important as it details the flow of the mercury after release.

Flue gas/air flow through the grate-kiln system is moved using a series of interconnected fans. Fired pellets are cooled using ambient air, drawn in by cooling fans, and a portion of this stream is used to pre-heat combustion air in the kiln, while the rest is exhausted to the atmosphere via a cooling vent stack. In the kiln, fuel (natural gas and biomass) is added to the heated air to initiate combustion and heat the taconite pellets.

Flue gas, resulting from the combustion of the fuel, flows through the kiln in the opposite direction as the flow of the pellets and through the pellet bed in the grate kiln. Gases from the pellet bed (within the preheat grates) are then routed to the front of the furnace section, transported through a series of multiclones, directed through a wet particulate scrubber, and sent to the stack.

As flue gas is transported through the system it entrains some taconite dust; some of which is removed in the multiclones. However a majority of the particulates are removed by the wet particulate scrubbers. The captured solids are then transported to a thickener. Oxidized mercury (Hg^{2+}) and particulate mercury (Hg^{P}) in the flue gas stream is believed to be captured mainly in the scrubber, while elemental mercury (Hg^0) is emitted through the stack. Line 3 uses a recirculating scrubber equipped with a recirculation tank. Fresh water is provided to the scrubber while the recirculation tank blowdown pumps prevent slurry build up. The pH of the scrubber slurry is amended with lime to neutralize acidity and to promote gypsum precipitation.

METHODS

The testing on Minntac Line 3 and sampling methods for the stack flue gas, scrubber slurry, green balls, and multiclone solid discharge are discussed below.

Testing on Minntac Line 3

Testing on Minntac Line 3 was performed over a period of three weeks from October 10, 2011 to October 28, 2011. Monitoring equipment was installed on October 11 and 12 and removed on October 27 and 28. The first stage of testing established pre-test baseline emissions; this took four days. Testing consisted of injecting brominated activated carbon (ESORB-HG-11) and PAC sorbents into the process flue gas using injection equipment supplied by a UND subcontractor (IAC International) and dosing the recirculation tank with the complexing/sequestering agents. Sorbents were supplied by Envergex LLC in 1000-lb bulk bags.

The sorbent injection equipment (Figures 1 and 2) consisted of a bulk bag handling system, a feeder to meter sorbent, a blower and a compressor to supply the conveying air, an eductor to pick up the sorbent discharged from the feeder, hoses to convey the sorbent, and distributors and injection lances to disperse the sorbent into the flue gas duct. The injection test agents, PAC and ESORB-HG-11, were transported through the hoses and distributors to the injection lances and into the flue gas using compressed air. The sorbent feed hopper was placed on a mass scale to determine additive injection rate. All the injection equipment was installed on a trailer; positioning the trailer was a challenge because of space constraints and uneven flooring; the final trailer location was several hundred feet from the target injection location, which was the preheat fans.

The first injection test ports were about 30 feet upstream of the preheat fan inlet. Injection of the sorbents upstream of the fans allowed for improved mixing and distribution of sorbent particles in the flue gas. Four ports were installed by Minntac personnel on each of the two ducts leading to the fans.

Initially, it was planned to inject upstream of the waste gas fan; however, due to the short residence time that would be available for mercury oxidation and capture, coupled with the low flue gas temperatures, it was anticipated that the mercury capture efficiencies would be low. Therefore, changing the injection location to the preheat zone wall was considered because this would provide a higher temperature. However, injection at this location would require redesigned injection lances that had cooling jackets, which could not be procured within the project schedule. Hence, as a compromise, a request was made to the MN DNR that the lances be placed on the edges of the preheat zone wall; the request was approved.



Figure 1. A close-up photo of the sorbent bulk-bag handling system. The bulk bag is placed on the top (upper arrow). The discharge pipe below (lower arrow) comes from the educator and is attached to a hose that connects to the distributors and injection lances.



Figure 2. Sorbent injection trailer with the bulk bag lifter assembled and the bulk bag in place. The IAC box in the foreground houses the blower and compressor that provide the pressurized air to conveying the sorbent into the flue gas duct.

To improve the removal of mercury in the scrubber liquids using DEDTC as a complexing agent during field testing, PAC and ESROB-11-HG were separately injected into the flue gas stream to increase the degree of oxidation of elemental mercury. It was deduced that a higher concentration of oxidized mercury present in the scrubber liquid would increase the effectiveness of DEDTC. Therefore, DEDTC was added to the scrubber by dosing the scrubber recirculation tank to a concentration of 7 mg/L. It was also noted that PAC and ESORB-HG-11 injected into the flue gas ended up in the recirculation tank, so no direct addition into the scrubber was needed. However, this subsequently slowed a return to baseline conditions because, being a recirculating scrubber, it would take almost 4 hours to replace one tank volume or more than 12 hours for the injected ESORB-HG-11/PAC to reduce to insignificant levels in the scrubber tank. Consequently, the sequestering properties of these additives kept the dissolved mercury concentrations lower than normal for most of the test period, except on Mondays (10/10/12, 10/17/12, and 10/24/12) as no injection was performed on weekends.

Stack Sampling

Stack measurements were performed by UND's sub-contractor, Western Kentucky University's (WKU) Institute for Combustion Science and Environmental Technology (ICSET). WKU used a PS Analytical (PSA) continuous mercury monitor (CMM) with a wet conversion system to obtain semi-continuous mercury concentrations in the flue gas and an extractive sampling method - ASTM D 6784 (commonly known as Ontario Hydro Method or OHM) to measure total and speciated mercury concentrations in the stack gases. Measurements were performed on the roof of the facility housing the stack. Several ports are located at the stack and two of these ports were used to set up the probes for the OHM and CMM. The OHM was the preferred measurement technique for evaluating performance of the additive, while the CMM was used to track trends during testing. The OHM method provides an average of all components of the mercury emission over the sampling period: Hg^0 , Hg^{2+} , and Hg^{P} . The sum of these components provides the total mercury concentration (Hg^{T}) in the stack gas. The OHM test was operated for approximately 1-2 hour periods during each run, with a sampled flue gas volume in the range of 0.70 to 0.90 m^3 . During a typical test day, one OHM sample was collected before (baseline) sorbent injection and at least one sample during the sorbent injection phase. This made it possible to obtain a baseline value and average mercury reductions for each test day. The CMM was operated continuously during each testing day; however it was taken offline at the end of the test day. Due to the long duration of each test, coupled with the fact that the CMM was not operated overnight, the stack mercury behavior at the end of each test day was not fully investigated; on some testing days the monitoring equipment was not always deployed immediately after performing the baseline OHM. As a result, the OHM baseline for these days might require a correction based on the CMM baseline just before monitoring began.

Impinger solutions obtained in the OHM test were immediately analyzed at the end of each test by ICSET's mobile laboratory. The quality of OHM data was ensured by using standard quality control procedures for laboratory and field analyses. Leak checks were performed during all runs and duplicate (and sometimes triplicate) samples were analyzed by ICSET mobile laboratory, along with sample spikes, standard samples, and sample blanks, to insure analytical precision and accuracy. The PSA monitor for semi-continuous mercury concentration measurement was calibrated at the beginning of each day and re-calibrated after any troubleshooting during sampling. Measurement accuracy was further checked by comparing OHM and CMM results at local O_2 concentrations (approximately 18%) and on a dry basis; they showed good agreement. Relative differences between OHM and CMM were less than 12%, except for one measurement (24%), which is considered good agreement when compared to data from similar mercury testing using OHM and CMM [Benson 2007].

Green Ball Sampling

Green balls were sampled to determine the daily average mercury concentration in the feed to the taconite furnace. Due to variability observed in green ball mercury concentrations

during previous research [Berndt, 2008], it was decided that the daily average mercury concentration of the green balls would be used for all mass balance calculations of that test day.

Green ball samples were collected by Minntac laboratory personnel and consisted of collecting a 5 minute composite sample in buckets from the roll feeders upstream of the grate. After collection the samples were delivered to the UND sampling team and the samples were transferred into clean plastic bags, labeled, and then stored until they were given to ICSET for mercury analysis. Samples were collected at three different time intervals each day. Composite green ball samples were analyzed using EPA Method D6722.

Scrubber Sampling

Scrubber samples were collected by the UND testing team from the scrubber recirculation tank from a valve located upstream of the scrubber blowdown pump. The slurry in the tank was agitated continuously, thus providing a well-mixed sample from the blowdown pump. For sample collection, the valve was first purged for at least 10 seconds before a sample was collected in a large bucket. The bucket was then transported to the filtration area. Here, the bucket was further agitated and a 500 mL sample was collected and filtered. The filtrate was then transferred into pre-washed containers containing nitric acid to maintain the $\text{pH} < 2$ and stored on ice. Another 500 mL sample was collected and filtered to determine total suspended solids (TSS). Initially, the filtrate samples were sent to ICSET for mercury analysis using EPA Method 7470. However, it was observed that most filtrate samples obtained during carbon injection testing had mercury concentration values below the detection limit for this method. Samples were then sent to Pace Analytical, which used a more sensitive method (EPA Method 1631) for obtaining mercury concentration in the filtrate obtained from the scrubber slurry. For filtrate samples analyzed by ICSET that were below the detection limit of $0.2 \mu\text{g/L}$, a default value of $0.2 \mu\text{g/L}$ was assumed during data analysis.

For quality control, duplicate samples and field blanks were taken. Field blanks were performed by transporting bottles of deionized water to the field site, transferring them into pre-cleaned sample bottles when other scrubber samples were processed, and analyzing them with the other scrubber samples. The analytical results for the field blanks were below the detection limits for both methods used (EPA Method 1631-low mercury analysis, and EPA Method 7470). Duplicate samples also showed good agreement.

Multiclone Solids Sampling

Multiclone solids were collected by the UND testing team from the multiclone blowdown system. Minntac Line 3 is equipped with 8 cyclones, each having its own blowdown port. Sampling from all ports required collecting a composite from each blowdown port consecutively. Multiclone dust samples were taken to provide an estimate of the mercury leaving the system through the multiclones. The blowdown rate (mass loading) was not able to be measured precisely and varied significantly during different sampling periods, with no substantial sample

amounts being collected during certain sampling periods. Additionally, analysis of multiclone dust samples showed large variability in mercury concentrations. An estimate of the blowdown rate was reached using the scrubber TSS and an assumed cyclone efficiency of 90%. The estimated value was calculated to be 390 lb/hr of solids and was combined with the highest multiclone mercury measurement of 450 ng/g to give a maximum possible mercury flux of 0.08 grams/hr through the blowdown, which is less than 3% of the average mercury (3.0 grams/hr) entering the system. This is consistent with measurements done by Berndt (Berndt 2003) that showed very low mercury content in multiclone blowdown.

The multiclones solids sampling technique involved collecting blowdown dust into a clean plastic bag and then transferring into a second plastic bag for storage. The location of the blowdown port required care during sampling to avoid the risk of contamination of collected samples by the water used to wash and transport the blowdown dust to a thickener located downstream of the multiclones. Collected samples were stored on ice for particulate bound mercury conducted by ICSET.

Field Testing Matrix

Table 1 summarizes the testing done at Minntac Line 3 and includes dates, times, test conditions, sorbent types, injection rates, injection locations, sampling locations, sampling types, and samples collected.

Table 1. Field Test Matrix

Date	Time	Test Condition	Sorbent Type	Injection Rate	Injection Location	Sampling Location	Sampling Type	Samples Collected
10/10/2011	7am -7 pm	Orientation by Minntac						
10/11/2011	7am -7 pm	Equipment Setup				Scrubber Stack		
	7am -7pm	Equipment Setup				Scrubber Stack		
10/12/2011	7am-7pm	Pre-Test				Scrubber Stack		
10/13/2011	7am -10am	Baseline				Scrubber Stack	CMM & OHM	Green Pellets, Scrubber Slurry
	10am - 1pm	Baseline				Scrubber Stack	CMM & OHM	
	1pm - 4pm	Baseline				Scrubber Stack		
	4pm - 7pm	Baseline				Scrubber Stack		
10/14/2011	7am – 4pm	Baseline				Scrubber Stack	CMM & OHM	Green Pellets, Scrubber Slurry, Multiclone solids
	4 pm - 5 pm	Condition 1	ESORB-HG-11	25 lb/hr	Preheat Fans	Scrubber Stack	CMM	
	5pm - 7pm	Condition 2		50 lb/hr		Scrubber Stack	CMM	
	7pm - 9pm	Condition 3		100 lb/hr		Scrubber Stack	CMM & OHM	
10/17/2011	7am - 10am	Baseline			Preheat Fans	Scrubber Stack	CMM & OHM	Green Pellets, Multiclone Solids, Scrubber Slurry
	10am - 2pm	Condition 2	ESORB-HG-11	50 lb/hr		Scrubber Stack		
	2pm - 4pm	Condition 3	ESORB-HG-11	100 lb/hr		Scrubber Stack	CMM	
	4pm - 7pm	Condition 4	ESORB-HG-11	150 lb/hr		Scrubber Stack	CMM & OHM	
10/18/2011	7am - 10am	Baseline	ESORB-HG-11		Preheat Fans	Scrubber Stack	CMM & OHM	Green Pellets, Multiclone Solids, Scrubber Slurry
	10am - 7pm	Condition 3	ESORB-HG-11	100 lb/hr		Scrubber Stack	CMM & OHM	
10/19/2011	7am -11am	Baseline			Preheat Fans	Scrubber Stack	CMM & OHM	Multiclone Solids, Scrubber Slurry
	11am - 2pm	Condition 1	DEDTC	0.7 mg/L		Scrubber Stack	CMM	
	2pm - 3pm	Condition 2	DEDTC	1.4 mg/L		Scrubber Stack	CMM	
	3pm -5pm	Condition 3	DEDTC	7.0 mg/L		Scrubber Stack	CMM	
	5pm – 9pm	Condition 4	DEDTC and ESORB-HG-11	BC = 50 lb/hr DEDTC = 7.0 mg/L		Preheat Fans	Scrubber Stack	CMM & OHM

Table 1. (Continued)

Date	Time	Test Condition	Sorbent Type	Injection Rate	Injection Location	Sampling Location	Sampling Type	Samples Collected
10/20/2011	7am - 11am	Baseline				Scrubber Stack	CMM & OHM	Multiclone Solids, Scrubber Slurry, Green Pellets
	11am - 12pm	Condition 1	PAC	50 lb/hr	Preheat Fans	Scrubber Stack	CMM	
	12pm - 3pm	Condition 2	PAC	100 lb/hr		Scrubber Stack	CMM & OHM	
	3pm -5pm	Condition 3	PAC	150 lb/hr		Scrubber Stack	CMM & OHM	
10/21/2011	7am -12pm	Baseline				Scrubber Stack	CMM & OHM	Green Pellets, Multiclone Solids, Scrubber Slurry
	12am - 5pm	Condition 4	ESORB-HG-11	150 lb/hr	Preheat Fans	Scrubber Stack		
10/24/2011	7am - 10am	Baseline				Scrubber Stack	CMM & OHM	Green Pellets, Multiclone Solids, Scrubber Slurry
	10am - 1 pm	Condition 5	ESORB-HG-11	75 lb/hr	Preheat Fans	Scrubber Stack	CMM & OHM	
10/25/2011	7pm - 10am	Baseline				Scrubber Stack	CMM & OHM	Green Pellets, Multiclone Solids, Scrubber Slurry
	10am - 12pm	Condition 1	ESORB-HG-11	50 lb/hr	preheat fans (4 inj. Lances) + Preheat zone (8 inj. Lances)	Scrubber Stack	CMM	
	12pm - 4pm	Condition 2	ESORB-HG-11	75 lb/hr		Scrubber Stack	CMM & OHM	
	4pm - 5pm	Condition 3	ESORB-HG-11	75 lb/hr	preheat fans (4 inj. Lances) + Preheat zone (4 inj. Lances)	Scrubber Stack	CMM	
10/26/2011	7pm - 10am	Baseline				Scrubber Stack	CMM & OHM	Green Pellets, Multiclone Solids, Scrubber Slurry
	10am -12pm	Condition 4	ESORB-HG-11	100 lb/hr	preheat fans (4 inj. Lances) + Preheat zone (4 inj. Lances)	Scrubber Stack	CMM	
	2pm -6pm	Condition 5	ESORB-HG-11	100 lb/hr	preheat fans (4 inj. Lances) + Preheat zone (4 inj. Lances)	Scrubber Stack	CMM & OHM	
10/27/2011	7am -7pm	Equipment Tear-Down				Scrubber Stack		
10/28/2011	7am -7 pm	Equipment Tear-Down				Scrubber Stack		

RESULTS

Results from the UND research team follow and include data and discussion pertaining to the sampling of green balls and baseline stack measurements, as well how the addition of ESORB-HG-11, PAC, and DEDTC reduced mercury emissions during taconite production.

Green Ball Sampling Data

Table 2 lists the green-ball mercury concentrations during the testing. Composite green-ball samples had mercury levels varying from 4 ng/g to 18 ng/g. The results for October 13 and 21 appear to be anomalously low. The analytical results on Table 2 were done at two separate times and there was variation in the results between the two testing periods. The low values obtained for samples collected on October 13th and 21st have been flagged on Table 2 as being outside the acceptable range of values and were not considered further.

The average mercury concentration in the green balls for the entire test period was 12.4 (± 2.9) ng/g (± 1 standard deviation). The average value showed good agreement with previous work conducted on Minntac Line 3 [Berndt 2008]. Additionally, it has also been reported that there could be a large daily variability in the green-ball mercury concentrations [Berndt 2003, 2005a & b, 2008]. The daily average green-ball concentrations were assumed to provide a sufficiently reliable estimate of the mercury entering the system; as such, they were used by the UND research team to calculate mercury reductions in the taconite production system by the addition of mercury-sorbing agents.

Table 2. Total Hg in green ball feed during testing period. Note: Only samples collected on days where additive testing showed promising results per the OHM were submitted for mercury analysis.

Date	Sample ID	Collection time	Mercury concentration ng/g	Daily Average, ng/g (Std Dev)
10/13/2011*	GB1	7:20 AM	6	
	GB2	10:50 AM	7	6.3
	GB3	2:55 PM	6	(0.6)
10/14/2011	GB4	7:10 AM	15	
	GB5	11:00 AM	13	14.3
	GB6	2:00 PM	15	(1.2)
10/17/2011	GB10	7:15 AM	12	
	GB11	10:45 AM	12	10.7
	GB12	1:40 PM	8	(2.3)
10/18/2011	GB13	7:15 AM	18	
	GB14	10:45 AM	15	16.3
	GB15	1:55 PM	16	(1.5)
10/19/2011	GB16	7:10 AM	12	
	GB17	10:50 AM	13	12.0
	GB18	1:25 PM	11	(1.0)
10/20/2011	GB19	7:15 AM	11	
	GB20	10:45 AM	15	11.0
	GB21	1:40 PM	7	(4.0)
10/21/2011*	GB22	7:23 AM	5	
	GB23	11:06 AM	5	4.7
	GB24	1:55 PM	4	(0.6)
10/24/2011	GB25	7:00 AM	11	
	GB26	11:00 AM	11	10.3
	GB27	2:00 PM	9	(1.2)

* Values flagged as out of range.

Baseline Stack Measurements

As a result of the fluctuations in mercury concentrations in the green ball metered to the grate kiln inlet, baseline emissions were considered crucial for the success of the project. Further, following recommendations and directions stipulated by the *Data Quality Assessment Worksheet* [Taconite Mercury QAPP, 2010], estimates of the annual mercury emissions with and without the sorption agents tested were required. Consequently, an entire day, October 13, was used to calculate baseline mercury emissions. These measurements were coupled with a baseline measurement performed every day before sorbent injection, to estimate the average plant baseline emission. The main technique used for measuring mercury concentrations was the Ontario Hydro Method (OHM), with the PS Analytical semi-continuous mercury monitor (CMM); both were used to track mercury trends during the test day so the effects of sorbent injection could be monitored.

The baseline emission data for the stack gases from the three-week testing period is summarized in Table 3. OHM provides information on mercury speciation, which is inclusive of particulate-bound mercury (Hg^{P}), and vapor phase mercury measured as the oxidized species (Hg^{2+}) and as elemental mercury (Hg^0). In this work, the sum of the oxidized and elemental

vapor mercury components is represented as total vapor mercury (Hg^{VT}). The sum of all the mercury components, including the particulate bound mercury, is the total mercury (Hg^{T}). Table 3 also lists the vapor phase mercury species concentrations, as measured using CMM. Hg^0 , Hg^{2+} and their sum Hg^{VT} , are calculated as an average of the CMM data during the period the OHM sampling was performed. The standard deviations of the CMM data are also calculated and presented.

Several observations can be made from the data shown in Table 3. Baseline Hg^{T} from the OHM data for stack emissions at Minntac Line 3 ranged from 3.5 to 8.2 $\mu\text{g}/\text{m}^3$, with most values between 4.0 and 6.2 $\mu\text{g}/\text{m}^3$ (dry basis). Hg^{P} emissions during baseline operation were minimal, with most values below 3% of the total mercury emitted. This indicates that the taconite dust has a low propensity to adsorb mercury during the time it is in contact with the flue gas in the ductwork leading to the scrubber and the stack. The predominant form of mercury in the stack emissions was Hg^0 with values ranging between 83 and 90 % of Hg^{T} , with the exception of one measurement. The high fraction of elemental mercury species in the stack gases validates the strategy taken in this study to oxidize the mercury for capture in the scrubber.

The CMM data only provides the vapor phase mercury concentrations. There was a reasonable correspondence between the CMM and the OHM measurements for the vapor phase mercury components. A specific example of the comparison between OHM and CMM data is for October 13, the full day of baseline measurements. During this test period, the three OHM measurements showed consecutive values of 4.45, 4.93 and 5.19 $\mu\text{g}/\text{m}^3$ for Hg^{VT} . For comparison, average CMM measurements during the same test periods were 4.24 (± 0.41), 3.88 (± 0.30) and 4.10 (± 0.32) $\mu\text{g}/\text{m}^3$, respectively. The average relative difference (Equation 1) between the OHM and CMM values was 8.7%. This trend was also seen during other test days.

$$\text{Average Relative Difference} = \frac{[\text{OHM} - \text{CMM}]}{[\text{OHM} + \text{CMM}]} * 100 \quad \dots (1)$$

On October 18 the CMM was undergoing troubleshooting during OHM baseline measurements. Troubleshooting also occurred on October 14 and 18, where the injection of ESORB-HG-11 did not begin immediately after baseline measurement.

Table 3. Baseline mercury concentrations in the stack gas (OHM and CMM averages) over the time OHM measurements were performed.

Date	OHM				CMM			
	Hg ⁰ µg/m ³	Hg ^{VT} µg/m ³	Hg ^P µg/m ³	Hg ^T µg/m ³	Hg ⁰ µg/m ³	Std Dev	Hg ^{VT} µg/m ³	Std Dev
13th	3.70	4.45	-	-	2.32	0.26	4.24	0.41
	3.98	4.93	-	-	2.58	0.13	3.88	0.30
	4.64	5.19	-	-	2.78	0.08	4.1	0.32
14th	5.86	6.69	-	-	4.20	0.19	5.51	0.27
17th	5.82	8.22	0.02	8.24	5.12	0.30	7.08	0.88
*18th	5.35	6.17	0.03	6.20	n/a	n/a	n/a	n/a
19th	4.63	4.86	0.07	4.93	4.08	0.13	5.19	0.15
20th	3.14	3.44	0.03	3.47	1.56	0.14	2.11	0.17
21st	4.50	5.04	0.02	5.06	3.12	0.50	3.96	0.13
24th	4.38	4.98	0.08	5.06	3.56	0.16	5.11	0.41
25th	3.35	3.81	0.20	4.01	3.11	0.29	4.39	0.39
26th	3.84	4.09	0.10	4.19	4.03	0.37	4.55	0.30

*CMM not running during OHM due to troubleshooting.

The baseline values as measured by the CMM showed larger-than-normal variations with standard deviations of around 10% of the mean value. These baseline results were taken on October 13 (Figure 3) and on October 17, 24, and 25 (Figure 4). The average Hg^{VT} during baseline test periods for the latter were 7.08 (± 0.88), 5.11 (± 0.41), and 4.39 (± 0.39) $\mu\text{g}/\text{m}^3$ respectively. These days had the highest standard deviations during the testing campaign.

More detailed, time-resolved CMM data are presented in Figures 5 through 8. The CMM baseline data for the period covering OHM baseline testing is represented by the vertical lines in each figure. Baseline CMM data for Oct 19 and 21 (Figure 5) indicated low and high mercury concentrations, respectively, at the start of the measurement period, while data for Oct 14, 20, and 26 (Figure 6) showed steady Hg concentrations.

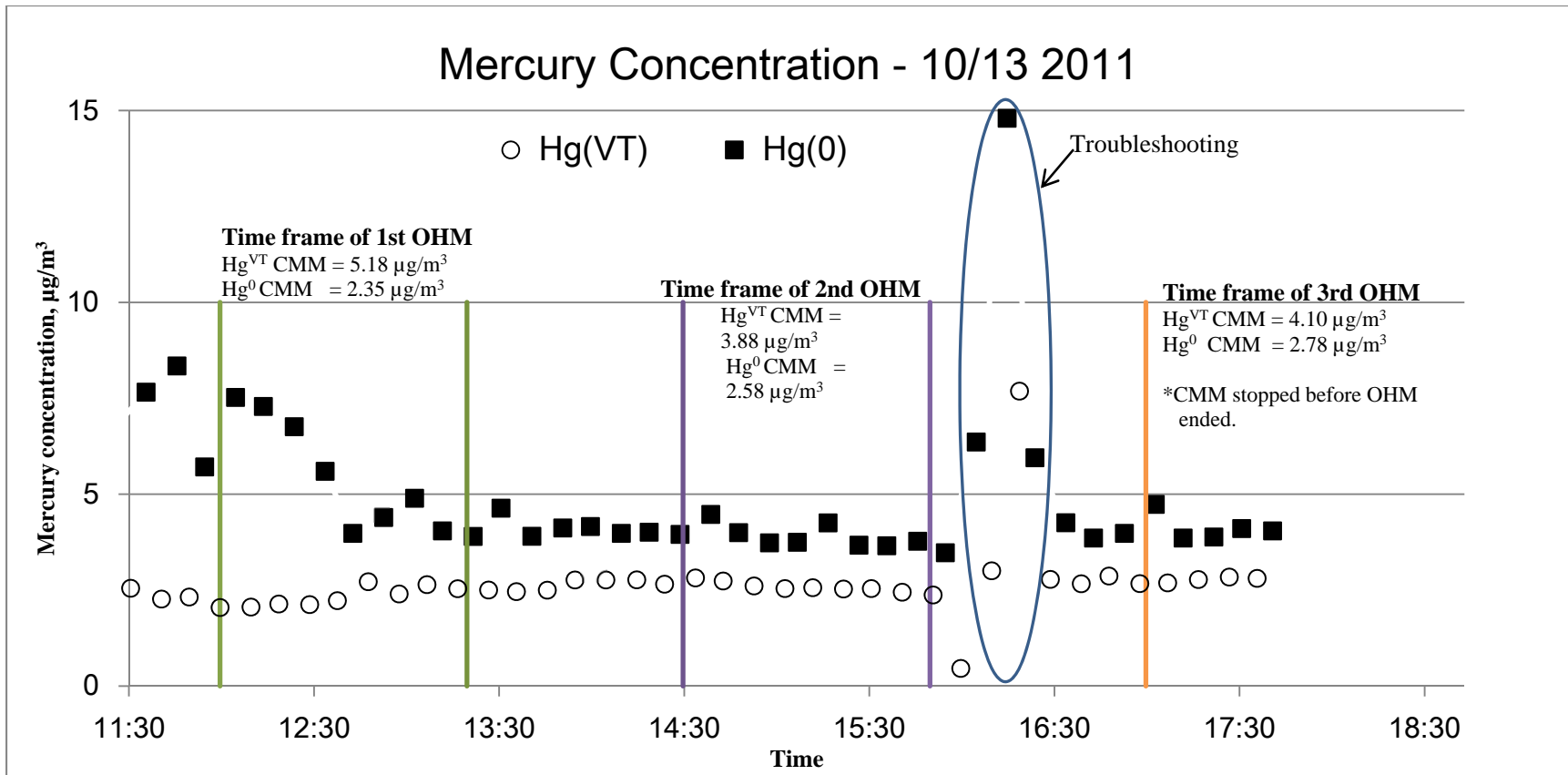


Figure 3. Average CMM measurements to determine baseline concentrations the day before testing.

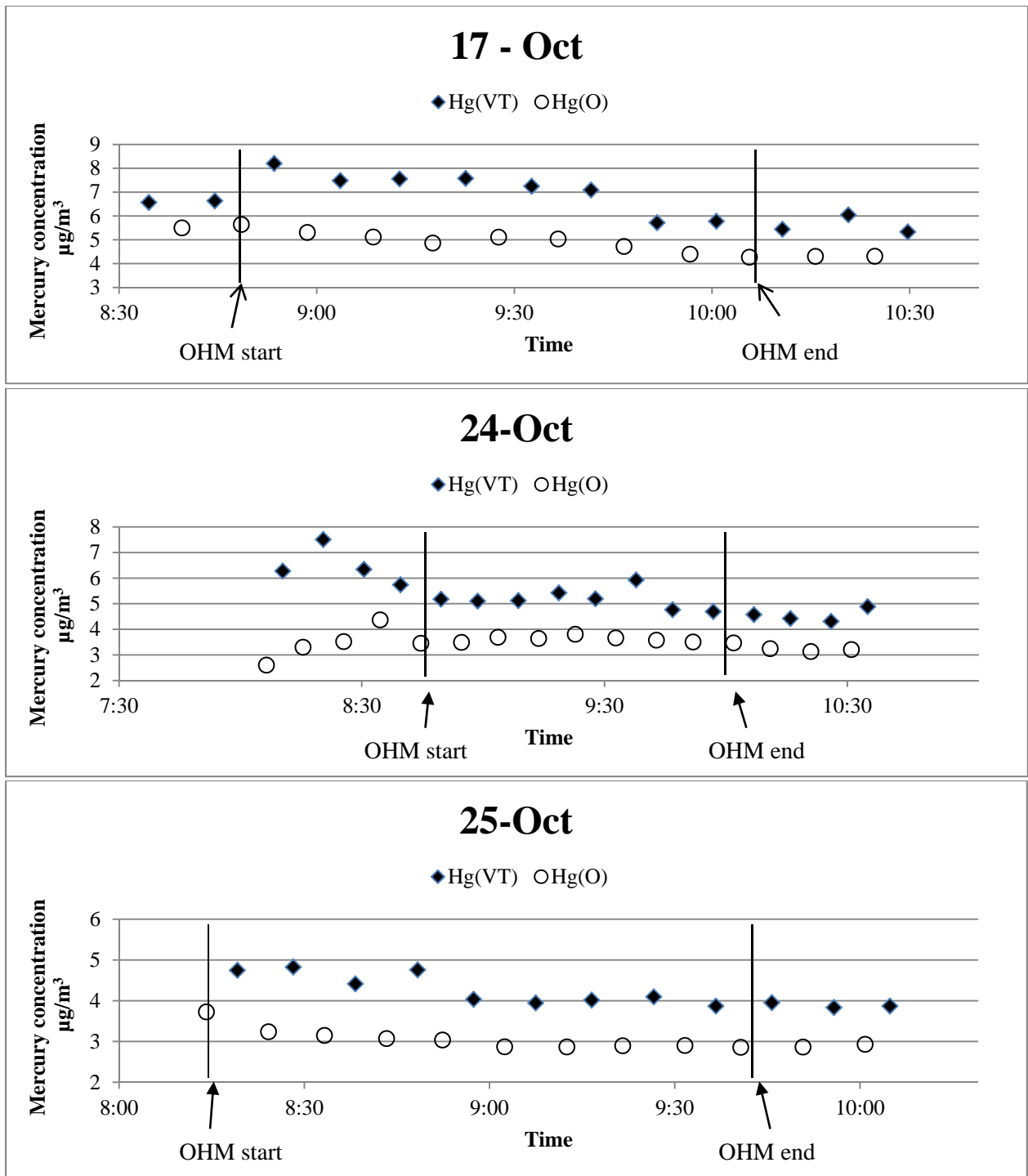


Figure 4. CMM baseline for Oct 17, 24, and 25. As can be observed the mercury concentrations was not steady especially for Oct 17 were the oxidized mercury (difference between Hg^{VT} and Hg^{O}) can be seen to increase. For Oct 24, the baseline shows a spike followed by a slight decrease slightly accounts for the high standard deviation of $0.41 \mu\text{g}/\text{m}^3$.

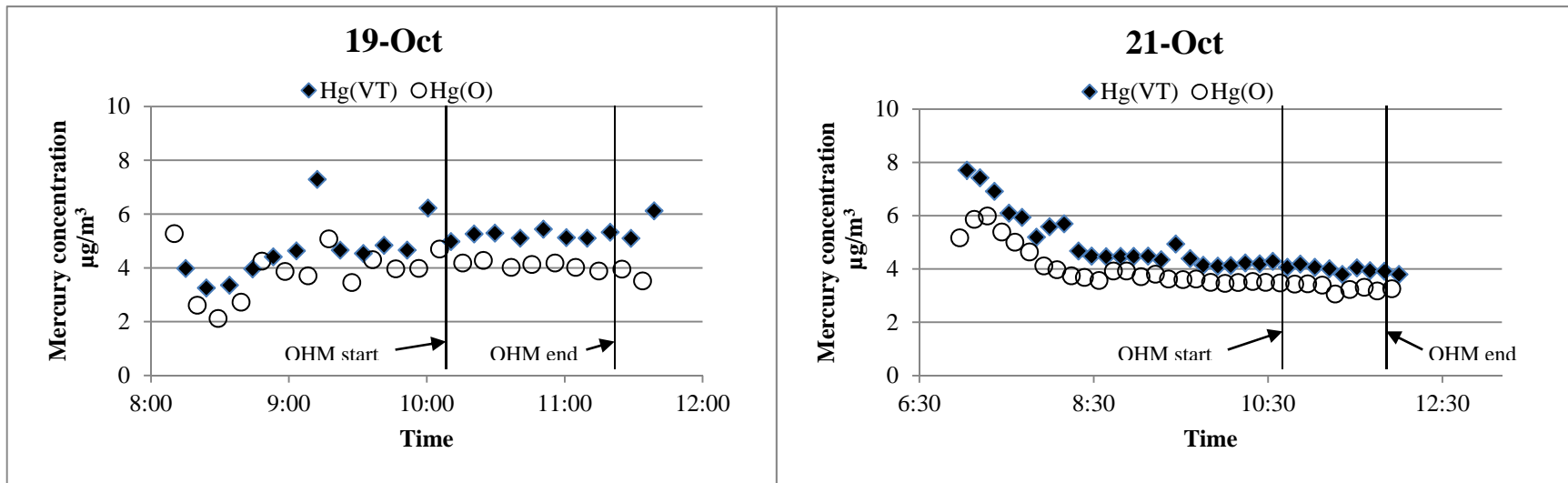


Figure 5. CMM baseline Hg concentrations for Oct 19 and 21, with low and high mercury concentrations at the start of measurements, respectively. In general, the baseline OHM mercury concentrations are steady for both days.

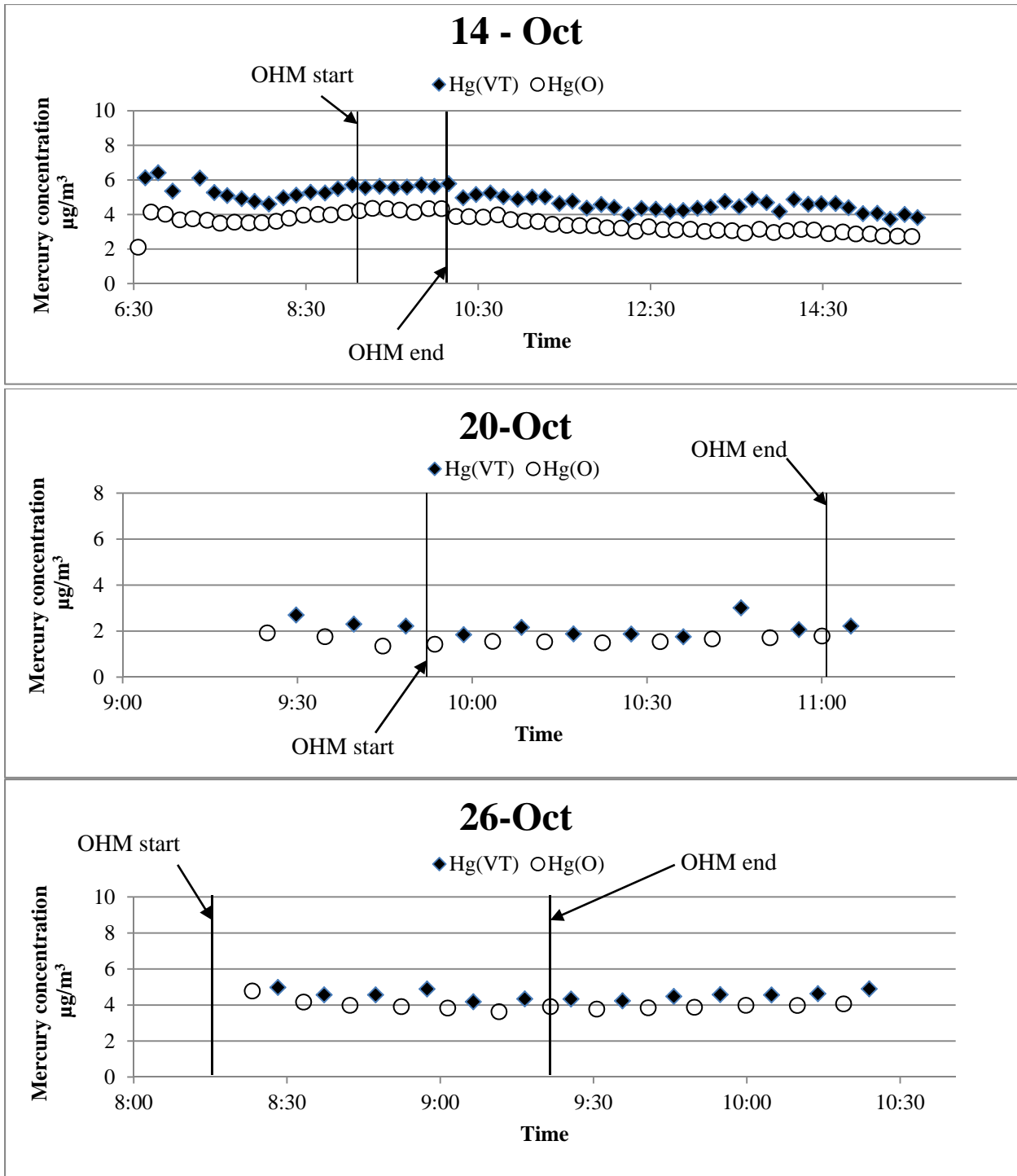


Figure 6. Data for Oct 14, 20, and 26. After the OHM on Oct 14, a problem with the injection equipment delayed testing by 5 hours after OHM. This is why the baseline period is a lot longer than other days. For Oct 26, OHM was started before the CMM started measuring stack mercury concentration. All three graphs show the steady values obtained during baseline OHM.

Figure 7 shows the total vapor phase mercury concentration values measured using the OHM method and tracked using the CMM. As can be seen, the OHM and CMM measurements showed close agreement, with OHM measurements slightly higher than CMM values in most cases. This difference, as mentioned earlier, has also been observed during mercury emission testing at coal-fired plant stack gases, [Benson 2007] and is believed to be due to differences in measurement techniques. On Oct 17, the total vapor mercury concentration showed a high baseline value; however, closer inspection of the OHM and CMM data on Figure 7 indicates that high oxidized mercury is the probable cause. This disparity can be attributed to some process abnormality. The variability in mercury emissions during the three-week testing period, from a low of 3.44 $\mu\text{g}/\text{m}^3$ (OHM data for Oct. 20) to a high of 8.22 $\mu\text{g}/\text{m}^3$ (OHM for Oct. 17), makes it difficult to estimate the baseline value that should to be used to determine reduction potentials of the sorption technologies tested. For individual test days, the respective OHM measurements were used to provide an estimate of actual reduction during testing as shown by Equation (2)

$$\% \text{ Hg Removal} = \frac{[\text{Hg}(1) - \text{Hg}(2)]}{\text{Hg}(1)} * 100 \quad \dots (2)$$

Where, Hg(1) is the OHM baseline total Hg concentration in $\mu\text{g}/\text{m}^3$ and Hg(2) is the OHM total mercury concentration, in $\mu\text{g}/\text{m}^3$ during additive injection and when stack mercury emissions are at steady state. The steady-state point was determined from the CMM charts..

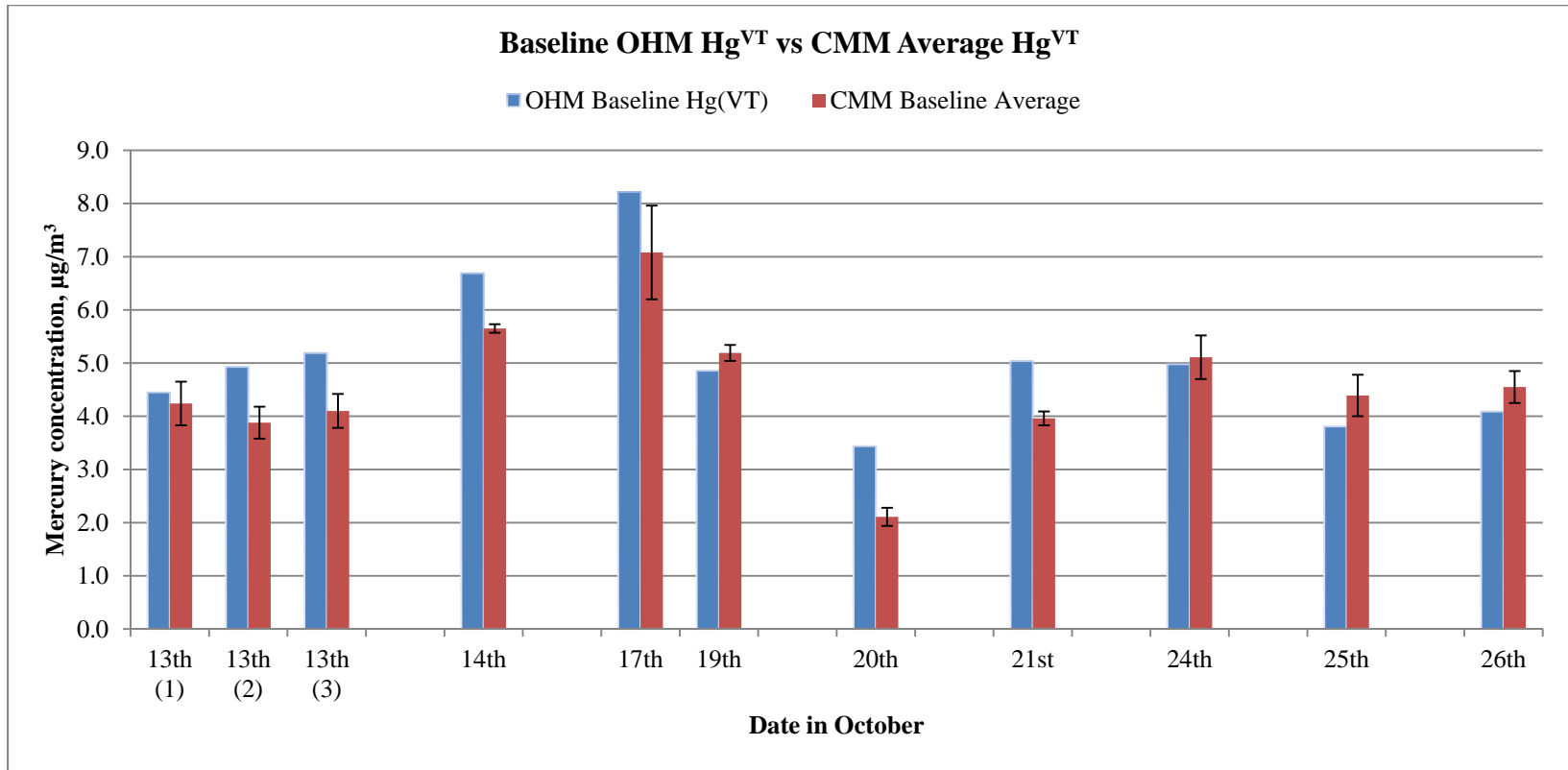


Figure 7. Summary of OHM and CMM baseline data. Error bars represent standard deviation of CMM averages.

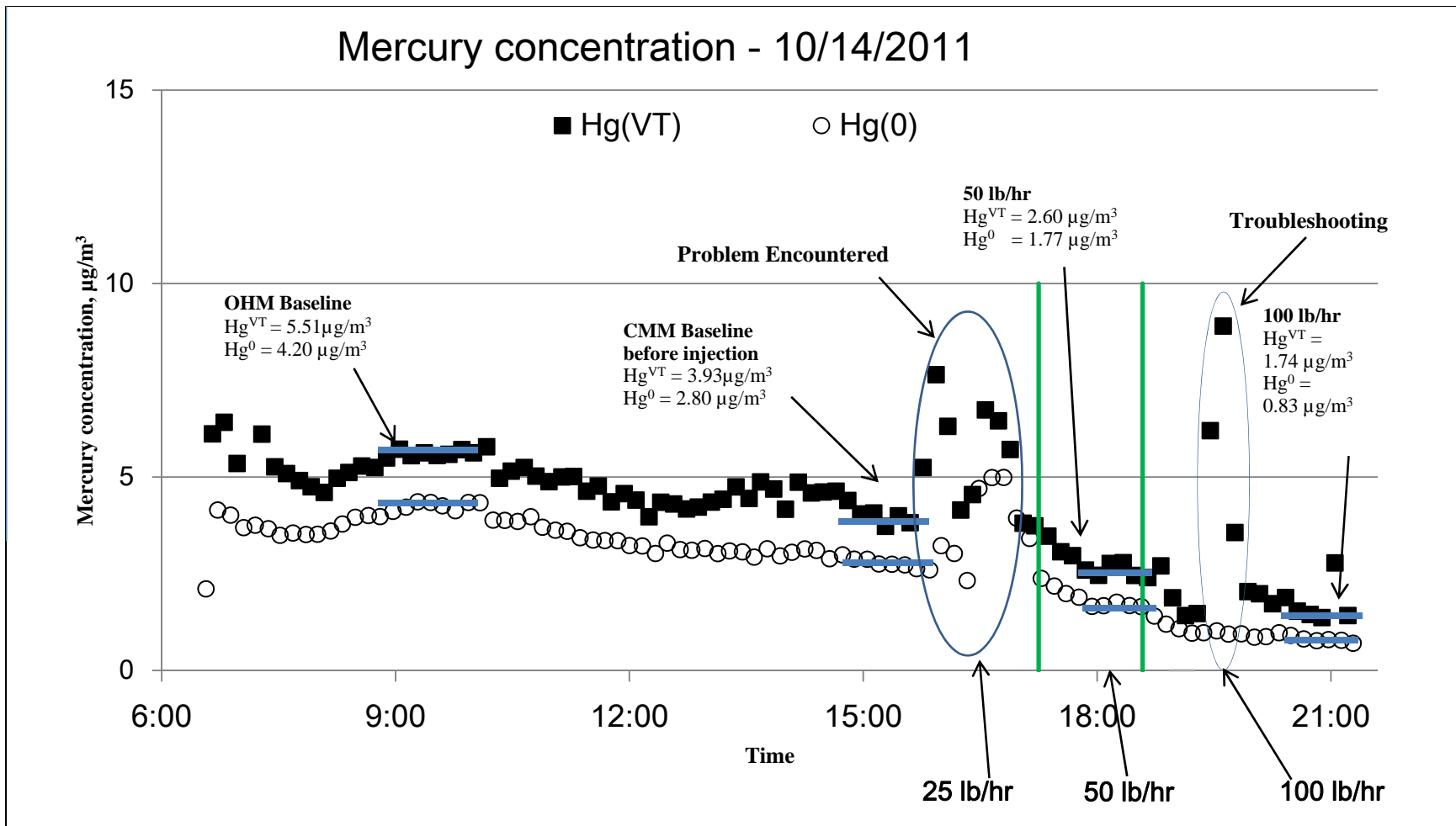


Figure 8. CMM data for Day 1 of ESORB-HG-11 injection. The average CMM mercury concentrations during OHM sampling are shown. It can be observed that the baseline decreased by approximately $1.50 \mu\text{g}/\text{m}^3$ during the time from baseline OHM to start of injection at 16:10. However, when injection started, a problem occurred on the CMM. As soon as the problem was corrected, injection was increased to 50 lb/hr.

ESORB-HG-11 Testing at Preheat Injection Location

As indicated earlier, the UND research team wanted to increase the oxidation and capture of mercury in the flue gas through injection of powdered activated carbon and brominated activated carbon. The proprietary halogenated PAC tested was ESORB-HG-11, provided by Envergen LLC.

A key aspect of the proposed technology was the identification and choice of a suitable injection location. While most sorbent injection approaches in the power industry have targeted the flue gas at low flue gas temperatures (around 120-150°C), the approach used in this study used injection of the sorbents at higher flue gas temperatures. The first injection test locations were located approximately 30 feet upstream of the preheat fan inlets. This was after the process gases have exited the preheater section of the grate kiln. Four ports were installed by Minntac personnel on each of the two ducts leading to the fans. This allowed the placement of a total of eight injection lances for sorbent introduction. Injection of the sorbent upstream of the fans provided the added benefit of enhanced mixing and improved distribution of the sorbent particles in the flue gas.

Filtrate from the slurry samples taken during the first four sampling days were analyzed using EPA Method 7470 which has a detection limit of 0.2 µg/L or 200 ng/L. Consequently, a 200 ng/L value was assigned as the default value for non-detect samples.

The first test day, Oct 14, involved injecting ESORB-HG-11. Baseline values from the OHM measurements showed Hg^{VT} of 6.69 µg/m³. The CMM trend and the OHM results are shown in Figure 8. As a result of a malfunction in the injection equipment, injection started five hours after the OHM baseline measurements were taken. During this time the CMM data decreased from Hg^{VT} of 5.51 µg/m³ (same time frame as OHM baseline) to 3.93 (± 0.10) µg/m³ just before the additive was injected. Because this was the first test run, the priority was to determine which injection rate showed greatest promise, so the drop in the CMM baseline was not considered critical during data evaluation.

The first injection rate investigated was 25 lb/hr of ESORB-HG-11. During this injection period, a problem occurred, as seen on the CMM chart, so no actual reduction was seen. After the effects of the problem on the CMM subsided, the injection rate was increased to 50 lb/hr, and Hg^{VT} , per the CMM, dropped to a steady value of approximately 2.60 µg/m³. The injection rate was then increased to 100 lb/hr and the OHM results showed Hg^{VT} of 2.85 (± 0.57) µg/m³, as shown on Figure 9.

Scrubber slurry samples were taken when the OHM measurements were done for the baseline condition and for the 100 lb/hr sorbent injection rate condition. The filtrate from the baseline sample showed the dissolved mercury concentration (Hg^{D}) to be = 1100 ng/L; however, the slurry sample corresponding to when the sorbent was injected at a rate of 100 lb/hr showed a non-detect ($\text{Hg}^{\text{D}} < 0.2$ µg/L). This suggests there was a large decrease in dissolved mercury after injection of ESORB-HG-11. These results are summarized in Figure 10.

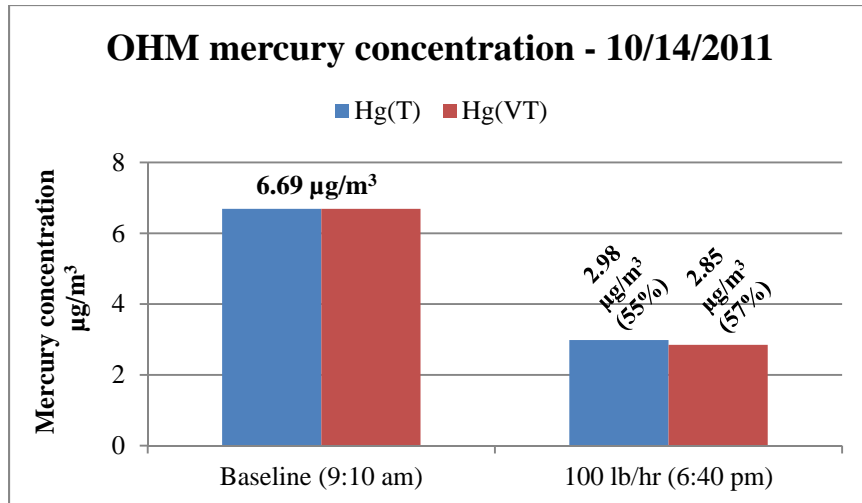


Figure 9. Step 1 testing of ESORB-HG-11 showing OHM results for baseline and 100 lb/hr injection on the 14th. Hg^T is total Hg in stack gas and Hg^{VT} is Hg^T minus particulate mercury, Hg^P, from probe filters. The time listed in brackets is the approximate start time of the OHM. Percent reduction for OHM shown in brackets by the final concentration is estimated from the baseline OHM. However, as will be seen in the CMM graph below, these reductions were calculated before the system came to steady state.

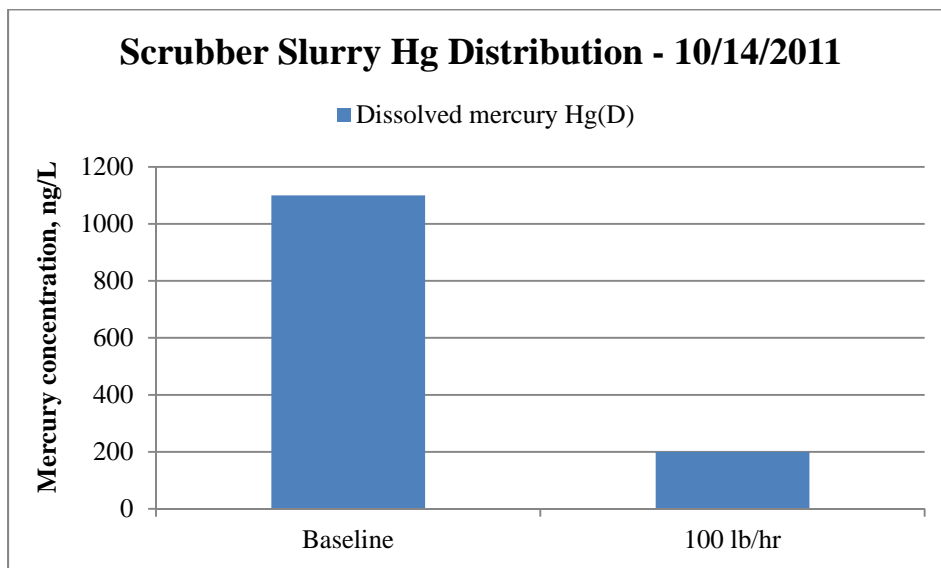


Figure 10. Bar chart showing behavior of mercury in scrubber slurry before and during testing. Dissolved mercury - Hg^D can be seen to decrease significantly with injection of ESORB-HG-11; ESORB-HG-11 is very efficient in sequestering mercury from solution and confirms results obtained in bench scale tests.

Day 2 of ESORB-HG-11 injection testing was Oct 17. The injection rates tested were 50, 100, and 150 lb/hr. OHM measurements were conducted for baseline conditions as well as for sorbent injection rates of 50 and 150 lb/hr. Figure 11 is a summary of the results, while Figure 12 summarizes the data for the 150-lb/hr injection rate. The OHM baseline Hg^{VT} was $8.22 \mu\text{g}/\text{m}^3$. The CMM average during the same period was $7.08 (\pm 0.88) \mu\text{g}/\text{m}^3$. However, looking more closely at the CMM trend depicted in Figure 13, a spike can be observed for the oxidized mercury from 8:50 am to 9:40 am, consistent with OHM data, which also shows an abnormally high oxidized mercury concentration of $2.40 \mu\text{g}/\text{m}^3$. OHM measurements for the 50 and 150 lb/hr injection rates yielded values for Hg^{VT} of 2.16 and $1.22 \mu\text{g}/\text{m}^3$, respectively. The total vapor mercury concentration does not include the particulate mercury component [Hg^{P}]. Hg^{T} from the OHM measurements for the 50 and 150 lb/hr injection rates were 2.22 and $1.81 \mu\text{g}/\text{m}^3$ (Figure 11). The disparity in results suggests that at the higher injection rates, some of the injected carbon (with the captured mercury) escapes the scrubber and contributes to the stack emissions as particulate mercury.

The CMM average Hg^{VT} concentration during the same time as the OHM sampling gave values of $2.93 (\pm 0.21) \mu\text{g}/\text{m}^3$ and $1.07 (\pm 0.29) \mu\text{g}/\text{m}^3$ for 50 and 150 lb/hr injection rates respectively. The relatively close agreement between OHM and CMM data validate the significant reduction in mercury emissions at each of the injection rates investigated. Based on the reductions in mercury emissions as a result of ESORB-HG-11 injection rates of 50 and 150 lb/hr, the Minntac line 3 test matrix was updated to include long term testing at these specified injection rates.

With regard to mercury distribution in the scrubber slurry samples, the results mirrored those obtained on Day 1 with a high Hg^{D} of 4000 ng/L during baseline operation. This value decreased significantly with injection of ESORB-HG-11, suggesting sequestration of the mercury captured in the scrubber to the scrubber solids. Figure 12 summarizes these results.

The first step of ESOR-HG-11 testing was conducted on Oct 14 and 17 and was aimed at determining the performance of each injection rate over a short term (≤ 3 hours). From the results above, the rates of 75, 100, and 150 lb/hr were selected for long-term testing (> 3 hours).

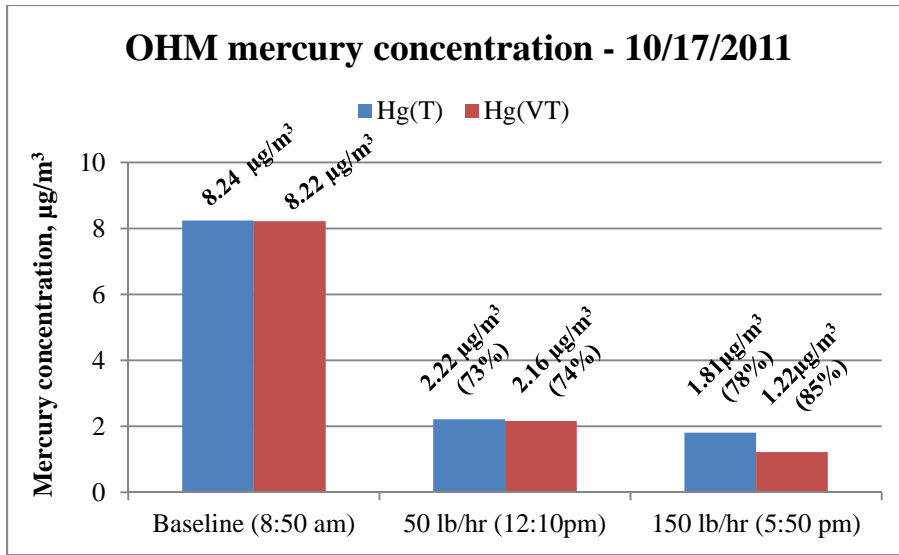


Figure 11. OHM results for Day 2 ESORB-HG-11 testing. OHM performed for baseline, 50 and 150 lb/hr injection rates. Baseline concentrations are believed to be higher than actual due to an unexplained increase observed in oxidized mercury during the measurement period. Results for 150 lb/hr suggest Hg^P emissions increase with increase in injection rate, suggesting ESORB-HG-11 has a higher penetration through the scrubber than taconite dust. As is the case with Oct 14, percent reduction for OHM shown in brackets by the final concentration is estimated from the baseline OHM and is calculated before the system came to steady state.

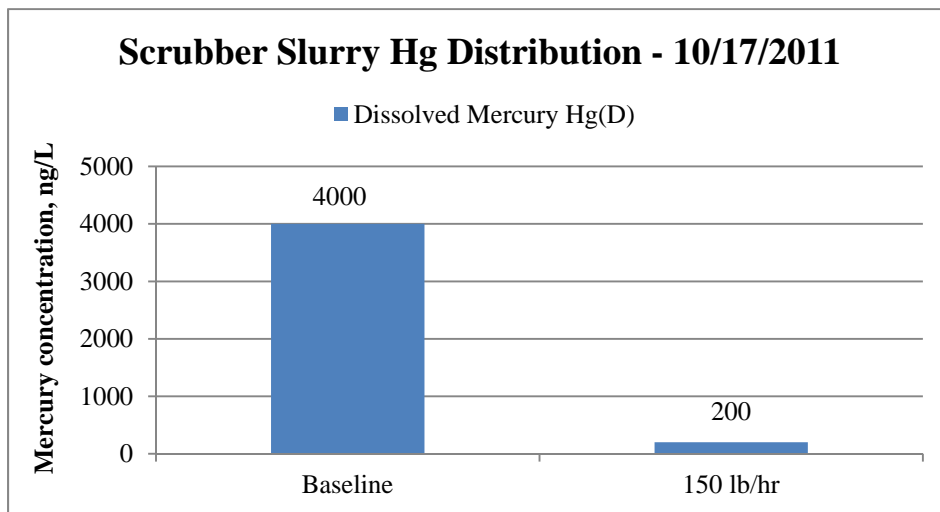


Figure 12. Bar chart showing behavior of mercury in scrubber slurry during ESORB-HG-11 injection. Hg^D concentrations decreased significantly from 4000 ng/L to < detection (200 ng/L) during 150 lb/hr.

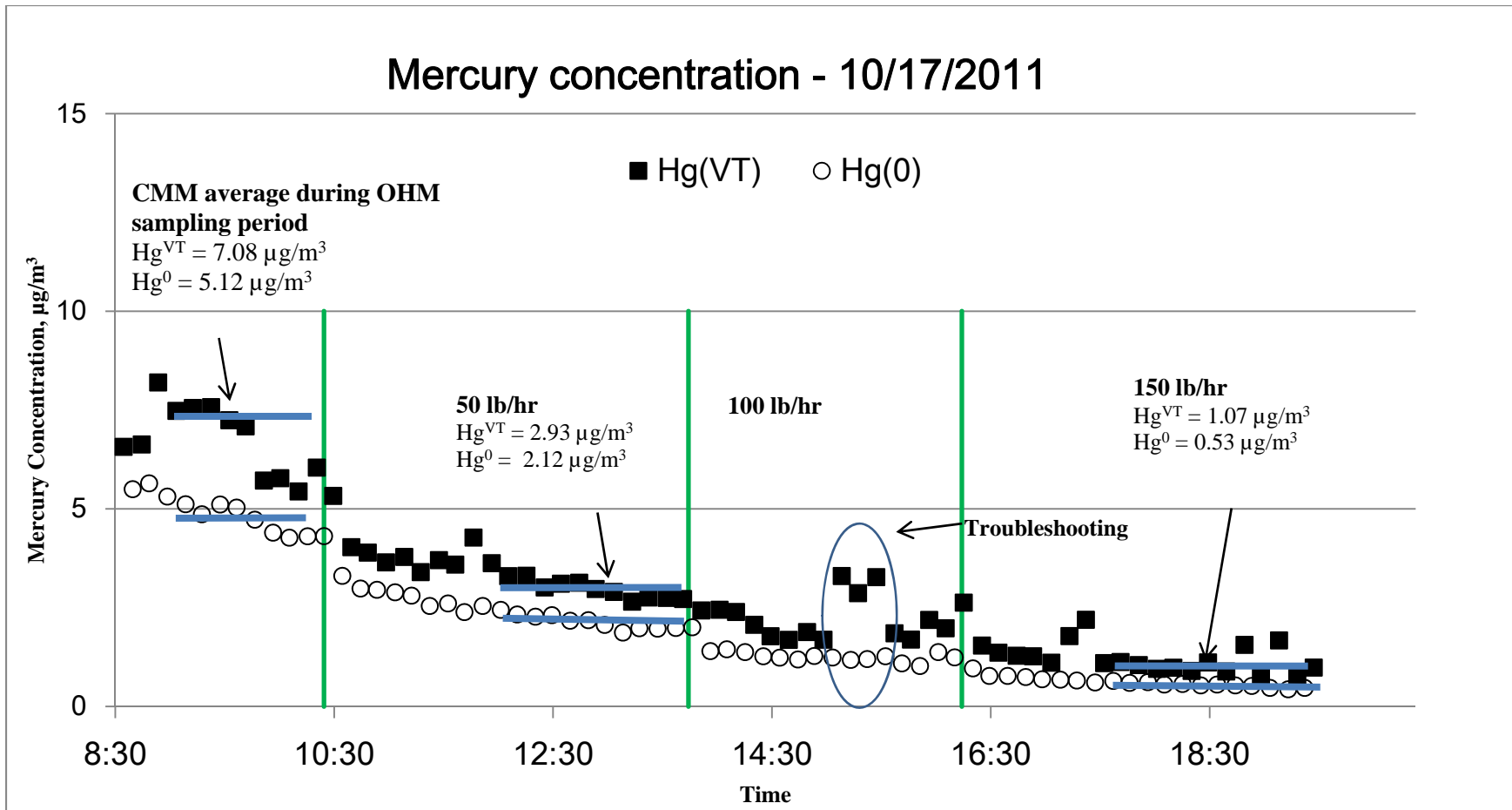


Figure 13. CMM data for Day 2. Injection rates of ESORB-HG-11 of 50, 100, and 150 lb/hr were investigated. Baseline measurements show increase in oxidized mercury as observed in OHM data; the reason for this increase is not known. Significant reductions in Hg emissions observed during testing suggested that these injection rates should be investigated further during long-term sorbent injection testing during Step 2.

On Day 3 (Oct18), a longer-term test that included injection of ESORB-HG-11 at a rate of 100 lb/hr was performed. The test duration was 5 hours and three OHM measurements were performed. These OHM measurements included the baseline as well as 3 and 5 hours after injection was started. The baseline value for the total vapor mercury concentration, before injection was started, was $6.17 \mu\text{g}/\text{m}^3$. Hg^{T} for the baseline condition was $6.20 \mu\text{g}/\text{m}^3$, as shown on Figure 14. Figure 15 shows the dissolved mercury decreased with the addition of 100 lb/hr of ESORB-HG-11.

Injection did not start immediately following the baseline OHM measurement because of troubleshooting of the CMM analyzer. The analyzer was subsequently brought back online for two hours before sorbent injection was started. The mercury concentration as measured by the CMM during this hour of baseline testing was stable at an average of $5.06 (\pm 0.22) \mu\text{g}/\text{m}^3$ (Figure 16). A reasonable agreement between this average and the OHM baseline value suggests that the baseline mercury emissions did not change significantly. The OHM baseline value was thus used to compute the percent mercury reduction.

OHM data showed that the stack values for mercury concentration decreased over time (Figure 16), suggesting that steady-state performance took time to achieve. This is likely because the system comprising the gas ducts and other surfaces continue to accumulate a portion of the injected sorbent and provide additional reduction in the mercury concentrations with time. The stack gas Hg^{VT} at the end of about 5 hours of injection as determined by OHM measurements was $1.4 \mu\text{g}/\text{m}^3$, representing a 77% reduction from baseline values. The corresponding value for Hg^{VT} determined from the CMM data was $1.15 \mu\text{g}/\text{m}^3$.

The contribution from particulate bound mercury changed Hg^{T} to $1.95 \mu\text{g}/\text{m}^3$, as shown on Figure 14. When compared to baseline values, this resulted in a 69% overall reduction for total mercury emissions. These results suggest that the brominated carbon sorbent, ESORB-HG-11, penetrates the scrubber in this unit, carrying with it a portion of the captured mercury. Therefore, greater mercury emission reductions may be obtained with improved scrubber operation.

With regard to the scrubber slurry taken during the long-term sorbent injection at 100 lb/hr, it was observed that the baseline filtrate sample was 600 ng/L, lower than baseline values obtained during previous short-term injection tests (Figure 15). The lower baseline filtrate result suggests that ESORB-HG-11 was still present in the system. Even with the lower levels of ESORB-HG-11, there was some sequestration still taking place in the recirculation tank. When long-term sorbent injection was started, the dissolved mercury concentration in the scrubber filtrate decreased to very low values ($\sim 50 \text{ ng}/\text{L}$), confirming the sequestration ability of ESORB-HG-11. Mass balance calculations suggest it would take several hours for ESORB-HG-11 present in the scrubber tank to be reduced to insignificant levels. This was further confirmed by the fact that the baseline Hg^{D} for Oct 17, a Monday, was significantly higher (4000 ng/L) as the ESORB-HG-11 previously injected into the system on the previous Friday most likely reduced to insignificant levels in the recirculation tank.

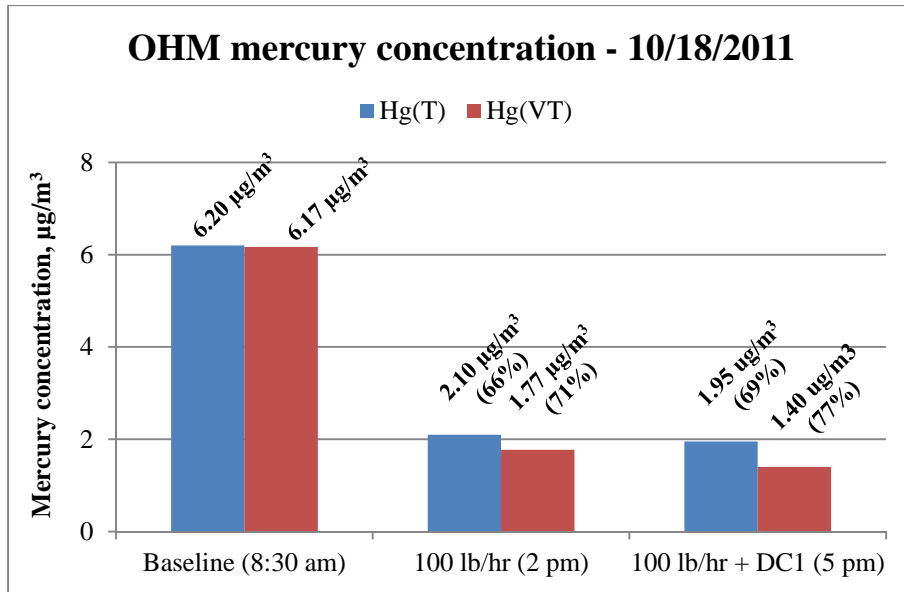


Figure 14. OHM results for Day 3 testing. OHM measurements were performed for baseline, and 3 hrs and 5 hrs into injection. Assuming OHM baseline is still valid at the start of injection, significant reductions can be observed for both Hg^T and Hg^{VT} . Results are also consistent with observation that Hg^P increased during technology testing; suggesting that ESORB-HG-11 penetrated the scrubber.

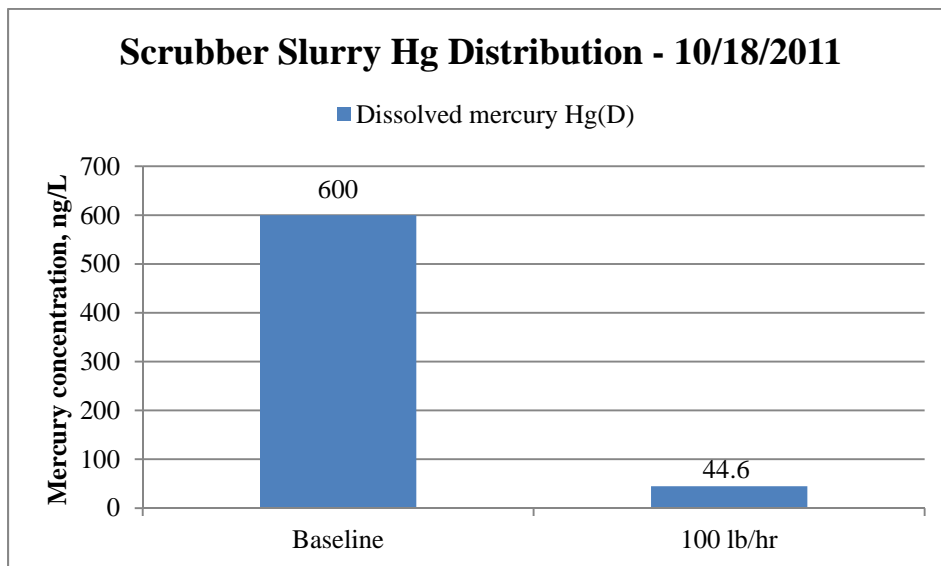


Figure 15. Scrubber mercury distribution during long term testing of ESORB-HG-11 with an injection rate of 100 lb/hr. Hg^D decreases with additive injection.

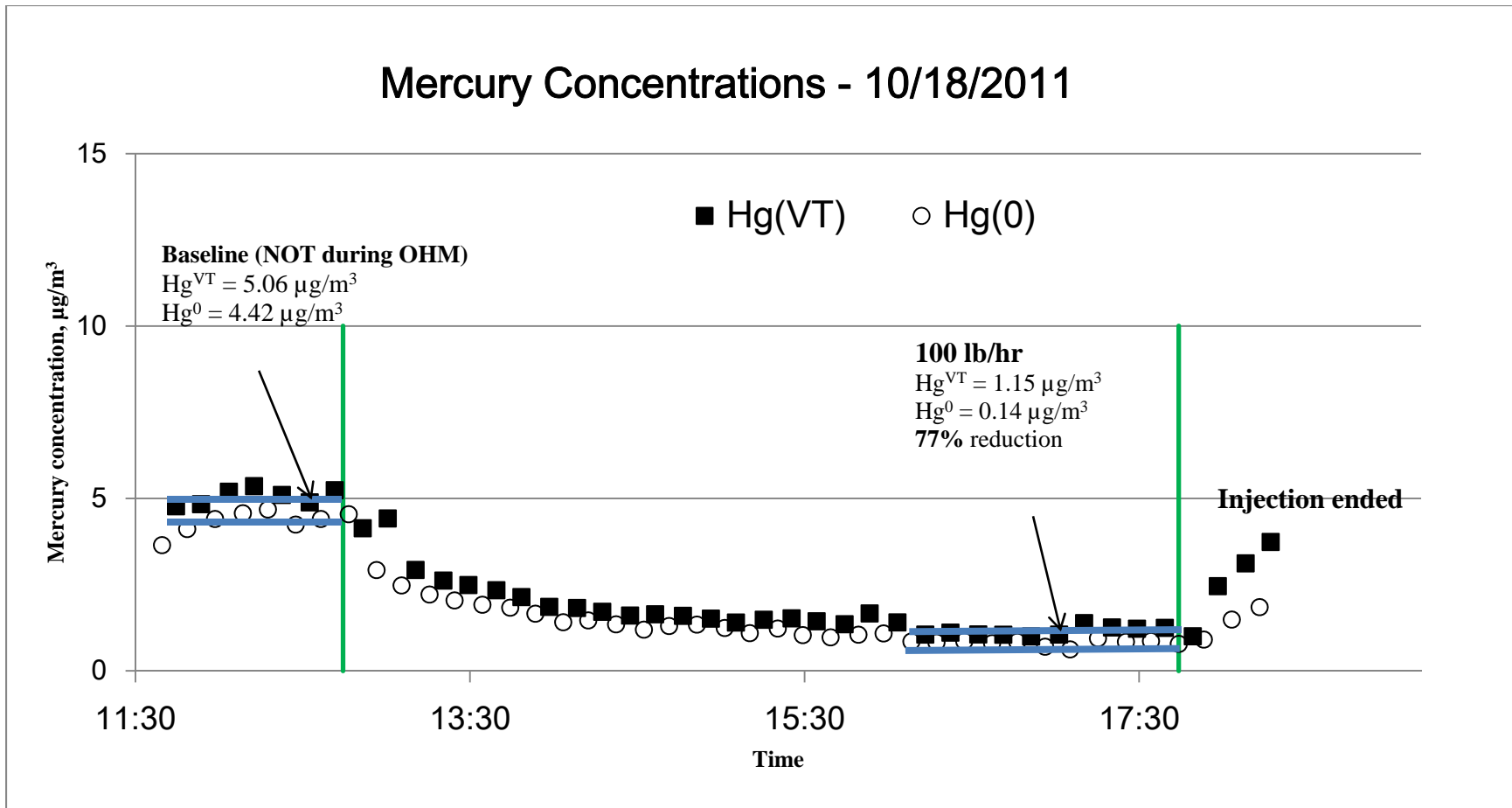


Figure 16. CMM data for Day 3. The CMM average baseline depicted is 3 hours after OHM baseline. Hg^{VT} average during 100 lb/hr injection was calculated over the same time the third OHM measurement was performed this day. OHM average, $1.40 \mu\text{g}/\text{m}^3$, and CMM average, $1.15 (\pm 0.14) \mu\text{g}/\text{m}^3$, agree closely.

Testing performed on Day 4 and 5 involved the injection of the scrubber additive, diethyl dithiocarbamate (DEDTC), and plain powdered activated carbon (PAC). These results are discussed later.

ESORB-HG-11 testing was resumed on day 6, October 21st with an injection rate of 150 lb/hr. Two OHM measurements were performed; one for the baseline, and the other started 4 hours into the injection schedule. The baseline OHM measurement showed a value for Hg^{VT} of $5.04 \mu\text{g}/\text{m}^3$ as shown on Figure 17. After 5 hours of injection, the OHM value was $0.83 \mu\text{g}/\text{m}^3$ corresponding to a reduction of 84% for Hg^{VT} . Figure 18 shows that the dissolved mercury decreased with the addition of 150 lb/hr of ESORB-HG-11. The CMM values for the stack Hg^{VT} was steady and near $0.61 \mu\text{g}/\text{m}^3$, as shown on Figure 19. Hg^{T} in the stack gas at this test condition, as measured by the OHM method was $1.50 \mu\text{g}/\text{m}^3$, corresponding to a 70% reduction from the baseline value. When compared to previous tests where sorbent injection rates were lower, Hg^{P} increased at this higher injection rate. Filters for both the CMM and OHM showed evidence of carbon penetration through the scrubber potentially contributing to Hg^{P} emission in the stack gas. This further corroborates the possibility that a portion of the sorbent laden with mercury penetrates the scrubber, and thereby increases the mercury emission rates.

Hg^{D} in the scrubber slurry decreased as a result of ESORB-HG-11 injection (Figure 18), which is consistent with previous tests. However, the baseline value was very low to start with, probably as a result of PAC still present in system from the run on the previous day. The dissolved mercury concentration in the scrubber liquids during ESORB-HG-11 injection at a rate of 150 lb/hr was 20 ng/L.

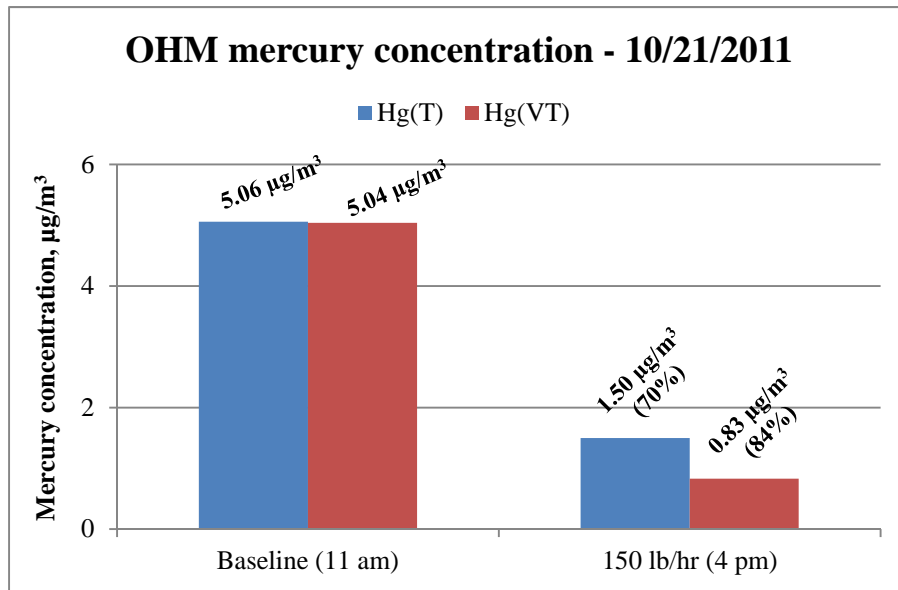


Figure 17. OHM results for Day 6 testing. OHM performed for baseline and 5 hrs into injection. Time listed in brackets is for OHM start. Hg^P increased significantly with higher injection rate as compared to Day 3, with 100 lb/hr injection rate.

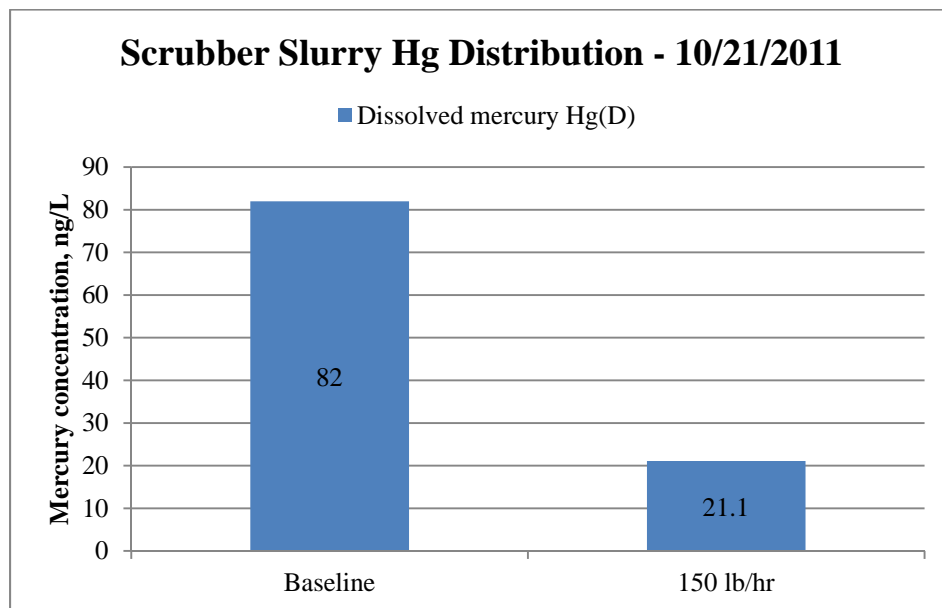


Figure 18. Slurry mercury distribution during injection of 150 lb/hr ESORB-HG-11. Hg^D is low but still decreased from 82 ng/L to 21 ng/L. The low baseline is probably because of residual PAC in the recirculation tank from testing on the previous day.

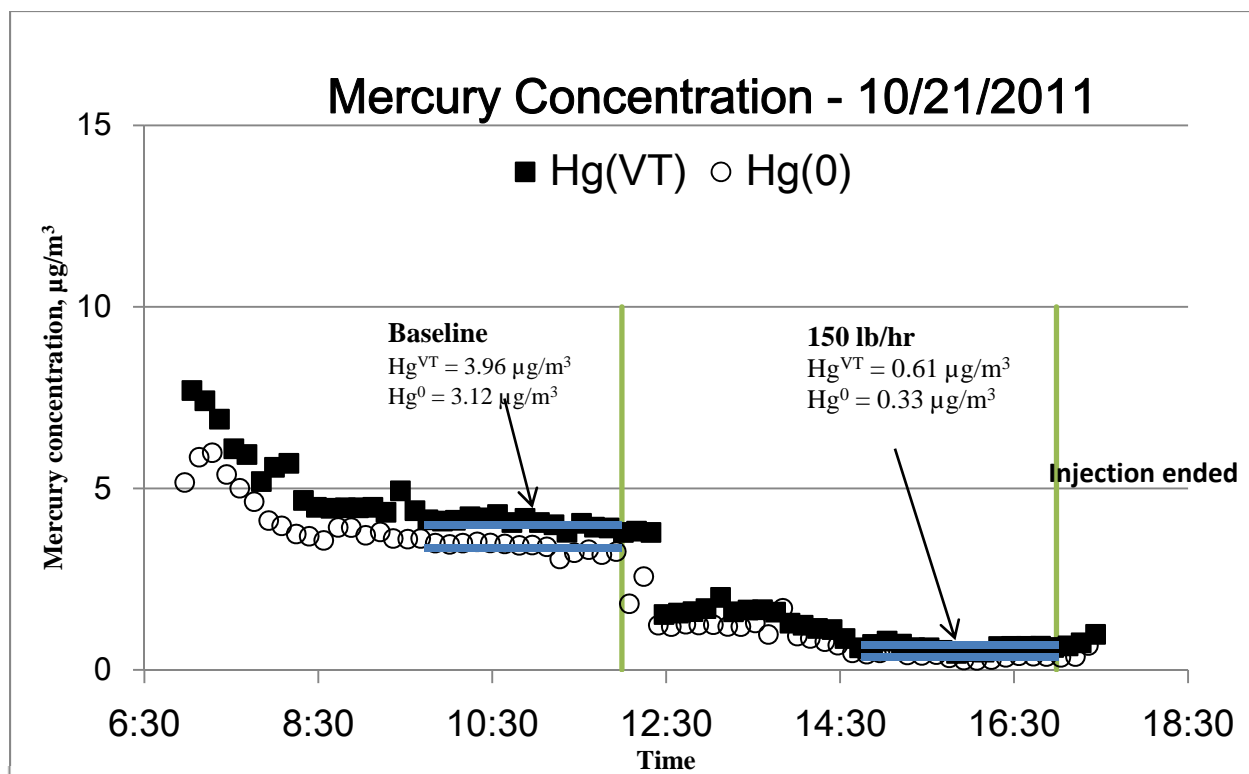


Figure 19. CMM data for Day 6. Injecting 150 lb/hr for 5 hrs shows Hg^{VT} decreased significantly to < 1 µg/m³. Average values showed in graph were computed during the same period the OHM measurement was performed.

Oct 24 was the last test day of ESORB-HG-11 performance at the preheat fan inlet injection location. A new injection rate (75 lb/hr) was investigated for a time of 5 hours. The goal was to investigate if a lower feed rate would still produce significant reductions in mercury emissions. As shown in Figure 20, the OHM baseline value for Hg^{VT} was 4.98 µg/m³. ESORB-HG-11 injection started 20 minutes after the OHM baseline measurement was completed. Reductions of 56% and 66% for Hg^{VT} were observed for OHM measurements performed 2 hours and 4 hours after injection. After the initial drop in the mercury concentration over a 30-minute ESORB-HG-11 injection period, the values remained nearly steady at an average of 2.70 µg/m³ for the rest of the injection period. A gradual increase was observed in Hg^{VT}, which corresponded to the process recovering after injection stopped. However, measurement using the CMM was stopped well before the stack mercury emissions returned to baseline values. Hg^P was significantly higher during this test condition than previously observed, even though the injection rate investigated here was lower than for previous tests.

Hg^D for the scrubber slurry during the baseline run was 4370 ng/L, suggesting the scrubber system had returned to baseline values over the weekend (Figure 21). The levels of Hg^D decreased once ESORB-HG-11 injection at a rate of 75 lb/hr was started. Hg^D did not drop as significantly as it did on previous days when sorbent injection started. This was an unexpected trend similar with the stack mercury concentration that showed a lower decrease than that observed for the 50 lb/hr injection test.

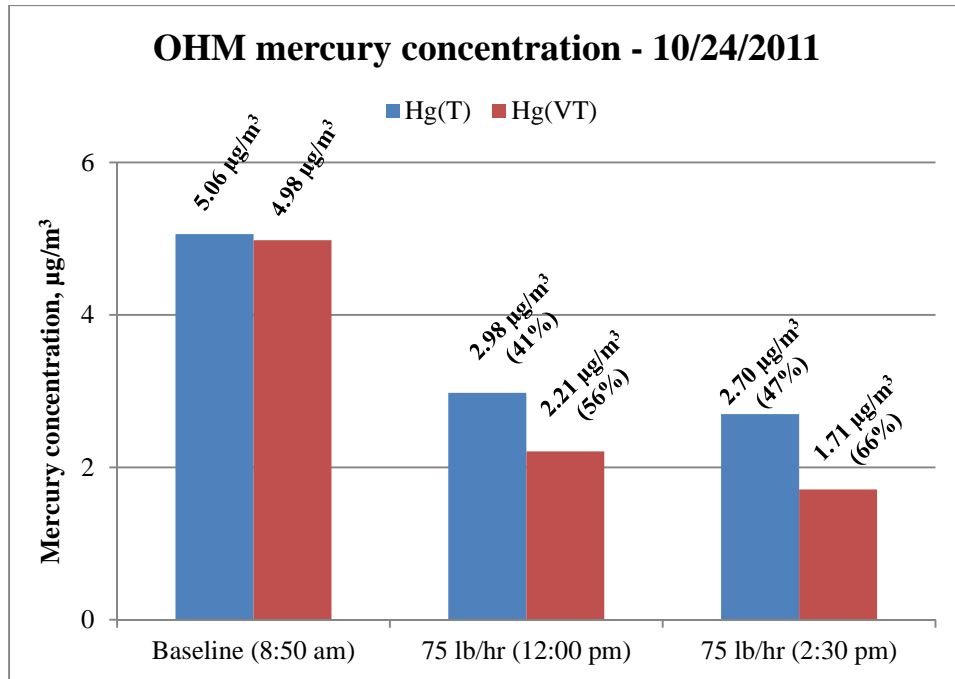


Figure 20. OHM results for testing on the 24th. OHM performed for baseline, 2 hrs and 4 hrs into injection. Time listed in brackets is for OHM start. Hg^P increased by 15% and 19%.

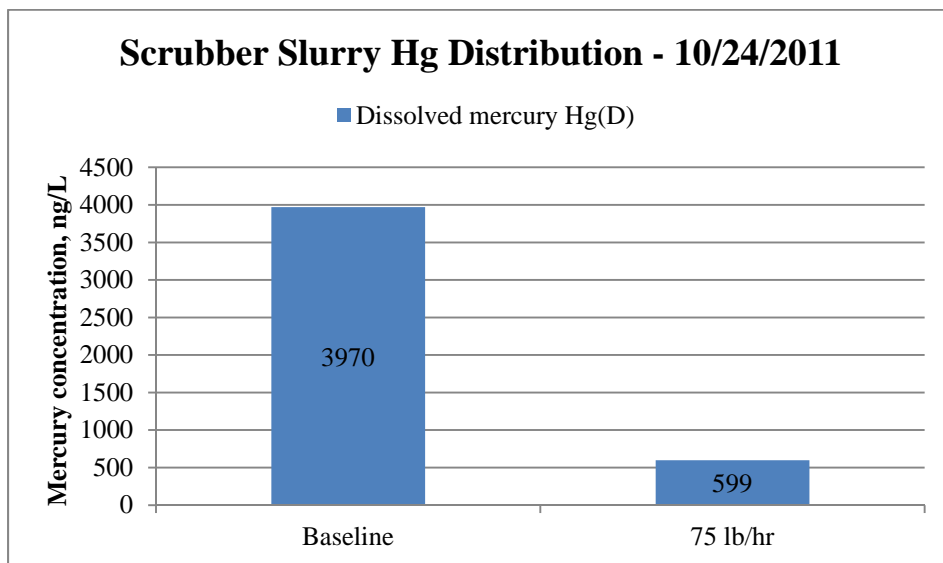


Figure 21. Scrubber mercury distribution during the injection of 75 lb/hr. Hg^D is seen to decrease but the final value after 6 hours of injection was higher than expected. Correspondingly high Hg^P stack emissions may suggest less ESORB-HG-11 was captured.

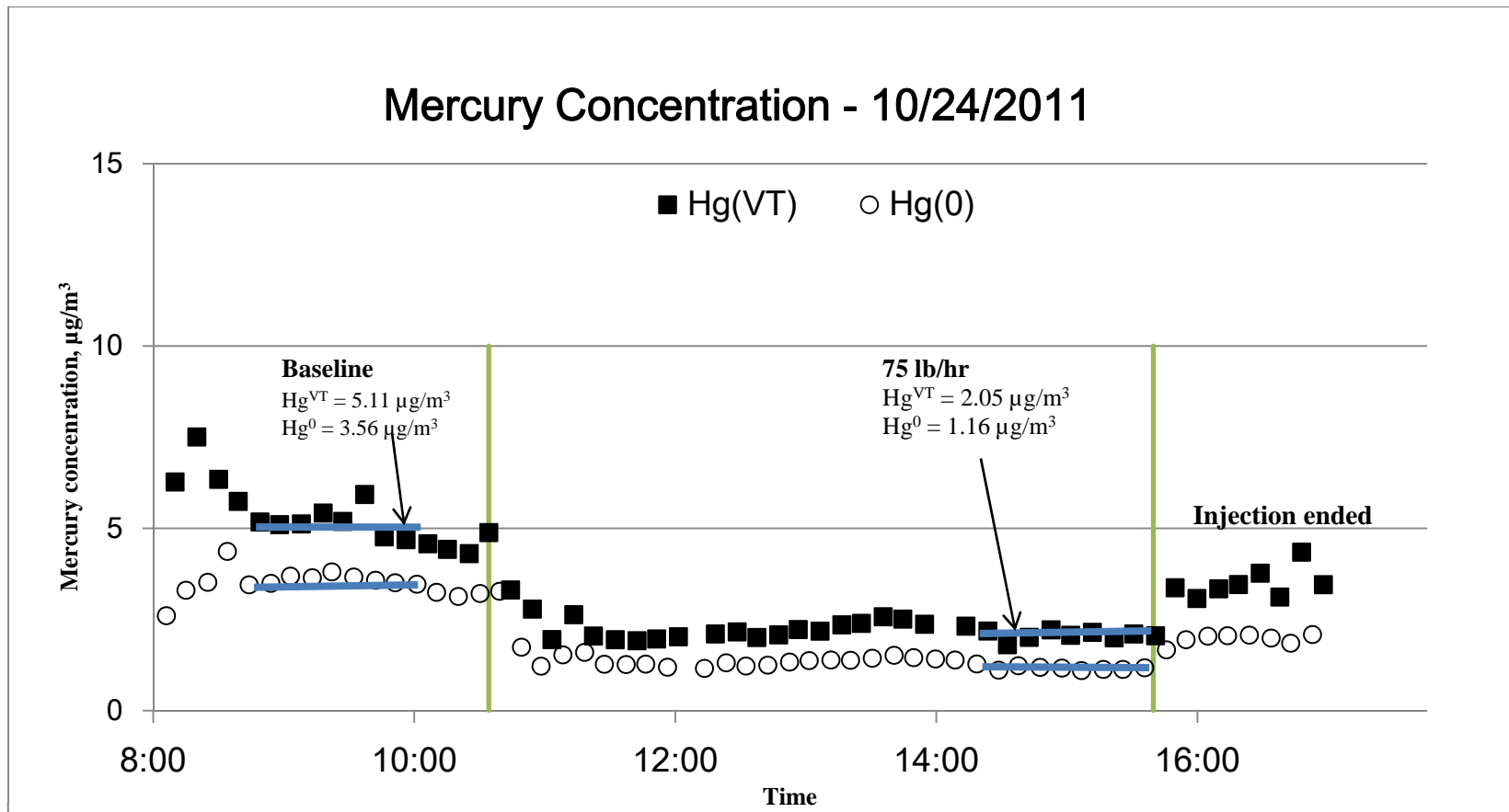


Figure 22. CMM for tests on the 24th at an injection rate of 75 lb/hr for 5 hrs. A sharp decrease can be observed followed by a stable value throughout the injection period.

Conclusion – ESORB-HG-11 Testing at Preheat Fan Inlet Location

ESORB-HG-11 testing at the preheat fan inlet injection location showed significant reductions in Hg^{VT} . At ESORB-HG-11 injection rates of 100 and 150 lb/hr, there were 77% and 84% reduction in stack mercury emissions from baseline, respectively. While there were significant reductions in stack vapor phase mercury emissions, Hg^{P} in the stack gases were seen to increase as a result of the penetration of ESORB-HG-11 through the plant scrubber. This was confirmed by visual inspection of the probe filters for both the OHM and CMM. The Hg^{P} emissions increased the Hg^{T} in the stack gas for the 100 and 150 lb/hr injection rates to 1.95 and 1.50 $\mu\text{g}/\text{m}^3$, respectively. The corresponding total stack mercury emission reductions for the 100 and 150 lb/hr injection rates compared to the baseline emissions were 69% and 71%, respectively. Baseline emission values on the day these tests were performed were 6.2 and 5.06 $\mu\text{g}/\text{m}^3$, respectively. At an injection rate of 75 lb/hr, Hg^{VT} reported a reduction of 66%, with its Hg^{P} emissions being the most significant during the entire testing period. While there are significant reductions in stack mercury emissions as a result of ESORB-HG-11 injection, the contribution from particulate bound mercury to the sorbent cannot be ruled out. It is suggested that identifying ways of improving the particulate capture efficiency of the scrubber may result in further reductions of stack mercury emissions, especially during ESORB-HG-11 injection.

Scrubber slurry analysis showed reductions in the levels of Hg^{D} as a result of ESORB-HG-11 injection. The captured mercury was associated with the non-magnetic portion of the scrubber slurry, in this case ESORB-HG-11. This confirms the sequestering ability of ESORB-HG-11. Minntac Line 3 slurry solids are discharged and not recycled, so captured mercury has been removed from the process permanently.

The reductions mentioned above were determined based on the baseline OHM concentrations of the respective test days and OHM concentrations taken during sorbent injection. The differences in the baseline average values as outlined earlier may require that another reduction calculation method be considered for overall additive performance that takes into consideration an average baseline emission, rather than a value determined for a particular period.

ESORB-HG-11 Testing at Preheat Grate Injection Location

The second sorbent injection location investigated at Minntac Line 3 was injection at the preheat zone. The goal was to test whether changing to an upstream location and using low injection rates could achieve reductions comparable or greater than those seen during injection at the preheat fan inlet zone. These tests were conducted on October 25 and 26. Injection into the preheat zone was also chosen with the idea that longer residence times would provide longer contact times between the sorbent and the mercury, with the expectation of improving the performance of ESORB-HG-11. Ports located at the base of the preheat zone wall were used, which enabled injection of ESORB-HG-11 directly into the preheat section upstream of the grate. However, the location of the ports on the walls of the zone coupled with the lack of suitable high temperature injection lances that could be inserted into the grate and withstand the high temperatures did not allow for effective distribution of the injected material into the flue gas above the pellet bed. At this location, injection rates of 50, 75, and 100 lb/hr were investigated, as shown

in Figures 23 – 26; however, no CMM measurements were done for the 50 lb/hr rate. For the other two rates, OHM and CMM baseline measurements showed good agreement during testing; however, reductions from baseline values were lower than 50%. As summarized in Figures 23 and 24, for 75 lb/hr and 100 lb/hr, respectively, stack mercury emission reductions ranged from 43 to 50% for Hg^{VT} and 25 to 31% for Hg^{T} . Results from these test runs suggest that injected carbon is transported in the flue gas and is not fully combusted in preheat zone. However, lower reductions than previous test results conducted at 75 lb/hr of ESORB-HG-11 injection suggest that the poor distribution of the sorbent in the preheat zone could be responsible for the diminished effectiveness.

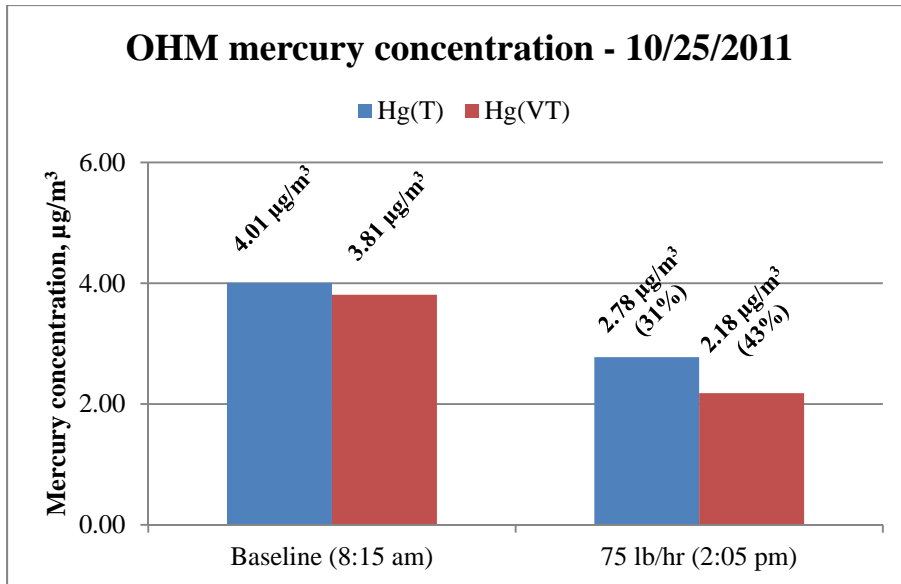


Figure 23. OHM results during preheat zone injection testing of 75 lb/hr of ESORB-HG-11. Reduction was < 50% for both Hg^T and Hg^{VT}. Significant Hg^P emissions during testing were also observed. This suggests that injected carbon is transported by flue gas and not combusted in the preheat zone. However, lower reductions than previous testing suggest distribution of ESORB-HG-11 into preheat zone is poor.

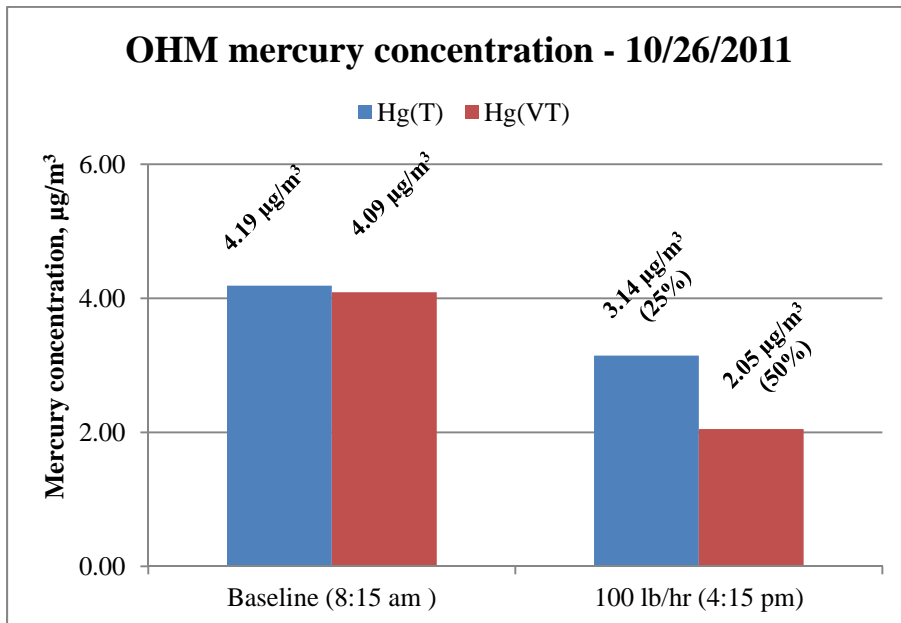


Figure 24. OHM results during preheat zone injection at 100 lb/hr of ESORB-HG-11. Hg^P was significant after injection began for close to 7 hrs.

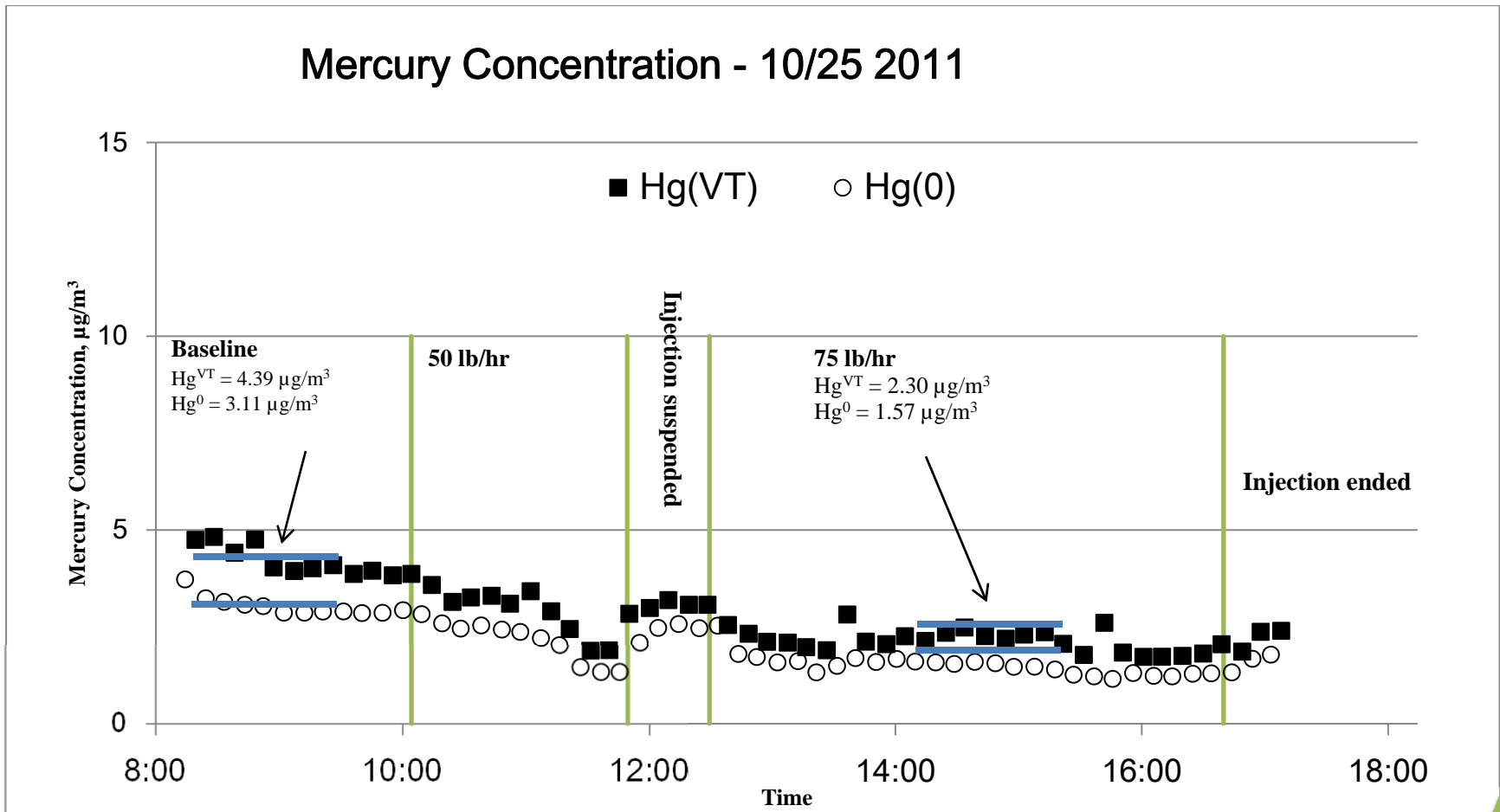


Figure 25. CMM data during preheat zone testing of 50 lb/hr and 75 lb/hr of ESORB-HG-11. Average values calculated during period OHM measurements were carried out.

Mercury Concentration - 10/26/2011

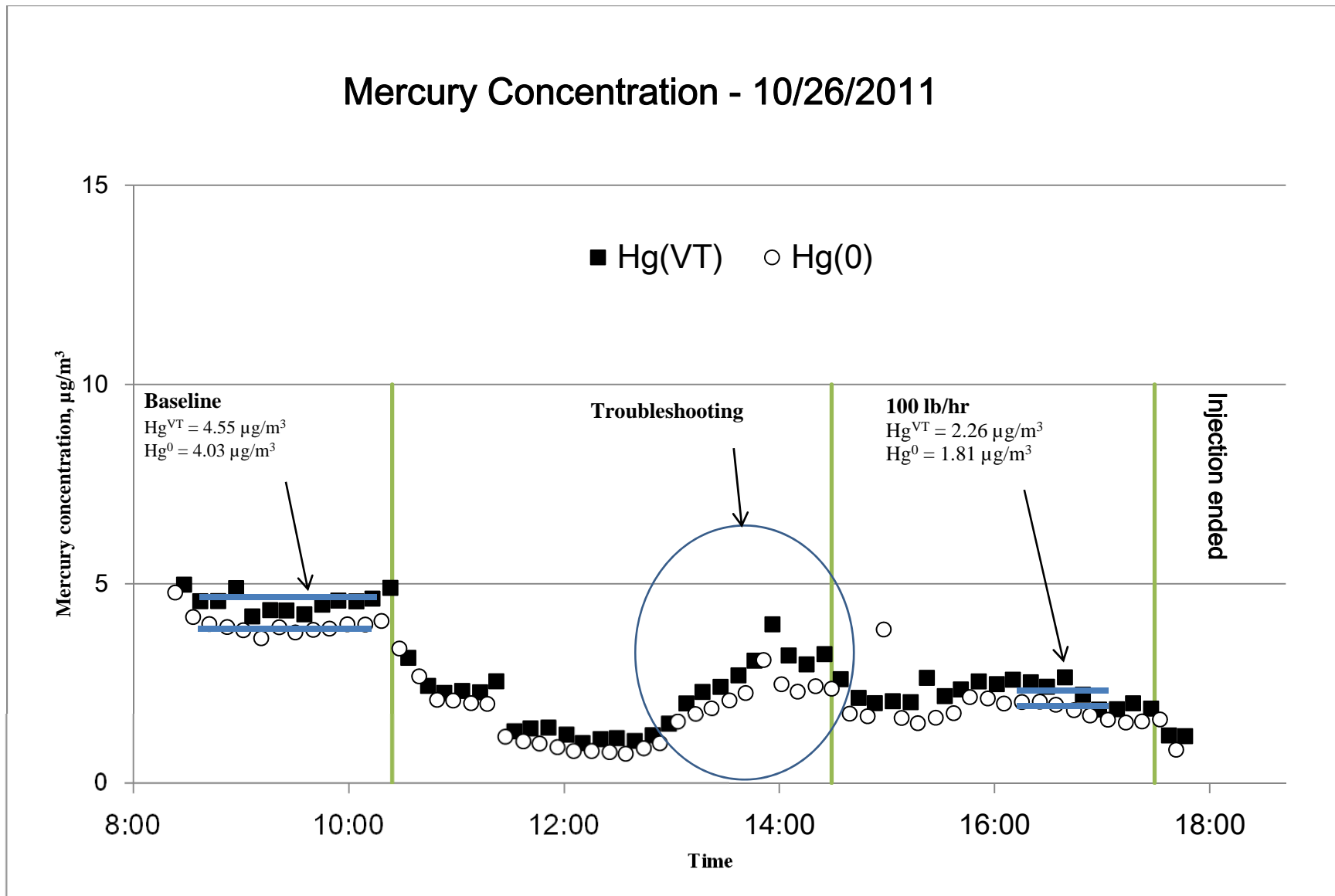


Figure 26. CMM data during preheat zone injection testing at 100 lb/hr. Some reduction observed but reduction was not significant.

Conclusion – ESORB-HG-11 Testing at Preheat Zone Injection Location

Injection of the brominated sorbent into the preheat zone showed less effectiveness in mercury emission reduction when compared to the preheat fan inlet injection for similar injection rates. This is believed to be largely due to the poor distribution of ESORB-HG-11 at this injection location, given that injection was at the preheat zone wall and not over the entire bed cross-section. In order to deliver a more uniform coverage of the sorbent into the flue gas at the high temperatures in the preheat zone, cooled lances that can be inserted further into the grate area will be required.

As a result of the lower stack mercury emission reduction from injection testing at this location, further analyses of other samples collected were not performed. It is believed that improving the injection distribution in the preheat zone using high temperature-tolerant lances and better port locations should lead to better reduction percentages.

PAC testing at Preheat Fan Inlet Location

On October 20, short-term tests using plain powdered activated carbon (PAC) were performed. The injection rates investigated were 50, 100 and 150 lb/hr. Baseline OHM results showed a low stack Hg^{VT} value of $3.44 \mu\text{g}/\text{m}^3$, which was the lowest baseline for the entire testing period. These results are summarized in Figures 27 - 29. CMM baseline results were also lower, averaging $2.11 \mu\text{g}/\text{m}^3$. The CMM trend for this test period is shown in Figure 29. Injection with PAC showed very little reduction in stack mercury emissions measured using the OHM method and reported on Figure 27. The CMM trend as shown in Figure 29 shows nearly no reductions in stack mercury emissions. PAC is effective in oxidizing mercury and capturing it if oxidizing components (like halogens) are present in the flue gas. Presumably, the flue gas from taconite processing at this plant did not contain sufficient concentrations of such oxidizing components. In as much, the Hg^{P} did not increase during PAC injection as was observed when injecting ESORB-HG-11. This could be explained either by the fact that the PAC did not capture any mercury species or by the fact that the PAC was more easily captured by the scrubber as compared to ESORB-HG-11.

PAC also exhibits mercury sequestering capabilities; hence even though stack mercury emissions did not decrease, its presence in the system affected mercury speciation in the slurry. Analysis of scrubber samples collected during testing confirmed this trend as shown on Figure 28. Baseline dissolved Hg^{D} was reported as a non-detect value; hence, a default of $0.2 \mu\text{g}/\text{L}$ was reported, which corresponds to the method detection limit. Other samples were analyzed using low-level mercury analysis (EPA Method 1631). Results indicated that Hg^{D} decreased during injection of PAC, confirming bench and pilot testing that showed that PAC also has the capacity to effectively capture and sequester mercury from the scrubber liquids.

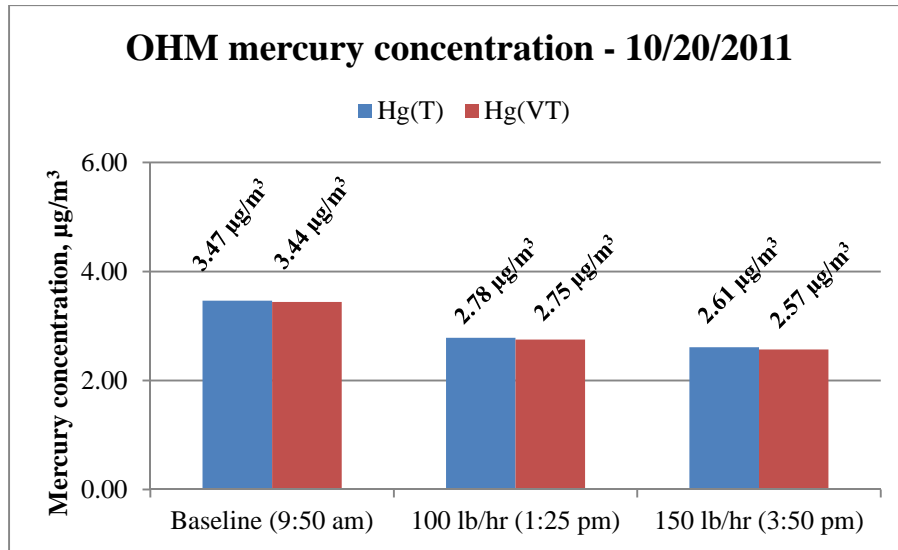


Figure 27. OHM concentrations during PAC testing. Decreases in Hg^T and Hg^{VT} shown on this figure are not believed to be due to injection of PAC, but rather due to baseline fluctuations during the test period. No significant increase in Hg^P observed during injection.

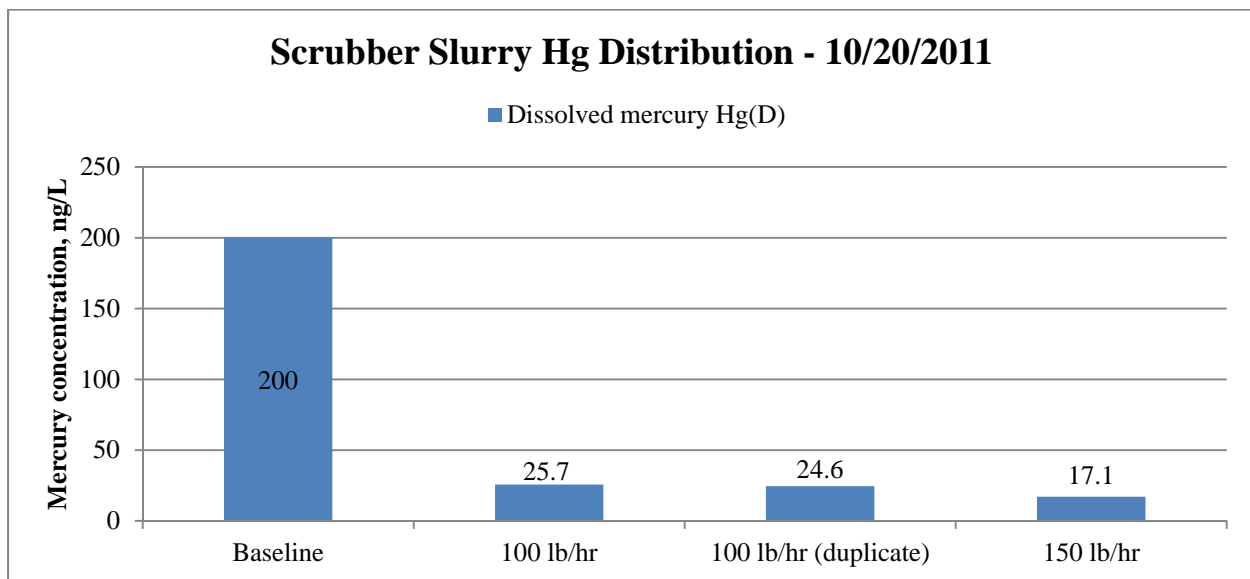


Figure 28. Hg^D values in the scrubber slurry during PAC injection. Hg^D is seen to decrease with injection of PAC. The 100 lb/hr samples were analyzed in duplicate. Hg^D sample for baseline was estimated at 200 ng/L. Meanwhile, Hg^D for 100 lb/hr and 150 lb/hr were 25.2 ng/L (average of 25.7 and 24.6) and 17.1 ng/L. The low Hg^D baseline is believed to be caused by ESORB-HG-11 that was added to the system on the Oct 19 during DEDTC testing.

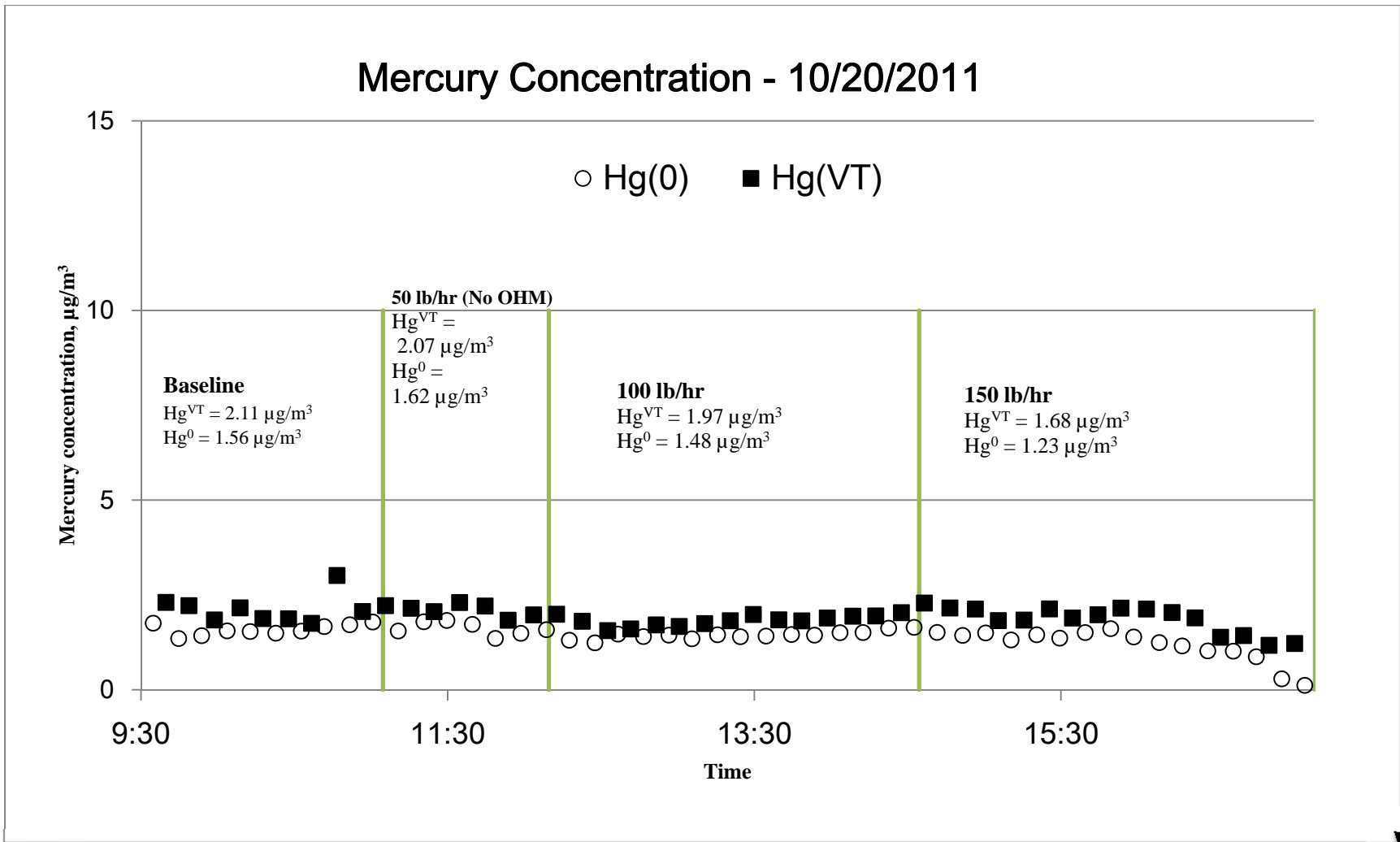


Figure 29. CMM data during PAC testing. The trend suggests that PAC did not increase oxidation of mercury in the system.

Conclusion for PAC injection at preheat fan location

Test results for short-term injection of plain powdered activated carbon (PAC) indicated that PAC did not significantly reduce stack mercury emissions. Even though PAC showed sequestering capabilities in the scrubber slurry, it would not be sufficient to attain the goal of 75% reduction in stack mercury emissions. Consequently, PAC was not investigated further in the test program.

DEDTC addition to scrubber slurry

The last technology tested was the addition of a scrubber additive diethyl dithiocarbamate (DEDTC); the test was performed on Oct 19. DEDTC is a mercury complexing agent used to improve oxidized mercury capture in the scrubber by reducing Hg^D concentrations. Testing of DEDTC was performed in two steps. The first step involved testing DEDTC without any other additive or sorbent. This test was conducted to determine whether DEDTC could improve the capture of oxidized mercury not already captured by scrubber liquids. The second step of testing involved DEDTC as well as ESORB-HG-11 to aid in mercury oxidation in the flue gas. The idea behind the second step was that injection of ESORB-HG-11 at 50lb/hr would increase oxidation of mercury species upstream of the scrubber while DEDTC would capture the oxidized mercury in the scrubber liquids. The results from these two steps would also be compared to test results from Oct 17 during which ESORB-HG-11 was injected at a rate of 50 lb/hr .injection.

In the first step, DEDTC was added to the scrubber recirculation tank by dosing to maintain a concentration of 1.4 mg/L, which was later increased to 7.0 mg/L. Scrubber slurry samples were collected at least one hour after dosing the recirculation tank. Stack mercury concentrations and slurry analysis during this test period showed no impact on mercury emissions after dosing of scrubber slurry with DEDTC. The results are shown in Figures 30 - 32. On the contrary, the Hg^D increased from low baseline values. This was attributed to left over ESORB-HG-11 from the previous test conducted on Oct 18 and not the chelating effects of DEDTC.

In the second stage of testing, which involved both the addition of the DEDTC to the scrubber recirculation tank and the injection of ESORB-HG-11 at the preheat fan inlet location, the mercury concentration in the stack gases decreased as expected. This is shown in Figure 31. However, the reduction in mercury emissions was similar with and without the addition of DEDTC to the scrubber slurry. This indicates that the entire impact on the mercury concentrations was from the injection of the brominated sorbent. Injection of ESORB-HG-11 also decreased Hg^D in the scrubber slurry filtrate after just two hours of injection (Figure 30). In summary, injection of the scrubber additive DEDTC did not improve mercury capture or mercury sequestration.

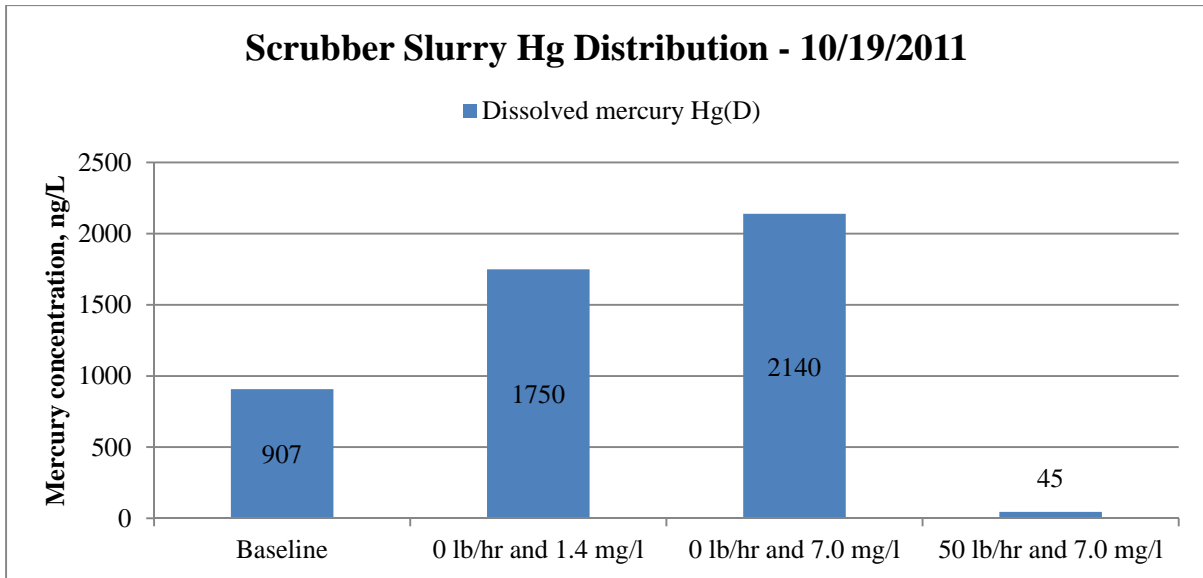


Figure 30. Hg^D is seen to increase even after addition of DEDTC up to 7.0 mg/L. The scrubber slurry two hours into injection of ESORB-HG-11 at 150 lb/hr saw Hg^D drop from 2140 to 45 ng/L.

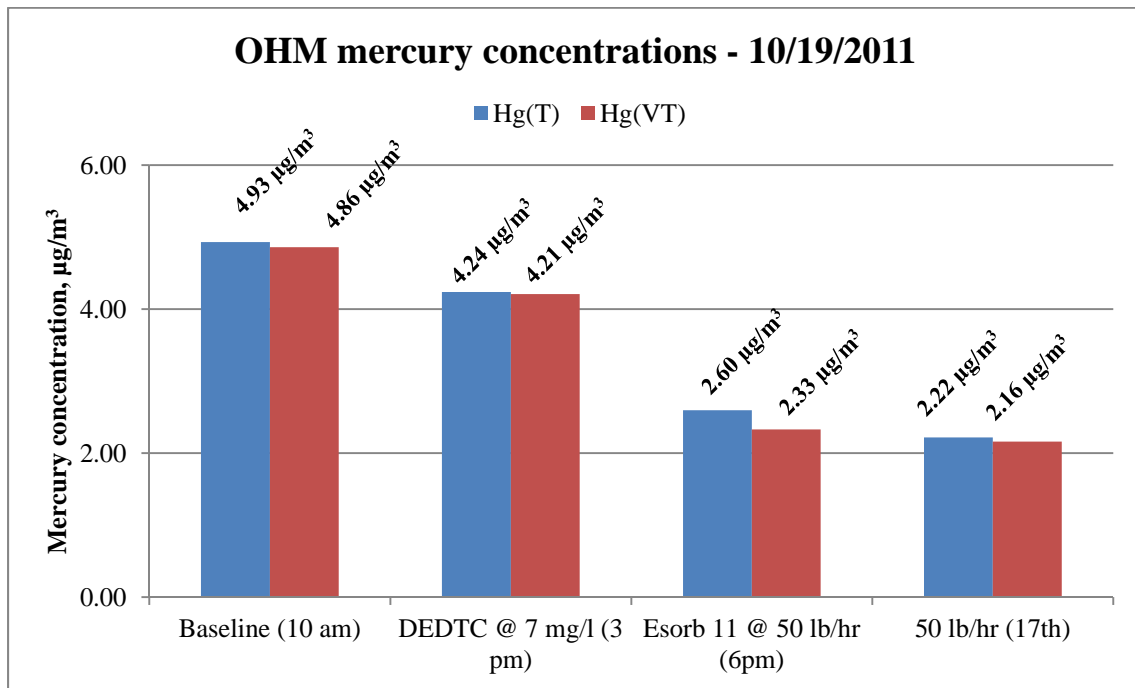


Figure 31. OHM during DEDTC testing and comparing 50 lb/hr injection with that of Oct 17th. Decrease in OHM measurements for DEDTC at 7 mg/L is assumed to be based on fluctuations in the system as confirmed by the CMM chart below. Comparing both 50-lb/hr tests suggests that DEDTC + ESORB-HG-11 shows similar reduction as for ESORB-HG-11 only.

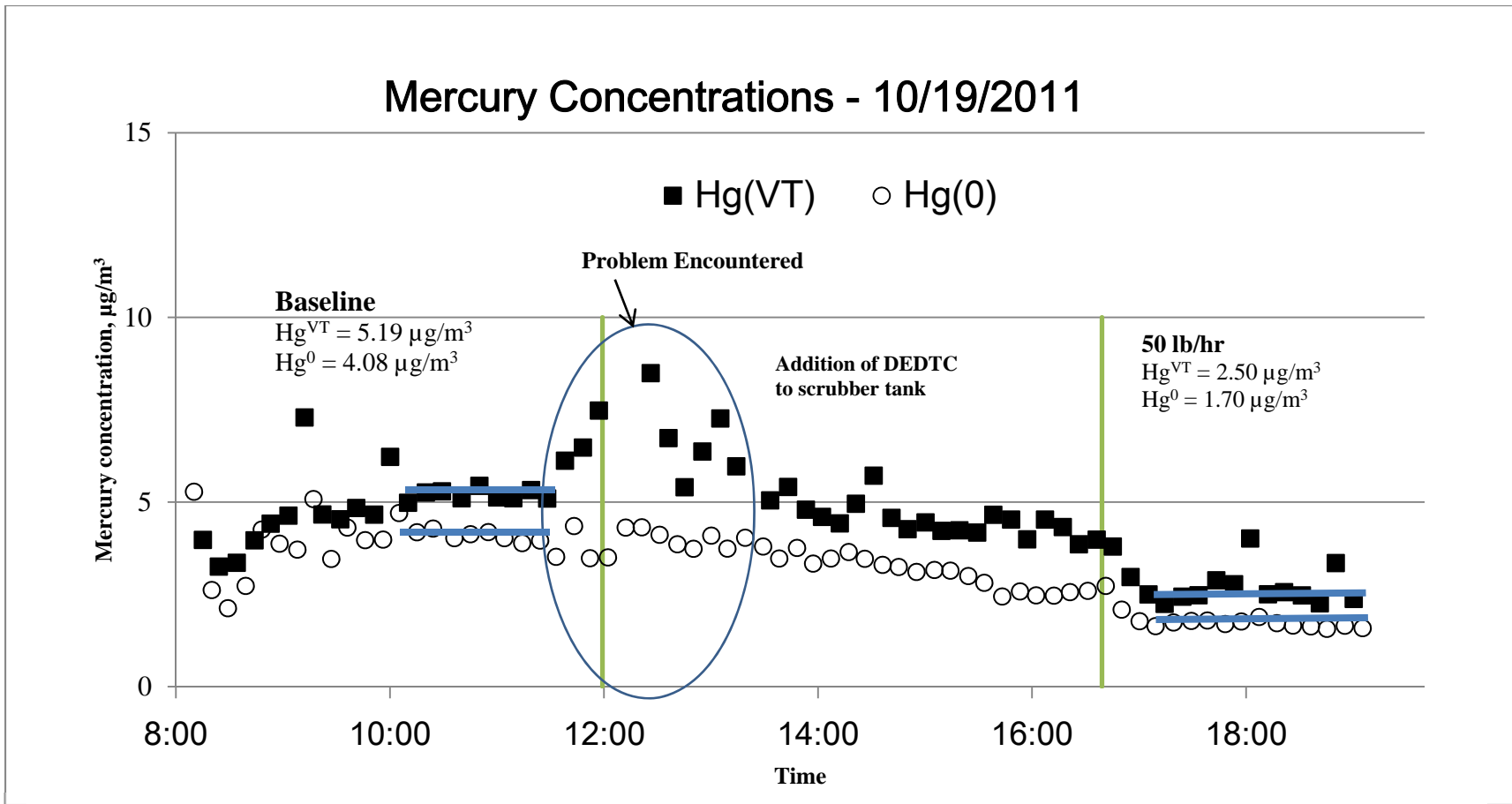


Figure 32. Showing CMM data during addition of DEDTC to scrubber followed by injection of 50 lb/hr of ESORB-HG-11 to the preheat fan inlet. After the problem with the CMM analyzer, the Hg^{VT} values decreased only slightly, if at all. However, once ESORB-HG-11 injection is started, mercury concentrations are seen to decrease sharply.

Conclusion on testing of DEDTC

Addition of the scrubber additive, DEDTC to the scrubber waters resulted in no observable effects on the mercury concentration/speciation in either the taconite process flue gases or the dissolved mercury concentration in the scrubber slurry.

Mercury Reductions with Average Baseline Mercury Emissions

From the tests conducted, ESORB-HG-11 was the only additive that showed the potential to attain the objective of 75% reduction in mercury emissions. However, to fully estimate the actual reduction potential of ESORB-HG-11 as a function of injection loading, it is first necessary to estimate a baseline Hg emission rate for the plant. This is calculated by taking the average of all baseline Hg^{T} measurements obtained during the test period (Oct 13 - 26). The result of averaging out the baseline measurements was $\text{Hg}^{\text{T}} = 5.20 (\pm 1.30) \mu\text{g}/\text{m}^3$. The percent reduction as a function of additive injection rate was then estimated using Equation (3):

$$\% \text{ Hg Reduction} = \frac{\text{HgB}_{\text{ave}} - \text{HgS}_{\text{ave}}}{\text{HgB}_{\text{ave}}} * 100 \quad \dots (3)$$

Where HgB_{ave} is the average baseline Hg^{T} and HgS_{ave} is the final stack Hg^{T} concentration during long-term injection.

Long-term testing at 150 lb/hr of ESORB HG-11 gave a final stack concentration of Hg^{T} of $1.50 \mu\text{g}/\text{m}^3$, which corresponds to a 71% reduction. ESORB-HG-11 injection at 100 lb/hr gave Hg^{T} of $1.95 \mu\text{g}/\text{m}^3$, which corresponds to a 63% reduction.

In addition, there was a significant increase in Hg^{P} during injection of ESORB-HG-11. The increase was attributed to poor capture of ESORB-HG-11 by the scrubber. Improving the capture of Hg^{P} in the scrubber should provide a further decrease in the stack mercury emissions. From the total vapor phase mercury (Hg^{VT}) concentrations taken at ESORB-HG-11 injection rates of 150 lb/hr and 100 lb/hr, the respective stack concentrations were $0.83 \mu\text{g}/\text{m}^3$ and $1.40 \mu\text{g}/\text{m}^3$, which correspond to stack emissions reductions of 82% and 73%, respectively. This suggests that improving particulate capture in the scrubber would further improve the reduction of mercury emissions. Figure 33 summarizes the reductions discussed as well as the significant contributions from Hg^{P} .

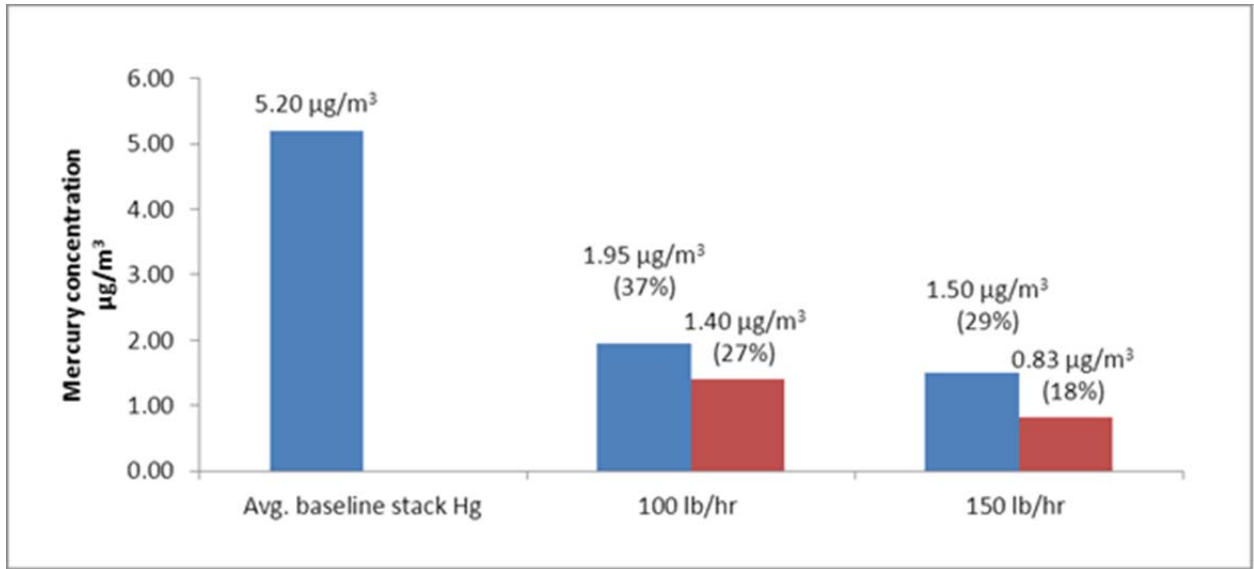


Figure 33. Potential reductions from ESORB-HG-11 as a function of long-term testing with injection rates of 100 lb/hr and 150 lb/hr.

CONCLUSION

Of all the additives tested, ESORB-HG-11 showed the greatest potential to attain target mercury reductions of 75% at injection rates of 100 to 150 lb/hr. The Hg^{VT} concentrations in the stack gases were $1.40 \mu\text{g}/\text{m}^3$ and $0.83 \mu\text{g}/\text{m}^3$ for 100 lb/hr and 150 lb/hr injection rates, respectively; compared to average baseline values of $5.20 \mu\text{g}/\text{m}^3$. However, Hg^{P} increased with injection of ESORB-HG-11, indicating that ESORB-HG-11 penetrates the scrubber. This resulted in Hg^{T} of $1.50 \mu\text{g}/\text{m}^3$ and $1.95 \mu\text{g}/\text{m}^3$ for 150 lb/hr and 100 lb/hr injection rates, respectively. Hg^{P} consists of mercury bound to ESORB-HG-11, a form which could be considered environmentally benign; however, additional research needs to be conducted for confirmation. The higher particulate mercury concentrations with sorbent injection decrease the potential mercury emission control effectiveness of the proposed technology. At an ESORB-HG-11 injection rate of 150 lb/hr, the emission reduction decreased from 84% to 70% and for the 100 lb/hr injection rate, the emission reduction decreased from 72% to 63%. Improved sorbent performance will require improved scrubber operation to increase particulate capture efficiencies.

Analysis of the scrubber slurry during testing showed significant decreases in dissolved mercury [Hg^{D}] during ESORB-HG-11 injection. These results point out the Hg^{D} sequestration capability of ESORB-HG-11. A majority of the injected ESORB-HG-11 that does not burn or coat the flue gas ducts gets captured by the scrubber waters and serves as an adsorbent for the dissolved mercury. This can be corroborated by the fact that ESORB-HG-11 was still present in the recirculation tank on days that were preceded by ESORB-HG-11 injection. As a result, Hg^{D} concentrations remained low for almost all test days except for days when the system had fully recovered (mainly occurring after a two-day weekend) and in the first week of testing. Consequently, use of ESORB-HG-11 for mercury capture ensures that recycling of scrubber waters does not increase the mercury released in the furnace and keeps stack emissions low by avoiding mercury build up in the system and through re-emission from the scrubber liquid.

REFERENCES

- Benson, S.A. *Controlling Mercury Emissions for Utilities Firing Lignites From North America*, Summary Report, 2007.
- Berndt, M. *Mercury and Mining in Minnesota*, Minerals Coordinating Committee, Department of Natural Resources (DNR), Minnesota, 2003.
- Berndt, M.; Engesser J.; Berquo, T.S. *Mercury Chemistry and Mossbauer Spectroscopy of Iron Oxides During Taconite Processing on Minnesota's Iron Range*, Department of Natural Resources (DNR), Minnesota, 2005.
- Berndt, M.; Engesser, J.; Johnson, A. *On the Distribution of Mercury in Taconite Plant Scrubber Systems*, Department of Natural Resources (DNR), Minnesota, 2003.
- Berndt, M.; Engesser, J. *Mercury Transport in Taconite Processing Facilities: (II) Fate of Mercury Captured by Wet Scrubbers*, Department of Natural Resources (DNR), Minnesota, 2005a.
- Berndt, M.; Engesser, J. *Mercury Transport in Taconite Processing Facilities: (II) Fate of Mercury Captured by Wet Scrubbers*, Department of Natural Resources (DNR), Minnesota, 2005b.
- Berndt, M.; Engesser, J. *Mercury Transport in Taconite Processing Facilities: (I) Release and Capture During Induration*, Department of Natural Resources (DNR), Minnesota, 2005a.
- Berndt, M. *On the Measurement of Stack Emissions at Taconite Processing Plants*, Department of Natural Resources (DNR), Minnesota, 2008.
- Galbreath, K.C. *Mercury Vaporization Characteristics of Taconite Pellets*, Final Report for the Minnesota Department of Natural Resources (Mn. DNR), 2005.
- Quality Assurance Project Plan*, prepared by the Minnesota Department of Natural Sources (Mn. DNR) August 2010

APPENDIX A: BENCH AND PILOT RESULTS

Bench Testing Summary

The bench scale tests consisted of dosing several 200 mL scrubber slurries, obtained from U.S. Steel Minntac Line 3, to a mercury concentration of 62.5 µg/L using mercuric chloride. A concentration of 62.5 µg/L was chosen based on mercury mass balance estimates from literature [Berndt and Engesser, 2005a and 2005b]. To each of these solutions, the additives were added on a mass basis following a low, mid and high level. Once added, the solutions were stirred for 10 minutes, an estimate of mercury residence time in the scrubber; filtered, and the filtrates submitted for mercury analyses. The resulting mercury concentrations provided an initial estimate for best loadings to be used in the pilot tests. See Figure A-1. From the bench tests, ESORB-HG-11 showed the best removal efficiencies for all the loadings tested. The other additives showed appreciable removal, too.

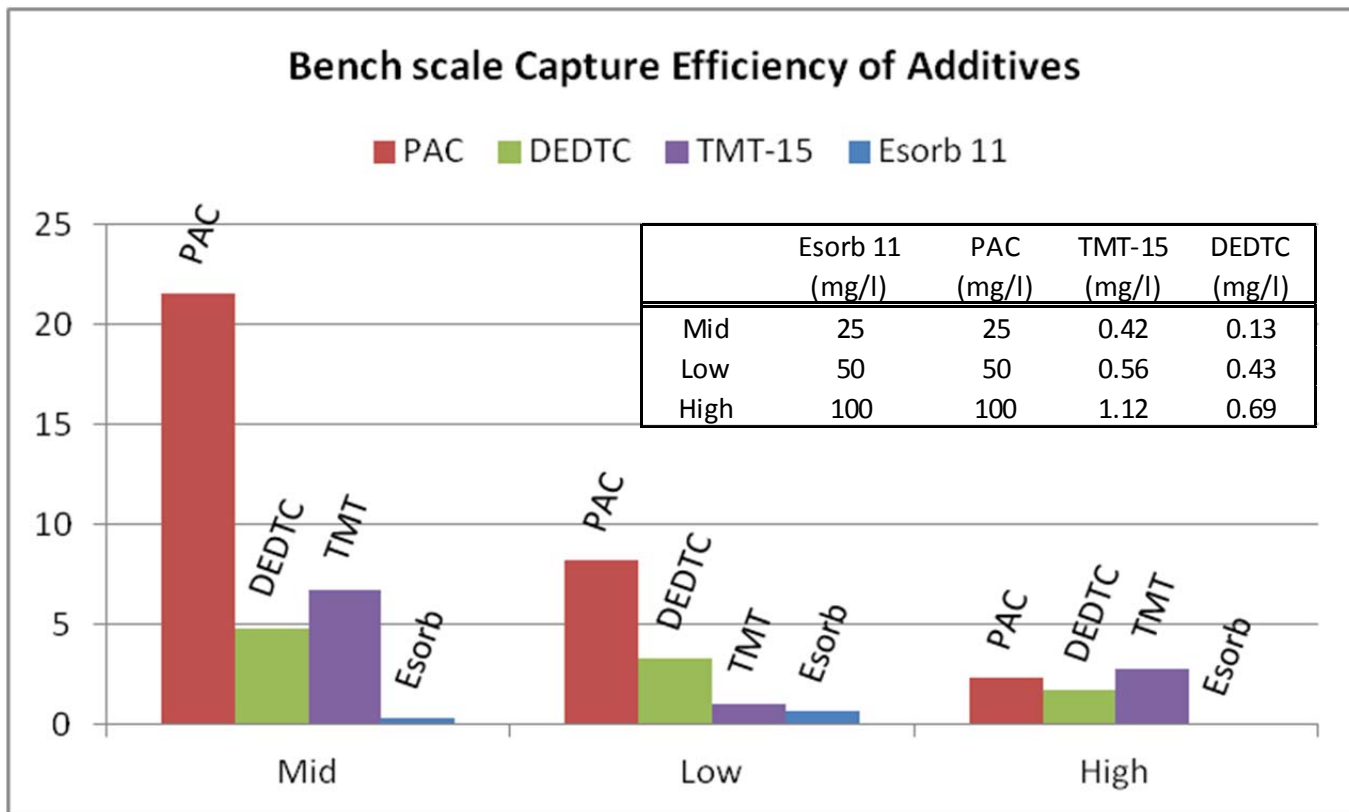


Figure A-1. Bench scale mercury test results for three levels of additive testing. Test involved spiking 200 mL of scrubber slurry with HgCl_2 to obtain a mercury concentration of $62.5 \mu\text{g/L}$. The four additives above were then added to solution and stirred for 10 minutes, filtered, and filtrate analyzed for Hg^{D} . Table in graph provides additive loading for the three levels analyzed. For ESORB-HG-11, 100 mg/L loading reduced mercury to non-detect levels. PAC, DEDTC and ESORB-HG-11 show increasing mercury capture with increase in loading, however, TMT-15 does not show any trend in mercury capture at loadings used.

Pilot Testing Summary

The pilot test consisted of a glass counter current scrubber with of a 30 L tank at the bottom and a 6 ft high scrubbing tower. The tank was connected to a diaphragm pump which circulated slurry from Minntac Line 3 through the scrubber when turned on. Flue gas generated from burning natural gas with a flow rate of approximately 40 L/min was used to simulate plant waste gas. The flue gas flowed through the scrubber from bottom to top with a sample obtained from sample ports at the top of the tower through two heated PFA (a substitute for Teflon™) tubes to a dual channel wet chemistry pre-treatment unit used to condition the sample gases before analysis by Cold Vapor Atomic Absorption Spectroscopy (CVAAS) in a dual channel Horiba DM-6B Continuous Mercury Monitor (CMM). Once the baseline mercury concentration was steady (region A in Figures A-2 to A-5), the flue gas was then spiked continuously with mercuric chloride generated using certified Dynacal permeation tubes and a constant temperature chamber called a Dynacalibrator, both manufactured by VICI Metronics; until a new steady state concentration was obtained (region B). The pump was then turned on with scrubber slurry from U.S.

Steel Minntac line 3 in the scrubber tank to obtain a new steady mercury concentration in the flue gas (region C). Once steady, the additive to be tested was added to the scrubber tank by dosing up to a concentration based on the bench tests. The mercury concentration in the scrubbed flue gas was then monitored. Each additive was tested twice. From the results obtained from testing all four additives, Figures B-2 to B-5, ESORB-HG-11 tested at a scrubber slurry concentration of 200 mg/L, was seen to be the most effective additive in the capture and sequestration of mercury for both tests carried out (Figure A-2). For the first test, a steady mercury concentration of approximately $20 \mu\text{g}/\text{m}^3$ was attained during mercury injection and slurry operation for both regions B and C, meanwhile, test 2 showed an increase in the Hg^{T} steady state value from region B to C, followed by a third increase in region C only. However, addition of ESORB-HG-11 led to a gradual decrease of 75% and 68% for tests 1 and 2 respectively. ESORB-HG-11 also showed lowest final Hg^{T} concentration for both tests, confirming it is the most effective additive for sequestration.

For the PAC test, Figure A-3, both tests showed an increase in mercury baseline when scrubbing started (region C). In the first test, PAC concentration in the scrubber slurry was initially 100 mg/L but very little reduction was observed (D'). It was then increased to 200mg/L and a 39% drop was observed. For the second test, a drop of 53% was observed.

Diethyl dithiocarbamate (DEDTC) also showed an increase in mercury baseline when scrubbing started (region C of Figure A-4). DEDTC concentration for the first test was 1.1 mg/L, had a higher steady state concentration of mercury and a final reduction of 46% when DEDTC. Test 2 showed a reduction of just 31% after using a higher DEDTC concentration of 2.2 mg/L.

Tests using TMT-15 used concentrations 10 and 20 mg/L, Figure A-5. During the first test (10 mg/L), a decrease in steady state mercury concentration was observed (region C). This was the only test that showed this behavior and the possible cause is unknown. However, Test 1 showed decreases in mercury concentration of 58%. Test 2 did show a lower reduction potential for TMT-15 of 36%, even though the concentration of TMT-15 was increased from 10 to 20 mg/L.

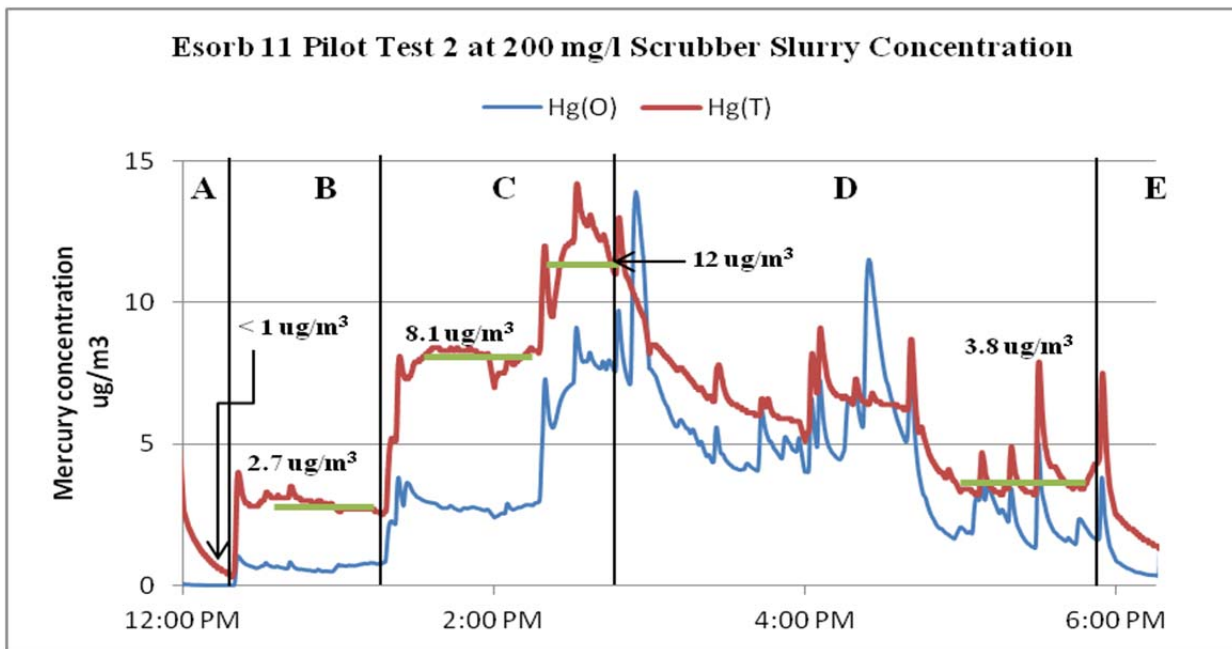
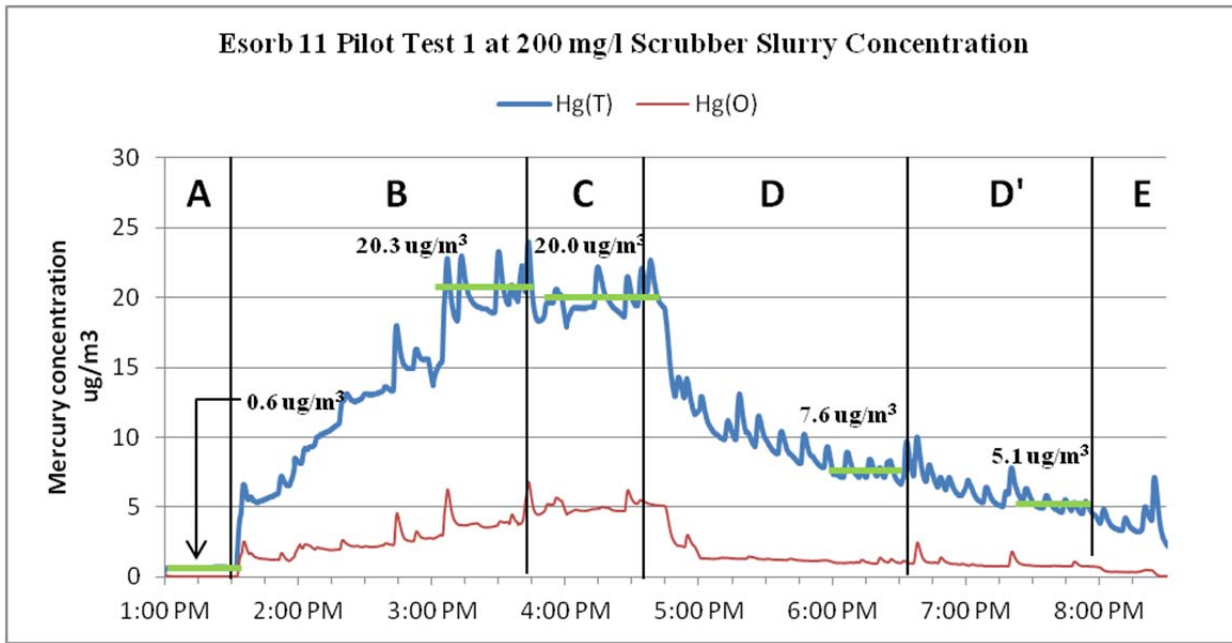


Figure A-2. Pilot scale test results when testing ESORB-HG-11 at 200 mg/L in scrubber slurry. Region A is scrubber baseline mercury concentration; B injection of mercuric chloride into scrubber flue gas until steady state; region C, scrubbing using line 3 slurry; D addition of ESORB-HG-11 by dosing the slurry to a concentration of 100 mg/L for test 1 and 200 mg/L for test 2; D' for test 1 only, increased ESORB-HG-11 concentration in slurry from 100mg/L to 200 mg/L; E Injection of mercury stopped.

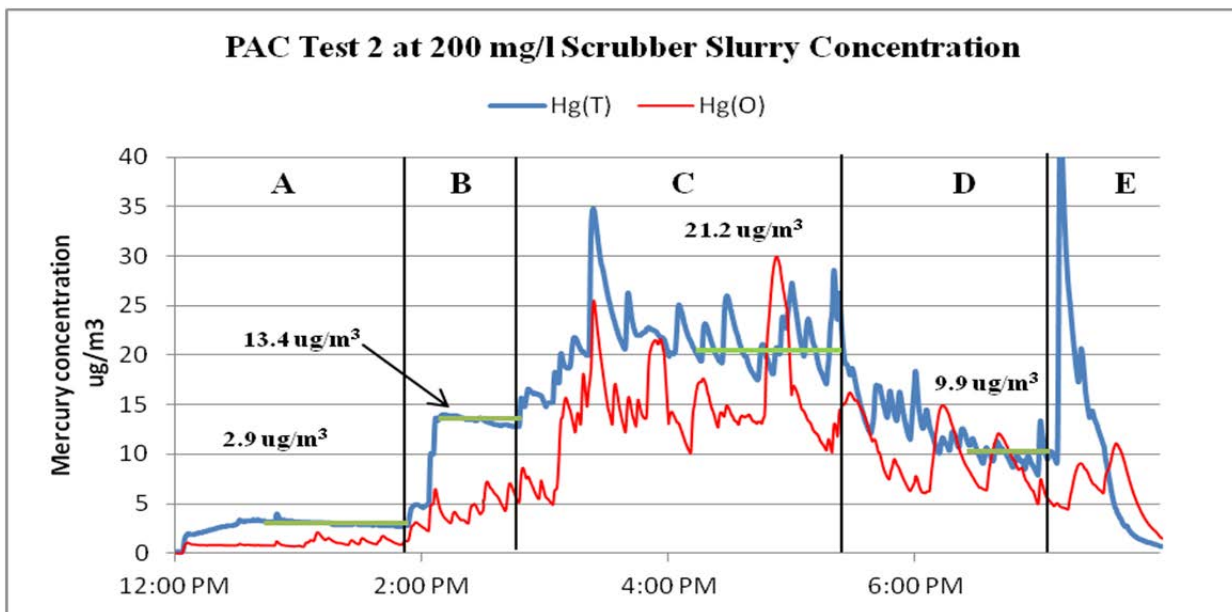
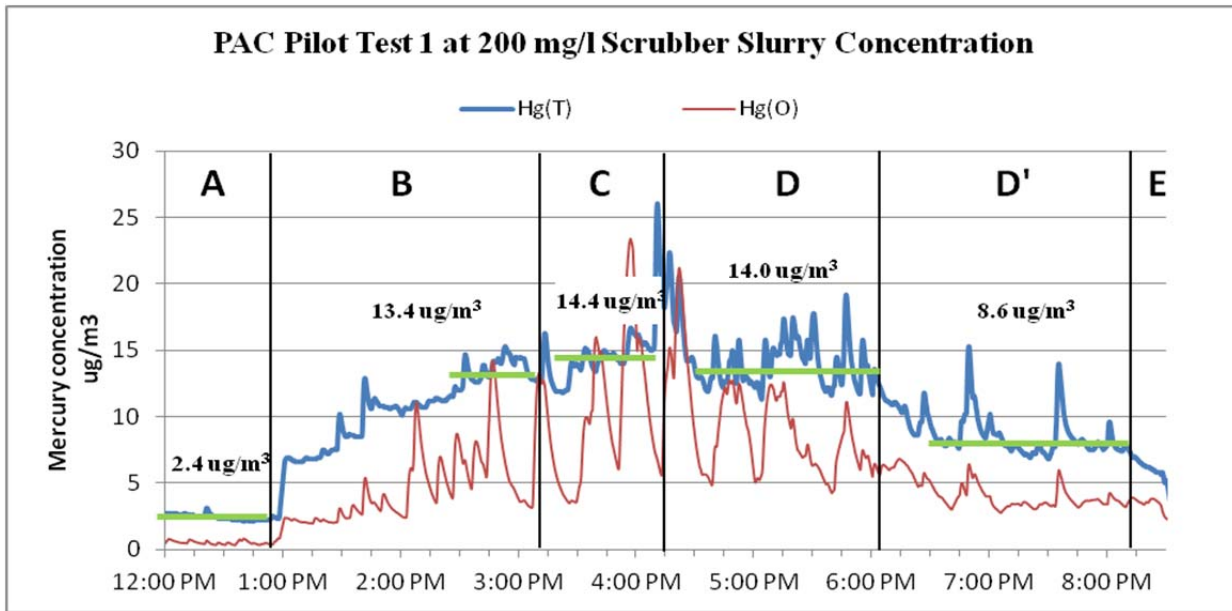


Figure A-3. showing two pilot scale test results when testing PAC at 200 mg/L in scrubber slurry. Region A is scrubber baseline mercury concentration; B injection of mercuric chloride into scrubber flue gas until steady state; region C, scrubbing using line 3 slurry; D addition of PAC by dosing the slurry to a concentration of 100 mg/L for test 1 and 200 mg/L for test 2; D' for test 1 only, increased PAC concentration in slurry from 100mg/L to 200 mg/L; E Injection of mercury stopped.

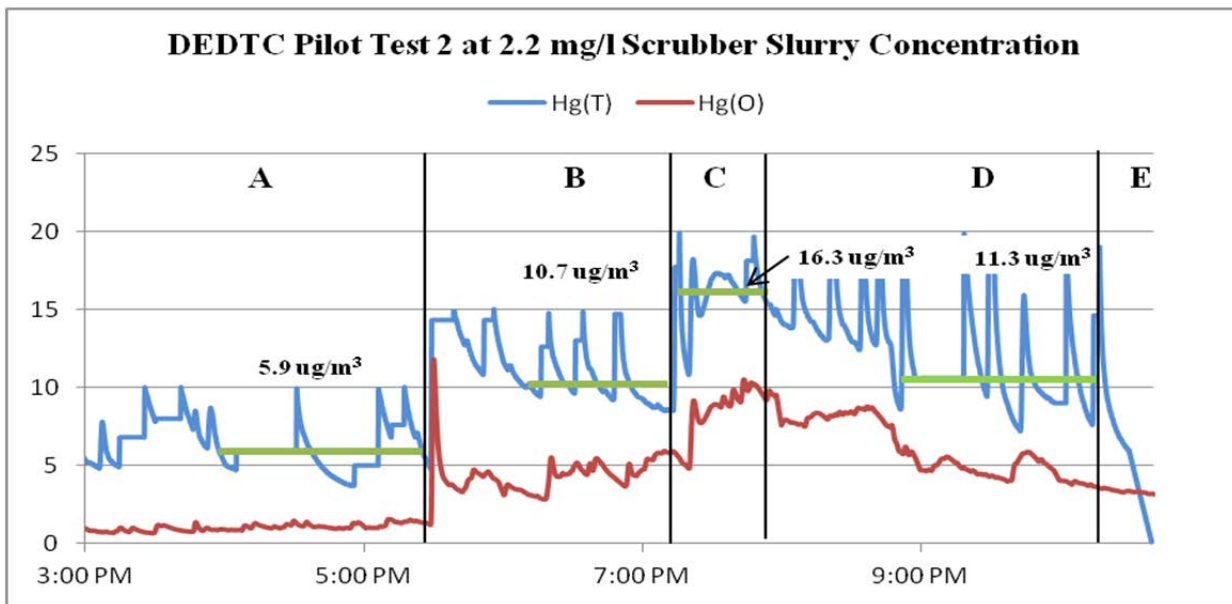
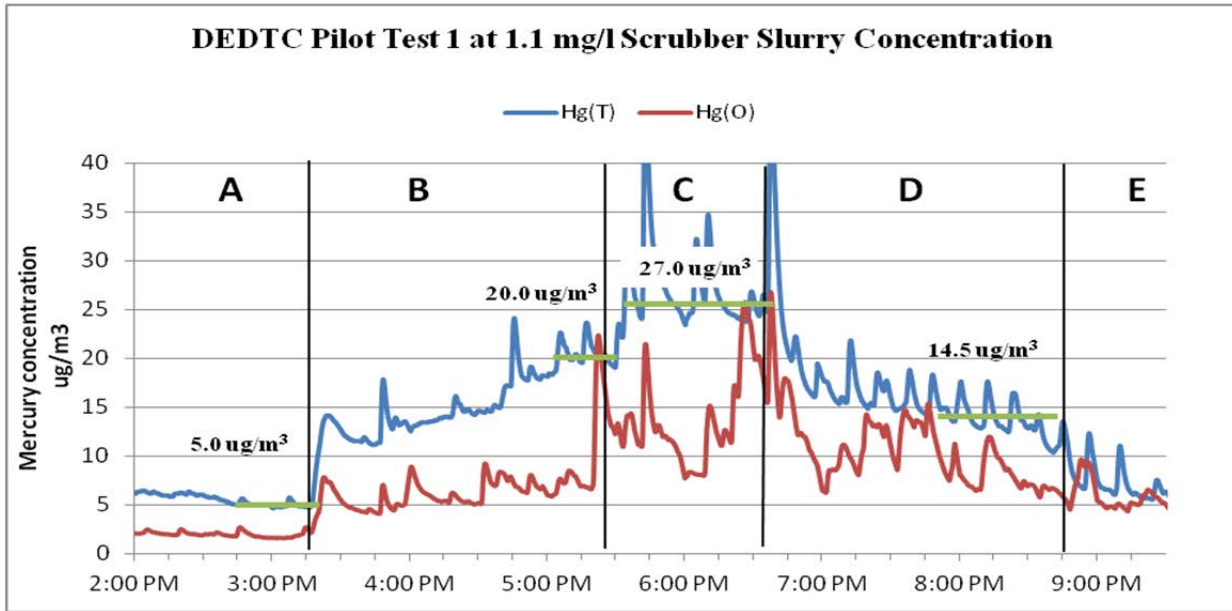


Figure A-4. Pilot scale test results when testing DEDTC at 1.1 and 2.2 mg/L in scrubber slurry. Region A is scrubber baseline mercury concentration; B injection of mercuric chloride into scrubber flue gas until steady state; region C, scrubbing using line 3 slurry started; D addition of DEDTC by dosing the slurry to a concentration of 1.1 or 2.2 mg/L; E Injection of mercury stopped.

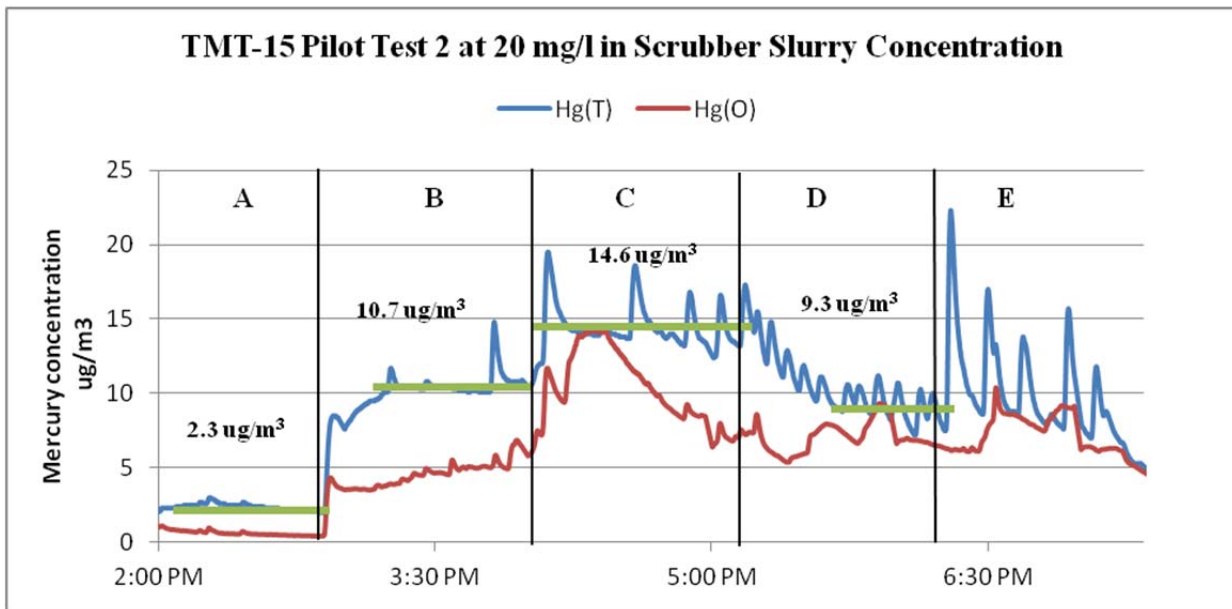
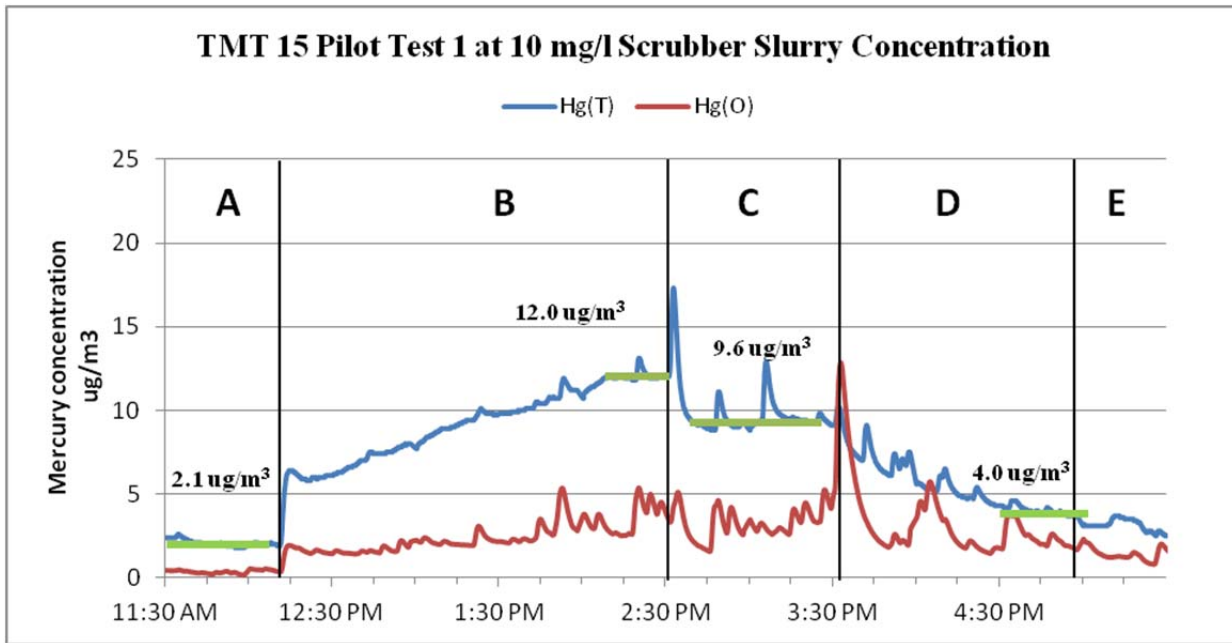


Figure A-5. Pilot scale test results when testing TMT 15 at 10 and 20 mg/L in scrubber slurry. Region A is scrubber baseline mercury concentration; B injection of mercuric chloride into scrubber flue gas until steady state; region C, scrubbing using line 3 slurry started; D addition of TMT-15 by dosing the slurry to a concentration of 10 or 20 mg/L; E Injection of mercury stopped.

APPENDIX B – ADDITIONAL FIELD DATA

Table B-1. OHM raw data for all test days.

DATE	Run	Hg ²⁺ (µg/m ³)	Hg ⁰ (µg/m ³)	Hg ^{VT} (µg/m ³)	Hg ^P (µg/m ³)	Hg ^T (µg/m ³)
20111013**	Baseline 1	0.75	3.70	4.45	n/a	4.45
	Baseline 2	0.95	3.98	4.93	n/a	4.93
	Baseline 3	0.55	4.64	5.19	0.00	5.19
20111014**	Baseline	0.83	5.86	6.69	n/a	6.69
	100lb/hr ESORB-HG-11	0.49	2.36	2.85	0.13	2.98
20111017	Baseline***	2.40	5.82	8.22	0.02	8.24
	50 lb/hr ESORB-HG-11	0.45	1.71	2.16	0.06	2.22
	150 lb/hr ESORB-HG-11	0.08	1.14	1.22	0.59	1.81
20111018	Baseline	0.82	5.35	6.17	0.03	6.20
	100 lb/hr ESORB-HG-11	0.37	1.40	1.77	0.33	2.10
	100 lb/hr ESORB-HG-11	0.33	1.07	1.4	0.55	1.95
20111019	Baseline	0.23	4.63	4.86	0.07	4.93
	DEDTC at 7 mg/l	0.31	3.90	4.21	0.03	4.24
	50 lb/hr ESORB-HG-11	0.24	2.09	2.33	0.27	2.60
20111020	Baseline	0.30	3.14	3.44	0.03	3.47
	100 lb/hr PAC	0.24	2.51	2.75	0.03	2.78
	150 lb/hr PAC	0.26	2.31	2.57	0.04	2.61
20111021	Baseline	0.54	4.5	5.04	0.02	5.06
	150 lb/hr ESORB-HG-11	0.22	0.61	0.83	0.67	1.50
20111024	Baseline	0.60	4.38	4.98	0.08	5.06
	75 lb/hr ESORB-HG-11	0.30	1.91	2.21	0.77	2.98
	75 lb/hr ESORB-HG-11	0.21	1.5	1.71	0.99	2.70
20111025	Baseline	0.46	3.35	3.81	0.20	4.01
	75 lb/hr ESORB-HG-11	0.27	1.91	2.18	0.60	2.78
20111026	Baseline	0.25	3.84	4.09	0.10	4.19
	75 lb/hr ESORB-HG-11	0.40	1.65	2.05	1.09	3.14

* Under local O2 concentration, dry basis.

** Hg(P) is for entire test period.

*** Hg(2+) is unusually high.

Table B-2. Multiclone Hg(P) concentration. No samples were collected on the 14th because sampling location inaccessible. NA refers to sample collection periods where no significant samples were collected from scrubber blowdown dust.

Date collected	Time collected	Hg(P) ng/g
10/14/2011	No Samples Collected	
	1:00 PM	139
10/17/2011	4:00 PM	82
	6:00 PM	42
	9:50 AM	NA
10/18/2011	2:40 PM	212
	5:30 PM	NA
	10:30 AM	45
10/19/2011	2:30 PM	15
	4:10 PM	26
	5:55 PM	90
	8:50 AM	90
10/20/2011	12:20 PM	NA
	2:00 PM	182
	4:20 PM	451
10/21/2011	11:15 AM	65
	4:05 PM	86
	10:00 AM	47
10/24/2011	12:45 PM	NA
	3:30 PM	40

Table B-3. OHM results and CMM concentrations during the same time period.

Date	Time	Loading	OHM	CMM		OHM	CMM	
			Hg ⁰ (µg/m ³)	Hg ⁰ (µg/m ³)	Std Dev	Hg ^{VT} (µg/m ³)	Hg ^{VT} (µg/m ³)	Std Dev
20111026	8:15am to 9:20am	Baseline	3.84	4.03	0.37	4.09	4.55	0.30
	4:15pm to 5:15pm	100 lb/hr-ESORB-HG-11	1.65	1.81	0.21	2.05	2.3	0.3
20111025	8:15am to 9:15am	Baseline	3.35	3.11	0.29	3.81	4.39	0.39
	2:05pm to 3:10pm	75 lb/hr-ESORB-HG-11	1.91	1.57	0.07	2.18	2.30	0.11
20111024	8:50am to 10:08am	Baseline	4.38	3.56	0.16	4.98	5.11	0.41
	12:00pm to 1:00pm	75 lb/hr-ESORB-HG-11	1.91	1.26	0.08	2.21	2.11	0.08
	2:30pm to 3:35pm	75 lb/hr-ESORB-HG-11	1.5	1.16	0.04	1.71	2.05	0.13
20111021	10:55am to 11:58am	Baseline	4.50	3.12	0.50	5.04	3.96	0.13
	4:00pm to 5:08pm	150 lb/hr-ESORB-HG-11	0.61	0.33	0.05	0.83	0.61	0.07
20111020	9:50am to 11:00am	Baseline	3.14	1.56	0.14	3.44	2.11	0.38
	1:25pm to 2:25pm	100 lb/hr-PAC	2.51	1.48	0.07	2.75	1.97	0.15
	3:50pm to 5:10pm	150 lb/hr-PAC	2.31	1.23	0.26	2.57	1.68	0.42
20111019	10:15am to 11:20am	Baseline	4.63	4.08	0.13	4.86	5.19	0.15
	3:20pm to 4:20pm	7 mg/l-DEDTC	3.9	2.68	0.27	4.21	4.29	0.28
	6:00pm to 7:20pm	50 lb/hr-ESORB-HG-11	2.09	1.68	0.11	2.33	2.43	0.12
20111018	8:30am to 9:50am	Baseline	5.35	n/a	n/a	6.17	n/a	n/a
	2:15pm to 3:40pm	100 lb/hr-ESORB-HG-11	1.4	1.22	0.15	1.77	1.53	0.11
	4:40pm to 5:45pm	100 lb/hr-ESORB-HG-11	1.07	0.80	0.10	1.4	1.15	0.14
20111017	8:50am to 10:10am	Baseline	5.82	5.12	0.30	8.22	7.08	0.88
	12:10pm to 1:40pm	50 lb/hr-ESORB-HG-11	1.71	2.12	0.16	2.16	2.93	0.21
	5:50pm to 7:20pm	150 lb/hr-ESORB-HG-11	1.14	0.53	0.06	1.22	1.07	0.29
20111014	9:10am to 10:25am	Baseline	5.86	4.26	0.10	6.69	5.65	0.08
	6:40pm to 7:50pm	100 lb/hr-ESORB-HG-11	2.36	1.16	0.25	2.85	1.98	0.57
20111013	12:00am to 1:20pm	Baseline 1	3.70	2.32	0.26	4.45	4.24	0.41
	2:30pm to 3:50pm	Baseline 2	3.98	2.58	0.13	4.93	3.88	0.30
	5:00pm to 6:20pm	Baseline 3	4.64	2.78	0.08	5.19	4.1	0.32

Table B-4. Scrubber slurry sample analysis results.

Date	Time collected	Hg ^D ng/L	TSS (%)	Comments	
10/13/2011	6:00 PM	5000	NA*	Replicate	
	6:00 PM	5000	NA*		
10/14/2011	10:05 AM	1100	0.68	Hg ^D below MDL	
	8:20 PM	< 200	0.68		
10/17/2011	9:35 AM	< 200	ND**	Blank, Hg ^D below MDL	
	9:45 AM	600	0.67		
	12:45 PM	NA	0.58		
	3:55 PM	NA	0.64		
	6:20 PM	< 200	0.59		
10/18/2011	10:00 AM	< 200	ND**	Blank, Hg ^D below MDL	
	10:00 AM	600	0.88		
	2:40 PM	45	0.65		
	5:10 PM	NA*	0.75		
10/19/2011	11:05 AM	907	0.39		
	2:00 PM	1750	0.78		
	3:55 PM	2140	0.99		
	6:20 PM	45	1.04		
10/20/2011	9:05 AM	< 200	0.76	Hg ^D below MDL	
	12:10 PM	NA*	0.65		
	2:05 AM	25.7	0.69		
	2:15 PM	24.6	ND**		Duplicate
	4:30 PM	17.1	0.67		
10/21/2011	11:10 AM	NA*	ND**	Blank	
	11:10 AM	82	0.59		
	4:15 PM	21.1	0.36		
10/24/2011	9:30 AM	3970	0.77	Blank	
	12:25 PM	NA*	0.64		
	3:15 PM	NA*	ND**		
	3:15 PM	599	0.80		

*Not analyzed. For 10/13/2011, TSS was not determined. For all other days, due to large volume of samples collected, only samples deemed necessary submitted for analysis. Necessity determined by collection period, steady state of CMM measurements, and injection condition.

**Not determined because either not applicable (blanks) or required samples not analyzed.

Appendix B-2-3

Mercury Control for Taconite Plants Using Gas-Phase Brominated Sorbents

July 9, 2012



Mercury Control for Taconite Plants Using Gas-Phase Brominated Sorbents

Final Report

**CFMS Contract No. B50921
T-Number 1029E**

Prepared by J. Miller, M. Zerangue, Z. Tang and R. Landreth

Edited by R. Landreth

7/9/2012

Table of Contents

1. Abstract	3
2. Project Purpose	4
3. Project Scope	4
4. Hibbing Taconite Process Description	5
5. Experimental	7
a. Albemarle Mobile Demonstration Unit	
b. Sorbent Distribution and lance System	
c. Mercury Monitors	
d. Solid Sample Mercury Analysis	
e. Water Sample Mercury Analysis	
f. LOI Analysis	
g. Hg Removal Calculation Method	
6. Field Trial Test Plan – Final	18
a. Baseline Measurements	
b. Parametric Testing	
c. Continuous Run	
d. Schedule	
7. Results and Discussion	20
a. Pre-Trial Testing	
b. Baseline Measurements	
c. Parametric Testing	
d. Continuous Run	
e. Green Ball Analysis	
f. Multiclone Dust Analysis	
g. Scrubber Water Analysis	
8. Summary and Conclusions	43
9. Recommendations	44
10. References	45
11. Appendices	46

Abstract

In 2011, Albemarle Environmental Division personnel conducted a field trial at Hibbing Taconite to demonstrate the effectiveness of gas-phase brominated sorbents in controlling mercury emissions from taconite facilities. There was a preliminary site visit in March 2011 followed by pre-trial testing in early June 2011. The pre-trial testing determined that the mercury sorbent would have to be injected into both the Windox Exhaust flue gas stream and the Hood Exhaust flue gas stream in order to achieve the desired result of 75% mercury removal from the baseline condition.

The equipment was prepared for the trial and the demonstration conducted in September and October 2011. The parametric testing demonstrated that the 75% Hg removal target could be achieved with a gas-phase brominated sorbent injection rate of about 3 lb/MMacf (126 lb/hr). It was demonstrated in a two-week long continuous injection run that this removal rate could be achieved over time. This injection rate is higher than expected to achieve the 75% mercury removal but it does not appear to be a problem of the control technique. Rather, the sorbent distribution was sub-optimal due to project limitations. The better the sorbent distribution, the better the mercury removal results.

Grab samples of green balls, multiclone dust and scrubber water were taken to identify any trends. The green ball mercury content averaged about 15 ng/g and varied randomly by nearly a factor of two from high to low concentration measured. Sorbent was injected before the multiclone and there was a concern that some sorbent would be captured there and decrease the overall Hg removal rate. It was discovered that some sorbent was captured by the multiclone but that its impact on the mercury removal rate was probably small. The Hg content of the scrubber water did not increase during the trial and varied between the high and low levels observed in the baseline testing. Filtering the scrubber water greatly reduced the mercury content since the sorbent contained in the scrubber solids still had Hg capacity.

Project Purpose

The purpose of this effort is to demonstrate that the Minnesota Department of Natural Resources (MN DNR) goal of reducing taconite flue gas mercury emissions by 75% from current levels can be achieved by the use of gas-phase brominated mercury sorbents. Gas-phase brominated sorbents have been proven very effective in mercury capture in similar applications.

Project Scope

In order to achieve this task, Albemarle Environmental Division conducted a six-task trial. Task 1 was the preliminary site visit to Hibbing Taconite, which was conducted on March 1, 2011. Hibbing Taconite was selected by the MN DNR as the host for the trial. Task 2 involved pre-trial testing, which was conducted at Hibbing Taconite between May 30 and June 4, 2011. Pre-trial testing determined the sources of Hg generation, as well as the sorbent injection and Hg measurement locations.

Task 3 of the project was for equipment preparation while Task 4 was the field trial, which began on 9/13/2011 and ended on 10/22/2011. Task 5 was the analysis of the samples and data collected during the field trial while Task 6 was final report preparation.

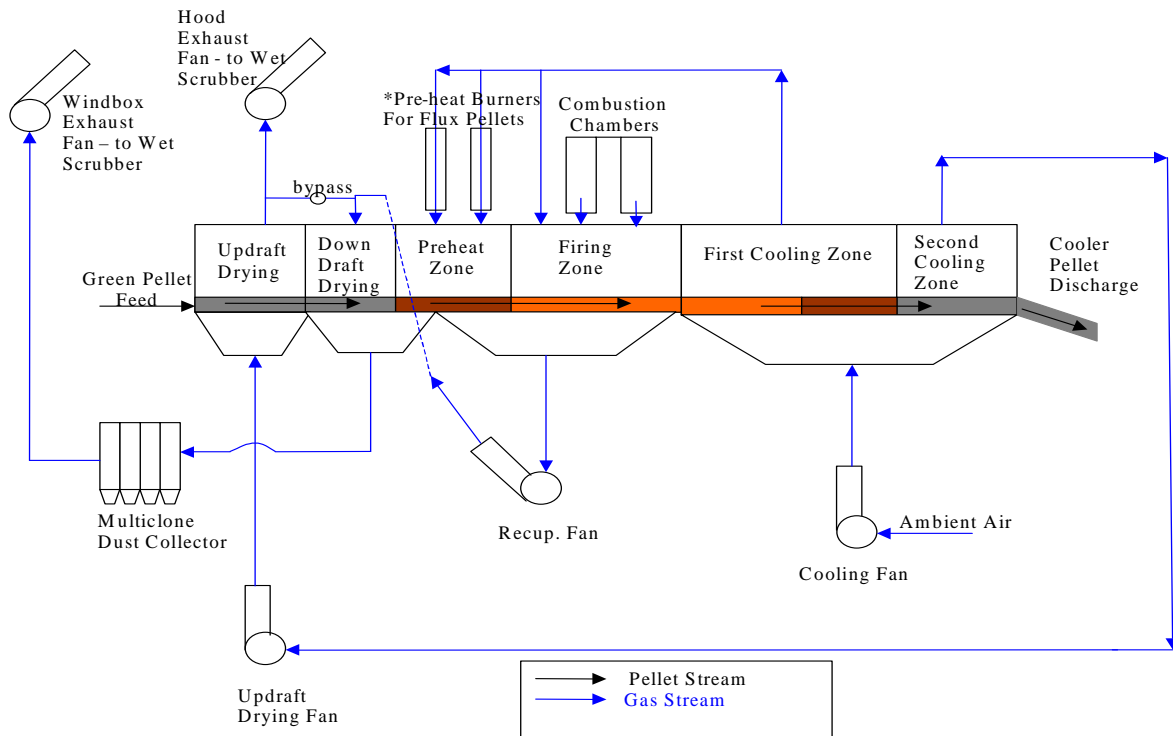
Hibbing Taconite Process Description

Hibbing Taconite, located near Hibbing, MN, fires greenballs made of taconite in straight-grate furnaces. Large combustion chambers firing natural gas, located in the center of each furnace, provide heat to pellets that move past the firing zone on a large grate. Outside air, heated as it cools the fired pellets in the second cooling zone, dries and heats fresh greenballs in the up-draft drying zone. Meanwhile, air introduced in the combustion chambers and/or in the first cooling zone passes through the pellet bed in the firing and preheat zones, and then again in the down-draft drying zone. Operation in this manner provides for thermal efficiency.

The drying, heating, and firing procedures are all performed on the grate in a straight-grate facility, however, a “hearth layer” consisting of pre-fired pellets is added beneath fresh greenballs to protect the grate from the intense heat used in the firing zones.

A schematic of the Hibbing Taconite pellet firing equipment is shown in Figure 1.

Figure 1. Diagram of the Hibbing Taconite Pellet Firing Equipment



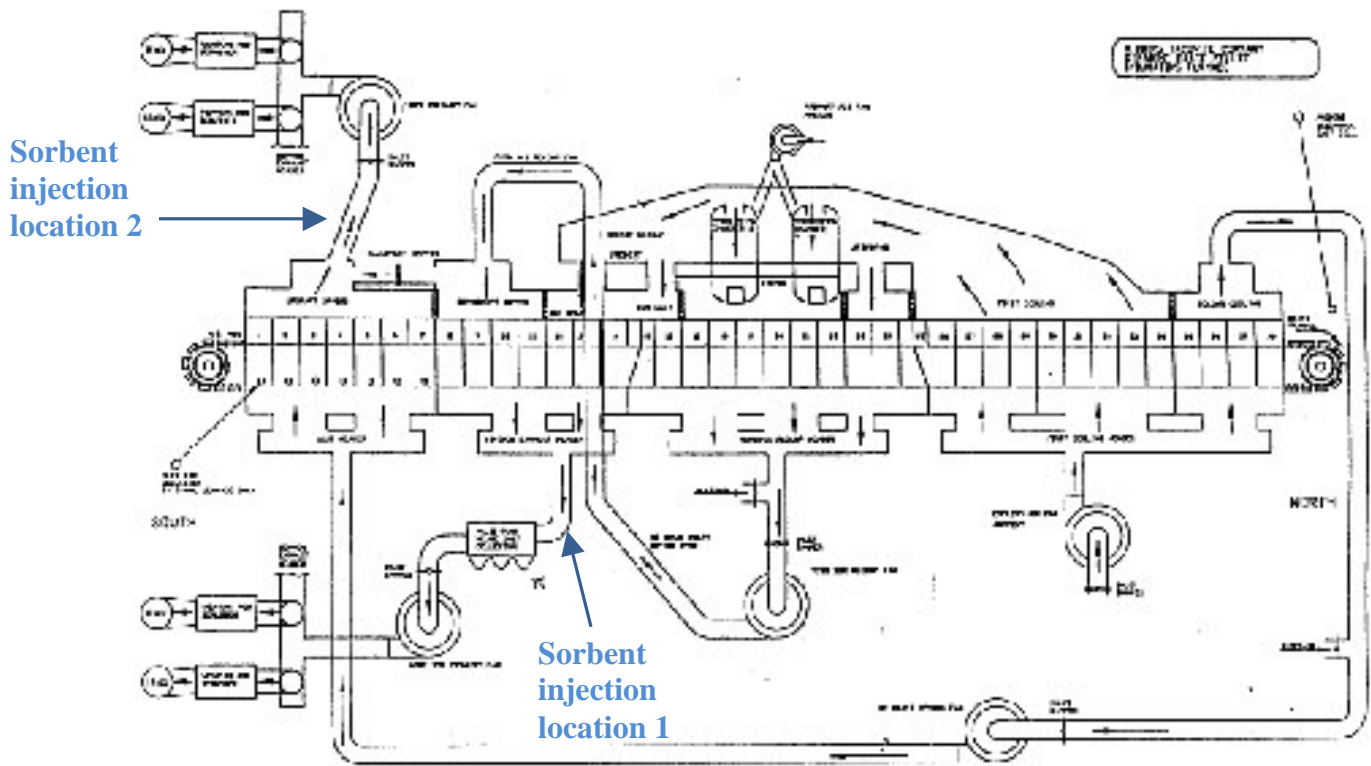
The furnace has two flue gas streams (Windbox and Hood Exhaust). Four single-pass scrubbers connected by a common duct are used for particulate control. The flue gas flow through each stack is 350-400 KSCFM.

Production Line 1 was used for this demonstration test. Injection ports were installed upstream and downstream of the multiclones in the Windbox Exhaust ductwork prior to the test since it was unclear which location would provide the best results. Unfortunately, it was discovered during equipment set up that the ports after the multiclones in the Windbox Exhaust ductwork were not usable due to obstructions in the ductwork. Therefore, only the injection ports upstream of the multiclone were utilized.

The injection locations in the Hood Exhaust ductwork were more straight forward to define.

The injection locations used during the trial are shown in Figure 2.

Figure 2. Sorbent Injection Locations

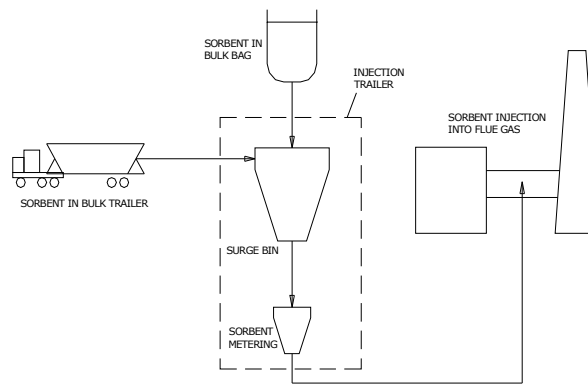


Experimental

Albemarle Mobile Demonstration Unit

The sorbent injection system design took into consideration both the desires of our host sites and the Albemarle's Environmental Division previous full-scale mercury testing experience. Customer sites typically have space constraints. Thus, the testing design incorporated the use of pneumatic tankers for the storage of large quantities of sorbent. The difficulty of building an injection system on site had been clearly demonstrated in the previous full-scale tests at other locations. The need for gravimetric control rather than volumetric control had also been demonstrated. The injection system was design to fit inside a trailer and be fully mobile. A diagram of the mobile demonstration unit appears in Figure 3.

Figure 3. Diagram of the Mobile Demonstration Unit



The functions of the sorbent injection system are as follows:

1. To provide for sorbent loading to a day storage hopper from either super sacks or pneumatic trucks.
2. To deliver the sorbent from the day storage hopper to a feeder system hopper.
3. To gravimetrically feed sorbent at selected rates into an eductor injection system.
4. To provide dilute phase conveying of the sorbent through the sorbent distributor and to the injection lances.

The day storage hopper, feeder hopper, gravimetric feeder and eductor are all enclosed in a trailer. A bin vent filter is provided to capture any dust generated by material handling. This filter is located on top of the day hopper. Blowers are used to provide the air flow necessary to convey the sorbent from a tanker to the

day storage hopper and to convey the sorbent from the feeder to the injection lances. The first of these blowers is located outside of the trailer while the other is located inside. All controls for the operation of the injection system are in an isolated area within the trailer. The injection trailer is shown in below in Photograph 1.

Photograph 1. Albemarle Mobile Demonstration Unit



The injection system has a PLC based control system, which controls all of the injection system operations. The control system monitors the amount of sorbent in the feeder system hopper and activates the screw feed system associated with the day storage hopper to provide refills as necessary. The control system can also refill the day storage hopper from the tanker.

The injection system was designed with the ease of installation and disassembly in mind. Only electricity and injection ports are required by the host site to support its operation.

The injection system was designed to have a sorbent injection rate range from as low as 15 lb/hr to a high of over 500 lb/hr. This range was selected in order to be able to provide testing at a variety of size systems and applications. For tests requiring a significant amount of sorbent, as was this one, the sorbent is provided by tanker truck. Only the plain powdered activated carbon (PAC) was fed to the day hopper from a super sack.

Sorbent Distribution and Lance System

The sorbent distribution and lance system designed for the Hibbing Taconite trial was based on injection into multiple ducts using a single sorbent feeder and a pneumatic conveyance system. Each of the ducts had multiple injection locations and two injection lances at each injection location. The control of material flow to the multiple injection lances was controlled by orifices.

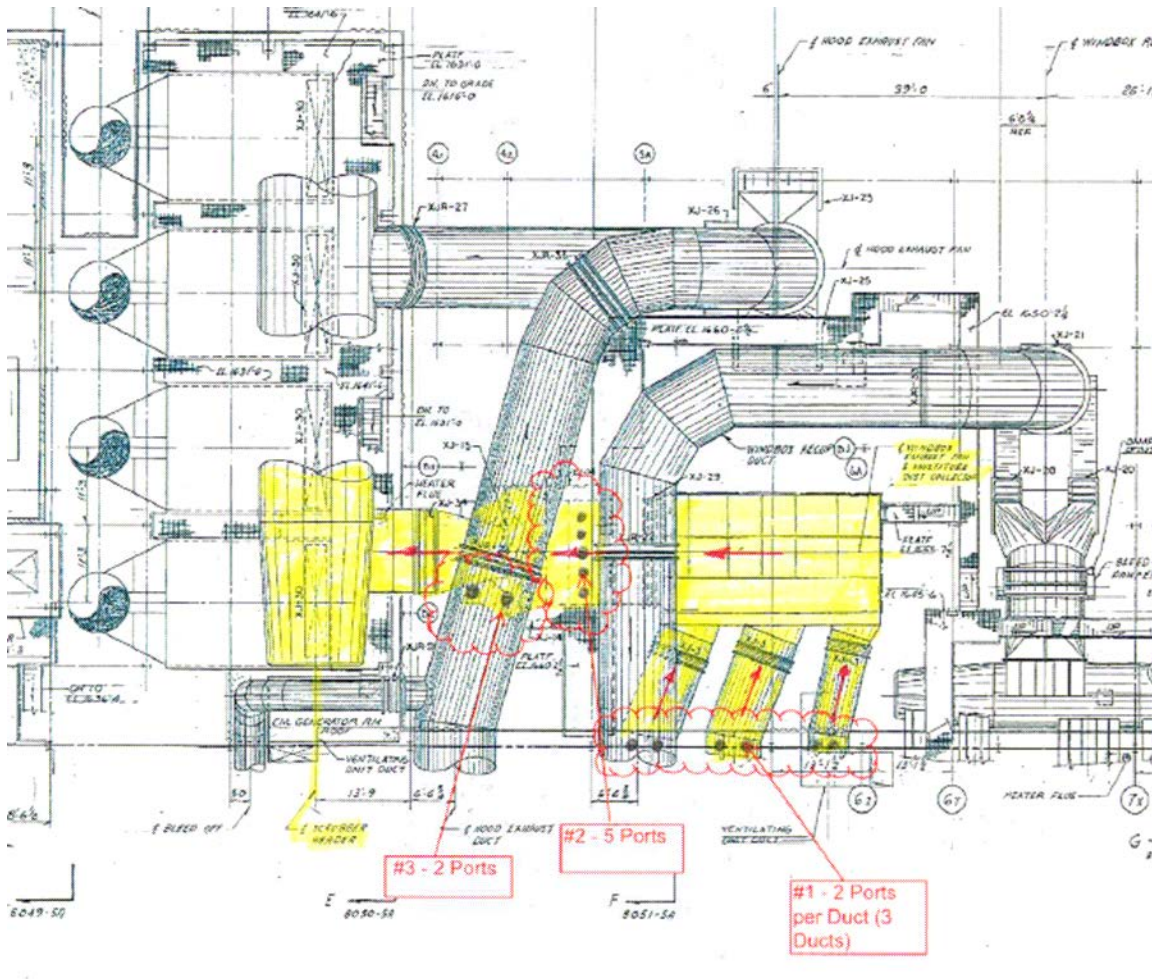
The injection lances are incorporated into injection modules, which bolt onto 4" flanged injection ports. Each injection port establishes an injection point in the exhaust gas. Two (2) lance testing modules were used at Hibbing Taconite. Testing modules are intended for short term applications but are designed with the same features as Albemarle's permanent injection modules. The main features of these systems are:

1. Multiple lances per injection module.
2. An orifice for each lance to control sorbent flow to the lance.
3. One port for each lance to allow installation of a PACFlow™ flow measurement probe.
4. Modules installed in series across a duct with spool pieces creating a manifold.
5. An inlet wye, two 180° bends, and connecting lines to create an equalization loop which delivers the sorbent to lances through the manifold.

In most applications Albemarle uses its proprietary X-a-Lance™ technology to increase the distribution of sorbent in the treated gas. The X-a-Lance™ design is an open ended, non-plugging lance design which uses specially designed exit holes to increase the dispersion of sorbent particles within the gas stream. The injection modules at Hibbing Taconite were equipped with X-a-Lances™.

Sorbent injection locations at three different areas on the furnace exhaust ducts were used at Hibbing Taconite as shown in Figure 4. Location #1 is on the Windbox Exhaust ducts immediately downstream of the furnace windbox. At this location three (3) ducts carry the hot gas and two (2) injection points per duct are identified. Each of these six (6) points is supplied with four (4) inch ports into which two (2) injection lances of different lengths are inserted. Therefore, at injection Location #1, twelve (12) injection lances deliver sorbent into the gas stream.

Figure 4. Injection Locations



Location #2 is on the Windbox Exhaust duct also but on the outlet of the multiclone particulate collection device. This device is designed to collect larger particles of iron compounds but should not remove particles of sorbent, which have a d50 particle size of 20 µm. However, due to the uncertainty of sorbent removal in the multiclone collector, injection Location #2 was designed as an alternative to Location #1. At Location #2, five (5) injection ports, or points, were designed and spaced across the duct perpendicular to the gas flow. Each of these ports is designed for two (2) injection lances of different lengths.

Unfortunately, during the lance installation period it was discovered that turning vanes exist inside the duct at Location #2, which was not known and did not appear on the drawings. Therefore Location #2 could not be used for sorbent injection testing.

Location #3 is on the Hood Exhaust duct after the duct exits the building but before the ID fan. At this location two (2) injection ports were installed in the ductwork and each port was designed to receive two (2) injection lances.

Due to plant outage scheduling constraints, the injection ports at Hibbing Taconite were chosen and installed before the pre-trial testing was conducted. At the time of the injection location design, it was believed that little mercury would be present in the Hood Exhaust gas. The reasoning was that the low temperature of 550° F present in the Hood Exhaust would not be expected to cause mercury to release from the green balls. Therefore, only two sorbent injection points were designed for the Hood Exhaust duct. However, the data gathered in the pre-trial testing proved the assumption concerning the mercury release from the green balls was incorrect in that more than 25% of the total gas phase mercury was in the Hood Exhaust gas. Unfortunately, it was not possible to put more injection points into the Hood Exhaust duct after the pretrial testing, so the control testing was performed with just two injection points in the hood exhaust duct.

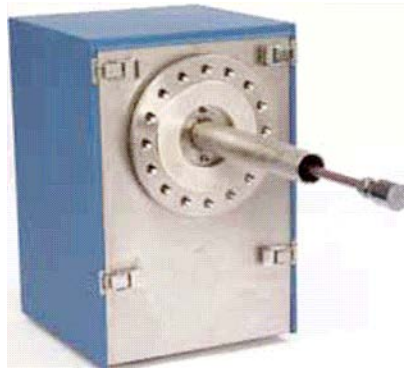
Additionally, due to ductwork constraints, the orientation of the installed injection ports on the hood exhaust duct was suboptimal. Both of the injection ports were installed on the centerline of the duct instead of across the duct as was done on all other ducts.

It is believed that fewer injection points and the suboptimal port orientation could have contributed to lower mercury capture in the Hood Exhaust gas than what was observed in the Windbox Exhaust gas.

Mercury Monitors

The latest version of the Tekran mercury monitoring equipment was used for this test program. Two types of particulate separator probes were utilized in this trial. One is a simple filter designed for use after wet scrubbers while the second is an inertial separator. A photograph of the filter probe is shown in below.

Photograph 2. Filter Probe



In an inertial separator, flue gas is drawn into the system by means of an eductor. The flow rate is measured by a Venturi meter and adjusted to provide an axial gas flow through the inertial separator of 70 – 100 feet per second. A gas sample is extracted at a low inertial filter face velocity of 0.006 feet per second. The particulate matter follows the gas stream and is thus separated from the gas sample. The gas removed from the duct is returned after use. The entire inertial separator is in an enclosure and maintained at 400^oF to avoid any condensation issues. The gas sample is conveyed through a heated line to the conversion module where the oxidized mercury is either converted to elemental mercury in order to provide a total gas phase mercury measurement or removed from the gas to allow for the measurement of elemental mercury.

The gas from the mercury conversion module is directed to a mercury analyzer. The gas sample is drawn across a gold trap in which the mercury is collected. After a prescribed sampling time, the trap is heated in order to release the mercury, which is measured by atomic fluorescence. The system was calibrated at least once per day using mercury standards. The analyzer provides one mercury measurement every two and one half (2.5) minutes, thus the name semi-continuous emission monitor. If both elemental and oxidized mercury are being analyzed, the measurements are five (5) minutes apart. The Tekran mercury conversion module and mercury CEM is shown in Photograph 3.

Photograph 3. Tekran Mercury Conversion Module and CEM



An Appendix K Mercury sorbent trap system was also used in this trial to measure the total mercury content of the flue gas. Albemarle manufactures its own Appendix K traps using our brominated sorbents. These traps are easier to analyze than those made using iodinated carbon. These traps are used to verify the mercury readings obtained by the Tekran Analyzer. A photo of a trap and the Appendix K controller appear below in Photograph 4.

Photograph 4. Appendix K Mercury Trap



The Appendix K samples were taken from all four stacks during the trial but mostly from Stacks 1 and 4, since they provided the extremes in the mercury concentration.

Solid Sample Mercury Analysis

The Appendix K traps, greenballs, and dust were analyzed for mercury content using an Ohio Lumex carbon trap Mercury Analyzer. The Ohio Lumex mercury analyzer is an atomic absorption spectrometer with Zeeman background correction. The Zeeman background correction eliminates the need for gold traps to concentrate the mercury. The instrument is calibrated with NIST standards. The detection limit is 50 µg/g. The Ohio Lumex unit is shown in Photograph 5.

Photograph 5. Ohio Lumex Carbon Trap Mercury Analyzer



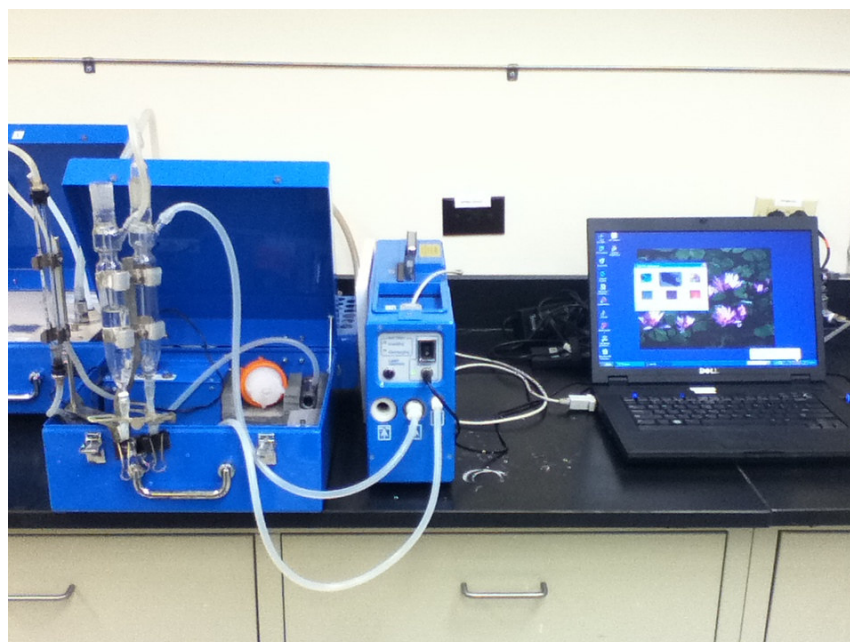
Water Sample Mercury Analysis

The water samples were analyzed using Ohio Lumex RA-915+ mercury analyzer. The analytical system consists of the RA-915+ analyzer itself, the RP-91 attachment for determination of mercury content in aqueous solutions using the "cold vapor" technique, and the RP-91C attachment for measuring mercury concentration in liquid and solid samples with a complex composition using the pyrolysis technique. Basic analytical characteristics of the system are given in the Table 1. The filtering of the water samples was performed at the Albemarle PDC using a 0.4 µm glass filter.

Table 1. Ohio Lumex Aqueous Sample Detection Limits

Subject	Detection limit	Sample parameters (flow rate, volume, weight)	Detection technique	Complete set
Ambient air	2 ng/m ³	20 l/min	Direct	RA-915+
Natural and industrial gases	2 - 500 ng/m ³	1 - 20 l/min		
Water	0.5 ng/l	20 ml	"Cold vapor" technique	RA-915+ RP-91
Urine	5 ng/l	1 ml		
Solid samples (soils, rocks)	0.5 µg/kg	0.2 g	Pyrolysis technique	RP-91C RA-915+
Biological samples (tissues, liver, etc.)	5 µg/kg	0.02 g		
Hair	20 µg/kg	0.01 g		
Oil and oil products	50 µg/kg	0.01 g		
Plants	2 µg/kg	0.05g		
Foodstuff	2 - 10 µg/kg	0.005 - 0.05 g		

Photograph 6. Ohio Lumex Model RA-915+ Mercury Analyzer with Liquid Sample Analysis Attachment



LOI Analysis

LOI analysis was performed on all dust samples taken from the multiclone. This was done to determine the carbon content present within the dust and whether any of the injected sorbent was captured.

All dust samples were individually weighed and placed into a crucible. Seven random samples were dried for 3 hours in an oven at 120°C. After drying the samples were weighed and the average weight variation calculated. The average weight variation for all seven samples was 0.00076%. It was therefore determined that the moisture content was extremely low, and drying before the actual LOI analysis would not be needed.

The dust samples were then placed into an oven at 800°C for 2 hours. The samples were weighed before and after being placed in the oven. The sample LOI was calculated by taking the percentage weight loss or gain of the sample after exiting the oven.

Hg Removal Calculation Method

Mercury removal is the key parameter to be calculated in this trial. The calculation is complicated by the fact that there are significant emissions from both the Windbox Exhaust and the Hood Exhaust, which report to four stacks. Fortunately, the four stacks are connected by a common duct, causing nearly identical flue gas flow through each stack.

The baseline and parametric testing was conducted by measuring the mercury emissions in two of these stacks (#1 and #4), which had the most divergent Hg emissions. The Hg concentrations were then averaged to provide the average Hg emission for the time period.

The following equation was used to calculate the Hg removal percentage:

$$Hg \text{ removal}(\%) = \left(1 - \frac{\text{Controlled gas mercury concentration}}{\text{Uncontrolled gas mercury concentration}} \right) \times 100$$

The uncontrolled gas mercury concentration was the average mercury emission rate derived from the baseline testing data.

The controlled gas mercury concentrations for the parametric tests were the average for the period after injection began once the Hg level reached a near stable level.

The mercury emission concentration was established in the parametric tests below which both stacks being monitored would have to be maintained in order to reach 75% mercury control. Thus, it was only necessary to monitor one stack during the continuous two-week run and make sure that a Hg emission level below the desired was maintained.

Field Trial Test Plan - Final

The field trial was divided into three phases: Baseline Measurements, Parametric Testing and Continuous Injection Run.

Baseline Measurements

Baseline flue gas mercury emissions from the facility were measured after the monitoring equipment was installed. The data from this period was used as a basis for determining the mercury reduction percentages achieved in the next phases of the project.

Parametric Testing

Both plain PAC and gas-phase brominated PACs were utilized during the parametric testing. A parametric injection test lasted for up to 6 hours at one or more injection rates. The injection was then terminated to allow the mercury to return to baseline levels. The injection runs with the brominated sorbents were usually shorter due to the high mercury capacity of these sorbents, which precludes returning to baseline mercury levels if injected for too long a period of time.

The sorbent injection trials started at an injection rate of 1 lb/MMacf on the first day that each sorbent was used and was increased as needed to achieve the mercury target. Plain PAC was not expected to be able to achieve the target and its injection rate was limited to a maximum of 5 lb/MMacf. There was a lay day between the plain PAC and brominated PAC runs.

Continuous Run

After the parametric testing, there was a continuous injection run with the gas-phase brominated sorbent at a selected rate for a two-week time period. This run was to approximate the results that might be achieved in continuous commercial operation.

Schedule

The schedule for the field test conducted at Hibbing Taconite is presented in Table 2.

Table 2. Schedule for Testing at Hibbing Taconite

<u>Schedule for Albemarle Project Entitled</u>	
<u>"Mercury Control for Taconite Plants Using Gas-Phase Brominated Sorbents"</u>	
<u>Activity</u>	<u>Date</u>
Travel to Hibbing Taconite	September 13, 2011
Equipment Installation	September 14-17, 2011
Baseline Measurements	September 17-21, 2011
Parametric Testing	September 22-26, 2011
Test Break/Plant Down	September 27 – October 6, 2011
Continuous Run	October 7 - October 22, 2011
Equipment Disassembly	October 22, 2011
Personnel Leave Site	October 23, 2011

Results and Discussion

Pre-Trial Testing

From May 30 through June 4, 2011, members of the Albemarle field testing team visited the Hibbing Taconite plant in order to define the mercury split between the two primary exhaust gas streams (Windbox and Hood) and determine where it would be best to install the injection ports. Sorbents traps were collected from the flue gas in both the Windbox and Hood Exhaust streams as well as from the flue gas in each of the four interconnected stacks. This testing would help determine if it would be necessary to inject into both the Windbox and Hood Exhaust gas ductwork in order to achieve the 75% mercury reduction target.

The data from the sorbent traps collected in Production Line 1 are presented in Table 3. All concentration data presented is in $\mu\text{g}/\text{Nm}^3$.

Table 3. Hg Test at HibTac Line 1 May-June, 2011

<u>Location</u>	<u>Gaseous Hg</u>	<u>Particulate Hg</u>	<u>Total Hg</u>	<u>% Particulate</u>
Windbox	3.59	0.00	3.59	0.0%
Hood	2.20	0.47	2.67	17.7%
	2.24	0.34	2.57	13.1%
	2.40	0.15	2.54	5.7%
Stack 1	1.45	0.32	1.76	17.9%
Stack 2	2.65	0.13	2.77	4.5%
Stack 3	3.49	0.34	3.83	9.0%
Stack 4	3.63	0.42	4.05	10.3%
	4.34	0.45	4.80	9.4%

In these tests, the front wool section of the sorbent trap was analyzed separately and designated as particulate mercury. It is known that fine iron oxide can act as a sorbent to capture mercury, and, thus, it is expected that some of the mercury captured on the filter was really gaseous mercury captured on the wool by iron oxide. The particulate mercury levels varied from 0.0% to 17.9% and averaged nearly 10%. In a typical application the naturally occurring particulate mercury is less than 1%.

The stack flue gas flow rates are nearly the same since there is a common duct connecting them. The flue gas from the Hood Exhaust reports to Stacks 1 and 2, while that from the Windbox Exhaust reports to Stacks 3 and 4. From the data in Table 3, it can be seen that the mercury content in Stacks 1 and 2 are similar as is the mercury content in Stacks 3 and 4. It was expected that most of the

mercury would be in the Windbox Exhaust gas. While the Windbox Exhaust gas does contain more mercury than the Hood Exhaust gas, it only contains 70% of the mercury. Thus, injecting sorbent only into the Window Exhaust gas stream could not achieve the mercury reduction target of 75%.

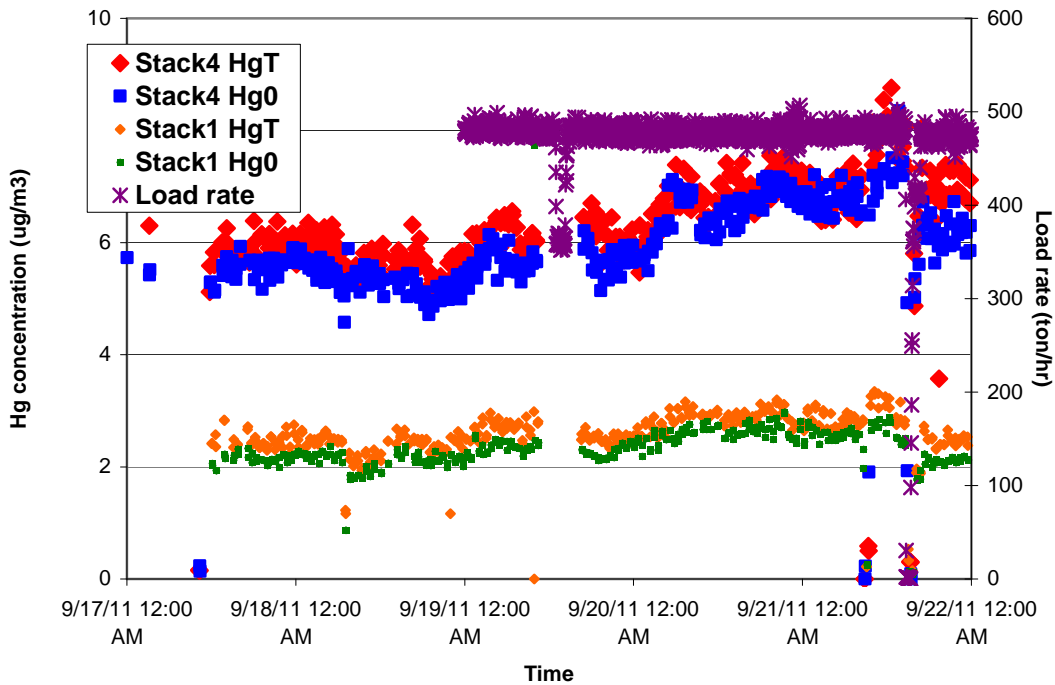
The preferred injection locations were also selected during the pre-trial testing and these were discussed previously in the section on sorbent distribution and lance system.

Baseline Measurements

Baseline measurements were conducted on Line 1 from Sept. 17 through end of day Sept. 21, 2011. The Tekran CEM was used for analyzing Stacks 1 & 4. The purpose of the baseline period was to analyze mercury emissions and establish the average mercury content of the flue gas without sorbent injection in both the Windbox and Hood Exhaust flue gas streams. These baseline mercury content values would then be used to judge the effectiveness of B-PAC™ once it was introduced into the gas stream during the parametric testing.

Figure 5 shows the baseline mercury emissions data from Line 1. The load rate data provided by Hibbing Taconite was also included.

Figure 5. Stacks 1 & 4 Baseline Mercury Data with Load Rate



As seen in the pre-trial testing, the mercury content of the flue gas was less in Stack 1 (Hood Exhaust) than in Stack 4 (Windbox Exhaust). The average total mercury concentration in Stack 4 over the 5-day baseline period was $6.32 \mu\text{g}/\text{Nm}^3$ while the average concentration in Stack 1 was $2.58 \mu\text{g}/\text{Nm}^3$. The combined average mercury concentration for the two stacks was $4.45 \mu\text{g}/\text{Nm}^3$. For all subsequent calculations contained in this report, this average mercury concentration will represent baseline conditions and will be referred to as 0% Hg removal.

It should be noted that there was a problem with the Hg CEM equipment on September 19 (10:25-16:35) during a plant slowdown, which caused the loss of 6 hours of data. The missing data was not used to compute the average mercury

content over the baseline period. There were two periods on September 21 when there was a reduction in total mercury measured. The first was likely due to completion of the sorbent injection system set-up. Residual sorbent present in the distribution hoses was probably pulled into the flue gas stream by the negative pressure Windbox and Hood Exhaust ducts causing the slight drop in mercury levels. The second drop in mercury concentration on that day was caused by a brief shutdown of the plant. The mercury emissions followed the production rate down to zero during this time. The mercury data exhibits the typical meander in mercury emissions caused by variation in the raw material mercury concentration.

Sorbent traps were taken from all four stacks during the baseline period. The results were very consistent with the Hg concentration in Stacks 1 and 2 being nearly identical as were the concentrations in Stacks 3 and 4. This is the same as the data shown in Table 3.

The results from the sorbent traps taken on Stacks 2 and 3 during the baseline period are presented in Table 4 relative to results from Stacks 1 and 4, respectively. The results for Stack 3 are very close to the results obtained by the CEM on Stack 4 during the sampling time. There was some variability in the traps taken on Stack 2 compared to the CEM data for Stack 1.

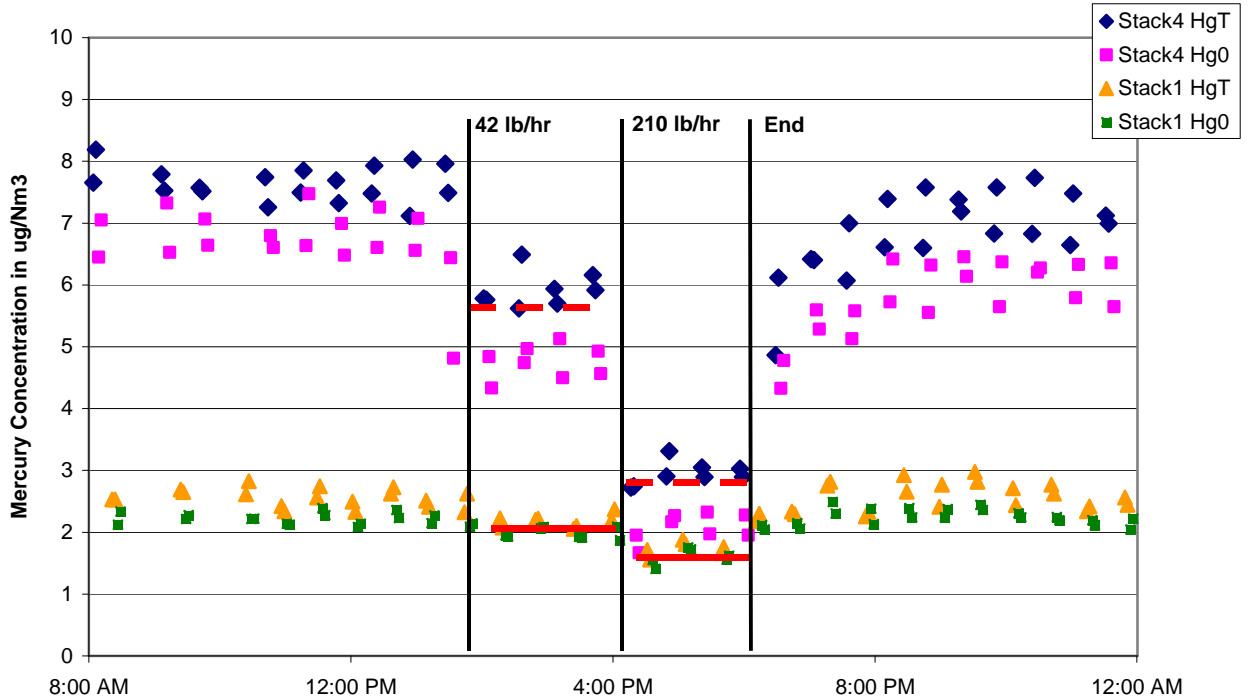
Table 4. Baseline Sorbent Traps, Stacks 2 & 3

Baseline Sorbent Trap Results				
Date	Stack 2 (Using Stack 1 Baseline)		Stack 3 (Using Stack 4 Baseline)	
	Analyzed w/ Filter	Analyzed w/o Filter	Analyzed w/ Filter	Analyzed w/o Filter
9/18/2011 15:07-16:07			+4%	+1%
9/19/2011 11:32-14:05	+53%	+46%		
9/20/2011 10:51-13:41	+77%	+71%		

Parametric Tests

The parametric testing began on 9/22/2011 with the injection of plain PAC. Two injection rates were utilized: 42 and 210 lb/hr. This translates into approximately 1 and 5 lb/MMacf, respectively. Injection rates are typically shown in lb/MMacf, since sorbent distribution is a primary factor controlling Hg removal. The mercury monitor data for this day is presented in Figure 6.

Figure 6. Injection of Plain PAC on 9/22/2011



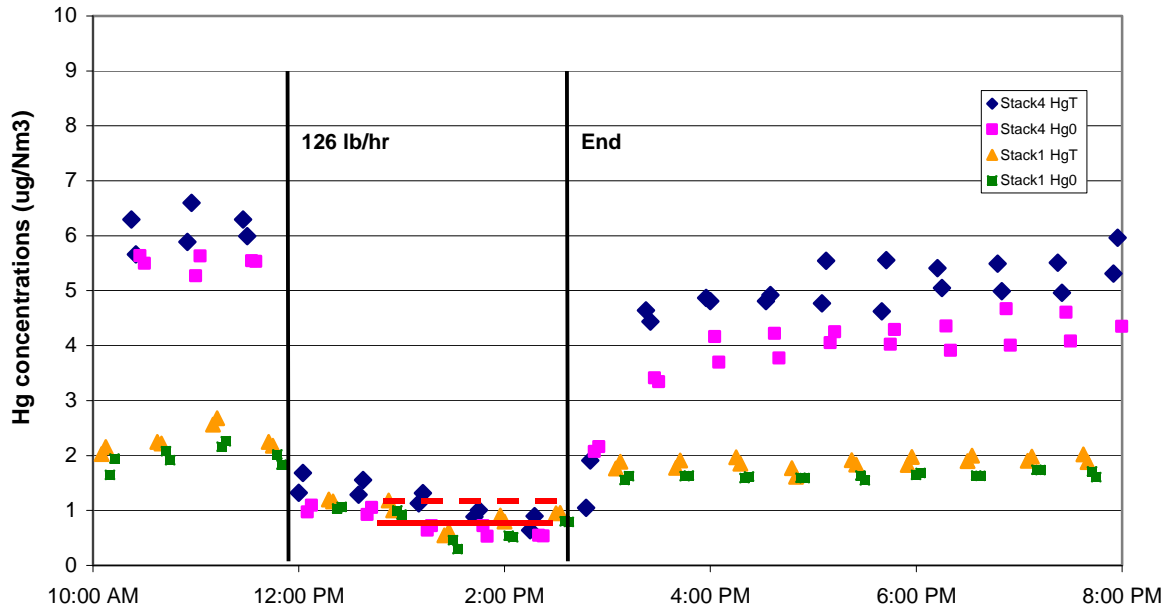
The mercury concentration in both stacks 1 and 4 are shown since the mercury emissions from both must be controlled in order to meet the 75% mercury reduction target. The combined average is used in the mercury reduction calculations since the stack flows are the same. It should be noted that a very high percentage of the Hg emissions is in elemental form. This is not surprising due the lack of acid gases in the taconite flue gases. The primary acid gases in flue gas are SO_3 and HCl. The acid gases are formed by converting SO_2 and NaCl, respectively, that are present in fuels and raw materials. Since taconite plants are natural gas fired and since the raw materials are low in sulfur and chloride impurities, very low levels of acid gases are expected in the flue gas.

Once injection began, the mercury emissions were very rapidly reduced. The red lines are shown as the average Hg levels for a given injection rates. After the injection stopped, the Hg emissions did not recover immediately to the baseline mercury level. This is due to sorbent on the walls continuing to remove mercury.

In fact, in trials using B-PAC, which has a much higher mercury capacity than plain PAC, the impact can be seen for a longer period.

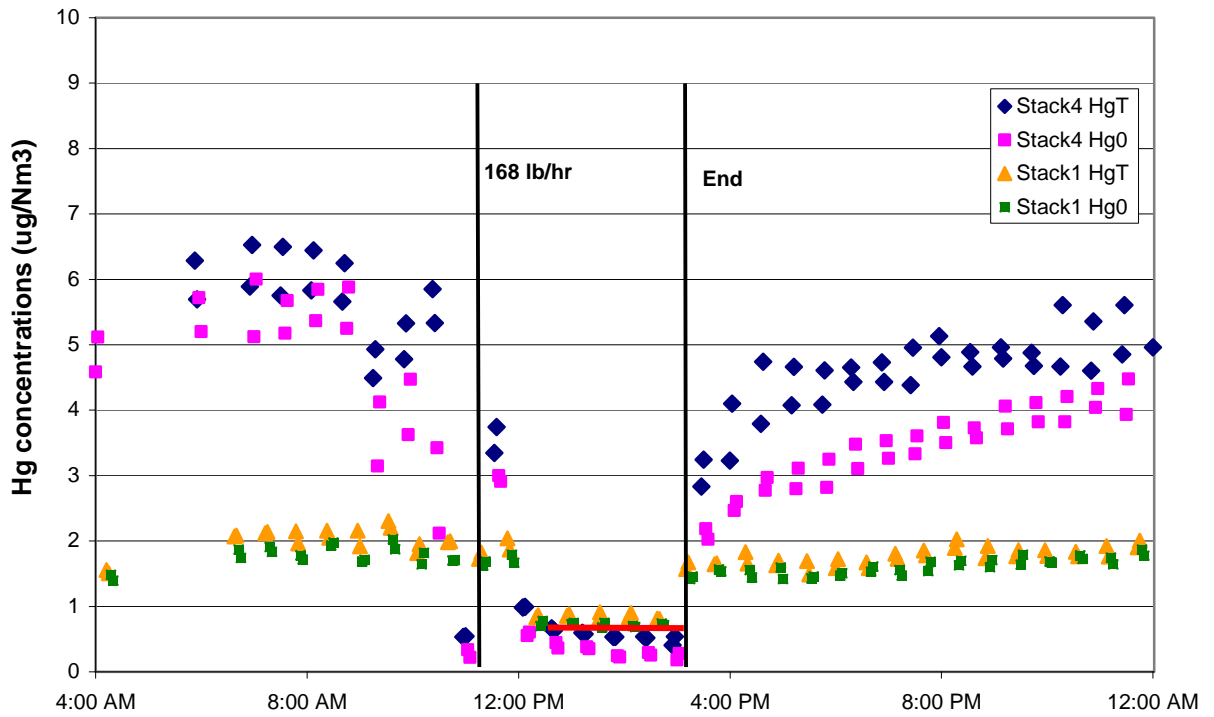
Several more days of parametric injection tests were conducted using B-PAC. The Hg monitor data for those days is presented in Figure 7 to 9.

Figure 7. Injection of B-PAC™ on 9/24/2011



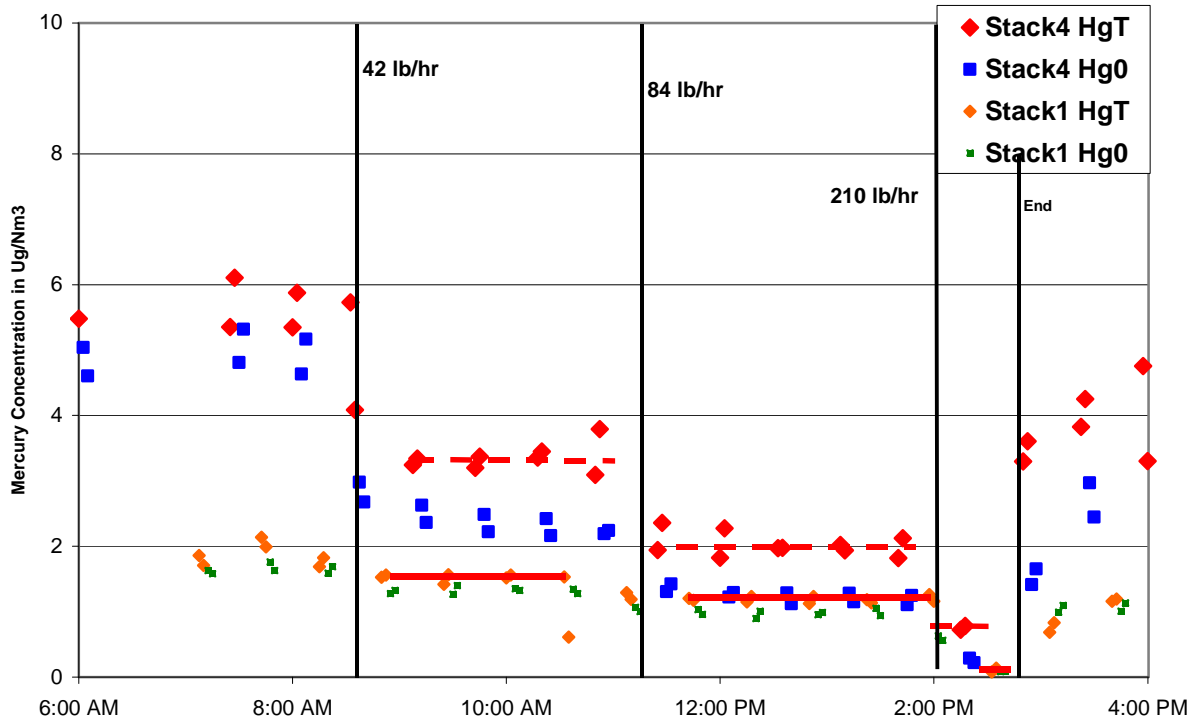
The mercury reduction is very rapid when the injection of B-PAC begins on September 24, 2011 at a rate of 126 lb/hr. The mercury recovery after the injection ceased is not rapid.

Figure 8. Injection of B-PAC™ on 9/25/2011



The B-PAC injection rate on September 25, 2011 was 168 lb/hr or approximately 4 lb/MMacf. Again the recover to baseline after the test is slow.

Figure 9. Injection of B-PAC™ on 9/26/2011



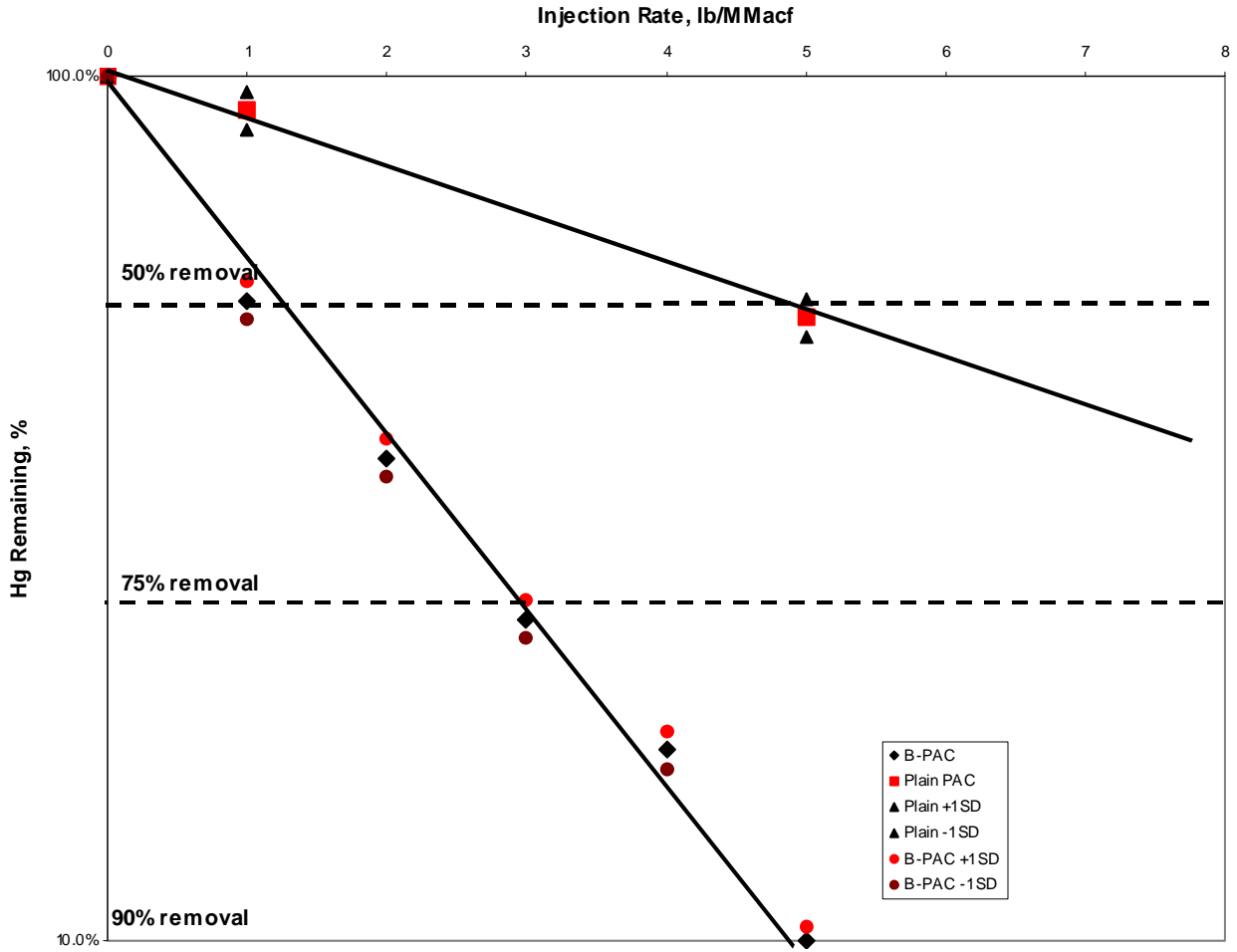
There were three injection rates tested on September 26, 2011: 42, 84 and 210 lb/hr. The highest of these injection rates provided a mercury removal rate in excess of the 75% mercury reduction target.

The results from all of the parametric sorbent injection tests are presented graphically in Figure 10.

The results are presented on a semi-log plot with the percent mercury remaining shown on the y-axis and the injection rate in terms of lb/MMacf shown on the x-axis. Shown in this manner, the results form straight lines since removal is a first order rate. The lines are trend lines and not regression lines. Both lines start at the origin: 100% Hg remaining (zero mercury reduction) and 0 lb/MMacf injection. Thus, mercury removal solely due to the sorbent is being presented. In addition to the measured mercury removal, values for ± 1 standard deviation of the mercury data is also presented. The data fits the trend lines fairly well.

The plain PAC performed as expected. The 75% removal target was not achieved even at the highest injection rate attempted. It is projected that a plain PAC injection rate >10 lb/MMacf would have been required to reach the target reduction, if at all possible. The B-PAC was able to achieve the 75% Hg reduction rate at about 3 lb/MMacf (126 lb/hr) or less than a third that of plain PAC. This is typical of the difference in performance of plain PAC and gas-phase brominated B-PAC in other applications. Mercury removal rates higher than 75% were achievable. Based upon these results, an injection rate of 3 lb/MMacf was selected for use in the continuous run.

Figure 10. Parametric Injection Test Results



The Hg removal results from all of the parametric tests are presented in Table 5.

Table 5. Parametric Test Results

<u>Sorbent</u>	<u>Injection Rate</u>		<u>Hg Remaining</u>		
	<u>lb/hr</u>	<u>lb/MMacf</u>	<u>%</u>	<u>+1 SD</u>	<u>-1 SD</u>
Plain PAC	42	1	91.2%	95.8%	86.7%
Plain PAC	210	5	52.5%	55.2%	50.0%
B-PAC	126	3	23.5%	24.8%	22.4%
B-PAC	168	4	16.6%	17.5%	15.8%
B-PAC	42	1	54.9%	57.8%	52.3%
B-PAC	84	2	36.2%	38.0%	34.4%
B-PAC	210	5	10.0%	10.4%	9.6%

The mercury data used to make these calculations is shown in Table 6.

Table 6. Parametric Testing CEM Hg Data

Sorbent	Injection Rate		Level	Level	Average	Baseline	Hg
	lb/hr	lb/MMacf	Stack 1	Stack 4	$\mu\text{g}/\text{Nm}^3$	$\mu\text{g}/\text{Nm}^3$	Remaining
Plain PAC	42	1	5.94	2.18	4.06	4.45	91.2%
Plain PAC	210	5	2.94	1.73	2.34	4.45	52.5%
B-PAC	126	3	0.93	1.16	1.05	4.45	23.5%
B-PAC	168	4	0.85	0.63	0.74	4.45	16.6%
B-PAC	42	1	1.53	3.36	2.45	4.45	54.9%
B-PAC	84	2	1.19	2.03	1.61	4.45	36.2%
B-PAC	210	5	0.11	0.75	0.43	4.45	9.7%

Appendix K sorbent traps were collected during the parametric testing. The data from these traps was also used to calculate the mercury removal rate at each injection rate. The calculated mercury removal rates for these two measurement methods are shown in Table 7.

Table 7. CEM and Appendix K Trap Hg Removal Data

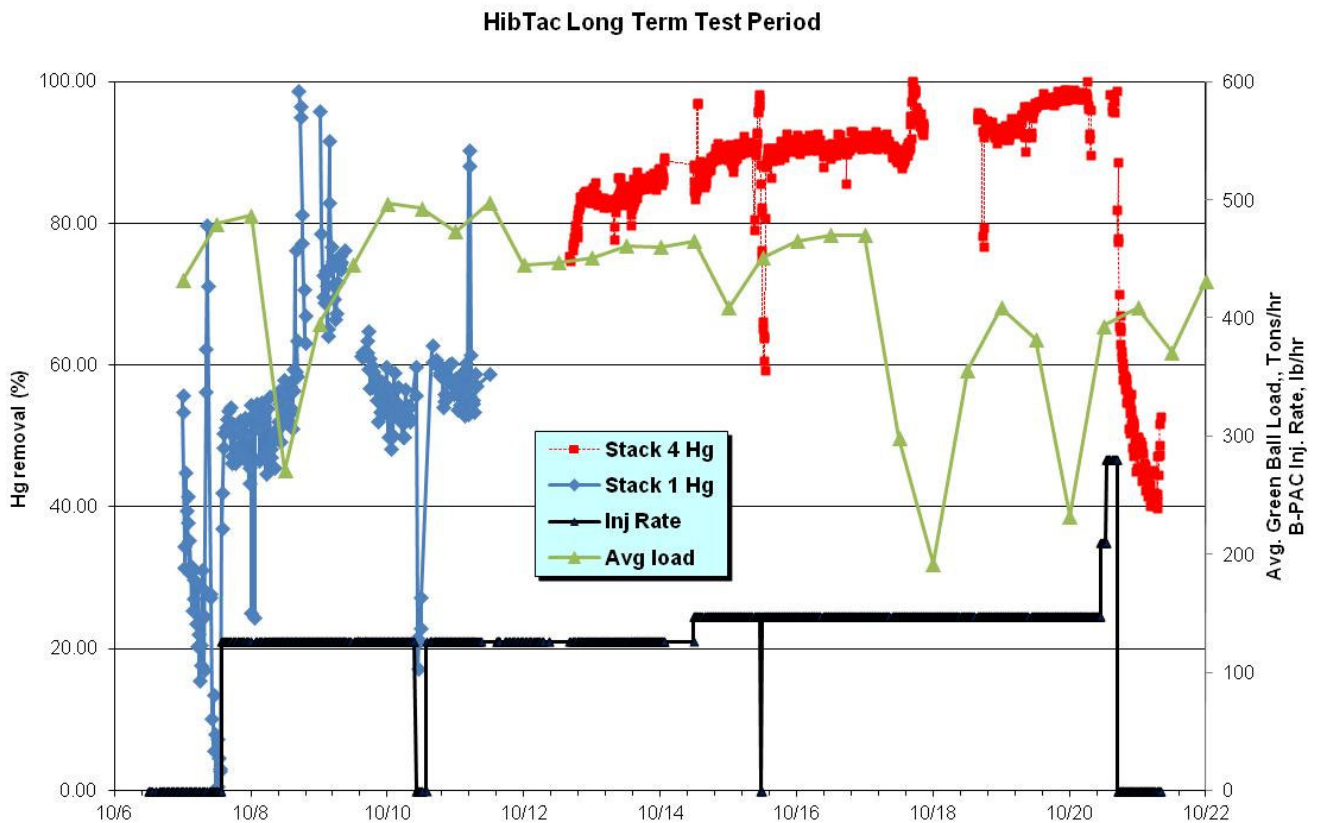
Sorbent	Injection Rate		Hg Remaining	
	lb/hr	lb/MMacf	CEM	Trap
Plain PAC	42	1	91.2%	81.5%
Plain PAC	210	5	52.5%	55.5%
B-PAC	126	3	23.5%	14.5%
B-PAC	168	4	16.6%	21.5%
B-PAC	42	1	54.9%	49.2%
B-PAC	84	2	36.2%	36.2%
B-PAC	210	5	10.0%	16.7%

The comparison of the mercury removal data is fairly good considering the difficulties associated with collecting sorbent traps in a wet stack. All of the removals appear to be in line except for the B-PAC injection rates of 3 and 4 lb/MMacf, but even these are within 10% of each other.

Continuous Run

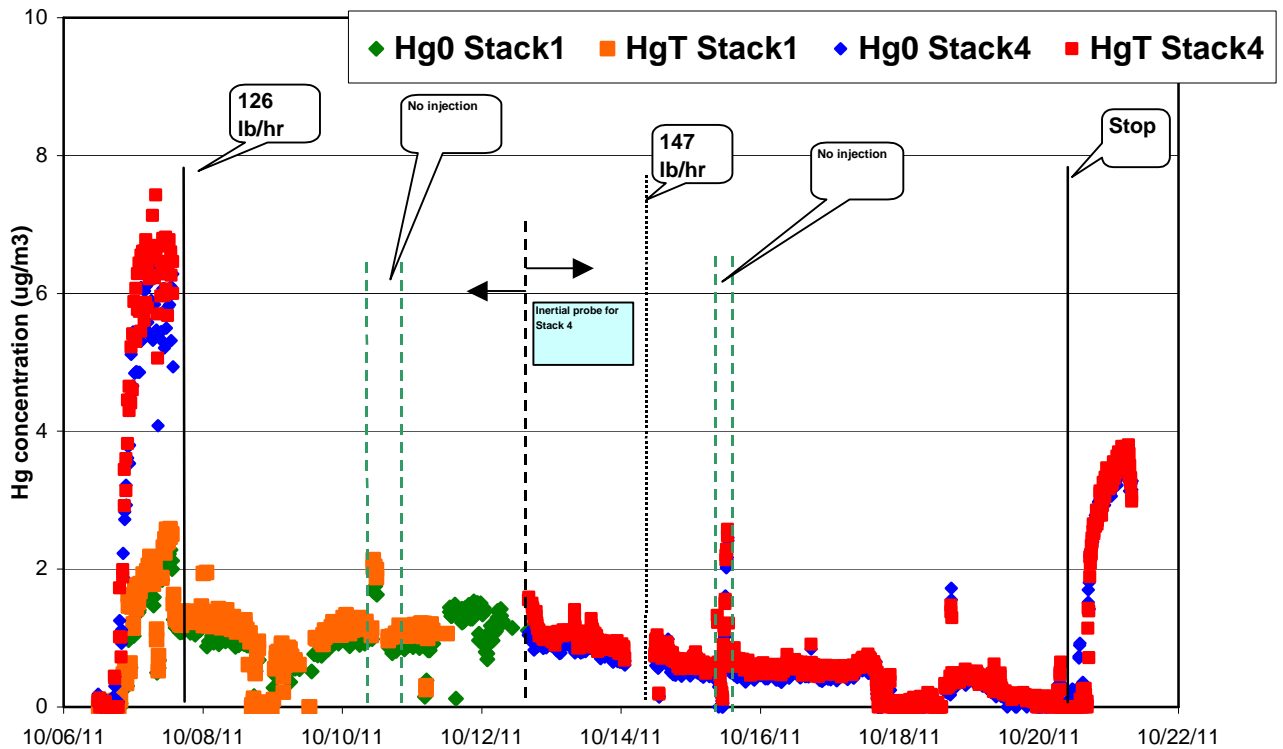
Albemarle began the long term testing at Hibbing Taconite on October 7 following a one-week break from sorbent injection. Like the other tests, the continuous run was on Line 1. The test period began with the CEM wet stack probe in Stack 4 and the CEM inertial filter probe in Stack 1. The CEM analyzer took alternating total and elemental mercury measurements from Stack 1 and Stack 4. The cycle time for each measurement is 2.5 minutes. Each stack was sampled for 30 minutes before switching to sample from the other stack. In Figure 11 below, the reduction of total mercury, as measured by the Hg CEM, is plotted along with the B-PAC™ injection rates, and the twelve-hour average green ball Hg load.

Figure 11. Continuous Run Mercury Removal



Both inertial and wet stack CEM probes were inserted into the emission gas stream on different stacks and used for drawing filtered gas samples for measurement in the CEM. In Figure 11 above, the percent mercury removal data gathered by only the inertial filter probe is plotted. No data collected by the wet probe is shown.

Figure 12. Continuous Run Mercury Concentrations



At the beginning of the continuous run, the wet probe was inserted into Stack 4 and the inertial probe into Stack 1. However, after day two of the long term test program, it was determined that the sample gas supplied by the wet stack probe had a negative mercury bias, meaning the probe was absorbing some of the mercury carried by the sample furnace gas to the CEM.

The bias of the sampling probes is determined by a calibration procedure called mercury recovery. In this procedure, the CEM monitor sends a known concentration of elemental mercury calibration gas to the intake portion of the sampling probe. From here it is drawn through the probe and back to the CEM for measurement. In a probe with no bias toward mercury absorption or mercury release, the CEM will measure 100% of the mercury supplied by the CEM with an accuracy of +/- 5%.

During the early part of the continuous run, the wet stack probe on Stack 4 began to show a steady increase of negative bias during mercury recovery calibrations. This probe uses an inline particle filter with blowback cleaning to separate solid particles from the sampling gas. As evidenced by the filter media color change, fine particles were accumulating on the filter and the blowback cleaning option was not able to dislodge these particles from the filter media. The mercury recovery procedure verified that during the first two days of long term testing, the particles captured on the filter media were increasingly absorbing mercury from out of the sampling gas. This situation is consistent with the theory that some B-

PAC™ particles were escaping from the scrubber collector and depositing on the wet probe filter media. While this negative bias was not seen on the wet probe during the short parametric tests, the continuous injection of B-PAC™ during long term testing overwhelmed the wet stack filter cleaning capability. Therefore, the data collected with the wet stack during the long term testing was not used in the data set of this report. The inertial filter probe was used to collect data on Stack 1 from October 7 – 11 and then physically moved to Stack 4 for the remainder of the long term test period. A mercury bias was not seen while sampling gas with the inertial filter probe.

The injection of B-PAC™ was started at 13:30 on October 7 at a rate of 126 lb/hr. This rate is equivalent to 3 lb B-PAC™/MMacf of furnace gas. The reduction of mercury was measured on Stack 1 by the CEM. The beginning of B-PAC™ injection is clearly visible in Figure 11 on October 7 as the mercury removal quickly jumped to 50%. The average removal measured on Stack 1 from October 7 to October 11 was 57%. The average Hg removal was 74% during the 24 hour period from 16:00 on October 8 to 16:00 on October 9. It should be noted that a higher mercury removal was always observed in Stack 4 as compared to Stack 1 due to the reduced number of lances and, subsequently sorbent delivered to that side. As can be seen by the Stack 4 data in Figure 11, a much higher mercury removal was achieved there and the combined removal would exceed 75%.

On October 10, the data set in Figure 11 switches to mercury removal on Stack 4. Removal on Stack 4 is significantly higher than removal on Stack 1 which is caused by a lower B-PAC™ mass injection rate in the Hood Exhaust stream as compared with the Windbox Exhaust stream. Mercury removal on Stack 4 is shown to increase steadily through the continuous run test period. An increase in mercury reduction over time has often been observed in mercury control tests and generally attributed to a build-up of mercury sorbent particles on surfaces within the gas flow path.

The average mercury removal on Stack 4 with 126 lb/hr (3 lb/MMacf) of B-PAC™ was 84%. This rate of injection was maintained until October 14 at 12:00.

In order to compensate for the lower removal rates measured on Stack 1, the injection rate of B-PAC™ was increased to 147 lb/hr, or 3.5 lb/MMacf, on October 14 at 12:00. The increase in injection rate resulted in an immediate increase in the mercury removal rate. The average mercury removal rate at 147 lb/hr was 92% in Stack 4. The Line 1 furnace was stopped unexpectedly for repairs on October 20 at 7:00 and this ended the 147 lb/hr test period.

Because October 20 was the last scheduled continuous run test day, the B-PAC™ injection rate was increased in increments from 210 lb/hr to 280 lb/hr to empty the MDU storage bin. The time weighted average injection rate during this 6-hour period, ending at 17:00 on October 20, was 255 lb/hr. The average

mercury removal during the high injection rate period far exceeded the 75% target.

B-PAC™ injection was stopped at 17:00 on October 20 but the mercury CEM continued to collect data from Stack 4 until October 21 at 8:00. The change in mercury removal due to the end of B-PAC™ injection is clearly seen in the data set in Figure 11 as the mercury removal drops sharply to as low as 40%. However, the mercury does not recover to the low removal level seen at the start of the continuous run test period. This is often observed in B-PAC™ injection tests and can be contributed to the presence of still active B-PAC™ collected in the ductwork and scrubber.

Green Ball Analysis

Green ball samples were taken during the test and analyzed for Hg. The samples were all grab samples and, thus, any conclusions made based upon the analysis are tentative. The results are shown in are Table 8. The Hg content of the green balls was measured at Albemarle's Hg R&D lab, which is located at Process Development Center (PDC) in Baton Rouge, LA using the Ohio Lumex analyzer.

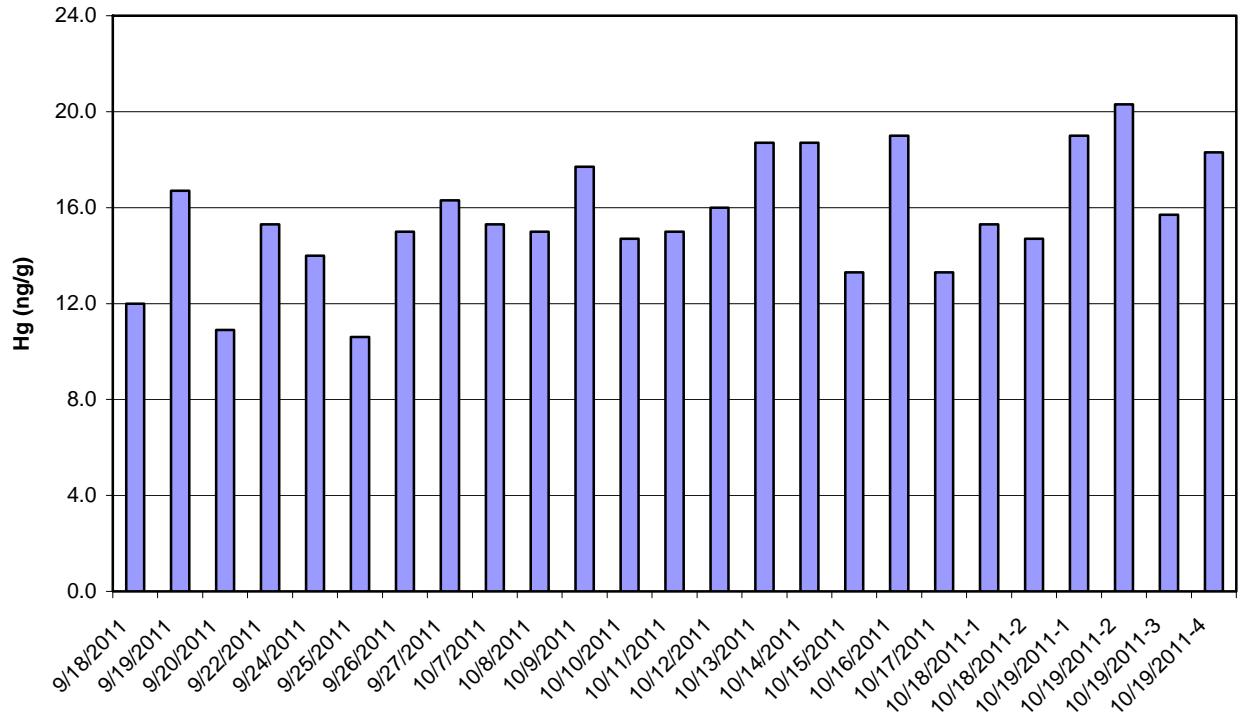
Table 8. Green Ball Hg Analyses

Date	Time	Operation	Result (ng/g)
9/18/2011	2:00pm	Baseline	12.0
9/19/2011	4:00pm	Baseline	16.7
9/20/2011	8:40am	Baseline	10.9
9/22/2011	5:10pm	Plain AC (5lb/MMacfm)	15.3
9/24/2011	1:40pm	Parametric (2lb/MMacfm)	14.0
9/25/2011	2:20pm	Parametric (4lb/MMacfm)	10.6
9/26/2011	12:30pm	Parametric (2lb/MMacfm)	15.0
9/27/2011	9:35am	Parametric (5lb/MMacfm)	16.3
10/7/2011	2:40pm	Long term (3lb/MMacfm)	15.3
10/8/2011	12:40pm	Long term (3lb/MMacfm)	15.0
10/9/2011	4:30pm	Long term (3lb/MMacfm)	17.7
10/10/2011	5:00pm	Long term (3lb/MMacfm)	14.7
10/11/2011	3:50pm	Long term (3lb/MMacfm)	15.0
10/12/2011	3:45pm	Long term (3lb/MMacfm)	16.0
10/13/2011	3:15pm	Long term (3lb/MMacfm)	18.7
10/14/2011	2:50pm	Long term (3.5lb/MMacfm)	18.7
10/15/2011	2:15pm	Long term (3.5lb/MMacfm)	13.3
10/16/2011	4:15pm	Long term (3.5lb/MMacfm)	19.0
10/17/2011	4:20pm	Long term (3.5lb/MMacfm)	13.3
10/18/2011-1	4:40pm	Long term (3.5lb/MMacfm)	15.3
10/18/2011-2	4:40pm	Long term (3.5lb/MMacfm)	14.7
10/19/2011-1	10:45am	Long term (3.5lb/MMacfm)	19.0
10/19/2011-2	10:45am	Long term (3.5lb/MMacfm)	20.3
10/19/2011-3	3:30pm	Long term (3.5lb/MMacfm)	15.7
10/19/2011-4	3:30pm	Long term (3.5lb/MMacfm)	18.3

The green ball Hg content varied from a low of 10.6 ng/g to a high of 20.3 ng/g, or nearly by a factor of two.

The data is presented graphically in Figure 13. The variation in green ball mercury level is easier to observe in this format.

Figure 13. Hg Content in Green Ball Samples



Multiclone Dust Analysis

The multiclone dust samples collected during the trial are listed in Table 9.

Table 9. Multiclone Dust Samples Collected during the Trial

Date	Time	Operation	Analysis
9/18/2011	2:15pm	Baseline	Hg, LOI
9/19/2011	3:30pm	Baseline	Hg, LOI
9/20/2011	9:00am	Baseline	Hg, LOI
9/22/2011	5:20pm	Plain AC (5lb/MMacfm)	Hg, LOI
9/24/2011	1:45pm	Parametric (2lb/MMacfm)	Hg, LOI
9/25/2011	2:20pm	Parametric (4lb/MMacfm)	Hg, LOI
9/26/2011	12:30pm	Parametric (2lb/MMacfm)	Hg, LOI
9/27/2011	9:45am	Parametric (5lb/MMacfm)	Hg, LOI
10/7/2011	2:30pm	Long term (3lb/MMacfm)	Hg, LOI
10/8/2011	12:45pm	Long term (3lb/MMacfm)	Hg, LOI
10/9/2011	4:25pm	Long term (3lb/MMacfm)	Hg, LOI
10/10/2011	5:00pm	Long term (3lb/MMacfm)	Hg, LOI
10/11/2011	3:45pm	Long term (3lb/MMacfm)	Hg, LOI
10/12/2011	3:45pm	Long term (3lb/MMacfm)	Hg, LOI
10/13/2011	3:15pm	Long term (3lb/MMacfm)	Hg, LOI
10/14/2011	2:30pm	Long term (3.5lb/MMacfm)	Hg, LOI
10/15/2011	2:15pm	Long term (3.5lb/MMacfm)	Hg, LOI
10/16/2011	4:15pm	Long term (3.5lb/MMacfm)	Hg, LOI
10/17/2011	4:20pm	Long term (3.5lb/MMacfm)	Hg, LOI
10/18/2011	4:40pm	Long term (3.5lb/MMacfm)	Hg, LOI
10/18/2011	4:40pm	Long term (3.5lb/MMacfm)	Hg, LOI
10/19/2011	10:45am	Long term (3.5lb/MMacfm)	Hg, LOI
10/19/2011	10:45am	Long term (3.5lb/MMacfm)	Hg, LOI
10/19/2011	3:30pm	Long term (3.5lb/MMacfm)	Hg, LOI
10/19/2011	3:30pm	Long term (3.5lb/MMacfm)	Hg, LOI

The LOI values should be a negative number since weight is expected to be lost during the heating process. However, the multiclone dust is composed primarily of various forms of iron oxide as can be seen in Table 10.

Table 10. XRD Analysis of Multiclone Dust

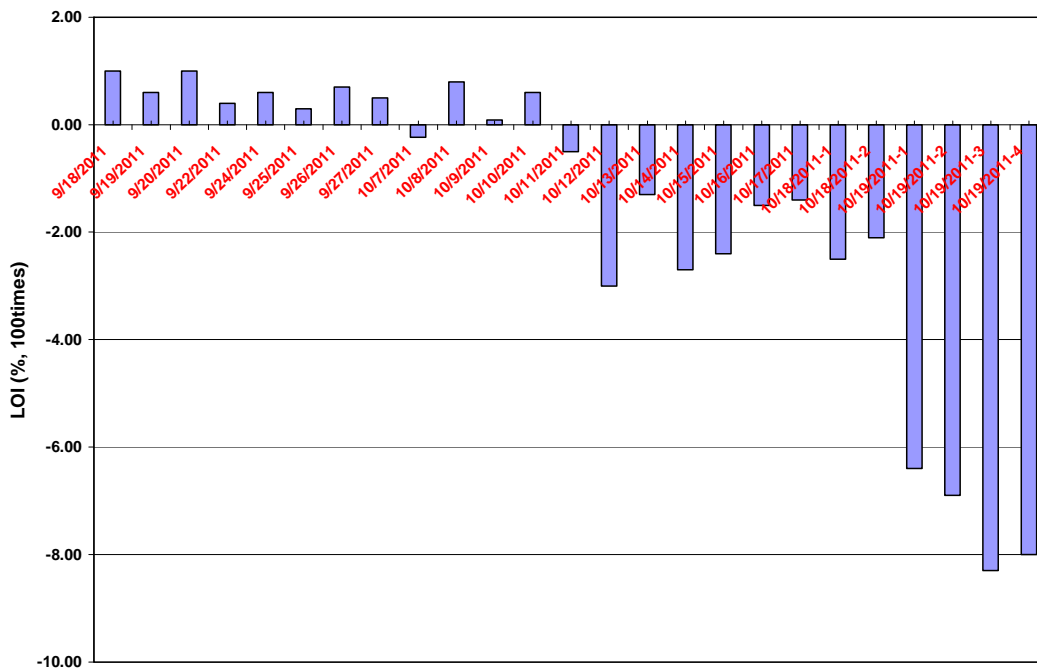
Sample	Magnetite (wt%)	Hematite (wt%)	Silicon Oxide (wt%)
9-19 sample	62.6	30.8	6.6
9-23 sample	58.4	33.3	8.4
10-13 sample	53.0	40.7	6.3
10-16 sample	53.6	39.4	7.0

At the high temperature conditions present in LOI analyses, magnetite (Fe₃O₄) can be converted to hematite (Fe₂O₃) as by Equation 1 to cause a weight gain of 3.5% for each magnetite particle oxidized.



It can be seen from Table 8 that the multiclone dust has a high percentage of magnetite and, thus, a weight gain in the analysis might be expected. The LOI results for the multiclone dust samples are presented in Figure 14.

Figure 14. LOI Results for Multiclone Dust Samples

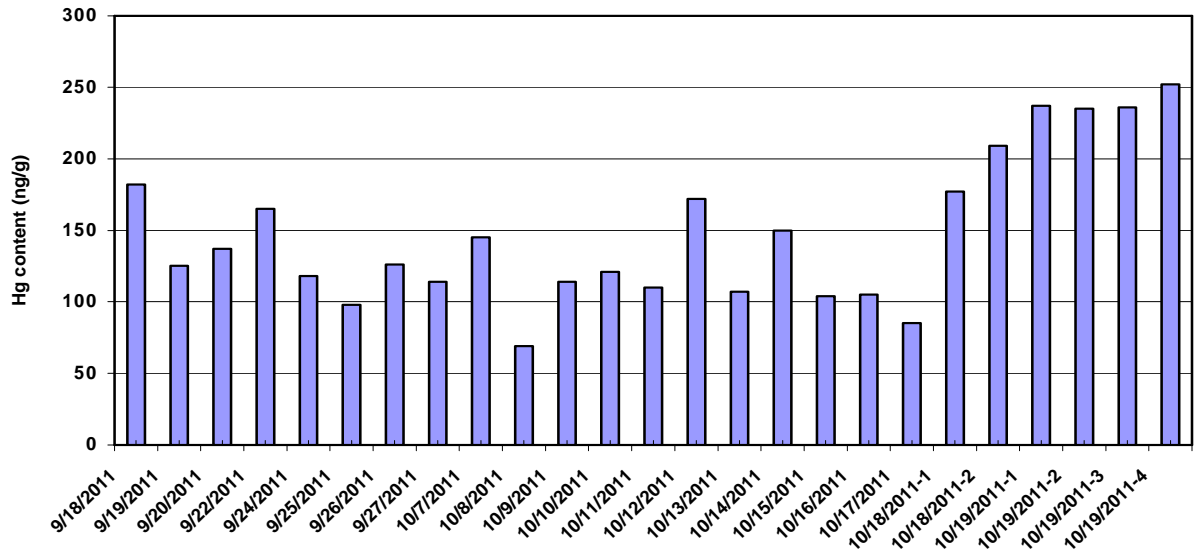


The LOI analyses of the dust samples did provide positive values up until the time of the continuous run when sorbent injection was around the clock. At that point, the LOI turned negative indicating that some of the B-PAC™ sorbent was being collected in the multiclone. This probably had a detrimental impact upon mercury removal since some of the sorbent was removed after a very short residence time and did not have an opportunity to fully capture mercury.

The mercury data from the multiclone samples is shown in Figure 15. The mercury content of the multiclone dust samples bounced around the average of all samples until the LOI content jumped well into the continuous run. Then the mercury content of the multiclone dust jumped to as high as 70% above the average mercury content of all samples. Thus, the sorbent being captured in the multiclone was capturing mercury but not as effectively as if it had more

residence time in the ductwork. The overall impact on the mercury removal rate was probably small.

Figure 15. Hg Content of Multiclone Dust Samples



Scrubber Water Analysis

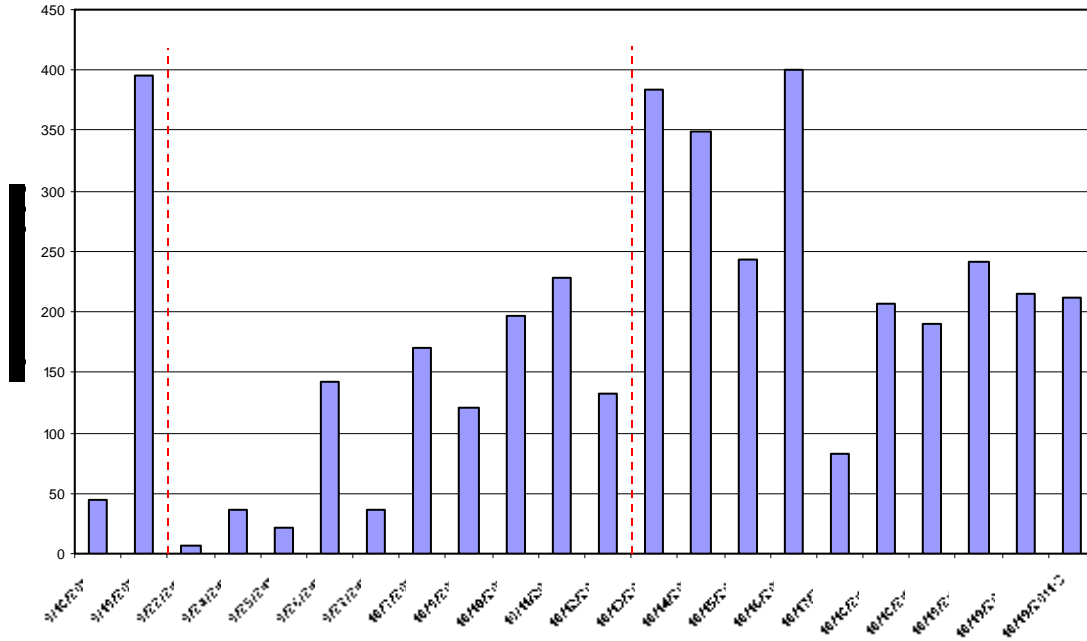
All of the scrubber water samples that were collected during the test period are listed in Table 11. In the last days of the trial, additional samples were taken in order to evaluate the impact of different treatment and storage methods. It should be noted that all samples are grab samples since representative sampling was not possible nor in the scope of the project.

Table 11. List of Scrubber Water samples

Date	Time	Storage Temperature	Operation	Analysis
9/18/2011	2:15pm	Room	Baseline	Hg
9/19/2011	3:30pm	Room	Baseline	Hg
9/22/2011	5:15pm	Room	Plain AC (5lb/MMacfm)	Hg
9/24/2011	1:40pm	Room	Parametric (2lb/MMacfm)	Hg
9/25/2011	2:20pm	Room	Parametric (4lb/MMacfm)	Hg
9/26/2011	12:30pm	Room	Parametric (2lb/MMacfm)	Hg
9/27/2011	9:35am	Room	Parametric (5lb/MMacfm)	Hg
10/7/2011	2:35pm	Room	Long term (3lb/MMacfm)	Hg
10/9/2011	4:30pm	Room	Long term (3lb/MMacfm)	Hg
10/10/2011	5:00pm	Room	Long term (3lb/MMacfm)	Hg
10/11/2011	3:50pm	Room	Long term (3lb/MMacfm)	Hg
10/12/2011	3:45pm	Room	Long term (3lb/MMacfm)	Hg
10/13/2011	3:15pm	Room	Long term (3lb/MMacfm)	Hg
10/14/2011	2:50pm	Room	Long term (3.5lb/MMacfm)	Hg
10/15/2011	2:15pm	Room	Long term (3.5lb/MMacfm)	Hg
10/16/2011	4:15pm	Room	Long term (3.5lb/MMacfm)	Hg
10/17/2011	4:20pm	Room	Long term (3.5lb/MMacfm)	Hg
10/18/2011	4:30pm	4°C	DI water	Hg
10/18/2011	4:30pm	4°C, w/HNO3	DI water	Hg
10/18/2011	4:30pm	Room	DI water	Hg
10/18/2011	4:50pm	4oC	Long term (3.5lb/MMacfm)	Hg
10/18/2011	4:50pm	4°C, w/HNO3	Long term (3.5lb/MMacfm)	Hg
10/18/2011	4:50pm	Room	Long term (3.5lb/MMacfm)	Hg
10/18/2011	4:50pm	Room	Long term (3.5lb/MMacfm)	Hg
10/19/2011	10:45am	4°C, w/HNO3	Long term (3.5lb/MMacfm)	Hg
10/19/2011	10:45am	4oC	Long term (3.5lb/MMacfm)	Hg
10/19/2011	10:45am	Room	Long term (3.5lb/MMacfm)	Hg
10/19/2011	10:45am	Room, w/HNO3	Long term (3.5lb/MMacfm)	Hg
10/19/2011	3:30pm	4°C, w/HNO3	Long term (3.5lb/MMacfm)	Hg
10/19/2011	3:30pm	4oC	Long term (3.5lb/MMacfm)	Hg
10/19/2011	3:30pm	Room	Long term (3.5lb/MMacfm)	Hg
10/19/2011	3:30pm	Room	Long term (3.5lb/MMacfm)	Hg

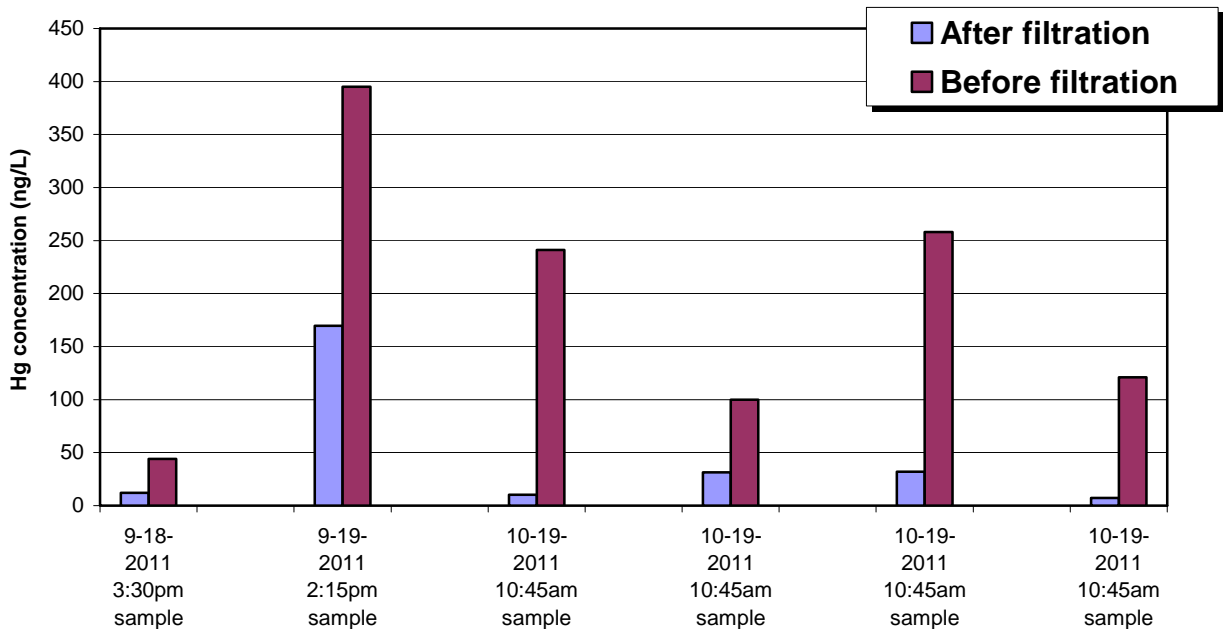
The mercury content of the water samples is presented in Figure 16.

Figure 16. Hg Content in Scrubber Water Samples



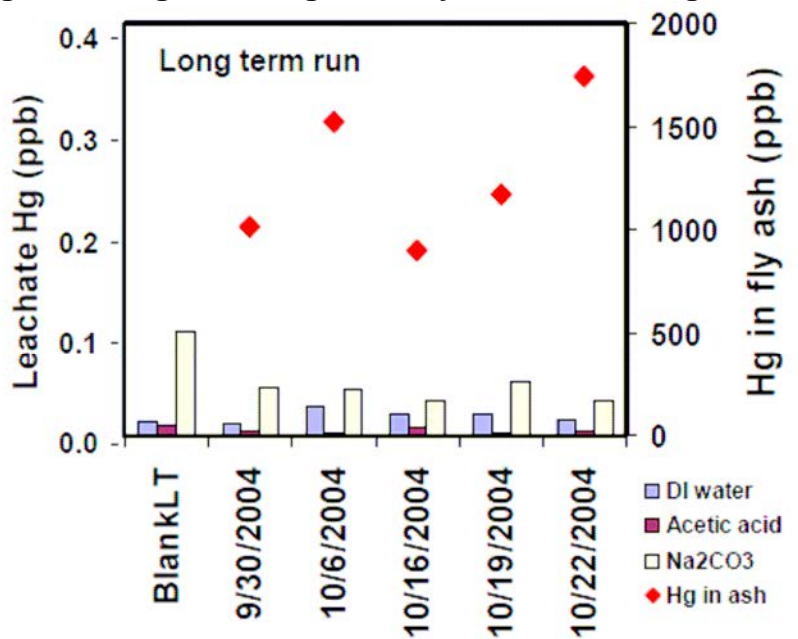
The mercury content of the scrubber water varied between the baseline low value and the baseline high value. The lack of mercury in the scrubber water is not surprising. B-PAC™ is a sorbent that can also capture mercury from water. The impact of filtration on the water samples can be seen in Figure 17.

Figure 17. The Impact of Filtration on Scrubber Water Hg Concentration



The samples were all filtered after the trial using a 0.4 mm glass filter. Filtration greatly reduced the scrubber water mercury concentration. This could be expected since the sorbent had additional capacity onto which the mercury could be captured. This is very similar to the results found when fly ash containing B-PAC™ is put through the U.S. EPA leachate tests. The results from one such series of tests are presented in Figure 18.⁽¹⁾

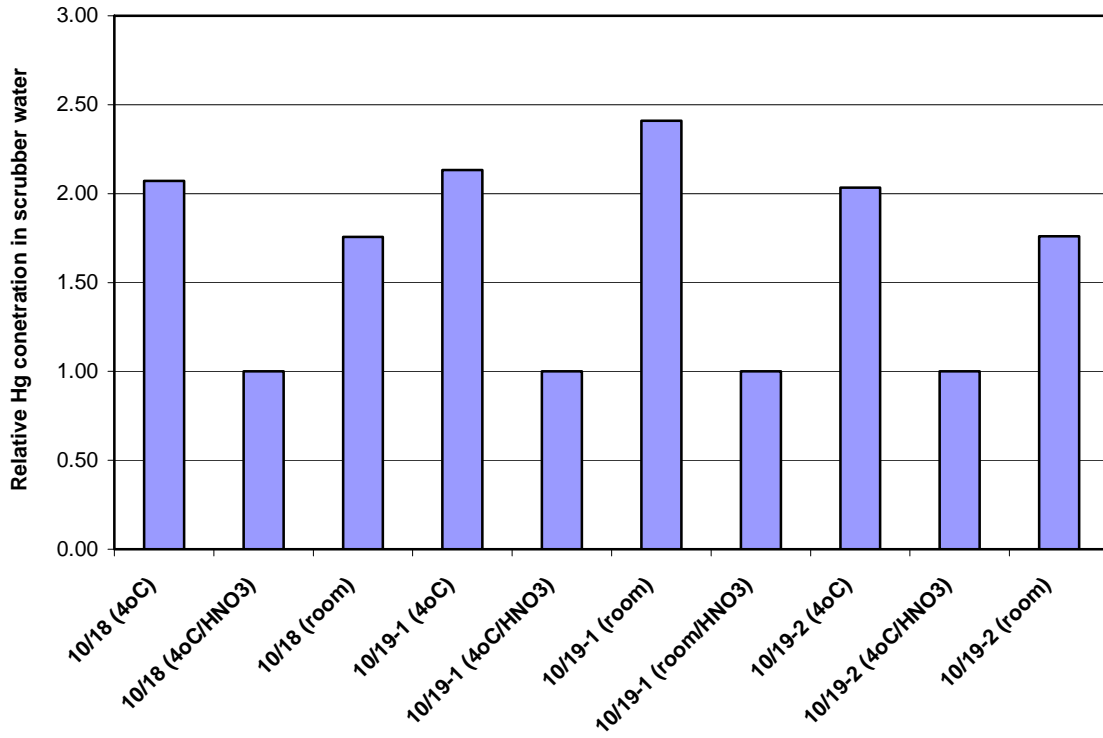
Figure 18. Hg Leaching from Fly Ash Containing B-PAC™



The mercury content of the leachates was below that of the blank in this test series since the sorbent had available mercury capacity and used it on the mercury in the water.

One last evaluation was performed with water samples. The mercury content of samples that had been stored at room temperature were compared to those stored at 4°C. In addition, the mercury content of samples that had been acidified with nitric acid was compared to those that had not. The results of these analyses are presented in Figure 19. There does not appear to be any difference in mercury content of samples stored at room temperature versus those stored at 4°C. This was expected. What was not expected was the impact of acidification. It was thought that acidification would stabilize any mercury in the liquid yielding higher mercury values. Just the opposite was the case. Acidification appears to have driven the mercury into the solids contained in the liquid.

Figure 19. Hg Content of Scrubber Water Treated in Different Manners



Summary and Conclusions

Sorbent testing using both plain and gas-phase brominated B-PAC™ was conducted in 2011 at Hibbing Taconite Line 1. The test program was divided into six tasks. Task 1 was the preliminary site visit to Hibbing Taconite, which was conducted on March 1, 2011. Hibbing Taconite had been selected by MN DNR as the host for the trial. Task 2 of the project was the pre-trial testing which was conducted at Hibbing Taconite from May 30 through June 4, 2011. Task 3 of the project was for equipment preparation while Task 4 was the field trial, which began on 9/13/2011 and ended on 10/22/2011. Task 5 was the analysis of the samples and data collected during the field trial while Task 6 was final report preparation of this report.

The following conclusions were made:

1. It was necessary to inject sorbent into both the Windbox and Hood Exhaust gas streams in order to achieve the target of 75% mercury removal.
2. The target of 75% mercury removal was achieved with an injection rate of about 3 lb/MMacf of B-PAC™.
3. It is believed that even better performance would have been achieved if the desired injection locations could have been utilized, since some sorbent was captured in the multiclone.
4. The 75% mercury reduction target was achieved throughout the two-week continuous run.
5. The scrubber water mercury content did not increase during sorbent injection but the mercury content in the scrubber solids did increase.
6. Storage temperature had no impact on the measured mercury concentration in the scrubber liquor samples but acidification did.
7. The four stacks at Hibbing Taconite Line 1 were very wet making mercury analysis a challenge, especially for sorbent traps and for some particulate separators associated with Hg CEMs.

Recommendations

The trial discussed in this report had limitations which should be addressed in a future trial. The next trial should address the following:

1. The current trial had a continuous run of only two weeks at one plant. A trial lasting several months should be conducted to further verify the long-term performance of the gas phase brominated sorbent at a different taconite facility.
2. Representative green ball and scrubber liquor samples should be collected in order to complete a mercury balance of the system.
3. Better sampling techniques should be developed for sorbent traps.
4. Better injection locations should be utilized in order to obtain better sorbent distribution and, thus, better mercury removal.

References

1. Landreth, R.R., "Advanced Utility Mercury-Sorbent Field-Testing Program", Final Report to the United States Department of Energy, September 15, 2011.

APPENDICES

- A. List of Figures
- B. List of Tables
- C. List of Photographs
- D. DQAW

Appendix A

List of Figures

List of Figures

1. Diagram of the Hibbing Taconite Pellet Firing Equipment
2. Sorbent Injection Locations
3. Diagram of the Mobile Demonstration Unit
4. Injection Locations
5. Stacks 1 & 4 Baseline Mercury Data with Load Rate
6. Injection of Plain PAC on 9/22/2011
7. Injection of B-PAC™ on 9/24/2011
8. Injection of B-PAC™ on 9/25/2011
9. Injection of B-PAC™ on 9/26/2011
10. Parametric Injection Test Results
11. Continuous Run Mercury Removal
12. Continuous Run Mercury Concentrations
13. Hg Content in Green Ball Samples
14. LOI Results for Multiclone Dust Samples
15. Relative Hg Content of Multiclone Dust Samples
16. Relative Hg Content in Scrubber Water Samples
17. The Impact of Filtration on Scrubber Water Hg Concentration
18. Hg Leaching from Fly Ash Containing B-PAC™
19. Hg Content of Scrubber Water Treated in Different Manners

Appendix B

List of Tables

List of Table

1. Ohio Lumex Aqueous Sample Detection Limits
2. Schedule for Testing at Hibbing Taconite
3. Hg Tests at HibTac Line 1 May-June 2011
4. Baseline Sorbent Traps, Stacks 2 & 3
5. Parametric Test Results
6. Parametric Testing CEM Hg Data
7. CEM and Appendix K Trap Hg Removal Data
8. Green Ball Hg Analyses
9. Multiclone Dust Samples Collected during the Trial
10. XRD Analysis of Multiclone Dust
11. List of Scrubber Water Samples

Appendix C

List of Photographs

List of Photographs

1. Albemarle Mobile Demonstration Unit
2. Filter Probe
3. Tekran Mercury Conversion Module and CEM
4. Appendix K Sorbent Trap
5. Ohio Lumex Carbon Trap Mercury Analyzer
6. Ohio Lumex Model RA-915+ Mercury Analyzer with Liquid Sample Analysis Attachment

Appendix D

DQAW

Title of Project: Mercury Control for Taconite Plants Using Gas-Phase Brominated Sorbents

Project Leader: Ron Landreth

Date Submitted: May 10, 2011, Rev 5 Final

(1) Method Description/Key Parameters:

- a. For which taconite plants are the test results from this study most applicable?
 - i. Testing will be performed on the Hibbing Taconite Plant but it is believed that this B-PAC™ technology may be viable for all the plants in this project.
 - ii. Provide an explanation.
 1. Brominated powdered activated carbon, B-PAC™, has been injected into wet and dry scrubbers to successfully control mercury emissions in the utility industry. It has been shown that the mercury captured on the carbon does not leach in wet environments such as scrubbers. It is believed that the B-PAC™ can work similarly in the exhaust gas scrubbing systems of taconite plants.
- b. What specific equations are being used to evaluate Hg removal efficiency from the process stream in your experiment or test?
 - i. Percent reduction basis – for a single pellet product and each B-PAC injection rate, establish percent mercury reduction of stack emissions as measured by a mercury CEM, continuous emission monitor. Uncontrolled mercury emission concentration is measured in a pre-injection test period.

$$Hg \text{ removal}(\%) = \left(1 - \frac{\text{Controlled gas mercury concentration}}{\text{Uncontrolled gas mercury concentration}} \right) \times 100$$

(2) Data Quality Assessment for key variables:

- a. For all variables in the equation for 1(b), what are the baseline values for these parameters in the uncontrolled process stream? Provide an estimate of the uncertainty in these variables (1 SD) and describe how this uncertainty was obtained or estimated.
 - i. The uncontrolled mercury concentration will be measured during a period before injection of B-PAC™. This pre-injection concentration will be used for calculating the percent reduction of mercury during sorbent injection.
 - ii. Uncertainty :
CEM accuracy: 5% uncertainty (1SD) (provided by instrument vendor)

- b. For all variables in the equation for 1(c), what are the baseline values for these parameters in the uncontrolled process stream? Provide an estimate of the uncertainty in these variables (1 SD) and describe how this uncertainty was obtained or estimated.
- c. For each variable in 2a and 2b provide the location of raw data and field logs. These records will be kept for a period of at least three years following acceptance of the final report. See section D in this QAPP for information on how these files will be used.
 - i. Raw data and field logs to be kept electronically in Baton Rouge at Albemarle Corporation's Product Development Center.

(3) Mercury Removal Estimates:

- a. Quantitative estimates: For a taconite plant currently emitting 100 units of mercury per unit time, what do the test results suggest mercury emission rates would be with application of the technology? Using the values in (2), calculate the error (1 SD) in this estimate. As an example, a value of "25 +/- 5" implies 25 units of mercury would be emitted per unit time and that the error in this estimate is 5 units (1 SD) of mercury per unit time).
 - i. Estimated mercury reduction based on utility plant testing, >75% with B-PAC™ injection rate of 2 to 4 lb/MMacf of exhaust gas
 - ii. The uncertainty (1SD) of the Tekran Hg CEM measurement is 5%. For a taconite plant currently emitting 100 units of mercury per unit time, to reach 75% Hg removal, the final stack hg emission is 25 unit+/-1.25 unit, the estimated measurement error is 1.25 units.
- b. Qualitative Factors: For the tests being considered, list critical components of experimental design that were not quantified but which may affect mercury removal in the actual process. For example, if certain components are known to contaminate or interfere with chemical additives, these should be listed.
 - i. Sulfur trioxide, SO₃, in the Windbox exhaust gas could compete with mercury for capture sites on the B-PAC™. SO₃ will be measured in the Windbox exhaust gas during the testing.
 - ii. Iron oxide interactions with mercury vapor could affect mercury speciation in sampling gas stream.

Appendix B-2-4

Developing Cost-Effective Solutions to Reduce Mercury Emissions from Minnesota Taconite Plants. ArcelorMittal Minorca Mine Inc. Plant

September 2012

Developing Cost-Effective Solutions to Reduce Mercury Emissions from Minnesota Taconite Plants

ArcelorMittal Minorca Mine Inc. Plant

Final Report

Prepared by:

ADA Environmental Solutions

9135 S Ridgeline Blvd., Ste 200
Highlands Ranch, CO 80129
Richard Schlager, VP, Technology Services
Jerry Amrhein, Project Manager
Kyle Bowell, Engineer II
(303) 734-1727

Prepared for:

Minnesota Department of Natural Resources

500 Lafayette Rd N
St. Paul, MN 55101
(651) 296-6157

ADA Document No. 2011-0227

ADA-ES Project No. 10-8088

August, 2012

Revised September 2012



DISCLAIMER

ADA, INCORPORATED ASSUMES NO LIABILITY WITH RESPECT TO THE USE OF, OR FOR DAMAGES RESULTING FROM THE USE OF, ANY INFORMATION, METHOD OR PROCESS DISCLOSED OR CONTAINED IN THIS REPORT ISSUED UNDER THE APPLICABLE CONTRACT. ADA, INCORPORATED EXPRESSLY DISCLAIMS AND EXCLUDES ANY AND ALL WARRANTIES, EITHER EXPRESS OF IMPLIED, WHICH MIGHT ARISE UNDER LAW OR EQUITY OR CUSTOM OF TRADE, INCLUDING AND WITHOUT LIMITATION, WARRANTIES OF MERCHANTABILITY AND OF FITNESS FOR SPECIFIED OR INTENDED PURPOSE.

Summary of Acronyms, Abbreviations, and Chemical Symbols

AC	Activated Carbon
ADA-ES or ADA	ADA Environmental Solutions
EPA	Environmental Protection Agency
Hg	Mercury
H _r	Relative Humidity
KT	Kepner-Tregoe
MnDNR	Minnesota Department of Natural Resources
MIM	Mercury Index Method
MTMCAC	Minnesota Taconite Mercury Control Advisory Committee
RPD	Relative Percent Difference
STM	Sorbent Trap Method, modified EPA Method 30B
TMDL	Total Maximum Daily Load

Executive Summary

In 2009, the Minnesota Pollution Control Board developed an Implementation Plan to reduce Minnesota's statewide mercury Total Maximum Daily Load (TMDL). As part of this plan, the taconite industry set a target of 75% reduction in the 2010 mercury air emissions by 2025¹. ADA Environmental Solutions (ADA) proposed a project to The Minnesota Department of Natural Resources (MnDNR) to develop cost-effective solutions to meet the industry goal by reducing mercury emissions from taconite plants by 75%. ADA was contracted to determine if activated carbon (AC) was a viable sorbent to control mercury in process gas from taconite plants when used in a fixed-bed application. The project was funded by the United States Environmental Pollution Agency (US-EPA), facilitated by the MnDNR, and coordinated by the Minnesota Taconite Mercury Control Advisory Committee (MTMCAC). Field testing was conducted at three taconite plants. This report applies specifically to ArcelorMittal Taconite, Virginia, Minnesota.

There were four main tasks defined in the Work Scope for Part 1. The four tasks are listed below.

- Task 1. Slipstream Testing. Screening tests included the relative performance of test materials in actual process gas, impact of relative humidity on performance, and impact of process gas on mercury capture performance compared to controlled laboratory conditions.
- Task 2. Develop a Full-Scale, Integrated Fixed-Bed Process Concept
- Task 3. Techno-Economic Analysis of Mercury Control Options
- Task 4. Pilot-Scale Fixed-Bed Design

Task 1 - Sorbent Screening Slipstream Testing

Screening was conducted using the Mercury Index Method (MIM), a tool based on EPA Reference Method 30B that was developed by ADA for the project. Stack gas from a taconite process was drawn through tubes containing AC sorbents. Each tube contained two sections, the first containing the AC under evaluation mixed with sand, and the second containing a standard EPA Method 30B AC. The Method 30B AC was sufficient to capture all the mercury contained in the sample gas for several days to weeks. The effectiveness of the test AC was determined by measuring the mercury captured in both sections and determining the fraction that passed through the first section into the section containing the Method 30B AC.

Results from Task 1 indicate that all test AC sorbents were effective for mercury removal at ArcelorMittal. Test sorbents included a sulfonated, granular, coconut shell-based carbon; an untreated, pelletized, anthracite-coal based carbon; and a sulfonated, pelletized, anthracite-coal based carbon. The material that comparatively captured the most mercury was the sulfur-treated coconut-shell (CR612C-Hg). Performance sensitivity to changes in process conditions will affect the full-scale design. Therefore, CR612C-Hg was tested in process gas with relative humidity between 50% and 81%. There was no significant impact in mercury capture performance as a result of changes to the relative humidity. Also, mercury removal results

from laboratory testing in dry nitrogen were very similar to results from slipstream tests at ArcelorMittal, indicating that nothing in the process gas at ArcelorMittal during the test period negatively impacted the mercury removal effectiveness. These results are consistent with results from testing conducted at the other two taconite plants.

Task 2 - Develop a Full-Scale, Integrated Fixed-Bed Process Concept

Task 1 screening results and full-scale design criteria were used by activated carbon applications expert Ray Johnson, PhD, to develop a full-scale fixed-bed conceptual design for ArcelorMittal using a design flow of 854,000 ACFM. The design incorporates 22 vessels containing beds of carbon that are each 47 feet long and 12-feet wide and 3 feet deep. An estimated 1,377,288 lbs of AC are required to fill the beds. The estimated pressure drop across is 6 to 12 inches of water. The amount of carbon that would be used per year to maintain 100% mercury capture was projected to be 117,403 lbs. This initial concept design would need to be validated through longer-term pilot testing.

Task 3 - Techno-Economic Analysis

The relative technical and economic characteristics of seven mercury control technologies were compared using a Kepner-Tregoe (KT) decision-making approach by Stantec Consulting Ltd. The fixed-bed method to control mercury was determined to provide good performance but at relatively high cost compared to other options. The high cost was a result of several factors including the number of vessels required and the associated plant integration, and the expected pressure drop across the beds. AC injection was identified as the most promising technology using this approach.

Task 4 - Pilot Plant Design

The estimated cost of a pilot-scale fixed-bed system appropriate to collect detailed information required for a robust full-scale design is \$50,000. All testing costs would be in addition to the cost of the equipment.

Task 1 results indicate fixed-beds of activated carbon can reliably achieve the taconite industry's goal of 75% mercury control. However, based on the Task 2 concept design and the Task 3 relative comparison of technical and economic factors, a fixed-bed approach to control mercury from the process gas at ArcelorMittal is expected to be more costly than other approaches and require multiple, large, interconnected vessels. Therefore, ADA does not recommend continued development and testing of fixed-bed technologies for mercury control from the process gas at ArcelorMittal. Based on results from Task 3, ADA recommends consideration of AC injection as a lower cost option to apply AC to meet the industry goal of 75% mercury control.

Table of Contents

1. Project Overview	1
2. Technical Approach	2
Task 1. Sorbent Screening	2
Phase 1: Relative Efficacy of Various AC Types	2
Phase 2: Evaluate the Effect of Relative Humidity	3
Phase 3: Impacts of Process Gas Constituents.....	3
STM Sampling.....	3
Task 2. Integrated Full-Scale Fixed-Bed Process Concept.....	4
Task 3. Techno-Economic Assessment	4
Task 4. Pilot-Scale Design.....	4
3. ArcelorMittal Taconite Plant System Description	5
4. Test Methods and Materials	6
EPA Method 30B and Sorbent Trap Method.....	6
Mercury Index Method	6
Mercury Analysis.....	7
Quality Assurance.....	8
Sorbent Descriptions.....	8
5. Results and Discussion	10
Task 1: Screening Tests	10
Phase 1: Relative Efficacy of Various AC Types.....	10
Phase 2: Effect of Relative Humidity	12
Phase 3: Impacts of Process Gas Constituents.....	13
STM Stack Sampling Results	14
Task 2. Integrated Full-Scale Fixed-Bed Process Concept.....	15
Task 3. Techno-Economic Summary.....	15
Task 4. Pilot-Scale Design.....	16
6. Conclusions and Recommendations	17
7. References	18
8. Appendices	19



List of Figures

Figure 1: ArcelorMittal Process Flow Diagram.....	5
Figure 2: MIM Sorbent Trap.....	7
Figure 3: Breakthrough after 1-Hour	10
Figure 4: Breakthrough after 3-Hours.....	11
Figure 5: Breakthrough after 10-Hours.....	11
Figure 6: Relative Humidity Comparison for Sabre 8% Br Standard	12
Figure 7: Relative Humidity Comparison for CR612C-Hg Test AC	13
Figure 8: Comparison of Field (Sorbent Screening) and Lab MIM Results.....	14
Figure 9: Sketch of Full-Scale Fixed-Bed Module	15

List of Tables

Table 1: Key STM QA/QC Criteria and Corrective Action	8
Table 2: Sorbent Screening Test Schedule	10
Table 3: Sorbent Performance Decision Matrix	11
Table 4: Average Mercury Concentration of ArcelorMittal’s Stacks.....	15
Table 5: Kepner-Tregoe Decision Matrix.....	16

1. Project Overview

In 2009, the Minnesota Pollution Control Board developed an Implementation Plan to reduce Minnesota's statewide mercury Total Maximum Daily Load (TMDL). As part of this plan, the taconite industry set a target of 75% reduction in the 2010 mercury air emissions by 2025¹. ADA Environmental Solutions (ADA) proposed a project to The Minnesota Department of Natural Resources (MnDNR) to develop cost-effective solutions to reduce meet the industry goal by reducing mercury emissions from taconite plants by 75%. The ADA proposal was a three-part study to assess the use of activated carbon based technologies. The first part of the study (Part 1) was to determine if activated carbon (AC) was a viable sorbent to control mercury in process gas from taconite plants. Part 2 was pilot-scale testing, and Part 3 was full-scale validation. Only Part 1 of ADA's proposal was approved, and ADA was contracted to focus on fixed-bed applications of AC. The project was funded by the United States Environmental Pollution Agency (US-EPA), facilitated by the MnDNR, and coordinated by the Minnesota Taconite Mercury Control Advisory Committee (MTMCAC). Field testing was conducted at three taconite plants. This report applies specifically to ArcelorMittal Taconite, Virginia, Minnesota.

There were four main tasks defined in the Work Scope for this project, and the key Task 1 objectives, are listed below.

Task 1. Sorbent Screening Tests

- Compare the performance of different AC and select the best performer based on mercury adsorption capacity and break through.
- Study the effects of relative humidity (H_r) on the performance of AC.
- Determine if any constituent in taconite process gas negatively impacts mercury capture.

Task 2. Develop a Full-Scale, Integrated Fixed-Bed Process Concept

Task 3. Techno-Economic Analysis of Mercury Control Options

Task 4. Pilot-Scale Fixed-Bed Design

2. Technical Approach

Task 1. Sorbent Screening

ADA developed the Mercury Index Method (MIM) and performed sorbent screening tests on commercially available AC on Stack D at ArcelorMittal's production line. The MIM is a derivative of EPA Method 30B², an industry standard for measuring mercury in a process gas. During MIM testing, stack gas from a taconite process was drawn through tubes containing AC sorbents. Each tube contained two sections, the first containing the AC under evaluation mixed with sand, and the second containing a standard EPA Method 30B AC. The Method 30B AC was sufficient to capture all the mercury contained in the sample gas for several days to weeks. The effectiveness of the test AC was determined by measuring the mercury captured in both sections and determining the fraction that passed through the first section into the section containing the Method 30B AC. The percent mercury contained in the second section is classified as the percent breakthrough from the first trap to the second trap. No breakthrough (0%) indicates all mercury was captured in the section of test AC. Full breakthrough (100%) indicates that the test AC did not capture any mercury and it all passed to the section containing the Method 30B carbon. A description of the MIM method is included in Section 4, Test Methods and Materials.

In the MIM trap, the first section AC is replaced with a mixture of inert material and small amounts of the powdered AC under evaluation. Although granular or pelletized carbon is typically used in a full-scale fixed-bed system, powdered AC is used for screening tests so that the mass of AC used can be limited to manage the test duration to hours rather than weeks or months. Screening tests to determine viability and relative performance are often conducted prior to investing resources into long-term field testing. A typical fixed-bed pilot-scale test would be designed so that breakthrough on a single carbon may take weeks or months, which can add unnecessary time and costs when the goal is initial screening. While long-duration tests are not appropriate for a screening tool, these are required to collect the information required for a robust and detailed full-scale design and would be appropriate if the project progressed to Part 2, pilot testing.

Task 1 included three objectives. The Task 3 activities were divided into three phases to address the three objectives. These phases are described below.

Phase 1: Relative Efficacy of Various AC Types

To achieve the first Task 1 objective, ADA tested four carbons at one, three, and ten hour periods to determine the relative performance of the materials. The criteria established compare relative performance was breakthrough from the section of test AC to the section of Method 30B AC. Percent breakthrough is defined as the mass of mercury in the second trap section divided by the total collected in both sections. It was determined in the lab before the test that a ten hour period was sufficient to assure significant breakthrough. Tests were repeated on separate days as a quality assurance measure. For all tests in Phase 1, the relative humidity, H_r , was maintained at 50%, and each trap was sampled at the same gas extraction rate. Once sampling was complete,

the traps were returned to ADA's laboratory in Littleton, CO and analyzed with the Ohio Lumex analyzer.

Phase 2: Evaluate the Effect of Relative Humidity

The second Task 1 objective was to determine the effect of H_r on carbon performance in fixed beds. High H_r is known in the industry to negatively impact performance. The effect of H_r may have important ramifications on the design of a full-scale fixed-bed system. If high humidity reduces mercury adsorption, a costly preheating or drying system may be required upstream of the fixed bed system.

The best performing sorbent from Phase 1 testing and the standard were tested simultaneously at each H_r levels for one, three, and ten hour periods. H_r levels included one representing the maximum H_r recommended in the industry (50%), one median H_r (75%), and one representing the H_r for a minimum temperature increase of 5°F over stack conditions (81%). H_r was easily adjusted by changing the operating temperature of the aluminum heating block at the tip of the MIM probe containing the sorbent traps. This approach was based on the assumption that the stack gas, which is downstream of a venturi scrubber, would be saturated ($H_r = 100\%$), and daily wet bulb/dry bulb measurements showed that the actual H_r averaged about 94%. The traps were returned to ADA for analysis.

Phase 3: Impacts of Process Gas Constituents

The final Task 1 objective was to determine if any constituent in taconite process gas could negatively impact carbon performance. Constituents such as sulfur trioxide have been shown to impact the effectiveness of AC for mercury capture in the utility industry³.

Performance data from MIM testing at ArcelorMittal was compared to similar tests performed at ADA under ideal lab conditions using mercury in dry nitrogen. Nine traps were run and the results averaged. These results were then compared to MIM field data collected at ArcelorMittal. Any significant decrease in sorbent screening performance could then be attributed to a constituent in the gas that prevented or decreased mercury capture on the carbon. The laboratory test apparatus consisted of standard Method 30B equipment, and a Thermo Fisher 81i Mercury Calibrator to generate a gas stream with a steady mercury concentration of $10\mu\text{g}/\text{m}^3$. This mercury concentration was selected based on prior discussions with the plant and was decided to be a safe, high-end representative of the expected mercury emissions. The same type of MIM traps were used in the laboratory and in the field.

STM Sampling

ADA also performed sorbent trap method (STM) measurements on the three stacks which were not used for MIM testing, Stacks A, B, and C. The test was done to determine the mercury variability between stacks. A description of the STM is included in Section 4 Test Methods and Materials.

Although the MIM results provide valuable insights, it should be stressed that the results do not provide all the information needed to design a full-scale fixed-bed system, nor can they be

used to directly predict full-scale fixed-bed performance. For example, 100% mercury capture cannot be definitively demonstrated using the MIM technique because the calculated breakthrough will always be $> 0\%$ due to the trace levels of mercury present in the section 2 trap prior to exposure to process gas.

Task 2. Integrated Full-Scale Fixed-Bed Process Concept

ADA contracted with Ray Johnson, PhD, the principal consultant with Activated Carbon Technologies, LLC, to develop a full-scale integrated fixed-bed process concept based on results from screening tests from ArcelorMittal in combination with other data available in the industry, and a Design Guide developed by the U. S. Army Corps of Engineers⁴. Dr. Johnson has been in the activated carbon industry for 40 years, and he has first-hand knowledge of the two primary carbon production processes, chemical and thermal activation, plus thermal reactivation/recycle of previously used carbon.

Screening tests, such as those conducted during Task 1, can and are utilized to identify gas streams unsuitable for mercury removal by AC. For gas streams where AC is suitable, industry standard design criteria provides for excess mercury removal capacity so that for a well-designed fixed-bed system, 100% mercury removal is achieved until initial breakthrough occurs. Commercial fixed-bed systems are designed to assure that beds are replaced or recharged well before initial mercury breakthrough is expected. Pilot tests are typically conducted to collect the data necessary, including breakthrough characterization, to complete the design engineering of the full-scale systems.

Task 3. Techno-Economic Assessment

ADA subcontracted Stantec Consulting Ltd. to compare the different technical and economic aspects of seven mercury control technologies using a Kepner-Tregoe (KT) decision-making approach⁵. The selected control technologies were identified by ADA as options for mercury control at taconite facilities and presented to the industry for approval during an industry update meeting on April 2, 2012. This presentation is included in Appendix D for reference. The selected technologies were: 1) monolithic polymer resin adsorber, 2) AC injection, 3) oxidant chemical addition, 4) AC injection + fabric filter; 4) AC fixed-bed adsorber, 5) AC fixed-bed adsorber + fabric filter, and 6) AC monolith.

Task 4. Pilot-Scale Design

Dr. Johnson prepared a design and parts list for a pilot system to complete the obligations of this project.

3. ArcelorMittal Taconite Plant System Description

The ArcelorMittal Taconite Plant processes taconite and is located along the Mesabi Iron Range near the town of Virginia, Minnesota. The plant uses a natural gas-fired straight grate furnace for its indurating process. ArcelorMittal operates one straight grate furnace line which has four stack vents. Figure 1 is a flow diagram of the ArcelorMittal processing plant.

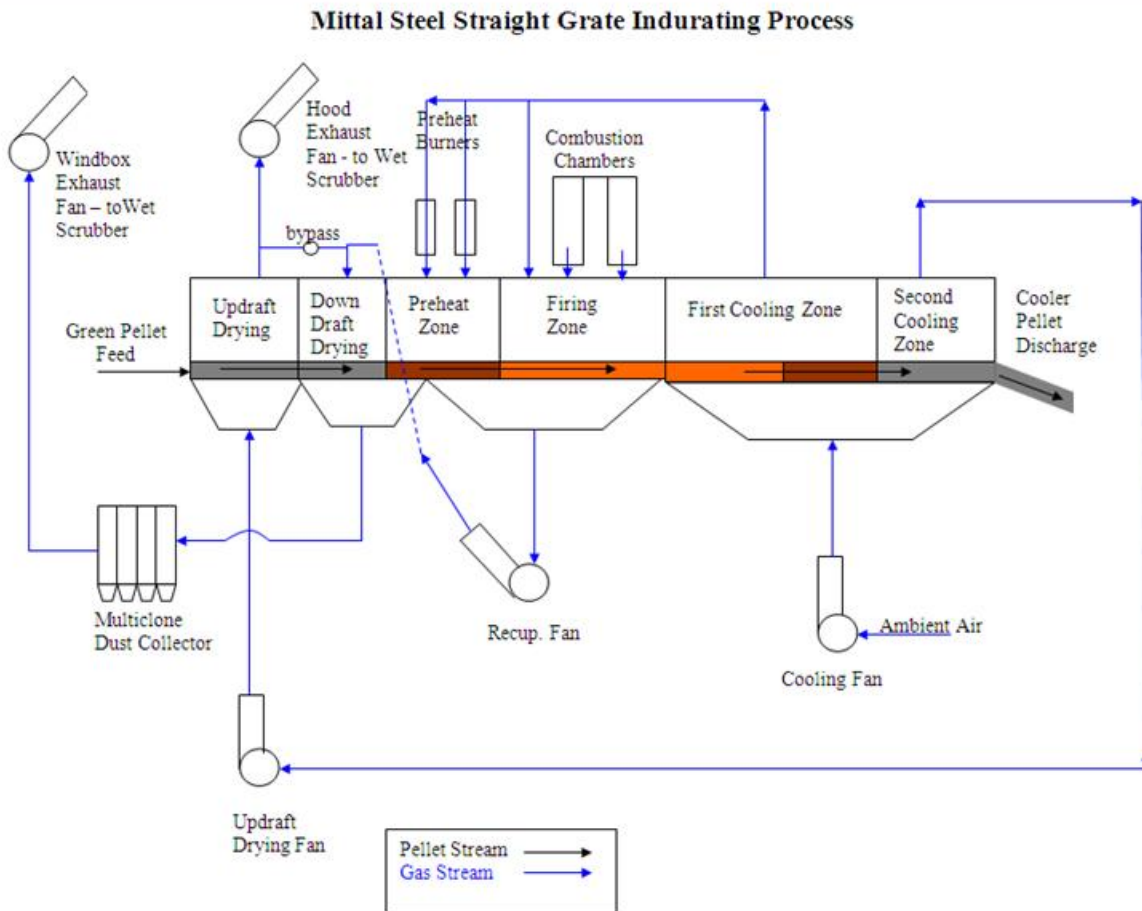


Figure 1: ArcelorMittal Process Flow Diagram

ADA performed all testing on the stacks downstream of the venturi wet scrubber. This was determined by the MnDNR, ArcelorMittal and ADA to be the best test location because it typically has the highest Hg concentration and is most representative of the gas stream that would be routed to a retrofitted fixed-bed treatment system. Test equipment was installed at existing sample ports on Stack D. Two sample ports were used on Stack D so that four sorbents could be run simultaneously. STM measurements were also performed on Stacks A, B, and C to confirm that this stack had the highest Hg concentration.

4. Test Methods and Materials

This section describes the testing methods that were used by ADA, including the Quality Assurance (QA) Program, and descriptions of the selected sorbents.

EPA Method 30B and Sorbent Trap Method

EPA Reference Method 30B² is commonly used in the electric utility industry to measure gas-phase mercury in flue gas. ADA's Sorbent Trap Method (STM) is Method 30B with slight modifications to some of the quality assurance criteria.

Both methods utilize two sections of 10 mm diameter glass tubes loaded with AC (trap) to capture mercury. Two carbon-filled glass tubes are inserted into the tip of the sampling probe which is then inserted directly into the gas stream. A measured volume of gas is drawn through the glass tubes, or mercury traps, at a constant flow rate. Mercury is captured by the AC. The traps are then analyzed for mercury in the laboratory using standard analytical techniques that meet specifications described Method 30B. For the traps used in this program, the carbon was heated to thermally desorb the mercury and the mercury was measured using atomic absorption spectroscopy. The concentration of mercury in the gas is calculated by dividing the mass captured by the gas volume drawn through the trap.

Each trap section normally contains enough carbon to adsorb several weeks of mercury. The second section of AC is used as a back-up for the first trap to capture any mercury that breaks through. If more than 10% of the total mercury is measured in the second section, the trap does not pass the quality assurance criteria. This is an EPA Method 30B criterion and effectively sets the upper limit for the relative amount of mercury that can be present in the "blank" carbon used to fill the traps. A more detailed description of the STM technique and a table showing the differences between the STM and Method 30B is included in Appendix E.

Mercury Index Method

ADA developed the Mercury Index Method (MIM) as a relatively simple method to quickly compare the mercury capture characteristics of various sorbents under a variety of process conditions. The MIM is a derivative of EPA Method 30B where the Method 30B AC in first section of the sampling tube is replaced with a very small amount of test AC mixed with an inert medium. The second section of the glass tube is the standard Method 30B AC-filled tube. The amount of test AC in the first section is limited so that the test AC will become completely saturated with mercury within a few hours. Any mercury that passes through the first section is captured by the AC in the second section. Figure 2 shows a MIM sorbent trap with the sections labeled.

The goal of the MIM screening tests is to achieve typically more than 20% and less than 80% breakthrough from the first (test) trap to the second (Method 30B AC) trap so that the relative performance of different test AC materials can be compared. Other key operating procedures are similar to the EPA Method 30B testing protocol.

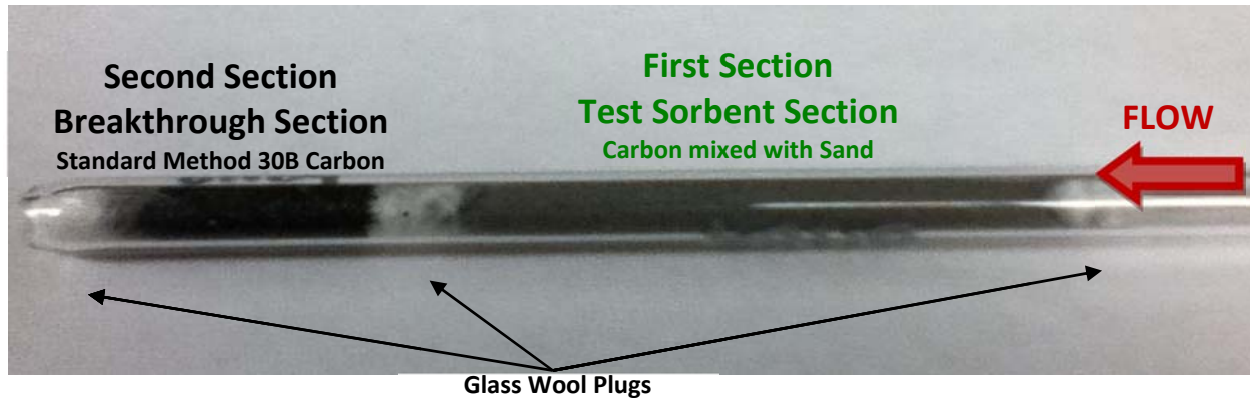


Figure 2: MIM Sorbent Trap

ADA assembled each of the test traps in a clean lab, beginning with empty, 10 mm diameter, standard, Method 30B glass tubes. The four sorbents were each ground and sieved until 95% by weight passed through a 325 mesh (45 μ m) screen and then mixed with an inert medium. The mixture was put into separate traps and backed up with a standard carbon section. Sections of the trap were separated by glass wool plugs.

Standard Method 30B sampling systems, model Hg-324K by the Environmental Supply Company, were used for the MIM tests. These systems consist of a probe, sample line, water knock outs and gas measurement and control console. Two MIM sorbent traps were inserted into the tip of each of two probes so that four sorbents could be tested simultaneously. Test duration, sample flow rate, and test bed temperature were controlled independently for each pair of traps.

Using the MIM test, the relative performance of a variety of AC samples under various operating conditions can be quickly determined. This allows the researchers to accurately determine the overall suitability of AC for mercury control with actual process gas conditions. Performance can also be compared to results in a controlled laboratory environment with mercury-laden laboratory gas to determine if the actual process gas introduces any trace elements that may interfere with mercury capture by the AC.

Mercury Analysis

Mercury captured in the AC traps was analyzed using an Ohio Lumex RA-915+ mercury analyzer. The procedure meets the requirements of EPA Method 30B and is the typical analytical technique used for this method. The principle of operation is atomic adsorption spectrometry. The two sections of each test trap were analyzed separately in the RP-C91 furnace attachment. The glass wool plugs and any ash drawn into the trap were analyzed with the subsequent trap section. In the RP-C91 furnace attachment, mercury is vaporized and the gas passes through the RA-915+ analyzer. The RA-915+ produces a desorption curve and the mass of mercury emitted from the sample is determined by comparing the area under the curve to a calibration curve created using NIST traceable mercury standards.



Quality Assurance

ADA’s Quality Assurance (QA) Program focused on maintaining consistency and accuracy of the sorbent screening and laboratory sampling equipment, the procedures used to collect the samples, and the laboratory equipment and procedures used to analyze the samples. The QA/QC Criteria for this program along with the corresponding corrective action is shown in Table 1. The Data Quality Assessment Worksheet (DQAW) for this program and additional QA information and records are included in Appendix F.

Table 1: Key STM QA/QC Criteria and Corrective Action

	QA/QC Specification (performed by)	Acceptance Criteria	Frequency and Requirement	Corrective Action
STM	Pre-test Leak-check (ADA-ES)	≤4% of target sampling rate	Prior to sampling, sampling lines and probe with sorbent traps in place and capped	Repair Leak. Do not start test until leak check is passed
	Post-test Leak-check (ADA-ES)	≤4% of average sampling rate	After sampling, sampling lines and probe with sorbent traps in place and capped	Flag data repeat run if necessary
	Dry Gas Meter Calibration (Environmental Supply)	Calibration factor (Y) within ±5% of average value from initial (3-point)	Prior to Initial Use: at 3 orifice settings; then Quarterly: at 1 setting	Recalibrate the meter at 3 orifice settings to determine new value of Y.
	Temperature Sensor Calibration (Environmental Supply)	Absolute temperature from sensor within ±1.5% of a reference sensor	Prior to Initial Use: then Quarterly	Recalibrate. Sensor not to be used until criteria is met.
	Barometer Calibration (Environmental Supply)	Absolute pressure by instrument within ±10mm Hg or reading with a mercury barometer	Prior to Initial Use: then Quarterly	Recalibrate. Instrument not to be used until criteria is met.
	Flowmeter Calibration (Environmental Supply)	Calibrate instrument voltage to reference flow until linear	Prior to Initial Use: then Quarterly	Recalibrate. Instrument not to be used until criteria is met.
	Flowmeter check (ADA-ES)	Total flow by instrument ±10% of a reference flowmeter	After Initial Use; then after each testing period, not to exceed Quarterly.	Recalibrate. Instrument not to be used until criteria is met.
Lab	Ohio Lumex Calibration (ADA-ES)	Mass of mercury measured within ±10% of mercury standard (≥3 point)	Prior to Initial Use; then daily	Recalibrate. Instrument not to be used until criteria is met.
	Ohio Lumex check (ADA-ES)	Mass of mercury measured within ±10% of mercury standard	After every 10-15 testing runs	Recalibrate. Instrument not to be used until criteria is met.

Note: Additional steps were taken while handling the traps to eliminate possible contamination. The sorbent traps were sealed at both ends with a tight cap and kept inside a sealed plastic bag until ready for use, at which time a clean pair of sampling gloves was worn during handling. The caps were not removed until the last possible moment before inserting the trap in the probe or the stack.

Sorbent Descriptions

Four different sorbents obtained from Carbon Resources, an industry provider of carbon for fixed-bed systems, were selected for Task 1 sorbent screening.

- Sabre 8% Br: Fine-grain, brominated, lignite-based. This sorbent was selected by ADA as the standard sorbent because it is known by ADA to have excellent mercury absorption

capacity. However, fine grain material is not appropriate for fixed-bed applications because of the high pressure drop associated with beds of fine material and the likelihood that fine material will be carried out of the bed. Bromination enhances mercury capture of gaseous elemental mercury and may provide better performance at higher temperatures (>325°F) than untreated sorbents. It was ground and sieved for use in the MIM traps.

- CR4AN: Pelletized, untreated, anthracite-based. This carbon is pelletized for use in full-scale applications to provide a large surface area and high mechanical hardness. CR4AN is also noted to have excellent pore volume and chemical stability. It was ground and sieved for use in the MIM traps.
- CR4AN-Hg: Pelletized, sulfonated, anthracite-based. Similar to CR4AN but impregnated with sulfur to react with mercury to form mercuric sulfide. It was ground and sieved for use in the MIM traps.
- CR612C-Hg: Coarse-grained, sulfonated, coconut shell-based. This carbon is also designed to react with mercury to form mercuric sulfide. It was chosen as being different from the other two in that it is granular and coconut shell based. It was ground and sieved for use in the MIM traps.

5. Results and Discussion

Task 1: Screening Tests

Table 2 shows the project schedule for Task 1 as it was actually conducted.

Table 2: Sorbent Screening Test Schedule

ArcelorMittal Taconite Test Schedule		9/5/2011	9/6/2011	9/7/2011	9/8/2011	9/9/2011	9/10/2011	9/11/2011
		M	T	W	Th	F	S	S
Test Description								
1	Arrive/Site Safety Orientation (7:00)		X					
2	Install Test Equipment		X					
3	Phase 1 - AC Comparison Test on Stack D		X	X				
4	Send traps to ADA for analysis				X			
5	Conduct STM Tests on Stacks A, B, and C				X			
6	Phase 2 - Relative Humidity Test on Stack D					X	X	X
7	Demobilization							X
8	Phase 3 - Gas Contaminate Study at ADA Lab							

Phase 1: Relative Efficacy of Various AC Types

Phase 1 testing occurred from September 6, 2011 until September 7, 2011 on Stack D of the single production line at ArcelorMittal. The results of Phase 1, shown Figures 3 through 5, are the percent breakthrough (mass of mercury in the second trap section divided by the total mass in both sections) for each of the test runs and duplicate tests (Run 1 and 2, respectively). The “best” performer is defined as the sorbent with the lowest percent breakthrough. The results from Phase 1 were also used to determine which sorbents to use in Phase 2. The AC sorbents are identified as follows: 1) Sabre 8% Br, 2) CR4AN, 3) CR4AN-Hg, 4) CR612C-Hg.

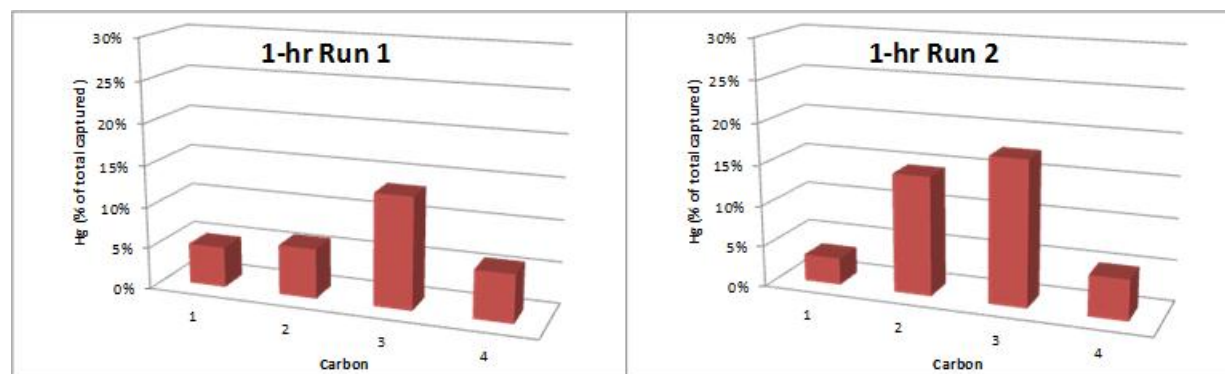


Figure 3: Breakthrough after 1-Hour

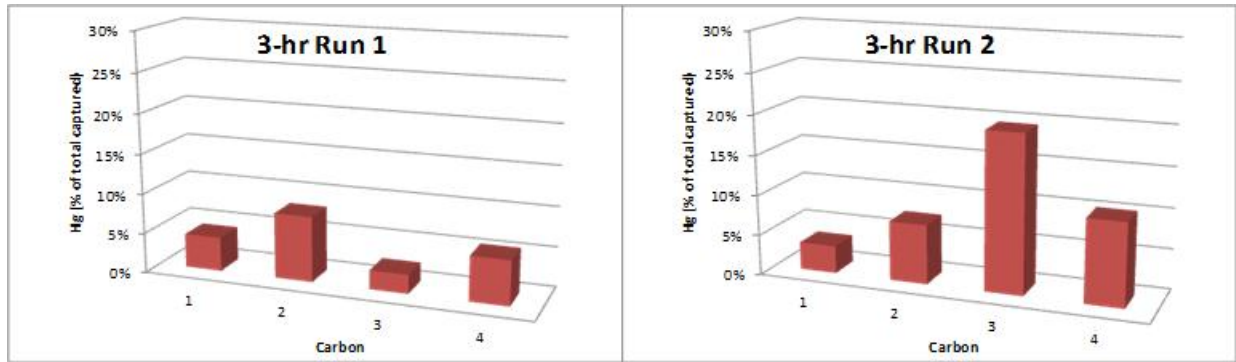


Figure 4: Breakthrough after 3-Hours

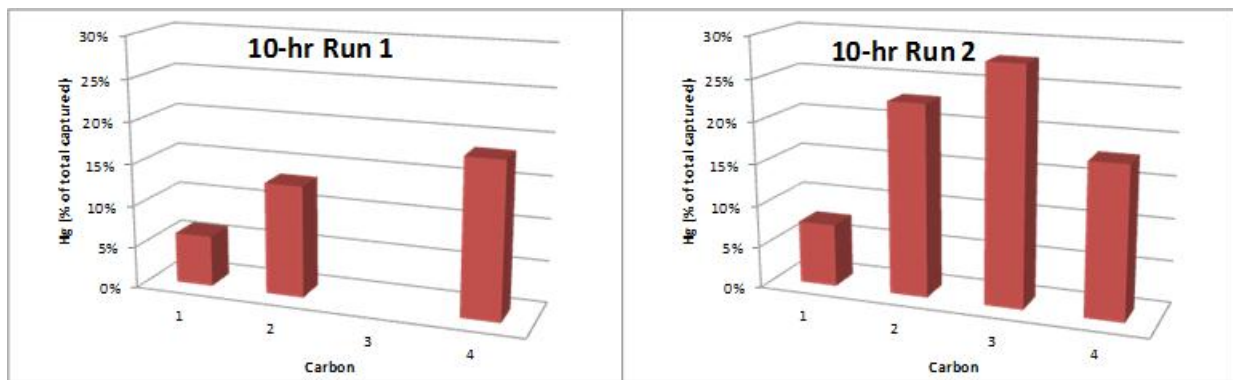


Figure 5: Breakthrough after 10-Hours

The Sabre 8% Br standard carbon had low percent breakthrough, which was expected because it was the benchmark standard chosen for the test. However this product is only offered commercially in powdered form and is therefore not appropriate for use in fixed beds unless it was pelletized. A decision matrix was developed to rank the performance of the three remaining fixed-bed test sorbents

In Table 3, results from each test run were analyzed separately and each of the three test ACs was given a score based on its comparative performance to the other two ACs. If the AC had the lowest percent breakthrough it was given a score of 3, the median percent breakthrough scored 2, and the highest percent breakthrough scored 1. These scores were then weighted by multiplying them by the test length hours. Weighting was deemed necessary because the ten hour tests are comparatively more important than the shorter tests. The scores for each carbon were then summed, and CR612C-Hg (Carbon 4) was identified as the best performer.

Table 3: Sorbent Performance Decision Matrix

RUN 1					RUN 2						
Weighted Multiplier					Weighted Multiplier						
CARBON	1	3	10	SCORE	CARBON	1	3	10	SCORE	CARBON	TOTAL SCORE
2	2	3	30	35	2	2	9	20	31	2	66
3	1	9	10	20	3	1	3	10	14	3	34
4	3	6	20	29	4	3	6	30	39	4	68

2: CR4AN, 3: CR4AN-Hg, 4: CR612C-Hg

Similar results were obtained at the two other taconite plants tested by ADA confirming that CR612C-Hg was the best performer. CR612C-Hg was used in Phase 2.

Phase 2: Effect of Relative Humidity

Phase 2 testing occurred from September 9, 2011 to September 11, 2011 on Stack D of ArcelorMittal’s single production line. Figures 6 and 7 show the mercury capture (the mass of mercury in each section divided by the total mass of mercury in the trap) at 81%, 75%, and 50% H_r for the standard sorbent and for CR612C-Hg. The figures show that there is no significant decrease in performance for increased H_r.

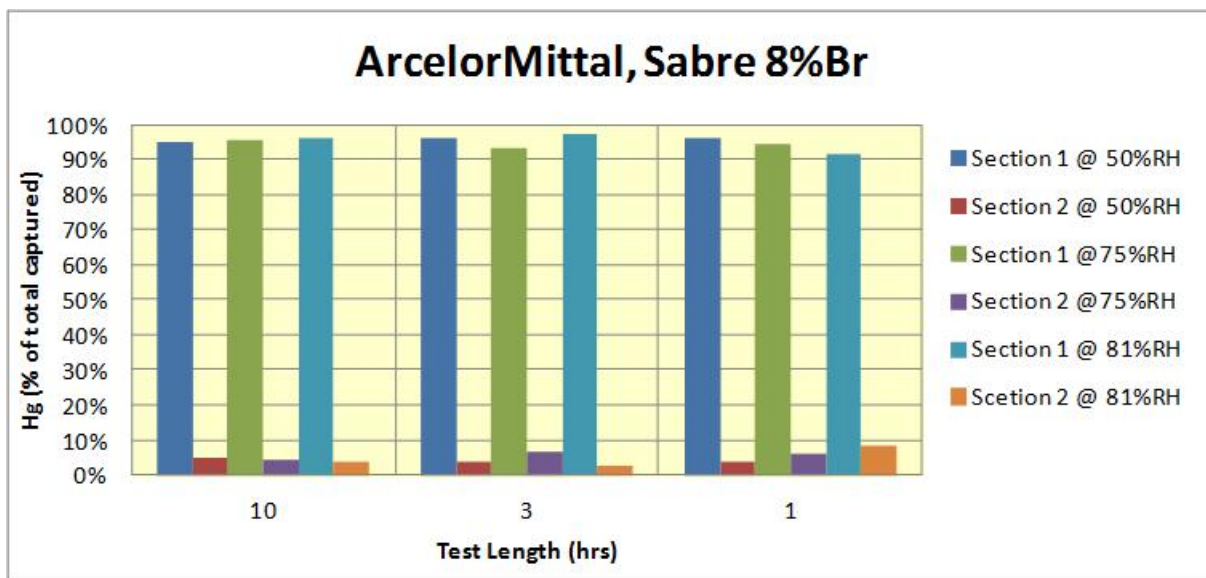


Figure 6: Relative Humidity Comparison for Sabre 8% Br Standard

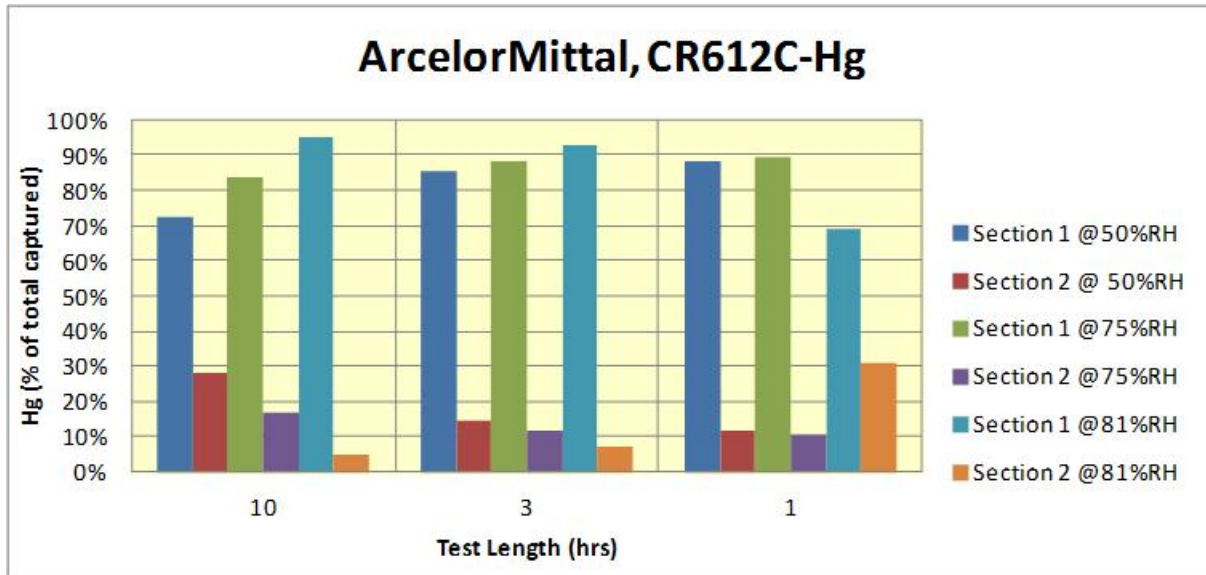


Figure 7: Relative Humidity Comparison for CR612C-Hg Test AC

Phase 3: Impacts of Process Gas Constituents

Figure 8 shows the average mercury capture of the lab tests compared to the MIM field tests. The data indicates that mercury capture was not significantly reduced in the actual process gas compared to laboratory gas. This indicates that there was no contaminating constituent in the taconite process gas that affected the mercury capture performance of the AC during the testing period.

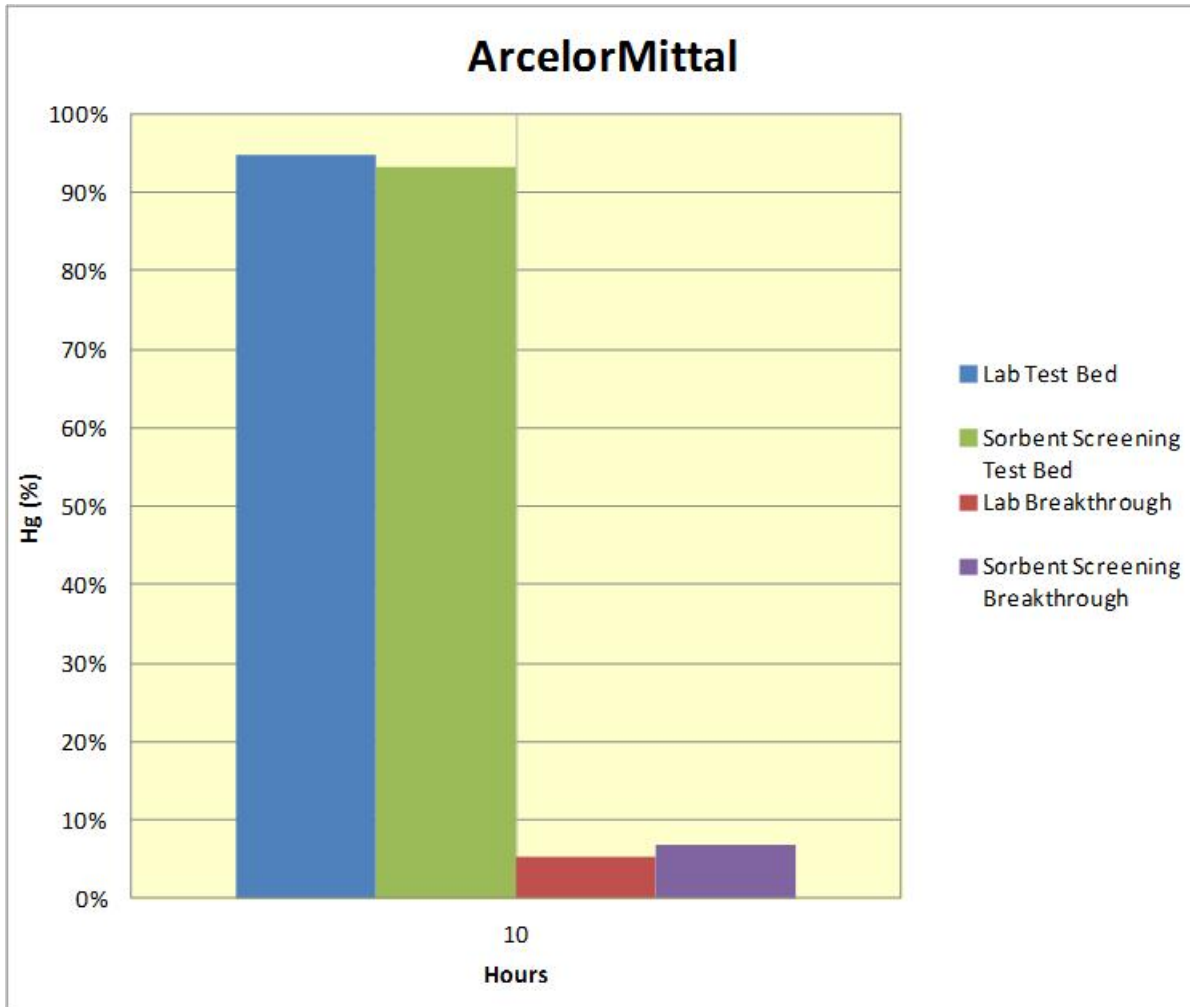


Figure 8: Comparison of Field (Sorbent Screening) and Lab MIM Results

STM Stack Sampling Results

On 9/8/11, ADA performed STM measurements on the three stacks which were not used for MIM testing, Stacks A, B, and C. These measurements were done to determine if there was mercury variability between stacks. Three STM pairs were collected during one-hour runs (raw data presented in Appendix E). The average mercury concentration of each stack is summarized in Table 4. Calculated total mercury from CR612C-Hg (Carbon 4) testing in Phases 1 and 2 is included in the average for Stack D and shown in Table 4. Samples were collected on Stack A and B simultaneously, and Stack A and C simultaneously. In general, Stacks A and B resulted in the lower mercury and Stacks C and D resulted in the higher mercury. Note that the units [ng/l]_{dry} are identical to µg/dscm.

Table 4: Average Mercury Concentration of ArcelorMittal’s Stacks

Stack	Hg _{AVG} [ng/L] _{dry}
A	2.81
B	3.96
C	6.90
D	6.75

Note: Hg concentrations may not be representative of long term operation.

Task 2. Integrated Full-Scale Fixed-Bed Process Concept

Based on an operating process gas flow of 854,000 ACFM at ArcelorMittal, Dr. Johnson recommended 22 fixed-beds of carbon with dimensions of 47-feet long, 12-feet wide, and 3 feet deep in separate cylindrical vessels, as shown in Figure 9. Approximately 1,377,288 lbs of carbon would be required to fill the beds. The estimated pressure drop across the beds is 6 to 12 inches of water. The amount of carbon that would be used per year, based on results from the Task 1 screening tests, is projected to be 117,403 lbs. This would need to be validated through pilot testing. For an actual full-scale design, ArcelorMittal would need to specify the desired design flow condition. Dr. Johnson’s design report is included as Appendix A.

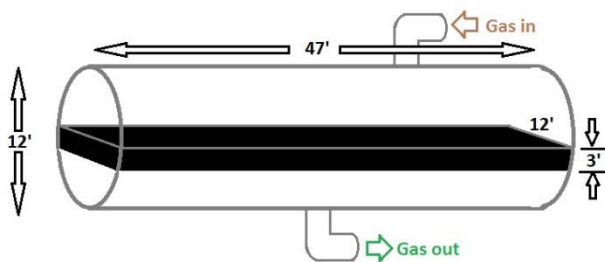


Figure 9: Sketch of Full-Scale Fixed-Bed Module

Task 3. Techno-Economic Summary

Stantec compared the technologies for both a general straight-grate taconite process and a grate kiln process and ranked them using a Kepner-Tregoe decision-making approach. Rankings were based on various technical and economic factors. The results of the assessment are summarized in Table 5, where the maximum possible score for any technology option is 1000. There was no difference in the score for the straight grate or grate kiln process. Two technology options, the polymer monolith and the AC monolith, are not included in the table because neither is currently offered commercially.

Based on this assessment and comparison to other technology options, the fixed-bed was determined to provide good performance but was expected to have a relatively high cost. The high cost was a result of several factors including the number of vessels required and the



associated plant integration, and the expected pressure drop across the beds. The Stantec report is included as Appendix C.

Table 5: Kepner-Tregoe Decision Matrix

Technology	Grand Total	Positive Attributes	Negative Attributes
ACI Injection	713	Reasonable performance at very low cost.	Questionable performance, limited specific experience.
Oxidant Chemical Addition	716-706	Reasonable performance at very low cost. Has been trialed on actual waste gas.	Mixed results with many difference oxidants.
ACI + Fabric Filter	686	Good performance. Good co-benefits.	Large footprint, high pressure drop.
Fixed-bed Adsorber	587	Good performance.	Very large footprint, high pressure drop. Very high capital cost.
Fixed-bed Adsorber + Fabric Filter	515.5	Good performance. Good co-benefits.	Largest footprint, highest pressure drop. Very high capital cost.

Task 4. Pilot-Scale Design

Dr. Johnson prepared a design and parts list for a pilot system to complete the obligations of Task 4 of this project. He estimated the parts could be purchased for less than \$20,000. Although not included in Dr. Johnson’s estimate, it is reasonable to assume that the labor to assemble the parts and check-out the operation will result in a multiplier of 2 to 2.5, resulting in an overall cost of nominally \$50,000. This estimate only included the pilot-scale equipment. Therefore, all testing costs would be in addition to the cost of the equipment. The pilot-scale design report is included as Appendix B.

6. Conclusions and Recommendations

Results from Task 1 indicate fixed-beds of activated carbon can achieve the taconite industry's goal of 75% mercury control, with the caveat that these results were obtained from short-duration screening tests. Specific objectives from Task 1: Slipstream Testing and the related observations are shown below:

Objective 1: Relative differences in sorbent performance:

- All test samples showed some initial calculated breakthrough at one hour. This may have been a result of mercury present on the carbon in the second section trap prior to exposure to process gas.
- The sulfur-treated coconut-shell (CR612C-Hg) performed best of all fixed-bed candidates.

Objective 2: Effects of Relative Humidity

- No significant reduction in mercury capacity of the best-performing AC (CR612C-Hg) was observed when changing the relative humidity between 81%, 75%, and 50%. This is consistent with the results from the test standard AC (Sabre 8% Br). Pilot-scale testing is recommended to confirm this result.

Objective 3: Process Gas Impacts

- MIM evaluations conducted using a slipstream of gas from ArcelorMittal compared well to MIM tests conducted using mercury in dry nitrogen in the laboratory. This indicates that nothing in the process gas at ArcelorMittal during the test period negatively impacted the mercury removal effectiveness of the activated carbons included in the test program.

Analysis of test results for Tasks 2 and 3 show that a fixed-bed approach is not the most cost-effective application of activated carbon. Based on the findings in Task 2 and 3, ADA does not recommend continued development and testing of fixed-bed technologies for mercury control from taconite plants. Based on results from Task 3, ADA recommends industry consideration of activated carbon injection as a lower cost option to apply AC to meet the industry mercury control goals.

7. References

- 1) Implementation Plan of Minnesota’s Statewide Mercury Total Maximum Daily Load. Minnesota Pollution Control Agency Publication wq-iw4-01p. October 2009.
- 2) METHOD 30B – DETERMINATION OF TOTAL VAPOR PHASE MERCURY EMISSIONS FROM COAL-FIRED COMBUSTION SOURCES USING CARBON SORBENT TRAPS - <http://www.epa.gov/ttn/emc/promgate/Meth30B.pdf> accessed 8/2/2012
- 3) Campbell et al. “Mercury Control with Activated Carbon: Results from Plants with High SO₃” Paper #08-A-174. Presented at the Power Plant Air Pollutant Control “Mega” Symposium, Baltimore, MD, August 25-28, 2008.
- 4) Adsorption Design Guide, Design Guide No. 1110-1-2, Department of the Army U. S. Army Corps of Engineers, 2001.
- 5) *The Rational Manager: A Systematic Approach to Problem Solving and Decision-Making* Charles H. Kepner, Benjamin B. Tregoe June 1965.

8. Appendices

Appendix A: Full-Scale Design Proposal

Appendix B: Fixed-bed Pilot-Scale Cost Estimate

Appendix C: Techno-Economic Analysis

Appendix D: Slides from April 2, 2012 Industry Meeting

Appendix E: Sorbent Trap Method Testing

Appendix F: Quality Assurance Program

9. Appendix A: Full-Scale Design Proposal

FIXED BED/ACTIVATED CARBON MERCURY REMOVAL-CONCEPTUAL DESIGN

FOR: ArcelorMittal Minorca Mine

Virginia, Minnesota

PREPARED BY: ACTIVATED CARBON TECHNOLOGIES, LLC

209 Clearwater Drive

Covington, VA 24426

H. Ray Johnson, PhD

CONSULTANT

SUMMARY AND RECOMMENDATION

Fixed bed/activated carbon technology has been successfully used for over 80 years to capture compounds from gas streams. Based on the information presented below and my 40+ years experience in the activated carbon field, it is my professional opinion that fixed bed/activated carbon technology can be successfully implemented and used to remove mercury from taconite process off-gases. It is recommended that the fixed bed carbon technology investigation move to the next stage; an activated carbon pilot system test.

BACKGROUND-FIXED BED/ACTIVATED CARBON SYSTEMS

Activated Carbon has been applied in Fixed Bed Adsorption Equipment for many years, beginning in the 1920's in Europe for recovery of organic solvents according to some historical information presented by Donau Carbon (1). The recovery of solvents by activated carbon also began in the U.S. in 1925 according to a historical timeline from Barnebey Sutcliffe (2), now part of Calgon Carbon. Thus, activated carbon has been successfully used in fixed bed, gas phase applications for over 80 years.

As a more recent example of fixed bed activated carbon technology, MeadWestvaco (MWV) commercialized a fixed bed system around 1980 for capture of corrosive gases such as H₂S. The initial fixed bed systems treated air flows up to 3,000 SCFM and utilized a 3 foot deep bed of impregnated, 3 or 4 mm pellet carbon or large granular carbon, such as 4 X 10 mesh size. The capture of H₂S and other sulfur gases occurred through chemical reaction with the impregnant material resulting in a high capacity for H₂S adsorption and carbon service life up to several years, 3-5 years in many cases. Based

on experience and a review of published literature, there seem to be several similarities between fixed bed/activated carbon performance for capture of H₂S and for capture of mercury. These similarities could potentially be exploited to increase the probability of commercial success for fixed bed/activated carbon capture of mercury from taconite process off gases.

Another example of fixed bed/activated carbon processes dates to the late 1980's when MWW commercialized unique pelletized carbons, 3 and 4 mm diameter, for organic solvent recovery applications. These products were used worldwide in solvent recovery systems designed and built by several different equipment manufacturers. These fixed bed systems typical employed a carbon bed that was also about 3 feet deep but in many cases a single vessel was sized to treat up to about 40-50,000 SCFM solvent laden air. After the carbon became saturated with adsorbed solvent in a matter of a few hours, the solvent is then removed by steaming and another adsorption cycle can begin. In most cases the carbon remains in service in the fixed bed for a period of years. Many features of the fixed bed design and operating features that have evolved over decades in the solvent recovery application can be applied in designing and operating a fixed bed/activated carbon system for mercury removal.

A more recent fixed bed type technology, developed within the past 5-10 years, uses an impregnated honeycomb carbon matrix; in place of carbon pellets or carbon granules, to capture corrosive gases such as H₂S (3). MeadWestvaco has commercialized systems utilizing the honeycomb technology treating gas flows up to about 30-40,000 SCFM. The honeycomb systems have faster removal kinetics, lower pressure drop, and operate at superficial velocities of 500 ft. /min., 5 times higher velocity compared to the typical 100 ft. /min. maximum for conventional activated carbon fixed beds for gas purification.

MeadWestvaco has provided systems with the honeycomb technology for corrosion control to the Flint Hills Resources Pine Bend Refinery in Rosemount, Minnesota. This installation would seem to offer a convenient site to gain more insight into the potential of mercury capture from taconite process off-gases using impregnated carbon technology.

Corning, Incorporated is also developing an impregnated honeycomb type filter to remove mercury from flue gas (4). Additional information on the development program for the Corning technology is described in a National Energy Technology Laboratory publication (5).

DESIGN CONSIDERATIONS-FIXED BED/ACTIVATED CARBON SYSTEM FOR MERCURY REMOVAL

ArcelorMittal Minorca Mine

The following design information will in general follow the steps presented in Appendix B-2-English Units of the ADSORPTION DESIGN GUIDE, Design Guide No. 1110-1-2 by the U. S. Army Corps of Engineers (6).

a. Parameters

* Flow Rate of Gas to be treated: 854,000 ACFM

* Temperature of Gas to Fixed Bed: 125 F°

* Run Time between carbon changes: (See design calculations below)

- * Number of Carbon Vessels: (See design calculations below)
- * Atmospheric Pressure: 14.7 psia
- * Moisture content in gas: 13.98 %
- * Mercury Concentration: 10 µg/m³
- * Total Mercury per Year: 180.8 lb Hg/yr (calculated from mercury concentration and flow rate)
- * Carbon Capacity for Mercury Adsorption (X/M): 0.00154 lb Hg/lb C

Other carbon capacity data for mercury capture can be found in several publications including the following data.

- (7) “Carbon Bed Mercury Emissions Control for Mixed Waste Treatment”: 0.19 lb Hg/lb C, and
- (8) “Long-Term Performance of Sulfur-Impregnated, Granulated Activated Carbon (GAC) for Mercury Removal from NWCF Off-Gas”: .035 to .072 lb Hg/lb C based on analysis of carbon samples.
- (9) Mersorb carbon containing impregnated sulfur was used for the studies in both publications. The carbon manufacturer, Nucon, predicts Mersorb to have capacity of about 0.20 lb Hg/lb C.

b. Design Steps

- (1) Determine the amount of carbon needed.

Considering several factors including:

- CR612C-HG, a sulfonated coconut shell carbon, performed best of the 4 carbons tested in the field by ADA Environmental Solutions. The supplier, Carbon Resources, has a specification for 12% minimum sulfur content for the CR612C-HG. The measured Mercury Index Method mercury adsorption capacity (X/M) for this carbon was 0.00154 lb Hg/lb carbon.
- Relevant publications and another sulfur impregnated carbon supplier, Nucon, indicate sulfur impregnated carbon capacity of about 0.2 lb Hg/lb Carbon.
- The carbon is in a fixed bed, expected to be exposed to the off gas containing mercury for extended time period, and under conditions that allow for the carbon in the upstream part of the bed to at least approach its saturation capacity for adsorbing mercury, 0.20 lb Hg/lb Carbon.

Potential carbon usage rates, based only on potential mercury adsorption capacity, could be:

<u>Mercury Adsorbed, lb/yr</u>	<u>Assumed Carbon Capacity, lb Hg/lb C</u>	<u>Carbon Usage, lb/yr</u>
180.8	0.00154	117,403
180.8	0.035	5,166
180.8	0.100	1,808

These calculated carbon usage numbers based on literature values are very minimal, but based on a somewhat similar type of process using impregnated carbon for removal of H₂S through reaction with an impregnant; the usage numbers could be reasonable and expected based on broad experience with H₂S removal over several thousand different installations.

However, it should also be noted that contaminants, adsorption of other compounds, temperature, relative humidity, etc. could vary significantly and impact the carbon usage rate. Larger scale pilot tests could provide more definitive information on the potential effects of these parameters.

(2) Determine the size of the carbon adsorption vessels

Relatively large fixed bed carbon adsorption systems/vessels have been used in solvent recovery applications for many years. Based on the extensive design/operating experience in this application area and my knowledge of this area, I will base the vessel sizing and number of vessels on solvent recovery experience.

One solvent recovery equipment manufacturer with decades of experience is AMCEC, Inc. located in Lisle, Illinois. One of the case studies listed on AMCEC's web site is "Pollution Control That Pays Its Way" covering a system installed in 1982 and still in operation (10).

The system includes 4 fixed bed carbon vessels with each adsorption vessel having a diameter of 12 feet and a length of 47 feet. Each vessel contains 43,000 pounds of CECA-AC35 activated carbon pellets. Assuming a cross-sectional area for the carbon bed of 12 feet X 47 feet or 564 ft², the carbon bed depth is in the range of 2.5 to 3 feet depending on the packing density of the carbon. See Figure 1 below.

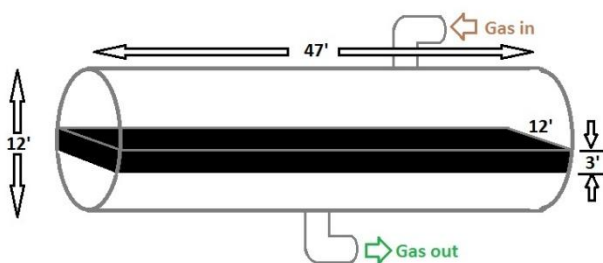


Figure 1: Carbon Vessel Design

In my experience this size vessel, up to about 12 feet diameter and 45-50 feet long, can be shop fabricated and transported to the job site by special tractor/trailer. There are many advantages to using a cylindrical vessel design and shop fabrication.

For subsequent calculations, I will assume a vessel size of 12 feet diameter, 47 feet long, and carbon bed cross sectional/bed surface area of 564 feet².

(3) Number of Adsorption Vessels

The typical range for gas flow velocities in fixed bed applications is on the order of 50-100 feet per minute. At this point, I would suggest a superficial gas velocity of 75 ft/minute and I will assume a bed cross sectional area of 564 ft² from above.

Each vessel will then treat 75 ft/minute times 564 ft² equals 42,300 ACFM.

Number of vessels on line at one time = 854,000 ACFM/ 43,200 ACFM/Vessel = ~20 Vessels.

An additional 1 or 2 vessels would be needed to provide back-up for maintenance, etc.

(4) Total Amount of Carbon

A typical carbon bed depth for a fixed bed application of this type is about 3 feet and I will use this depth.

Carbon bed volume/vessel = 564 ft² X 3 ft = 1692 ft³

Calgon gives an Apparent Density of 37 lb/ft³ for sulfur impregnated HGR grade carbon.

Carbon amount per vessel = 1692 ft³ X 37 lb /ft³ = 62,604 pounds.

Total installed carbon (22 vessels) = 1,377,288 pounds.

(5) Pressure Drop Across Carbon Bed

Pressure drop for gas flow through a packed bed of carbon is dependent on the packing characteristics; and the limiting pressure drop curves are measured by many manufacturers for “dense pack” (maximum pressure drop for a given superficial velocity) and for “loose pack “(minimum pressure for a given superficial velocity). In some cases the “loose pack pressure drop is only about ½ the “dense pack” pressure drop. As an example Calgon’s data (11) for BPL 4 X 10 Mesh product shows a pressure drop of ~ 1.5 inches water/foot bed at a superficial velocity of 75 ft./min for “loose pack” while the pressure drop is ~ 3.5 inches water/ft. bed at the same velocity for “dense pack.”

In NUCON MERSORB BULLETIN 11B28-2010 (12), Nucon does not indicate the packing characteristic but gives a pressure drop of ~ 2 inches water/ft.bed at 75 ft./min for 4 mm pellet and ~ 4 inches water/ft.bed for 3 mm pellet.

At this conceptual stage, it seems appropriate to assume that the pressure drop for the fixed bed of carbon will be in the range of 2-4 inches water/ft bed.

Assuming a 3 foot deep bed from section (4) above, the total pressure drop for the carbon bed is expected to be 6 to 12 inches of water.

(6) Other Pressure Drops

Pressure drop across other parts of the system such as flow control valves ductwork, inlet/exit flow losses, etc. will not be evaluated at this stage of the conceptual design.

(7) Blower

Pressure drop, horsepower and other characteristics of the blower will not be evaluated at this stage of the conceptual design.

POTENTIAL ALTERNATE DESIGN CONSIDERATIONS-HONEYCOMB MODULE/ACTIVATED CARBON SYSTEM FOR MERCURY REMOVAL

MeadWestvaco Corporation

MeadWestvaco (MWV) Corporation has provided deep bed (~ 3 feet nominal depth) carbon pellet systems for over 30 years and installed over 3,000 of these systems in industrial and municipal applications (13). The impregnated carbon systems are designed primarily for removal of corrosive acid gases, such as H₂S, from air/gas streams. The process of removing of H₂S by impregnated carbons seems to have many similarities to the process for removing Mercury using impregnated carbons.

Within about the past 5 years, MWV has developed and commercially introduced a new impregnated Honeycomb Matrix (HM[®]) Media to replace the traditional carbon pellet media. According to MWV, the Honeycomb Media Has several advantages when compared to traditional pellet media. These advantages include:

- 1) Superficial velocities of air can be 500 ft./min. for the honeycomb system compared to 100 ft./min. for pellet systems
- 2) Even with higher velocities, honeycomb media achieves higher removal efficiencies with lower bed depths.
- 3) Improved performance with lower maintenance and cost.

More details on the honeycomb matrix systems are available in the following documents that can be downloaded from the MWV web site, MWV.com under the Specialty Chemicals, Air Purification Section.

* Clean Air Update March 2010 (PDF)

* Clean Air Update January 2010 (PDF)

* Air Purifications Brochure

MWV does not currently provide the honeycomb matrix system for air purification applications to remove Mercury but I recommend that this technology be considered as the evaluation of fixed bed carbon technology evolves.

MWV does have the honeycomb matrix technology installed and operating for corrosion control at Flint Hills Resources Pine Bend Refinery in Rosemount, Minnesota. I would expect that a site visit to view this installation could be arranged for ADA-ES and Minnesota DNR representatives.

Corning Incorporated

Corning Incorporated is also developing honeycomb media and has several U. S. patents and patent applications on the use of sulfur-impregnated honeycomb media for mercury capture. Corning patents in this general area include U. S. Patents 6, 136,749; 6,187,713; 6,258,334; 6,372,289 and others. Some recent patent application numbers by Corning relative to mercury removal include 20080207443; 20110020202 and others.

Corning's development of this media is mentioned in a Chemical and Engineering News article titled "Getting Rid of Mercury" dated November 24, 2008 (4).

According to a National Energy Technology Laboratory (NETL) project fact sheet the Corning honeycomb media is undergoing development in an integrated system to remove trace metals including mercury (5).

CONCLUSION

Conventional fixed bed/activated carbon systems have been used for over 80 years to remove target compounds from gas streams including off-gases from many types of processes. Systems employing impregnated carbons, as an example, have been utilized in many thousands of installations to remove corrosive gases, such as H₂S, employing 3 foot deep beds of carbon pellets or large carbon granules. Pilot studies utilizing impregnated carbon pellets/granular particles have demonstrated the potential for using deep fixed carbon beds for capture of mercury from different types of process off gases. There seems to be many similarities between the removal of H₂S employing impregnated carbons and the capture of mercury by impregnated carbons.

In view of the historical success using impregnated carbons in fixed bed systems and based on my broad experience in activated carbon technology, it is my professional opinion that fixed bed activated carbon technology can be successfully applied to mercury capture from taconite process off gases.

Furthermore, I recommend that a pilot system investigation be performed to demonstrate the performance of this technology and develop additional information for design and installation of full scale systems.

REFERENCES

1. www.donau-carbon.com , " Our history at a glance"

2. www.bsicarbon.com, "historical timeline, 1919 to present for Barnebey Sutcliffe, A Calgon Carbon Company
3. www.mwv.com, MWV Specialty Chemicals Division, Air Purification Group, Vol. 1, Issue 2, March 2010"
4. Chemical & Engineering News, "Getting Rid of Mercury", Volume 86, Number 47, pp 22-23, November 24, 2008.
5. National Energy Technology Laboratory, "Monolith Traps for Mercury and Trace Metal Control in Advanced Gasification Units", Project 393, August 2009.
6. Department of the Army, U. S. Army Corps of Engineers, "Engineering and Design ADSORPTION DESIGN GUIDE", Design Guide No. 1110-1-2, March 1, 2001.
7. Soelberg, Nick; Enneking, Joe, "Carbon Bed Mercury Emissions Control for Mixed Waste Treatment", Journal of the Air & Waste Management Association, Volume 60 November 2010, pages 1341-1352.
8. Del Debbio, J. A.; Watson, T.L.; Heintzelman, J. B., " Long-Term Performance of Sulfur-Impregnated, Granulated Activated Carbon (GAC) for Mercury Removal from NWCF Off-Gas, Idaho National Engineering and Environmental Laboratory, September 2003
9. MERSORB® Mercury Adsorbents, "Design and Performance Characteristics", Nucon International, Inc.
10. www.amcec.com, "Pollution Control That Pays Its Way", By Martin Decker, Pradkash, Naik, and Mike Worrall, Reprinted from Industrial Wastes
11. BPL 4X10 Granular Activated Carbon, Product Data Sheet, Pressure Drop Curve, Calgon Carbon Corporation
12. Nucon Mersorb Bulletin 11B28-2010, Nucon International, Inc.
13. www.mwv.com, MWV Specialty Chemicals Division, Air Purification Group, Vol. 1, Issue 1, January 2010"

FIXED BED/ACTIVATED CARBON MERCURY REMOVAL

INTEGRAL PROCESS DESIGN CONCEPT

FOR: ArcelorMittal Minorca Mine

Virginia, Minnesota

PREPARED BY: ACTIVATED CARBON TECHNOLOGIES, LLC

209 Clearwater Drive

Covington, VA 24426

H. Ray Johnson, PhD

CONSULTANT

DESCRIPTION OF PROCESS DESIGN CONCEPT

The attached block diagram presents a concept for integrating the new fixed bed carbon adsorption system into the existing plant process. The design concept includes four separate, but identical lines to treat a total waste gas flow of 854,000 ACFM at 125 F° with 13.98 % moisture.

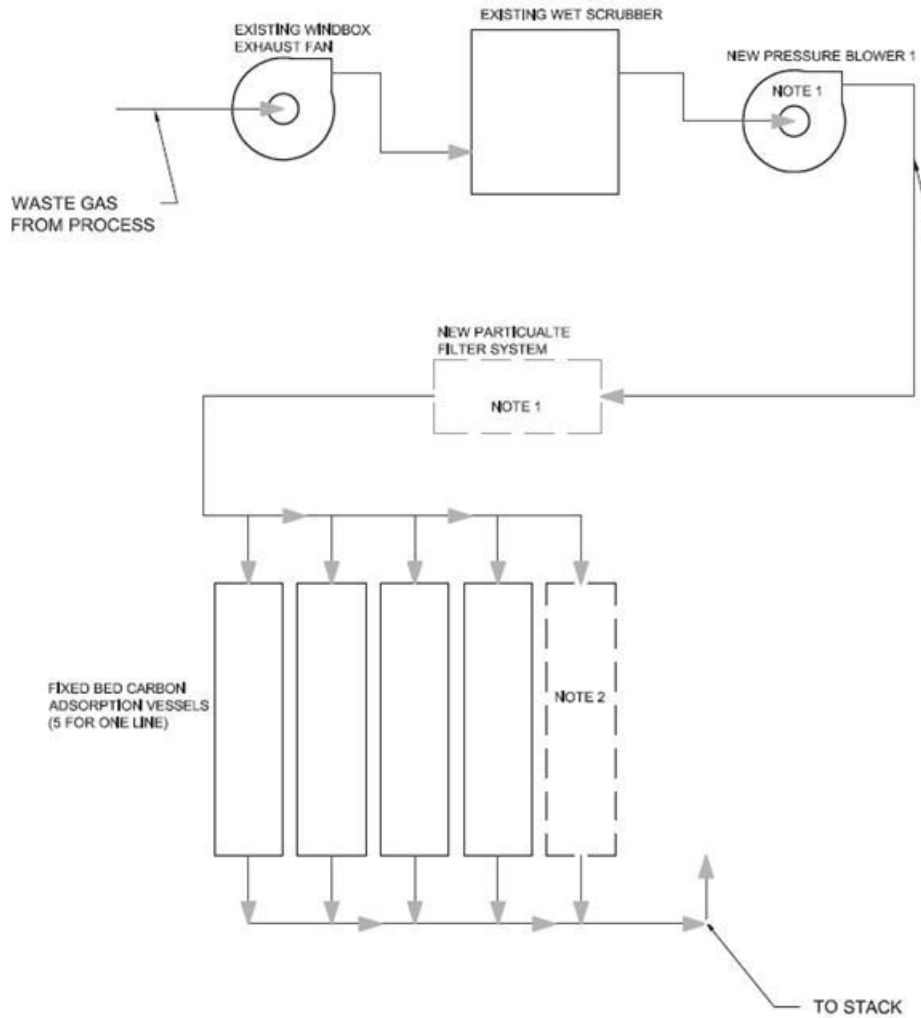
For each line, waste gas from an existing wet scrubber will be diverted prior to exiting the existing stack to a new pressure blower. Although the proposed design concept includes only one large pressure blower, ArcelorMittal's operating philosophy and strategy may favor more than one pressure blower for each line.

The design concept presented includes a new particulate filter system downstream of the pressure blower to remove particulate matter to a level that eliminates potential problems with particulates clogging the fixed carbon beds and increasing pressure drop above maximum design level. Design information for the particulate filter system and level of particulate removal required should be developed during a pilot system test program. Although the concept includes a new filter system, the potential for increasing the efficiency of the existing wet scrubber should be evaluated as a possible means of eliminating the need for a new filter. Also, the carbon adsorption vessels might include the potential for filtering particulates with periodic removal of the captured particulate matter.

The filtered waste gas is then treated in the fixed bed carbon adsorption vessels. The design concept includes multiple carbon adsorption vessels, 5 vessels for each of the four lines. Depending on ArcelorMittal's operating strategy, one of the five vessels could be typically off-line and designated as a

spare vessel, to be used as needed for maintenance purposes, reduce blower pressure requirements, etc. It is also possible that the fifth vessel in each line could be eliminated leaving only four vessels, but reducing operating margins from some standpoints. The design concept includes adsorption vessels of a size that can be shop fabricated, however, the potential for on-site fabrication of larger, but fewer number adsorption vessels can be considered by ArcelorMittal.

The cleaned off-gas from the carbon adsorption vessels for each line is routed to the existing stacks and emitted to the atmosphere.



**ARCELOR MITTAL MINORCA MINE
CARBON FIXED BED ADSORPTION
PROCESS DESIGN CONCEPT
(TYPICAL CONCEPT FOR ONE OF
FOUR LINES)**

NOTE 1: REQUIREMENT AND DESIGN PARAMETERS TO BE DEFINED DURING PILOT TESTING PHASE.

NOTE 2: ONE ADSORPTION VESSEL CAN NORMALLY BE KEPT OFF LINE AS A SPARE.

DRAWN BY	DATE
RMJ	REVISED: 2-1-2012
SHEET: 1 OF 1	SCALE: NOT TO SCALE

10. Appendix B: Fixed Bed Pilot-Scale Cost Estimate

ADA-ES PROJECT-MERCURY REMOVAL FROM TACONITE OFF GAS

PILOT SYSTEM DESIGN AND COST ESTIMATION

PREPARED BY: ACTIVATED CARBON TECHNOLOGIES, LLC

209 Clearwater Drive
Covington, Virginia 24426
H. Ray Johnson, PhD
CONSULTANT

DESCRIPTION OF PILOT SYSTEM

The fixed bed, activated carbon pilot system will include a 4 inch nominal, 316 SS pipe, 5 feet long to serve as the column or vessel for the fixed bed of carbon particles. The design basis will provide for carbon bed depths of 3 feet with provisions made to withdraw gas samples at bed depths of 0,1,3,6,12, and 24 inches to monitor the mercury adsorption wave front. Superficial gas velocities through the 4 inch column will be in the range of 50-100 ft./minute for a flow of about 5-10 ACFM. Provisions for filtering particulate matter from the inlet gas, monitoring and controlling total gas flow through the column. Measuring temperatures and pressures will be included. A pressure blower rated for a static pressure of 50 inches water and flows up to several hundred ACFM is included. Provisions for mounting, weatherizing and other installation details can be included as more details on the actual site for the pilot system becomes available.

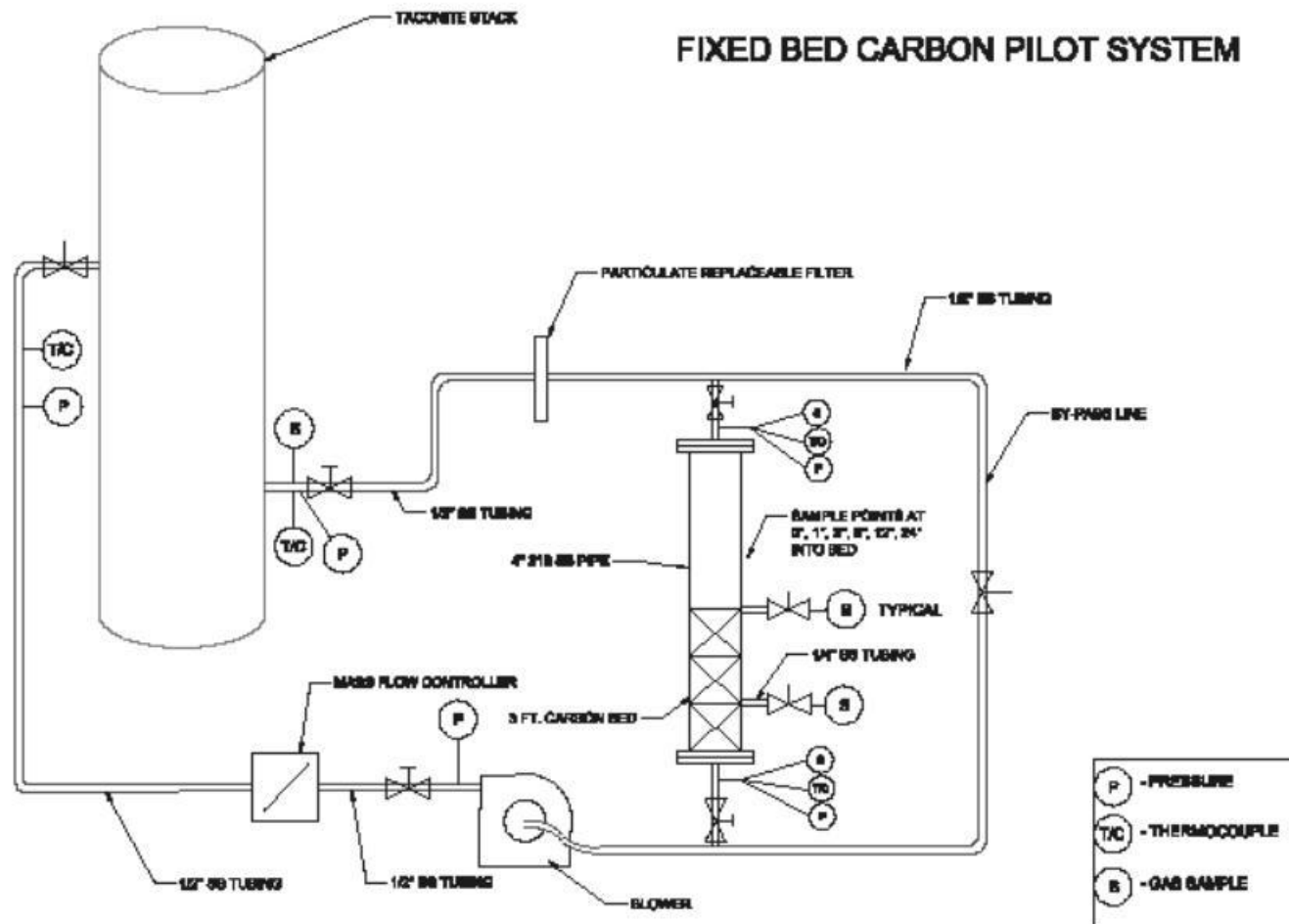
The present pilot system proposed design can be easily modified/added to by adding one or more adsorber vessels (4 inch pipe) to evaluate more than one carbon grade at the same time, as an example. Since plugging of a carbon bed with particulates in an unfiltered off-gas can be a concern, modification of the system to include another carbon column receiving unfiltered off-gas can be easily accomplished. Other modifications can be considered.

The estimated cost to date for a single column system is in the range of about 14,000 to 19,000 dollars not including a contingency estimate. The major components and their cost estimate are listed on the following page. Manufacturers spec sheets for some of the major components are attached. Other suppliers' information is available as needed. A simple drawing of a single column pilot system is provided in the attachment.

PILOT SYSTEM COMPONENTS/COST ESTIMATE

COMPONENT	BRIEF DESCRIPTION	ESTIMATED COST		SOURCE OF ESTIMATE
		Low	High	
1. Column ,	4 inch, sch.40 ,316 SS pipe,5 feet long, inlet,outlet flanges ,6 sampling connections	750	850	Creative Fab., Covington,VA
2. Flow Controller	Sierra Max-Trak Model 180M (See Spec Sheet)	2800	3500	JOBE & Company,Richmond,VA
3. Pressure Blower	Cincinnati Fan Model HP-6E26 (See Spec Sheet) 10 HP Motor	3000	3200	Prime Air Products,Lynchburg,VA
4. Swagelok Tubing Fittings	1/2 inch,316 SS, ball valves 6@ 211.10 each	1267	1300	Diebert Valve,Richmond,VA
	1/4 inch,316 SS, ball valves 10@ 174.60 each	1746	1800	
	1/2 inch, 316 SS tubing tees 8@ 44.90 each	359	375	
	1/4 inch,316 SS male to tubing fittings 8@ 7.10 each	57	70	
	1/2 inch,316 SS tubing 40 ft.@ 10.69/ft	428	450	
	1/4 inch, 316 SS tubing 40 ft@ 6.00/ft	240	250	
5. Magnehelic Pressure Gages	Series 2000 for P/DP 6@ 70 each	420	450	Dwyer Web Site
6. Thermocouples	Type J 4@ 22 each	88	100	Omega Web Site
7 Temperature Data Logger	1 @ 999 each	999	1000	Omega Web Site
8. Insulation-4 inch column	2-3ft lengths @ 26.05 each	52	60	Granger Web Site
9. Cartridge Filter	Compressed air filter 55 SCFM Max Flow	200	300	Filtersource Web Site
10. Assembly,Enclosure, Weather Protection as needed.		2000	5000	HRJ Estimate
		14406	18705	

FIXED BED CARBON PILOT SYSTEM



DRAWN BY	DATE
RMJ	REVISED: 11-28-2011
SHEET: 1 OF 1	SCALE: NOT TO SCALE

Appendix C: Techno-Economic Analysis



**EVALUATION OF MERCURY
CONTROL OPTIONS
TACONITE INDUSTRY**

Revision F

Prepared for:
ADA Environmental Solutions
9135 S. Ridgeline Blvd., Suite 200
Highlands Ranch, CO 80129
USA

Prepared by:
Stantec Consulting Ltd.
Clean Coal Centre of Excellence
701 – 2010 – 11th Avenue
Regina, Saskatchewan
Canada, S4P 0J3

Project No. 111100111

August 14, 2012

Revision	Rev. Date	Description	Created By	Initial	Approved By	Initial
A	June 4, 2012	Issued for Review	M. Richard			
B	June 20, 2012	Issued for Review	M. Richard			
C	June 29, 2012	Issued	M. Richard			
D	July 13, 2012	Issued	M. Richard			
F	August 14, 2012	Issued	M. Richard			

Table of Contents

Revision History.....	i
1.0 INTRODUCTION.....	1
2.0 TECHNOLOGIES CONSIDERED	2
3.0 EVALUATION TECHNIQUE.....	4
4.0 GENERIC PLANT.....	8
5.0 EVALUATION RESULTS	9
6.0 DISCUSSION.....	11
7.0 APPENDICES.....	12
APPENDIX A TECHNOLOGY DATA SHEETS.....	12
APPENDIX B EVALUATION BACKUP INFORMATION.....	12

List of Tables

Table 4-1 Generic Taconite Plant	8
Table 5-1 Ranking and General Appraisal for Generic Plants	9

List of Figures

Figure 1 Relative Capital Costs	10
Figure 2 Relative Operating Costs.....	10

1.0 Introduction

Stantec Consulting Ltd. has been tasked by ADA Environmental Solutions (ADA-ES) to assist them in a high-level evaluation of technologies that show potential for controlling mercury emissions from taconite processing facilities as listed below:

- Keewatin Taconite (Keetac) - located near Keewatin, Minnesota
- Hibbing Taconite (Hibtac) - located near Hibbing, Minnesota
- ArcelorMittal - located near Virginia, Minnesota
- USS Minntac (Minntac) - located near Mountain Iron, Minnesota
- United Taconite (U-Tac) - located near Eveleth, Minnesota

Stantec has elected to use a Kepner-Tregoe style qualitative analysis to rank the technologies being considered. The details of this method are expanded upon within this report.

2.0 Technologies Considered

Seven mercury control technologies, as provided by ADA-ES, were to be assessed using the Kepner-Tregoe technique. ADA conducted fixed bed screening tests to determine the relative performance of activated carbon for mercury control on process gas slipstreams from three taconite plants. The other technologies were considered options because of their application for mercury control in other industries.

Activated Carbon Injection (ACI)

Powdered Activated Carbon (PAC) is used as a sorbent to adsorb the mercury. It is injected and mixed with the waste gas in the duct prior to the existing wet scrubber. Since it is in-duct capture, residence time of the AC will depend upon the configuration of the plant and distance from the injection points to the particulate control device as well as the type of particulate control device. The spent AC is removed from the treated gas in the wet scrubber by scrubbing water and discharged with scrubber blowdown.

Activated Carbon Injection with Fabric Filter

PAC is used as a sorbent to adsorb the mercury. It is injected and mixed with the waste gas in new ductwork leading to the fabric filter, which is used for filtering the spent carbon out of the system. In this evaluation, the fabric filter will replace the existing wet scrubber.

Fixed Bed Adsorption

PAC is packed in a fixed bed adsorption vessel. The waste gas leaves the wet scrubber and passes through a series of horizontally cylindrical vessels where the fixed carbon beds remove the mercury from the waste gas. The spent beds will be removed for potential off-site regeneration.

Fixed Bed Adsorption with Fabric Filter

Waste gas passes through a fabric filter to remove particulate matter to a level that eliminates potential problems with clogging the fixed carbon beds. The dedusted waste gas will be introduced to a series of fixed bed carbon adsorption vessels, which will remove the mercury from the waste gas. The spent beds will be removed for off-site regeneration. Functionally no different from the fixed bed application; the fabric filter only serves to protect the fixed beds. The fabric filter allows the existing scrubber to be eliminated.

Monolithic Honeycomb Adsorption

Activated carbon is mechanically fixed into a honeycomb structure that may include additives to enhance mercury capture. The cells of the monolith are plugged at their ends intermittently to force gas flow through the walls of the structure.

Evaluation of this technology was halted, but a data sheet for it can be found in the appendices of this report. During the course of the evaluation, the monolithic honeycomb adsorption technology was found to be no longer in commercial development.

Monolithic Polymer Resin Adsorption

Activated Carbon Fluoropolymer Composite (CFC) materials are used to chemically adsorb mercury from the flue gas stream. The treated activated carbon powder is combined with chemicals, such as elemental sulfur or alkaline metal iodides, to enhance the mercury removal efficiency and the fluoropolymer. The mixture is then calendered into CFC sheets under elevated temperature. The CFC sheet is stretched extensively to develop the microporous structure that will allow rapid chemical oxidation of Hg^0 and binding of Hg^{2+} to the active sites of the fibre. This technology is evaluated as contained within a stand-alone adsorber tower but can also be retrofitted into an existing wet scrubber.

Oxidative Chemical Addition

A chemical additive is added in the waste gas to enhance mercury oxidization converting Hg^0 (insoluble) to Hg^{2+} (water-soluble). An increase in the percentage of Hg^{2+} or particulate-bound mercury at the inlet of the wet scrubber will improve the mercury removal from the process. The oxidant can be added into the process gas during the induration or into the scrubber water at the wet scrubber. This evaluation assumes induration injection, and we have selected calcium bromide as the oxidant.

3.0 Evaluation Technique

The technique used in this evaluation is a modified, high-level Kepner-Tregoe style WANTS analysis, which can be found in full in their book “The New Rational Manager.” The process involves a decision analysis that uses a scoring technique to apply a series of qualitative assessments of an option to arrive at a more quantitative score. The technologies for mercury control will be assessed individually using this technique, then ranked to determine which ones show the most promise.

The process typically begins with establishing criteria of importance. These criteria are generally divided into two categories, MUSTS and WANTS. MUSTS represent features that must be achievable by the technology. For this specific evaluation, there were no clear MUSTS as any technology that does not meet the MUSTS list is discounted immediately, and there was a desire for all technologies to make it forward to the more detailed WANTS analysis. Still, the following MUSTS were generally followed:

- Technology MUST be capable of 75% mercury capture or better.
- Technology MUST be commercially available in 2012 or on track for commercial availability before 2014.

Between these two MUSTS, the polymer resin monolith and honeycomb monolith technologies did not pass. Although the monolithic polymer resin adsorption technology has been successfully piloted and scheduled for a larger scale pilot testing in 2013, it may not be commercially ready before 2014. Unlike the polymer resin monolith technology, an attempt to commercially develop the honeycomb monolith technology for mercury removal application for utility flue gases was terminated, since it was most likely not cost-effective.

The remaining technologies then proceed to the WANTS analysis. Here the technology is given a score in several different categories, grouped as follows:

- Economic

These criteria are related to the capital and operating costs of the systems, as assessed from the high-level aspect of this study.

1. *Capital Cost* - Systems with the highest capital costs were given the worst score and the lowest the best; all systems in-between were scored relatively between them.
2. *Operating Cost* - Similar to capital cost, the highest and lowest yearly operating costs were given the worst and best scores, respectively, with technologies in-between scored relatively.

- Risk

These criteria are related to the apparent risk of retrofitting the technologies to an existing facility.

1. *Turndown* - This criterion assesses the technologies capability to load follow downward while maintaining performance. Technologies that feature multiple parallel reactors score well because as gas flow is reduced, modules can be shutdown. Technologies that depend on the existing scrubber depend on its turndown capabilities to maintain particulate control, which is likely unique to each scrubber.
2. *Availability/Reliability* - This criterion assesses the uptime of a given system. Systems with many moving parts or unreliable components score poorly.
3. *Erosion/Corrosion/Plugging/Scaling* - This criterion assigns a score based on how susceptible the system is to attack from the harshness of the flow or chemicals used. A high score is impervious to these issues, while a low one may be at risk.
4. *Simplicity* - Generally, a simplified system will be more successful in long-term performance and ease of operability. High scoring systems would have relatively simple flow sheets.
5. *Modularization* - To minimize system costs, in-shop fabrication of modularized gas treatment equipment is often beneficial. High scoring systems would have systems delivered to site ready for installation; low scoring systems will require much more field work.
6. *Technology Maturity* - A mature technology scores high as the long operation history increases the likelihood of avoiding design or operational problems.
7. *Commercial Scale* - Systems available today, at the scale required, score high in this category. If significant scale-up is required from systems readily available today, then a low score will result.
8. *Construction Schedule* - Technologies with fewer pieces of equipment (e.g., injection lances or chemical silo) are likely to meet the construction schedule and keep the schedule short. These technologies will score higher than those requiring multiple parallel trains of vessels.
9. *Retrofit Integration* - The ease of integrating new equipment is assessed in this category. Equipment that can be installed in the gas path with minimal impact to the operating plant scores high, while systems needing significant shutdowns for integration score low.
10. *Safety* - Systems using dangerous, toxic chemicals with many confined spaces, excessive temperatures, and pressures would score poorly here.

11. *Materials of Construction* - Systems that feature high steel alloys score poorly here. Due to being installed after existing wet scrubbers, some systems will have to be constructed of corrosion-resistant material (e.g., stainless steel) as the waste gas would be near saturated conditions.
12. *Maintenance* - Systems requiring frequent maintenance, adsorbent change outs, and bag replacements score lower here.

- Performance

The performance section seeks to rank the technologies on how well they will accomplish their primary function to control mercury in waste gas. It also assesses how susceptible they are to performance hindrance, due to expected upset conditions that will undoubtedly arise.

1. *Scrubber Compatible* - If the technology has a limited impact to the scrubber, it scores well in this category. If it changes how the existing scrubber works or performs, it scores progressively worse as impact increases.
2. ΔP - The pressure drop of the technology is assessed here. Higher pressure drops require more fan power than lower pressure drops, and score worse than technologies with relatively lower resistance to gas flow.
3. *Footprint* - Systems with large footprints score poor in this category, as it is our understanding that space limitations may be present at many of the possible host plants.
4. *Suitability to Induration Type* - If the technology performance depends on the induration type present at the host plant, it will be scored well or poorly based on information available thus far. Specific analysis is included for the two induration types considered in this study.
5. *Sensitivity to Flue Gas Compositions* - Flue gas compositions (e.g., SO_x, NO_x and moisture) can reduce the mercury removal efficiency by reducing the adsorption capacity of adsorbents or reacting with oxidative chemicals directly. Technologies with adsorbents/chemicals insensitive to these flue gas compositions score well here.
6. *Regeneration Capability* - Technologies with regenerable adsorbents score well here as they typically have lower operation costs.
7. *Impact on Scrubber Solid Recycle* - Adding adsorbents/chemicals at or before the existing wet scrubber or the new fabric filter can contaminate scrubber solid recycling to the green ball feed with mercury. Technologies that remove mercury downstream of the wet scrubber tend to avoid solid contamination and score well.

8. *Impact on Iron Chemistry During Induration Process* - If the technology interacts or interferes with iron chemistry during the induration process, it is scored poorly here.
 9. *Possibility of Mercury Re-emission/Desorption* - Based on information provided on the technologies considered, some display a risk of re-emission of mercury. Technologies that feature this risk to performance are scored poorer than those that feature robust and stable adsorbents.
- Environmental
- While the whole analysis focuses on the technologies capabilities with regards to mercury, the environmental category looks at co-benefits or waste emission increased due to the incorporation of new emission control equipment.
1. *Particulate Co-Benefits/Fugitive Emissions* - Technologies that may increase the emission of particulate by increased loading on the existing scrubber, or introduce new emissions to the gas path, are scored lower than technologies that do not increase emissions or assist in controlling existing emissions even further.
 2. *Waste Quantity* - Technologies that produce waste streams that must be handled score poorer than those that either have regenerable adsorbents or do not produce significant wastes.

Each category is subdivided into further individual criteria, each of which is given a weight. The weight, a value between 1 and 10, indicates the relative importance of each criteria (10 being of high importance; 1 being of minimal importance). When the technology is evaluated, it is given a score from 1 to 10 for each criteria (10 being an excellent score; 1 being a poor score). The weight and the score are multiplied to arrive at a weighted score, and then all weighted scores are tallied to give a grand total. The highest grand totals are then recommended as attractive technologies for further study.

4.0 Generic Plant

In order to calculate some rough sizing and costs for the technologies to evaluate, it was necessary to develop generic plants that could represent the actual plant data provided.

As shown in Table 4-1, two generic plants, Plant 1 (Straight Grate) and Plant 2 (Grate Kiln), are established to represent the taconite facilities in Minnesota for evaluation. Based on process data received from five taconite plants, both generic plants are co-fire natural gas and coal with a recirculating wet venturi-type scrubber, as an existing particulate matter control device. Scrubber solids are recycled back to the process at the green ball feed. Other process parameters of the generic plants (e.g., waste gas flow rate, SO_x/NO_x stack emission rate) are selected to represent the worst-case scenario of the process. However, the generic plants do not cover the differences between each plant such as pre-heat burners. A full process description of these generic plants can be found in Appendix B. As can be seen in the end, the generic plants are very similar, differing only in induration type. At this high-level it was not necessary to delve any deeper into the unique features of each individual processing line. All other factors of the plants did not play a role in determining the scoring of the technologies evaluated.

Table 4-1 Generic Taconite Plant

Parameter		Unit	Generic Taconite Plant 1 Straight Grate	Generic Taconite Plant 2 Grate Kiln
Induration Type		(-)	Straight Grate	Grate Kiln
Existing PM Control Device		(-)	Wet Venturi-Type Scrubber	Wet Venturi-Type Scrubber
Scrubber Type		(-)	Recirculating	Recirculating
Solid Recycle to the Process		(-)	Yes	Yes
Recycle Location		(-)	Green Ball Feed	Green Ball Feed
Fuel Type		(-)	Coal/Natural Gas	Coal/Natural Gas
Waste Gas After Scrubber		(scfm)	854000	854000
Gaseous Composition After Scrubber	• Moisture	(%)	15.27	15.27
	• Mercury	(µg/m ³)	10	10
SO ₂ Emission Rate		(lb/hr)	272	272
NO _x Emission Rate		(lb/hr)	311	311

5.0 Evaluation Results

Table 5.1 is generated from the generic plants and demonstrates the ranking and general appraisal of the technologies after completion of scoring. The ranges reflect the subtle variants in scoring due to the separate analysis for the two induration types from the generic plants, which in the end were not substantial.

Table 5-1 Ranking and General Appraisal for Generic Plants

Technology	Grand Total	Positive Attributes	Negative Attributes
ACI Injection	713	Reasonable performance at very low cost.	Limited specific experience.
Oxidant Chemical Addition	716-706	Reasonable performance at very low cost. Has been trialed on actual waste gas.	Mixed results with many difference oxidants.
ACI + Fabric Filter	640	Good performance. Good co-benefits.	Large footprint, high pressure drop.
Fixed Bed Adsorption	597	Good performance.	Very large footprint, high pressure drop. Very high capital cost.
Fixed Bed Adsorption + Fabric Filter	475.5	Good performance. Good co-benefits.	Largest footprint, highest pressure drop. Highest capital cost.

The full scoring can be found in the appendices of this report along with notes explaining the scores.

A high-level appraisal of costs was conducted for these systems as applied to the generic plant. Cost estimation accounted for the cost of equipment, material, labour, engineering and construction management, project contingency and Operational & Maintenance (O&M). It excluded the demolition cost of the existing equipment and other owner's costs, such as commissioning and start-up costs. The following figures demonstrate the relative results of this analysis:

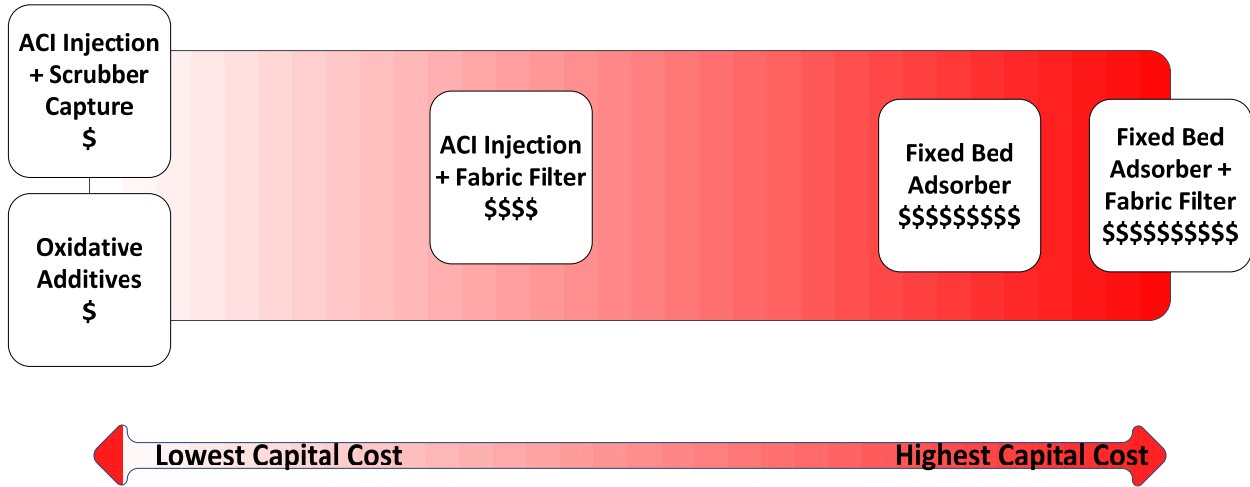


Figure 1 Relative Capital Costs

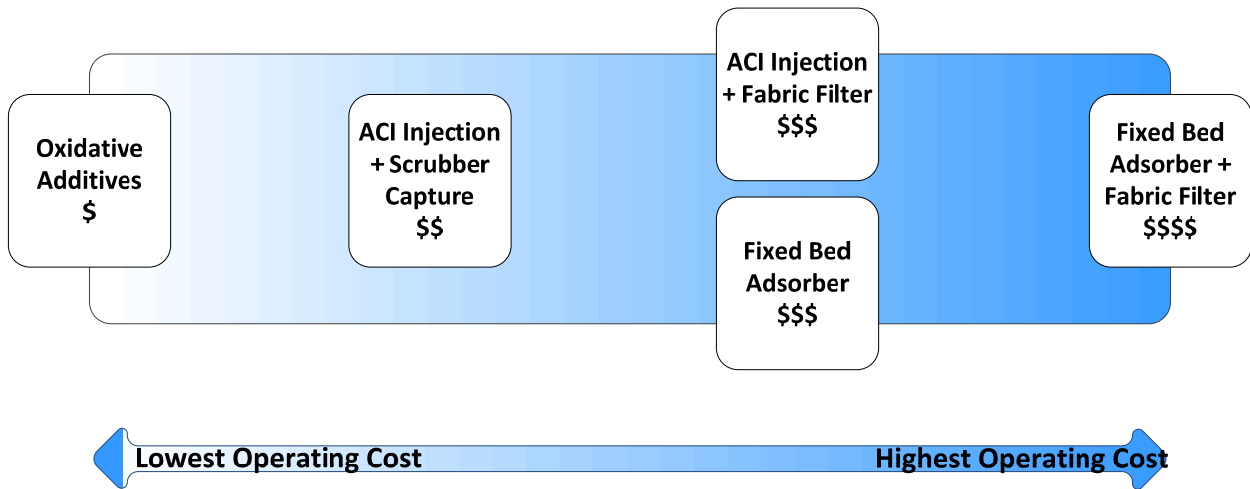


Figure 2 Relative Operating Costs

6.0 Discussion

Based on this high-level screening, the most attractive technologies are the simplified injection technologies, be they activated carbon injection into the existing scrubber or with a new fabric filter, or the special oxidant additives. However, the spent AC, or the chemical additives, can contaminate the recycle solids allowing mercury to be re-emitted back to the atmosphere. Some possible solutions are proposed to reduce the impact of these sorbents on the recycle solids:

- Sending the recycle solids to the grinding mill, instead of the green ball feed, may help reduce the mercury concentration in the solids, since only the magnetic fraction of these solids are recovered, and mercury, which tends to adsorb to the non-magnetic fraction of the solids, will be disposed.
- Proper separation techniques should be used to separate the sorbents from the scrubber solid prior to recycle.

The fixed bed options, while offering predictable performance, have high capital cost, due to the large number of parallel trains required to treat a waste gas volume of this size, and high quality materials of construction to withstand any potential corrosion environment in the process. However, it is possible to lower the cost by reducing the quality of materials if selected for this analysis, which can be confirmed in detailed design. If the waste gas from kilns is not corrosive, carbon steel can be used at a significant savings.

7.0 Appendices

Appendix A Technology Data Sheets

Appendix B Evaluation Backup Information

Stantec

ADA Environmental Solutions
EVALUATION OF MERCURY CONTROL OPTIONS
TACONITE INDUSTRY
August 14, 2012

APPENDIX A

Technology Data Sheets

Stantec

ADA Environmental Solutions
EVALUATION OF MERCURY CONTROL OPTIONS
TACONITE INDUSTRY
August 14, 2012

APPENDIX B

Evaluation Backup Information

Stantec

ADA Environmental Solutions
EVALUATION OF MERCURY CONTROL OPTIONS
TACONITE INDUSTRY
August 14, 2012

APPENDIX A

Technology Data Sheets

Technology Survey: Activated Carbon Injection (ACI) and Wet Scrubber

Date of Technology Assessment: May 08, 2012

Equipment Summary:

1. Activated Carbon (AC)
2. AC silo
3. Feeder
4. Injection lance

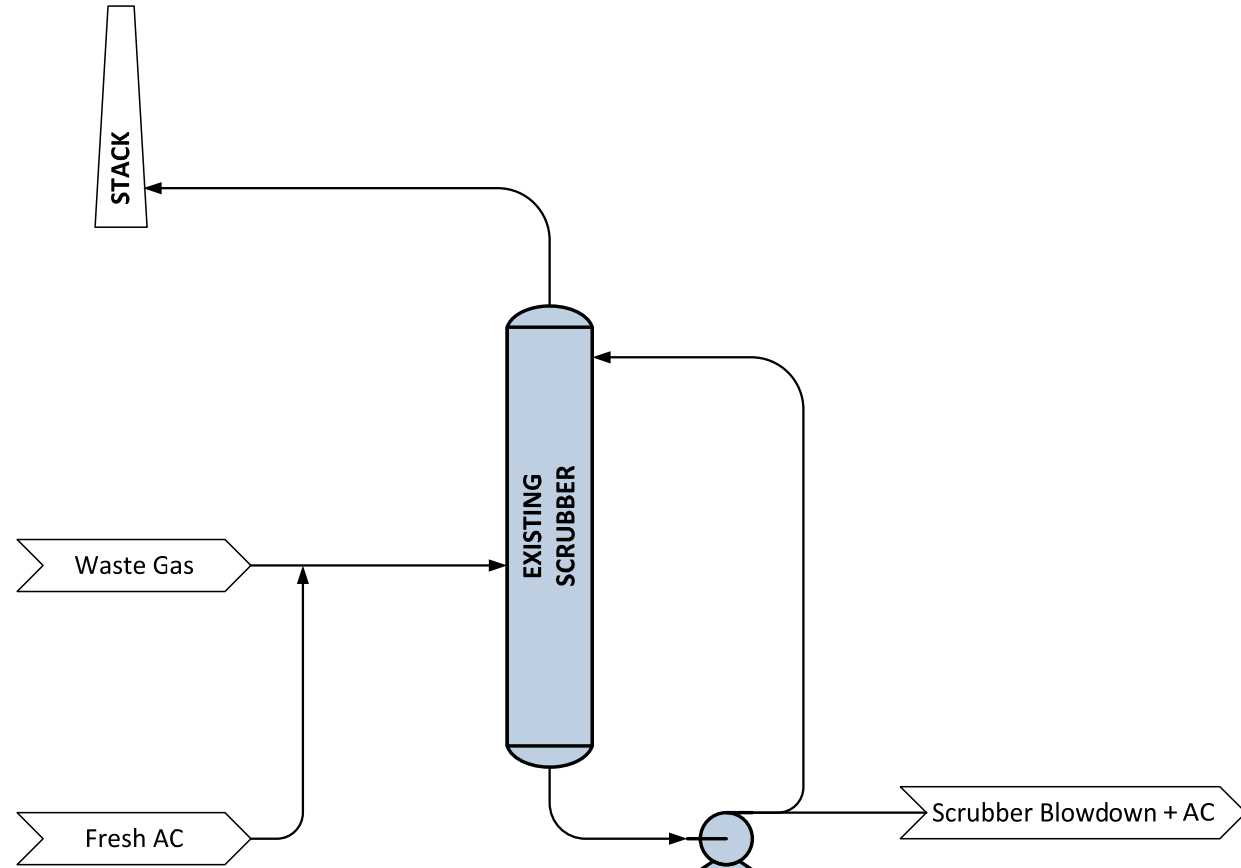
Detailed Description:

Powdered activated carbon is used as a sorbent to adsorb the mercury. It is injected and mixed with the waste gas in the duct prior to the wet scrubber. Residence time varies with the configuration of the plant and distance to the particulate control device, as well as the type of particulate control device. In this technology, the existing wet scrubber is used for removing the spent carbon, which will be taken out of the treated gas by scrubbing water and discharged from the scrubber with scrubber blowdown. Note that the results referenced in this datasheet were obtained from pilot testings at coal-fired power plants where an electrostatic precipitator or a fabric filter was used as a particulate control device. Unlike the utility sector, the wet scrubber was a primary particulate control device in the taconite processing plants and was not designed to handle additional AC injected to the system. As a result, any introduced AC could likely result in an increase in particulate emissions and actual mercury removal may differ.

Potential for Use with Generic Taconite Plant:

Injection lance prior to existing scrubbers. Lances for individual scrubbers or for the entire waste gas duct to be determined in detail design.

Flow Sheet:





Technology Survey: Activated Carbon Injection (ACI) and Wet Scrubber

- Scrubber Compatible: No. The spent AC can increase particulate loading of the scrubber. A further evaluation on particulate removal efficiencies required.
- Pressure Drop: Small
- Footprint: 2500 ft² for one processing line (756000 acfm flue gas)
- Size: Small
- Power Usage: Small. No additional fan power is required.
- Suitability for Induration Type: Straight Grate/Grate Kiln
- Suitability for Fuel Type: High-rank coal (e.g., bituminous coals); the mercury control can be increased if brominated (treated) AC is used.
- Susceptibility to Flue Gas Compositions: (i) Water vapor; SO₃; SO₂/NO₂ (reduce the equilibrium sorption capacity)
(ii) Cl; NO_x; NO_x/NO₂ and HCl (increase the equilibrium sorption capacity)
- Regeneration Capability: No
- Chemistry b/w Mercury and Additives or Sorbents: Well-understood since it has been extensively tested in coal-fired systems.
- Possibility of Mercury Re-emission/Desorption: Possible if a very high level of SO_x, NO_x, and HCl control is not obtained.

Maturity/Risk Comments:

Mature technology in coal-fired utility applications, commercially available.

State of Development:

- Conceptual
 Bench Scale
 Pilot Scale
 Full Scale
 Commercially Available & Performance Guaranteed

List of Users/Pilot Sites (include size of plant and type of fuel):

Power Plant	Fuel Type	ACI Rate (lb/hr)
1. E.C. Gaston	Low sulfur bituminous	750
2. Pleasant Prairie	Powder River Basin (PRB) subbituminous	750
3. Brayton Point	Low sulfur bituminous	750
4. Salem Harbor	Low sulfur bituminous	750

Projected to be Commercially Available on:

ACI technology is currently commercially available for utility industries.

Path to Commercial Availability:

Multiple ACI technology providers for utility industry as listed below;

Company	% Mercury removal	Experience	ACI system
1. ADA Environmental Solutions (CO, USA)	+90%	10+ years with >60 full-scale demonstrations (>16,000 MW of ACI systems under contract)	Standard and custom designed ACI systems
2. Norit Americas Inc (TX, USA)	+90%	15+ year	Standard and custom designed ACI systems
3. Dustex Cooperation (GA, USA)	+90%	Not given	Standard and custom designed ACI systems
4. APC Technologies Inc. (PA, USA)	+90%	Not given	Not given

Other suppliers include Clyde Bergemann Delta Ducon, Inc. (PA, USA) and FLSmidth (PA, USA).



Technology Survey: Activated Carbon Injection (ACI) and Wet Scrubber

Cost Summary:

Cap	Staffing	Maint.	Aux. Power	Disposal	By Product	Reagent	Fuel	Total O&M Cost

Total Installed Cost:

Total Annual O&M:

Source(s) of Cost Data:

Comments on Costs:

Low cost option. Impact of scrubber waste water contamination not considered.

Integration Potential:

Integrates easily, except for impacts to scrubber waste water/solid reuse.

Imposed Operational Limitations/Plant Impact:

- Impact on Scrubber Solid Recycle: Yes, the spent AC can contaminate the scrubber solid. Therefore, recycling these solids could result in very high (and increasing) levels of mercury being recycled. However, it is possible to minimize this impact if the scrubber solids are recycled to the grinding mill rather than the green ball feed. Since mercury tends to absorb to the nonmagnetic fraction of the scrubber solids, it will be discarded at the grinding mill where only the magnetic fraction of these solids are recovered. Or, other separation techniques (e.g. magnetic separation) may be used to separate the spent AC from the scrubber solids before recycling to the green ball feed.
- Impact on Iron Chemistry During the Induration Process: No, the activated carbon is added after induration.
- Others: the long-term balance-of-plant impacts is unknown when more expensive treated (brominated) AC is used to achieve desired mercury control, especially when high elemental Hg concentration is generated at taconite plants.

Other Technologies:

ACI technologies can be used with other particulate control devices (e.g., fabric filter) to help remove spent AC from the gas stream.

Materials of Construction (erosion, corrosion, etc.):

Corrosion resistant lances required due to presence of acidic species and humidity, although waste gas is not saturated.

Safety Comments:

Entry into AC silo requires assurance of breathable atmosphere. Entry will be rare.



Technology Survey: Activated Carbon Injection (ACI) and Wet Scrubber

General Comments:

ACI technology is a commercially proven technology for coal-fired power plants (>90% mercury removal) and has been tested for mercury control in the taconite facilities. Integration of the ACI technology to the taconite process is straightforward due to small footprint and small pressure drop (no need for additional fan power). Among other technologies, it is considered a low-cost option even though it is a throwaway process. However, spent AC can possibly impact the scrubber solid and wastewater and may worsen particulate emission of poorly functioning scrubbers.

Benefits and Drawbacks:

Benefits

- No additional duckwork is required, except for the injection lances. Equipment such as AC silo and feeder can be placed outside the process building.
- All equipment can be purchased directly from vendors and is very reliable.
- Depending on the amount of AC used, the annual labour cost for operating and maintaining the equipment is quite low.

Drawbacks

- Since mercury removal by the ACI technology is in-duct capture, optimization of the injection location is required to maximize the residence time. In addition, a flow profile and simulation of the duct may be necessary to ensure good distribution of AC and to determine the proper location of the lances.
- The amount of AC must be increased in order to achieve the same mercury removal level as would be when an electrostatic precipitator or a fabric filter is present.
- Additional AC could potentially increase particulate emissions.
- It can impact scrubber solids recycling and/or chemistry.

References:

1. Laudal, D.L., Dunham, G.E. Mercury Control Technologies for the Taconite Industry (2007).
2. Sjostrom, A.; Durham, M.; Bustard, C.J. Activated Carbon Injection for Mercury Control: Overview. Fuel 89 (2010), pp.1320 – 1322.

Technology Survey: Activated Carbon Injection (ACI) and Fabric Filter

Date of Technology Assessment: May 08, 2012

Equipment Summary:

1. Activated Carbon (AC)
2. AC silo
3. Feeder
4. Injection lance
5. Fabric filter

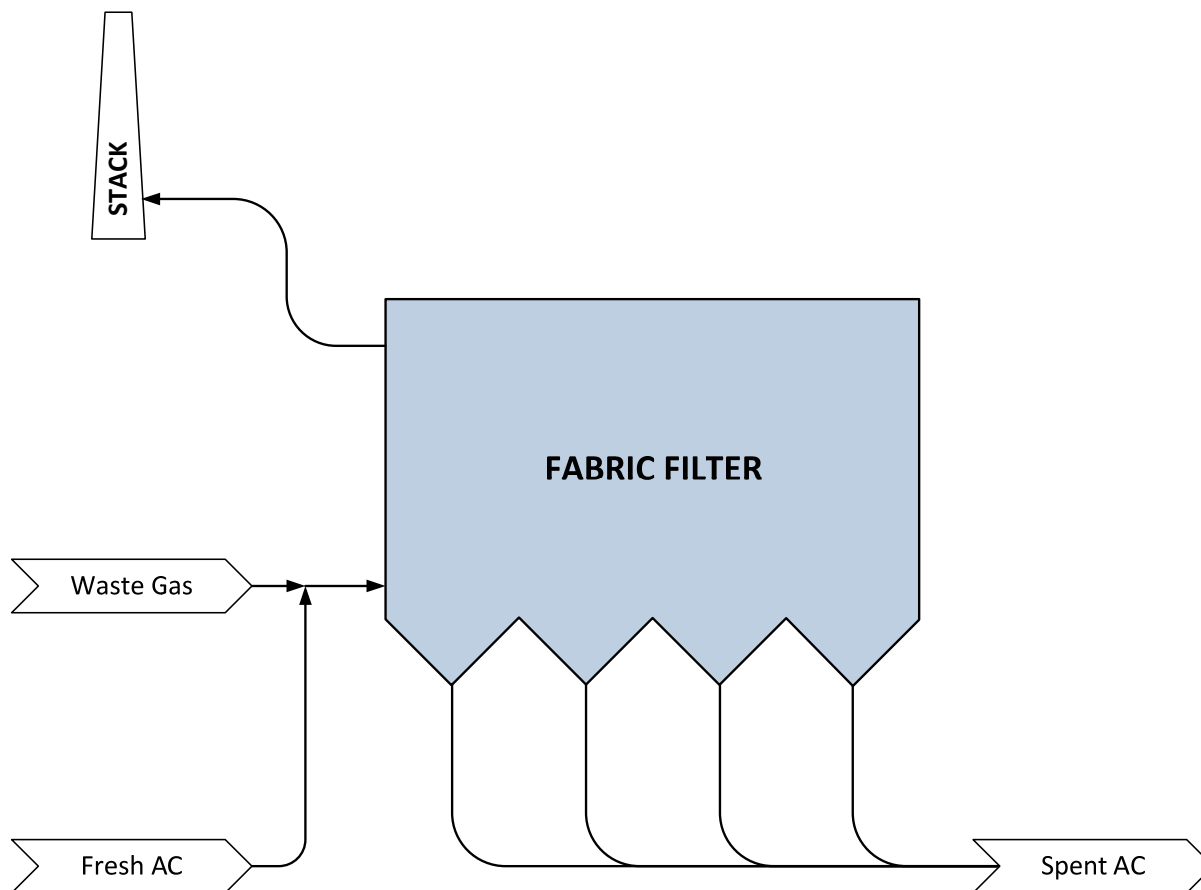
Detailed Description:

Powdered activated carbon is used as a sorbent to adsorb the mercury. It is injected and mixed with the waste gas in new ductwork leading to a fabric filter that will replace the existing wet scrubber. The fabric filter is used to filter the spent carbon out of the system.

Potential for Use with Generic Taconite Plant:

Injection lance prior to a new fabric filter. Lances for the entire waste gas duct and a specification of a fabric filter to be determined in detail design.

Flow Sheet:





Technology Survey: Activated Carbon Injection (ACI) and Fabric Filter																																																					
<ul style="list-style-type: none"> Scrubber Compatible: No. The fabric filter replaces the existing wet scrubber. Pressure Drop: High Footprint: 4500 ft² for one processing line (756000 acfm flue gas) Size: Small ACI system and 75 ft by 60 ft for fabric filter Power Usage: 3000 hp Suitability for IndurationType: Straight Grate/Grate Kiln Suitability for Fuel Type: See ACI technology Susceptibility to Flue Gas Compositions: See ACI technology Regeneration Capability: No Chemistry Between Mercury and Chemical Additive or Sorbents: See ACI technology Possibility of Mercury Re-emission/Desorption: Possible if a very high level of SO₂, NO_x, and HCl control is not obtained. 																																																					
<p>Maturity/Risk Comments: Mature technology, commercially available.</p>																																																					
<p>State of Development: <input type="checkbox"/> Conceptual <input type="checkbox"/> Bench Scale <input type="checkbox"/> Pilot Scale <input type="checkbox"/> Full Scale <input checked="" type="checkbox"/> Commercially Available & Performance Guaranteed</p>																																																					
<p>List of Users/Pilot Sites (include size of plant and type of fuel): Multiple utility + industrial applications.</p>																																																					
<p>Projected to be Commercially Available on: Both ACI technology and fabric filter are currently commercially available.</p>																																																					
<p>Path to Commercial Availability: Multiple ACI technology providers (See ACI technology) and fabric filter suppliers.</p>																																																					
<p>Cost Summary:</p> <table border="1" style="width: 100%; border-collapse: collapse; text-align: center;"> <thead> <tr> <th style="width: 11%;">Cap</th> <th style="width: 11%;">Staffing</th> <th style="width: 11%;">Maint.</th> <th style="width: 11%;">Aux. Power</th> <th style="width: 11%;">Disposal</th> <th style="width: 11%;">By Product</th> <th style="width: 11%;">Reagent</th> <th style="width: 11%;">Fuel</th> <th style="width: 11%;">Total O&M Cost</th> </tr> </thead> <tbody> <tr><td> </td><td> </td><td> </td><td> </td><td> </td><td> </td><td> </td><td> </td><td> </td></tr> <tr><td> </td><td> </td><td> </td><td> </td><td> </td><td> </td><td> </td><td> </td><td> </td></tr> <tr><td> </td><td> </td><td> </td><td> </td><td> </td><td> </td><td> </td><td> </td><td> </td></tr> <tr><td> </td><td> </td><td> </td><td> </td><td> </td><td> </td><td> </td><td> </td><td> </td></tr> </tbody> </table>									Cap	Staffing	Maint.	Aux. Power	Disposal	By Product	Reagent	Fuel	Total O&M Cost																																				
Cap	Staffing	Maint.	Aux. Power	Disposal	By Product	Reagent	Fuel	Total O&M Cost																																													
Total Installed Cost:				Total Annual O&M:																																																	
<p>Source(s) of Cost Data:</p>																																																					
<p>Comments on Costs: Middle cost option.</p>																																																					
<p>Integration Potential: Medium integration potential. Replacing the existing scrubber involves substantial duct work rearrangement.</p>																																																					

Technology Survey: Activated Carbon Injection (ACI) and Fabric Filter
<p>Imposed Operational Limitations/Plant Impact:</p> <ul style="list-style-type: none"> • Impact on Scrubber Solid Recycle: Yes, recycling solids will be mixed with the spent AC. To minimize the impact, the mixture should be recycled to the grinding mill, instead of the green ball feed, or it must be separated before recycle. • Impact on Iron Chemistry During the Induration Process: No, the activated carbon is added after induration. • Others: the long-term balance-of-plant impacts is unknown when more expensive treated (brominated) AC is used to achieve the desired mercury control, especially when high elemental Hg concentration is generated at taconite plants.
<p>Other Technologies:</p>
<p>Materials of Construction (erosion, corrosion, etc.): Corrosion resistant lances required due to presence of acidic species and humidity, although waste gas is not saturated. Stainless steel assumed for a fabric filter. However, the quality of materials may be reduced, which can be confirmed in detail design. If the waste gas from kilns is not corrosive, carbon steel can be used at a significant savings.</p>
<p>Safety Comments: Entry into AC silo requires assurance of breathable atmosphere. Entry will be rare.</p>
<p>General Comments: Each individual technology is a commercially proven technology for coal-fired power plants. In this particular application, the ACI technology removes mercury from the waste gas whereas the fabric filter filters spent AC out of the system, mitigating the particulate stack emission problem. Integration to the taconite process has a medium potential considering extra space, ductwork and fan power to accommodate the fabric filter in addition to the ACI system. Among other technologies, it is considered a middle-cost option due to additional equipment costs.</p>
<p>Benefits and Drawbacks:</p> <p><u>Benefits</u></p> <ul style="list-style-type: none"> • It increases particulate control. • It can achieve a high mercury control level with a relatively low amount of sorbents compared to the ACI technology. <p><u>Drawbacks</u></p> <ul style="list-style-type: none"> • Since mercury removal by the ACI technology is in-duct capture, optimization of the injection location is required to maximize the residence time. In addition, a flow profile and simulation of the duct may be necessary to ensure good distribution of AC and to determine the proper location of the lances. • Required space is large. • It can impact scrubber solids recycling and/or chemistry • Increased fan power is required.
<p>References: 1. Laudal, D.L., Dunham, G.E. Mercury Control Technologies for the Taconite Industry (2007).</p>

Technology Survey: Fixed Bed Adsorption

Date of Technology Assessment: May 08, 2012

Equipment Summary:

1. Activated Carbon (AC)
2. Carbon adsorption vessels

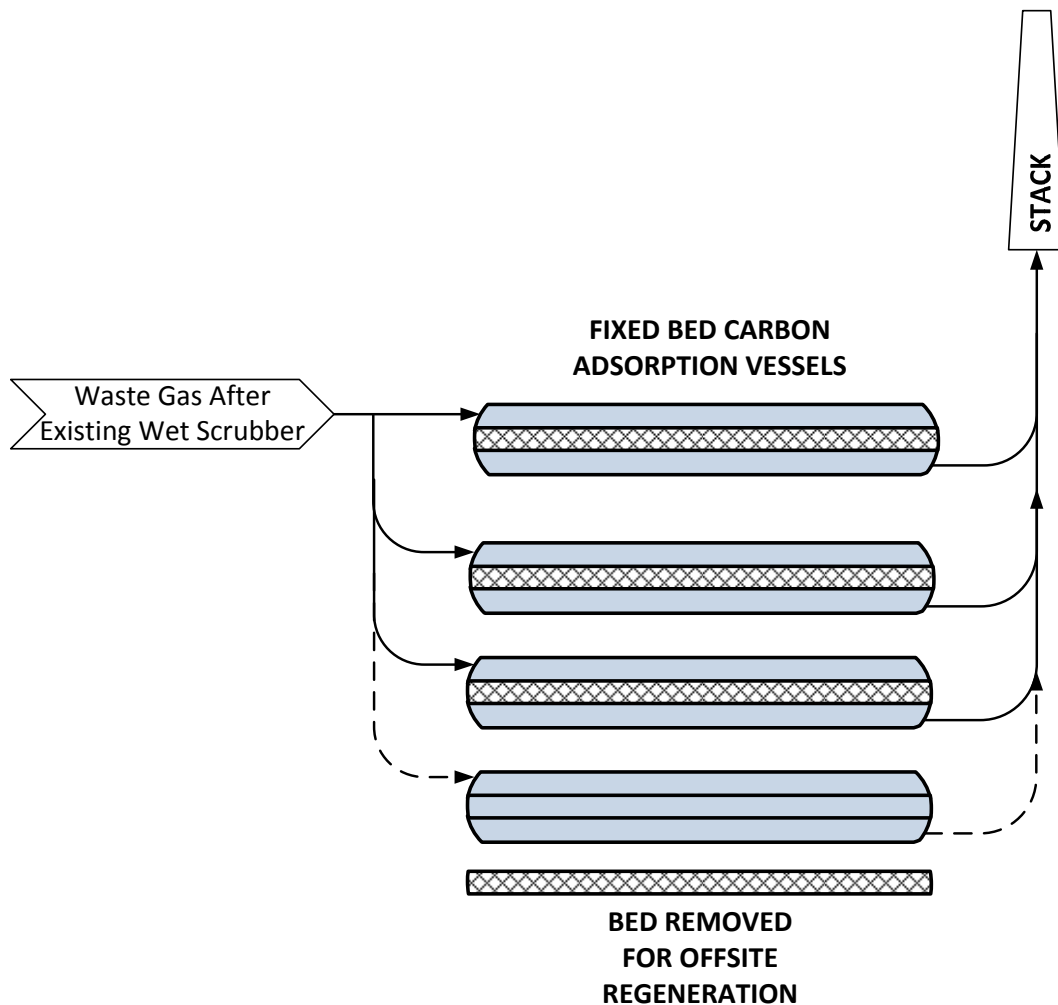
Detailed Description:

Powdered activated carbon is packed in a fixed-bed adsorption vessel. The waste gas leaving the wet scrubber passes through a series of these vessels where the fixed-carbon beds will remove the mercury from the waste gas. The spent beds will be removed for potential off-site regeneration.

Potential for Use with Generic Taconite Plant:

A series of adsorption vessels after existing wet scrubbers. Extensive amount of ductwork required. The number and size of vessels, the amount of AC initial fill and off-site regeneration to be determined in detail design.

Flow Sheet:



Technology Survey: Fixed Bed Adsorption

- Scrubber Compatible: Yes
- Pressure Drop: 6 – 12 in H₂O⁽²⁻⁴⁾ for one adsorption vessel (42300 acfm)
- Footprint: 42900 ft² for one processing line (756000 acfm flue gas)
- Size: 12 ft dia. and 47 ft long for one adsorption vessel (42300 acfm) (Require multiple vessels)
- Power Usage: 3000 hp (756000 acfm flue gas)
- Suitability for Induration Type: Straight Grate/Grate Kiln
- Suitability for Fuel Type: See ACI technology
- Susceptibility to Flue Gas Compositions: See ACI technology / Post scrubber corrosion concern due to wet gas
- Regeneration Capability: Yes
- Chemistry b/w Mercury and Additives or Sorbents: See ACI technology
- Possibility of Mercury Re-emission/Desorption: Possible if a very high level of SO₂, NO_x, and HCl control is not obtained or bed is replaced.

Maturity/Risk Comments:

Used in other industries. Piloting recommended.

State of Development:

- Conceptual
 Bench Scale
 Pilot Scale
 Full Scale
 Commercially Available & Performance Guaranteed

List of Users/Pilot Sites (include size of plant and type of fuel):

Plant	Application	Waste gas flow rate
1. Armak (MI, USA)	Solvent recovery system	125,000 scfm

Projected to be Commercially Available on:

The fixed-carbon bed technology is currently commercially available for several industries such as solvent recovery systems and waste-to-energy plants. A full-scale conceptual design for a taconite processing plant was performed in 2012 by ADAES.

Path to Commercial Availability:

Multiple fixed-bed adsorption technology providers as listed below;

Company	% Removal	Application
1. APC Technologies Inc. (PA, USA)	99% (mercury)	Wastewater treatment plants (sludge incinerators), hospital waste incinerators, municipal waste incinerators, waste-to-energy plants, fossil fuel fired boilers, taconite plants, retort furnaces, fluorescent bulb manufacturing, chlor-alkali plants, chemical plants and specialty refineries
2. AMCEC Inc. (IL, USA)	+99% (Organic solvents)	Solvent recovery systems
3. MEGTEC System Inc. (WI, USA)	+99% (Organic solvents)	Solvent recovery systems
4. Fusion Environmental Corporation (GA, USA)	+99% (Organic solvents, e.g., VOCs)	Solvent recovery systems

Technology Survey: Fixed Bed Adsorption

Cost Summary:

Cap	Staffing	Maint.	Aux. Power	Disposal	By Product	Reagent	Fuel	Total O&M Cost

Total Installed Cost:

Total Annual O&M:

Source(s) of Cost Data:

Comments on Costs:

High cost option due to large number of parallel trains, extensive ductwork and additional fan power to overcome back pressure exerted by the fixed bed. Cost can be decreased if the lower quality of materials of construction than stainless steel (assumed in this evaluation) is used.

Integration Potential:

Difficult, much ductwork rerouting required, and high space requirement.

Imposed Operational Limitations/Plant Impact:

- Impact on Scrubber Solid Recycle: No, the fixed carbon adsorption technology is applied after the scrubber. Therefore, the scrubber solid recycle is not affected.
- Impact on Iron Chemistry During the Induration Process: No, there is no need for the fixed bed technology to add any AC or additives during the induration process.
- Others: Very high pressure drop

Other Technologies:

In case of poor-efficiency wet scrubbers, installing particulate control devices (e.g., fabric filter) upstream of the adsorption vessel help reduce particulate clogging the fixed beds, but increase system pressure drop at the same time. Additional fan power is needed.

Materials of Construction (erosion, corrosion, etc.):

Post scrubber installation has acid dew point corrosion concerns. Stainless steel assumed in this evaluation. However, the quality of materials to resist corrosion may be reduced, which can be confirmed in detail design.

Safety Comments:

Entry to the fixed bed vessels is moderately frequent since entry is required each time the top layer of the bed needed to be changed, but manually entering the confined space may not be necessary depending on techniques used.

General Comments:

Although the fixed-carbon bed adsorption technology has been used in several industries (e.g., chlor-alkali plants and solvent recovery systems) to remove organic solvents from the gaseous streams with >99% removal, pilot testing with waste gas from the taconite processing plants is recommended. Since this technology requires large space to house several parallel trains, extensive ductwork and extra fan power, it makes the integration to the taconite process relatively difficult and expensive. However, this technology will not impact the existing wet scrubber.



Technology Survey: Fixed Bed Adsorption

Benefits and Drawbacks:

Benefits

- Increased particulate emissions can be avoided.
- Impact to scrubber solids recycling can be avoided since the technology is installed after the wet scrubber.

Drawbacks

- Additional fan power is required to overcome the pressure drop across the fixed-bed reactor.
- Required footprint is substantially large.
- Due to space limitation, the fixed-bed reactor would have to be located outside the process plant. Therefore, duct modification is required to direct the waste gas from the wet scrubber and back to the stack.
- High relative humidity can impact the carbon performance in fixed beds. A waste gas pretreatment may be required to get rid of excess water vapor.
- Material disposal (e.g., spent AC bed) should be taken into consideration.

References:

1. Laudal, D.L., Dunham, G.E. Mercury Control Technologies for the Taconite Industry (2007).
2. ADA Environmental Solutions (ADA-ES), Developing Cost-Effective Solutions to Reduce Mercury Emissions from Minnesota Taconite Plants: United Taconite Plant (2012).
3. ADA Environmental Solutions (ADA-ES), Developing Cost-Effective Solutions to Reduce Mercury Emissions from Minnesota Taconite Plants: Hibbing Taconite Plant (2012).
4. ADA Environmental Solutions (ADA-ES), Developing Cost-Effective Solutions to Reduce Mercury Emissions from Minnesota Taconite Plants: ArcelorMittal Minorca Mine Inc. Plant (2012).

Technology Survey: Fixed Bed Adsorption and Fabric Filter

Date of Technology Assessment: May 08, 2012

Equipment Summary:

1. Activated Carbon (AC)
2. Carbon adsorption vessels
3. Fabric Filter

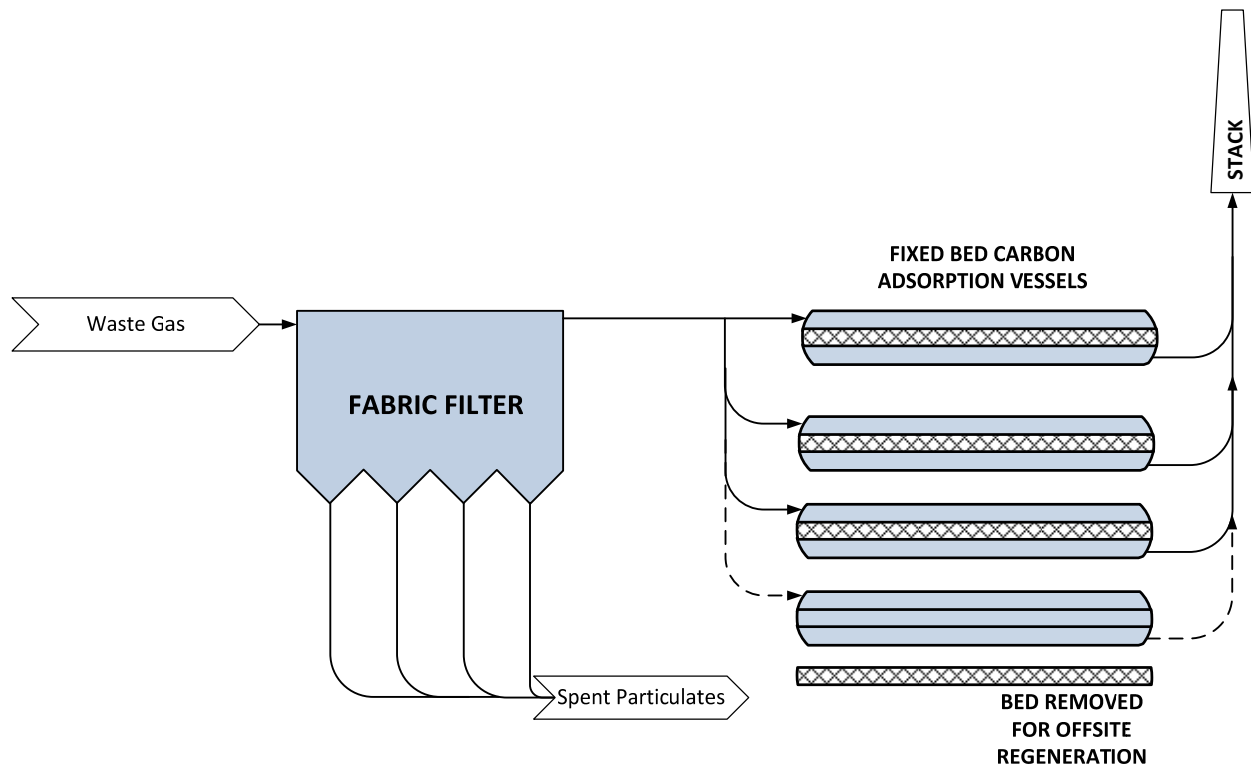
Detailed Description:

Waste gas passes through a fabric filter, which replaces the existing wet scrubber, to remove particulate matter to a level that eliminates potential problems with clogging the fixed carbon beds. The dedusted waste gas is then introduced to a series of fixed-bed carbon adsorption vessels, which will remove the mercury from the waste gas. The spent beds will be removed for off-site regeneration.

Potential for Use with Generic Taconite Plant:

Fabric filter and a series of adsorption vessels. Extensive amount of ductwork required. The number and size of vessels, the amount of AC initial fill and off-site regeneration as well as fabric filter sizing to be determined in detail design.

Flow Sheet:





Technology Survey: Fixed Bed Adsorption and Fabric Filter

- Scrubber Compatible: No. The fabric filter replaces the existing wet scrubber.
- Pressure Drop: Greater than the fixed bed technology (>6 – 12 in H₂O)
- Footprint: 47400 ft² for one processing line (756000 acfm flue gas)
- Size: 12 ft dia. and 47 ft long for one adsorption vessel (42300 acfm) (Require multiple vessels) and 75 ft by 60 ft for fabric filter
- Power Usage: 3900 hp (756000 acfm flue gas)
- Suitability for IndurationType: Straight Grate/Grate Kiln
- Suitability for Fuel Type: See ACI technology
- Susceptibility to Flue Gas Compositions: See ACI technology
- Regeneration Capability: Yes
- Chemistry Between Mercury and Chemical Additive or Sorbents: See ACI technology
- Possibility of Mercury Re-emission/Desorption: Possible if a very high level of SO₂, NO_x, and HCl control is not obtained or bed is replaced.

Maturity/Risk Comments:
Similar to the fixed-bed technology.

State of Development:
 Conceptual Bench Scale Pilot Scale Full Scale Commercially Available & Performance Guaranteed

List of Users/Pilot Sites (include size of plant and type of fuel):
Similar to the fixed-bed technology.

Projected to be Commercially Available on:
Similar to the fixed-bed technology.

Path to Commercial Availability:
Multiple fixed-carbon bed technology providers (see the fixed-bed technology) and fabric filter suppliers.

Cost Summary:

Cap	Staffing	Maint.	Aux. Power	Disposal	By Product	Reagent	Fuel	Total O&M Cost

Total Installed Cost: _____ **Total Annual O&M:** _____

Source(s) of Cost Data:

Comments on Costs:
Highest cost option due to large number of parallel trains, the fabric filter, extensive ductwork and additional fan power to overcome back pressure exerted by the fixed bed and the fabric filter. Cost can be decreased if the lower quality of materials of construction than stainless steel (assumed in this evaluation) is used.

Technology Survey: Fixed Bed Adsorption and Fabric Filter
<p>Integration Potential: Difficult, extensive space and ductwork modification required.</p>
<p>Imposed Operational Limitations/Plant Impact:</p> <ul style="list-style-type: none"> • Impact on Scrubber Solid Recycle: Yes, recycling solids will be mixed with the spent AC. To minimize the impact, the mixture should be recycled to the grinding mill, instead of the green ball feed, or it must be separated before recycle. • Impact on Iron Chemistry During the Induration Process: No, there is no need for the fixed bed technology to add any AC or additives during the induration process. • Others: Very high pressure drop.
<p>Other Technologies:</p>
<p>Materials of Construction (erosion, corrosion, etc.): Stainless steel assumed. However, the quality of materials may be reduced, which can be confirmed in detail design. If the waste gas from kilns is not corrosive, carbon steel can be used at a significant savings.</p>
<p>Safety Comments: Entry to fixed bed vessels is moderately frequent since the entry is required each time the top layer of the bed needed to be changed, but manually entering the confined space may not be necessary depending on techniques used.</p>
<p>General Comments: Similar to the fixed-bed technology. With an addition of the fabric filter, particulate clogging of the fixed carbon bed is eliminated but difficulty in process integration and cost is increased.</p>
<p>Benefits and Drawbacks:</p> <p><u>Benefits</u></p> <ul style="list-style-type: none"> • Increased particulate emissions can be avoided. • Clogging in the fixed-bed carbon vessel due to particulate matter is reduced. <p><u>Drawbacks</u></p> <ul style="list-style-type: none"> • Higher fan power than the fixed-bed technology to overcome the pressure drop across both fabric filter and fixed-bed reactors. • Required footprint is substantially larger than the fixed-bed technology. • Due to space limitation, both fabric filter and fixed-bed reactors would have to be located outside the process plant. Therefore, duct modification is required to direct the waste gas from the wet scrubber and back to the stack. • High relative humidity can impact the carbon performance in fixed beds. A waste gas pretreatment may be required to get rid of excess water vapor. • It can impact scrubber solids recycling and/or chemistry. • Material disposal (e.g., spent AC bed) should be taken into consideration.
<p>References:</p> <ol style="list-style-type: none"> 1. Laudal, D.L., Dunham, G.E. Mercury Control Technologies for the Taconite Industry (2007).

Technology Survey: Monolithic Polymer Resin Adsorption

Date of Technology Assessment: May 08, 2012

Equipment Summary:

- Adsorption vessels
- Activated-carbon polymer resin monoliths

Detailed Description:

Activated carbon fluoropolymer composite (CFC) materials are used to chemically adsorb mercury from the flue gas stream. The treated activated carbon powder is combined with chemicals such as elemental sulfur or alkaline metal iodides to enhance the mercury efficiency and the fluoropolymer (e.g., polymertetrafluoroethylene - PTFE). The mixture is then calendered into CFC sheets under elevated temperature. The CFC sheet is stretched extensively to develop the microporous structure that will allow rapid chemical oxidation of Hg^0 and binding of Hg^{2+} to the active sites of the fiber. Fig. 1 shows the microscopic structure of the CFC material where the solid nodes represent the activated carbon and the lines represent PTFE polymer fibrils. The mercury molecules in the flue gas will be chemically adsorbed on the activated carbon active sites. These sites do not saturate with SO_2 since SO_2 molecules adsorbed on the activated carbon are converted to H_2SO_4 with the presence of O_2 and H_2O , expelled from the activated carbon through the polymer fibril networks due to a high water repellency of PTFE and then collected at the outlet. Without SO_2 saturating the active sites, it is possible to achieve long-term operation before the activated carbon becomes saturated by mercury and sorbent regeneration may not be required in the lifetime of the adsorbent. When interviewed, the vendor indicates that adsorbent removal and replacement can be built into the supply contract and will be carried out periodically and automatically. The limited commercial experience with this technology does not allow prediction of service life at this time.

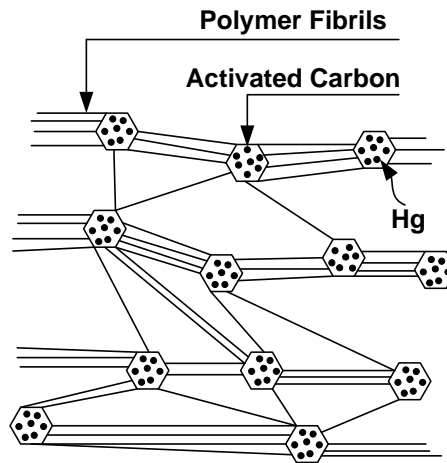


Figure 1. Microscopic structure of a CFC material

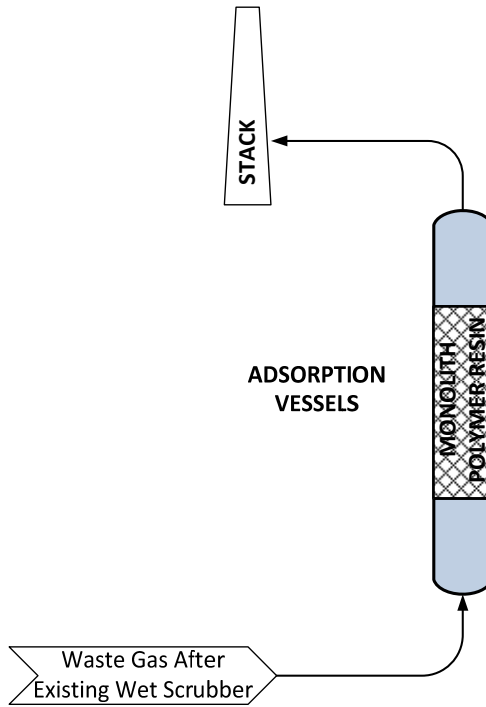
Both sides of the CFC surface can be laminated with extra porous membranes to enhance the PM2.5 filtration capability. The CFC sheets can be fixed on a solid frame in parallel with the same distance between the sheets to form a sorbent module, which will be stacked in the sorbent house. Alternatively, the CFC materials made into granular, rod or other shapes can be used as a packing material to form a packed-bed system [1,2]. Pressure drop created by this technology is expected to be lower than the fixed-bed technology since CFC sheets can be made into various shapes and forms, including an open-channel design.

Potential for Use with Generic Taconite Plant:

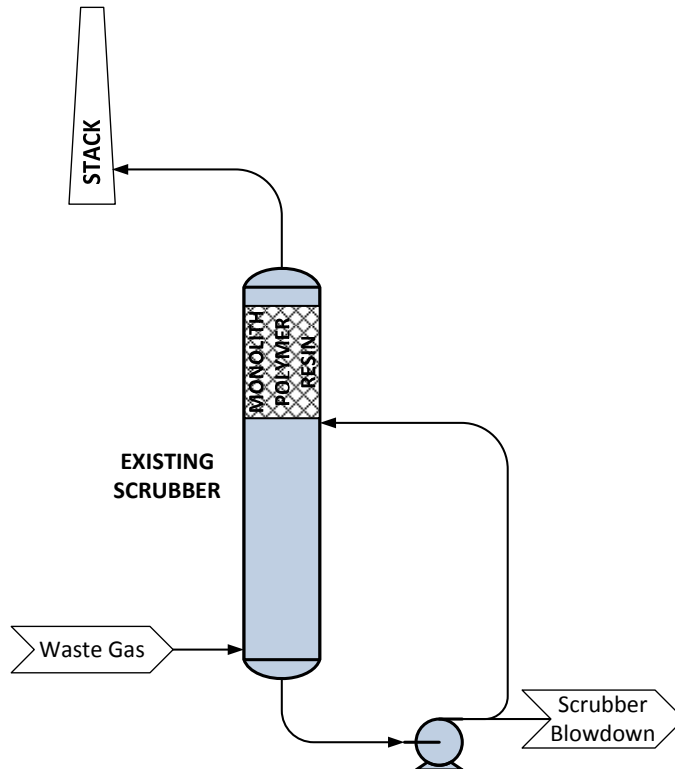
The monolith may be installed in a new adsorber vessel, or possibly integrated directly into the existing scrubber. In this evaluation, an installation of a new adsorber vessel is assumed.

Technology Survey: Monolithic Polymer Resin Adsorption

Flow Sheet:



(a) Adsorption vessels packed with the polymer resin monoliths is used to treat the waste gas after wet scrubber.



(b) the polymer resin monoliths are installed within the wet scrubber.



Technology Survey: Monolithic Polymer Resin Adsorption

- Scrubber Compatible: Yes
- Pressure Drop: Expected to have lower pressure drop than the fixed bed design due to open-channel Design (based on preliminary vendor commentary).
- Footprint: 6400 ft² for post scrubber installation. The foot print can be reduced if the monoliths are installed in the scrubber.
- Size: A single vessel with 32 ft by 32 ft square by 30 ft tall
- Power Usage: Fan power required
- Suitability for IndurationType: Unknown. Never been tested in the taconite processing plants.
- Suitability for Fuel Type: Need further testing
- Susceptibility to Flue Gas Compositions: No
- Regeneration Capability: No need for regeneration
- Chemistry Between Mercury and Chemical Additive or Sorbents: Need further testing
- Possibility of Mercury Re-emission/Desorption: No

Maturity/Risk Comments:

Immature technology has been piloted successfully, larger scale pilot planned for 2013. The site has not been announced.

State of Development:

Conceptual Bench Scale Pilot Scale (small) Full Scale Commercially Available & Performance Guaranteed

List of Users/Pilot Sites (include size of plant and type of fuel):

Power Plant	Coal Type	Flue Gas	CPC Tape	%Hg Removal	Ref
1. Plant Yates	low sulfur, eastern bituminous coal	Slip stream after wet scrubber			3-5
		<ul style="list-style-type: none"> • 5.0 acfm, 100% humidity and 123°F • 13.0 and 24.7 acfm, 100% humidity and 123°F 	Four 5" wide, 5' long strips	~60% for 60 days	
			Eight 6" deep, 3.8" diameter cylindrical modules	>90% for 120 days	

Projected to be Commercially Available on:

Full-scale demonstration is proposed in 2013 [5].

Path to Commercial Availability:

Company	% Mercury Removal	Application
1. W. L. Gore & Associates, Inc. (DE, USA)	Up to 95%	Coal-fired power plants

Cost Summary:

Cap	Staffing	Maint.	Aux. Power	Disposal	By Product	Reagent	Fuel	Total O&M Cost

Total Installed Cost:

Total Annual O&M:

Technology Survey: Monolithic Polymer Resin Adsorption
Source(s) of Cost Data:
Comments on Costs: It offers low operating cost due to long module life time (very high mercury storage capacity) and simple operation (no adjustments needed to account for changes in mercury concentration or speciation, little to no maintenance or energy required to operate, no regeneration).
Integration Potential: Extra space to install a single adsorption vessel and ductwork modification required unless the in-scrubber installation is considered.
Imposed Operational Limitations/Plant Impact: <ul style="list-style-type: none"> • Impact on Scrubber Solid Recycle: No, the polymer resin monolith is applied after the scrubber. Therefore, the scrubber solid recycle is not affected. • Impact on Iron Chemistry During the Induration Process: No, there is no need for the monolithic polymer resin adsorption technology to add any additives during the induration process. • Others: May adsorb SO₂ as H₂SO₄, and add this acid to the scrubber water. It is unclear if this waste stream is already acidic, and if a lower pH is an issue.
Other Technologies:
Materials of Construction (erosion, corrosion, etc.): Must be constructed of corrosion resistant materials.
Safety Comments: Minimal.
General Comments: This developing technology requires further testing with the taconite waste gas. Data from pilot testing with coal-fired flue gases showed positive results of up to 95% mercury removal without sorbent regeneration. It is considered a low cost option compared with other technologies.
Benefits and Drawbacks: <u>Benefits</u> <ul style="list-style-type: none"> • No frequent regeneration required since the bed is not deactivated by SO_x or other acid gases [3]. • It offers co-benefit of SO₂ and PM2.5 reduction since most of SO₂ will be converted to H₂SO₄ (aq) (~37%wt) and PM2.5 can be filtered out [1]. • The pressure drop due to the CPC sheet or CPC in modular forms is reasonably low [3]. • The CPC sheet can be used to capture PM2.5 by surface filtration mechanism, and SO_x and other acid gases by converting them into aqueous acid solutions and expelled to the outer surfaces of the CPC sheet [1,3] • The peripheral equipment such as silos and lances and procedures associated with PAC injection, collection, and disposal not required [2]. • It is insensitive to flue gas compositions (SO₃, halogen content, VOCs) [5]. • It is possible to use within a wet scrubber to prevent mercury re-emissions from the scrubber and provide



Technology Survey: Monolithic Polymer Resin Adsorption

SO_x polishing [5].

- Since mercury reduction is determined by the number of the CPC modules, it allows a flexibility to meet future regulations or process changes by simply adding additional layer of modules.

Drawbacks

- The technology is immature and requires full-scale demonstration.
- Impact of condensing acids on scrubber water is unknown.

References:

1. Lu, X-C; Wu, X. Flue Gas Purification Process Using a Sorbent Polymer Composite Material. U.S. Patent No. 7,442,352 B2 (2008).
2. Durante, V.A.; Stark, S.; Gebert, R.; Xu, Z.; Bucher, R., Keeney, R.; Ghorishi, B. A Novel Technology to Immobilize Mercury from Flue Gases. Paper # 232 (2003).
3. Darrow, J.R. Options for PM, Dioxin/Furan and Mercury Control Using ePTFE Technologies. Presentation (2011).
4. Lu, X.S.; Xu, Z.; Stark, S.; Gebert, R.; Machalek, T.; Richardson, C.; Paradis, J.; Chang, R.; Looney, B. Matthews, M. Flue Gas Mercury Removal Using Carbon Polymer Composite Material. Presented at EUEC, Jan 31 – Feb 2, 2011.
5. Darrow, J.; Kolde, J. Gore ® Mercury Control System. Presentation (2012).

Technology Survey: Oxidative Chemical Addition

Date of Technology Assessment: May 08, 2012

Equipment Summary:

1. Chemical additives – Several potential chemical additives were considered as listed below;
 - Sodium and calcium chloride (NaCl and CaCl_2)
 - Sodium and calcium bromide (NaBr and CaBr_2)
 - Hydrogen peroxide (H_2O_2)
 - EPA's proprietary oxidant
 - EERC's proprietary additive
 - Ozone
 - Sodium bicarbonate (NaHCO_3)

Note that an H_2O_2 solution can capture about 10 – 15% of the mercury in the process gas. It is not a likely candidate for taconite processing plants and it even interferes with the background mercury oxidation process that takes place when no oxidant is added to the water. However, the proprietary EPA oxidant achieved above 80% removal.

2. Chemical silo

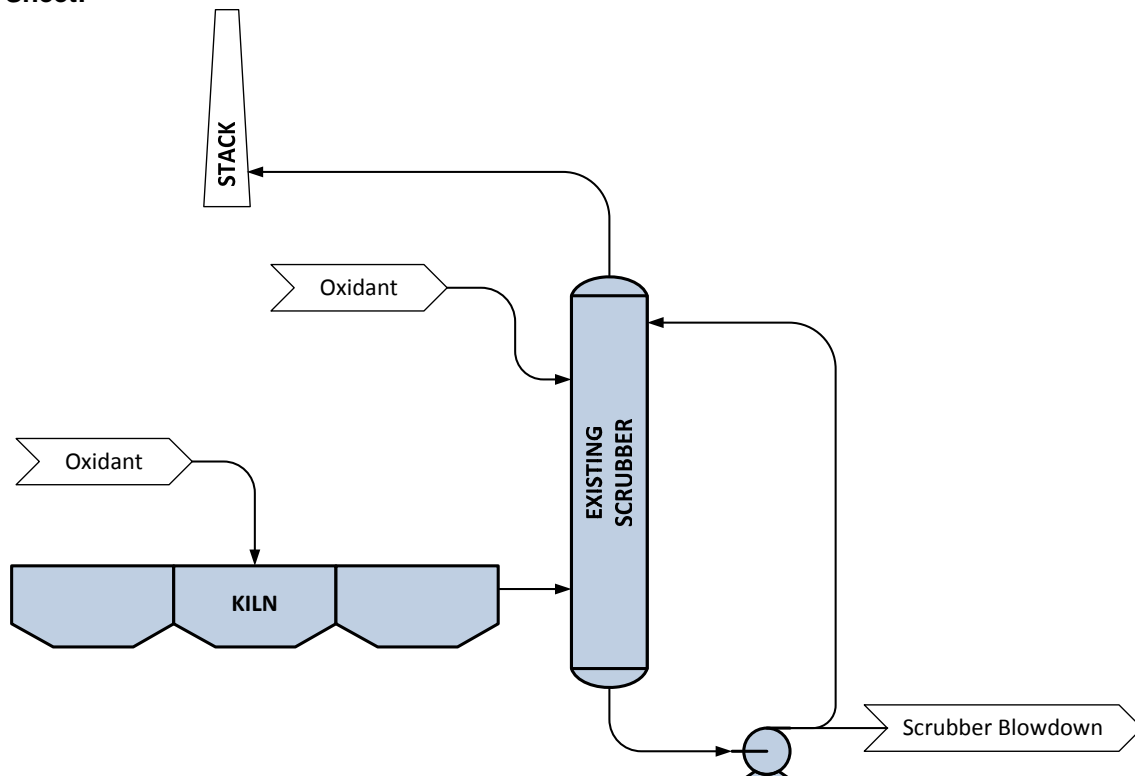
Detailed Description:

A chemical additive is added in the waste gas to enhance mercury oxidization converting Hg^0 (insoluble) to Hg^{2+} (water-soluble). An increase in the percentage of Hg^{2+} or particulate-bound mercury at the inlet of the wet scrubber will improve the mercury removal from the process.

Potential for Use with Taconite Plant:

Short-term tests has been conducted at the taconite plants for mercury reduction from stack emissions in 2007. A series of experiments was performed on slipstream gases from an operating taconite facility to investigate the effect of chemical oxidants on capture efficiency for elemental mercury. CaBr_2 is assumed as the oxidant for this analysis.

Flow Sheet:





Technology Survey: Oxidative Chemical Addition

- Scrubber Compatible: No. Oxidants will impact scrubber solid recycle/effluent.
- Pressure Drop: No change to current pressure drop.
- Footprint: 2500 ft² for one processing line (756000 acfm flue gas)
- Size: Small
- Power Usage: Small. No additional fan power is required.
- Suitability for Induration Type: Grate Kiln
- Suitability for Fuel Type: Need further testing
- Susceptibility to Flue Gas Compositions: EPA_{ox} reacts extensively with SO_x and NO_x.
- Regeneration Capability: No
- Chemistry b/w Mercury and Additive or Sorbents: Partially studied
- Possibility of Mercury Re-emission/Desorption: Yes

Maturity/Risk Comments:

Commercially emerging technology has been tested in the coal-fired power plants. Pilot testing is recommended. High potential for corrosion and erosion when the halogenated additives are used.

State of Development:

Conceptual
 Bench Scale
 Pilot Scale
 Full Scale
 Commercially Available & Performance Guaranteed

List of Users/Pilot Sites (include size of plant and type of fuel):

Taconite Plant	Fuel Type	Production Rate (Lt/hr)	Induration Type	Pellet	Scrubber Type	Chemical Additive
1. U-Tac	Natural gas /Coal	200 - 450	Grate Kiln	Standard	Recirculating	NaCl to greenball
2. Hibtac	Natural gas	300 - 350	Straight Grate	Standard	Once through	NaCl, NaBr, CaCl ₂ and CaBr ₂ to greenball and process gas
3. KeeTac	Natural gas /Coal	700	Grate Kiln	Standard	Recirculating	H ₂ O ₂ and EPA's proprietary oxidant to scrubber liquid

Projected to be Commercially Available on:

Path to Commercial Availability:

Multiple oxidative chemical suppliers.

Cost Summary:

Cap	Staffing	Maint.	Aux. Power	Disposal	By Product	Reagent	Fuel	Total O&M Cost

Total Installed Cost:

Total Annual O&M:



Technology Survey: Oxidative Chemical Addition
<p>Source(s) of Cost Data:</p>
<p>Comments on Costs: Least expensive option.</p>
<p>Integration Potential: Integrates easily, except for impacts to iron and scrubber waste water/solid reuse.</p>
<p>Imposed Operational Limitations/Plant Impact:</p> <ul style="list-style-type: none"> • Impact on Scrubber Solid Recycle: Yes, chemical additives increase the mercury concentration in the scrubber solids. To minimize the impact, the scrubber solids should be recycled to the grinding mill, instead of the green ball feed. • Impact on Iron Chemistry During the Induration Process: Possible for the additives added directly to the kiln. • Others: There is a potential for corrosion and erosion, especially when the halogenated (Br and Cl) additives are used due to a generation of halogen gases (Br₂ and Cl₂). If the tests for halide addition yielded positive results for mercury control, corrosion studies and cost analysis would be required prior to considering a viable technology.
<p>Other Technologies:</p>
<p>Materials of Construction (erosion, corrosion, etc.): Corrosion resistant materials may be needed if the halogenated (Br and Cl) additives are used.</p>
<p>Safety Comments: Most oxidants are very safe. H₂O₂, if considered, is hazardous. Oxygen stored for ozone production hazardous (compressed gas).</p>
<p>General Comments: It is a commercially emerging technology with relatively simple process integration to the taconite processing plant. It is the least expensive option among other technologies. Further testing is recommended to understand the effect of oxidative chemicals on the chemistry of iron product, mercury reemission, scrubber liquids/solids and corrosion.</p>
<p>Benefits and Drawbacks:</p> <p><u>Benefits</u></p> <ul style="list-style-type: none"> • For in-scrubber oxidation, the equipment required is inexpensive and simple since it involves only a tank to contain the oxidant and a small pump to feed the material in the scrubber system. <p><u>Drawbacks</u></p> <ul style="list-style-type: none"> • The EPA oxidant can react extensively with NO_x and SO_x. This implies both a higher consumption rate for the oxidant and a potential for high NO₃⁻ in the scrubber effluent, which may lead to a water treatment problem. • It can impact scrubber solids recycling and/or chemistry.



Technology Survey: Oxidative Chemical Addition
<ul style="list-style-type: none">• It is likely to impact iron chemistry, especially when the additive is added during the induration process.
<p>References:</p> <ol style="list-style-type: none">1. Laudal, D.L., Dunham, G.E. Mercury Control Technologies for the Taconite Industry (2007).2. Berndt, M.E., Engesser, J. Mercury Transport in Taconite Processing Facilities: (III) Control Method Test Results (2007).

Technology Survey: Monolithic Honeycomb Adsorption

Date of Technology Assessment: May 08, 2012

Equipment Summary:

- Adsorption vessels
- Honeycomb monoliths

Detailed Description:

A series of activated carbon honeycomb catalyst monoliths is used to remove mercury from the flue gas. The honeycomb monolith is usually made of an activated carbon powder and catalyst (e.g. elemental sulfur). It comprises multiple opening cells and plugs, which are interconnected by porous walls extending from the inlet to the outlet. Each cell is preferably plugged only at one end. This plugging configuration in Fig. 1(a) will improve intimate contact between the flue gas and the porous wall of the monolith. Fig. 1(b) shows that the flue gas enters the monolith through the opening cells at the inlet end, then through the porous cell walls and out of the monolith through the open cells at the outlet end.

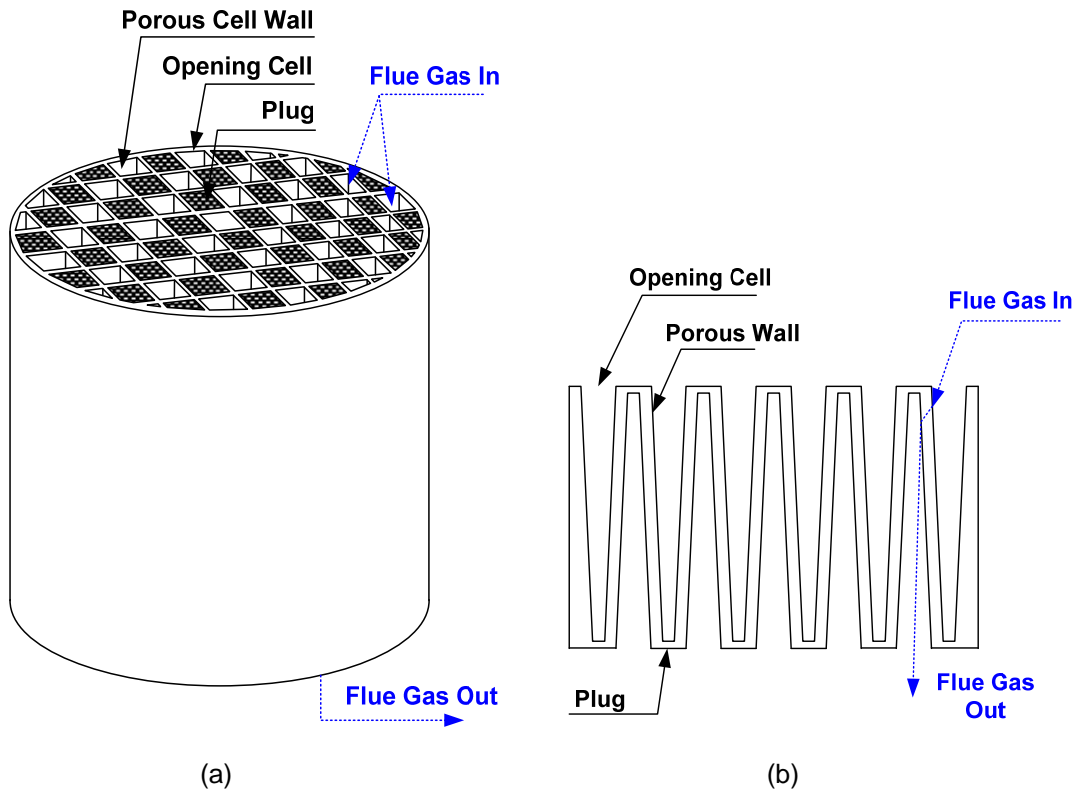


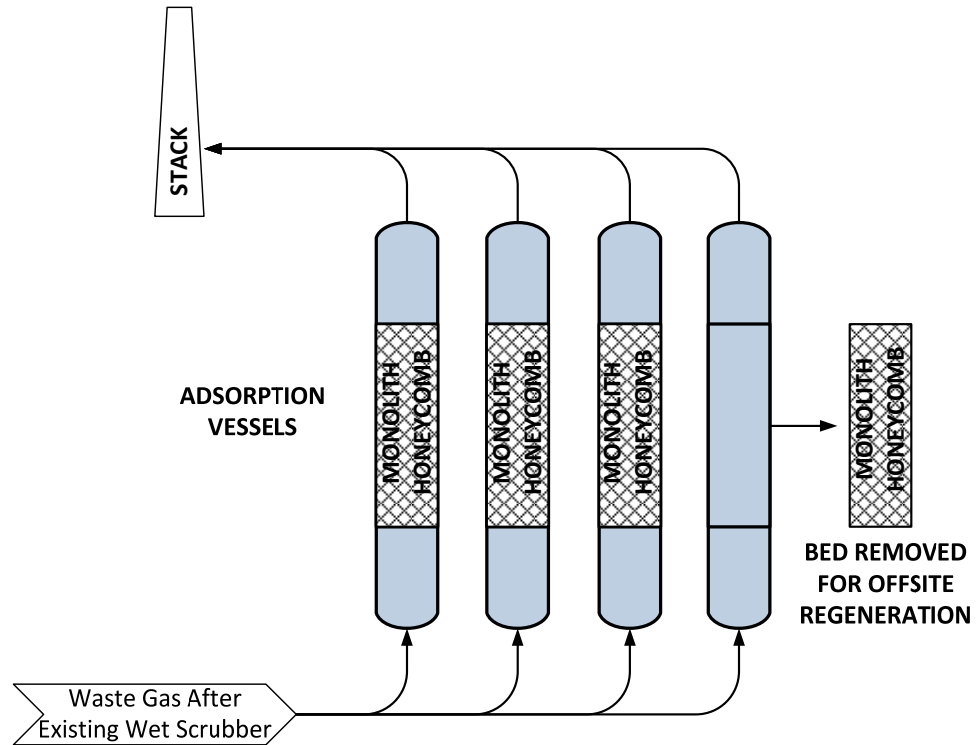
Figure 1 (a) Plugged wall flow honeycomb monolith, (b) Cross-sectional view of plugged wall flow honeycomb monolith

Potential for Use with Generic Taconite Plant:

This technology is no longer being commercially developed, thus further evaluation has been halted.

Technology Survey: Monolithic Honeycomb Adsorption

Flow Sheet:



- Scrubber Compatible:
- Pressure Drop:
- Footprint:
- Size:
- Power Usage:
- Suitability for IndurationType:
- Suitability for Fuel Type:
- Susceptibility to Flue Gas Compositions:
- Regeneration Capability:
- Chemistry Between Mercury and Chemical Additive or Sorbents:
- Possibility of Mercury Re-emission/Desorption:

Maturity/Risk Comments:

No longer commercially developed.

State of Development:

- Conceptual
 Bench Scale
 Pilot Scale
 Full Scale
 Commercially Available & Performance Guaranteed

List of Users/Pilot Sites (include size of plant and type of fuel):

Projected to be Commercially Available on:



Technology Survey: Monolithic Honeycomb Adsorption

Path to Commercial Availability:

The honeycomb technology is no longer considered a commercially viable technology for mercury control. The technology developers were MeadWestvaco and Corning Incorporated.

Cost Summary:

Cap	Staffing	Maint.	Aux. Power	Disposal	By Product	Reagent	Fuel	Total O&M Cost

Total Installed Cost:

Total Annual O&M:

Source(s) of Cost Data:

Comments on Costs:

Integration Potential:

Imposed Operational Limitations/Plant Impact:

- Impact on Scrubber Solid Recycle:
- Impact on Iron Chemistry During the Induration Process:
- Others:

Other Technologies:

Materials of Construction (erosion, corrosion, etc.):

Safety Comments:

General Comments:



Technology Survey: Monolithic Honeycomb Adsorption

Benefits and Drawbacks:

Benefit

- > 90% of Hg⁰ removal efficiency without adding active materials such as activated carbon powder or ammonia to the system [1].
- No a particulate matter such as FF and ESP required to remove the active material added [1].
- Compared to ACI, Lower amount of contaminated activated carbon material being regenerated with low hazardous waste disposal cost [1].

References:

1. Gadkaree, K.P.; He, L.; Shi, Y. Activated Carbon Honeycomb Catalyst Beds and Methods for the Use Thereof. U.S. Patent No. 7,722,705 B2 (2010).

Stantec

ADA Environmental Solutions
EVALUATION OF MERCURY CONTROL OPTIONS
TACONITE INDUSTRY
August 14, 2012

APPENDIX B

Evaluation Backup Information

PARAMETER		UNIT	KEEWATIN TACONITE (KEETAC)	HIBBING TACONITE (HIBTAC)			ARCELOR MITTAL	USS MINNTAC (MINNTAC)					UNITED TACONITE (U-TAC)		GENERIC TACONITE PLANT 1 - STRAIGHT GRATE	GENERIC TACONITE PLANT 2 - GRATE KILN	
LOCATION			Keewatin	Hibbing			Virginia	Mountain Iron					Eveleth				
STACK RELATIVE HUMIDITY		(%)	Not given	70 ^(a)	Not given	Not given	94 ^(a)	Not given					Not given	67 ⁽¹⁾	70	70	
STACK TEMPERATURE		(°F)	Not given	124 ^(a)	Not given	Not given	125 ^(a)	125 ^(e)					Not given	140 ⁽¹⁾	125	125	
LINE NO.		(-)	2 ^(e)	1	2	3	1	3	4	5	6	7	1	2	1	1	
INDURATION TYPE		(-)	Grate Kiln	Straight Grate	Straight Grate	Straight Grate	Straight Grate	Grate Kiln	Grate Kiln	Grate Kiln	Grate Kiln	Grate Kiln	Grate Kiln	Grate Kiln	Straight Grate	Grate Kiln	
PELLET TYPE		(-)	Standard	Standard	Standard	Standard	Flux	Standard/Flux ^(e)	Standard/Flux ^(e)	Standard/Flux ^(e)	Standard/Flux ^(e)	Standard/Flux ^(e)	Standard	Standard	Standard	Standard	
EXISTING PM CONTROL DEVICE	• Wet Venturi Type Scrubber	(-)	Yes	Yes	Yes	Yes	Yes	Yes	Yes	Yes	Yes	Yes	Yes	Yes	Yes	Yes	
	• Multiclone	(-)	Yes	Yes	Yes	Yes	Yes	Yes ^(e)	Yes ^(e)	Yes ^(e)	Yes ^(e)	Yes ^(e)	No	No	No	No	
	• Lime Neutralization	(-)	Yes	No	No	No	No	Yes	No	No	No	No	No	No	No	No	
SCRUBBER TYPE		(-)	Recirculating	Once through	Once through	Once through	Recirculating	Recirculating	Once Through	Once Through	Once Through	Once Through	Recirculating	Recirculating	Recirculating	Recirculating	
SCRUBBER LIQUID		(gpm)	7250 ^(b)	3500 ^(b)	3500 ^(b)	3500 ^(b)	4000 ^(b)	2500 ^(e)	3000 ^(b)	3000 ^(b)	3000 ^(b)	3000 ^(b)	Not given	5800 ^(b)	7250	7250	
WASTE GAS TO SCRUBBER		(scfm)	570000 ^(b)	500000 ^(b)	500000 ^(b)	500000 ^(b)	350000 ^(b)	225000 ^(e)	410000 ^(b)	410000 ^(b)	400000 ^(b)	400000 ^(b)	Not given	580000 ^(b)	580000	580000	
WASTE GAS AFTER SCRUBBER		(scfm)	570000 ^(e)	756000 ^(f)	756000 ^(f)	756000 ^(f)	854000 ⁽³⁾	225000 ^(e)	410000 ^(e)	410000 ^(e)	410000 ^(e)	410000 ^(e)	292000 ^(e)	636000 ^(e)	854000	854000	
GASEOUS COMPOSITION AFTER SCRUBBER	• Moisture	(%)	15 ^(e)	9.96 ^(f)	9.96 ^(f)	9.96 ^(f)	13.98 ^(c)	15 ^(e)	15 ^(e)	15 ^(e)	15 ^(e)	15 ^(e)	Not given	15.27 ^(g)	15.27	15.27	
	• Mercury	(µg/m ³)	Not given	10 ^(f)	10 ^(f)	10 ^(f)	10 ^(c)	Not given	Not given	Not given	Not given	Not given	Not given	10 ^(g)	10	10	
SCRUBBER BLOWDOWN		(gpm)	375 ^(b)	Not given	Not given	Not given	350 ^(b)	100 ^(e)	Not given	Not given	Not given	Not given	Not given	800 ^(b)	800	800	
% SOLIDS IN SCRUBBER BLOWDOWN		(%)	Not given	Not given	Not given	Not given	Not given	Not given	0.07 ^(b)	0.07 ^(b)	0.07 ^(b)	0.07 ^(b)	Not given	2 ^(b)	2	2	
SOLID RECYCLE TO THE PROCESS		(-)	No	Yes	Yes	Yes	Yes	No	Yes ^(e)	Yes ^(e)	Yes ^(e)	Yes ^(e)	Not given	Yes	Yes	Yes	
RECYCLE LOCATION		(-)	N/A	Grinding Mills	Grinding Mills	Grinding Mills	Thickener ^(e)	N/A	Thickener ^(e)	Thickener ^(e)	Thickener ^(e)	Thickener ^(e)	Not given	Green Ball Feed	Green Ball Feed	Green Ball Feed	
SOLID DISPOSAL		(-)	Landfill	N/A	N/A	N/A	N/A	Settling Pond	N/A	N/A	N/A	N/A	Not given	N/A	N/A	N/A	
PRODUCTION RATE		(Lt/hr)	700 ^(d)	300-350 ^(d)	300-350 ^(d)	300-350 ^(d)	350 ^(d)	200-250 ^(d)	400-450 ^(d)	400-450 ^(d)	400-450 ^(d)	400-450 ^(d)	200-250 ^(d)	400-450 ^(d)	700	700	
FUEL TYPE	• Coal	(-)	Yes (Power River Basin Coal)									Yes (Power River Basin Coal)	Yes (Power River Basin Coal)	Yes (Eastern bit.)	Yes (Eastern bit.)	Yes (PRB Subbit. Coal)	Yes (PRB Subbit. Coal)
	• Natural Gas	(-)	Yes	Yes	Yes	Yes	Yes	Yes	Yes	Yes	Yes	Yes	Yes ^(e)	Yes ^(e)	Yes	Yes	
	• Wood	(-)							Yes	Yes	Yes ^(e)	Yes ^(e)			No	No	
	• Petroleum Coke	(-)											Yes	Yes	No	No	
AIR FLOW RATE		(kscfm)	550-650 ^(d)	350-400 ^(d)	350-400 ^(d)	350-400 ^(d)	350 ^(d)	180-250 ^(d)	370-450 ^(d)	370-450 ^(d)	370-450 ^(d)	370-450 ^(d)	180-250 ^(d)	450-600 ^(d)	650	650	
PM EMISSION RATE	• Dry Catch Only (Filterable)	(lb/hr)		17 ^(a)	Not given	Not given	29.7 ^(a, Note 1)	Not given	Not given	54 ^(e)	Not given	25 ^(e)	12	19.7	54	54	
	• Dry Catch Only (Filterable) + Organic Condensibles	(lb/hr)		21 ^(a)	Not given	Not given	36.1 ^(a, Note 1)	Not given	Not given	56 ^(e)	Not given	25 ^(e)	13	20.3	56	56	
	• Dry Catch Only (Filterable) + Organic Cond. + Inorganic Cond.	(lb/hr)		Not given	Not given	Not given	Not given	Not given	Not given	62 ^(e)	Not given	29 ^(e)	Not given	26.1	62	62	
	• Dry Catch Only (Filterable) + Organic Cond. + Aq. Phase Cond.	(lb/hr)	N/A ^(e)	28 ^(a)	Not given	Not given	Not given	N/A ^(e)	N/A ^(e)	N/A ^(e)	N/A ^(e)	N/A ^(e)	Not given	Not given	28	28	
SO ₂ EMISSION RATE		(lb/hr)	272 ^(e)	55 ^(a)	Not given	Not given	Not given	Not given	Not given	Not given	Not given	Not given	Not given	Not given	272	272	
NO _x EMISSION RATE		(lb/hr)	Not given	311 ^(a)	Not given	Not given	Not given	Not given	Not given	Not given	Not given	Not given	Not given	Not given	311	311	

^(a) Stack data received from Task Force via email on April 20, 2012

Note ⁽¹⁾ It is a sum of Stack A - D. Since no unit is given in the stack data table, "lb/hr" is assumed.

^(b) Data from "Taconite Processes.docx" on February 17, 2012

^(c) ADAES, Draft final report "Developing Cost-Effective solutions to Reduce Mercury Emissions from Minnesota Taconite Plants - ArcelorMittal Minorna Mine Inc.Plant", February 28, 2012

^(d) Berndt, M., Technical report "Mercury Control Technologies for the Taconite Industry", June, 2007

^(e) Data from Task Force's comments on May 30, 2012

^(f) ADAES, Draft final report "Developing Cost-Effective solutions to Reduce Mercury Emissions from Minnesota Taconite Plants - Hibbing Taconite Plant", February 28, 2012

^(g) ADAES, Draft final report "Developing Cost-Effective solutions to Reduce Mercury Emissions from Minnesota Taconite Plants - United Taconite Plant", February 28, 2012

Technology Survey (Generic Taconite Plant 1 - Straight Grate)

Stantec Project # 111100111
 Prepared by: MER
 Date: 14-Aug-12

Desirable Criteria	Weight	Activated Carbon Injection (ACI) - Scrubber Capture			ACI - Fabric Filter			Fixed Bed Adsorption			Fixed Bed Adsorption - Fabric Filter			Oxidative Chemical Addition			
		Sc	Wt Sc	Notes	Sc	Wt Sc	Notes	Sc	Wt Sc	Notes	Sc	Wt Sc	Notes	Sc	Wt Sc	Notes	
1.0	Economic - 20%																
1.1	Capital Cost	10	10	100	6	60		2	20		1	10		10	100		
1.2	Operating Cost	10	4	40	3	30		2	20		1	10		10	100		
	SUB-TOTAL	20		140		90			40			20			200		
2.0	Risk - 30%																
2.1	Turndown	1	8	8	Limited by existing scrubber	10	10	Not limited by existing scrubber. Fabric filter replaces scrubber.	10	10	Multiple vessels give flexibility	10	10	Multiple vessels give flexibility	8	8	Limited to turndown of entire system
2.2	Availability / Reliability	1	10	10	Minimal moving parts	8	8	Minimal moving parts / Bag changes	6	6	Carbon bed replacement	5	5	Carbon bed replacement / Bag changes	10	10	Minimal moving part
2.3	Erosion / Corrosion / Plugging / Scaling	3	8	24	Existing scrubber should be able to handle particulate	9	27	Proper design necessary to avoid bag blinding	5	15	Susceptible to plugging from residual particulate	6	18	Fabric filter protects fixed bed.	3	9	Corrosion risk due to halide gas generation
2.4	Simplicity	3	10	30	Just lances	8	24	Lances / fabric filter	3	9	Multiple vessels	1	3	Multiple vessels / fabric filter	10	30	Just lances
2.5	Modularization	2	10	20		8	16		9	18		8	16	Fabric filter typically field erected.	10	20	
2.6	Technology Maturity	3	8	24	Well tested in utilities	8	24	Well tested in utilities	7	21	Tested in other industries (e.g., solvent recovery / VOC emission control)	7	21	Tested in other industries (e.g., solvent recovery / VOC emission control)	5	15	Emerging technology, but tested with the taconite flue gas
2.7	Commercial Scale	1	10	10		10	10		6	6	The number of parallel trains indicative of scale issues	6	6	The number of parallel trains indicative of scale issues	8	8	
2.8	Construction Schedule	0.5	10	5	Just lances	7	3.5	Fabric filter / ductwork	2	1	Many pieces of equipment	1	0.5	Many pieces of equipment	10	5	Just lances
2.9	Retrofit Integration	2.5	8	20	Impacts scrubber	7	17.5	Ductwork required	6	15	Significant ductwork required	6	15	Significant ductwork required	8	20	Impacts scrubber
2.10	Safety	10	9	90	Entry into AC silo required, but rare	9	90	Entry into AC silo required, but rare	8	80	Vessel entry likely required.	8	80	Vessel entry likely required.	9	90	Some chemical storage required
2.11	Materials of Construction	1	10	10	Just lances	8	8		4	4	Many pieces of stainless steel equipment	3	3		10	10	Just lances
2.12	Maintenance	2	10	20	Just lances	7	14	Bag changes	5	10	Carbon bed replacement	3	6	Carbon bed replacement / Bag changes	10	20	Just lances
	SUB-TOTAL	30		271		252			195			183.5			245		
3.0	Performance - 40%																
3.1	Scrubber Compatible	8	4	32	Particulate loading increase	6	48	Replace scrubber	8	64	No scrubber impact	6	48	Replace scrubber	2	16	Oxidant may upset scrubber operation
3.2	ΔP (Energy use)	7	10	70	Just lances	5	35	Fabric filter	3	21	Multiple vessels	1	7	Multiple vessel / Farbric filter	10	70	Just lances
3.3	Footprint	6	10	60	Just lances	5	30	Fabric filter	3	18	Multiple vessels	1	6	Multiple vessels	10	60	Just lances
3.4	Suitability for Induration Type	2	10	20		10	20		10	20		10	20		5	10	Score 10 for the other induration type
3.5	Sensitivity to Flue Gas Compositions (e.g., SO _x , NO _x and Moisture)	2	6	12	Water vapor / SO _x	6	12	Water vapor / SO _x	5	10	Water vapor / SO _x	5	10	Water vapor / SO _x	8	16	Potential reaction with waste gas
3.6	Regeneration Capability	2	1	2	Throwaway sorbent	1	2	Throwaway sorbent	10	20	Yes	10	20	Yes	1	2	Not possible to regenerate
3.7	Impact on Scrubber Solid Recycle	6	2	12	Contaminate scrubber solid	2	12	Contaminate scrubber solid	10	60	After scrubber	2	12	Contaminate scrubber solid	2	12	Increase mercury concentration in the scrubber solid
3.8	Impact on Iron chemistry During the Induration Process	5	10	50	No impact	10	50	No impact	10	50	No impact	10	50	No impact	3	15	Some impact to process
3.9	Possibility of Mercury Reemission/Desorption	2	7	14	Possible mercury desorption if a very high level of SO ₂ , NO _x , and HCl control is not obtained.	7	14	Possible mercury desorption if a very high level of SO ₂ , NO _x , and HCl control is not obtained.	7	14	Possible mercury desorption if a very high level of SO ₂ , NO _x , and HCl control is obtained or bed is not replaced.	7	14	Possible mercury desorption if a very high level of SO ₂ , NO _x , and HCl control is obtained or bed is not replaced.	5	10	Further testing required.
	SUB-TOTAL	40		272		223			277			187			211		
4.0	Environmental - 5%																
4.1	Particulate Co-Benefits / Fugitive Emissions	5	1	5	May overload poor scrubbers	10	50	Fabric filter should capture PM	8	40	Should capture PM, may emit attrited AC	8	40	Should capture PM, may emit attrited AC	3	15	Possible oxidant emission
4.2	Waste Quantity	5	5	25	Spent AC	5	25	Spent AC	9	45	Spent AC is sent to off-site regeneration.	9	45	Spent AC is sent to off-site regeneration.	7	35	Contaminates scrubber waste water.
	SUB-TOTAL	10		30		75			85			85			50		
	GRAND-TOTAL	100		713		640			597			475.5			706		

Notes: Score assigned by project team (0 = least, 10 = best).
 Weighted score is the product of the 'weight' and the 'score'.

Technology Survey (Generic Taconite Plant 2 - Grate Kiln)

Stantec Project # 111100111
 Prepared by: MER
 Date: 14-Aug-12

Desirable Criteria	Weight	Activated Carbon Injection (ACI) - Scrubber Capture			ACI - Fabric Filter			Fixed Bed Adsorption			Fixed Bed Adsorption - Fabric Filter			Oxidative Chemical Addition			
		Sc	Wt Sc	Notes	Sc	Wt Sc	Notes	Sc	Wt Sc	Notes	Sc	Wt Sc	Notes	Sc	Wt Sc	Notes	
1.0	Economic - 20%																
1.1	Capital Cost	10	10	100	6	60		2	20		1	10		10	100		
1.2	Operating Cost	10	4	40	3	30		2	20		1	10		10	100		
	SUB-TOTAL	20		140		90			40			20			200		
2.0	Risk - 30%																
2.1	Turndown	1	8	8	Limited by existing scrubber	10	10	Not limited by existing scrubber. Fabric filter replaces scrubber.	10	10	Multiple vessels give flexibility	10	10	Multiple vessels give flexibility	8	8	Limited to shutdown of entire system
2.2	Availability / Reliability	1	10	10	Minimal moving parts	8	8	Minimal moving parts / Bag changes	6	6	Carbon bed replacement	5	5	Carbon bed replacement / Bag changes	10	10	Minimal moving part
2.3	Erosion / Corrosion / Plugging / Scaling	3	8	24	Existing scrubber should be able to handle particulate	9	27	Proper design necessary to avoid bag blinding	5	15	Susceptible to plugging from residual particulate	6	18	Fabric filter protects fixed bed.	3	9	Corrosion risk due to halide gas generation
2.4	Simplicity	3	10	30	Just lances	8	24	Lances / fabric filter	3	9	Multiple vessels	1	3	Multiple vessels / fabric filter	10	30	Just lances
2.5	Modularization	2	10	20		8	16		9	18		8	16	Fabric filter typically field erected.	10	20	
2.6	Technology Maturity	3	8	24	Well tested in utilities	8	24	Well tested in utilities	7	21	Tested in other industries (e.g., solvent recovery / VOC emission control)	7	21	Tested in other industries (e.g., solvent recovery / VOC emission control)	5	15	Emerging technology, but tested with the taconite flue gas
2.7	Commercial Scale	1	10	10		10	10		6	6	The number of parallel trains indicative of scale issues	6	6	The number of parallel trains indicative of scale issues	8	8	
2.8	Construction Schedule	0.5	10	5	Just lances	7	3.5	Fabric filter / ductwork	2	1	Many pieces of equipment	1	0.5	Many pieces of equipment	10	5	Just lances
2.9	Retrofit Integration	2.5	8	20	Impacts scrubber	7	17.5	Impacts scrubber	6	15	Significant ductwork required	6	15	Significant ductwork required	8	20	Impacts scrubber
2.10	Safety	10	9	90	Entry into AC silo required, but rare	9	90	Entry into AC silo required, but rare	8	80	Vessel entry likely required.	8	80	Vessel entry likely required.	9	90	Some chemical storage required
2.11	Materials of Construction	1	10	10	Just lances	8	8		4	4	Many pieces of stainless steel equipment	3	3		10	10	Just lances
2.12	Maintenance	2	10	20	Just lances	7	14	Bag changes	5	10	Carbon bed replacement	3	6	Carbon bed replacement / Bag changes	10	20	Just lances
	SUB-TOTAL	30		271		252			195			183.5			245		
3.0	Performance - 40%																
3.1	Scrubber Compatible	8	4	32	Particulate loading increase	6	48	Replace scrubber	8	64	No scrubber impact	6	48	Replace scrubber	2	16	Oxidant may upset scrubber operation
3.2	ΔP (Energy use)	7	10	70	Just lances	5	35	Fabric filter	3	21	Multiple vessels	1	7	Multiple vessel / Fabric filter	10	70	Just lances
3.3	Footprint	6	10	60	Just lances	5	30	Fabric filter	3	18	Multiple vessels	1	6	Multiple vessels	10	60	Just lances
3.4	Suitability for Induration Type	2	10	20		10	20		10	20		10	20		10	20	
3.5	Sensitivity to Flue Gas Compositions (e.g., SO _x , NO _x and Moisture)	2	6	12	Water vapor / SO _x	6	12	Water vapor / SO _x	5	10	Water vapor / SO _x	5	10	Water vapor / SO _x	8	16	Potential reaction with waste gas
3.6	Regeneration Capability	2	1	2	Throwaway sorbent	1	2	Throwaway sorbent	10	20	Yes	10	20	Yes	1	2	Not possible to regenerate
3.7	Impact on Scrubber Solid Recycle	6	2	12	Contaminate scrubber solid	2	12	Contaminate scrubber solid	10	60	After scrubber	2	12	Contaminate scrubber solid	2	12	Increase mercury concentration in the scrubber solid
3.8	Impact on Iron chemistry During the Induration Process	5	10	50	No impact	10	50	No impact	10	50	No impact	10	50	No impact	3	15	Some impact to process
3.9	Possibility of Mercury Reemission/Desorption	2	7	14	Possible mercury desorption if a very high level of SO ₂ , NO _x , and HCl control is not obtained.	7	14	Possible mercury desorption if a very high level of SO ₂ , NO _x , and HCl control is not obtained.	7	14	Possible mercury desorption if a very high level of SO ₂ , NO _x , and HCl control is obtained or bed is not replaced.	7	14	Possible mercury desorption if a very high level of SO ₂ , NO _x , and HCl control is obtained or bed is not replaced.	5	10	Further testing required.
	SUB-TOTAL	40		272		223			277			187			221		
4.0	Environmental - 5%																
4.1	Particulate Co-Benefits / Fugitive Emissions	5	1	5	May overload poor scrubbers	10	50	Fabric filter should capture PM	8	40	Should capture PM, may emit attrited AC	8	40	Should capture PM, may emit attrited AC	3	15	Possible oxidant emission
4.2	Waste Quantity	5	5	25	Spent AC	5	25	Spent AC	9	45	Spent AC is sent to off-site regeneration.	9	45	Spent AC is sent to off-site regeneration.	7	35	Contaminates scrubber waste water.
	SUB-TOTAL	10		30		75			85			85			50		
	GRAND-TOTAL	100		713		640			597			475.5			716		

Notes: Score assigned by project team (0 = least, 10 = best).
 Weighted score is the product of the 'weight' and the 'score'.

Appendix D: Slides from April 2, 2012 Industry Meeting

Developing Cost-Effective Solutions to Reduce Mercury Emissions from Minnesota Taconite Plants

Industry Update Meeting
April 2, 2012



Sharon M. Sjostrom, P.E. – Chief Technology Officer, ADA-ES

Kyle S. Bowell – Project Engineer, ADA-ES

H. Ray Johnson, PH.D. – Activated Carbon Technologies

©2012 ADA-ES, Inc.
All rights reserved.



Topics for Discussion

- Program overview
- Technical Approach
- Results from Screening Tests
- Review of Technology Options
 - Description of Fixed-Bed Design
 - Description of Fixed-Bed Pilot
- Recommended Path Forward
- Discussion

©2012 ADA-ES, Inc.
All rights reserved.



Program Overview

Program Goal: Develop cost-effective solutions to reduce mercury emissions from Minnesota taconite plants

- Options:
- Hg oxidation and capture in WFGD
 - Sorbent injection and capture in WFGD
 - Sorbent injection and capture in FF
 - Activated carbon bed



©2012 ADA-ES, Inc.
All rights reserved.



ADA Feasibility Project

Question: Is activated carbon a viable mercury control approach for the industry?

Sorbent Screening

- Slipstream Testing
- Develop an Integrated Process Concept
- Pilot Plant Design
- Techno-Economic Analysis

Pilot Scale Testing

Full Scale Testing

©2012 ADA-ES, Inc.
All rights reserved.



General Approach

- Determine if process gas negatively impacts performance of activated carbon

Lab results and other commercial applications indicate activated carbon (fixed bed and powdered injection) can be effective at controlling mercury

- Determine most cost effective option to achieve mercury control goals
- Pilot test appropriate control options

©2012 ADA-ES, Inc.
All rights reserved.



Sorbent Screening: Technical Approach

Compare mercury capture characteristics of four activated carbon sorbents in actual process gas from three plants

Key Questions:

Do some sorbents perform better than others?

Is sorbent performance negatively impacted by process gas?

What is the effect of relative humidity on performance?

©2012 ADA-ES, Inc.
All rights reserved.



Plants Included in Screening

	United Taconite	Hibbing Taconite	ArcelorMittal Mineorca
Grate	Grate/Kiln	Straight Grate	Straight Grate
APC Equipment	Recirculating scrubber with no lime neutralization	Multiclone + once through scrubbers	Multiclone + recirc scrubber with no lime neutralization
Pellet Type	Std pellets with an organic binder	Standard pellets	Fluxed pellets



© David Schauer, Used with Permission

©2012 ADA-ES, Inc.
All rights reserved.



Potential Differences in Key Process Gas Characteristics

Pellets	Description	SO ₂ Emissions Factors (Gas-Fired) (lb/ton)	
Standard	Ore + binder	Grate/kiln ^a	0.29
		Grate/kiln, with wet scrubber ^a	0.053
		Straight grate	ND
		Straight grate, with wet scrubber ^b	0.1
Flux	1 to 10% limestone	Grate/kiln, with wet scrubber ^a	0.14
		Straight grate	ND

Emissions of NO_x and SO₂ generally are higher with flux pellets due to additional heating requirements

^aAir Pollution Emissions Test, Eveleth Taconite, Eveleth, MN, EMB 76-IOB-3,

U. S. Environmental Protection Agency, Research Triangle Park, NC, November 1975

^bResults Of The May 5-7, 1987, Atmospheric Emission Tests On The Induration Furnaces At The Hibbing Taconite Company In Hibbing, MN, Interpoll, Inc., Circle Pines, MN, May 14, 1987.

©2012 ADA-ES, Inc.
All rights reserved.



Screening Test Method

Specially prepared sorbent beds

Grind AC samples to <325 mesh (powder)

Mix with sand to manage pressure and channeling

Meter flow through beds

Measure collected mercury in beds



©2012 ADA-ES, Inc.
All rights reserved.



Bed Preparation

Sorbent ground until 95% by weight passed through a 325 mesh (45 μ m) screen.

Ground sorbents mixed with sand

Ratio of 20 milligrams of sorbent to 50 grams of sand

Found to be highest carbon content without clogging

Sample traps contained 4 grams of the sand/sorbent mixture in the test beds

1.6 milligrams of sorbent present in the traps

©2012 ADA-ES, Inc.
All rights reserved.



Screening Test Method

Test four samples simultaneously

Draw process gas through the beds using EPA M30B sampling consoles

Conduct tests at 3 sample durations for improved characterization

Repeat each test



©2012 ADA-ES, Inc.
All rights reserved.



Sorbents

Bromine-Treated, high activity, low ash, coal-based (**HA-Br**)

Note that bromine-treated AC is not a practical choice for fixed bed systems

Anthracite-based (**A**)

Carbon Resources CR4AN

Sulfur-treated, anthracite-based (**A-S**)

Carbon Resources CR4AN-Hg

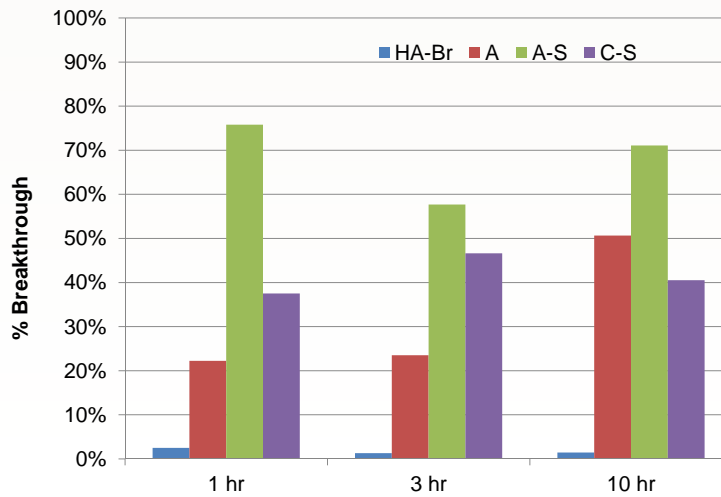
Sulfur-treated, coconut-shell based (**C-S**)

Carbon Resources CT612C-Hg

©2012 ADA-ES, Inc.
All rights reserved.



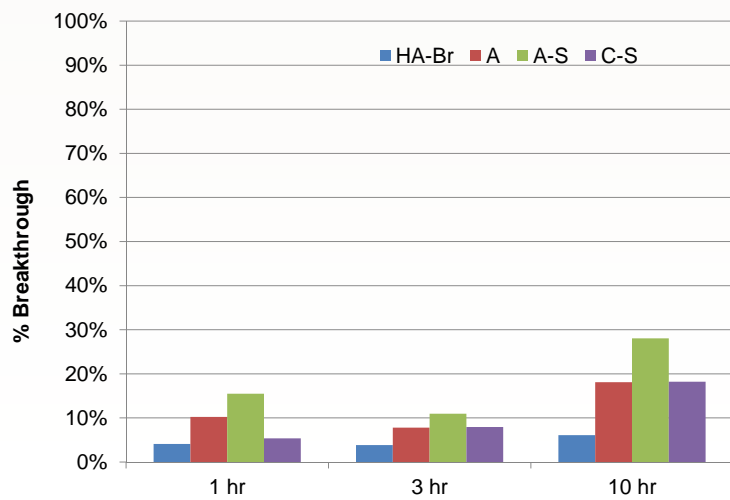
United Taconite Results



©2012 ADA-ES, Inc.
All rights reserved.



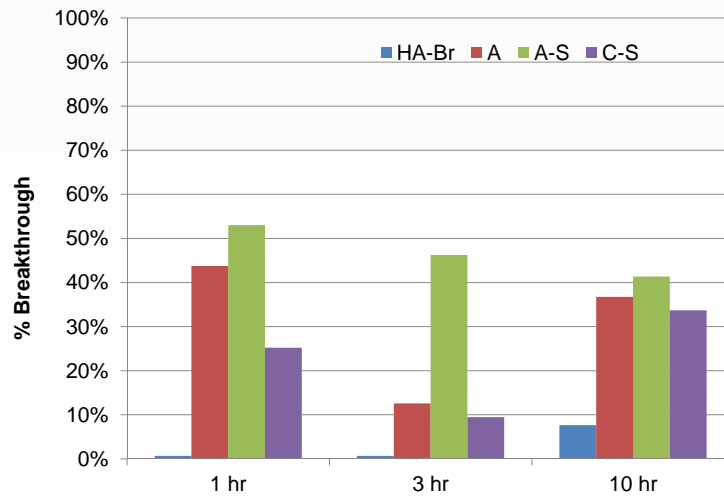
ArcelorMittal Results



©2012 ADA-ES, Inc.
All rights reserved.



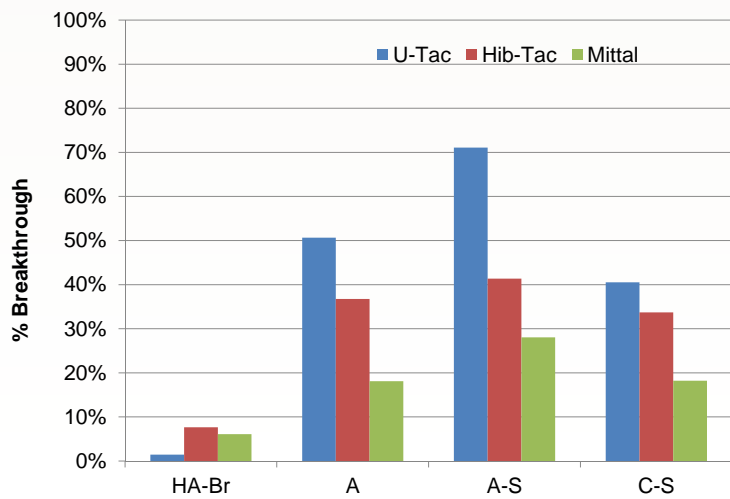
Hibbing Taconite Results



©2012 ADA-ES, Inc.
All rights reserved.



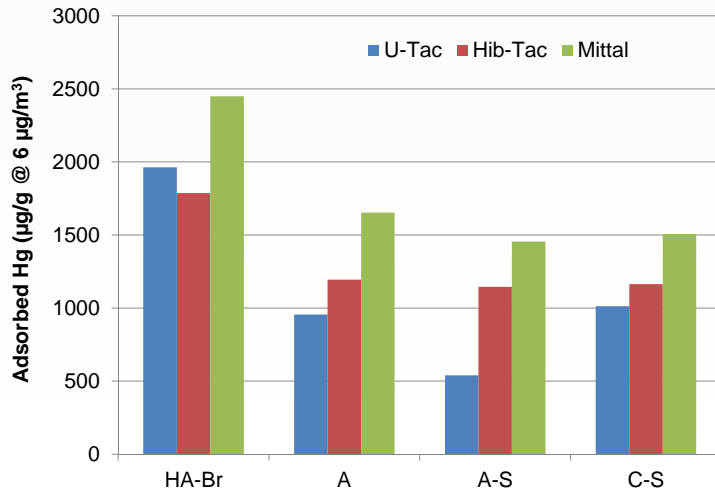
10-hr Comparison - Breakthrough



©2012 ADA-ES, Inc.
All rights reserved.

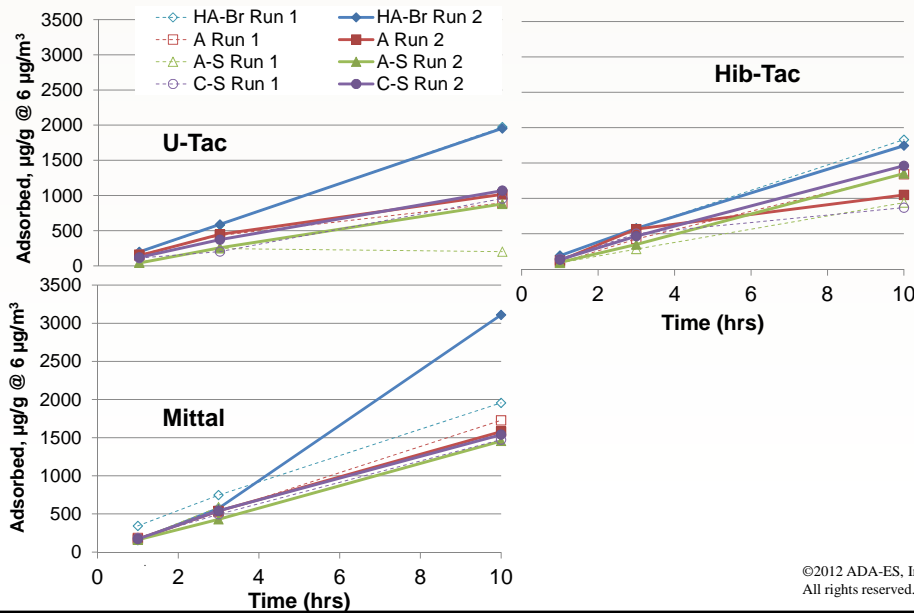


10-hr Comparison - Adsorption



©2012 ADA-ES, Inc.
All rights reserved.

Adsorption Comparison



©2012 ADA-ES, Inc.
All rights reserved.



Comparison of AC

Relative differences in sorbent performance were consistent across all sites

All test samples showed initial breakthrough at 1 hr.

1 hr breakthrough on sulfur-treated carbons typically higher than at 3 hr. This could indicate a “conditioning” effect.

Sulfur-treated anthracite showed highest breakthrough for all sites.

Sulfur-treated coconut-shell presented least sensitivity to differences in process gas.

In general, sulfur-treated coconut-shell performed best of all fixed-bed candidates.

©2012 ADA-ES, Inc.
All rights reserved.



Site-specific performance differences

United Tac beds showed highest breakthrough

Grate/kiln, standard pellets, no multiclone, recirculating scrubber with no lime neutralization

ArcelorMittal showed lowest breakthrough

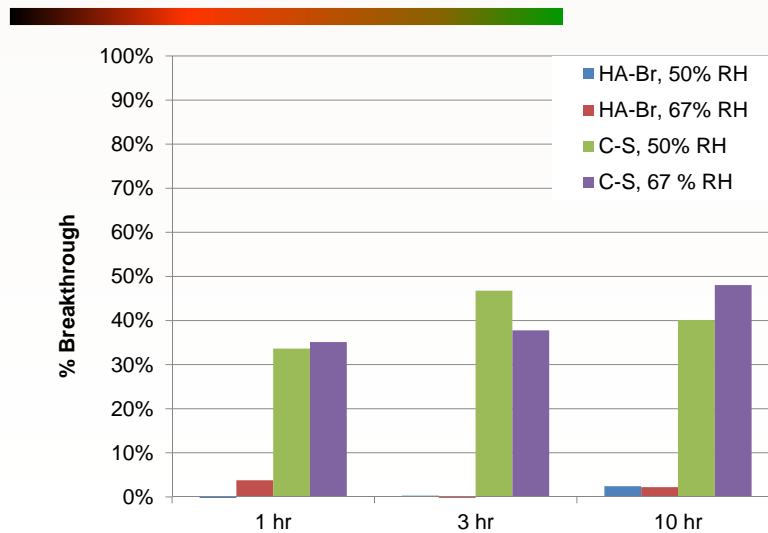
Straight grate, flux pellets, multiclone, recirculating scrubber with no lime neutralization

*SO₂ concentration at United Taconite expected to be lower than ArcelorMittal
Are there other differences in process gas?*

©2012 ADA-ES, Inc.
All rights reserved.



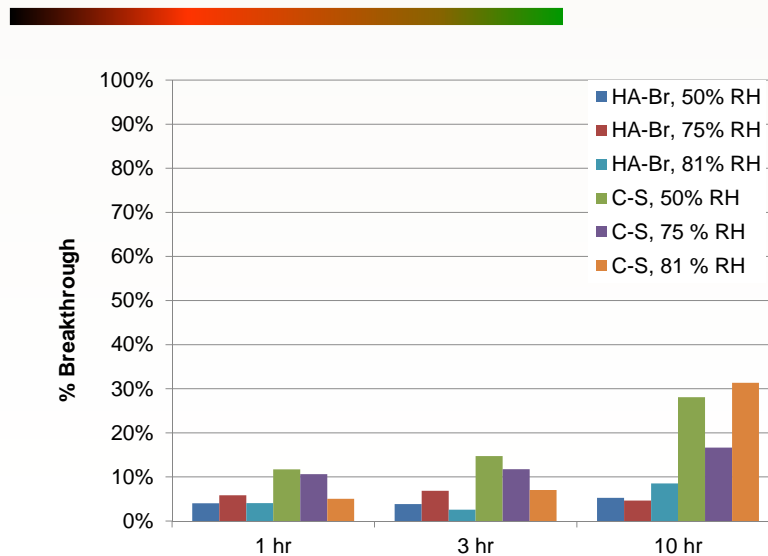
United Taconite RH Results



©2012 ADA-ES, Inc.
All rights reserved.



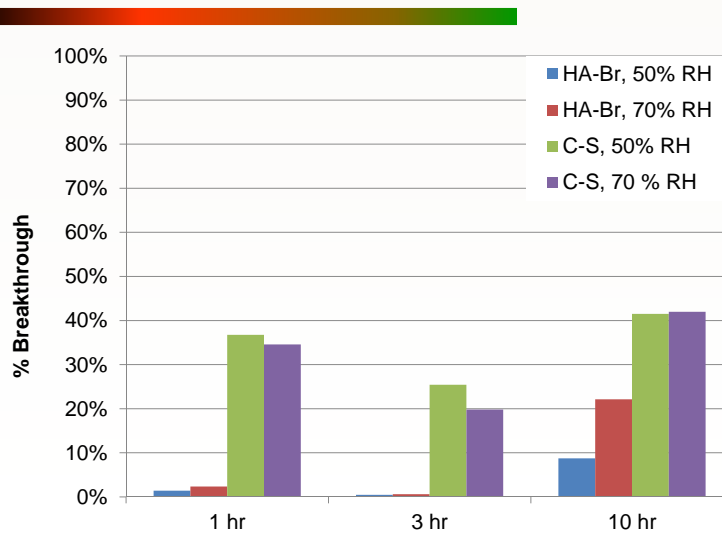
ArcelorMittal RH Results



©2012 ADA-ES, Inc.
All rights reserved.



Hibbing Taconite RH Results



©2012 ADA-ES, Inc.
All rights reserved.



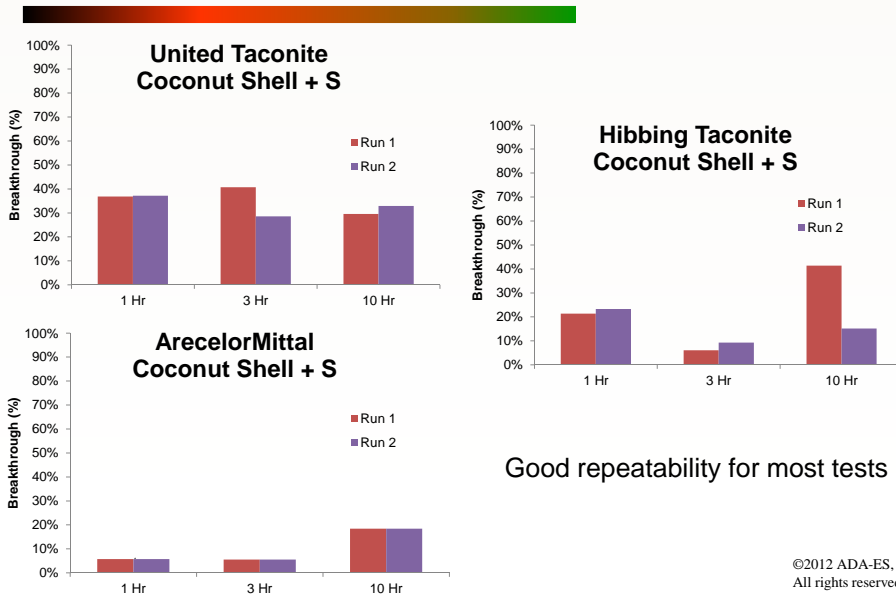
Screening Summary – RH Tests

- No impact on sorbent performance resulting from increased relative humidity (50 to 81%)

©2012 ADA-ES, Inc.
All rights reserved.



Repeatability - Example



Comparison to Other Testing

- 2009 Fixed Bed Lab Study by EERC
- Test Details
 - Bromine-treated, lignite carbon and Sulfur-treated bituminous carbon evaluated
 - 1000 hour test
 - 2 ppm HCl and 20 ppm NO₂ in simulated gas
 - Temp ~ 180°F
- 100% removal achieved throughout test for both sorbents

Dunham 2009, Demonstration of Mercury Capture in a Fixed Bed

©2012 ADA-ES, Inc.
All rights reserved.



Comparison to Other Testing

- 2002 Test by ADA Technologies
 - Temperature ~ 100°F
 - Sulfur-treated carbon
 - N₂, Hg and 25% moisture
- Good capture noted
- Increasing RH from 25% to 50% improved Hg removal

Broderic, 2002, Spallation Neutron Source Carbon Adsorption Tests

©2012 ADA-ES, Inc.
All rights reserved.



Techno-Economic Analysis

- Define industry economic goals
- Compare the technical and economic aspects of potential AC technology options, determine applicability to each plant and impact on plant operations
- Compare the technical and economic aspects of all available technology options to AC-based solutions, including oxidizing chemicals and scrubber additives

*This Task is < 5% complete and **Currently on Hold***

©2012 ADA-ES, Inc.
All rights reserved.



Review of Technology Options

- Hg oxidation and capture in WFGD
- Sorbent injection and capture in WFGD
- Sorbent injection and capture in FF
- Activated carbon bed
- Others?



©2012 ADA-ES, Inc.
All rights reserved.



Sorbent Injection

- Commercially available
- Removal expected to be limited without baghouse
- May increase PM emissions unless baghouse added
- Addition of baghouse may increase costs above fixed-bed system



©2012 ADA-ES, Inc.
All rights reserved.



Sorbent Monolith Approach

- Activated carbon based and polymer-based
- Not applied commercially for mercury at required scale

Costs uncertain

Polymer developer (Gore) estimates polymer-based system cost-competitive with ACI for in-scrubber application

- Lower pressure drop expected

©2012 ADA-ES, Inc.
All rights reserved.



Carbon Honeycomb

MeadWestvaco

30-40,000 SCFM systems in commercial operation
(5 + years) *No commercial mercury systems in service*

Fast removal kinetics, low pressure drop,
high velocity ~ 500 ft. /min. (5 x typical fixed bed)

Example: Flint Hills Resources Pine Bend Refinery in
Rosemount, Minnesota

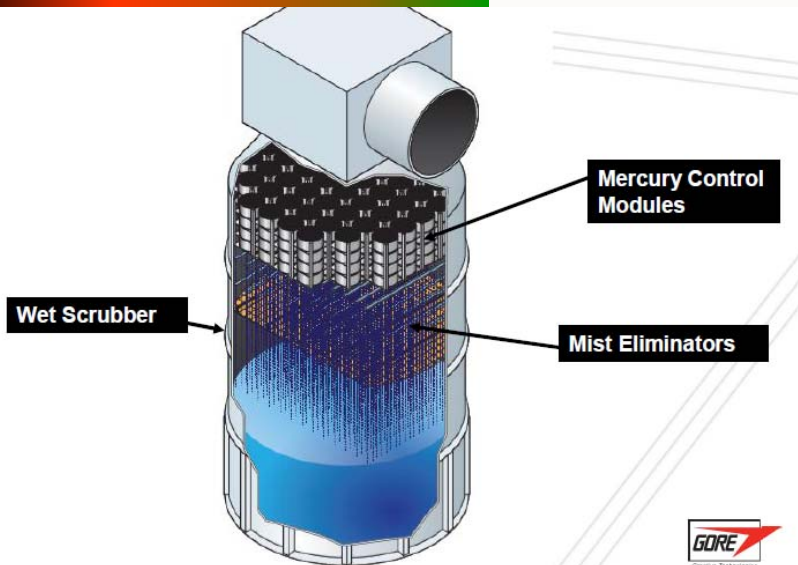
Corning, Inc. System in Development



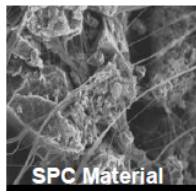
©2012 ADA-ES, Inc.
All rights reserved.



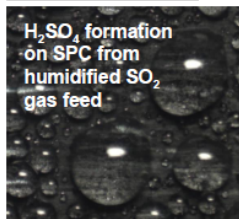
Polymer Design (Gore)



Sorbent Polymer Composite (SPC) material developed by Gore efficiently captures Hg for long periods of time even in the presence of high acid gas concentrations



SPC Material



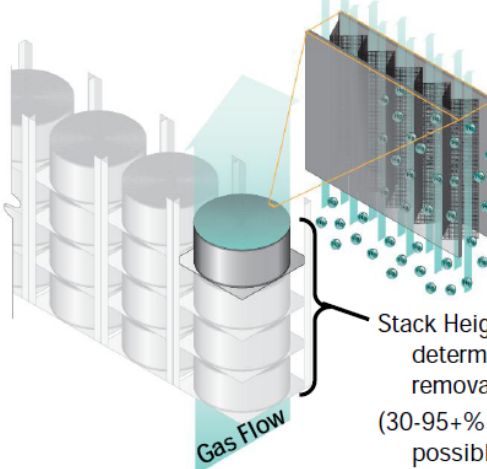
H₂SO₄ formation on SPC from humidified SO₂ gas feed

W. L. Gore & Associates

SPC tape is incorporated in discrete modules (2' wide x 1' high)

Open channel design:

- Low Pressure Drop
- Resists Fouling by dust



Stack Height determines mercury removal efficiency (30-95+% Hg removal possible)



Sorbent Bed Approach

- Commercially available at required scale

Fixed bed systems

Moving bed systems

- Higher cost than sorbent injection alone
- Higher pressure drop across system expected



©2012 ADA-ES, Inc.
All rights reserved.



Fixed-Bed AC Systems

- Commercial use for 80+ years
- Large systems/vessels used in solvent recovery applications for many years

Example: AMCEC (inst. 1982, still operating)

Vessels are 12 feet diam x 47 feet long

43,000 lbs AC pellets/vessel

©2012 ADA-ES, Inc.
All rights reserved.



Fixed Bed Design Parameters

	ArcelorMittal	Hibbing Taconite	United Taconite
Total Flow (ACFM)	854,000	756,000	493,000
Temperature (F°)	125	123	140
Hg Concentration ($\mu\text{g}/\text{m}^3$)	10	10	10
Total Hg (lb/yr)	180.8	222.32	140.87
Gas flow per vessel (acfm)	43,000	43,000	43,000
# Vessels	22	20	13
Bed Depth (ft)	3	3	3
Pressure drop (in H ₂ O, est)	6 to 12	6 to 12	6 to 12
Total Carbon (lbs)	1,368,553	1,225,874	842,970
AC Life	TBD*	TBD*	TBD*

* Based on lab results, estimated carbon ~ 35,000 to 100,000 lbs/yr; Life est > 10 yrs

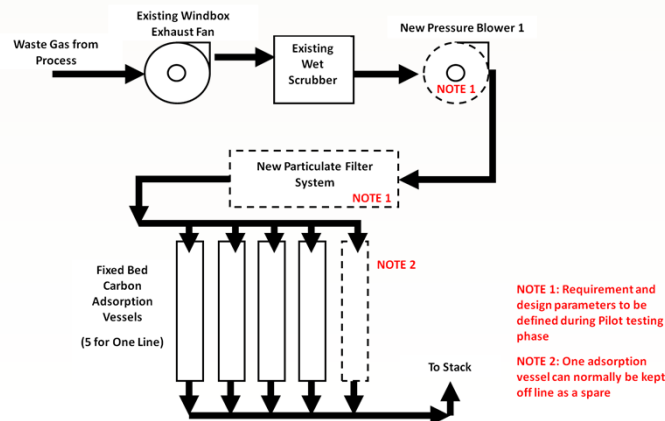
H. Ray Johnson, PH.D., Activated Carbon Technologies

©2012 ADA-ES, Inc.
All rights reserved.



Full-Scale Fixed Bed Design

CARBON FIXED BED ADSORPTION PROCESS DESIGN CONCEPT
(TYPICAL CONCEPT FOR ONE OF FOUR LINES)



H. Ray Johnson, PH.D., Activated Carbon Technologies

©2012 ADA-ES, Inc.
All rights reserved.



Key Considerations for Fixed-Bed

- Mercury capacity from pilot testing
 - System capital costs
- If particulate filter is required, costs will likely be higher than ACI + FF
- Sorbent characteristics will determine bed pressure drop. Fan power must be included

©2012 ADA-ES, Inc.
All rights reserved.

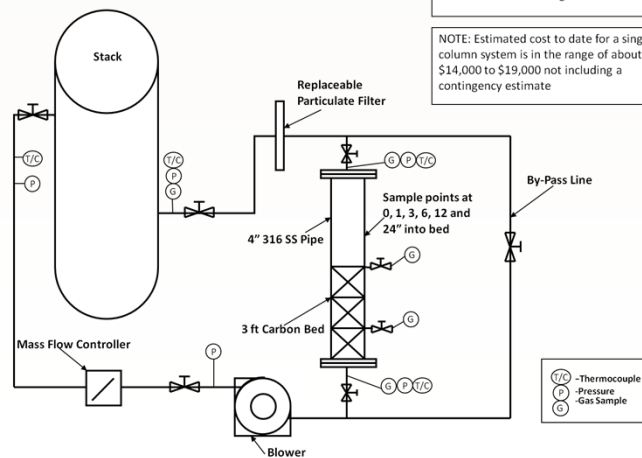


Pilot Scale Design

FIXED BED CARBON PILOT SYSTEM

NOTE: Easily modified by adding one or more adsorber vessels (4 inch pipe) to evaluate more than one carbon grade at the same time

NOTE: Estimated cost to date for a single column system is in the range of about \$14,000 to \$19,000 not including a contingency estimate



H. Ray Johnson, PH.D., Activated Carbon Technologies

©2012 ADA-ES, Inc.
All rights reserved.



Pilot Testing Recommendations

- Conduct extended slipstream test (1000 hrs+) on actual process gas
- Use most promising AC based on economics (expected Hg capacity, cost/lb, pressure characteristics, etc)
- Sample Hg at multiple locations (example 0, 1, 3, 6, 12, and 24 inches) to monitor the mercury adsorption wave front
- Monitor temperatures and pressures

©2012 ADA-ES, Inc.
All rights reserved.



Recommended Next Steps

Techno-economic assessment is required prior to determining path forward

Oxidation technologies may be lowest cost option. Confirm sufficient and reliable mercury removal with minimal balance-of-plant issues

Confirm removal effectiveness, particulate emissions, and impacts to scrubber solution for sorbent injection alone (ACI)

Fixed beds should be pursued if costs are competitive. Pilot-scale testing is required for design engineering

Moving beds systems and polymer-based monolith costs should be considered for comparison

©2012 ADA-ES, Inc.
All rights reserved.



Tasks and Budget Status

Project Tasks	Estimated % Complete
Gather Site-Specific Information and Conduct Screening Tests	100%
Develop Integrated Process Concept	100%
Techno-Economic Analysis	5%
Pilot Plant Design and Test Plan	100%
Reporting	50%

Contract Amount: \$350,000
Invoiced Through February 2012: \$210,000

©2012 ADA-ES, Inc.
All rights reserved.

Questions and Discussion



ADA Environmental Solutions
Sharon M. Sjostrom
Kyle S. Bowell
Activated Carbon Technologies
H. Ray Johnson



12. Appendix E: Sorbent Trap Method Testing

This project employed the EPA Method 30B titled “Determination of Total Vapor Phase Mercury Emissions from Coal-Fired Combustion Sources Using Carbon Sorbent Traps”. When using this mercury measurement method, the operator extracted a known volume of process gas from a duct through a dry sorbent trap (containing a specially treated form of activated carbon) as a single-point sample, with a nominal flow rate which was varied based on process gas mercury concentrations. The sample rate typically varies between 250 cm³/min to 1000 cm³/min of dry gas. The sampling flow rate was held constant (+/- 25%) during testing. The dry sorbent trap, which was in the process gas stream during testing, represents the entire mercury sample. Each trap was analyzed in an offsite laboratory for total mercury using an Ohio Lumex 915+ RP-M. Samples can be collected over time periods ranging from less than an hour to weeks in duration. The test result provides a total vapor-phase mercury measurement of the process gas stream for the time period of the test.

STM testing requires that paired samples be collected in the field. The analysis results of the paired sample trains are compared and are typically in agreement within 5-20% relative percent difference (RPD). Another built-in quality assurance measure is achieved through the analysis of two trap sections in series. Each trap has two separate mercury sorbent sections, as shown in Figure 9 the “B” section is analyzed to evaluate whether any mercury breakthrough occurred. Low B section mercury, in conjunction with a field blank trap, is used to confirm overall sample handling quality.

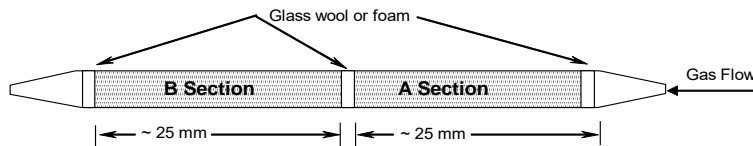


Figure 1: Sorbent Trap Side View

The STM sample train is fairly simple. Major components are a sorbent trap mounted directly on the end of a probe, a moisture knockout is located in series with each channel of sampling train outside the duct, and a console that controls the sampling rate and meters the gas, as well as recording data in a data logger. Key temperatures, sampling volume, and barometric pressure are recorded on field sampling data sheets and/or by a data logger for each sample run. A picture of the STM sampling console is shown in Figure 10 and a figure of the sampling train arrangement is shown in Figure 11.



Figure 2: STM Sampling Console Setup at a Stack Sampling Location

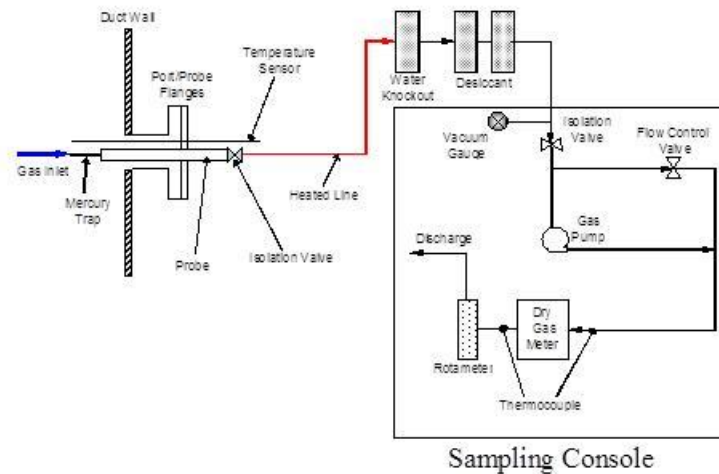


Figure 3: Sorbent Trap Method Sampling Train STM

STM testing collects a mass of mercury on the trap media. Using stack gas flow rate, gaseous data from the plant's CEMS, and coal ultimate analysis (or EPA Method 19 F-Factors if ultimate analysis is unavailable), mercury concentration are calculated and typically reported in lb/TBtu.

Method 30B versus STM QA Criteria

QA/QC Test or Spec	Acceptance Criteria	Method 30B Frequency	STM Frequency	Consequences
Gas flow meter calibration (3 settings)	Calibration factor (Yi) at each flow rate must be within ±2% of the average value (Y)	Prior to initial use and when post-test check is not within ±5% of Y	Prior to initial use and when post-test check is not within ±5% of Y	Recalibrate at 3 points until the acceptance criteria are met
Gas flow meter post-test calibration check	Calibration factor (Yi) must be within ±5% of the Y value from the most recent 3 point calibration	After each field test. For mass flow meters, must be done onsite, using stack gas	After each field test, mass flow meter volume is verified using a totalizer	Recalibrate gas flow meter at 3 points to determine a new value of Y. For mass flow meters, must be done on-site, using stack gas. Apply the new Y value to the field test data
Temperature sensor calibration	Absolute temperature measured by sensor within ± 1.5% of a reference sensor	Prior to initial use and before each test thereafter	Prior to initial use. Before each test thereafter or quarterly, sensor is checked against calibration standard	Recalibrate; sensor may not be used until specification is met
Barometer calibration	Absolute pressure measured by instrument within ± 10 mm Hg of reading with a mercury barometer	Prior to initial use and before each test thereafter	Prior to initial use, then quarterly	Recalibrate; instrument may not be used until specification is met
Pre-test leak check	≤ 4% of target sampling rate	Prior to sampling	Prior to sampling	Sampling shall not commence until the leak check is passed
Post-test leak check	≤ 4% of target sampling rate	After sampling	After sampling	Sample invalidated
Analytical bias test	Average recovery between 90% and 110% for Hg0 and HgCl2 at each of the 2 spike concentration levels	Prior to analyzing field samples and prior to use of new sorbent media	Annual test with both Hg0 and HgCl2. Prior to analyzing field samples and prior to use of new sorbent media analyzer is tested with HgCl2.	Field samples shall not be analyzed until the percent recovery criteria has been met
Multipoint analyzer calibration	Each analyzer reading within ± 10% of true value and r2 ≥ 0.99	On the day of analysis, Before analyzing any samples	On the day of analysis, Before analyzing any samples	Recalibrate until successful
Analysis of independent calibration standard	Within ± 10% of true value	Following daily calibration, prior to analyzing field samples	Following daily calibration, prior to analyzing field samples	Recalibrate and repeat independent standard analysis until successful
Analysis of continuing calibration verification standard (CCVS)	Within ± 10% of true value	Following daily calibration, After analyzing ≤ 10 field samples, and at end of each set of analyses	Following daily calibration, After analyzing ≤ 10 field samples, and at end of each set of analyses	Recalibrate and repeat independent standard analysis, reanalyze samples until successful, if possible; for destructive techniques, samples invalidated
Test run total sample volume	Within ± 20% of total volume sampled during field recovery test	Each individual sample	Spike recovery test (i.e. field recovery) not conducted	Sample invalidated
Sorbent trap section 2 breakthrough	< 10% of section 1 Hg mass for Hg concentrations > 1 µg/dscm; ≤ 20% of section 1 Hg mass for Hg concentrations ≤ 1 µg/dscm	Every sample	Every sample	Sample invalidated
Paired sorbent trap agreement	≤ 10% Relative Deviation (RD) mass for Hg concentrations > 1 µg/dscm; ≤ 20% RD or < 0.2 µg/dscm absolute difference for Hg concentrations ≤ 1 µg/dscm	Every run	Every run	Run invalidated
Sample analysis	Within valid calibration range (within calibration curve)	All Section 1 samples where stack Hg concentration is ≥ 0.5 µg/dscm	All Section 1 samples where stack Hg concentration is ≥ 0.5 µg/dscm Is ≥ 0.5 µg/dscm	Reanalyze at more concentrated level if possible, samples invalidated if not within calibrated range
Sample analysis	Within bounds of Hg0 and HgCl2 Analytical Bias Test	All Section 1 samples where stack Hg concentration is ≥ 0.5 µg/dscm	All Section 1 samples where stack Hg concentration is ≥ 0.5 µg/dscm	Expand bounds of Hg0 and HgCl2 Analytical Bias Test; if not successful, samples invalidated
Field recovery test	Average recovery between 85% and 115% for Hg0	Once per field test	Spike recovery test (i.e. field recovery) not conducted	Field sample runs not validated without successful field recovery test

Appendix F: Quality Assurance Program

F.1 Data Quality Assessment Worksheet

F.2 Quality Assurance Discussion Slides

F.3 STM Equipment Calibrations

 Thermocouple Calibrations

 DGM Calibrations

 Mercury Analyzer Calibrations

F.4 Raw Data

Data Quality Assessment Worksheet

Title of Project: Developing Cost-Effective Solutions to Reduce Mercury Emissions from Minnesota Taconite Plants: ArcelorMittal

Project Leader: Richard Schlager

Date Submitted : July 9, 2012

(1) Method Description/Key Parameters:

- a. Screening tests were conducted at ArcelorMittal, Hibbing Taconite, and United Taconite Unit 2. Results are specific to these plants, but can be applied to similarly-configured plants.
- b. The Mercury Index Method (MIM) screening tool used for testing was based on EPA Method 30B. In particular, equation 30B-2 in section 12.3 Calculation of Breakthrough, equation 30B-3 in section 12.4 Calculation of Hg Concentration, and equation 30B-5 in section 12.6 Calculation of Paired Trap Agreement will be utilized. These are shown below. Mercury removal efficiency for the screening tests is determined based on breakthrough.

12.1 Nomenclature. The terms used in the equations are defined as follows:

B = Breakthrough (%).

C_a = Concentration of Hg for the sample collection period, for sorbent trap "a" ($\mu\text{g}/\text{dscm}$).

C_b = Concentration of Hg for the sample collection period, for sorbent trap "b" ($\mu\text{g}/\text{dscm}$).

m_1 = Mass of Hg measured on sorbent trap section 1 (μg).

m_2 = Mass of Hg measured on sorbent trap section 2 (μg).

RD = Relative deviation between the Hg concentrations from traps "a" and "b" (%).

V_t = Total volume of dry gas metered during the collection period (dscm); for the purposes of this method, standard temperature and pressure are defined as 20° C and 760 mm Hg, respectively.

DATA QUALITY ASSESSMENT WORKSHEET FOR PROJECT 3

12.3 Calculation of Breakthrough. Use Equation 30B-2 to calculate the percent breakthrough to the second section of the sorbent trap.

$$B = \frac{m_2}{m_1} \times 100 \quad \text{Eq. 30B-2}$$

12.4 Calculation of Hg Concentration. Calculate the Hg concentration measured with sorbent trap “a”, using Equation 30B-3.

$$C_a = \frac{(m_1 + m_2)}{V_t} \quad \text{Eq. 30B-3}$$

For sorbent trap “b”, replace “C_a” with “C_b” in Equation 30B-3. Report the average concentration, i.e., $\frac{1}{2}(C_a + C_b)$.

12.6 Calculation of Paired Trap Agreement. Calculate the relative deviation (RD) between the Hg concentrations measured with the paired sorbent traps using Equation 30B-5.

$$RD = \frac{|C_a - C_b|}{C_a + C_b} \times 100 \quad \text{Eq. 30B-5}$$

- c. The phase of the project funded to-date is limited to Slipstream Testing at a very small scale. Mercury removal efficiency for full scale can be projected using the slipstream screening results, within the limitations of the technique. For the tests conducted during the Slipstream Testing, the mercury measured in the second trap section (m_2 in equation 30B-2), which is packed with standard 30B carbon trap, was never zero. This is a result of mercury present on the “blank” traps prior to exposure to process gas. Because the amount of mercury captured during testing was very low, m_1 in equation 30B-2, the resultant calculated breakthrough was always less than 100%. EPA Method 30B allows the breakthrough calculated using equation 30B-2 to be up to 10% before the test is considered failing. Thus, within the limitations of the method, 100% actual mercury capture in the first section trap of the MIM that contained the test carbon would be reported as up to 10% breakthrough, or $\geq 90\%$ mercury removal.

Results from Slipstream Testing were extrapolated to full-scale operation by calculating the capacity of the carbon for mercury using the equation below:

Capacity = $m_1/M1$, where

m_1 is the mass of Hg measured in the first section trap and

M1 = mass of carbon in first section trap

As carbon in the first section becomes saturated with mercury and begins to break through to the second section, m_1 will begin to approach a constant mass and the capacity will approach the equilibrium capacity for the material. For the estimated carbon required for the full-scale application, the capacity calculated during the 10 hour MIM sample run was utilized because it was the best representation of the equilibrium capacity for the data collected. Full scale design details, including the amount of carbon that will be required per year to assure the full-scale fixed bed does not reach breakthrough, must be determined using pilot-testing.

(2) Data Quality Assessment for key variables:

- a. EPA Method 30B is an EPA reference method for vapor-phase mercury emissions. Due to the design of the testing in this program, all Method 30B results and all MIM results provided are collected in the uncontrolled gas stream. To determine the mercury concentration in the uncontrolled gas stream, EPA Method 30B measurements were conducted. Relative difference between the duplicate, simultaneous, Method 30B samples were calculated and all results met the goal of < 10% relative difference. All MIM samples were collected in a quad, simultaneous manner (4 tests conducted simultaneously). The relative difference for these tests was calculated by determined the average of all four simultaneous (Ca in equation 30B-5) and comparing each separate test to the quad average using equation 30B-5. These results are included in the Quality Assurance Program appendix of the final report. Calibration records for the dry gas meters used during testing (V_t in equation 30B-3) and analytical records of m_1 and m_2 on equations 30B-2 and 30B-3 are included in the Quality Assurance Program appendix of the final report.
- b. Contributions to the scale-up uncertainty using the approach in 1(c) include: 1) the measurement uncertainty of carbon in the trap (M1) and 2) the measurement of the mercury collected (m_1). The precision of the carbon mass measurement is 0.25% based on the accuracy of the balance. However, because the sample preparation technique requires mixing the carbon with sand and utilizing a portion of the mixture for the test, the primary uncertainty is related to how homogenous the sample mixture is. This cannot be measured directly. To quantify the accuracy of the results and include any variability resulting from sample mixing, all tests conducted in the field were repeated and the standard deviation of the sample pairs was calculated. The average SD for the ArcelorMittal pairs was 3%, and the maximum SD for a single pair was 14%. This demonstrates good repeatability and suggests low uncertainty for the sample preparation. Quality control standards were used during mercury analysis. Standards were analyzed nominally every tenth sample. On average, the QC standards analyzed during the ArcelorMittal MIM trap analyses were within 5% of the standard value. The maximum difference for a single sample was 13%.

- c. Relevant raw data records are included in the Quality Assurance Program appendix of the final report.
- (3) Mercury Removal Estimates:
- a. A fixed-bed device for this industry would be designed to capture all incoming mercury within the bed. Therefore, the mercury emissions from a unit currently emitting 100 units of mercury per unit time would be 0 lbs of mercury. For the tests conducted during the Slipstream Testing, the mercury measured in the second trap section was never zero, in part due to mercury present on the “blank” traps prior to exposure to process gas. Due to the design of the test, this introduced some uncertainty into the breakthrough analysis because, according to equation 30B-2, some breakthrough was always calculated. EPA Method 30B allows up to 10% breakthrough before the test is considered failing. Thus, within the limitations of this screening test, the mercury emissions from a taconite plant currently emitting 100 units of mercury per unit time would be 0 +10 units of mercury per unit time.
 - b. Process gas components such as sulfuric acid were not measured during the program but may affect the mercury removal effectiveness of activated carbon. Results from field MIM tests were compared to tests conducted in the laboratory. There was an insignificant difference between the laboratory and the field results. This data is included in the QA presentation included in the Quality Assurance Program appendix of the final report.
 - c. The mercury measured on the Sabre carbon and section 2 trap was consistently lower than the mercury measured from any test carbon + section 2 trap. An analytical bias is suspected that is related to the thermal decomposition technique used to analyze the traps. No problems were noted with any of the test carbons or the standard Method 30B carbon traps, thus this problem did not affect the overall conclusions of the study.

Quality Assurance Assessment

©2012 ADA-ES, Inc.
All rights reserved.

Developing Cost-Effective Solutions to Reduce Mercury Emissions from Minnesota Taconite Plants

**Industry Update Meeting
April 2, 2012**



PROVIDING THE SOLUTIONS FOR EMISSIONS COMPLIANCE

Sharon M. Sjostrom, P.E. – Chief Technology Officer, ADA-ES

Kyle S. Bowell – Project Engineer, ADA-ES

H. Ray Johnson, PH.D. – Activated Carbon Technologies

©2012 ADA-ES, Inc.
All rights reserved.



QA Objectives

- Determine mercury concentration in the untreated flue gas with sufficient accuracy and precision to validate results;
- Run a sufficient number of tests to verify data are representative of long-term operation at a taconite plant with no mercury control;
- Use the Sorbent Trap Method to evaluate comparability of data;
- Collect data on mercury present downstream of a sorbent bed for each sorbent tested;
- Perform a comparison of sorbents tested at each plant to determine the best sorbents for later pilot and full scale testing in subsequent Phases of this program if funded.

©2012 ADA-ES, Inc.
All rights reserved.



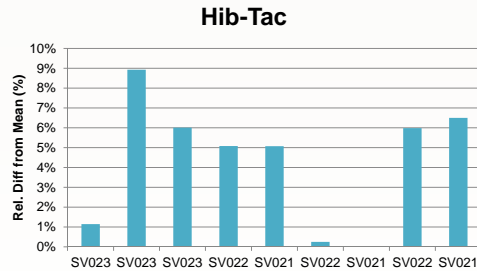
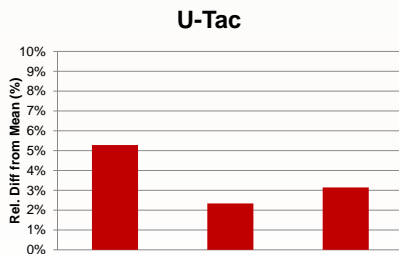
QA Results

- ✓ Determine mercury concentration in the untreated flue gas with sufficient accuracy and precision to validate results
Used calibrated DGM, flowmeters, and thermocouples (NIST traceable)
- ✓ Use the Sorbent Trap Method to evaluate comparability of data
Relative Difference for EPA 30B sorbent traps within QA Criteria of < 10% RD
Total mercury measured by EPA 30B representative of total mercury measured using test beds

©2012 ADA-ES, Inc.
All rights reserved.

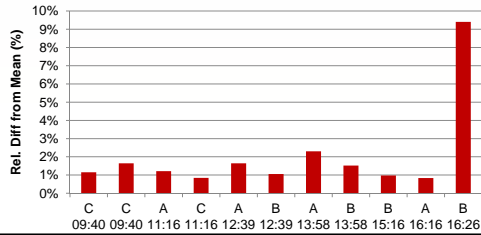


30B Rel. Diff: Paired Traps



Mittal

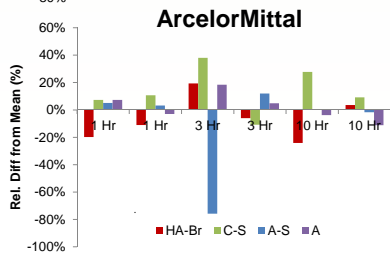
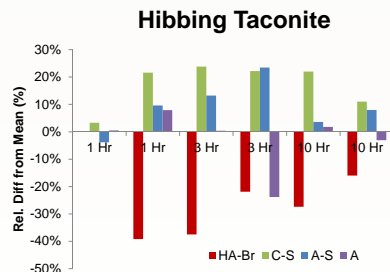
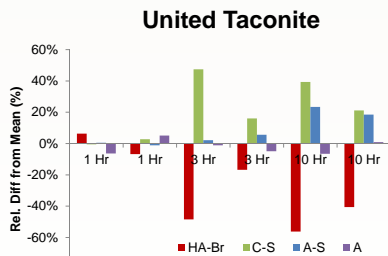
Goal: <10% RD



©2012 ADA-ES, Inc. All rights reserved.



Comparison of Quad Samples: Total Hg (Concentration)



Consistently low relative recovery for HA-Br Analytical bias suspected (thermal decomposition)

Note: Breakthrough analysis conducted by correcting data to quad average

©2012 ADA-ES, Inc. All rights reserved.



QA Results

- ✓ Run a sufficient number of tests to verify data are representative of long-term operation at a taconite plant with no mercury control

Tests were designed to compare relative sorbent performance, indicate impacts of process gas on sorbent performance, and indicate effect of relative humidity on performance.

4 sorbents x 3 time conditions x 2 tests = 24 tests
(Each timed test repeated for each condition)

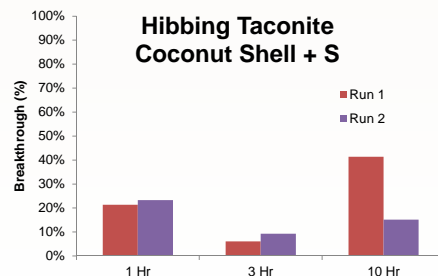
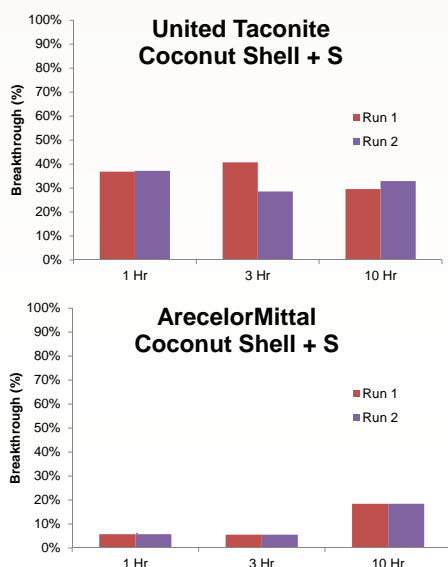
2 sorbents x 2 RH/sorbent x 3 times = 12 relative humidity tests

→ **At least 36 tests conducted per site**

©2012 ADA-ES, Inc.
All rights reserved.



QA Results: Repeatability

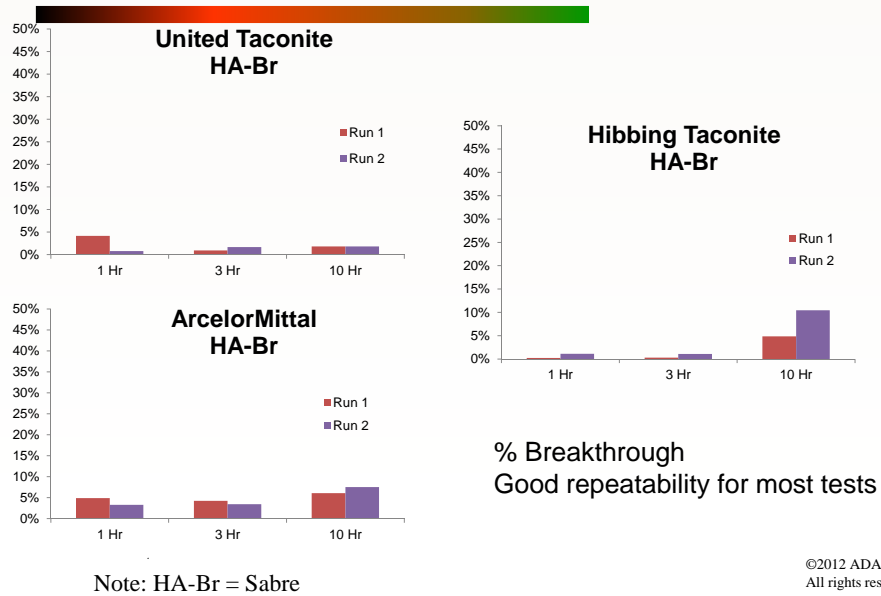


Good repeatability for most tests

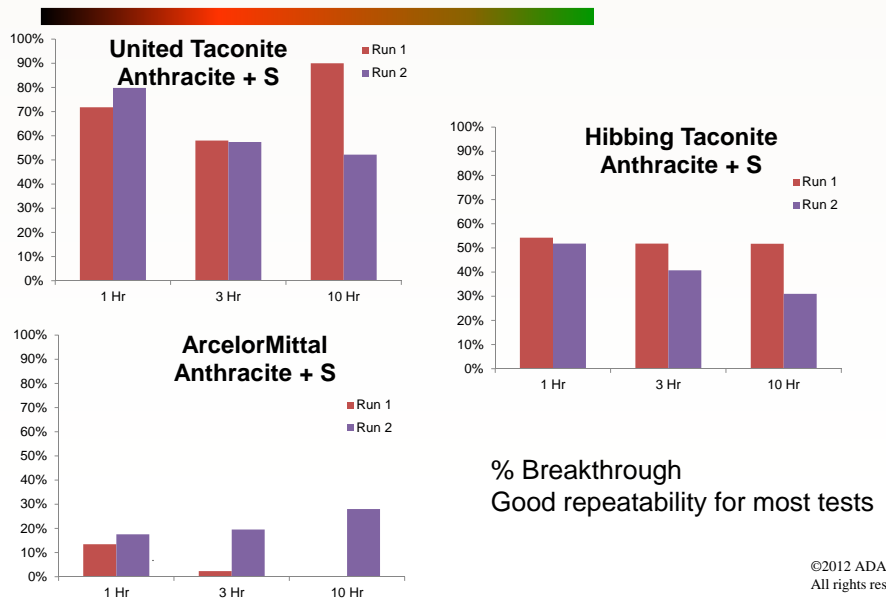
©2012 ADA-ES, Inc.
All rights reserved.



QA Results: Repeatability

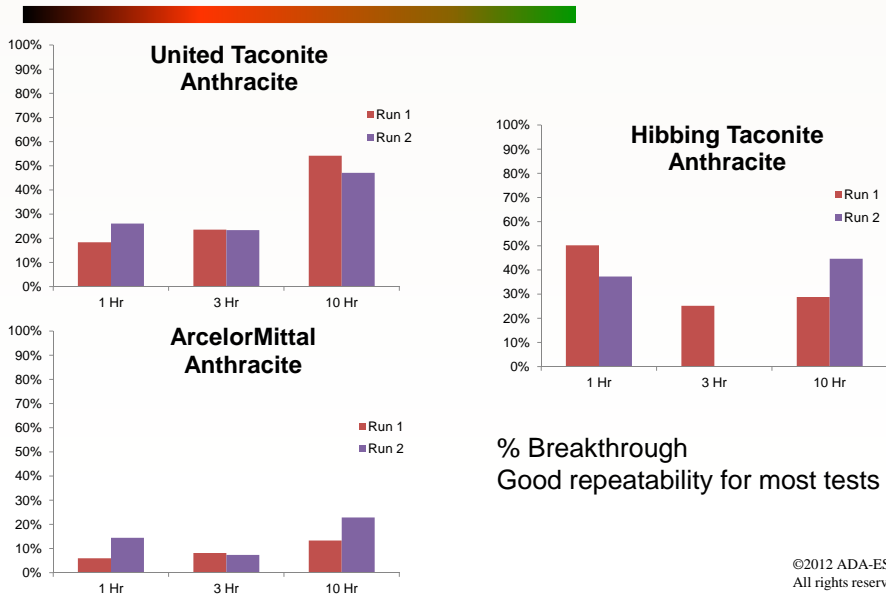


QA Results: Repeatability





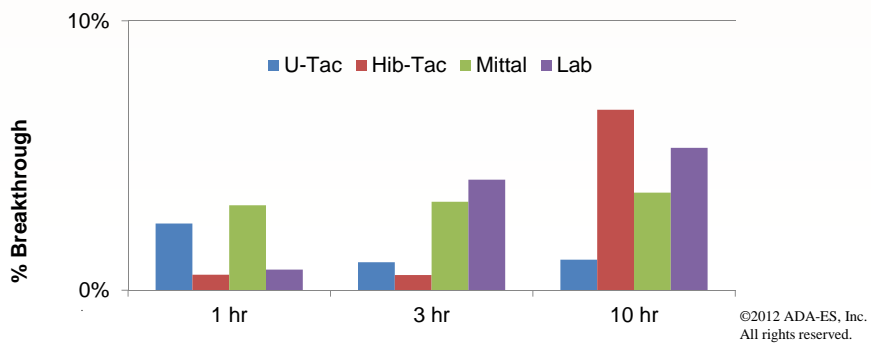
QA Results: Repeatability



Comparison with Lab Results

HA-Br characterized in lab (mercury in dry nitrogen) for up to 10 hours

Insignificant difference in lab and field results





QA Results

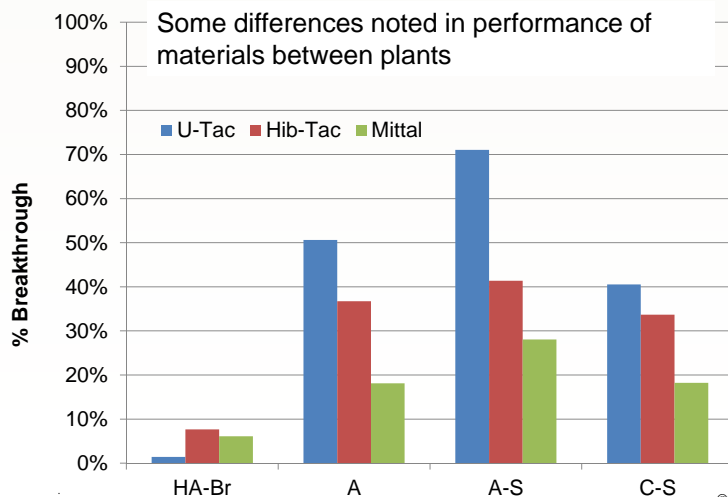
- ✓ Collect data on mercury present downstream of a sorbent bed for each sorbent tested

Mercury breakthrough was measured for all tests by collecting and analyzing all mercury exiting the test traps in a standard EPA M30B sorbent trap

©2012 ADA-ES, Inc.
All rights reserved.



10-hr Hg Breakthrough Comparison



©2012 ADA-ES, Inc.
All rights reserved.



QA Objectives

- ✓ Perform a comparison of sorbents tested at each plant to determine the best sorbents for later pilot and full scale testing

Four sorbents were tested and performance was compared. Final determination of material for scale-up should factor in cost and physical characteristics that may impact equipment design.

©2012 ADA-ES, Inc.
All rights reserved.

F.3 STM Equipment Calibrations

ADA used two separate sets of STM equipment to conduct testing. These boxes are identified as HG-324K-1026 and HG-324K-1064. Before either box was utilized in the field they were sent to the manufacturer, Environmental Supply Company, for calibration. The calibration of the two Dry Gas Meters, the thermocouple, barometer, and flowmeter for both boxes is presented in the following pages in the report format received from Environmental Supply.

NOTE: While both calibrations took place several months before testing, their Initial Use (as specified in the QA Program) was not until August 1st, 2011.



Environmental Supply Company, Inc.

Quality Source Sampling Systems & Accessories

DGM Reference Calibration

Date: May 4, 2011

Reference Meter: Shinagawa Wet Test Meter

Pbar: 29.70 in. Hg

Model: W-NK-1A

S/N: 538787

Dry Gas Meter: Actaris ACD G1.6

AVG γ : 1.005

S/N: 3750037

Counter
Scale

Counts Per Liter (CPL): 500

Factor: 2.0000 at dP 1.000

RUN #	Flow (lpm)	DGM (liters)	DGM (°F)	WTM Initial	WTM final	WTM (liters)	WTM (°F)	DGM Gamma (γ)	Diff (%)
1	0.400	12.084	71.9	716.588	728.644	12.056	70.4	1.000	-0.41
2	0.600	12.056	72.4	728.644	740.692	12.048	70.5	1.003	-0.17
3	0.800	15.876	72.7	740.692	756.667	15.975	70.6	1.010	0.58

Assigned To: HG-324K-1026 Ch-1


Signature

05/04/11
Date



DGM Reference Calibration

Date: May 4, 2011

Reference Meter: Shinagawa Wet Test Meter
Model: W-NK-1A
S/N: 538789

Pbar: 29.70 in. Hg

Dry Gas Meter: Actaris ACD G1.6
S/N: 3750038

AVG γ : 1.003

Counts Per Liter (CPL): 520

Counter Scale Factor: 1.9231 at dP 1.000

RUN #	Flow (lpm)	DGM (liters)	DGM (°F)	WTM initial	WTM final	WTM (liters)	WTM (°F)	DGM Gamma (γ)	Diff (%)
1	0.400	12.029	72.8	145.290	157.282	11.992	70.4	1.001	-0.13
2	0.600	11.996	73.2	157.282	169.249	11.967	70.5	1.003	0.01
3	0.800	15.919	73.5	169.249	185.141	15.892	70.5	1.004	0.13

Assigned To: HG-324K-1026 Ch-2

Signature

05/04/11
Date



HG-324K THERMOCOUPLE CALIBRATION

Date: May 3, 2011

Reference Thermocouple: PIE Thermocouple

Console S/N: HG-324K- 1026

Serial Number: 104547 (NIST Traceable)

Model: 520

TC Simulator Output (°F)	Stack T/C Reading (°F)	Sorbent T/C Reading (°F)	Probe T/C Reading (°F)	Condenser T/C Reading (°F)	Max % Diff	Min % Diff
30	30.49	30.49	30.49	30.60	2.00	1.62
60	60.51	60.49	60.50	60.62	1.03	0.81
120	120.45	120.45	120.45	120.61	0.51	0.37
250	250.45	250.43	250.43	250.58	0.23	0.17
500	500.58	500.56	500.57	500.72	0.14	0.11

HG-324K BAROMETER CALIBRATION

Reference Barometer: Compact Digital Barometer from Control Company

Serial Number: 72402089 (NIST Traceable)

Model: 61161-396

ES Elevation: 379' above sea level

Date	Time	Reference (in Hg)	HG-324K (in Hg)	Difference (in Hg)	% Diff.
3-May-11	13:25	29.71	29.694	0.016	0.05

HG-324K FLOWMETER CALIBRATION

Reference Flowmeter DryCal Technologies

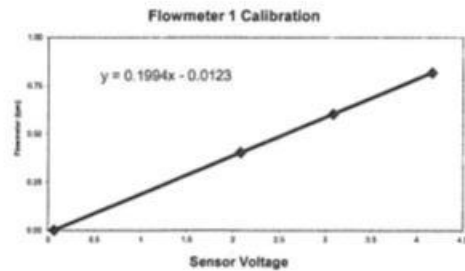
Serial Number: 112234 (NIST Traceable)

Model: Definer 220

Flowmeter 1	
Sensor Voltage	Reference Meter Flow (lpm)
0.064	0.000
2.0819	0.404
3.0866	0.603
4.1601	0.817

SLOPE 0.1994

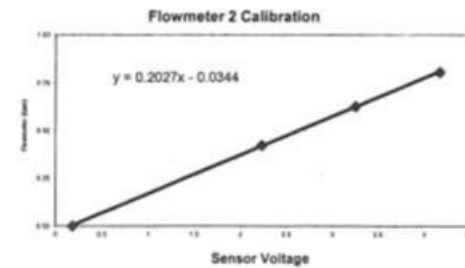
INTERCEPT -0.0123



Flowmeter 2	
Sensor Voltage	Reference Meter Flow (lpm)
0.1819	0.000
2.2327	0.423
3.2501	0.626
4.1633	0.806

SLOPE 0.2027

INTERCEPT -0.0344





Environmental Supply Company, Inc.

Quality Source Sampling Systems & Accessories

DGM Reference Calibration

Date: February 4, 2011

Reference Meter: Shinagawa Wet Test Meter

Pbar: 29.90 in. Hg

Model: W-NK-1A

S/N: 538787

Dry Gas Meter: Actaris ACD G1.6

AVG γ : 1.003

S/N: 3600875

Counter
Scale

Counts Per Liter (CPL): 545

Factor: 1.8349 at dP 1.000

RUN #	Flow (lpm)	DGM (liters)	DGM (°F)	WTM initial	WTM final	WTM (liters)	WTM (°F)	DGM Gamma (γ)	Diff (%)
1	0.400	11.903	69.4	904.119	916.014	11.895	67.6	1.003	0.01
2	0.600	11.855	69.8	916.014	927.863	11.849	67.8	1.003	0.07
3	0.800	15.882	70.0	927.863	943.710	15.847	67.7	1.002	-0.07

Assigned To: HG-324K-1064 Ch-1

Signature

02/04/11
Date



DGM Reference Calibration

Date: February 4, 2011

Reference Meter: Shinagawa Wet Test Meter

Pbar: 29.90 in. Hg

Model: W-NK-1A

S/N: 538789

Dry Gas Meter: Actaris ACD G1.6

AVG γ : 1.004

S/N: 3600876

Counts Per Liter (CPL): 535

Counter Scale Factor: 1.8692 at dP 1.000

RUN #	Flow (lpm)	DGM (liters)	DGM (°F)	WTM initial	WTM final	WTM (liters)	WTM (°F)	DGM Gamma (γ)	Diff (%)
1	0.400	12.029	69.7	546.621	558.641	12.020	67.6	1.003	-0.04
2	0.600	11.924	70.1	558.641	570.567	11.926	67.8	1.005	0.09
3	0.800	15.962	70.1	570.567	586.509	15.942	67.8	1.003	-0.05

Assigned To: HG-324K-1064 Ch-2

Troy Baker
Signature

02/04/11
Date



HG-324K THERMOCOUPLE CALIBRATION

Date: February 3, 2011

Reference Thermocouple: PIE Thermocouple

Serial Number: 104547 (NIST Traceable)

Console S/N: HG-324K- 1064

Model: 520

TC Simulator Output (°F)	Stack T/C Reading (°F)	Sorbent T/C Reading (°F)	Probe T/C Reading (°F)	Condenser T/C Reading (°F)	Max % Diff	Min % Diff
30	30.60	30.63	30.69	30.68	2.29	2.00
60	60.57	60.58	60.61	60.62	1.03	0.95
120	120.55	120.58	120.55	120.61	0.51	0.46
250	250.50	250.51	250.50	250.56	0.22	0.20
500	500.48	500.50	500.55	500.59	0.12	0.10

HG-324K BAROMETER CALIBRATION

Reference Barometer: Compact Digital Barometer from Control Company

Serial Number: 72402089 (NIST Traceable)

Model: 61161-396

ES Elevation: 378' above sea level

Date	Time	Reference (in Hg)	HG-324K (in Hg)	Difference (in Hg)	% Diff.
3-Feb-11	14:55	29.91	29.972	0.062	0.21

HG-324K FLOWMETER CALIBRATION

Reference Flowmeter: DryCal Technologies

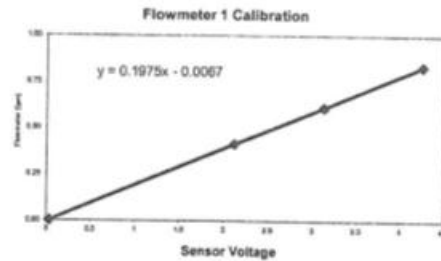
Serial Number: 112234 (NIST Traceable)

Model: Definer 220

Flowmeter 1	
Sensor Voltage	Reference Meter Flow (lpm)
0.0344	0.000
2.1183	0.412
3.1246	0.610
4.2477	0.833

SLOPE 0.1975

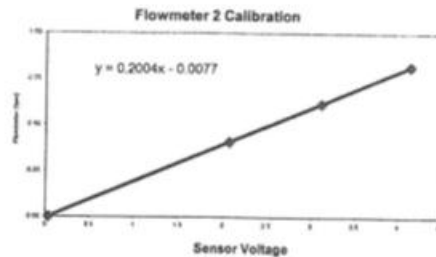
INTERCEPT -0.0067



Flowmeter 2	
Sensor Voltage	Reference Meter Flow (lpm)
0.0368	0.000
2.0754	0.407
3.1166	0.617
4.133	0.821

SLOPE 0.2004

INTERCEPT -0.0077



F.3.1 Flowmeter checks

ADA performed a flowmeter check, confirming the validity of all data gathered. A handheld reference flowmeter (Aalborg) was placed in line with the fully assembled STM equipment, and a 5 minute test was run using stack gas to confirm the accuracy of the instrument's flowmeter, the results of the tests for both channels of both sets of equipment is presented in Table F-1.

Table F-1: STM Equipment Flowmeter Quality Check

Date	STM Box	Channel	Visual Check		Totalizer vs GFM			GFM Temp (F)	B.P. (Hg)	Time (min)	Inst Calc (L STP)	Results	
			Aalborg (L/min)	Instrument (L/min)	Inst (L STP)	Inst (L nom)	Aalborg (L)					Visual % diff	Volume % diff
9/11/2011	1064	A1	0.74	0.784	3.073	3.266	3.10	73.186	28.343	5	3.075	5.95	0.79
		A2	0.75	0.792	3.715	3.948	3.66	72.984	28.343	5	3.719	5.60	1.61
		E1	0.76	0.789	3.707	3.956	3.69	74.273	28.242	5	3.704	3.82	0.39
	1026	E2	0.75	0.796	3.662	3.927	3.61	75.998	28.243	5	3.665	6.13	1.53

The QA Program allows for up to a 10% difference between the reference flowmeter (Aalborg) total volume reading and the instrument's flowmeter total volume reading, but as seen in Table F-1, 1.61% was the highest observed.

F.3.2 Leak checks

Pre and Post-Test Leak-Checks were performed before and after each test. If the Pre-Test Leak-Check failed, the leak was found and repaired until the Leak-Check passed and the test was begun. If the Post-Test Leak-Check failed then the data for that individual test was discarded and the test was repeated. The results of the Leak-Checks are presented in Table F-2.

Table F-2: Pre and Post-Test Leak-Checks

Date	Start Time	End Time	Trap ID	Leak Test _i (Pass/Fail)	Leak Test _f (Pass/Fail)	DGM [L (STP)]
09/06/11	19:19	20:19	04135	PASS	PASS	47.331
			01125	PASS	PASS	47.088
			02127	PASS	PASS	46.732
			03138	PASS	PASS	46.736
09/06/11	20:34	06:34	04128	PASS	PASS	431.288
			01126	PASS	PASS	454.519
			02124	PASS	PASS	464.297
			03132	PASS	PASS	442.546
09/07/11	06:47	09:47	04134	PASS	PASS	135.822
			01129	PASS	PASS	133.488
			02125	PASS	FAIL	135.966
			03139	PASS	PASS	123.125
09/07/11	10:36	11:36	04137	PASS	PASS	37.862
			01111	PASS	PASS	44.402
			02104	PASS	PASS	44.829
			03135	PASS	PASS	41.053
09/07/11	11:50	14:50	04138	PASS	PASS	136.260
			01124	PASS	PASS	134.018
			03130	PASS	PASS	136.304
			02123	PASS	PASS	125.998
09/07/11	15:12	01:12	04129	PASS	PASS	773.634
			01128	PASS	PASS	455.662
			02126	PASS	PASS	461.154
			03136	PASS	PASS	439.439
09/08/11	09:40	10:40	100924	PASS	PASS	45.456
			100953	PASS	PASS	45.229
			100959	PASS	PASS	45.580
			100962	PASS	PASS	44.363
09/08/11	11:16	12:16	100906	PASS	PASS	45.554
			100920	PASS	PASS	45.137
			100955	PASS	PASS	45.327
			100966	PASS	PASS	43.702
09/08/11	12:39	13:39	100910	PASS	PASS	44.942
			100941	PASS	PASS	44.875
			100957	PASS	PASS	45.185
			101029	PASS	PASS	42.855
09/08/11	13:58	14:58	100911	PASS	PASS	49.369
			100915	PASS	PASS	44.961
			100932	PASS	PASS	45.474
			100935	PASS	PASS	43.466
09/08/11	15:16	16:16	100902	PASS	PASS	45.825
			100912	PASS	PASS	44.445
09/08/11	16:16	17:16	98870	PASS	PASS	44.735
			98916	PASS	PASS	44.958
09/08/11	16:26	17:26	100904	PASS	PASS	45.788
			100965	PASS	PASS	44.509
09/09/11	21:19	07:19	04136	PASS	PASS	455.461
			03137	PASS	PASS	451.333
			04133	PASS	PASS	455.951
			03133	PASS	PASS	433.551
09/10/11	07:33	10:33	04131	PASS	PASS	135.618
			03131	PASS	PASS	134.874
			04139	PASS	PASS	136.670
			03134	PASS	PASS	127.337
09/10/11	10:55	11:55	04118	PASS	PASS	43.757
			03119	PASS	PASS	43.397
			04120	PASS	PASS	41.176
			03129	PASS	PASS	41.596
09/10/11	12:03	13:03	04123	PASS	PASS	43.566
			03116	PASS	PASS	43.839
09/10/11	12:03	15:03	04132	PASS	PASS	128.114
			03128	PASS	PASS	128.806
09/10/11	15:32	01:32	04130	PASS	PASS	455.266
			03120	PASS	PASS	433.311

F.3.3 Mercury Analyzer Calibrations

Mercury analyzer analytical bias test 3/24/2011

Spike recovery study certificate 3/24/2011

Mercury Analyzer Calibration Certificate and gas bottle certificate of analysis 3/27/2011

Mercury Analyzer Calibration Certificate and gas bottle certificate of analysis 6/15/2012

Ohio Lumex Co.

9263 Ravenna Rd, Unit A-3

Twinsburg Ohio 44087

Tel. 1-888-876-2611

Email: Mail@Ohiolumex.com

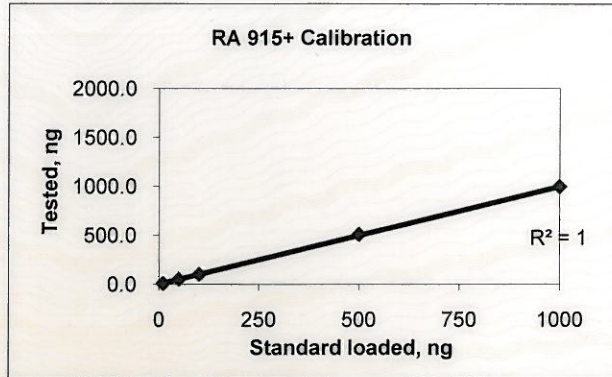
Analyzer # 1364 Certificate

Testing is based on EPA Method 30B QA/QC requirements

No.	Standard (ng)	Tested (ng)
1	10	10.0
2	50	52
3	100	104
4	500	511
5	1000	1000
6	2000	1990

Flow= 2.0 L/min

% RSD= 2.2



Initial Calibration Response Factor = 182.8 (Area/ng)

Method Detection Limit Test

No.	Standard (ng)	Tested (ng)
1	3.0	3.1
2	3.0	3.2
3	3.0	3.1
4	3.0	2.9
5	3.0	3.3
6	3.0	3.0
7	3.0	3.1
8	3.0	3.0

Std Dev = 0.125ng

MDL= 0.374 ng

Bias Test

Hg	Trap No.	Spiked (ng)	Tested (ng)	Recovery (%)	Rec. Ave (%)
Hg(0)	81779	10	9.9	99	100
	80468	10	10	100	
	80469	10	10	100	
	21165	1900	1930	102	101
	21506	1900	1950	103	
	21437	1900	1860	98	
Hg(2+)	0000-1	10	11	110	101
	0000-2	10	10	100	
	0000-3	10	9.2	92	
	0001-1	1900	1890	99	100
	0001-2	1900	1910	101	
	0001-3	1900	1920	101	

Analyst: [Signature]

QA/QC manager: [Signature]
Date: 3/24/2011

All standards used are NIST traceable, certificates attached.

Method Detection Limit (MDL) is defined by "40 CFR, part 136, Appendix B"

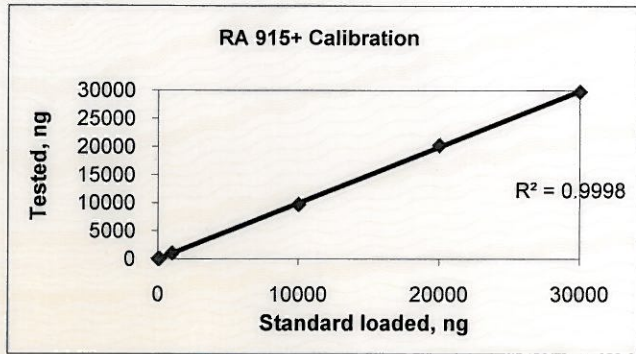
This certification will expire on March 24, 2012

Ohio Lumex Co.
 9263 Ravenna Rd, Unit A-3
 Twinsburg Ohio 44087
 Tel. 1-888-876-2611
 Email: Mail@Ohiolumex.com

Spike Recovery Study Certificate for Analyzer # 1364

Testing is based on EPA Method Appendix K QA/QC requirements

No.	Standard (ng)	Tested (ng)
1	10	10
2	100	92
3	1000	1050
4	10000	9760
5	20000	20300
6	30000	29800



Flow= 4.0 L/min

% RSD= 4.8

Initial Calibration Response Factor = 108.6 (Area/ng)

Spiked Traps Recovery Tests

Hg0	Trap No.	Spiked (ng)	Received (ng)	Recovery (%)	Rec. Ave (%)
Level 1	67838	50	46	92	94
	67846	50	47	94	
	67850	50	48	96	
Level 2	57186	3000	2780	93	95
	57074	3000	2910	97	
	57090	3000	2840	95	
Level 3	51861	30000	28500	95	94
	51889	30000	28400	95	
	51869	30000	28100	94	

Analyst: *[Signature]*

QA/QC manager: *[Signature]*

Date: 3/24/2011

All standards used are NIST traceable, certificates attached.
 Spiking procedure followed EPA CFR 40 Part 75 requirements
 This certification will expire on March 24, 2012

THE LINDE GROUP



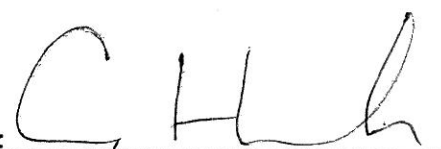
**CERTIFICATE
OF
ANALYSIS**

SALES#:	107702332	CYLINDER # :	CC-266087
PRODUCTION#:	1157050	CYLINDER PRES:	2000 psig
CERTIFICATION DATE:	11/04/2010	CYLINDER VALVE:	CGA 660
P.O.# :	101110JS	PRODUCT EXPIRATION DATE:	05/03/2011
BLEND TYPE:	CERTIFIED		

ANALYTICAL ACCURACY: + / - 10%

<u>COMPONENT</u>	<u>REQUESTED GAS CONC</u>	<u>ANALYSIS</u>
Mercury	6.5 ug/m3	6.7 ug/m3
Air	Balance	Balance

1 ATM/20 °C

ANALYST: 
 Cody Hamlin

DATE: 11/04/2010

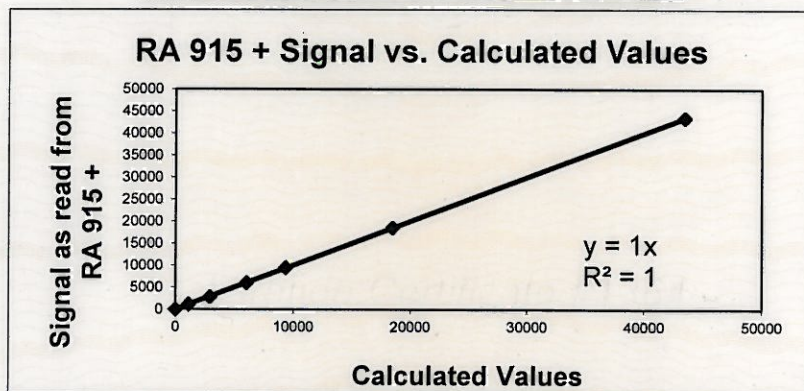
Linde Gas North America LLC

(908) 329-9700 Main (908) 329-9740 Fax
www.Lindeus.com

Ohio Lumex Co.
 9263 Ravenna Rd, Unit A-3
 Twinsburg Ohio 44087
 Tel. 1-888-876-2611
 Email: Mail@Ohiolumex.com

Calibration Certificate #1364
RA 915 +

Standard #	Temp C	Calculated value	Signal (10m cell)
1	20.5	0	0
2	20.5	1122	1145
3	20.5	2907	2827
4	20.5	6016	5966
5	20.5	9341	9445
6	20.5	18453	18537
7	20.5	43470	43423



Spectra Gas certified value: 6.7ug/m3
 Calibration Parameter A : 656

Reading observed: 6.7ug/m3.
 Calibration Parameter B : 38400

CALIBRATION DATE: 03/27/11 NEXT CALIBRATION DUE: 03/27/12

ON THE DATE CALIBRATED, THIS UNIT OPERATED WITHIN SPECIFIED TOLERANCES

Digital Barometer: Cert. # 4245-3250914, Cal. Due: 10/26/2012

Digital Thermometer: Cert. # 4245-3250914, Cal. Due: 10/26/2012

Set of Calibrated Saturated Mercury Vapor Cells, Due: 12/15/2011

Gas NIST traceable Standard: SpectraGas Calibration cylinder #: CC-266087

Concentration: 6.7ug/m3, Analytical Accuracy: +/- 10%. Expiration date: 05/03/2011

SERVICE TECHNICIAN: J.S. *J. Sipos*

RECOMMENDATION NOTE: INSTRUMENT SHOULD BE RECALIBRATED EVERY 12 MONTHS OR SOONER, IF EXPOSED TO EXTREME CONDITIONS OR DAMAGE IS SUSPECTED

THE LINDE GROUP



SHIPPED TO: Ohio Lumex Company
9263 Ravenna Rd Unit A-3
Twinsburg, OH 44087

PAGE: 1 of 1

CERTIFICATE OF ANALYSIS

Sales#: 108894131
Production#: 1215054
Certification Date: May-18-2012
P.O.# : VERBAL JOSEPH
Blend Type: CERTIFIED
Material#: 24086892

Expiration Date: Nov-13-2012
Do NOT use under: 150 psig

Cylinder Size: 2A (8" X 47.5")
Cylinder # : CC-270699
Cylinder Pressure: 2000 psig
Cylinder Valve: CGA 660 / Steel
Cylinder Volume: 29.5 Liter
Cylinder Material: Aluminum
Gas Volume: 4000 Liter
Blend Tolerance: 20% Relative
Analytical Accuracy: 10% Relative

<u>COMPONENT</u>	<u>REQUESTED CONC</u>	<u>CERTIFIED CONC</u>
Mercury	7.0 ug/m3	6.7 ug/m3
Air	Balance	Balance

1 ATM/20°C

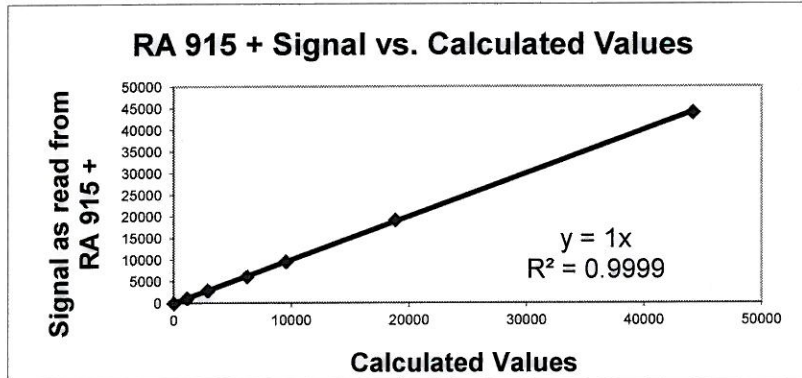
ANALYST: Justin Kutz
Justin Kutz

DATE: May-18-2012

Ohio Lumex Co.
 9263 Ravenna Rd. Unit A-3
 Twinsburg Ohio 44087
 Tel. 1-888-876-2611
 Email: Mail@Ohiolumex.com

Calibration Certificate #1364
RA 915 +

Standard #	Temp C	Calculated value	Signal (10m cell)
1	24	0	0
2	24	1131	1125
3	24	2896	2881
4	24	6214	6149
5	24	9531	9573
6	24	18814	19176
7	24	44150	43996



Spectra Gas certified value: 6.7 ug/m3 Reading observed: 6.7 ug/m3.
 Calibration Parameter A : 851 Calibration Parameter B : 48888

CALIBRATION DATE: 06/15/12 NEXT CALIBRATION DUE: 06/15/13

ON THE DATE CALIBRATED, THIS UNIT OPERATED WITHIN SPECIFIED TOLERANCES

Digital Barometer: Cert. # 4245-3250914, Cal. Due: 10/26/2012
Digital Thermometer: Cert. # 4245-3250914, Cal. Due: 10/26/2012
Gas NIST traceable Standard: SpectraGas Calibration cylinder #: CC-270699
 Concentration: 6.7 ug/m3, Analytical Accuracy: +/- 10%. Expiration date: 11/13/2012

SERVICE TECHNICIAN: J.S.
QC Check: YB

RECOMMENDATION NOTE: INSTRUMENT SHOULD BE RECALIBRATED EVERY 12 MONTHS OR SOONER, IF EXPOSED TO EXTREME CONDITIONS OR DAMAGE IS SUSPECTED

F.4 Raw Data

Tables F-3 and F-4 which follow present all data collected and used by ADA to generate this report. Table F-4 is the raw data from the Ohio Lumex analyzer and is organized chronologically by the times in which the samples were run.

NOTE: The carbon sorbents in Table F-3 are denoted as:

1. Sabre 8% Br (STD)
2. CR4AN
3. CR4AN-Hg
4. CR612C-Hg

Table F-3: Data Validation and

Taconite Project #: 8088-11 Plant: ArcelorMittal Boiler ID: none Sampling Location: Stack D, unless otherwise noted Ohio Lumex ID:																	
Run	Date	Start Time	End Time	Flow Rate [cc/min]	DGM Trap ID [L (STP)]	Stack Wet Bulb Temp (F)	Stack Dry Bulb Temp (F)	Stack RH (%)	STM Box Set Temp (F)	Trap RH (%)	Test Task	Carbon	Test Length (hrs)	Analysis			Comments
														M _{SO2} [ng]	M _{SO4} [ng]	H ₂ O [%]	
1	09/06/11	19:19	20:19	800	04135 46.372	123	125	94.17	147	50	1	1	1	2719	14.0	13.98	
2					01125 45.422	123	125	94.17	147	50	1	2	1	360	23.0	13.98	
3	09/06/11	20:34	06:34	800	03138 45.182	123	125	94.17	147	50	1	4	1	359	22.0	13.98	
4					04128 43.096	123	125	94.17	147	50	1	1	10	1463	95.0	13.98	
5					01126 45.412	123	125	94.17	147	50	1	2	10	1809	278.0	13.98	
6					02124 46.4291	123	125	94.17	147	50	1	3	10				Error in Lab analysis for 02124
7					03132 44.2539	123	125	94.17	147	50	1	4	10	2200	498.0	13.98	
8	09/07/11	06:47	09:47	800	04134 135.819	123	125	94.17	147	50	1	1	3	899	40.0	13.98	
9					01129 133.479	123	125	94.17	147	50	1	2	3	841	75.0	13.98	
10					02125 135.958	123	125	94.17	147	50	1	3	3	186	45	13.98	
11					03139 123.122	123	125	94.17	147	50	1	4	3	930	55.0	13.98	
12					04137 36.537	123	125	94.17	147	50	1	1	1	267	9.1	13.98	
13	09/07/11	10:36	11:36	800	01111 44.393	123	125	94.17	147	50	1	2	1	313	51.0	13.98	
14					02104 44.820	123	125	94.17	147	50	1	3	1	324	69.0	13.98	
15					03135 41.046	123	125	94.17	147	50	1	4	1	367	19.0	13.98	
16					04138 136.258	123	125	94.17	147	50	1	1	3	870	31.0	13.98	
17	09/07/11	11:50	14:50	800	01124 134.008	123	125	94.17	147	50	1	2	3	916	73.0	13.98	
18					02123 77.3634	123	125	94.17	147	50	1	3	3	799	194.0	13.98	
19					03130 136.301	123	125	94.17	147	50	1	4	3	767	88.0	13.98	
20					04128 45.466	123	125	94.17	147	50	1	2	3	916	73.0	13.98	
21	09/07/11	15:12	01:12	800	02126 46.1069	123	125	94.17	147	50	1	3	10	2353	878.0	13.98	
22					03136 43.9427	123	125	94.17	147	50	1	4	10	2718	595.0	13.98	
23	09/08/11	09:40	10:40	800	100924 45.454	122	124	94.130			na	na	1	297	22.0	13.66	Stack C
24					100953 45.222	122	124	94.130			na	na	1	293	21.0	13.66	Stack C
25					100959 45.574	122	124	94.130			na	na	1	291	20.0	13.66	Stack C
26					100952 44.356	122	124	94.130			na	na	1	288	21.0	13.66	Stack A
27	09/08/11	11:16	12:16	800	100906 45.231	122	124	94.130			na	na	1	114	12.0	13.66	Stack C
28					100920 44.838	122	124	94.130			na	na	1	112	9.9	13.66	Stack C
29					100955 45.319	122	124	94.130			na	na	1	286	21.0	13.66	Stack A
30					100956 43.691	122	124	94.130			na	na	1	279	22.0	13.66	Stack A
31	09/08/11	12:39	13:39	800	100910 44.933	122	124	94.130			na	na	1	105	11.0	13.66	Stack B
32					100957 45.180	122	124	94.130			na	na	1	166	16.0	13.66	Stack B
33					100911 44.971	122	124	94.130			na	na	1	153	16.0	13.66	Stack A
34					100929 42.851	122	124	94.130			na	na	1	75	8.7	13.66	Stack B
35	09/08/11	13:58	14:58	800	100952 45.467	122	124	94.130			na	na	1	72	7.9	13.66	Stack B
36					100955 43.464	122	124	94.130			na	na	1	126	11.0	13.66	Stack B
37	09/08/11	15:16	16:16	800	100902 45.820	122	124	94.130			na	na	1	123	12.0	13.66	Stack B
38					100912 44.442	122	124	94.130			na	na	1	164	16.0	13.66	Stack A
39	09/08/11	16:16	17:16	800	98870 44.721	122	124	94.130			na	na	1	124	12.0	13.66	Stack A
40					100904 45.782	122	124	94.130			na	na	1	123	12.0	13.66	Stack B
41	09/08/11	16:26	17:26	800	100954 44.504	122	124	94.130			na	na	1	142	15.0	13.66	Stack B
42					04136 45.5254	124	126	94.200	148	50	2	1	10	2342	129.0	14.46	65%RH 148F
43	09/09/11	21:19	07:19	800	03137 45.133	124	126	94.200	148	50	2	4	10	2180	845.0	14.46	75%RH 134F
44					04133 45.5949	124	126	94.200	134	75	2	1	10	2213	107.0	14.46	65%RH 148F
45					03133 43.348	124	126	94.200	134	75	2	4	10	980	369.0	14.46	65%RH 148F
46	09/10/11	07:33	10:33	800	04131 135.613	124	126	94.200	148	50	2	1	3	703	28.0	14.46	65%RH 148F
47					04139 136.666	124	126	94.200	134	75	2	1	3	370	27.0	14.46	75%RH 134F
48					03134 127.333	124	126	94.200	134	75	2	4	3	1112	147.0	14.46	65%RH 148F
49	09/10/11	10:55	11:55	800	04118 43.755	124	126	94.200	148	50	2	1	1	192	8.0	14.46	65%RH 148F
50					03119 43.395	124	126	94.200	134	75	2	1	1	240	31.7	14.46	75%RH 134F
51	09/10/11	12:03	13:03	800	04120 41.176	124	126	94.200	134	75	2	4	1	162	10.0	14.46	65%RH 148F
52					03129 41.596	124	126	94.200	131	81	2	1	1	187	7.9	14.46	65%RH 148F
53	09/10/11	12:03	13:03	800	04123 43.312	124	126	94.200	131	81	2	1	3	494	13.0	14.46	65%RH 148F
54					04132 128.107	124	126	94.200	131	81	2	1	3	690	56.0	14.46	65%RH 148F
55	09/10/11	15:32	01:32	800	03128 128.806	124	126	94.200	131	81	2	1	10	1649	153.0	14.46	65%RH 148F
56					04130 45.158	124	126	94.200	131	81	2	1	10	1938	592.0	14.46	65%RH 148F

Table F-4: Ohio Lumex Hg Analyzer Produced Raw Data

Description	M, mg	C, ng/g	Area	Description	M, mg	C, ng/g	Area	Description	M, mg	C, ng/g	Area
BLANK	1	0.0	16	02123 9/7/11 stack D 3 3hr E2 carbon bed	1	194	12100	100953 S2	1	21	3370
Std_ 100	1	9.5	970	03130 9/7/11 stack D 4 3hr E1 sand pt1 (wet)	1	522	32500	100959 S1	1	291	44900
Std_ 1000	1	93	9380	03130 9/7/11 stack D 4 3hr E1 sand pt2 (wet)	1	245	15300	100959 S2	1	20	3220
Std_ 500	1	808	80900	03130 9/7/11 stack D 4 3hr E1 carbon bed (wet)	1	88	5510	100962 S1	1	288	44500
QC_ 200	1	454	45500	QC_ 1000	1	1090	67800	100962 S2	1	21	3270
QC_ 200	1	197	19800	QC_ 500	1	495	30800	Std_ 300	1	292	45000
QC_ 200	1	201	20200	Std_ 100, RL = 3%	1	103	9890	Std_ 10, RL = -5%	1	9.5	821
03132 10hr 4 E2 Sand pt 1	1	1800	181000	Std_ 1000, RL = -1%	1	987	94500	Std_ 100, RL = 0%	1	100	8690
03132 10hr 4 E2 Carbon Bed	1	498	49900	Std_ 500, RL = 4%	1	523	50100	Std_ 500, RL = 5%	1	529	45800
03132 10hr 4 E2 Sand pt 2	1	400	40100	Std_ 10, RL = 0%	1	10	1040	Std_ 1000, RL = -1%	1	985	85300
01126 10hr 2 A2 Sand pt 1	1	1690	170000	R.F. 5; R.F = 105.8	1	5.5	529	Std_ 2; R.F. Point	1	2.7	233
01126 10hr 2 A2 Sand pt 2	1	119	12000	QC_ 200	1	179	17200	QC_ 200	1	207	18000
01126 10hr 2 A2 Carbon Bed	1	278	27900	QC_ 200	1	187	17900	04136 A1 9-9-11 10hr Task 2 Stack D sand pt1	1	2040	177000
04128 10 hr 1 A1 Sand pt1	1	526	52700	04120 1 hour Amittal Stack D 9-10-11 Sand Part 1	1	120	11500	04136 A1 9-9-11 10hr task 2 stack D sand pt2	1	302	26200
04128 10 hr 1 A1 Sand pt2	1	937	93800	04120 1 hour Amittal Stack D 9-10-11 Sand Part 2	1	42	4070	04136 A1 9-9-11 10hr task 2 stack D carbon bed	1	129	11200
04128 10 hr 1 A1 Carbon bed	1	95	9610	04120 1 hour Amittal Stack D 9-10-11 Carbon Bed	1	10	992	03137 A2 9-9-11 10hr task 2 stack D sand pt 1	1	1820	158000
QC_ 200	1	198	19900	03129 1 hour Amittal Stack D 9-10-11 Sand Part 1	1	53	5100	03137 A2 9-9-11 10hr task 2 stack D sand pt 2	1	360	31200
04134 1 3 hr A1 Sand pt 1	1	874	76000	03129 1 hour Amittal Stack D 9-10-11 Sand Part 2	1	167	16000	03137 A2 9-9-11 10hr task 2 stack D Carbon bed	1	845	73200
04134 1 3 hr A1 Sand pt 2	1	25	2240	03129 1 hour Amittal Stack D 9-10-11 Carbon Bed	1	26	2570	100069 Sand	1	6.7	580
04134 1 3 hr A1 Carbon bed	1	40	3510	04130 10 hr 81% RH Stack D 9-10-11 Sand part 1	1	239	22900	QC_ 200	1	216	18700
01129 2 3 hr A2 Sand pt 1	1	760	66100	04130 10 hr 81% RH Stack D 9-10-11 Sand part2	1	1410	135000	04133 E1 9-9-11 10hr task 2 stack D Sand Pt1	1	2200	191000
01129 2 3 hr A2 Sand pt 2	1	81	7060	04130 10 hr 81% RH Stack D 9-10-11 Carbon Bed	1	153	14700	04133 E1 9-9-11 10hr task 2 stack D Sand Pt2	1	13	1150
01129 2 3 hr A2 Carbon Bed	1	75	6580	QC_ 200	1	183	17600	04133 E1 9-9-11 10hr task 2 stack D Carbon Bed	1	107	9340
02125 3 3 hr E1 Sand pt 1 (Wet)	1	27	2350	QC_ 2000	1	1800	173000	03133 E2 9-9-11 10hr task 2 stack D Sand pt1	1	1640	142000
02125 3 3 hr E1 Sand pt 2 (WET)	1	159	11200	03120 10 hr 81% RH Stack D 9-10-11 Sand part 1	1	1160	111000	03133 E2 9-9-11 10hr task 2 stack D Sand pt2	1	220	19100
02125 3 3 hr E1 Carbon bed (WET)	1	4.5	390	03120 10 hr 81% RH Stack D 9-10-11 Sand part 2	1	148	14200	03133 E2 9-9-11 10hr task 2 stack D Carbon Bed	1	369	32000
03139 4 3 hr E2 Sand pt 1	1	790	68700	03120 10 hr 81% RH Stack D 9-10-11 Carbon Bed	1	592	56700	04132 E1 9-10-11 3hr task 2 stack D sand pt1	1	438	38000
03139 4 3 hr E2 Sand pt 2	1	140	12200	100904 mittal 9-8-11 stack A&B Run 6 Carbon Bed 1	1	142	13600	04132 E1 9-10-11 3hr task 2 stack D sand pt2	1	56	4910
03139 4 3 hr E2 Carbon Bed	1	55	4820	100904 mittal 9-8-11 stack A&B Run 6 Carbon Bed 2	1	19	1900	04132 E1 9-10-11 3hr task 2 stack D carbon bed	1	13	1170
QC_ 200	1	201	17500	100965 mittal 9-8-11 stack A&B Run 6 CB 1	1	169	16200	QC_ 200	1	225	19500
QC_ 200	1	199	17400	100965 mittal 9-8-11 stack A&B Run 6 CB 2	1	20	1970	QC_ 500	1	470	40700
04135 1 1hr A1 Sand pt 1	1	266	18800	QC_ 200	1	195	18700	03128 E2 9-10-11 3hr task 2 stack D Sand pt1	1	603	52200
04135 1 1hr A1 Sand pt 2	1	5.9	418	Std_ 10, RL = 0%	1	10	1660	03128 E2 9-10-11 3hr task 2 stack D Sand pt2	1	87	7580
04135 1 1hr A1 carbon bed	1	14	1020	Std_ 50, RL = 4%	1	52	8040	03128 E2 9-10-11 3hr task 2 stack D Carbon Bed	1	52	4520
01125 2 1hr A2 Sand pt 1	1	221	15600	Std_ 100, RL = 5%	1	105	16300	01123 A1 9-10-11 1hr task 2 stack D sand pt 1	1	122	10600
01125 2 1hr A2 Sand pt 2	1	139	9810	Std_ 500, RL = 2%	1	514	79300	01123 A1 9-10-11 1hr task 2 stack D sand pt 2	1	65	5650
01125 2 1hr A2 Carbon Bed	1	23	1690	Std_ 1000, RL = 0%	1	992	153000	01123 A1 9-10-11 1hr task 2 stack D Carbon Bed	1	7.9	685
02127 2 1hr E1 Sand pt 1	1	269	19000	QC_ 200 SS	1	204	31600	03116 A2 9-10-11 1hr task 2 stack D sand pt1	1	210	18200
02127 2 1hr E1 Sand pt 2	1	53	3780	Std_ 2 RF-198	1	2.6	396	03116 A2 9-10-11 1hr task 2 stack D sand pt2	1	37	3270
02127 2 1hr E1 Carbon Bed	1	50	3540	Std_ 40	1	40	6270	03116 A2 9-10-11 1hr task 2 stack D Carbon Bed	1	13	1150
03139 3 1 HR E2 SAND PT 1	1	282	19900	100902 S1	1	166	25700	QC_ 400			
03139 3 1 HR E2 SAND PT 2	1	77	5470	100902 S2	1	16	2510	Std_ 10	1	9.8	841
03139 3 1 HR E2 CARBON BED	1	22	1600	100912 S1	1	164	25300	Std_ 100	1	99	8540
QC_ 200	1	204	14400	100912 S2	1	16	2540	Std_ 500	1	495	42600
QC_ 200	1	196	16400	98870 S1	1	124	19200	Std_ 1000	1	1000	86100
04137 9/7/11 1 1hr A1 stack D Sand pt1	1	250	20900	98870 S2	1	12	2000	R.F. 5 R.F pt = 97.2	1	5.7	486
04137 9/7/11 1 1hr A1 stack D Sand pt2	1	17	1480	98916 S1	1	123	19000	QC_ 300	1	287	24700
04317 9/7/11 1 1hr A1 stack D carbon bed	1	9.1	810	98916 S2	1	16	2530	QC_ 200	1	194	16700
01111 9/7/11 2 1hr A2 stack D sand pt1	1	288	24100	100915 S1	1	72	11200	QC_ 200	1	192	16500
01111 9/7/11 2 1hr A2 stack D sand pt2	1	25	2150	100916 S2	1	7.9	1220	04118 1 hour 9 10 11 Stack D 50% RH	1	154	13300
01111 9/7/11 2 1hr A2 stack D carbon bed	1	53	4520	Std_ 10, RL = 10%	1	11	1770	04118 1 HOUR sand pt 2	1	38	3320
02104 9/7/11 3 1hr E1 stack D sand pt1	1	282	23600	Std_ 100, RL = 2%	1	102	15800	04118 carbon bed	1	4.2	358
02104 9/7/11 3 1hr E1 stack D sand pt2	1	42	3580	Std_ 250, RL = 3%	1	258	39800	04118 carbon bed pt 2	1	3.8	323
02104 9/7/11 3 1hr E1 stack D carbon bed	1	69	5860	Std_ 500, RL = 1%	1	508	78300	03119 1 hour 50% RH sand pt 1	1	206	17700
03135 9/7/11 4 1hr E2 stack D sand pt1	1	345	28800	Std_ 1000, RL = 0%	1	993	153000	03119 sand pt 2	1	34	2970
03135 9/7/11 4 1hr E2 stack D sand pt2	1	22	1920	Std_ 200 SS	1	200	30900	03119 Carbon Bed	1	29	2520
03135 9/7/11 4 1hr E2 stack D carbon bed	1	19	1690	Std_ 3 RF-139	1	2.7	417	03119 Carbon bed pt 2	1	2.7	228
QC_ 200	1	185	15500	100911 S1	1	75	11700	QC_ 200	1	191	14900
BLANK	1	-28		100911 S2	1	8.7	1340	Std_ 200	1	210	16400
Std_ 10	1	13	1000	100935 S1	1	123	19000	Std_ 10, RL = 20%, RL = 20%	1	12	1220
Std_ 100	1	107	8100	100935 S2	1	12	1920	Std_ 100, RL = 6%, RL = 6%	1	106	10100
Std_ 500	1	532	40200	100932 S1	1	126	19500	Std_ 500, RL = -9%, RL = -9%	1	451	43000
Std_ 5000	1	4970	376000	100932 S2	1	11	1810	Std_ 1000, RL = 2%, RL = 2%	1	1020	97100
QC_ 1000	1	1070	81400	100955 S1	1	286	44100	Std_ 750, RL = 2%, RL = 2%	1	766	72900
QC_ 200	1	219	16600	100955 S2	1	21	3270	Std_ 300, RL = -10%	1	269	25600
QC_ 200	1	219	16600	100906 S1	1	114	17700	QC_ 500	1	505	48100
04129 9/7/11 stack D 1 10hr A1 sand pt1	1	1620	101000	100906 S2	1	12	1890	QC_ 250	1	238	22700
04129 9/7/11 stack D 1 10hr A1 sand pt2	1	3500	218000	Std_ 100	1	97	15000	04131 AM 91011 3-hr Task2 stkD Sand Bed 1	1	635	60500
04129 9/7/11 stack D 1 10hr A1 carbon bed	1	416	25900	Std_ 200	1	194	29900	04131 AM 91011 3-hr Task2 stkD Sand Bed 2	1	68	6550
01128 9/7/11 stack D 2 10hr A2 sand pt1	1	1410	87800	100966 S1	1	279	43000	04131 AM 91011 3-hr Task2 stkD Carbon Bed 1	1	28	2730
01128 9/7/11 stack D 2 10hr A2 sand pt2	1	741	46100	100966 S2	1	22	3460	03131 AM 91011 3-hr Task2 stkD Sand Bed 1	1	554	52800
01128 9/7/11 stack D 2 10hr A2 carbon bed	1	638	39700	100920 S1	1	112	17400	03131 AM 91011 3-hr Task2 stkD Sand Bed 2	1	75	7140
02126 9/7/11 stack D 3 10hr E1 sand pt1	1	1640	102000	100920 S2	1	9.9	1530	03131 AM 91011 3-hr Task2 stkD Carbon Bed 1	1	108	10300
02126 9/7/11 stack D 3 10hr E1 sand pt2	1	613	38100	100910 S1	1	105	16300	04139 AM 91011 3-hr Task2 stkD Sand Bed 1	1	317	30200
02126 9/7/11 stack D 3 10hr E1 carbon bed	1	878	54600	100910 S2	1	11	1720	04139 AM 91011 3-hr Task2 stkD Sand Bed 2	1	53	5110
03136 9/7/11 stack D 4 10hr E2 sand pt1	1	2070	129000	101029 S1	1	153	23700	04139 AM 91011 3-hr Task2 stkD Carbon Bed 1	1	27	2630
03136 9/7/11 stack D 4 10hr E2 sand pt2	1	648	40300	101029 S2	1	16	2600	Std_ 100, RL = -20%, RL = 4%	1	101	7650
03136 9/7/11 stack D 4 10hr E2 carbon bed	1	595	37000	100941 S1	1	110	17000	Std_ 350, RL = -20%, RL = 0%	1	351	26400
QC_ 200	1	207	12800	Std_ 150 SS	1	163	25200	Std_ 650, RL = -21%, RL = 0%	1	649	48800
QC_ 200	1	200	12400	100941 S2	1	9.7	1490	QC_ 400	1	401	30200
QC_ 1000	1	1020	63100	100957 S1	1	166	25700	03134 AM 91011 3-hr Task2 stkD Sand Bed 1	1	312	23500
04138 9/7/11 stack D 1 3hr A1 sand pt1	1	762	47400	100957 S2	1	16	2580	03134 AM 91011 3-hr Task2 stkD Sand Bed 2	1	724	54500
04138 9/7/11 stack D 1 3hr A1 sand pt2	1	108	6750	100924 S1	1	297	45800	03134 AM 91011 3-hr Task2 stkD Sand Bed 3	1	76	5730
04138 9/7/11 stack D 1 3hr A1 carbon bed	1	31	1990	100924 S2	1	22	3470	03134 AM 91011 3-hr Task2 stkD Carbon Bed 1	1	147	11100
01124 9/7/11 stack D 2 3hr A2 sand pt1	1	664	41300	100953 S1	1	293	45200	QC_ 500	1	516	38800
01124 9/7/11 stack D 2 3hr A2 sand pt2	1	252	15700								
01124 9/7/11 stack D 2 3hr A2 carbon bed	1	73	4590								
02123 9/7/11 stack D 3 3hr E2 sand pt1	1	648	40300								
02123 9/7/11 stack D 3 3hr E2 sand pt2	1	151	9460								

F.4.1 Sample Trap Preparation

The sample traps were prepared by ADA with the following parameters:

- Each sorbent was ground until 95% by weight passed through a 325 mesh (45 μ m) screen.
- The ground sorbents were mixed with sand with a ratio of 20 milligrams of sorbent to 50 grams of sand
- The sample traps each contained 4 grams of the sand/sorbent mixture in the test beds, meaning 1.6 milligrams of sorbent was present in the traps.

F.4.2 Sorbent Trap Method Raw Data

On 9/8/11, ADA performed a modified Method 30B test on Stacks A, B, and C. Three pairs of standard Ohio Lumex made STM traps were collected during 1-hour runs on Stacks A, B, and C and the results are presented in Table F-5. The total mass of mercury captured in each pair is used to calculate the mercury concentration of the process gas (column Hg-STM) and then averaged together. The relative difference (RD) between the paired traps is required to be less than 10%.

Table F-5: STM Results

Date	Start Time	End Time	Stack	DGM [L (STP)]	M _{Sect1} [ng]	M _{Sect2} [ng]	%Break Through	Hg-STM [ng/L] _{dry}	Hg-STM _{AVG} [ng/L] _{dry}	RD [%]	RD Pass/Fail
09/08/11	09:40	10:40	Stack C	45.454	297	22.0	6.9	7.02	6.98	0.53	PASS
				45.222	293	21.0	6.7	6.94			
			Stack C	45.574	291	20.0	6.4	6.82	6.90		
				44.356	288	21.0	6.8	6.97			
09/08/11	11:16	12:16	Stack A	45.231	114	12.0	9.5	2.79	2.75	1.22	PASS
				44.838	112	9.9	8.1	2.72			
			Stack C	45.319	286	21.0	6.8	6.77	6.83		
				43.691	279	22.0	7.3	6.89			
09/08/11	12:39	13:39	Stack A	44.933	105	11.0	9.5	2.58	2.62	1.64	PASS
				44.868	110	9.7	8.1	2.67			
			Stack B	45.180	166	16.0	8.8	4.03	3.99		
				42.851	153	16.0	9.5	3.94			
09/08/11	15:16	16:16	Stack B	45.820	166	16.0	8.8	3.97	4.01	0.97	PASS
				44.442	164	16.0	8.9	4.05			
09/08/11	16:16	17:16	Stack A	44.721	124	12.0	8.8	3.04	3.07	0.83	PASS
				44.951	123	16.0	11.5	3.09			
09/08/11	16:26	17:26	Stack B	45.782	142	19.0	11.8	3.52	3.88	9.40	PASS
				44.504	169	20.0	10.6	4.25			

Appendix B-2-5

Evaluation of a Slipstream Baghouse for the Taconite Industry

January 2012



EERC[®]

Energy & Environmental Research Center

UNIVERSITY OF NORTH DAKOTA

15 North 23rd Street — Stop 9018 / Grand Forks, ND 58202-9018 / Phone: (701) 777-5000 Fax: 777-5181
Web Site: www.undeerc.org

January 25, 2012

Dr. Michael Berndt
Research Scientist
Minnesota Department of Natural Resources
Division of Lands and Minerals
500 Lafayette Road
Saint Paul, MN 55155-4045

Dear Dr. Berndt:

Subject: Revised Final Report Entitled "Project 4: Evaluation for a Slipstream Baghouse for the Taconite Industry"; EERC Fund 15726

Please find enclosed the revised subject final report.

If you have any questions or require clarification of any point, please contact me by phone at (701) 777-5138 or by e-mail at dlaudal@undeerc.org.

Sincerely,

Dennis L. Laudal
Senior Research Advisor

DLL/kal

Enclosures

c/enc: Ryan Siats, U.S. Steel

PROJECT 4: EVALUATION OF A SLIPSTREAM BAGHOUSE FOR THE TACONITE INDUSTRY

Revised Final Report

Prepared for:

Michael Berndt

Minnesota Department of Natural Resources
Division of Lands and Minerals
500 Lafayette Road
Saint Paul, MN 55155-4045

Prepared by:

Dennis L. Laudal

Energy & Environmental Research Center
University of North Dakota
15 North 23rd Street, Stop 9018
Grand Forks, ND 58202-9018

2012-EERC-01-05

January 2012

EERC DISCLAIMER

LEGAL NOTICE This research report was prepared by the Energy & Environmental Research Center (EERC), an agency of the University of North Dakota, as an account of work sponsored by the Minnesota Department of Natural Resources. Because of the research nature of the work performed, neither the EERC nor any of its employees makes any warranty, express or implied, or assumes any legal liability or responsibility for the accuracy, completeness, or usefulness of any information, apparatus, product, or process disclosed or represents that its use would not infringe privately owned rights. Reference herein to any specific commercial product, process, or service by trade name, trademark, manufacturer, or otherwise does not necessarily constitute or imply its endorsement or recommendation by the EERC.

PROJECT 4: EVALUATION OF A SLIPSTREAM BAGHOUSE FOR THE TACONITE INDUSTRY

ABSTRACT

Over the past 20 years, there has been a concerted effort by national and state agencies to reduce mercury emissions from all sources. In November of 2011, the U.S. Environmental Protection Agency (EPA) is required to issue an air toxic rule that will include mercury based on maximum achievable control technology (MACT) requirements for the coal-fired power industry. Although utilities are the largest source of anthropogenic mercury emissions, they are not the only source. In Minnesota, one of these sources is the taconite industry. As a result, the Energy & Environmental Research Center tested a mercury control technology utilizing a slipstream baghouse with activated carbon injection at the United States Steel Corporation, Minnesota Ore Operations – Keetac Plant. Results showed that by using as little as 2.2 lb/Macf of standard activated carbon or 1.1 lb/Macf of a treated carbon >75% mercury removal can be achieved.

ACKNOWLEDGMENTS

The authors of this report would like to thank Mike Berndt of the Minnesota Department of Natural Resources for all of his support and input. We would also like to thank Region 5 EPA for providing funding for the project. In addition, we thank Keith Hanson of Barr Engineering. Lastly, we gratefully acknowledge and thank Ryan Siats and Keetac for supporting this project and allowing the installation of the slipstream baghouse at their site.

TABLE OF CONTENTS

LIST OF FIGURES	iii
LIST OF TABLES	iv
NOMENCLATURE	v
EXECUTIVE SUMMARY	vi
1.0 INTRODUCTION AND BACKGROUND	1
2.0 PROJECT OBJECTIVES	2
3.0 EXPERIMENTAL APPROACH	2
3.1 Description of Equipment.....	3
3.1.1 EERC Portable Slipstream Baghouse	3
3.1.2 Activated Carbon Injection System	4
3.1.3 Mercury Measurement Equipment	5
3.2 Project Test Plan	5
4.0 RESULTS AND DISCUSSION	6
4.1 Operation of the Slipstream Baghouse	6
4.2 Particulate Control	8
4.3 Mercury Control	9
4.3.1 Baseline Results	10
4.3.2 Mercury Removal Using Standard Activated Carbon	12
4.3.3 Mercury Removal Using Bromine-Treated Activated Carbon	12
4.3.4 Comparison of the Mercury Removal Between the CMMs and Sorbent Traps	14
4.4 Preliminary Economic Evaluation	15
4.4.1 Installation and Operating Costs for a Pulse-Jet Baghouse	15
4.4.2 Installation and Operating Costs for an ACI System.....	16
5.0 QUALITY ASSURANCE/QUALITY CONTROL	17
5.1 K-Tron Activated Carbon Feeder	17
5.2 Particulate Samples.....	18
5.3 Mercury Measurements	19
5.3.1 Calibration of the CMMs	19
5.3.2 QA/QC Requirements for the Sorbent Traps.....	19
5.3.3 Comparison of CMMs to Sorbent Trap Mercury Measurements	20

Continued . . .

TABLE OF CONTENTS (continued)

6.0 CONCLUSIONS AND RECOMMENDATIONS 26

7.0 REFERENCES 27

SAMPLE CALCULATIONS Appendix A

DUST-LOADING DATA SHEETS Appendix B

COMPLETE SORBENT TRAP AND CMM COMPARISON DATA Appendix C

LIST OF FIGURES

1	Photograph of the EERC baghouse, trailer, and control room.....	4
2	Bag layout of the EERC slipstream baghouse resulting in an air-to-cloth ratio of 5.45 ft/min.....	5
3	Slipstream baghouse operating temperatures	7
4	Slipstream baghouse pressure drop and gas flow rate.....	9
5	Initial baseline mercury results	10
6	Results showing mercury reemission after shutting off the ACI	11
7	Mercury results utilizing standard activated carbon	11
8	Mercury results utilizing bromine-treated activated carbon at a feed rate of 0.6 lb/Macf	13
9	Mercury results utilizing bromine-treated activated carbon at a feed rate of 1.1 lb/Macf	13
10	Calibration of the K-Tron activated carbon feed system	18

LIST OF TABLES

1	Project Test Plan.....	6
2	Actual Tests Conducted at Keetac.....	7
3	Particulate Sampling Across the Slipstream BH at Keetac.....	9
4	Mercury Removal Using a Slipstream BH and Standard Activated Carbon	12
5	Mercury Removal Using a Slipstream Baghouse and Bromine-Treated Activated Carbon.....	14
6	Comparison of Sorbent Trap and CMM Results.....	14
7	Capital Cost for a Pulse-Jet Baghouse at Keetac	15
8	Baghouse Annual Operating and Maintenance Costs for Keetac	16
9	Estimated Sorbent Costs at Keetac with a Pulse-Jet Baghouse	17
10	Particulate Sampling Isokinetic Determination.....	19
11	CMM Calibration Requirements.....	19
12	Multipoint Linearity Checks	20
13	Baghouse Inlet CMM Zero and Span Data	21
14	Baghouse Outlet CMM Zero and Span Data	22
15	Baghouse Inlet CMM Calibration Data	23
16	Baghouse Outlet CMM Calibration Data.....	24
17	OhioLumex Calibration Results.....	24
18	QC Check Standard Results for the OhioLumex	25
19	QA/QC Comparison of CMMs to Sorbent Traps.....	25

NOMENCLATURE

AC	activated carbon
ACI	activated carbon injection
BH	baghouse
C_a and C_b	mercury concentrations measured by the paired sorbent traps
C_m	meter constant
CMM	continuous mercury monitor
CVAA	cold vapor atomic adsorption
CVAF	cold-vapor atomic fluorescence
EERC	Energy & Environmental Research Center
EPA	U.S. Environmental Protection Agency
FOB	freight on board
ISP	inertial separation probe
Keetac	United States Steel Corporation, Minnesota Ore Operations – Keetac
Lt	long ton
Macf	million actual cubic feet
MACT	maximum achievable control technology
MNDNR	Minnesota Department of Natural Resources
NIST	National Institute of Standards and Technology
PAC	powdered activated carbon
PPS	polyphenylene sulfide
PRB	Powder River Basin
QA/QC	quality assurance/quality control
RSD	relative standard difference
scfm	standard cubic feet per min
TPE	total purchased equipment

PROJECT 4: EVALUATION OF A SLIPSTREAM BAGHOUSE FOR THE TACONITE INDUSTRY

EXECUTIVE SUMMARY

Introduction

Over the past 20 years, there has been a concerted effort by national and state agencies to reduce mercury emissions from all sources. In December of 2011, the U.S. Environmental Protection Agency (EPA) issued an air toxic rule for the coal-fired power industry. This rule will include mercury and is based on maximum achievable control technology requirements.

Although utilities are the largest source of anthropogenic mercury, they are not the only source. In Minnesota, one of these sources is the taconite industry. Taconite processing has two potential sources of mercury: mercury released from processing the ore and mercury released from the fuels used during processing. The greatest percentage of mercury emissions results from mercury inherent in the ore, which is related to the ore's geographical location in the Biwabik Iron Formation.

The taconite industry formed a working group to evaluate and help fund research to reduce mercury emissions. This group, the Minnesota Taconite Mercury Control Advisory Committee, along with the Minnesota Department of Natural Resources and EPA, funded five projects. One of those projects was an Energy & Environmental Research Center (EERC) project to evaluate the use of a slipstream baghouse (BH) with activated carbon injection (ACI) to reduce mercury emissions.

Although the technology would be expected to provide effective mercury control for any of the taconite plants (straight grate or grate kilns), in reality, the technology would only be economical for those plants where, in addition to mercury, particulate control is a potential concern. The plant chosen for this project was the United States Steel Corporation, Minnesota Ore Operations – Keetac (Keetac) Plant. The primary goal of the project was to provide a minimum of 75% reduction in mercury emissions, where mercury reduction is defined by:

$$(\text{BH Inlet Hg Conc.} - \text{BH Outlet Hg Conc.}) \div \text{BH Inlet Hg Conc.} \times 100\% \quad [\text{Eq. 1}]$$

The EERC slipstream baghouse is a trailer-mounted baghouse that was transported to the test site and connected in slipstream fashion to allow for testing “real” flue gases under actual operating conditions. Because the slipstream baghouse was located after a wet scrubber, the flue gas at the inlet was saturated at about 132°F. To avoid wetting the bags and fan, an additional drip leg and heating elements were installed to raise the inlet flue gas temperature to about 165°F. For a full-scale unit, it would be expected that a portion of the flow (prior to the wet scrubber) would be routed to the baghouse to maintain a temperature above the water dew point.

For the Keetac test, the baghouse was operated at a nominal air-to-cloth ratio of 6 ft/min (actual ft³/min of gas per ft² of cloth). The bags that were used for this test were Ryton[®] PPS

(polyphenylene sulfide). Because the gas flow rate was about 600 scfm (720 acfm at 190°F), a total of seven bags were needed to maintain an actual air-to-cloth ratio of 5.45. A picture of the portable baghouse is shown in Figure ES-1. Ports were installed so that the mercury concentrations at both the baghouse inlet and outlet could be measured using continuous mercury monitors (CMMs) and sorbent traps.

Approach

The original test plan is shown in Table ES-1. However, several problems were encountered during this testing that altered the overall test plan as originally proposed. It was planned that most, if not all, of the testing would occur when coal was fired, but the plant had difficulty operating its coal feed unit. As a result, more testing was conducted when natural gas was fired than was planned. In a taconite plant, the mercury emitted by the fuel is only a fraction of the total mercury, so the mercury control technology could still be evaluated. The second problem that occurred was a result of the shutdown of the Minnesota state government on July 1, 2011. Therefore, the project ended somewhat earlier than intended. Finally, the mercury removal was such that the tests using the higher add rates were not necessary. The actual tests that were completed are shown in Table ES-2.



Figure ES-1. Baghouse, trailer, and control room.

Table ES-1. Project Test Plan

Test	Carbon	Carbon Feed Rate, lb/Macf	Test Duration, days
1	Standard ACI	4	2
2	Standard ACI	2	2
3	Standard ACI	1	2
4	Treated ACI	4	2
5	Treated ACI	2	2
6	Treated ACI	1	2
7	Contingency tests		3

Table ES-2. Actual Tests Conducted at Keetac

Test	Date/Time Start	Date/Time End	Fuel	Sorbent	Add Rate, g/hr	Add ¹ Rate, lb/Macf	Run Time, hrs
1	6/17/11 17:30	6/19/11 12:05	Natural gas	Baseline	0	0	42.5
2	6/19/11 12:41	6/23/11 08:57	Natural gas	Standard	21.27	1.1	92.3
3	6/23/11 08:57	6/24/11 12:36	Natural gas	Standard	39.40	2	27.6
4	6/24/11 12:36	6/24/11 16:10	Natural gas	Standard	42.50	2.2	3.6
5	6/24/11 16:10	6/26/11 08:28	Natural gas	Baseline	0	0	40.7
6	6/26/11 09:05	6/27/11 10:59	Natural gas	Bromine-treated	12.11	0.6	25.9
7	6/27/11 10:59	6/27/11 18:31	PRB ²	Bromine-treated	12.11	0.6	7.5
8	6/27/11 18:31	6/28/11 16:00	Natural gas	Bromine-treated	12.11	0.6	21.3 ³
9	6/28/11 08:26	6/28/11 08:39	PRB	Bromine-treated	12.11	0.6	0.2
10	6/28/11 16:00	6/29/11 10:07	Natural gas	Bromine-treated	21.36	1.1	18.1
11	6/29/11 14:37	6/29/11 23:33	PRB	Bromine-treated	21.36	1.1	9.1
12	6/29/11 23:33	6/30/11 06:28	Natural gas	Bromine-treated	21.36	1.1	6.5
13	6/30/11 06:28	7/1/11 07:57	PRB	Bromine-treated	21.36	1.1	25.4

¹Based on an actual gas flow rate of 720 acf.

²Powder River Basin coal

³Does not include the short time the coal was on (Test 9).

Results and Discussion

The slipstream baghouse operated very well, and particulate emissions were very low during the entire test period. There were no unplanned down periods. However, additional external heaters and insulation were needed to prevent wetting of the bags. In a full-scale installation of a baghouse to control mercury, a wet scrubber bypass of about 18%–20% of the flow would be needed to prevent condensation.

The primary goal of this project was to provide a minimum of 75% reduction in mercury emissions utilizing a slipstream baghouse with two different types of activated carbon. The first was a standard activated carbon and the second a bromine-treated activated carbon (DARCO Hg-LH). The mercury reductions achieved were determined by measuring the mercury at the inlet and the outlet of the slipstream baghouse utilizing CMMs and sorbent traps. The mercury

removals achieved are shown in Table ES-3, where it can be seen that the goal of 75% removal can be achieved consistently using 2.0 lb/Macf of standard activated carbon or 1.1 lb/Macf of treated activated carbon.

A preliminary cost estimate was also made. The results showed that the capital costs for purchasing and installing a pulse-jet baghouse and activated carbon systems at Keetac would be between \$10 million and \$12 million for the baghouse and \$1.5 million – \$2 million for an ACI system. The yearly operating cost for the baghouse would be about \$2.0 million. The operating cost for the ACI system is greatly impacted by the cost of the sorbent and selected injection rates. Based on the results above and current costs, the annual operating cost would be about \$725,000/yr using the treated carbon at an injection rate of 1.1 lb/Macf or about \$870,000/yr with standard activated carbon (2 lb/Macf).

Conclusions and Recommendations

Based on the results of the testing, the following conclusions can be made:

- 75% mercury removal can be achieved at the Keetac Plant with either standard or bromine-treated activated carbon at feed rates of 2 lb/Macf and 1.1 lb/Macf, respectively.
- Very low particulate emissions are achieved.
- Because of the relatively high cost of installing a fabric filter, the most economic installation would be for those taconite facilities that require fuel flexibility and/or have concerns about particulate emissions.
- If a baghouse is to be installed at the Keetac taconite plant, about 18%–20% of the flue gas would need to bypass the wet particulate scrubber to prevent wetting of the bags.

Table ES-3. Mercury Removal Using a Slipstream BH at Keetac

Type of Activated Carbon	Fuel	Feed Rate, lb/Macf	Inlet Hg Conc., $\mu\text{g}/\text{Nm}^3$	Outlet Hg Conc., $\mu\text{g}/\text{Nm}^3$	Mercury Removal, %	Std. Dev., %
Standard	Natural gas	1.1	6.00	1.42	76.3	6.3
Standard	Natural gas	2.0	5.99	0.93	84.5	7.7
Standard	Natural gas	2.2	5.18	0.47	91.0	1.6
Treated	Natural gas*	0.60	5.18	0.89	82.9	4.9
Treated	PRB coal	0.60	5.25	0.60	88.6	2.3
Treated	Natural gas	1.1	4.55	0.55	88.1	4.8
Treated	PRB coal	1.1	4.38	0.19	95.6	2.0

* Only the last 28 hours of the test was considered.

If this is to be a viable technology, the following recommendations are made for future testing:

- Longer-term testing is needed to determine the resultant steady-state pressure drop across the baghouse as a function of air-to-cloth ratio.
- Longer-term tests are also needed to ensure that required mercury control will be maintained over time.
- The economic evaluation presented in this report is based on a model developed for utilities and may or may not be totally valid for a taconite plant. Therefore, more specific economic data are needed.

PROJECT 4: EVALUATION OF A SLIPSTREAM BAGHOUSE FOR THE TACONITE INDUSTRY

1.0 INTRODUCTION AND BACKGROUND

Mercury is a naturally occurring element that is ubiquitous in the Earth's crust. Both anthropogenic activities such as combustion and mining processes and natural sources such as volcanoes release mercury into the atmosphere. Through transport and deposition, some mercury enters the aquatic systems, resulting in an increase in mercury loading in fish. Over the past 20 years, there has been a concerted effort by national and state agencies to reduce anthropogenic mercury emissions from all sources. For example, in December of 2011, the U.S. Environmental Protection Agency (EPA) issued an air toxic rule for the coal-fired power industry that will include mercury. This rule was based on maximum achievable control technology (MACT) requirements.

Although utilities are the largest source of anthropogenic mercury, they are not the only source. In Minnesota, one of these sources is the taconite industry. It has been estimated that these plants emit 250–350 kg of mercury a year into the atmosphere (1). Taconite processing has two potential sources of mercury: mercury released from processing the ore and mercury released from the fuels used when the ore is processed. Unlike coal-fired utilities, the major source of mercury is not the combustion fuel but the processing of the ore into taconite pellets. Even for those facilities that fire coal, it only takes 20–30 lb of coal to process 1 long ton (Lt) of green balls. The concentration of mercury in the unprocessed ore is related to the ore's geographical location in the Biwabik Iron Formation.

Because of EPA's intent to issue a small boiler MACT and continued pressure on the Minnesota Pollution Control Agency to regulate mercury emissions from taconite plants. The taconite industry formed a working group to evaluate and help fund research to reduce mercury emissions. This group, the Minnesota Taconite Mercury Control Advisory Committee, along with the Minnesota Department of Natural Resources (MNDNR) and EPA, funded five projects. One of those was an Energy & Environmental Research Center (EERC) project to evaluate the potential of using a slipstream baghouse (BH) with activated carbon injection (ACI) to reduce mercury emissions.

Although the technology would be expected to provide effective mercury control for any of the taconite plants (straight grate or grate kilns), in reality, the technology would only be economical for those plants where, in addition to mercury, particulate control is a potential concern. All Minnesota taconite plants have rod-type venturi scrubbers for particulate control. For plants with a straight grate configuration, the only fuel that can be utilized is natural gas, and therefore, these scrubbers provide enough control so that particulate emissions are not usually a concern. However, for plants using grate kilns and burn coal, there is the potential for increased particulate emissions. Because the United States Steel Corporation, Minnesota Ore Operations – Keetac (Keetac) Plant has a grate kiln and burns coal, it volunteered to host the EERC project. The Keetac Plant has the following configuration:

- Line type: grate kiln
- Number of lines: one
- Production: 700 Lt/hr
- Pellets: acid
- Fuel: natural gas and Powder River Basin (PRB) coal
- Gas flow rate: 550–650 kscfm
- Particulate control: rod-type venturi scrubber (may also add lime to control SO₂ emissions)

This report provides the results of the EERC project.

2.0 PROJECT OBJECTIVES

The primary goal of this project was to provide a minimum of 75% reduction in mercury emissions, where mercury reduction is defined by:

$$(\text{BH Inlet Hg Conc.} - \text{BH Outlet Hg Conc.}) \div \text{BH Inlet Hg Conc.} \times 100\% \quad [\text{Eq. 1}]$$

Specific objectives of the project are as follows:

- Determine the effectiveness of a slipstream baghouse to reduce mercury utilizing both a standard activated carbon (DARCO[®] Hg) and a bromine-treated activated carbon (DARCO[®] Hg-LH).
- Determine the required feed rate for the two types of carbon to meet the goal of 75% mercury removal.
- Determine the mercury speciation (elemental and oxidized mercury) at both the inlet and outlet of the baghouse.
- Determine the particulate removal across the slipstream baghouse.

3.0 EXPERIMENTAL APPROACH

As stated previously, the overall approach was to install a slipstream baghouse at the outlet of the wet scrubber at the Keetac taconite plant. Activated carbon would then be fed into the inlet piping of the slipstream baghouse. Mercury would be continuously measured at the inlet and outlet of the baghouse, thereby determining the mercury removal. Because this is a true

slipstream of the plant gas flow, the mercury removal obtained during the testing should be directly comparable to that obtained if the plant installed a full-scale baghouse.

3.1 Description of Equipment

All of the equipment used for testing at Keetac was owned by the EERC. However, help was provided by the plant and its contractors to install the slipstream baghouse at Keetac.

3.1.1 EERC Portable Slipstream Baghouse

The EERC slipstream baghouse is a trailer-mounted baghouse that was transported to the test site and connected in slipstream fashion to the existing duct at the outlet of the wet scrubber to allow for testing “real” flue gases under actual operating conditions. The slipstream baghouse chamber was designed to accommodate up to twelve 6-inch bags, with lengths of 12 feet. This equates to 226 ft² of filtration area. To connect the slipstream baghouse to the plant ducting, two separate 10-inch flanges were installed, one at the immediate exit of the wet scrubber and the other directly into the stack.

A variable-speed blower capable of drawing between 450 and 2700 acfm of flue gas (~300°F) through the baghouse was provided as part of the mobile unit. In this way, the filter face velocity could be varied between 2 and 12 ft/min. An 8-inch baghouse bypass line and an orifice meter were utilized to control and to maintain isokinetic flow at the inlet nozzle for all test conditions. In addition, pipe velocities were maintained near 75 ft/sec, preventing dropout of fly ash particles. The baghouse chamber and inlet piping runs were insulated and heat-traced.

Because the slipstream baghouse was located after a wet scrubber, the flue gas at the inlet was saturated at about 132°F. To avoid condensation and the resulting wetting of the bags and fan, an additional drip leg and heating elements were installed. This allowed the inlet flue gas temperature to be maintained at approximately 165°F. The baghouse chambers were heated to maintain a temperature of about 215°F at the baghouse outlet. For a full-scale unit, it would be expected that a portion of the flow (prior to the scrubber) would be routed to the baghouse to maintain a temperature above the water dew point.

Most of the parameters of the slipstream baghouse were controlled using an automated data acquisition system; however, the temperature of the inlet ducting and baghouse were maintained through manual inputs. The unit was designed so that the temperature of the bottom, middle, and top of the baghouse could be independently set. Cleaning of the bags was achieved by the use of medium-pressure pulse-jets that could be computer-controlled or operated manually. All baghouse operational parameters were recorded by the computer and later downloaded to a flash drive. Emptying of the baghouse hopper was achieved through a manual gate valve. Hopper ash was collected in barrels placed under the hopper. For this project, the baghouse hoppers were emptied at the end of each test. Ports were installed at both the inlet and outlet of the baghouse, so mercury measurements could be taken using continuous mercury monitors (CMMs) and carbon traps. A picture of the portable baghouse is shown in Figure 1.



Figure 1. Photograph of the EERC baghouse, trailer, and control room.

For the Keetac project, the baghouse was operated at a nominal air-to-cloth ratio of 6 ft/min (ft³/min of gas at actual temperatures and pressures per ft² of cloth). The bags that were used for this test were Ryton[®] PPS (polyphenylene sulfide). These are relatively standard bags used in pulse-jet baghouse installations because of their chemical resistance. The gas flow rate averaged 584 scfm. The actual gas flow was based on the average temperature at the inlet to the baghouse (165°F) and at the outlet (215°F), or 190°F, resulting in an actual gas flow rate of 719 acfm. This would require between six and seven bags to provide an air-to-cloth ratio of 6 ft/min. For these tests, the more conservative approach was taken, and seven bags were installed, resulting in an actual air-to-cloth ratio of 5.45 ft/min. The bag layout is shown in Figure 2. Cleaning of the bags was computer-controlled and based on a set differential pressure. The calculations for air-to-cloth ratio are shown in Appendix A.

3.1.2 Activated Carbon Injection System

Activated carbon was injected into the slipstream baghouse using a K-Tron feed system. The K-Tron is a dual-screw feeder that has been used in a number of projects to continuously inject sorbents into flue gas entering the slipstream baghouse. From the feeder, the sorbent was introduced into baghouse inlet piping via an Air-Vac eductor driven by compressed air. The feeder was filled with activated carbon as needed; however, none of the tests required the feeder to be filled more than once a day. The feed rate was set using a controller and was also bucket-calibrated.

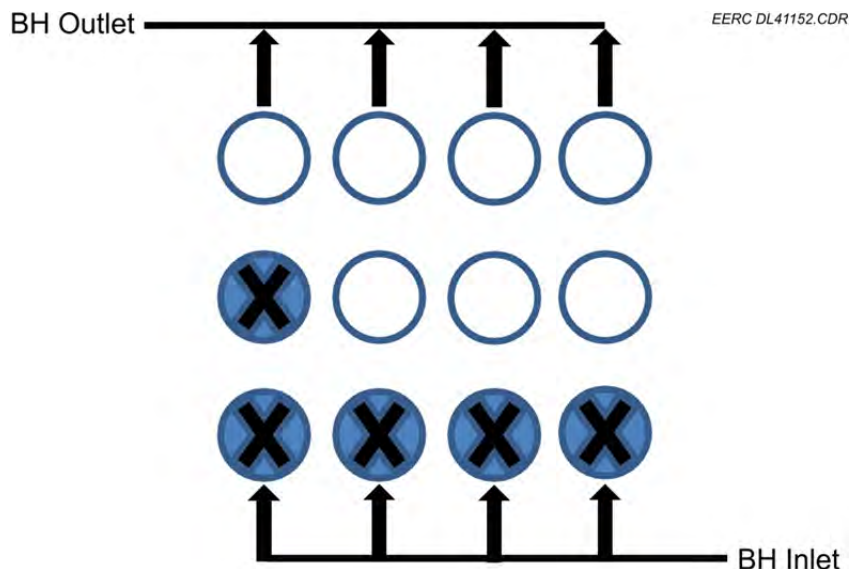


Figure 2. Bag layout of the EERC slipstream baghouse resulting in an air-to-cloth ratio of 5.45 ft/min (open circles are the bags).

3.1.3 Mercury Measurement Equipment

The CMMs used for these tests were Tekran instruments. A Tekran analyzes mercury using cold-vapor atomic fluorescence (CVAF) techniques and has gold traps that are used to capture and concentrate the mercury. The system consists of three parts. The first is the inertial separation probe (ISP), which is designed to remove particles with minimal contact with the flue gas. The second section is the pretreatment and conversion system. These instruments only measure elemental mercury, and the gold trap can be poisoned by some of the gases that are typically found in both utility and industrial processes. These include HCl, NO₂, and SO₂. Therefore, the pretreatment and conversion system must take out or greatly reduce these gases as well as convert all the mercury to elemental mercury. The Tekran uses dilution and thermal conversion to accomplish these tasks. The final section of the instrument is the CVAF mercury analyzer.

Mercury was also measured utilizing sorbent traps by pulling flue gas through the trap using a pump and then measuring the gas flow with a dry gas meter. The sorbent traps were then analyzed for mercury using an OhioLumex analyzer, which is a cold-vapor atomic adsorption analyzer that uses a thermal attachment to release the mercury captured on the sorbent trap. The mercury is then carried by a gas stream into the analyzer. All of the equipment for conducting sorbent trap mercury measurements was used in compliance with the protocols outlined in EPA Method 30B.

3.2 Project Test Plan

Once the slipstream baghouse and CMMs were installed and the temperatures set so that wetting of the bags/fan did not occur, actual testing began (June 17, 2011). The original test plan

is shown in Table 1. However, several problems were encountered that altered the overall test plan as originally proposed. It was planned that most, if not all, of the testing would occur when coal was fired, but the plant had difficulty operating its coal feed unit. As a result, more testing was conducted when natural gas was fired than was planned. In a taconite plant, the mercury emitted by the fuel is only a fraction of the total mercury, so the mercury control technology could still be evaluated. The second problem that occurred was a shutdown of the Minnesota state government on July 1, 2011. As a result, the project ended earlier than intended. Finally, the mercury removal was such that the tests using the higher rates of sorbents, 4 lb/Macf for the standard activated carbon and 2 and 4 lb/Macf for the bromine-treated activated carbon, were not necessary. As will be discussed later, much higher mercury removals than 75% were achieved at these lower ACI rates. The actual tests that were completed are shown in Table 2. Test 4 was intended to be overnight to reestablish the baseline conditions prior to beginning the tests using the treated activated carbon. However, as will be discussed in Section 4, this took substantially longer than was planned.

4.0 RESULTS AND DISCUSSION

4.1 Operation of the Slipstream Baghouse

The slipstream baghouse operated very well during the entire test period. There were no unplanned down periods. As discussed earlier, a major concern was the potential for wetting of the bags as a result of the saturated gas exiting the wet scrubber. However, by adding additional external heaters and extra insulation to prevent cold spots, the inlet temperature of the flue gas was increased such that no wetting took place. Figure 3 shows the baghouse inlet and outlet temperatures were relatively constant over the entire project.

In a full-scale installation of a baghouse to control mercury emissions, external heaters would not be possible. Therefore, a wet scrubber bypass would be required to provide additional heat to prevent water condensation on the bags. If the following assumptions are made:

- Total flue gas flow rate is 600,000 scfm.
- The temperature of the gas entering the wet scrubber is 300°F.

Table 1. Project Test Plan

Test	Carbon	Carbon Feed Rate, lb/Macf	Test Duration, days
1	Standard ACI	4	2
2	Standard ACI	2	2
3	Standard ACI	1	2
4	Treated ACI	4	2
5	Treated ACI	2	2
6	Treated ACI	1	2
7	Contingency tests		3

Table 2. Actual Tests Conducted at Keetac

Test	Date/Time Start	Date/Time End	Fuel	Sorbent	Add Rate, g/hr	Add ¹ Rate, lb/Macf	Run Time, hr
1	6/17/11 17:30	6/19/11 12:05	Natural gas	Baseline	0	0	42.5
2	6/19/11 12:41	6/23/11 08:57	Natural gas	Standard	21.27	1.1	92.3
3	6/23/11 08:57	6/24/11 12:36	Natural gas	Standard	39.40	2	27.6
4	6/24/11 12:36	6/24/11 16:10	Natural gas	Standard	42.50	2.2	3.6
5	6/24/11 16:10	6/26/11 08:28	Natural gas	Baseline	0	0	40.7
6	6/26/11 09:05	6/27/11 10:59	Natural gas	Bromine-treated	12.11	0.6	25.9
7	6/27/11 10:59	6/27/11 18:31	PRB ²	Bromine-treated	12.11	0.6	7.5
8	6/27/11 18:31	6/28/11 16:00	Natural gas	Bromine-treated	12.11	0.6	21.3 ³
9	6/28/11 08:26	6/28/11 08:39	PRB	Bromine-treated	12.11	0.6	0.2
10	6/28/11 16:00	6/29/11 10:07	Natural gas	Bromine-treated	21.36	1.1	18.1
11	6/29/11 14:37	6/29/11 23:33	PRB	Bromine-treated	21.36	1.1	9.1
12	6/29/11 23:33	6/30/11 06:28	Natural gas	Bromine-treated	21.36	1.1	6.5
13	6/30/11 06:28	7/1/11 07:57	PRB	Bromine-treated	21.36	1.1	25.4

¹Based on an actual gas flow rate of 720 acf.

²Powder River Basin coal.

³Does not include the short time the coal was on (Test 9).

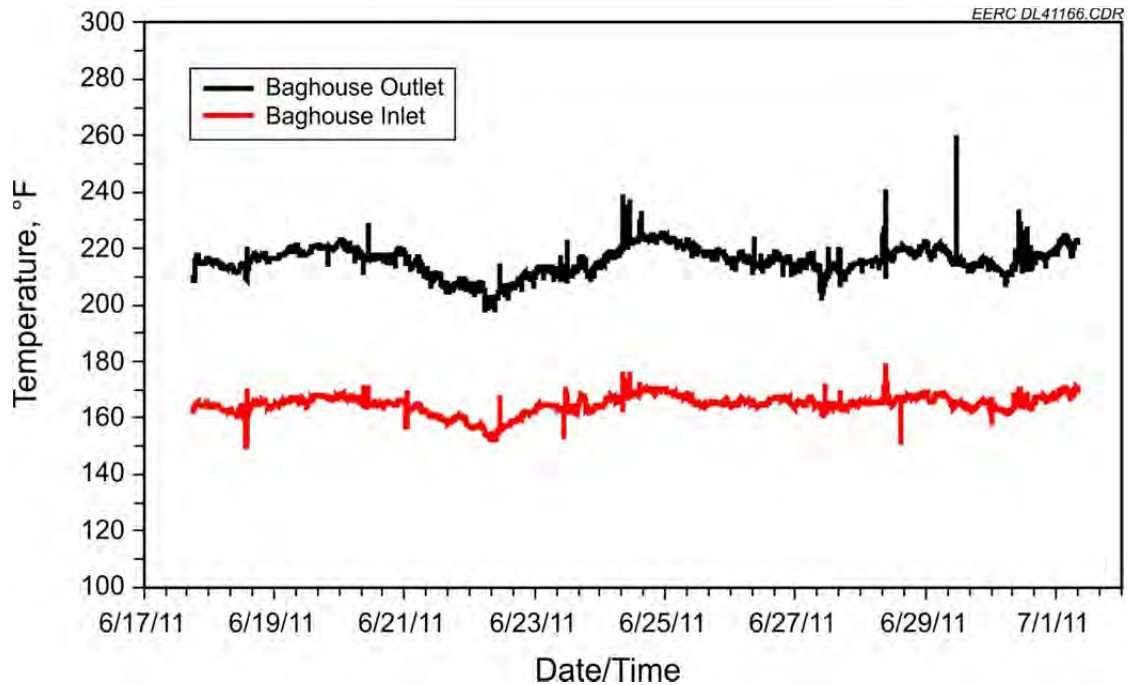


Figure 3. Slipstream baghouse operating temperatures.

- The temperature of the gas exiting the wet scrubber is saturated at 135°F.
- All water droplets are small, with little impact on the thermodynamics.
- The temperature of the gas entering the baghouse must be $\geq 155^{\circ}\text{F}$ to ensure no wetting of the bags.

The amount of reheat that would be needed would require that 18.2% of the flow bypass the wet scrubber (calculations are shown in Appendix A). If relatively large water droplets exist, the percentage of bypass needed may be greater. Therefore, to minimize the amount of flue gas bypass, it will be important to minimize and reduce the size of any water droplets exiting the wet scrubber. This may necessitate using enhanced mist eliminators and/or adding a drip leg at the outlet of the scrubber.

Another important operational variable for any baghouse is the pressure drop across the bags. This impacts the needed fan capacity, the footprint (air-to-cloth ratio) of the baghouse, the particulate collection efficiency, bag life, and overall economics. This project was not designed to determine the final pressure drop that would be experienced under “normal” operation, as the tests were too short to reach any steady-state condition. Often this can take several months before a reasonable steady state is reached. These tests were designed simply to facilitate the mercury measurement, and therefore, the pulsing of the bags was done on a regular basis and at a reasonably low pressure drop set point. Between each test, the baghouse was pulsed off-line to facilitate cleaning. Figure 4 shows the baghouse pressure drop and gas flow rate over the length of the project. When Keetac was firing natural gas, the bags were pulsed when the pressure drop reached 3 in. W.C. However, a higher set point was used, first 4 and then 6 in. W.C. when a PRB coal was the fuel. It is clear that longer-term testing is needed to determine the ultimate pressure drop that will be experienced. This will obviously determine what air-to-cloth ratio is needed to maintain a reasonable pressure drop.

4.2 Particulate Control

Because the baghouse was installed following a particulate scrubber, it was expected that the inlet dust loading was going to be very low, and this was the case. Also, as expected, the baghouse inlet dust loading was higher when coal was fired. In either case, the dust loading at the outlet of the baghouse was exceedingly low and, therefore, would allow for flexibility in the use of fuel as well as flexibility in overall plant operations without greatly impacting particulate emissions. The results of EPA Method 5 particulate sampling is shown in Table 3. The calculations are shown in Appendix A, and the dust-loading data sheets are provided in Appendix B. As Table 3 shows, the actual particulate removal was somewhat higher when coal was fired. This may be the result of a dust cake forming on the bags. Because the baghouse inlet dust loadings are so low, especially for tests firing natural gas, the particulate removal efficiency is somewhat misleading. Very small changes in the outlet particulate concentration have a major effect on the particulate removal efficiency.

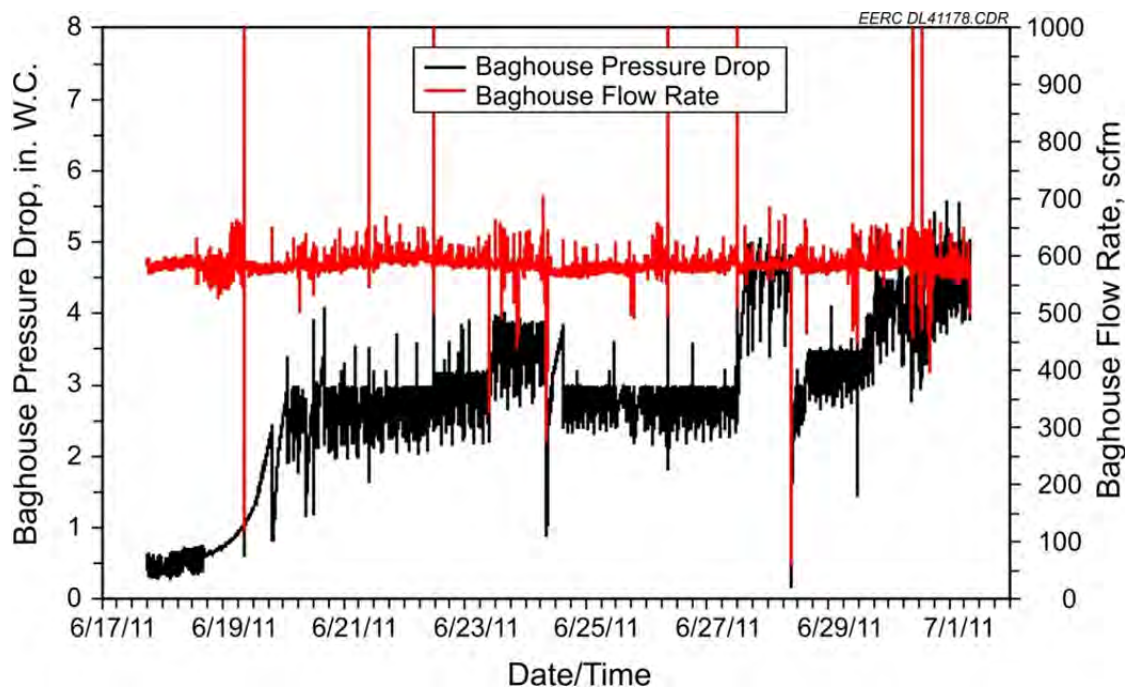


Figure 4. Slipstream baghouse pressure drop and gas flow rate.

Table 3. Particulate Sampling Across the Slipstream BH at Keetac

Date	Fuel	Time	Sample Pt.	Sample		H ₂ O, %	Isokinetic, %	Dust Loading, grains/scf	Removal, %
				Time, min					
06/16/11	Natural gas	14:10	BH in	40		15.6	105.6	0.0026	–
06/18/11	Natural gas	14:51	BH in	120		16.3	104.1	0.0027	
06/18/11	Natural gas	14:47	BH out	120		16.2	104.2	0.0006	80.8
06/20/11	Natural gas	13:50	BH in	120		16.1	99.3	0.0022	
06/20/11	Natural gas	13:41	BH out	120		16.0	100.5	0.0009	59.1
06/30/11	PRB coal	09:43	BH in	180		16.0	98.3	0.0040	
06/30/11	PRB coal	09:35	BH out	180		16.1	103.3	0.0004	90.0
06/30/11	PRB coal	16:17	BH in	180		17.2	101.1	0.0045	
06/30/11	PRB coal	16:08	BH out	180		17.2	103.9	0.0003	93.3

4.3 Mercury Control

The primary goal of this project was to provide a minimum of 75% reduction in mercury emissions utilizing a slipstream baghouse with both a standard and bromine-treated activated carbon. The mercury reductions achieved (see Equation 1 in Section 2.0) were evaluated by measuring the mercury at the inlet and the outlet of the slipstream baghouse utilizing CMMs and sorbent traps. The CMMs also provided the mercury speciation at each location. An example of the mercury calculations is provided in Appendix A.

4.3.1 Baseline Results

The baseline results are shown in Figure 5, which shows there was no mercury removal across the baghouse without activated carbon addition. In fact, the outlet mercury concentration was somewhat higher than at the inlet. Although new bags were used for this project, most likely there was some carbon attached to the walls of the baghouse from previous tests which resulted in a small amount of offgassing of mercury. Initially the inlet and outlet mercury concentrations were about the same, but then for a period of time, the outlet concentration was greater than the inlet. Near the end of the baseline test, the two concentrations again appeared to be about the same. This again supports the occurrence of mercury offgassing. The phenomenon of mercury offgassing was more prominent, as shown in Figure 6, when later in the project the carbon feed system was turned off prior to changing the type of carbon. The goal was to return to the baseline condition. Offgassing of mercury occurs when activated carbon becomes mercury-saturated and then other components in the flue gas, such as HCl, SO₂ and NO₂, replace the already-collected mercury (2). The sorbent trap samples that were taken during the initial baseline test support the CMM data indicating a higher mercury concentration at the outlet than at the inlet.

As would be expected following a wet scrubber, the mercury at the baghouse inlet was >80% elemental mercury. Under baseline conditions, at the outlet of the baghouse, the mercury speciation did not change.

The CMM mercury measurement results using the standard activated carbon are shown in Figure 7. Two ACI rates, 1.1 and 2.0 lb/Macf, were tested. Unfortunately, because the coal feeder was not operating properly at the plant and because of the state shutdown, we were unable

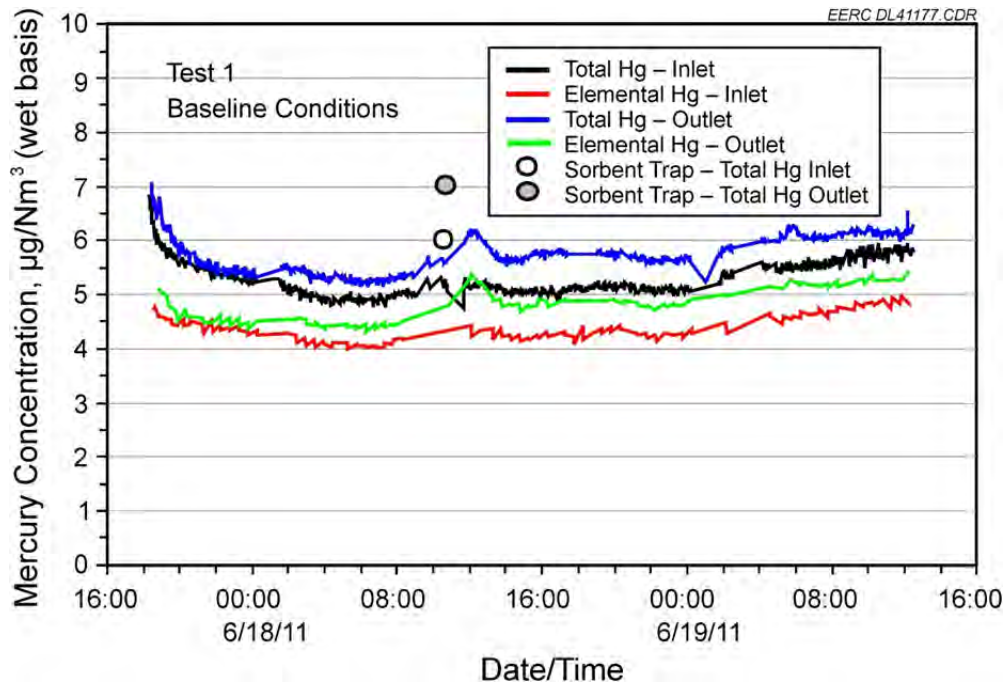


Figure 5. Initial baseline mercury results.

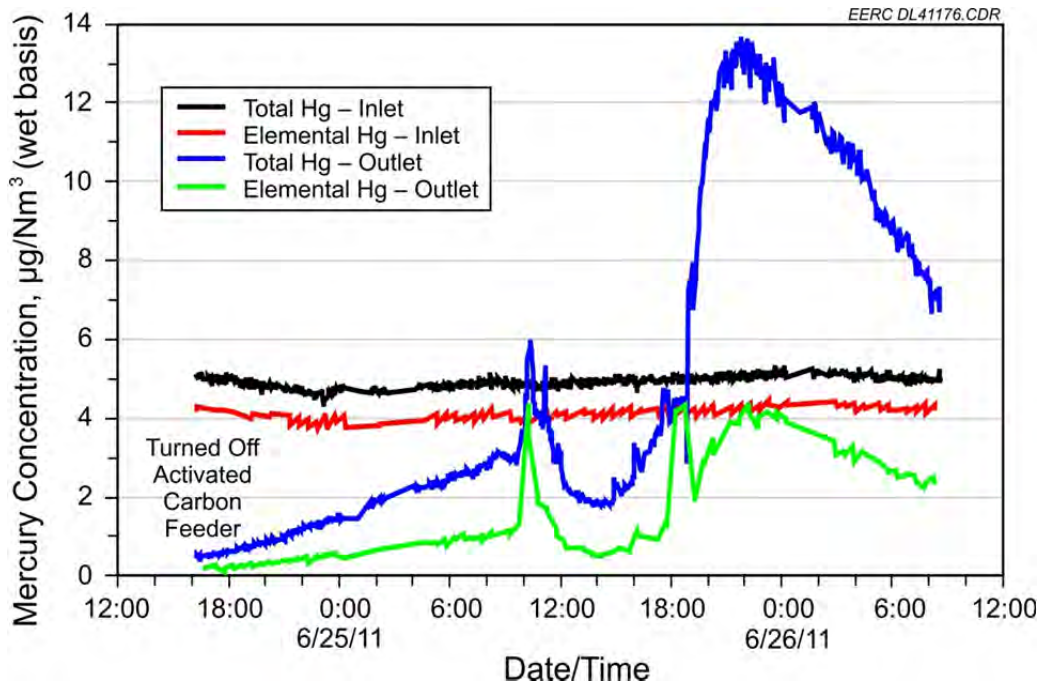


Figure 6. Results showing mercury reemission after shutting off the ACI.

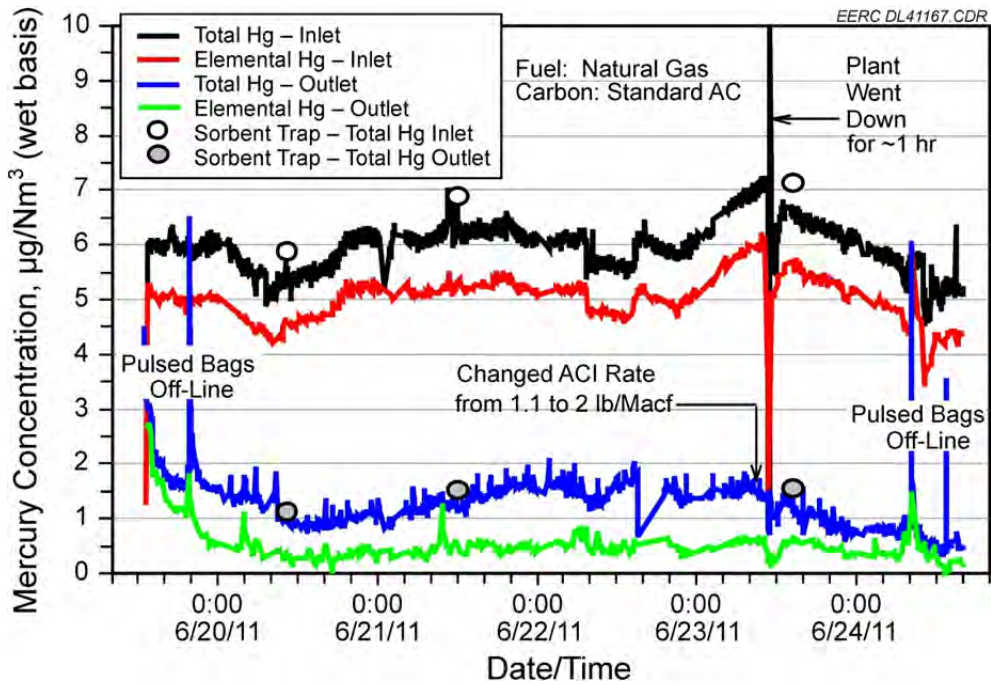


Figure 7. Mercury results utilizing standard activated carbon.

to test the standard activated carbon when coal was fired. Therefore, all of the tests were done firing natural gas.

4.3.2 Mercury Removal Using Standard Activated Carbon (DARCO Hg)

The CMM mercury measurement results using the standard activated carbon are shown in Figure 7. Two ACI rates, 1.1 and 2.0 lb/Macf, were tested. Unfortunately, because the coal feeder was not operating properly at the plant and because of the state shutdown, we were unable to test the standard activated carbon when coal was fired. Therefore, all of the tests were done with natural gas.

At an ACI rate of 1.1 lb/Macf, the mercury removal averaged 76.1% with a standard deviation of 6.3%. Therefore, the results were somewhat borderline as to whether the goal of 75% mercury removal was met. At an ACI rate of 2.0 lb/Macf, the mercury removal averaged 84.5% with a standard deviation of 8.5%. At this feed rate when natural gas was fired, the mercury removal goal was met. When the ACI rate was increased to 2.2 lb/Macf, mercury removal averaged 91.0%. A summary of the results is shown in Table 4.

Based on the mercury speciation measured by the CMM at the outlet of the baghouse, it appears that the activated carbon not only captured mercury but converted a percentage of the mercury not captured to oxidized mercury. At the outlet of the baghouse, the mercury being emitted was only about 35% elemental mercury. It is interesting to note that when the ACI rate was increased from 1.1 to 2.0 lb/Macf, the concentration of elemental mercury remained approximately the same. Therefore, the decrease in total mercury emissions is due to additional removal of the oxidized mercury.

4.3.3 Mercury Removal Using Bromine-Treated Activated Carbon (DARCO LH-Hg)

The CMM mercury measurement results using the bromine-treated activated carbon are shown in Figures 8 and 9. Figures 8 and 9 show the results when the ACI rate was 0.6 lb/Macf and 1.1 lb/Macf, respectively. During the time these tests were being conducted, both natural gas and PRB coal were fired. The results for these tests are summarized in Table 5.

As shown in Figure 8, once the bromine-treated ACI was started and natural gas was fired, there was a slow decrease in the mercury removal. This slow decrease may be related to the previous test when no activated carbon was injected and there was substantial offgassing of mercury (Figure 6). Because of this slow decrease in mercury, the mercury removal averaged only 74.2% with a very high standard deviation of 16.8%. It took almost 12 hours before the

Table 4. Mercury Removal Using a Slipstream BH and Standard Activated Carbon

Fuel	Feed Rate, lb/Macf	Inlet Hg Conc., $\mu\text{g}/\text{Nm}^3$	Outlet Hg Conc., $\mu\text{g}/\text{Nm}^3$	Mercury Removal, %	Std. Dev., %
Natural Gas	1.1	6.00	1.42	76.3	6.3
Natural Gas	2	5.99	0.93	84.5	7.7
Natural Gas	2.2	5.18	0.47	91.0	1.6

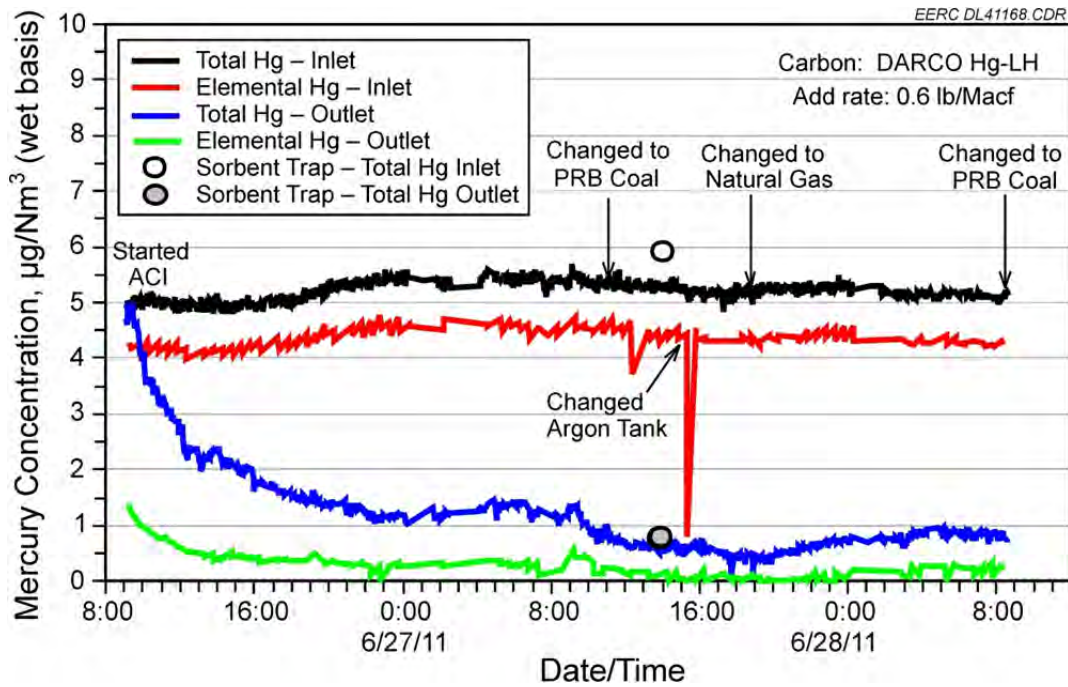


Figure 8. Mercury results utilizing bromine-treated activated carbon at a feed rate of 0.6 lb/Macf.

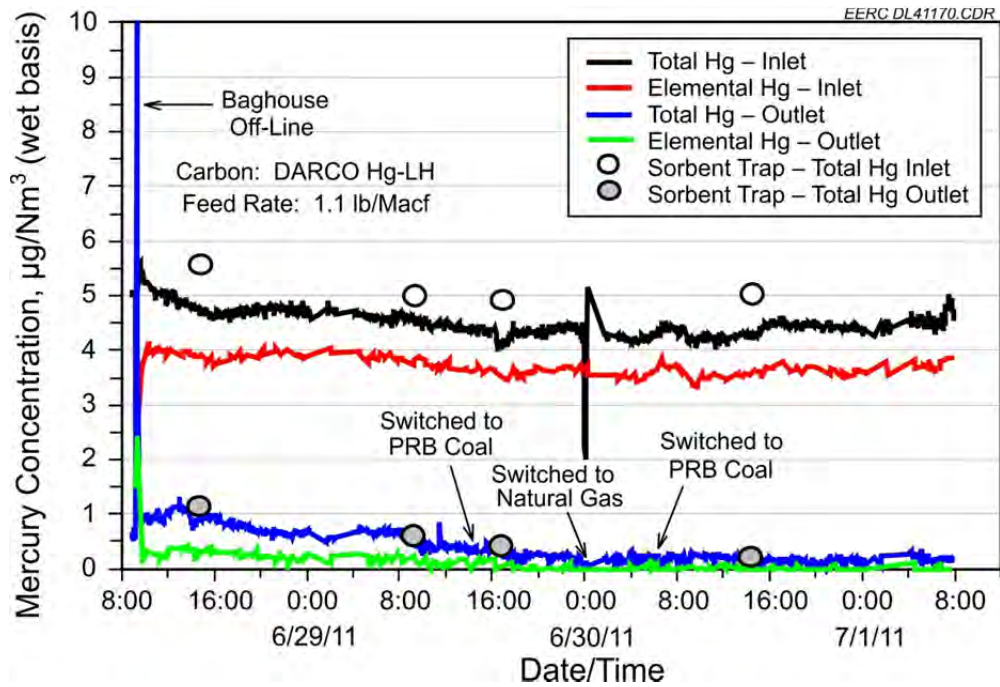


Figure 9. Mercury results utilizing bromine-treated activated carbon at a feed rate of 1.1 lb/Macf.

Table 5. Mercury Removal Using a Slipstream Baghouse and Bromine-Treated Activated Carbon

Fuel	Feed Rate, lb/Macf	Inlet Hg Conc., $\mu\text{g}/\text{Nm}^3$	Outlet Hg Conc., $\mu\text{g}/\text{Nm}^3$	Mercury Removal, %	Std. Dev., %
Natural Gas*	0.60	5.25	0.89	82.9	4.9
PRB Coal	0.60	5.25	0.60	88.6	2.3
Natural Gas	1.1	4.55	0.55	88.1	4.8
PRB Coal	1.1	4.38	0.19	95.6	2.0

* Only the last 28 hours of the test was considered.

mercury removal was >75%. For the remaining 28 hours of testing, the mercury removal was 82.9% with a standard deviation of only 4.9%. During this period, the goal of 75% mercury removal was met at a bromine-treated ACI rate of only 0.6 lb/Macf.

The mercury removal was higher when the PRB coal was fired compared to natural gas. Even at 0.6 lb/Macf of bromine-treated carbon, the mercury removal averaged 88.6% with a standard deviation of only 2.3%. Figure 9 shows the mercury results when the bromine-treated ACI rate was increased to 1.1 lb/Macf. With coal, a very high mercury removal of >95% was achieved. For the entire testing with bromine-treated activated carbon, the concentration of elemental mercury at the baghouse was very low at <0.5 $\mu\text{g}/\text{Nm}^3$.

4.3.4 Comparison of the Mercury Removal Between the CMMs and Sorbent Traps

The results of the sorbent trap sampling, along with the CMM results, were provided in Figures 5–9. Table 6 shows a comparison of the mercury removal measured by the two different mercury measurement methods. As shown, there was very good agreement between the two, but the measured removal was somewhat greater when using the CMMs. This may be a result of how each of the methods measures mercury, as will be discussed in Section 6.0.

Table 6. Comparison of Sorbent Trap and CMM Results

Fuel	Type Activated Carbon	Injection Rate, lb/Macf	Sorbent Trap Averages			CMM Averages		
			BH Inlet Hg Conc., $\mu\text{g}/\text{Nm}^3$	BH Outlet Hg Conc., $\mu\text{g}/\text{Nm}^3$	Hg Removal, %	BH Inlet Hg Conc., $\mu\text{g}/\text{Nm}^3$	BH Outlet Hg Conc., $\mu\text{g}/\text{Nm}^3$	Hg Removal, %
Natural Gas	None	Baseline	6.042	7.038	-16.5	5.18	5.669	-10.5
Natural Gas	Standard	1.1	5.900	1.140	80.7	5.34	0.908	83.0
Natural Gas	Standard	1.1	6.896	1.536	77.7	6.31	1.185	81.2
Natural Gas	Standard	2.0	7.151	1.577	77.9	6.55	1.179	82.0
PRB Coal	Treated	0.6	5.936	0.808	86.4	5.30	0.629	88.3
Natural Gas	Treated	0.6	5.590	1.163	79.2	4.70	0.929	80.2
Natural Gas	Treated	1.1	5.020	0.621	87.6	4.52	0.451	90.0
PRB Coal	Treated	1.1	4.930	0.441	91.1	4.21	0.290	93.1
PRB Coal	Treated	1.1	5.051	0.232	95.4	4.30	0.093	97.8

4.4 Preliminary Economic Evaluation

A very preliminary economic evaluation was done. The evaluation included the capital cost of purchasing and installing both a pulse-jet baghouse operating at an air-to-cloth ratio of 6 ft/min and an ACI system. All costs are based on 2011 dollars. Please note, the costs presented in this report were determined based on a model developed for the utility industry, and therefore, the economic information provided should be used for discussion purposes only. Site-specific cost information would need to be developed if a full-scale baghouse were to be installed.

4.4.1 Installation and Operating Costs for a Pulse-Jet Baghouse

The capital costs for purchasing and installing a baghouse at Keetac are shown in Table 7. The total capital cost would be between \$10,000,000 and \$12,000,000. The first-year operating cost for the baghouse is shown in Table 8. The estimated operating cost for the first year is \$2,044,920.

Table 7. Capital Cost for a Pulse-Jet Baghouse at Keetac

Capital Cost Items	Cost
Purchased Equipment	
Basic Fabric Filter	\$3,750,500
Insulation	\$244,930
Cages	\$105,670
Initial Bags (including spares)	\$466,000
Auxiliary Equipment (fan, ductwork, motor, starter, dampers, compressor, screw conveyor)	\$1,170,400
Instrument and Controls, %	\$345,000
Taxes, %	\$103,500
Freight, %	\$172,500
Total Purchased Equipment (TPE)	\$6,358,500
Installation Direct Costs (calculated as a % of TPE)	
Foundations and Supports	\$162,840
Erection and Handling	\$2,035,500
Electrical, %	\$325,680
Piping, %	\$84,900
Insulation for Ductwork	\$81,420
Painting	\$40,710
Total Installation Direct Costs	\$2,731,050
Total Direct Costs for Purchased Equipment and Installation	\$9,089,550
Indirect Costs (calculated as a % of TPE)	
Engineering and Supervision	\$844,750
Contingencies (project and process)	\$544,164
General Facilities	\$422,370
Total Indirect Costs	\$1,811,290
Total Capital Requirements	\$10,900,840

Table 8. Baghouse Annual Operating and Maintenance Costs for Keetac

Operating Item	Cost
Direct Annual Costs	
Operating and Supervision Labor	\$125,200
Replace Bags (labor and materials)	\$97,210
Utilities (fan and cleaning bags)	\$498,020
Total Annual Direct Cost	\$720,430
Indirect Annual Costs	
Taxes, Insurance and Administration	\$382,530
Capital Recovery	\$908,960
Total Annual Indirect Cost	\$1,291,490
Total Annual Cost	\$2,011,920

4.4.2 Installation and Operating Costs for an ACI System

A price quote was obtained from Norit Americas Inc. to provide a complete powdered activated carbon (PAC) injection system. The total capital cost (FOB) is \$1,220,410. Included in this price are the following items:

- PAC storage silo and all associated equipment
- Volumetric feeder, hopper, and associated equipment for two delivery lines
- Eductors and blowers
- All structural steel and piping
- Control panel and associated software and hardware
- Injection distribution system (injection lances) and flow/distribution modeling field support services. Norit would provide the services of a technician to support installation and start-up of the equipment.

In addition to capital equipment provided by a vendor, certain site preparation and infrastructure would be required by plant personnel. Based on information provided by Norit, an estimate of \$125,000 would be required to provide the following:

- Concrete foundations for the silo, feeders, and blowers
- Unloading and assembly of vendor-supplied equipment with support from the Norit Americas on-site technician
- Piping to provide dry compressed air (100 psi) to the feeder and silo

- Drainage and containment as required by the site to collect and dispose of wash-down and any other wastes generated by the PAC system
- Electrical service including single-phase 120-volt and three-phase 480-volt power
- Communication wiring to the plant process and data control system
- General lighting
- Applicable permits

The total capital cost for the PAC system, including both the vendor-supplied process equipment and site preparation work is \$1,345,410. The primary operating cost for the ACI system is the cost of the sorbent and the sorbent feed rate. Based on the results for this test, to ensure meeting the mercury reduction goal of 75%, the feed rate for standard activated carbon would be 2 lb/Macf and 1.1 lb/Macf if bromine-treated activated carbon were assumed. Table 9 presents the estimated sorbent costs at Keetac. These results also assume that the total gas flow rate for the plant is 600,000 scfm, the baghouse temperature at the ACI location is 155°F, and the plant has an operating factor of 0.90 (7884 hr/yr). Including maintenance costs and utilities for the ACI system, the total yearly operating cost would be \$861,700 if standard activated carbon is used and \$723,750 if the bromine-treated carbon is used. Again, operating cost of the ACI system are going to be very sensitive to sorbent costs.

5.0 QUALITY ASSURANCE/QUALITY CONTROL (QA/QC)

Prior to beginning the project, a quality assurance plan was submitted and approved by MNDNR and EPA. This document was used as a guideline for the project. All project data from the baghouse operation, CMMs, and other sampling was either downloaded from the computers to a flash drive or recorded onto data sheets. The data sheets were properly labeled, and chain-of-custody procedures were followed for all samples and data sheets.

5.1 K-Tron Activated Carbon Feeder

Prior to beginning the project, the EERC K-Tron feeder was calibrated. The results are shown in Figure 10. As can be seen, the calibration curve is highly linear and correlates directly with the rpm set point. In addition to the development of the initial calibration curve, several

Table 9. Estimated Sorbent Costs at Keetac with a Pulse-Jet Baghouse

Item	Standard Activated Carbon	Treated Activated Carbon
ACI Rate	2.0 lb/Macf	1.1 lb/Macf
Yearly Consumption	788,400 lb	394,200 lb
Cost per lb Delivered	\$0.85	\$1.35
Yearly Sorbent Costs	\$670,140	\$532,170

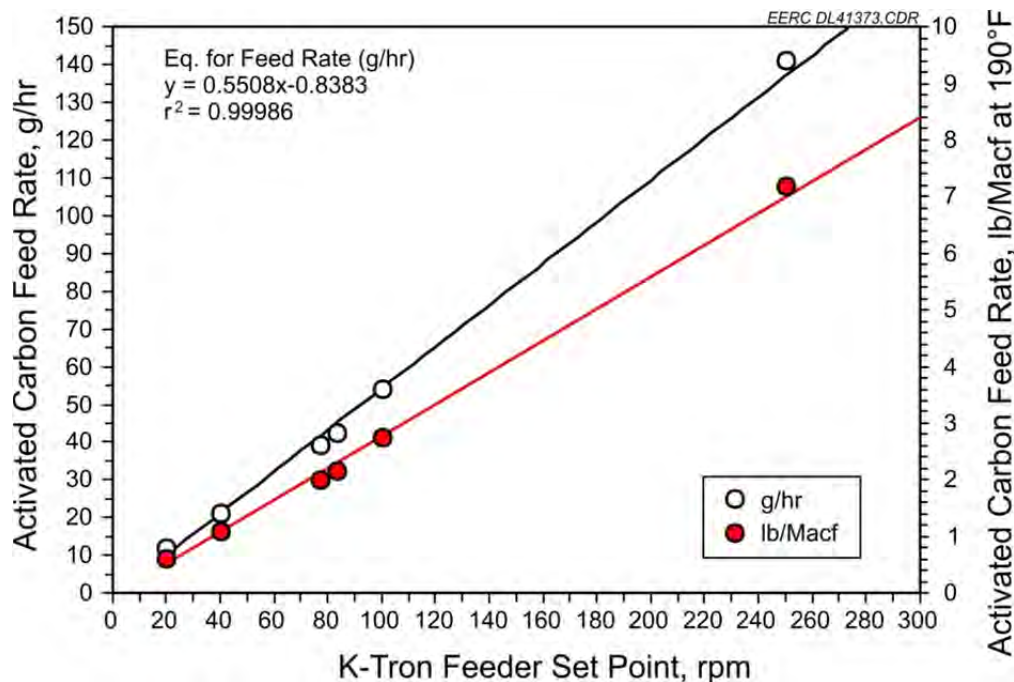


Figure 10. Calibration of the K-Tron activated carbon feed system.

times during the project, the feeder was bucket-calibrated to ensure the feed rate had remained constant, which it had.

5.2 Particulate Samples (EPA Method 5)

All particulate sampling followed the procedures outlined in EPA Method 5. The only exception was that the piping was not traversed as it was a slipstream and the piping was only 10 in. in diameter so stratification was not a concern. All sampling boxes were calibrated prior to arriving on-site, and a meter constant (C_m) was calculated. The primary sampling QC criteria are that the sampling be conducted in an isokinetic manner so particles captured on the filter are representative of those in the gas stream. The requirement is that all samples be isokinetic within 10%. As can be seen in Table 10, all samples met this criteria.

The filters were preweighed to a constant temperature and stored in labeled petri dishes. Once the dust loading was completed as prescribed in EPA Method 5, the filters were carefully removed from the filter holders, and any remaining dust was brushed onto the filters. The filters and any dust brushed from the filter holder were once again placed in labeled petri dishes and desiccated prior to weighing. The filters were weighed on-site using a calibrated five-place balance.

Table 10. Particulate Sampling Isokinetic Determination

Sample No.	Date	Fuel	Isokinetic, %
1	06/16/11	Natural gas	105.6
2	06/18/11	Natural gas	104.1
3	06/18/11	Natural gas	104.2
4	06/20/11	Natural gas	99.3
5	06/20/11	Natural gas	100.5
6	06/30/11	PRB coal	98.3
7	06/30/11	PRB coal	103.3
8	06/30/11	PRB coal	101.1
9	06/30/11	PRB coal	103.9

5.3 Mercury Measurements

Two different mercury measurements were made during the project. The primary measurements were provided by CMMs installed at the inlet and outlet of the baghouse. The second method used sorbent traps. These were taken for QA/QC purposes and to compare to the CMM results.

5.3.1 Calibration of the CMMs

The requirements for calibration, spanning, and zeroing of the CMMs are listed in Table 11. The leak check was <1% following installation of the two CMMs. The multipoint linearity checks are shown in Table 12. With the exception of the second check for the CMM located at the baghouse outlet, which was a bit high, they all were within 10% of the expected value. The daily zero and span results are shown in Tables 13 and 14.

In all cases, the span was within the required 90%–100% range, and the zero values were at or near zero. The internal calibration results are shown in Tables 15 and 16. The instrument was calibrated both at the probe tip and directly into the analyzer. Again, as was the case with the span data, all recoveries were within the 10% range.

5.3.2 QA/QC Requirements for the Sorbent Traps

An additional QA/QC for the CMMs was to compare the results to those obtained using sorbent traps. Sorbent traps are considered to be a reference method (EPA Method 30B). At least one paired sorbent trap sample was taken at the baghouse inlet and outlet for each test. The results were then compared to the CMM data taken over the same time period.

Table 11. CMM Calibration Requirements

Test	Criteria	How Often
Leak Check	>2% of total sample flow	Immediately after installation
Internal Zero and Span	Automatically adjusted by the instrument	Daily
Local and Probe Tip Calibration	90%–110% of anticipated value	Every other day or more as needed
Multipoint Span	Automatically adjusted by the instrument	Once a week

Table 12. Multipoint Linearity Checks

Baghouse Inlet CMM		Calibration Gas Recovery, %		
Date/Time	Side	Low 6.00 $\mu\text{g}/\text{Nm}^3$	Mid 8.00 $\mu\text{g}/\text{Nm}^3$	High 10.0 $\mu\text{g}/\text{Nm}^3$
6/17/11 3:27	A	102.88	104.45	103.71
	B	104.63	106.75	105.79
6/17/11 17:20	A	129.15	116.53	112.74
	B	120.31	114.71	109.93
6/23/11 13:42	A	95.85	97.68	98.49
	B	98.04	100.94	102.36
Baghouse Outlet CMM		Calibration Gas Recovery, %		
Date/Time	Side	Low 1.32 $\mu\text{g}/\text{Nm}^3$	Mid 3.32 $\mu\text{g}/\text{Nm}^3$	High 6.60 $\mu\text{g}/\text{Nm}^3$
6/17/11 3:27	A	106.53	100.76	100.44
	B	106.05	102.19	100.15
6/17/11 17:20	A	101.85	100.94	98.94
	B	96.95	102.65	101.43
6/23/11 13:42	A	94.64	94.54	95.66
	B	99.18	100.10	99.09

To measure the mercury adsorbed by the sorbent traps, an OhioLumex instrument was used. This instrument uses cold-vapor atomic absorption to measure the mercury that is desorbed from the traps using thermal techniques. This instrument is currently considered to be the standard for these types of measurements. Before beginning analysis of the samples, a five-point linear calibration curve is generated. This curve must have an R^2 of >99% before it is acceptable. Because the samples were taken back to the EERC for analysis, the samples were analyzed over two separate time periods. Therefore, two calibration curves were generated. Once a calibration curve has been generated, separate National Institute of Standards and Technology (NIST) traceable QC samples are used to check the calibration curve. The requirement is that the recovery of the QC standards be $\pm 10\%$, or a new curve must be generated.

The two calibration curves for this project are shown in Table 17. As shown, both calibration curves were acceptable.

In addition to the development of the calibration curve, for every ten samples and at least once a day, check standards must be analyzed. These also have to have recoveries within 10% of the known value or a new calibration curve must be developed. Table 18 presents the check standards that were completed for this project. All QA/QC check standards were within the acceptable range.

5.3.3 Comparison of CMMs to Sorbent Trap Mercury Measurements

For each test, at least one paired set of sorbent trap samples was taken at the baghouse inlet and outlet. These results were then compared to the results obtained using the CMMs. The

Table 13. Baghouse Inlet CMM Zero and Span Data

Date/Time	Side	Probe Zero, μg/Nm ³	Probe Tip, μg/Nm ³	Date/Time	Side	Probe Zero, μg/Nm ³	Probe Tip, μg/Nm ³
6/17/11 3:27	A	0.000		6/23/11 1:12	A	0.000	
	B	0.065			B	0.000	
6/17/11 7:27	A	0.000		6/23/11 1:32	A		100.17
	B	0.000			B		98.42
6/17/11 18:07	A		98.06	6/24/11 1:12	A	0.000	
	B		98.11		B	0.075	
6/18/11 1:10	A	0.571		6/24/11 1:32	A		99.87
	B	0.563			B		99.19
6/18/11 1:17	A		102.39	6/25/11 1:15	B	0.177	
	B		100.81		A	0.000	
6/18/11 9:10	A	0.234		6/25/11 1:35	B		97.96
	B	0.097			A		102.30
6/18/11 9:30	A		97.40	6/26/11 1:12	A	0.000	
	B		98.63		B	0.000	
6/18/11 9:55	A	0.000		6/26/11 1:32	A		100.63
	B	0.000			B		99.88
6/18/11 10:15	A		98.87	6/27/11 1:15	B	0.000	
	B		99.67		A	0.000	
6/19/11 1:12	A	0.000		6/27/11 1:35	B		96.93
	B	0.082			A		101.70
6/19/11 1:32	A		96.34	6/28/11 1:15	B	0.000	
	B		100.14		A	0.000	
6/19/11 3:57	A		101.94	6/28/11 1:35	B		99.83
	B		99.11		A		103.86
6/20/11 1:32	A		101.94	6/29/11 1:12	A	0.132	
	B		99.11		B	0.000	
6/21/11 1:12	B	0.061		6/29/11 1:32	A		98.02
	A	0.052			B		99.73
6/21/11 1:32	A		99.17	6/30/11 1:12	A	0.000	
	B		98.36		B	0.000	
6/22/11 1:12	A	0.000		6/30/11 1:32	A		98.72
	B	0.000			B		100.73
6/22/11 1:32	A		102.60	7/1/11 1:12	A	0.000	
	B		102.48		B	0.000	
				7/1/11 1:32	A		97.56
					B		99.66

comparison was shown previously in Section 4.3, Figures 5–9. This section discusses the QA/QC associated with those comparisons.

Table 14. Baghouse Outlet CMM Zero and Span Data

Date/Time	Side	Probe Zero, $\mu\text{g}/\text{Nm}^3$	Probe Tip, $\mu\text{g}/\text{Nm}^3$	Date/Time	Side	Probe Zero, $\mu\text{g}/\text{Nm}^3$	Probe Tip, $\mu\text{g}/\text{Nm}^3$
6/17/2011 11:00	B	0.149		6/22/2011	A	0.000	
	A	0.000			B	0.000	
6/17/2011 11:15	B		108.05	6/22/2011	A		102.76
	A		110.32		B		102.37
6/17/2011 12:40	B	0.193		6/23/2011	B	0.000	
	A	0.000			A	0.000	
6/17/2011 12:55	B		103.00	6/23/2011	B		100.38
	A		104.25		A		99.39
6/17/2011 13:15	B	0.027		6/24/2011	B	0.000	
	A	0.066			A	0.000	
6/17/2011 13:30	B		101.06	6/24/2011	B		96.37
	A		102.46		A		96.14
6/17/2011 18:00	A	0.199		6/25/2011	B	0.000	
	B	0.201			A	0.000	
6/17/2011 18:15	A		100.21	6/25/2011	B		98.07
	B		102.58		A		98.34
6/18/2011 1:07	A	0.047		6/26/2011	B	0.000	
	B	0.000			A	0.000	
6/18/2011 1:22	A		96.71	6/26/2011	B		104.16
	B		98.16		A		101.33
6/18/2011 9:07	A	0.000		6/27/2011	B	0.000	
	B	0.000			A	0.000	
6/18/2011 9:27	A		94.54	6/27/2011	B		96.69
	B		95.07		A		99.30
6/18/2011 9:55	B	0.000		6/28/2011	B	0.000	
	A	0.000			A	0.000	
6/18/11 10:15	B		99.90	6/28/2011	B		106.80
	A		101.79		A		106.46
6/18/2011 18:52	A	0.000		6/29/2011	A	0.000	
	B	0.000			B	0.000	
6/19/2011 1:10	A	0.045		6/29/2011	A		96.02
	B	0.000			B		99.67
6/19/2011 1:30	A		98.97	6/30/2011	B	0.000	
	B		101.36		A	0.000	
6/20/2011 1:10	B	0.000		6/30/2011	B		98.25
	A	0.000			A		101.29
6/20/2011 1:30	B		98.87	7/1/2011 1:07	A	0.000	
	A		102.40		B	0.000	
6/21/2011 1:10	A	0.000		7/1/2011 1:27	A		96.57
	B	0.000			B		98.41
6/21/2011 1:30	A		100.03				
	B		103.33				

Table 15. Baghouse Inlet CMM Calibration Data

Directly into Analyzer		At the Probe Tip		Directly into Analyzer		At the Probe Tip	
Date/Time	Recovery, %	Date/Time	Recovery, %	Date/Time	Recovery, %	Date/Time	Recovery, %
6/19/11 3:00	100.64	6/19/11 3:30	101.84	6/27/11 3:02	101.23	6/27/11 3:32	100.88
6/19/11 3:02	99.20	6/19/11 3:32	99.97	6/27/11 3:05	102.06	6/27/11 3:35	102.49
6/19/11 3:05	100.72	6/19/11 3:35	102.03	6/27/11 3:07	101.18	6/27/11 3:37	101.02
6/19/11 3:07	99.72	6/19/11 3:37	98.93	6/27/11 3:10	102.24	6/27/11 3:40	102.52
6/19/11 3:10	101.46	6/19/11 3:40	101.22	6/27/11 3:12	101.34	6/27/11 3:42	101.45
6/19/11 3:12	100.01	6/19/11 3:42	98.14	6/27/11 3:15	102.30	6/27/11 3:45	101.81
6/23/11 3:00	102.40	6/23/11 3:30	102.20	6/29/11 3:00	101.73	6/29/11 3:30	102.90
6/23/11 3:02	101.41	6/23/11 3:32	101.59	6/29/11 3:02	101.42	6/29/11 3:32	102.12
6/23/11 3:05	102.53	6/23/11 3:35	101.47	6/29/11 3:05	101.84	6/29/11 3:35	101.67
6/23/11 3:07	101.39	6/23/11 3:37	99.98	6/29/11 3:07	101.26	6/29/11 3:37	101.45
6/23/11 3:10	102.47	6/23/11 3:40	101.83	6/29/11 3:10	102.14	6/29/11 3:40	101.57
6/23/11 3:12	101.58	6/23/11 3:42	100.97	6/29/11 3:12	101.68	6/29/11 3:42	100.42
6/25/11 3:02	99.34	6/25/11 3:32	101.51	7/1/11 3:00	102.30	7/1/11 3:30	104.17
6/25/11 3:05	100.34	6/25/11 3:35	102.52	7/1/11 3:02	101.78	7/1/11 3:32	102.41
6/25/11 3:07	99.99	6/25/11 3:37	99.75	7/1/11 3:05	102.26	7/1/11 3:35	103.43
6/25/11 3:10	100.97	6/25/11 3:40	101.90	7/1/11 3:07	101.86	7/1/11 3:37	102.21
6/25/11 3:12	100.74	6/25/11 3:42	99.47	7/1/11 3:10	102.39	7/1/11 3:40	102.94
6/25/11 3:15	101.66	6/25/11 3:45	99.81	7/1/11 3:12	101.75	7/1/11 3:42	101.92

To be a valid paired sample, the paired sorbent traps must have a relative standard difference (RSD) of $\leq 20\%$, where the RSD is defined by:

$$RSD = \frac{|C_a - C_b|}{C_b + C_b} \times 100\% \quad [\text{Eq. 2}]$$

where C_a and C_b are the mercury concentration measured by the paired sorbent traps.

As shown in Table 19, all the sorbent trap paired sample RSD values were substantially less than the requirements of $<20\%$ outlined in EPA Method 30B. In addition, to be a valid sample, the amount of mercury captured in the back half (breakthrough) cannot be $>5\%$ of the total mercury captured by the sorbent trap. With the exception of one sample that was 3.6% in the second half, all samples had a breakthrough that was $<1\%$.

The comparison between the sorbent trap samples and the CMMs is also provided in Table 19. With the exception of the last three baghouse outlet samples, a comparison between the mercury concentrations measured using the sorbent traps and those measured using the CMMs had an RSD of $<15\%$. The last three mercury concentrations measured at the baghouse outlet were very low, and very small differences in concentrations result in higher RSDs, but in terms of mercury removal across the baghouse, these differences have little meaning.

Table 16. Baghouse Outlet CMM Calibration Data

Directly into Analyzer		At the Probe Tip		Directly into Analyzer		At the Probe Tip	
Date/Time	Recovery, %	Date/Time	Recovery, %	Date/Time	Recovery, %	Date/Time	Recovery, %
6/17/11 9:52	100.31	6/17/11 10:17	100.53	6/23/11 3:07	101.03	6/23/11 3:37	102.43
6/17/11 9:55	99.40	6/17/11 10:20	99.03	6/23/11 3:10	100.61	6/23/11 3:40	101.42
6/17/11 9:57	100.21	6/17/11 10:22	99.44	6/25/11 2:57	102.25	6/25/11 3:27	100.72
6/17/11 10:00	99.42	6/17/11 10:25	97.99	6/25/11 3:00	100.89	6/25/11 3:30	100.44
6/17/11 10:02	99.85	6/17/11 10:27	99.62	6/25/11 3:02	101.93	6/25/11 3:32	101.84
6/18/11 17:55	98.99	6/18/11 18:25	100.38	6/25/11 3:05	100.89	6/25/11 3:35	100.17
6/18/11 17:57	99.86	6/18/11 18:27	99.27	6/25/11 3:07	101.34	6/25/11 3:37	100.97
6/18/11 18:00	99.14	6/18/11 18:30	99.46	6/25/11 3:10	101.31	6/25/11 3:40	98.76
6/18/11 18:02	99.88	6/18/11 18:32	99.12	6/27/11 2:57	102.29	6/27/11 3:27	102.23
6/18/11 18:05	99.16	6/18/11 18:35	99.44	6/27/11 3:00	101.09	6/27/11 3:30	99.80
6/18/11 18:07	99.52	6/18/11 18:37	98.88	6/27/11 3:02	102.05	6/27/11 3:32	101.46
6/19/11 2:57	100.93	6/19/11 3:27	102.32	6/27/11 3:05	101.24	6/27/11 3:35	100.66
6/19/11 3:00	99.51	6/19/11 3:30	101.17	6/27/11 3:07	101.47	6/27/11 3:37	101.46
6/19/11 3:02	100.72	6/19/11 3:32	101.96	6/27/11 3:10	101.02	6/27/11 3:40	100.72
6/19/11 3:05	100.13	6/19/11 3:35	99.71	6/29/11 2:57	101.99	6/29/11 3:27	100.98
6/19/11 3:07	101.22	6/19/11 3:37	100.97	6/29/11 3:00	101.38	6/29/11 3:30	100.84
6/19/11 3:10	100.24	6/19/11 3:40	98.23	6/29/11 3:02	102.05	6/29/11 3:32	100.67
6/21/11 2:57	101.77	6/21/11 3:27	102.50	6/29/11 3:05	100.75	6/29/11 3:35	100.81
6/21/11 3:00	101.16	6/21/11 3:30	102.03	6/29/11 3:07	101.71	6/29/11 3:37	100.44
6/21/11 3:02	101.98	6/21/11 3:32	102.51	6/29/11 3:10	101.40	6/29/11 3:40	99.10
6/21/11 3:05	100.81	6/21/11 3:35	102.69	7/1/11 2:57	101.52	7/1/11 3:27	102.50
6/21/11 3:07	101.71	6/21/11 3:37	102.89	7/1/11 3:00	100.72	7/1/11 3:30	101.46
6/21/11 3:10	100.72	6/21/11 3:40	101.41	7/1/11 3:02	101.78	7/1/11 3:32	101.86
6/23/11 2:57	101.30	6/23/11 3:27	102.11	7/1/11 3:05	101.21	7/1/11 3:35	100.65
6/23/11 3:00	100.51	6/23/11 3:30	101.65	7/1/11 3:07	101.57	7/1/11 3:37	101.79
6/23/11 3:02	101.37	6/23/11 3:32	102.04	7/1/11 3:10	100.78	7/1/11 3:40	99.86
6/23/11 3:05	101.05	6/23/11 3:35	100.58				

Table 17. OhioLumex Calibration Results

Calibration Curve 1		Calibration Curve 2	
Known Mass, ng	Calculated Mass, ng	Known Mass, ng	Calculated Mass, ng
Blank	0.0	Blank	0
10	9.7	10	10
10	10.0	10	9.3
100	103	100	100
100	92		
250	231	250	247
250	241		
500	508	500	500
500	496	500	500
R ²	0.9993	R ²	1.00

Table 18. QC Check Standard Results for the OhioLumex

Known Mass, ng	Measured Mass, ng	Recovery, %	Known Mass, ng	Measured Mass, ng	Recovery, %
40	38	95	20	20	100
400	390	98	400	394	99
250	250	100			
20	18	90	100	108	108
400	406	102	450	475	95
550	556	101	200	198	99
100	106	106	40	42	105
500	492	98	100	104	104
			400	399	100
10	11	110	10	10	100
100	98	98	200	203	102
200	190	95	500	526	105
500	533	107			
10	10	100	20	21	105
100	105	105	200	198	99
200	190	95	400	419	105
500	493	99			
20	20	100			
500	510	102			
100	106	106			
400	386	97			

Table 19. QA/QC Comparison of CMMs to Sorbent Traps

Date	Sample Location	C _a , µg/Nm ³	C _b , µg/Nm ³	Paired Trap	Sorbent Trap	CMM	
				RSD, %	Average, µg/Nm ³	Average, µg/Nm ³	RSD, %
6/18/11	BH inlet	6.033	6.050	0.14	6.042	5.184	7.64
6/18/11	BH outlet	7.041	7.036	0.04	7.038	5.669	10.77
6/20/11	BH inlet	5.784	6.017	1.98	5.900	5.341	4.98
6/20/11	BH outlet	1.166	1.115	2.20	1.140	0.908	11.36
6/21/11	BH inlet	6.946	6.846	0.73	6.896	6.306	4.47
6/21/11	BH outlet	1.544	1.529	0.51	1.536	1.185	12.90
6/23/11	BH inlet	7.311	6.991	2.24	7.151	6.554	4.35
6/23/11	BH outlet	1.568	1.587	0.58	1.577	1.179	14.45
6/27/11	BH inlet	5.850	6.023	1.45	5.936	5.300	5.66
6/27/11	BH outlet	0.814	0.802	0.75	0.808	0.629	12.46
6/28/11	BH inlet	5.598	5.582	0.15	5.590	4.701	8.64
6/28/11	BH outlet	1.156	1.171	0.67	1.163	0.929	11.20
6/29/11	BH inlet	4.966	5.074	1.07	5.020	4.521	5.23
6/29/11	BH outlet	0.619	0.623	0.25	0.621	0.451	15.85
6/29/11	BH inlet	4.979	4.880	1.00	4.930	4.212	7.85
6/29/11	BH outlet	0.448	0.434	1.64	0.441	0.290	20.59
6/30/11	BH inlet	5.098	5.004	0.93	5.051	4.299	8.05
6/30/11	BH outlet	0.234	0.231	0.51	0.232	0.093	43.04

Although small, there appears to be a bias in the measurements. The sorbent trap mercury measurements were in all cases greater than the CMM results. This almost certainly is a result of differences in how the two measurement methods deal with particulate matter. The sorbent trap samples have a quartz wool plug prior to the mercury sorbent. When the analysis is done, the quartz wool is analyzed with the first sorbent section. Therefore, any mercury captured by the particulate matter on the quartz plug is considered to be part of the overall measured concentration. However, with a CMM, the ISP helps ensure only gas-phase mercury is measured. The fact that the bias is greater at the baghouse inlet where the particulate concentration is the greatest supports this. Based on previous testing done at taconite plants, it has been found that the high iron content of the dust results in mercury capture (3).

The complete sorbent trap data along with the CMM comparison information is presented in Appendix C.

6.0 CONCLUSIONS AND RECOMMENDATIONS

Based on the results of the testing conducted using a slipstream baghouse at Keetac, the following conclusions can be made:

- Mercury removal of >75% can be achieved at Keetac with either standard or bromine-treated activated carbon.
- To ensure >75% removal when natural gas is fired, 2.0 lb/Macf is needed when using standard activated carbon.
- To ensure >75% removal when natural gas is fired, 1.1 lb/Macf is needed when using bromine-treated activated carbon.
- To ensure >75% removal when a PRB coal is fired, only 0.6 lb/Macf of bromine-treated activated carbon is needed.
- Very low particulate emissions can be achieved.
- Because of the relatively high cost of installing a fabric filter, the most economical installation would be for those taconite facilities that require fuel flexibility and/or where particulate emissions are a concern.
- If a baghouse is to be installed at Keetac, 18%–20% flue would need to bypass the wet particulate scrubber to prevent wetting of the bags.
- As expected, the mercury at the outlet of the scrubber is ~80% elemental mercury.
- It appears that if the ACI is turned off, there is the potential of high mercury emissions as a result of reemission.

- Overall, the slipstream baghouse and CMMs operated well during the test period.

If this is to be a viable technology, the following recommendations are made for future testing.

- Longer-term testing is needed to determine the resultant steady-state pressure drop across the baghouse as a function of air-to-cloth ratio.
- Longer-term tests are also needed to ensure that required mercury control will be maintained.
- It appeared that the bromine-treated activated carbon worked better when firing coal compared to natural gas. The same may be true using standard activated carbon. Therefore, additional coal tests are needed.
- The economic evaluation presented in this report is based on the utility requirements and may or may not be the same for a taconite plant. Therefore, more specific economic data are needed.
- There may be a need to evaluate or update the existing wet scrubber mist eliminators.

7.0 REFERENCES

1. Berndt, M.; Engesser, J.; Johnson, A. *On Distribution of Mercury in Taconite Plant Scrubber Systems*; Submitted to the Minnesota Pollution Control Agency, Oct 2003.
2. Pavlish, J.H.; Sondreal, E.A.; Mann, M.D.; Olson, E.S.; Galbreath, K.C.; Laudal, D.L.; Benson, S.A. Status Review of Mercury Control Options for Coal-Fired Power Plants. *Fuel* **2003**, 82, 89–165.
3. Laudal, D.L. *Methods Testing for Measurement of Mercury Speciation for High Reactive Dust*; Report to the Minnesota Pollution Control Agency; Energy & Environmental Research Center: Grand Forks, ND, March 2007.

APPENDIX A
SAMPLE CALCULATIONS

SAMPLE CALCULATIONS

1.0 AIR-TO-CLOTH RATIO

Gas flow rate = 584 scfm

Pressure = 1 atm.

Temperature at baghouse inlet = 165°F

Temperature at baghouse outlet = 215°F

Average temperature = $(165+215)/2 = 190^\circ\text{F}$

Standard temperature = 68°F

Actual gas flow rate = $(584)*(190+460)/(68+460) = 719$ acfm

Bag diameter = 6 in

Bag length = 12 ft

No. of bags = 7

Total bag surface area = $\pi*(6/12)*12*7 = 131.95$ ft²

Air-to-cloth ratio = $719/131.95 = \underline{5.45}$ ft/min

2.0 ACTIVATED CARBON FEED RATE IN lb/Macf

Activated carbon feed rate = 42.5 g/hr

Actual gas flow rate = 719 acfm

Activated carbon feed rate = $42.5/(454*719*60)*10^6 = \underline{2.17}$ lb/Macf

3.0 FLUE GAS BYPASS CALCULATION FOR REHEAT

Saturated gas temperature = 135°F = 57.22°C

Gas flow rate = 600,000 scfm (68°F) = 15,830.4 scm/min (0°C) = 19,148.4 m³/min (actual)

Desired gas temperature to prevent bag wetting = 155°F = 68.33°C

Temperature of flue gas prior to wet scrubber = 300°F = 148.89°C

Flue gas molecular weight = 30.4 kg-moles/m³

Molecular weight of water = 18.01 kg-moles/m³

Ideal gas law = 1kg-mole/22.4 m³ at standard pressure (1 atm.) and temp. (0°C)

Pressure = 1 atm. = $1*101.325 = 101.325$ kPa

From steam table the moisture vapor pressure at 135°F = 17.49 kPa

Gas vapor pressure = $101.325-17.49 = 83.83$ kPa

Gas flow rate (mass basis) = $15,830.4*(30.4/22.4)*(83.83/100) = 18,010.1$ kg/min

Moisture flow rate (mass basis) = $15,830.4*(18.01/22.4)*(17.50/100) = 2227.4$ kg/min

Flue gas heat capacity = 1.01 kJ/kg/°K

Moisture heat capacity = 1.87 kJ/kg/°K

Energy needed to heat gas to desired temp. = $18,010.1*1.01*(68.33-57.22) = 202,093.1$ kJ/min

Energy needed to heat moisture = $2227.4*1.87*(68.33-57.22) = 46,275.8$ kJ/min

High temperature dilution gas needed = $(202,093.1+46,275.8)/1.01/(148.89-68.33) = 3052.5$ kg/min

Dilution gas volume flow rate = $3052.5 \times (22.4/30.4) \times (148.89+273)/273 = 3475.9 \text{ m}^3/\text{min}$ (actual)
 % bypass needed of high-temperature gas = $3475.9/19148.4 \times 100 = \underline{18.2\%}$

4.0 PARTICULATE-SAMPLING CALCULATIONS

4.1 Volume of Gas Sample

$V_m(\text{std})$ = Volume of gas sample measured by the dry gas meter, connected to standard conditions, dscf

$$V_m(\text{std})(\text{dscf}) = \frac{K_1 \times V_m \times C_m \times P_m}{T_m + 460}$$

$$V_m(\text{std}) = \frac{17.64 \times 81.588 \times 1.010 \times 28.15}{70 + 460} = 77.207 \text{ dscf}$$

Where:

K_1 = 17.64 R/in. Hg

V_m = Volume of gas sample as measured by dry gas meter corrected for C_m = meter calibration coefficient) (dcf)

P_m = Meter pressure (in. Hg)

T_m = Meter temperature ($^{\circ}\text{F}$)

4.2 Volume of Water Vapor

$V_w(\text{std})$ = Volume of water vapor in the gas sample, corrected to standard conditions, scf

$$V_w(\text{std})(\text{scf}) = K_2 \times H_2O(g)$$

$$V_w(\text{std}) = 0.04715 \times 314.7 = 14.813 \text{ scf}$$

Where:

K_2 = 0.04715 ft^3/g

$H_2O(g)$ = Mass of liquid collected in impingers and silica gel (g)

4.3 Water Vapor in the Gas Stream

B_{ws} = Water vapor in the gas stream, proportion by volume

$$B_{ws} = \frac{V_w(\text{std})}{V_m(\text{std}) + V_w(\text{std})}$$

$$B_{ws} = \frac{14.813}{77.207 + 14.813} = 0.1613$$

4.4 Molecular Weight

$$M_w = 30 \times (1 - B_{ws}) + 18 \times B_{ws} = 30 \times (1 - 0.1613) + 18 \times 0.1613 = 28.06$$

4.5 Average Stack Gas Velocity

V_s = Average stack gas velocity, ft/sec

$$V_s \text{ (ft/sec)} = K_3 \times C_p \times (\Delta p)^{1/2} (\text{avg}) \times \left[\frac{T_s + 460}{P_s \times M_s} \right]^{1/2}$$

$$V_s = 85.49 \times 0.84 \times 0.40 \times \left[\frac{165 + 460}{28.09 \times 28.06} \right]^{1/2} = 25.58 \text{ ft/sec}$$

Where:

$$K_3 = 85.49 \text{ ft/sec} \times \left[\frac{\frac{lb}{lb-mole} \times in. Hg}{R \times in. H_2O} \right]^{1/2}$$

C_p = Pitot tube coefficient, dimensionless

Δp = Velocity head of stack gas (in. Hg)

$(\Delta p)^{1/2} (\text{avg})$ = Average of the square root of Δp values

T_s = Stack gas temperature ($^{\circ}F$)

P_s = Stack pressure (in. Hg)

4.6 Isokinetic Sampling Rate

I = Percent of isokinetic sampling, %

$$I (\%) = \frac{K_4 \times (T_s + 460) \times V_m(\text{std}) \times 144}{P_s \times V_s \times A_n \times \theta \times (1 - Bws)}$$

$$I = \frac{0.09450 \times (165 + 460) \times 77.207 \times 144}{28.07 \times 25.58 \times 0.06158 \times 180 \times (1 - 0.1613)} = 98.3\%$$

Where:

$$K_4 = \frac{0.09450\% (\text{in. Hg})(\text{min})}{R \times \text{sec}}$$

A_n = Cross-sectional area of nozzle (in.^2)

θ = Total sampling time (min)

4.7 Dust Loading

Filter tare weight = 0.23651 g

Final filter weight = 0.25662 g

Net weight on filter = 0.25662 - 0.23651 = 0.02011 g

Petri dish tare weight = 0.74168 g
 Petri dish and probe dust = 0.74182 g
 Net weight on petri dish = 0.74182 - 0.74168 = 0.00014 g
 Total dust collected = 0.02011 + 0.00014 = 0.02025 g = 0.02025 * 15.43 = 0.31246 grains
 Gas volume sampled = 77.207 dscf
 Dust loading = 0.31246 / 77.027 = 0.0041 grains/dscf

5.0 MERCURY SAMPLING

5.1 Mercury Concentration in Flue Gas Based on Sorbent Traps (Sample 7A)

Volume of gas sampled = 50.277 L (dry)
 Moisture in flue gas = 16.2% (from dust loading sample)
 Volume of moisture sampled = 50.277 * (1 - 0.162) = 9.719 L
 Total gas sampled = 50.277 + 9.719 = 59.996 L (wet)
 Tm = 65°F
 Pb (barometric) = 28.35 in Hg
 Elevation = 20 ft
 Cm = 1.015
 N (normal conditions) = 68°F and 29.92 in Hg
 Vt (corrected) = 59.996 * 1.015 * (29.92 / [28.35 - 20/1000]) * 528 / (65 + 460) =
 57.990 NL (wet)
 Section 1 Hg = 288 ng
 Section 2 Hg = 0 ng
 Back plug = 0 ng
 Total Hg collected = 288 ng
 Breakthrough = 0 / 288 * 100 = 0%
 Total Hg conc. in gas stream = 288 / 57.990 = 4.966 ng/NL = 4.966 µg/Nm³

5.2 Paired Sorbent Trap Calculations (7A and 7B)

Hg concentration from Trap 7A = 4.966 µg/Nm³
 Hg concentration from Trap 7B = 5.074 µg/Nm³
 Relative standard difference = ABS[(5.074 - 4.966)] / (5.074 + 4.966) * 100 = 1.07%

5.3 Mercury Removal Across Slipstream Baghouse (Sample 7 sorbent trap and CMM average over the time the sorbent trap sample was taken)

Sorbent trap avg. Hg at the BH inlet = (4.966 + 5.074) / 2 = 5.020 µg/Nm³
 Sorbent trap avg. Hg at the BH outlet = (0.619 + 0.623) / 2 = 0.621 µg/Nm³
 CMM avg. Hg at the BH inlet = 4.52 µg/Nm³
 CMM avg. Hg at the BH outlet = 0.451 µg/Nm³
 Hg removal based on sorbent traps = (5.020 - 0.621) / 5.020 * 100 = 87.6%
 Hg removal based on CMMs = (4.52 - 0.451) / 4.52 * 100 = 90.0%

APPENDIX B
DUST-LOADING DATA SHEETS

OPERATORS		RS								
ID		KEETAC-BHIN-M5-1			Vwstd	0.697	SCF			
RUN #					Vmstd	6.297	SCF			
DATE		6/15/2011			Vtstd	6.994	SCF			
TIME		15:24			% H2O	10.0	%			
FUND #		15726			% Isokin	38.3	%			
DUST LOADING DATA SHEET					DCL	#VALUE!	grains/SCF			
Sample Pt.		DWN LEG BH IN								
Traverse Pt.		3' IN			Ps =	28.87	in. Hg Abs.			
Pb (Barometric Press.)		28.97	in Hg		Ts =	608	°R			
Elevation correction		20 ft (1 in Hg / 1000 ft)								
Ps (Stack Pressure)		-1.1 in H2O			VS (Stack Velocity)		1706	ft/min		
Dn (Nozzle Diam.)		0.280 in			QN (Nozzle Flow Rate)		0.7296	ACFM		
Est. ΔP (Pitot)		0.21 in H2O			QM (Meter Flow Rate)		0.5227	ACFM		
Cm		1.010			ΔH (orifice)		0.70	in H2O		
Cp		0.84 (Type S=.84, Std=.99)			Seconds/Rev		11.5			
Est. Ts (Stack Temp)		148 °F								
Est. % H2O		15					O2 %			
ΔH@		1.46					CO ppm			
Tm (Est)		60 °F					NO ppm			
ΔH (Est)		0.80 in Hg					NO2 ppm			
							SO2 ppm			
							CO2 %			
							coal CO2=18.6*(21-02%)/21			
<i>Note: Standard Temperature and Pressure are 68 oF and 29.92 in. Hg</i>										
Time (min.)	Temp stack	Gas Meter (ft3)	Tm Inlet	Tm Outlet	ΔH	ΔP Pitot	Pump Vac in Hg	Temp Probe	Temp Box	Temp Impinger
0	140	65.091	50	50	0.80	0.21	3.0	250		OK
30	140	71.331	54	54	0.80	0.21	5.0	250		OK
30					0.50					
Averages:	140	6.240	52		0.70	0.21	4.0	250	#DIV/0!	#DIV/0!
Comment										

Sample Pt.	DWN LEG BH IN		Date	6/15/2011
			Run #	0
Train Type			Fund #	15726
			Cost Center #	
STOPPER TYPE	TYPE OF SOLUTION	INITIAL WT. (g)	FINAL WT. (g)	NET WT. (g)
Straight	DI	645.3	655.3	10.0
Straight	DI	614.3	616.0	1.7
Impinger	DRY	637.7	638.7	1.0
Straight	SIL GEL	958.7	960.7	2.0
Straight		616.2	616.3	0.1
Straight				0.0
Impinger				0.0
Straight				0.0
			TOTAL H2O (g)	14.8
FILTER		wet	wet	#VALUE!
				0.00000
Additional Dust				0.00000
			TOTAL DUST (g)	#VALUE!
Vwstd	0.697	SCF		
Vmstd	6.297	SCF		
Vtstd	6.994	SCF		
% H2O	10.0	%		
% Isokinetic	38.3	%		
DCL	#VALUE!	grains/SCF		
DCL - Metric	#VALUE!	grams/SCM = grains/SCF*2.288		
DUST LOADING CALCULATIONS (Concentration Basis)				
Inlet DCL				grains/SCF
% Efficiency = (Inlet DCL - Outlet DCL) * 100			#VALUE!	%
	Inlet DCL			
Pipe Area				ft2
ACFM = VS * Pipe Area (ft2)			0.0000	ACFM
SCFM = ACFM * PS/TS * 17.64			0.0	SCFM
lbs/hour = grains/scf * 0.000143 * SCFM * 60			#VALUE!	lbs/hour

Equations		
Page 1		
PS (Stack Pressure)	=PB + (PS in H2O / 13.6) - elevation/1000	in. Hg Abs.
TS (Stack Temperature)	=average TS oF + 460	oR
VS (Stack Velocity)ft/min	=60*85.49 * Cp * sqrt(P * TS oR / PS in Hg Abs / MS)	ft/min
MS	=30 * (1-%H2O/100) + 18 * %H2O/100	g/mol
QN (Nozzle Flow Rate)	=VS * pi * DN2 / 576	ACFM
QM (Meter Flow Rate)	=QN * TM * PS in Hg Abs/(Cm * TS oR * (HM /13.6)) - (1-%H2O/100)	ACFM
H (orifice)	=QM2 * H@ * (PB + HM /13.6)/(0.03175 * (TM + 460))	in H2O
Seconds/Rev	=1/(QM / 0.1 / 60)	
Page 2		
VWstd	=0.04707 * (H2O g)	SCF
VMstd	=17.64 * VWstd * Cm * (PB+ HM /13.6 - Elevation/1000)	SCF
VTstd	=VWstd + VMstd	SCF
% H2O	=(VWstd / VTstd) * 100	%
% Isokinetic	= 0.0945 * TS oR * VMstd * 60 sec/min * 144 in2/ft2 (PS in Hg Abs * VS * (DN2/4*pi) * time min * (1-%H2O/100)	%
DCL	=15.43 * (dust g) / VMstd	grains/SCF
% Efficiency	=(Inlet DCL - Outlet DCL) / Inlet DCL * 100	%
ACFM	=VS * Pipe Area (ft2)	ACFM
SCFM	=ACFM * PS / TS * 17.64	SCFM
lbs/hour	=grains/SCF * 0.000143 * SCFM * 60 min/hr	lbs/hour
PPM Calculation		
PPM	=Conc mg/L * Vol mL * L/1000 mL * 2.205e-6 lb/mg * 387 ft3/mol / VTstd * e6	
Stack Vel ft./sec.	Vs=85.49*Cp*SQRT Dp*SQRT(Ts/Ps/Mw)	
Mol Wt. Wet	Mw=30*(1-Bws)+18*Bws	

ID			
Run #			
Start Time			
Fund #			
Vt Std			ft ³
Volume of Sample			mL
Concentration			mg/L or ppm
Molecular Weight			g/mole
Molecular Weights (g/mole)			
SO3	80.06		
SO2	64.06		
NH3	17.04		
Cl2	70.90		
HCl	36.46		
F2	38.00		
HF	20.02		
Hg	200.59		
#DIV/0!	ppm in flue gas		
<i>387 ft³/mol at 68oF</i>			

DATE	ID	SAMPLE PORT	SAMPLER	START TIME	TEST TIME	BARO PRESS (in Hg)	STACK PRESS (in H2O)	TEMP (F)	O2%	ΔP	NOZ DIA	GAS METER VOL (cf)	TOTAL H2O	TOTAL DUST	VTSTD (SCF)	% H2O	METER TEMP	ΔH	% ISO	DLC GRAINS/SCF
6/15/2011	KEETAC-BHIN-MS-1	DWN LEG BH IN	RS	15:24	30	28.97	-1.1	140	0.0	0.21	0.280	6.240	14.8	#VALUE!	6.994	10.0	52	0.70	36.3	#VALUE!

OPERATORS		RS									
ID		KEETAC-BHOUT-M5-6-2			Vwstd	15.971	SCF				
RUN #		2			Vmstd	76.845	SCF				
DATE		6/30/2011			Vtstd	92.816	SCF				
TIME		16:08			% H2O	17.2	%				
FUND #		15726			% Isokin	#VALUE!	%				
DUST LOADING DATA SHEET					DCL	0.0003	grains/SCF				
Sample Pt.		BH OUT DWN LG									
Traverse Pt.		3' BIN			Ps =	27.52	in. Hg Abs.				
Pb (Barometric Press.)		28.05	in Hg		Ts =	676	°R				
Elevation correction		5 ft (1 in Hg / 1000 ft)									
Ps (Stack Pressure)		-7.2	in H2O		VS (Stack Velocity)		1613	ft/min			
Dn (Nozzle Diam.)		0.280	in		QN (Nozzle Flow Rate)		0.6896	ACFM			
Est. ΔP (Pitot)		0.16	in H2O		QM (Meter Flow Rate)		0.4390	ACFM			
Cm		1.040			ΔH (orifice)		0.49	in H2O			
Cp		0.84 (Type S=.84, Std=.99)			Seconds/Rev		13.7				
Est. Ts (Stack Temp)		216	°F								
Est. % H2O		16			O2 %		16.9				
ΔH@		1.57			CO ppm		3				
Tm (Est)		85	°F		NO ppm		83				
ΔH (Est)		0.50	in Hg		NO2 ppm		2				
					SO2 ppm		12				
					CO2 %						
					coal CO2=18.6*(21-02%)/21						
<i>Note: Standard Temperature and Pressure are 68 oF and 29.92 in. Hg</i>											
Time (min.)	Temp stack	Gas Meter (ft3)	Tm Inlet	Tm Outlet	ΔH	ΔP Pitot	Pump Vac in Hg	MUFF	Temp Box	Temp Impinger	
0	216	308.770	80	79	0.53	0.16	2.0	254		OK	
15	216	315.410	83	78	0.55	0.16	2.0	249		OK	
30	216	322.130	83	78	0.55	0.16	2.0	250		OK	
45	216	328.950	83	76	0.55	0.16	2.0	249		OK	
60	216	335.600	81	78	0.52	0.16	2.0	249		OK	
75	216	342.160	82	76	0.52	0.16	2.0	252		OK	
90	216	348.990	83	82	0.52	0.16	2.1	247		OK	
105	216	355.720	81	76	0.52	0.16	2.1	252		OK	
120	216	362.440	81	77	0.52	0.16	2.1	250		OK	
135	216	369.140	80	76	0.52	0.16	2.1	247		OK	
150	216	375.840	81	75	0.52	0.16	2.2	255		OK	
165	216	382.530	81	76	0.52	0.16	2.2	255		OK	
180	216	389.197	80	74	0.52	0.16	2.2	254		OK	
Averages:	216	80.427	79		0.53	0.16	2.1	251	#DIV/0!	#DIV/0!	
Comments	Leak ck OK										

Sample Pt.	BH OUT DWN LG		Date	6/30/2011
			Run #	2
Train Type			Fund #	15726
			Cost Center #	
STOPPER TYPE	TYPE OF SOLUTION	INITIAL WT. (g)	FINAL WT. (g)	NET WT. (g)
Straight	DI	799.7	999.6	199.9
Straight	DI	641.6	756.8	115.2
Impinger	DRY	668.3	673.8	5.5
Straight	SIL GEL	1015.6	1034.3	18.7
Straight				0.0
Straight				0.0
Impinger				0.0
Straight				0.0
			TOTAL H2O (g)	339.3
FILTER		0.24056	0.24147	0.00091
		0.79902	0.79951	0.00049
Additional Dust				0.00000
			TOTAL DUST (g)	0.00140
Vwstd	15.971	SCF		
Vmstd	76.845	SCF		
Vtstd	92.816	SCF		
% H2O	17.2	%		
% Isokinetic	#VALUE!	%		
DCL	0.0003	grains/SCF		
DCL - Metric	0.0006	grams/SCM = grains/SCF*2.288		
DUST LOADING CALCULATIONS (Concentration Basis)				
Inlet DCL			0.0045	grains/SCF
% Efficiency = (Inlet DCL - Outlet DCL) * 100			93.7531	%
Inlet DCL				
Pipe Area				ft2
ACFM = VS * Pipe Area (ft2)			0.0000	ACFM
SCFM = ACFM * PS/TS * 17.64			0.0	SCFM
lbs/hour = grains/scf * 0.000143 * SCFM * 60			0.0000	lbs/hour

Equations		
Page 1		
PS (Stack Pressure)	=PB + (PS in H2O / 13.6) - elevation/1000	in. Hg Abs.
TS (Stack Temperature)	=average TS oF + 460	oR
VS (Stack Velocity)ft/min	=60*85.49 * Cp * sqrt(P * TS oR / PS in Hg Abs / MS)	ft/min
MS	=30 * (1-%H2O/100) + 18 * %H2O/100	g/mol
QN (Nozzle Flow Rate)	=VS * pi * DN2 / 576	ACFM
QM (Meter Flow Rate)	=QN * TM * PS in Hg Abs/(Cm * TS oR * (HM /13.6)) - (1-%H2O/100)	ACFM
H (orifice)	=QM2 * H@ * (PB + HM /13.6)/(0.03175 * (TM + 460))	in H2O
Seconds/Rev	=1/(QM / 0.1 / 60)	
Page 2		
VWstd	=0.04707 * (H2O g)	SCF
VMstd	=17.64 * VWstd * Cm * (PB+ HM /13.6 - Elevation/1000)	SCF
VTstd	=VWstd + VMstd	SCF
% H2O	=(VWstd / VTstd) * 100	%
% Isokinetic	= 0.0945 * TS oR * VMstd * 60 sec/min * 144 in2/ft2 (PS in Hg Abs * VS * (DN2/4*pi) * time min * (1-%H2O/100)	%
DCL	=15.43 * (dust g) / VMstd	grains/SCF
% Efficiency	=(Inlet DCL - Outlet DCL) / Inlet DCL * 100	%
ACFM	=VS * Pipe Area (ft2)	ACFM
SCFM	=ACFM * PS / TS * 17.64	SCFM
lbs/hour	=grains/SCF * 0.000143 * SCFM * 60 min/hr	lbs/hour
PPM Calculation		
PPM	=Conc mg/L * Vol mL * L/1000 mL * 2.205e-6 lb/mg * 387 ft3/mol / VTstd * e6	
Stack Vel ft./sec.	Vs=85.49*Cp*SQRT Dp*SQRT(Ts/Ps/Mw)	
Mol Wt. Wet	Mw=30*(1-Bws)+18*Bws	

ID			
Run #			
Start Time			
Fund #			
Vt Std			ft ³
Volume of Sample			mL
Concentration			mg/L or ppm
Molecular Weight			g/mole
Molecular Weights (g/mole)			
SO3	80.06		
SO2	64.06		
NH3	17.04		
Cl2	70.90		
HCl	36.46		
F2	38.00		
HF	20.02		
Hg	200.59		
#DIV/0!	ppm in flue gas		
387 ft ³ /mol at 68oF			

DATE	ID	SAMPLE PORT	SAMPLER	START TIME	TEST TIME	BARO PRESS (in Hg)	STACK PRESS (in H2O)	TEMP (F)	O2%	ΔP	NOZ DIA	GAS METER VOL (cf)	TOTAL H2O	TOTAL DUST	VMSTD (SCF)	VTSTD	% H2O	METER TEMP	ΔH	% ISO	DLC GRAINS/SCF
6/30/2011	KEETAC-BHOUT-MSBH	OUT DYN LG	RS	16:08	180	28.05	-7.2	216	15.9	0.16	0.280	80.427	339.3	0.0014	76.845	92.816	17.2	79	0.53	#VALUE!	0.0003

OPERATORS		RS									
ID		KEETAC-BHOUT-M5-5			Vwstd	14.629	SCF				
RUN #					Vmstd	76.326	SCF				
DATE		6/30/2011			Vtstd	90.955	SCF				
TIME		9:35			% H2O	16.1	%				
FUND #		15726			% Isokin	103.3	%				
DUST LOADING DATA SHEET					DCL	0.0004	grains/SCF				
Sample Pt.		BH OUT DWN LG									
Traverse Pt.		3' BIN			Ps =	27.59	in. Hg Abs.				
Pb (Barometric Press.)		28.11	in Hg		Ts =	676	*R				
Elevation correction		5 ft (1 in Hg / 1000 ft)									
Ps (Stack Pressure)		-7.0		in H2O	VS (Stack Velocity)		1611	ft/min			
Dn (Nozzle Diam.)		0.280		in	QN (Nozzle Flow Rate)		0.6887	ACFM			
Est. ΔP (Pitot)		0.16		in H2O	QM (Meter Flow Rate)		0.4264	ACFM			
Cm		1.040			ΔH (orifice)		0.48	in H2O			
Cp		0.84 (Type S=.84, Std=.99)			Seconds/Rev		14.1				
Est. Ts (Stack Temp)		216		*F							
Est. % H2O		16			O2 %		17.2				
ΔH@		1.57			CO ppm		3				
Tm (Est)		70		*F	NO ppm		101				
ΔH (Est)		0.60		in Hg	NO2 ppm		0				
					SO2 ppm		7				
					CO2 %						
					coal CO2=18.6*(21-02%)/21						
<i>Note: Standard Temperature and Pressure are 68 oF and 29.92 in. Hg</i>											
Time (min.)	Temp stack	Gas Meter (ft3)	Tm Inlet	Tm Outlet	ΔH	ΔP Pitot	Pump Vac in Hg	MUFF	Temp Box	Temp Impinger	
0	216	230.378	70	69	0.48	0.16	2.0	251		OK	
15	216	236.620	71	67	0.48	0.16	2.0	247		OK	
30	216	243.140	71	65	0.51	0.16	2.0	249		OK	
45	216	249.670	72	65	0.51	0.16	2.0	247		OK	
60	216	256.220	72	67	0.51	0.16	2.0	254		OK	
75	216	262.720	72	66	0.51	0.16	2.0	256		OK	
90	216	268.920	71	67	0.51	0.16	2.0	248		OK	
105	216	275.750	73	67	0.51	0.16	2.0	247		OK	
120	216	282.390	73	68	0.51	0.16	2.1	253		OK	
135	216	288.900	75	69	0.51	0.16	2.1	248		OK	
150	216	295.440	73	69	0.51	0.16	2.2	250		OK	
165	216	302.000	76	70	0.51	0.16	2.2	254		OK	
180	216	308.754	75	71	0.51	0.16	2.2	255		OK	
Averages:	216	78.376	70		0.51	0.16	2.1	251	#DIV/0!	#DIV/0!	
Comments	Leak ck OK										

Sample Pt.	BH OUT DWN LG		Date	6/30/2011
			Run #	0
Train Type			Fund #	15726
			Cost Center #	
STOPPER TYPE	TYPE OF SOLUTION	INITIAL WT. (g)	FINAL WT. (g)	NET WT. (g)
Straight	DI	788.5	996.4	207.9
Straight	DI	641.5	721.3	79.8
Impinger	DRY	668.3	673.8	5.5
Straight	SIL GEL	981.8	999.4	17.6
Straight				0.0
Straight				0.0
Impinger				0.0
Straight				0.0
			TOTAL H2O (g)	310.8
FILTER		0.23657	0.23741	0.00084
		0.79765	0.79902	0.00137
Additional Dust				0.00000
			TOTAL DUST (g)	0.00221
Vwstd	14.629	SCF		
Vmstd	76.326	SCF		
Vtstd	90.955	SCF		
% H2O	16.1	%		
% Isokinetic	103.3	%		
DCL	0.0004	grains/SCF		
DCL - Metric	0.0010	grams/SCM = grains/SCF*2.288		
DUST LOADING CALCULATIONS (Concentration Basis)				
Inlet DCL			0.0040	grains/SCF
% Efficiency = (Inlet DCL - Outlet DCL) * 100			88.8307	%
Inlet DCL				
Pipe Area				ft2
ACFM = VS * Pipe Area (ft2)			0.0000	ACFM
SCFM = ACFM * PS/TS * 17.64			0.0	SCFM
lbs/hour = grains/scf * 0.000143 * SCFM * 60			0.0000	lbs/hour

Equations		
Page 1		
PS (Stack Pressure)	$=PB + (PS \text{ in H}_2\text{O} / 13.6) - \text{elevation}/1000$	in. Hg Abs.
TS (Stack Temperature)	$=\text{average TS of} + 460$	oR
VS (Stack Velocity)ft/min	$=60*85.49 * C_p * \text{sqrt}(P * TS \text{ oR} / PS \text{ in Hg Abs} / MS)$	ft/min
MS	$=30 * (1-\%H_2O/100) + 18 * \%H_2O/100$	g/mol
QN (Nozzle Flow Rate)	$=VS * \pi * DN^2 / 576$	ACFM
QM (Meter Flow Rate)	$=QN * TM * PS \text{ in Hg Abs}/(C_m * TS \text{ oR} * (HM /13.6)) - (1-\%H_2O/100)$	ACFM
H (orifice)	$=QM^2 * H@ * (PB + HM /13.6)/(0.03175 * (TM + 460))$	in H2O
Seconds/Rev	$=1/(QM / 0.1 / 60)$	
Page 2		
VWstd	$=0.04707 * (H_2O \text{ g})$	SCF
VMstd	$=17.64 * VWstd * C_m * (PB+ HM /13.6 - \text{Elevation}/1000)$	SCF
VTstd	$=VWstd + VMstd$	SCF
% H2O	$=(VWstd / VTstd) * 100$	%
% Isokinetic	$= 0.0945 * TS \text{ oR} * VMstd * 60 \text{ sec}/\text{min} * 144 \text{ in}^2/\text{ft}^2$ $(PS \text{ in Hg Abs} * VS * (DN^2/4*\pi) * \text{time min} * (1-\%H_2O/100))$	%
DCL	$=15.43 * (\text{dust g}) / VMstd$	grains/SCF
% Efficiency	$=(\text{Inlet DCL} - \text{Outlet DCL}) / \text{Inlet DCL} * 100$	%
ACFM	$=VS * \text{Pipe Area (ft}^2)$	ACFM
SCFM	$=ACFM * PS / TS * 17.64$	SCFM
lbs/hour	$=\text{grains}/\text{SCF} * 0.000143 * \text{SCFM} * 60 \text{ min}/\text{hr}$	lbs/hour
PPM Calculation		
PPM	$=\text{Conc mg}/\text{L} * \text{Vol mL} * \text{L}/1000 \text{ mL} * 2.205\text{e-}6 \text{ lb}/\text{mg} * 387 \text{ ft}^3/\text{mol} / VTstd * e6$	
Stack Vel ft./sec.	$V_s=85.49*C_p*\text{SQRT } D_p*\text{SQRT}(T_s/P_s/M_w)$	
Mol Wt. Wet	$M_w=30*(1-B_{ws})+18*B_{ws}$	

ID			
Run #			
Start Time			
Fund #			
Vt Std			ft^3
Volume of Sample			mL
Concentration			mg/L or ppm
Molecular Weight			g/mole
Molecular Weights (g/mole)			
SO3	80.06		
SO2	64.06		
NH3	17.04		
Cl2	70.90		
HCl	36.46		
F2	38.00		
HF	20.02		
Hg	200.59		
#DIV/0!	ppm in flue gas		
387 ft3/mol at 68oF			

DATE	ID	SAMPLE PORT	SAMPLER	START TIME	TEST TIME	BARO PRESS (in Hg)	STACK PRESS (in H2O)	TEMP (F)	O2%	ΔP	NOZ DIA	GAS METER VOL (cf)	TOTAL H2O	TOTAL DUST	VMSTD (SCF)	VTSTD (SCF)	% H2O	METER TEMP	ΔH	% ISO	DLC GRAINS/SCF
6/30/2011	KEETAC-BHOUT-MS9H	OUT	DWN LG	9:35	180	28.11	-7	216	17.2	0.16	0.280	78.376	310.8	0.00221	76.326	90.955	15.1	70	0.51	103.3	0.0004

OPERATORS		RS									
ID	KEETAC-BHOUT-M5-4			Vwstd	9.565	SCF					
RUN #				Vmstd	50.122	SCF					
DATE	6/20/2011			Vtstd	59.687	SCF					
TIME	13:41			% H2O	16.0	%					
FUND #	15726			% Isokin	100.5	%					
DUST LOADING DATA SHEET				DCL	0.0009	grains/SCF					
Sample Pt.	BH OUT DWN LG										
Traverse Pt.	3' BIN			Ps =	27.83	in. Hg Abs.					
Pb (Barometric Press.)	28.17 in Hg			Ts =	684	°R					
Elevation correction	5 ft (1 in Hg / 1000 ft)										
Ps (Stack Pressure)	-4.6 in H2O			VS (Stack Velocity)		1613	ft/min				
Dn (Nozzle Diam.)	0.280 in			QN (Nozzle Flow Rate)		0.6898	ACFM				
Est. ΔP (Pitot)	0.16 in H2O			QM (Meter Flow Rate)		0.4247	ACFM				
Cm	1.040			ΔH (orifice)		0.48	in H2O				
Cp	0.84 (Type S=.84, Std=.99)			Seconds/Rev		14.1					
Est. Ts (Stack Temp)	224 °F										
Est. % H2O	16			O2 %		17.9					
ΔH@	1.57			CO ppm		4					
Tm (Est)	70 °F			NO ppm		250					
ΔH (Est)	0.70 in Hg			NO2 ppm		5					
				SO2 ppm		0					
				CO2 %							
				coal CO2=18.6*(21-02%)/21							
<i>Note: Standard Temperature and Pressure are 68 oF and 29.92 in. Hg</i>											
Time (min.)	Temp stack	Gas Meter (ft3)	Tm Inlet	Tm Outlet	ΔH	ΔP Pitot	Pump Vac in Hg	251	Temp Box	Temp Impinger	
0	224	179.509	63	63	0.49	0.16	1.6	248		OK	
15	224	185.730	64	63	0.49	0.16	1.8	251		OK	
30	224	192.050	66	62	0.49	0.16	1.8	251		OK	
45	224	198.430	67	61	0.49	0.16	1.9	251		OK	
60	224	204.870	67	63	0.49	0.16	1.9	251		OK	
75	224	211.260	68	62	0.49	0.16	1.9	251		OK	
90	224	217.590	68	63	0.49	0.16	1.9	250		OK	
105	224	224.010	68	63	0.49	0.16	1.9	250		OK	
120	224	230.333	68	64	0.49	0.16	1.9	250		OK	
120											
Averages:	224	50.824	65		0.49	0.16	1.8	250	#DIV/0!	#DIV/0!	
Comments											

Sample Pt.	BH OUT DWN LG		Date	6/20/2011
			Run #	0
Train Type			Fund #	15726
			Cost Center #	
STOPPER TYPE	TYPE OF SOLUTION	INITIAL WT. (g)	FINAL WT. (g)	NET WT. (g)
Straight	DI	801.1	965.8	164.7
Straight	DI	641.3	665.1	23.8
Impinger	DRY	668.0	671.5	3.5
Straight	SIL GEL	970.7	981.9	11.2
Straight				0.0
Straight				0.0
Impinger				0.0
Straight				0.0
			TOTAL H2O (g)	203.2
FILTER		0.23764	0.23956	0.00192
		0.79651	0.79767	0.00116
Additional Dust				0.00000
			TOTAL DUST (g)	0.00308
Vwstd	9.565	SCF		
Vmstd	50.122	SCF		
Vtstd	59.687	SCF		
% H2O	16.0	%		
% Isokinetic	100.5	%		
DCL	0.0009	grains/SCF		
DCL - Metric	0.0022	grams/SCM = grains/SCF*2.288		
DUST LOADING CALCULATIONS (Concentration Basis)				
Inlet DCL			0.0022	grains/SCF
% Efficiency = (Inlet DCL - Outlet DCL) * 100 Inlet DCL			56.9011	%
Pipe Area				ft2
ACFM = VS * Pipe Area (ft2)			0.0000	ACFM
SCFM = ACFM * PS/TS * 17.64			0.0	SCFM
lbs/hour = grains/scf * 0.000143 * SCFM * 60			0.0000	lbs/hour

Equations		
Page 1		
PS (Stack Pressure)	=PB + (PS in H2O / 13.6) - elevation/1000	in. Hg Abs.
TS (Stack Temperature)	=average TS oF + 460	oR
VS (Stack Velocity)ft/min	=60*85.49 * Cp * sqrt(P * TS oR / PS in Hg Abs / MS)	ft/min
MS	=30 * (1-%H2O/100) + 18 * %H2O/100	g/mol
QN (Nozzle Flow Rate)	=VS * pi * DN2 / 576	ACFM
QM (Meter Flow Rate)	=QN * TM * PS in Hg Abs/(Cm * TS oR * (HM /13.6)) - (1-%H2O/100)	ACFM
H (orifice)	=QM2 * H@ * (PB + HM /13.6)/(0.03175 * (TM + 460))	in H2O
Seconds/Rev	=1/(QM / 0.1 / 60)	
Page 2		
VWstd	=0.04707 * (H2O g)	SCF
VMstd	=17.64 * VWstd * Cm * (PB+ HM /13.6 - Elevation/1000)	SCF
VTstd	=VWstd + VMstd	SCF
% H2O	=(VWstd / VTstd) * 100	%
% Isokinetic	= 0.0945 * TS oR * VMstd * 60 sec/min * 144 in2/ft2 (PS in Hg Abs * VS * (DN2/4*pi) * time min * (1-%H2O/100)	%
DCL	=15.43 * (dust g) / VMstd	grains/SCF
% Efficiency	=(Inlet DCL - Outlet DCL) / Inlet DCL * 100	%
ACFM	=VS * Pipe Area (ft2)	ACFM
SCFM	=ACFM * PS / TS * 17.64	SCFM
lbs/hour	=grains/SCF * 0.000143 * SCFM * 60 min/hr	lbs/hour
PPM Calculation		
PPM	=Conc mg/L * Vol mL * L/1000 mL * 2.205e-6 lb/mg * 387 ft3/mol / VTstd * e6	
Stack Vel ft./sec.	Vs=85.49*Cp*SQRT Dp*SQRT(Ts/Ps/Mw)	
Mol Wt. Wet	Mw=30*(1-Bws)+18*Bws	

ID			
Run #			
Start Time			
Fund #			
Vt Std			ft ³
Volume of Sample			mL
Concentration			mg/L or ppm
Molecular Weight			g/mole
Molecular Weights (g/mole)			
SO3	80.06		
SO2	64.06		
NH3	17.04		
Cl2	70.90		
HCl	36.46		
F2	38.00		
HF	20.02		
Hg	200.59		
#DIV/O!	ppm in flue gas		
387 ft ³ /mol at 68oF			

DATE	ID	SAMPLE PORT	SAMPLER	START TIME	TEST TIME	BARO PRESS (in Hg)	STACK PRESS (in H2O)	TEMP (F)	O2%	ΔP	NOZ DIA	METER VOL (cf)	GAS METER VOL (cf)	TOTAL H2O	TOTAL DUST	VMSTD (SCF)	VTSTD (SCF)	% H2O	METER TEMP	ΔH	ISO	%	DLC GRAINS/SCF
6/20/2011	KEETAC-BHOUT-M5BH	OUT DWN LG	RS	13:41	120	28.17	-4.6	224	17.9	0.16	0.280	50.824	50.824	203.2	0.00308	50.122	59.667	16.0	65	0.49	100.5		0.0009

OPERATORS		RS								
ID		KEETAC-BHOUT-M5-3			Vwstd	10.087	SCF			
RUN #					Vmstd	51.992	SCF			
DATE		6/17/2011			Vtstd	62.079	SCF			
TIME					% H2O	16.2	%			
FUND #		15726			% Isokin	104.2	%			
DUST LOADING DATA SHEET					DCL	0.0006	grains/SCF			
Sample Pt.		BH OUT DWN LG								
Traverse Pt.		3' BIN			Ps =	27.97	in. Hg Abs.			
Pb (Barometric Press.)		28.20	in Hg		Ts =	684	°R			
Elevation correction		5 ft (1 in Hg / 1000 ft)								
Ps (Stack Pressure)		-3.0 in H2O			VS (Stack Velocity)		1607	ft/min		
Dn (Nozzle Diam.)		0.280 in			QN (Nozzle Flow Rate)		0.6871	ACFM		
Est. ΔP (Pitot)		0.16 in H2O			QM (Meter Flow Rate)		0.4400	ACFM		
Cm		1.040			ΔH (orifice)		0.50	in H2O		
Cp		0.84 (Type S=.84, Std=.99)			Seconds/Rev		13.6			
Est. Ts (Stack Temp)		224 °F								
Est. % H2O		16			O2 %		17.9			
ΔH@		1.57			CO ppm		4			
Tm (Est)		85 °F			NO ppm		228			
ΔH (Est)		0.70 in Hg			NO2 ppm		2			
					SO2 ppm		0			
					CO2 %					
					coal CO2=18.6*(21-02%)/21					
<i>Note: Standard Temperature and Pressure are 68 oF and 29.92 in. Hg</i>										
Time (min.)	Temp stack	Gas Meter (ft3)	Tm Inlet	Tm Outlet	ΔH	ΔP Pitot	Pump Vac in Hg	Temp Probe	Temp Box	Temp Impinger
0	224	126.170	71	71	0.53	0.16	1.5	249		OK
30	224	139.530	73	68	0.53	0.16	1.5	250		OK
60	224	152.370	75	67	0.53	0.16	1.5	250		OK
90	224	166.130	76	69	0.53	0.16	1.5	250		OK
120	224	179.470	73	67	0.53	0.16	1.5	250		OIK
120										
Averages:	224	53.300	71		0.53	0.16	1.5	250	#DIV/0!	#DIV/0!
Comments										

Sample Pt.	BH OUT DWN LG		Date	6/17/2011
			Run #	0
Train Type			Fund #	15726
			Cost Center #	
STOPPER TYPE	TYPE OF SOLUTION	INITIAL WT. (g)	FINAL WT. (g)	NET WT. (g)
Straight	KCl	838.8	1009.9	171.1
Straight	KCl	637.6	662.4	24.8
Impinger	KCl	616.1	623.8	7.7
Straight	H2O2	986.0	996.7	10.7
Straight	KMnO4			0.0
Straight	KMnO4			0.0
Impinger	KMnO4			0.0
Straight	Silica Gel			0.0
			TOTAL H2O (g)	214.3
FILTER		0.24222	0.24357	0.00135
				0.00000
Additional Dust		0.79573	0.79643	0.00070
			TOTAL DUST (g)	0.00205
Vwstd	10.087	SCF		
Vmstd	51.992	SCF		
Vtstd	62.079	SCF		
% H2O	16.2	%		
% Isokinetic	104.2	%		
DCL	0.0006	grains/SCF		
DCL - Metric	0.0014	grams/SCM = grains/SCF*2.288		
DUST LOADING CALCULATIONS (Concentration Basis)				
Inlet DCL			0.0027	grains/SCF
% Efficiency = (Inlet DCL - Outlet DCL) * 100 / Inlet DCL			77.4670	%
Pipe Area				ft2
ACFM = VS * Pipe Area (ft2)			0.0000	ACFM
SCFM = ACFM * PS/TS * 17.64			0.0	SCFM
lbs/hour = grains/scf * 0.000143 * SCFM * 60			0.0000	lbs/hour

Equations		
Page 1		
PS (Stack Pressure)	=PB + (PS in H2O / 13.6) - elevation/1000	in. Hg Abs.
TS (Stack Temperature)	=average TS oF + 460	oR
VS (Stack Velocity)ft/min	=60*85.49 * Cp * sqrt(P * TS oR / PS in Hg Abs / MS)	ft/min
MS	=30 * (1-%H2O/100) + 18 * %H2O/100	g/mol
QN (Nozzle Flow Rate)	=VS * pi * DN2 / 576	ACFM
QM (Meter Flow Rate)	=QN * TM * PS in Hg Abs/(Cm * TS oR * (HM /13.6)) - (1-%H2O/100)	ACFM
H (orifice)	=QM2 * H@ * (PB + HM /13.6)/(0.03175 * (TM + 460))	in H2O
Seconds/Rev	=1/(QM / 0.1 / 60)	
Page 2		
VWstd	=0.04707 * (H2O g)	SCF
VMstd	=17.64 * VWstd * Cm * (PB+ HM /13.6 - Elevation/1000)	SCF
VTstd	=VWstd + VMstd	SCF
% H2O	=(VWstd / VTstd) * 100	%
% Isokinetic	= 0.0945 * TS oR * VMstd * 60 sec/min * 144 in2/ft2 (PS in Hg Abs * VS * (DN2/4*pi) * time min * (1-%H2O/100)	%
DCL	=15.43 * (dust g) / VMstd	grains/SCF
% Efficiency	=(Inlet DCL - Outlet DCL) / Inlet DCL * 100	%
ACFM	=VS * Pipe Area (ft2)	ACFM
SCFM	=ACFM * PS / TS * 17.64	SCFM
lbs/hour	=grains/SCF * 0.000143 * SCFM * 60 min/hr	lbs/hour
PPM Calculation		
PPM	=Conc mg/L * Vol mL * L/1000 mL * 2.205e-6 lb/mg * 387 ft3/mol / VTstd * e6	
Stack Vel ft./sec.	Vs=85.49*Cp*SQRT Dp*SQRT(Ts/Ps/Mw)	
Mol Wt. Wet	Mw=30*(1-Bws)+18*Bws	

ID			
Run #			
Start Time			
Fund #			
Vt Std			ft ³
Volume of Sample			mL
Concentration			mg/L or ppm
Molecular Weight			g/mole
Molecular Weights (g/mole)			
SO3	80.06		
SO2	64.06		
NH3	17.04		
Cl2	70.90		
HCl	36.46		
F2	38.00		
HF	20.02		
Hg	200.59		
#DIV/0!	ppm in flue gas		
387 ft ³ /mol at 68oF			

DATE	ID	SAMPLE PORT	SAMPLER	START TIME	TEST TIME	BARO PRESS (in Hg)	STACK PRESS (in H2O)	TEMP (F)	O2%	ΔP	NOZ DIA	GAS METER VOL (cf)	TOTAL H2O	TOTAL DUST	VTSTD (SCF)	% H2O	METER TEMP	ΔH	% ISO	DLC GRAINS/SCF	
6/7/2011	KEETAC-BHOUT-MESH	OUT DWN LG	RS	0:00	1:20	28.20	-3	224	17.9	0.16	0.280	53.300	214.3	0.00205	51.992	62.079	16.2	71	0.53	104.2	0.00068

OPERATORS		RS									
ID	KEETAC-BHIN-M5-6-2					Vwstd	16.296	SCF			
RUN #	2					Vmstd	78.373	SCF			
DATE	6/30/2011					Vtstd	94.669	SCF			
TIME	16:17					% H2O	17.2	%			
FUND #	15726					% Isokin	101.1	%			
DUST LOADING DATA SHEET						DCL	0.0045	grains/SCF			
Sample Pt.	BHIN DWN LG										
Traverse Pt.	3' IN					Ps =	28.02	in. Hg Abs.			
Pb (Barometric Press.)	28.05 in Hg					Ts =	626	°R			
Elevation correction	20 ft (1 in Hg / 1000 ft)										
Ps (Stack Pressure)	-0.2 in H2O					VS (Stack Velocity)		1538	ft/min		
Dn (Nozzle Diam.)	0.280 in					QN (Nozzle Flow Rate)		0.6577	ACFM		
Est. ΔP (Pitot)	0.16 in H2O					QM (Meter Flow Rate)		0.4654	ACFM		
Cm	1.010					ΔH (orifice)		0.52	in H2O		
Cp	0.84 (Type S=.84, Std=.99)					Seconds/Rev		12.9			
Est. Ts (Stack Temp)	166 °F										
Est. % H2O	16					O2 %		16.8			
ΔH@	1.46					CO ppm		3			
Tm (Est)	75 °F					NO ppm		85			
ΔH (Est)	0.60 in Hg					NO2 ppm		3			
						SO2 ppm		10			
						CO2 %					
						coal CO2=18.6*(21-02%)/21					
<i>Note: Standard Temperature and Pressure are 68 oF and 29.92 in. Hg</i>											
Time (min.)	Temp stack	Gas Meter (ft3)	Tm Inlet	Tm Outlet	ΔH	ΔP Pitot	Pump Vac in Hg	Temp Probe	Temp Box	Temp Impinger	
0	166	288.248	75	75	0.52	0.16	3.0	248		OK	
15	166	295.740	78	75	0.53	0.16	3.0	251		OK	
30	166	302.650	80	76	0.54	0.16	3.0	250		OK	
45	166	309.760	81	77	0.54	0.16	3.0	249		OK	
60	166	316.720	82	78	0.54	0.16	3.5	249		OK	
75	166	323.730	83	78	0.54	0.16	4.0	252		OK	
90	166	330.750	82	79	0.54	0.16	4.5	260		OK	
105	166	337.790	82	78	0.54	0.16	5.0	260		OK	
120	166	344.830	83	79	0.54	0.16	5.5	258		OK	
135	166	351.750	83	79	0.54	0.16	5.5	254		OK	
150	166	358.740	81	78	0.54	0.16	5.5	249		OK	
165	166	365.760	81	78	0.54	0.16	6.0	250		OK	
180	166	372.742	80	77	0.54	0.16	6.0	250		OK	
Averages:	166	84.494	79		0.54	0.16	4.4	252	#DIV/0!	#DIV/0!	
Comments	Leak ck OK										

Sample Pt.	BHIN DWN LG		Date	6/30/2011
			Run #	2
Train Type			Fund #	15726
			Cost Center #	
STOPPER TYPE	TYPE OF SOLUTION	INITIAL WT. (g)	FINAL WT. (g)	NET WT. (g)
Straight	DI	802.2	1014.3	212.1
Straight	DI	641.7	739.7	98.0
Impinger	DRY	618.4	627.4	9.0
Straight	SIL GEL	993.5	1020.6	27.1
Straight				0.0
Straight				0.0
Impinger				0.0
Straight	Silica Gel			0.0
			TOTAL H2O (g)	346.2
FILTER		0.24493	0.26753	0.02260
		0.74182	0.74194	0.00012
Additional Dust				0.00000
			TOTAL DUST (g)	0.02272
Vwstd	16.296	SCF		
Vmstd	78.373	SCF		
Vtstd	94.669	SCF		
% H2O	17.2	%		
% Isokinetic	101.1	%		
DCL	0.0045	grains/SCF		
DCL - Metric	0.0102	grams/SCM = grains/SCF*2.288		
DUST LOADING CALCULATIONS (Concentration Basis)				
Inlet DCL				grains/SCF
% Efficiency = (Inlet DCL - Outlet DCL) * 100			#DIV/0!	%
Inlet DCL				
Pipe Area				ft2
ACFM = VS * Pipe Area (ft2)			0.0000	ACFM
SCFM = ACFM * PS/TS * 17.64			0.0	SCFM
lbs/hour = grains/scf * 0.000143 * SCFM * 60			0.0000	lbs/hour

Equations		
Page 1		
PS (Stack Pressure)	=PB + (PS in H2O / 13.6) - elevation/1000	in. Hg Abs.
TS (Stack Temperature)	=average TS oF + 460	oR
VS (Stack Velocity)ft/min	=60*85.49 * Cp * sqrt(P * TS oR / PS in Hg Abs / MS)	ft/min
MS	=30 * (1-%H2O/100) + 18 * %H2O/100	g/mol
QN (Nozzle Flow Rate)	=VS * pi * DN2 / 576	ACFM
QM (Meter Flow Rate)	=QN * TM * PS in Hg Abs/(Cm * TS oR * (HM /13.6)) - (1-%H2O/100)	ACFM
H (orifice)	=QM2 * H@ * (PB + HM /13.6)/(0.03175 * (TM + 460))	in H2O
Seconds/Rev	=1/(QM / 0.1 / 60)	
Page 2		
VWstd	=0.04707 * (H2O g)	SCF
VMstd	=17.64 * VWstd * Cm * (PB+ HM /13.6 - Elevation/1000)	SCF
VTstd	=VWstd + VMstd	SCF
% H2O	=(VWstd / VTstd) * 100	%
% Isokinetic	= 0.0945 * TS oR * VMstd * 60 sec/min * 144 in2/ft2 (PS in Hg Abs * VS * (DN2/4*pi) * time min * (1-%H2O/100)	%
DCL	=15.43 * (dust g) / VMstd	grains/SCF
% Efficiency	=(Inlet DCL - Outlet DCL) / Inlet DCL * 100	%
ACFM	=VS * Pipe Area (ft2)	ACFM
SCFM	=ACFM * PS / TS * 17.64	SCFM
lbs/hour	=grains/SCF * 0.000143 * SCFM * 60 min/hr	lbs/hour
PPM Calculation		
PPM	=Conc mg/L * Vol mL * L/1000 mL * 2.205e-6 lb/mg * 387 ft3/mol / VTstd * e6	
Stack Vel ft./sec.	Vs=85.49*Cp*SQRT Dp*SQRT(Ts/Ps/Mw)	
Mol Wt. Wet	Mw=30*(1-Bws)+18*Bws	

ID			
Run #			
Start Time			
Fund #			
Vt Std			ft ³
Volume of Sample			mL
Concentration			mg/L or ppm
Molecular Weight			g/mole
Molecular Weights (g/mole)			
SO3	80.06		
SO2	64.06		
NH3	17.04		
Cl2	70.90		
HCl	36.46		
F2	38.00		
HF	20.02		
Hg	200.59		
#DIV/0!	ppm in flue gas		
387 ft ³ /mol at 68oF			

DATE	ID	SAMPLE PORT	SAMPLER	START TIME	TEST TIME	BARO PRESS (in Hg)	STACK PRESS (in H2O)	TEMP (F)	O2%	ΔP	NOZ DIA	GAS METER VOL (cf)	TOTAL H2O	TOTAL DUST	VMSTD (SCF)	VTSTD (SCF)	% H2O	METER TEMP	ΔH	ISO	DLC GRAINS/SCF
6/30/2011	KEETAC-BHIN-M5-6	BHIN DWN LG	RS	16:17	180	28.05	-0.2	166	16.8	0.16	0.280	84.494	346.2	0.02272	78.373	94.669	17.2	79	0.54	101.1	0.0045

OPERATORS		RS									
ID		KEETAC-BHIN-M5-5			Vwstd	14.813	SCF				
RUN #					Vmstd	77.207	SCF				
DATE		6/30/2011			Vtstd	92.020	SCF				
TIME		9:43			% H2O	16.1	%				
FUND #		15726			% Isokin	98.3	%				
DUST LOADING DATA SHEET					DCL	0.0040	grains/SCF				
Sample Pt.		BHIN DWN LG									
Traverse Pt.		3' IN			Ps =	28.07	in. Hg Abs.				
Pb (Barometric Press.)		28.11	in Hg		Ts =	625	°R				
Elevation correction		20 ft (1 in Hg / 1000 ft)									
Ps (Stack Pressure)		-0.3	in H2O		VS (Stack Velocity)		1535	ft/min			
Dn (Nozzle Diam.)		0.280	in		QN (Nozzle Flow Rate)		0.6566	ACFM			
Est. ΔP (Pitot)		0.16	in H2O		QM (Meter Flow Rate)		0.4565	ACFM			
Cm		1.010			ΔH (orifice)		0.51	in H2O			
Cp		0.84 (Type S=.84, Std=.99)			Seconds/Rev		13.1				
Est. Ts (Stack Temp)		165	°F								
Est. % H2O		16			O2 %		17.1				
ΔH@		1.46			CO ppm		3				
Tm (Est)		65	°F		NO ppm		102				
ΔH (Est)		0.60	in Hg		NO2 ppm		0				
					SO2 ppm		8				
					CO2 %						
					coal CO2=18.6*(21-02%)/21						
<i>Note: Standard Temperature and Pressure are 68 oF and 29.92 in. Hg</i>											
Time (min.)	Temp stack	Gas Meter (ft3)	Tm Inlet	Tm Outlet	ΔH	ΔP Pitot	Pump Vac in Hg	Temp Probe	Temp Box	Temp Impinger	
0	165	206.629	64	65	0.51	0.16	2.0	251		OK	
15	165	213.240	67	64	0.52	0.16	2.0	251		OK	
30	165	219.980	69	65	0.52	0.16	2.0	250		OK	
45	165	226.770	71	66	0.52	0.16	2.0	250		OK	
60	165	233.560	72	67	0.52	0.16	2.5	250		OK	
75	165	240.330	71	67	0.52	0.16	3.0	253		OK	
90	165	247.130	72	68	0.52	0.16	3.0	249		OK	
105	165	253.890	73	69	0.52	0.16	3.5	251		OK	
120	165	260.850	73	69	0.52	0.16	3.5	249		OK	
135	165	267.670	73	69	0.52	0.16	4.0	251		OK	
150	165	274.480	74	69	0.52	0.16	4.5	249		OK	
165	165	281.42	75	70	0.52	0.16	5	252		OK	
180	165	288.217	76	71	0.52	0.16	5.5	251		OK	
Averages:	165	81.588	70		0.52	0.16	3.3	251	#DIV/0!	#DIV/0!	
Comments	Leak check OK										

Sample Pt.	BHIN DWN LG		Date	6/30/2011
			Run #	0
Train Type			Fund #	15726
			Cost Center #	
STOPPER TYPE	TYPE OF SOLUTION	INITIAL WT. (g)	FINAL WT. (g)	NET WT. (g)
Straight	DI	821.7	1025.0	203.3
Straight	DI	640.5	724.2	83.7
Impinger	DRY	618.5	626.0	7.5
Straight	SIL GEL	980.5	1000.7	20.2
Straight				0.0
Straight				0.0
Impinger				0.0
Straight	Silica Gel			0.0
			TOTAL H2O (g)	314.7
FILTER		0.23651	0.25662	0.02011
		0.74168	0.74182	0.00014
Additional Dust				0.00000
			TOTAL DUST (g)	0.02025
Vwstd	14.813	SCF		
Vmstd	77.207	SCF		
Vtstd	92.020	SCF		
% H2O	16.1	%		
% Isokinetic	98.3	%		
DCL	0.0040	grains/SCF		
DCL - Metric	0.0093	grams/SCM = grains/SCF*2.288		
DUST LOADING CALCULATIONS (Concentration Basis)				
Inlet DCL				grains/SCF
% Efficiency = (Inlet DCL - Outlet DCL) * 100 Inlet DCL			#DIV/0!	%
Pipe Area				ft2
ACFM = VS * Pipe Area (ft2)			0.0000	ACFM
SCFM = ACFM * PS/TS * 17.64			0.0	SCFM
lbs/hour = grains/scf * 0.000143 * SCFM * 60			0.0000	lbs/hour

Equations		
Page 1		
PS (Stack Pressure)	=PB + (PS in H2O / 13.6) - elevation/1000	in. Hg Abs.
TS (Stack Temperature)	=average TS oF + 460	oR
VS (Stack Velocity)ft/min	=60*85.49 * Cp * sqrt(P * TS oR / PS in Hg Abs / MS)	ft/min
MS	=30 * (1-%H2O/100) + 18 * %H2O/100	g/mol
QN (Nozzle Flow Rate)	=VS * pi * DN2 / 576	ACFM
QM (Meter Flow Rate)	=QN * TM * PS in Hg Abs/(Cm * TS oR * (HM /13.6)) - (1-%H2O/100)	ACFM
H (orifice)	=QM2 * H@ * (PB + HM /13.6)/(0.03175 * (TM + 460))	in H2O
Seconds/Rev	=1/(QM / 0.1 / 60)	
Page 2		
VWstd	=0.04707 * (H2O g)	SCF
VMstd	=17.64 * VWstd * Cm * (PB+ HM /13.6 - Elevation/1000)	SCF
VTstd	=VWstd + VMstd	SCF
% H2O	=(VWstd / VTstd) * 100	%
% Isokinetic	= 0.0945 * TS oR * VMstd * 60 sec/min * 144 in2/ft2 (PS in Hg Abs * VS * (DN2/4*pi) * time min * (1-%H2O/100))	%
DCL	=15.43 * (dust g) / VMstd	grains/SCF
% Efficiency	=(Inlet DCL - Outlet DCL) / Inlet DCL * 100	%
ACFM	=VS * Pipe Area (ft2)	ACFM
SCFM	=ACFM * PS / TS * 17.64	SCFM
lbs/hour	=grains/SCF * 0.000143 * SCFM * 60 min/hr	lbs/hour
PPM Calculation		
PPM	=Conc mg/L * Vol mL * L/1000 mL * 2.205e-6 lb/mg * 387 ft3/mol / VTstd * e6	
Stack Vel ft./sec.	Vs=85.49*Cp*SQRT Dp*SQRT(Ts/Ps/Mw)	
Mol Wt. Wet	Mw=30*(1-Bws)+18*Bws	

ID			
Run #			
Start Time			
Fund #			
Vt Std			ft ³
Volume of Sample			mL
Concentration			mg/L or ppm
Molecular Weight			g/mole
Molecular Weights (g/mole)			
SO3	80.06		
SO2	64.06		
NH3	17.04		
Cl2	70.90		
HCl	36.46		
F2	38.00		
HF	20.02		
Hg	200.59		
#DIV/0!	ppm in flue gas		
387 ft ³ /mol at 68oF			

DATE	ID	SAMPLE PORT	SAMPLER	START TIME	TEST TIME	BARO		STACK		NOZ DIA	GAS		VTSTD	% H2O	METER TEMP	DLC			
						PRESS (in Hg)	PRESS (in H2O)	TEMP (F)	TEMP (F)		METER VOL (cf)	TOTAL H2O					TOTAL DUST	VMSTDI (SCF)	% H2O
6/30/2011	KEETAC-BHIN-M5-5	BHIN DWN LG	RS	9:43	180	28.11	-0.3	165	17.1	0.16	81.588	314.7	77.207	92.020	16.1	70	0.52	98.3	0.0040

OPERATORS		RS									
ID	KEETAC-BHIN-M5-4			Vwstd	9.969	SCF					
RUN #				Vmstd	52.138	SCF					
DATE	6/20/2011			Vtstd	62.107	SCF					
TIME	13:50			% H2O	16.1	%					
FUND #	15726			% Isokin	99.3	%					
DUST LOADING DATA SHEET				DCL	0.0022	grains/SCF					
Sample Pt.	DWN LG BHIN										
Traverse Pt.	3' IN			Ps =	28.14	in. Hg Abs.					
Pb (Barometric Press.)	28.17 in Hg			Ts =	622	°R					
Elevation correction	20 ft (1 in Hg / 1000 ft)										
Ps (Stack Pressure)	-0.2 in H2O			VS (Stack Velocity)	1530		ft/min				
Dn (Nozzle Diam.)	0.280 in			QN (Nozzle Flow Rate)	0.6542		ACFM				
Est. ΔP (Pitot)	0.16 in H2O			QM (Meter Flow Rate)	0.4552		ACFM				
Cm	1.010			ΔH (orifice)	0.51		in H2O				
Cp	0.84 (Type S=.84, Std=.99)			Seconds/Rev	13.2						
Est. Ts (Stack Temp)	162 °F										
Est. % H2O	16			O2 %	17.9						
ΔH@	1.46			CO ppm	3						
Tm (Est)	63 °F			NO ppm	253						
ΔH (Est)	0.80 in Hg			NO2 ppm	6						
				SO2 ppm	0						
				CO2 %							
				coal CO2=18.6*(21-02%)/21							
<i>Note: Standard Temperature and Pressure are 68 oF and 29.92 in. Hg</i>											
Time (min.)	Temp stack	Gas Meter (ft3)	Tm Inlet	Tm Outlet	ΔH	ΔP Pitot	Pump Vac in Hg	Temp Probe	Temp Box	Temp Impinger	
0	162	152.282	58	58	0.53	0.16	1.0	250		OLK	
15	162	159.080	61	59	0.50	0.16	1.0	249		OK	
30	162	165.850	62	59	0.50	0.16	1.0	252		OK	
45	163	172.660	64	60	0.50	0.16	1.0	250		OK	
60	162	179.430	66	62	0.50	0.16	1.0	252		OK	
75	162	186.170	67	63	0.50	0.16	1.0	251		OK	
90	162	192.890	68	64	0.50	0.16	1.5	251		OK	
105	162	199.630	68	64	0.50	0.16	2.0	251		OK	
120	162	206.586	68	64	0.50	0.16	2.0	251		OK	
120											
Averages:	162	54.304	63		0.50	0.16	1.3	251	#DIV/0!	#DIV/0!	
Comments											

Sample Pt.	DWN LG BHIN		Date	6/20/2011
			Run #	0
Train Type			Fund #	15726
			Cost Center #	
STOPPER TYPE	TYPE OF SOLUTION	INITIAL WT. (g)	FINAL WT. (g)	NET WT. (g)
Straight	DI	811.1	980.1	169.0
Straight	DI	640.4	666.2	25.8
Impinger	DRY	618.2	623.8	5.6
Straight	SIL GEL	969.3	980.7	11.4
Straight				0.0
Straight				0.0
Impinger				0.0
Straight	Silica Gel			0.0
			TOTAL H2O (g)	211.8
FILTER		0.23076	0.23762	0.00686
		0.74072	0.74139	0.00067
Additional Dust				0.00000
			TOTAL DUST (g)	0.00753
Vwstd	9.969	SCF		
Vmstd	52.138	SCF		
Vtstd	62.107	SCF		
% H2O	16.1	%		
% Isokinetic	99.3	%		
DCL	0.0022	grains/SCF		
DCL - Metric	0.0051	grams/SCM = grains/SCF*2.288		
DUST LOADING CALCULATIONS (Concentration Basis)				
Inlet DCL				grains/SCF
% Efficiency = (Inlet DCL - Outlet DCL) * 100			#DIV/0!	%
Inlet DCL				
Pipe Area				ft2
ACFM = VS * Pipe Area (ft2)			0.0000	ACFM
SCFM = ACFM * PS/TS * 17.64			0.0	SCFM
lbs/hour = grains/scf * 0.000143 * SCFM * 60			0.0000	lbs/hour

Equations		
Page 1		
PS (Stack Pressure)	=PB + (PS in H2O / 13.6) - elevation/1000	in. Hg Abs.
TS (Stack Temperature)	=average TS oF + 460	oR
VS (Stack Velocity)ft/min	=60*85.49 * Cp * sqrt(P * TS oR / PS in Hg Abs / MS)	ft/min
MS	=30 * (1-%H2O/100) + 18 * %H2O/100	g/mol
QN (Nozzle Flow Rate)	=VS * pi * DN2 / 576	ACFM
QM (Meter Flow Rate)	=QN * TM * PS in Hg Abs/(Cm * TS oR * (HM /13.6)) - (1-%H2O/100)	ACFM
H (orifice)	=QM2 * H@ * (PB + HM /13.6)/(0.03175 * (TM + 460))	in H2O
Seconds/Rev	=1/(QM / 0.1 / 60)	
Page 2		
VWstd	=0.04707 * (H2O g)	SCF
VMstd	=17.64 * VWstd * Cm * (PB+ HM /13.6 - Elevation/1000)	SCF
VTstd	=VWstd + VMstd	SCF
% H2O	=(VWstd / VTstd) * 100	%
% Isokinetic	= 0.0945 * TS oR * VMstd * 60 sec/min * 144 in2/ft2 (PS in Hg Abs * VS * (DN2/4*pi) * time min * (1-%H2O/100)	%
DCL	=15.43 * (dust g) / VMstd	grains/SCF
% Efficiency	=(Inlet DCL - Outlet DCL) / Inlet DCL * 100	%
ACFM	=VS * Pipe Area (ft2)	ACFM
SCFM	=ACFM * PS / TS * 17.64	SCFM
lbs/hour	=grains/SCF * 0.000143 * SCFM * 60 min/hr	lbs/hour
PPM Calculation		
PPM	=Conc mg/L * Vol mL * L/1000 mL * 2.205e-6 lb/mg * 387 ft3/mol / VTstd * e6	
Stack Vel ft./sec.	Vs=85.49*Cp*SQRT Dp*SQRT(Ts/Ps/Mw)	
Mol Wt. Wet	Mw=30*(1-Bws)+18*Bws	

ID			
Run #			
Start Time			
Fund #			
Vt Std			ft ³
Volume of Sample			mL
Concentration			mg/L or ppm
Molecular Weight			g/mole
Molecular Weights (g/mole)			
SO3	80.06		
SO2	64.06		
NH3	17.04		
Cl2	70.90		
HCl	36.46		
F2	38.00		
HF	20.02		
Hg	200.59		
#DIV/O!	ppm in flue gas		
387 ft ³ /mol at 68oF			

DATE	ID	SAMPLE PORT	SAMPLER	START TIME	TEST TIME	BARO PRESS (in Hg)	STACK PRESS (in H2O)	TEMP (F)	O2%	ΔP	NOZ DIA	GAS METER VOL (cf)	TOTAL H2O	TOTAL DUST	VMSTD (SCF)	VTSTD (SCF)	% H2O	METER TEMP	ΔH	% ISO	DLC GRAINS/SCF
6/20/2011	KEETAC-BHIN-M5-4	DWN LG BHIN	RS	13:50	120	28.17	-0.15	162	17.9	0.16	0.280	54.304	211.8	0.00753	52.138	62.107	16.1	63	0.50	99.3	0.0022

OPERATORS		RS								
ID		KEETAC-BHIN-M5-3				Vwstd	10.770	SCF		
RUN #						Vmstd	55.416	SCF		
DATE		6/18/2011				Vtstd	66.186	SCF		
TIME		14:51				% H2O	16.3	%		
FUND #		15726				% Isokin	104.1	%		
DUST LOADING DATA SHEET						DCL	0.0027	grains/SCF		
Sample Pt.		BH IN DWN LG								
Traverse Pt.		3' IN				Ps =	28.17	in. Hg Abs.		
Pb (Barometric Press.)		28.20	in Hg			Ts =	605	°R		
Elevation correction		20	ft (1 in Hg / 1000 ft)							
Ps (Stack Pressure)		-0.2	in H2O			VS (Stack Velocity)		1506	ft/min	
Dn (Nozzle Diam.)		0.280	in			QN (Nozzle Flow Rate)		0.6440	ACFM	
Est. ΔP (Pitot)		0.16	in H2O			QM (Meter Flow Rate)		0.4614	ACFM	
Cm		1.010				ΔH (orifice)		0.53	in H2O	
Cp		0.84	(Type S=.84, Std=.99)			Seconds/Rev		13.0		
Est. Ts (Stack Temp)		145	°F							
Est. % H2O		16				O2 %		17.8		
ΔH@		1.46				CO ppm		4		
Tm (Est)		60	°F			NO ppm		233		
ΔH (Est)		0.80	in Hg			NO2 ppm		2		
						SO2 ppm		0		
						CO2 %				
						coal CO2=18.6*(21-02%)/21				
<i>Note: Standard Temperature and Pressure are 68 oF and 29.92 in. Hg</i>										
Time (min.)	Temp stack	Gas Meter (ft3)	Tm Inlet	Tm Outlet	ΔH	ΔP Pitot	Pump Vac in Hg	Temp Probe	Temp Box	Temp Impinger
0	145	93.415	67	67	0.60	0.16	3.0	251		OK
30	145	107.390	75	69	0.60	0.16	3.0	250		OK
60	145	122.970	79	72	0.60	0.16	4.0	248		OK
90	145	137.390	80	74	0.60	0.16	4.0	248		OK
120	145	152.253	81	75	0.60	0.16	4.0	250		OK
120										
Averages:	145	58.838	74		0.60	0.16	3.6	249	#DIV/0!	#DIV/0!
Comments										

Sample Pt.	BH IN DWN LG		Date	6/18/2011
			Run #	0
Train Type			Fund #	15726
			Cost Center #	
STOPPER TYPE	TYPE OF SOLUTION	INITIAL WT. (g)	FINAL WT. (g)	NET WT. (g)
Straight	KCl	854.5	1016.3	161.8
Straight	KCl	636.1	681.8	45.7
Impinger	KCl	641.3	647.9	6.6
Straight	H2O2	948.7	963.4	14.7
Straight	KMnO4			0.0
Straight	KMnO4			0.0
Impinger	KMnO4			0.0
Straight	Silica Gel			0.0
			TOTAL H2O (g)	228.8
FILTER		0.23647	0.24528	0.00881
		0.74021	0.74072	0.00051
Additional Dust		0.74021	0.74072	0.00051
			TOTAL DUST (g)	0.00983
Vwstd	10.770	SCF		
Vmstd	55.416	SCF		
Vtstd	66.186	SCF		
% H2O	16.3	%		
% Isokinetic	104.1	%		
DCL	0.0027	grains/SCF		
DCL - Metric	0.0063	grams/SCM = grains/SCF*2.288		
DUST LOADING CALCULATIONS (Concentration Basis)				
Inlet DCL			0.0060	grains/SCF
% Efficiency = (Inlet DCL - Outlet DCL) * 100			54.3678	%
Inlet DCL			76.60%	
Pipe Area				ft2
ACFM = VS * Pipe Area (ft2)			0.0000	ACFM
SCFM = ACFM * PS/TS * 17.64			0.0	SCFM
lbs/hour = grains/scf * 0.000143 * SCFM * 60			0.0000	lbs/hour

Equations		
Page 1		
PS (Stack Pressure)	=PB + (PS in H2O / 13.6) - elevation/1000	in. Hg Abs.
TS (Stack Temperature)	=average TS oF + 460	oR
VS (Stack Velocity)ft/min	=60*85.49 * Cp * sqrt(P * TS oR / PS in Hg Abs / MS)	ft/min
MS	=30 * (1-%H2O/100) + 18 * %H2O/100	g/mol
QN (Nozzle Flow Rate)	=VS * pi * DN2 / 576	ACFM
QM (Meter Flow Rate)	=QN * TM * PS in Hg Abs/(Cm * TS oR * (HM /13.6)) - (1-%H2O/100)	ACFM
H (orifice)	=QM2 * H@ * (PB + HM /13.6)/(0.03175 * (TM + 460))	in H2O
Seconds/Rev	=1/(QM / 0.1 / 60)	
Page 2		
VWstd	=0.04707 * (H2O g)	SCF
VMstd	=17.64 * VWstd * Cm * (PB+ HM /13.6 - Elevation/1000)	SCF
VTstd	=VWstd + VMstd	SCF
% H2O	=(VWstd / VTstd) * 100	%
% Isokinetic	= 0.0945 * TS oR * VMstd * 60 sec/min * 144 in2/ft2 (PS in Hg Abs * VS * (DN2/4*pi) * time min * (1-%H2O/100)	%
DCL	=15.43 * (dust g) / VMstd	grains/SCF
% Efficiency	=(Inlet DCL - Outlet DCL) / Inlet DCL * 100	%
ACFM	=VS * Pipe Area (ft2)	ACFM
SCFM	=ACFM * PS / TS * 17.64	SCFM
lbs/hour	=grains/SCF * 0.000143 * SCFM * 60 min/hr	lbs/hour
PPM Calculation		
PPM	=Conc mg/L * Vol mL * L/1000 mL * 2.205e-6 lb/mg * 387 ft3/mol / VTstd * e6	
Stack Vel ft./sec.	Vs=85.49*Cp*SQRT Dp*SQRT(Ts/Ps/Mw)	
Mol Wt. Wet	Mw=30*(1-Bws)+18*Bws	

ID			
Run #			
Start Time			
Fund #			
Vt Std			ft ³
Volume of Sample			mL
Concentration			mg/L or ppm
Molecular Weight			g/mole
Molecular Weights (g/mole)			
SO3	80.06		
SO2	64.06		
NH3	17.04		
Cl2	70.90		
HCl	36.46		
F2	38.00		
HF	20.02		
Hg	200.59		
#DIV/0!	ppm in flue gas		
387 ft ³ /mol at 68oF			

DATE	ID	SAMPLE PORT	SAMPLER	START TIME	TEST TIME	BARO PRESS (in Hg)	STACK PRESS (in H2O)	TEMP (F)	O2%	ΔP	NOZ DIA	GAS METER VOL (cf)	TOTAL H2O	TOTAL DUST	VMSTD (SCF)	VTSTD (SCF)	% H2O	METER TEMP	ΔH	ISO	DLG GRAINS/SCF
6/18/2011	KEETAC-BHIN-M5-3	BH IN DWN LG	RS	14:51	120	28.20	-0.15	145	17.8	0.16	0.280	58.838	228.8	0.00883	55.416	66.186	15.3	74	0.60	104.1	0.0027

OPERATORS		RS									
ID	KEETAC-BHIN-M5-2				Vwstd	4.024	SCF				
RUN #					Vmstd	21.826	SCF				
DATE	6/16/2011				Vtstd	25.851	SCF				
TIME	14:10				% H2O	15.6	%				
FUND #	15726				% Isokin	105.6	%				
DUST LOADING DATA SHEET					DCL	0.0026	grains/SCF				
Sample Pt.	DWN LEG BH IN										
Traverse Pt.	3' IN				Ps =	28.90	in. Hg Abs.				
Pb (Barometric Press.)	29.00 in Hg				Ts =	608	°R				
Elevation correction	20 ft (1 in Hg / 1000 ft)										
Ps (Stack Pressure)	-1.1 in H2O				VS (Stack Velocity)		1705	ft/min			
Dn (Nozzle Diam.)	0.280 in				QN (Nozzle Flow Rate)		0.7293	ACFM			
Est. ΔP (Pitot)	0.21 in H2O				QM (Meter Flow Rate)		0.5248	ACFM			
Cm	1.010				ΔH (orifice)		0.70	in H2O			
Cp	0.84 (Type S=.84, Std=.99)				Seconds/Rev		11.4				
Est. Ts (Stack Temp)	148 °F										
Est. % H2O	15						O2 %				
ΔH@	1.46						CO ppm				
Tm (Est)	62 °F						NO ppm				
ΔH (Est)	0.50 in Hg						NO2 ppm				
							SO2 ppm				
							CO2 %				
							coal CO2=18.6*(21-02%)/21				
<i>Note: Standard Temperature and Pressure are 68 oF and 29.92 in. Hg</i>											
Time (min.)	Temp stack	Gas Meter (ft3)	Tm Inlet	Tm Outlet	ΔH	ΔP Pitot	Pump Vac in Hg	Temp Probe	Temp Box	Temp Impinger	
0	148	71.320	59	59	0.80	0.21	3.0	250		OK	
30	148		68	61	0.70	0.21	4.0	250		OK	
40	148	93.385	68	62	0.60	0.21	4.5	250		OK	
40					0.50						
Averages:	148	22.065	63		0.65	0.21	3.8	250	#DIV/0!	#DIV/0!	
Comments											

Sample Pt.	DWN LEG BH IN		Date	6/16/2011
			Run #	0
Train Type			Fund #	15726
			Cost Center #	
STOPPER TYPE	TYPE OF SOLUTION	INITIAL WT. (g)	FINAL WT. (g)	NET WT. (g)
Straight	DI	654.8	702.5	47.7
Straight	DI	615.8	636.3	20.5
Impinger	DRY	639.0	645.2	6.2
Straight	SIL GEL	960.5	971.6	11.1
Straight				0.0
Straight				0.0
Impinger				0.0
Straight				0.0
			TOTAL H2O (g)	85.5
FILTER		0.21974	0.22343	0.00369
				0.00000
Additional Dust				0.00000
			TOTAL DUST (g)	0.00369
Vwstd	4.024	SCF		
Vmstd	21.826	SCF		
Vtstd	25.851	SCF		
% H2O	15.6	%		
% Isokinetic	105.6	%		
DCL	0.0026	grains/SCF		
DCL - Metric	0.0060	grams/SCM = grains/SCF*2.288		
DUST LOADING CALCULATIONS (Concentration Basis)				
Inlet DCL				grains/SCF
% Efficiency = (Inlet DCL - Outlet DCL) * 100			#DIV/0!	%
Inlet DCL				
Pipe Area				ft2
ACFM = VS * Pipe Area (ft2)			0.0000	ACFM
SCFM = ACFM * PS/TS * 17.64			0.0	SCFM
lbs/hour = grains/scf * 0.000143 * SCFM * 60			0.0000	lbs/hour

Equations		
Page 1		
PS (Stack Pressure)	=PB + (PS in H2O / 13.6) - elevation/1000	in. Hg Abs.
TS (Stack Temperature)	=average TS of + 460	oR
VS (Stack Velocity)ft/min	=60*85.49 * Cp * sqrt(P * TS oR / PS in Hg Abs / MS)	ft/min
MS	=30 * (1-%H2O/100) + 18 * %H2O/100	g/mol
QN (Nozzle Flow Rate)	=VS * pi * DN2 / 576	ACFM
QM (Meter Flow Rate)	=QN * TM * PS in Hg Abs/(Cm * TS oR * (HM /13.6)) - (1-%H2O/100)	ACFM
H (orifice)	=QM2 * H@ * (PB + HM /13.6)/(0.03175 * (TM + 460))	in H2O
Seconds/Rev	=1/(QM / 0.1 / 60)	
Page 2		
VWstd	=0.04707 * (H2O g)	SCF
VMstd	=17.64 * VWstd * Cm * (PB+ HM /13.6 - Elevation/1000)	SCF
VTstd	=VWstd + VMstd	SCF
% H2O	=(VWstd / VTstd) * 100	%
% Isokinetic	= 0.0945 * TS oR * VMstd * 60 sec/min * 144 in2/ft2 (PS in Hg Abs * VS * (DN2/4*pi) * time min * (1-%H2O/100)	%
DCL	=15.43 * (dust g) / VMstd	grains/SCF
% Efficiency	=(Inlet DCL - Outlet DCL) / Inlet DCL * 100	%
ACFM	=VS * Pipe Area (ft2)	ACFM
SCFM	=ACFM * PS / TS * 17.64	SCFM
lbs/hour	=grains/SCF * 0.000143 * SCFM * 60 min/hr	lbs/hour
PPM Calculation		
PPM	=Conc mg/L * Vol mL * L/1000 mL * 2.205e-6 lb/mg * 387 ft3/mol / VTstd * e6	
Stack Vel ft./sec.	Vs=85.49*Cp*SQRT Dp*SQRT(Ts/Ps/Mw)	
Mol Wt. Wet	Mw=30*(1-Bws)+18*Bws	

ID			
Run #			
Start Time			
Fund #			
Vt Std			ft ³
Volume of Sample			mL
Concentration			mg/L or ppm
Molecular Weight			g/mole
Molecular Weights (g/mole)			
SO3	80.06		
SO2	64.06		
NH3	17.04		
Cl2	70.90		
HCl	36.46		
F2	38.00		
HF	20.02		
Hg	200.59		
#DIV/O!	ppm in flue gas		
387 ft ³ /mol at 68oF			

DATE	ID	SAMPLE PORT	SAMPLER	START TIME	TEST TIME	BARO PRESS (in Hg)	STACK PRESS (in H2O)	STACK TEMP (F)	O2%	ΔP	NOZ DIA	GAS METER VOL (cf)	TOTAL H2O	TOTAL DUST	VMSTD (SCF)	% H2O	METER TEMP	ΔH	% ISO	DLC GRAINS/SCF	
6/16/2011	KEETAC-BHIN-M5-2	DWN LEG BH IN	RS	14:10	40	29.00	-1.1	148	0.0	0.21	0.280	22.065	85.5	0.00369	21.826	25.851	15.6	63	0.65	105.6	0.0026

APPENDIX C

COMPLETE SORBENT TRAP AND CMM COMPARISON DATA

(Copies of the original sorbent trap data sheets and the CMM data are available upon request.)

Table C-1. Complete Sorbent Trap and CMM Comparison Data

Sample No.	Units	1A	1B	1A	1B	2A	2B	2A	2B	3A	3B	3A	3B
Trap ID		88413	88410	88425	88419	88443	88406	88423	88376	88402	88417	88420	88385
Date		6/18/11	6/18/11	6/18/11	6/18/11	6/20/11	6/20/11	6/20/11	6/20/11	6/21/11	6/21/11	6/21/11	6/21/11
Time		10:29	10:29	10:36	10:38	10:20	10:22	10:13	10:15	12:02	12:04	11:55	11:57
Location		BH-in	BH-in	BH-out	BH-out	BH-in	BH-in	BH-out	BH-out	BH-in	BH-in	BH-out	BH-out
Duration	min	60	60	60	60	60	60	60	60	60	60	60	60
Vm	dL	61.705	65.522	60.949	65.515	61.673	62.727	118.32	115.60	60.816	67.876	119.099	117.688
Pb	in Hg	28.14	28.14	28.14	28.14	28.17	28.17	28.17	28.17	28.02	28.02	28.02	28.02
Elev Corr.	ft	20	20	20	20	20	20	20	20	20	20	20	20
Tm	°F	65	67	63	64	61	63	59	61	64	66	63	65
Cm	–	1.0150	1.0050	1.0000	1.0000	1.0150	1.0050	1.0000	1.0000	1.0150	1.0050	1.0000	1.0000
Moisture	%	16.3	16.3	16.2	16.2	16.1	16.1	16.0	16.0	16.2	16.2	16.1	16.1
Vw	L	12.017	12.760	11.825	12.711	11.792	11.994	22.581	22.061	11.757	13.122	22.855	22.584
Front Wool+Plug	ng	0.0	0.0	0.0	0.0	0.0	0.0	0.0	0.0	0.0	0.0	0.0	0.0
Sect 1	ng	426	448	486	521	411	429	157	146	482	523	200	201
Sect 2 w/Plug	ng	0.7	0.2	0.2	0.2	0.2	0.2	0.2	0.4	0.5	0.5	7.1	0.8
Back Plug	ng	0	0	0	0	0	0	0	0	0.2	0	0	0
Breakthrough	%	0.2	0.0	0.0	0.0	0.0	0.0	0.1	0.3	0.1	0.1	3.6	0.4
Vt (corrected)*	NL(wet)	70.728	74.081	69.050	74.081	71.098	71.327	134.87	131.25	69.461	76.469	134.114	132.020
Hg(wet)	µg/Nm ³	6.033	6.050	7.041	7.036	5.784	6.017	1.166	1.115	6.946	6.846	1.544	1.529
Hg Avg (wet)	µg/Nm ³		6.042		7.038		5.900		1.140		6.896		1.536
RSD (paired traps)	%		0.14		0.04		1.98		2.20		0.73		0.51
Removal (sorbent trap)	%	-16.5				80.7				77.7			
No. CMM Data Points		8		6		21		20		18		18	
Average	µg/Nm ³	5.18		5.669		5.34		0.908		6.31		1.185	
Std. Dev.	µg/Nm ³	0.081		0.136		0.153		0.029		0.210		0.078	
RSD (sorbent trap to CMM)	%	7.640		10.268		4.981		11.358		4.469		12.903	
Removal (CMM)	%	-9.5				83.0				81.2			

Continued . . .

C-1

Table C-1. Complete Sorbent Trap and CMM Comparison Data (continued)

Sample No.	Units	4A	4B	4A	4B	5A	5B	5A	5B	6A	6B	6A	6B
Trap ID		88405	88421	88440	88438	88442	88414	88404	88417	88422	88399	88412	88396
Date		6/23/11	6/23/11	6/23/11	6/23/11	6/27/11	6/27/11	6/27/11	6/27/11	6/28/11	6/28/11	6/28/11	6/28/11
Time		14:30	14:32	14:20	14:20	13:55	13:57	13:48	13:50	14:42	14:44	14:35	14:37
Location		BH-in	BH-in	BH-out	BH-out	BH-in	BH-in	BH-out	BH-out	BH-in	BH-in	BH-out	BH-out
Duration	min	60	60	60	60	60	60	60	60	60	60	60	60
Vm	dL	58.741	65.936	120.16	117.45	61.361	66.886	123.23	124.12	63.876	65.065	129.29	125.69
Pb	in Hg	28.08	28.08	28.08	28.08	28.02	28.02	28.02	28.02	28.35	28.35	28.35	28.35
Elev Corr.	ft	20	20	20	20	20	20	20	20	20	20	20	20
Tm	°F	60	63	59	60	65	68	62	63	76	79	70	71
Cm	–	1.0150	1.0050	1.0000	1.0000	1.0150	1.0050	1.0000	1.0000	1.0150	1.0050	1.0000	1.0000
Moisture	%	16.2	16.2	16.1	16.1	16.2	16.2	16.1	16.1	16.2	16.2	16.1	16.1
Vw	L	11.356	12.747	23.059	22.539	11.862	12.930	23.648	23.819	12.348	12.578	24.811	24.120
Front Wool+Plug	ng	0.0	0.0	0.0	0.0	0.0	0.0	0.0	0.0	0.0	0.0	0.0	0.0
Sect 1	ng	495	523	214	210	409	452	113	112	404	404	168	165
Sect 2 w/Plug	ng	0.3	0.4	0.3	1.5	0.2	0.1	0.2	0.1	0.0	0.0	0.0	0.2
Back Plug	ng	0	0	0	0	0	0	0	0	0	0	0	0
Breakthrough	%	0.1	0.1	0.1	0.7	0.0	0.0	0.2	0.1	0.0	0.0	0.0	0.1
Vt (corrected)*	NL(wet)	67.752	74.869	136.64	133.31	69.950	75.068	139.03	139.77	72.163	72.377	145.36	141.04
Hg(wet)	µg/Nm ³	7.311	6.991	1.568	1.587	5.850	6.023	0.814	0.802	5.598	5.582	1.156	1.171
Hg Avg (wet)	µg/Nm ³		7.151		1.577		5.936		0.808		5.590		1.163
RSD (paired)	%		2.24		0.58		1.45		0.75		0.15		0.67
Removal (sorbent trap)	%	77.9				86.4				79.2			
No. CMM Data Points		21		21		21		21		21		21	
Average	µg/Nm ³	6.55		1.179		5.30		0.629		4.70		0.929	
Std. Dev.	µg/Nm ³	0.092		0.128		0.082		0.058		0.053		0.036	
RSD (sorbent trap to CMM)	%	4.35		14.454		5.663		12.457		8.644		11.196	
Removal (CMM)	%	82.0				88.1				80.2			

Continued . . .

C-5

Table C-1. Complete Sorbent Trap and CMM Comparison Data (continued)

Sample No.	Units	7A	7B	7A	7B	8A	8B	8A	8B	9A	9B	9A	9B
Trap ID		88326	88415	88407	88413	88389	88398	88408	88377	88397	88386	88403	88388
Date		6/29/11	6/29/11	6/29/11	6/29/11	6/29/11	6/29/11	6/29/11	6/29/11	6/30/11	6/30/11	6/30/11	6/30/11
Time		9:15	9:17	9:04	9:05	16:52	16:54	16:45	16:47	14:22	14:23	14:17	14:19
Location		BH-in	BH-in	BH-out	BH-out	BH-in	BH-in	BH-out	BH-out	BH-in	BH-in	BH-out	BH-out
Duration	min	46	45	60	60	60	60	60	60	60	60	60	60
Vm	dL	50.277	53.715	121.181	119.469	62.370	65.610	123.327	120.354	61.901	62.808	143.270	143.830
Pb	in Hg	28.35	28.35	28.35	28.35	28.32	28.32	28.32	28.32	28.05	28.05	28.05	28.05
Elev Corr.	ft	20	20	20	20	20	20	20	20	20	20	20	20
Tm	°F	65	67	65	67	78	81	79	81	77	80	76	77
Cm	–	1.0150	1.0050	1.0000	1.0000	1.0150	1.0050	1.0000	1.0000	1.0150	1.0150	1.0000	1.0000
Moisture	%	16.2	16.2	16.1	16.1	16.0	16.0	16.1	16.1	17.2	17.2	17.2	17.2
Vw	L	9.719	10.384	23.254	22.926	11.873	12.490	23.637	23.068	12.871	13.060	29.790	29.906
Front	ng	0.0	0.0	0.0	0.0	0.0	0.0	0.0	0.0	0.0	0.0	0.0	0.0
Wool+Plug													
Sect 1	ng	288	310	85	84	348	353	61	57	356	351	37	37
Sect 2 w/Plug	ng	0.0	0.1	0.2	0.1	0.3	0.6	0.0	0.4	0.4	2.0	0.3	0.0
Back Plug	ng	0	0	0	0	0	0	0	0	0	0	0	0
Breakthrough	%	0.0	0.0	0.2	0.1	0.1	0.2	0.0	0.7	0.1	0.6	0.8	0.0
Vt (corrected)*	NL(wet)	57.990	61.112	137.541	135.083	69.952	72.457	136.170	132.396	69.908	70.538	159.708	160.034
Hg(wet)	µg/Nm ³	4.966	5.074	0.619	0.623	4.979	4.880	0.448	0.434	5.098	5.004	0.234	0.231
Hg Avg (wet)	µg/Nm ³		5.020		0.621		4.930		0.441		5.051		0.232
RSD (paired traps)	%		1.07		0.25		1.00		1.64		0.93		0.51
Removal (sorbent trap)	%	87.6				91.1				95.4			
No. CMM Data Points		20		20		21		22		21		20	
Average	µg/Nm ³	4.52		0.451		4.21		0.290		4.30		0.093	
Std. Dev.	µg/Nm ³	0.076		0.078		0.123268		0.055		0.066525		0.056	
RSD (sorbent trap to CMM)	%	5.231		15.846		7.847127		20.594		8.049454		43.042	
Removal (CMM)	%	90.0				93.1				97.8			

C-3

Appendix B-2-6

Phase Two Final Report

July 26, 2012

UNIVERSITY OF NORTH DAKOTA

PHASE TWO FINAL REPORT

Project 5

**Steven A. Benson, Nicholas Lentz, Shuchita Patwardhan, Junior Nasah, Charles Thumbi
and Harry Feilen.**

**University of North Dakota
Institute for Energy Studies
Upson II Room 366
243 Centennial Drive, Stop 8153
Grand Forks, ND 58202-8153**

**Srivats Srinivasachar
Envergex, LLC
7/26/2012**

Table of Contents

1. List of Figures	iii
2. List of Tables	vii
3. Summary	1
4. Background	2
a) Problem	2
b) Green Ball Production	2
c) Proposed Technology	3
5. Approach	3
a) Green ball Production for Phase 2 Testing	3
b) Pellet Testing Equipment	6
c) Test Matrix	8
d) Analytical Methods	9
6. Results and Discussion	9
a) Data Quality Assessment	9
b) Minntac Test Results	10
c) Utac Test Results	14
d) Arcelor Mittal Test Results	17
e) Keetac Test Results	20
f) Hibtac Test Results	23
g) Additional Analyses	26
7. Conclusions	33
8. Future Work	34
9. References	35
10. Appendix A – Results	36
a) Minntac Baseline Results:	36
b) Minntac 0.1wt% Loading Runs:	37
c) Minntac 0.5wt% Loading Results:	38
d) Utac Baseline Results:	40
e) Utac 0.1wt% Loading Results:	41

f) Utac 0.5wt% Loading Results:	41
g) Arcelor Mittal Baseline Results:	43
h) Arcelor Mittal 0.1wt% Loading Results:	44
i) Arcelor Mittal 0.5wt% Loading Results:	45
j) Keetac Baseline Test Results:	47
k) Keetac 0.1wt% Loading Results:	48
l) Keetac 0.5wt% Test Results:	49
m) Hibtac Standard Green Ball Baseline Test Results:	50
n) Hibtac Standard Green Ball 0.1wt% Loading Test Results:	51
o) Hibtac Standard Green Ball 0.5wt% Loading Test Results:	52
p) Hibtac High Compression Green Ball Baseline Test Results:	54
q) Hibtac High Compression Green Ball 0.1wt% Test Results:	56
r) Hibtac High Compression Green Ball 0.5wt% Test Results:	57
11. Appendix B – Batch Balling Results Report	59
12. Appendix C – Data Quality Assessment Worksheet	64

List of Figures

Figure	Page
1. Picture of “Balling” tire assembly.	5
2. Pictures showing a) green ball “seeds” b) Sieved green balls.	5
3. Schematic of testing equipment.	6
4. Pictures showing reactor vessel, Wet-chemistry impinger train, Horiba DM-6B mercury analyzer.	7
5. Mercury release profile for a Minntac baseline run.	12
6. Mercury release profile for a Minntac 0.1wt% loading run.	12
7. Minntac total mercury (Hg^T) percentage release profile for baseline, 0.1wt% and 0.5wt%; as a function of temperature.	13

8. Minntac elemental mercury (Hg^0) percentage release profile for Baseline, 0.1wt% and 0.5wt%.....	13
9. Mercury release profile for Utac baseline run.	16
10. Mercury release profile for Utac 0.1wt% run.	16
11. Mercury release profile for Utac 0.5wt% run.	17
12. Mercury release profile for Arcelor Mittal baseline run.	18
13. Mercury release profile for Arcelor Mittal 0.1wt% run.....	19
14. Arcelor Mittal total mercury (Hg^T) percentage release profile for baseline, 0.1wt% and 0.5wt%; as a function of temperature.	19
15. Utac elemental mercury (Hg^0) percentage release profile for Baseline, 0.1wt% and 0.5wt%.....	20
16. Mercury release profile for Keetac baseline run.....	21
17. Mercury release profile for Keetac 0.1wt% run.....	22
18. Mercury release profile for Keetac 0.5wt% run.....	22
19. Mercury release profile for Hibtac standard green ball baseline run.....	24
20. Mercury release profile for Hibtac standard green ball 0.1wt% run.....	25
21. Mercury release profile for Hibtac standard green ball 0.5wt% run.....	25
22. TGA-DSC curve for carbon-containing Utac green ball.	29
23. a) TGA-DSC curve for carbon-free Minntac green balls. b) TGA-DSC curve for carbon-containing Minntac green balls.	30
24. XRD results for Utac green ball sample at a) baseline b) 400°C c) 700°C, and d) 1000°C.	31

25. XRD results for Minntac green ball with no carbon at a) baseline b) 400°C c) 700°C, and d) 1000°C.....	31
26. XRD results for Minntac green ball with 0.1wt% carbon at a) baseline b) 400°C c) 700°C, and d) 1000°C.....	32
27. Carbon-containing Minntac 400°C sample showing a) SEM image magnified at 700x. b) Back scattered analysis of SEM image showing presence of iron. No discernible difference on iron surface.	33
28. Reduction potential observed for 0.1wt% and 0.5wt% loading of ESORB-HG-11.	34
29. Mercury release profile for Minntac second baseline run.	36
30. Mercury release profile for Minntac replicate batch first baseline run.....	36
31. Mercury release profile for Minntac replicate batch second baseline run.	37
32. Mercury release profile for Minntac second 0.1wt% run.	37
33. Mercury release profile for Minntac third 0.1wt% run.	38
34. Mercury release profile for Minntac first 0.5wt% run.....	38
35. Mercury release profile for Minntac second 0.5wt% run.	39
36. Mercury release profile for Minntac third 0.5wt% run.....	39
37. Mercury release profile for Utac first baseline run.....	40
38. Mercury release profile for Utac third baseline run.....	40
39. Mercury release profile for Utac third 0.1wt% run.....	41
40. Mercury release profile for Utac first 0.5wt% run.....	41
41. Mercury release profile for Utac second 0.5wt% run.	42
42. Mercury release profile for Utac replicate second 0.5wt% run.	42
43. Mercury release profile for Arcelor Mittal baseline run.	43

44. Mercury release profile for Arcelor Mittal third baseline run.	43
45. Mercury release profile for Arcelor Mittal first 0.1wt% loading run.	44
46. Mercury release profile for Arcelor Mittal second 0.1wt% loading run.....	44
47. Mercury release profile for Arcelor Mittal second 0.1wt% replicate loading run.....	45
48. Mercury release profile for Arcelor Mittal first 0.5wt% loading run.	45
49. Mercury release profile for Arcelor Mittal second 0.5wt% loading run.....	46
50. Mercury release profile for Arcelor Mittal third 0.5wt% loading run.	46
51. Mercury release profile for Keetac first baseline run.	47
52. Mercury release profile for Keetac second baseline run.....	47
53. Mercury release profile for Keetac second 0.1wt% run.	48
54. Mercury release profile for Keetac replicate first 0.1wt% run.	48
55. Mercury release profile for Keetac replicate second 0.1wt% run.....	49
56. Mercury release profile for Keetac second 0.5wt% run.	49
57. Mercury release profile for Keetac third 0.5wt% run.	50
58. Mercury release profile for Hibtac standard green ball second baseline run.....	50
59. Mercury release profile for Hibtac standard green ball third baseline.....	51
60. Mercury release profile for Hibtac standard green ball second 0.1wt% run.	51
61. Mercury release profile for Hibtac standard green ball third 0.1wt% run.	52
62. Mercury release profile for Hibtac standard green ball third 0.5wt% run.	52
63. Mercury release profile for Hibtac standard green ball second 0.5wt% run.	53
64. Mercury release profile for Hibtac standard green ball second 0.5wt% replicate run.....	53
65. Mercury release profile for Hibtac high compression green ball baseline run.	54
66. Mercury release profile for Hibtac high compression green ball second baseline run.	54

67. Mercury release profile for Hibtac compression green ball first replicate baseline run. . .	55
68. Mercury release profile for Hibtac compression green ball second replicate run.	55
69. Mercury release profile for Hibtac compression green ball first 0.1wt% run.	56
70. Mercury release profile for Hibtac compression green ball second 0.1wt% run.....	56
71. Mercury release profile for Hibtac compression green ball third 0.1wt% run.	57
72. Mercury release profile for Hibtac compression green ball first 0.5wt% run.	57
73. Mercury release profile for Hibtac compression green ball second 0.5wt% run.....	58
74. Mercury release profile for Hibtac compression green ball third 0.5wt% run.	58

List of Tables

Table	Page
1. Summary of Phase 2 Runs.	8
2. Results for Minntac Green Ball Testing.	11
3. Oxidation Results for Utac Green Ball Testing.	15
4. Oxidation Results for Arcelor Mittal Green Ball Testing.....	18
5. Results for Keetac Green Ball Testing.....	21
6. Results for Hibtac Standard Green Ball Testing.	23
7. Results for Hibtac High Compression Green Ball Testing.....	24
8. Mercury Concentration in Green Balls Heated to Specific Temperatures.	26
9. Mössbauer Results for Utac Samples Containing 0.1wt% ESORB-HG-11.....	28
10. Mössbauer Results for Heated Minntac Samples not Containing ESORB-HG-11	28
11. Mössbauer Results for Heated Minntac Samples Containing 0.1wt% ESORB-HG-11...	29

12. Reduction Potential of ESORB-HG-11 for Each Taconite Facility. 65

Summary

Green balls produced from concentrate/filter cake and additives obtained from five of the taconite facilities operating on the Mesabi Iron Range were combined with trace amounts of ESORB-HG-11. ESORB-HG-11 is a proprietary brominated powdered activated carbon. The green balls containing ESORB-HG-11 were then subjected to heating experiments to determine the mercury oxidation potential of the additive.

Heating tests of the green balls from four of the facilities gave mercury oxidation levels ranging between 43% and 78%, with averages of 52% ($\pm 8\%$) and 58% ($\pm 11\%$) for additive amounts of 0.1weight% and 0.5wt%, respectively. Baseline oxidations averaged 18% ($\pm 6\%$), while oxidation due to ESORB-HG-11 averaged 42% ($\pm 9\%$) and 48% ($\pm 13\%$) for the 0.1wt% and 0.5wt% additive loading respectively. The results confirm preliminary results obtained in Phase 1 of this project, and indicate that the 0.1weight% ESORB-HG-11 loading is optimal for mercury oxidation, and is recommended for any potential future work involving the technology. The results obtained from a fifth facility, United Taconite, were not included in determining the averages, as they showed significantly lower mercury oxidation increases for ESORB-HG-11-containing green balls. The oxidation levels observed were approximately 10% to 15% lower than those observed for the other plants. The possible reason for this difference was not conclusively established during the testing.

The green balls were produced by the Coleraine Minerals Research Laboratory (CMRL) of the Natural Resources Research Institute (NRRI) and were subjected to industry-standard, Batch Balling tests to determine the possible effects the additive might have on the physical properties of the green balls. The physical properties investigated consisted of the moisture content, wet drop number, and dry compressive strength. For the samples with 0.1weight% additive, no significant difference due to addition of ESORB-HG-11 was observed with respect to the baseline standard during the batch balling tests. Slight differences from the baseline standard were observed with the 0.5weight% additive loading, suggesting that the 0.1weight% is the optimal additive loading.

Preliminary tests performed during Phase 1 of this project determined that there was little or no gas-phase mercury oxidation occurring during tests performed using the bench scale apparatus. This suggests that the mercury oxidation observed during these tests is a solid phase phenomenon occurring most likely on the carbon surface and within the green ball. Previous work indicates that gas-phase mercury oxidation does occur in taconite facilities with bromide addition to the green ball which enhances baseline (no bromide addition) mercury oxidation values. Consequently, a full-scale demonstration of the technology might result in higher levels of mercury oxidation than observed during the bench scale tests in this project. No tests were performed in this project to determine the impact of the carbon additive on the fired taconite pellet; this aspect should be investigated in future testing.

Background

Problem

The taconite industry has been identified as one of the major contributors of atmospheric mercury in the Lake Superior basin by the Lake Superior Lakewide Management Plan (LAMP) [Taconite Mercury QAPP]. Mercury is a leading concern among the air toxic metals addressed in the 1990 Clean Air Act Amendments because of its volatility, persistence and bioaccumulation as methylmercury in the environment, and its neurological health impacts.

In order to address this problem, the Minnesota taconite industry set a goal of achieving a 75% reduction in mercury emissions from the industry by the year 2025, with current industry wide emissions estimated at 440 to 880 lb/yr [Berndt 2003]. Several projects were then selected by the Minnesota Taconite Mercury Control Advisory Committee (MTMCAC) to identify the different existing mercury control technologies that show a potential to achieve 75% reduction.

Previous research work done at taconite processing plants by the Minnesota Department of Natural Resources (DNR) identified the ore as the main source of mercury during taconite processing [Berndt 2003]. This ore undergoes a series of beneficiation steps through which it is processed into small spherical balls referred to as green balls. Mercury is released during induration (heat processing) of these green balls to a final product referred to as taconite pellets. Previous work suggests that the release starts at temperatures of approximately 200°C and continues well up to temperatures of 600°C [Galbreath et al 2005], which corresponds to temperatures seen in the pre-heat zone of the induration furnaces.

In order to address this mercury emission problem, an approach was proposed by the University of North Dakota (UND) team in response to a Request for Proposals (RFP) issued by the Minnesota DNR. This approach explores the possibility of oxidizing the mercury before it is released from the green balls.

Green Ball Production

To produce green balls taconite ore undergoes a series of beneficiation steps which can be subdivided into [EPA]:

- Liberation, which involves crushing followed by grinding to release the desired ore from the gangue material.
- Concentration, here magnetism and/or flotation are used to separate the ore from the rest of the gangue material.
- Agglomeration, in which the concentrated ore mixed with water, a binder and certain additives; is ‘tumbled’ in a balling drum or disc to produce green balls.

The final chemistry of the green balls before induration depends on the concentrated ore composition and the additives used in the agglomeration step. Taconite facilities employ different formulations during their respective agglomeration steps. These formulations control

the type of binder used, binder/concentrate ratio, moisture content of the pellets, and additives used. The final chemistry of the green balls is considered important with respect to the proposed technology for mercury oxidation within the green balls.

This study focuses on five of the taconite facilities currently operating on the Mesabi Iron Range: United State Steel's Minntac and Keetac; United Taconite (Utac), Arcelor Mittal and Hibbing Taconite (Hibtac). This report details the results obtained when a mercury oxidizing additive – ESORB-HG-11, is combined with green balls from each taconite facility. The green balls/ESORB-HG-11 combination is produced according to the formulations of each respective facility.

Proposed Technology

The proposed technology employs a low-corrosivity carbon based mercury oxidizing agent/additive. The additive is a proprietary enhanced Powdered Activated Carbon (PAC) known as ESORB-HG-11, and is to be added in trace quantities to green balls prior to induration. ESORB-HG-11 is a proven effective catalytic oxidation agent that then acts as a fixed bed catalyst for mercury oxidation. ESORB-HG-11 contains only trace amounts of halogens thus reducing the possible occurrence of halogen driven corrosion.

This report is a follow up to the Phase 1 report that focused on establishing the potential and optimum loading of ESORB-HG-11 to oxidize mercury present in green balls. This report focuses on laboratory scale work performed to establish the extent oxidation achievable when ESORB-HG-11 was included in the formulation of green balls obtained from five taconite facilities. ESORB-HG-11 loadings of 0.1wt% and 0.5wt% were used for the duration of the test, based on optimum loading established during the Phase 1 testing. The main goals of these tests were:

- Establish potential oxidation levels achievable by including ESORB-HG-11 in green ball formulations.
- Perform chemical analyses on test products to better understand mechanism of mercury oxidation.

Green balls used for the testing were prepared by the Coleraine Minerals Research Laboratory (CMRL). Preparation was done according to a batch balling procedure established by CMRL and based on the green ball formulations of each respective facility.

Approach

Green ball Production for Phase 2 Testing

Phase 2 tests employed green ball samples produced by CMRL. The balls were produced following a “Batch Balling” procedure established by CMRL, which used the formulations of each respective plant to produce the green balls. CMRL is an established testing facility for iron

ore related bench and pilot scale experiments. Several different tests related to the taconite industry are performed by CMRL including batch balling studies. Their batch balling procedure is known and accepted by the taconite industry.

The CMRL balling procedure involved first obtaining concentrates from each respective facility and performing a moisture test. Minntac provided a filter cake that was received as a slurry and pressure filtered to the facility's required moisture standard. The green ball chemistry and moisture content were adjusted to be representative of each respective taconite facility's standard, as determined necessary. The ESORB-HG-11 was then added to the concentrate batch by sprinkling, followed by hand blending in a mixing bowl. The blending technique has been employed exhaustively as a method of adding small quantities of additives to green ball formulations; it is a proven and reliable combination method. Loading rates used for ESORB-HG-11 in the green balls were 0.1wt% and 0.5wt%.

The binder was added along with ESORB-HG-11 during the sprinkling method. Once blended, small amounts of the new concentrate containing the additive and binder were then introduced into a balling tire, see Figure 1. "Seed" balls of -3 to +4 mesh were then produced, as seen in Figure 2. A specified amount of the "seed" balls (170 to 250g) was used to "grow" the green balls by gradually adding concentrate to the seeds until they reached the target size. The "growing" step took on average 3 minutes, and was followed by a "rolling" step that lasted for a minute. Final green ball sizes were -1/2" +3/8", see Figure 2. A size distribution of the green balls was also determined; this distribution is a relative value and is used as a measure of the green ball growth rate during batch balling.

Once the green balls were formed, they were screened to determine the size distribution. A sample of the green balls prepared, approximately 200-300g, was placed in a drying oven to determine the moisture content; meanwhile another sample of 10 green balls was subjected to an 18" wet drop test. Ten of the dried green balls from the moisture test were then subjected to a dry compressive strength test. The results of the different tests are presented in Appendix B. The remaining green balls were stored in plastic bags and transported back to the University of North Dakota (UND) for oxidation testing.

Green balls were produced for all the facilities. For each facility a batch was prepared containing no additive (baseline), 0.1wt% additive and 0.5wt% additive. A replicate of either the baseline, 0.1wt% or 0.5wt% batch, was also prepared, depending on the facility. This gave a total of four batches per facility except for Hibtac. Hibtac uses two different formulations for their green balls, so two different sets of batches were made for Hibtac, for a total of 8 batches.



Figure 1. Picture of “Balling” tire assembly.



Figure 2. Pictures showing a) green ball “seeds” b) Sieved green balls.

Pellet Testing Equipment

The bench-scale apparatus is illustrated in Figures 3 and 4. It consisted of a tube furnace, reaction vessel, gas metering system, gas conditioning system, mercury pretreatment system, and mercury analyzer. The testing procedure involved placing approximately 100g of green balls into the reaction vessel and heating the green balls up to 700°C. During the heating process, air flow to the vessel was maintained at 7.5 Lpm to ensure the system was under positive air pressure negating any effects of leaks on mercury concentration in sample gas. A portion of the flow leaving the reaction vessel was sampled through heated PFA tubing to a pretreatment system, and then directly to the analyzer for elemental mercury determination. Excess air was vented through a carbon bed. Initial experiments were conducted with an air flow rate of 5 Lpm and a final temperature of 700°C before modifications were made to the test system including an increase in the air flow rate to ensure constant positive air pressure in the system.

Before each run, the Horiba mercury analyzer was either calibrated or its calibration verified. While the analyzer was calibrated, the PFA tubing and other parts that would contact reactor outlet gases were preheated to 150°C to prevent condensation or reduction of oxidized mercury in the lines during the experiment. The furnace reactor was also preheated to 700°C and then allowed to cool to 250°C to drive out any residual mercury in the furnace. During testing, once the green balls were added to the reactor the temperature of the reactor was increased to 700°C at a ramp rate of 20°C/min based on full-scale conditions. Note that due to heat losses in the bench scale assembly, the actual ramp rate decreased as the temperature of the reactor bed increased, resulting in a slower overall ramp rate when compared with full-scale conditions.

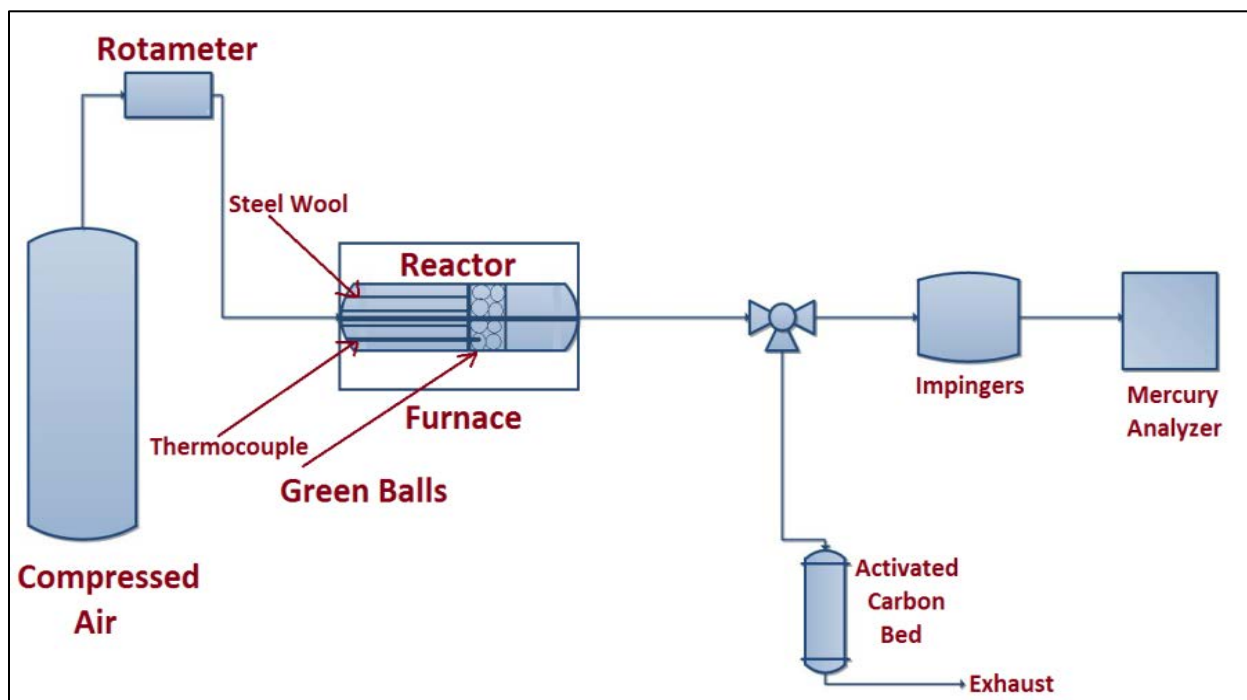


Figure 3. Schematic of testing equipment.

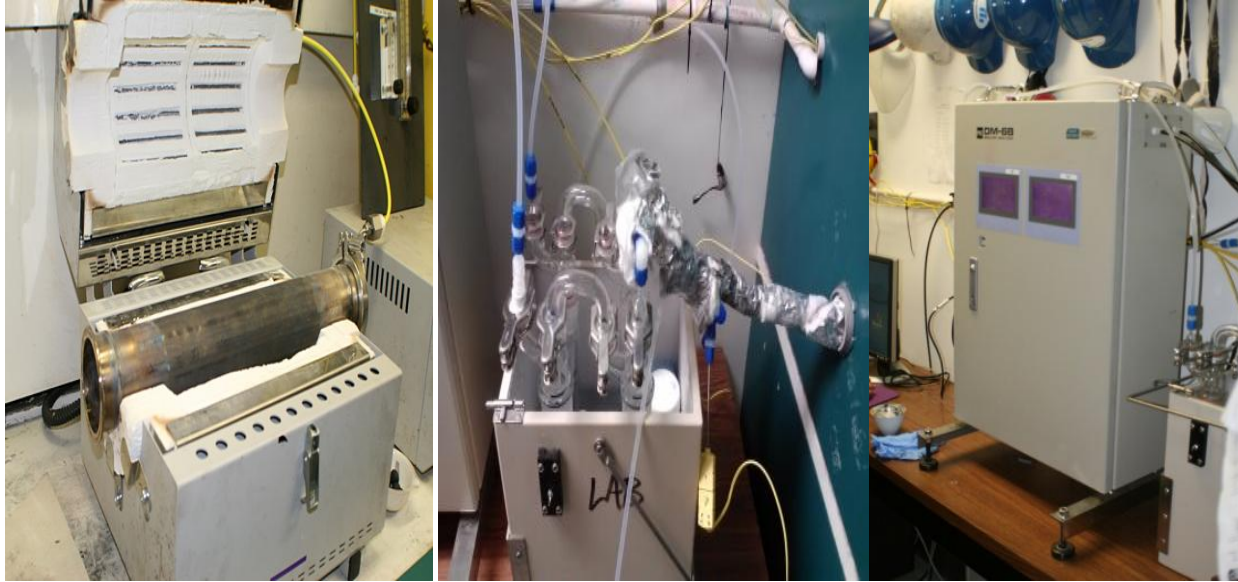


Figure 4. Pictures showing reactor vessel, Wet-chemistry impinger train, Horiba DM-6B mercury analyzer.

A wet chemistry pre-treatment system was used to condition the sample gases before mercury analysis. It consisted of two parallel sets of impingers: one for determining Hg^0 concentration in sample gas, while the other for determining Hg^T concentration in the sample gas. The set-up was designed based on a modified wet chemistry PS Analytical pre-treatment conversion system and ASTM D6784-02 (also known as the Ontario Hydro [OH] method). In this design, the first impinger train is for conditioning the elemental mercury stream. It consists of two impingers in series sitting in an ice bath. The first impinger contains a 150 mL of 10% w/v potassium chloride (KCl) and 0.8% w/v $\text{Na}_2\text{S}_2\text{O}_3$ solution that captures the oxidized mercury in order to obtain only elemental mercury concentration, while the second impinger traps all moisture present in the gas sample before analysis by the mercury analyzer. The second impinger train is for conditioning the total mercury stream. Here, the first impinger contains 150 mL of 0.8% w/v stannous chloride (SnCl_2) solution and 20% w/v of NaOH. The SnCl_2 reduces the oxidized mercury in order to obtain a total mercury measurement of the flue gas. This impinger train also sits in an ice bath. The second impinger traps all moisture present in the gas sample before analysis. The trains were modified from a continuous flow to a batch system.

The Horiba mercury analyzer simultaneously and continuously measures both total and elemental mercury. The difference between the total and elemental is taken as oxidized mercury. The mercury measurements are plotted on an XY curve at an interval of 10 seconds per measurement. The mercury measured can then be estimated by calculating the area under the curve for both Hg^0 and Hg^T . With the calculated values, the percent oxidation and mercury

concentration of the green balls can be estimated. Gas flow rates are measured with rotameters and were validated with mass flow controllers.

Test Matrix

Table 1 summarizes the test matrix for Phase 2 testing. All batches prepared by CMRL were tested in triplicates except for replicate batches which were tested in duplicates. During test runs, the total mercury concentration [Hg^{T}] and elemental mercury concentration [Hg^0] were measured and used to estimate the percent mercury oxidation, which was assumed to be an estimate of the removal potential if there was a wet scrubber present downstream of the test equipment. The equation for estimating percent mercury oxidation/removal is discussed in the *Data Quality Assessment* section and in Appendix C.

Table 1. Summary of Phase 2 Runs.

Facility	Pellet Type	Loading (wt.%)	Number of Runs
Minntac	Flux	Baseline	2
		Baseline Replicate	2
		0.1	3
		0.5	3
Keetac	Flux (low level limestone)	Baseline	3
		0.1	2
		0.1 Replicate	2
		0.5	3
Arcelor Mittal	Standard	Baseline	3
		0.1	2
		0.1 Replicate	2
		0.5	3
Utac	Standard	Baseline	3
		0.1	3
		0.5	2
		0.5 Replicate	2
Hibtac	Standard	Baseline	3
		0.1	3
		0.5	2
		0.5 Replicate	2
Hibtac	High Compression	Baseline	2
		Baseline Replicate	2
		0.1	3
		0.5	3

Analytical Methods

To obtain insight on the mechanism governing mercury oxidation i.e. surface chemistry of green balls during oxidation, a series of analytical tests were carried out. The tests consisted of Mössbauer spectroscopy, X-ray diffraction (XRD), scanning electron microscopy (SEM) and thermogravimetric analysis-differential scanning calorimetry (TGA-DSC). The tests sought to investigate the changes occurring as the green balls were heated, and determine possible effect the changes had on mercury release. Results from these analyses are discussed later in this report.

Results and Discussion

The results obtained during Phase 2 testing are sub-divided into 5 sections, each section representing the results from each taconite facility. Some graphs are included in this section for illustration purposes while the rest of the graphs can be found in appendix A. A total of ten runs were done for each type of pellet produced by the facilities.

Batch balling tests were also conducted on the green balls produced to compare the physical quality of the green balls prepared with the additives. No significant differences were observed during the tests between the 0.1wt% loading and the baseline standard used for comparison. However, for the 0.5wt%, a few differences were observed such as the size distributions which were slightly larger (+1/2" size fraction) than the baseline. The size distribution is a measure of the green ball growth rate, meaning that the green balls apparently "grew" faster when containing more additive as compared to the additive-free green balls. The next difference observed was the dry compression test results for Hibbing Taconite standard green balls and Keewatin Taconite green balls which were lower for the high additive load rate. The data used was not sufficient to conclusively determine that these differences were significant. The full report is presented in Appendix B.

The Batch Balling Test results suggest that the 0.1wt% is the optimal loading for testing as no significant difference between additive green balls and baseline green balls was observed during these tests. More tests are however recommended to investigate if there is any effect of the additive on the quality of fired green balls (taconite pellet).

Data Quality Assessment

A key objective of the bench tests was to provide a possible estimate of the potential reduction capability of the technology if deployed at an actual taconite facility. To estimate this reduction potential, the average oxidation due to addition of ESORB-HG-11 only was estimated. This required assumption that all oxidized mercury released from the taconite processes would get captured by the scrubber system and that any mercury re-emission from the scrubber waters is negligible. The equation used to determine reduction potential was:

$$\text{Reduction Potential} = \frac{\text{Hg}[2] - \text{Hg}[1]}{100 - \text{Hg}[1]} * 100 \dots\dots\dots[1]$$

Where,

- Hg[1] is the average mercury oxidation for baseline runs for respective facility, expressed as a percentage.
- Hg[2] is the average mercury oxidation for 0.1wt% ESORB-HG-11 runs for respective facility, expressed as a percentage.

Certain factors are not accounted for when using the bench scale results to estimate potential mercury oxidation. The first is gas phase oxidation. Phase 1 testing established that little or no oxidation was observed when bromine salts were added to carbon-free green balls. This suggested that there was little or no gas phase oxidation during bench tests. However, gas phase oxidation is considered to occur during field tests [Berndt, Engesser 2005]. Consequently, it is very possible that the reduction potential observed during bench tests would be lower than those observed during potential full-scale testing.

Secondly, the goal of increasing the ratio of oxidized mercury to total mercury is to increase the amount of mercury that could get captured in the wet scrubbers. This approach would prove successful only for facilities that discharge their scrubber solids and/or liquids, providing an “exit” for the mercury captured by the system. Recycling of both scrubber solids and liquids re-introduces the captured mercury back into the process, negating the benefits of using the technology. The results obtained for each facility are presented below.

Minntac Test Results

Table 2 presents the results for all Minntac tests performed and Figures 5 and 6 show the release profile for the baseline and 0.1wt% run respectively. The baseline batch obtained from CMRL was replicated, so duplicate runs of each baseline batch were performed. Both baseline batches showed very good agreement with average oxidation values of 25.7% and 22.3%. Good agreement of the results confirms the reliability of the “Batch Balling” production technique.

Results for ESORB-HG-11-containing batches, 0.1wt% and 0.5wt%, showed very close agreement with mercury oxidation averages of 61.6% and 62.9% respectively. With a baseline oxidation average of 24%, the ESORB-HG-11 reduction potential was estimated to be 49.4% and 51.2% for the 0.1wt% and 0.5wt% loading respectively. The small relative difference between results of both loadings confirms the results obtained during the Phase 1 tests that suggested 0.1wt% to be the optimum loading of ESORB-HG-11 in green balls. All the additive runs showed oxidation levels greater than 50%.

To better understand the effect of temperature on the mercury release profile for Minntac, plots of the percentage of mercury evolved (elemental and total) against the pellet core

temperature were made in Figures 7 and 8. The release profiles for duplicate/triplicate runs during Minntac testing were consistent. Consequently, percentage mercury evolved of one run from a particular loading, say 0.1wt%, is representative of the other loadings. Figures 7 and 8 show curves of three runs: baseline, 0.1wt% and 0.5wt%. The percentage of Hg⁰ and Hg^T evolved was plotted against the temperature of the pellet core. This plot generated a curve that shows the “rate” at which mercury is evolved as a function of temperature.

Table 2. Results for Minntac Green Ball Testing.

Green Ball	Additive	Additive Loading (wt.%)	Observed Oxidation		Reduction Potential	
			Test Runs (%)	Average	(%)	Average
Minntac	ESORB-HG-11	Baseline Replicate	17.3	22.3	N/A	N/A
			27.4			
Minntac	ESORB-HG-11	Baseline	26.8	25.7	N/A	N/A
			24.7			
Minntac	ESORB-HG-11	0.1	64.2	61.6	52.9	49.4
			53.5		38.8	
			67.1		56.7	
Minntac	ESORB-HG-11	0.5	68.0	62.9	57.9	51.2
			61.2		48.9	
			59.6		46.8	

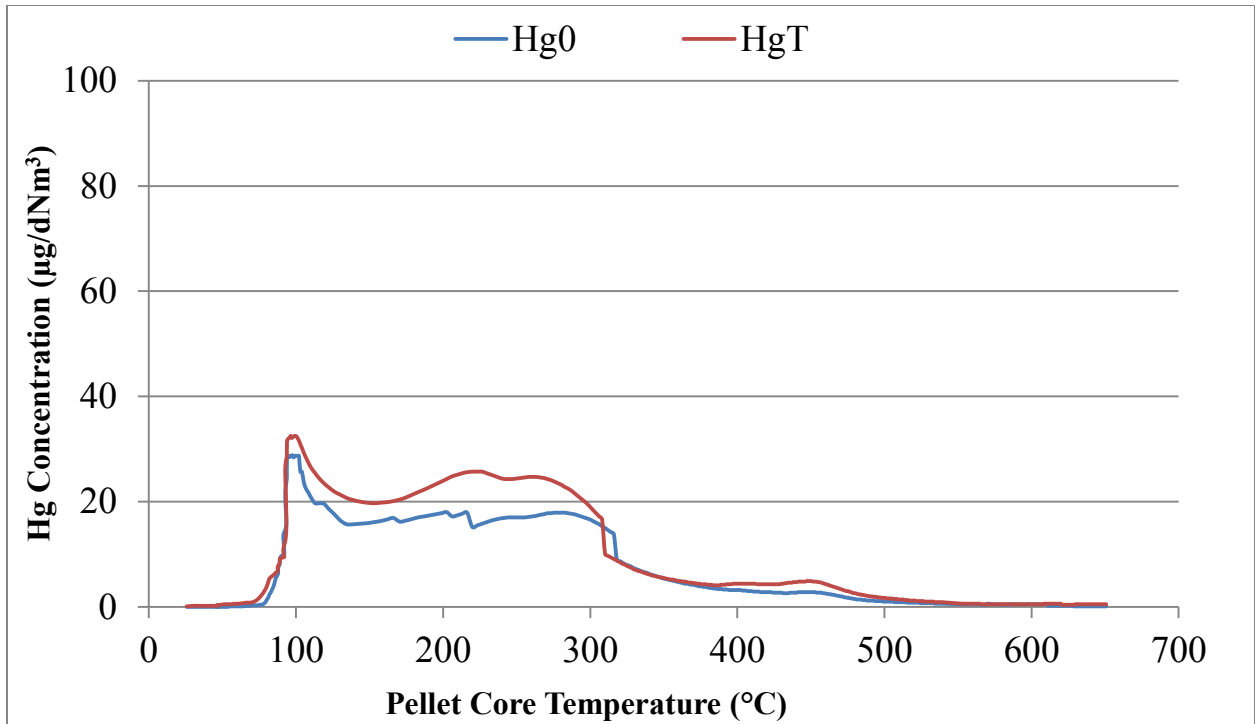


Figure 5. Mercury release profile for a Minntac baseline run.

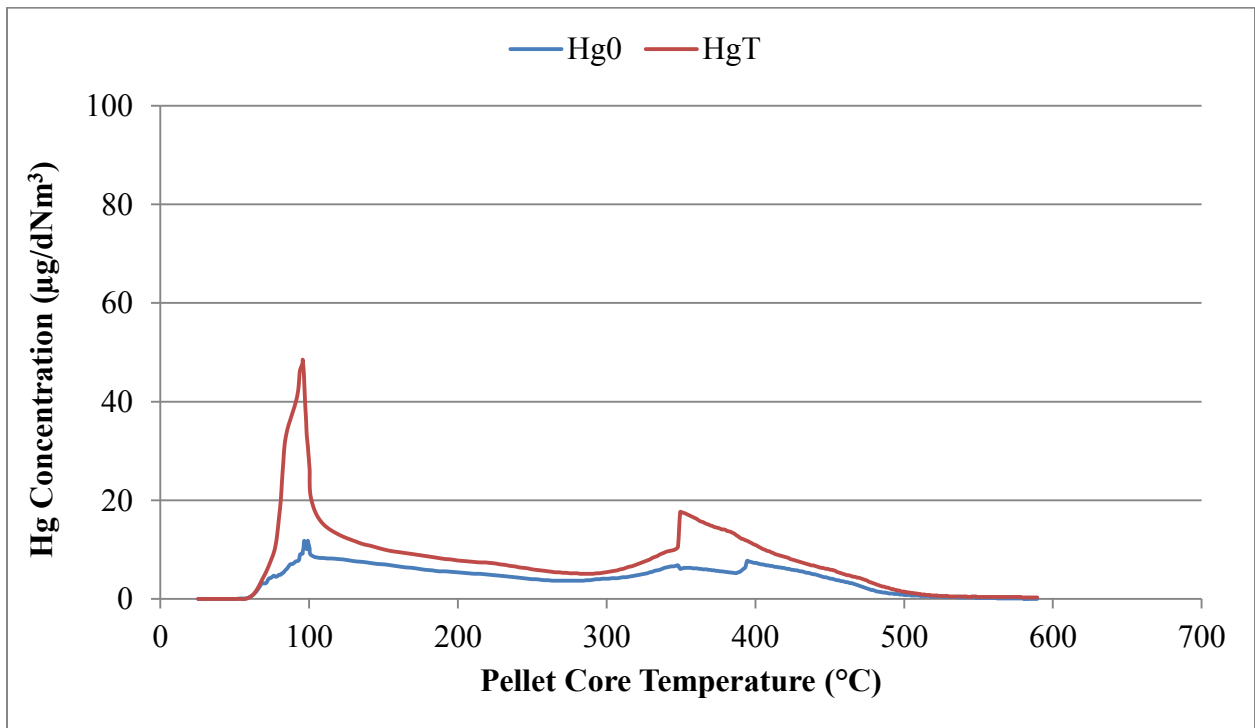


Figure 6. Mercury release profile for a Minntac 0.1wt% loading run.

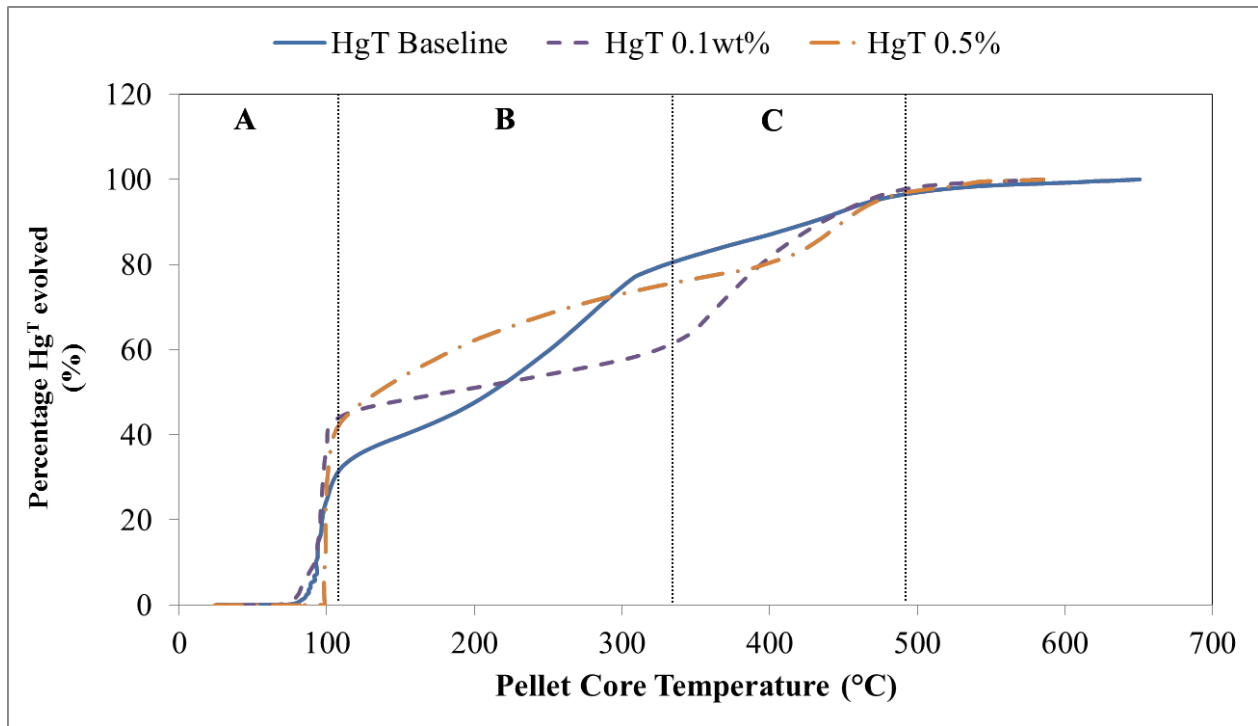


Figure 7. Minntac total mercury (Hg^T) percentage release profile for baseline, 0.1wt% and 0.5wt%; as a function of temperature.

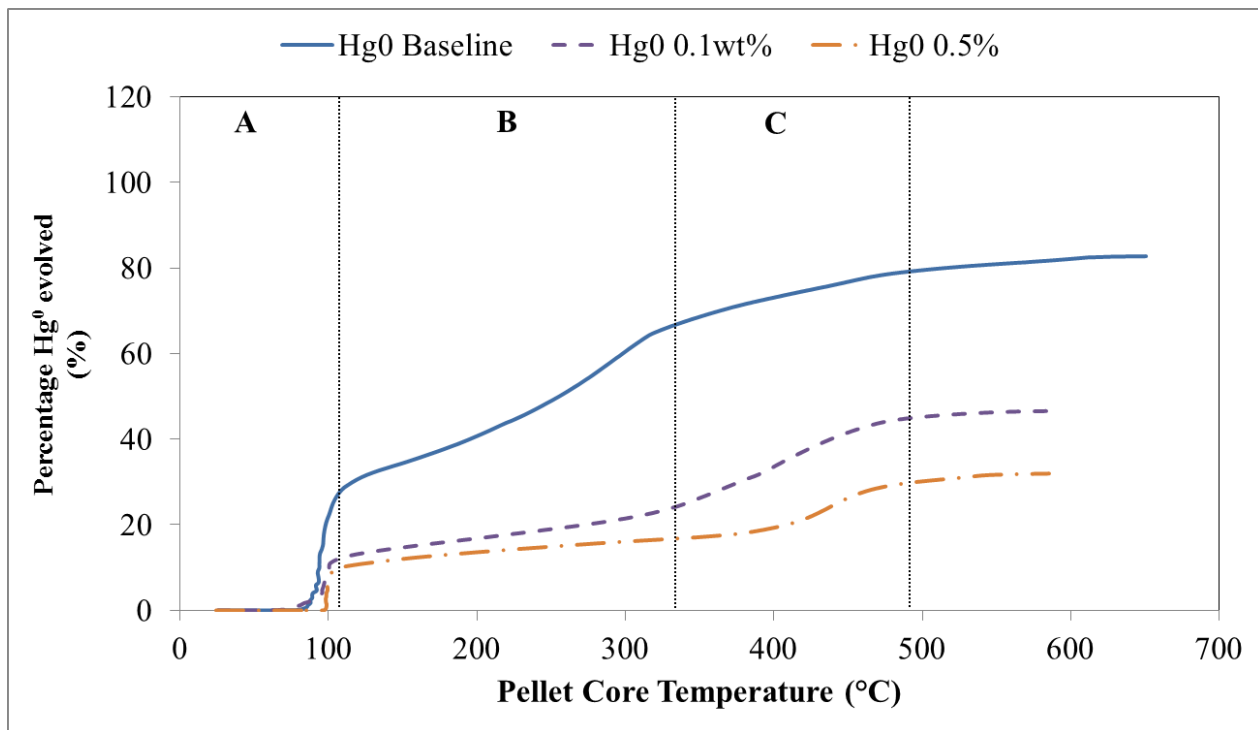


Figure 8. Minntac elemental mercury (Hg⁰) percentage release profile for Baseline, 0.1wt% and 0.5wt%.

The percentage plots are divided into three regions: A, B and C. Region A corresponds to the start of heating. In this region the green balls are inserted into the furnace pre-heated to 250°C. The furnace is pre-heated to ensure that the feed air is approximately at 200°C before contacting the inserted green balls. 3 to 5 minutes after the green balls are inserted, a significant mercury release is observed, see Figures 5 to 8. This mercury released is considered to be mercury associated with the surface of the pellets. Recall that the furnace is pre-heated to 250°C, and using a ramp rate of 20°C/min, the temperature of the surface of the green balls during this release is believed to be at least 300°C. In Figures 7 and 8, the release is represented by the steep slope of the curves in region A.

In Figure 7, the percentage of Hg released in region A was higher for both the 0.1wt% and 0.5wt% when compared to the baseline. This seemed to suggest that more mercury was released at the start of the experiment for ESORB-HG-11-containing green balls; however, analysis of the percentage mercury release profiles before pellet core temperatures reached 200°C, for all the runs determined that this behavior was not consistent. So no immediate conclusion was drawn from it.

In region B, the curves appear to “flatten” suggesting that most of the mercury associated with the surface of the pellets has been released. The “flatter” profile suggests mercury release is now occurring from deeper within the pellet as it gradually heats up. Closer observation of the individual curves show that baseline curves are steeper in region B than for 0.1wt%/0.5wt% curves. In region C, the trend is reversed – baseline curves are “flatter” than the 0.1wt%/0.5wt% curves. This phenomenon is possibly due to the oxidation effects of ESORB-HG-11. The mechanism of mercury oxidation by ESORB-HG-11 is believed to consist of a “capture” step, where the mercury is bound to the surface of the carbon; followed by an oxidation step, where the “captured” mercury is then oxidized by the bromine atoms present at the active sites. Therefore in region B, capture of mercury by the carbon slows the rate of mercury release; meanwhile in the baseline curve the absence of carbon does not hinder the mercury release. In region C, the pellet temperature is approximately 350°C, a temperature at which the carbon can probably no longer hold on to the mercury. So all captured mercury is then released from the carbon, as seen for the 0.1wt%/0.5wt% curves, and the carbon no longer exhibits any oxidation capacity as seen in Figures 5 and 6 where no oxidation occurs after 400°C.

This trend is consistent with the other Minntac runs. Graphs displaying the trends are found in Appendix A. The Minntac runs show oxidation of mercury released from green balls during heating tests, with percent oxidations observed as high as 68%. The percentage mercury release curves also give a possible insight into the oxidation mechanism and its dependence on temperature.

Utac Test Results

Table 3 summarizes the results obtained for testing with Utac green balls. 10 runs were performed for Utac testing; however, the results of one run were discarded due to a problem

identified with the test equipment during quality control measures. The issue was resolved before testing proceeded. Each batch obtained for Utac testing was tested in triplicates or duplicates and showed good agreement. The average oxidation observed for baseline runs was 21.7%; meanwhile 0.1wt%, 0.5wt% and 0.5wt% replicate runs showed average oxidation levels of 36.8, 34.2 and 37.1% respectively. The reduction potential of the additive only was calculated to be 16.3%, 16.0% and 19.8% for 0.1wt%, 0.5wt% and 0.5wt% replicate respectively. Oxidation for additive-containing green balls ranged from 34% to 37%, approximately 15% decrease from oxidation observed in other facilities. Figures 9, 10 and 11 better illustrate the lower oxidation observed. The possible reason for the lower oxidation observed with Utac samples were not established during testing.

A percentage release plot for Utac data was not included. There was less similarity between release profiles for duplicate/triplicate runs of specific loadings. Consequently, percentage plots for one run of a particular loading are not be representative of the other runs. This makes comparison of runs of different loadings not possible.

Table 3. Oxidation Results for Utac Green Ball Testing.

Green Ball	Additive	Additive Loading (wt.%)	Observed Oxidation		Reduction Potential	
			Test Runs (%)	Average	(%)	Average
Utac	ESORB-HG-11	Baseline	25.7	21.7	N/A	N/A
			19.7			
			19.6			
Utac	ESORB-HG-11	0.1	32.9	36.8	14.3	19.3
			40.7		24.3	
Utac	ESORB-HG-11	0.5	33.9	34.2	15.6	16.0
			34.5		16.4	
Utac	ESORB-HG-11	0.5 Replicate	28.1	37.1	8.2	19.8
			46.2		31.3	

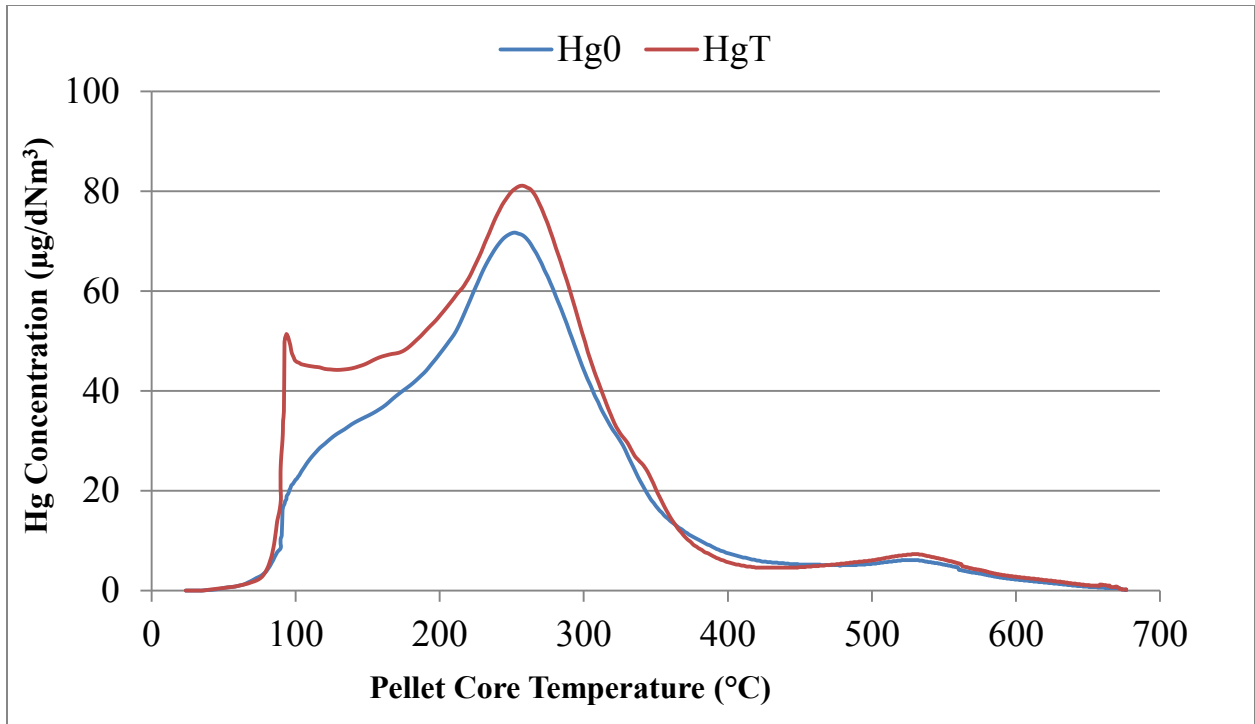


Figure 9. Mercury release profile for Utac baseline run.

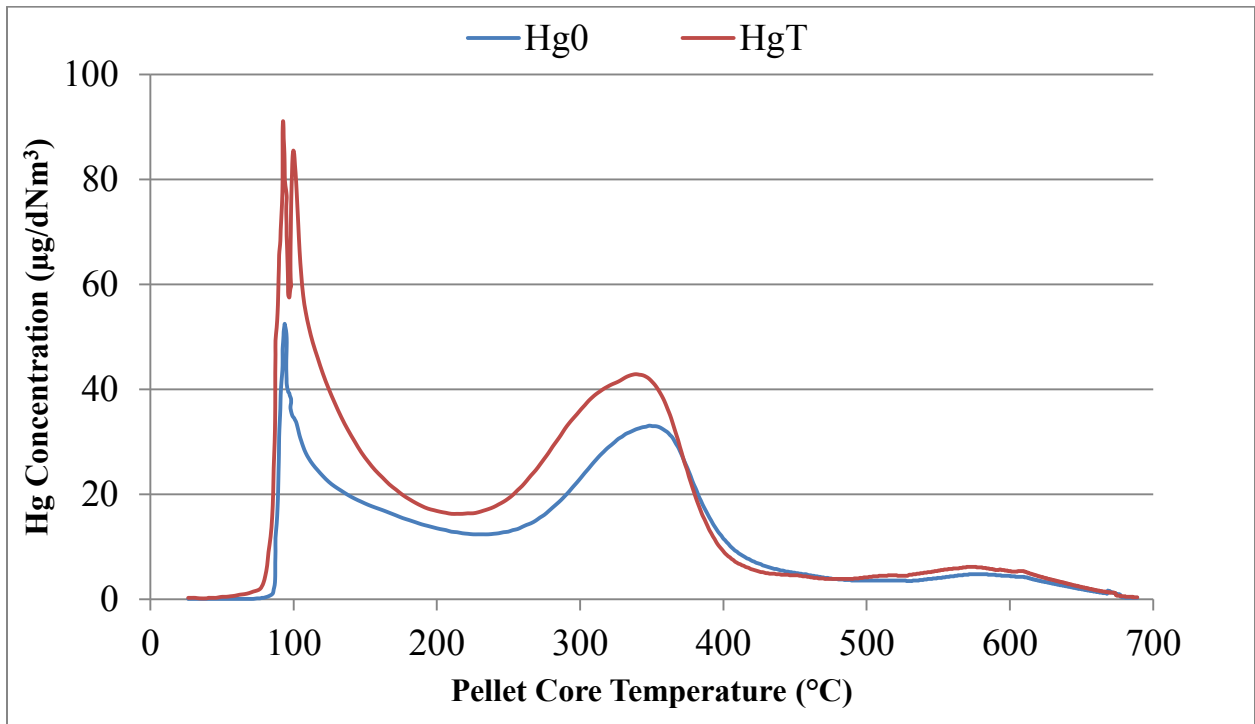


Figure 10. Mercury release profile for Utac 0.1wt% run.

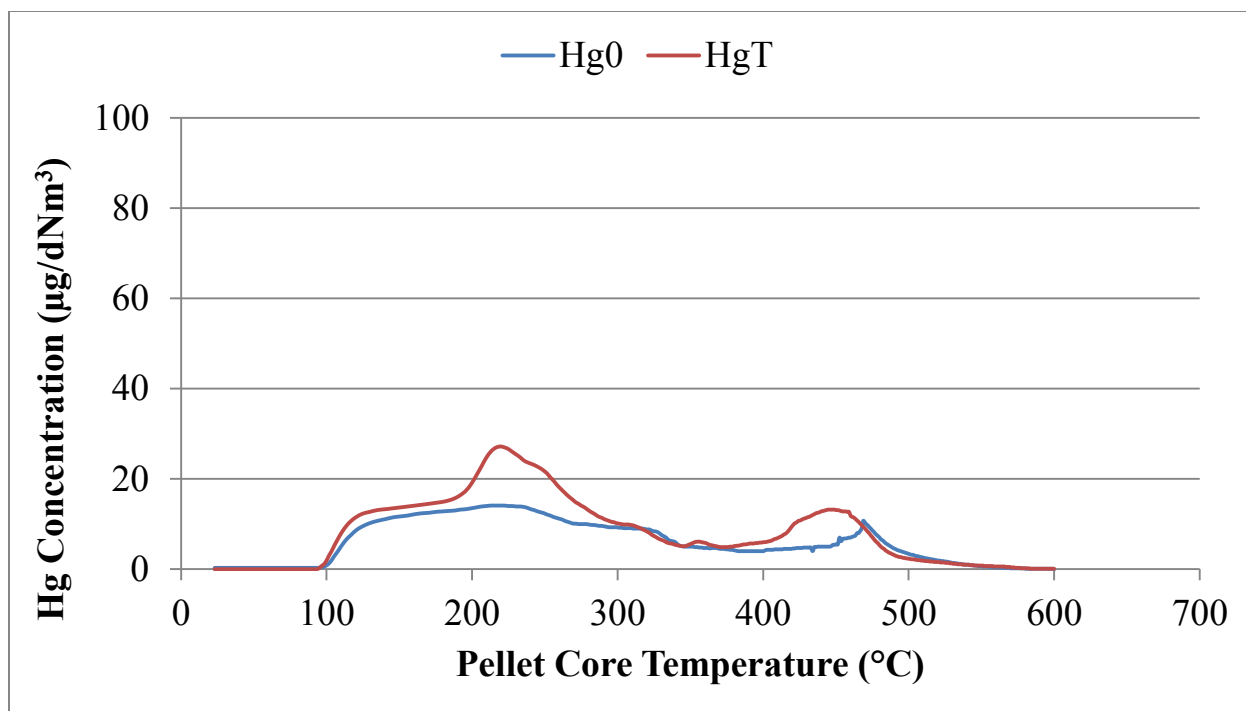


Figure 11. Mercury release profile for Utac 0.5wt% run.

Arcelor Mittal Test Results

The results for Arcelor Mittal are presented in Table 4 and Figures 12 to 15. The average baseline oxidation was 19.9% and showed very good agreement between runs. There were two 0.1wt% green ball batches; each batch gave an average oxidation of 56.9% and 48.2%, with ESORB-HG-11 reduction potential estimated to be 46.2% and 35.4% respectively. The 0.5wt% runs gave an average of 53.3%, with the reduction potential of ESORB-HG-11 only of 41.7%. Looking at the ESORB-HG-11 oxidation only, the difference between the 0.1wt% loading and the 0.5wt% loading was not significant as expected.

Arcelor Mittal runs have similar release profiles for respective loadings as was the case with Minntac. The percentage release plots in Figures 14 and 15 also show curves consistent with those of Minntac. Region C of the plots shows that the increase in the slope for 0.1wt% and 0.5wt% occurs between 400°C and 500°C. Meanwhile in Region A, the amount of mercury released at the start of the run was higher for the carbon runs than the baseline run. Looking at the release profiles for these runs (Figures 12, 13, 40 to 47), for the additive runs, more release and oxidation occurs at the start of the run. Runs were performed randomly and on different test days, so a possible cause of this was not fully determined.

Table 4. Oxidation Results for Arcelor Mittal Green Ball Testing.

Green Ball	Additive	Additive Loading (wt.%)	Observed Oxidation		Reduction Potential	
			Test Runs (%)	Average	(%)	Average
Arcelor Mittal	ESORB-HG-11	Baseline	20.0	21.7	N/A	N/A
			20.8			
			18.8			
Arcelor Mittal	ESORB-HG-11	0.1	66.4	56.9	58.1	46.2
			47.4		34.4	
Arcelor Mittal	ESORB-HG-11	0.1 Replicate	53.4	48.2	41.8	35.4
			43.0		28.9	
Arcelor Mittal	ESORB-HG-11	0.5	49.9	53.3	37.5	41.7
			60.1		50.1	
			49.9		37.5	

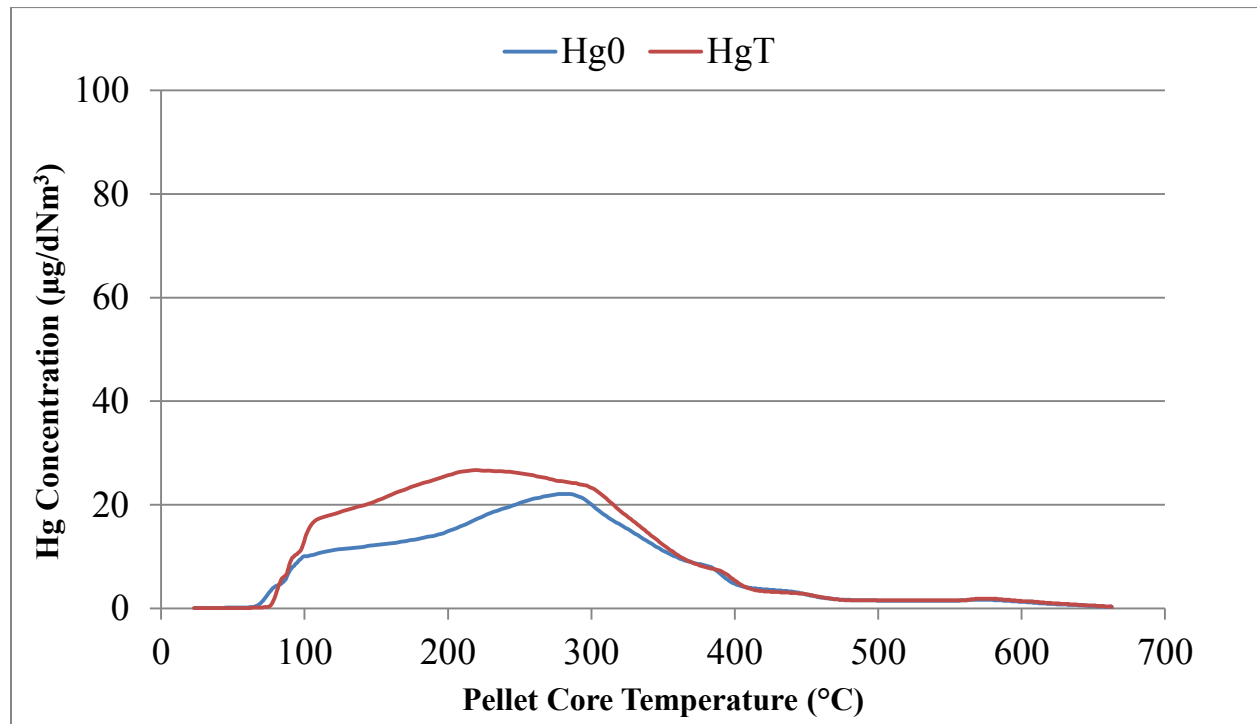


Figure 12. Mercury release profile for Arcelor Mittal baseline run.

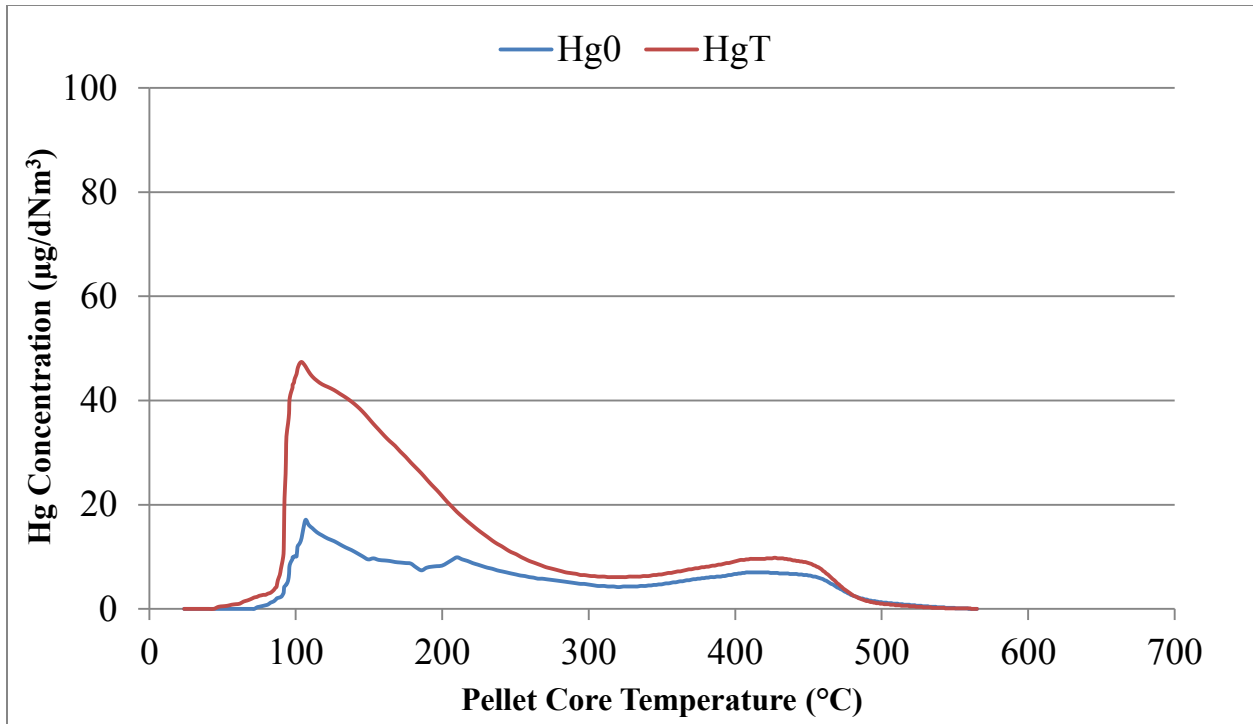


Figure 13. Mercury release profile for Arcelor Mittal 0.1wt% run.

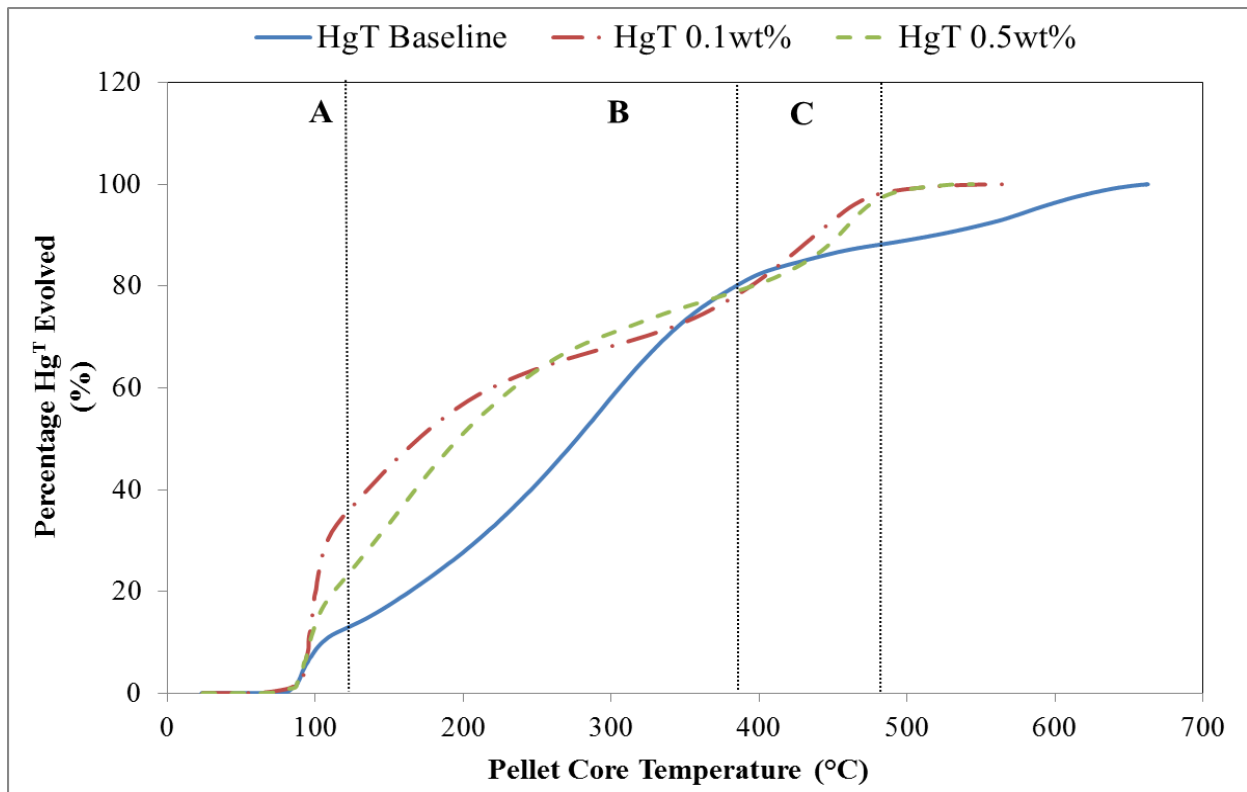


Figure 14. Arcelor Mittal total mercury (Hg^T) percentage release profile for baseline, 0.1wt% and 0.5wt%; as a function of temperature.

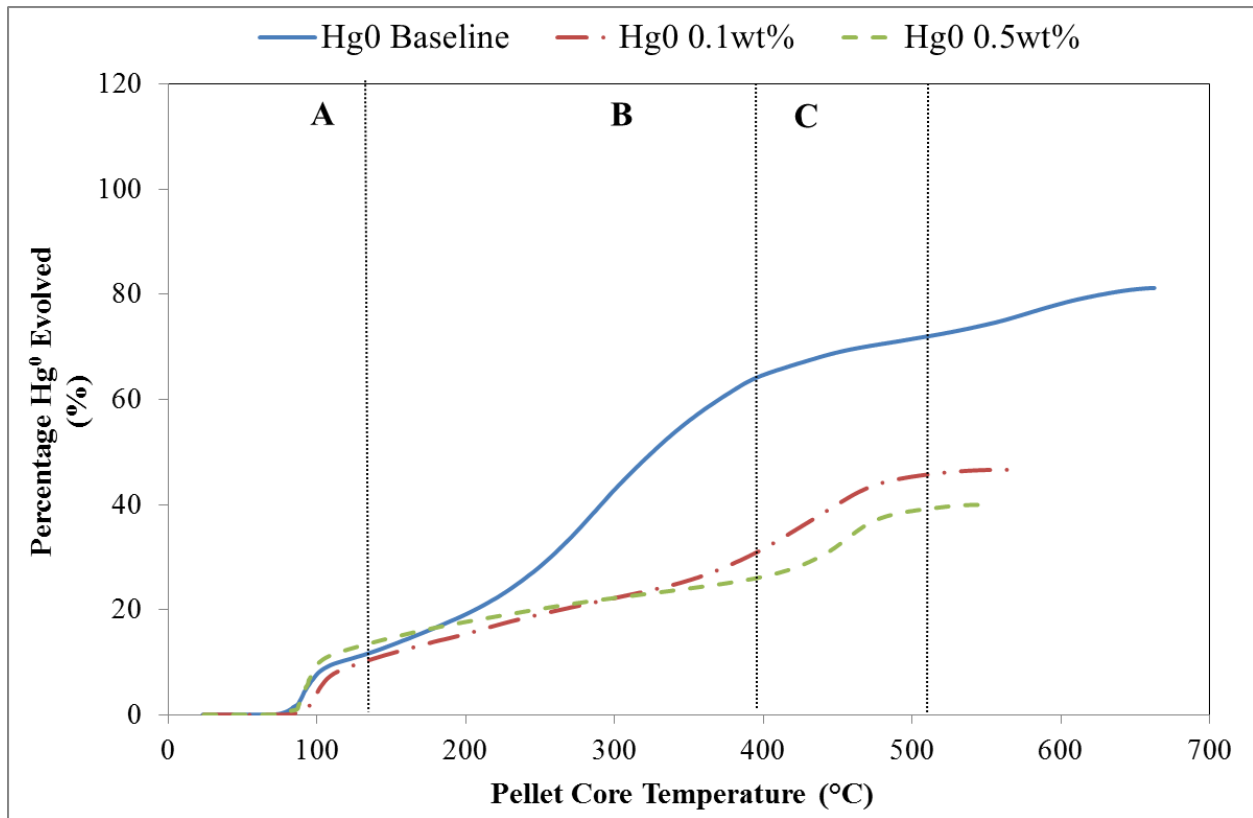


Figure 15. Utac elemental mercury (Hg⁰) percentage release profile for Baseline, 0.1wt% and 0.5wt%.

Keetac Test Results

The result's averages are summarized in Table 5. Baseline runs showed good agreement for mercury oxidation with an average of 15.1%. Keetac baseline average mercury oxidation was lower than that for Minntac, Utac and Arcelor Mittal. The 0.1wt% batch was replicated and all runs showed very good agreement with an average oxidation of 45.8%. 0.5wt% loading showed slightly higher mercury oxidation with an average of 52.3%. The 0.1wt% and 0.5wt% loadings showed ESORB-HG-11 reduction potential of 38.6% and 43.9% respectively.

Figures 16 to 18 show release profiles for baseline, 0.1wt% and 0.5wt%. A percentage release analysis of Keetac data was not performed because like Utac, there is less similarity between release profiles for duplicate/triplicate runs of particular loadings. Consequently, percentage plots of a particular loading are not consistent.

Keetac results show oxidation results close to values observed for Minntac and Arcelor Mittal confirming further that the additive is also as effective for mercury oxidation for Keetac green balls.

Table 5. Results for Keetac Green Ball Testing.

Green Ball	Additive	Additive Loading (wt.%)	Observed Oxidation		Reduction Potential	
			Test Runs (%)	Average	(%)	Average
Keetac	ESORB-HG-11	Baseline	-00.4*			
			16.9	21.7	N/A	N/A
			13.3			
Keetac	ESORB-HG-11	0.1	43.6	43.7	33.6	33.7
			43.8		33.8	
Keetac	ESORB-HG-11	0.1 Replicate	44.2	47.8	34.3	38.6
			51.5		42.9	
			51.5		42.9	
Keetac	ESORB-HG-11	0.5	46.5	52.3	37.0	43.9
			59.0		51.7	

* Run not included in average calculation.

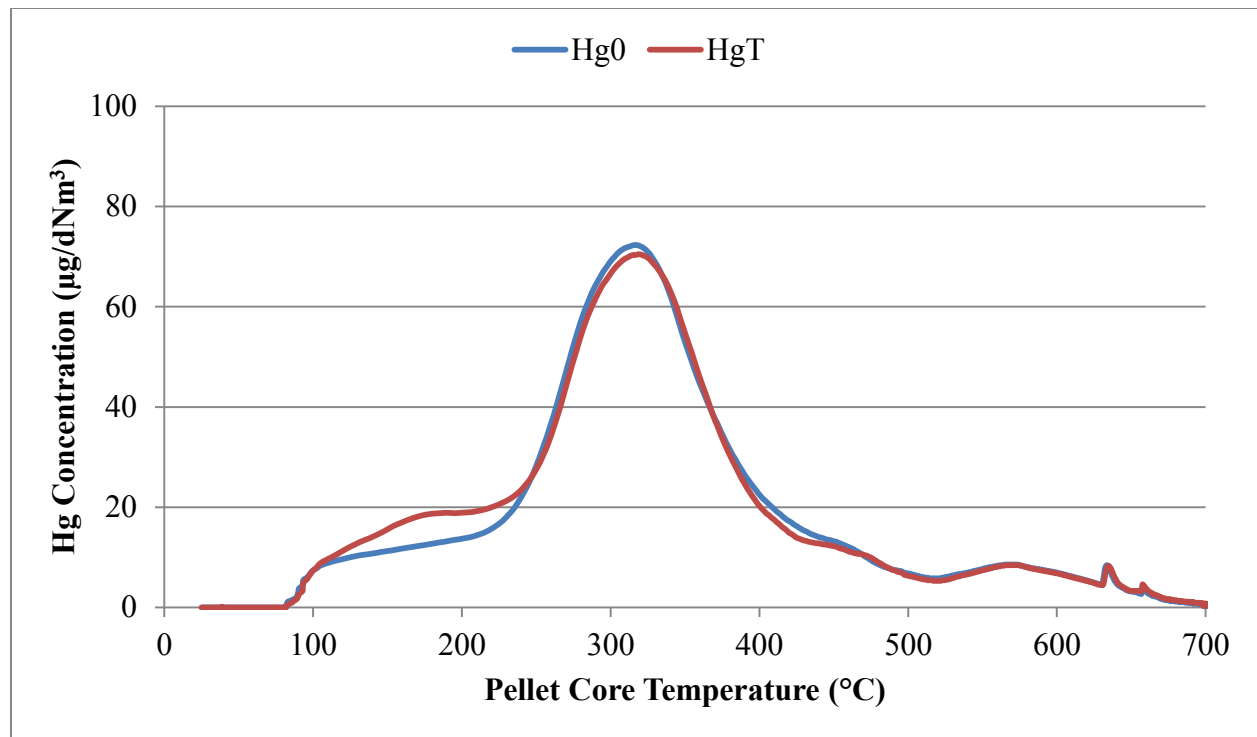


Figure 16. Mercury release profile for Keetac baseline run.

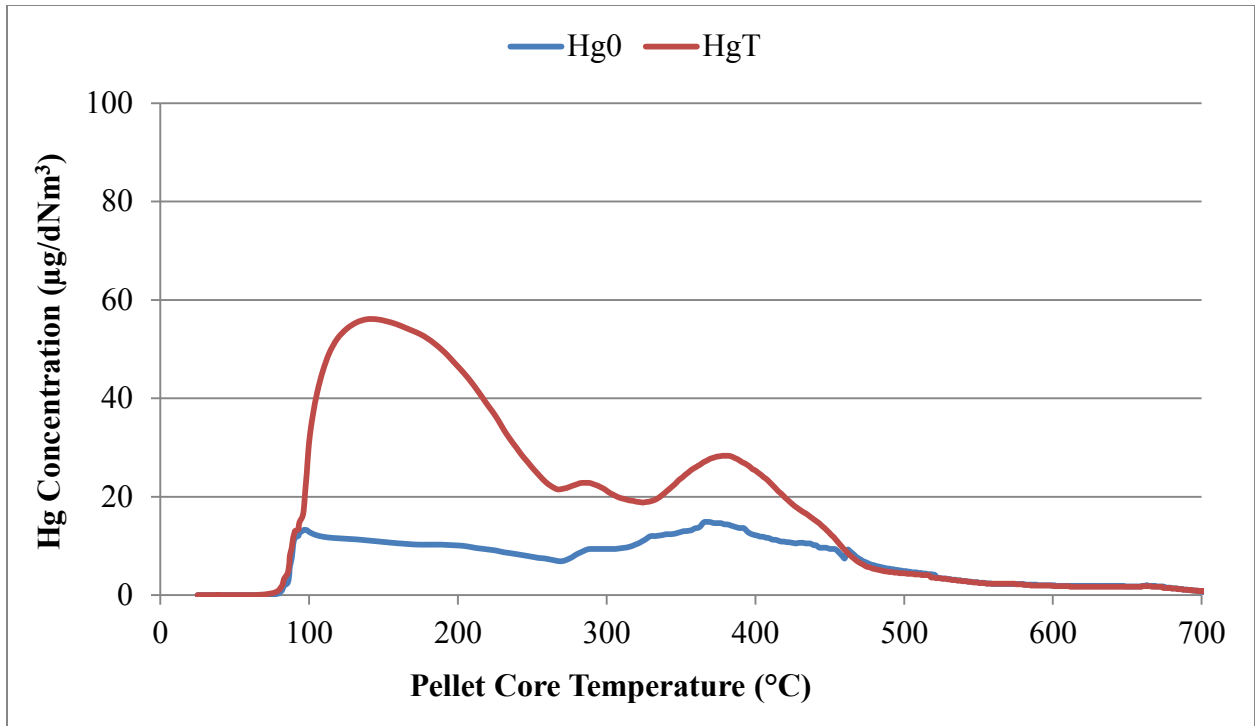


Figure 17. Mercury release profile for Keetac 0.1wt% run.

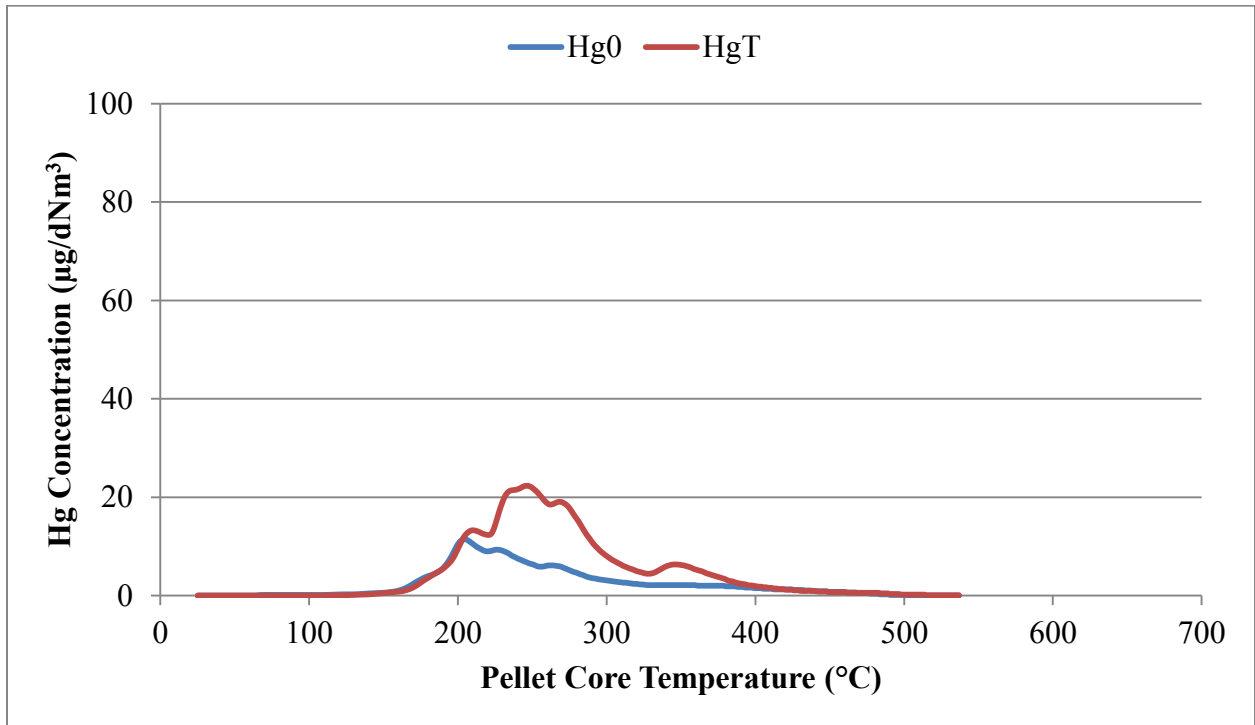


Figure 18. Mercury release profile for Keetac 0.5wt% run.

Hibtac Test Results

Results for Hibtac tests are found in Table 6 (standard green balls) and Table 7 (high compression green balls). For the standard green balls, results for different loadings showed slightly larger differences when compared to results of other plants, with differences also observed with the plots of individual runs for a particular loading as seen in Figures 19 to 21. Baseline runs averaged 17.1%, which is good agreement with the baselines of other plants. Runs for 0.1wt%, 0.5wt% and 0.5wt% replicate additive loadings averaged 54.6%, 60.9% and 56.7% respectively. The ESORB-HG-11 reduction potential estimated was 39.7% and 55.5% respectively.

The high compression green ball results showed good agreement with the standard green ball result (Table 7). The baseline runs averaged 16%, the 0.1wt% loading averaged 50% and the 0.5wt% loading averaged 63%. ESORB-HG-11 reduction potential was 39.7% and 55.5% for 0.1wt% and 0.5wt% respectively. The oxidation levels suggest no significant effect of the type of green ball (standard or high compression) on the oxidation capabilities of the added sorbent. Figures for the high compression green ball tests are presented in Appendix A.

The release profiles for the runs were also dissimilar, making a percentage mercury release plot not feasible as was the case with Utac and Keetac. The results however, show very good agreement with results for Minntac, Arcelor Mittal and Keetac.

Table 6. Results for Hibtac Standard Green Ball Testing.

Green Ball	Additive	Additive Loading (wt.%)	Observed Oxidation		Reduction Potential	
			Test Runs (%)	Average	(%)	Average
Hibtac	ESORB-HG-11	Baseline	12.5	14.0	N/A	N/A
			21.6			
			8.0			
Hibtac	ESORB-HG-11	0.1	52.7	54.6	45.0	47.2
			58.8			
			52.2			
Hibtac	ESORB-HG-11	0.5	44.1	60.9	35.0	54.6
			77.7			
			74.1			
Hibtac	ESORB-HG-11	0.5	44.7	56.7	35.7	49.7
			68.8			
			63.7			

Table 7. Results for Hibtac High Compression Green Ball Testing.

Green Ball	Additive	Additive Loading (wt.%)	Observed Oxidation		Reduction Potential	
			Test Runs (%)	Average	(%)	Average
Minntac	ESORB-HG-11	Baseline Replicate	15.1	10.1	N/A	N/A
			5.1			
Minntac	ESORB-HG-11	Baseline	22.0	22.6	N/A	N/A
			23.2			
Minntac	ESORB-HG-11	0.1	45.1	49.5	34.4	39.7
			47.6		37.4	
			55.9		47.3	
Minntac	ESORB-HG-11	0.5	46.8	62.8	36.4	55.5
			75.1		70.2	
			66.5		60.0	

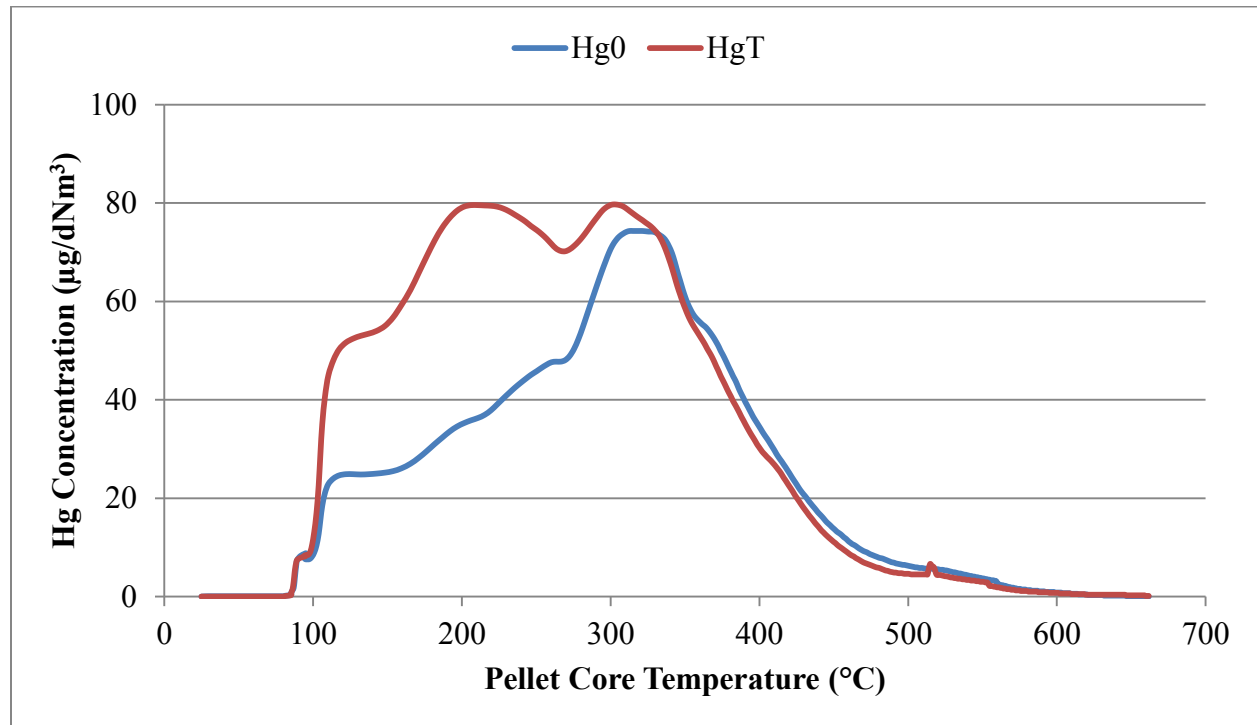


Figure 19. Mercury release profile for Hibtac standard green ball baseline run.

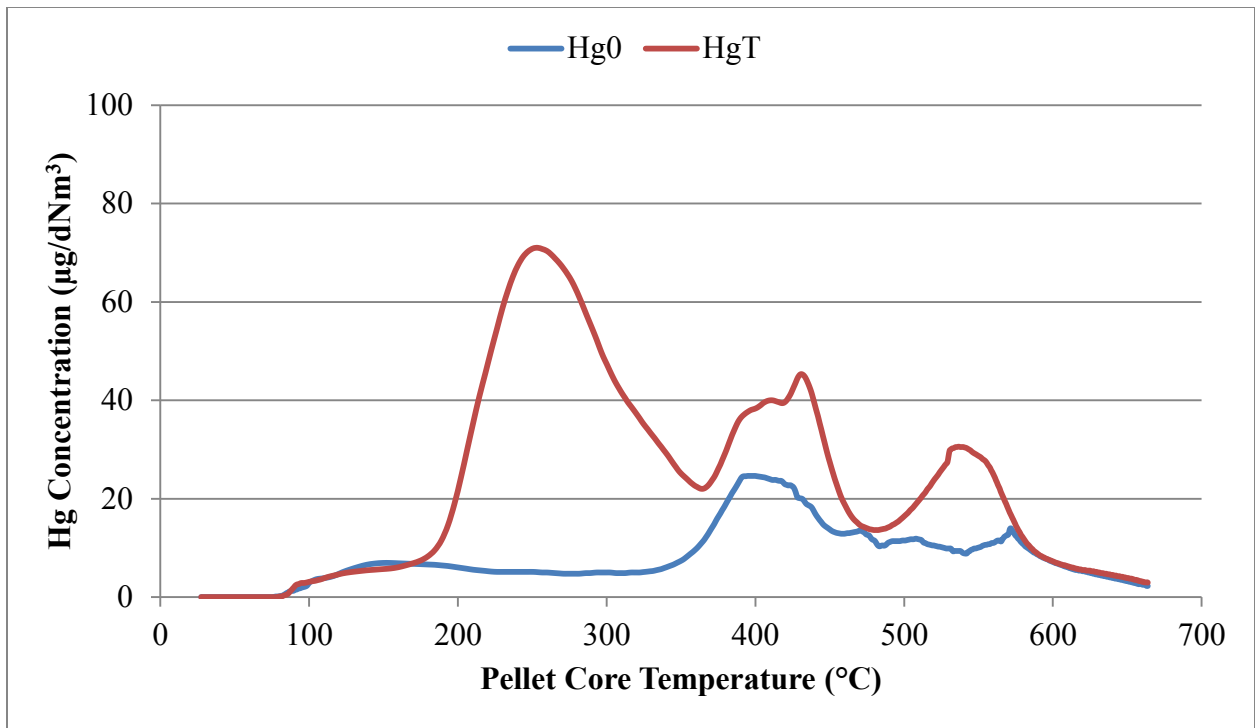


Figure 20. Mercury release profile for Hibtac standard green ball 0.1wt% run.

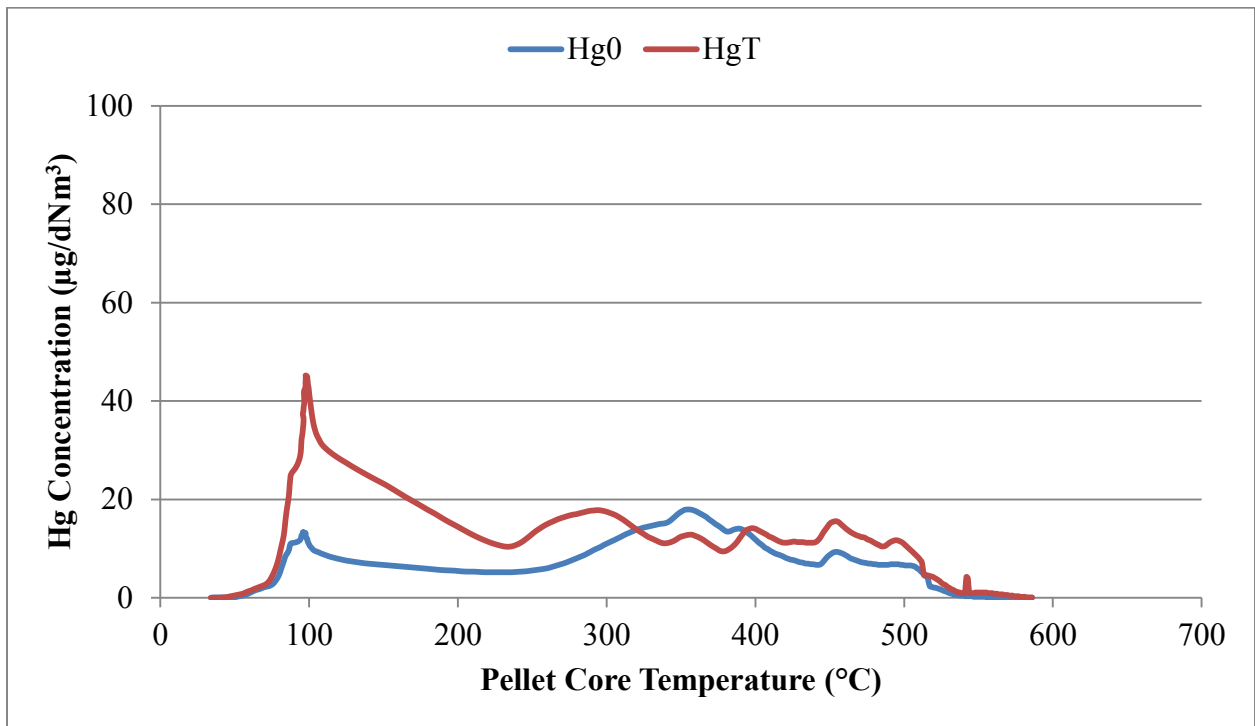


Figure 21. Mercury release profile for Hibtac standard green ball 0.5wt% run.

Additional Analyses

Additional analyses of green balls (unfired and fired) from Minntac (no carbon and 0.1wt%) and Utac were performed to possibly provide some insight into the mechanism involving mercury oxidation and/or release from the green balls as they were heated. Green ball samples at four different temperatures of 25°C (unheated), 400°C, 700°C and 1000°C were subjected to different analyses. Three of these analyses looked at the temperatures at which oxidation of magnetite occurs. Mössbauer spectroscopy provided qualitative and quantitative information on the type of iron oxide (hematite, magnetite or maghemite) present and their respective compositions. X-ray diffraction (XRD) is a qualitative analysis for identifying the compounds present in the different samples. Thermogravimetric analysis – Differential Scanning Calorimetry – was used to determine mass change as a function of temperature, providing possible temperature at which oxidation starts. The samples were also analyzed to determine their mercury concentration.

Mercury concentration analysis of the samples was done using EPA method 7471 – Mercury in Solid or Semisolid Waste. The results are summarized in Table 8. The results obtained for the heated samples were either low or non-detect, and close to the method detection limit. This suggests that by 400°C most of the mercury associated with the initial green balls has been released, a trend that agrees with release data for almost all runs that show that 75% of the mercury is released by 400°C.

Table 8. Mercury Concentration in Green Balls Heated to Specific Temperatures.

Green Ball	Additive Loading (wt.%)	Hg Concentration (ng/g) in GB at Temperature			
		25°C	400°C	700°C	1000°C
Minntac	0	6.6	ND	ND	ND
Minntac	0.1	25	5.2	5.0	ND
Utac	0.1	26	5.9	ND	ND

ND = Non detect; NA = Not analyzed.

Mössbauer results, Table 9 to 11, identified Hematite in small concentrations present in the 400°C sample (largest concentration identified was 22%) and increasing. For the 1000°C sample only hematite (not shown in tables) was identified. The 400°C temperature is the temperature of the pellet core, meaning the surface of the pellet is at an even higher temperature. This suggests that magnetite oxidation by hematite starts at around 400°C, an observation also seen in the TGA-DSC and XRD results. Mössbauer results did not conclusively identify the maghemite to be present in the any of the samples; however, the data seemed to suggest the possible presence of maghemite in the 400°C and 700°C sample. Maghemite has been identified in partially fired green ball samples collected under the induration grate of some of the taconite

facilities. It is also believed to play a role in the oxidation of mercury in taconite processes [Berndt et al, 2005].

TGA analysis, Figures 22 and 23, consisted of heating the samples to 1100°C in air at a ramp rate of 20°C/min and held at 1100°C for 10 min. Two significant drops in weight were observed at the start of the heating and also at 700°C. The first drop was attributed to moisture loss. The second drop was considered to be due to calcination of carbonate species (limestone or dolomite) present in the sample. A significant drop was not observed in the Utac sample, most likely due to the low level of limestone used in Utac green ball formulations. Heating the samples in nitrogen to 800°C followed by heating in air showed only a mass increase which started between 350°C and 400°C. This same increase can also be seen in the samples heated in air. This confirms the observation made in the Mössbauer analysis that oxidation to hematite starts around 400°C.

Finally, XRD analysis showed an increase in hematite concentration from 400°C to 1000°C agreeing with the Mössbauer results. The XRD results (not shown) also confirmed that the disappearance of carbonate species for the 1000°C sample, confirming the observation that the weight loss seen in the TGA-DSC analysis is due to calcination of carbonate species.

The most important observation from these additional analyses is the fact that the oxidation of magnetite to hematite seems to begin at around 400°C with less than 25% mercury observed in the 400°C samples. Meanwhile, by 400°C, 75% of the mercury has been released for more than 80% of the runs performed. This agrees with work done by Benner [2003] who also observed that most of the mercury associated with green balls is out by 400°C. This would suggest that the mercury release from the green balls during the bench tests is not a function of the magnetite oxidation to hematite. Previous work performed by Berndt [2005] suggested that the oxidation of the magnetite in green balls to a maghemite/magnetite solution followed by hematite plays a role in the capture/release/oxidation of mercury in taconite facilities. Air flow patterns in taconite facilities are a lot more complex than those involved in the bench tests. Air from a hotter section of the processes is usually used to heat up colder sections, meaning mercury released in the system re-contacts the green balls and might explain the different conclusions observed between these bench tests and previous field work.

Table 9. Mössbauer Results for Utac Samples Containing 0.1wt% ESORB-HG-11.

Sample	I.D.	Magnetite A/B Ratio	Percent Total
Baseline	Magnetite A	0.62	36.89
	Magnetite B		46.60
	Magnetite B		12.62
	Unknown		3.88
Total			100.00
400°C	Magnetite A	0.60	28.00
	Magnetite B		41.00
	Magnetite B		6.00
	Hematite		21.00
	Unknown		4.00
Total			100.00
700°C	Magnetite A	0.95	18.81
	Magnetite B		13.86
	Magnetite B		5.94
	Hematite		58.42
	Unknown		2.97
Total			100.00

Table 10: Mössbauer Results for Heated Minntac Samples not Containing ESORB-HG-11

Sample	I.D.	Magnetite A/B Ratio	Percent Total
Baseline	Magnetite A	0.73	40.57
	Magnetite B		50.71
	Magnetite B		5.07
	Unknown		3.65
Total			100.00
400°C	Magnetite A	0.65	32.97
	Magnetite B		44.82
	Magnetite B		5.98
	Hematite		12.95
	Unknown		3.39
Total			100.00
700°C	Magnetite A	1.0	27.72
	Magnetite B		21.78
	Magnetite B		5.94
	Hematite		44.55
Total			100.00

Table 11. Mössbauer Results for Heated Minntac Samples Containing 0.1wt% ESORB-HG-11.

Sample	I.D.	Magnetite A/B Ratio	Percent Total
Baseline	Magnetite A	0.4	40.82
	Magnetite B	0.48	48.98
	Magnetite B	0.07	7.14
	Unknown	0.03	3.06
Total		0.98	100.00
400°C	Magnetite A	0.31	30.88
	Magnetite B	0.4	39.84
	Magnetite B	0.09	8.96
	Hematite	0.17	16.93
	Unknown	0.034	3.39
Total		1.004	100.00
700°C	Magnetite A	0.28	28.28
	Magnetite B	0.21	21.21
	Magnetite B	0.06	6.06
	Hematite	0.44	44.44
Total		0.99	100.00

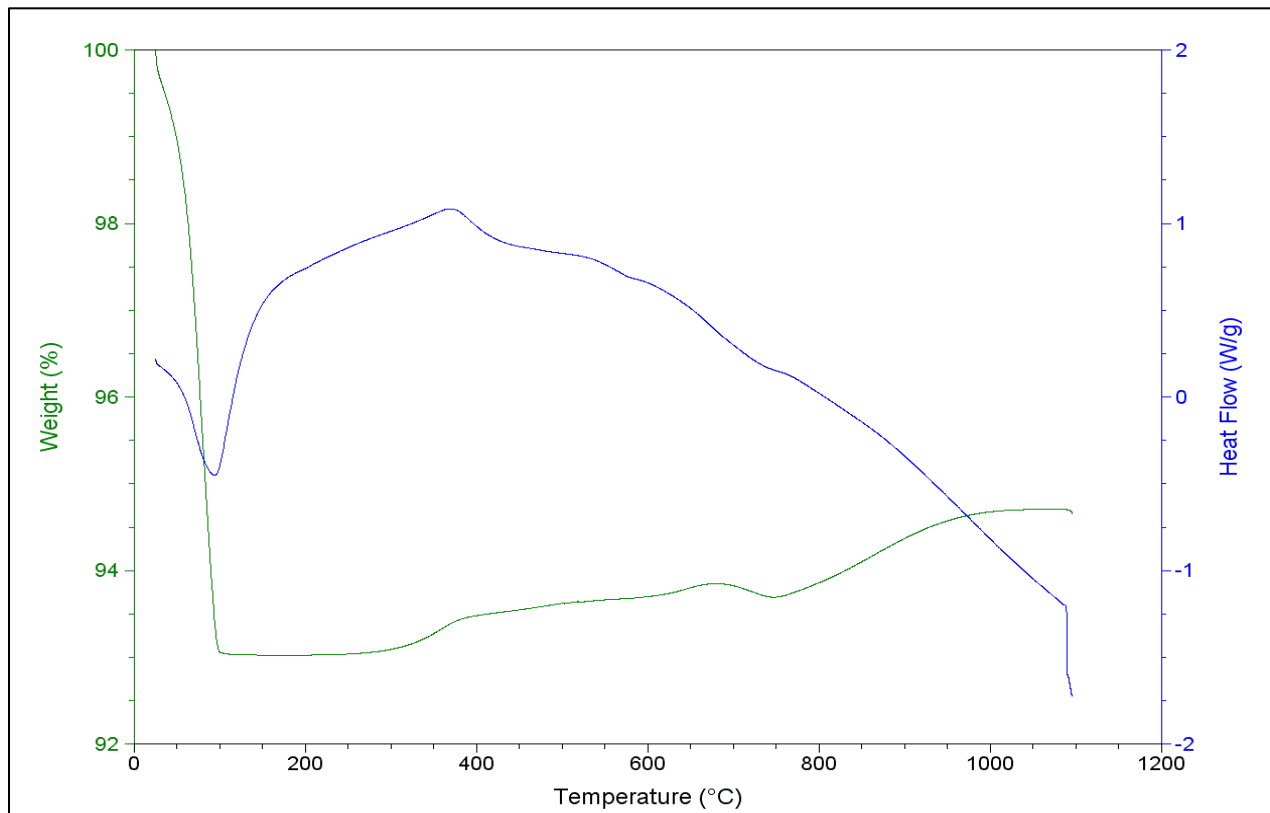


Figure 22. TGA-DSC curve for carbon-containing Utac green ball.

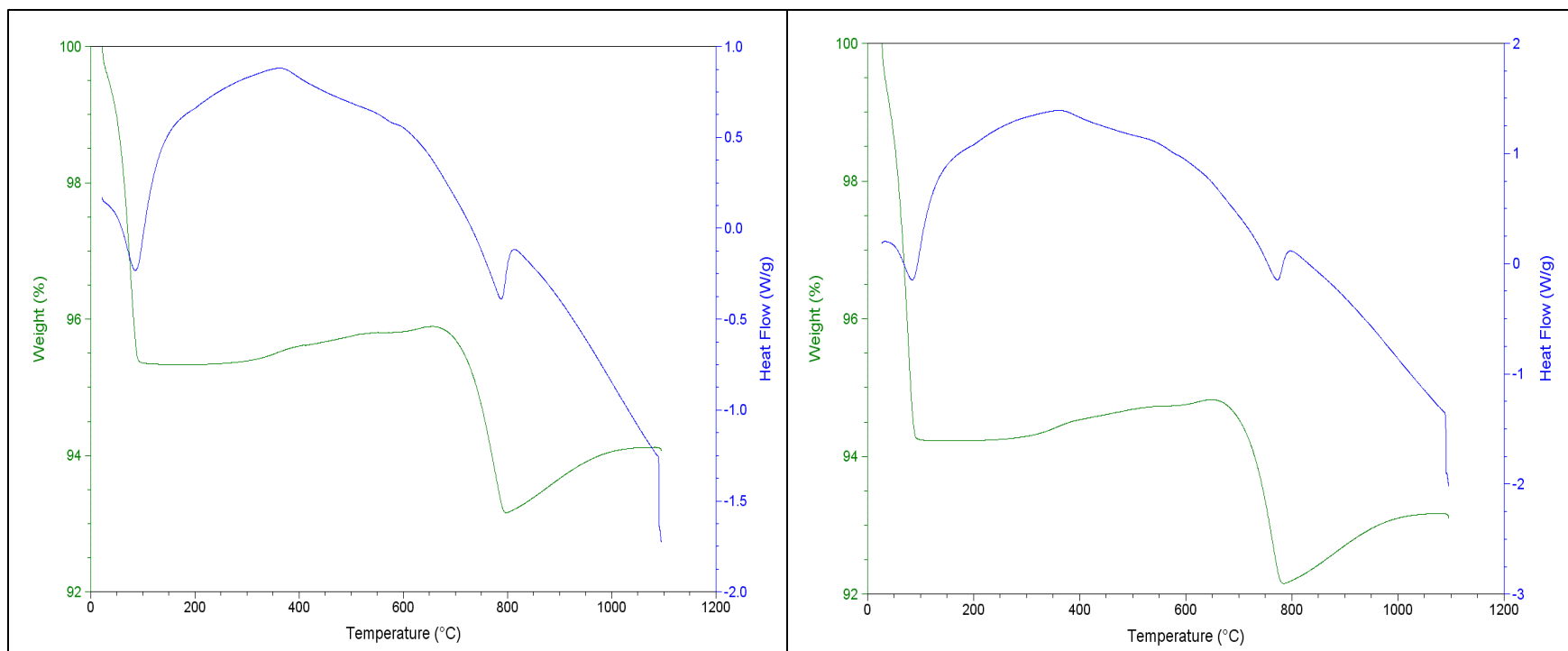


Figure 23. a) TGA-DSC curve for carbon-free Minntac green balls. b) TGA-DSC curve for carbon-containing Minntac green balls.

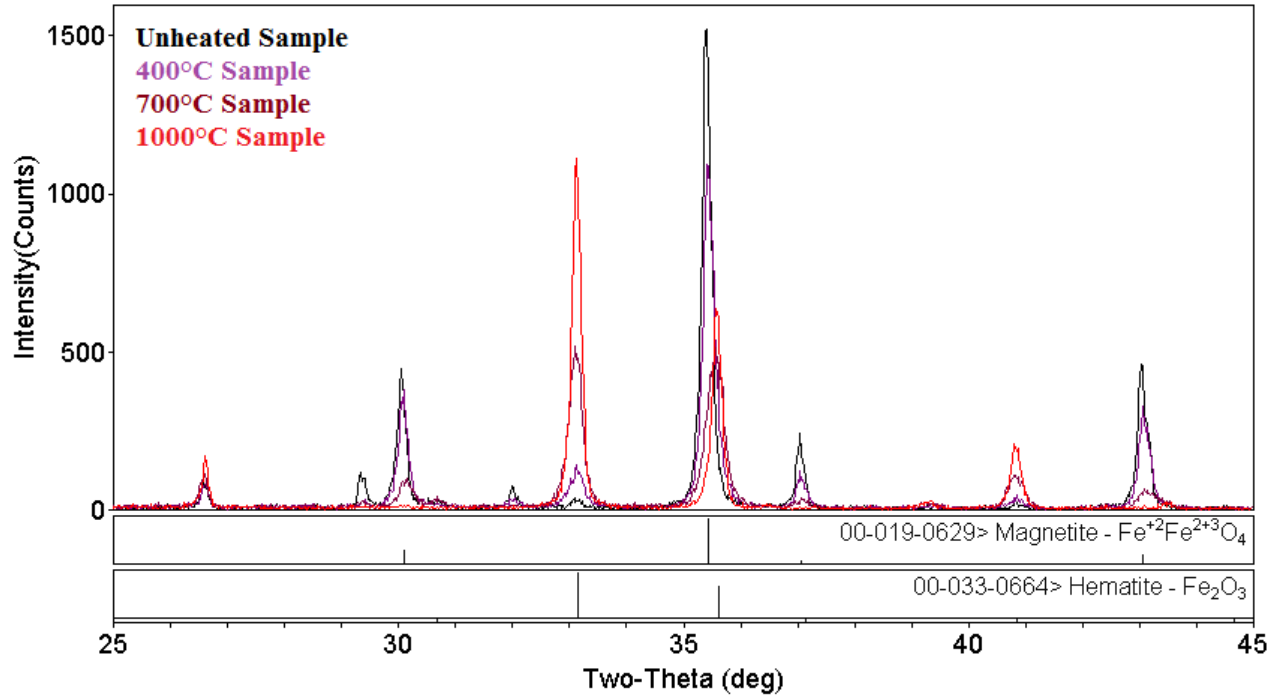


Figure 24. XRD results for Utac green ball sample at a) baseline b) 400°C c) 700°C, and d) 1000°C.

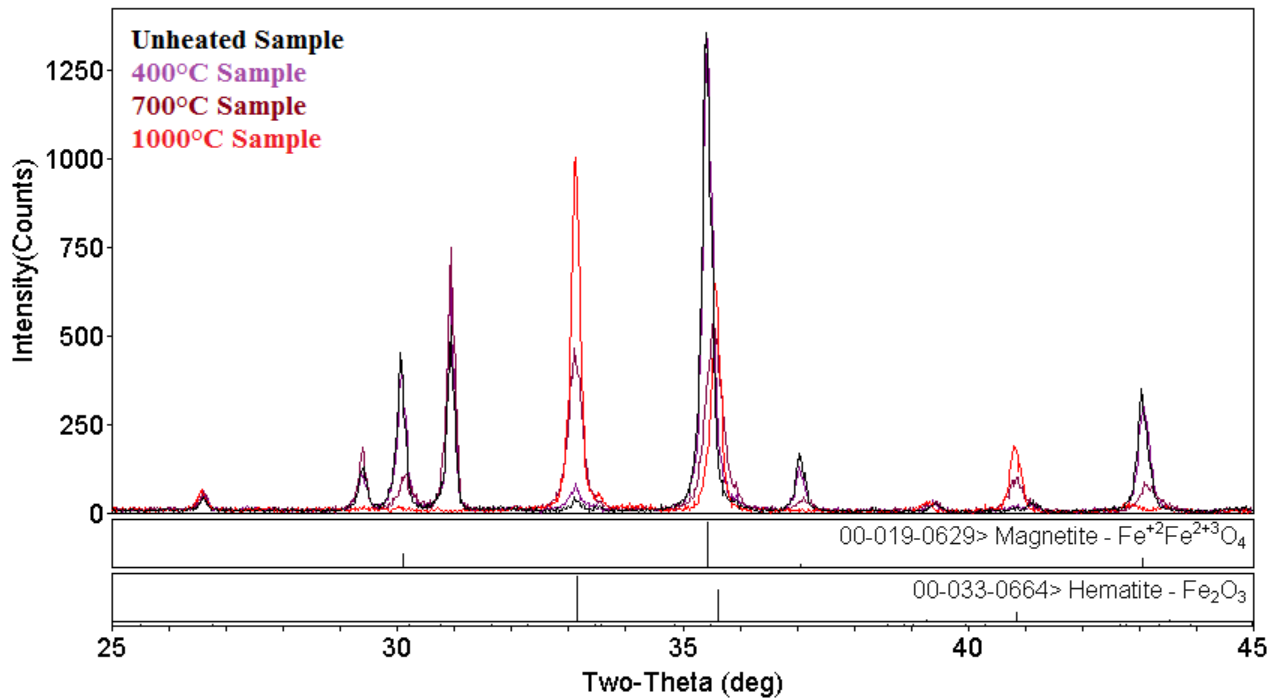


Figure 25. XRD results for Minntac green ball with no carbon at a) baseline b) 400°C c) 700°C, and d) 1000°C.

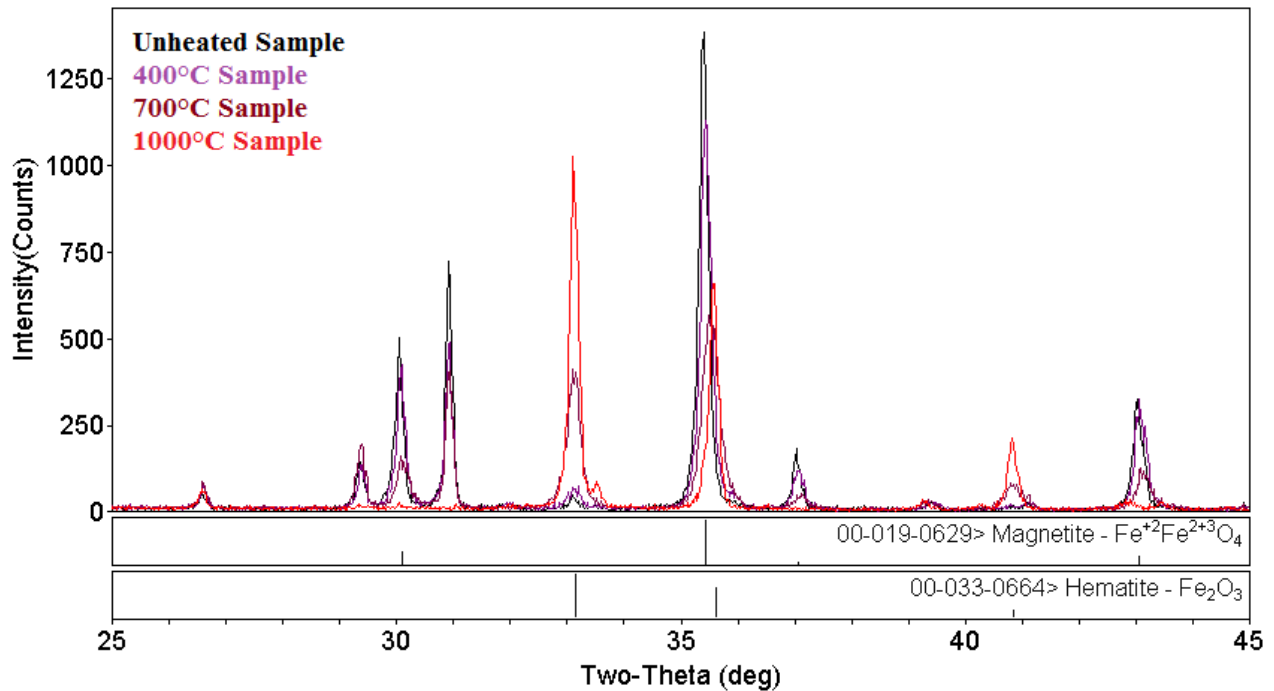


Figure 26. XRD results for Minntac green ball with 0.1wt% carbon at a) baseline b) 400°C c) 700°C, and d) 1000°C.

SEM analysis was aimed at observing how oxidation of magnetite to hematite was propagated as the green ball was heated. Samples analyzed using SEM were ground down to a 200 mesh size and suspended in an epoxy resin to enable polishing of the sample using a diamond polishing wheel. The images obtained, Figure 24, didn't show any observable difference on the surface of the iron particles. Forsmo suggested that oxidation of magnetite to hematite occurs from the surface of the particle first with oxidation of magnetite in the core controlled by the diffusion of oxygen into the particle lattice. This could explain why the SEM images obtained do not show any discernible magnetite or hematite.

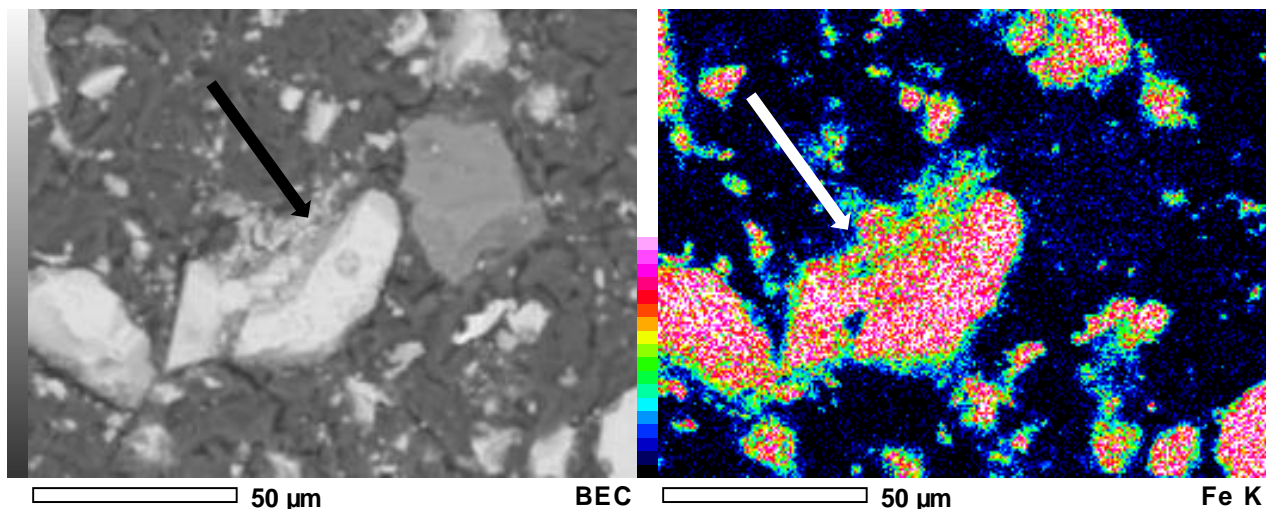


Figure 27. Carbon-containing Minntac 400°C sample showing a) SEM image magnified at 700x. b) Back scattered analysis of SEM image showing presence of iron. No discernible difference on iron surface.

Conclusions

Testing of green balls for all five Taconite facilities operating on the Mesabi Iron Range demonstrated that the additive – ESORB-HG-11 (a brominated activated carbon) has the ability to improve mercury oxidation as the mercury thermally desorbs. Green balls containing ESORB-HG-11 showed oxidation due to the additive alone (or, mercury reduction potential – using a scrubber to capture oxidized mercury) ranging from 29% to 74%, except for green balls obtained from United Taconite. Average oxidation values obtained for all plants are presented in Figure 28.

Baseline oxidations gave an average of 18% for all the runs, with a standard deviation of 6%. Additive loadings of 0.1wt% gave a reduction potential of 42% with a standard deviation of 9%, and, additive loading of 0.5wt% gave a reduction potential of 48% with a standard deviation of 13%. United Taconite data were not included in determining averages. The close agreement between results of different plants confirms that ESORB-HG-11 is effective in promoting mercury oxidation. The mercury oxidation observed for ESORB-HG-11 – containing green balls is considered to occur as a solid phase reaction on the surface of the green ball pellets. Gas phase oxidation reactions are not considered significant during the bench testing. This implies that there is a potential for higher oxidation levels to be observed for full-scale testing of the technology, as previous testing at taconite facilities [Berndt, Engesser 2005] suggest that gas phase mercury oxidation contributes to the final oxidation observed. Moreover, ESORB-HG-11 has proven to show good gas phase oxidation capabilities when tested at Minntac line 3 [Taconite Mercury Emission Control Studies - Project 1].

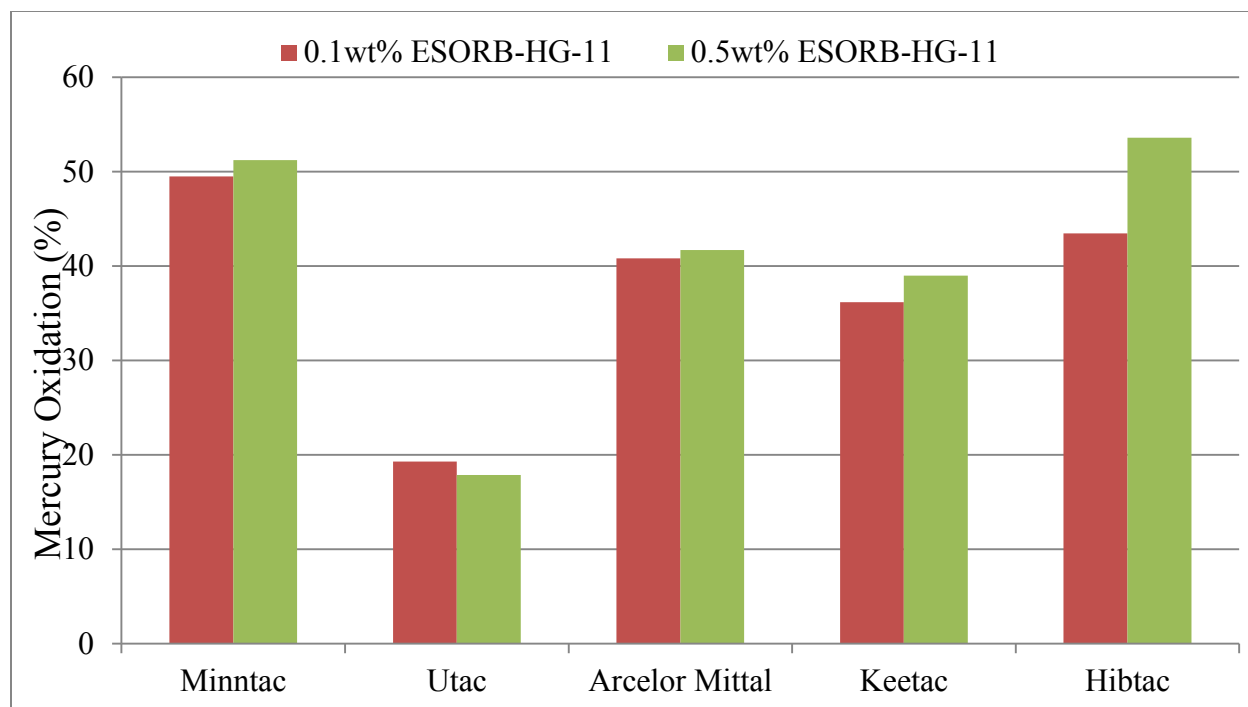


Figure 28. Reduction potential observed for 0.1wt% and 0.5wt% loading of ESORB-HG-11.

The green balls tested were produced by the Coleraine Minerals Research Laboratory (CMRL) of the Natural Resources Research Institute (NRRI) and were subjected to industry-standard, Batch Balling tests to evaluate the effect the additive had on the moisture content, wet drop number, and dry compressive strength. For the samples with 0.1weight% additive, no significant difference due to addition of ESORB-HG-11 was observed with respect to the baseline standard during the batch balling tests. Slight differences from the baseline standard were observed with the 0.5weight% additive loading. The 0.1weight% loading was determined to be the optimum loading for potential full-scale testing of the technology.

Future Work

Suggested future work for this project primarily consists of conducting Fired Pellet Quality Tests on carbon-containing green balls to ensure that addition of ESORB-HG-11 to the green ball does not affect the physical properties of the taconite pellets.

If the tests confirm that addition of ESORB-HG-11 to green balls has no significant negative effect on the physical properties of the taconite pellets, then full-scale testing of the technology is recommended to determine actual reduction potential.

References

- Benner, B. (2005) *Mercury release from taconite during heating*. CMRL report TR-05-06/NRRI/TR-2005-17, 3 pages.
- Berndt, M. E. *Mercury and Mining in Minnesota*, Report, MN Dept. of Natural Resources, 2003.
- Berndt, M.E.; Engesser, J. E. *Mercury Transport in Taconite Processing Facilities: (II) Release and Capture during Induration*, Report, MN Dept. of Natural Resources, 2005.
- Berndt, M. E.; Engesser, J. E. *Mercury Transport in Taconite Processing Facilities: (III) Control Method Test Results*, Report, MN Dept. of Natural Resources, 2007.
- Berndt, M. E.; Engesser, J. E.; Berquó, T. S. *Mercury Chemistry and Mössbauer Spectroscopy of Iron Oxides During Taconite Processing on Minnesota's Iron Range*, Report, MN Dept. of Natural Resources, 2005b.
- Environmental Protection Agency, *AP 42: Compilation of Air Pollutant Emission Factors*, CH. 11, Volume 1, Fifth Edition; <http://www.epa.gov/ttnchie1/ap42/ch11/final/c11s23.pdf> (Accessed June 10, 2012).
- Forsmo, S. *Influence of Green Pellet Properties on Pelletizing of Magnetite Iron Ore*, Doctoral Thesis, Luleå University of Technology, Luleå, Sweden, 2007.
- Galbreath, K. C. *Mercury Vaporization Characteristics of Taconite Pellets*, Final Report, MN Dept. of Natural Resources, 2005.
- QAPP for Taconite Mercury Control Studies: Phase I*, Minnesota Department of Natural Resources, 2010.

Appendix A – Results

Minntac Baseline Results:

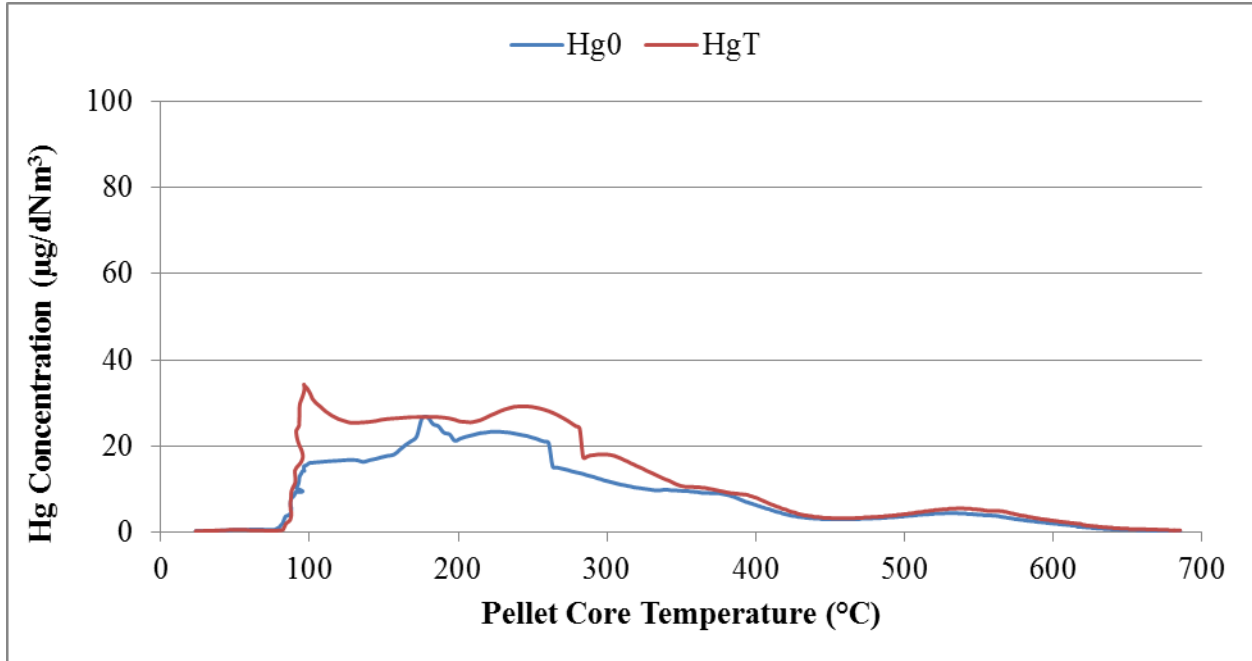


Figure 29. Mercury release profile for Minntac second baseline run.

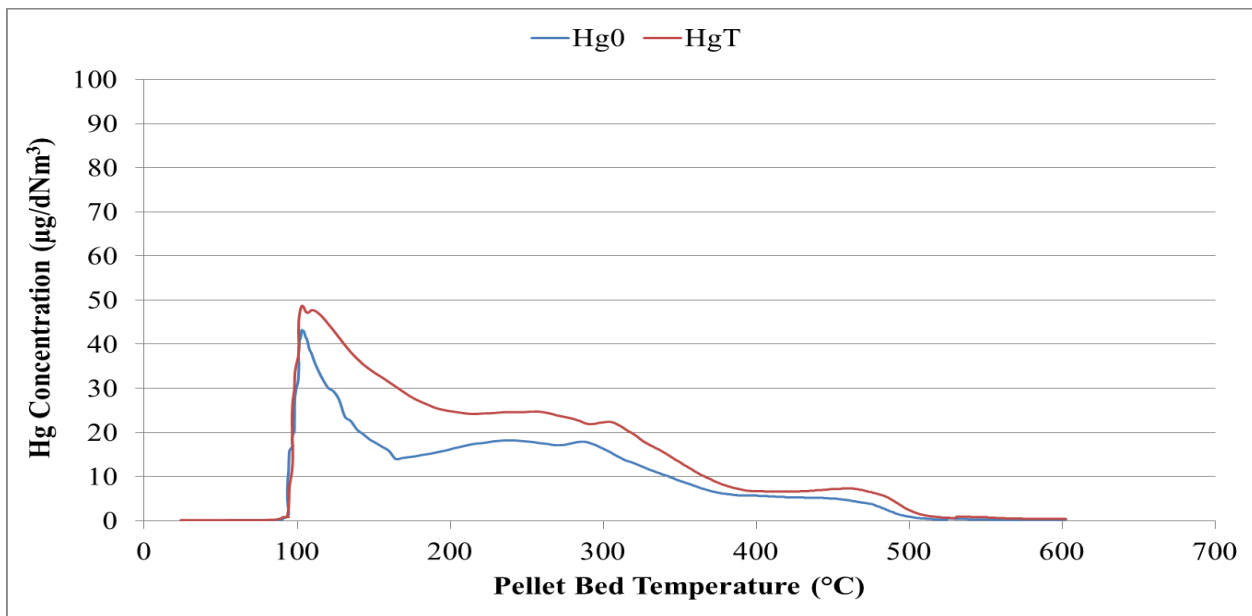


Figure 30. Mercury release profile for Minntac replicate batch first baseline run.

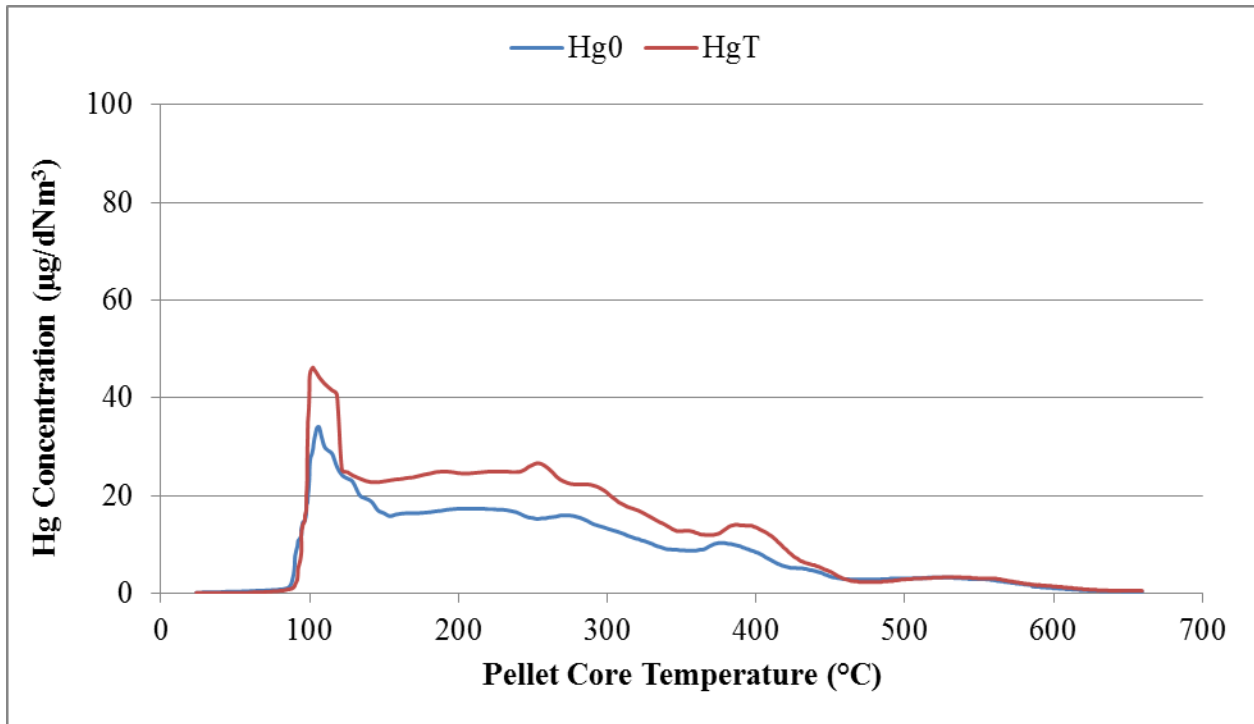


Figure 31. Mercury release profile for Minntac replicate batch second baseline run.

Minntac 0.1wt% Loading Runs:

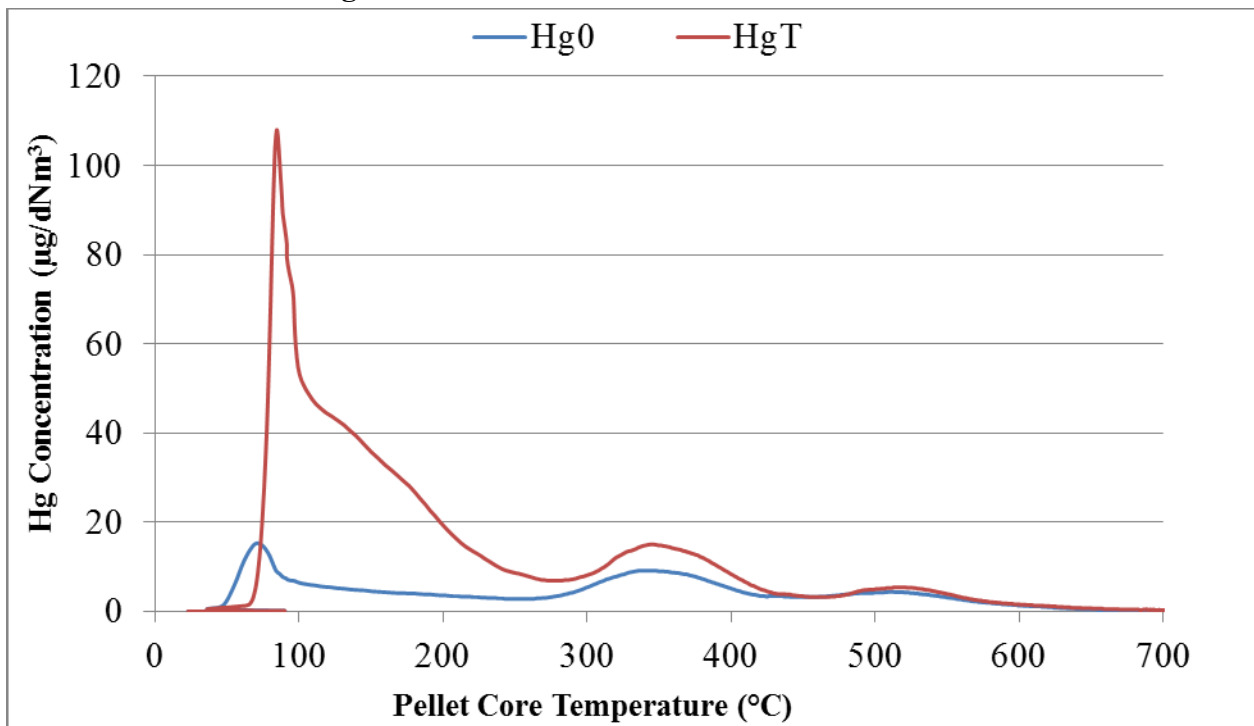


Figure 32. Mercury release profile for Minntac second 0.1wt% run.

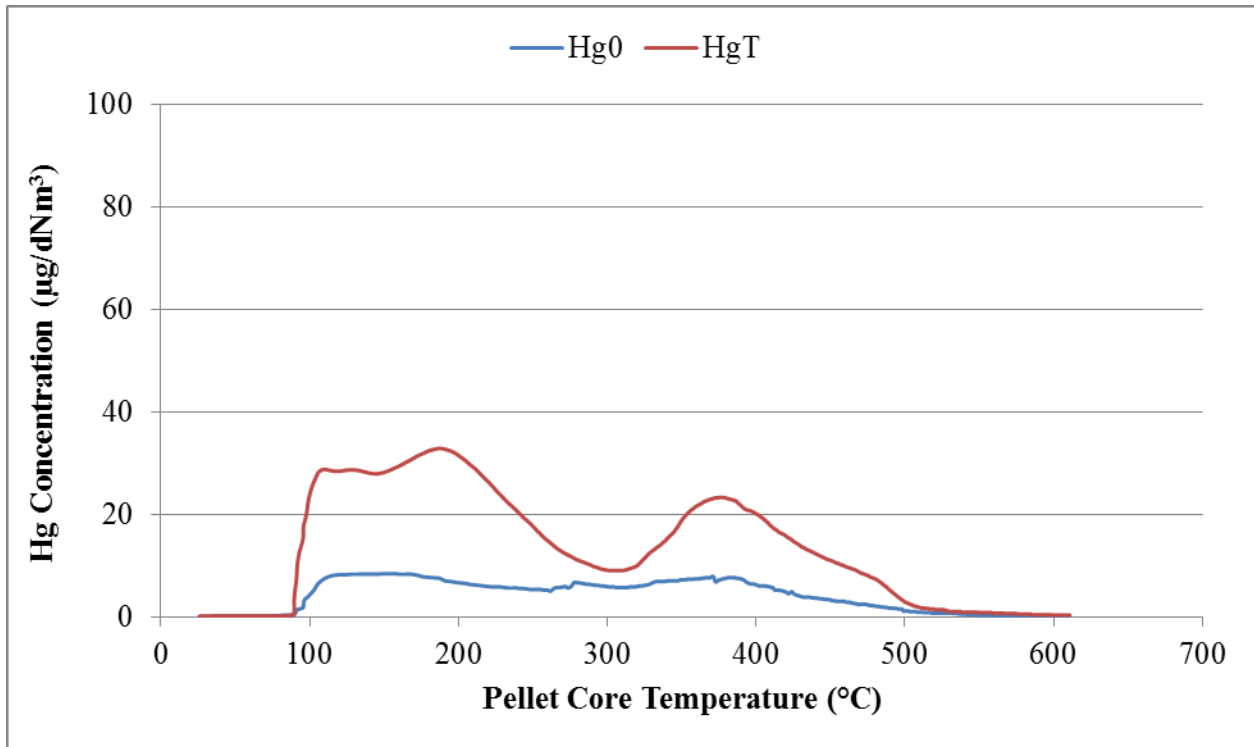


Figure 33. Mercury release profile for Minntac third 0.1wt% run.

Minntac 0.5wt% Loading Results:

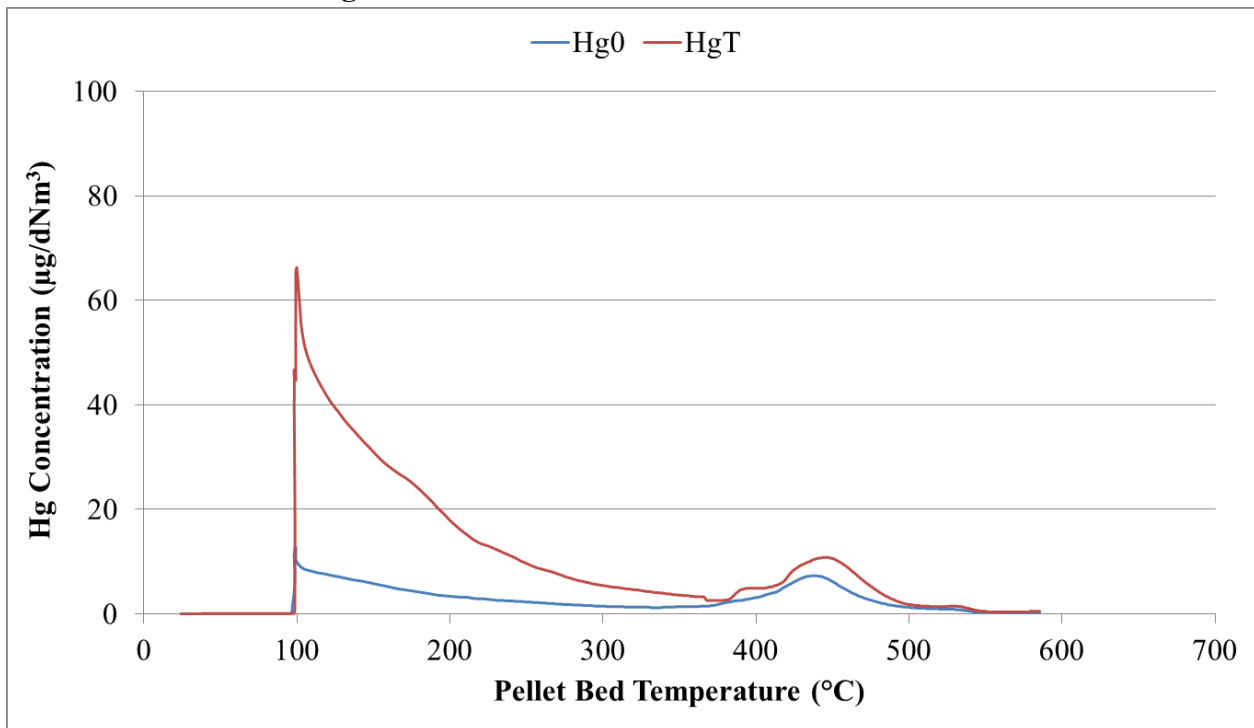


Figure 34. Mercury release profile for Minntac first 0.5wt% run.

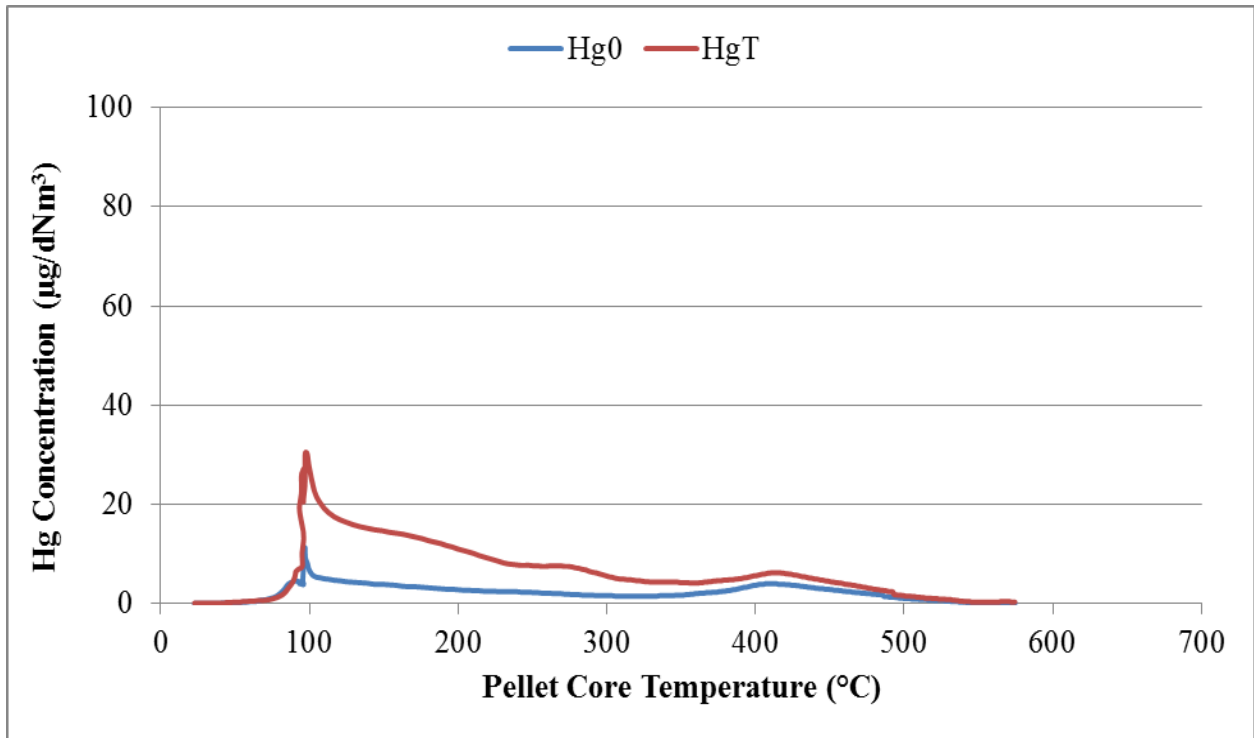


Figure 35. Mercury release profile for Minntac second 0.5wt% run.

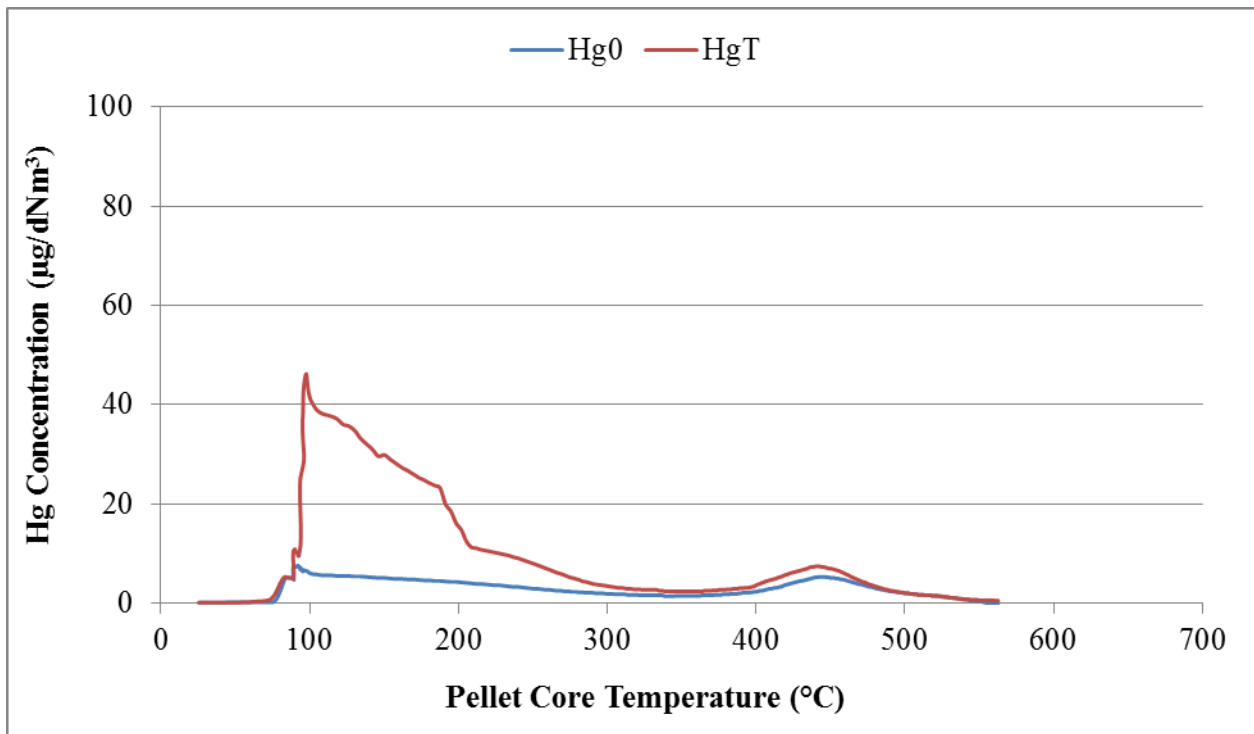


Figure 36. Mercury release profile for Minntac third 0.5wt% run.

Utac Baseline Results:

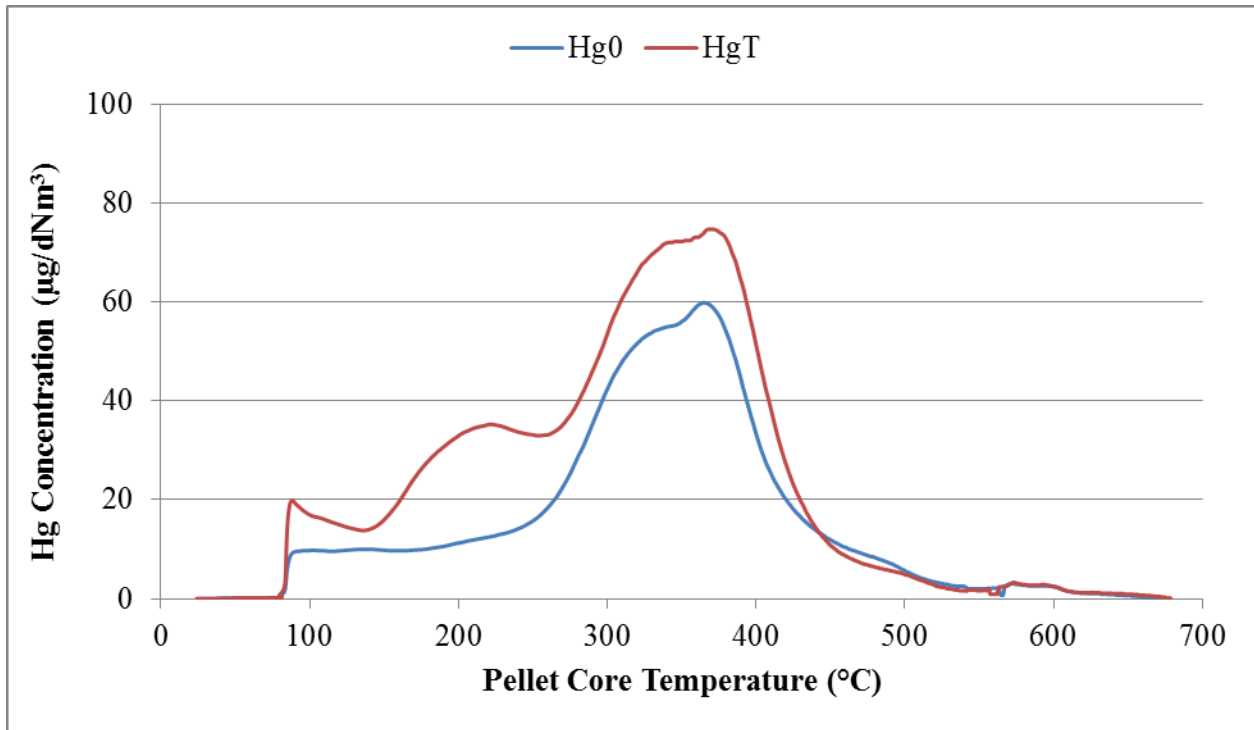


Figure 37. Mercury release profile for Utac first baseline run.

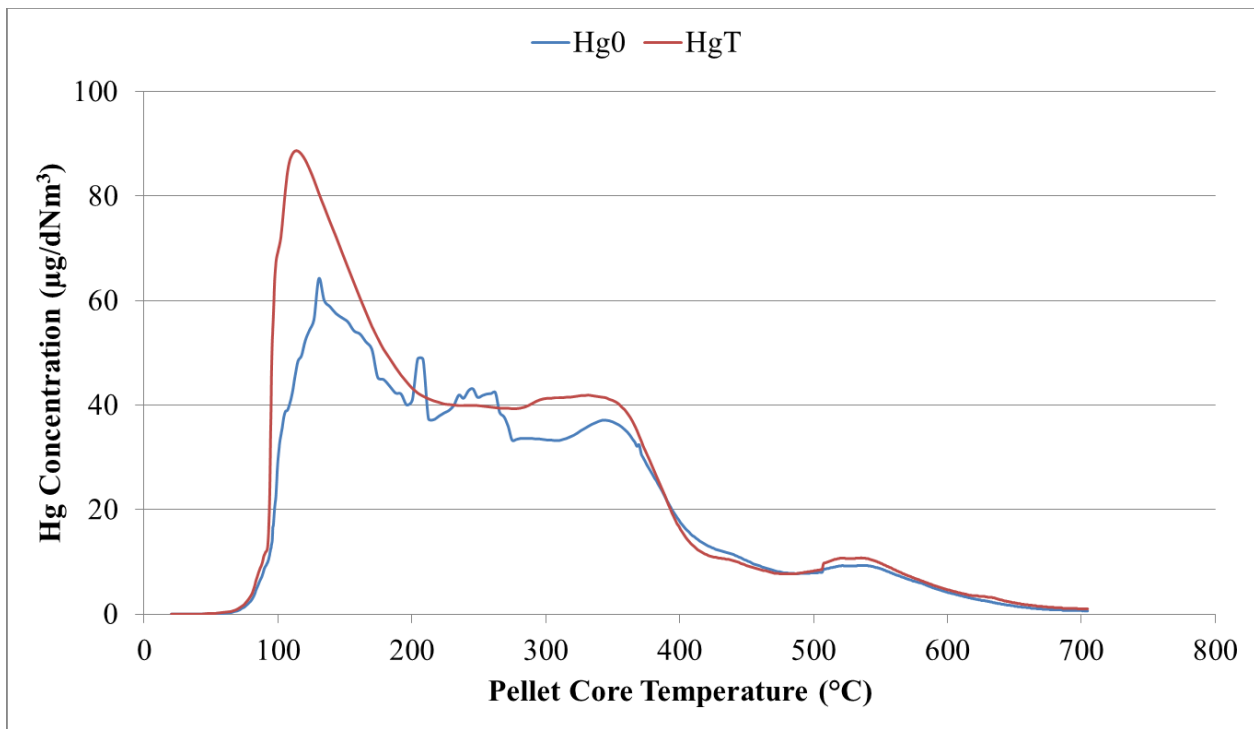


Figure 38. Mercury release profile for Utac third baseline run.

Utac 0.1wt% Loading Results:

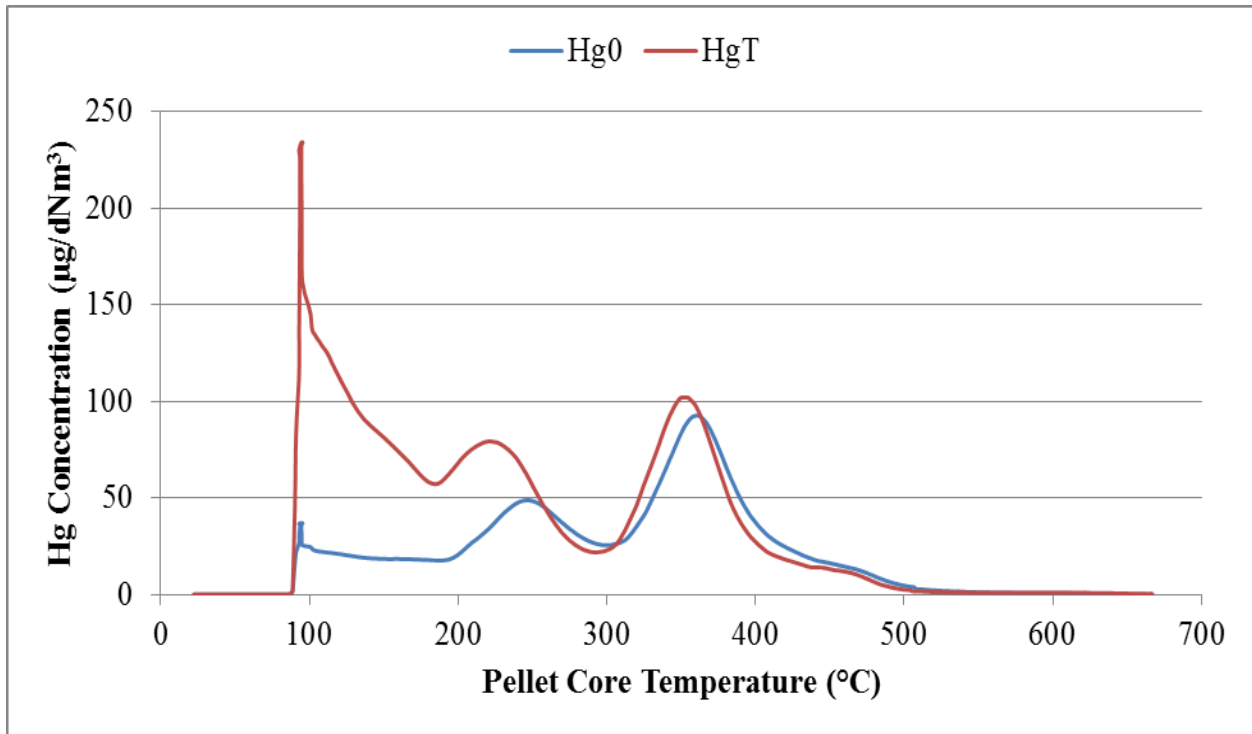


Figure 39. Mercury release profile for Utac third 0.1wt% run.

Utac 0.5wt% Loading Results:

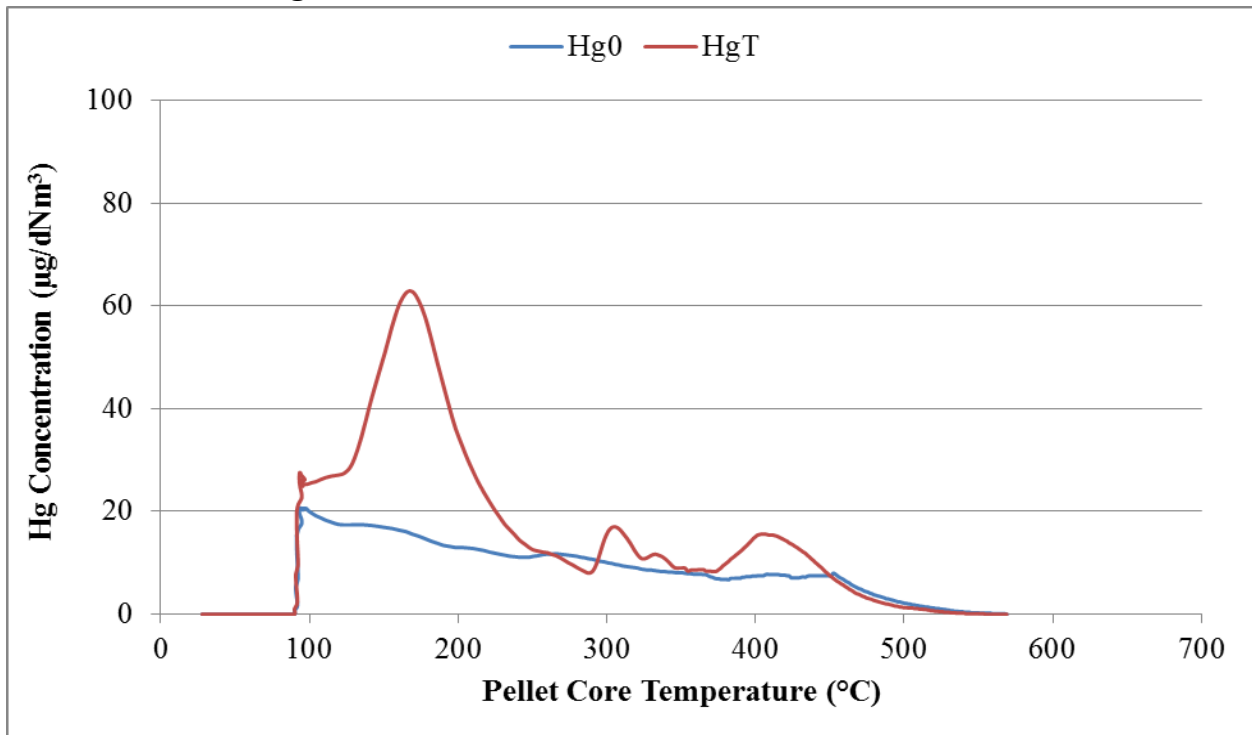


Figure 40. Mercury release profile for Utac first 0.5wt% run.

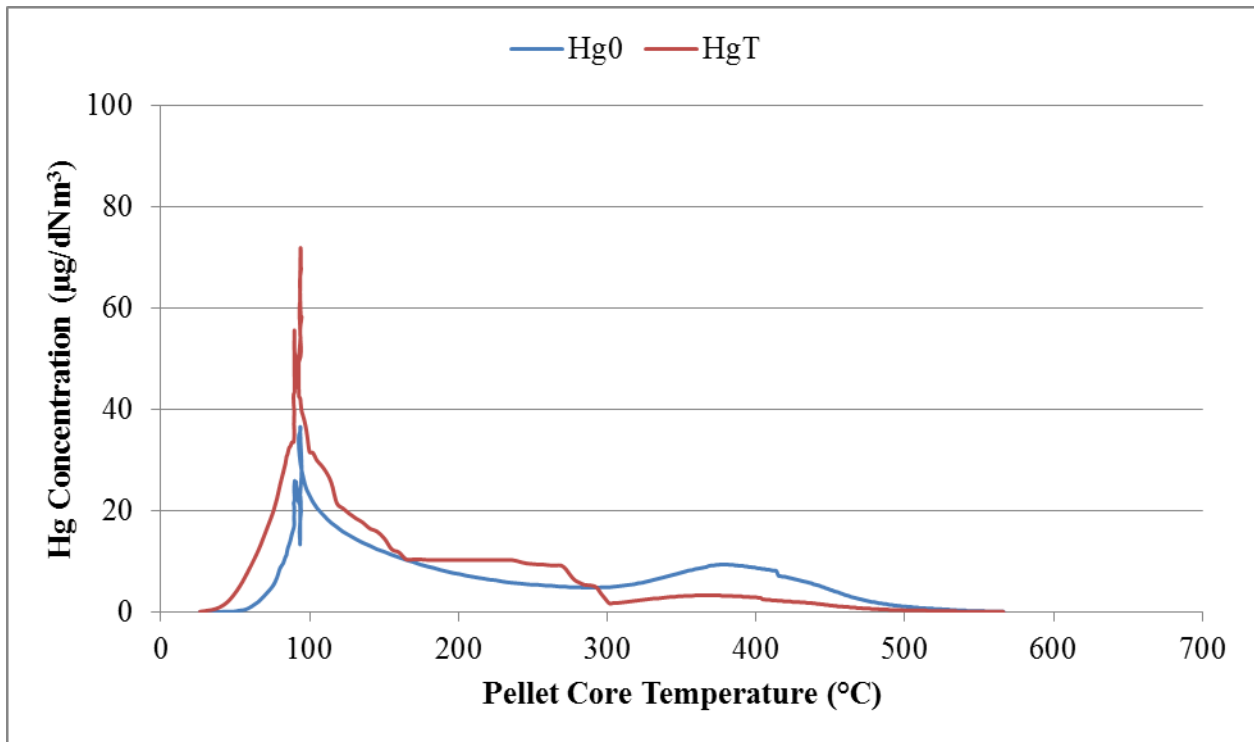


Figure 41. Mercury release profile for Utac second 0.5wt% run.

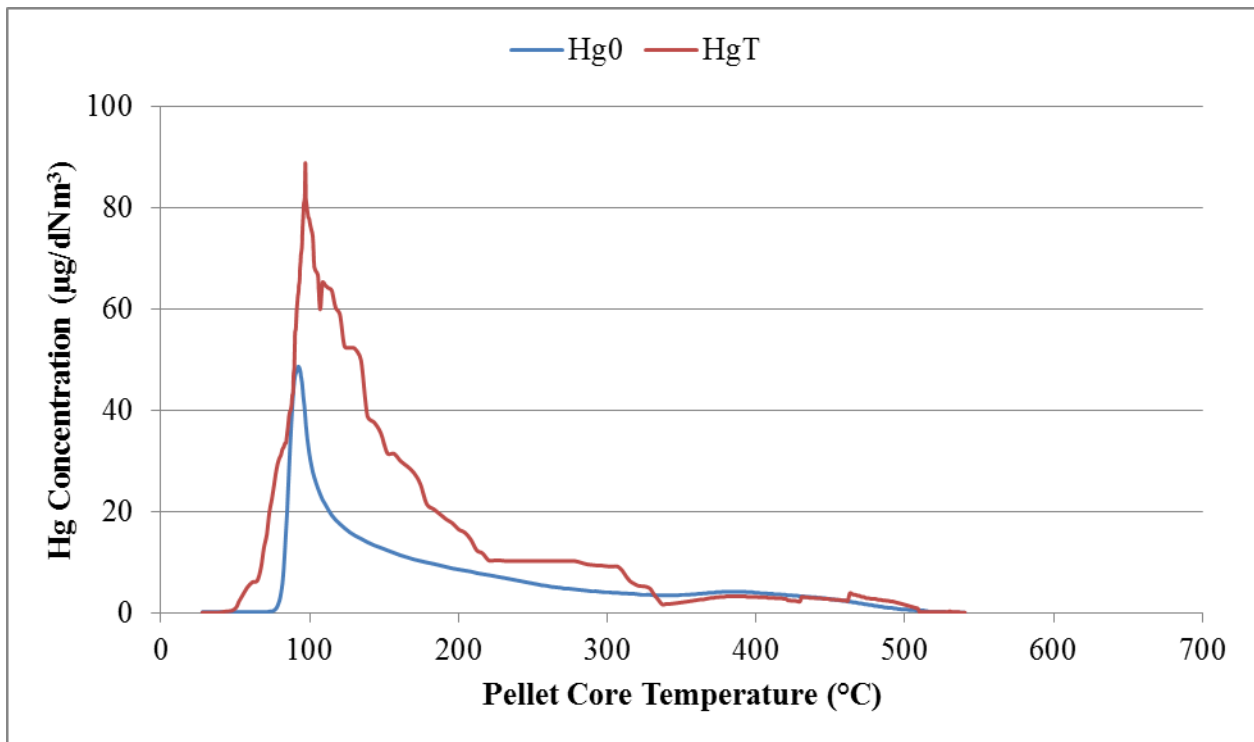


Figure 42. Mercury release profile for Utac replicate second 0.5wt% run.

Arcelor Mittal Baseline Results:

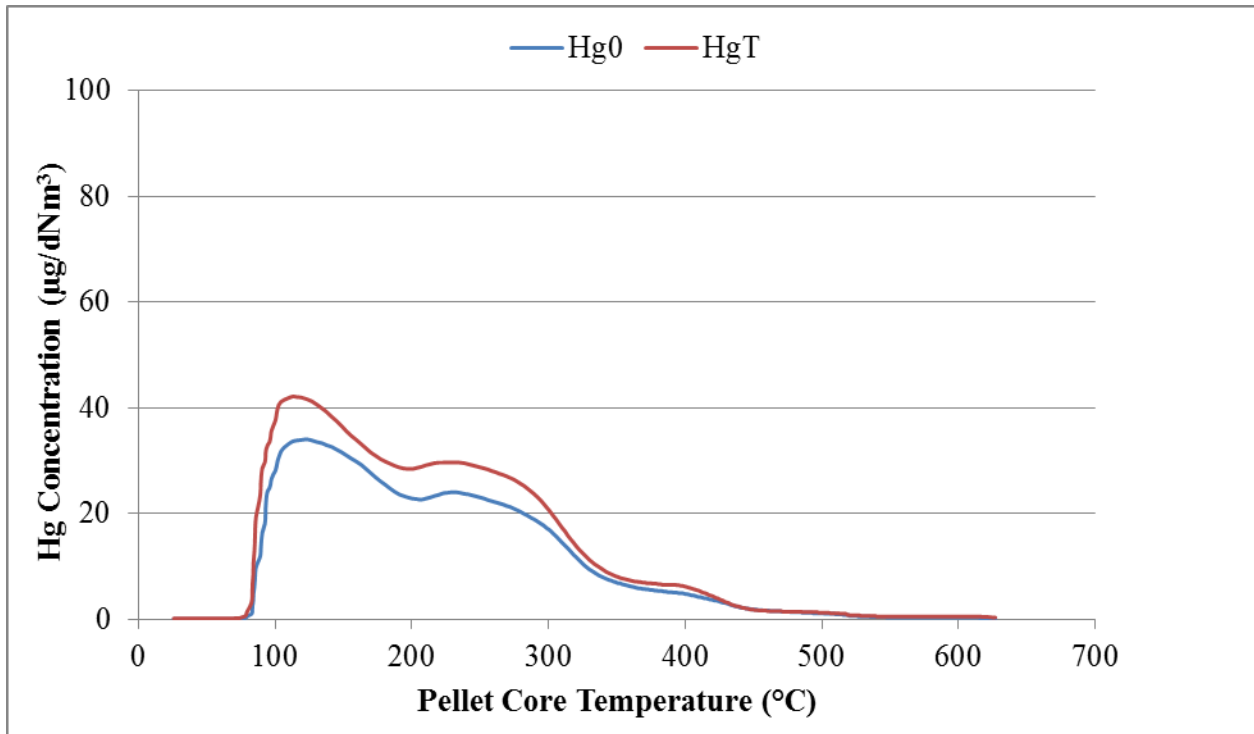


Figure 43. Mercury release profile for Arcelor Mittal baseline run.

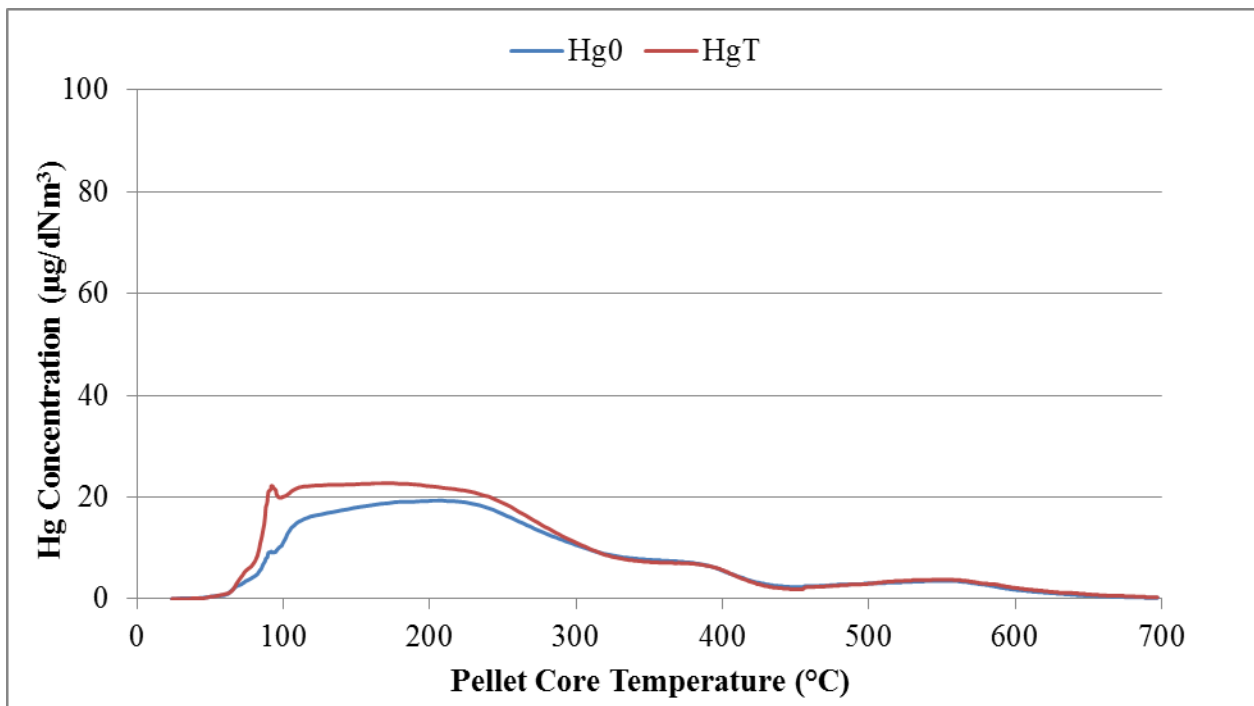


Figure 44. Mercury release profile for Arcelor Mittal third baseline run.

Arcelor Mittal 0.1wt% Loading Results:

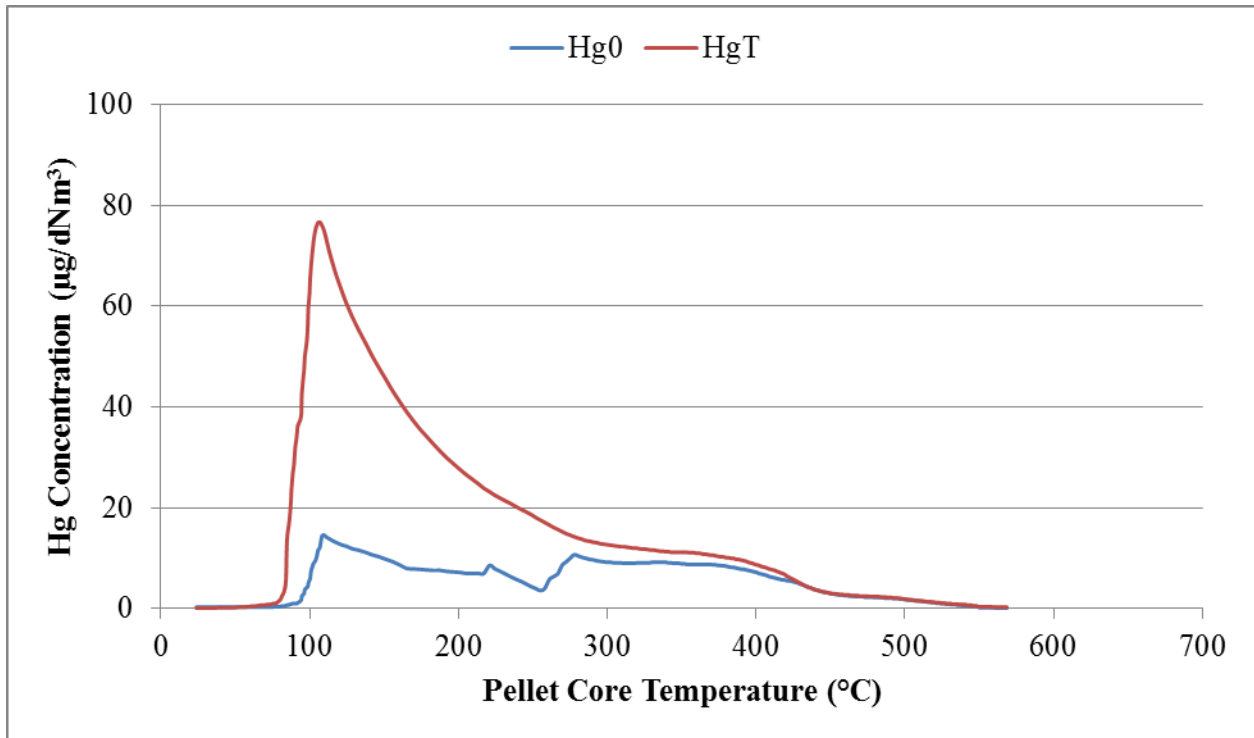


Figure 45. Mercury release profile for Arcelor Mittal first 0.1wt% loading run.

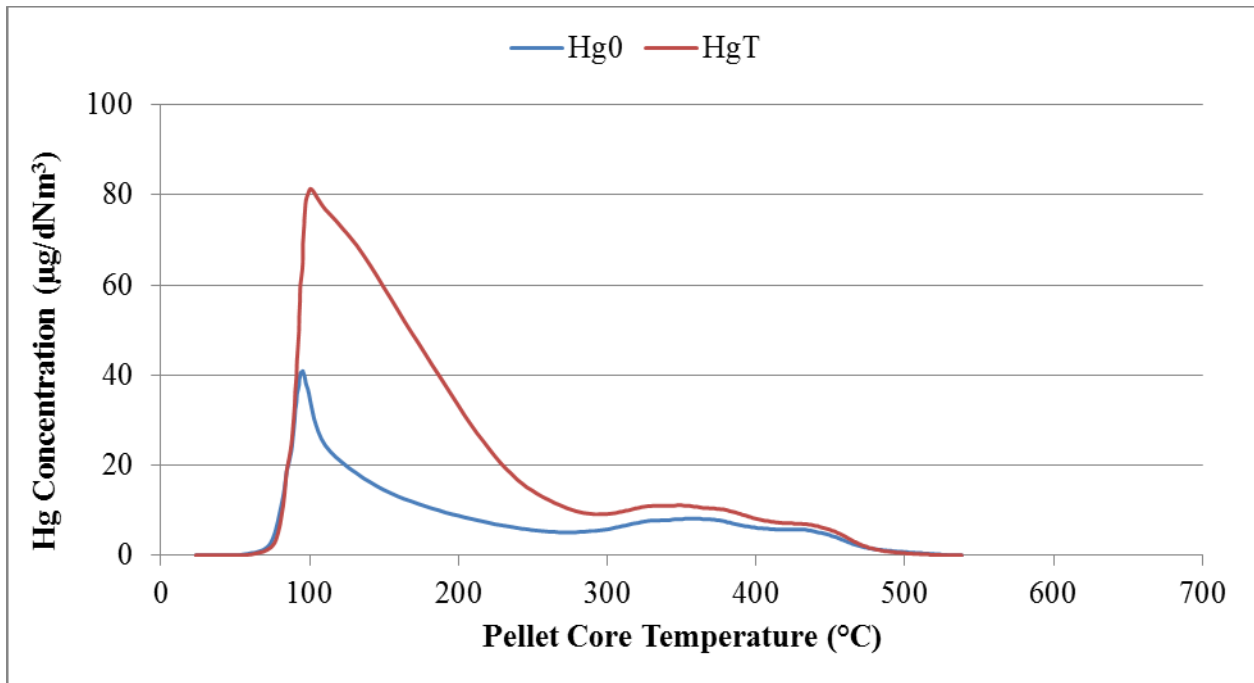


Figure 46. Mercury release profile for Arcelor Mittal second 0.1wt% loading run.

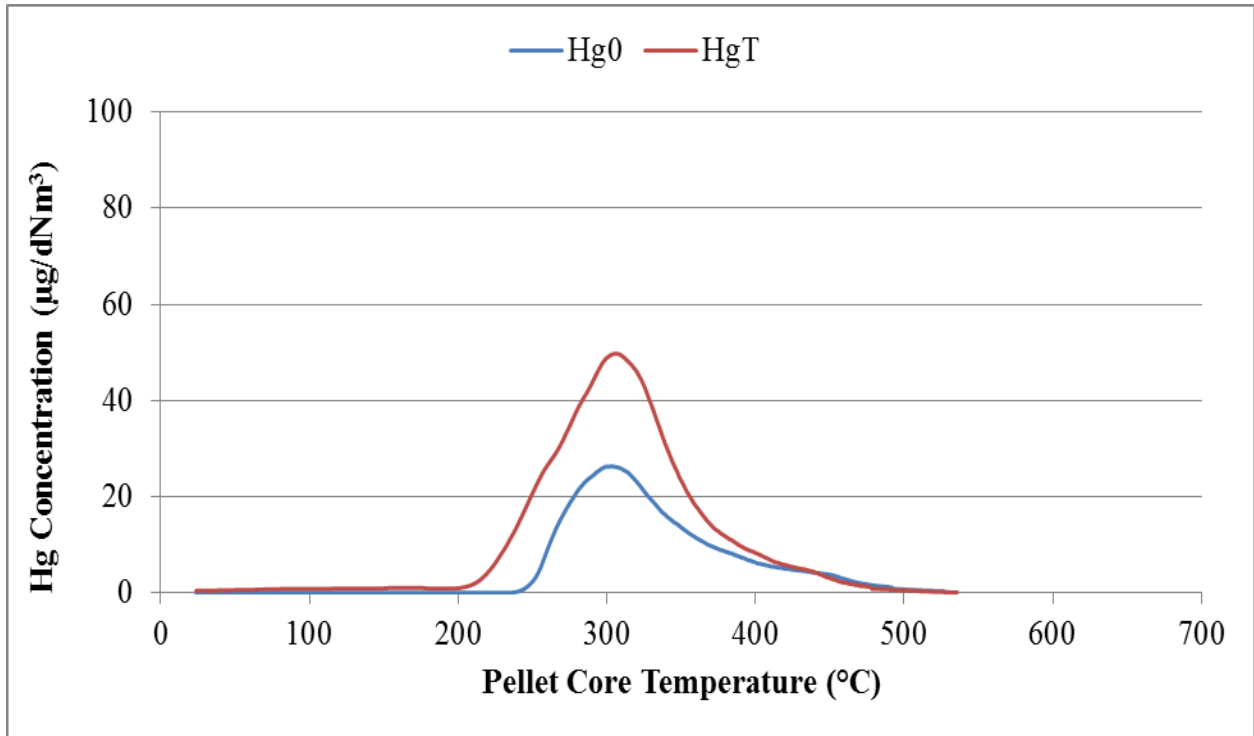


Figure 47. Mercury release profile for Arcelor Mittal second 0.1wt% replicate loading run.

Arcelor Mittal 0.5wt% Loading Results:

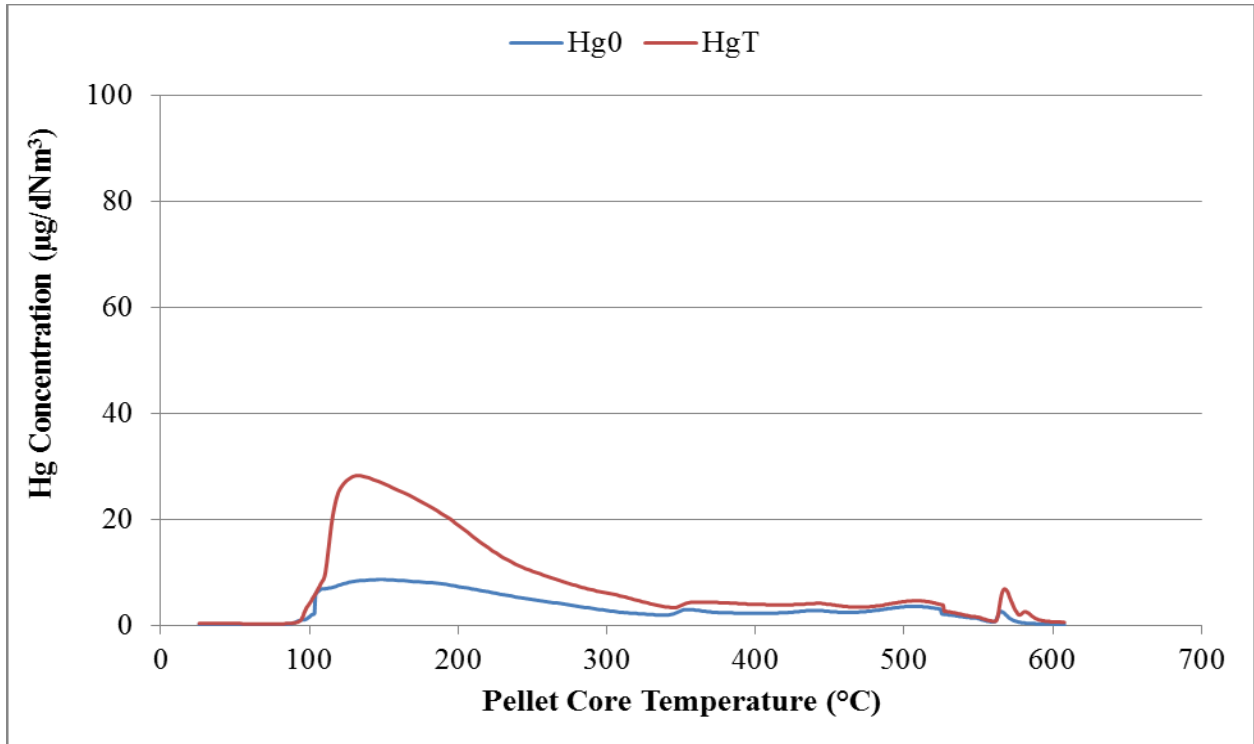


Figure 48. Mercury release profile for Arcelor Mittal first 0.5wt% loading run.

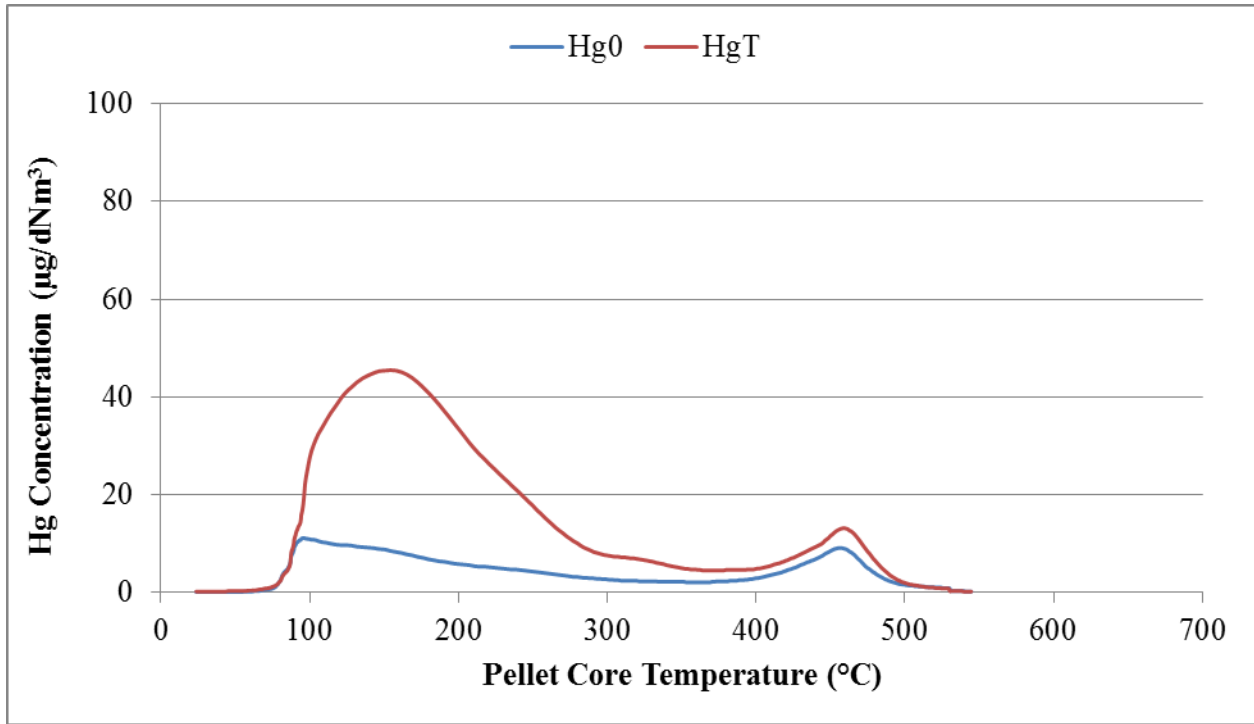


Figure 49. Mercury release profile for Arcelor Mittal second 0.5wt% loading run.

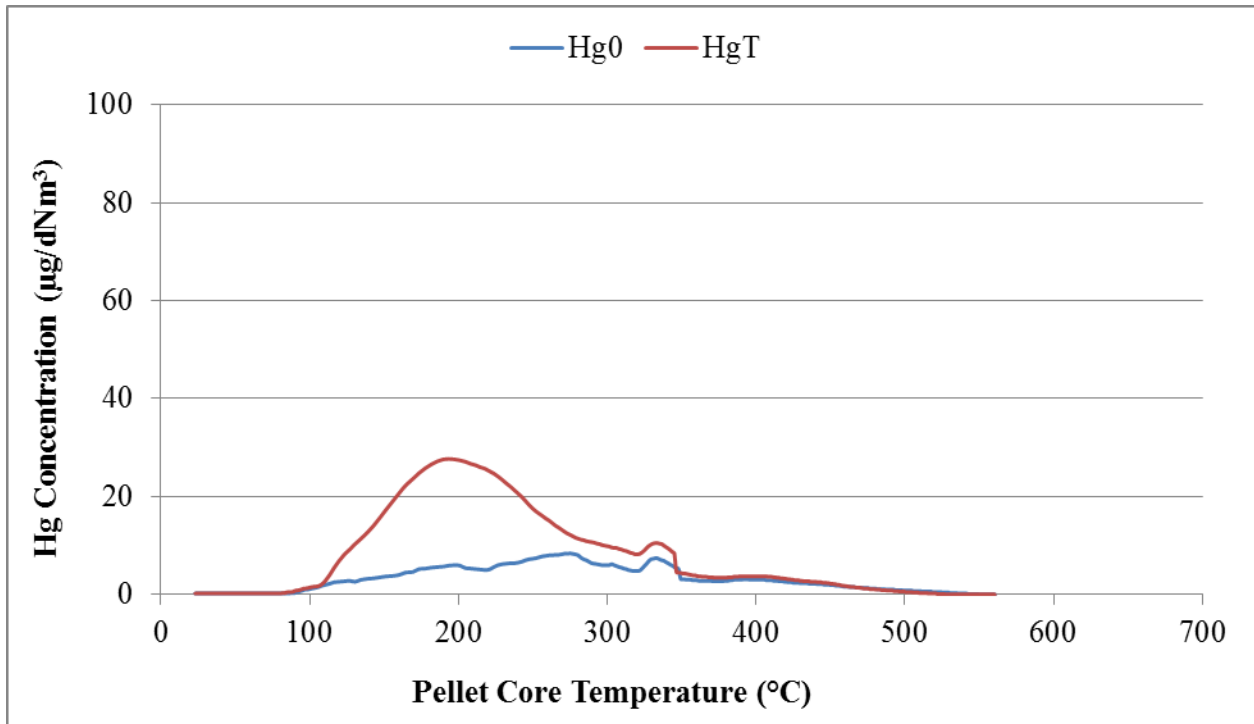


Figure 50. Mercury release profile for Arcelor Mittal third 0.5wt% loading run.

Keetac Baseline Test Results:

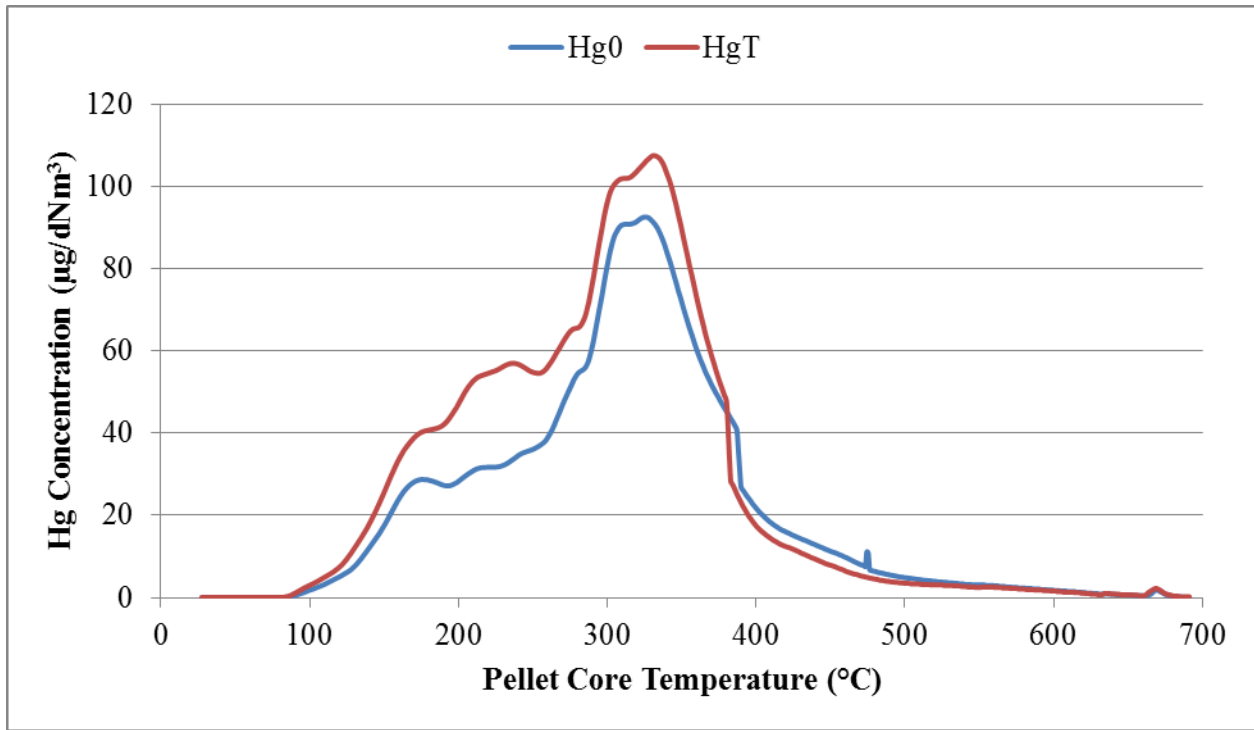


Figure 51. Mercury release profile for Keetac first baseline run.

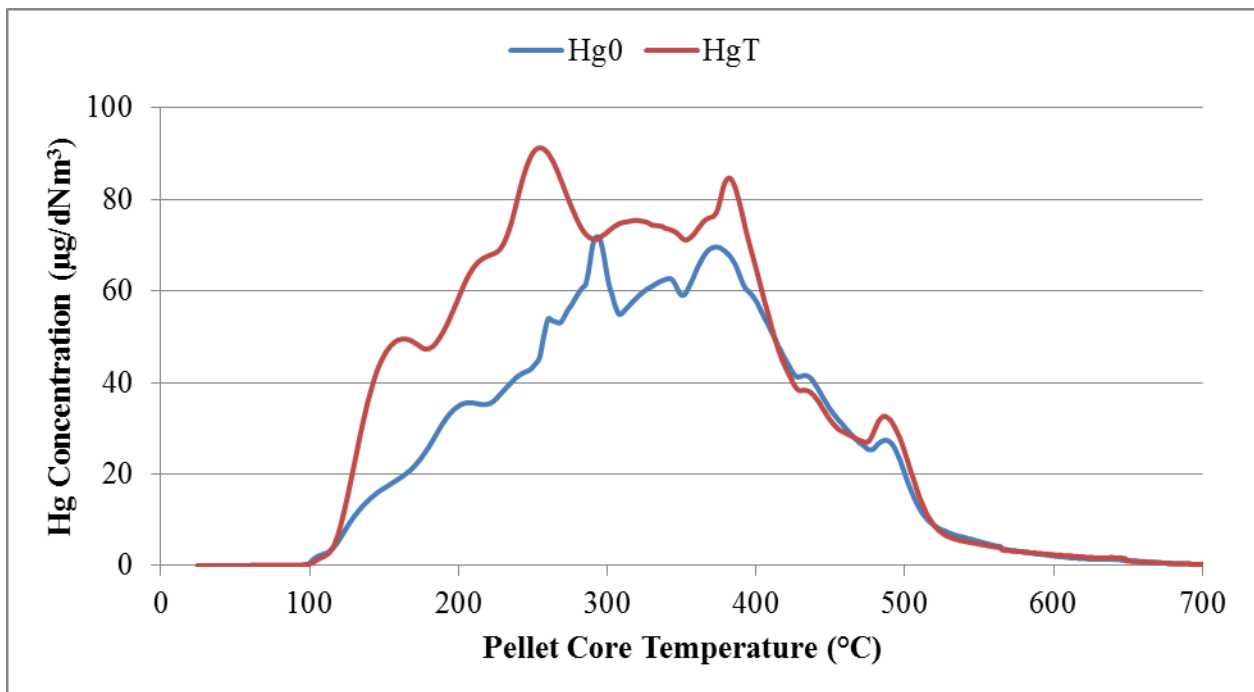


Figure 52. Mercury release profile for Keetac second baseline run.

Keetac 0.1wt% Loading Results:

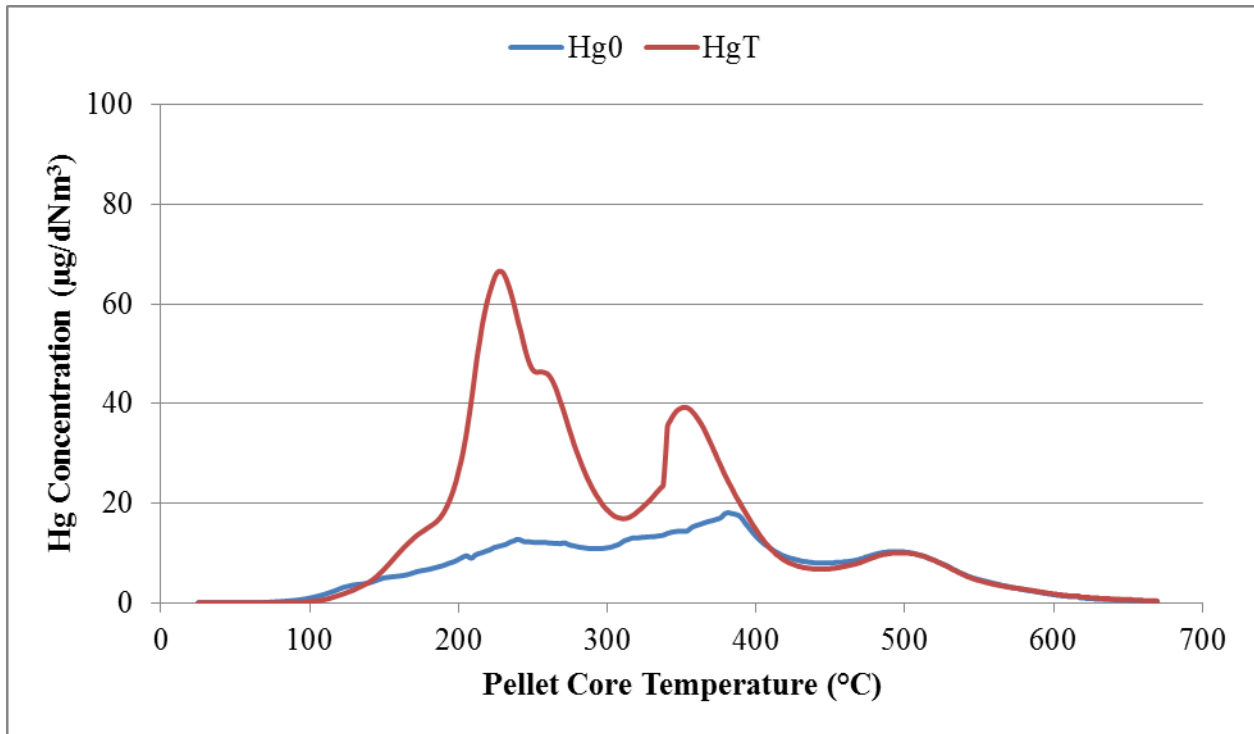


Figure 53. Mercury release profile for Keetac second 0.1wt% run.

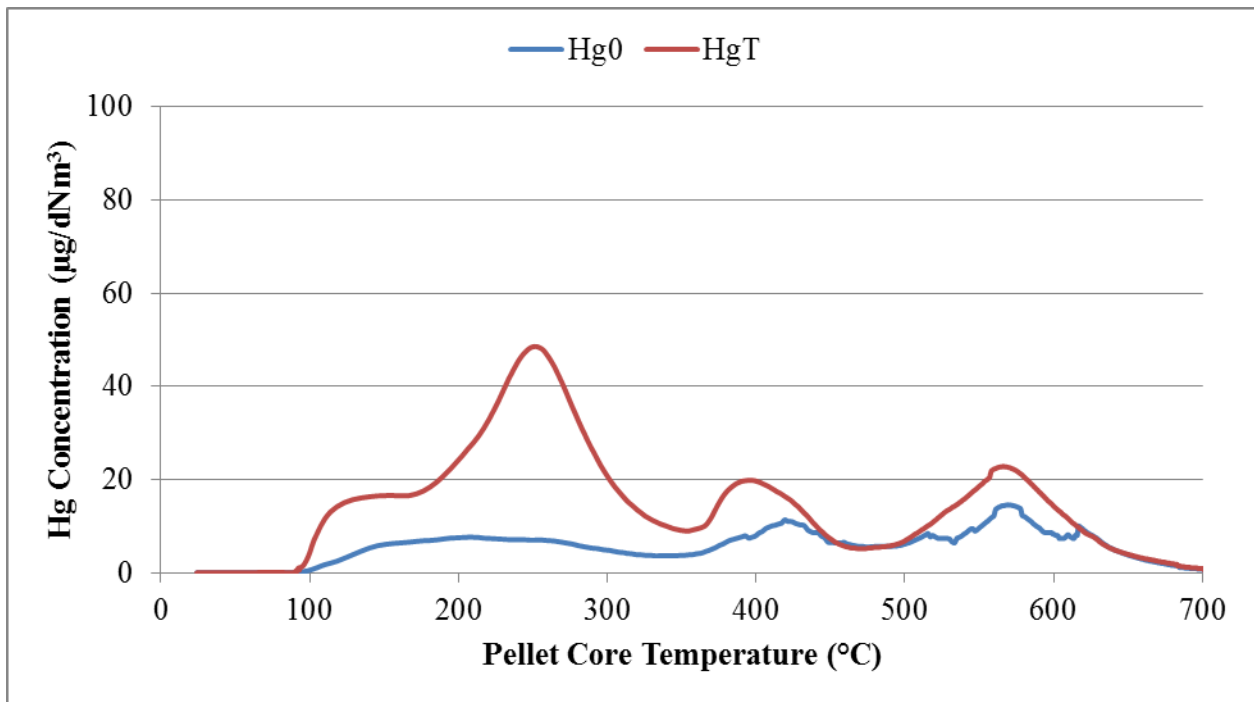


Figure 54. Mercury release profile for Keetac replicate first 0.1wt% run.

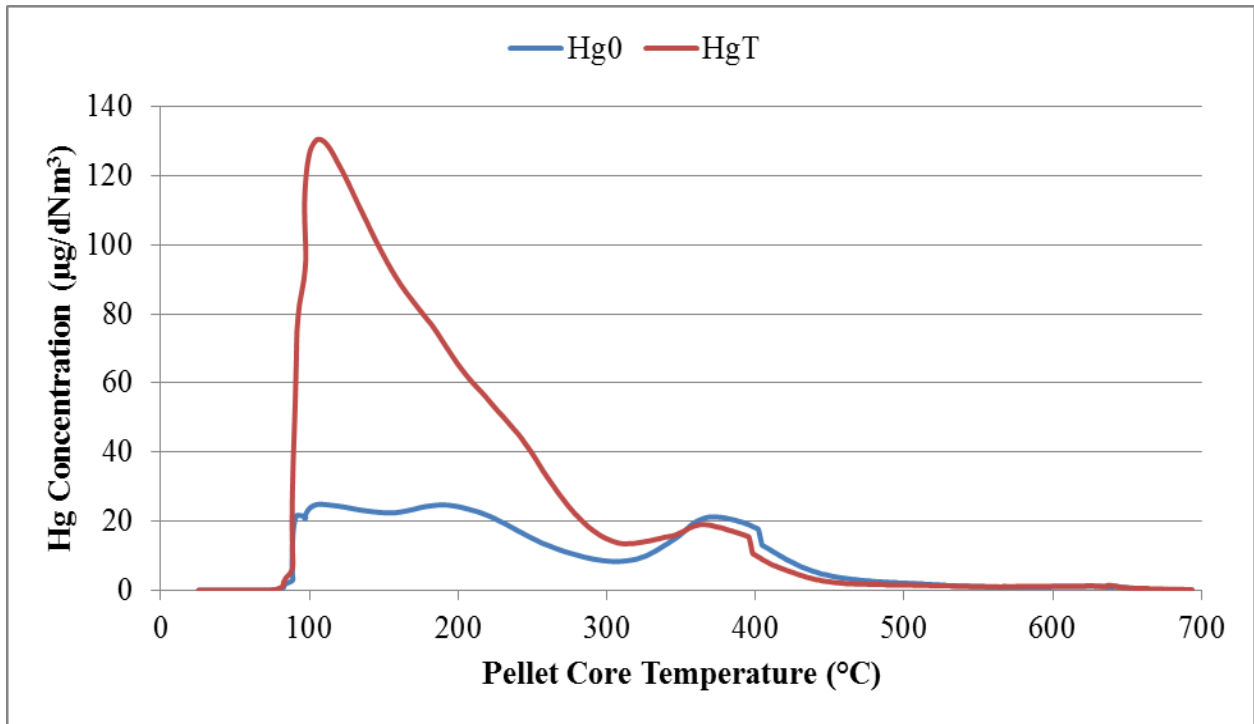


Figure 55. Mercury release profile for Keetac replicate second 0.1wt% run.

Keetac 0.5wt% Test Results:

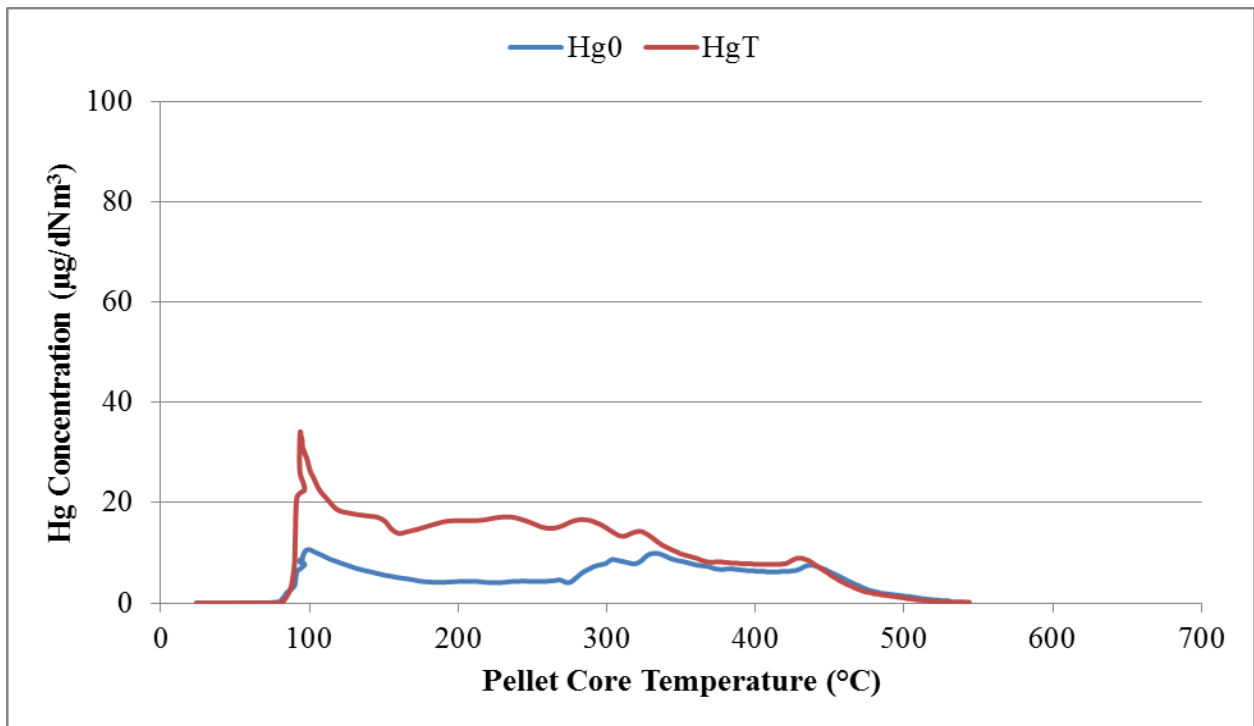


Figure 56. Mercury release profile for Keetac second 0.5wt% run.

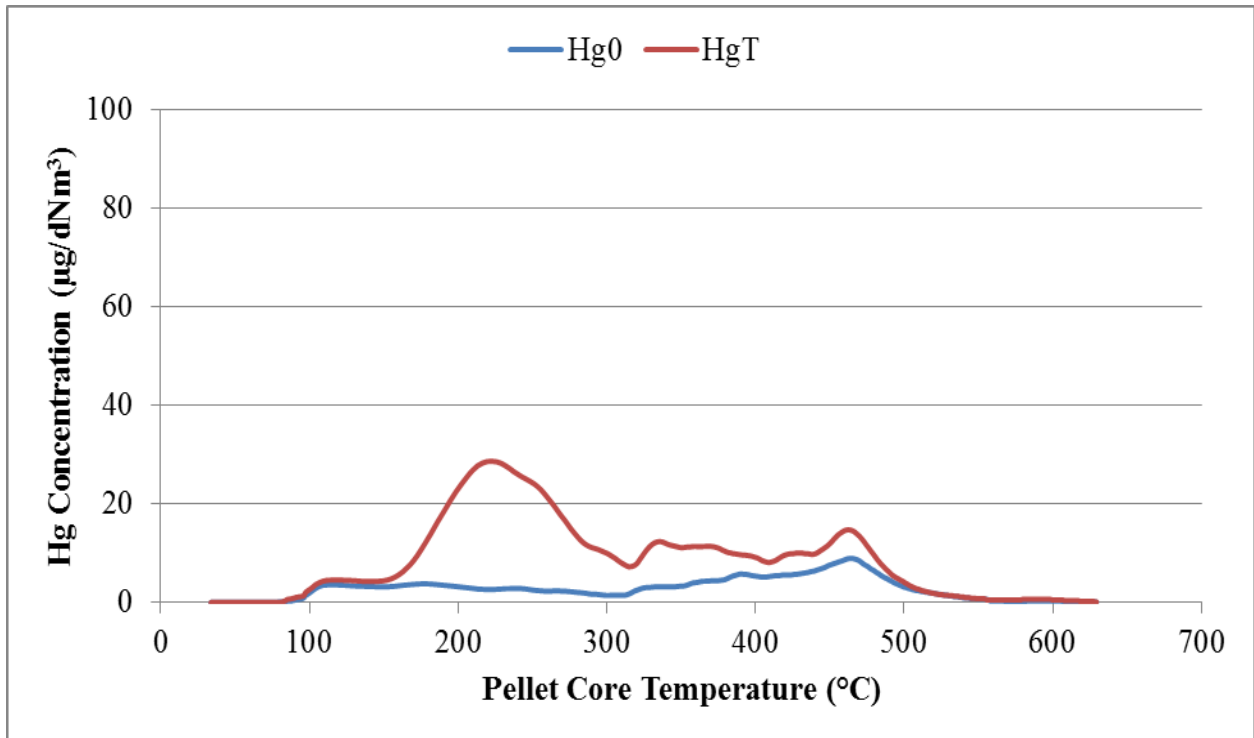


Figure 57. Mercury release profile for Keetac third 0.5wt% run.

Hibtac Standard Green Ball Baseline Test Results:

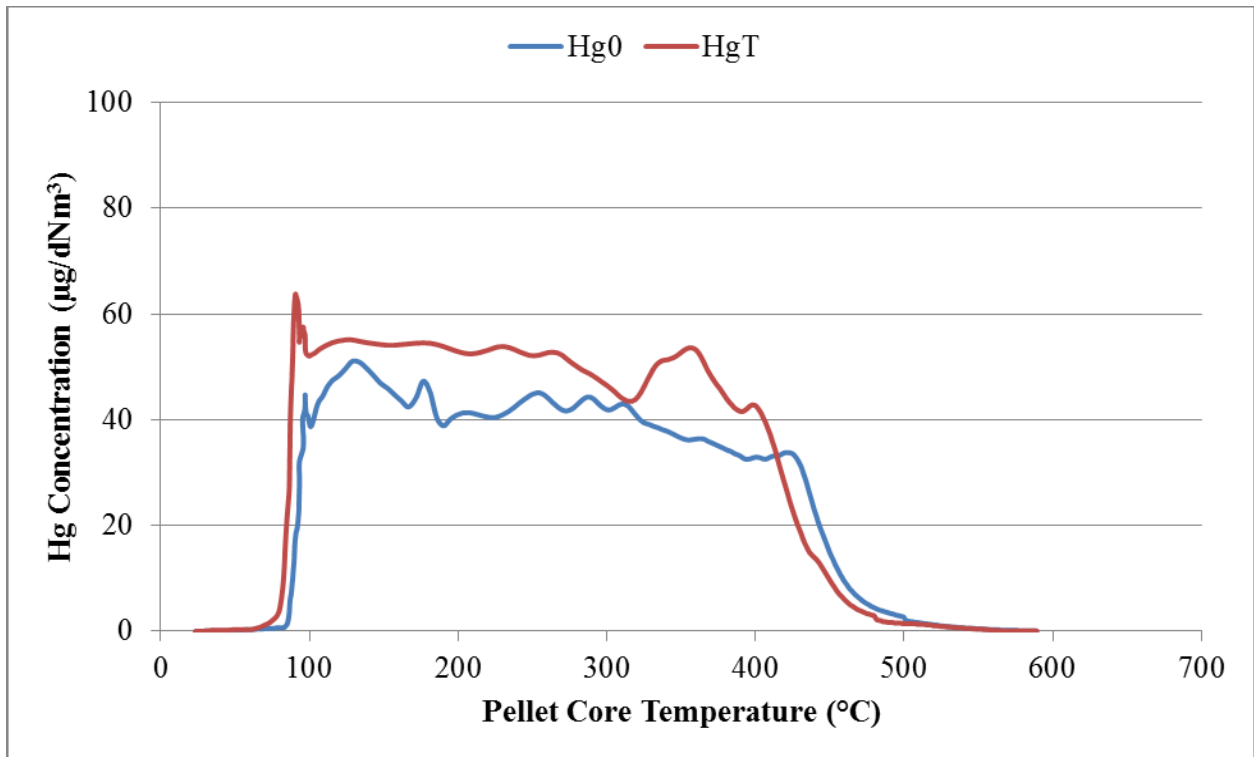


Figure 58. Mercury release profile for Hibtac standard green ball second baseline run.

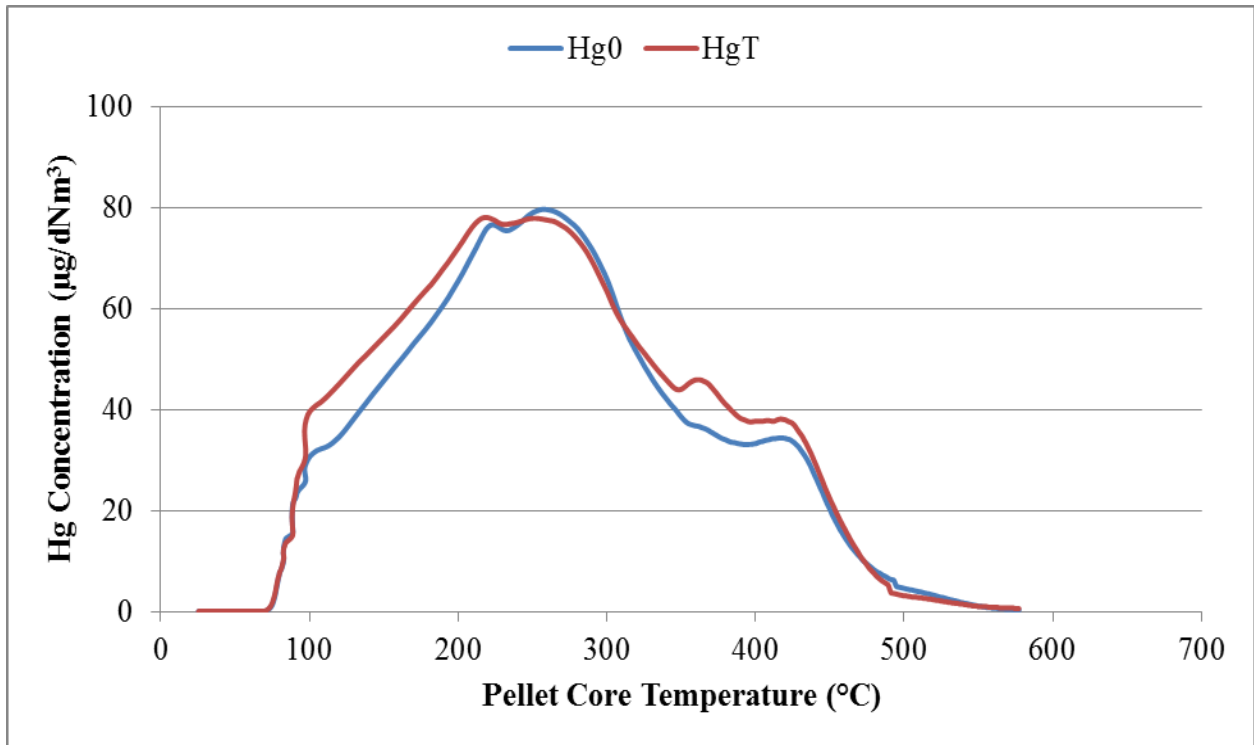


Figure 59. Mercury release profile for Hibtac standard green ball third baseline.

Hibtac Standard Green Ball 0.1wt% Loading Test Results:

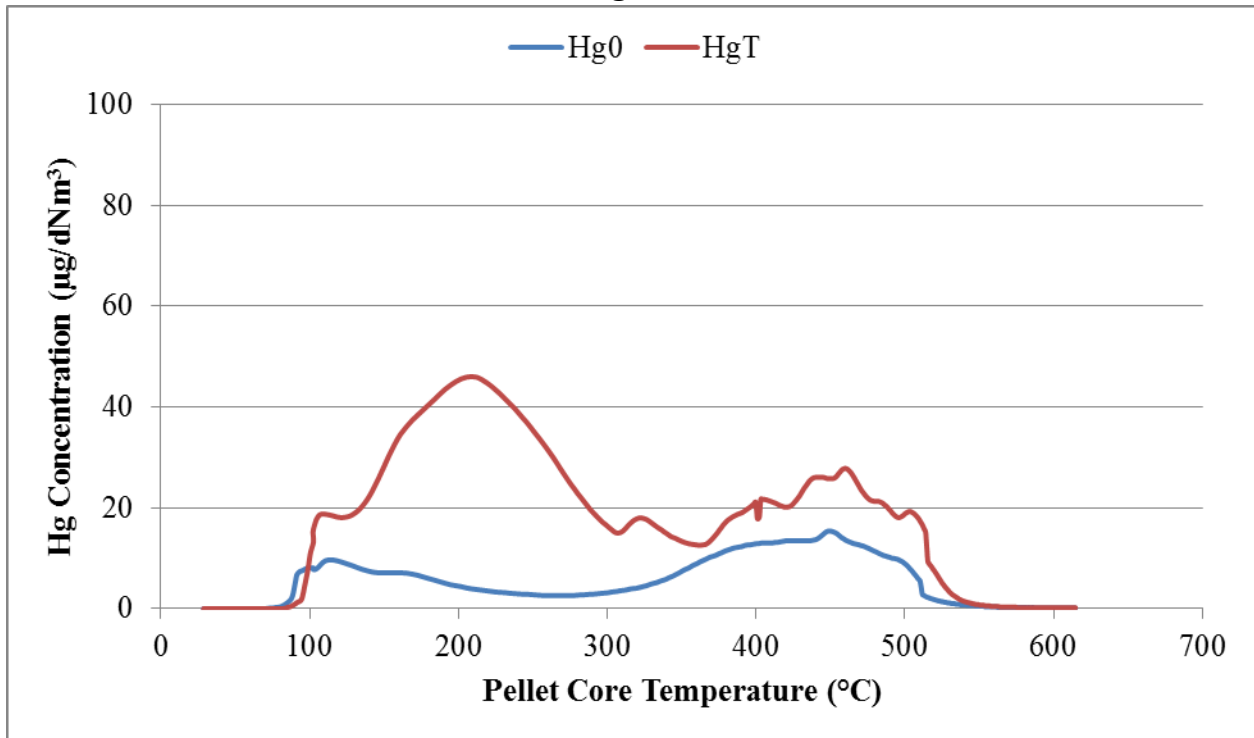


Figure 60. Mercury release profile for Hibtac standard green ball second 0.1wt% run.

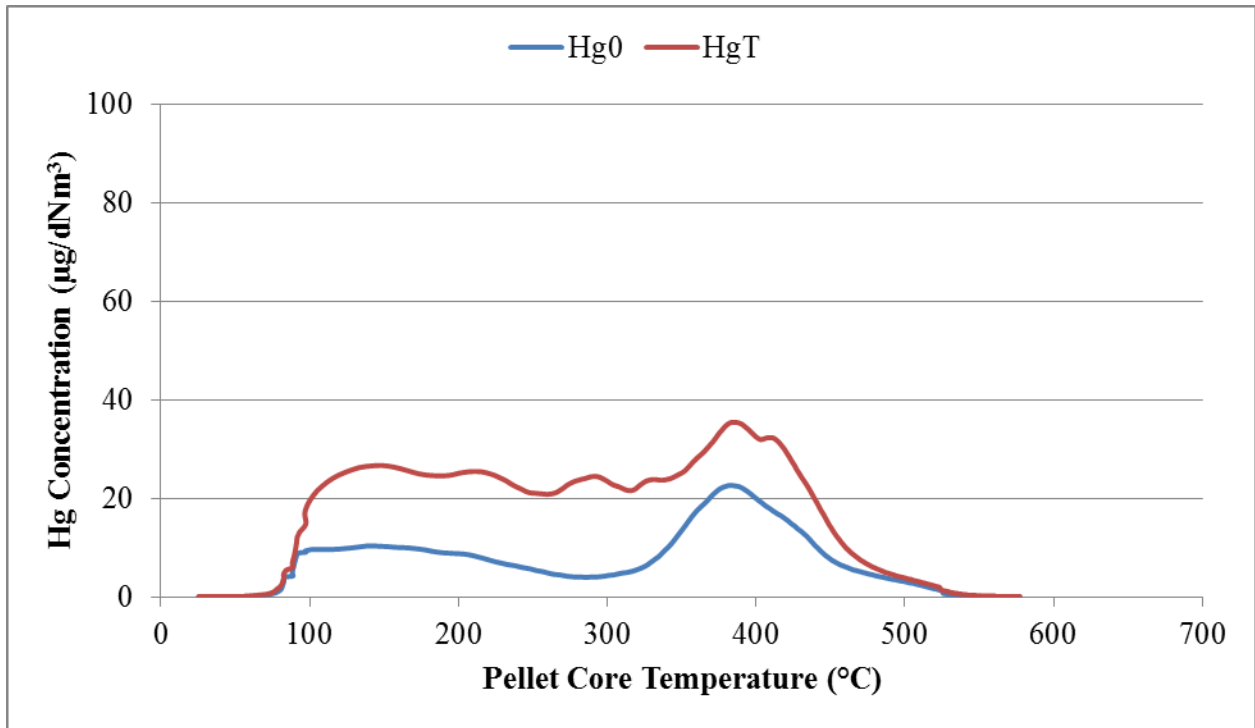


Figure 61: Mercury release profile for Hibtac standard green ball third 0.1wt% run.

Hibtac Standard Green Ball 0.5wt% Loading Test Results:

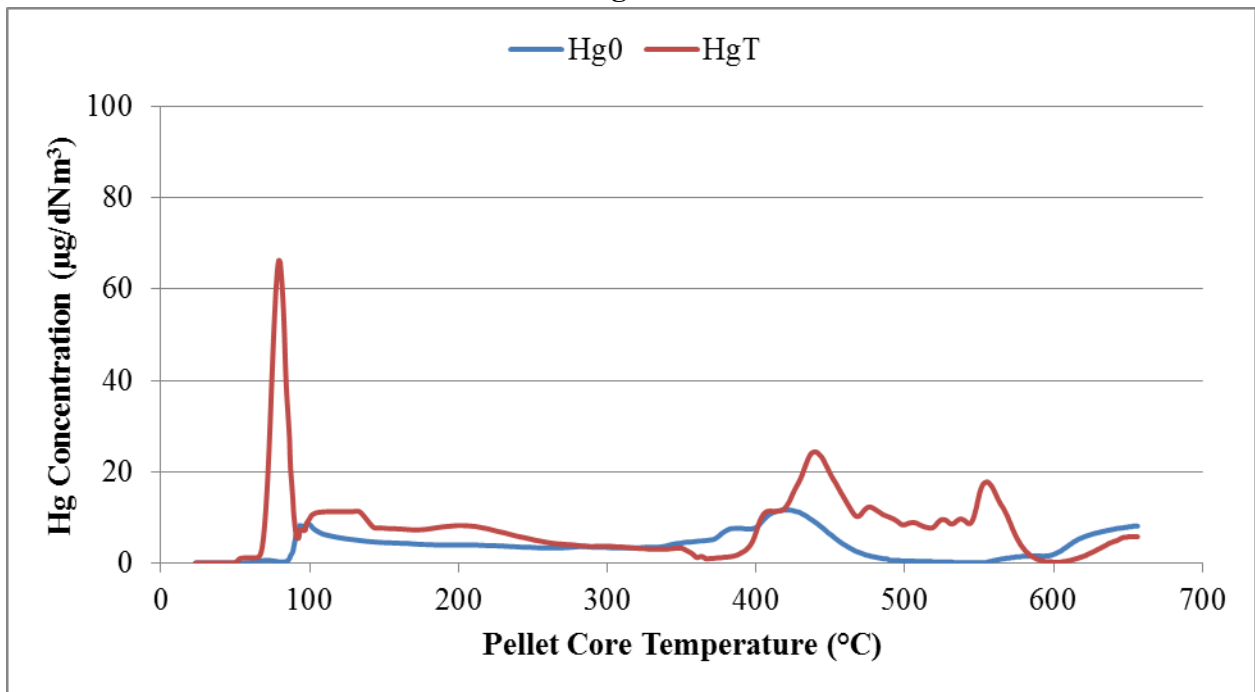


Figure 62. Mercury release profile for Hibtac standard green ball third 0.5wt% run.

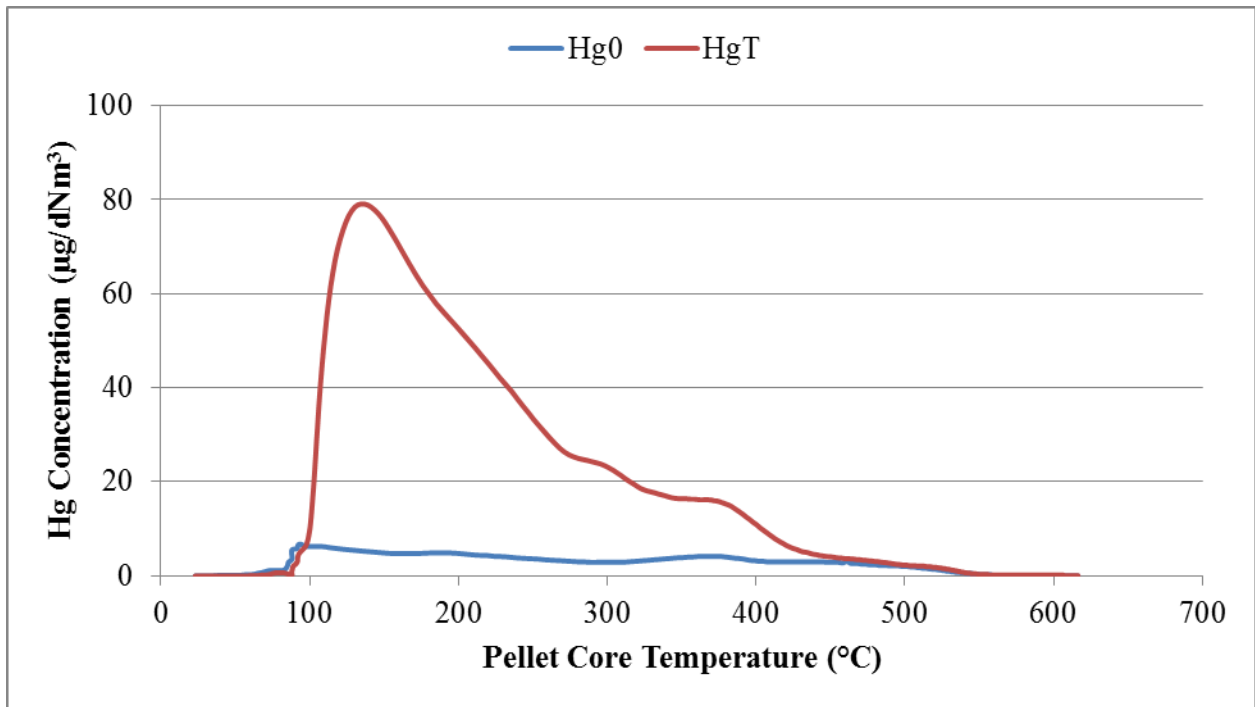


Figure 63. Mercury release profile for Hibtac standard green ball second 0.5wt% run.

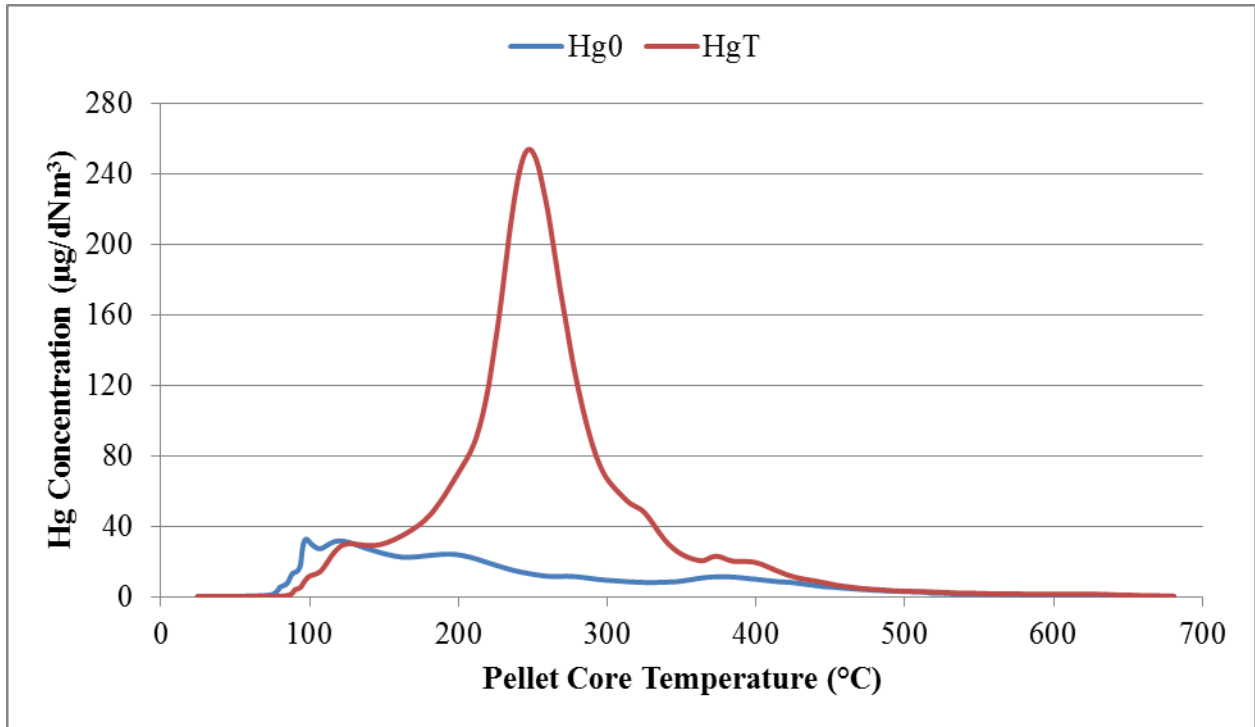


Figure 64. Mercury release profile for Hibtac standard green ball second 0.5wt% replicate run.

Hibtac High Compression Green Ball Baseline Test Results:

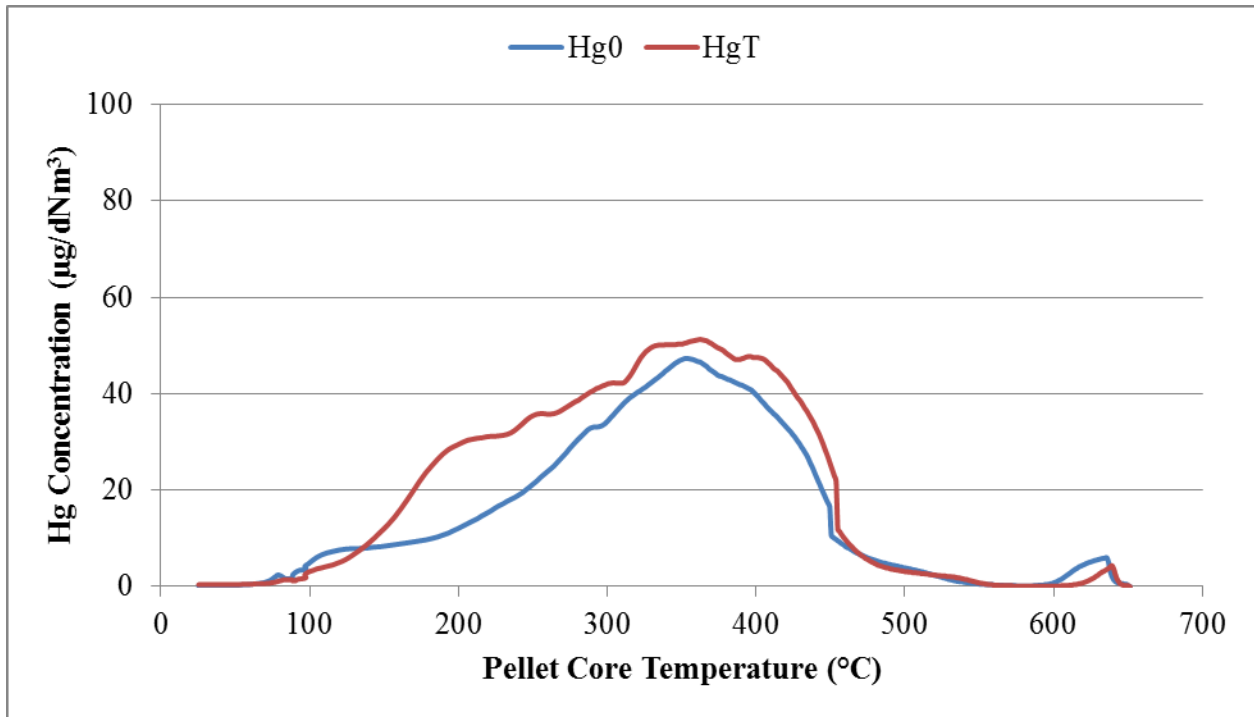


Figure 65. Mercury release profile for Hibtac high compression green ball baseline run.

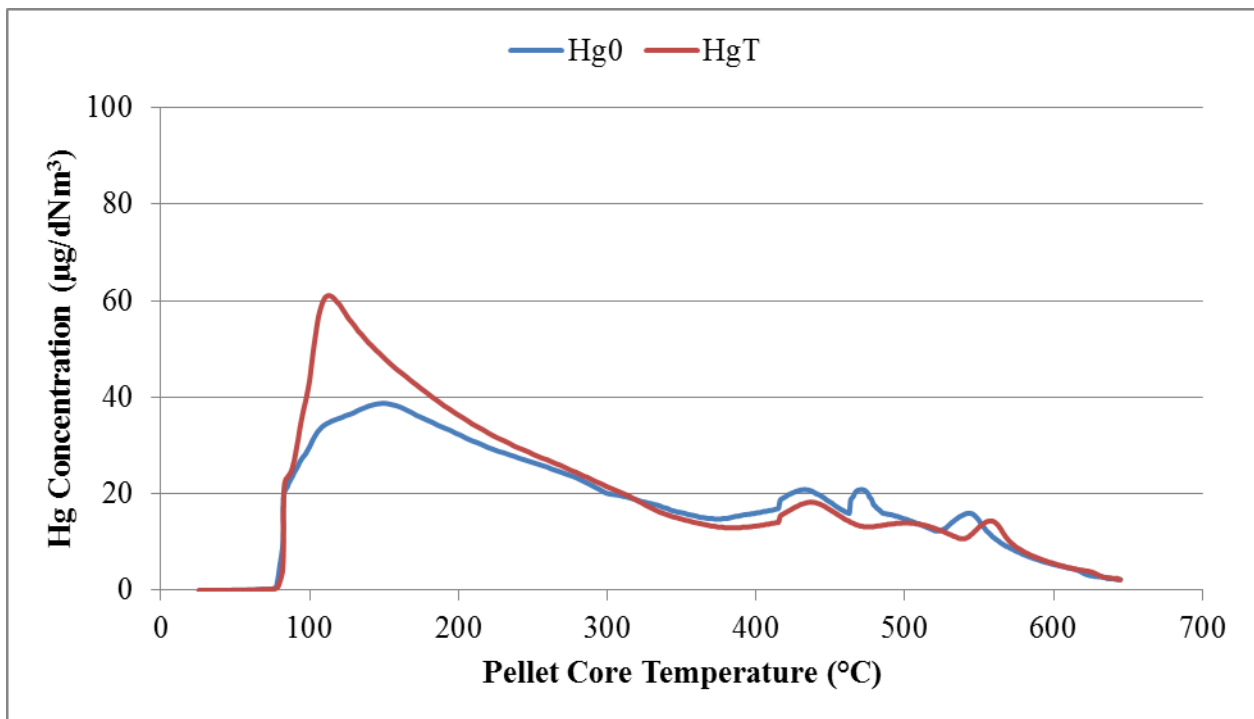


Figure 66. Mercury release profile for Hibtac high compression green ball second baseline run.

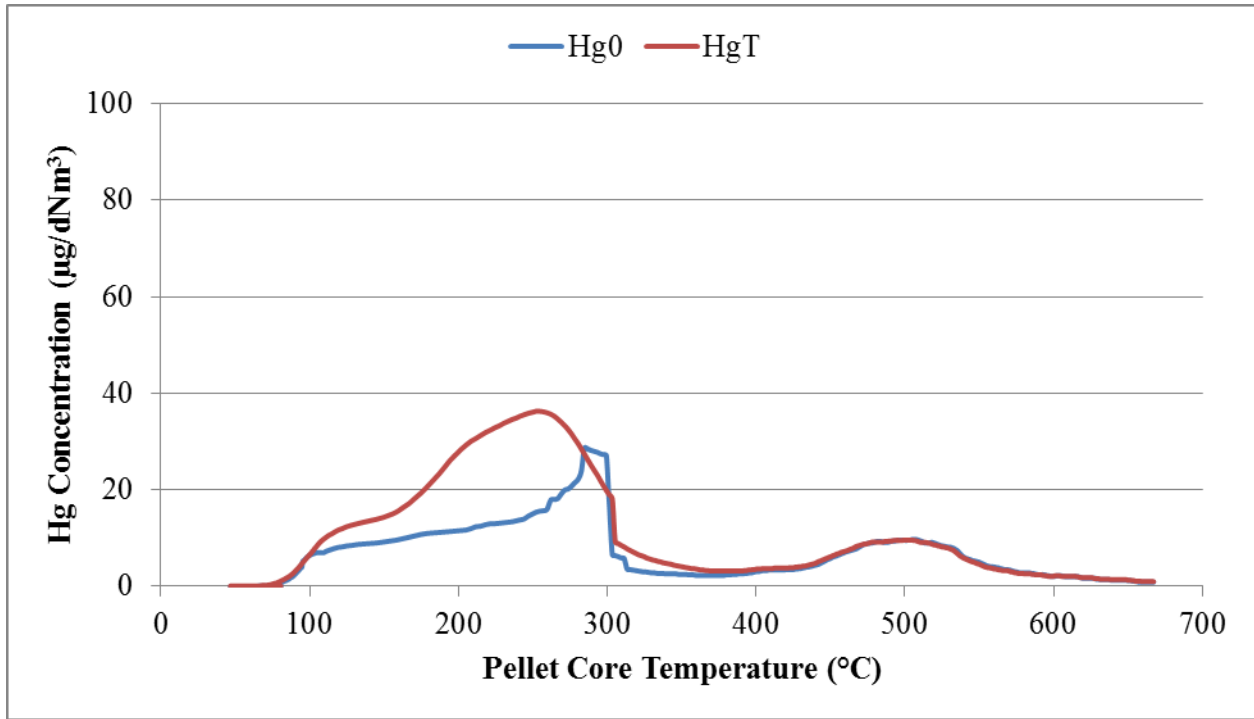


Figure 67. Mercury release profile for Hibtac compression green ball first replicate baseline run.

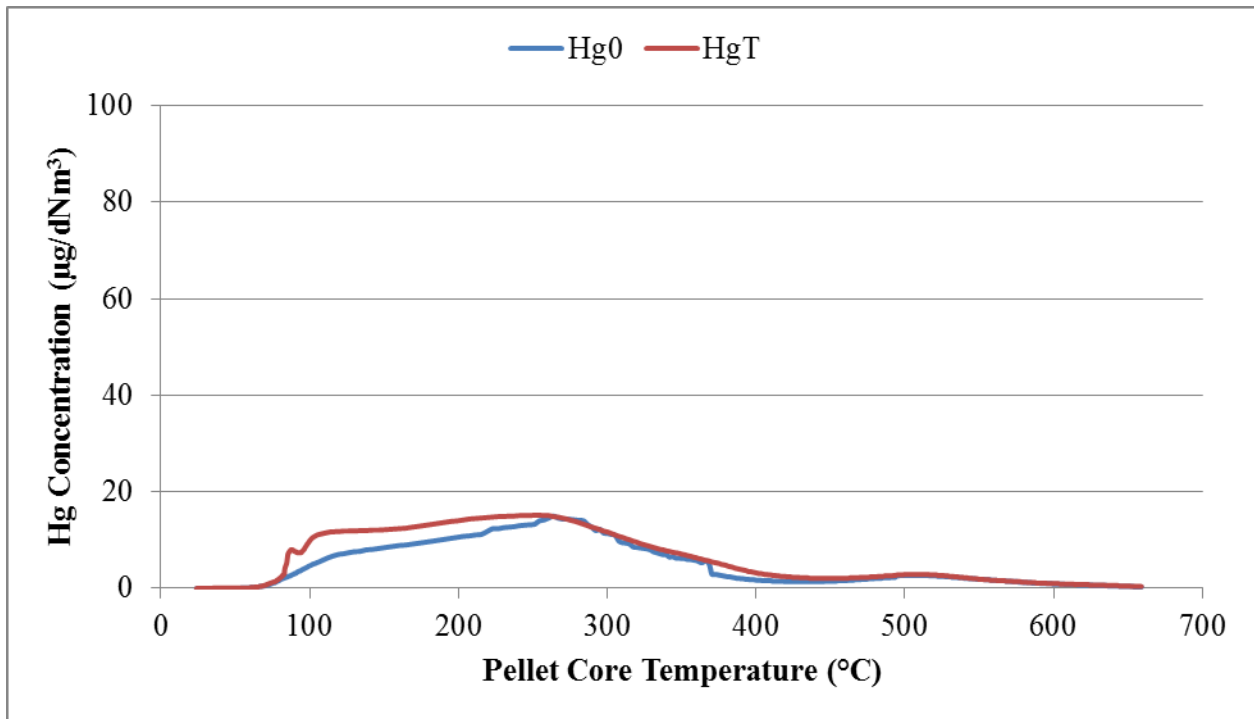


Figure 68. Mercury release profile for Hibtac compression green ball second replicate run.

Hibtac High Compression Green Ball 0.1wt% Test Results:

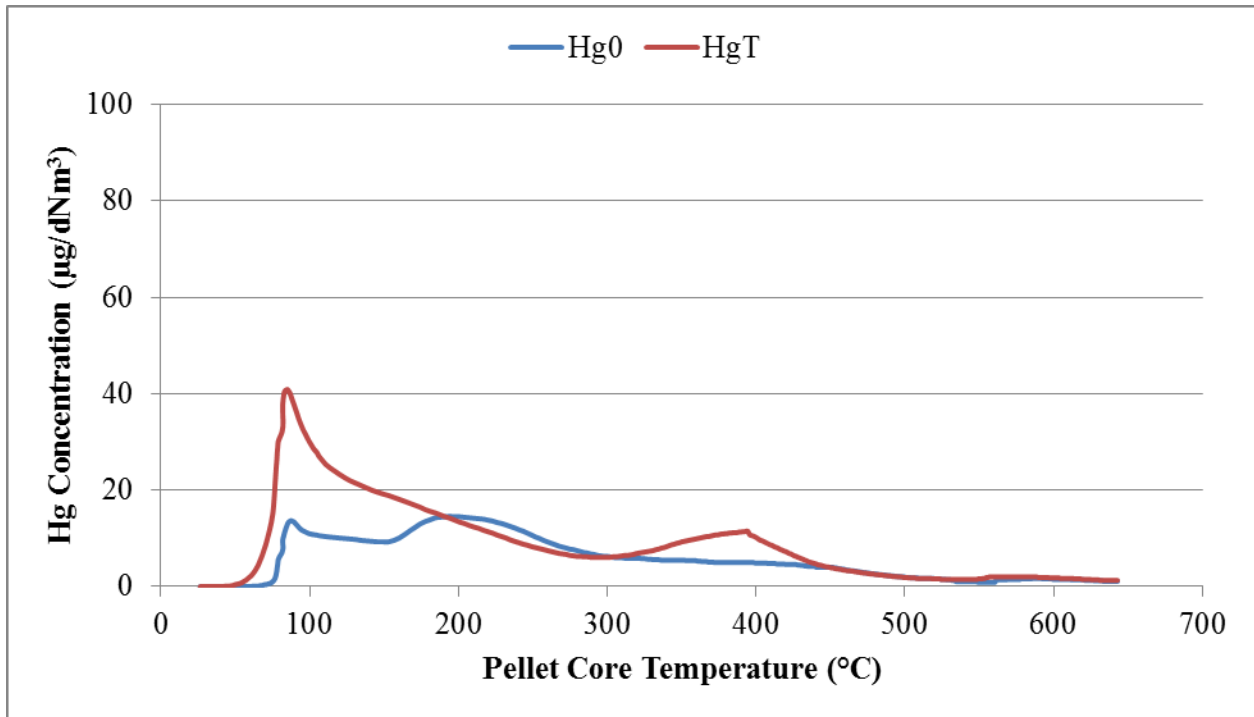


Figure 69. Mercury release profile for Hibtac compression green ball first 0.1wt% run.

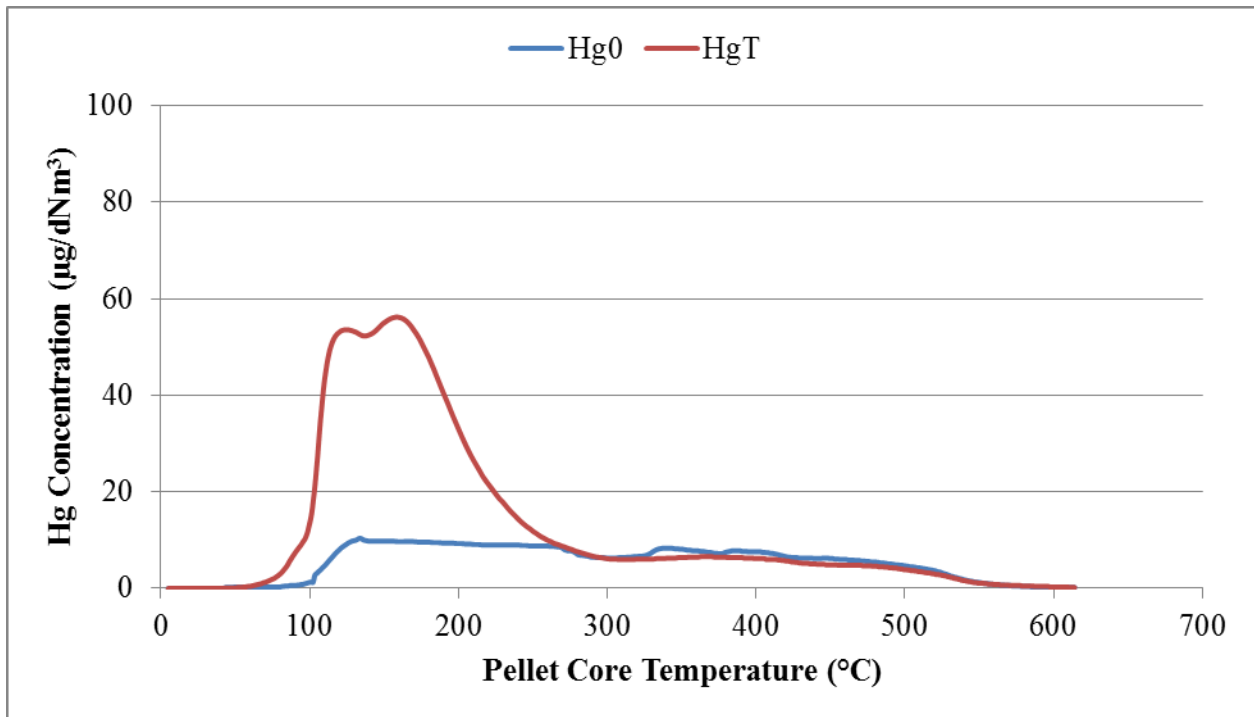


Figure 70. Mercury release profile for Hibtac compression green ball second 0.1wt% run.

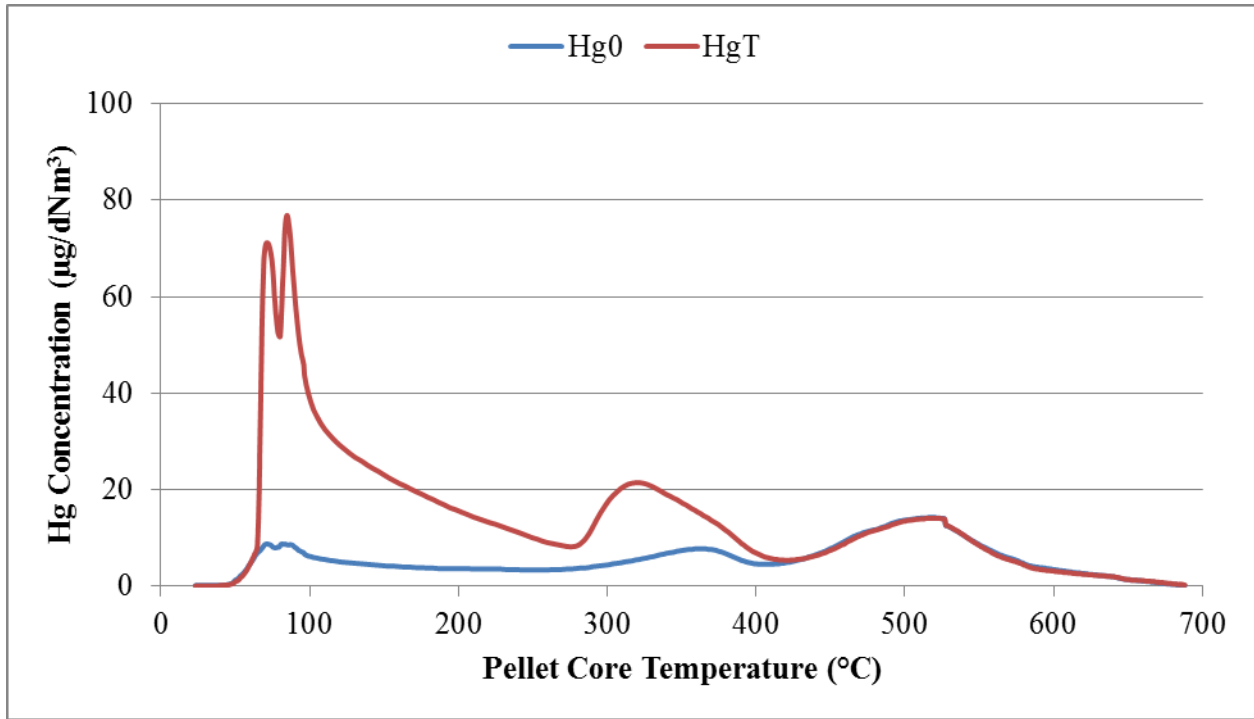


Figure 71. Mercury release profile for Hibtac compression green ball third 0.1wt% run.

Hibtac High Compression Green Ball 0.5wt% Test Results:

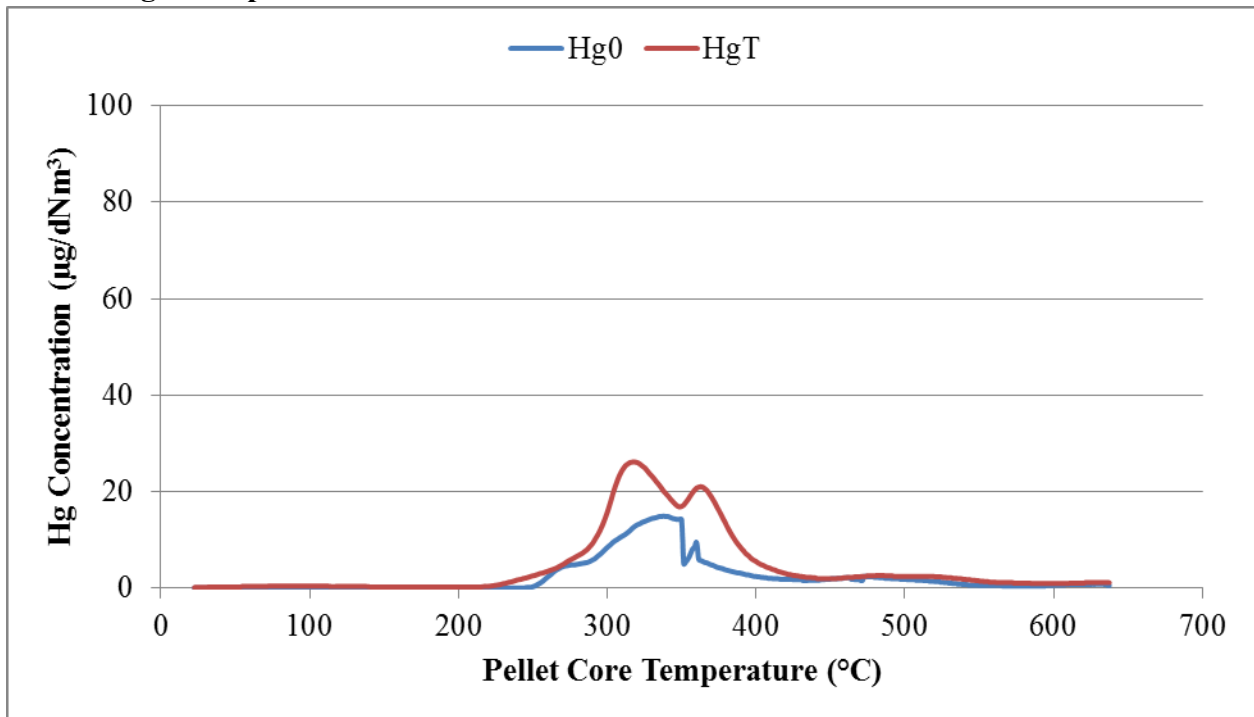


Figure 72. Mercury release profile for Hibtac compression green ball first 0.5wt% run.

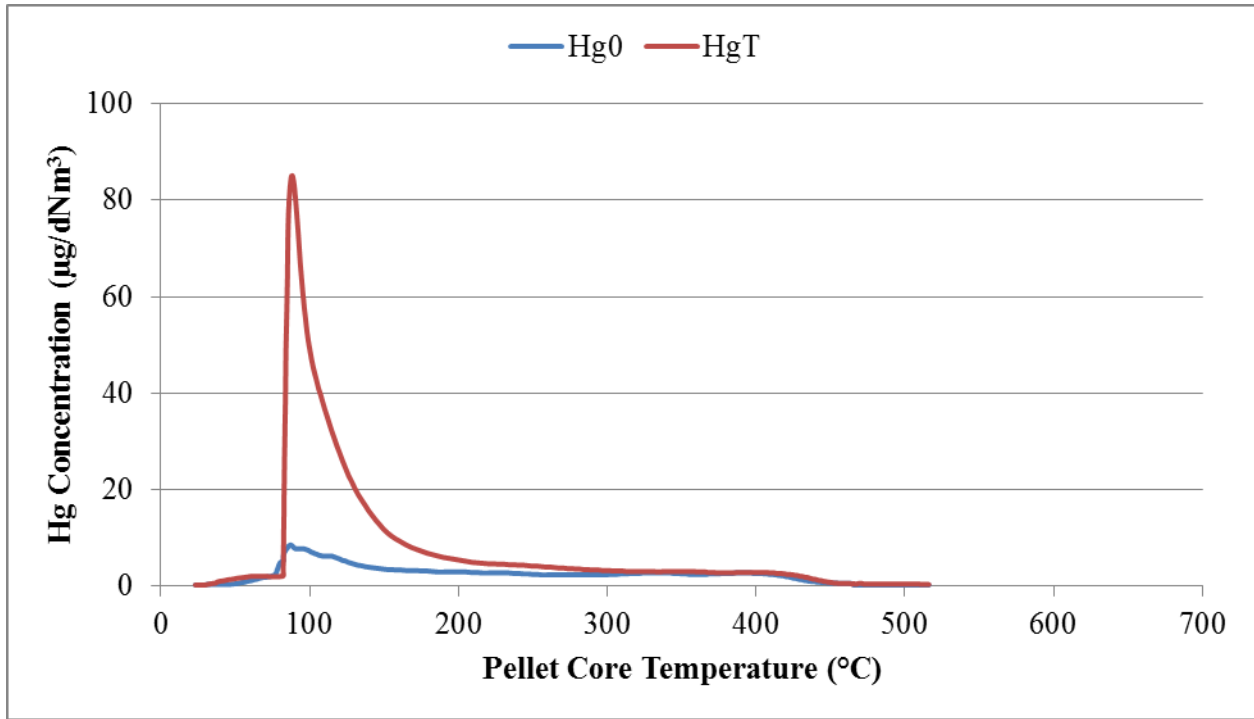


Figure 73. Mercury release profile for Hibtac compression green ball second 0.5wt% run.

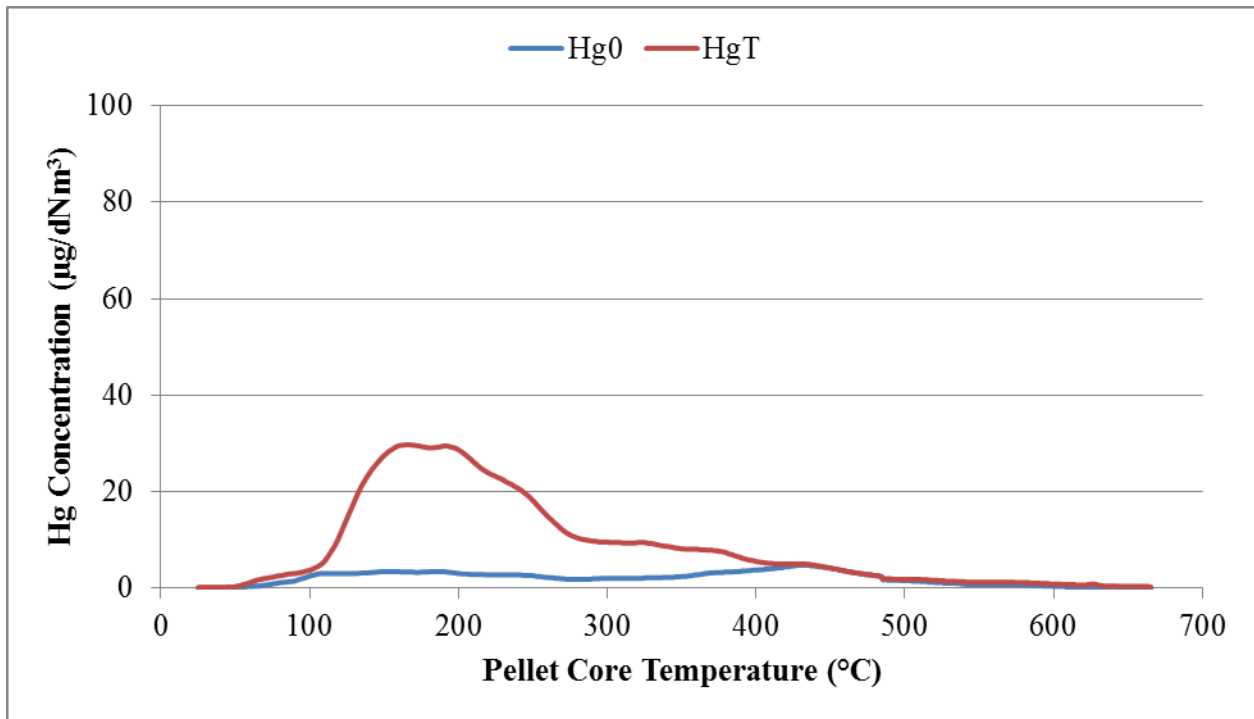


Figure 74. Mercury release profile for Hibtac compression green ball third 0.5wt% run.

Appendix B – Batch Balling Results Report

Duluth Campus

*Coleraine Minerals Research
Laboratory*

Natural Resources Research Institute

*Box 188
One Gayley Avenue
Coleraine, Minnesota 55722*

*218-245-4201
Fax: 218-245-4219*

July 6, 2012

Nicholas Lentz, Ph.D.

Associate Director for Energy Technology Applications

Shuchita Patwardhan

Graduate Research Assistant

Institute for Energy Studies
The University of North Dakota
243 Centennial Drive Stop 8153
Upton II Room 366L
Grand Forks, ND 58202
(701)-777-2684

RE: Batch Balling Tests with University of North Dakota Carbon Additive

Introduction

A series of batch balling tests were conducted from 6/25 – 6/28/2012 to evaluate a carbon based additive supplied by the University of North Dakota (UND) to green taconite agglomerates and compare them to a standard baseline to determine an influence on the green ball properties. The testing sequence consisted of three tests and one repeat (4 tests total) for each of six Taconite Mining Operations in Northern Minnesota. The three tests consisted of a low and high level carbon additive rate of 0.1% and 0.5% and a baseline with 0.0% additive. The repeat test appears to be random and was supplied by UND. The basis for each of the six operations, Arcelor-Mittal Minorca, U.S. Steel Keewatin Taconite, Hibbing Taconite, U.S. Steel Minntac and United Taconite was determined from current plant operations and prior batch balling testing conducted at the Coleraine Minerals Research Laboratory.

Discussion

Batch balling tests were conducted to compare the physical quality of green balls prepared with the concentrates and additives described in the attached table. The raw materials were all

collected fresh from the respective plants in the weeks prior to testing and were used “as received” except for the Minntac which sent a filter cake that required filtering prior to use. Low level fluxstone addition was done as necessary in blended in a dry state to ensure proper green ball chemistry representative of the specific plant operation.

Batch Balling Procedure:

The mixes are prepared on a dry weight basis of 3000 g iron ore concentrate including the limestone/fluxstone addition. Binders are added in excess of the concentrate blends on the basis of lbs./Dry Long Ton (DLT) concentrate. The binder addition rates used in this study were used within the acceptable guidelines of typical plant operations. The binders (bentonite or organic) were added with the carbon additive. The carbon sorbent was added in several “small portions” sprinkled into the concentrate and blended by hand in a lab mixing bowl. This technique has been compared to low intensity mixing, typical of most operations, with no significant variance. Once the mixes are blended, they are pushed through a laboratory shredder to eliminate any micro agglomerates to prepare them for agglomeration in the balling tire. Figure 1 shows the batch balling test equipment and arrangement, consisting of a shredder and balling tire.



Figure 1. Batch balling test equipment and arrangement

The concentrate blend is initially added to the balling tire in small amounts to produce “seed” balls. Seed balls are screened at -3Mesh +4Mesh. Each plant operation requires a specified amount of seeds (typically between 170 and 250g) to duplicate plant green ball quality. The green balls for testing are then grown from the seeds by slowly adding concentrate to build them up to target size. The procedure requires the addition of the remaining concentrate blend over a period of 3 minutes, followed by a 1 minute “roll”. Target sized green balls are -1/2” + 3/8”.

Analysis:

The green balls are screened to obtain a size distribution used for comparative purposes and for measuring relative growth rate. It should be noted that this may or may not be representative of actual plant green balls size distribution. A sample is placed in a drying oven to determine moisture content. Separate samples of the green balls are measured for 18” wet drop number. Once green the balls are dried, the moisture is calculated and the dried balls are then measured for dry compressive strength.

Results / Conclusions

Results of these tests are provided in the attached table. Green ball quality is a key parameter in the operation of an induration furnace from the standpoint of bed permeability, airflow, and dust generation. The data shows that the addition of the UND carbon additive at both low and high level addition has no significant effect on green ball moisture or wet drop number when compared to a baseline standard. In addition, the additive shows no significant influence on dry compression strength of green balls prepared with fluxstone addition or the standard green ball prepared with the organic binder for United Taconite. The standard green balls prepared for Hibbing Taconite (with a very low level limestone addition) and Keewatin taconite (no limestone) show a slight decrease in the dry compression at the higher dosage rate of 0.5%. It should be noted that these two operations also have much coarser particle size distribution due to their relative location on the Minnesota Iron Range and the transition in the silica liberation characteristics of the ore body. In some cases, the data also indicates the relative green ball size distribution is slightly larger (+1/2” size fraction) with the higher additive rate, however this should be further studied as it is not fully verified by the data.

Richard Kiesel
Deputy Director
High Temperature Processing and Bio-Energy Conversion
University of Minnesota Duluth
Natural Resources Research Institute
Coleraine Minerals Research lab
PO Box 188
One Gayley Ave.
Coleraine, MN 55722
Ph: 218-245-4207
Fax: 218-245-4219
e-mail: rkiesel@nrri.umn.edu

Table 1: Results of Batch Balling Tests

Test #	Iron Ore Concentrate	Description	Binder	Additive (s)	UND Carbon Additive, %	Green Ball Quality			Green Ball Sizing, %		
						Moist, %	18" Drop	Dry Comp	+1/2"	-1/2" +7/16"	-7/16" +3/8"
B12576	Arcelor Mittal	Fluxed	Bentonite	Limestone-Dolomite	0.0	9.8	7.5	7.8	0.5	44.0	55.6
B12577	Arcelor Mittal	Fluxed	Bentonite	Limestone-Dolomite	0.1	9.9	8.2	9.0	1.1	48.4	50.5
B12578	Arcelor Mittal	Fluxed	Bentonite	Limestone-Dolomite	0.5	9.8	7.2	7.1	1.8	55.8	42.4
B12579	Arcelor Mittal	Fluxed	Bentonite	Limestone-Dolomite	0.1	9.7	7.1	7.9	7.3	64.2	28.5
Std Deviation						0.1	0.5	0.8			
B12580	Keetac	Std	Bentonite	--	0.0	9.4	4.8	6.8	11.7	49.2	39.0
B12581	Keetac	Std	Bentonite	--	0.1	9.5	4.9	5.6	6.8	46.4	46.8
B12582	Keetac	Std	Bentonite	--	0.5	9.2	4.5	3.1	14.8	43.2	42.0
B12583	Keetac	Std	Bentonite	--	0.1	9.5	5.7	5.7	7.7	52.2	40.1
Std Deviation						0.1	0.5	1.6			
B12584	Hibtac	Std Pellet	Bentonite	Low Level Limestone	0.0	9.7	6.5	8.8	1.8	46.9	51.2
B12585	Hibtac	Std Pellet	Bentonite	Low Level Limestone	0.1	9.6	6.3	8.4	3.5	51.3	45.2
B12586	Hibtac	Std Pellet	Bentonite	Low Level Limestone	0.5	9.5	6.2	3.9	10.2	47.1	42.7
B12587	Hibtac	Std Pellet	Bentonite	Low Level Limestone	0.5	9.6	6.0	4.3	4.6	46.4	49.0
Std Deviation						0.1	0.2	2.6			
B12588	Hibtac	High Comp	Bentonite	Low Level Limestone	0.0	9.6	6.8	7.2	2.8	52.4	44.8
B12589	Hibtac	High Comp	Bentonite	Low Level Limestone	0.1	9.7	6.1	9.0	1.7	35.0	63.3
B12590	Hibtac	High Comp	Bentonite	Low Level Limestone	0.5	9.6	6.3	7.9	6.1	57.1	36.7
B12591	Hibtac	High Comp	Bentonite	Low Level Limestone	0.0	9.5	6.5	8.8	2.9	48.6	48.5
Std Deviation						0.1	0.3	0.8			
B12592	Minntac	Fluxed	Bentonite	Limestone-Dolomite	0.0	9.5	6.8	8.6	0.3	33.6	66.0
B12593	Minntac	Fluxed	Bentonite	Limestone-Dolomite	0.1	9.6	6.5	8.1	0.7	47.2	52.1
B12594	Minntac	Fluxed	Bentonite	Limestone-Dolomite	0.5	9.2	5.9	6.0	3.3	54.7	42.0
B12595	Minntac	Fluxed	Bentonite	Limestone-Dolomite	0.0	9.2	6.2	8.8	0.5	37.4	62.1
Std Deviation						0.2	0.4	1.3			
B12596	Utac	Std	Organic	Low Level Limestone	0.0	9.9	5.0	2.1	25.2	40.1	34.6
B12597	Utac	Std	Organic	Low Level Limestone	0.1	10.1	5.5	2.8	7.6	50.5	41.9
B12598	Utac	Std	Organic	Low Level Limestone	0.5	10.2	5.9	3.1	11.4	49.2	39.3
B12599	Utac	Std	Organic	Low Level Limestone	0.5	9.7	5.5	2.6	12.1	39.5	48.4
Std Deviation						0.2	0.4	0.4			

Appendix C – Data Quality Assessment Worksheet

1) Method Description/Key Parameters:

- a) Test results from these studies would be most applicable for US Steel’s Minnesota Taconite and Keewatin Taconite; Arcelor Mittal and Hibbing Taconite. Testing consists of bench scale experiments performed on green balls obtained from all five taconite facilities, with the four facilities listed above showing best results. United Taconite oxidation results were lower than for other facilities.
- b) Mercury oxidation is determined by calculating the difference between the total mercury (Hg^T) and elemental mercury (Hg^0) release during bench testing of green balls. Oxidized mercury tends to be captured by taconite wet scrubber systems, so the percent mercury oxidation is used as an estimate of the percent mercury reduction. Full-scale testing of the technology would be necessary to determine the actual reduction potential of the technology.

- Oxidation formula:

$$\% \text{ Hg Oxidation} = \frac{\{Hg^T - Hg^0\}}{Hg^T} * 100 \dots\dots\dots[1]$$

Where,

- Hg^T is the total mercury emission during the test run.
- Hg^0 is the total elemental mercury emission during the test run. Hg^T and Hg^0 are measured using a Horiba DM-6B Cold Vapor Atomic Absorption Spectroscopy CMM.

- Sample calculation using Minntac 0.1wt% results:

- Hg^T = Average total mercury concentration = 7.2 ng Hg/g GB
- Hg^0 = Average elemental mercury concentration = 2.7 ng Hg/g GB

$$\% \text{ Hg Oxidation} = \frac{\{7.2 - 2.7\} * 100}{7.2} = \underline{62.9\%}$$

- c) The mercury reduction potential of the technology is determined using equation 2 below.
- Equation 2:

$$\text{Reduction Potential} = \frac{\text{Hg}[2] - \text{Hg}[1]}{100 - \text{Hg}[1]} * 100 \dots\dots\dots[2]$$

Where,

- Hg[1] is the average mercury oxidation obtained for baseline runs of respective facility.
 - Hg[2] is the average mercury oxidation obtained for 0.1wt% ESORG-HG-11 runs or respective facility.
- Example using Minntac baseline and 0.1wt% average oxidations observed:
 - Hg[1] = Minntac baseline average oxidation = 24%
 - Hg[2] = Minntac 0.1wt% oxidation average = 62%

$$\% \text{ Hg Oxidation} = \frac{\{62 - 24\} * 100}{\{100 - 24\}} = \underline{50\%}^*$$

*Values might change slightly from values in report body and table below due to rounding.

2) Data Quality Assessment for Key Variables:

- a) Not applicable. Mercury oxidation calculated based on results of each individual run.
- b) Average values obtained for Hg[1] and Hg[2] are listed in Table 12 below.
- c) Data will be stored at University of North Dakota – Institute for Energy Studies.

3) Mercury Removal Estimates:

- a) Reduction potential for each plant is summarized in Table 13 below.

Table 12. Reduction Potential of ESORB-HG-11 for Each Taconite Facility.

Facility	Hg[1] (SD), %	Hg[2] (SD), %	Reduction Potential (SD), %
Minntac	24 (4.6)	62 (7.2)	49 (9.4)
Keetac	15 (2.5)	46 (3.8)	36 (4.5)
Arcelor Mittal	20 (1.0)	53 (10.2)	41 (12.7)
Utac	22 (3.5)	37 (5.5)	19 (7.1)
Hibtac*	15 (7.2)	52 (5.1)	43 (6.5)

Note: 1) The oxidation estimates, Hg[1] and Hg[2], are averages obtained during bench tests, and Hg[2] is assumed to estimate a “minimum” possible reduction expected for stack mercury emissions during full-scale scale work. 2) Only results for 0.1wt% ESORB-HG-11 loading are used to determine Hg[2] as this is considered the optimum loading. *Results for both standard and compression pellets averaged.

b) Qualitative Factors:

Gas phase oxidation was not quantifiable using bench scale test equipment, see report. Consequently, actual full-scale test reduction potential of the technology tested could be higher than that observed during bench tests.

c) Problems Encountered:

No significant problems were encountered during technology testing.

Appendix B-2-7

Continuation of Corrosion Potential of Bromide Injection under Taconite Operating Conditions

March 2012



EERC

Energy & Environmental Research Center

UNIVERSITY OF NORTH DAKOTA

15 North 23rd Street — Stop 9018 / Grand Forks, ND 58202-9018 / Phone: (701) 777-5000 Fax: 777-5181
Web Site: www.undeerc.org

March 29, 2012

Dr. Michael Berndt
Research Scientist
Division of Lands and Minerals
Minnesota Department of Natural Resources
500 Lafayette Road
Saint Paul, MN 55155-4045

Dear Dr. Berndt:

Subject: EERC Final Report Entitled "Continuation of Corrosion Potential of Bromide Injection Under Taconite Operating Conditions"; EERC Fund 15727

Enclosed please find the subject final report. If you have any questions, please contact me by phone at (701) 777-5236 or by e-mail at yzhuang@undeerc.org.

Sincerely,

Ye Zhuang
Research Manager

YZ/sh

Enclosure

CONTINUATION OF CORROSION POTENTIAL OF BROMIDE INJECTION UNDER TACONITE OPERATING CONDITIONS

Final Report

Prepared for:

Michael Berndt

Division of Lands and Minerals
Minnesota Department of Natural Resources
500 Lafayette Road
Saint Paul, MN 55155-4045

Prepared by:

Ye Zhuang
David J. Dunham
John H. Pavlish

Energy & Environmental Research Center
University of North Dakota
15 North 23rd Street, Stop 9018
Grand Forks, ND 58201-9018

EERC DISCLAIMER

LEGAL NOTICE This research report was prepared by the Energy & Environmental Research Center (EERC), an agency of the University of North Dakota, as an account of work sponsored by Minnesota Department of Natural Resources. Because of the research nature of the work performed, neither the EERC nor any of its employees makes any warranty, express or implied, or assumes any legal liability or responsibility for the accuracy, completeness, or usefulness of any information, apparatus, product, or process disclosed or represents that its use would not infringe privately owned rights. Reference herein to any specific commercial product, process, or service by trade name, trademark, manufacturer, or otherwise does not necessarily constitute or imply its endorsement or recommendation by the EERC.

TABLE OF CONTENTS

LIST OF FIGURES	ii
LIST OF TABLES	iii
BACKGROUND	1
OBJECTIVES	3
EXPERIMENTAL APPROACH.....	3
THERMODYNAMIC PERSPECTIVE.....	6
RESULTS AND DISCUSSIONS.....	11
Preexposure Baseline Analysis	11
Postexposure Analysis.....	14
Minorca Coupon.....	14
Minntac Coupon.....	17
Low-Carbon Steel	21
CONCLUSIONS.....	24
REFERENCES	25

LIST OF FIGURES

1	Temperature cycle in hot zone	4
2	Temperature cycle in cool zone	4
3	Halogen-induced active oxidation mechanisms	7
4	Phase-stability diagrams of Fe–O ₂ –Br ₂ and Fe–O ₂ –Cl ₂	7
5	Phase-stability diagrams of Ni–O ₂ –Br ₂ and Ni–O ₂ –Cl ₂	8
6	Phase-stability diagrams of Cr–O ₂ –Br ₂ and Cr–O ₂ –Cl ₂	9
7	Phase-stability diagrams of Minntac–O ₂ –Br ₂ and Minntac–O ₂ –Cl ₂	10
8	Morphology of the Minntac coupon prior to the test: unpolished surface and polished surface	12
9	Morphology of Minorca coupon prior to the test: unpolished surface and polished surface	13
10	Surface morphology of the low-carbon steel coupon prior to the test	14
11	Surface of the Minorca coupon after exposure	15
12	Cross section of the Minorca coupon after HCl exposure.....	15
13	Cross section of the Minorca coupon after HBr exposure	16
14	Variation of Fe, Cr, and Ni across the Minorca coupon	17
15	Surface of the Minntac coupon after exposure.....	18
16	Cross section of the Minntac coupon after HCl exposure.....	18
17	Cross section of the Minntac coupon after HBr exposure.....	19
18	Variation of Fe, Cr, and Ni across the Minntac coupon.....	20
19	Surface of low-carbon steel coupon after exposure	21
20	Cross section of the low-carbon steel coupon after HCl exposure	22

Continued...

LIST OF FIGURES (continued)

21	Cross section of the low-carbon steel coupon after HBr exposure	22
22	Variation of Fe across the low-carbon steel coupon	23
23	Changes of specimen weight during the thermal cycle exposure	23

LIST OF TABLES

1	Simulated Taconite Flue Gas Composition.....	5
2	Experiment Parameters of Exposure Test	6
3	Summary of T4, Melting Point, Volatility Ranks of Metal Compounds	10
4	Elemental Composition of the Testing Coupons.....	11

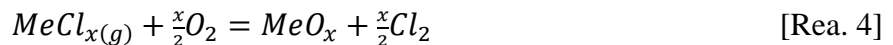
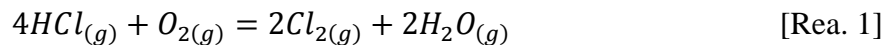
CONTINUATION OF CORROSION POTENTIAL OF BROMIDE INJECTION UNDER TACONITE OPERATING CONDITIONS

BACKGROUND

The state of Minnesota is targeting an overall 90% mercury reduction. As a result, mercury emissions from taconite plants, the second largest mercury source next to coal-fired utility plant, have to be reduced to meet the state regulation.

Among various mercury reduction technologies being developed, halogens, such as chlorine and bromine species, have been widely applied and proven effective to convert elemental mercury (Hg^0) to either oxidized mercury (Hg^{2+}) and/or particulate-bound mercury ($\text{Hg}[\text{p}]$) in coal flue gas environments (1–4). Both $\text{Hg}[\text{p}]$ and Hg^{2+} then can be removed from the gas stream with particulate matter control devices and/or wet scrubbers. Both chloride and bromide compounds have been added into the induration furnace, the green ball feed system, and the scrubber liquids to evaluate their effectiveness on mercury reduction in taconite flue gas (5–7). So far, mercury reduction using bromine has shown to be the most promising and cost-effective control option that can be directly applied to taconite facilities.

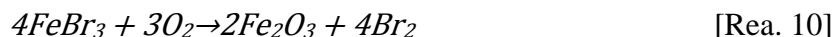
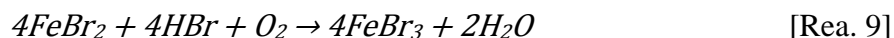
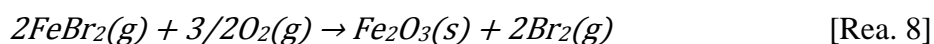
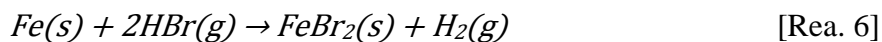
One major concern about applying halogens such as bromide or chloride as a mercury reduction agent is that they could induce corrosion and/or accelerate corrosion rates on taconite processing equipment, such as the feed grate and ducting system. Extensive studies have been performed to understand chlorine-induced corrosion in coal combustion environments. It is well accepted that HCl will attack metal surfaces at temperatures over 200°C through the following reactions (8):



At the metal–oxide interface where the oxygen partial pressure is low, metal chlorides are the thermoequilibrium-preferred reaction products. Depending on the temperature dependence of the vapor pressure with formed metal chlorides, the chlorides evaporate and diffuse toward the gas–scale interface. Within the scale, the oxygen partial pressure increases, and upon reaching regions with higher oxygen partial pressures, the gaseous chlorides will react with oxygen to form solid oxides releasing gaseous chlorine, described as active oxidation corrosion. For temperatures below 100°C, dew point corrosion by hydrochloric acid occurs on metal surfaces.

Bromine species do not naturally exist in taconite processing, and its corrosion characteristics on metal alloy is not well established. It has been proposed that bromine-induced corrosion is similar to that of chlorination and can be categorized as hydrobromic acid dew point

corrosion and active oxidation corrosion (9). Bromine-induced dew point corrosion occurs on metal surfaces as flue gas temperature is below a corresponding hydrobromic acid dew point. At temperatures over the hydrobromic acid dew point, active oxidation takes place as gaseous bromine diffuses through the oxide layer to the scale–metal interface where it reacts with base metals forming metallic bromides. For example, bromine species can react with iron to form iron bromide following reactions:



By Reactions 8 and 10, the formed free bromine is either released to the bulk gas or diffuses back to the scale–metal interface, and thus a cycle is formed. Limited studies on bromine-induced corrosion were performed at static temperatures below 700°C, not a representative taconite processing condition (10).

The EERC had previously performed a 30-day laboratory corrosion to evaluate bromine-induced corrosion on taconite grate bar under temperatures of 500°C, 300°C, and 150°C, respectively (11). Postanalysis indicates minor bromine deposition and losses of Fe, Cr, and Ni of the testing coupons but mainly is confined to the coupon surface. However, these corrosion experiments were conducted under static temperature conditions while actual taconite equipment’s experience thermal cycling, which may magnify and accelerate corrosion and greatly impact the test results. Therefore, these preliminary data are not necessarily enough to provide a completed perspective of possible bromine-induced corrosion issue in actual taconite processing condition.

Based upon feedback from the taconite industry, the Energy & Environmental Research Center (EERC) proposes additional bench-scale coupon corrosion tests under continuous thermal cycling with wider temperature regimes and extended exposure time. Moreover, materials other than grate bar, such as low carbon alloy used in ducting systems, also need to be investigated for bromine corrosion under low-temperature regime.

The Phase II corrosion experiments proposed by the EERC will help the taconite industry to understand and evaluate the potential side effects that may result from applying bromide-related mercury control technology to the taconite industry.

OBJECTIVES

The overall goal of this project is to characterize bromine-induced corrosion on taconite processing equipment under simulated but representative taconite processing conditions. Specific objectives of this project include the following:

- Determine Br-induced corrosion on grate bars and ductwork materials in simulated taconite flue gas containing HBr under thermal cycling conditions.
- Compare the corrosion rates induced by bromine and chlorine, respectively.
- Estimate the life span of test coupons in taconite flue gas containing bromine species.

EXPERIMENTAL APPROACH

To meet these objectives, the EERC proposed a series of bench-scale corrosion experiments in which selected metal coupons were placed in a temperature-controlled chamber filled with simulated taconite flue gas containing HBr and in a parallel stream containing HCl. The exposure chamber is divided into two different temperature zones: hot zone and cool zone. Representative grate bar and low carbon steel coupons were placed in the hot zone and cool zone, respectively.

The temperature profile was originally proposed as cycling between 500° and 1200°C hourly in the hot zone to mimic the heat profile of grate bars experienced in the actual taconite processing condition, while temperatures within the cool zone will be varied between 65° and 250°C daily to simulate downstream ductwork. Having started the project, the EERC has revised temperature cycling profiles based on the requirement from the taconite industry. As for the hot zone, temperatures varied from 80° to 950°C within a 3-hour cycle: 1 hour heating up, a half hour at peak temperature, 1 hour cooling off, and a half hour at a lower temperature, as plotted in Figure 1. The temperature cycle in the cool zone was revised to be varied from 50° to 200°C within a 2½-hour cycle: a half hour heating up, 1 hour at peak temperature, a half hour cooling off, and a half hour at a lower temperature, as plotted in Figure 2.

At the request of the taconite industry, instead of one grate coupon originally proposed, two different grate coupons (Minorca and Minntac) were included in the corrosion experiment under the hot-zone condition. The grate bar coupons were provided by the taconite industry. The Minorca coupon has 5% Ni, 27% Cr, and balanced Fe content compared to 17% Ni, 27% Cr, and balanced Fe content in Minntac coupons. The grate bar coupons in the hot zone were covered with an iron oxide–limestone mixture to simulate the taconite processing environment. The low-carbon steel coupons (C1018) were obtained from ASPI Inc.

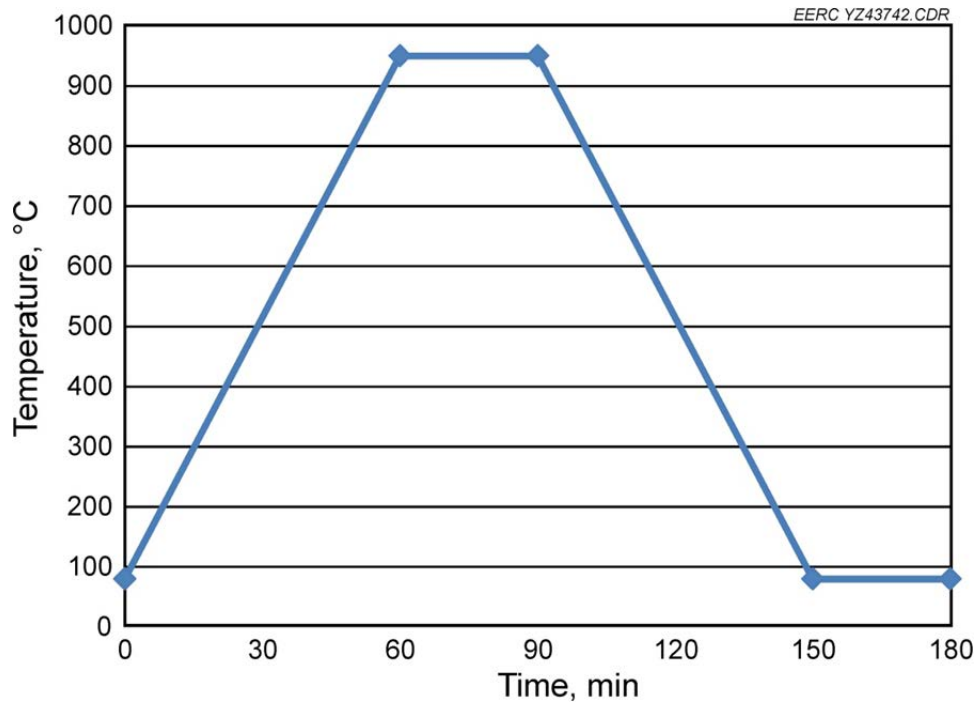


Figure 1. Temperature cycle in hot zone.

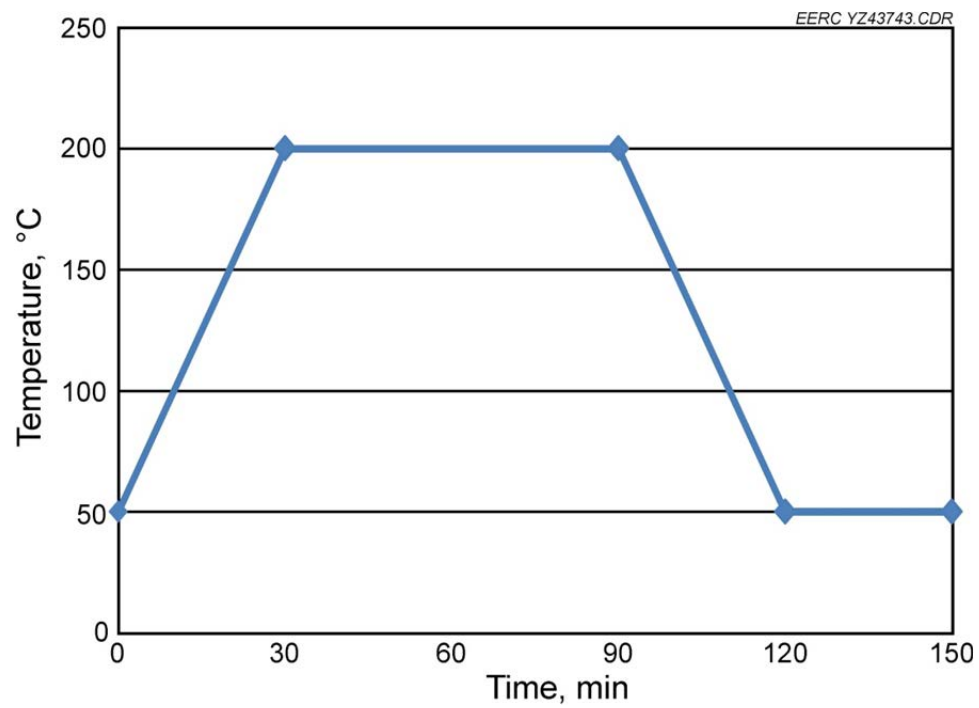


Figure 2. Temperature cycle in cool zone.

Table 1 shows the simulated taconite flue gas composition used in the exposure experiments. The gas delivery system of the EERC's Environmental Chemistry Laboratory was used to provide the flue gas matrix for the test. The system uses mass flow controllers to meter appropriate amounts of each gas constituent. The mass flow controllers are backed up by rotary meters to provide a visual check on the gas flows into the mixing manifold. A National Instruments LabVIEW program was written for the test to control the mass flow controllers to provide required flow rate of each flue gas component. The acid gases, air, balance nitrogen, and carbon dioxide were mixed in the heated manifold before being sent to the test tubes in a heated line. The moisture for the gas matrix was created in a steam generator and combined with a small portion of the balance nitrogen before being sent to the test apparatus in a heated line. The moisture content was regulated with a peristaltic pump that fed the steam generator. Note that the taconite flue gas usually has high concentrations of O₂ (~16%) and H₂O (~20%) and very low SO₂ as a result of taconite plants using low sulfur fuel and moisture from drying the green balls.

The coupons were exposed to the flue gas for 3 months and recovered every 30 days during the test for weight measurement. The collected coupons were treated following the standard ASTM International G1-03 method before the weight measurement. The weight gain/loss was determined by comparing to previous weight measurements.

In addition to the bromine-induced corrosion testing, a parallel exposure experiment was also conducted in which the metal coupons were exposed to similar simulated taconite flue gas containing 20 ppm HCl instead of HBr. The flue gas compositions are listed in Table 1. Similar metal coupons experienced the same temperature cycles in the 20-ppm HCl-containing taconite flue gas as that in HBr-laden flue gas for 3 months. The metal coupons were periodically removed for weight measurement to determine the chlorine corrosion rate, and the results were compared to the corrosion rate derived from bromine corrosion testing. The detailed test parameters are shown in Table 2.

Table 1. Simulated Taconite Flue Gas Composition

Flue Gas Constituent	Flue Gas I	Flue Gas II
O ₂ , %	14	14
CO ₂ , %	4.0	4.0
H ₂ O, %	20	20
N ₂ , %	Balance	Balance
NO, ppm	600	600
NO ₂ , ppm	10	10
CO, ppm	40	40
SO ₂ , ppm	10	10
HBr, ppm	20	NA*
HCl, ppm	NA	20

*Not applicable.

Table 2. Experiment Parameters of Exposure Test

Test No.	Temperature Zone	Exposure Time	Flue Gas Composition	Coupon Material	Deposit
T-1	80°–950°C (3-hour cycle)	3 months	Flue gas I	Grate bar	Iron oxide/ limestone
T-2	80°–950°C (3-hour cycle)	3 months	Flue gas II	Grate bar	Iron oxide/ limestone
T-3	50°–200°C (2.5-hour cycle)	3 months	Flue gas I	Low-carbon steel	None
T-4	50°–200°C (2.5-hour cycle)	3 months	Flue gas II	Low-carbon steel	None

At the end of the exposure experiments, the recovered metal coupons were analyzed for morphology as well as the elemental compositions.

THERMODYNAMIC PERSPECTIVE

The main corrosion mechanism induced by halogens on metal is that the formed metal chloride or metal bromide are much volatile than the corresponding metal oxide. At high temperature, metal halides at the metal–oxide interface evaporate and diffuse outward. As a result, a nonprotective scale layer is subsequently formed, and the halogens can continuously attack metals. The temperature, oxygen/halogen ratio, and metal matrix of the material will influence corrosion behavior. Figure 3 describes the halogen corrosion mechanisms.

Plotted in Figures 4–6 are the thermodynamic phase-stability diagrams that were constructed under metal–oxygen–chlorine and metal–oxygen–bromine systems for iron, nickel, and chromium, respectively, which are the three main elements of taconite grate materials. Since temperatures play a critical role in metal corrosion, the phase-stability diagrams were plotted in 500° and 950°C, respectively. Also included in the phase-stability diagrams are the points representing the oxygen and bromine or chlorine partial pressure of the experimental gas conditions, marked as the square dots.

For all three elements being considered at 500°C, the scales formed on the scale–gas interface were predominantly oxides because of the high partial pressure of oxygen in the testing taconite flue gas, 14% O₂ vs. 20 ppm HCl or HBr. However, halides could be thermodynamically favored as the oxygen potential was reduced, for example, at the scale–metal interface. Based on the phase-stability diagrams, the predominant metal compounds at low oxygen conditions, i.e., scale–metal interface, are FeBr₂/FeCl₂, Ni/NiBr₂/NiCl₂, and CrBr₂/CrCl₂/CrCl₃ for Fe, Ni, and Cr, respectively. Most formed metal halides remained at their solid states at 500°C, implying that active oxidation should be at minimum levels. The calculated results under 500°C condition agreed with the experimental observations in Phase I, in which only minor Br-induced corrosion was detected on the surface of the coupon exposed below 500°C.

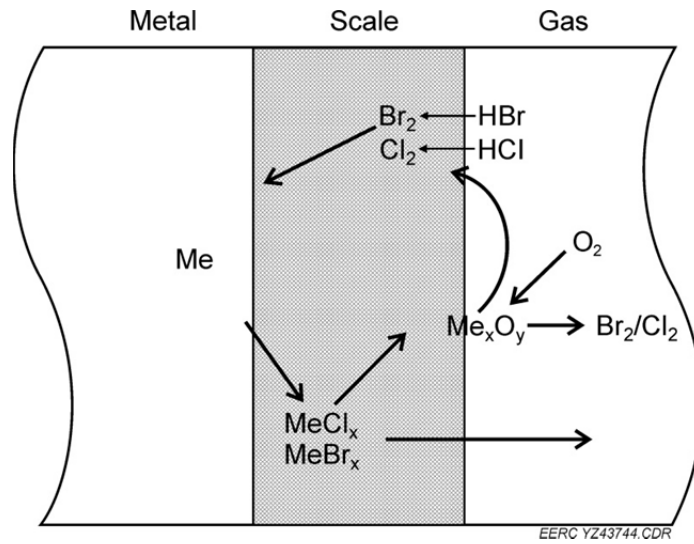


Figure 3. Halogen-induced active oxidation mechanisms.

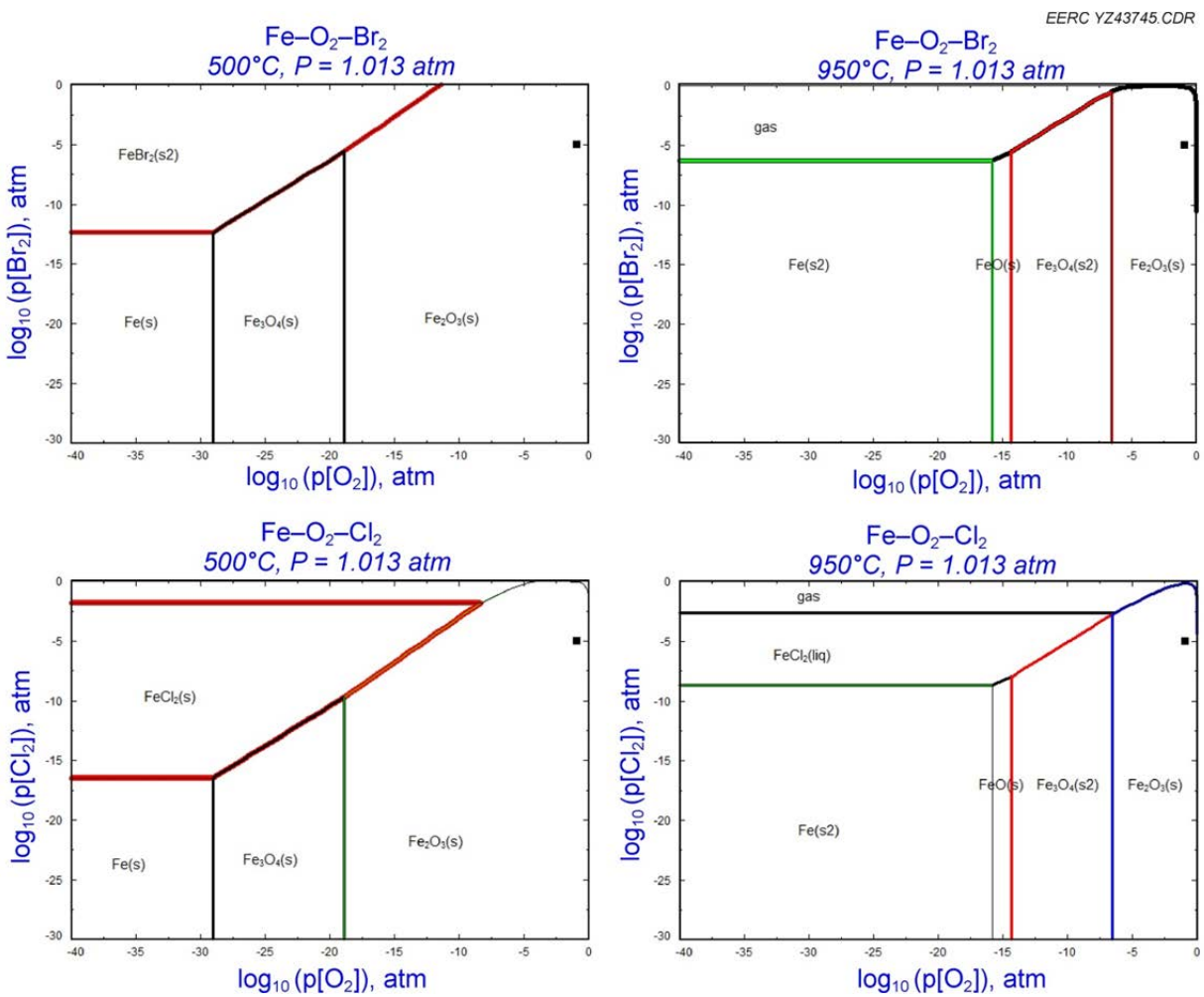


Figure 4. Phase-stability diagrams of Fe-O₂-Br₂ and Fe-O₂-Cl₂, respectively.

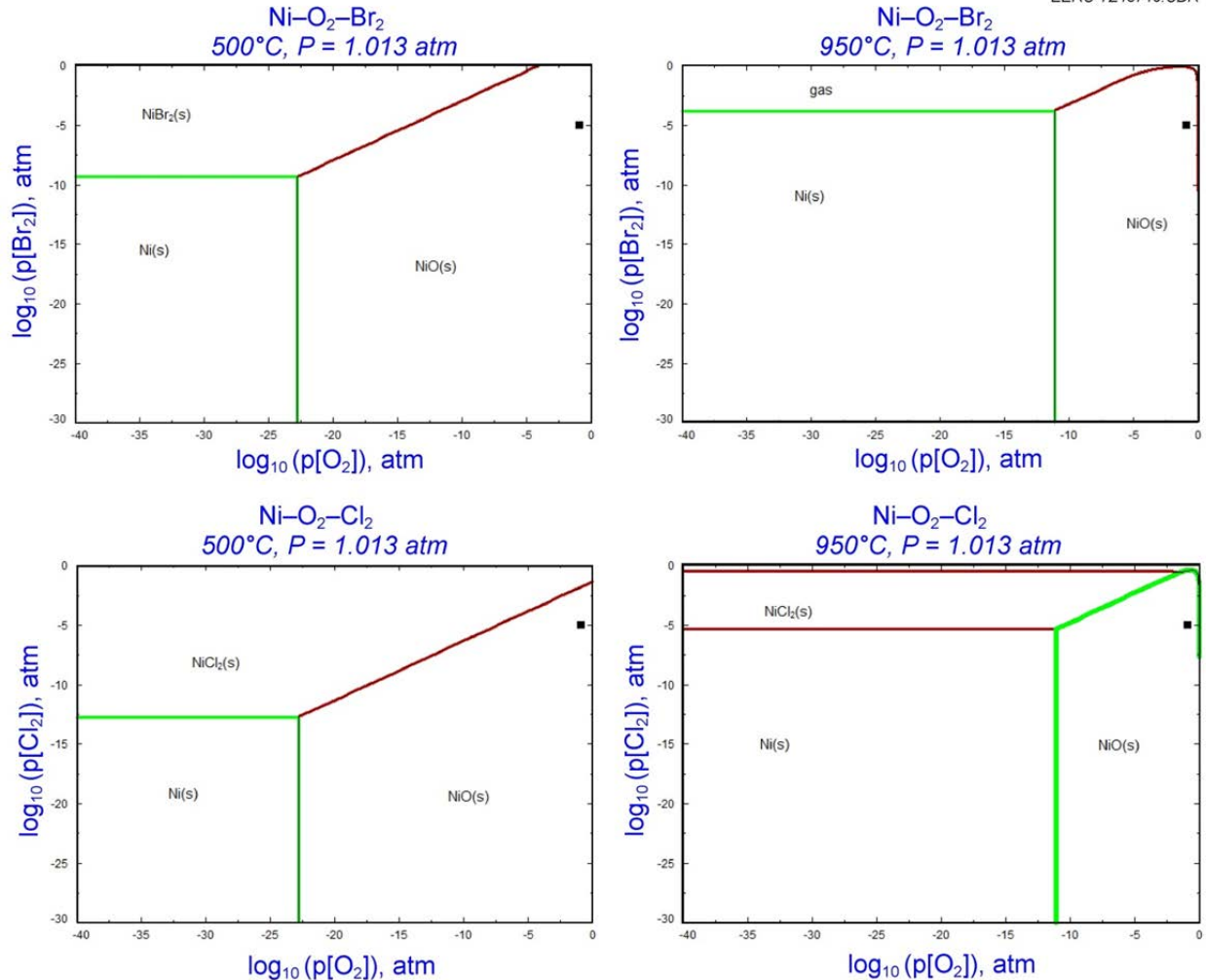


Figure 5. Phase-stability diagrams of Ni–O₂–Br₂ and Ni–O₂–Cl₂, respectively.

With the temperature increasing to 950°C, FeBr₂ becomes vapor and FeCl₂ changes to liquid with elevated vapor pressure under low oxygen conditions, which could affect corrosion progress. It is expected that FeBr₂ would diffuse outward through the oxide layer, cause spallation of the oxide layer, and form blisters. Similar back diffusion with subsequent active oxidation occurred for FeCl₂, while the extent of corrosion is less severe than that caused by FeBr₂ since a less amount of gaseous FeCl₂ is formed than FeBr₂. FeBr₂ or FeCl₂ reaching scale–gas interface converts to oxides such as Fe₂O₃/FeO/Fe₃O₄, as shown in the phase diagram and other reports (10), because of the high oxygen potential, while the halogens release either into the gas phase or they reattack metals. The phase diagrams indicate that NiO solid is predominant on metal surfaces at 950°C, while Ni remains in an elemental state at a low oxygen potential for bromine and NiCl₂ solid is formed with chlorine exposure. Nickel seems to be immune to a bromine attack at 950°C. CrBr₂ solid is thermodynamically stable, while CrCl₂ at liquid phase becomes the dominant chloride compound at a low oxygen potential under 950°C. Formed CrBr₂ and CrCl₂ can convert to oxide at a much lower oxygen partial pressure than needed to convert nickel bromide and chloride to nickel oxide.

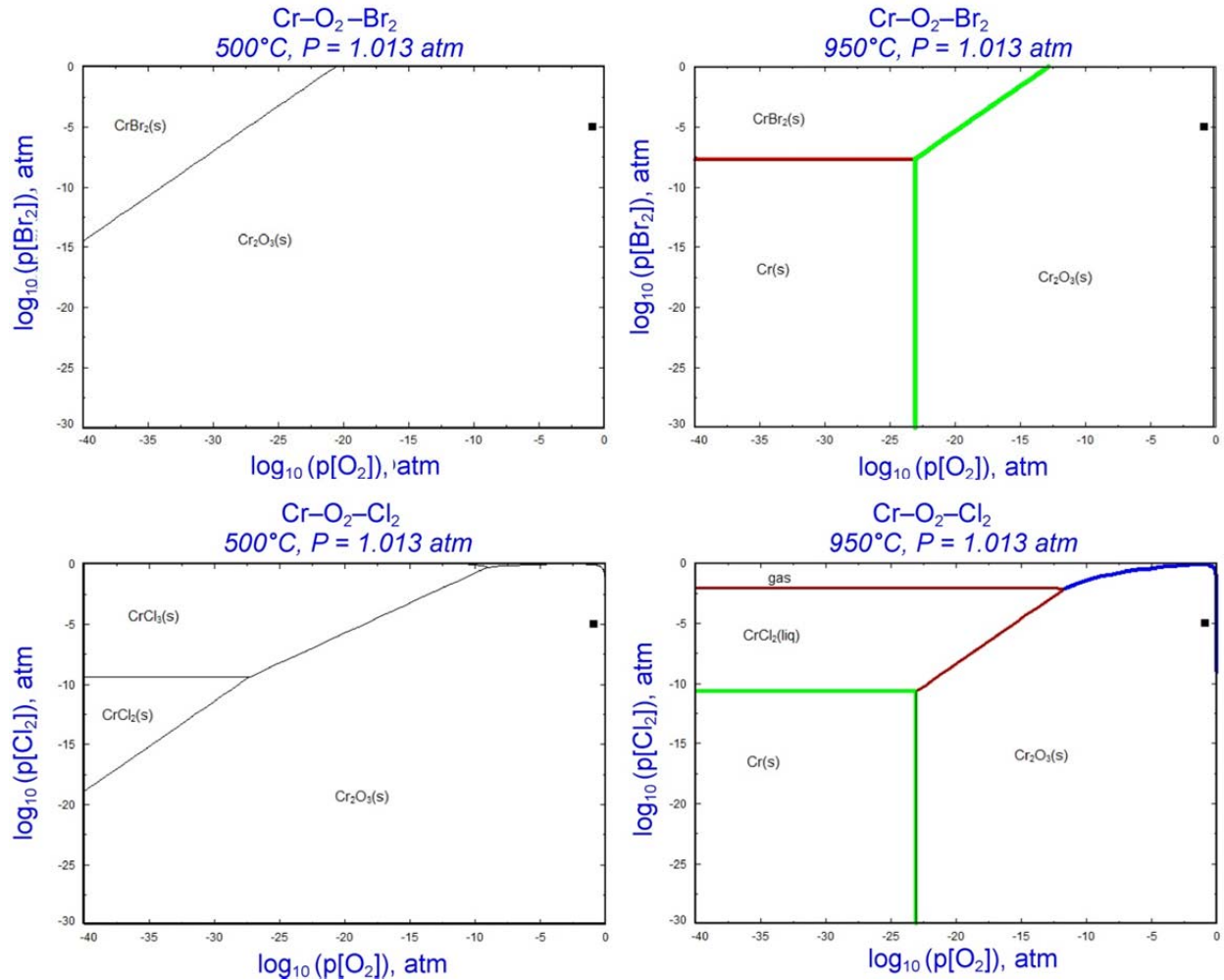


Figure 6. Phase-stability diagrams of Cr–O₂–Br₂ and Cr–O₂–Cl₂, respectively.

For a taconite grate bar that consists of varying amounts of Fe–Cr–Ni, a complex metal oxide scale is the predominant compound on the metal–gas interface, as shown in Figure 7 and reported by others (12).

The extent of active oxidation heavily depends on the volatilization of the formed compounds, which can be characterized with temperature T₄, defined as the temperature at which the vapor pressure reaches 10⁻⁴ atm. It is widely agreed that as the exposure temperature exceeds the corresponding T₄, active oxidation would become the dominant corrosion mechanism (13). Table 3 lists the T₄ and melting points of metal bromides, chlorides, and oxides that could be formed in the taconite process according to the phase-stability diagrams.

Note that the T₄s of the formed chloride, bromide, and oxide compounds are higher than 500°C, which indicates that the quantities of the volatile species produced and diffused outward to the gas stream are small at temperatures below 500°C. As a result, the oxide scale will remain

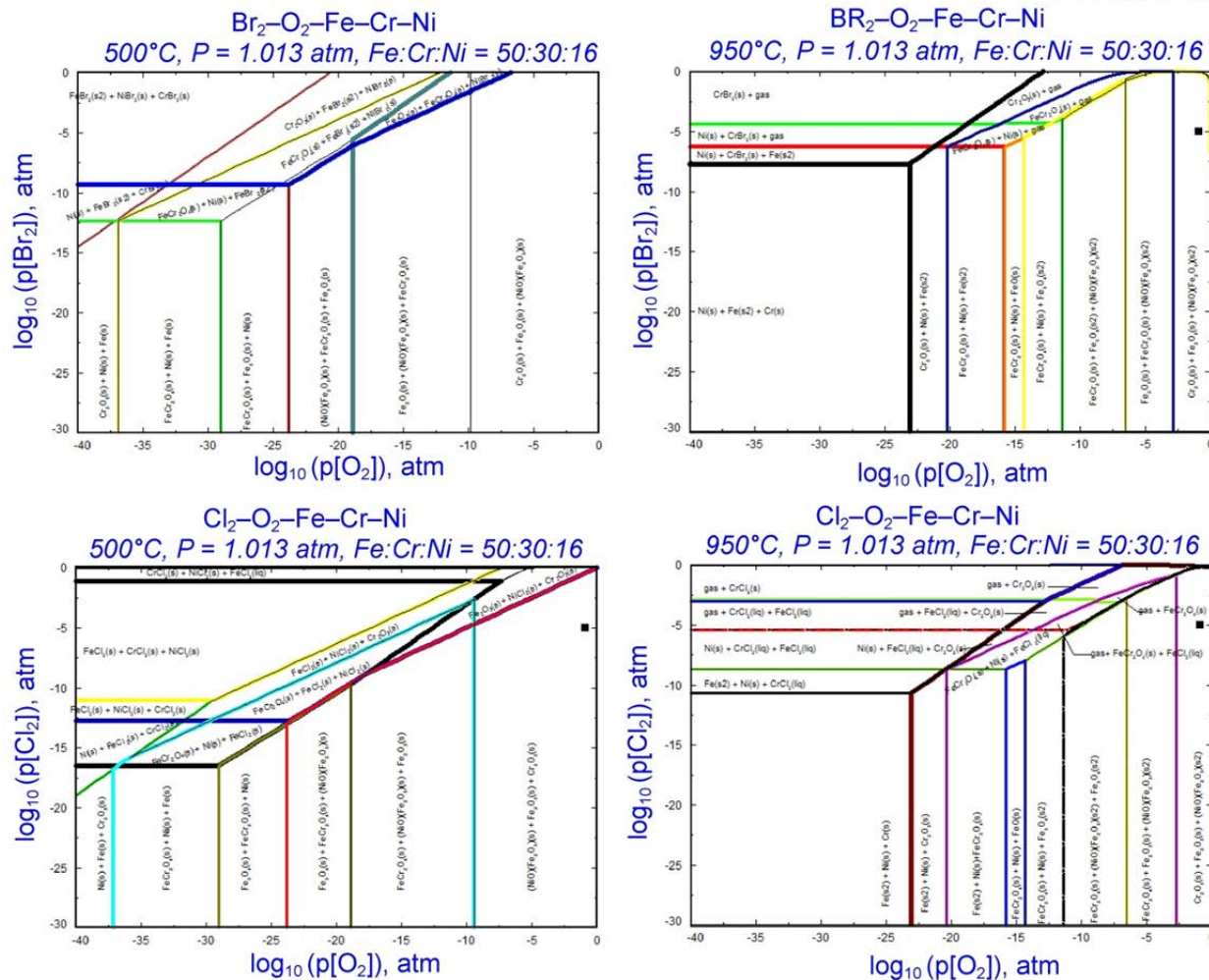


Figure 7. Phase-stability diagrams of Minntac–O₂–Br₂ and Minntac–O₂–Cl₂, respectively.

Table 3. Summary of T4, Melting Point, Volatility Ranks of Metal Compounds

Metal Compounds	T4, °C	Melting Point, °C	Volatility Rank
FeBr ₂	509	689	1
FeCl ₂	536	677	2
NiBr ₂	567	963	3
NiCl ₂	587*	1009	4
CrCl ₃	607	1152	5
CrBr ₂	716	NA	6
CrCl ₂	747	824	7
Fe ₂ O ₃	NA	1565	8
NiO	NA	1955	9
Cr ₂ O ₃	NA	2435	10

intact and minimize further chlorine- or bromine-induced active oxidation. Slight weight gain is expected for the materials below this temperature because of halogen deposition as observed for the testing coupons in Phase I exposure experiments where temperatures were controlled below 500°C. Similar observations have also been reported elsewhere (14).

As shown in Table 3, T4 of iron bromide/chloride are the lowest, followed with nickel bromide/chloride and chromium chloride/bromide, indicating that most metal bromides have relatively higher volatilities than the corresponding chloride followed by oxides. As the exposure temperature reaches 950°C, active oxidation would occur to some different degrees for all three elements. It is estimated that iron would have poor resistance to halogens under the high temperature condition, while bromine-induced corrosion on iron would be worse than that of chlorine. Chromium compound is much less mobile than Fe and Ni and easier to convert to chromium oxide, which forms a protective scale. Therefore, Cr is likely to be the most resistant to active oxidation induced by halogens, followed by Ni, while Fe is susceptible to an attack by halogens.

RESULTS AND DISCUSSIONS

Preexposure Baseline Analysis

Two taconite grate bars (Minntac and Minorca) and one low carbon steel coupon were exposed in simulated taconite flue gas containing HBr and HCl, respectively, for 3 months. Table 4 lists the main composition of each material prior to the test. The Minntac coupon has a much higher Ni content (9.92%–16.41%) than that of Minorca coupon (1.3%–4.55%). Cr content was 31.61% for the Minntac coupon (polished side), slightly higher than the 26.58% between the two grate materials. Based upon the above thermodynamic calculations, it is expected that the Minntac coupon would be more resistant than the Minorca coupon to HCl and HBr attacks. The unpolished surface of the Minorca coupon has higher levels of impurities of Ca and Si, and the impurities mainly remain on the surface in comparison to the polished surface. The low-carbon steel mainly consists of iron. As a result of high contents of Cr and Ni in alloy, the heat-resistant grate bars are expected to have a better resistance to acid gases of HCl and HBr than the low-carbon steel. Morphology of the coupon surface prior to the exposure tests is referred as baseline (Figures 8–10).

Table 4. Elemental Composition of the Testing Coupons

Coupon Type	Fe	Cr	Ni	Si	Mo	Ca	Zr
Minorca (unpolished)	61.25	22.64	1.30	4.48	0.26	5.48	4.16
Minorca (polished)	66.58	26.58	4.55	1.30	0.14	0.11	0
Minntac (unpolished)	62.29	19.75	9.92	2.15	0.45	0.54	1.92
Minntac (polished)	49.94	31.61	16.41	1.32	0.17	0.14	0.04
Low Carbon Steel	99.03	0.01	0.00	0.05	0.12	0	0

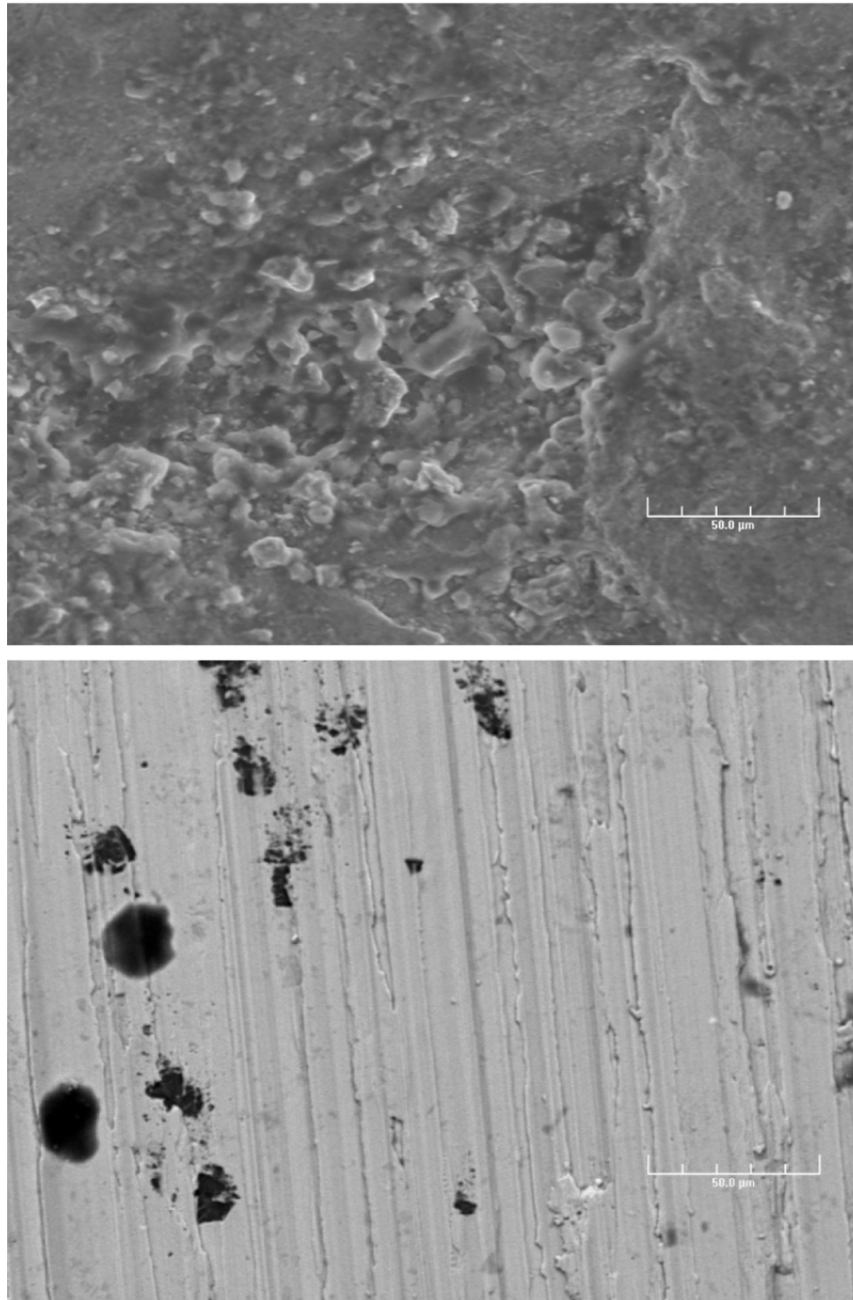


Figure 8. Morphology of the Minntac coupon prior to the test: unpolished surface (top) and polished surface (bottom).

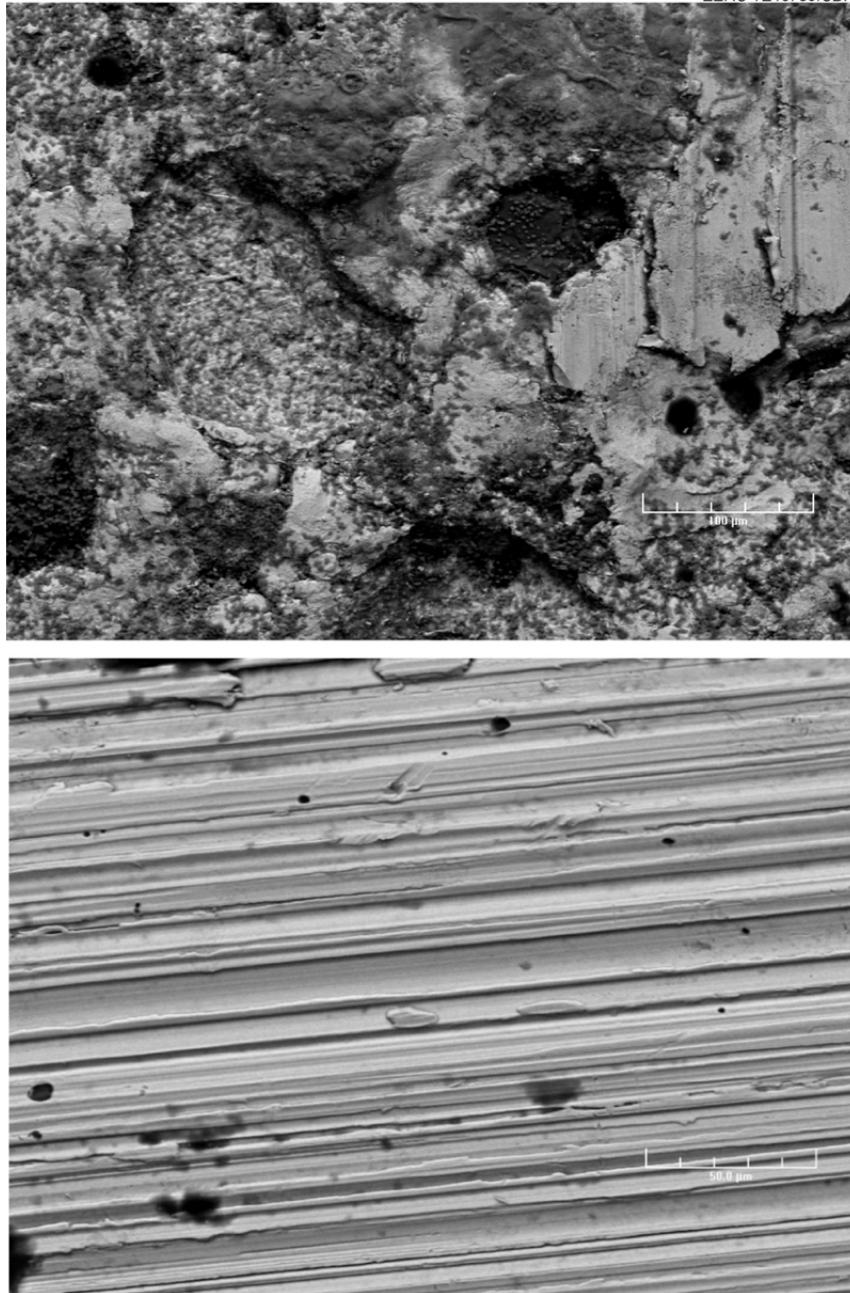


Figure 9. Morphology of Minorca coupon prior to the test: unpolished surface (top) and polished surface (bottom).

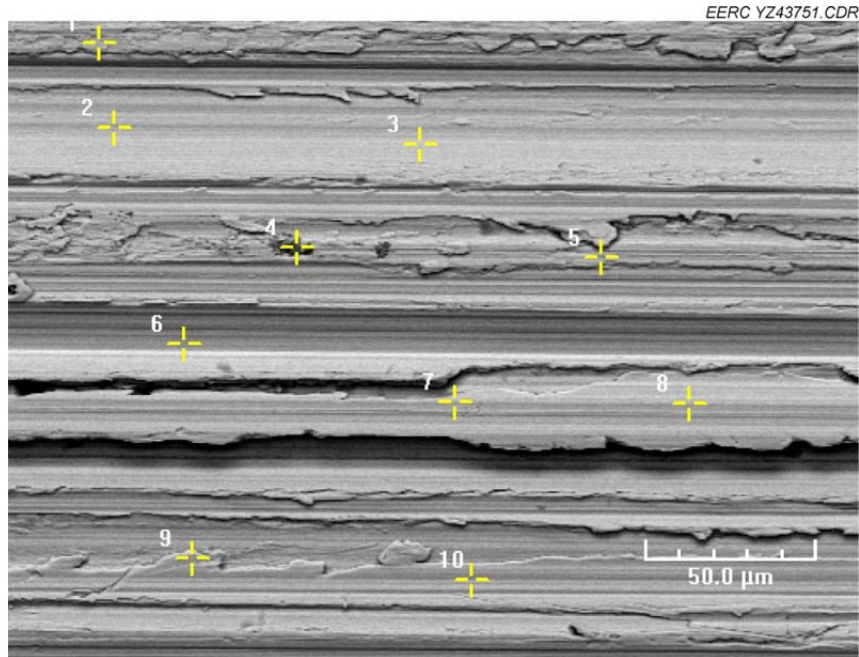


Figure 10. Surface morphology of the low-carbon steel coupon prior to the test.

Postexposure Analysis

Upon completion of the 3-month exposure test, the coupons were removed and prepared for morphology and elemental analysis using scanning electron microscopy energy-dispersive spectroscopy. The results are discussed below.

Minorca Coupon

Shown in Figure 11 are the images of the Minorca coupon surface after 3 months of exposure to flue gas containing HCl and HBr, respectively. The coupon that has been exposed to the flue gas containing HCl virtually maintains its integrity on the surface after the 3-month test, which agreed with the corresponding cross-section analysis shown in Figure 12. A minor depletion of Fe was found on the scale–gas interface (Points 1 and 2), with corresponding enrichment of either Ni or Cr on the interface. Meanwhile, a slightly elevated Cl presence was also observed. According to thermodynamic calculation, even though FeCl_2 might become volatile, the formed NiCl_2 , $\text{CrCl}_2/\text{CrCl}_3$ would remain immobile as a solid phase under the current thermal cycle, and the scale would maintain its integrity. As a result, no significant cracking was observed beneath the surface, proving that the formed Fe–Cr–Ni complex scale is resistant to HCl attack and restricts chlorine-induced active oxidation within the interface.

On the other hand, the Minorca coupons exposed to HBr have shown blistering and tiny pinholes on the surface (shown in Figure 11), indicating volatiles have emerged beneath the surface and were released through the scale during the exposure experiment. Corresponding cross-section morphology (Figure 13) showed that local microcracking has been developed

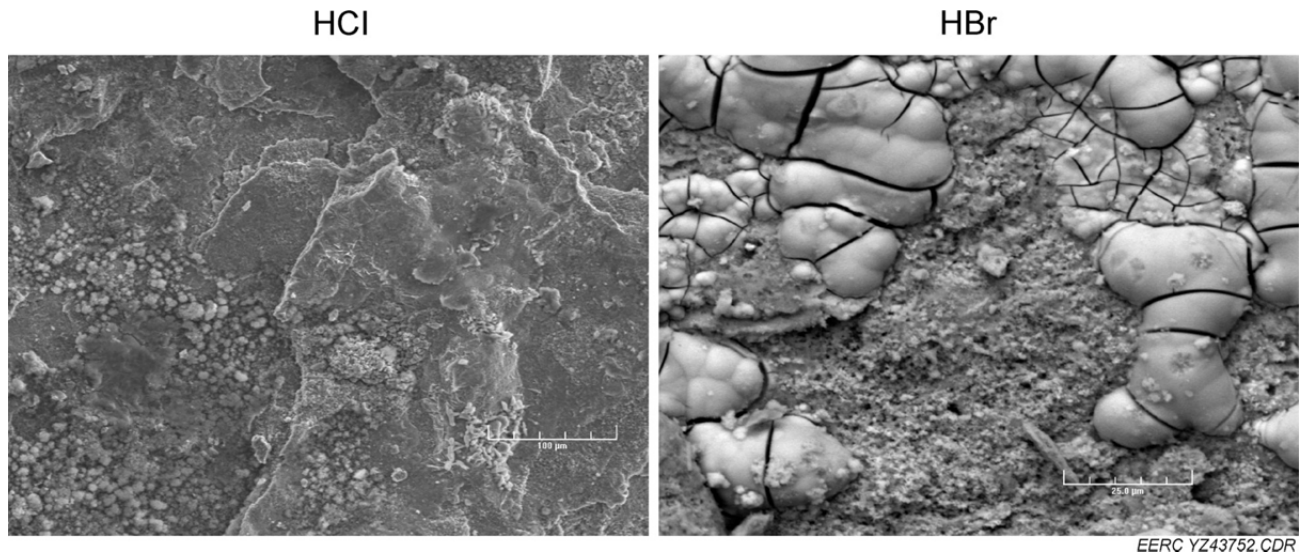


Figure 11. Surface of the Minorca coupon after exposure.

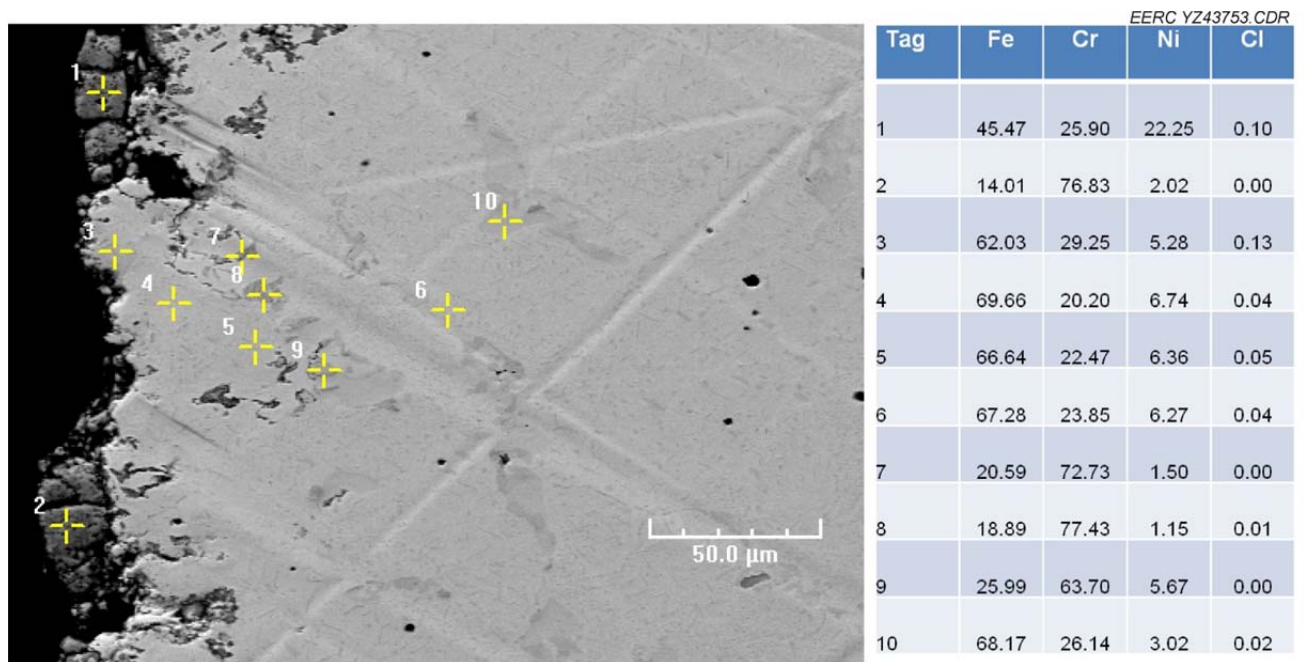


Figure 12. Cross section of the Minorca coupon after HCl exposure.

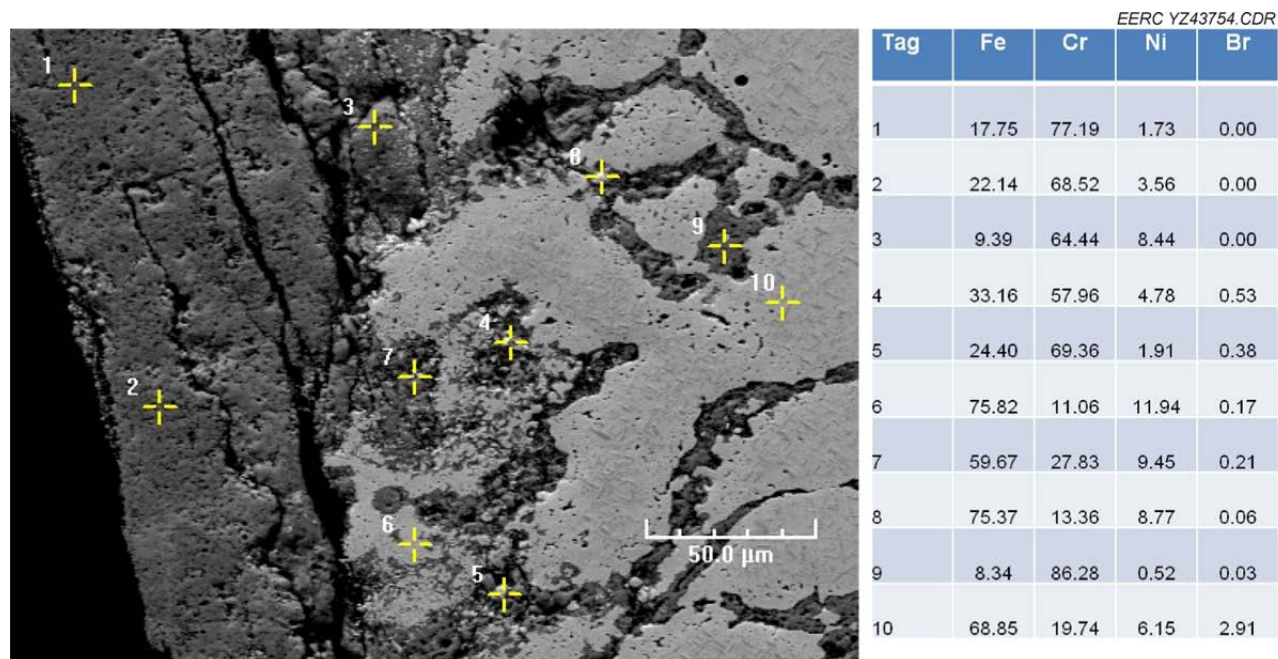


Figure 13. Cross section of the Minorca coupon after HBr exposure.

beneath the scale. Further elemental analysis on the selected points within the cross section indicated that Fe depletion took place not only within the scale but also along the microcracking beneath the surface. As a result of Fe depletion, the concentrations of Cr and Ni to some degree were elevated accordingly. When bromine gas reacts with metals, forming metallic bromide with no oxygen present, iron bromide is the most volatile compared to chromium bromide and nickel bromide because of its low T₄ among the three metal bromides. Therefore, a fair amount of iron bromide evaporated, diffused through the scale, and escaped into the gas stream. Meanwhile, chromium bromide and nickel bromide remained immobile as solid, resulting in the observed enrichment beneath the scale. The outward diffusion of iron bromide was the main reason for the local microcracking. At the scale–gas interface, metallic bromide compounds would be converted to oxides in the presence of oxygen and bromine gas either released into the gas stream or diffused back to metal. Therefore, no bromine was present within the scale.

To further differentiate the impact of HCl and HBr on metal corrosion, elemental analysis of the three elements was performed along a randomly selected line within the cross section. As shown in Figure 14, the partitioning of Fe, Cr, and Ni for the coupon under HCl exposure was similar to that in the baseline condition. The coupon that was under HBr exposure showed appreciable Fe depletion with corresponding enrichment of Cr and/or Ni within the first 50 μm from the scale–gas interface, and no significant changes of distribution of the three elements was observed beyond 200 μm from the surface, indicating that bromine-induced corrosion was minor for the Minorca coupon under the testing conditions.

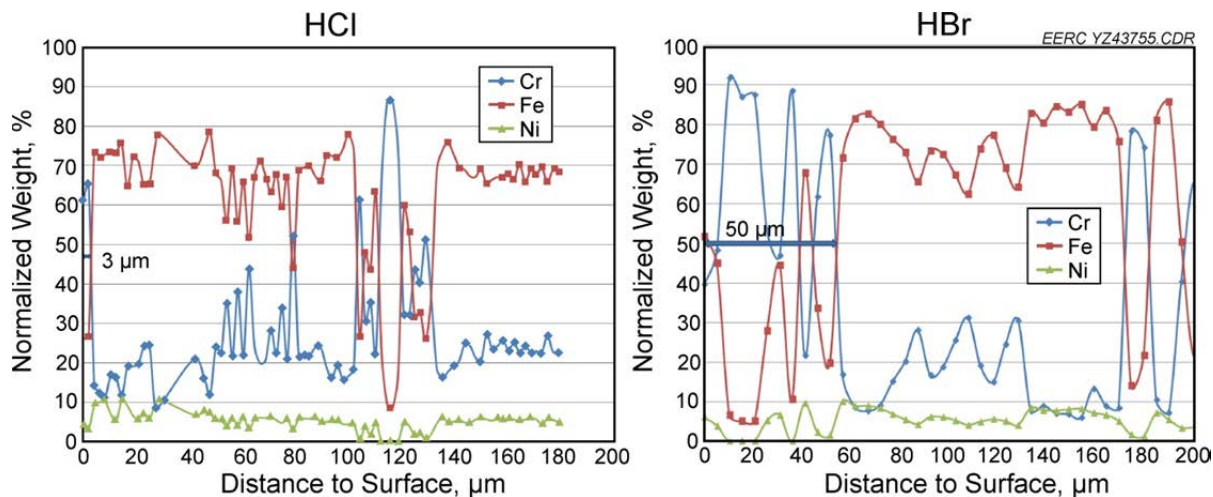


Figure 14. Variation of Fe, Cr, and Ni across the Minorca coupon.

Results of both surface and cross-section analysis on the Minorca coupons agree with the thermodynamic expectation that bromine is more corrosive than chlorine, mainly because iron bromide is more volatile than iron chloride. With the presence of chromium and nickel, however, the corrosion is somewhat slowed down since chromium bromide and nickel bromide remained solid and did not diffuse outward to the gas–scale interface under current thermal cycles.

Minntac Coupon

The Minntac coupon was exposed with the same flue gas and thermal cycles as that of the Minorca coupon. As shown in Figure 15, coupons that have been respectively exposed to HCl and HBr maintain good integrity after 3 months of exposure. Although not showing spalling or blistering as did the Minorca coupon, tiny pinholes were observed on the surface of the Minntac coupons after being exposed to HBr, suggesting that volatile gas was released during the HBr experiment.

Cross-section morphology of the Minntac coupon under a HCl exposure test showed that no significant HCl-induced active oxidation occurred. However, microcracking was occasionally found that originated from the coupon surface and penetrated $\sim 100\ \mu\text{m}$ as shown in Figure 16. In addition to Fe depletion, Ni concentration was also reduced from $\sim 16.4\%$ of the pretest to $1\%–8\%$ on the coupon surface and along the microcracking as well, indicating that both Fe and Ni were partially released into the gas stream during the exposure experiment. This was most likely a result of the vaporization of FeCl_2 and NiCl_2 as suggested by thermodynamic calculations. Meanwhile, Cr maintained as solid on the surface to minimize a HCl attack.

Similar to the results of the Minorca coupons, more microcracking was observed beneath the Minntac coupon surface under exposure to HBr than HCl. Plots in Figure 17 show typical cracking with their associated elemental distributions of the Minntac coupon under HBr exposure. Fe and Ni were found to be coincidentally depleted with Cr enrichment along the microcracking.

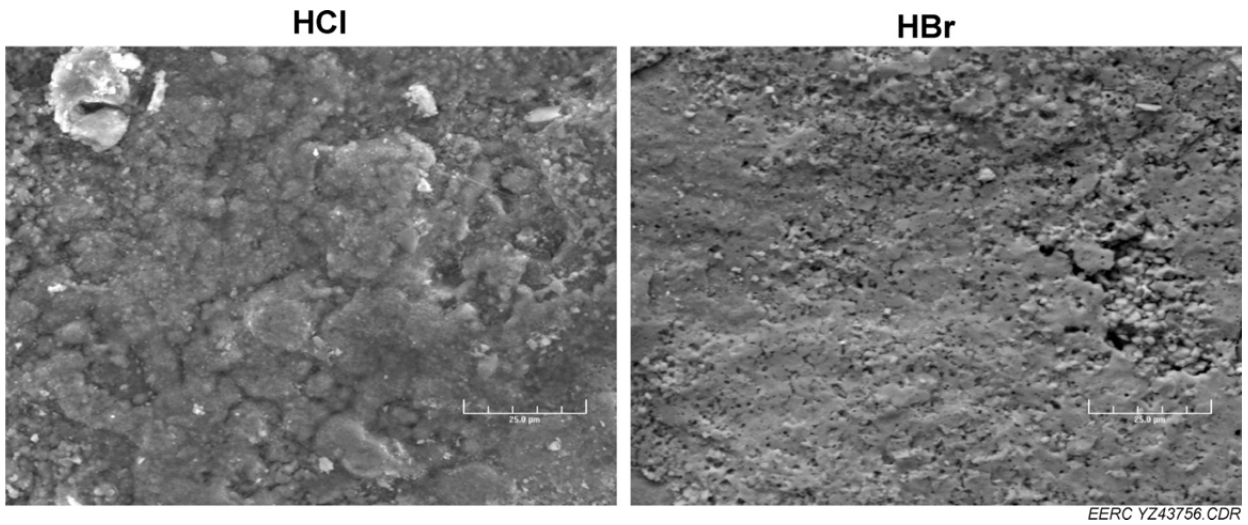


Figure 15. Surface of the Minntac coupon after exposure.

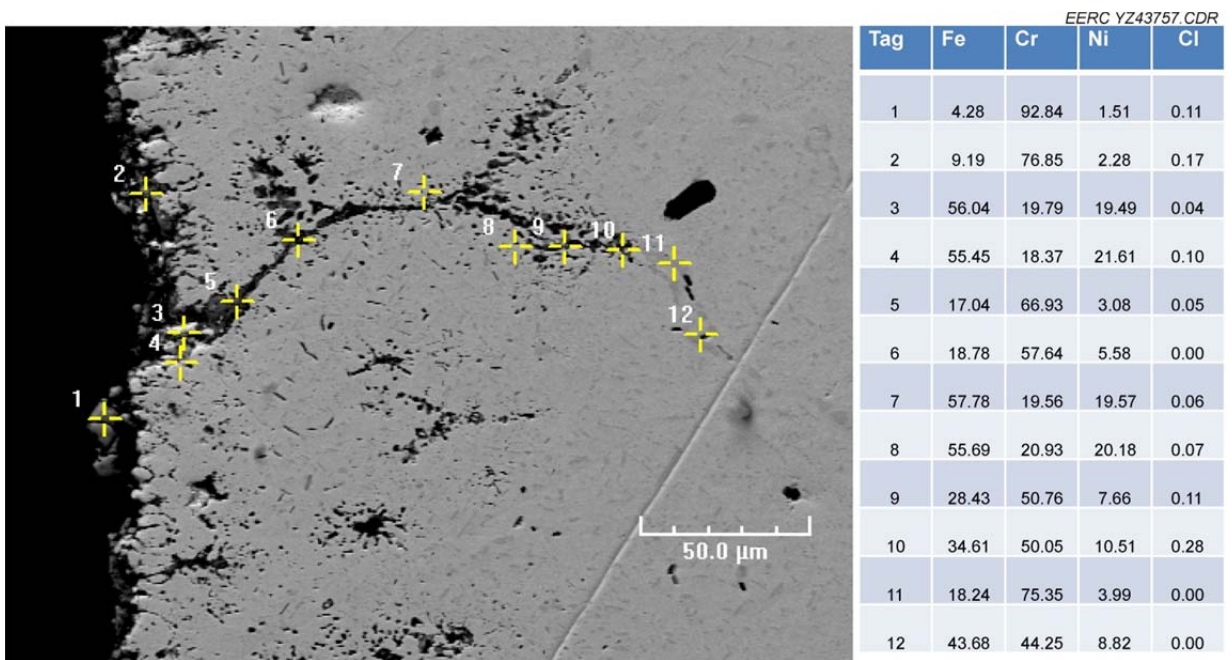
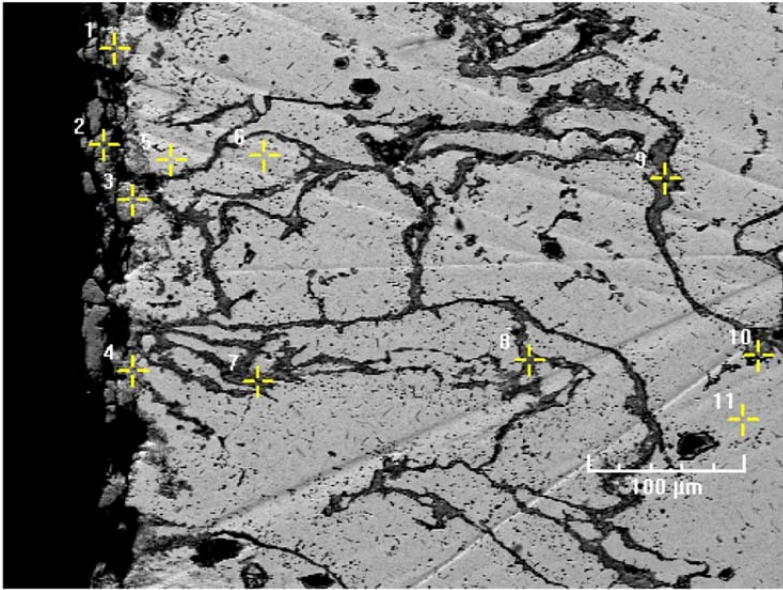
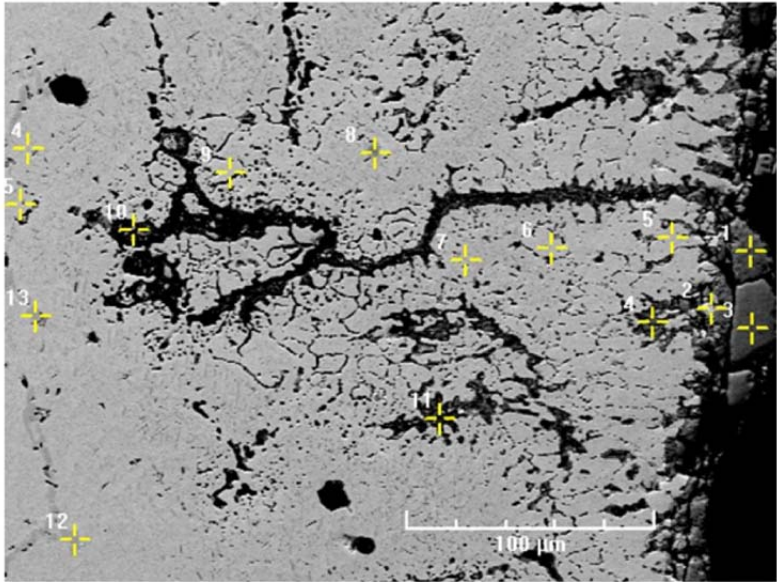


Figure 16. Cross section of the Minntac coupon after HCl exposure.



Tag	Fe	Cr	Ni	Br
1	29.60	49.54	18.21	0.13
2	21.21	70.20	5.51	0.53
3	39.01	21.41	36.49	0.00
4	25.74	50.47	20.97	0.00
5	57.63	11.22	29.66	0.00
6	56.38	20.50	21.23	0.00
7	8.07	83.84	2.16	0.55
8	8.55	87.90	1.91	0.18
9	6.35	90.63	1.31	0.00
10	9.34	63.92	2.48	0.00



Tag	Fe	Cr	Ni	Br
1	8.76	86.20	1.51	0.00
2	26.30	57.22	10.78	0.27
3	2.36	95.56	0.32	0.00
4	10.98	80.93	4.63	0.13
5	58.89	12.56	26.37	0.12
6	60.87	14.42	22.97	0.35
7	52.76	25.27	19.55	0.15
8	38.93	40.52	16.45	0.50
9	59.55	17.93	20.22	0.18
10	22.29	62.91	6.04	0.25
11	19.50	49.94	5.91	0.21
12	44.35	36.92	15.91	0.21
13	34.10	38.63	11.94	0.10
14	51.69	26.50	18.72	0.18
15	58.80	19.80	18.37	0.27

Figure 17. Cross section of the Minntac coupon after HBr exposure.

As suggested by thermodynamic calculation, iron bromide that was formed beneath the surface in the absence of oxygen was the most volatile and evaporated through the scale, causing the depletion of Fe. Chromium bromide, the least volatile bromide compound, remained as solid and immobile within the coupon during the thermal cycle. In comparison to iron bromide and chromium bromide, nickel bromide has an intermediate volatility based upon its T4 and seemed to show some degree of volatilization with a final Ni content along the crack, stabilizing between 1% and 8%. At the scale–gas interface, metallic bromide compounds would be converted to oxides in the presence of oxygen, and bromine gas was either released into the gas stream or diffused back to metal. Therefore, no bromine was present within the scale.

Elemental analysis along a randomly selected line was performed, and the resulting elemental distributions for the coupon exposed to HCl and HBr stream, respectively, are plotted in Figure 18. The elemental partitioning of the coupon exposed to HCl showed depletion of Fe and Ni with respective Cr enrichment for the first 5 μm below the surface and recovered to the baseline condition, indicating resistance to HCl-induced corrosion. HBr, on the other hand, showed deeper $\sim 20\text{-}\mu\text{m}$ penetration through the coupons with enrichment of Cr and depletion of Fe and Ni. The coincident depletion of Fe and Ni seems to suggest that a Fe–Ni complex halide may be formed during the exposure. Further study on species of metal halides would facilitate an understanding of the reaction pathways. Since nickel bromide is less volatile than iron bromide and the iron content of the Minntac coupon is lower than the Minorca coupon, the overall active oxidation induced by HBr is less severe in the Minntac coupon than in the Minorca coupon, which explains why no obvious blistering was observed in the Minntac coupon surface.

Both thermodynamic calculation and experimental data suggested that HBr is more corrosive than HCl to metals, and experimental data of Minorca and Minntac coupons prove that, in comparison to Fe and Ni, Cr is the most resistant element to HCl and HBr attack during the present thermal cycle. Thermodynamic calculation also showed chromium chloride/bromide can convert to oxide at a very low oxygen partial pressure and a much higher oxygen partial pressure

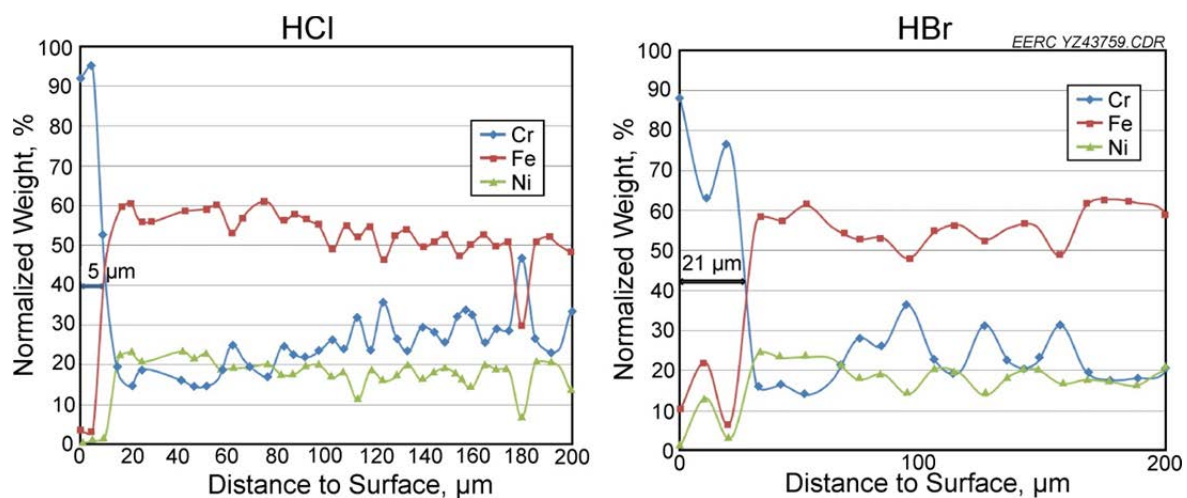


Figure 18. Variation of Fe, Cr, and Ni across the Minntac coupon.

is needed to convert nickel chloride/bromide to nickel oxide. The presence of chromium on the coupon surface ensures the integrity of a formed protective scale and slow downs or minimizes further HCl and/or HBr corrosion.

Low-Carbon Steel

Plotted in Figures 19–22 are the morphology analysis (surface and cross section) with associate elemental distribution of the low-carbon steel coupons that have been exposed in HBr and HCl containing flue gas with temperature cycling between 50° and 200°C. Both low-carbon steel coupons showed no significant HCl-and/or HBr-induced blistering, and iron concentrations below the scale remained constant under the low-temperature thermal cycle. Cross-section morphology also indicated no microcracking below the scale. The main reasons can be ascribed to the fact that iron bromide and iron chloride remained as solid, and no vaporization of metal bromide and chloride took place under the low-temperature thermal cycles.

Loose condensate was found above the normal oxide scales of low-carbon steel coupons exposed to HBr streams (Figure 21). Further elemental analysis data showed that fair amounts of Ni and Br elements were detected within the condensate, indicating that nickel bromide compounds evaporated from the upstream heat-resistant coupons (Minorca and Minntac coupons) during the high-temperature cycles and recondensed on the low-carbon steel surface where the temperature was cycled between 50° and 200°C.

All tested coupons were periodically recovered during the exposure experiment for weight measurement, and the temporal variation of coupons weighed were plotted in Figure 23.

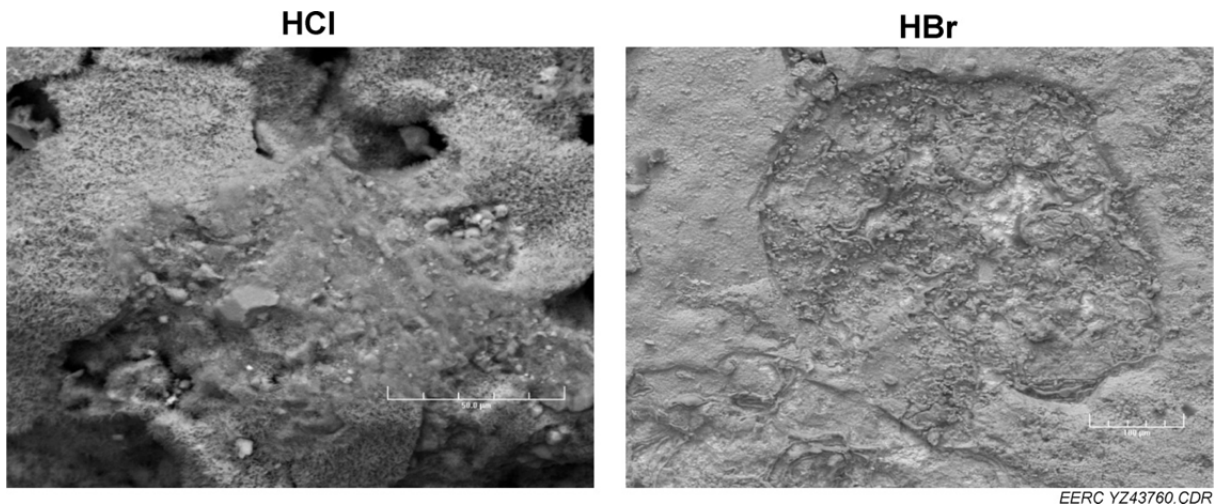


Figure 19. Surface of low-carbon steel coupon after exposure.

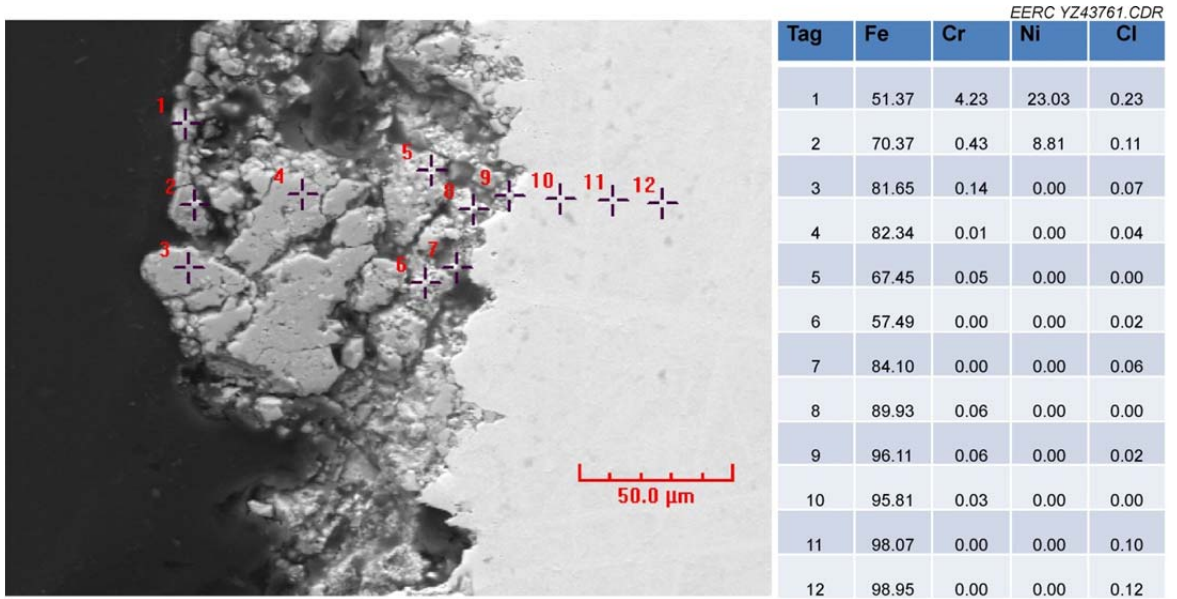


Figure 20. Cross section of the low-carbon steel coupon after HCl exposure.

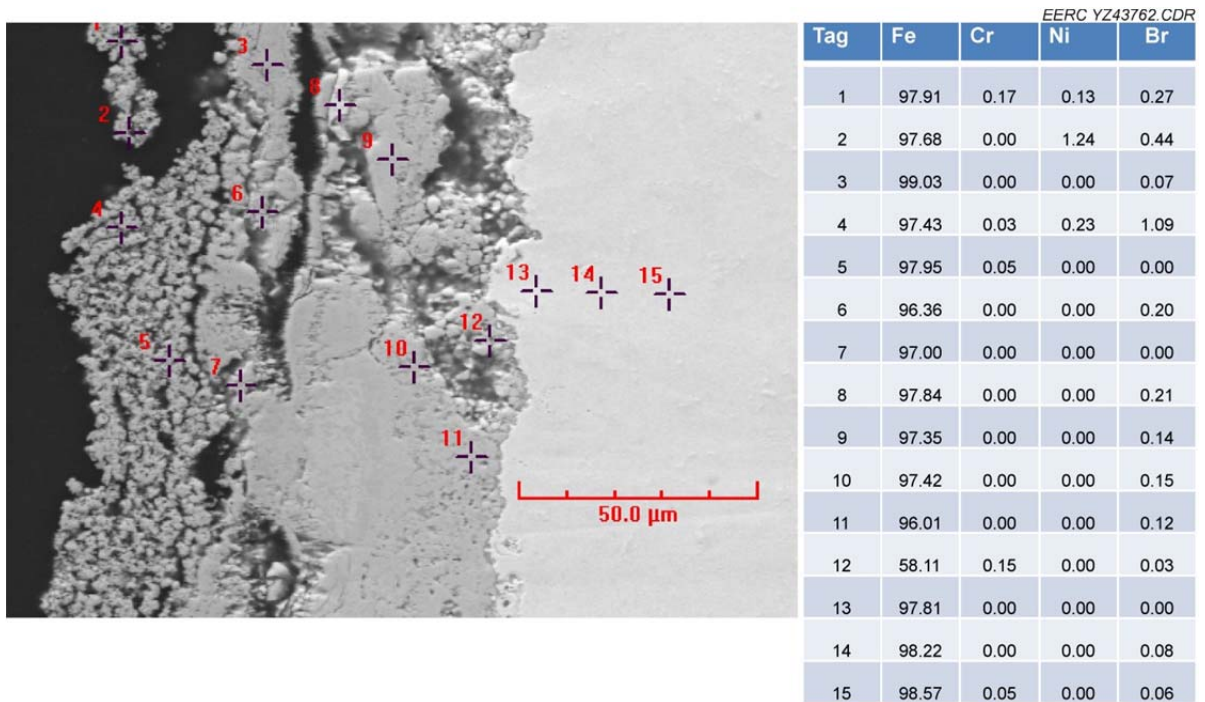


Figure 21. Cross section of the low-carbon steel coupon after HBr exposure.

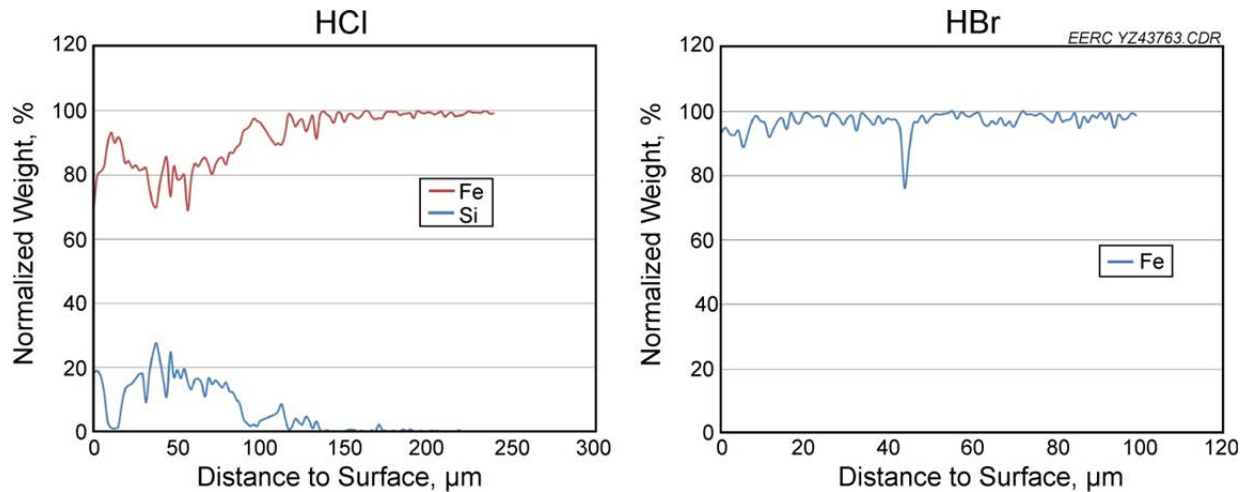


Figure 22. Variation of Fe across the low-carbon steel coupon.

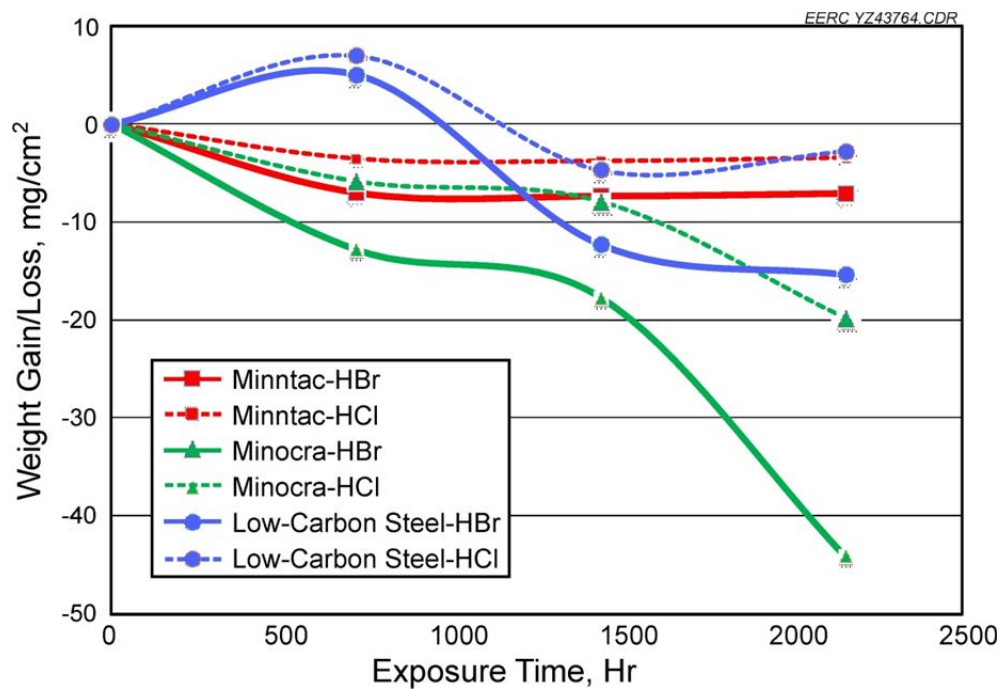


Figure 23. Changes of specimen weight during the thermal cycle exposure.

Both the Minntac and Minorca coupons initially showed weight loss. However, after 30 days, the weight of the Minntac coupon became stable while the Minorca coupon continuously lost weight until the end of the 3-month test, indicating the Minntac coupon was better protected from a HCl/HBr attack than the Minorca coupon. The Minntac coupon lost less weight than the Minorca coupon under the HBr and HCl exposure experiment, respectively, mainly because the Minntac coupon has a higher content of chromium than the Minorca coupon,

which remained solid under the high-temperature cycle and prevented further weight loss. Another reason for the better corrosion resistance is the formation of chromium oxide scales with a significantly denser morphology. Accordingly, less diffusion paths exist for the transport of chlorine or bromine from the gas phase to the metal and for the transport of gaseous metal chlorides and bromide from the metal–scale interface outward, allowing less active oxidation. HBr clearly showed more impact on the weight change of coupons than HCl, suggesting that HBr resulted in more material loss than HCl when both were kept at the same levels. The reason is ascribed to a more volatile bromide compound that evaporated during the present high-temperature thermal cycles.

The low-carbon steel coupon, under a low-temperature cycle, showed weight gain, initially followed with subsequent loss, and maintained its weight at the end of the test.

CONCLUSIONS

- Comparison between bromine- and chlorine-induced metal corrosion was made under simulated taconite operating conditions.
- Active oxidation was the main corrosion mechanism under elevated temperatures of 500°–950°C, while HBr showed a higher corrosion rate than HCl under current simulated conditions.
- Blisters and/or pinholes observed on the surface of the grate bar indicate that volatile compounds were formed, mainly iron chloride or iron bromide compounds.
- Under the same level of halogen exposure with the same thermal cycles, both the Minntac and Minorca grate bar showed more microfracture in the bromine condition than in the chlorine test.
- Depletion of iron is the main reason for weight loss.
- Temperature is very critical to corrosion, and the maximum temperature seems to be the most important factor.
- No significant corrosion was observed for the low-carbon steel since it only experienced low temperatures of 50°–200°C.

Note that the completed corrosion exposure tests were carried out in a bench-scale experimental system that cannot precisely simulate actual operating conditions in the taconite process. Therefore, the project results can be regarded as the first-step effort to address the potential bromine-induced corrosion as bromine is applied to the taconite facility for mercury reduction. Large-scale field testing is recommended in the future to account for the difference between bench-scale and full-scale systems.

REFERENCES

1. Zhuang, Y.; Laumb, J.D.; Holmes, M.J.; Liggett, R.R.; Pavlish, J.H. Impacts of Acid Gases on Mercury Oxidation Across SCR Catalyst. *Fuel Process. Technol.* **2007**, *88*, 929–934.
2. Zhuang, Y.; Thompson, J.S.; Zygarlicke, C.J.; Pavlish, J.H. Impact of Calcium Chloride Addition on Mercury Transformations and Control in Coal Flue Gas. *Fuel* **2007**, *86*, 2351–2359.
3. Pavlish, J.H.; Sondreal, E.A.; Mann, M.D.; Olson, E.S.; Galbreath, K.C.; Laudal, D.L.; Benson, S.A. A Status Review of Mercury Control Options for Coal-Fired Power Plants. Special Mercury Issue of *Fuel Process. Technol.* **2003**, *82* (2–3), 89–165.
4. Liu, S.; Yan, N.; Liu, Z. Using Bromine Gas to Enhance Mercury Removal from Flue Gas of Coal-Fired Power Plants. *Environ. Sci. Technol.* **2007**, *41* (4), 1405–1412.
5. Berndt, M.E.; Engesser, J. *Mercury Transport in Taconite Processing Facilities: (III) Control Method Test Results*; Final Report to Iron Ore Cooperative Research; Minnesota Department of Natural Resources: Hibbing, MN, 2007.
6. Berndt, M.E. *On the Measurement of Stack Emissions at Taconite Processing Plants*; Progress Report to Minnesota Control Agency; Minnesota Department of Natural Resources: Hibbing, MN, 2008.
7. Pavlish, J.H.; Zhuang, Y. *Proof-of-Concept Testing of Novel Mercury Control Technology for a Minnesota Taconite Plant*. Technical Report to Minnesota Department of Natural Resources; Energy & Environmental Research Center: Grand Forks, ND, 2008.
8. Zahs, A.; Spiegel, M.; Grabke, H.J. Chloridation and Oxidation of Iron, Chromium, Nickel and their Alloys in Chloridizing and Oxidizing Atmospheres at 400±700°C. *Corrosion Science* **2000**, *42*, 1093–1122.
9. Zhuang, Y.; Chen, C.; Timpe, R.C.; Pavlish, J.H. Investigations on Bromine Corrosion Associated with Mercury Control Technologies in Coal Flue Gas. *Fuel* **2009**, *88*, 1692–1697.
10. Lee, S.; Maemura, K.; Yamamura, T.; Nakazawa, S.; Lee, K.H.; Chang, D.; Ahn, J.-H.; Chung, H. Corrosion Behavior of Metals in Flowing Ar-42.6%O₂-14.7%Br₂ Gas Mixture at 700°C. *Corrosion Science Section* **2006**, *62* (1), 13–28.
11. Zhuang, Y.; Dunham, D.J.; Pavlish, J.H. *Assessment of Potential Corrosion Induced by Bromine Species Used for Mercury Reduction in a Taconite Facility*. Report to Minnesota Department of Natural Resources; Energy & Environmental Research Center: Grand Forks, ND, 2009.
12. Stott, F.H.; Shih, C.Y. High-Temperature Corrosion of Iron-Chromium Alloys in Oxidizing-Chloridizing Conditions. *Oxidation of Metals* **2000**, *54* (5/6), 425–443.

13. Grabke, H.J.; Bryers, R.W. *Incinerating Municipal and Industrial Waste*. New York: Hemisphere, 1989.
14. Tu, J.P.; Li, Z.Z.; Mao, Z.Y. Reaction Mechanism of Preoxidized Nickel-Chromium-Cerium Alloy with Chlorine Gas in the Temperature Range 400°C to 700°C. *Corrosion Science Section* **1997**, 53 (4), 312–318.

Appendix B-3

Phase II – Extended Testing of Activated Carbon Injection

Contents

B-3-1: Minnesota Taconite Phase II Research – Evaluation of Carbon Injection to Increase Mercury Capture. ArcelorMittal Minorca Mine Inc. (May 16, 2014)	B-3-1
B-3-2: Minnesota Department of Natural Resources Review of Phase II Hg Control Reports (October 31, 2014)	B-3-87

Appendix B-3-1

Minnesota Taconite Phase II Research – Evaluation of Carbon
Injection to Increase Mercury Capture.
ArcelorMittal Minorca Mine Inc.

May 16, 2014



MINNESOTA TACONITE PHASE II RESEARCH - EVALUATION OF CARBON INJECTION TO INCREASE MERCURY CAPTURE

ARCELORMITTAL MINORCA MINE INC.

Final Report

Prepared For: Iron Mining Association of Minnesota
324 West Superior Street, Suite 502
Duluth, MN 55802

Prepared By: Kyle Bowell, Andrew Bertelson, Gerald Amrhein, Maxine Biggs

ADA-ES, Inc.
9135 South Ridgeline Boulevard, Suite 200
Highlands Ranch, CO 80129

ADA Document Number: ADA-ES: 2013-0237

ADA Project Number: 8155-13

Date: May 16, 2014



DISCLAIMER

ADA-ES, INC. ASSUMES NO LIABILITY WITH RESPECT TO THE USE OF, OR FOR DAMAGES RESULTING FROM THE USE OF, ANY INFORMATION, METHOD OR PROCESS DISCLOSED OR CONTAINED IN THIS REPORT ISSUED UNDER THE APPLICABLE CONTRACT. ADA-ES, INC. EXPRESSLY DISCLAIMS AND EXCLUDES ANY AND ALL WARRANTIES, EITHER EXPRESS OF IMPLIED, WHICH MIGHT ARISE UNDER LAW OR EQUITY OR CUSTOM OF TRADE, INCLUDING AND WITHOUT LIMITATION, WARRANTIES OF MERCHANTABILITY AND OF FITNESS FOR SPECIFIED OR INTENDED PURPOSE.



EXECUTIVE SUMMARY

ADA-ES, Inc. (ADA) was awarded a contract to test Activated Carbon Injection (ACI) at five taconite ore processing plants in northern Minnesota as part of the Minnesota Taconite Mercury Reduction Research Phase II Program. The purpose of Phase II is to determine the level of mercury reduction possible using ACI. This report presents the results of the Phase II ACI test at the ArcelorMittal Minorca plant (Minorca).

Three commercially available powdered activated carbons (PACs) were tested in a PAC Screening Test from 6/24/13 to 6/27/13 to determine the best PAC to use for the Phase II test. Albemarle's BPAC was selected because it performed better than the other PACs and achieved 91% HgG reduction in stack D and 67% HgG reduction in stack B at an ACI rate of 3 lb/mmcf.

Phase II Testing was conducted from 7/10/13 to 8/8/13 using BPAC at 3 lb/mmcf and injecting only into the Windbox Exhaust. The ACI rate was constant except during minor plant outages and for ACI equipment maintenance. ADA installed one Hg-CEMS in stack D for the entirety of testing and another was moved between stacks A, B, and C. Barr Engineering performed weekly particulate testing on the stack during Phase II testing.

The results of Phase II testing showed that the gas phase mercury (HgG) reduction, as measured by the mercury continuous emission monitor system (Hg-CEMS), and considering all four stacks, was 76% at 3 lb/mmcf. However, the total mercury (HgT) reduction calculated using the MM30B sorbent trap data was 54%. Therefore, the test indicates that the target of 75% Hg reduction is not obtainable at Minorca with the current system configuration.

Throughout this report it is important to distinguish between gas phase mercury (HgG), as measured by the mercury continuous emission monitor system (Hg-CEMS), and total mercury (HgT) which is the sum of the particulate bound or particulate phase mercury (HgP) and HgG. Hg-CEMS cannot measure HgP, but ADA also used a modified EPA Method 30B (MM30B) procedure during Phase II that can be used to estimate HgP. It is important note that ADA often uses the MM30B as a research tool to independently verify the operations of the Hg-CEMS and to measure mercury in gas streams where no Hg-CEMS data is available. Mercury reductions will be reported as HgG when measured with the Hg-CEMS, and as HgT when measured by the MM30B when available.

Barr will provide a separate report of the particulate tests conducted at Minorca.

ACRONYMS

PM	Particulate Matter
Hg	Mercury
HgT	Total Mercury
Hg0	Elemental Mercury
Hg2	Oxidized Mercury
HgG	Gas Phase Mercury
HgP	Particulate Bound Mercury
Hg-CEMS	Mercury Continuous Emissions Monitor System
SO ₂	Sulfur Dioxide
NO _x	Nitrogen Oxide(s)
ACI -	Activated Carbon Injection
PAC -	Powdered Activated Carbon
HPAC	Albemarle's High Temp Brominated PAC
BPAC	Albemarle's Brominated PAC
FPP	Fast PAC Premium - ADA-CS's Ground Brominated PAC
PPPP	Power PAC Premium Plus - ADA-CS's Double Brominated PAC
ADA-CS	ADA-Carbon Solutions
ADA	ADA-ES, Inc.
Barr	Barr Engineering Co.
AMUSA	ArcelorMittal
USS	United States Steel Corp.
Cliffs	Cliffs Natural Resources
Hibtac	Hibbing Taconite Facility
Utac	United Taconite Facility
Minntac	Minnesota Taconite Facility
Keetac	Keewatin Taconite Facility
Minorca	Minorca Taconite Facility
PST	PAC Screening Test
OL	Ohio Lumex Mercury Analyzer
MM30B	Modified EPA Method 30B
acfm	Actual cubic feet per minute of gas
scfm	Standard cubic feet per minute of gas
µg/wscm	Micrograms of Hg per wet standard cubic meter of gas
ng/g	Nanograms of Hg per gram of sample
lb/mmacf	Pounds of PAC per million actual cubic feet of gas
ME	Mist Eliminator

Table of Contents

EXECUTIVE SUMMARY	iii
ACRONYMS	iv
1.0 INTRODUCTION	1
1.1 Project Purpose and Scope	1
1.2 Facility Description	4
1.3 Test Plan	5
1.3.1 ACI Injection Port Locations	7
1.3.2 Mercury Measurement Port Locations	7
1.3.3 Test Chronology	8
2.0 METHODS	9
2.1 ACI System	9
2.2 Mercury Measurement Techniques	12
2.2.1 EPA Method 29	12
2.2.2 Ontario Hydro	13
2.2.3 Hg-CEMS	14
2.2.4 EPA Method 30B - And ADA's Modifications	17
2.3 Solids Sampling and Analysis	20
2.4 Ohio Lumex	20
3.0 PAC SCREENING TEST (PST)	21
3.1 Description	21
3.2 Results	22
4.0 PHASE II TESTING	26
4.1 Description	26
4.2 Results	26
4.2.1 Phase II Testing	26
4.2.2 Stack MM30B Data	32
4.2.3 Inlet MM30B Data	37
4.2.4 Sample Carbon Analysis	38
4.2.5 Solids Analyses for Hg	41
4.3 QA/QC	49
4.3.1 Sample Calculations	49
4.3.2 MM30B and Hg-CEMS Comparison	50
5.0 CONCLUSIONS	51
6.0 APPENDIX A - Hg-CEMS Data (Electronic)	52
7.0 APPENDIX B - Hg-CEMS Calibration Data	53
8.0 APPENDIX C - Ohio Lumex Data	61
9.0 APPENDIX D - MM30B Data	76

List of Figures

Figure 1. Minorca Gas Stream and Sampling Locations	4
Figure 2. Process Diagram with Sampling Locations.....	6
Figure 3. PAC Injection Location	7
Figure 4. PST and Phase II Testing ACI Lance Arrangements at Minorca	7
Figure 5. DemoPAC Injection Equipment.....	9
Figure 6. ADA Portable Injection Silo (Mini Silo)	10
Figure 7. PAC Blower	11
Figure 8. Method 29 Sample Train	13
Figure 9. Ontario Hydro Method	14
Figure 10. Hg-CEMS Diagram	16
Figure 11. Method 30B Sample Train.....	18
Figure 12. Environmental Supply Company HG-324K System	19
Figure 13. MM30B Two Section Sorbent Trap	19
Figure 14. HPAC Screening Test Results	22
Figure 15. BPAC Screening Test Results	23
Figure 16. 2013N Screening Test Results	23
Figure 17. Comparison of the PAC Screening Test Results for HgG	25
Figure 18. Minorca Gas Stream and Sampling Locations	25
Figure 19. Phase II Testing Baseline Stack Data.....	27
Figure 20. Phase II Testing - Stack D and A Emissions.....	28
Figure 21. Phase II Testing - Stack D and B Emissions.....	29
Figure 22. Phase II Testing - Stack D and C Emissions.....	30
Figure 23. Phase II Testing - Stack Emissions	31
Figure 24. Stack A MM30B Data vs. Hg-CEMS	33
Figure 25. Stack B MM30B Data vs. Hg-CEMS	34
Figure 26. Stack C MM30B Data vs. Hg-CEMS	35
Figure 27. Stack D MM30B Data vs. Hg-CEMS	36
Figure 28. Inlet MM30B Data with Greenball Hg Data	37
Figure 29. Process Diagram with Sampling Locations	38
Figure 30. Phase II Testing Multiclone Carbon Analysis	39
Figure 31. Phase II Testing Thickener Overflow Carbon Analysis.....	39
Figure 32. Phase II Testing Fine Tails Carbon Analysis	40
Figure 33. Phase II Testing Green Ball Carbon Analysis.....	40
Figure 34. Phase II Testing Fired Pellets Carbon Analysis	41
Figure 35. ADA Green Ball Hg Analyses	42
Figure 36. Independent Phase II Testing Green Ball Hg Analysis	43
Figure 37. ADA Thickener Overflow Hg Analysis	44
Figure 38. Independent Phase II Testing Thickener Overflow Hg Analysis	45
Figure 39. ADA Multiclone Hg Analyses	46
Figure 40. Independent Phase II Testing Multiclone Hg Analysis	46



Figure 41. ADA Fine Tailings Hg Analyses 47
 Figure 42. Independent Phase II Testing Fine Tailings Hg Analysis..... 47
 Figure 43. ADA Fired Pellets Hg Analysis 48

List of Tables

Table 1. Minorca Test Chronology 8
 Table 2. Technical Specifications for the Mini Silo 10
 Table 3. Technical Specifications for the PAC Blower 11
 Table 4. Summary of the PAC Screening Test at Minorca 24
 Table 5. Phase II Testing Mercury Reduction Summary via Hg-CEMS and MM30B..... 32
 Table 6. M30B Relative Deviation 49
 Table 7. Hg-CEMS Relative Accuracy..... 49
 Table 8. MM30B Data and RD, RA, AMD Calculations 77



1.0 INTRODUCTION

1.1 Project Purpose and Scope

ADA-ES, Inc. (ADA) was awarded a contract to test Activated Carbon Injection (ACI) at five taconite ore processing plants in northern Minnesota as part of the Minnesota Taconite Mercury Reduction Research Phase II Program which broadened the scope of testing to medium-term operations (roughly a one month timespan) at multiple facilities. The purpose of Phase II is to determine the level of mercury reduction.

The five sites selected for this program are:

- Cliffs Natural Resources (Cliffs)
 - Line 3 at Hibbing Taconite (Hibtac)
 - Line 2 at United Taconite LLC (Utac)
- United States Steel Corp (USS)
 - Agglomerator Line 7 at Minntac
 - Keetac
- ArcelorMittal (AMUSA)
 - Minorca Mine (Minorca)

At each site, the ACI test was divided into three phases: Set-up, the PAC Screening Tests (PST), and Phase II testing. During Set-up, ADA installed the ACI equipment and mercury monitoring systems needed to accomplish the goals of the project.

The purpose of the PST was to develop a performance curve for each commercially available, brominated, powdered activated carbon (PAC) tested and determine which PAC would perform the best at each site. The PST involved testing each PAC for one day at three to four injection rates. The data from the PST was then used to select a PAC and ACI rate for Phase II testing. During the PST, the host site subcontracted Barr Engineering Co. (Barr) to conduct particulate matter (PM) loading tests at each injection rate.

The Mercury Phase II project team (ADA, host site reps and Barr) selected three PACs to be used for the PST at Minorca. One of the standard PACs tested at the first two sites was replaced with a coarse ground PAC for this test to determine if particulate collection efficiency across the scrubber could be improved by using a coarser material.

- Albemarle
 - HPAC - A brominated PAC developed for higher temperature applications
 - BPAC - A standard brominated PAC
- ADA-Carbon Solutions (ADA-CS) - ADA-CS is not affiliated with ADA-ES.
 - ACS DEV 2013N (2013N) - A coarse ground enhanced brominated PAC.

At the completion of the PST, the project team reviewed the data and selected a PAC and ACI rate to be used during Phase II testing.

The purpose of Phase II testing was to investigate the longer term effects of recycle and process changes with ACI. Most of the five test sites recycle material collected downstream of the furnace back into the process. Therefore, it was anticipated that PAC, and the mercury (Hg) absorbed on the PAC, could also end up back in the Green Balls and affect product quality or provide a recycle loop for the mercury that could reduce Hg reduction efficiency. Phase II testing at Minorca was allotted a maximum of 30-days.

During Phase II testing, the host site collected periodic samples at various locations throughout the plant. These samples were dewatered by the host site and the solids were provided to ADA for Hg analysis. Results provided initial insight into whether mercury was infiltrating the process streams as a result of recycling. Barr was also contracted by the host site to periodically conduct PM testing on the stacks.

Throughout the PST and Phase II testing, ADA employed the ThermoFisher mercury continuous emission monitor system (Hg-CEMS) to measure mercury emission at the stack. ADA also used a modified EPA Method 30B (MM30B) to periodically measure the Hg concentration of the inlet gas (before ACI), and to validate the performance of the Hg-CEMS at the stack. Throughout this report it is important to distinguish between gas phase mercury (HgG) and total mercury (HgT) which is the sum of the particulate bound or particulate phase mercury (HgP) and HgG. Hg-CEMS cannot measure HgP, but the MM30B can be used to estimate HgP. For this project, ADA used the MM30B as a research tool to independently verify the operations of the Hg-CEMS and to measure mercury in gas streams where no Hg-CEMS data was available. The modification to the M30B procedure included taking only single pairs of measurements instead of multiple pairs, and the use of two section sorbent traps instead of three-section spiked traps (see Section 2.2.4). Mercury reductions will be reported as HgG when measured with the Hg-CEMS, and as HgT when measured by the MM30B when available.



To calculate Hg reduction using Hg-CEMS data, a baseline (no ACI) HgG stack emission was determined by averaging data over a period time (30 minutes to several hours) before ACI was initiated and when the process was deemed to be operating normally. The same process was then used to determine HgG emission with ACI. The two HgG averages were then used to calculate HgG reduction. Minorca splits the waste gas between four stacks, so this process was repeated on each stack to calculate an overall Hg reduction.

To calculate HgT reduction using the sorbent trap data, all available stack data taken before ACI began and when the process was deemed to be operating normally was averaged to give a baseline value for HgT. The same was done for any data taken with ACI. The two HgT averages were then used to calculate HgT reduction.

This report only pertains to the testing conducted at the ArcelorMittal Minorca plant.



1.2 Facility Description

The indurating furnace at the Arcelor Mittal Minorca Mine is a straight grate furnace that can burn either natural gas or fuel oil. Unfired pellets from the balling disks are screened for size before entering the furnace. The pellets travel through the updraft, downdraft and preheat sections before reaching their peak temperature (2450°F) in the firing zone. The pellets then pass through the first and second cooling zones before being discharged to the stockpile.

Figure 1 depicts the gas streams and sampling locations for Minorca. Two separate exhaust gas streams exit the furnace: the Hood Exhaust and the Windbox Exhaust. The two exhaust streams are driven by separate fans, after which they combine at a common header and then split into four streams that pass through recirculating venturi scrubbers and exit through four stacks. Particulate control devices downstream of the furnace consist of a multiclone dust collector on the Windbox Exhaust and the four recirculating venturi scrubbers. At Minorca, solids from the scrubbers are recirculated back directly to the concentrate thickener.

However, solids from the multiclone dust collectors were discharged from the process to a settling pond during testing. The gas flow rate for the Hood and Windbox Exhausts are about 535,000 acfm each, for a total of 1,070,000 acfm.

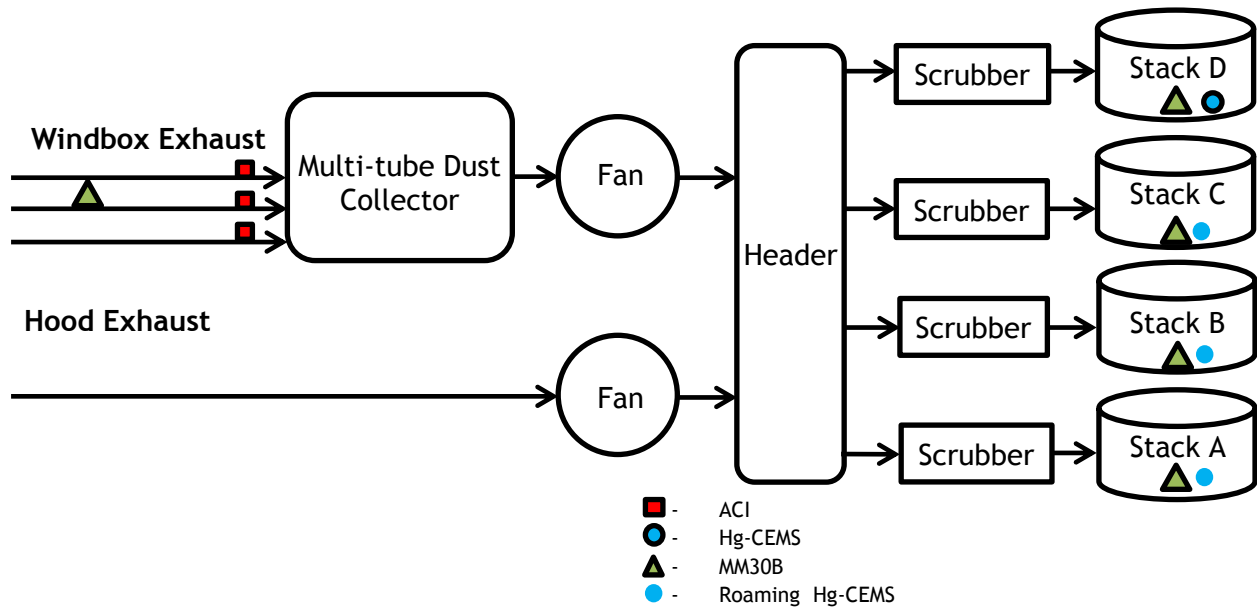


Figure 1. Minorca Gas Stream and Sampling Locations

1.3 Test Plan

The ACI test was divided into three phases: Set-up, the PAC Screening Tests (PST), and Phase II testing. The purpose of the PST was to develop a performance curve for each commercially available, brominated, powdered activated carbon (PAC) tested and determine which PAC would perform the best at each site. The PST involved testing each PAC for one day at three or four injection rates. Data from the PST was used to select a PAC and ACI rate for Phase II testing.

At Minorca, the original plan called for testing each of the proposed PACs at 3, 5, and 7 lb/mmacf (pounds of PAC per million actual cubic feet of gas) during the PST. However, results at Hibtac, with a similar exhaust gas configuration as Minorca, indicated that testing at 1, 3 and 5 lb/mmacf would be sufficient to achieve a goal of 75% HgG reduction during the PST. Each ACI rate was run for several hours during which Barr performed PM testing on Stack D only. Hg reduction was based on baseline Hg-CEMS concentration measured at the beginning of each day and the Hg concentration averaged over at least 30-minutes of steady operation of the Hg-CEMS during each run.

During previous testing at Hibtac, the Hood Exhaust was found to contain low mercury emissions, lacked the surface area associated with the multiclone, and had reduced residence time compared to the Windbox Exhaust. Therefore, for Phase II testing at Minorca, the project team decided to forgo PAC injection into the Hood Exhaust, and instead focus completely on mercury capture in the Windbox Exhaust to maximize the effectiveness of the PAC.

Based on the results of the PST, the project team decided to use BPAC at 3 lb/mmacf for the Phase II testing. The Phase II test continued for the full 30 days due to the extensive solids sample testing the plant was conducting. The following samples were collected and analyzed by ADA.

- Green Balls - Every day
- Multi-tube Collector drop out - Twice during Phase II testing
- Concentrate Thickener Overflow - Twice during Phase II testing
- Pellets - Twice during Phase II testing
- Fine Tailings - Twice during Phase II testing

Minorca collected a larger number of samples and analyzed them for both carbon and mercury. The data was shared with ADA and included in this report. The process samples included:

- Green Balls - Twice Daily on Week Days during Phase II testing
- Pellets- Twice Daily on Week Days during Phase II testing
- Multiclone drop out - Twice Daily on Week Days during Phase II testing
- Thickener Overflow - Twice Daily on Week Days during Phase II testing
- Fine Tailings - Twice Daily on Week Days during Phase II testing

Figure 2 and Figure 3 indicate with a red “X” where the above samples were collected.

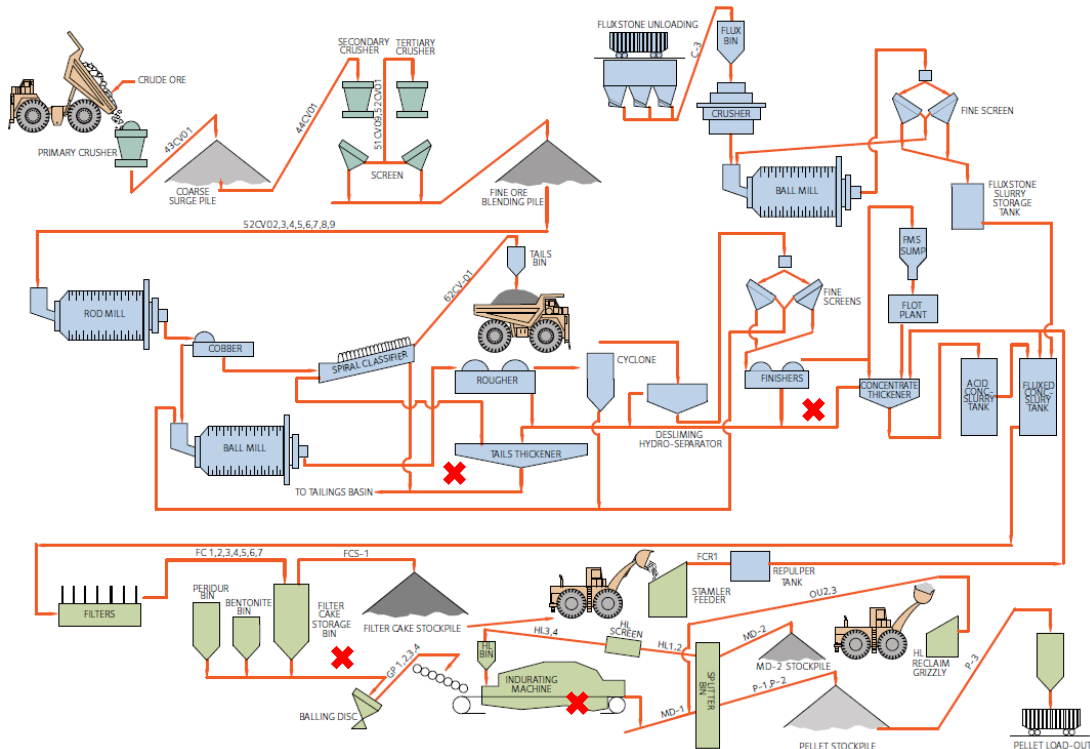


Figure 2. Process Diagram with Sampling Locations

Since Minorca has four stacks, two Hg-CEMS were used to record the mercury emission trends. Based on initial testing, stacks C and D had the highest Hg emissions and the team decided to dedicate one Hg-CEMS to stack D, and the other was periodically moved between the other three stacks A, B, and C. The Hg-CEMS only recorded data on stacks B and D during the PST, but one was moved between stacks A, B, and C during Phase II testing. Barr collected weekly PM data during Phase II testing.

1.3.1 ACI Injection Port Locations

As shown in Figure 1 and Figure 3 (blue “X”), ACI ports were installed upstream of the Multi-tube Collector on the Windbox Exhaust. Figure 4 shows the lance arrangement used at Minorca during PST and Phase II testing. The red “X” indicates where the multiclone samples were taken.

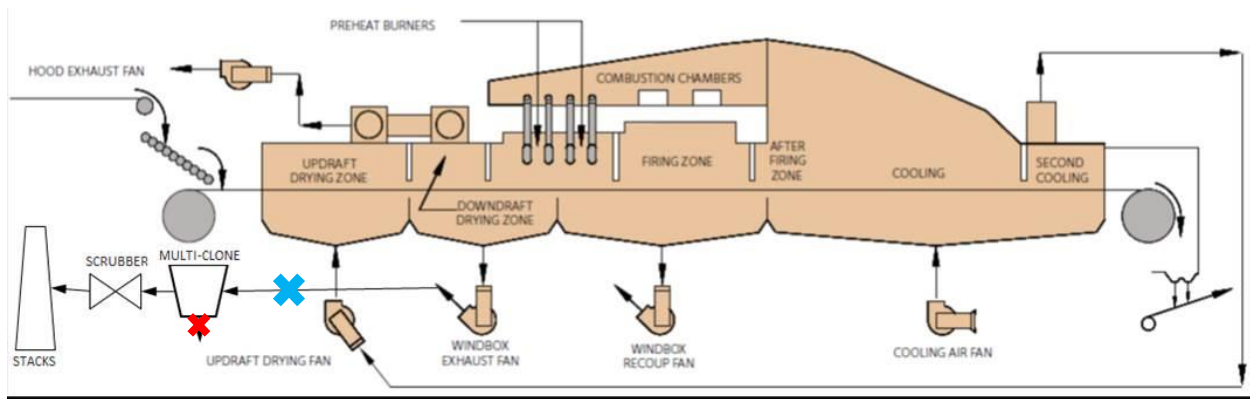


Figure 3. PAC Injection Location

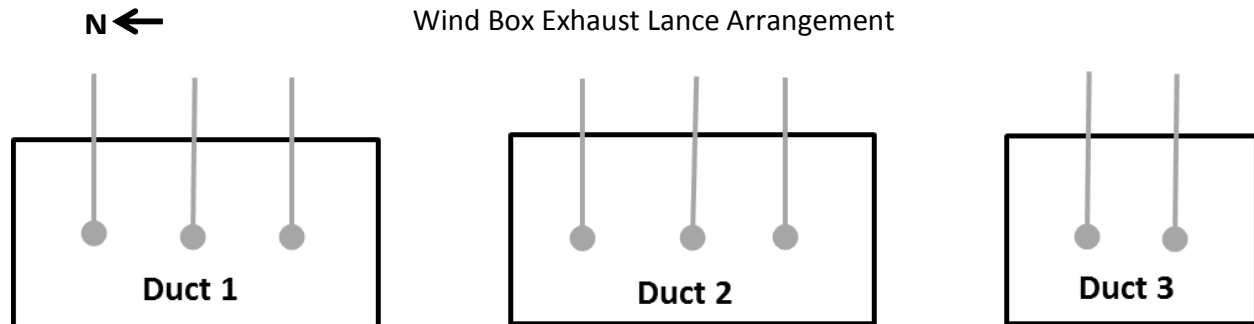


Figure 4. PST and Phase II Testing ACI Lance Arrangements at Minorca

1.3.2 Mercury Measurement Port Locations

Sample ports for the Hg-CEMS and MM30B were available on all four stacks. Ports for inlet MM30B sampling were installed prior to the ACI ports on the Windbox Exhaust duct.



1.3.3 Test Chronology

The major events that occurred during the test at Minorca are shown below in Table 1.

Table 1. Minorca Test Chronology

Day	Date	Description
Monday	06/17/13	ADA begins installation of equipment and Hg-CEMS
Monday	06/24/13	HPAC tested at 1, 3, 6 lb/mmcf. Barr performed PM test at stack at each rate
Wednesday	06/26/13	BPAC tested at 1, 3, 5 lb/mmcf. Barr performed PM test at stack at each rate
Thursday	06/27/13	2013N tested at 1, 5, 7 lb/mmcf. Barr performed PM test at stack at each rate
Wednesday	07/03/13	Project team decides to use BPAC at 3 lb/mmcf (192 lb/hr)
Wednesday	07/10/13	Started Phase II Testing with BPAC at 3 lb/mmcf (192 lb/hr)
Thursday	08/08/13	Phase II Testing completed
Tuesday	08/13/13	Demobilization completed



2.0 METHODS

2.1 ACI System

Since Phase II testing had not ended at Hibtac when the PST was scheduled to commence at Minorca, ADA’s smaller DemoPAC injection system was used for the PST. After Hibtac concluded, the Mini-Silo was installed and used at Minorca for Phase II testing. DemoPAC, shown in Figure 5, is a small system that is easy to transport and setup, but has a lower sorbent capacity, only holding one supersack (1000 lb) at a time. The DemoPAC is approximately 16-ft high (two 8-ft sections), with a 6-ft x 6-ft footprint and has an empty weight of approximately 2,000 lbs.



Figure 5. DemoPAC Injection Equipment

The Mini-Silo, shown in Figure 6, is approximately 25-ft high, has an 8-ft x 8-ft footprint, an empty weight of 14,000 lb and a capacity of 17,000 lb of PAC. It can be loaded either with supersacks or from a bulk truck as was done at Minorca. Table 2 gives the specifications for the Mini Silo. The sorbent injection system also includes PAC conveying lines and injection lances. The silo was installed outdoors next to the Windbox and Hood Exhaust fans.

Temporary sorbent transport hoses were installed between the silo and the injection lances.



Figure 6. ADA Portable Injection Silo (Mini Silo)

Table 2. Technical Specifications for the Mini Silo

Utility	Specification
Electrical	480VAC / 3PH / 100A
Air	Clean, Dry Air at 90-100 psi and 15 scfm
I&C	4-20 mA signal (production rate)
Dimensions	~ 8-ft x 8-ft x 25-ft (L x W x H)
Weight	~14,000 lb empty
Installation	Anchor skid, lift top portion and bolt to lower portion
Location	Set up at grade below injection point

ADA purchased all sorbents and arranged for shipment and delivery. Sorbent can be provided in 1000 lb supersacks as was done during the PST or 50,000 lb pneumatic tank trucks as was done during Phase II testing. A supersack is loaded into the silo via a hoist that raises it to the top of the silo where it is dumped through an opening into the silo. The Mini-Silo and the DemoPAC have a Programmable Logic Controller and computer program system that controls

the system operation and adjusts the variable speed screw feeder to meter sorbent injection rates.

Motive air is supplied by a positive displacement blower, shown in Figure 7. The technical specifications for the blower are summarized in Table 3. Flexible hose carries the sorbent from the feeder to a distribution manifold located near the injection grid. At Minorca, the primary conveying hose was split into two secondary lines that were further divided into four legs each to create the eight-lance arrangements discussed above in Figure 4.



Figure 7. PAC Blower

Table 3. Technical Specifications for the PAC Blower

Utility	Specification
Electrical	480VAC / 3PH / 60A, 120VAC
Dimensions	6-ft x 4-ft x 6-ft (L x W x H)
Weight	2,750 lb
Installation	Place on level surface
Location	≤ 20 feet from Silo

2.2 Mercury Measurement Techniques

This section discusses several of the most common methods used to measure mercury emissions from waste gas streams. A short explanation of each method will be presented along with the pros and cons. More specifically, the following methods will be considered:

- EPA Method 29 (M29)
- EPA Method 30B (M30B) - And ADA's modifications
- Ontario Hydro (O-H) Method or ASTM Method D6784-02
- Mercury Analyzers or Mercury Continuous Emission Monitoring Systems (Hg-CEMS)

For this project ADA used Hg-CEMS and MM30B. The Hg-CEMS were used to continuously monitor speciated mercury emissions from the stack. MM30B was used for two purposes. First, it was used to track the Hg concentration in the waste gas at the furnace exit prior to the ACI grid to determine if inlet mercury concentration changed due to the effect of recycle or from process changes. Also, MM30Bs were used to check the performance of the Hg-CEMS at the stack. It is important to note that in the original test plan, the data collected from MM30Bs were not intended to be used to calculate the Hg reduction performance of the process. However, as the project progressed, additional MM30B tests were added to the project scope in the hope of being able to do so.

2.2.1 EPA Method 29

EPA Method 29 (M29) is an isokinetic, wet chemistry, batch sampling method developed to measure metal emissions in waste gas streams. Up to 17 different metallic species can be measured with M29, including mercury. Figure 8 shows the sample train used in this method. The gas sample is drawn isokinetically into a heated sample probe, through a heated glass fiber filter, and then through a series of glass impingers submerged in an ice bath. The sample nozzle, probe, and filter collect the particulate matter in the gas sample. The first set of impingers contains an acidified aqueous solution of hydrogen peroxide. A blank impinger is placed between the impinger sets to prevent carryover. The second impinger set contains an acidified aqueous solution of potassium permanganate that absorbs all of the metal species including mercury. The last impinger contains silica gel to remove the moisture from the gas sample. Finally, the gas passes through a dry gas meter that measures the total dry gas sample volume. The solutions are then recovered and analyzed by various spectroscopy methods for the elements of interest. A two hour minimum sampling time is recommended for Method 29. Increasing the sample time can improve the detection limits. All glassware components must be rinsed during sample recovery and the rinsate analyzed for additional mercury. Pre- and post-test leak-checks must be performed and the method requires multiple runs for quality assurance/quality control.

Method 29 can be used to estimate HgP by separately reporting the mercury collected with the particulate in or on the nozzle, probe, and filter. However, the particulate may absorb some of the HgG, misrepresenting the partitioning of mercury between particulate and gas phases. The absorption of HgG on the filter substrate is dependent upon the nature and constituents of the collected particulate matter. However, the sum of HgG and HgP accurately represents the total mercury emissions.

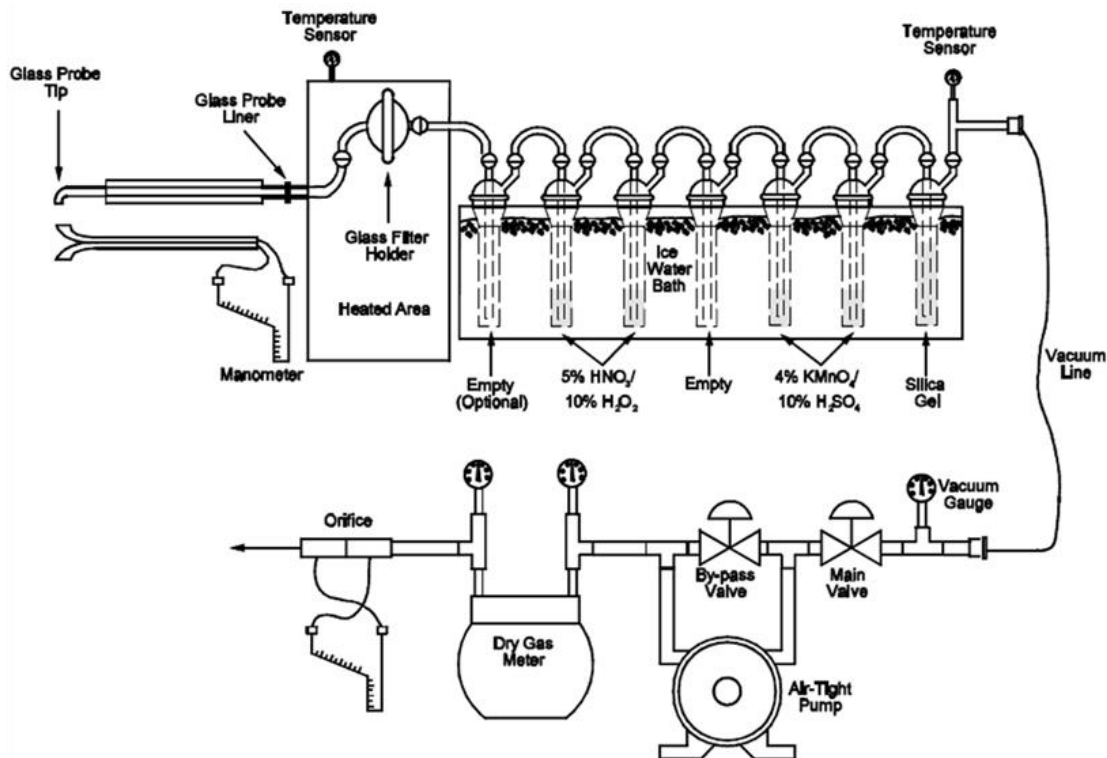


Figure 8. Method 29 Sample Train

2.2.2 Ontario Hydro

The Ontario-Hydro Method (O-H) is similar to Method 29 however; it was developed to separately measure both the oxidized (Hg₂) and elemental (Hg₀) mercury species in the gas sample. Any system that can measure both mercury species is said to be able to “speciate” the mercury. Figure 9 shows the sample train used in this method. The sample console is identical and the sample collection train is very similar to M29. For the O-H method, the first impinger set contains aqueous potassium chloride solution which selectively removes the Hg₂ from the gas sample. Hg₀ is then captured in the following impingers containing either acidified aqueous potassium permanganate or acidified hydrogen peroxide. The final impinger contains silica gel desiccant to remove moisture from the gas sample. All glass elements of the system must be rinsed during sample recovery, and the rinsate is recovered

and analyzed for additional mercury. A leak check is performed before and after the test. The nozzle, probe, filter, and impingers are recovered and sent to a lab to be analyzed by various spectroscopy methods. A high level of quality assurance/quality control is required to properly conduct the O-H method.

This batch method has a higher detection limit than other wet chemistry methods, but can measure the HgP and speciated gaseous mercury levels in a sample. A two hour minimum sampling time is recommended for the O-H method. Increasing the sample time can improve the detection limits. However, particulate matter on the filter may absorb some of the gas phase mercury and can also change the speciation of the sampled mercury, misrepresenting the partitioning of mercury between particulate and gas phases or the mercury speciation. The absorption of HgG on the filter substrate is dependent up on the nature and constituents of the collected particulate matter.

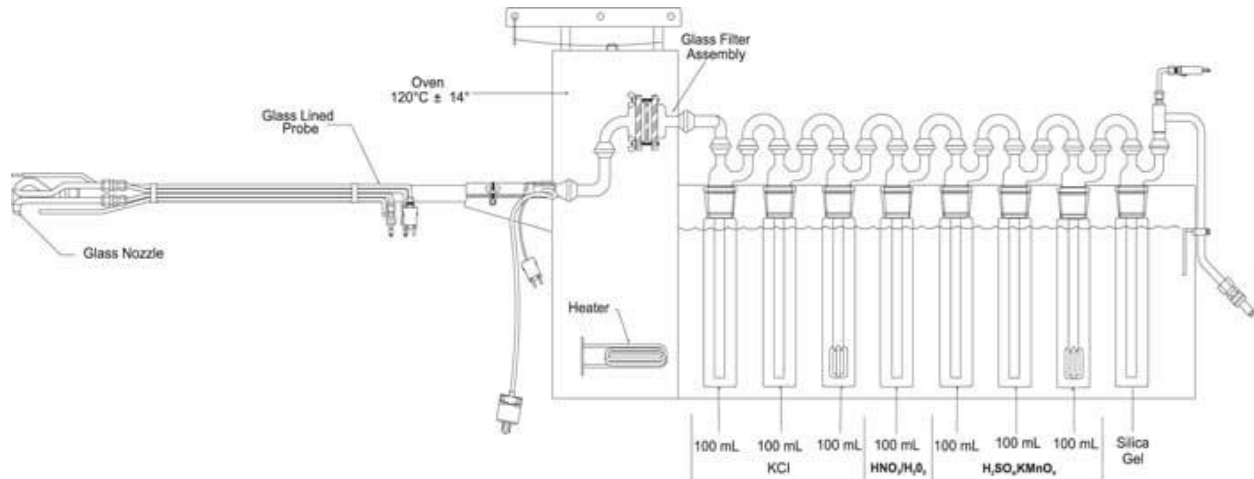


Figure 9. Ontario Hydro Method

2.2.3 Hg-CEMS

Mercury Continuous Emission Monitoring Systems (Hg-CEMS) were developed to provide continuous, real time measurements of speciated gas phase mercury. This is the only measurement method that provides continuous Hg measurement. However, because they rely on real time spectroscopy measurement for mercury detection, they cannot be used to measure HgP. The discussion below mostly pertains to the ThermoFisher (Thermo) system that ADA is most familiar with. Other suppliers, such as Tekran and Ohio Lumex, also provide Hg-CEMS that operate on slightly different principles, but, in general, the main components and operations are similar. For example, Tekran employs a wet chemical system to speciate mercury whereas Thermo developed a dry system.

A diagram of the Thermo system used for both Hg-CEMS is shown in Figure 10. It is comprised of an analyzer, calibrator, controller, and an extraction probe along with additional

peripheral components such as a zero air supply and heated umbilical. The Thermo probe contains an inertial particulate filter, a nitrogen dilution module (40:1 dilution typical), a splitter to divide the diluted sample into two streams; one for measuring gas phase elemental mercury (Hg₀) and one for measuring total gas phase mercury (Hg_G), and a converter to convert all of the Hg in the gas sample to Hg₀. The inertial filter is an important component of the probe. It was designed so that a gas sample can be extracted from a stream containing particulates without passing the sample through a filter cake as is done in the other measurement methods.

The design basis for detecting Hg in the Hg-CEMS is atomic spectroscopy whereby the gas sample is exposed to ultraviolet light at 253.7 nm so that an electron in the outer most orbital of Hg₀ absorbs a photon, becomes excited, then decays back to the ground energy state, emitting (fluorescing) a photon of light at the same wavelength. To detect mercury, analyzers can either measure the amount of light absorbed (Cold Vapor Atomic Absorption Spectroscopy or CVAAS), or the amount of light that fluoresces (Cold Vapor Atomic Fluorescence Spectroscopy or CVAFS), as is done in the Thermo system. Since Hg₂ does not have electrons in the outer orbital, it cannot be measured by this technique. Therefore, in order to speciate Hg, the system divides the sample into two streams one of which is further treated to convert all of the Hg to Hg₀. These two streams are alternately analyzed so that one produces a value for Hg₀ only and the other Hg_T (gas phase only). Hg₂ is then calculated by the difference.

The calibrator produces a gas stream with a selectable Hg₀ concentration. The cal gas is transported to the probe and enters the system before the inertial filter. During cals, the probe is isolated so that only cal gas is flowing through the probe. ADA checks the system calibration at least once a day. All calibration checks and adjustments are provided in Appendix B. MM30B data at the stack is included in Appendix D along with comparisons to the Hg-CEMS data.

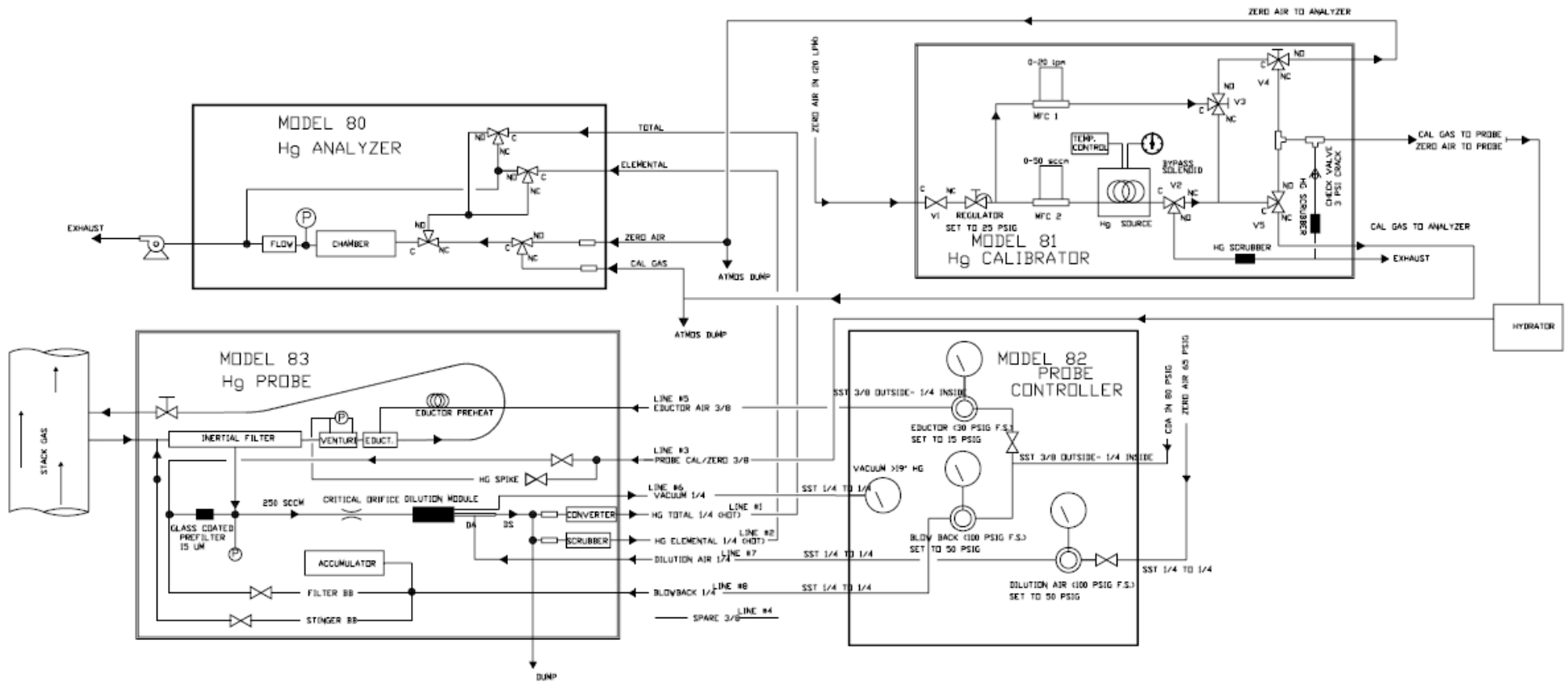


Figure 10. Hg-CEMS Diagram

2.2.4 EPA Method 30B - And ADA's Modifications

EPA Method 30B (M30B) was developed by the Electric Power Research Institute, with assistance from ADA, as a simpler method for measuring Hg than M29 and O-H. M30B specifies that it is to be used in low particulate gas streams and was designed to measure only HgT assuming HgP was negligible. However, for this project, ADA separately analyzed the first glass wool section of the sorbent trap that theoretically contains all of the HgP to provide an estimate for both HgP and HgG.

Figure 11 is a schematic of M30B sample system and Figure 12 is a diagram of the HG-324K System manufactured by the Environmental Supply Company and used by ADA for this project. The system consists of a temperature controlled, two channel probe, sample dryers, and a console that controls the sampling rate, measures the gas sample, and records operating data including temperatures, sampling volume, and barometric pressure. For the procedure, two sample traps (shown in Figure 13) are inserted into the end of the probe and the probe is inserted into the gas stream. A sample is drawn at a constant sample rate through the traps, dried, and measured. The traps are then recovered and the various sections are analyzed. ADA analyzed the traps on-site using the 915+ mercury analyzer by Ohio Lumex. Sample times can vary from as little as 30 minutes to as long as 30-days. ADA ran all traps for 60 minutes.

M30B sorbent traps consist of three sections of specially treated PAC separated by glass wool. The primary purpose of the glass wool is to retain and separate the carbon sections in the glass sample tube. However, the first glass wool section also acts to filter particulate matter from the gas sample. The first PAC section contains enough material to absorb the mercury in a typical gas sample for at least 30 days. The second PAC section is used for QA/QC purposes and is often called the "breakthrough" section. To meet QA/QC requirements, the Hg in this section must be less than 10% of the total Hg. The third PAC section contains a spiked quantity of Hg and is used for QA/QC. Upon analysis, the measured mercury in this section must agree with the spiked amount. The final glass wool section keeps the PAC from being sucked into the probe during sampling. For this project, ADA used a two section trap which did not contain the spiked section. This is the main reason the method is referred to as a modified M30B - MM30B in this report.

In a typical analysis of sorbent traps, the first glass wool and PAC sections are analyzed together to produce a single value for HgT. The second and third glass wool and second PAC sections are also analyzed together and used for QA/QC purposes to demonstrate that no breakthrough occurred during sampling. However, ADA often analyzes the first glass wool section and accompanying particulate matter separately to ascertain an estimate for HgP. However, there are two caveats to the procedure. First, the particulate matter that collects on the first glass wool section may absorb some of the HgG, misrepresenting the partitioning

of mercury between particulate and gas phases. The absorption of HgG on the glass wool substrate is dependent upon the nature and constituents of the collected particulate matter. Secondly, as it is not designed nor intended to measure HgP, M30B is not done isokinetically so does not collect a true representative sample of particulate matter in the gas stream. At best, the M30B provides an estimate of HgP and the partitioning of mercury between particulate and gas phases in the stack gas stream.

At Minorca, HgP was found to be a significant portion of HgT when ACI was operating. This is important for several reasons. First, since the Hg-CEMS cannot measure HgP the data from Hg-CEMS data could not be used to calculate the total Hg reduction during ACI operation. Also, in order to assess if the Hg-CEMS are operating properly by use of the MM30B, only the HgG component of the trap data could be compared to the Hg-CEMS values for QA/QC purposes. However, if the particulates collected in the sorbent trap scrub a significant portion of the Hg from the sample gas, the trap HgG will still not agree well with the Hg-CEMS values. In this case as long as the Hg-CEMS values falls between the trap HgT and HgG the only thing that can be ascertained is that it is likely that the particulates in the trap are scrubbing Hg. If the Hg-CEMS values fall below the trap HgG, it is likely that the Hg-CEMS is not operating properly.

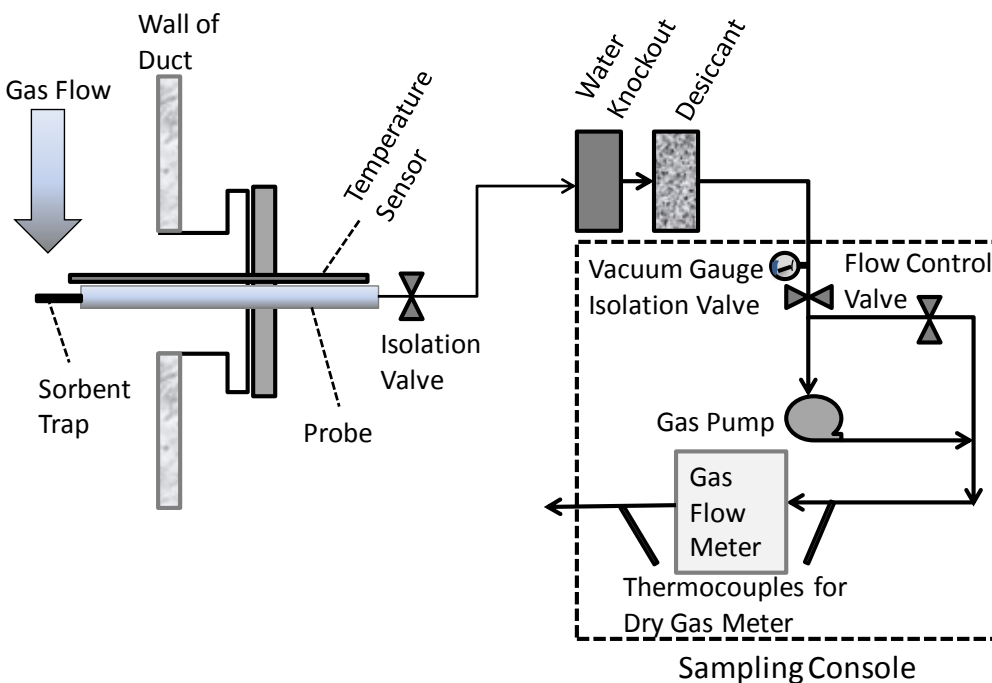


Figure 11. Method 30B Sample Train

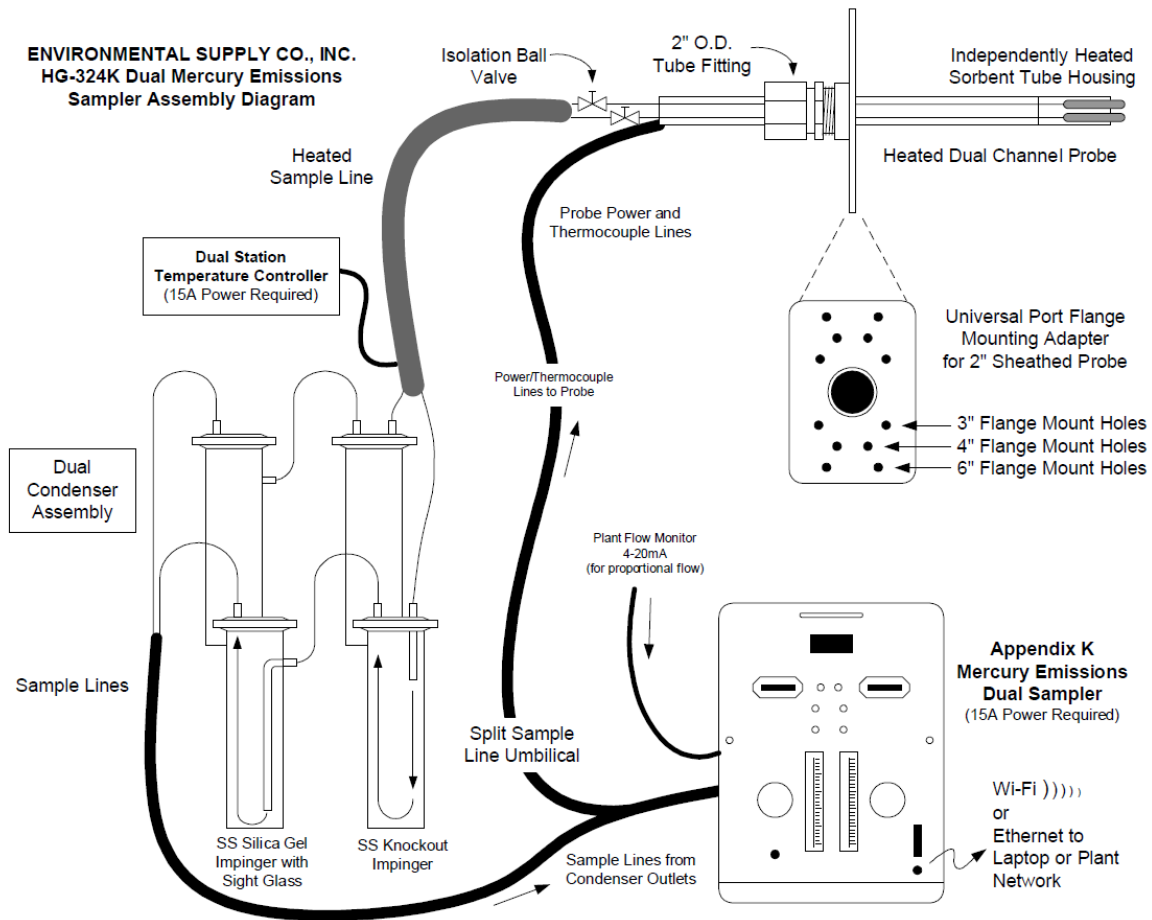


Figure 12. Environmental Supply Company HG-324K System

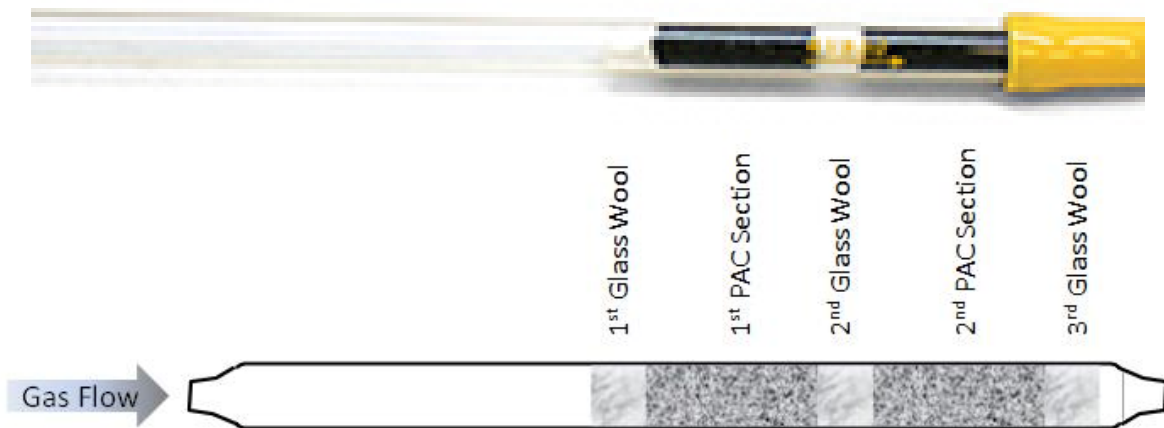


Figure 13. MM30B Two Section Sorbent Trap

2.3 Solids Sampling and Analysis

As discussed above, several of the host sites, including Minorca, recycle the process solids back to different points in the process. At Minorca, solids from the scrubber are recycled directly back to the concentrate thickener tank, however for this test solids from the multitube collector were disposed of. Therefore, it is likely that PAC, and the Hg absorbed on the PAC, would also be recycled into the green balls and the Hg would be re-released during the induration process. To investigate the possible effect of recycle, the host site sampled and analyzed several process streams on a regular basis. ADA received a split of selected samples twice during the test for analysis with the Ohio Lumex (OL). ADA received the independent analysis results conducted by Minorca for all the samples for both carbon and Hg analysis. Results of the analysis are included in Section 4.

Samples were collected from the following locations:

- Green Balls
- Multi-tube Collector drop out
- Concentrate Thickener Overflow
- Pellets
- Fine Tailings

2.4 Ohio Lumex

ADA used the OL RA-915+ to quantitatively recover and quantify Hg from sorbent traps and process samples. The analyzer meets the requirements for analysis specified in M30B. It utilizes differential atomic absorption spectrometry (Zeeman Effect) to measure mercury. The trap sections are inserted into the RP-91C furnace attachment and heated to 800C to vaporize and convert the mercury from a bound state to an atomic state. Organic compounds are completely burned to produce non-interfering carbon dioxide and water. The analyzer produces a desorption curve from which the mass of mercury emitted can be determined by comparison to desorption curves produced from National Institute of Standards and Technology traceable mercury standards. Samples containing 0.2 ppb to 30,000 ppm Hg can be analyzed. Results are obtained in minutes allowing for near real-time, onsite sample analysis. All of the raw data obtained with the OL for process samples and sorbent traps are included in Appendix C.

3.0 PAC SCREENING TEST (PST)

3.1 Description

The goals of the PAC Screening Test were:

- Determine which of several commercially available PACs performed the best.
- Determine what PAC rate was needed to achieve 75% Hg reduction.
- Perform PM stack tests for each PAC at each rate tested on stack D only.

The original plan called for testing PAC rates of 3, 5 and 7 lb/mmacf. However, because ADA had previously tested at Hibtac, which has a very similar exhaust gas layout as at Minorca, it was discovered that the higher rates of injection were not needed when a multi-tube dust collector is present. Therefore, rates of 1, 3 and 5 lb/mmacf were tested for the three candidate PACs.

A typical day of PAC screening involves:

1. Calibrate the Hg-CEMS
2. Obtain Hg-CEMS baseline data
3. Begin testing at the first ACI rate
4. Barr PM Test (when steady conditions are reached as determined by the Hg-CEMS)
5. Change ACI rate and repeat Step 4
6. Continue until all three rates have been tested

Each PAC was tested during a single day and the system was allowed to recover overnight. At Minorca, Hg levels returned to the original baseline conditions after running without ACI overnight. However, Hg reduction was calculated using baseline data obtained shortly before ACI began each day.

3.2 Results

Figure 14 through Figure 16 show the results of the PST at Minorca. Each figure has six traces and four shaded areas. The shaded areas represent the period during which the Hg-CEMS data was averaged in order to determine the HgG reduction.

- Black Dots - Plant Production Rate
- Red Dots - Stack D Hg-CEMS gas phase total Hg, $\mu\text{g}/\text{wscm}$
- Pink Dots - Stack D Hg-CEMS gas phase elemental Hg, $\mu\text{g}/\text{wscm}$
- Dark Green Dots - Stack B Hg-CEMS gas phase total Hg, $\mu\text{g}/\text{wscm}$
- Light Green Dots - Stack B Hg-CEMS gas phase elemental Hg, $\mu\text{g}/\text{wscm}$
- Purple Line - PAC Rate, lb/mmactf
- Grey Shade - Data period averaged to calculate baseline Hg
- Blue Shade - Data period averaged to calculate Hg at low ACI rate
- Red Shade - Data period averaged to calculate Hg at medium ACI rate
- Green Shade - Data period averaged to calculate Hg at high ACI rate

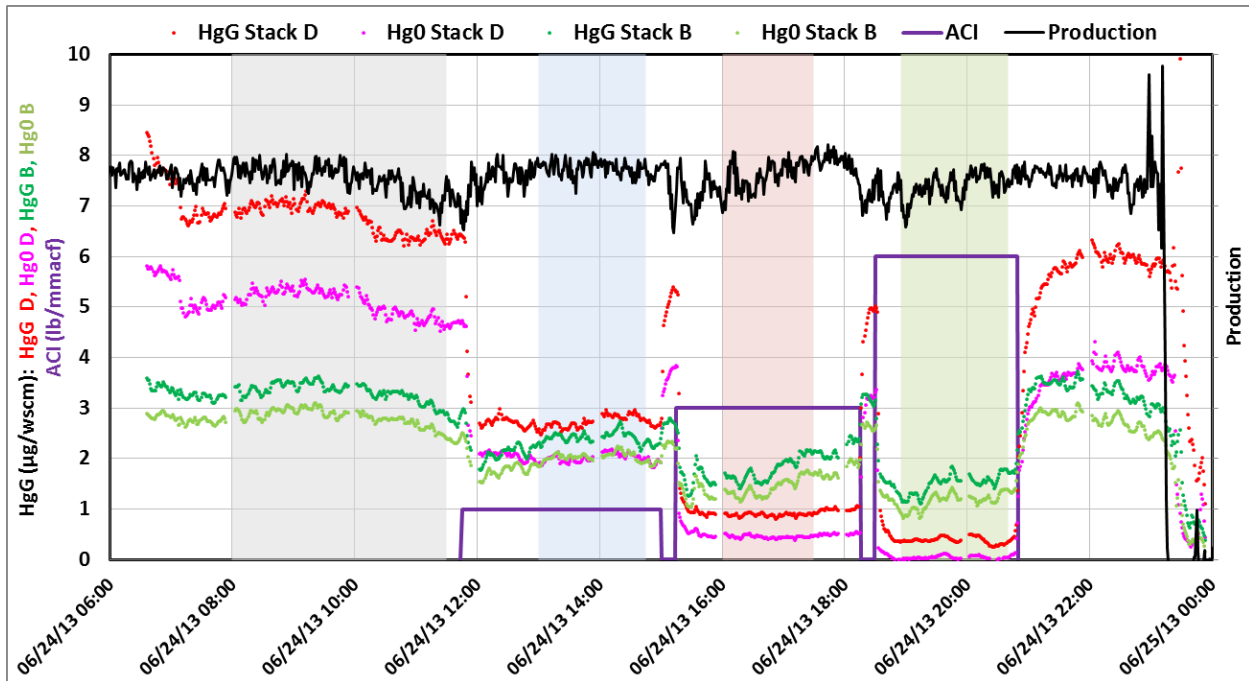


Figure 14. HPAC Screening Test Results

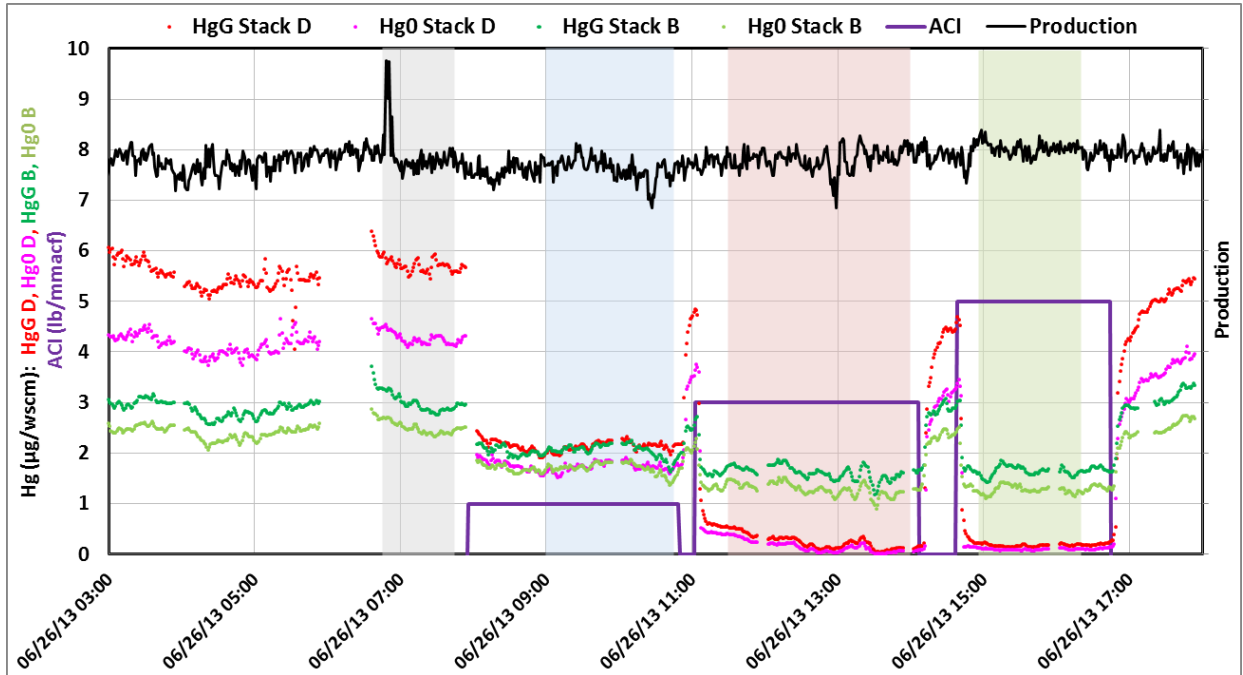


Figure 15. BPAC Screening Test Results

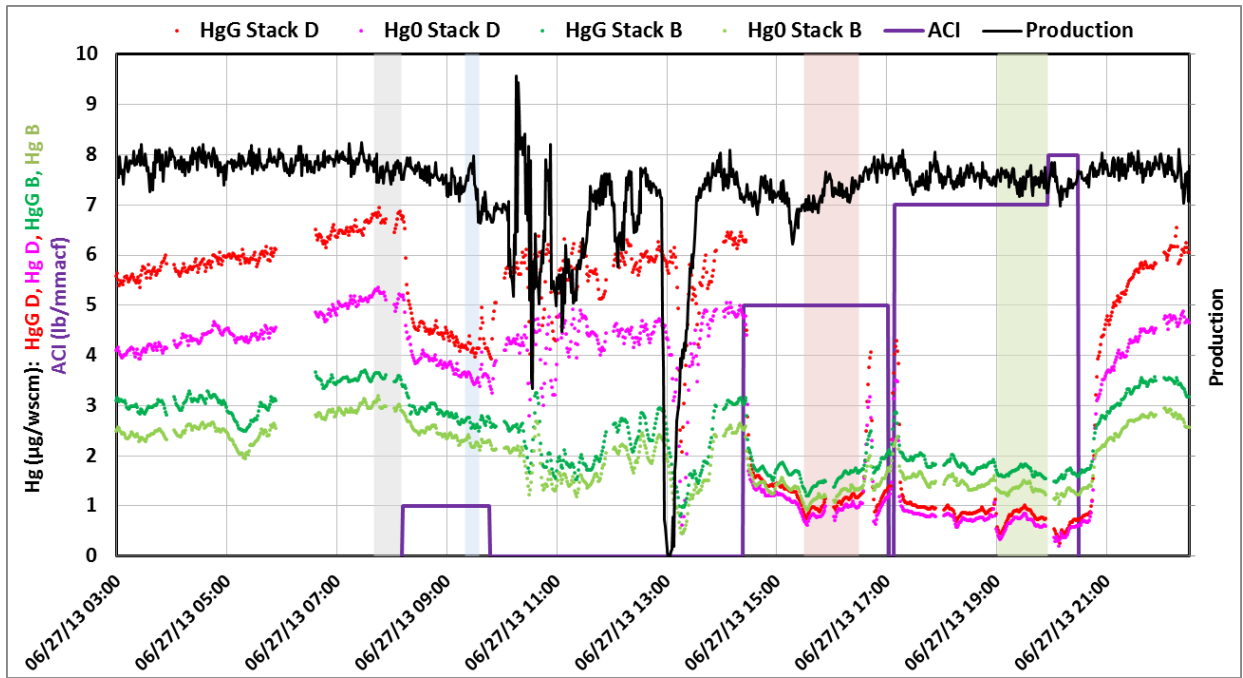


Figure 16. 2013N Screening Test Results

Table 4 is a compilation of the PST results showing the HgG baseline and test values for each PAC and ACI rate tested for both stacks D and B along with the calculated HgG reduction for each test as measured by the Hg-CEMS. Hg reduction was plotted in Figure 17 to produce a comparison of PAC performance. The figure shows that all of the PACs achieved 75% HgG reduction on stack D at 5 lb/mmcf. However, the coarser PAC did not perform as well in stack D as the other two PACs.

All of the PACs showed moderate reduction on stack B, but none reached 75% reduction. As shown in Figure 18, no injection occurs in the Hood Exhaust so there is no stack reduction for stacks A and B except from the limited mixing that occurs in the header.

BPAC was selected for Phase II testing at 3 lb/mmcf because it performed as well as the other PACs on stack B and much better on stack D. It is also a moderately priced, readily available sorbent.

Table 4. Summary of the PAC Screening Test at Minorca

Hg-CEMS, µg/wscm	HPAC	BPAC	2013N
Baseline Stack D	6.75	5.70	6.73
Baseline Stack B	3.32	2.96	3.57
With ACI			
1 lb/mmcf Stack D HgG (µg/wscm)	2.73	2.12	4.14
1 lb/mmcf Stack B HgG (µg/wscm)	2.42	2.05	2.63
Removal Stack D	60%	63%	39%
Removal Stack B	27%	31%	26%
3 lb/mmcf Stack D HgG (µg/wscm)	0.88	0.23	n/a
3 lb/mmcf Stack B HgG (µg/wscm)	1.76	1.60	n/a
Removal Stack D	87%	96%	n/a
Removal Stack B	47%	46%	n/a
5 lb/mmcf Stack D HgG (µg/wscm)	n/a	0.17	1.03
5 lb/mmcf Stack B HgG (ug/wscm)	n/a	1.63	1.50
Removal Stack D	n/a	97%	85%
Removal Stack B	n/a	45%	58%
6 lb/mmcf Stack D HgG (µg/wscm)	0.37	n/a	n/a
6 lb/mmcf Stack B HgG (ug/wscm)	1.49	n/a	n/a
Removal Stack D	94%	n/a	n/a
Removal Stack B	55%	n/a	n/a
7 lb/mmcf Stack D HgG (µg/wscm)	n/a	n/a	0.78
7 lb/mmcf Stack B HgG (ug/wscm)	n/a	n/a	1.66
Removal Stack D	n/a	n/a	88%
Removal Stack B	n/a	n/a	53%

ug/wscm - micrograms of Hg per wet standard cubic meter of gas.
 n/a - system was not tested at this rate.

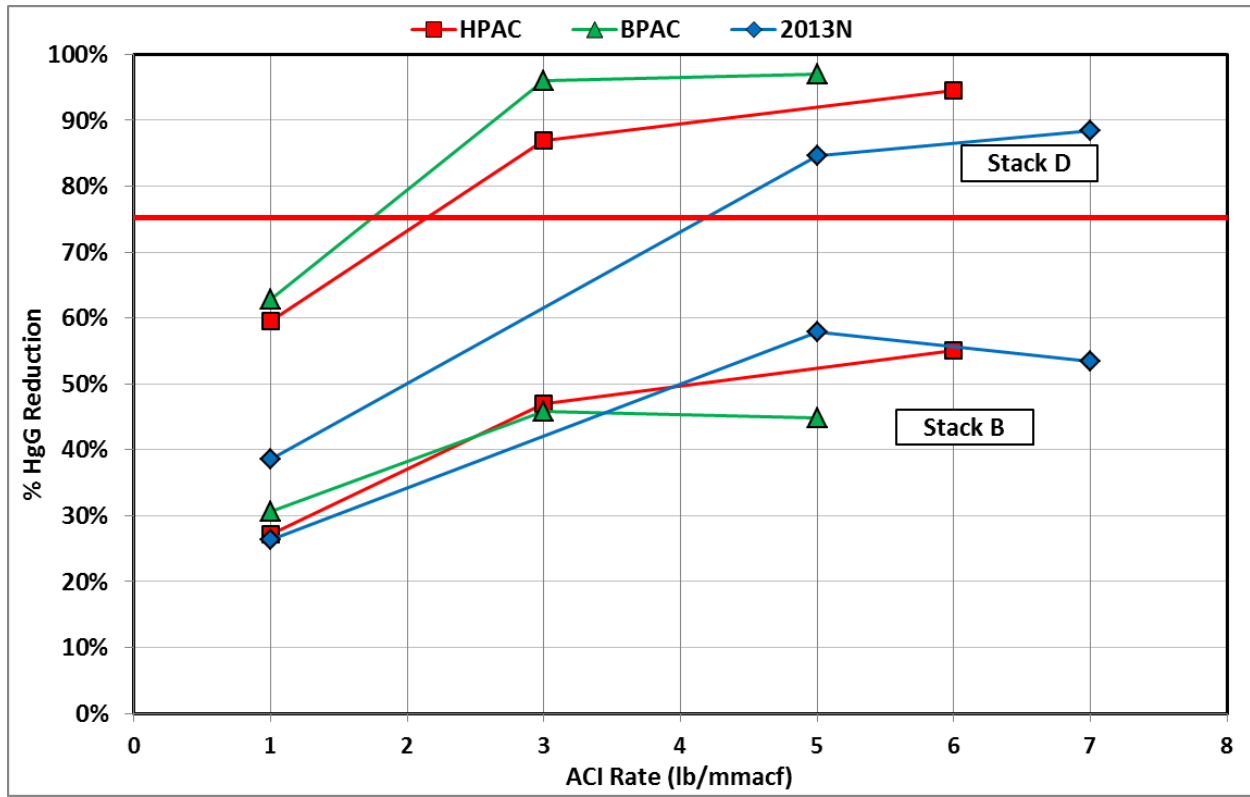


Figure 17. Comparison of the PAC Screening Test Results for HgG

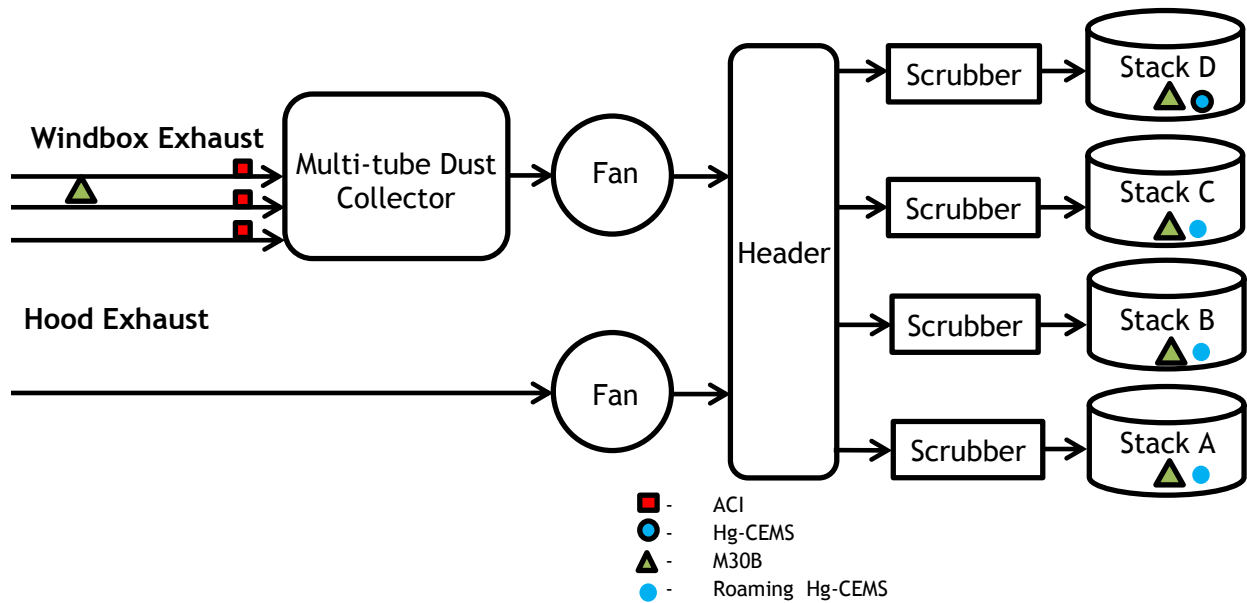


Figure 18. Minorca Gas Stream and Sampling Locations

4.0 PHASE II TESTING

4.1 Description

The goals of Phase II testing were:

- Determine the long term Hg reduction performance for BPAC at 3 lb/mmacf
- Determine the effects of PAC/Hg recycle on the mercury concentration in the process streams and the effects on Hg reduction
- Perform periodic PM tests at the Stack (Barr)

A typical day of Phase II testing involves:

1. Calibrate the Hg-CEMS
2. Collect and analyze samples
3. Collect and analyze MM30B sorbent traps

Phase II Testing commenced on 7/10/13 and was completed on 8/8/13 as scheduled. The ACI rate was held at 3 lb/mmacf except for short periods when the plant was off-line or minor maintenance was required on the Hg-CEMS or Mini-Silo. Barr performed weekly PM testing during Phase II testing.

4.2 Results

4.2.1 Phase II Testing

Figure 19 through Figure 23 show the data collected prior to and during Phase II testing. The shaded areas represent the periods during which the Hg-CEMS data were averaged in order to determine the HgG reduction. The figures use the following color designations:

- Black Dots - Plant Production Rate
- Red Dots - Stack D Hg-CEMS total gas phase Hg, $\mu\text{g}/\text{wscm}$
- Green Dots - Stack B Hg-CEMS total gas phase Hg, $\mu\text{g}/\text{wscm}$
- Orange Dots - Stack C Hg-CEMS total gas phase Hg, $\mu\text{g}/\text{wscm}$
- Blue Dots - Stack A Hg-CEMS total gas phase Hg, $\mu\text{g}/\text{wscm}$
- Purple Line - PAC Rate, lb/mmacf
- Pink Line - Approximate shift in baseline
- Light Red Shade - Data period averaged to calculate Stack D total gas phase Hg
- Light Green Shade - Data period averaged to calculate Stack B total gas phase Hg
- Light Orange Shade - Data period averaged to calculate Stack C total gas phase Hg
- Light Blue Shade - Data period averaged to calculate Stack A total gas phase Hg

Figure 19 shows the baseline HgG data for all four stacks during the 10 days before Phase II testing began. The shaded sections in Figure 19 were the baselines chosen for each stack (C and D have the same time period). These periods represent relatively steady operation for production and Hg levels and were close to the beginning of the testing period.

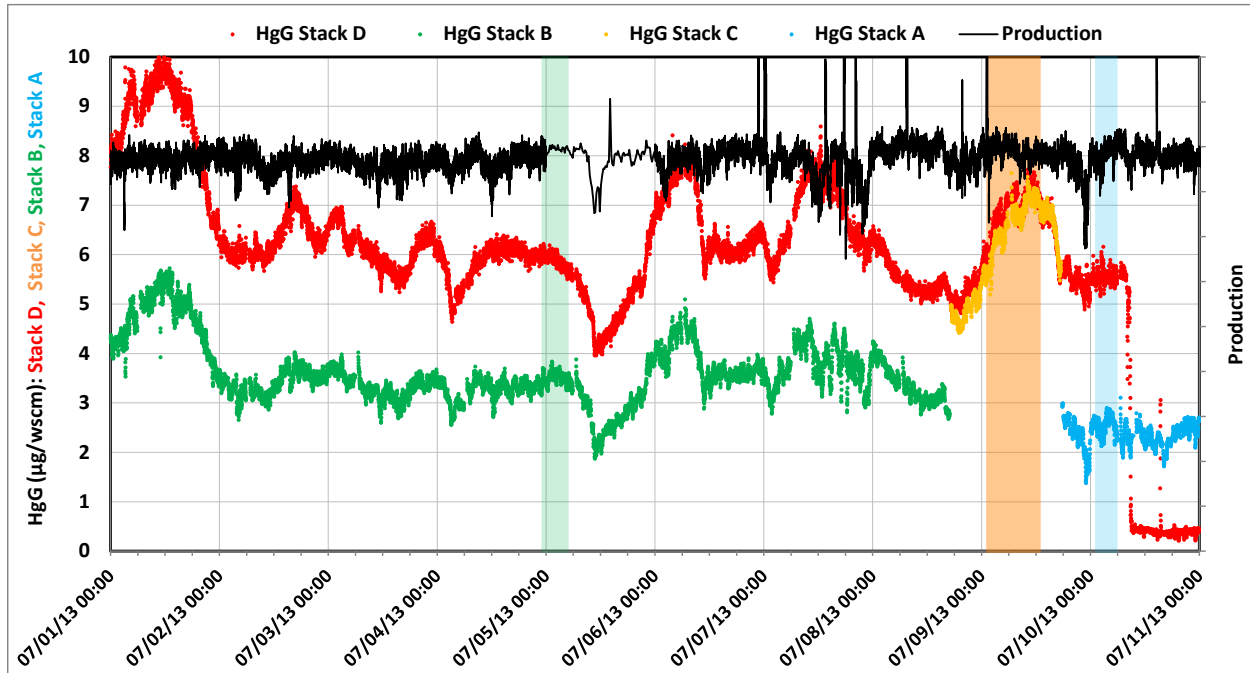


Figure 19. Phase II Testing Baseline Stack Data

Figure 20 through Figure 23 show the results of Phase II testing at Minorca. The figures show the mercury trend of the two stacks being sampled at any given time. Figure 23 shows all the stack data on a single graph. One Hg-CEMS probe was positioned in stack D for the duration of Phase II testing, and the second was rotated between stacks A, B, and C every two to three days. When ACI commenced, Figure 22 shows immediate and significant reduction in HgG emissions in stack D and C, and Figure 20 and Figure 21 show more gradual and less significant reduction in stacks A and B. This was expected because PAC was only being injected into the Windbox Exhaust that preferentially exits through stacks C and D. The data shows that some minimal mixing must occur between the Windbox and Hood Exhaust gas in the common header based on the HgG reductions measured in stacks A and B. HgG emissions in stack D were fairly stable with values usually under $1.0 \mu\text{g/wscm}$ during testing.

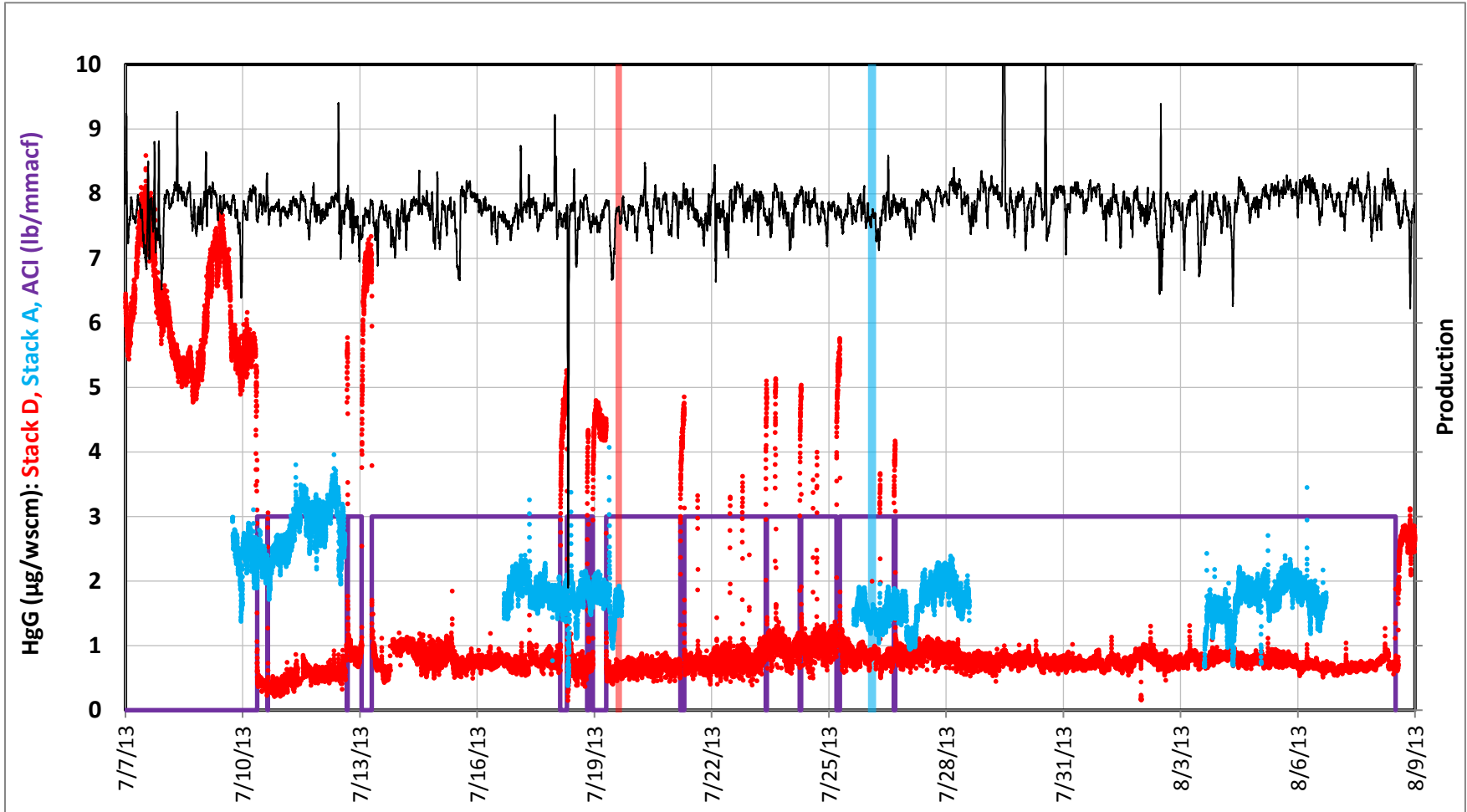


Figure 20. Phase II Testing - Stack D and A Emissions

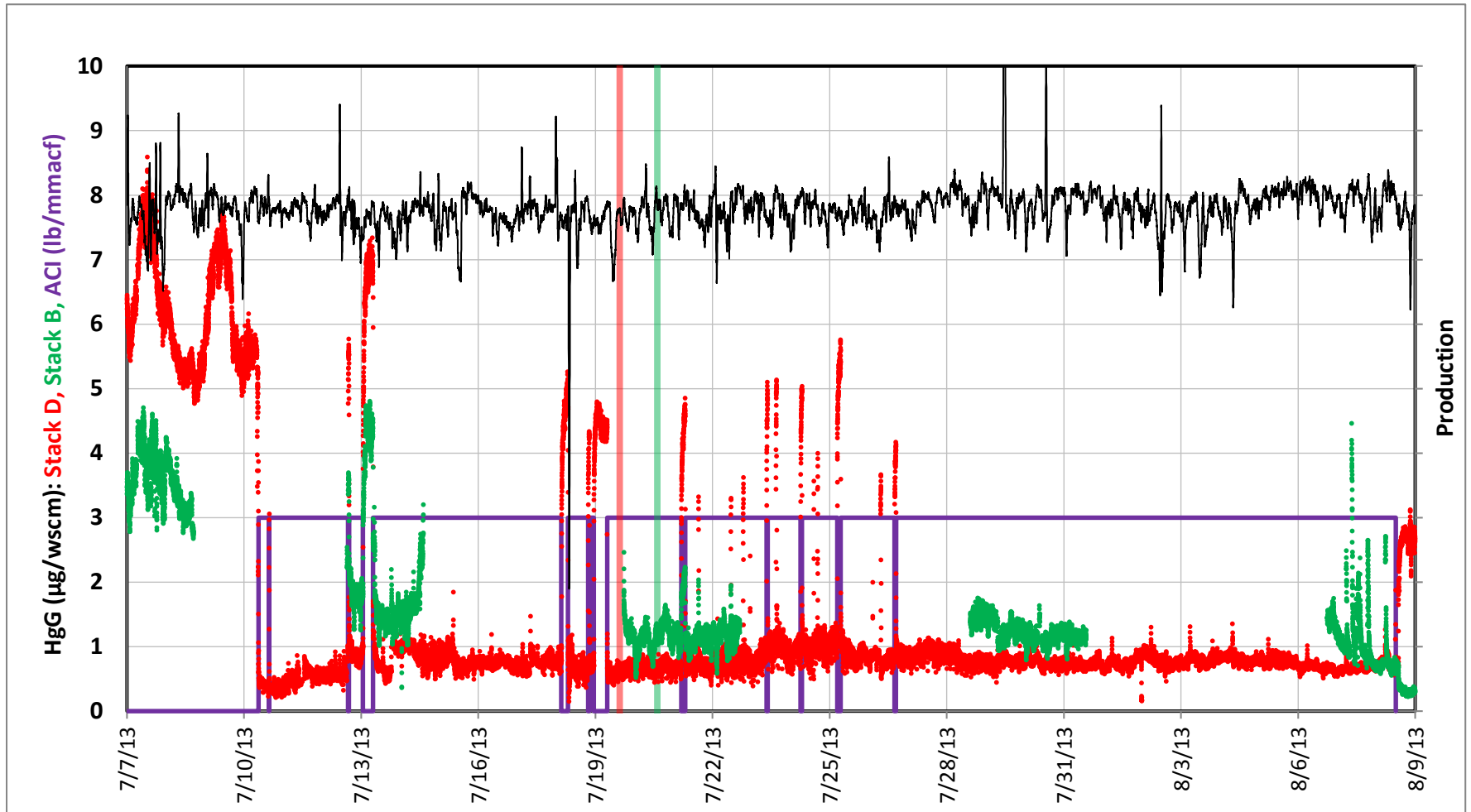


Figure 21. Phase II Testing - Stack D and B Emissions

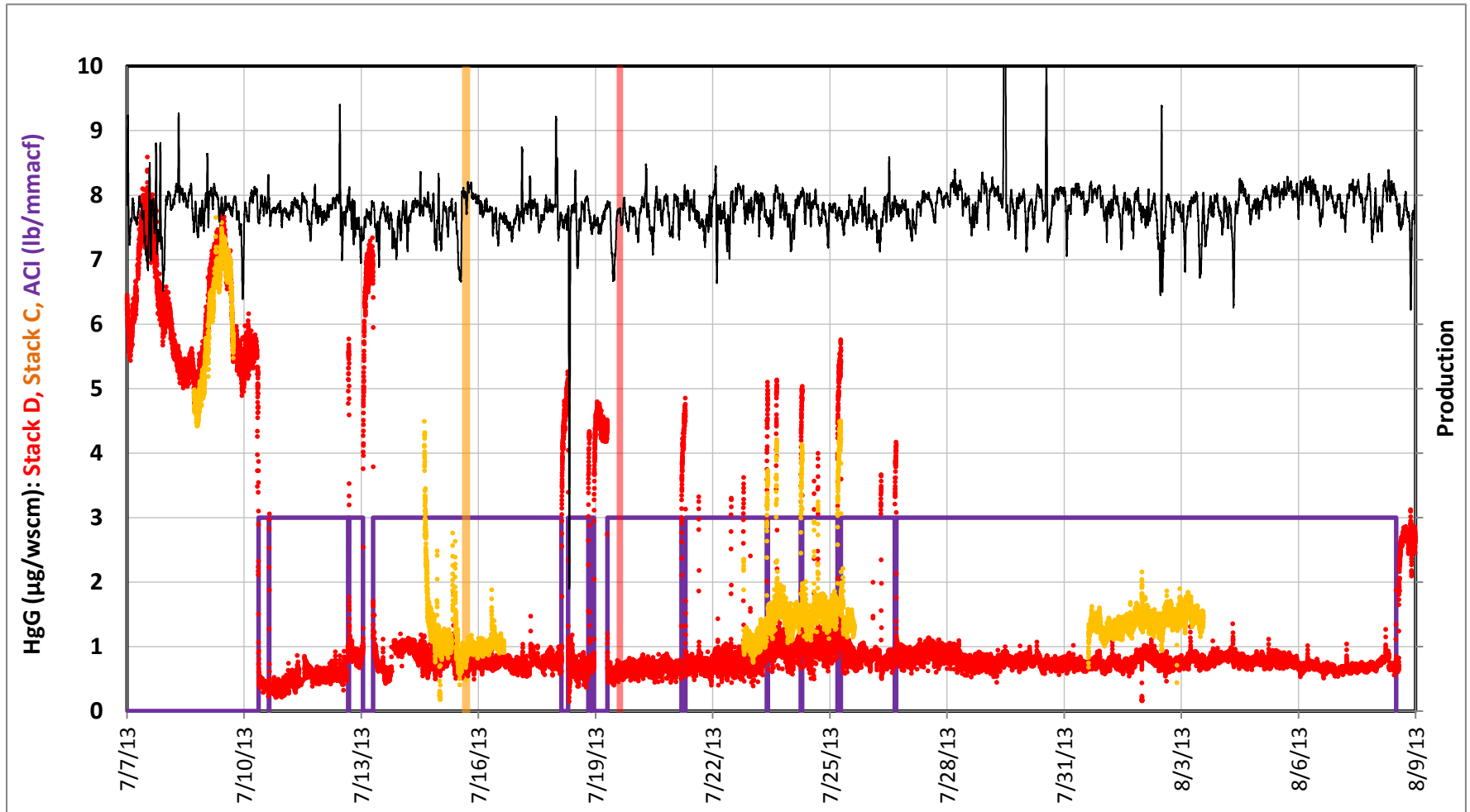


Figure 22. Phase II Testing - Stack D and C Emissions

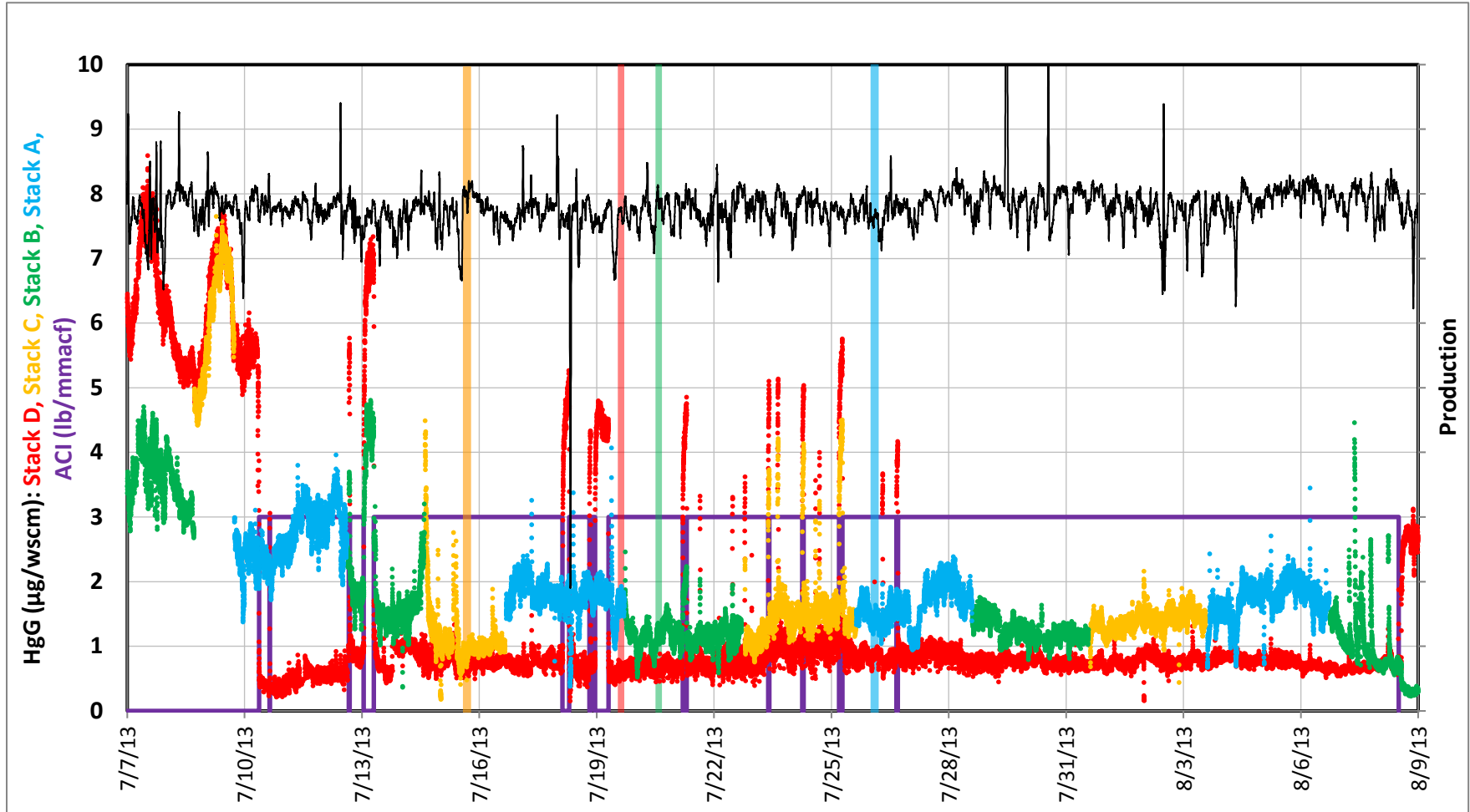


Figure 23. Phase II Testing - Stack Emissions

The results of Phase II testing, summarized in Table 5, list the Baseline and ACI Hg emissions, as well as the calculated Hg reductions, for the Hg-CEMS and MM30B measurements. Hg-CEMS data represent the HgG reduction whereas the MM30B data represents HgT reduction and includes particulate bound mercury (HgP). The table shows that stacks C and D had the highest baseline values and the highest reduction percentages. The total HgG reduction, considering all four stacks, was 76%. However, the HgT reduction based on MM30B data was 54%.

Table 5. Phase II Testing Mercury Reduction Summary via Hg-CEMS and MM30B

CEMS Hg-Gas Phase (ug/wscm)	Stack D	Stack C	Stack B	Stack A	Total
Baseline	7.26	5.85	3.02	3.51	19.64
With ACI	0.39	0.72	0.94	1.71	3.77
Reduction	95%	88%	69%	51%	76%

MM30B Hg-Total (ug/wscm)	Stack D	Stack C	Stack B	Stack A	Total
Baseline	11.11	6.74	3.46	4.07	25.38
With ACI	3.50	3.13	1.72	2.28	10.64
Reduction	68%	54%	50%	44%	54%

4.2.2 Stack MM30B Data

Figure 24 through Figure 27 show a comparison of the stack MM30B and Hg-CEMS data for each of the four stacks. The figure presents the MM30B data in three parts; HgT-dark symbol, HgG-medium colored symbol, and HgP-light symbol. Hg-CEMS values are shown as a line in the same color as the MM30B symbol for HgG. This was done because it was discovered that HgP was a significant portion of HgT as determined by analyzing the first glass wool section of the sorbent trap, which is assumed to contain all of the particulate, separately from the two sorbent sections. The Hg-CEMS can only measure gas phase mercury, so if the gas contains a significant fraction of HgP, the Hg-CEMS and MM30B will not agree well. The figure shows that the Hg-CEMS values agreed well with the MM30B HgG data for all stacks and the HgP was a major fraction of the mercury leaving Stacks C and D. The values for this graph were used in Table 5. This topic is discussed further in the QA/QC section and in Appendix D.

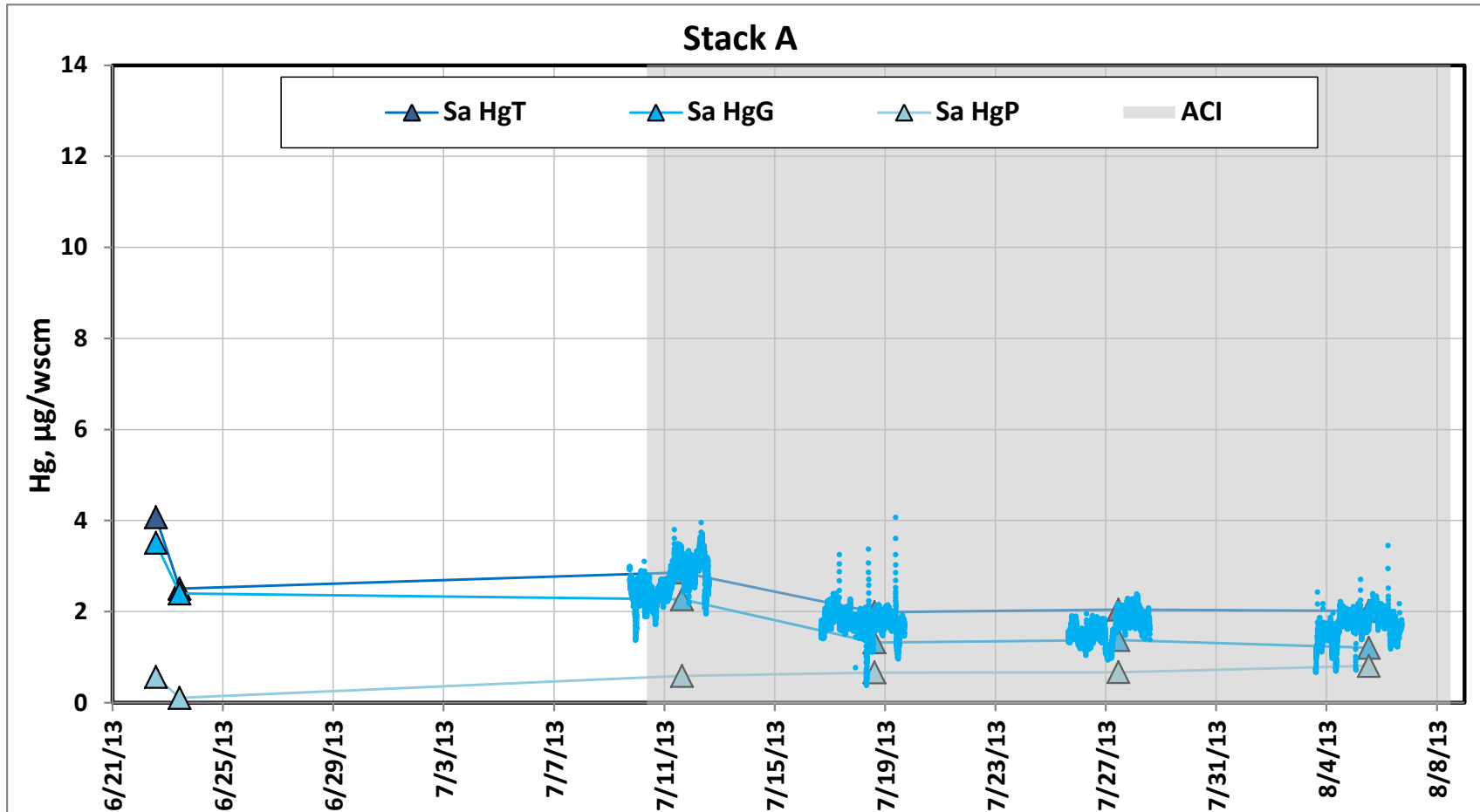


Figure 24. Stack A MM30B Data vs. Hg-CEMS

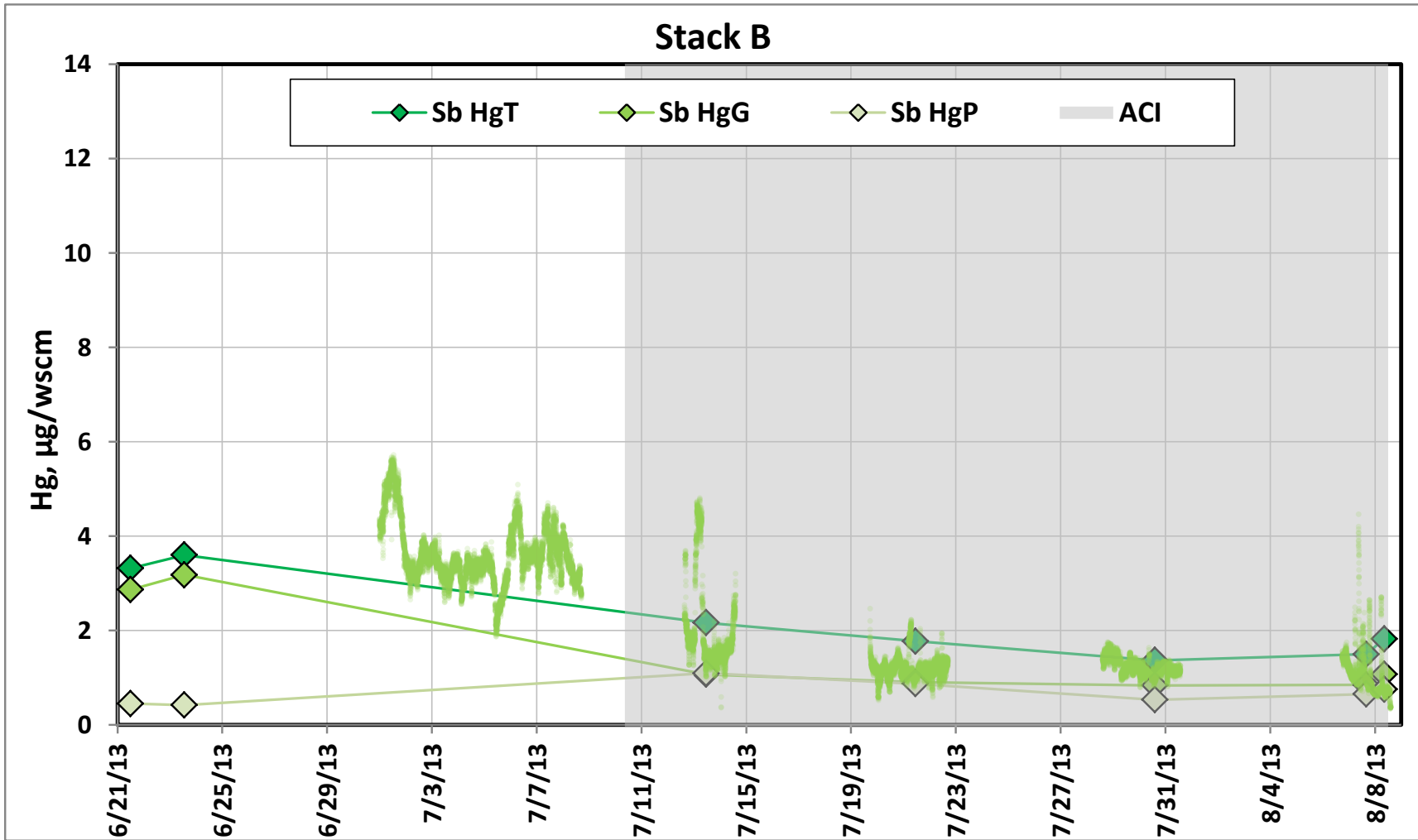


Figure 25. Stack B MM30B Data vs. Hg-CEMS

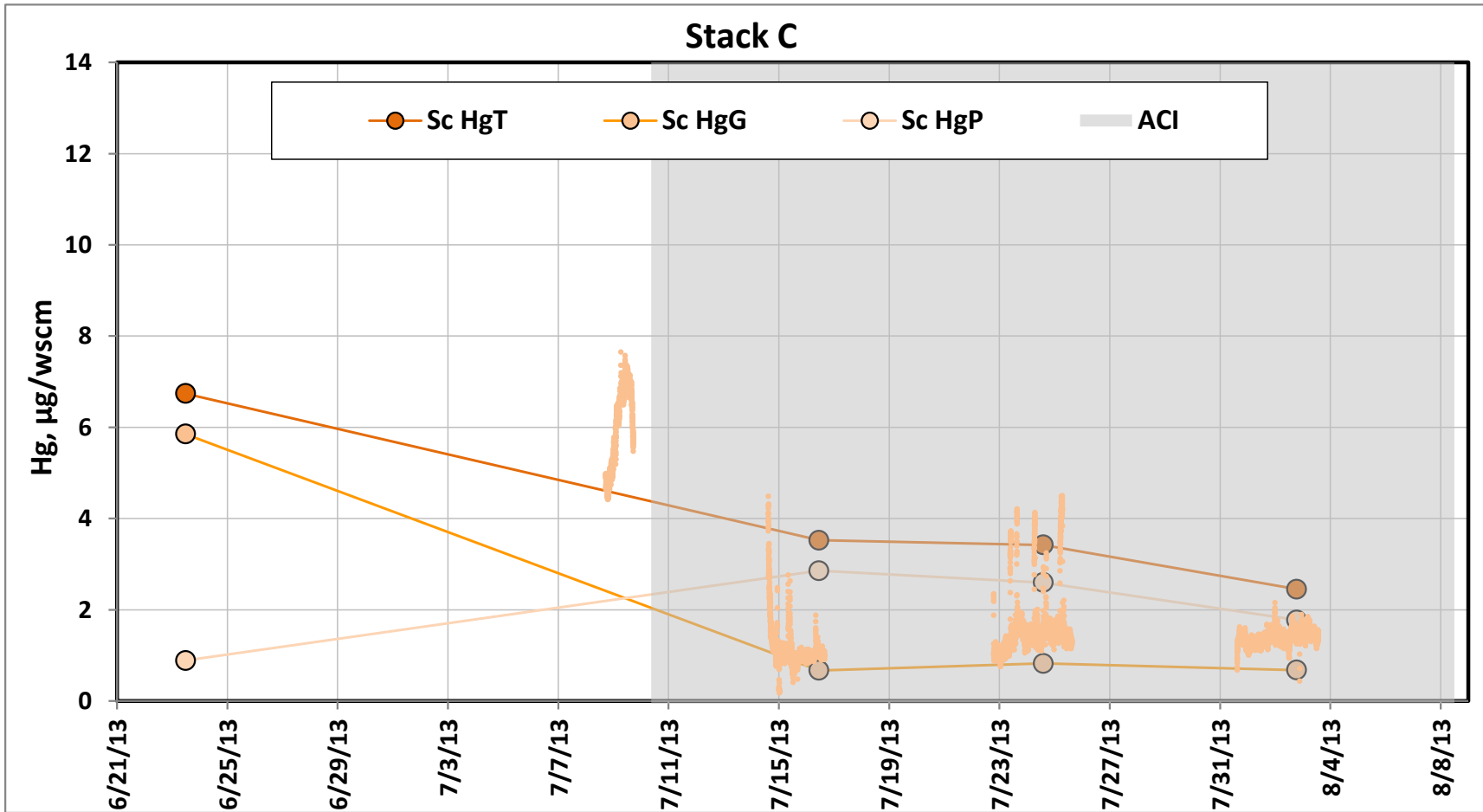


Figure 26. Stack C MM30B Data vs. Hg-CEMS

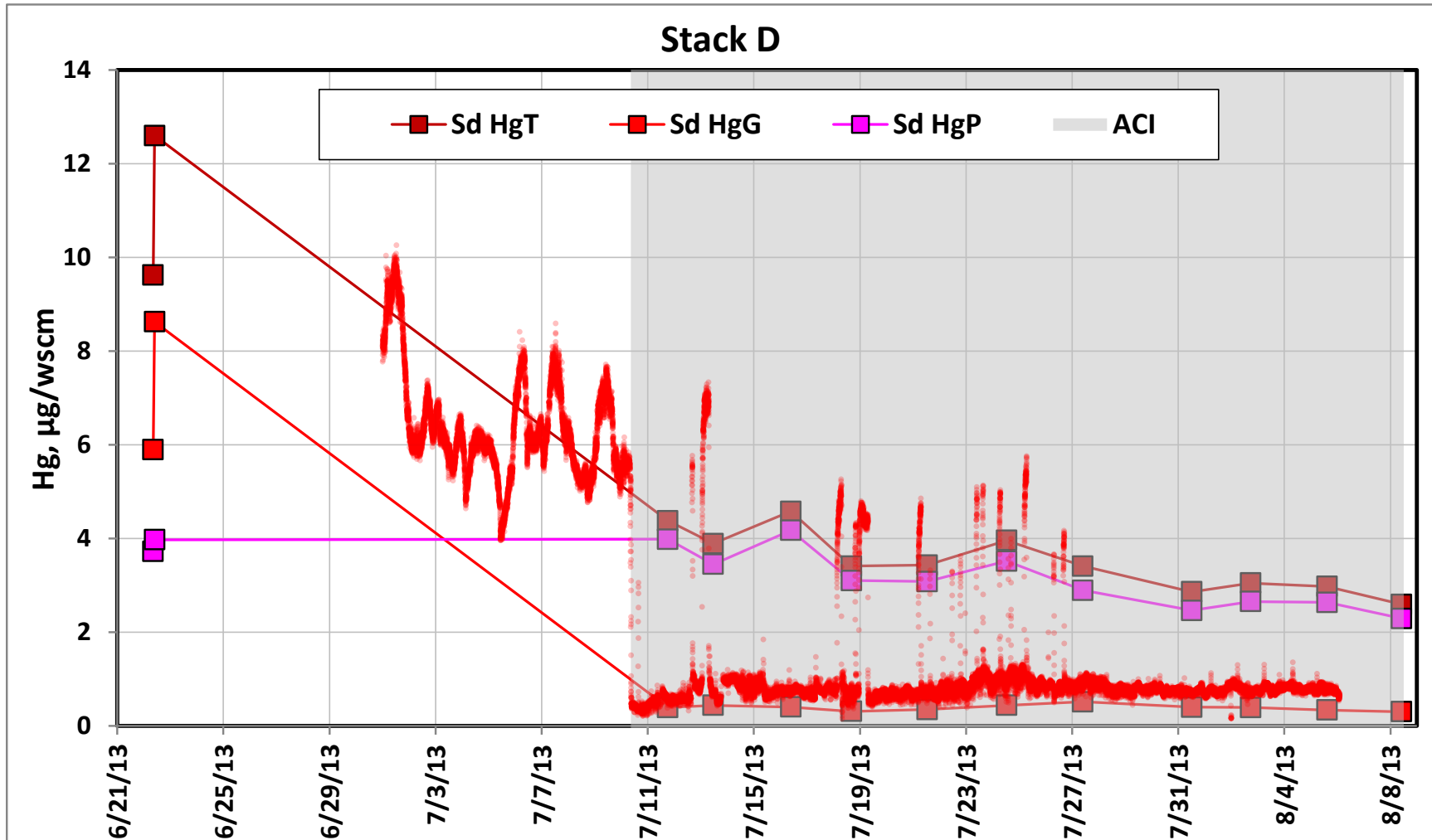


Figure 27. Stack D MM30B Data vs. Hg-CEMS

4.2.3 Inlet MM30B Data

Figure 28 shows the results of the MM30B sorbent traps that were collected upstream of the ACI grid including tests in each of the four inlet ducts prior to the PST. The gray shaded area represents Phase II testing. The red markers represent Hg concentration in the Green Balls. The figure shows that during the limited 30-day test, there was little or no increase in the inlet mercury concentration from Hg/PAC recycled back to the process. The inlet mercury corresponded well with changes in the Hg concentration of the Green Balls. Extended testing would be required to further identify long-term, inlet mercury concentration changes.

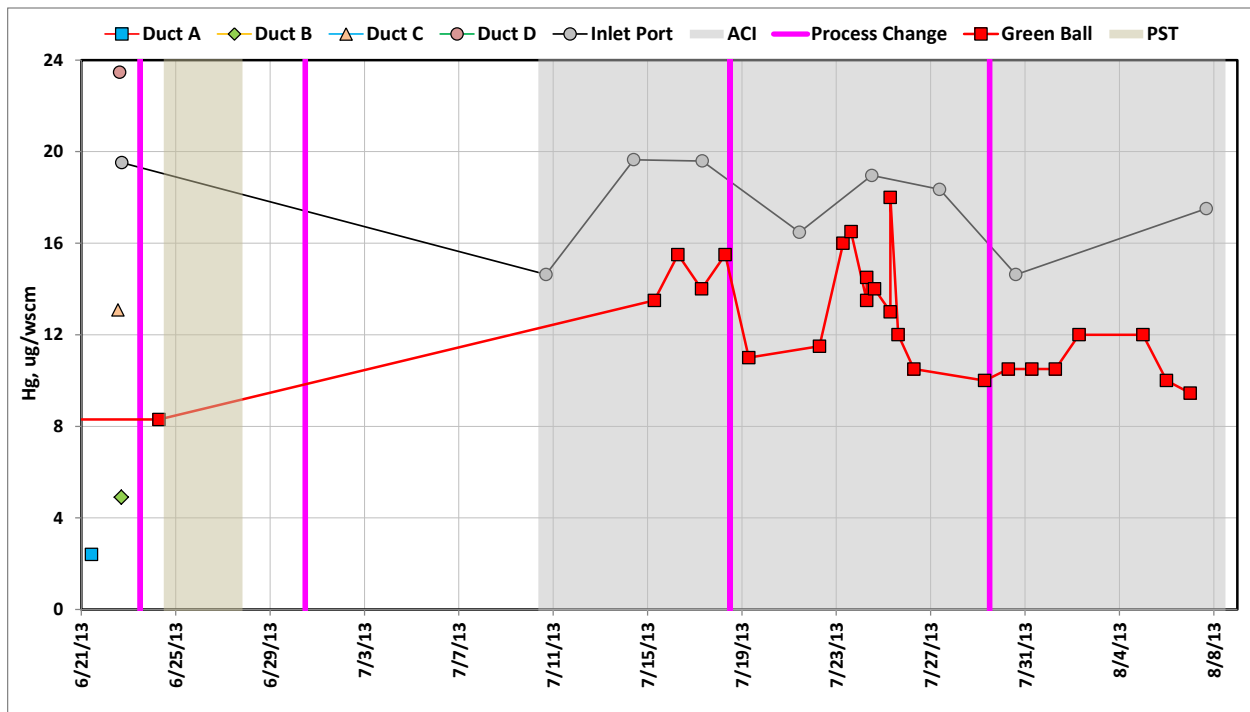


Figure 28. Inlet MM30B Data with Greenball Hg Data

4.2.4 Sample Carbon Analysis

Several samples were analyzed, as shown in Figure 29, for carbon content in an effort to track the Hg. It is believed that by tracing the carbon through the process it can be determined where the Hg is going because it is attached to the carbon and difficult to leach.

Multiclone, Thickener Overflow, Fine Tails, Green Balls, and Fired Pellets samples were analyzed by an independent lab for total carbon. Figure 30 through Figure 34 show the results of the analysis. Figure 30 and Figure 31 indicate the multiclone collector and thickener overflow sample carbon content had risen slightly. However, Figure 32, Figure 33, and Figure 34 do not show any significant increase in fine tails, green balls, or pellets.

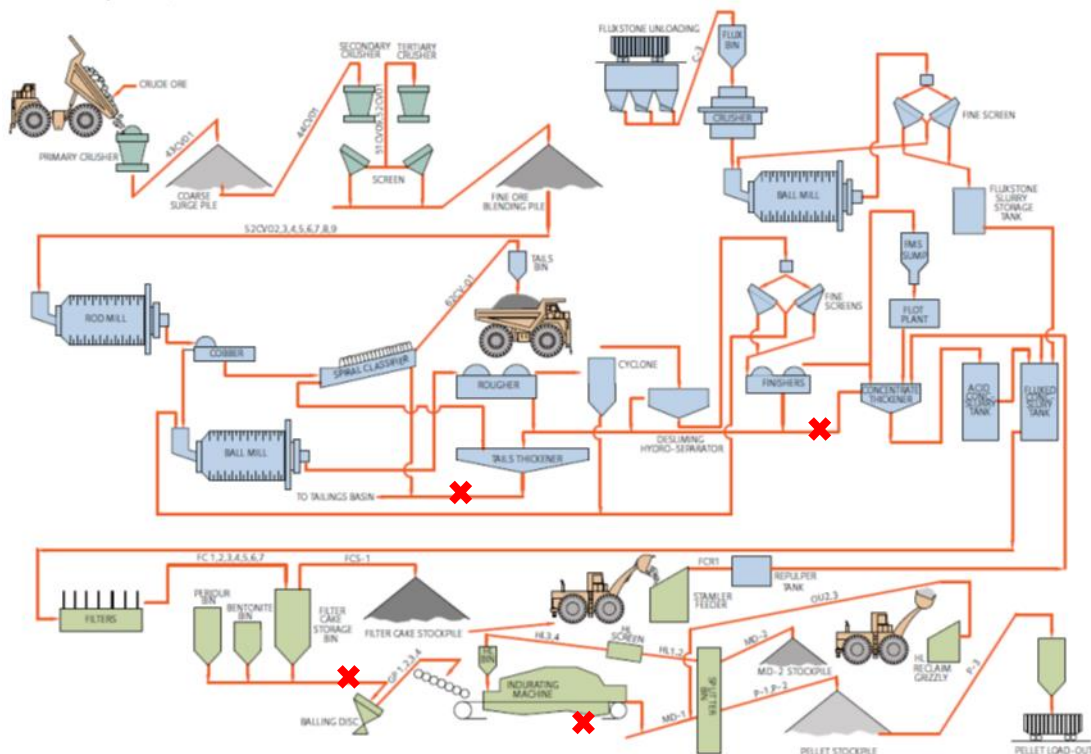


Figure 29. Process Diagram with Sampling Locations

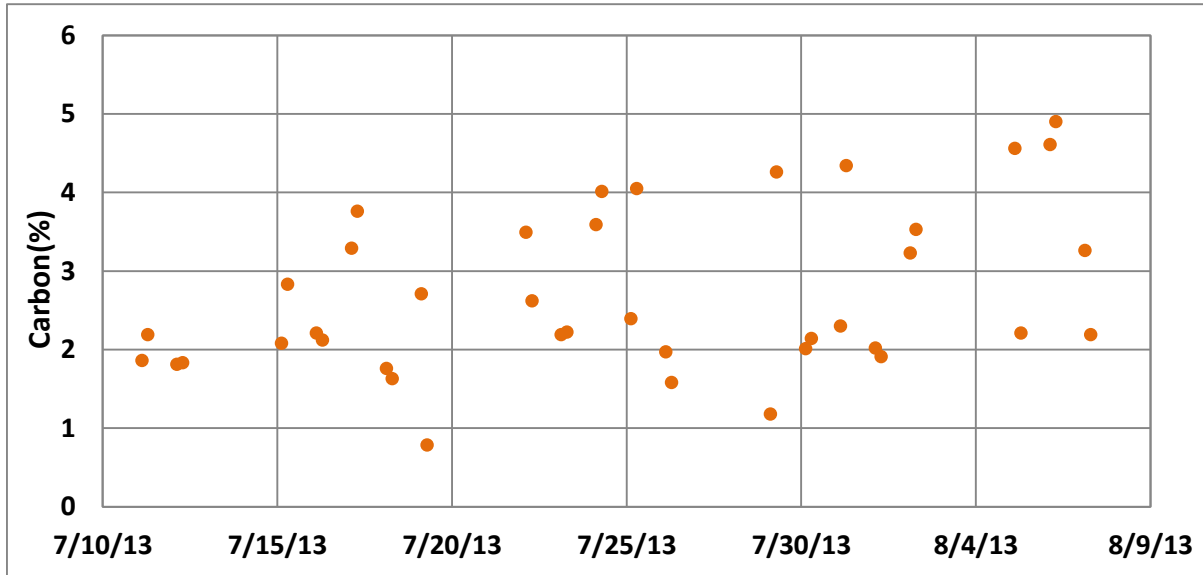


Figure 30. Phase II Testing Multiclone Carbon Analysis

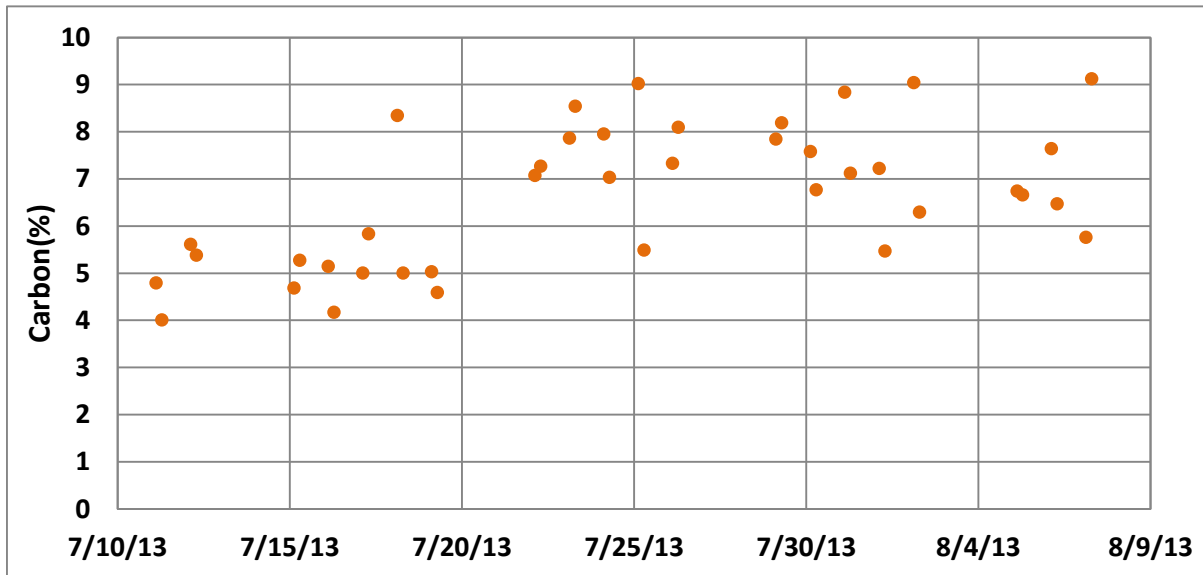


Figure 31. Phase II Testing Thickener Overflow Carbon Analysis

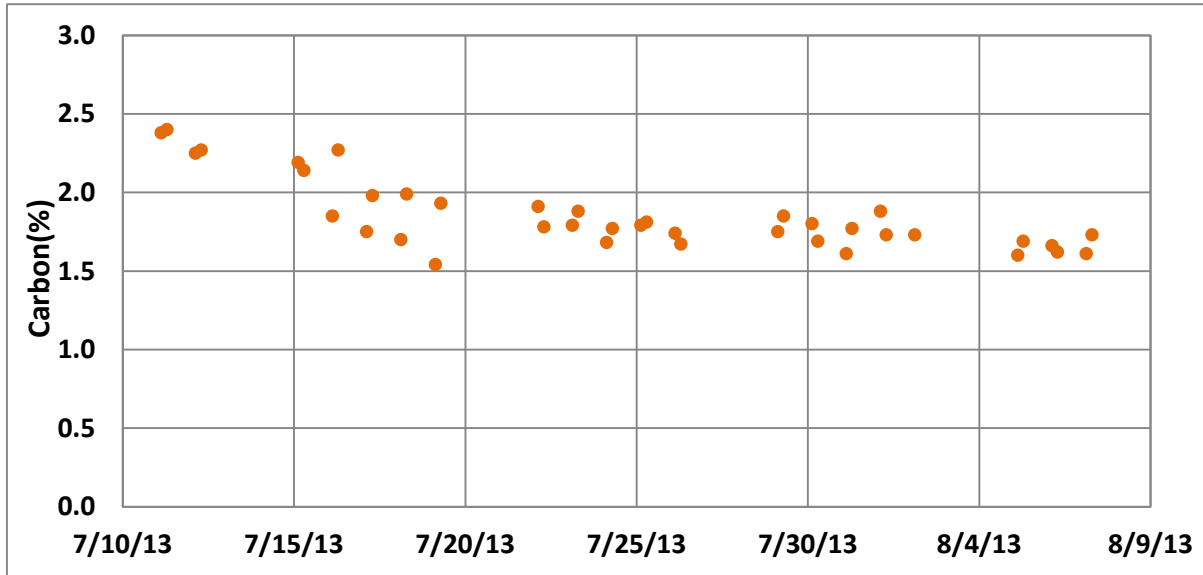


Figure 32. Phase II Testing Fine Tails Carbon Analysis

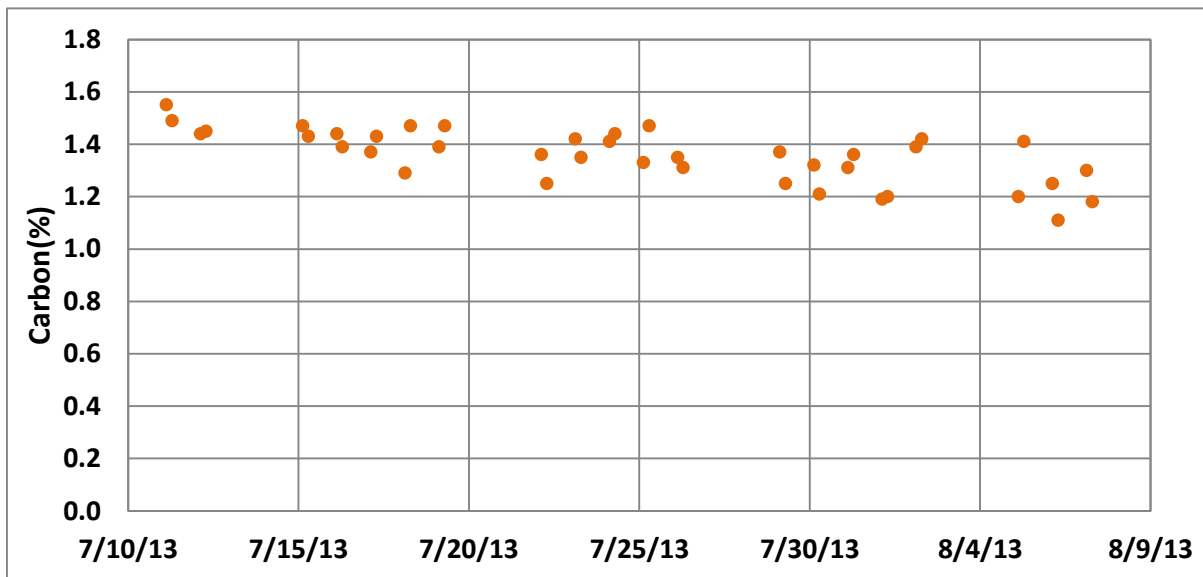


Figure 33. Phase II Testing Green Ball Carbon Analysis

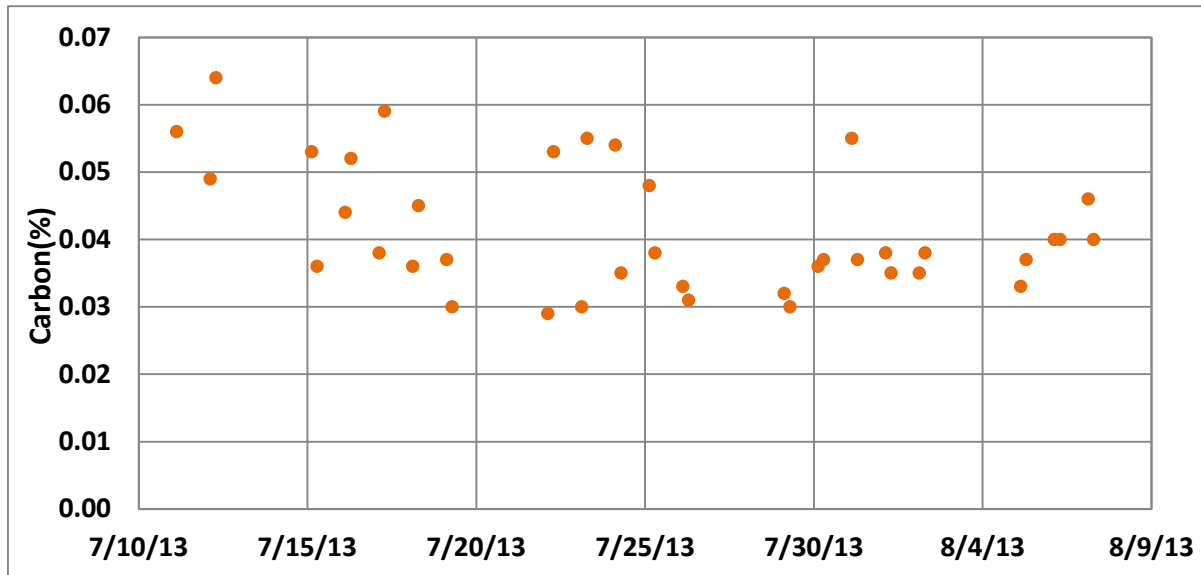


Figure 34. Phase II Testing Fired Pellets Carbon Analysis

4.2.5 Solids Analyses for Hg

Minorca recycles the solids collected in the scrubber back to the concentrate thickener; there is no magnetic separator in this recycle loop. Therefore, it is possible that PAC, and the Hg absorbed by the PAC, could also be recycled into the green balls and the Hg would be re-released during the induration process. Since the scrubber water is recycled back to the concentrate thickener directly, it is possible the mercury could exit the process with the fine tailings (see Figure 29). The Phase II testing (30 days) was of sufficient length for PAC concentrations to reach steady levels in the internal process vessels; however, there are external influences that would require much longer test periods to determine the ultimate fate of Hg collected on the PAC.

To determine the fate of mercury recycled with the PAC in the scrubber water, several process streams were sampled on a regular basis. The host site contracted an independent lab to analyze the samples and provided ADA with a split on several occasions for analysis with the OL.

ADA received samples according to the schedule below.

- Green Balls - Every day
- Pellets - Twice during Phase II testing
- Multiclone drop out - Twice during Phase II testing
- Thickener Overflow - Twice during Phase II testing
- Fine Tailings - Twice during Phase II testing

Minorca had the following samples analyzed for mercury.

- Green Balls - Twice Daily on Week Days during Phase II testing
- Pellets- Twice Daily on Week Days during Phase II testing
- Multiclone drop out - Twice Daily on Week Days during Phase II testing
- Thickener Overflow - Twice Daily on Week Days during Phase II testing
- Fine Tailings - Twice Daily on Week Days during Phase II testing

Figure 35 through Figure 43 show the results of the ADA OL Hg analysis and the independent lab Hg analysis of the solid samples in nanograms of mercury per gram of solid sample (ng/g) on a dry basis. Due to the relatively short test duration and small sample data set, more testing is needed to evaluate long-term Hg trend in the test samples. It is important to take notice of the range of the y-axis because what may appear to be a significant change in the Hg concentration may not be very significant compared to Hg concentrations in the other samples.

Figure 35 shows the ADA measured Hg concentration in the Green Ball samples from before the Screening Test to the end of Phase II testing. Figure 36 displays the Green Ball Hg concentration obtained by the independent lab for Phase II testing only. In general, Hg in the Green Balls was relatively stable and the two analyses agreed well.

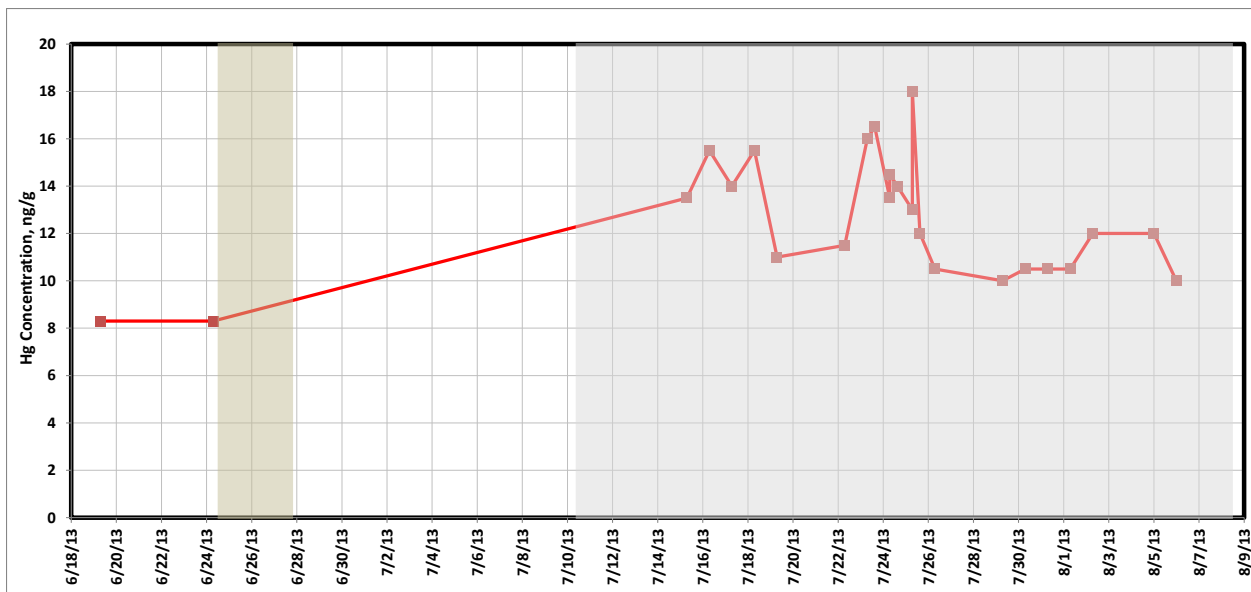


Figure 35. ADA Green Ball Hg Analyses

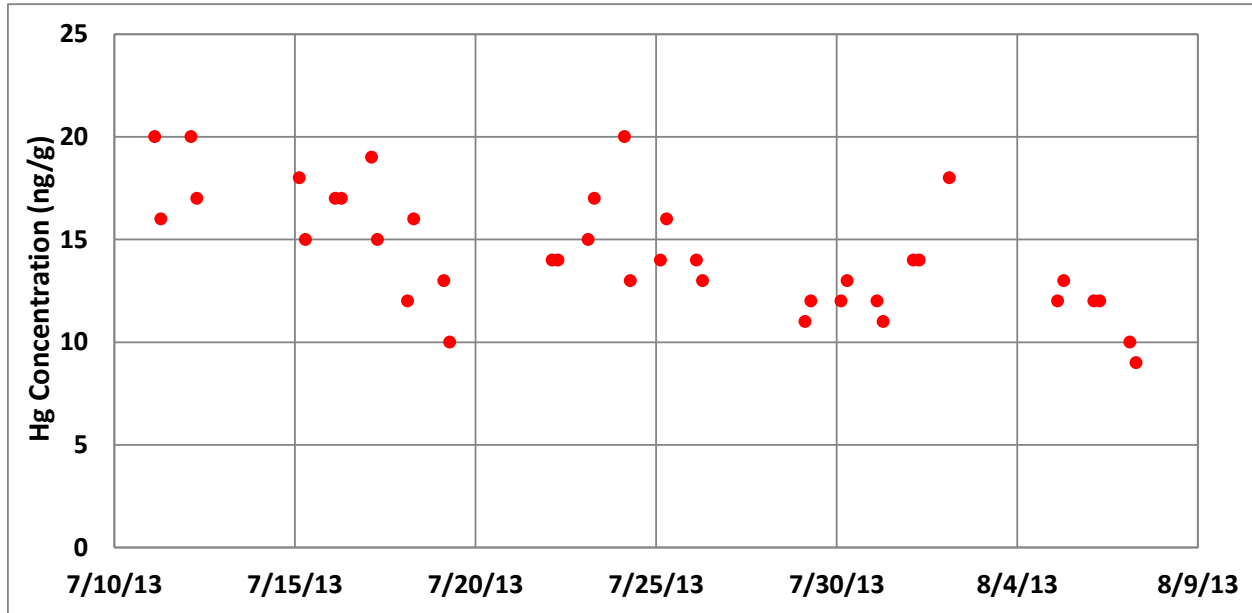


Figure 36. Independent Phase II Testing Green Ball Hg Analysis

Figure 37 shows the ADA measured Hg concentration in the Thickener Overflow from before and during Phase II testing. Figure 38 displays the independent lab results from the Thickener Overflow Phase II testing Hg analysis. Both analyses of the limited data set show elevated Hg during Phase II testing with a downward trend towards the end of Phase II testing. Note that the mercury concentration in this sample was higher than the other samples. PAC is smaller and less dense than taconite particulates so it is reasonable to find high Hg concentrations in these samples. Extended testing is needed to further evaluate the long term trends.

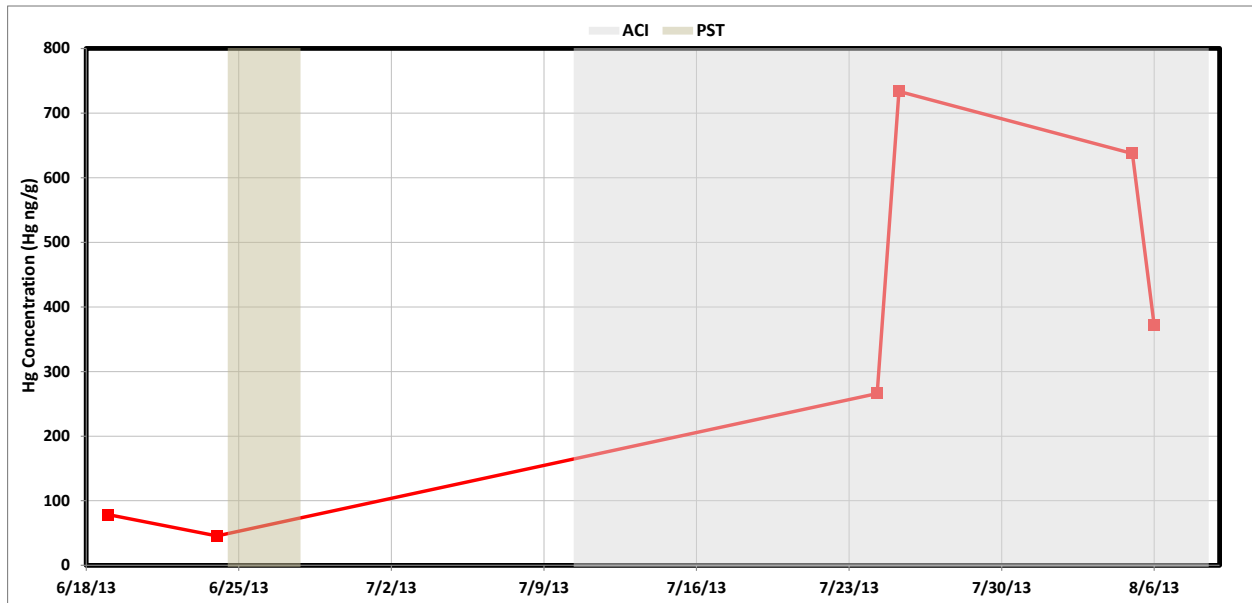


Figure 37. ADA Thickener Overflow Hg Analysis

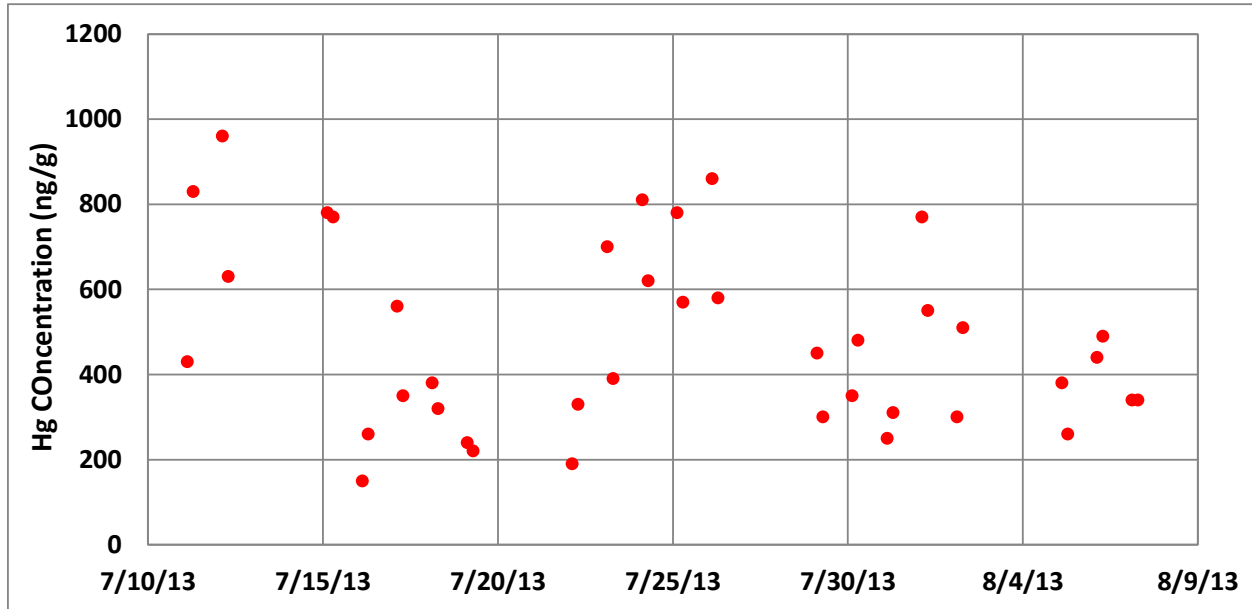


Figure 38. Independent Phase II Testing Thickener Overflow Hg Analysis

Figure 39 shows the ADA measured Hg concentration of the Multiclone solid samples which were collected at the drop out valves. Figure 40 displays the Hg analysis results from the independent lab for Phase II testing only. Both analyses show higher Hg concentration during Phase II testing, however, the analysis obtained by the independent lab shows less Hg concentration than some of ADA's results.

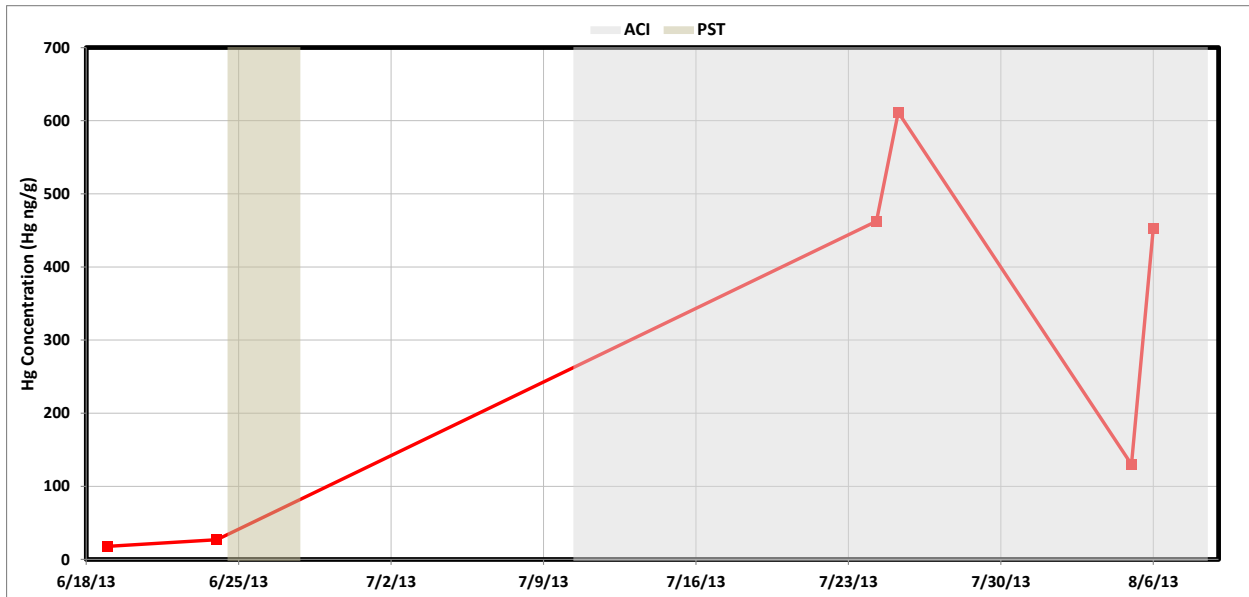


Figure 39. ADA Multiclone Hg Analyses

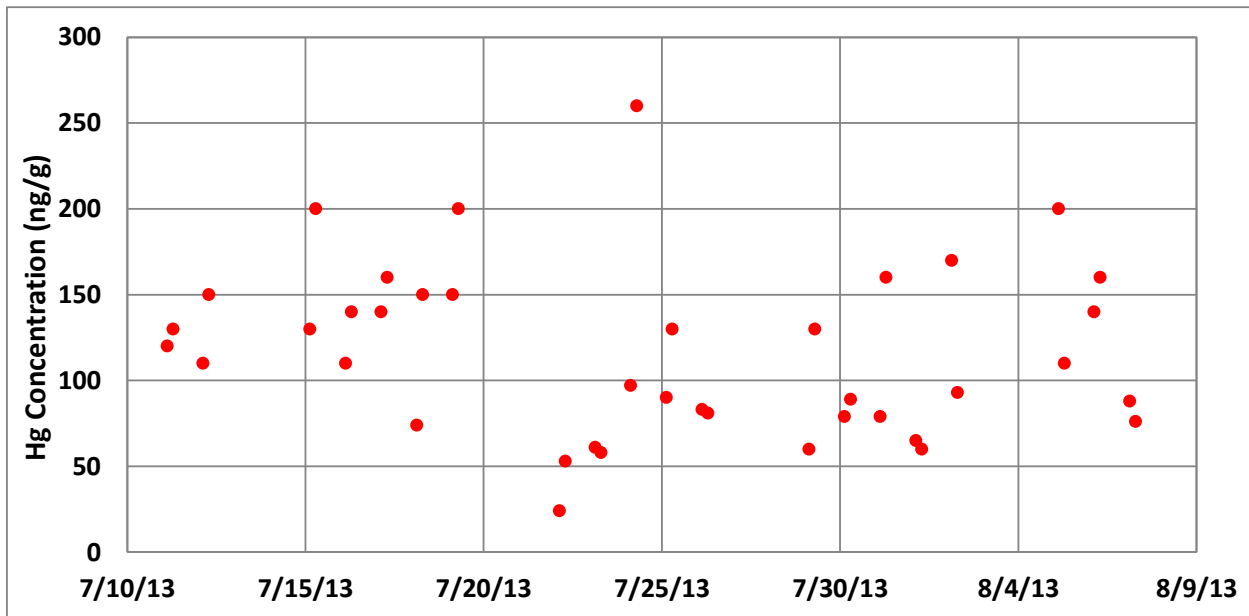


Figure 40. Independent Phase II Testing Multiclone Hg Analysis

Figure 41 shows the ADA obtained Hg concentration in the Fine Tailings. Figure 42 displays the Hg concentration acquired by the independent lab. Both analyses indicate higher concentrations at the beginning of Phase II testing but the available data appear to decrease toward the end of Phase II testing.

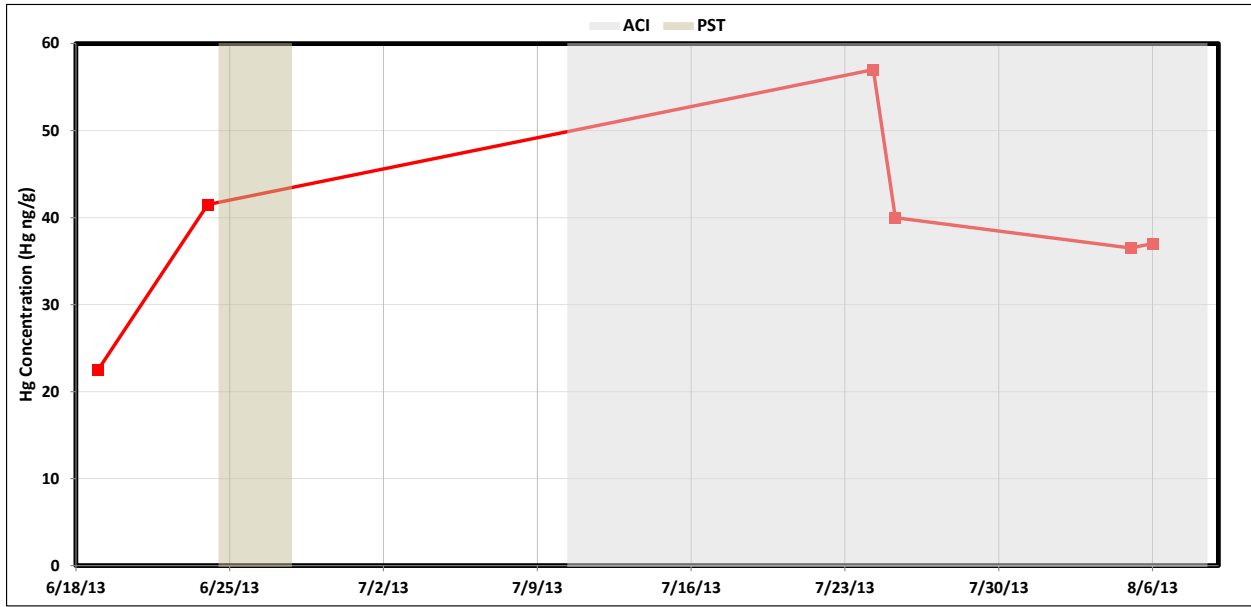


Figure 41. ADA Fine Tailings Hg Analyses

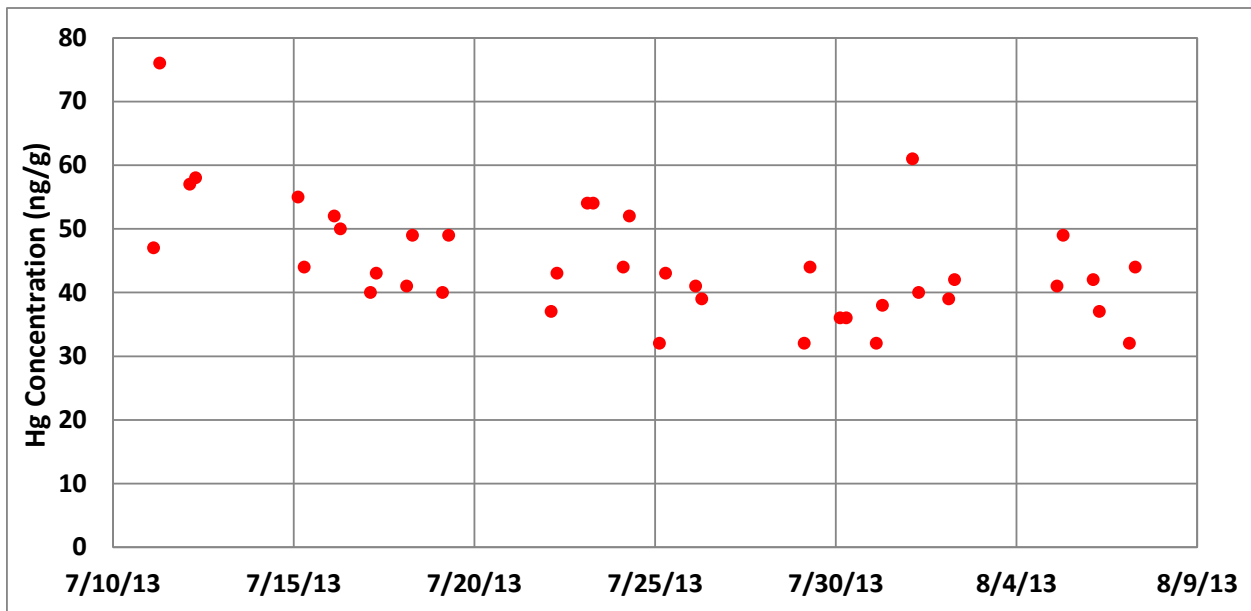


Figure 42. Independent Phase II Testing Fine Tailings Hg Analysis

Figure 43 shows the ADA measured Hg concentration in the fired Pellets. The figure shows no significant change in the relatively small amount of measured Hg within the Pellets as compared to the two data points from before the ACI injection. Little mercury was expected in this sample because the mercury should volatilize at the high temperatures in the furnace. The independent lab results showed all non-detects so the data is not presented.

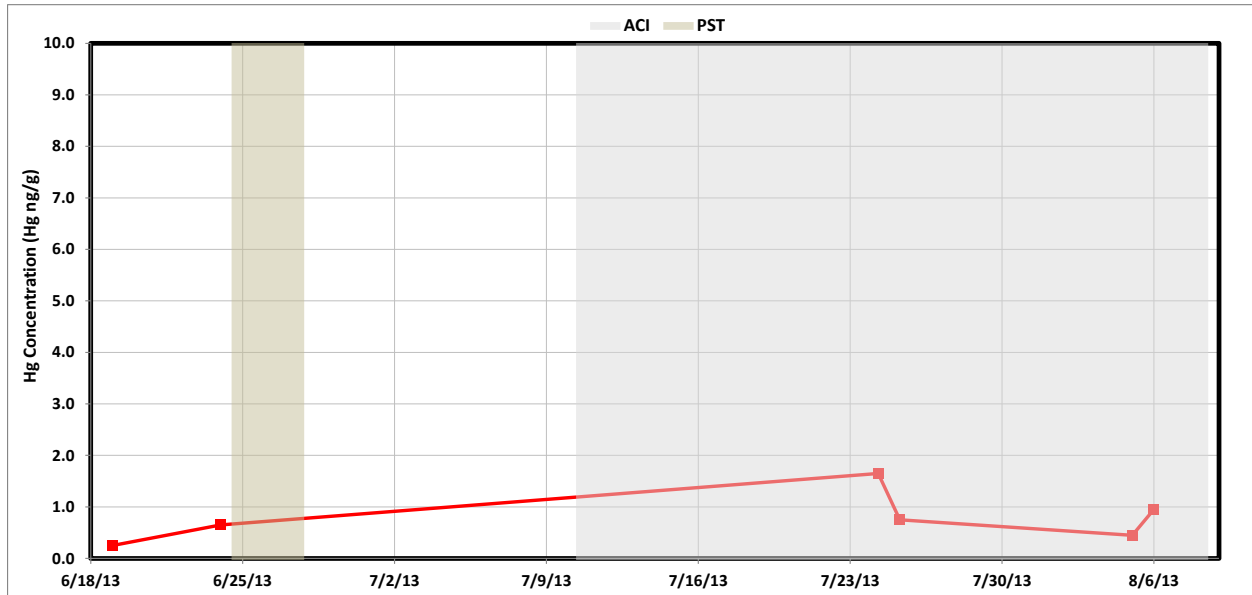


Figure 43. ADA Fired Pellets Hg Analysis

4.3 QA/QC

4.3.1 Sample Calculations

Modified Method 30B QA/QC Procedures

To provide assurance that the reported Hg-CEMS concentrations are accurate, ADA uses sorbent trap measurements as a quality control check. As a reference method, the paired sorbent trap measurements must meet a self-consistency criterion, and the average Hg-CEMS measurement must satisfy a relative accuracy criterion compared to the MM30B results. The criteria described below are derived from Title 40, CFR Part 75.

The paired sorbent trap results shall agree with each other according to Table 6.

Table 6. M30B Relative Deviation

Concentration Range	Criteria
C > 1 µg/dscm	Relative Deviation shall not exceed 10%
C < 1 µg/dscm	Relative Deviation shall not exceed 20%

To determine the concentration range for selecting the appropriate criteria, the average of the two sorbent trap concentrations, C, results shall be used.

Relative Deviation (RD) is defined in Title 40, CFR Part 75, Appendix K as:

$$RD = 100 \times \frac{|C_a - C_b|}{C_a + C_b}$$

Where: C_a and C_b are the paired MM30B concentrations of a sample run.

The average Hg-CEMS concentration shall agree with the average MM30B concentration, C, according to Table 7.

Table 7. Hg-CEMS Relative Accuracy

Concentration Range	Criteria
C > 5 µg/dscm	Relative Accuracy shall not exceed 20%
C < 5 µg/dscm	Absolute Mean Difference shall not exceed 1 µg/dscm

To determine the concentration range for selecting the appropriate criteria, average MM30B concentration, C, shall be used.

Relative Accuracy (RA) is defined as:

$$RA = 100 \times \frac{|C - C_{CEM,ave}|}{C}$$

Absolute Mean Difference (AMD) is defined as:

$$AMD = |C - C_{CEM,ave}|$$

The average Hg-CEMS concentration, $C_{CEM,ave}$, shall be determined by numerically averaging the available concentration data from the period during which the MM30B measurements were obtained.

4.3.2 MM30B and Hg-CEMS Comparison

Appendix D contains all of the MM30B data obtained during the test at Minorca. The table also shows the average Hg-CEMS data at the stacks and the results of the comparison to corresponding MM30B data.

This comparison was done with one significant exception to the QA/QC procedure described above. The RA/AMD procedure assumes that there is no significant HgP in the stack gas. However, ADA discovered that with ACI operating at Minorca, HgP was a significant portion of the total mercury. This was determined by analyzing the first glass wool section of the sorbent trap, which is assumed to contain all of the particulate, separately from the other two sorbent sections. This allowed ADA to calculate a value for MM30B gas phase mercury ($HgG = HgT - HgP$) which was then used to perform the RA/AMD calculations. It is important to note that Hg-CEMS can only measure HgG. As Figure 27 shows, the MM30B HgG compared well with Hg-CEMS, but the MM30B HgT did not; indicating a significant amount of HgP.

The gas moisture at the Hood Exhaust was 6.1% and at the Windbox Exhaust was 8.5%. The moisture at stacks A, B, C, and D was 11.5%, 12.2%, 13.6%, and 14.9% respectively based on stack measurements by Barr during testing.

5.0 CONCLUSIONS

The Screening Test was conducted by injecting three different PACs at three rates into the Windbox Exhaust via an injection grid with 8 lances. Phase II testing ran for 30 days, injecting BPAC into only the Wind Box Exhaust at a rate of 3 lb/mmacf. Various solids samples were collected and analyzed for carbon and Hg to assess the fate of mercury recycled back to the process with the scrubber water.

The following conclusions can be drawn from the ACI tests at Minorca:

- Albemarle's BPAC performed well in the Screening Test and was selected for Phase II testing due to its performance and relatively low cost.
- The coarser ground PAC did not perform as well as the standard PACs in Stack D. The results of the PM tests with this material will be presented by Barr in a separate report.
- MM30B results, using the modified M30B procedure, show that total Hg reduction at 3 lb/mmacf of ACI was 54%; and therefore, the goal of 75% **total Hg reduction** is not obtainable at Minorca with the current system configuration.
- The Hg-CEMS showed the **gas phase Hg reduction** was 76% at 3 lb/mmacf.
- Particulate phase HgP in the stack gas significantly increased with ACI in Stacks C and D. Sorbent traps can be analyzed in such a way to give an estimate of HgP whereas the Hg-CEMS cannot. The Hg-CEMS values (HgG) agreed well with HgG MM30B data, but not with the total MM30B HgT values due to the particulate mercury (HgP).
- Mercury concentrations measured in the process samples during the 30-day trial provide an initial indication that most of the Hg recycled back to the process with the scrubber water does not end up in the green balls.
- Multiclone solids showed an increase in Hg with ACI.
- A three to four week period is not sufficient to determine the effects of all the external processes of ore type, green ball composition, plant operations, holding basin water recycle, etc. A longer period of time with a more rigorous effluent sampling plan would be required to determine the ultimate fate of mercury captured by the PAC.



6.0 APPENDIX A - HG-CEMS DATA (ELECTRONIC)

All Hg-CEMS data was sent to the ArcelorMittal Minorca Project Manager electronically with the Final Report.





7.0 APPENDIX B - HG-CEMS CALIBRATION DATA

FULL RAK CEMS CALIBRATION RECORD																	
DATE	TIME	TYPE	LEVEL	SPAN	ELEM ZERO		ELEM SPAN		TOTAL ZERO		TOTAL SPAN		OCOEFF	TCOEFF	OBKG	TBKG	DILF
6/19	8:26	iMCAL	5.0	10	--	--	--	--	--	--	--	--	1.000	1.000	0.00	0.00	1.00
6/19	9:00	iMUP	--	--	--	--	--	--	--	--	--	--	1.000	1.000	0.04	0.04	1.00
6/19	9:00	iCALC	--	--	--	--	--	--	--	--	--	--	--	--	--	--	--
6/19	9:01	iMCAL	10.0	10	--	--	--	--	--	--	--	--	1.000	1.000	0.04	0.04	1.00
6/19	9:37	iMUP	--	--	--	--	--	--	--	--	--	--	1.014	1.002	0.04	0.04	1.00
6/19	9:37	iCALC	--	--	--	--	--	--	--	--	--	--	--	--	--	--	--
6/19	9:38	iCHK	10.0	10	0.00	0.0%	9.98	-0.2%	0.00	0.0%	10.01	0.1%	1.014	1.002	0.04	0.04	1.00
6/19	10:05	iCALC	--	--	--	--	--	--	--	--	--	--	1.016	0.999	0.04	0.04	1.00
6/19	10:06	iCHK	9.0	10	0.00	0.0%	9.04	0.4%	0.00	0.0%	9.04	0.4%	1.014	1.002	0.04	0.04	1.00
6/19	10:52	iCALC	--	--	--	--	--	--	--	--	--	--	1.009	1.003	0.04	0.04	1.00
6/19	11:00	CHG	--	--	--	--	--	--	--	--	--	--	0.989	0.934	1.19	0.98	29.50
6/19	13:07	MCAL	10.0	10	0.47	4.7%	7.66	-23%	0.94	9.4%	7.45	-26%	1.000	1.000	0.00	0.00	29.50
6/19	13:41	MUP	--	--	--	--	--	--	--	--	--	--	1.000	1.000	1.42	1.49	29.50
6/19	13:41	CALC	--	--	--	--	--	--	--	--	--	--	1.374	1.032	1.70	2.95	29.50
6/19	13:43	MCAL	10.0	10	0.10	1.0%	9.94	-0.6%	0.48	4.8%	10.22	2.2%	1.000	1.000	1.42	1.49	37.70
6/19	14:16	MUP	--	--	--	--	--	--	--	--	--	--	1.011	0.996	1.48	1.81	37.70
6/19	14:16	CALC	--	--	--	--	--	--	--	--	--	--	1.015	1.012	1.54	2.03	37.70
6/19	14:18	CHK	10.0	10	0.06	0.6%	10.18	1.8%	0.15	1.5%	10.24	2.4%	1.011	0.996	1.48	1.81	37.70
6/19	14:49	CALC	--	--	--	--	--	--	--	--	--	--	0.999	0.999	1.52	1.94	37.70
6/19	16:00	CHK	9.0	10	-0.02	-0.2%	8.54	-4.6%	-0.03	-0.3%	8.64	-3.6%	1.011	0.996	1.48	1.81	37.70
6/19	16:29	CALC	--	--	--	--	--	--	--	--	--	--	1.063	0.983	1.54	1.84	37.70
6/19	17:11	oCHK	10.0	10	-0.12	-1.2%	20.08	101%	-0.48	-4.8%	19.15	92%	1.011	0.996	1.48	1.81	37.70
6/19	17:40	oCALC	--	--	--	--	--	--	--	--	--	--	0.500	1.025	0.68	0.68	37.70
6/20	6:00	CHK	9.0	10	-0.04	-0.4%	8.59	-4.1%	-0.20	-2.0%	8.68	-3.2%	1.011	0.996	1.48	1.81	37.70
6/20	6:29	CALC	--	--	--	--	--	--	--	--	--	--	1.053	0.969	1.50	1.63	37.70
6/20	10:31	LIN	3.0	--	--	--	2.84	-6.1%	--	--	2.89	-4.7%	1.011	0.996	1.48	1.81	37.70
6/20	10:46	LIN	5.0	--	--	--	4.90	-2.1%	--	--	4.87	-2.7%	1.011	0.996	1.48	1.81	37.70
6/20	11:10	LIN	9.0	--	--	--	9.18	2.0%	--	--	9.11	1.2%	1.011	0.996	1.48	1.81	37.70
6/21	8:15	CHK	9.0	10	-0.12	-1.2%	9.37	3.7%	-0.41	-4.1%	9.12	1.2%	1.011	0.996	1.48	1.81	37.70
6/21	8:44	CALC	--	--	--	--	--	--	--	--	--	--	0.959	0.991	1.29	1.32	37.70
6/22	6:00	CHK	9.0	10	-0.07	-0.7%	9.75	7.5%	-0.32	-3.2%	9.57	5.7%	1.011	0.996	1.48	1.81	37.70
6/22	6:29	CALC	--	--	--	--	--	--	--	--	--	--	0.927	0.989	1.30	1.35	37.70
6/22	7:22	CHG	--	--	--	--	--	--	--	--	--	--	0.927	0.989	1.30	1.35	37.70
6/23	6:00	CHK	9.0	10	0.03	0.3%	8.86	-1.4%	0.06	0.6%	9.12	1.2%	0.927	0.989	1.30	1.35	37.70
6/23	6:29	CALC	--	--	--	--	--	--	--	--	--	--	0.945	0.964	1.35	1.40	37.70
6/24	6:00	CHK	9.0	10	0.05	0.5%	9.79	7.9%	0.06	0.6%	9.74	7.4%	0.927	0.989	1.30	1.35	37.70
6/24	6:29	CALC	--	--	--	--	--	--	--	--	--	--	0.856	0.995	1.24	1.31	37.70
6/24	7:11	CHG	--	--	--	--	--	--	--	--	--	--	0.856	0.995	1.24	1.31	37.70
6/24	21:52	DILP	CHANGE FROM 44 psi -- DOWN TO 40 psi AT 6/24 22:02 -- STABLE TO 43 psi AT 6/24 22:08														
6/25	3:45	DILP	CHANGE FROM 43 psi -- STABLE TO 45 psi AT 6/25 03:51														
6/25	6:00	CHK	9.0	10	0.02	0.2%	9.12	1.2%	0.06	0.6%	9.35	3.5%	0.856	0.995	1.24	1.31	37.70
6/25	6:29	CALC	--	--	--	--	--	--	--	--	--	--	0.847	0.974	1.25	1.33	37.70
6/25	14:24	DILP	CHANGE FROM 43 psi -- DOWN TO 43 psi AT -- STABLE TO 46 psi AT 6/25 14:30														
6/25	23:50	DILP	CHANGE FROM 46 psi -- STABLE TO 44 psi AT 6/25 23:56														
6/26	6:00	CHK	9.0	10	0.04	0.4%	9.19	1.9%	0.08	0.8%	9.44	4.4%	0.856	0.995	1.24	1.31	37.70
6/26	6:29	CALC	--	--	--	--	--	--	--	--	--	--	0.842	0.973	1.26	1.34	37.70
6/26	7:18	DILP	CHANGE FROM 46 psi -- DOWN TO 43 psi AT 6/26 07:22 -- STABLE TO 46 psi AT 6/26 07:31														
6/27	6:00	CHK	9.0	10	0.04	0.4%	9.12	1.2%	0.05	0.5%	9.36	3.6%	0.856	0.995	1.24	1.31	37.70
6/27	6:29	CALC	--	--	--	--	--	--	--	--	--	--	0.848	0.971	1.27	1.31	37.70
6/28	6:00	CHK	9.0	10	0.04	0.4%	9.52	5.2%	0.01	0.1%	9.49	4.9%	0.856	0.995	1.24	1.31	37.70
6/28	6:29	CALC	--	--	--	--	--	--	--	--	--	--	0.812	0.996	1.21	1.26	37.70
6/28	14:51	CHG	--	--	--	--	--	--	--	--	--	--	0.812	0.996	1.21	1.26	37.70
6/29	6:00	CHK	9.0	10	0.00	0.0%	9.24	2.4%	0.04	0.4%	9.31	3.1%	0.812	0.996	1.21	1.26	37.70
6/29	6:29	CALC	--	--	--	--	--	--	--	--	--	--	0.791	0.993	1.18	1.27	37.70
6/29	13:59	CNVT	CHANGE FROM 760°C -- UP TO 771°C AT 6/29 13:59 -- STABLE TO 761°C AT 6/29 14:05														
6/30	6:00	CHK	9.0	10	0.05	0.5%	9.27	2.7%	0.09	0.9%	9.16	1.6%	0.812	0.996	1.21	1.26	37.70
6/30	6:29	CALC	--	--	--	--	--	--	--	--	--	--	0.792	1.014	1.23	1.34	37.70
7/1	6:00	CHK	9.0	10	0.06	0.6%	8.85	-1.5%	0.18	1.8%	8.91	-0.9%	0.812	0.996	1.21	1.26	37.70





ArcelorMittal
Minorca Mine
ACI Test

7/1	6:29	CALC	--	--	--	--	--	--	--	--	--	--	0.832	1.002	1.30	1.48	37.70
7/2	6:00	CHK	9.0	10	0.10	1.0%	9.39	3.9%	0.16	1.6%	9.28	2.8%	0.812	0.996	1.21	1.26	37.70
7/2	6:29	CALC	--	--	--	--	--	--	--	--	--	--	0.787	1.014	1.27	1.40	37.70
7/3	6:00	CHK	9.0	10	0.08	0.8%	9.40	4.0%	0.11	1.1%	9.21	2.1%	0.812	0.996	1.21	1.26	37.70
7/3	6:29	CALC	--	--	--	--	--	--	--	--	--	--	0.784	1.020	1.25	1.36	37.70
7/3	20:39	DILP	CHANGE FROM 46 psi — DOWN TO 44 psi AT 7/3 20:41 — STABLE TO 45 psi AT 7/3 20:48														
7/3	23:13	DILP	CHANGE FROM 45 psi — DOWN TO 43 psi AT 7/3 23:14 — STABLE TO 47 psi AT 7/3 23:20														
7/4	6:00	CHK	9.0	10	0.10	1.0%	9.46	4.6%	0.11	1.1%	9.36	3.6%	0.812	0.996	1.21	1.26	37.70
7/4	6:29	CALC	--	--	--	--	--	--	--	--	--	--	0.781	1.008	1.26	1.33	37.70
7/5	6:00	CHK	9.0	10	0.08	0.8%	9.36	3.6%	0.13	1.3%	9.26	2.6%	0.812	0.996	1.21	1.26	37.70
7/5	6:29	CALC	--	--	--	--	--	--	--	--	--	--	0.787	1.013	1.25	1.37	37.70
7/6	6:00	CHK	9.0	10	0.06	0.6%	9.43	4.3%	0.12	1.2%	9.25	2.5%	0.812	0.996	1.21	1.26	37.70
7/6	6:29	CALC	--	--	--	--	--	--	--	--	--	--	0.780	1.022	1.22	1.36	37.70
7/7	6:00	CHK	9.0	10	0.04	0.4%	8.85	-1.5%	0.13	1.3%	8.79	-2.1%	0.812	0.996	1.21	1.26	37.70
7/7	6:29	CALC	--	--	--	--	--	--	--	--	--	--	0.829	1.013	1.28	1.44	37.70
7/7	10:52	CNVT	CHANGE FROM 752°C — UNSTABLE 728°C TO 779°C — STABLE TO 758°C AT 7/7 11:04														
7/7	11:59	DILP	CHANGE FROM 47 psi — DOWN TO 42 psi AT 7/7 12:28 — STABLE TO 47 psi AT 7/7 12:43														
7/7	14:46	DILP	CHANGE FROM 47 psi — DOWN TO 44 psi AT 7/7 14:58 — STABLE TO 46 psi AT 7/7 15:04														
7/8	6:00	CHK	9.0	10	0.06	0.6%	9.29	2.9%	0.10	1.0%	9.17	1.7%	0.812	0.996	1.21	1.26	37.70
7/8	6:29	CALC	--	--	--	--	--	--	--	--	--	--	0.791	1.014	1.23	1.35	37.70
7/9	6:00	CHK	9.0	10	0.11	1.1%	9.71	7.1%	0.17	1.7%	9.49	4.9%	0.812	0.996	1.21	1.26	37.70
7/9	6:29	CALC	--	--	--	--	--	--	--	--	--	--	0.761	1.027	1.23	1.38	37.70
7/9	8:05	CHG	--	--	--	--	--	--	--	--	--	--	0.761	1.027	1.23	1.38	37.70
7/10	0:28	CNVT	CHANGE FROM 759°C — UNSTABLE 554°C TO 770°C — STABLE TO 759°C AT 7/10 00:45														
7/10	1:18	CNVT	CHANGE FROM 759°C — UNSTABLE 584°C TO 786°C — STABLE TO 739°C AT 7/10 01:33														
7/10	1:45	CNVT	CHANGE FROM 739°C — UNSTABLE 618°C TO 770°C — STABLE TO 755°C AT 7/10 01:57														
7/10	1:58	CNVT	CHANGE FROM 755°C — UNSTABLE 636°C TO 763°C — STABLE TO 750°C AT 7/10 02:09														
7/10	6:00	CHK	9.0	10	0.07	0.7%	8.85	-1.5%	0.07	0.7%	8.97	-0.3%	0.761	1.027	1.23	1.38	37.70
7/10	6:29	CALC	--	--	--	--	--	--	--	--	--	--	0.780	1.014	1.33	1.47	37.70
7/11	8:00	CHK	9.0	10	0.04	0.4%	7.88	-11%	-0.01	-0.1%	8.40	-6.0%	0.761	1.027	1.23	1.38	37.70
7/11	8:29	CALC	--	--	--	--	--	--	--	--	--	--	0.874	0.957	1.46	1.46	37.70
7/11	9:40	MCAL	9.0	10	-0.26	-2.6%	5.60	-34%	-0.32	-3.2%	6.34	-27%	0.761	1.027	1.23	1.38	37.70
7/11	9:49	DILP	CHANGE FROM 47 psi — DOWN TO 41 psi AT 7/11 09:56 — STABLE TO 48 psi AT 7/11 10:06														
7/11	10:14	MUP	--	--	--	--	--	--	--	--	--	--	0.761	1.027	0.93	1.05	37.70
7/11	10:14	CALC	--	--	--	--	--	--	--	--	--	--	1.169	0.903	1.48	1.43	37.70
7/11	10:36	iCHK	9.0	10	0.01	0.1%	10.31	13%	0.01	0.1%	10.41	14%	1.014	1.002	0.04	0.04	1.00
7/11	10:47	iCALC	--	--	--	--	--	--	--	--	--	--	0.886	0.992	0.04	0.04	1.00
7/11	10:53	CHG	--	--	--	--	--	--	--	--	--	--	0.761	1.027	0.93	1.05	37.70
7/11	11:58	MCAL	9.0	10	0.04	0.4%	6.06	-29%	0.01	0.1%	6.36	-26%	0.761	1.027	0.93	1.05	37.70
7/11	12:27	MUP	--	--	--	--	--	--	--	--	--	--	1.136	0.974	1.43	1.49	37.70
7/11	12:27	CALC	--	--	--	--	--	--	--	--	--	--	1.138	0.973	1.45	1.50	37.70
7/11	12:30	CHK	9.0	10	-0.01	-0.1%	8.99	-0.1%	0.00	0.0%	9.15	1.5%	1.136	0.974	1.43	1.49	37.70
7/11	12:59	CALC	--	--	--	--	--	--	--	--	--	--	1.136	0.957	1.42	1.46	37.70
7/12	7:30	CHK	9.0	10	0.00	0.0%	7.86	-11%	0.09	0.9%	8.13	-8.7%	1.136	0.974	1.43	1.49	37.70
7/12	7:59	CALC	--	--	--	--	--	--	--	--	--	--	1.299	0.952	1.64	1.76	37.70
7/12	9:38	MCAL	9.0	10	-0.02	-0.2%	8.35	-6.5%	0.05	0.5%	8.54	-4.6%	1.136	0.974	1.43	1.49	37.70
7/12	10:10	MUP	--	--	--	--	--	--	--	--	--	--	1.221	0.959	1.50	1.58	37.70
7/12	10:10	CALC	--	--	--	--	--	--	--	--	--	--	1.221	0.960	1.52	1.63	37.70
7/12	10:15	CHK	9.0	10	0.00	0.0%	9.14	1.4%	0.02	0.2%	9.13	1.3%	1.221	0.959	1.50	1.58	37.70
7/12	10:44	CALC	--	--	--	--	--	--	--	--	--	--	1.203	0.961	1.48	1.58	37.70
7/12	15:02	PRBT	CHANGE FROM 220°C — DOWN TO 117°C AT 7/12 15:21 — STABLE TO 220°C AT 7/12 15:49														
7/12	15:02	DILP	CHANGE FROM 48 psi — DOWN TO 1.4 psi AT 7/12 15:37 — STABLE TO 48 psi AT 7/12 15:45														
7/12	17:20	CHK	9.0	10	0.00	0.0%	9.23	2.3%	0.06	0.6%	9.32	3.2%	1.221	0.959	1.50	1.58	37.70
7/12	17:49	CALC	--	--	--	--	--	--	--	--	--	--	1.191	0.956	1.47	1.59	37.70
7/13	7:30	CHK	9.0	10	0.03	0.3%	9.67	6.7%	0.06	0.6%	9.52	5.2%	1.221	0.959	1.50	1.58	37.70
7/13	7:59	CALC	--	--	--	--	--	--	--	--	--	--	1.140	0.977	1.43	1.56	37.70
7/13	8:16	CHG	--	--	--	--	--	--	--	--	--	--	1.140	0.977	1.43	1.56	37.70
7/13	18:00	CHK	9.0	10	-0.13	-1.3%	7.03	-20%	-0.15	-1.5%	7.24	-18%	1.140	0.977	1.43	1.56	37.70
7/13	18:29	CALC	--	--	--	--	--	--	--	--	--	--	1.433	0.946	1.64	1.71	37.70
7/13	18:41	MCAL	9.0	10	0.92	9.2%	6.95	-21%	0.81	8.1%	7.13	-19%	1.140	0.977	1.43	1.56	37.70





ArcelorMittal
Minorca Mine
ACI Test

7/13	18:47	iCHK	5.0	10	0.01	0.1%	4.91	-0.9%	0.01	0.1%	4.89	-1.1%	1.014	1.002	0.04	0.04	1.00
7/13	19:01	iCALC	--	--	--	--	--	--	--	--	--	--	1.034	1.006	0.04	0.04	1.00
7/13	19:27	MUP	--	--	--	--	--	--	--	--	--	--	1.000	1.000	1.65	1.80	37.70
7/13	19:27	CALC	--	--	--	--	--	--	--	--	--	--	1.703	0.931	3.51	3.38	37.70
7/13	19:29	MCAL	9.0	10	0.03	0.3%	9.08	0.8%	-0.04	-0.4%	9.49	4.9%	1.000	1.000	1.65	1.80	54.00
7/13	19:58	MUP	--	--	--	--	--	--	--	--	--	--	0.993	0.953	1.65	1.68	54.00
7/13	19:58	CALC	--	--	--	--	--	--	--	--	--	--	0.994	0.950	1.67	1.66	54.00
7/13	20:15	CHK	9.0	10	0.01	0.1%	8.92	-0.8%	0.03	0.3%	8.93	-0.7%	0.993	0.953	1.65	1.68	54.00
7/13	20:44	CALC	--	--	--	--	--	--	--	--	--	--	1.003	0.954	1.68	1.73	54.00
7/14	7:30	CHK	9.0	10	-0.01	-0.1%	8.85	-1.5%	0.08	0.8%	9.16	1.6%	0.993	0.953	1.65	1.68	54.00
7/14	7:59	CALC	--	--	--	--	--	--	--	--	--	--	1.008	0.930	1.67	1.74	54.00
7/15	7:30	CHK	9.0	10	-0.02	-0.2%	8.80	-2.0%	-0.01	-0.1%	8.93	-0.7%	0.993	0.953	1.65	1.68	54.00
7/15	7:59	CALC	--	--	--	--	--	--	--	--	--	--	1.012	0.942	1.66	1.68	54.00
7/16	7:30	CHK	9.0	10	-0.24	-2.4%	8.90	-1.0%	-0.20	-2.0%	9.08	0.8%	0.993	0.953	1.65	1.68	54.00
7/16	7:59	CALC	--	--	--	--	--	--	--	--	--	--	0.978	0.939	1.39	1.43	54.00
7/17	3:05	CNVT	CHANGE FROM 746°C — UNSTABLE 568°C TO 777°C — STABLE TO 759°C AT 7/17 03:17														
7/17	5:11	CNVT	CHANGE FROM 759°C — DOWN TO 681°C AT 7/17 05:16 — STABLE TO 752°C AT 7/17 05:24														
7/17	7:30	CHK	9.0	10	-0.23	-2.3%	8.47	-5.3%	-0.18	-1.8%	8.81	-1.9%	0.993	0.953	1.65	1.68	54.00
7/17	7:59	CALC	--	--	--	--	--	--	--	--	--	--	1.026	0.923	1.47	1.49	54.00
7/17	8:11	CHG	--	--	--	--	--	--	--	--	--	--	1.026	0.923	1.47	1.49	54.00
7/18	7:25	CNVT	CHANGE FROM 760°C — UNSTABLE 390°C TO 811°C — STABLE TO 735°C AT 7/18 07:42														
7/18	8:24	CNVT	CHANGE FROM 735°C — UNSTABLE 233°C TO 821°C — STABLE TO 734°C AT 7/18 08:39														
7/18	9:00	CHK	9.0	10	0.02	0.2%	9.28	2.8%	-0.05	-0.5%	9.22	2.2%	1.026	0.923	1.47	1.49	54.00
7/18	9:29	CALC	--	--	--	--	--	--	--	--	--	--	0.997	0.923	1.45	1.40	54.00
19-Jul	8:30	CHK	9	10	0.02	0.20%	9.64	6.40%	-0.04	-0.40%	9.24	2.40%	1.026	0.923	1.47	1.49	54
19-Jul	8:59	CALC	--	--	--	--	--	--	--	--	--	--	0.959	0.957	1.39	1.4	54
20-Jul	7:30	CHK	9	10	0.04	0.40%	8.84	-1.60%	0.07	0.70%	9.1	1.00%	0.959	0.957	1.39	1.4	54
20-Jul	7:59	CALC	--	--	--	--	--	--	--	--	--	--	0.981	0.933	1.46	1.47	54
7/21	8:30	CHK	9.0	10	0.08	0.8%	9.21	2.1%	0.09	0.9%	9.33	3.3%	0.959	0.957	1.39	1.40	54.00
7/21	8:59	CALC	--	--	--	--	--	--	--	--	--	--	0.945	0.945	1.45	1.45	54.00
7/22	7:30	CHK	9.0	10	0.06	0.6%	8.93	-0.7%	0.05	0.5%	9.11	1.1%	0.959	0.957	1.39	1.40	54.00
7/22	7:59	CALC	--	--	--	--	--	--	--	--	--	--	0.973	0.937	1.47	1.45	54.00
7/23	7:30	CHK	9.0	10	0.06	0.6%	9.00	0.0%	0.04	0.4%	9.13	1.3%	0.959	0.957	1.39	1.40	54.00
7/23	7:59	CALC	--	--	--	--	--	--	--	--	--	--	0.966	0.941	1.46	1.43	54.00
24-Jul	8:30	CHK	9	10	0.09	0.90%	9.06	0.60%	0.08	0.80%	9.23	2.30%	0.959	0.957	1.39	1.4	54
24-Jul	8:59	CALC	--	--	--	--	--	--	--	--	--	--	0.962	0.939	1.48	1.46	54
7/25	7:30	CHK	9.0	10	0.08	0.8%	9.33	3.3%	0.08	0.8%	9.41	4.1%	0.959	0.957	1.39	1.40	54.00
7/25	7:59	CALC	--	--	--	--	--	--	--	--	--	--	0.933	0.949	1.43	1.43	54.00
7/26	6:40	CHK	9.0	10	0.08	0.8%	9.62	6.2%	0.07	0.7%	9.67	6.7%	0.959	0.957	1.39	1.40	54.00
7/26	7:09	CALC	--	--	--	--	--	--	--	--	--	--	0.905	0.950	1.38	1.37	54.00
7/26	7:41	CHG	--	--	--	--	--	--	--	--	--	--	0.905	0.950	1.38	1.37	54.00
7/26	21:39	CNVT	CHANGE FROM 758°C — UNSTABLE 732°C TO 775°C — STABLE TO 758°C AT 7/26 21:48														
7/27	6:40	CHK	9.0	10	0.04	0.4%	8.91	-0.9%	0.02	0.2%	8.81	-1.9%	0.905	0.950	1.38	1.37	54.00
7/27	7:09	CALC	--	--	--	--	--	--	--	--	--	--	0.919	0.959	1.44	1.43	54.00
7/28	3:47	CNVT	CHANGE FROM 760°C — UNSTABLE 747°C TO 773°C — STABLE TO 760°C AT 7/28 03:54														
7/28	5:40	CNVT	CHANGE FROM 760°C — UNSTABLE 733°C TO 768°C — STABLE TO 758°C AT 7/28 05:48														
7/28	6:40	CHK	9.0	10	0.08	0.8%	9.04	0.4%	0.06	0.6%	9.09	0.9%	0.905	0.950	1.38	1.37	54.00
7/28	7:09	CALC	--	--	--	--	--	--	--	--	--	--	0.909	0.942	1.47	1.42	54.00
7/29	6:40	CHK	9.0	10	0.09	0.9%	9.46	4.6%	0.05	0.5%	9.46	4.6%	0.905	0.950	1.38	1.37	54.00
7/29	7:09	CALC	--	--	--	--	--	--	--	--	--	--	0.870	0.946	1.42	1.36	54.00
7/30	6:40	CHK	9.0	10	0.06	0.6%	9.63	6.3%	0.06	0.6%	9.64	6.4%	0.905	0.950	1.38	1.37	54.00
7/30	7:09	CALC	--	--	--	--	--	--	--	--	--	--	0.851	0.949	1.36	1.34	54.00
7/30	9:12	CHG	--	--	--	--	--	--	--	--	--	--	0.851	0.949	1.36	1.34	54.00
7/30	9:49	CNVT	CHANGE FROM 760°C — STABLE TO 757°C AT 7/30 09:55														
7/30	23:06	RFINT	CHANGE FROM 50933 Hz — DOWN TO 49502 Hz AT 7/30 23:10 — STABLE TO 50858 Hz AT 7/30 23:16														
7/31	5:00	CHK	9.0	10	0.01	0.1%	8.95	-0.5%	0.01	0.1%	9.01	0.1%	0.851	0.949	1.36	1.34	54.00
7/31	5:29	CALC	--	--	--	--	--	--	--	--	--	--	0.857	0.942	1.38	1.35	54.00
8/1	5:00	CHK	9.0	10	0.03	0.3%	9.11	1.1%	0.03	0.3%	9.04	0.4%	0.851	0.949	1.36	1.34	54.00
8/1	5:29	CALC	--	--	--	--	--	--	--	--	--	--	0.843	0.957	1.37	1.37	54.00
8/2	5:00	CHK	9.0	10	0.03	0.3%	9.15	1.5%	0.07	0.7%	9.09	0.9%	0.851	0.949	1.36	1.34	54.00





ArcelorMittal
Minorca Mine
ACI Test

8/2	5:29	CALC	--	--	--	--	--	--	--	--	--	--	0.840	0.960	1.37	1.41	54.00
8/2	10:28	CNVT	CHANGE FROM 760°C — UNSTABLE 736°C TO 783°C — STABLE TO 755°C AT 8/2 10:36														
8/2	16:25	CNVT	CHANGE FROM 755°C — UP TO 795°C AT 8/2 16:26 — STABLE TO 762°C AT 8/2 16:32														
8/3	5:00	CHK	9.0	10	0.07	0.7%	9.21	2.1%	0.08	0.8%	9.23	2.3%	0.851	0.949	1.36	1.34	54.00
8/3	5:29	CALC	--	--	--	--	--	--	--	--	--	--	0.838	0.949	1.40	1.40	54.00
8/4	7:05	CHK	9.0	10	0.08	0.8%	9.36	3.6%	0.13	1.3%	9.36	3.6%	0.851	0.949	1.36	1.34	54.00
8/4	7:34	CALC	--	--	--	--	--	--	--	--	--	--	0.825	0.955	1.39	1.44	54.00
8/5	5:00	CHK	9.0	10	0.08	0.8%	9.28	2.8%	0.09	0.9%	9.32	3.2%	0.851	0.949	1.36	1.34	54.00
8/5	5:29	CALC	--	--	--	--	--	--	--	--	--	--	0.833	0.946	1.41	1.40	54.00
8/6	5:00	CHK	9.0	10	0.06	0.6%	9.36	3.6%	0.09	0.9%	9.49	4.9%	0.851	0.949	1.36	1.34	54.00
8/6	5:29	CALC	--	--	--	--	--	--	--	--	--	--	0.823	0.940	1.38	1.37	54.00
8/7	5:00	CHK	9.0	10	0.06	0.6%	9.28	2.8%	0.11	1.1%	9.28	2.8%	0.851	0.949	1.36	1.34	54.00
8/7	5:29	CALC	--	--	--	--	--	--	--	--	--	--	0.830	0.954	1.38	1.42	54.00
8/8	5:00	CHK	9.0	10	0.09	0.9%	9.58	5.8%	0.16	1.6%	9.59	5.9%	0.851	0.949	1.36	1.34	54.00
8/8	5:29	CALC	--	--	--	--	--	--	--	--	--	--	0.807	0.955	1.38	1.43	54.00
8/8	7:42	CHG	--	--	--	--	--	--	--	--	--	--	0.807	0.955	1.38	1.43	54.00
8/9	5:00	CHK	9.0	10	0.04	0.4%	9.50	5.0%	0.03	0.3%	9.18	1.8%	0.807	0.955	1.38	1.43	54.00
8/9	5:29	CALC	--	--	--	--	--	--	--	--	--	--	0.768	0.988	1.35	1.44	54.00





ArcelorMittal
Minorca Mine
ACI Test

MODRAK CEMS CALIBRATION RECORD																	
DATE	TIME	TYPE	LEVEL	SPAN	ELEM ZERO		ELEM SPAN		TOTAL ZERO		TOTAL SPAN		OCOE	TCOE	OBKG	TBKG	DILF
6/18	17:09	CHG	--	--	--	--	--	--	--	--	--	--	1.028	0.987	10.29	10.12	52.50
6/18	18:13	VAC	CHANGE FROM 21 inHg — DOWN TO 2.2 inHg AT 6/18 18:18 — STABLE TO 22 inHg AT 6/18 18:39														
6/18	18:14	ORFP	CHANGE FROM 0.4 psi — UP TO 0.5 psi AT 6/18 18:29 — STABLE TO 0.4 psi AT 6/18 18:37														
6/18	22:35	PMTV	CHANGE FROM 586V — STABLE TO 569V AT 6/18 22:53														
6/19	8:26	iMCAL	5.0	10	--	--	--	--	--	--	--	--	1.000	1.000	0.00	0.00	52.50
6/19	9:10	iMUP	--	--	--	--	--	--	--	--	--	--	1.000	1.000	0.18	0.18	52.50
6/19	9:10	iCALC	--	--	--	--	--	--	--	--	--	--	--	--	--	--	
6/19	9:11	iMCAL	10.0	10	--	--	--	--	--	--	--	--	1.000	1.000	0.18	0.18	
6/19	10:29	iMUP	--	--	--	--	--	--	--	--	--	--	0.960	1.000	0.14	0.14	
6/19	10:29	iCALC	--	--	--	--	--	--	--	--	--	--	--	--	--	--	
6/19	10:30	iCHK	10.0	10	0.00	0.0%	9.93	-0.7%	0.00	0.0%	9.90	-1.0%	0.960	1.001	0.14	0.14	
6/19	10:53	iCALC	--	--	--	--	--	--	--	--	--	--	0.967	1.003	0.14	0.14	
6/19	10:54	iCHK	9.0	10	0.00	0.0%	8.83	-1.7%	0.00	0.0%	8.81	-1.9%	0.960	1.001	0.14	0.14	
6/19	11:30	iCALC	--	--	--	--	--	--	--	--	--	--	0.978	1.003	0.14	0.14	
6/19	11:35	CHG	--	--	--	--	--	--	--	--	--	--	1.028	0.987	10.29	10.12	
6/19	13:09	iMCAL	5.0	10	--	--	--	--	--	--	--	--	0.960	1.001	0.14	0.14	
6/19	13:29	iMUP	--	--	--	--	--	--	--	--	--	--	1.003	1.003	0.14	0.14	
6/19	13:29	iCALC	--	--	--	--	--	--	--	--	--	--	--	--	--	--	
6/19	13:30	iCHK	10.0	10	0.00	0.0%	10.30	3.0%	0.00	0.0%	10.30	3.0%	1.003	1.003	0.14	0.14	
6/19	14:12	iCALC	--	--	--	--	--	--	--	--	--	--	0.974	1.003	0.14	0.14	
6/19	14:18	MCAL	10.0	10	2.01	20%	12.17	22%	3.74	37%	12.34	23%	1.000	1.000	0.00	0.00	
6/19	14:52	MUP	--	--	--	--	--	--	--	--	--	--	1.000	1.000	7.24	7.13	
6/19	14:52	CALC	--	--	--	--	--	--	--	--	--	--	0.993	1.171	13.82	12.90	
6/19	14:54	MCAL	10.0	10	0.02	0.2%	10.07	0.7%	0.00	0.0%	10.39	3.9%	1.000	1.000	7.24	7.13	
6/19	15:26	MUP	--	--	--	--	--	--	--	--	--	--	0.994	0.968	7.20	6.86	
6/19	15:26	CALC	--	--	--	--	--	--	--	--	--	--	0.995	0.967	7.22	6.86	
6/19	16:15	CHK	10.0	10	0.01	0.1%	9.79	-2.1%	-0.02	-0.2%	9.83	-1.7%	0.994	0.968	7.20	6.86	
6/19	16:44	CALC	--	--	--	--	--	--	--	--	--	--	1.016	0.961	7.36	6.94	
6/19	17:11	oCHK	10.0	10	-0.01	-0.1%	16.87	69%	-0.01	-0.1%	16.80	68%	0.994	0.968	7.20	6.86	
6/19	17:41	oCALC	--	--	--	--	--	--	--	--	--	--	0.588	0.973	4.25	4.08	
6/20	6:00	CHK	9.0	10	-0.05	-0.5%	8.67	-3.3%	0.01	0.1%	8.78	-2.2%	0.994	0.968	7.20	6.86	
6/20	6:29	CALC	--	--	--	--	--	--	--	--	--	--	1.026	0.963	7.37	7.06	
6/20	10:18	LIN	3.0	--	--	--	3.04	1.3%	--	--	3.21	7.1%	0.994	0.968	7.20	6.86	
6/20	10:31	LIN	3.0	--	--	--	2.82	-6.2%	--	--	2.90	-3.7%	0.994	0.968	7.20	6.86	
6/20	10:46	LIN	5.0	--	--	--	4.74	-5.2%	--	--	4.86	-2.8%	0.994	0.968	7.20	6.86	
6/20	11:11	LIN	9.0	--	--	--	8.81	-2.1%	--	--	8.85	-1.7%	0.994	0.968	7.20	6.86	
6/20	11:46	LIN	9.0	--	--	--	8.73	-3.0%	--	--	8.81	-2.1%	0.994	0.968	7.20	6.86	
6/20	18:15	PMTV	CHANGE FROM 569V — UNSTABLE 568V TO 570V — STABLE TO 569V AT 6/20 18:22														
6/21	8:45	CHK	9.0	10	0.01	0.1%	8.64	-3.6%	-0.02	-0.2%	8.75	-2.5%	0.994	0.968	7.20	6.86	52.50
6/21	9:14	CALC	--	--	--	--	--	--	--	--	--	--	1.036	0.954	7.51	7.03	52.50
6/21	15:47	DILP	CHANGE FROM 44.2 psi — STABLE TO -11.1 psi AT 6/21 15:53														
6/21	17:10	DILP	CHANGE FROM -11 psi — STABLE TO 45 psi AT 6/21 17:16														
6/22	11:30	CHK	9.0	10	0.00	0.0%	8.79	-2.1%	0.06	0.6%	8.91	-0.9%	0.994	0.968	7.20	6.86	52.50
6/22	11:59	CALC	--	--	--	--	--	--	--	--	--	--	1.017	0.962	7.37	7.04	52.50
6/23	6:00	CHK	9.0	10	-0.12	-1.2%	8.64	-3.6%	0.04	0.4%	8.73	-2.7%	0.994	0.968	7.20	6.86	52.50
6/23	6:29	CALC	--	--	--	--	--	--	--	--	--	--	1.022	0.975	7.28	7.14	52.50
6/23	11:47	PRBT	CHANGE FROM 220°C — DOWN TO 186°C AT 6/23 11:54 — STABLE TO 220°C AT 6/23 12:41														
6/23	11:48	DILP	CHANGE FROM 45 psi — DOWN TO 1.2 psi AT 6/23 11:55 — STABLE TO 45 psi AT 6/23 12:02														
6/24	6:00	CHK	9.0	10	0.01	0.1%	8.79	-2.1%	0.05	0.5%	8.85	-1.5%	0.994	0.968	7.20	6.86	52.50
6/24	6:29	CALC	--	--	--	--	--	--	--	--	--	--	1.019	0.965	7.39	7.06	52.50
6/24	7:10	CHG	--	--	--	--	--	--	--	--	--	--	1.019	0.965	7.39	7.01	52.50
6/25	6:00	CHK	9.0	10	0.00	0.0%	8.96	-0.4%	0.07	0.7%	9.09	0.9%	1.019	0.965	7.39	7.01	52.50
6/25	6:29	CALC	--	--	--	--	--	--	--	--	--	--	1.023	0.958	7.42	7.06	52.50
6/26	6:00	CHK	9.0	10	-0.05	-0.5%	8.98	-0.2%	0.03	0.3%	9.07	0.7%	1.019	0.965	7.39	7.01	52.50
6/26	6:29	CALC	--	--	--	--	--	--	--	--	--	--	1.015	0.965	7.31	7.02	52.50
6/26	17:04	DILP	CHANGE FROM 44 psi — DOWN TO 1.2 psi AT 6/26 17:11 — STABLE TO 44 psi AT 6/26 17:18														
6/27	6:00	CHK	9.0	10	-0.03	-0.3%	8.85	-1.5%	0.05	0.5%	9.08	0.8%	1.019	0.965	7.39	7.01	52.50
6/27	6:29	CALC	--	--	--	--	--	--	--	--	--	--	1.032	0.950	7.45	7.04	52.50





ArcelorMittal
Minorca Mine
ACI Test

6/28	6:00	CHK	9.0	10	0.05	0.5%	8.69	-3.1%	0.05	0.5%	9.14	1.4%	1.019	0.965	7.39	7.01	52.50
6/28	6:29	CALC	--	--	--	--	--	--	--	--	--	--	1.062	0.917	7.75	6.99	52.50
6/28	19:26	DILP	CHANGE FROM 45 psi — DOWN TO 37 psi AT 6/28 19:31 — STABLE TO 44 psi AT 6/28 19:42														
6/29	6:00	CHK	9.0	10	0.01	0.1%	8.76	-2.4%	0.08	0.8%	9.11	1.1%	1.019	0.965	7.39	7.01	52.50
6/29	6:29	CALC	--	--	--	--	--	--	--	--	--	--	1.048	0.935	7.61	7.07	52.50
6/30	6:00	CHK	9.0	10	0.08	0.8%	8.92	-0.8%	0.14	1.4%	9.18	1.8%	1.019	0.965	7.39	7.01	52.50
6/30	6:29	CALC	--	--	--	--	--	--	--	--	--	--	1.037	0.944	7.60	7.12	52.50
7/1	6:00	CHK	9.0	10	0.05	0.5%	9.08	0.8%	0.13	1.3%	9.31	3.1%	1.019	0.965	7.39	7.01	52.50
7/1	6:29	CALC	--	--	--	--	--	--	--	--	--	--	1.016	0.949	7.42	7.00	52.50
7/2	6:00	CHK	9.0	10	0.04	0.4%	9.11	1.1%	0.10	1.0%	9.36	3.6%	1.019	0.965	7.39	7.01	52.50
7/2	6:29	CALC	--	--	--	--	--	--	--	--	--	--	1.012	0.944	7.38	6.91	52.50
7/3	6:00	CHK	9.0	10	-0.03	-0.3%	8.93	-0.7%	0.06	0.6%	9.05	0.5%	1.019	0.965	7.39	7.01	52.50
7/3	6:29	CALC	--	--	--	--	--	--	--	--	--	--	1.024	0.961	7.40	7.08	52.50
7/4	6:00	CHK	9.0	10	0.02	0.2%	8.85	-1.5%	0.12	1.2%	9.22	2.2%	1.019	0.965	7.39	7.01	52.50
7/4	6:29	CALC	--	--	--	--	--	--	--	--	--	--	1.038	0.937	7.54	7.05	52.50
7/5	6:00	CHK	9.0	10	0.10	1.0%	8.91	-0.9%	0.16	1.6%	9.23	2.3%	1.019	0.965	7.39	7.01	52.50
7/5	6:29	CALC	--	--	--	--	--	--	--	--	--	--	1.041	0.937	7.65	7.11	52.50
7/6	6:00	CHK	9.0	10	0.11	1.1%	8.96	-0.4%	0.15	1.5%	9.25	2.5%	1.019	0.965	7.39	7.01	52.50
7/6	6:29	CALC	--	--	--	--	--	--	--	--	--	--	1.035	0.940	7.62	7.09	52.50
7/7	6:00	CHK	9.0	10	0.06	0.6%	8.91	-0.9%	0.17	1.7%	9.16	1.6%	1.019	0.965	7.39	7.01	52.50
7/7	6:29	CALC	--	--	--	--	--	--	--	--	--	--	1.037	0.949	7.58	7.19	52.50
7/8	1:49	PMTV	CHANGE FROM 568V — UP TO 571V AT — STABLE TO 569V AT 7/8 01:55														
7/8	6:00	CHK	9.0	10	0.13	1.3%	8.86	-1.4%	0.21	2.1%	9.06	0.6%	1.019	0.965	7.39	7.01	52.50
7/8	6:29	CALC	--	--	--	--	--	--	--	--	--	--	1.050	0.952	7.74	7.34	52.50
7/8	16:56	PRBT	CHANGE FROM 220°C — DOWN TO 190°C AT 7/8 17:08 — STABLE TO 220°C AT 7/8 17:41														
7/8	17:02	DILP	CHANGE FROM 44 psi — DOWN TO 1.3 psi AT 7/8 17:08 — STABLE TO 44 psi AT 7/8 17:14														
7/9	6:00	CHK	9.0	10	0.24	2.4%	8.97	-0.3%	0.22	2.2%	9.18	1.8%	1.019	0.965	7.39	7.01	52.50
7/9	6:29	CALC	--	--	--	--	--	--	--	--	--	--	1.050	0.941	7.86	7.26	52.50
7/9	17:31	PRBT	CHANGE FROM 220°C — DOWN TO 193°C AT 7/9 17:39 — STABLE TO 220°C AT 7/9 18:20														
7/10	6:00	CHK	8900.0	8900	-0.08	0.0%	16.23	-100%	-0.05	0.0%	16.69	-100%	1.019	0.965	7.39	7.01	52.50
7/10	6:29	CALC	--	--	--	--	--	--	--	--	--	--	556.018	0.940	3988.37	3701.95	52.50
7/10	9:30	CHK	9.0	10	0.14	1.4%	8.94	-0.6%	0.23	2.3%	9.29	2.9%	1.019	0.965	7.39	7.01	52.50
7/10	9:59	CALC	--	--	--	--	--	--	--	--	--	--	1.042	0.938	7.70	7.20	52.50
7/11	8:00	CHK	9.0	10	0.11	1.1%	9.05	0.5%	0.24	2.4%	9.36	3.6%	1.019	0.965	7.39	7.01	52.50
7/11	8:29	CALC	--	--	--	--	--	--	--	--	--	--	1.026	0.945	7.56	7.16	52.50
7/12	7:30	CHK	9.0	10	0.20	2.0%	8.99	-0.1%	0.26	2.6%	9.35	3.5%	1.019	0.965	7.39	7.01	52.50
7/12	7:59	CALC	--	--	--	--	--	--	--	--	--	--	1.043	0.933	7.77	7.20	52.50
7/12	14:48	PRBT	CHANGE FROM 220°C — DOWN TO 161°C AT 7/12 14:56 — STABLE TO 220°C AT 7/12 15:47														
7/12	14:48	DILP	CHANGE FROM 44 psi — DOWN TO 1.2 psi AT 7/12 15:02 — STABLE TO 44 psi AT 7/12 15:17														
7/13	7:30	CHK	9.0	10	0.21	2.1%	8.94	-0.6%	0.31	3.1%	9.59	5.9%	1.019	0.965	7.39	7.01	52.50
7/13	7:59	CALC	--	--	--	--	--	--	--	--	--	--	1.051	0.907	7.85	7.10	52.50
7/13	8:25	CHG	--	--	--	--	--	--	--	--	--	--	1.051	0.907	7.85	7.10	52.50
7/13	18:00	CHK	9.0	10	-0.09	-0.9%	8.84	-1.6%	-0.07	-0.7%	8.89	-1.1%	1.051	0.907	7.85	7.10	52.50
7/13	18:29	CALC	--	--	--	--	--	--	--	--	--	--	1.060	0.904	7.83	7.07	52.50
7/14	7:30	CHK	9.0	10	-0.06	-0.6%	8.76	-2.4%	-0.04	-0.4%	8.84	-1.6%	1.051	0.907	7.85	7.10	52.50
7/14	7:59	CALC	--	--	--	--	--	--	--	--	--	--	1.073	0.900	7.96	7.15	52.50
7/14	14:12	PRBT	CHANGE FROM 220°C — DOWN TO 163°C AT 7/14 14:21 — STABLE TO 220°C AT 7/14 15:07														
7/14	14:12	DILP	CHANGE FROM 44 psi — DOWN TO 1.1 psi AT 7/14 14:29 — STABLE TO 44 psi AT 7/14 14:42														
7/15	7:30	CHK	9.0	10	-0.06	-0.6%	7.19	-18%	-0.07	-0.7%	8.70	-3.0%	1.051	0.907	7.85	7.10	52.50
7/15	7:59	CALC	--	--	--	--	--	--	--	--	--	--	1.304	0.751	9.66	7.22	52.50
7/15	8:25	MCAL	9.0	10	-0.84	-8.4%	5.33	-37%	-0.38	-3.8%	6.92	-21%	1.051	0.907	7.85	7.10	52.50
7/15	8:58	MUP	--	--	--	--	--	--	--	--	--	--	1.501	0.741	9.85	7.37	52.50
7/15	8:58	CALC	--	--	--	--	--	--	--	--	--	--	1.533	0.766	10.23	8.28	52.50
7/15	9:00	CHG	--	--	--	--	--	--	--	--	--	--	1.501	0.741	9.85	7.37	52.50
7/15	9:05	CHK	9.0	10	0.07	0.7%	8.51	-4.9%	-0.06	-0.6%	8.97	-0.3%	1.501	0.741	9.85	7.37	52.50
7/15	9:34	CALC	--	--	--	--	--	--	--	--	--	--	1.599	0.693	10.56	7.29	52.50
7/15	9:58	CHG	--	--	--	--	--	--	--	--	--	--	1.599	0.693	10.56	7.29	52.50
7/15	16:05	DILP	CHANGE FROM 44 psi — DOWN TO 8.4 psi AT 7/15 16:12 — STABLE TO 44 psi AT 7/15 16:19														
7/16	7:30	CHK	9.0	10	-0.03	-0.3%	10.42	14%	-0.04	-0.4%	9.01	0.1%	1.599	0.693	10.56	7.29	52.50
7/16	7:59	CALC	--	--	--	--	--	--	--	--	--	--	1.377	0.800	9.07	7.21	52.50





ArcelorMittal
Minorca Mine
ACI Test

7/16	8:30	MCAL	9.0	10	-0.06	-0.6%	10.19	12%	-0.06	-0.6%	8.96	-0.4%	1.599	0.693	10.56	7.29	52.50
7/16	9:01	MUP	--	--	--	--	--	--	--	--	--	--	1.407	0.788	9.25	7.25	52.50
7/16	9:01	CALC	--	--	--	--	--	--	--	--	--	--	1.404	0.788	9.21	7.22	52.50
7/16	9:03	CHG	--	--	--	--	--	--	--	--	--	--	1.407	0.788	9.25	7.25	52.50
7/16	9:05	CHK	9.0	10	0.02	0.2%	8.92	-0.8%	0.06	0.6%	9.03	0.3%	1.407	0.788	9.25	7.25	52.50
7/16	9:34	CALC	--	--	--	--	--	--	--	--	--	--	1.424	0.782	9.38	7.34	52.50
7/16	15:43	PRBT	CHANGE FROM 220°C — DOWN TO 128°C AT 7/16 15:55 — STABLE TO 221°C AT 7/16 16:41														
7/16	15:43	DILP	CHANGE FROM 44.1 psi — STABLE TO 5.5 psi AT 7/16 15:51														
7/16	16:20	DILP	CHANGE FROM 5.5 psi — STABLE TO 44.2 psi AT 7/16 16:28														
7/17	7:30	CHK	9.0	10	0.01	0.1%	9.97	9.7%	0.02	0.2%	9.08	0.8%	1.407	0.788	9.25	7.25	52.50
7/17	7:59	CALC	--	--	--	--	--	--	--	--	--	--	1.271	0.867	8.36	7.23	52.50
7/17	8:14	CHG	--	--	--	--	--	--	--	--	--	--	1.271	0.867	8.36	7.23	52.50
7/18	9:00	CHK	9.0	10	0.02	0.2%	9.07	0.7%	0.05	0.5%	8.86	-1.4%	1.271	0.867	8.36	7.23	52.50
7/18	9:29	CALC	--	--	--	--	--	--	--	--	--	--	1.265	0.889	8.34	7.43	52.50
19-Jul	8:30	CHK	9	10	0.05	0.50%	9.27	2.70%	0.07	0.70%	8.92	-0.80%	1.271	0.867	8.36	7.23	52.5
19-Jul	8:59	CALC	--	--	--	--	--	--	--	--	--	--	1.24	0.904	8.21	7.43	52.5
20-Jul	7:30	CHK	9	10	-0.02	-0.20%	8.84	-1.60%	-0.02	-0.20%	8.83	-1.70%	1.271	0.867	8.36	7.23	52.5
20-Jul	7:59	CALC	--	--	--	--	--	--	--	--	--	--	1.291	0.868	8.47	7.33	52.5
7/21	8:30	CHK	9.0	10	-0.02	-0.2%	8.87	-1.3%	-0.01	-0.1%	8.93	-0.7%	1.271	0.867	8.36	7.23	52.50
7/21	8:59	CALC	--	--	--	--	--	--	--	--	--	--	1.287	0.862	8.45	7.26	52.50
7/22	7:30	CHK	9.0	10	0.06	0.6%	8.54	-4.6%	0.07	0.7%	8.65	-3.5%	1.271	0.867	8.36	7.23	52.50
7/22	7:59	CALC	--	--	--	--	--	--	--	--	--	--	1.349	0.856	8.95	7.65	52.50
7/22	16:49	DILP	CHANGE FROM 44 psi — DOWN TO 1.1 psi AT 7/22 16:56 — STABLE TO 44 psi AT 7/22 17:34														
7/22	16:51	PRBT	CHANGE FROM 221°C — DOWN TO 85°C AT 7/22 17:15 — STABLE TO 220°C AT 7/22 18:07														
7/22	17:09	CNVT	CHANGE FROM 756°C — DOWN TO 720°C AT 7/22 17:10 — STABLE TO 757°C AT 7/22 17:21														
7/23	7:30	CHK	9.0	10	-0.01	-0.1%	8.47	-5.3%	-0.04	-0.4%	8.90	-1.0%	1.271	0.867	8.36	7.23	52.50
7/23	7:59	CALC	--	--	--	--	--	--	--	--	--	--	1.349	0.822	8.86	7.23	52.50
24-Jul	8:30	CHK	9	10	0.13	1.30%	9.17	1.70%	0.1	1.00%	9.15	1.50%	1.349	0.822	8.86	7.23	52.5
24-Jul	8:59	CALC	--	--	--	--	--	--	--	--	--	--	1.344	0.821	8.96	7.29	52.5
7/25	3:12	INTT	CHANGE FROM 28°C — UP TO 30°C AT 7/25 03:16 — STABLE TO 28°C AT 7/25 03:31														
7/25	7:30	CHK	9.0	10	0.18	1.8%	9.29	2.9%	0.18	1.8%	9.15	1.5%	1.349	0.822	8.86	7.23	52.50
7/25	7:59	CALC	--	--	--	--	--	--	--	--	--	--	1.333	0.835	8.94	7.44	52.50
7/25	15:02	PRBT	CHANGE FROM 220°C — DOWN TO 183°C AT 7/25 15:11 — STABLE TO 220°C AT 7/25 15:53														
7/25	15:04	DILP	CHANGE FROM 44 psi — DOWN TO 1.2 psi AT 7/25 15:12 — STABLE TO 44 psi AT 7/25 15:20														
7/26	6:40	CHK	9.0	10	0.07	0.7%	9.41	4.1%	0.07	0.7%	8.98	-0.2%	1.349	0.822	8.86	7.23	52.50
7/26	7:09	CALC	--	--	--	--	--	--	--	--	--	--	1.300	0.862	8.61	7.38	52.50
7/27	6:40	CHK	9.0	10	-0.05	-0.5%	7.24	-18%	-0.01	-0.1%	6.76	-22%	1.349	0.822	8.86	7.23	52.50
7/27	7:09	CALC	--	--	--	--	--	--	--	--	--	--	1.666	0.885	10.88	9.61	52.50
7/27	7:17	MCAL	9.0	10	-0.49	-4.9%	6.45	-26%	-0.32	-3.2%	6.11	-29%	1.349	0.822	8.86	7.23	52.50
7/27	7:52	MUP	--	--	--	--	--	--	--	--	--	--	1.774	0.881	11.09	9.78	52.50
7/27	7:52	CALC	--	--	--	--	--	--	--	--	--	--	1.748	0.887	10.85	9.67	52.50
7/27	8:10	CHK	9.0	10	0.18	1.8%	8.53	-4.7%	0.12	1.2%	8.91	-0.9%	1.774	0.881	11.09	9.78	52.50
7/27	8:39	CALC	--	--	--	--	--	--	--	--	--	--	1.912	0.837	12.14	10.14	52.50
7/28	6:40	CHK	9.0	10	0.14	1.4%	9.21	2.1%	0.03	0.3%	9.41	4.1%	1.774	0.881	11.09	9.78	52.50
7/28	7:09	CALC	--	--	--	--	--	--	--	--	--	--	1.760	0.852	11.14	9.41	52.50
7/28	8:52	DILP	CHANGE FROM 45 psi — DOWN TO 39 psi AT — STABLE TO 45 psi AT 7/28 08:58														
7/28	14:24	PRBT	CHANGE FROM 220°C — STABLE TO 220°C AT 7/28 14:30														
7/29	6:40	CHK	9.0	10	0.25	2.5%	9.59	5.9%	0.19	1.9%	9.90	9.0%	1.774	0.881	11.09	9.78	52.50
7/29	7:09	CALC	--	--	--	--	--	--	--	--	--	--	1.708	0.848	10.91	9.24	52.50
7/29	7:23	CHG	--	--	--	--	--	--	--	--	--	--	1.708	0.848	10.91	9.24	52.50
7/29	22:55	INTT	CHANGE FROM 28°C — UP TO 30°C AT 7/29 23:02 — STABLE TO 28°C AT 7/29 23:17														
7/30	5:43	INTT	CHANGE FROM 28°C — UP TO 30°C AT 7/30 05:48 — STABLE TO 29°C AT 7/30 05:54														
7/30	6:40	CHK	9.0	10	-0.01	-0.1%	8.79	-2.1%	0.05	0.5%	8.72	-2.8%	1.708	0.848	10.91	9.24	52.50
7/30	7:09	CALC	--	--	--	--	--	--	--	--	--	--	1.748	0.860	11.16	9.64	52.50
7/30	7:59	DILP	CHANGE FROM 45 psi — DOWN TO 1.2 psi AT 7/30 08:06 — STABLE TO 44 psi AT 7/30 08:15														
7/30	8:21	CHK	9.0	10	-0.02	-0.2%	10.99	20%	0.02	0.2%	11.30	23%	1.708	0.848	10.91	9.24	52.50
7/30	8:50	CALC	--	--	--	--	--	--	--	--	--	--	1.397	0.827	8.91	7.38	52.50
7/30	9:16	MCAL	9.0	10	-0.13	-1.3%	11.28	23%	-0.15	-1.5%	11.29	23%	1.708	0.848	10.91	9.24	52.50
7/30	9:50	MUP	--	--	--	--	--	--	--	--	--	--	1.346	0.849	8.49	7.21	52.50
7/30	9:50	CALC	--	--	--	--	--	--	--	--	--	--	1.347	0.846	8.50	7.15	52.50





ArcelorMittal
Minorca Mine
ACI Test

7/30	10:00	CHK	9.0	10	0.02	0.2%	8.91	-0.9%	0.01	0.1%	8.97	-0.3%	1.346	0.849	8.49	7.21	52.50
7/30	10:29	CALC	--	--	--	--	--	--	--	--	--	--	1.363	0.843	8.62	7.25	52.50
7/31	5:00	CHK	9.0	10	0.07	0.7%	9.06	0.6%	0.06	0.6%	8.89	-1.1%	1.346	0.849	8.49	7.21	52.50
7/31	5:29	CALC	--	--	--	--	--	--	--	--	--	--	1.349	0.863	8.59	7.40	52.50
7/31	13:42	DILP	CHANGE FROM 44.2 psi — STABLE TO 1.2 psi AT 7/31 13:50														
7/31	13:43	PRBT	CHANGE FROM 220°C — DOWN TO 108°C AT 7/31 14:07 — STABLE TO 221°C AT 7/31 15:04														
7/31	14:07	CNVT	CHANGE FROM 748°C — DOWN TO 724°C AT — STABLE TO 756°C AT 7/31 14:13														
7/31	14:44	DILP	CHANGE FROM 1.2 psi — STABLE TO 44.2 psi AT 7/31 14:52														
8/1	5:00	CHK	9.0	10	0.05	0.5%	8.69	-3.1%	0.04	0.4%	8.84	-1.6%	1.346	0.849	8.49	7.21	52.50
8/1	5:29	CALC	--	--	--	--	--	--	--	--	--	--	1.403	0.834	8.90	7.42	52.50
8/2	5:00	CHK	9.0	10	0.06	0.6%	8.71	-2.9%	0.01	0.1%	8.84	-1.6%	1.346	0.849	8.49	7.21	52.50
8/2	5:29	CALC	--	--	--	--	--	--	--	--	--	--	1.401	0.832	8.90	7.35	52.50
8/3	5:00	CHK	9.0	10	0.13	1.3%	8.88	-1.2%	0.04	0.4%	8.99	-0.1%	1.346	0.849	8.49	7.21	52.50
8/3	5:29	CALC	--	--	--	--	--	--	--	--	--	--	1.384	0.831	8.87	7.30	52.50
8/3	13:32	DILP	CHANGE FROM 44.2 psi — STABLE TO 1.2 psi AT 8/3 13:40														
8/3	13:33	PRBT	CHANGE FROM 220°C — DOWN TO 122°C AT 8/3 13:50 — STABLE TO 221°C AT 8/3 14:55														
8/3	14:28	DILP	CHANGE FROM 1.2 psi — STABLE TO 44.2 psi AT 8/3 14:36														
8/4	5:00	CHK	9.0	10	0.08	0.8%	9.25	2.5%	0.07	0.7%	8.85	-1.5%	1.346	0.849	8.49	7.21	52.50
8/4	5:29	CALC	--	--	--	--	--	--	--	--	--	--	1.321	0.887	8.41	7.46	52.50
8/5	5:00	CHK	9.0	10	0.11	1.1%	9.58	5.8%	0.07	0.7%	8.88	-1.2%	1.346	0.849	8.49	7.21	52.50
8/5	5:29	CALC	--	--	--	--	--	--	--	--	--	--	1.281	0.912	8.19	7.43	52.50
8/5	7:51	CHG	--	--	--	--	--	--	--	--	--	--	1.281	0.912	8.19	7.43	52.50
8/6	5:00	CHK	9.0	10	0.06	0.6%	8.92	-0.8%	0.05	0.5%	8.92	-0.8%	1.281	0.912	8.19	7.43	52.50
8/6	5:29	CALC	--	--	--	--	--	--	--	--	--	--	1.302	0.911	8.39	7.60	52.50
8/7	5:00	CHK	9.0	10	-0.05	-0.5%	12.56	36%	-0.06	-0.6%	12.57	36%	1.281	0.912	8.19	7.43	52.50
8/7	5:29	CALC	--	--	--	--	--	--	--	--	--	--	0.914	0.910	5.81	5.25	52.50
8/7	8:16	CHK	9.0	10	-0.06	-0.6%	12.23	32%	0.01	0.1%	13.27	43%	1.281	0.912	8.19	7.43	52.50
8/7	8:49	CALC	--	--	--	--	--	--	--	--	--	--	0.938	0.845	5.96	5.05	52.50
8/7	12:14	PRBT	CHANGE FROM 221°C — DOWN TO 205°C AT 8/7 12:21 — STABLE TO 220°C AT 8/7 12:51														
8/8	5:00	CHK	9.0	10	0.06	0.6%	10.24	12%	0.09	0.9%	12.40	34%	1.281	0.912	8.19	7.43	52.50
8/8	5:29	CALC	--	--	--	--	--	--	--	--	--	--	1.132	0.754	7.29	5.50	52.50



8.0 APPENDIX C - OHIO LUMEX DATA

No	Description: 6/22/13	M, mg	C, ng/g	Area	Maximum	Time
1	Std__10	1	9.8	7340	820	2:47:19 PM
2	Std__50	1	49	36600	3350	2:51:07 PM
3	Std__100	1	100	75100	6450	2:55:47 PM
4	Std__150	1	148	111000	14400	3:00:28 PM
5	Std__200	1	199	149000	19300	3:04:04 PM
6	Std__250	1	250	187000	15700	3:08:10 PM
7	Std__100 QA, RL = 3%	1	103	77300	6510	3:23:18 PM
	Standard__100, R = 0%		103			
8	Std__100 SS, RL = 4%	1	104	77800	9330	3:29:01 PM
9	172276 FP	1	217	162000	17900	3:37:52 PM
13	172276 Section 1	1	243	182000	18400	3:52:05 PM
14	172276 Section 2	1	10	7540	280	3:53:59 PM
20	173282 FP	1	74	55900	4170	4:15:21 PM
21	173282 Section 1	1	361	270000	29600	4:18:55 PM
22	173282 Section 2	1	15	11200	505	4:21:30 PM
23	172358 FP	1	120	89700	7350	4:42:16 PM
24	172358 Section 1	1	222	166000	16500	4:44:56 PM
25	172358 Section 2	1	10	7970	298	4:47:24 PM
26	172485 FP	1	166	124000	7060	5:02:21 PM
27	Std__100 QA, RL = 1%	1	101	75900	5730	5:05:00 PM
28	172485 Section 1	1	207	155000	18100	5:08:27 PM
29	172485 Section 2	1	14	10800	453	5:13:08 PM
30	172458 FP	1	6.1	4570	327	5:26:58 PM
31	172458 Section 1	1	116	86700	10000	5:29:53 PM
32	172458 Section 2	1	1.2	920	40	5:31:57 PM
33	172474 FP	1	5.1	3840	339	5:42:53 PM
35	12474 Section 1	1	132	99200	12300	5:46:10 PM
36	12474 Section 2	1	1.0	750	62	5:48:25 PM
37	173272 FP	1	22	16600	1310	5:58:25 PM
38	173272 Section 1	1	120	90200	12100	6:00:42 PM
39	Std__100 QA, RL = 5%	1	105	78600	7090	6:04:53 PM
40	173272 Section 2	1	7.3	5430	294	6:07:36 PM
41	173281 FP	1	20	15500	1010	6:17:06 PM
42	173281 Section 1	1	125	94000	12500	6:19:35 PM
43	173281 Section 2	1	7.4	5510	244	6:21:19 PM
44	173296FP	1	42	31600	2410	6:31:13 PM
45	173296 Section 1	1	644	481000	51300	6:34:31 PM
46	173296 Section 2	1	6.6	4930	343	6:39:03 PM
47	173273 FP	1	38	28800	2640	6:48:26 PM



48	173273 Section 1	1	633	473000	53600	6:51:48 PM
49	173273 Section 2	1	7.9	5920	351	6:56:11 PM
50	Std__100 QA, RL = 3%	1	103	77500	7070	6:59:50 PM
51	173262 FP	1	0.7	550	32	7:10:58 PM
52	173262 Section 1	1	167	125000	13500	7:13:09 PM
53	173262 Section 2	1	0.3	202	14	7:16:19 PM
54	173265 FP	1	0.9	684	35	7:28:18 PM
55	173265 Section 1	1	191	143000	16300	7:30:26 PM
56	173265 Section 2	1	0.4	326	17	7:32:22 PM
57	172122 FP	1	6.5	4850	403	7:40:08 PM
58	172122 Section 1	1	451	337000	41900	7:43:05 PM
59	172122 Section 2	1	2.3	1700	144	7:45:23 PM
61	173268 FP	1	4.3	3220	199	7:52:46 PM
62	173268 Section 1	1	478	357000	43000	7:56:05 PM
63	173268 Section 2	1	3.5	2590	213	7:58:00 PM
65	172205 FP	1	80	60000	3680	8:06:46 PM
67	172205 Section 1	1	686	512000	51400	8:10:44 PM
68	172205 Section 2	1	3.4	2560	102	8:13:30 PM
69	172341 FP	1	79	59000	4680	8:20:20 PM
71	172341 Section 1	1	781	583000	51600	8:24:00 PM
73	172341 Section 2	1	5.4	4040	193	8:26:16 PM
74	Std__100 QC, RL = 7%	1	107	80100	8430	8:29:04 PM
No	Description: 6/23/13	M, mg	C, ng/g	Area	Maximum	Time
1	Std__10	1	9.8	7340	820	2:47:19 PM
2	Std__50	1	49	36600	3350	2:51:07 PM
3	Std__100	1	100	75100	6450	2:55:47 PM
4	Std__150	1	148	111000	14400	3:00:28 PM
5	Std__200	1	199	149000	19300	3:04:04 PM
6	Std__250	1	250	187000	15700	3:08:10 PM
7	Std__100 QA, RL = 3%	1	103	77300	6510	3:23:18 PM
	Standard__100, R = 0%		103			
8	Std__100 SS, RL = 4%	1	104	77800	9330	3:29:01 PM
9	172276 FP	1	217	162000	17900	3:37:52 PM
13	172276 Section 1	1	243	182000	18400	3:52:05 PM
14	172276 Section 2	1	10	7540	280	3:53:59 PM
20	173282 FP	1	74	55900	4170	4:15:21 PM
21	173282 Section 1	1	361	270000	29600	4:18:55 PM
22	173282 Section 2	1	15	11200	505	4:21:30 PM
23	172358 FP	1	120	89700	7350	4:42:16 PM





24	172358 Section 1	1	222	166000	16500	4:44:56 PM
25	172358 Section 2	1	10	7970	298	4:47:24 PM
26	172485 FP	1	166	124000	7060	5:02:21 PM
27	Std__100 QA, RL = 1%	1	101	75900	5730	5:05:00 PM
28	172485 Section 1	1	207	155000	18100	5:08:27 PM
29	172485 Section 2	1	14	10800	453	5:13:08 PM
30	172458 FP	1	6.1	4570	327	5:26:58 PM
31	172458 Section 1	1	116	86700	10000	5:29:53 PM
32	172458 Section 2	1	1.2	920	40	5:31:57 PM
33	172474 FP	1	5.1	3840	339	5:42:53 PM
35	12474 Section 1	1	132	99200	12300	5:46:10 PM
36	12474 Section 2	1	1.0	750	62	5:48:25 PM
37	173272 FP	1	22	16600	1310	5:58:25 PM
38	173272 Section 1	1	120	90200	12100	6:00:42 PM
39	Std__100 QA, RL = 5%	1	105	78600	7090	6:04:53 PM
40	173272 Section 2	1	7.3	5430	294	6:07:36 PM
41	173281 FP	1	20	15500	1010	6:17:06 PM
42	173281 Section 1	1	125	94000	12500	6:19:35 PM
43	173281 Section 2	1	7.4	5510	244	6:21:19 PM
44	173296FP	1	42	31600	2410	6:31:13 PM
45	173296 Section 1	1	644	481000	51300	6:34:31 PM
46	173296 Section 2	1	6.6	4930	343	6:39:03 PM
47	173273 FP	1	38	28800	2640	6:48:26 PM
48	173273 Section 1	1	633	473000	53600	6:51:48 PM
49	173273 Section 2	1	7.9	5920	351	6:56:11 PM
50	Std__100 QA, RL = 3%	1	103	77500	7070	6:59:50 PM
51	173262 FP	1	0.7	550	32	7:10:58 PM
52	173262 Section 1	1	167	125000	13500	7:13:09 PM
53	173262 Section 2	1	0.3	202	14	7:16:19 PM
54	173265 FP	1	0.9	684	35	7:28:18 PM
55	173265 Section 1	1	191	143000	16300	7:30:26 PM
56	173265 Section 2	1	0.4	326	17	7:32:22 PM
57	172122 FP	1	6.5	4850	403	7:40:08 PM
58	172122 Section 1	1	451	337000	41900	7:43:05 PM
59	172122 Section 2	1	2.3	1700	144	7:45:23 PM
61	173268 FP	1	4.3	3220	199	7:52:46 PM
62	173268 Section 1	1	478	357000	43000	7:56:05 PM
63	173268 Section 2	1	3.5	2590	213	7:58:00 PM
65	172205 FP	1	80	60000	3680	8:06:46 PM
67	172205 Section 1	1	686	512000	51400	8:10:44 PM





68	172205 Section 2	1	3.4	2560	102	8:13:30 PM
69	172341 FP	1	79	59000	4680	8:20:20 PM
71	172341 Section 1	1	781	583000	51600	8:24:00 PM
73	172341 Section 2	1	5.4	4040	193	8:26:16 PM
74	Std__100 QC, RL = 7%	1	107	80100	8430	8:29:04 PM
75	Std__100 QC, RL = 5%	1	105	78500	6950	2:09:12 PM
76	173255 FP	1	5.7	4250	322	2:37:17 PM
77	173255 Section 1	1	82	61400	5550	2:40:04 PM
78	173255 Section 2	1	3.5	2600	155	2:43:06 PM
79	173288 FP	1	2.6	1910	115	2:52:51 PM
80	173288 Section 1	1	98	73200	5360	2:55:15 PM
81	173288 Section 2	1	4.4	3250	177	2:57:25 PM
82	173267 FP	1	15	11800	808	3:06:57 PM
83	173267 Section 1	1	115	85900	8120	3:09:29 PM
84	173267 Section 2	1	5.2	3910	174	3:11:31 PM
85	173274 FP	1	17	13000	764	3:23:39 PM
86	173274 Section 1	1	116	87100	11600	3:26:44 PM
88	Std__100 QA, RL = 5%	1	105	78900	7980	3:35:34 PM
90	173274 Section 2	1	5.8	4320	167	3:38:35 PM
91	173259 FP	1	36	27100	1180	3:49:39 PM
92	173259 Section 1	1	205	153000	17300	3:52:52 PM
93	173259 Section 2	1	7.1	5270	214	3:55:13 PM
94	173261 FP	1	30	22800	1680	4:03:46 PM
96	173261 Section 1	1	215	161000	18400	4:07:43 PM
97	173261 Section 2	1	7.9	5860	199	4:10:39 PM
98	Std__100 QA, RL = 5%	1	105	78800	8280	4:17:16 PM
No	Description: 7/12/13	M, mg	C, ng/g	Area	Maximum	Time
1	Std__5, RL = -11%	1	4.4	1560	177	11:47:51 AM
2	Std__10, RL = -13%	1	8.7	3070	324	11:49:42 AM
3	Std__100, RL = -2%, RL = -2%	1	98	34900	3510	11:51:34 AM
4	Std__50, RL = -2%, RL = -2%	1	49	17600	2160	11:53:49 AM
5	Std__500, RL = 0%, RL = 0%	1	500	177000	18400	11:56:06 AM
6	Std__5, RL = 0%	1	5.0	1760	161	12:10:58 PM
7	Std__10, RL = -1%	1	9.8	3450	389	12:12:43 PM
8	Std__250 SS, RL = 0%	1	249	88300	9360	12:16:41 PM
9	OL 173271 Sec 1 Plug Stack A	1	20	7350	387	12:24:06 PM
10	OL 173271 Sec 1	1	82	29200	2990	12:26:08 PM
11	OL 173271 Sec 2 and Plug	1	4.5	1600	85	12:28:07 PM
12	OL 173300 Sec 1 Plug Stack A	1	24	8550	640	12:32:35 PM





13	OL 173300 Sec 1	1	79	28000	3820	12:34:15 PM
14	OL 173300 Sec 2 and Plug	1	4.6	1640	80	12:36:05 PM
15	OL 173276 Sec 1 Plug Stack D	1	158	56200	6250	12:40:47 PM
16	OL 173276 Sec 1	1	7.5	2670	291	12:42:20 PM
17	OL 173276 Sec 2 and Plug	1	6.1	2150	113	12:44:25 PM
18	OL 173284 Sec 1 Plug Stack D	1	150	53400	3620	12:47:23 PM
19	OL 173284 Sec 1	1	8.6	3060	422	12:49:45 PM
20	OL 173284 Sec 2 and Plug	1	8.0	2840	179	12:52:01 PM
21	OL 173257 Sec 1 Plug Inlet	1	33	11700	1020	12:54:28 PM
22	OL 173257 Sec 1	1	460	163000	18900	12:56:46 PM
23	OL 173257 Sec 2 and Plug	1	10	3820	287	12:58:24 PM
24	OL 173275 Sec 1 Plug Inlet	1	35	12500	773	1:02:15 PM
25	OL 173275 Sec 1	1	494	175000	21800	1:04:22 PM
26	OL 173275 Sec 2 and Plug	1	13	4720	304	1:06:10 PM
27	Std__300 Chk, RL = 1%	1	305	108000	13500	1:10:15 PM
No	Description: 7/14/13	M, mg	C, ng/g	Area	Maximum	Time
1	Std__5, RL = -4%	1	4.8	1550	165	11:24:33 AM
2	Std__10, RL = 0%	1	10	3290	307	11:26:58 AM
3	Std__100, RL = 3%	1	103	33300	2830	11:29:00 AM
4	Std__500, RL = 0%	1	499	161000	17700	11:31:38 AM
5	Std__500 SS, RL = 4%	1	520	168000	13200	11:34:27 AM
6	OL 165245 Sec 1 Plug	1	42	13600	1530	11:48:53 AM
7	OL 165245 Sec 1	1	613	198000	20100	11:50:58 AM
8	OL 165345 Sec 2 and Plug	1	12	4100	178	11:52:36 AM
9	OL 165389 Sec 1 Plug	1	45	14800	1510	11:59:42 AM
10	OL 165389 Sec 1	1	688	222000	31500	12:01:35 PM
11	OL 165389 Sec 2	1	17	5640	440	12:03:07 PM
12	OL 165482 Sec 1 Plug	1	131	42500	3090	12:17:01 PM
13	OL 165482 Sec 1	1	9.1	2920	278	12:18:31 PM
14	OL 165482 Sec 2	1	8.4	2700	175	12:19:57 PM
15	OL 165484 Sec 1 Plug	1	133	43000	4680	12:29:10 PM
16	OL 165484 Sec 1	1	8.6	2790	321	12:30:53 PM
17	OL 165484 Sec 2	1	7.4	2380	124	12:32:25 PM
18	OL 165385 Sec 1 Plug	1	40	13200	782	12:39:59 PM
19	OL 165385 Sec 1	1	38	12400	1400	12:41:43 PM
20	OL 165385 Sec 2	1	4.7	1530	83	12:43:29 PM
21	OL 165726 Sec 1 Plug	1	43	14000	1160	12:45:18 PM
22	OL 165726 Sec 1	1	34	11200	1430	12:47:02 PM
23	OL 165726 Sec 2	1	4.4	1410	71	12:48:19 PM





24	Std__700 Chk, RL = 1%	1	713	230000	24100	12:52:53 PM
No	Description: 7/17/13	M, mg	C, ng/g	Area	Maximum	Time
1	Std__5, RL = 8%	1	5.4	1690	135	9:13:56 AM
2	Std__10, RL = 0%, RL = 0%	1	10	3430	381	9:15:58 AM
3	Std__5, RL = 5%, RL = 5%	1	5.3	1660	207	9:19:14 AM
4	Std__100, RL = 8%, RL = 8%	1	108	34000	3360	9:22:26 AM
5	Std__1000, RL = 0%, RL = 0%	1	999	313000	33700	9:24:56 AM
6	Std__1000 SS, RL = 2%	1	1020	320000	35100	9:30:26 AM
7	OL 173258 Sec 1 Plug	1	161	50700	3940	9:36:52 AM
8	OL 173258 Sec 1	1	7.9	2490	260	9:38:50 AM
9	OL 173258 Sec 2 and Plug	1	8.0	2510	175	9:40:11 AM
10	OL 173292 Sec 1 Plug	1	166	52200	2560	9:43:53 AM
11	OL 173292 Sec 1	1	7.5	2340	221	9:45:44 AM
12	OL 173292 Sec and Plug	1	8.3	2590	189	9:47:39 AM
13	OL 171696 Sec 1 Plug	1	112	35100	2900	9:51:09 AM
14	OL 171696 Sec 1	1	19	5960	768	9:52:43 AM
15	OL 171696 Sec 2 and Plug	1	7.6	2380	182	9:54:04 AM
16	OL 171706 Sec 1 Plug	1	109	34200	2670	9:58:26 AM
17	OL 171706 Sec 1	1	18	5810	704	10:00:26 AM
18	OL 171706 Sec 2 and Plug	1	7.3	2290	164	10:02:12 AM
19	OL 173264 Sec 1 Plug	1	43	13500	1280	10:05:39 AM
20	OL 173264 Sec 1	1	663	208000	22500	10:08:09 AM
21	OL 173264 Sec 2 and Plug	1	23	7240	601	10:10:21 AM
22	OL 171680 Sec 1 Plug	1	25	8030	523	10:12:59 AM
23	OL 171680 Sec 1	1	648	203000	22900	10:15:18 AM
24	OI 171680 Sec 2 and Plug	1	17	5340	381	10:17:02 AM
25	Std__700 Chk, RL = 7%	1	753	236000	27000	10:21:11 AM
No	Description: 7/20/13	M, mg	C, ng/g	Area	Maximum	Time
1	Std__100, RL = 5%	50	105	1820	221	8:06:47 PM
2	Std__100, RL = -2%	100	98	3410	410	8:09:43 PM
3	Std__1000, RL = 0%	50	999	17300	2290	8:11:53 PM
4	GB-202 - 1	1066	14	5250	248	9:24:49 PM
5	GB-202 - 2	1387	13	6400	314	9:28:17 PM
6	GB-203 - 1	1838	15	9760	441	9:31:20 PM
7	GB-203 - 2	1093	16	6280	347	9:34:37 PM
8	GB-204 - 1	1295	13	6050	309	10:03:28 PM
9	GB-204 - 2	1621	15	8540	371	10:06:35 PM
10	GB-205 - 1	1120	18	7240	323	10:09:10 PM





11	GB-205 - 2	1276	13	5970	300	10:12:43 PM
12	GB-206 - 1	1264	11	4880	250	10:23:23 PM
13	GB-206 - 2	1329	11	5130	227	10:26:23 PM
14	Std__100, RL = 1%	100	101	3500	463	10:33:05 PM
No	Description: 7/21/13	M, mg	C, ng/g	Area	Maximum	Time
1	Std__5, RL = -4%	1	4.8	1650	190	11:47:26 PM
2	Std__10, RL = 0%	1	9.9	3410	366	12:23:41 AM
3	Std__50, RL = 0%	1	50	17400	1930	12:25:47 AM
4	Std__100, RL = 1%	1	101	35000	3870	12:28:25 AM
5	Std__250, RL = 2%	1	257	89100	10800	12:42:23 AM
6	Std__500, RL = 2%	1	511	177000	19500	12:45:20 AM
7	Std__1000, RL = 0%	1	991	343000	29200	12:48:19 AM
8	Std__30, RL = 0%	1	30	10500	1310	12:55:34 AM
9	171708 FP	1	24	8430	597	1:06:36 AM
10	171708 Section 1	1	45	15700	1930	1:08:45 AM
11	171708 Section 2	1	3.6	1240	59	1:11:01 AM
12	172004 FP	1	24	8630	662	1:18:06 AM
13	172004 Section 1	1	43	15000	1800	1:19:56 AM
14	172004 Section 2	1	4.1	1430	60	1:21:50 AM
15	172187 FP	1	121	42200	4510	1:31:45 AM
16	172187 Section 1	1	5.7	1980	234	1:33:48 AM
17	172187 Section 2	1	4.8	1660	84	1:35:26 AM
18	172200 FP	1	112	39000	3670	1:37:32 AM
20	Std__30, RL = 0%	1	30	10600	1290	1:42:40 AM
21	172200 Section 1	1	6.8	2370	327	1:44:40 AM
22	172200 Section 2	1	5.9	2030	77	1:48:06 AM
23	171596 FP	1	32	11100	1090	1:56:28 AM
24	171596 Section 1	1	525	182000	19000	1:58:52 AM
25	171596 Section 2	1	13	4550	364	2:01:20 AM
26	172073 FP	1	33	11600	1510	2:15:33 AM
27	172073 Section 1	1	540	187000	20400	2:18:58 AM
28	172073 Section 2	1	11	3860	331	2:21:10 AM
29	171590 FP	1	32	11300	1100	2:23:54 AM
30	171590 Section 1	1	29	10300	1250	2:28:21 AM
31	Std__30, RL = 0%	1	30	10500	1200	2:30:54 AM
32	171590 Section 2	1	3.2	1090	53	2:42:56 AM
33	172237 FP	1	31	10800	966	2:44:44 AM
34	172237 Section 1	1	30	10600	1300	2:46:40 AM
35	172237 Section 2	1	3.0	1050	35	2:49:02 AM





36	171682 FP	1	115	39800	3460	2:57:35 AM
37	171682 Section 1	1	7.5	2610	298	2:59:58 AM
38	171682 Section 2	1	6.0	2080	93	3:02:04 AM
39	171683 FP	1	115	39900	3570	3:07:43 AM
40	171683 Section 1	1	6.8	2350	283	3:10:47 AM
41	171683 Section 2	1	5.8	1990	90	3:12:42 AM
42	Std__30, RL = 0%	1	30	10600	1220	3:14:56 AM
No	Description: 7/25/13	M, mg	C, ng/g	Area	Maximum	Time
1	Std__5, RL = -4%	1	4.8	1560	161	10:53:08 AM
2	Std__10, RL = 0%	1	10	3370	281	10:54:51 AM
3	Std__100, RL = 2%	1	102	33200	3020	10:56:51 AM
4	Std__500, RL = 3%	1	517	167000	13300	10:58:47 AM
5	Std__1000, RL = 0%	1	992	320000	32400	11:02:30 AM
6	Std__1000 SS, RL = -3%	1	964	311000	26800	11:04:41 AM
7	OL 172080 Sec 1 Plug	1	95	30900	1870	11:19:08 AM
8	OL 172080 Sec 1	1	26	8610	913	11:20:50 AM
9	OL 172080 Sec 2 and Plug	1	7.2	2310	145	11:22:50 AM
10	OL 171698 Sec 1 Plug	1	103	33400	2950	11:25:02 AM
11	OL 171698 Sec 1	1	24	7770	940	11:28:02 AM
12	OL 171698 Sec 2 and Plug	1	5.4	1730	113	11:29:58 AM
13	OL 171679 Sec 1 Plug	1	134	43300	2950	11:33:28 AM
14	OL 171679 Sec 1	1	9.9	3180	354	11:35:57 AM
15	OL 171679 Sec 2 and Plug	1	6.7	2160	130	11:37:15 AM
16	OL 173013 Sec 1 Plug	1	133	43000	4110	11:42:15 AM
17	OL 173013 Sec 1	1	10	3300	349	11:44:32 AM
18	OL 173013 Sec 2 and Plug	1	6.8	2190	94	11:46:19 AM
19	OL 171689 Sec 1 Plug	1	48	15600	838	11:49:34 AM
20	OL 171689 Sec 1	1	595	192000	22200	11:51:21 AM
21	OL 171689 Sec 2 and Plug	1	17	5520	325	11:54:09 AM
22	OL 172182 Sec 1 Plug	1	59	19200	832	11:57:52 AM
23	OL 172182 Sec 1	1	604	195000	19900	11:59:28 AM
24	OL 172182 Sec 2 and Plug	1	19	6350	453	12:01:11 PM
25	Std__600, RL = 4%	1	626	202000	18200	12:06:21 PM
No	Description: 7/26/13	M, mg	C, ng/g	Area	Maximum	Time
1	Std__100, RL = 5%	50	105	1670	167	8:01:14 AM
2	Std__100, RL = 4%	100	104	3290	333	8:03:10 AM
3	Std__1000, RL = 5%	50	1050	16600	1650	8:05:33 AM
4	Std__1000, RL = 3%	100	1030	32600	3500	8:07:39 AM





5	Std__10000, RL = 5%	50	10500	167000	14500	8:12:51 AM
6	Std__10000, RL = -1%	100	9850	311000	34000	8:15:35 AM
7	Pellets 7-24-2013 A	655	1.1	235	13	8:28:56 AM
8	Pellets 7-24-2013 B	1029	1.3	438	20	8:31:27 AM
9	Fine Tailings AM 7-24-2013 A	881	51	14400	867	8:33:57 AM
10	Fine Tailings AM 7-24-2013 B	847	40	10900	572	8:36:30 AM
11	Multiclone AM 7-24-2013 A	406	552	70800	4010	8:48:36 AM
12	Multiclone AM 7-24-2013 B	445	554	77800	4620	8:51:03 AM
13	Green Balls AM 7-24-2013 A	1091	16	5660	309	8:53:37 AM
14	Green Balls AM 7-24-2013 B	531	19	3340	211	8:55:26 AM
15	Conc Thick Overflow W AM 7-24-2013 A	420	353	46800	3500	9:09:26 AM
16	Conc Thick Overflow W AM 7-24-2013 B	652	354	72900	5100	9:12:51 AM
17	Multiclone PM 7-24-2013 A	655	362	74900	4350	9:17:02 AM
18	Multiclone PM 7-24-2013 B	700	360	79600	4630	9:19:36 AM
19	Pellets PM 7-24-2013 A	497	3.1	487	24	10:06:47 AM
20	Pellets PM 7-24-2013 B	855	2.4	655	29	10:08:55 AM
21	Green Balls PM 7-24-2013 A	646	19	3880	209	10:11:22 AM
22	Green Balls PM 7-24-2013 B	1206	25	9680	510	10:13:31 AM
23	Fine Tailings PM 7-24-2013 A	676	42	9120	543	10:26:11 AM
24	Fine Tailings PM 7-24-2013 B	522	43	7170	481	10:28:23 AM
25	Conc Thick Overflow W PM 7-24-2013 A	458	816	118000	7420	10:31:06 AM
26	Conc Thick Overflow W PM 7-24-2013 B	515	824	134000	8750	10:34:29 AM
27	Green Balls AM 7-25-2013 A	637	20	4110	275	10:52:40 AM
28	Green Balls AM 7-25-2013 B	716	16	3640	219	10:54:49 AM
29	Fine Tailings AM 7-25-2013 A	885	41	11600	627	10:57:09 AM
30	Fine Tailings AM 7-25-2013 B	867	41	11300	596	11:00:00 AM
31	Conc Thick Overflow W AM 7-25-2013 A	701	290	64300	4420	11:10:33 AM
32	Conc Thick Overflow W AM 7-25-2013 B	507	285	45700	3010	11:13:15 AM
33	Pellets AM 7-25-2013 A	1163	0.7	273	10	11:15:27 AM
34	Pellets AM 7-25-2013 B	923	0.5	141	8	11:16:58 AM
35	Multiclone AM 7-25-2013 A	689	667	145000	8680	12:19:02 PM
36	Multiclone AM 7-25-2013 B	932	666	196000	10300	12:22:10 PM
37	Pellets PM 7-25-2013 A	1033	0.3	111	7	12:24:13 PM
38	Pellets PM 7-25-2013 B	741	0.9	215	7	12:30:03 PM
39	Green Balls PM 7-25-2013 A	917	16	4810	266	12:40:58 PM
40	Green Balls PM 7-25-2013 B	862	14	4030	211	12:44:24 PM
41	Conc Thick Overflow W PM 7-25-2013 A	622	708	139000	8260	12:47:00 PM
42	Conc Thick Overflow W PM 7-25-2013 B	424	696	93200	5840	12:49:38 PM
43	Multiclone PM 7-25-2013 A	698	177	39000	2750	1:01:05 PM
44	Multiclone PM 7-25-2013 B	705	173	38600	2490	1:03:24 PM





45	Fine Tailings PM 7-25-2013 A	537	54	9270	576	1:05:59 PM
46	Fine Tailings PM 7-25-2013 B	1011	33	10800	566	1:08:28 PM
47	Std__1000, RL = 9%	100	1090	34400	3770	1:13:54 PM
No	Description: 7/27/13	M, mg	C, ng/g	Area	Maximum	Time
1	Std__100, RL = 1%	50	101	1770	184	9:35:50 PM
2	Std__100, RL = -1%	100	99	3480	428	9:37:55 PM
3	Std__1000, RL = 0%	50	1000	17500	2060	9:40:56 PM
4	GB-207-1	1497	11	6000	331	10:06:47 PM
5	GB-207-2	1217	13	5650	357	10:08:58 PM
6	GB-208-1	1371	13	6430	368	10:12:10 PM
7	GB-208-2	1683	19	11200	544	10:15:32 PM
8	GB-209-1	1563	18	9900	672	10:28:14 PM
9	GB-209-2	1656	15	8960	512	10:31:12 PM
10	GB-210-1	1442	14	7530	443	10:33:56 PM
11	GB-210-2	1216	13	5900	335	10:37:05 PM
12	GB-212-1	977	13	4770	246	10:53:59 PM
13	GB-212-2	1253	53	23400	2340	10:56:58 PM
14	GB-211-1	1537	14	7710	459	10:59:35 PM
15	GB-211-2	1277	14	6310	387	11:02:47 PM
16	GB-213-1	1786	11	7160	394	11:09:13 PM
17	GB-213-2	791	13	3740	206	11:11:57 PM
18	GB-214-1	1399	11	5580	302	11:14:55 PM
19	GB-214-2	1383	10	5250	291	11:18:38 PM
No	Description: 7/28/13	M, mg	C, ng/g	Area	Maximum	Time
1	Std__5, RL = 8%, RL = 8%	1	5.4	1800	156	9:59:54 AM
2	Std__50, RL = 10%	1	55	18400	1590	10:01:42 AM
3	Std__500, RL = 5%, RL = 5%	1	526	175000	19300	10:03:57 AM
4	Std__1000, RL = -1%, RL = -1%	1	986	328000	32300	10:06:34 AM
5	Std__50, RL = 2%	1	51	17200	1660	10:12:16 AM
	Std__1000 SS, RL = -1%	1	989	329000	30500	10:14:26 AM
1	OL 171676 Sec 1 Plug	1	45	15100	811	10:20:09 AM
2	OL 171676 Sec 1	1	622	207000	16400	10:22:16 AM
3	OL 171676 Sec 2 and Plug	1	17	5790	235	10:24:31 AM
4	OL 172483 Sec 1 Plug	1	53	17900	1040	10:28:03 AM
5	OL 172483 Sec 1	1	613	204000	25600	10:30:10 AM
6	OL 172483 Sec 2 and Plug	1	19	6600	350	10:32:02 AM
7	OL 171588 Sec 1 Plug	1	101	33900	3030	10:35:58 AM
8	OL 171588 Sec 1	1	17	5840	569	10:38:17 AM





9	OL 171588 Sec 2 and Plug	1	7.1	2360	135	10:40:56 AM
10	OL 171710 Sec 1 Plug	1	118	39400	3070	10:44:38 AM
11	OL 171710 Sec 1	1	11	3930	411	10:46:57 AM
12	OL 171710 Sec 2 and Plug	1	3.9	1280	76	10:48:59 AM
13	OL 171621 Sec 1 Plug	1	27	9160	441	10:52:39 AM
14	OL 171621 Sec 1	1	48	16200	1580	10:55:30 AM
15	OL 171621 Sec 2 and Plug	1	4.8	1580	103	10:57:12 AM
16	OL 171707 Sec 1 Plug	1	24	8180	525	10:59:39 AM
17	OL 171707 Sec 1	1	48	16200	1760	11:01:20 AM
18	OL 171707 Sec 2 and Plug	1	4.3	1430	129	11:02:58 AM
19	Std__650 Chk, RL = 4%	1	676	225000	23300	11:07:46 AM
No	Description: 8/2/13	M, mg	C, ng/g	Area	Maximum	Time
1	Std__10, RL = -1%	1	9.8	3390	378	8:45:16 AM
2	Std__100, RL = -1%	1	99	34600	3550	8:48:51 AM
3	Std__50, RL = -2%	1	49	17000	1980	8:57:10 AM
4	Std__250, RL = 0%	1	251	87100	10800	9:01:42 AM
5	Std__500, RL = 0%	1	499	173000	19000	9:06:26 AM
6	Std__250 SS, RL = -2%	1	245	85100	10800	9:12:38 AM
7	171685 S1	1	10	3800	585	9:21:07 AM
8	171685 P1	1	95	33200	2650	9:24:29 AM
9	171685 S2 P2	1	3.7	1270	54	9:31:19 AM
10	173001 S1	1	12	4380	668	9:37:34 AM
11	173001 P1	1	92	32100	2140	9:40:28 AM
12	173001 S2 P2	1	4.5	1550	85	9:45:03 AM
13	172111 S1	1	30	10500	1560	9:51:41 AM
14	172111 P1	1	21	7390	425	9:54:17 AM
15	172111 S2 P2	1	2.7	947	61	9:59:34 AM
16	Std__100, RL = -2%	1	98	34000	3740	10:04:46 AM
17	172235 S1	1	29	10200	1470	10:14:57 AM
18	172235 P1	1	20	7050	442	10:17:32 AM
19	172235 S2 P2	1	2.8	986	74	10:21:49 AM
20	172241 S1	1	450	156000	20100	10:30:25 AM
21	172241 P1	1	35	12200	1250	10:34:40 AM
22	172241 S2 P2	1	14	5190	477	10:39:20 AM
23	172495 S1	1	453	157000	21100	10:44:46 AM
24	172495 P1	1	54	18800	1180	10:48:50 AM
25	172495 S2 P2	1	14	5170	460	10:52:47 AM
26	Std__100	1	96	33500	3510	10:57:56 AM





ArcelorMittal
 Minorca Mine
 ACI Test

No	Description: 8/4/13	M, mg	C, ng/g	Area	Maximum	Time
1	Std__10, RL = 0%	1	10	3400	402	1:26:06 PM
2	Std__100, RL = -1%	1	99	33500	3800	1:29:23 PM
3	Std__50, RL = -2%	1	49	16800	1840	1:34:19 PM
4	Std__500, RL = 0%	1	497	168000	17800	1:38:06 PM
5	Std__250, RL = 2%	1	257	87000	10400	1:44:23 PM
6	Std__SS 250	1	248	83900	10300	1:49:09 PM
7	K 173016 s1	1	192	65000	8340	1:56:01 PM
8	K 173016 P1	1	13	4600	261	1:58:03 PM
9	K 173016 S2 P2	1	0.2	67	8	2:01:31 PM
10	K 172496 S1	1	199	67300	8930	2:32:37 PM
11	K 172496 P1	1	8.9	3000	186	2:35:57 PM
12	K 172496 S2 P2	1	0.3	92	7	2:39:35 PM
13	K 171717 S1	1	180	60900	7770	2:46:01 PM
14	K 171717 P1	1	7.6	2560	157	2:51:21 PM
15	K 171717 S2 P2	1	0.3	102	9	2:54:58 PM
16	K 172231 S1	1	181	61400	8680	2:59:22 PM
17	Std__100	1	101	34400	3470	3:04:58 PM
18	K 172231 P1	1	9.9	3350	191	3:10:54 PM
19	K172231 S2 P2	1	0.3	89	9	3:14:39 PM
20	172217 S1	1	11	3820	504	3:18:55 PM
21	172217 P1	1	107	36400	2360	3:22:38 PM
22	172217 S2 P2	1	4.8	1630	99	3:27:25 PM
23	171693 S1	1	22	7590	989	3:33:36 PM
24	171693 P1	1	69	23500	1400	3:36:00 PM
25	171693 S2 P2	1	5.4	1810	86	3:39:49 PM
26	171684 S1	1	20	6930	1000	3:46:22 PM
27	171684 P1	1	71	24100	1730	3:48:51 PM
28	Std__100	1	102	34500	3690	3:53:15 PM
29	171684 S2 P2	1	5.9	2000	85	4:01:28 PM
30	171686 S1	1	586	198000	27300	4:07:24 PM
31	171686 P1	1	68	23300	1300	4:13:07 PM
32	171686 S2 P2	1	4.9	1670	134	4:17:44 PM
33	173009 S1	1	589	199000	23700	4:22:20 PM
34	173009 P1	1	85	29000	1450	4:25:42 PM
35	173009 S2 P2	1	4.1	1380	98	4:29:50 PM
36	Std__1000, RL = -8%	1	911	308000	36900	4:34:02 PM
No	Description: 8/7/13	M, mg	C, ng/g	Area	Maximum	Time
1	Std__100, RL = -4%	50	96	1600	180	5:44:13 PM





2	Std__100, RL = -4%	100	96	3200	369	5:46:46 PM
3	Std__1000	50	1000	16800	1800	5:49:31 PM
4	Std__1000, RL = 0%	50	1000	16600	1560	5:54:35 PM
	GB 8-2	970	11	3620	197	6:22:31 PM
1	GB 8-2	1338	13	5910	257	6:25:33 PM
2	GB 8-5	727	13	3350	166	6:27:56 PM
3	GB 8-5	678	11	2620	123	6:30:18 PM
4	GB 8-6	1102	35	12800	796	6:48:19 PM
5	GB 8-6	1096	9.1	3300	134	6:51:10 PM
6	GB 8-7	863	9.2	2630	102	6:53:35 PM
7	GB 8-7	1104	9.7	3530	127	6:56:34 PM
8	GB-SS 317	562	13	2570	110	7:04:38 PM
9	GB-SS 317	761	12	3050	141	7:07:08 PM
10	Std__100, RL = -3%	100	97	3230	214	7:10:00 PM
11	GB-SS 322	793	13	3640	161	7:28:01 PM
12	GB-SS 322	439	13	1910	91	7:30:28 PM
13	GB-SS 320	1120	0.5	203	8	7:32:24 PM
14	GB-SS 320	1702	0.4	211	8	7:34:32 PM
15	P-SS 325	1179	0.9	357	10	7:46:00 PM
16	P-SS 325	599	1.0	193	9	7:47:59 PM
17	FT-SS 323	888	36	10800	405	7:50:56 PM
18	FT-SS 323	388	38	4960	193	7:53:25 PM
19	FT-SS 318	355	33	3920	159	8:01:22 PM
20	FT-SS 318	840	40	11200	429	8:04:35 PM
21	Std__100, RL = -5%	100	95	3160	261	8:07:06 PM
No	Description: 8/8/13	M, mg	C, ng/g	Area	Maximum	Time
1	Std__10, RL = 0%	1	10.0	3310	344	2:00:24 PM
2	Std__100, RL = 0%	1	100	33500	3480	2:03:39 PM
3	Std__50, RL = 0%	1	50	16800	1620	2:07:04 PM
4	Std__500, RL = 0%	1	496	165000	15700	2:10:33 PM
5	Std__250, RL = 2%	1	255	84800	8940	2:14:56 PM
6	Std__250 SS, RL = 0%	1	250	83300	9160	2:18:34 PM
7	184732 s1	1	6.7	2210	322	2:25:22 PM
8	184732 p1	1	86	28900	2190	2:28:42 PM
9	184732 s2 p2	1	3.7	1230	70	2:33:45 PM
10	184920 s1	1	8.0	2670	384	2:38:44 PM
11	184920 p1	1	85	28300	2570	2:42:17 PM
12	184920 s2 p2	1	4.2	1410	59	2:46:10 PM
13	184627 s1	1	35	11800	1500	2:50:06 PM





ArcelorMittal
Minorca Mine
ACI Test

14	184627 p1	1	28	9450	693	2:52:44 PM
15	184627 s2 p2	1	3.9	1280	84	2:56:07 PM
16	184853 s1	1	35	11700	1330	3:00:19 PM
17	Std__100	1	102	34200	3360	3:36:12 PM
18	184853 p1	1	27	9150	610	3:46:51 PM
19	184853 s2 p2	1	4.4	1460	61	3:50:24 PM
20	171585 s1	1	44	14800	1910	4:09:31 PM
21	171585 p1	1	25	8590	939	4:12:01 PM
22	171585 s2 p2	1	3.8	1270	82	4:16:25 PM
23	172500 s1	1	36	12000	1860	4:19:35 PM
24	172500 p1	1	33	11200	1040	4:22:31 PM
25	172500 s2 p2	1	3.0	1010	43	4:25:20 PM
26	184614 s1	1	29	9820	1310	4:29:36 PM
27	184614 p1	1	25	8360	638	4:31:10 PM
28	Std__100	1	104	34700	3130	4:34:42 PM
29	184614 s2 p2	1	2.6	874	42	4:40:19 PM
30	184821 s1	1	28	9550	1340	4:43:32 PM
31	184821 p1	1	23	7940	665	4:45:37 PM
32	184821 s2 p2	1	2.7	904	39	4:48:31 PM
33	171678 s1	1	9.3	3090	424	4:53:49 PM
34	171678 p2	1	102	34100	3160	4:56:22 PM
35	171678 s2 p2	1	4.2	1410	63	5:00:37 PM
36	172218 s1	1	7.7	2550	286	5:03:47 PM
37	172218 p1	1	98	32600	3300	5:05:42 PM
38	172218 s2 p2	1	4.5	1490	60	5:08:29 PM
39	Std__100	1	101	33800	3950	5:14:47 PM
40	184646 s1	1	385	128000	17100	5:21:37 PM
41	184646 p1	1	59	19800	1990	5:25:26 PM
42	184646 s2 p2	1	13	4510	296	5:30:08 PM
43	184871 s1	1	409	136000	17100	5:34:58 PM
44	184871 p1	1	73	24300	1990	5:40:02 PM
45	184871 s2 p2	1	11	3890	290	5:43:50 PM
46	Std__100	1	102	34000	3130	5:47:32 PM
1	Std__100, RL = -3%	100	97	3340	342	5:57:10 PM
2	Std__100, RL = -2%	50	98	1680	175	5:59:36 PM
3	Std__1000, RL = 0%	50	1000	17100	2010	6:01:55 PM
4	8-6 1	1140	10	4030	205	6:09:37 PM
5	8-6 2	518	10	1800	97	6:13:59 PM
6	ss319 1	574	592	116000	8040	6:17:53 PM
7	ss319 2	336	583	66900	4740	6:21:08 PM





ArcelorMittal
Minorca Mine
ACI Test

8	ss325 1	307	372	39000	2800	6:25:28 PM
9	ss325 2	394	371	50000	3420	6:29:03 PM
10	ss327 1	460	726	114000	8490	6:32:57 PM
11	ss327 2	277	741	70100	5900	6:37:17 PM
12	ss326 1	301	452	46500	3820	6:41:49 PM
13	ss326 2	511	454	79300	5000	6:47:16 PM
14	ss321 1	444	131	19900	1380	6:49:46 PM
15	ss321 2	393	129	17400	1140	6:53:10 PM
16	bad 1000	100	943	32200	3110	6:56:59 PM
17	Std__1000	100	978	33400	3570	6:59:41 PM



9.0 APPENDIX D - MM30B DATA

Table 8 shows the average Hg-CEMS data at the stack and the results of the comparison to corresponding MM30B data.

This comparison was done with one significant exception to the QA/QC procedure described in Section 4.3.1. The RA/AMD procedure assumes that there is no significant particulate mercury (HgP) in the stack gas. However, ADA discovered that with ACI operating at Minorca, HgP was a significant portion of the total mercury. This was determined by analyzing the first glass wool section of the sorbent trap, which is assumed to contain all of the particulate, separately from the other two sorbent sections. This allowed ADA to calculate a value for MM30B gas phase mercury ($HgG = HgT - HgP$) which was then used to perform the RA/AMD calculations. It is important to note that Hg-CEMS can only measure HgG. As Figure 27 shows, the MM30B HgG compared well with Hg-CEMS but the MM30B HgT did not.

Also, the gas moisture at the Hood Exhaust was 6.1% and at the Windbox Exhaust was 8.5%. The moisture at stacks A, B, C, and D was 11.5%, 12.2%, 13.6%, and 14.9% respectively based on stack measurements by Barr during testing.



ArcelorMittal
Minorca Mine
ACI Test

Table 8. MM30B Data and RD, RA, AMD Calculations

Run	Sampling Location	Trap ID	Date	Start Time	End Time	Flow Rate cc/min	DGMI L	DGMf L	Volume L actual	Initial Leak Test Pass/Fail	Final Leak Test Pass/Fail	DGM L (STP)	M Plug 1 ONLY ng	M Sect 1 ONLY ng	M Plug 2 and Sect 2 ng	H ₂ O %	STM (dry) µg/dscm	STM µg/wscm	Total STM Avg µg/wscm	Gas Phase STM Hg µg/wscm	Gas Phase STM Avg Hg	Particulate STM Hg µg/wscm	Particulate STM Avg	RD %	Pass/Fail	CEM Avg µg/wscm	RA %	AMD µg/wscm	Pass/Fail
1	Stack B, STM 1064	173279, 173291	6/21/13	11:52	12:52	600	14538.2, 12597.8	14574.4, 12633.0	36.2, 35.2	PASS, PASS	PASS, PASS	32.697, 31.886	102, 99	5.7, 4.1	12.2, 12.2	3.29, 3.23	2.89, 2.84	3.32		2.87		0.45	0.93	PASS					
2	Stack C, STM 1064	172422, 172107	6/21/13	10:15	11:15	600	12561.9, 14501.1	12597.5, 14538.0	35.6, 36.9	PASS, PASS	PASS, PASS	32.434, 33.29	124, 140	6.3, 6.9	13.6, 13.6	4.02, 4.41	3.47, 3.81	3.64					4.69	PASS	5.39	48.00	1.75	FAIL	
3	Duct A, STM 1062	172108, 168921	6/21/13	10:22	11:22	600	8219.2, 110259.7	8252.9, 110293.0	33.7, 33.3	PASS, PASS	PASS, PASS	31.212, 29.742	78, 77	0.6, 0.4	6.1, 6.1	2.52, 2.60	2.36, 2.44	2.40					1.64	PASS					
4	Duct C, STM 1062	173268, 172122	6/22/13	13:25	14:25	600	110352.0, 8326.7	110387.1, 8365.0	35.1, 38.3	PASS, PASS	PASS, PASS	31.311, 35.155	4.3, 6.5	478, 451	3.5, 2.3	8.5, 8.5	15.52, 13.08	14.20, 11.97	13.08	14.07, 11.80	12.93	0.13, 0.17	0.15	8.52	PASS				
5	Duct A, STM 1062	172458, 172474	6/22/13	11:22	12:22	600	110314.3, 8286.2	110348.0, 8323.1	33.7, 36.9	PASS, PASS	PASS, PASS	29.893, 33.703	6.1, 5.1	116, 132	1.2, 1.0	6.1, 6.1	4.12, 4.10	3.87, 3.85	3.86		3.69	0.14	0.17	0.33	PASS				
6	Stack D, STM 1064	172358, 172485	6/22/13	08:21	09:21	600	14581.2, 12641.2	14616.0, 12675.4	34.8, 34.2	PASS, PASS	PASS, PASS	32.873, 32.561	120, 166	222, 207	10.0, 14.0	14.9, 14.9	10.72, 11.89	9.13, 10.11	9.62	6.02, 5.78	5.90	3.11, 4.34	3.72	5.14	PASS	8.41	42.65	2.51	FAIL
7	Stack D, STM 1064	172276, 173282	6/22/13	09:52	10:52	600	14616.4, 12675.6	14650.6, 12709.4	34.2, 33.8	PASS, PASS	PASS, PASS	31.271, 30.865	217, 74	243, 361	10.0, 15.0	14.9, 14.9	15.03, 14.58	12.79, 12.41	12.60	6.89, 10.37	8.63	5.91, 2.04	3.97	1.52	PASS	8.73	1.21	0.10	PASS
8	Stack A, STM 1064	173272, 173281	6/22/13	13:42	14:42	600	14690.0, 12749.0	14726.0, 12783.8	36.0, 34.8	PASS, PASS	PASS, PASS	33.12, 32.442	22, 20	120, 125	7.3, 11.5	4.51, 4.70	3.99, 4.16	4.07	3.40, 3.61	3.51	0.59, 0.55	0.57	2.06	2.06	PASS	2.97	15.30	0.54	PASS
9	Inlet MM30B Port, STM 1064	173273, 173296	6/22/13	17:14	18:14	600	14768.4, 12825.0	14804.9, 12860.1	36.5, 35.1	PASS, PASS	PASS, PASS	32.708, 31.615	38, 42	633, 644	7.9, 6.6	8.5, 8.5	20.76, 21.91	18.99, 20.05	19.52	17.93, 18.83	18.38	1.06, 1.22	1.14	2.70	PASS				
10	Duct B, STM 1062	173262, 173265	6/22/13	16:47	17:47	600	110422.5, 8403.8	110454.8, 8438.6	32.3, 34.8	PASS, PASS	PASS, PASS	31.669, 35.538	0.7, 0.9	167.0, 191.0	0.3, 0.4	8.5, 8.5	5.30, 5.41	4.85, 4.95	4.90	4.83, 4.93	4.88	0.02, 0.02	0.02	0.99	PASS				
11	Duct D, STM 1062	172205, 172341	6/22/13	15:06	16:06	600	110388.1, 8366.3	110422.3, 8403.3	34.2, 37.0	PASS, PASS	PASS, PASS	29.986, 33.749	80, 79	686.0, 781.0	3.4, 5.4	8.5, 8.5	25.66, 25.64	23.48, 23.46	23.47	21.04, 21.32	21.18	2.44, 2.14	2.29	0.03	PASS				
12	Stack A, STM 1064	173255, 173288	6/23/13	10:28	11:28	600	14809.0, 12864.5	14846.2, 12900.6	37.2, 36.1	PASS, PASS	PASS, PASS	36.236, 33.464	5.7, 2.6	82.0, 98.0	3.5, 4.4	11.5, 11.5	2.52, 3.14	2.23, 2.78	2.50	2.09, 2.71	2.40	0.14, 0.40	0.10	10.98	FAIL	2.65	10.54	0.25	PASS
13	Stack C, STM 1062	173267, 173274	6/23/13	13:13	14:13	600	110512.6, 8482.3	110549.2, 8518.2	36.6, 35.9	PASS, PASS	PASS, PASS	33.256, 33.558	15, 17	115.0, 116.0	5.2, 5.8	12.2, 12.2	4.07, 4.14	3.57, 3.63	3.60	3.17, 3.19	3.18	0.40, 0.44	0.42	0.86	PASS	3.58	12.58	0.40	PASS
14	Stack C, STM 1062	173259, 173261	6/23/13	11:40	12:40	600	110473.4, 8444.5	110508.8, 8479.0	35.4, 34.5	PASS, PASS	PASS, PASS	31.86, 32.374	36, 30	205, 215	7.1, 7.9	13.6, 13.6	7.79, 6.75	6.73, 6.75	6.74	5.75, 5.95	5.85	0.98, 0.80	0.89	0.16	PASS				
15	Inlet 30B Port, STM 1062	173257, 173275	7/10/13	16:40	17:40	600	110532.2, 8521.8	110588.5, 8558.9	35.3, 37.1	PASS, PASS	PASS, PASS	31.309, 34.034	33, 35	460, 494	10.0, 13.0	8.5, 8.5	16.07, 15.93	14.70, 14.57	14.64	13.74, 13.63	13.68	0.96, 0.94	0.95	0.44	PASS				
16	Stack A, STM 1064	173271, 173300	7/11/13	15:21	16:21	600	14850.5, 12905.0	14887.6, 12940.9	37.1, 35.9	PASS, PASS	PASS, PASS	33.596, 32.718	20, 24	82, 79	4.5, 4.6	11.5, 11.5	3.17, 3.29	2.81, 2.91	2.86	2.28, 2.26	2.27	0.53, 0.65	0.59	1.84	PASS	3.03	33.48	0.76	PASS
17	Stack D, STM 1064	173276, 173284	7/11/13	18:06	19:06	600	14887.9, 12941.2	14925.4, 12977.1	37.5, 35.9	PASS, PASS	PASS, PASS	33.513, 32.255	158, 150	7.5, 8.6	6.1, 8.0	14.9, 14.9	5.12, 5.17	4.36, 4.40	4.38	0.35, 0.44	0.39	4.01, 3.96	3.98	0.43	PASS	0.55	40.43	0.16	PASS
18	Stack D, STM 1064	165482, 165484	7/13/13	9:48	10:48	600	14927.6, 12979.4	14963.8, 13014.5	36.2, 35.1	PASS, PASS	PASS, PASS	33.06, 32.055	131, 133	9.1, 8.6	8.4, 7.4	14.9, 14.9	4.49, 4.65	3.82, 3.96	3.89	0.42, 1.11	0.44	3.53, 1.04	3.45	1.71	PASS	0.70	59.96	0.26	PASS
19	Stack B, STM 1064	165385, 165726	7/13/13	11:16	12:16	600	14964.5, 13015.0	15002.0, 13051.4	37.5, 36.4	PASS, PASS	PASS, PASS	33.92, 32.675	40, 43	38, 34	4.7, 4.4	12.2, 12.2	2.44, 2.49	2.14, 2.19	2.16	1.11, 1.03	1.07	1.04, 1.16	1.10	1.08	PASS	1.41	31.95	0.34	PASS
20	Inlet 30B Port, STM 1062	165245, 165389	7/14/13	09:57	10:57	600	110589.0, 8562.8	110625.0, 8599.0	36.0, 36.2	PASS, PASS	PASS, PASS	31.736, 34.204	42, 45	613, 688	12.0, 17.0	8.5, 8.5	21.02, 21.93	19.23, 20.06	19.65	18.02, 18.86	18.44	1.21, 1.20	1.21	2.12	PASS				
21	Stack D, STM 1064	173258, 173292	7/16/13	9:27	10:27	600	15005.0, 13054.9	15041.2, 13090.5	36.2, 35.6	PASS, PASS	PASS, PASS	33.629, 33.065	161, 166	7.9, 7.5	8.0, 8.3	14.9, 14.9	5.26, 5.50	4.48, 4.68	4.58	0.40, 0.41	0.40	4.07, 4.27	4.17	2.21	PASS	0.74	82.94	0.34	PASS
22	Stack C, STM 1062	171696, 171706	7/16/13	10:55	11:55	600	15041.8, 13090.8	15078.8, 13126.8	37.0, 36.0	PASS, PASS	PASS, PASS	33.816, 33.085	112, 109	19, 18	7.6, 7.3	13.6, 13.6	4.10, 4.06	3.54, 3.51	3.52	0.68, 0.66	0.67	2.86, 2.85	2.85	0.48	PASS	1.05	56.68	0.38	PASS
23	Inlet 30B Port, STM 1062	171680, 173264	7/17/13	07:39	08:39	600	110625.8, 8602.4	110661.8, 8640.0	36.0, 37.6	PASS, PASS	PASS, PASS	31.701, 34.624	25, 43	648.0, 663.0	17.0, 23.0	8.5, 8.5	21.77, 21.05	19.92, 19.27	19.59	19.19, 18.13	18.66	0.72, 1.14	0.93	1.66	PASS				
24	Stack A, STM 1064	171708, 172004	7/18/13	14:50	15:50	600	15082.7, 13130.7	15119.0, 13166.1	36.3, 35.4	PASS, PASS	PASS, PASS	32.471, 31.597	24, 24	45.0, 43.0	3.6, 4.1	11.5, 11.5	2.24, 2.25	1.98, 1.99	1.99	1.32, 1.32	1.32	0.65, 0.67	0.66	0.32	PASS	1.80	36.17	0.48	PASS





ArcelorMittal
Minorca Mine
ACI Test

Run	Sampling location	Trap ID	Date	Start Time	End Time	Flow Rate cc/min	DGMI L	DGMf L	Volume L actual	Initial Leak Test Pass/Fail	Final Leak Test Pass/Fail	DGM L (STP)	M Plug 1 ONLY ng	M Sect 1 ONLY ng	M Plug 2 and Sect 2 ng	H ₂ O %	STM (dry) µg/dscm	STM µg/wscm	Total STM Avg µg/wscm	Gas Phase STM Hg µg/wscm	Gas Phase STM Avg Hg	Particulate STM Hg µg/wscm	Particulate STM Hg Avg	RD %	Pass/Fail	CEM Avg µg/wscm	RA %	AMD µg/wscm	Pass/Fail
25	Stack D, STM 1064	172187 172200	7/18/13	16:20	17:20	600	15123.0 13169.7	15160.1 13205.1	37.1 35.4	PASS	PASS	32.66 31.271	121 112	5.7 6.8	4.8 5.9	14.9 14.9	4.03 3.99	3.43 3.39	3.41	0.27	0.31	3.15 3.05	3.10	0.48	PASS	0.66	113.18	0.35	PASS
26	Inlet, 30B Port, STM 1062	171596 172073	7/21/13	10:38	11:38	600	110662.4 8642.9	110697.6 8677.7	35.2 34.8	PASS	PASS	31.657 32.417	32 33	525.0 540.0	13.0 11.0	8.5 8.5	18.01 18.02	16.48 16.48	16.48	15.55	15.55	0.92 0.93	0.93	0.93	0.03	PASS			
27	Stack B, STM 1064	171590 172237	7/21/13	11:09	12:09	600	15164.1 13208.6	15198.5 13242.2	34.4 33.6	PASS	PASS	32.036 31.456	32 31	29.0 30.0	3.2 3.0	12.2 12.2	2.00 2.03	1.76 1.79	1.77	0.88 0.92	0.90	0.88 0.87	0.87	0.76	PASS	1.05	16.43	0.15	PASS
28	Stack D, STM 1064	171682 171683	7/21/13	12:55	13:55	600	15202.6 13245.7	15238.4 13280.6	35.8 34.9	PASS	PASS	32.137 31.388	115 115	7.5 6.8	6.0 5.8	14.9 14.9	4.00 4.07	3.40 3.46	3.43	0.36 0.34	0.35	3.05 3.12	3.08	0.83	PASS	0.71	103.12	0.36	PASS
29	Inlet, 30B Port, STM 1062	171689 172182	7/24/13	12:08	13:08	600	110702.2 8682.3	110737.7 8717.9	35.5 35.6	PASS	PASS	31.779 32.995	48 59	595 604	17.0 19.0	8.5 8.5	20.77 20.67	19.00 18.91	18.96	17.62 17.28	17.45	1.38 1.64	1.51	0.24	PASS				
30	Stack D, STM 1064	171679 173013	7/24/13	12:37	13:37	600	15241.5 13284.1	15277.9 13319.4	36.4 35.3	PASS	PASS	32.689 31.904	134 133	9.9 10	6.7 6.8	14.9 14.9	4.61 4.70	3.92 4.00	3.96	0.43 0.45	0.44	3.49 3.55	3.52	0.95	PASS	0.95	115.84	0.51	PASS
31	Stack C, STM 1062	171598 172080	7/24/13	14:08	15:08	600	15281.5 13323.0	15318.5 13358.7	37.0 35.7	PASS	PASS	31.394 32.456	103 95	24 26	5.4 7.2	13.6 13.6	3.96 3.95	3.43 3.41	3.42	0.76 0.88	0.82	2.66 2.53	2.60	0.19	PASS	1.72	109.19	0.90	PASS
32	Inlet, 30B Port, STM 1062	171676 172483	7/27/13	9:10	10:10	600	110738.0 8721.1	110774.8 8757.0	36.8 35.9	PASS	PASS	34.172 34.092	45 53	622 613	17.0 17.0	8.5 8.5	20.02 20.09	18.31 18.38	18.35	17.11 16.96	17.04	1.20 1.42	1.31	0.19	PASS				
33	Stack D, STM 1064	171588 171710	7/27/13	09:37	10:37	600	15324.5 13364.6	15358.6 13397.4	34.1 32.8	PASS	PASS	32.683 31.757	101 118	17 11	7.1 3.9	14.9 14.9	3.83 4.18	3.26 3.56	3.41	0.63 0.40	0.51	2.63 3.16	2.90	4.46	PASS	0.90	75.30	0.39	PASS
34	Stack A, STM 1064	171621 171707	7/27/13	11:03	12:03	600				PASS	PASS	34.033 33.546	27 24	48 48	4.8 4.3	11.5 11.5	2.34 2.27	2.08 2.01	2.04	1.37 1.38	1.38	0.70 0.63	0.67	1.52	PASS	1.82	32.23	0.44	PASS
35	Stack B, STM 1064	172111 172235	7/30/13	14:20	15:20	600	15404.2 13442.2	15442.2 13479.2	38.0 37.0	PASS	PASS	34.239 33.634	21 20	30 29	2.7 2.8	12.2 12.2	1.57 1.54	1.38 1.35	1.36	0.84 0.83	0.83	0.54 0.52	0.53	0.91	PASS	1.01	21.06	0.18	PASS
36	Inlet, 30B Port, STM 1062	172241 172495	7/30/13	14:43	15:43	600	110776.8 8760.6	110811.8 8795.6	35.0 35.0	PASS	PASS	31.321 32.474	35 54	450 453	14.0 14.0	8.5 8.5	15.93 16.04	14.58 14.68	14.63	13.56 13.16	13.36	1.02 1.52	1.27	0.35	PASS				
37	Stack D, STM 1064	171685 173001	7/31/13	12:11	13:11	600	15445.2 13482.1	15480.6 13516.7	35.4 34.6	PASS	PASS	32.64 31.934	95 92	10 12	3.7 4.5	14.9 14.9	3.33 3.40	2.83 2.89	2.86	0.36 0.44	0.40	2.48 2.45	2.46	1.00	PASS	0.71	78.19	0.31	PASS
38	Stack D, STM 1064	172217	8/2/13	17:27	18:27	600	15485.3	15523.8	38.5	PASS	PASS	34.288	107	11	4.8	14.9	3.58	3.05	3.05	0.39	0.39	2.66	2.66			0.71	81.06	0.32	PASS
39	Stack C, STM 1062	171684 171693	8/2/13	18:42	19:42	600	15526.4 13528.8	15565.6 13560.5	39.2 31.7	PASS	PASS	34.539 33.648	71 69	20 22	5.9 5.4	13.6 13.6	2.81 2.86	2.42 2.48	2.45	0.65 0.70	0.68	1.78 1.77	1.77	1.05	PASS	1.42	110.14	0.74	PASS
40	Inlet, 30B Port, STM 1062	171686 173009	8/4/13	14:10	15:10	600	110966.3 8945.5	111004.9 8982.9	38.6 37.4	PASS	PASS	34.755 35.1	68 85	586 589	4.9 4.1	8.5 8.5	18.96 19.32	17.35 17.68	17.51	15.56 15.46	15.51	1.79 2.22	2.00	0.94	PASS				
41	Stack A, STM 1064	171585 172500	8/5/13	12:57	13:57	600	15568.7 13569.0	15603.2 13602.8	34.5 33.8	PASS	PASS	32.173 31.45	25 33	44 36	3.8 3.0	11.5 11.5	2.26 2.29	2.00 2.03	2.01	1.31 1.10	1.21	0.69 0.93	0.81	0.58	PASS				
42	Stack D, STM 1064	171678 172218	8/5/13	14:39	15:39	600	15607.0 13606.4	15642.8 13641.2	35.8 34.8	PASS	PASS	32.681 31.842	102 98	9.3 7.7	4.2 4.5	14.9 14.9	3.53 3.46	3.01 2.95	2.98	0.35 0.33	0.34	2.66 2.62	2.64	1.05	PASS	0.80	136.13	0.46	PASS
43	Stack B, STM 1064	184614 184821	8/7/13	15:56	16:56	600	15646.2 13644.8	15681.2 13679.1	35.0 34.3	PASS	PASS	32.583 32.069	25 23	29 28	2.6 2.7	12.2 12.2	1.74 1.67	1.53 1.47	1.50	0.85 0.84	0.85	0.67 0.63	0.65	1.83	PASS	0.91	7.56	0.06	PASS
44	Inlet, 30B Port, STM 1062	184646 184871	8/7/13	16:30	17:30	600	111008.8 8988.6	111044.9 9025.6	36.1 37.0	PASS	PASS	31.815 33.957	59 73	385 409	13.0 11.0	8.5 8.5	14.36 14.52	13.14 13.28	13.21	11.45 11.32	11.38	1.70 1.97	1.83	0.53	PASS				
45	Stack B, STM 1064	184627 184853	8/8/13	8:32	09:32	600	15685.1 13682.2	15719.5 13716.2	34.4 34.0	PASS	PASS	32.399 31.836	28 27	35 35	3.9 4.4	12.2 12.2	2.06 2.09	1.81 1.83	1.82	1.05 1.09	1.07	0.76 0.74	0.75	0.50	PASS	0.65	39.27	0.42	PASS
46	Stack D, STM 1064	184732 184920	8/8/13	10:04	11:04	600	15723.1 13719.7	15758.0 13753.4	34.9 33.7	PASS	PASS	32.167 31.361	86 85	6.7 8	3.7 4.2	14.9 14.9	3.00 3.10	2.55 2.64	2.59	0.28 0.33	0.30	2.28 2.31	2.29	1.68	PASS	0.68	124.35	0.38	PASS



Appendix B-3-2

Minnesota Department of Natural Resources Review of Phase II Hg Control Reports

October 31, 2014

10/31/2014

Minnesota Department of Natural Resources

500 Lafayette Road • St. Paul, MN • 55155-40__



Hongming Jiang
Pollution Control Agency
520 Lafayette Road North
St Paul, MN 55155

RE: Review of Phase II Hg Control Reports

Five taconite mining companies recently submitted reports to the Minnesota Pollution Control Agency evaluating activated and brominated carbon injection to control Hg in stack emissions. Subsequently, your agency made a request to the DNR that I review these documents. It was agreed that I would provide a general, less detailed analyses of the reports, but that MPCA would provide more in-depth detailed analyses. This letter provides my overall assessment of the five reports that were originally submitted by ADA-ES to each of the companies conducting the tests.

My general findings are as follows:

M30B analysis indicates capture is much less than what is analyzed by CMS, however, the sampling method used for M30B was not done iso-kinetically and so may not be quantitative. Two primary methods were used for the analysis of stack gases during the five studies: M30B and CEMS. M30B is a method that relies on the sampling of stack gases through a tube containing glass wool and a sorbent material while CEMS is a continuous monitoring method that only analyzes mercury in the gaseous phase. The former has the advantage that Hg bound to particulates that is trapped in the glass wool can be quantified and added to the estimation of total mercury in any sample passing through the tube. The latter only analyzes what is present in the gas phase, but has the advantage that it provides continuous monitoring rather than just a periodic "spot check".

Ultimately, the M30B method results show that ACI reduces gaseous mercury but that a substantial amount of particulate bound mercury is formed during ACI injection and some of this particulate fraction escapes the wet scrubber and is emitted at the stack. I will defer to those with more experience in measuring particulates in stack emissions to determine how much weight to place on the HgP and HgT measurements that were made using the M30B method.

Potential Hg feedback loops likely provided an additional interference for making reduction estimates at Minntac, Utac, and ArcelorMittal. Previous studies have indicated that at least some Hg captured by wet scrubbers at these plants is attached to the dust particles that are returned eventually to the balling mills (Benner, 2008; Berndt and Engesser, 2005a; Berndt and Engesser, 2005b; Berndt et al., 2005). Although some mention of this potential was provided in the reports, it was not addressed with the rigor needed to allow determination of the quantitative impacts on reduction estimates in any of the reports. It is reasonable to assume, however, that removing the feedback loops during ACI injection would greatly improve the percentages of mercury captured compared to the estimates provided in the reports.

Measurements provided for the scrubbers were inadequate to allow Hg balance checks to be conducted during any of the tests. Thus, we don't really know the fate of the captured mercury or how permanent (or ephemeral) the mercury reductions are. A previous study performed at a taconite processing plant indicated that a considerable fraction of the gas-phase Hg was lost somewhere within the plant and ducts when CaBr₂ was injected into process gases (Berndt, 2008). Mercury lost in the ducts or plant would not show up in the scrubber at first but could ultimately show up somewhere else later. Thus, tests involving brominated carbons should measure the total load of Hg that is captured by the scrubbers before and after the method is applied. Ideally, one would hope that the load captured and "blown down" by the scrubbers would balance Hg in the feed, fuel, product, and stack. Without such tests, we cannot determine what fraction of the Hg decreases occurred as a result of temporary hold-ups within the furnace (e.g., non-steady state) and that which was caused by increased capture in the scrubber. Although ADA-ES made some attempt to evaluate materials in the scrubbers before and during the tests, the methods used to evaluate the effluent fell far short of allowing quantification. In order to do so, more information would be needed on scrubber flow rates and the concentrations of Hg in the scrubber solids and liquids would need to be analyzed using more refined methods.

These results need to be compared to results from other past studies. ACI testing was previously conducted at both Hibbing Taconite and US Steel, but results from those tests were not compared to results from the present tests (Benson et al., 2012; Miller et al., 2012). Also, as mentioned above, much work was done previously on scrubber water and scrubber solid characterization (Berndt and Engesser, 2005b). Measured correctly, the change in scrubber solid chemistry can be used as an alternative means to estimate or verify changes in Hg capture rates.

Despite the four criticisms mentioned above, the reports do provide relatively strong evidence that re-emission of particulate-bound mercury is a pervasive issue that must be solved before brominated activated carbon injection methods can be considered suitable for the taconite industry. This potential issue was also identified previously in Phase 1 (Benson et al., 2012). Please let me know if I can be of any further assistance as the MPCA finalizes its review of the industry's reports.

Regards,



Michael E. Berndt

References (all available at http://www.dnr.state.mn.us/lands_minerals/dnr_hg_research.html)

- Benner, B.R., 2008. Bench scale tests to separate mercury from wet-scrubber solids from taconite plants. Report submitted to the Minnesota Department of Natural Resources, St. Paul, MN, p. 26.
- Benson, S.A., Nasah, J., Thumbi, C., Patwardhan, S., Yarbrough, L., Feilen, H., Korom, S.F., Srinivasachar, S., 2012. Evaluation of Scrubber Additives and Carbon Injection to Increase Mercury Capture, Report submitted to the Minnesota Department of Natural Resources, St. Paul, MN, p. 67.
- Berndt, M., Engesser, J., 2005a. Mercury Transport in Taconite Processing Facilities: (I) Release and Capture During Induration. An Iron Ore Cooperative Research Final Report, Report submitted to the Minnesota Department of Natural Resources, St. Paul, MN, p. 60.

Berndt, M., Engesser, J., 2005b. Mercury Transport in Taconite Processing Facilities: (II) Fate of Mercury Captured by Wet Scrubbers, Report submitted to the Minnesota Department of Natural Resources, St. Paul, MN, p. 32.

Berndt, M., Engesser, J., Berquo, T.S., 2005. Mercury chemistry and Mossbauer spectroscopy of iron oxides during taconite processing on Minnesota's Iron Range, Air Quality V. Energy and Environmental Research Center, Washington, D. C. , p. 15.

Berndt, M.E., 2008. On the measurement of stack emissions at taconite processing plants - a progress report submitted to MPCA, Report submitted to the Minnesota Department of Natural Resources, St. Paul, MN, St. Paul, MN, p. 23.

Miller, J., Zerangue, M., Tang, Z., Landreth, R., 2012. Mercury control for taconite plants using gas-phase brominated sorbents, Report submitted to the Minnesota Department of Natural Resources, St. Paul, MN, St. Paul, MN, p. 55.

CC Jennifer Engstrom

Appendix B-4

Gore Technology Demonstrations

Contents

B-4-1: Minnesota Taconite Mercury Reduction Research. GORE™ Demonstrations Summary Report (September 24, 2015).....	B-4-1
--	-------

Appendix B-4-1

Minnesota Taconite Mercury Reduction Research. GORE™ Demonstrations Summary Report

September 24, 2015



Minnesota Taconite Mercury Reduction Research *GORE™ Demonstrations Summary Report*

Prepared for
Iron Mining Association
ArcelorMittal Minorca Mine Inc.
Hibbing Taconite
Northshore Mining Company
U. S. Steel Keetac
U. S. Steel Minntac
United Taconite LLC



September 24, 2015

Minnesota Taconite Mercury Reduction Research

GORE™ Demonstrations Summary Report

September 24, 2015

Contents

1.0	Introduction	1
2.0	Background	2
2.1	Total Maximum Daily Load (TMDL)	2
2.2	Air Quality Rules for Mercury Air Emission Reduction and Reporting Requirements.....	3
2.3	Phase I Summary.....	5
2.4	Phase II Summary	5
2.5	GORE™ Mercury Control System.....	7
3.0	GORE™ Mercury Control System Pilot Unit Demonstrations	8
3.1	Summary of Demonstrations.....	8
3.2	Results	8
3.3	Conclusions.....	9
4.0	Next Steps.....	11

List of Tables

Table 2-1	TMDL Implementation Plan Interim Goals for the Minnesota Taconite Processing Sector..2
Table 2-2	Average mercury reduction during Test Period of ACI for Minnesota Taconite Mercury Reduction Working Group facilities.....6
Table 3-1	GORE™ Demonstration Pilot Unit Mercury and SO ₂ Reduction8

List of Appendices

Appendix A	Facility Technical Report
Appendix B	GORE™ Demonstration Report
Appendix C	TRC Test Reports

1.0 Introduction

This report presents an overview of mercury emission reduction research efforts undertaken to date by the Minnesota taconite industry. Participating facilities representing Minnesota's taconite industry include: ArcelorMittal Minorca Mine; Cliffs Natural Resources' Hibbing Taconite, Northshore Mining Company and United Taconite LLC; and U. S. Steel Keetac and Minntac. The purpose of this report is to provide a high-level summary of the industry-wide effort to determine if a technology has the potential to meet the requirements of Minnesota Rule 7007.0502, and summarize the testing and results from each of the GORE™ Mercury Control System pilot unit demonstrations.

In addition to this report, full facility-specific technical reports have been prepared to document testing results from the GORE™ Mercury Control System pilot unit demonstration at the specific testing facility, including mercury reduction results, sulfur dioxide (SO₂) reduction results, and mercury concentration levels in the wash water from the cleaning cycle of the GORE units. The facility-specific reports are included as appendices.

2.0 Background

2.1 Total Maximum Daily Load (TMDL)

The Minnesota Pollution Control Agency (MPCA) developed a state-wide mercury Total Maximum Daily Load (TMDL) to address mercury concentrations in Minnesota’s lakes and streams, which was approved by the U.S. Environmental Protection Agency (EPA) in March 2007. The TMDL addresses impaired waters by evaluating the sources of mercury pollution, pollutant reduction necessary to meet water-quality standards, and the allowable levels of future pollution. In Minnesota, mercury is primarily introduced to surface waters through atmospheric deposition.

The TMDL specifies that in order to meet water quality standards, a 93% reduction from 1990 human-caused, air-deposited mercury levels is required. Attainment of this goal is only possible through global and national reductions as 90% of mercury deposition in Minnesota is from sources outside of Minnesota. In accordance with the TMDL, the taconite processing sector have committed to a goal of a 75% reduction of mercury emissions by 2025 with the understanding that those reductions must not negatively impact pellet quality, does not cause excessive corrosion, and that the technology is technically and economically feasible.

The TMDL Implementation Plan¹ notes that “mercury-reduction technology does not currently exist for use on taconite pellet furnaces. Therefore, achieving the 75% mercury reduction target will incorporate the concept of adaptive management by focusing on research to develop the technology in the near term and installation of mercury emission control equipment thereafter.” The Plan recommends the following interim goals to the Minnesota taconite processing sector as outlined in Table 2-1:

Table 2-1 TMDL Implementation Plan Interim Goals for the Minnesota Taconite Processing Sector

Year	Interim Goals
2013	Complete medium and longer-term testing of identified mercury-reduction technologies on at least one straight-grate furnace and one grate-kiln furnace.
2014	Begin the first full-scale installation of mercury emission control equipment on one existing furnace. The equipment installed will consist of the most promising technology to date.
2016	Operation and modification of the equipment installed in 2014 will continue for two years to fully commission and maximize its efficiency. Based on results of full-scale installation and optimization, provide a schedule for implementation at all other existing furnaces.
2025	Completed installation of control technology on all furnaces and achieved the 75% mercury reduction goal.

¹ Implementation Plant for Minnesota’s Statewide Mercury Total Maximum Daily Load, 2009, Minnesota Pollution Control Agency

Additionally, the TMDL Implementation Plan requires the control technology must be technically and economically feasible, it must not impair pellet quality, and it must not cause excessive corrosion to pellet furnaces and associated ducting and emission-control equipment, also known as adaptive management criteria. The factors for determining technical and economic feasibility will be developed through a collaborative effort by the taconite industry and the MPCA.

2.2 Air Quality Rules for Mercury Air Emission Reduction and Reporting Requirements

On September 29, 2014, the State of Minnesota amended the air quality rules related to mercury air emissions reporting and reductions. While the new rules implement some aspects of the mercury reduction activities identified in the TMDL, the new rules do not incorporate all four of the adaptive management criteria for consideration when evaluating mercury reduction technology for feasibility. Also, the new rules require submittal of mercury reduction plans by December 30, 2018, according to Minn. R. 7007.0502 Subp. 4B.

The new rules require mercury reduction plans to include the following:

7007.0502 Subp. 5. Mercury Emissions Reduction Plan Elements and Format

A. The owners or operators of an existing mercury emission source must submit a mercury emissions reduction plan that complies with this item:

(1) The plan must be submitted in a format specified by the commissioner and must contain:

- a. description of the specific control equipment, processes, materials, or work practices that will be employed to achieve the applicable control efficiencies,*
- b. the mercury reduction, control efficiency, or emission rate that each emissions unit will achieve once the Plan for that emissions unit is fully implemented;*
- c. a description of how operating parameters will be optimized to maintain the mercury control efficiency in the Plan;*
- d. a proposed periodic monitoring and record-keeping system for proposed control equipment, processes, materials, or work practices or citation to an applicable requirement for monitoring and record keeping consistent with chapter 7017. An evaluation of the use of a continuous mercury emission monitoring system must be included in the Plan;*
- e. if the Plan includes elements that meet the definition of a modification under part 7007.0100, subpart 14, or requires an air permit amendment or notification under part 7007.1150, a projected schedule for submitting the appropriate permit applications; and*

- f. *the date that the mercury reductions proposed in the Plan will be demonstrated. This date must be no later than January 1, 2025, or as specified in subpart 6.*

(2) if the owner or operator determines that the mercury reductions listed in subpart 6, if applicable, are not technically achievable by the identified compliance date, the owners or operators may submit an alternative plan to reduce mercury emissions, in a format specified by the commissioner. The alternative plan must contain:

- a. *the plan elements in item A, substituting the owners' or operators' proposed reduction for the requirements under subpart 6;*
- b. *a detailed explanation of why the mercury reductions listed in subpart 6 are not technically achievable;*
- c. *a demonstration that air pollution control equipment, work practices, or the use of alternative fuels or raw materials have been optimized such that the source is using the best controls for mercury that are technically feasible; and*
- d. *an estimate of the annual mass of mercury emitted under the requirements of subpart 6 and the proposed alternative plan.*

Minnesota's taconite industry must include in the plan the minimum mercury control requirements for source categories listed in Minn. R. 7007.0502, Subp. 6A:

7007.0502 Subp. 6. Mercury Control and Work Practices

A. For ferrous mining or processing:

- (1) the plan must address the indurating furnace or kiln of a taconite processing facility or the rotary hearth furnace of a direct-reduced iron facility and must demonstrate that by January 1, 2025, mercury emissions from the indurating furnace or kiln or rotary hearth furnace do not exceed 28 percent of the mercury emitted in 2008 or 2010, whichever is greater. The commissioner shall determine the mercury emitted in 2008 and 2010. If the facility held a Minnesota Pollution Control Agency construction permit but was operating in 2010 at less than 75 percent of full capacity, the operating furnace must not exceed 28 percent of the mercury potential to emit included in the permit authorizing construction; and*
- (2) the plan may accomplish reductions as:*
 - a. *28 percent of 2008 or 2010 emissions for each furnace;*
 - b. *28 percent of 2008 or 2010 emissions across all furnaces at a single stationary source; or*
 - c. *28 percent of 2008 or 2010 emissions across furnaces at multiple stationary sources.*

Owners of the stationary sources must enter into an enforceable agreement as provided by Minnesota Statutes, section 115.071, subdivision 1, to reduce mercury emissions between the stationary sources. If this option is selected, the reduction plan must include the enforceable agreement. Execution of an enforceable agreement under this part does not relieve the owner or operator of the obligation to obtain a permit or permit amendment if otherwise required under this chapter.

Once the mercury reduction plan is submitted for approval, the plan will be included in the facility's

operating permit or other enforceable document. The plan will also be posted electronically to the MPCA's internet site for public viewing and not public comment. Interested parties may request to receive notification from the MPCA when plans are received. The following summarizes the industry's efforts in researching mercury reduction technology and methods as part of the TMDL and to meet the requirements of Minnesota Rule 7007.0502.

2.3 Phase I Summary

To assist the taconite industry in achieving the TMDL goal of 75% reduction, research was conducted by the Minnesota Taconite Mercury Control Agency Advisory Committee (MTMCAC), consisting of industry, state (including MPCA and MNDNR), and academic technical experts. Research conducted by this group from 2010-2012 focused on testing activated and brominated carbon sorbents to improve mercury capture in existing taconite processing plants. Six projects were selected and conducted using combined funds from the Minnesota Department of Natural Resources' Environmental Cooperative Research Program (ECR), six Minnesota participating taconite companies, and the US Environmental Protection Agency, Great Lakes Restoration Initiative (EPA-GLRI).

The six projects conducted include:

- 1) Evaluation of Scrubber Additives and Carbon Injection to Increase Mercury Capture;
- 2) Mercury Control for Taconite Plants Using Gas-Phase Brominated Sorbents;
- 3) Developing Cost-Effective Solutions to Reduce Mercury Emissions from Minnesota Taconite Plants;
- 4) Evaluation of a Slipstream Baghouse for the Taconite Industry;
- 5) Evaluation of a Low Corrosion Method to Increase Mercury Oxidation and Scrubber Capture; and
- 6) Corrosion Potential of Bromide Injection Under Taconite Operating Conditions

The methodology and results of these projects are documented in the Minnesota Taconite Mercury Control Advisory Committee: Summary of Phase One Research (Minnesota Department of Natural Resources, 2012). Of the methods considered in these six short-term studies, direct carbon injection, fixed bed reactors, and post-scrubber bag houses were all found to have the potential to control mercury at levels needed for the industry to achieve its 75% reduction goal. Direct injection of activated and brominated carbons into process gas streams was considered to be the most technically and economically feasible of these methods; and therefore, was chosen for further research and testing in Phase II of the effort.

2.4 Phase II Summary

Based on the Phase I short-term testing of various mercury control technologies tests, the taconite industry decided to further evaluate the effectiveness of mercury reduction by the injection of brominated activated carbon through screening of specific activated carbon products and extended testing of the

most promising activated carbon products. The Minnesota Taconite Mercury Reduction Working Group (Working Group) was comprised of environmental and technical staff from and funded by:

1. ArcelorMittal Minorca Mine Inc.
2. Hibbing Taconite
3. Northshore Mining Company
4. U. S. Steel Keetac
5. U. S. Steel Minntac
6. United Taconite LLC

ADA-ES, Inc. performed screening tests at each facility for the purpose of determining which powdered activated carbon (PAC) products were most promising to be used in each facility’s 15 – 30 day test period (Test Period). Products chosen from the screening test for the Test Period were determined based upon the product’s mercury removal capabilities and particulate matter emissions. Consideration was also given to the product’s technical and economic feasibility.

Results from Test Period of Activated Carbon Injection (ACI) at each facility are identified in Table 2-2:

Table 2-2 Average mercury reduction during Test Period of ACI for Minnesota Taconite Mercury Reduction Working Group facilities

Facility	ACI (lb/mmacf)	M30B	Hg-CEM
		Total Hg % Reduction	Gas Phase Hg % Reduction
Minntac ¹	9	52	82
Hibtac ²	3	40	81
Minorca ³	3	54	81
Keetac ⁴	7	61	82
Utac ⁵	5-8	25	48

Notes:

- 1 The facility has five furnaces, of which one furnace was tested with one stack; The stack that was tested and the number of runs are: SV 151 (average of 4 baseline runs and 1 ACI run).
- 2 The facility has three furnaces, of which one furnace was tested with four stacks; The stacks that were tested and the number of successful runs are: SV 029 (0 baseline runs and 3 ACI runs), SV 030 (2 baseline runs and 1 ACI run), SV 031 (0 baseline runs and 2 ACI runs); SV 032 (2 baseline runs and 4 ACI runs). No baseline M30Bs were taken on two of the four stacks.
- 3 The facility has one furnace. Four stacks were tested – the average reflects a summation of removal efficiencies for each stack; The stacks that were tested and their number of runs are: SV014 (average of 1 baseline run and 4 ACI runs), SV015 (average of 2 baseline runs and average of 3 ACI runs), SV016 (average of 1 baseline

- run and average of 3 ACI runs); SV017 (average of 2 baseline runs and average of 9 ACI runs).
- 4 The facility has one furnace. One stack was tested and the runs on the stack were averaged; The stack that was tested and the number of runs are: SV 051 (average of 2 baseline runs and average of 2 ACI runs).
- 5 The facility has two furnaces, of which one furnace with two stacks was tested. Testing was focused on one stack SV048 (3 baseline runs and 4 ACI runs) with supplementary testing performed on stack SV049 (1 baseline run and 3 ACI runs).

Conclusions gathered from Phase II efforts include:

- ACI can achieve some mercury reduction but did not meet the minimum mercury control requirements listed in Minn. R. 7007.0502, Subp. 6A;
- Total mercury reduction from ACI varied from 25% to 61%;
- Results varied from site to site due to intrinsic differences in furnace design, configuration, and operation;
- Although no facility demonstrated non-compliance for PM during stack testing, significantly higher PM flow weighted averages were noted;
- The use of ACI would, at a minimum, require a major permit modification and possibly a Prevention of Significant Deterioration permit;
- Taconite furnace atmospheres are different than utility power boilers – thus results show different mercury reduction results and require higher rates of injection than utility facilities; and
- When utilizing carbon injection particulate phase mercury is present and cannot be measured by Method 30A (mercury CEMS).

During Phase II, the Mercury Reduction Working Group began investigating GORE™ Mercury Control System (GORE™) technology to determine the feasibility in reducing mercury air emissions from taconite processing. The GORE technology was identified in 2011 as an emerging mercury reduction technology for taconite indurating furnaces. GORE is comprised of a pleated PTFE (polytetrafluoroethylene –Teflon) sorbent polymer composite for mercury reduction. Section 3.0 presents the GORE pilot unit demonstration project and results.

2.5 GORE™ Mercury Control System

While the initial Phase II testing showed preliminary results below the mercury reduction goal of 75% outlined in the TMDL, the Working Group became aware of and decided to evaluate the GORE™ technology as a potential alternative mercury reduction technology. The industry was informed of a pilot test that was occurring at Sherco, a power plant operated by Xcel Energy in Becker, MN. Industry representatives toured the pilot test and made the decision to pursue similar testing of the technology on taconite furnaces.

3.0 GORE™ Mercury Control System Pilot Unit Demonstrations

3.1 Summary of Demonstrations

The GORE™ technology is a fixed sorbent polymer composite, which doesn't require injection of powder sorbents or chemicals, capturing both elemental and oxidized mercury, and removes SO₂ as a co-benefit. The system includes wash equipment to remove particulate material from the pleated sorbent panels. The panels are housed in modules that may be placed in series to increase the removal efficiency of the system.

Cox Industries (Cox) was contracted by the Working Group to design, fabricate, and supply the GORE™ pilot unit to demonstrate mercury reduction from a taconite furnace exhaust slip steam. Demonstrations took place on three different induration furnaces: Minntac – Line 7, Minorca, and United Taconite – Line 2. Minntac - Line 7 is a grate-kiln furnace capable of burning natural gas, coal, fuel oil and biomass, Minorca is a straight-grate furnace capable of burning natural gas and fuel oil, and United Taconite - Line 2 is grate-kiln furnace capable of burning natural gas, coal, petroleum coke, and fuel oil.

GORE™ Mercury Control Business representatives assisted facility representatives in operating the pilot unit and conducting the demonstrations. The GORE™ pilot unit pulled a slip stream of air through the test skid modules (updraft) and through a fan, which returned the slip stream into the waste gas stack. The facilities where the demonstration took place contracted with TRC Solutions Emissions Testing Services to perform the mercury and SO₂ analysis. Samples for mercury and SO₂ were taken before and after the test skid modules to determine the amount of reduction. The mercury samples were analyzed using Method 30B. All results were excluded from testing if the paired traps were not within 10% of each other. SO₂ was analyzed using a Continuous Emission Monitoring System (CEMS). Water was used in the system to spray the GORE™ modules to remove particulate and any other build-up. The results of the GORE™ pilot unit demonstrations are described in the following section.

3.2 Results

The facility demonstration at Minntac – Line 7 commenced on September 4, 2014, and was completed on November 16, 2014. The facility demonstration at United Taconite – Line 2 commenced on December 1, 2014, and was completed on January 23, 2015. The facility demonstration at Minorca commenced on February 3, 2015, and was completed on March 12, 2015. Results from each of the facility demonstrations are presented in Table 3-1:

Table 3-1 Range of Airstream Velocity, Mercury Reduction and SO₂ Reduction During Site-Specific GORE™ Demonstration

Facility	Velocity (fps)	Total Hg Reduction (%)	SO ₂ Reduction (%)
		M30B	SO ₂ -CEM
Minntac ¹	7.7 – 12.0	48.1 – 83.7	66.4 – 80.6
United Taconite ²	8.0 – 12.0	39.5 – 91.6	48.9 – 79.6
Minorca ³	6.7 – 11.0	26.1 – 63.7	41.7 – 74.1

- 1 The facility has five furnaces, of which one furnace, Line 7, with one stack (SV 151) which was tested.
- 2 The facility has two furnaces, of which one furnace, Line 2, with two stacks. Testing was focused on SV049
- 3 The facility has one furnace with four stacks. Testing was focused on SV017.

3.3 Conclusions

Conclusions gathered from the GORE™ pilot unit demonstrations include:

- While GORE™ can achieve some mercury reduction it has not demonstrated the ability to consistently meet the minimum mercury control requirements listed in Minn. R. 7007.0502, Subp. 6A;
- Mercury reduction, measured by M30B, from GORE™ pilot unit demonstrations varied from 26% to 92% depending on a number of site-specific factors including SO₂ loading, airflow rate, wash water timing/flow/location, furnace design/configuration/operation.
- SO₂ reduction, measured by SO₂ CEMS, from the GORE™ pilot unit demonstrations varied from 41% to 81% depending on a number of site-specific factors including SO₂ loading (ore variability, fuel type), airflow, wash water timing/flow/location, furnace design/configuration/operation
- Pressure drop and airflow are an important factor to the design of the GORE™ system when considering full-scale implementation, as pressure drop and airflow will determine whether or not fan changes will be required to maintain necessary airflow through the furnace;
- Comparing the results from the GORE™ pilot unit demonstrations as an indicator for full-scale use to meet the estimated mercury reduction required by Minn. R. 7007.0502, Subp. 6A, facilities would need to scale up the GORE™ pilot unit by a factor of 200 to 390, depending on the overall airflow of the specific indurating furnace. For example, the GORE™ pilot unit needed to operate at 8ft/s in order to achieve a 72% reduction in mercury air emissions from Utac’s Line 2 furnace. UTAC’s Line 2 furnace would require a scale up factor of roughly 390 times the size of the GORE™ pilot unit, or roughly 2,350 Gore modules, to achieve a 72% reduction in mercury air

emissions on Utac's Line 2 furnace (8 fps = 1920 ACFM, 750,000 acfm total airflow from Utac Line 2 furnace / 1920 ACFM = 391, 391 x 6 = 2,344 modules). Further site-specific engineering is required to estimate the total footprint required for a full scale installation;

- The frequency of wash cycles varied during the GORE™ pilot unit demonstrations. Site-specific results of mercury concentration in the GORE™ membrane wash water effluent ranged from 2460 ng/L – 30,300 ng/L. The wash water influent mercury concentrations ranged from non-detect to approximately 10 ng/L. This represents a significant increase in mercury loading to the plants' process water systems. Coupled with an increase in other constituents to the plant water system (TDS, sulfate), consideration of a full-scale implementation of the GORE™ technology for mercury reduction would require the evaluation of additional wastewater treatment for the increased loading of mercury, sulfate, TDS and other constituents that may be captured by the wash water.
- Material build-up in the GORE unit was witnessed frequently when the slip-stream had low SO₂ levels, resulting in lower mercury reductions and more frequent wash cycle requirements. The long term effects of increased build-up could cause unacceptable differential pressure increases across the GORE unit, thereby reducing indurating airflow and jeopardizing pellet quality production. Since the site visit of the pilot test at Sherco, a facility representative notified the taconite industry that the GORE™ test was only run for approximately 5 months (July to December 2013) before the test was discontinued and the GORE unit was removed. The Sherco GORE test experienced similar issues that the taconite industry observed: significant increased differential pressure and plugging across the GORE™ modules as a result of particulate loading and low SO₂ levels in the air stream; and
- More information is required to properly assess whether the GORE™ technology is feasible for mercury reduction from a taconite furnace.

4.0 Next Steps

In the continuation of the industry wide efforts to meet the requirements of Minnesota Rule 7007.0502, the Working Group intends to complete a comprehensive review of the best available mercury reduction technology for taconite processing based on research and testing summarized above:

- What is the full range of potentially applicable technologies to be considered?
- Which mercury reduction technologies are technically feasible?
- What is the effectiveness in reducing mercury for technologies that are technically feasible?
- What is the economic feasibility of the technologies?

During this process, the Working Group intends to identify potential gaps in previous researching and testing that would support further investigation in order to develop a mercury reduction plan, potentially including:

- What additional parameters to be tested are required?
- Which alternatives are preferred for extended testing?
- What are the permitting implications with preferred alternative(s)

Appendix B-5

Site-Specific Evaluations

See Appendix B-5_Minorca BAMRT and AMERP Final Contents

B-5-1: ArcelorMittal Minorca Mine Inc. Activated Carbon Injection Testing to Control Mercury Air Emissions: Results of Extended Testing (September 2018).....	B-5-1
B-5-2: Hibbing Taconite Company. 2017 Mercury Reduction Test Report. Phase III – Gap Analysis: Halide Injection on Furnace Line 2 (April 13, 2018).....	B-5-662
B-5-3: Minorca Mine – Scrubber Solids Mass Balance (December 5, 2018)	B-5-720
B-5-4: Summary of Emissions Speciation Change on Potential Mercury Loading to Northeast Minnesota (December 14, 2018).....	B-5-837